Computational and Mathematical Methods in Medicine

Leveraging Complexity and Heterogeneity in Multi-Omics Biomedical Data 2022

Lead Guest Editor: Min Tang
Guest Editors: Hong Zheng and Jialiang Yang

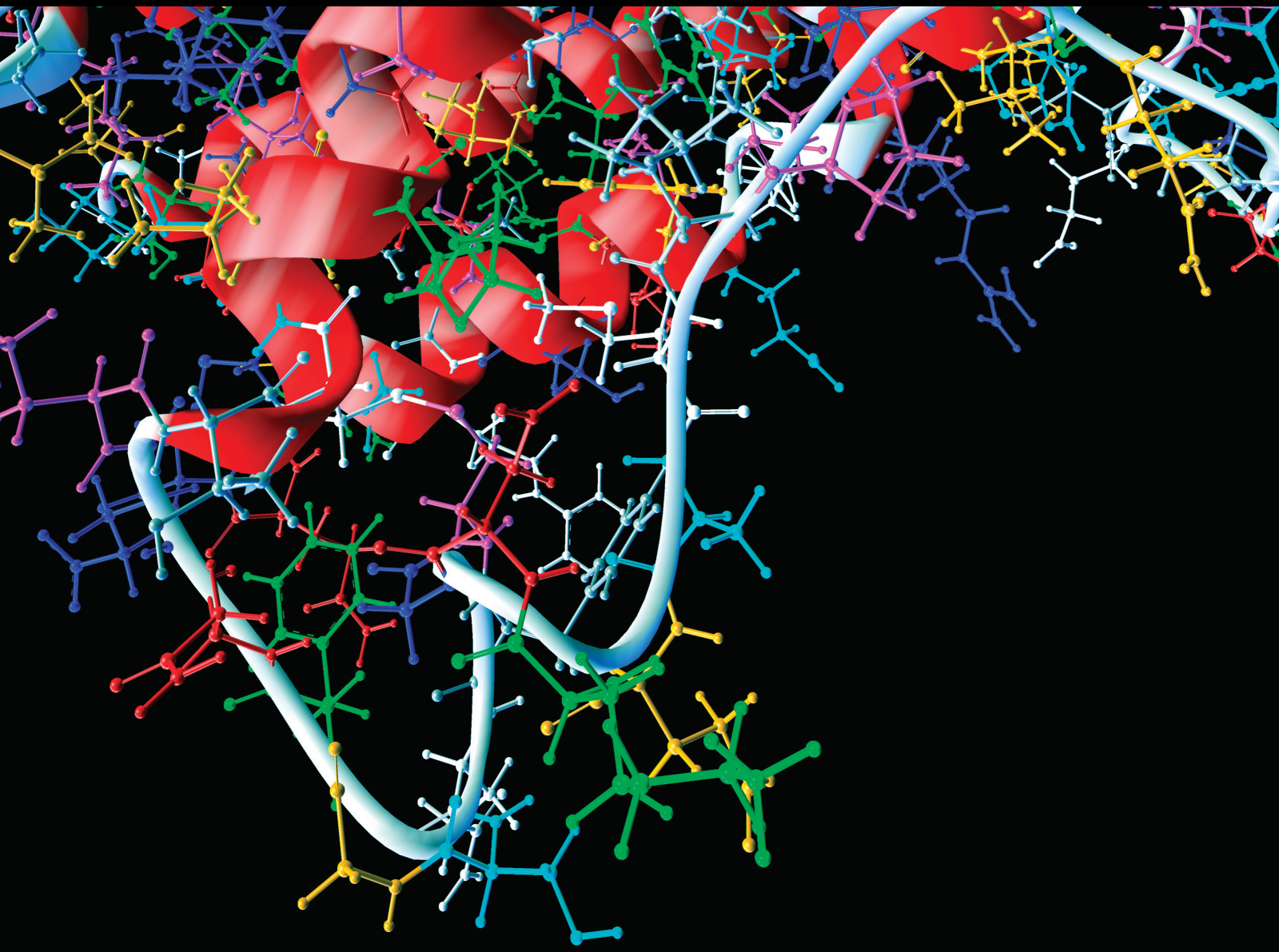

Leveraging Complexity and Heterogeneity in Multi-Omics Biomedical Data 2022

Computational and Mathematical Methods in Medicine

Leveraging Complexity and Heterogeneity in Multi-Omics Biomedical Data 2022

Lead Guest Editor: Min Tang
Guest Editors: Hong Zheng and Jialiang Yang

Contents

Retracted: Efficacy and Risk Factors of Pyrrotinib in Second- and Third-Line Treatments for HER2-Positive Advanced Breast Cancer
Computational and Mathematical Methods in Medicine
Retraction (1 page), Article ID 9868302, Volume 2023 (2023)

Retracted: A Systematic Review and Meta-Analysis of Influences of Chronic Kidney Disease on Patients after Percutaneous Coronary Intervention for Chronic Total Occlusions
Computational and Mathematical Methods in Medicine
Retraction (1 page), Article ID 9865637, Volume 2023 (2023)

Retracted: Continuous Renal Replacement Therapy for Hypertension Complicated by Refractory Heart Failure: An Analysis of Safety and Nursing Highlights
Computational and Mathematical Methods in Medicine
Retraction (1 page), Article ID 9864531, Volume 2023 (2023)

Retracted: Time to First Dressing Change after Peripherally Inserted Central Venous Catheter (PICC) Insertion in Breast Cancer Patients
Computational and Mathematical Methods in Medicine
Retraction (1 page), Article ID 9864257, Volume 2023 (2023)

Retracted: Analysis of the Relationship between Gut Flora Levels in Childhood Obese Population and Normal Healthy Population Based on Machine Learning
Computational and Mathematical Methods in Medicine
Retraction (1 page), Article ID 9861751, Volume 2023 (2023)

Retracted: Correlation Analysis of Serum Pepsinogen, Interleukin, and TNF-α with Hp Infection in Patients with Gastric Cancer: A Randomized Parallel Controlled Clinical Study
Computational and Mathematical Methods in Medicine
Retraction (1 page), Article ID 9856372, Volume 2023 (2023)

Retracted: Efficacy of TACE+Radiofrequency Ablation+Sorafenib in the Treatment of Patients with Recurrent Liver Cancer and Construction of Prediction Model
Computational and Mathematical Methods in Medicine
Retraction (1 page), Article ID 9850243, Volume 2023 (2023)

Retracted: circKMT2E Protect Retina from Early Diabetic Retinopathy through SIRT1 Signaling Pathway via Sponging miR-204-5p
Computational and Mathematical Methods in Medicine
Retraction (1 page), Article ID 9849304, Volume 2023 (2023)

Retracted: Relationship between Severity of Lumbar Spinal Stenosis and Ligamentum Flavum Hypertrophy and Serum Inflammatory Factors
Computational and Mathematical Methods in Medicine
Retraction (1 page), Article ID 9843748, Volume 2023 (2023)

Contents

Retracted: Comparison of the Effects of Laparoscopic Surgery and Traditional Open Surgery on Stone Clearance, Laboratory Indexes and Life Quality in Patients with Renal Calculi
Computational and Mathematical Methods in Medicine
Retraction (1 page), Article ID 9817359, Volume 2023 (2023)

Retracted: Application Value of Total Knee Arthroplasty plus Platelet-Rich Plasma Therapy in Traumatic Arthritis of the Knee
Computational and Mathematical Methods in Medicine
Retraction (1 page), Article ID 9808951, Volume 2023 (2023)

Retracted: Effect of Nursing Outcome-Oriented Intervention on Airway Management in Elderly Long-Term Bedridden Patients
Computational and Mathematical Methods in Medicine
Retraction (1 page), Article ID 9807415, Volume 2023 (2023)

Retracted: Berberine Inhibits Herpes Simplex Virus 1 Replication in HEK293T Cells
Computational and Mathematical Methods in Medicine
Retraction (1 page), Article ID 9806505, Volume 2023 (2023)

Retracted: Effects of Nifedipine and Labetalol Combined with Magnesium Sulfate on Blood Pressure Control, Blood Coagulation Function, and Maternal and Infant Outcome in Patients with Pregnancy-Induced Hypertension
Computational and Mathematical Methods in Medicine
Retraction (1 page), Article ID 9805202, Volume 2023 (2023)

Retracted: A Preliminary Study on the Value of Intestinal Flora in Predicting Major Adverse Cardiovascular and Cerebrovascular Events in Patients with Refractory Hypertension
Computational and Mathematical Methods in Medicine
Retraction (1 page), Article ID 9804870, Volume 2023 (2023)

Retracted: Impact of Small Incision Reduction and Suture Linked with Functional Appliance of Sufferers with Irrecoverable TMJ Anterior Disc Displacement
Computational and Mathematical Methods in Medicine
Retraction (1 page), Article ID 9795457, Volume 2023 (2023)

Retracted: Electroacupuncture Treats Myocardial Infarction by Influencing the Regulation of Substance P in the Neurovascular to Modulate PGI2/TXA2 Metabolic Homeostasis via PI3K/AKT Pathway: A Bioinformatics-Based Multiomics and Experimental Study
Computational and Mathematical Methods in Medicine
Retraction (1 page), Article ID 9793878, Volume 2023 (2023)

Retracted: Effects of Transcranial Magnetic Stimulation Combined with Computer-Aided Cognitive Training on Cognitive Function of Children with Cerebral Palsy and Dysgnosia
Computational and Mathematical Methods in Medicine
Retraction (1 page), Article ID 9790315, Volume 2023 (2023)

Contents

Retracted: Comparison of Effectiveness as well as Advantages and Disadvantages of Different Dimensions of Hysterosalpingo-Contrast Sonography for Diagnosis of Lesions Associated with Female Infertility
Computational and Mathematical Methods in Medicine
Retraction (1 page), Article ID 9757648, Volume 2023 (2023)

Retracted: Study on the Clinical Value of Noninvasive Prenatal Testing in Screening the Chromosomal Abnormalities of the Fetus in the Elderly Pregnant Women
Computational and Mathematical Methods in Medicine
Retraction (1 page), Article ID 9878617, Volume 2023 (2023)

Retracted: Effect of Enteral and Parenteral Nutrition Support on Pulmonary Function in Elderly Patients with Chronic Obstructive Pulmonary Disease Complicated by Respiratory Failure
Computational and Mathematical Methods in Medicine
Retraction (1 page), Article ID 9878450, Volume 2023 (2023)

Retracted: Influences of Antithrombotic Elastic Socks Combined with Air Pressure in Reducing Lower Extremity Deep Venous Thrombosis for Patients Undergoing Cardiothoracic Surgery
Computational and Mathematical Methods in Medicine
Retraction (1 page), Article ID 9863871, Volume 2023 (2023)

Retracted: The Significance of Implementing Bilevel Positive Airway Pressure under Cluster Nursing in Improving the Survival Possibility of Patients with Severe Pulmonary Infection Complicated by Respiratory Failure
Computational and Mathematical Methods in Medicine
Retraction (1 page), Article ID 9860406, Volume 2023 (2023)

Retracted: MDH1 and MDH2 Promote Cell Viability of Primary AT2 Cells by Increasing Glucose Uptake
Computational and Mathematical Methods in Medicine
Retraction (1 page), Article ID 9854393, Volume 2023 (2023)

Retracted: Acupuncture Enhances Gastrointestinal Motility and Improves Autonomic Nervous Function in Patients with Septic Gastrointestinal Dysfunction
Computational and Mathematical Methods in Medicine
Retraction (1 page), Article ID 9852615, Volume 2023 (2023)

Retracted: Identification of Molecular Targets and Underlying Mechanisms of Xiaoji Recipe against Pancreatic Cancer Based on Network Pharmacology
Computational and Mathematical Methods in Medicine
Retraction (1 page), Article ID 9758487, Volume 2023 (2023)

Retracted: The Relationship between Angiotensin–Neprilysin Treatment, Echocardiographic Parameters, and NT-proBNP Levels in HFpEF Patients with Acute Decompensated Heart Failure
Computational and Mathematical Methods in Medicine
Retraction (1 page), Article ID 9850396, Volume 2023 (2023)

Contents

Retracted: Mining of Potential Biomarkers and Pathway in Valvular Atrial Fibrillation (VAF) via Systematic Screening of Gene Coexpression Network
Computational and Mathematical Methods in Medicine
Retraction (1 page), Article ID 9823815, Volume 2023 (2023)

Retracted: Downregulation of miR-146a-5p Promotes Acute Pancreatitis through Activating the TLR9/NLRP3 Signaling Pathway by Targeting TRAF6 In Vitro Rat Model
Computational and Mathematical Methods in Medicine
Retraction (1 page), Article ID 9820687, Volume 2023 (2023)

Retracted: Effects of Hypoxia-Inducible Factor 1 (HIF-1) Signaling Pathway on Acute Ischemic Stroke
Computational and Mathematical Methods in Medicine
Retraction (1 page), Article ID 9819283, Volume 2023 (2023)

Retracted: Comparison of Efficacy and Psychology of Breast-Conserving Surgery and Modified Radical Mastectomy on Patients with Early Breast Cancer under Graded Nursing
Computational and Mathematical Methods in Medicine
Retraction (1 page), Article ID 9806902, Volume 2023 (2023)

Retracted: GINS2 Is Downregulated in Peripheral Blood of Patients with Intervertebral Disk Degeneration and Promotes Proliferation and Migration of Nucleus Pulposus Cells
Computational and Mathematical Methods in Medicine
Retraction (1 page), Article ID 9806791, Volume 2023 (2023)

Retracted: Influences of Airway Obstruction Caused by Adenoid Hypertrophy on Growth and Development of Craniomaxillofacial Structure and Respiratory Function in Children
Computational and Mathematical Methods in Medicine
Retraction (1 page), Article ID 9804692, Volume 2023 (2023)

Retracted: Mechanisms of Banxia Xiexin Decoction Underlying Chronic Atrophic Gastritis via Network Pharmacology, Molecular Docking, and Molecular Dynamics Simulations
Computational and Mathematical Methods in Medicine
Retraction (1 page), Article ID 9803037, Volume 2023 (2023)

Retracted: Multislice Computed Tomography Angiography Imaging Diagnosis of Lower Extremity Arteriosclerosis in Patients with Hypertension and Its Correlation with the Level of High-Sensitivity C-Reactive Protein
Computational and Mathematical Methods in Medicine
Retraction (1 page), Article ID 9796430, Volume 2023 (2023)

Retracted: To Study the Effect of Individualized Nursing Model Based on MDT Concept on Limb Function Recovery and Quality of Life in Patients with Breast Cancer
Computational and Mathematical Methods in Medicine
Retraction (1 page), Article ID 9790685, Volume 2023 (2023)

Contents

[Retracted] Effect of Dapagliflozin on Clinical Outcome after Drug-Eluting Stent Implantation in Elderly T2DM Patients: A Real-World Study
Yuan Lin, Fang Zhou, Xihu Wang, Yaju Guo, and Weiguo Chen
Research Article (5 pages), Article ID 8441396, Volume 2023 (2023)

[Retracted] Perioperative Effect of Single-Port Thoracoscopic Segmentectomy and Three-Port Thoracoscopic Segmentectomy in the Treatment of Early Non-Small-Cell Lung Cancer
Cong Zhang, Dexiong Jiang, Cuilian Luo, Dongdong Yuan, and Guansheng Shang
Research Article (6 pages), Article ID 7550317, Volume 2023 (2023)

[Retracted] A Systematic Review and Meta-Analysis of Influences of Chronic Kidney Disease on Patients after Percutaneous Coronary Intervention for Chronic Total Occlusions
Weifei Wu, Menghan Gao, and Xu Wu
Review Article (10 pages), Article ID 9450752, Volume 2023 (2023)

[Retracted] Individualized Management of Quality of Care in Orthopedic Nurses Based on Sensitive Indicators
Weiling Zhang, Xiaomin Huang, and Tianwen Huang
Research Article (8 pages), Article ID 1950220, Volume 2023 (2023)

[Retracted] Analysis of Efflux Pump System and Other Drug Resistance Related Gene Mutations in Tigecycline-Resistant *Acinetobacter baumannii*
Wenzheng Zheng, Yubo Huang, Wenbin Wu, Jiaxin Zhu, and Tiantuo Zhang
Research Article (12 pages), Article ID 8611542, Volume 2023 (2023)

[Retracted] An Eight-mRNA Prognostic Model to Predict Survival in Hepatic Cellular Cancer
Dong Xia, Xuebin Liao, and Huamao Zhang
Research Article (7 pages), Article ID 7278231, Volume 2023 (2023)

[Retracted] Role of GLI1 in Hypoxia-Driven Endometrial Stromal Cell Migration and Invasion in Endometriosis
Lili Wang, Jiaxin Liang, Siyi Bi, Yixuan Li, Wei Zhang, Wang Xiwen, Yi Liu, and Hengwei Liu
Research Article (9 pages), Article ID 6890790, Volume 2022 (2022)

[Retracted] Effects of Hypoxia-Inducible Factor 1 (HIF-1) Signaling Pathway on Acute Ischemic Stroke
Guoliang Li, Liang Tao, and Hui Wu
Research Article (8 pages), Article ID 1860925, Volume 2022 (2022)

[Retracted] Effect of Parecoxib Sodium Combined with Dexmedetomidine on Analgesia and Postoperative Pain of Patients Undergoing Hysteromyomectomy
Xiaowei Wang, Yongxue Chen, Yonglei Zhao, Zhigang Wang, Lu Zhao, Junde Hou, and Fei Liu
Research Article (7 pages), Article ID 5123933, Volume 2022 (2022)

Contents

[Retracted] Effect of Enteral and Parenteral Nutrition Support on Pulmonary Function in Elderly Patients with Chronic Obstructive Pulmonary Disease Complicated by Respiratory Failure
Liangge Wang, Wenxiu Rui, Si Chen, Yazhou Li, and Minhuan Ren
Research Article (8 pages), Article ID 4743070, Volume 2022 (2022)

[Retracted] Time to First Dressing Change after Peripherally Inserted Central Venous Catheter (PICC) Insertion in Breast Cancer Patients
Yinghua Zeng, Wenji Li, Xiaojin Li, and Lanlan Ma
Research Article (8 pages), Article ID 9380796, Volume 2022 (2022)

[Retracted] Outcome of Nursing Based on Health Belief United with Knowledge, Belief, and Practice Mode on Gastroscopy of Patients with Gastric Cancer
Junna Yang, Jing Yang, Dongmei Guo, Qingchao Zhao, and Yang Chen
Research Article (7 pages), Article ID 9491454, Volume 2022 (2022)

[Retracted] Analysis of Data on Fludarabine, Cyclophosphamide, and Rituximab Chemoimmunotherapy for Chronic Lymphocytic Leukemia Shows High Patient Heterogeneity and the Need for More Consideration of Individualized Treatment
Xiaoli Xu, Ying Zhao, Haiyan Ye, Yonglei Qi, Wenning Xu, Yiwen Ling, and Shaojiang Yang
Research Article (21 pages), Article ID 7451395, Volume 2022 (2022)

[Retracted] Mining of Potential Biomarkers and Pathway in Valvular Atrial Fibrillation (VAF) via Systematic Screening of Gene Coexpression Network
Fan Zou, Tiantian Chen, Xiuying Xiang, Chengjiang Peng, Shuai Huang, and Shaohong Ma
Research Article (21 pages), Article ID 3645402, Volume 2022 (2022)

[Retracted] circKMT2E Protect Retina from Early Diabetic Retinopathy through SIRT1 Signaling Pathway via Sponging miR-204-5p
Jilai Shi and Li Li
Research Article (12 pages), Article ID 7188193, Volume 2022 (2022)

[Retracted] Correlation of Serum M-CSF, CER, and TIMP-1 Levels with Liver Fibrosis in Viral Hepatitis
Hairong Yao, Xuan Yang, Man Yan, Xueqin Fang, Yange Wang, Hong Qi, and Li Sun
Research Article (8 pages), Article ID 6736225, Volume 2022 (2022)

[Retracted] Comparison of the Effects of Laparoscopic Surgery and Traditional Open Surgery on Stone Clearance, Laboratory Indexes and Life Quality in Patients with Renal Calculi
Qian Ai, Dong Tang, Yongfa Li, Yingjie Huang, and Junxian Yang
Research Article (9 pages), Article ID 8211389, Volume 2022 (2022)

[Retracted] Study on the Clinical Value of Noninvasive Prenatal Testing in Screening the Chromosomal Abnormalities of the Fetus in the Elderly Pregnant Women
Zhiping Gu, Mengmeng Du, Tianhui Xu, and Chunyan Jin
Research Article (7 pages), Article ID 2977128, Volume 2022 (2022)

Contents

[Retracted] Electroacupuncture Treats Myocardial Infarction by Influencing the Regulation of Substance P in the Neurovascular to Modulate PGI2/TXA2 Metabolic Homeostasis via PI3K/AKT Pathway: A Bioinformatics-Based Multiomics and Experimental Study
Ping Zhang, Yanyan Wang, Xiaomin Xing, Hu Li, Xiaojing Wang, Hanlin Zhang, Xin Wang, Xiubin Li, Yanju Li, and Qian Wang
Research Article (15 pages), Article ID 5367753, Volume 2022 (2022)

[Retracted] Expression of GMFB in High-Grade Cervical Intraepithelial Neoplasia and Its Role in Cervical Cancer
Jun Tian, Jianqing Wang, Yinxiu Chi, Zhongbao Han, Dongliang Zhang, and Hu Zhang
Research Article (8 pages), Article ID 7784921, Volume 2022 (2022)

[Retracted] Acupuncture Enhances Gastrointestinal Motility and Improves Autonomic Nervous Function in Patients with Septic Gastrointestinal Dysfunction
Lihong Ban, Yongpeng Pu, Huanyuan Huang, Bin You, Wei Chen, and Yanzhen Wang
Research Article (8 pages), Article ID 1653290, Volume 2022 (2022)

[Retracted] Hub Genes and Long Noncoding RNAs That Regulates It Associated with the Prognosis of Esophageal Squamous Cell Carcinoma Based on Bioinformatics Analysis
Jun Lu, Ruichao Li, Minghao Fang, and Shun Ke
Research Article (11 pages), Article ID 6027058, Volume 2022 (2022)

[Retracted] The Significance of Implementing Bilevel Positive Airway Pressure under Cluster Nursing in Improving the Survival Possibility of Patients with Severe Pulmonary Infection Complicated by Respiratory Failure
Xiao Fang and Haiyan Yang
Research Article (8 pages), Article ID 2324797, Volume 2022 (2022)

[Retracted] Efficacy and Prediction Model Construction of Drug-Coated Balloon Combined with Cutting Balloon Angioplasty in the Treatment of Drug-Eluting Stent In-Stent Restenosis
Haokun Wu, Tianhao Yu, Ting Fan, and Wenjun Liao
Research Article (8 pages), Article ID 9832622, Volume 2022 (2022)

[Retracted] Efficacy and Risk Factors of Pyrrotinib in Second- and Third-Line Treatments for HER2-Positive Advanced Breast Cancer
Xiaolei Wang, Yuxia Huang, Zhen Yang, Yang Yang, Fenfen Wei, Min Yan, and Fanfan Li
Research Article (8 pages), Article ID 7864114, Volume 2022 (2022)

[Retracted] Comparison of Effectiveness as well as Advantages and Disadvantages of Different Dimensions of Hysterosalpingo-Contrast Sonography for Diagnosis of Lesions Associated with Female Infertility
Rudi Pei
Research Article (7 pages), Article ID 7508880, Volume 2022 (2022)

Contents

[Retracted] The Relationship between Angiotensin–Neprilysin Treatment, Echocardiographic Parameters, and NT-proBNP Levels in HFpEF Patients with Acute Decompensated Heart Failure
Xiaoliang Zhang, Song Yang, and Zhonglin Xu
Research Article (6 pages), Article ID 4298644, Volume 2022 (2022)

[Retracted] To Study the Effect of Individualized Nursing Model Based on MDT Concept on Limb Function Recovery and Quality of Life in Patients with Breast Cancer
Yue Chen, Feng Luo, and Guo Shi
Research Article (6 pages), Article ID 1032503, Volume 2022 (2022)

[Retracted] Diagnostic Values of Advanced Glycation End Products and Homocysteine in Patients with Alzheimer's Disease and Sarcopenia
Xuelian Zhang, Yunxia Meng, Weiwei Zhang, Luhang Shi, Xia Liu, Lijuan Zhang, and Qiaoling Liu
Research Article (8 pages), Article ID 8949048, Volume 2022 (2022)

[Retracted] Cognitive Function and Vitamin D Status in the Chinese Hemodialysis Patients
Jing Zhang, Jun Hu, Ru Zhou, and Yuzhen Xu
Research Article (6 pages), Article ID 2175020, Volume 2022 (2022)

[Retracted] Identification of Molecular Targets and Underlying Mechanisms of Xiaoji Recipe against Pancreatic Cancer Based on Network Pharmacology
Cunbing Xia, Dexuan Chen, Gaoyuan Wang, Haijian Sun, Jingran Lin, Chen Chen, Tong Shen, Hui Cheng, Chao Pan, Dong Xu, Hongbao Yang, Yongkang Zhu, and Hong Zhu
Research Article (17 pages), Article ID 4640849, Volume 2022 (2022)

[Retracted] Effectiveness of Cognitive Behavior Therapy Combined with Eye Movement Desensitization and Reprocessing on Psychological Problems and Life Quality in Patients' Postfacial Trauma
Yue Lin, Wang Lv, Jun Xu, Yingying Jiang, and Zheyan Chen
Research Article (7 pages), Article ID 7822847, Volume 2022 (2022)

[Retracted] The Impact of Standardized Health Education in Patients with Ischemic Stroke on Patient Management Satisfaction and Quality of Clinical Management Services
Jing Chen and Lin Xiang
Research Article (6 pages), Article ID 5698400, Volume 2022 (2022)

[Retracted] Adverse Influences of Nonstrabismic Amblyopia on Quality of Life of Teenagers in China
Yakun Wang and Hong Wang
Research Article (6 pages), Article ID 2621991, Volume 2022 (2022)

[Retracted] MicroRNA-1306-5p Regulates the METTL14-Guided m6A Methylation to Repress Acute Myeloid Leukemia
Jiajia Li, Yanping Wu, Meng Wang, Xiaofeng Chen, Zhongyu Li, Xue Bai, and Haotian Wu
Research Article (12 pages), Article ID 5787808, Volume 2022 (2022)

Contents

[Retracted] Systematic Evaluation of the Efficacy of Acupuncture Associated with Physical and Mental Intervention when Treating Idiopathic Tinnitus and the Improvement of Tinnitus Symptoms
Yan Li, Di Sang, Zeting Wu, and Xuemei Cao
Research Article (10 pages), Article ID 6764909, Volume 2022 (2022)

[Retracted] Influence of Optimal Management of Hyperglycemia and Intensive Nursing on Blood Glucose Control Level and Complications in Patients with Postoperative Cerebral Hemorrhage
Dandan Sun, Liang Sun, and Fang Su
Research Article (7 pages), Article ID 8553539, Volume 2022 (2022)

[Retracted] Analysis of the Relationship between Gut Flora Levels in Childhood Obese Population and Normal Healthy Population Based on Machine Learning
Yaoqing Feng, Xia Si, Ruifang Zhu, Junxiang Chen, Wenting Zhao, Qian Wang, and Shifan Han
Research Article (9 pages), Article ID 6860940, Volume 2022 (2022)

[Retracted] Long Noncoding RNA LINC00473 Ameliorates Depression-Like Behaviors in Female Mice by Acting as a Molecular Sponge to Regulate miR-497-5p/BDNF Axis
Bo Li, Hongxia Zhao, and Junxia Sun
Research Article (12 pages), Article ID 4244425, Volume 2022 (2022)

[Retracted] Effects of Transcranial Magnetic Stimulation Combined with Computer-Aided Cognitive Training on Cognitive Function of Children with Cerebral Palsy and Dysgnosia
Jun Chen, Xiaoming Yu, and Guangjin Luo
Research Article (7 pages), Article ID 5316992, Volume 2022 (2022)

[Retracted] Meta-Analysis of the Effect of Nursing Intervention on Children with Type 2 Diabetes
Liying Tang, Zhen Xu, Ping Yao, and Huiqin Zhu
Research Article (10 pages), Article ID 6185739, Volume 2022 (2022)

[Retracted] A Preliminary Study on the Value of Intestinal Flora in Predicting Major Adverse Cardiovascular and Cerebrovascular Events in Patients with Refractory Hypertension
Jie Jiao, Yeping Zhang, Pengda Han, and Shuya Zhai
Research Article (7 pages), Article ID 7723105, Volume 2022 (2022)

[Retracted] Study on Strength and Quality Training of Youth Basketball Players
Qinghui Meng
Research Article (11 pages), Article ID 4676968, Volume 2022 (2022)

Hindawi
Computational and Mathematical Methods in Medicine
Volume 2023, Article ID 9897854, 1 page
https://doi.org/10.1155/2023/9897854

Retraction

Retracted: Correlation of Serum M-CSF, CER, and TIMP-1 Levels with Liver Fibrosis in Viral Hepatitis

Computational and Mathematical Methods in Medicine

Received 12 December 2023; Accepted 12 December 2023; Published 13 December 2023

This article has been retracted by Hindawi, as publisher, following an investigation undertaken by the publisher [1]. This investigation has uncovered evidence of systematic manipulation of the publication and peer-review process. We cannot, therefore, vouch for the reliability or integrity of this article.

Please note that this notice is intended solely to alert readers that the peer-review process of this article has been compromised.

Wiley and Hindawi regret that the usual quality checks did not identify these issues before publication and have since put additional measures in place to safeguard research integrity.

We wish to credit our Research Integrity and Research Publishing teams and anonymous and named external researchers and research integrity experts for contributing to this investigation.

The corresponding author, as the representative of all authors, has been given the opportunity to register their agreement or disagreement to this retraction. We have kept a record of any response received.

References

[1] H. Yao, X. Yang, M. Yan et al., "Correlation of Serum M-CSF, CER, and TIMP-1 Levels with Liver Fibrosis in Viral Hepatitis," *Computational and Mathematical Methods in Medicine*, vol. 2022, Article ID 6736225, 8 pages, 2022.

Hindawi
Computational and Mathematical Methods in Medicine
Volume 2023, Article ID 9895475, 1 page
https://doi.org/10.1155/2023/9895475

Retraction

Retracted: Analysis of Efflux Pump System and Other Drug Resistance Related Gene Mutations in Tigecycline-Resistant *Acinetobacter baumannii*

Computational and Mathematical Methods in Medicine

Received 12 December 2023; Accepted 12 December 2023; Published 13 December 2023

This article has been retracted by Hindawi, as publisher, following an investigation undertaken by the publisher [1]. This investigation has uncovered evidence of systematic manipulation of the publication and peer-review process. We cannot, therefore, vouch for the reliability or integrity of this article.

Please note that this notice is intended solely to alert readers that the peer-review process of this article has been compromised.

Wiley and Hindawi regret that the usual quality checks did not identify these issues before publication and have since put additional measures in place to safeguard research integrity.

We wish to credit our Research Integrity and Research Publishing teams and anonymous and named external researchers and research integrity experts for contributing to this investigation.

The corresponding author, as the representative of all authors, has been given the opportunity to register their agreement or disagreement to this retraction. We have kept a record of any response received.

References

[1] W. Zheng, Y. Huang, W. Wu, J. Zhu, and T. Zhang, "Analysis of Efflux Pump System and Other Drug Resistance Related Gene Mutations in Tigecycline-Resistant *Acinetobacter baumannii*," *Computational and Mathematical Methods in Medicine*, vol. 2023, Article ID 8611542, 12 pages, 2023.

Hindawi
Computational and Mathematical Methods in Medicine
Volume 2023, Article ID 9892159, 1 page
https://doi.org/10.1155/2023/9892159

Retraction

Retracted: Efficacy Analysis of Comprehensive Nursing in the Care of Ovarian Carcinoma Treated with Paclitaxel Combined with Nedaplatin

Computational and Mathematical Methods in Medicine

Received 12 December 2023; Accepted 12 December 2023; Published 13 December 2023

This article has been retracted by Hindawi, as publisher, following an investigation undertaken by the publisher [1]. This investigation has uncovered evidence of systematic manipulation of the publication and peer-review process. We cannot, therefore, vouch for the reliability or integrity of this article.

Please note that this notice is intended solely to alert readers that the peer-review process of this article has been compromised.

Wiley and Hindawi regret that the usual quality checks did not identify these issues before publication and have since put additional measures in place to safeguard research integrity.

We wish to credit our Research Integrity and Research Publishing teams and anonymous and named external researchers and research integrity experts for contributing to this investigation.

The corresponding author, as the representative of all authors, has been given the opportunity to register their agreement or disagreement to this retraction. We have kept a record of any response received.

References

[1] Y. Li, J. Wu, and G. Zhu, "Efficacy Analysis of Comprehensive Nursing in the Care of Ovarian Carcinoma Treated with Paclitaxel Combined with Nedaplatin," *Computational and Mathematical Methods in Medicine*, vol. 2022, Article ID 9398823, 6 pages, 2022.

Hindawi
Computational and Mathematical Methods in Medicine
Volume 2023, Article ID 9891370, 1 page
https://doi.org/10.1155/2023/9891370

Retraction

Retracted: Meta-Analysis of the Effect of Nursing Intervention on Children with Type 2 Diabetes

Computational and Mathematical Methods in Medicine

Received 12 December 2023; Accepted 12 December 2023; Published 13 December 2023

This article has been retracted by Hindawi, as publisher, following an investigation undertaken by the publisher [1]. This investigation has uncovered evidence of systematic manipulation of the publication and peer-review process. We cannot, therefore, vouch for the reliability or integrity of this article.

Please note that this notice is intended solely to alert readers that the peer-review process of this article has been compromised.

Wiley and Hindawi regret that the usual quality checks did not identify these issues before publication and have since put additional measures in place to safeguard research integrity.

We wish to credit our Research Integrity and Research Publishing teams and anonymous and named external researchers and research integrity experts for contributing to this investigation.

The corresponding author, as the representative of all authors, has been given the opportunity to register their agreement or disagreement to this retraction. We have kept a record of any response received.

References

[1] L. Tang, Z. Xu, P. Yao, and H. Zhu, "Meta-Analysis of the Effect of Nursing Intervention on Children with Type 2 Diabetes," *Computational and Mathematical Methods in Medicine*, vol. 2022, Article ID 6185739, 10 pages, 2022.

Hindawi
Computational and Mathematical Methods in Medicine
Volume 2023, Article ID 9891078, 1 page
https://doi.org/10.1155/2023/9891078

Retraction

Retracted: Effectiveness of Cognitive Behavior Therapy Combined with Eye Movement Desensitization and Reprocessing on Psychological Problems and Life Quality in Patients' Postfacial Trauma

Computational and Mathematical Methods in Medicine

Received 12 December 2023; Accepted 12 December 2023; Published 13 December 2023

This article has been retracted by Hindawi, as publisher, following an investigation undertaken by the publisher [1]. This investigation has uncovered evidence of systematic manipulation of the publication and peer-review process. We cannot, therefore, vouch for the reliability or integrity of this article.

Please note that this notice is intended solely to alert readers that the peer-review process of this article has been compromised.

Wiley and Hindawi regret that the usual quality checks did not identify these issues before publication and have since put additional measures in place to safeguard research integrity.

We wish to credit our Research Integrity and Research Publishing teams and anonymous and named external researchers and research integrity experts for contributing to this investigation.

The corresponding author, as the representative of all authors, has been given the opportunity to register their agreement or disagreement to this retraction. We have kept a record of any response received.

References

[1] Y. Lin, W. Lv, J. Xu, Y. Jiang, and Z. Chen, "Effectiveness of Cognitive Behavior Therapy Combined with Eye Movement Desensitization and Reprocessing on Psychological Problems and Life Quality in Patients' Postfacial Trauma," *Computational and Mathematical Methods in Medicine*, vol. 2022, Article ID 7822847, 7 pages, 2022.

Hindawi
Computational and Mathematical Methods in Medicine
Volume 2023, Article ID 9879478, 1 page
https://doi.org/10.1155/2023/9879478

Retraction

Retracted: The Effect of Microwave Ablation Combined with Anti-PD-1 Monoclonal Antibody on T Cell Subsets and Long-Term Prognosis in Patients Suffering from Non-Small-Cell Lung Cancer

Computational and Mathematical Methods in Medicine

Received 12 December 2023; Accepted 12 December 2023; Published 13 December 2023

This article has been retracted by Hindawi, as publisher, following an investigation undertaken by the publisher [1]. This investigation has uncovered evidence of systematic manipulation of the publication and peer-review process. We cannot, therefore, vouch for the reliability or integrity of this article.

Please note that this notice is intended solely to alert readers that the peer-review process of this article has been compromised.

Wiley and Hindawi regret that the usual quality checks did not identify these issues before publication and have since put additional measures in place to safeguard research integrity.

We wish to credit our Research Integrity and Research Publishing teams and anonymous and named external researchers and research integrity experts for contributing to this investigation.

The corresponding author, as the representative of all authors, has been given the opportunity to register their agreement or disagreement to this retraction. We have kept a record of any response received.

References

[1] W. Yu, J. Sun, T. Wang, and Y. Du, "The Effect of Microwave Ablation Combined with Anti-PD-1 Monoclonal Antibody on T Cell Subsets and Long-Term Prognosis in Patients Suffering from Non-Small-Cell Lung Cancer," *Computational and Mathematical Methods in Medicine*, vol. 2022, Article ID 7095423, 7 pages, 2022.

Hindawi
Computational and Mathematical Methods in Medicine
Volume 2023, Article ID 9879301, 1 page
https://doi.org/10.1155/2023/9879301

Retraction

Retracted: The Impact of Standardized Health Education in Patients with Ischemic Stroke on Patient Management Satisfaction and Quality of Clinical Management Services

Computational and Mathematical Methods in Medicine

Received 12 December 2023; Accepted 12 December 2023; Published 13 December 2023

This article has been retracted by Hindawi, as publisher, following an investigation undertaken by the publisher [1]. This investigation has uncovered evidence of systematic manipulation of the publication and peer-review process. We cannot, therefore, vouch for the reliability or integrity of this article.

Please note that this notice is intended solely to alert readers that the peer-review process of this article has been compromised.

Wiley and Hindawi regret that the usual quality checks did not identify these issues before publication and have since put additional measures in place to safeguard research integrity.

We wish to credit our Research Integrity and Research Publishing teams and anonymous and named external researchers and research integrity experts for contributing to this investigation.

The corresponding author, as the representative of all authors, has been given the opportunity to register their agreement or disagreement to this retraction. We have kept a record of any response received.

References

[1] J. Chen and L. Xiang, "The Impact of Standardized Health Education in Patients with Ischemic Stroke on Patient Management Satisfaction and Quality of Clinical Management Services," *Computational and Mathematical Methods in Medicine*, vol. 2022, Article ID 5698400, 6 pages, 2022.

Hindawi
Computational and Mathematical Methods in Medicine
Volume 2023, Article ID 9878272, 1 page
https://doi.org/10.1155/2023/9878272

Retraction

Retracted: Clinical Application of Digital 3D Reconstruction and 3D Printing Technology in Endometrial Cancer (EC) Surgery

Computational and Mathematical Methods in Medicine

Received 12 December 2023; Accepted 12 December 2023; Published 13 December 2023

This article has been retracted by Hindawi, as publisher, following an investigation undertaken by the publisher [1]. This investigation has uncovered evidence of systematic manipulation of the publication and peer-review process. We cannot, therefore, vouch for the reliability or integrity of this article.

Please note that this notice is intended solely to alert readers that the peer-review process of this article has been compromised.

Wiley and Hindawi regret that the usual quality checks did not identify these issues before publication and have since put additional measures in place to safeguard research integrity.

We wish to credit our Research Integrity and Research Publishing teams and anonymous and named external researchers and research integrity experts for contributing to this investigation.

The corresponding author, as the representative of all authors, has been given the opportunity to register their agreement or disagreement to this retraction. We have kept a record of any response received.

References

[1] F. Luo and Q. Yang, "Clinical Application of Digital 3D Reconstruction and 3D Printing Technology in Endometrial Cancer (EC) Surgery," *Computational and Mathematical Methods in Medicine*, vol. 2022, Article ID 9180216, 8 pages, 2022.

Hindawi
Computational and Mathematical Methods in Medicine
Volume 2023, Article ID 9868969, 1 page
https://doi.org/10.1155/2023/9868969

Retraction

Retracted: Perioperative Effect of Single-Port Thoracoscopic Segmentectomy and Three-Port Thoracoscopic Segmentectomy in the Treatment of Early Non-Small-Cell Lung Cancer

Computational and Mathematical Methods in Medicine

Received 12 December 2023; Accepted 12 December 2023; Published 13 December 2023

This article has been retracted by Hindawi, as publisher, following an investigation undertaken by the publisher [1]. This investigation has uncovered evidence of systematic manipulation of the publication and peer-review process. We cannot, therefore, vouch for the reliability or integrity of this article.

Please note that this notice is intended solely to alert readers that the peer-review process of this article has been compromised.

Wiley and Hindawi regret that the usual quality checks did not identify these issues before publication and have since put additional measures in place to safeguard research integrity.

We wish to credit our Research Integrity and Research Publishing teams and anonymous and named external researchers and research integrity experts for contributing to this investigation.

The corresponding author, as the representative of all authors, has been given the opportunity to register their agreement or disagreement to this retraction. We have kept a record of any response received.

References

[1] C. Zhang, D. Jiang, C. Luo, D. Yuan, and G. Shang, "Perioperative Effect of Single-Port Thoracoscopic Segmentectomy and Three-Port Thoracoscopic Segmentectomy in the Treatment of Early Non-Small-Cell Lung Cancer," *Computational and Mathematical Methods in Medicine*, vol. 2023, Article ID 7550317, 6 pages, 2023.

Hindawi
Computational and Mathematical Methods in Medicine
Volume 2023, Article ID 9868302, 1 page
https://doi.org/10.1155/2023/9868302

Retraction

Retracted: Efficacy and Risk Factors of Pyrrotinib in Second- and Third-Line Treatments for HER2-Positive Advanced Breast Cancer

Computational and Mathematical Methods in Medicine

Received 12 December 2023; Accepted 12 December 2023; Published 13 December 2023

This article has been retracted by Hindawi, as publisher, following an investigation undertaken by the publisher [1]. This investigation has uncovered evidence of systematic manipulation of the publication and peer-review process. We cannot, therefore, vouch for the reliability or integrity of this article.

Please note that this notice is intended solely to alert readers that the peer-review process of this article has been compromised.

Wiley and Hindawi regret that the usual quality checks did not identify these issues before publication and have since put additional measures in place to safeguard research integrity.

We wish to credit our Research Integrity and Research Publishing teams and anonymous and named external researchers and research integrity experts for contributing to this investigation.

The corresponding author, as the representative of all authors, has been given the opportunity to register their agreement or disagreement to this retraction. We have kept a record of any response received.

References

[1] X. Wang, Y. Huang, Z. Yang et al., "Efficacy and Risk Factors of Pyrrotinib in Second- and Third-Line Treatments for HER2-Positive Advanced Breast Cancer," *Computational and Mathematical Methods in Medicine*, vol. 2022, Article ID 7864114, 8 pages, 2022.

Hindawi
Computational and Mathematical Methods in Medicine
Volume 2023, Article ID 9865637, 1 page
https://doi.org/10.1155/2023/9865637

Retraction

Retracted: A Systematic Review and Meta-Analysis of Influences of Chronic Kidney Disease on Patients after Percutaneous Coronary Intervention for Chronic Total Occlusions

Computational and Mathematical Methods in Medicine

Received 12 December 2023; Accepted 12 December 2023; Published 13 December 2023

This article has been retracted by Hindawi, as publisher, following an investigation undertaken by the publisher [1]. This investigation has uncovered evidence of systematic manipulation of the publication and peer-review process. We cannot, therefore, vouch for the reliability or integrity of this article.

Please note that this notice is intended solely to alert readers that the peer-review process of this article has been compromised.

Wiley and Hindawi regret that the usual quality checks did not identify these issues before publication and have since put additional measures in place to safeguard research integrity.

We wish to credit our Research Integrity and Research Publishing teams and anonymous and named external researchers and research integrity experts for contributing to this investigation.

The corresponding author, as the representative of all authors, has been given the opportunity to register their agreement or disagreement to this retraction. We have kept a record of any response received.

References

[1] W. Wu, M. Gao, and X. Wu, "A Systematic Review and Meta-Analysis of Influences of Chronic Kidney Disease on Patients after Percutaneous Coronary Intervention for Chronic Total Occlusions," *Computational and Mathematical Methods in Medicine*, vol. 2023, Article ID 9450752, 10 pages, 2023.

Hindawi
Computational and Mathematical Methods in Medicine
Volume 2023, Article ID 9864531, 1 page
https://doi.org/10.1155/2023/9864531

Retraction

Retracted: Continuous Renal Replacement Therapy for Hypertension Complicated by Refractory Heart Failure: An Analysis of Safety and Nursing Highlights

Computational and Mathematical Methods in Medicine

Received 12 December 2023; Accepted 12 December 2023; Published 13 December 2023

This article has been retracted by Hindawi, as publisher, following an investigation undertaken by the publisher [1]. This investigation has uncovered evidence of systematic manipulation of the publication and peer-review process. We cannot, therefore, vouch for the reliability or integrity of this article.

Please note that this notice is intended solely to alert readers that the peer-review process of this article has been compromised.

Wiley and Hindawi regret that the usual quality checks did not identify these issues before publication and have since put additional measures in place to safeguard research integrity.

We wish to credit our Research Integrity and Research Publishing teams and anonymous and named external researchers and research integrity experts for contributing to this investigation.

The corresponding author, as the representative of all authors, has been given the opportunity to register their agreement or disagreement to this retraction. We have kept a record of any response received.

References

[1] M. Zhang and J. Li, "Continuous Renal Replacement Therapy for Hypertension Complicated by Refractory Heart Failure: An Analysis of Safety and Nursing Highlights," *Computational and Mathematical Methods in Medicine*, vol. 2022, Article ID 7951744, 8 pages, 2022.

Hindawi
Computational and Mathematical Methods in Medicine
Volume 2023, Article ID 9864257, 1 page
https://doi.org/10.1155/2023/9864257

Retraction

Retracted: Time to First Dressing Change after Peripherally Inserted Central Venous Catheter (PICC) Insertion in Breast Cancer Patients

Computational and Mathematical Methods in Medicine

Received 12 December 2023; Accepted 12 December 2023; Published 13 December 2023

This article has been retracted by Hindawi, as publisher, following an investigation undertaken by the publisher [1]. This investigation has uncovered evidence of systematic manipulation of the publication and peer-review process. We cannot, therefore, vouch for the reliability or integrity of this article.

Please note that this notice is intended solely to alert readers that the peer-review process of this article has been compromised.

Wiley and Hindawi regret that the usual quality checks did not identify these issues before publication and have since put additional measures in place to safeguard research integrity.

We wish to credit our Research Integrity and Research Publishing teams and anonymous and named external researchers and research integrity experts for contributing to this investigation.

The corresponding author, as the representative of all authors, has been given the opportunity to register their agreement or disagreement to this retraction. We have kept a record of any response received.

References

[1] Y. Zeng, W. Li, X. Li, and L. Ma, "Time to First Dressing Change after Peripherally Inserted Central Venous Catheter (PICC) Insertion in Breast Cancer Patients," *Computational and Mathematical Methods in Medicine*, vol. 2022, Article ID 9380796, 8 pages, 2022.

Hindawi
Computational and Mathematical Methods in Medicine
Volume 2023, Article ID 9861751, 1 page
https://doi.org/10.1155/2023/9861751

Retraction

Retracted: Analysis of the Relationship between Gut Flora Levels in Childhood Obese Population and Normal Healthy Population Based on Machine Learning

Computational and Mathematical Methods in Medicine

Received 12 December 2023; Accepted 12 December 2023; Published 13 December 2023

This article has been retracted by Hindawi, as publisher, following an investigation undertaken by the publisher [1]. This investigation has uncovered evidence of systematic manipulation of the publication and peer-review process. We cannot, therefore, vouch for the reliability or integrity of this article.

Please note that this notice is intended solely to alert readers that the peer-review process of this article has been compromised.

Wiley and Hindawi regret that the usual quality checks did not identify these issues before publication and have since put additional measures in place to safeguard research integrity.

We wish to credit our Research Integrity and Research Publishing teams and anonymous and named external researchers and research integrity experts for contributing to this investigation.

The corresponding author, as the representative of all authors, has been given the opportunity to register their agreement or disagreement to this retraction. We have kept a record of any response received.

References

[1] Y. Feng, X. Si, R. Zhu et al., "Analysis of the Relationship between Gut Flora Levels in Childhood Obese Population and Normal Healthy Population Based on Machine Learning," *Computational and Mathematical Methods in Medicine*, vol. 2022, Article ID 6860940, 9 pages, 2022.

Hindawi
Computational and Mathematical Methods in Medicine
Volume 2023, Article ID 9856372, 1 page
https://doi.org/10.1155/2023/9856372

Retraction

Retracted: Correlation Analysis of Serum Pepsinogen, Interleukin, and TNF-α with Hp Infection in Patients with Gastric Cancer: A Randomized Parallel Controlled Clinical Study

Computational and Mathematical Methods in Medicine

Received 12 December 2023; Accepted 12 December 2023; Published 13 December 2023

This article has been retracted by Hindawi, as publisher, following an investigation undertaken by the publisher [1]. This investigation has uncovered evidence of systematic manipulation of the publication and peer-review process. We cannot, therefore, vouch for the reliability or integrity of this article.

Please note that this notice is intended solely to alert readers that the peer-review process of this article has been compromised.

Wiley and Hindawi regret that the usual quality checks did not identify these issues before publication and have since put additional measures in place to safeguard research integrity.

We wish to credit our Research Integrity and Research Publishing teams and anonymous and named external researchers and research integrity experts for contributing to this investigation.

The corresponding author, as the representative of all authors, has been given the opportunity to register their agreement or disagreement to this retraction. We have kept a record of any response received.

References

[1] S. Hao, M. Shou, J. Ma, Y. Shu, and Y. Yu, "Correlation Analysis of Serum Pepsinogen, Interleukin, and TNF-α with Hp Infection in Patients with Gastric Cancer: A Randomized Parallel Controlled Clinical Study," *Computational and Mathematical Methods in Medicine*, vol. 2022, Article ID 9277847, 7 pages, 2022.

Hindawi
Computational and Mathematical Methods in Medicine
Volume 2023, Article ID 9850243, 1 page
https://doi.org/10.1155/2023/9850243

Retraction

Retracted: Efficacy of TACE+Radiofrequency Ablation +Sorafenib in the Treatment of Patients with Recurrent Liver Cancer and Construction of Prediction Model

Computational and Mathematical Methods in Medicine

Received 12 December 2023; Accepted 12 December 2023; Published 13 December 2023

This article has been retracted by Hindawi, as publisher, following an investigation undertaken by the publisher [1]. This investigation has uncovered evidence of systematic manipulation of the publication and peer-review process. We cannot, therefore, vouch for the reliability or integrity of this article.

Please note that this notice is intended solely to alert readers that the peer-review process of this article has been compromised.

Wiley and Hindawi regret that the usual quality checks did not identify these issues before publication and have since put additional measures in place to safeguard research integrity.

We wish to credit our Research Integrity and Research Publishing teams and anonymous and named external researchers and research integrity experts for contributing to this investigation.

The corresponding author, as the representative of all authors, has been given the opportunity to register their agreement or disagreement to this retraction. We have kept a record of any response received.

References

[1] A. Sun, S. Chen, M. Lin et al., "Efficacy of TACE+Radiofrequency Ablation+Sorafenib in the Treatment of Patients with Recurrent Liver Cancer and Construction of Prediction Model," *Computational and Mathematical Methods in Medicine*, vol. 2022, Article ID 6879035, 7 pages, 2022.

Hindawi
Computational and Mathematical Methods in Medicine
Volume 2023, Article ID 9849304, 1 page
https://doi.org/10.1155/2023/9849304

Retraction

Retracted: circKMT2E Protect Retina from Early Diabetic Retinopathy through SIRT1 Signaling Pathway via Sponging miR-204-5p

Computational and Mathematical Methods in Medicine

Received 12 December 2023; Accepted 12 December 2023; Published 13 December 2023

This article has been retracted by Hindawi, as publisher, following an investigation undertaken by the publisher [1]. This investigation has uncovered evidence of systematic manipulation of the publication and peer-review process. We cannot, therefore, vouch for the reliability or integrity of this article.

Please note that this notice is intended solely to alert readers that the peer-review process of this article has been compromised.

Wiley and Hindawi regret that the usual quality checks did not identify these issues before publication and have since put additional measures in place to safeguard research integrity.

We wish to credit our Research Integrity and Research Publishing teams and anonymous and named external researchers and research integrity experts for contributing to this investigation.

The corresponding author, as the representative of all authors, has been given the opportunity to register their agreement or disagreement to this retraction. We have kept a record of any response received.

References

[1] J. Shi and L. Li, "circKMT2E Protect Retina from Early Diabetic Retinopathy through SIRT1 Signaling Pathway via Sponging miR-204-5p," *Computational and Mathematical Methods in Medicine*, vol. 2022, Article ID 7188193, 12 pages, 2022.

Hindawi
Computational and Mathematical Methods in Medicine
Volume 2023, Article ID 9843748, 1 page
https://doi.org/10.1155/2023/9843748

Retraction

Retracted: Relationship between Severity of Lumbar Spinal Stenosis and Ligamentum Flavum Hypertrophy and Serum Inflammatory Factors

Computational and Mathematical Methods in Medicine

Received 12 December 2023; Accepted 12 December 2023; Published 13 December 2023

This article has been retracted by Hindawi, as publisher, following an investigation undertaken by the publisher [1]. This investigation has uncovered evidence of systematic manipulation of the publication and peer-review process. We cannot, therefore, vouch for the reliability or integrity of this article.

Please note that this notice is intended solely to alert readers that the peer-review process of this article has been compromised.

Wiley and Hindawi regret that the usual quality checks did not identify these issues before publication and have since put additional measures in place to safeguard research integrity.

We wish to credit our Research Integrity and Research Publishing teams and anonymous and named external researchers and research integrity experts for contributing to this investigation.

The corresponding author, as the representative of all authors, has been given the opportunity to register their agreement or disagreement to this retraction. We have kept a record of any response received.

References

[1] N. He, W. Qi, Y. Zhao, and X. Wang, "Relationship between Severity of Lumbar Spinal Stenosis and Ligamentum Flavum Hypertrophy and Serum Inflammatory Factors," *Computational and Mathematical Methods in Medicine*, vol. 2022, Article ID 8799240, 7 pages, 2022.

Hindawi
Computational and Mathematical Methods in Medicine
Volume 2023, Article ID 9837890, 1 page
https://doi.org/10.1155/2023/9837890

Retraction

Retracted: Effect of Dapagliflozin on Clinical Outcome after Drug-Eluting Stent Implantation in Elderly T2DM Patients: A Real-World Study

Computational and Mathematical Methods in Medicine

Received 12 December 2023; Accepted 12 December 2023; Published 13 December 2023

This article has been retracted by Hindawi, as publisher, following an investigation undertaken by the publisher [1]. This investigation has uncovered evidence of systematic manipulation of the publication and peer-review process. We cannot, therefore, vouch for the reliability or integrity of this article.

Please note that this notice is intended solely to alert readers that the peer-review process of this article has been compromised.

Wiley and Hindawi regret that the usual quality checks did not identify these issues before publication and have since put additional measures in place to safeguard research integrity.

We wish to credit our Research Integrity and Research Publishing teams and anonymous and named external researchers and research integrity experts for contributing to this investigation.

The corresponding author, as the representative of all authors, has been given the opportunity to register their agreement or disagreement to this retraction. We have kept a record of any response received.

References

[1] Y. Lin, F. Zhou, X. Wang, Y. Guo, and W. Chen, "Effect of Dapagliflozin on Clinical Outcome after Drug-Eluting Stent Implantation in Elderly T2DM Patients: A Real-World Study," *Computational and Mathematical Methods in Medicine*, vol. 2023, Article ID 8441396, 5 pages, 2023.

Hindawi
Computational and Mathematical Methods in Medicine
Volume 2023, Article ID 9835206, 1 page
https://doi.org/10.1155/2023/9835206

Retraction

Retracted: An Eight-mRNA Prognostic Model to Predict Survival in Hepatic Cellular Cancer

Computational and Mathematical Methods in Medicine

Received 12 December 2023; Accepted 12 December 2023; Published 13 December 2023

This article has been retracted by Hindawi, as publisher, following an investigation undertaken by the publisher [1]. This investigation has uncovered evidence of systematic manipulation of the publication and peer-review process. We cannot, therefore, vouch for the reliability or integrity of this article.

Please note that this notice is intended solely to alert readers that the peer-review process of this article has been compromised.

Wiley and Hindawi regret that the usual quality checks did not identify these issues before publication and have since put additional measures in place to safeguard research integrity.

We wish to credit our Research Integrity and Research Publishing teams and anonymous and named external researchers and research integrity experts for contributing to this investigation.

The corresponding author, as the representative of all authors, has been given the opportunity to register their agreement or disagreement to this retraction. We have kept a record of any response received.

References

[1] D. Xia, X. Liao, and H. Zhang, "An Eight-mRNA Prognostic Model to Predict Survival in Hepatic Cellular Cancer," *Computational and Mathematical Methods in Medicine*, vol. 2023, Article ID 7278231, 7 pages, 2023.

Hindawi
Computational and Mathematical Methods in Medicine
Volume 2023, Article ID 9834985, 1 page
https://doi.org/10.1155/2023/9834985

Retraction

Retracted: Expression of GMFB in High-Grade Cervical Intraepithelial Neoplasia and Its Role in Cervical Cancer

Computational and Mathematical Methods in Medicine

Received 12 December 2023; Accepted 12 December 2023; Published 13 December 2023

This article has been retracted by Hindawi, as publisher, following an investigation undertaken by the publisher [1]. This investigation has uncovered evidence of systematic manipulation of the publication and peer-review process. We cannot, therefore, vouch for the reliability or integrity of this article.

Please note that this notice is intended solely to alert readers that the peer-review process of this article has been compromised.

Wiley and Hindawi regret that the usual quality checks did not identify these issues before publication and have since put additional measures in place to safeguard research integrity.

We wish to credit our Research Integrity and Research Publishing teams and anonymous and named external researchers and research integrity experts for contributing to this investigation.

The corresponding author, as the representative of all authors, has been given the opportunity to register their agreement or disagreement to this retraction. We have kept a record of any response received.

References

[1] J. Tian, J. Wang, Y. Chi, Z. Han, D. Zhang, and H. Zhang, "Expression of GMFB in High-Grade Cervical Intraepithelial Neoplasia and Its Role in Cervical Cancer," *Computational and Mathematical Methods in Medicine*, vol. 2022, Article ID 7784921, 8 pages, 2022.

Hindawi
Computational and Mathematical Methods in Medicine
Volume 2023, Article ID 9832018, 1 page
https://doi.org/10.1155/2023/9832018

Retraction

Retracted: Efficacy of Xiyanping in the Treatment of Elderly Patients with Chronic Obstructive Pulmonary Disease and Its Effect on the Expression of GDF-15 and HIF-1α in Serum

Computational and Mathematical Methods in Medicine

Received 12 December 2023; Accepted 12 December 2023; Published 13 December 2023

This article has been retracted by Hindawi, as publisher, following an investigation undertaken by the publisher [1]. This investigation has uncovered evidence of systematic manipulation of the publication and peer-review process. We cannot, therefore, vouch for the reliability or integrity of this article.

Please note that this notice is intended solely to alert readers that the peer-review process of this article has been compromised.

Wiley and Hindawi regret that the usual quality checks did not identify these issues before publication and have since put additional measures in place to safeguard research integrity.

We wish to credit our Research Integrity and Research Publishing teams and anonymous and named external researchers and research integrity experts for contributing to this investigation.

The corresponding author, as the representative of all authors, has been given the opportunity to register their agreement or disagreement to this retraction. We have kept a record of any response received.

References

[1] J. X. Wang, Y. Zhang, S. F. Wang, J. Li, and P. C. Li, "Efficacy of Xiyanping in the Treatment of Elderly Patients with Chronic Obstructive Pulmonary Disease and Its Effect on the Expression of GDF-15 and HIF-1α in Serum," *Computational and Mathematical Methods in Medicine*, vol. 2022, Article ID 6193110, 8 pages, 2022.

Hindawi
Computational and Mathematical Methods in Medicine
Volume 2023, Article ID 9831697, 1 page
https://doi.org/10.1155/2023/9831697

Retraction

Retracted: MicroRNA-1306-5p Regulates the METTL14-Guided m6A Methylation to Repress Acute Myeloid Leukemia

Computational and Mathematical Methods in Medicine

Received 12 December 2023; Accepted 12 December 2023; Published 13 December 2023

This article has been retracted by Hindawi, as publisher, following an investigation undertaken by the publisher [1]. This investigation has uncovered evidence of systematic manipulation of the publication and peer-review process. We cannot, therefore, vouch for the reliability or integrity of this article.

Please note that this notice is intended solely to alert readers that the peer-review process of this article has been compromised.

Wiley and Hindawi regret that the usual quality checks did not identify these issues before publication and have since put additional measures in place to safeguard research integrity.

We wish to credit our Research Integrity and Research Publishing teams and anonymous and named external researchers and research integrity experts for contributing to this investigation.

The corresponding author, as the representative of all authors, has been given the opportunity to register their agreement or disagreement to this retraction. We have kept a record of any response received.

References

[1] J. Li, Y. Wu, M. Wang et al., "MicroRNA-1306-5p Regulates the METTL14-Guided m6A Methylation to Repress Acute Myeloid Leukemia," *Computational and Mathematical Methods in Medicine*, vol. 2022, Article ID 5787808, 12 pages, 2022.

Hindawi
Computational and Mathematical Methods in Medicine
Volume 2023, Article ID 9826193, 1 page
https://doi.org/10.1155/2023/9826193

Retraction

Retracted: Investigation of the Clinical Effect of New Shoulder Joint Abduction Frame in Humeral Fracture Patients after Arthroscopic Shoulder Surgery

Computational and Mathematical Methods in Medicine

Received 12 December 2023; Accepted 12 December 2023; Published 13 December 2023

This article has been retracted by Hindawi, as publisher, following an investigation undertaken by the publisher [1]. This investigation has uncovered evidence of systematic manipulation of the publication and peer-review process. We cannot, therefore, vouch for the reliability or integrity of this article.

Please note that this notice is intended solely to alert readers that the peer-review process of this article has been compromised.

Wiley and Hindawi regret that the usual quality checks did not identify these issues before publication and have since put additional measures in place to safeguard research integrity.

We wish to credit our Research Integrity and Research Publishing teams and anonymous and named external researchers and research integrity experts for contributing to this investigation.

The corresponding author, as the representative of all authors, has been given the opportunity to register their agreement or disagreement to this retraction. We have kept a record of any response received.

References

[1] G. Yu, M. Yu, S. Liu, H. Xue, and Y. Sun, "Investigation of the Clinical Effect of New Shoulder Joint Abduction Frame in Humeral Fracture Patients after Arthroscopic Shoulder Surgery," *Computational and Mathematical Methods in Medicine*, vol. 2022, Article ID 8764155, 7 pages, 2022.

Hindawi
Computational and Mathematical Methods in Medicine
Volume 2023, Article ID 9824960, 1 page
https://doi.org/10.1155/2023/9824960

Retraction

Retracted: Efficacy and Prediction Model Construction of Drug-Coated Balloon Combined with Cutting Balloon Angioplasty in the Treatment of Drug-Eluting Stent In-Stent Restenosis

Computational and Mathematical Methods in Medicine

Received 12 December 2023; Accepted 12 December 2023; Published 13 December 2023

This article has been retracted by Hindawi, as publisher, following an investigation undertaken by the publisher [1]. This investigation has uncovered evidence of systematic manipulation of the publication and peer-review process. We cannot, therefore, vouch for the reliability or integrity of this article.

Please note that this notice is intended solely to alert readers that the peer-review process of this article has been compromised.

Wiley and Hindawi regret that the usual quality checks did not identify these issues before publication and have since put additional measures in place to safeguard research integrity.

We wish to credit our Research Integrity and Research Publishing teams and anonymous and named external researchers and research integrity experts for contributing to this investigation.

The corresponding author, as the representative of all authors, has been given the opportunity to register their agreement or disagreement to this retraction. We have kept a record of any response received.

References

[1] H. Wu, T. Yu, T. Fan, and W. Liao, "Efficacy and Prediction Model Construction of Drug-Coated Balloon Combined with Cutting Balloon Angioplasty in the Treatment of Drug-Eluting Stent In-Stent Restenosis," *Computational and Mathematical Methods in Medicine*, vol. 2022, Article ID 9832622, 8 pages, 2022.

Hindawi
Computational and Mathematical Methods in Medicine
Volume 2023, Article ID 9821497, 1 page
https://doi.org/10.1155/2023/9821497

Retraction

Retracted: Role of GLI1 in Hypoxia-Driven Endometrial Stromal Cell Migration and Invasion in Endometriosis

Computational and Mathematical Methods in Medicine

Received 12 December 2023; Accepted 12 December 2023; Published 13 December 2023

This article has been retracted by Hindawi, as publisher, following an investigation undertaken by the publisher [1]. This investigation has uncovered evidence of systematic manipulation of the publication and peer-review process. We cannot, therefore, vouch for the reliability or integrity of this article.

Please note that this notice is intended solely to alert readers that the peer-review process of this article has been compromised.

Wiley and Hindawi regret that the usual quality checks did not identify these issues before publication and have since put additional measures in place to safeguard research integrity.

We wish to credit our Research Integrity and Research Publishing teams and anonymous and named external researchers and research integrity experts for contributing to this investigation.

The corresponding author, as the representative of all authors, has been given the opportunity to register their agreement or disagreement to this retraction. We have kept a record of any response received.

References

[1] L. Wang, J. Liang, S. Bi et al., "Role of GLI1 in Hypoxia-Driven Endometrial Stromal Cell Migration and Invasion in Endometriosis," *Computational and Mathematical Methods in Medicine*, vol. 2022, Article ID 6890790, 9 pages, 2022.

Hindawi
Computational and Mathematical Methods in Medicine
Volume 2023, Article ID 9819813, 1 page
https://doi.org/10.1155/2023/9819813

Retraction

Retracted: Systematic Evaluation of the Efficacy of Acupuncture Associated with Physical and Mental Intervention when Treating Idiopathic Tinnitus and the Improvement of Tinnitus Symptoms

Computational and Mathematical Methods in Medicine

Received 12 December 2023; Accepted 12 December 2023; Published 13 December 2023

This article has been retracted by Hindawi, as publisher, following an investigation undertaken by the publisher [1]. This investigation has uncovered evidence of systematic manipulation of the publication and peer-review process. We cannot, therefore, vouch for the reliability or integrity of this article.

Please note that this notice is intended solely to alert readers that the peer-review process of this article has been compromised.

Wiley and Hindawi regret that the usual quality checks did not identify these issues before publication and have since put additional measures in place to safeguard research integrity.

We wish to credit our Research Integrity and Research Publishing teams and anonymous and named external researchers and research integrity experts for contributing to this investigation.

The corresponding author, as the representative of all authors, has been given the opportunity to register their agreement or disagreement to this retraction. We have kept a record of any response received.

References

[1] Y. Li, D. Sang, Z. Wu, and X. Cao, "Systematic Evaluation of the Efficacy of Acupuncture Associated with Physical and Mental Intervention when Treating Idiopathic Tinnitus and the Improvement of Tinnitus Symptoms," *Computational and Mathematical Methods in Medicine*, vol. 2022, Article ID 6764909, 10 pages, 2022.

Hindawi
Computational and Mathematical Methods in Medicine
Volume 2023, Article ID 9817359, 1 page
https://doi.org/10.1155/2023/9817359

Retraction

Retracted: Comparison of the Effects of Laparoscopic Surgery and Traditional Open Surgery on Stone Clearance, Laboratory Indexes and Life Quality in Patients with Renal Calculi

Computational and Mathematical Methods in Medicine

Received 12 December 2023; Accepted 12 December 2023; Published 13 December 2023

This article has been retracted by Hindawi, as publisher, following an investigation undertaken by the publisher [1]. This investigation has uncovered evidence of systematic manipulation of the publication and peer-review process. We cannot, therefore, vouch for the reliability or integrity of this article.

Please note that this notice is intended solely to alert readers that the peer-review process of this article has been compromised.

Wiley and Hindawi regret that the usual quality checks did not identify these issues before publication and have since put additional measures in place to safeguard research integrity.

We wish to credit our Research Integrity and Research Publishing teams and anonymous and named external researchers and research integrity experts for contributing to this investigation.

The corresponding author, as the representative of all authors, has been given the opportunity to register their agreement or disagreement to this retraction. We have kept a record of any response received.

References

[1] Q. Ai, D. Tang, Y. Li, Y. Huang, and J. Yang, "Comparison of the Effects of Laparoscopic Surgery and Traditional Open Surgery on Stone Clearance, Laboratory Indexes and Life Quality in Patients with Renal Calculi," *Computational and Mathematical Methods in Medicine*, vol. 2022, Article ID 8211389, 9 pages, 2022.

Hindawi
Computational and Mathematical Methods in Medicine
Volume 2023, Article ID 9808951, 1 page
https://doi.org/10.1155/2023/9808951

Retraction

Retracted: Application Value of Total Knee Arthroplasty plus Platelet-Rich Plasma Therapy in Traumatic Arthritis of the Knee

Computational and Mathematical Methods in Medicine

Received 12 December 2023; Accepted 12 December 2023; Published 13 December 2023

This article has been retracted by Hindawi, as publisher, following an investigation undertaken by the publisher [1]. This investigation has uncovered evidence of systematic manipulation of the publication and peer-review process. We cannot, therefore, vouch for the reliability or integrity of this article.

Please note that this notice is intended solely to alert readers that the peer-review process of this article has been compromised.

Wiley and Hindawi regret that the usual quality checks did not identify these issues before publication and have since put additional measures in place to safeguard research integrity.

We wish to credit our Research Integrity and Research Publishing teams and anonymous and named external researchers and research integrity experts for contributing to this investigation.

The corresponding author, as the representative of all authors, has been given the opportunity to register their agreement or disagreement to this retraction. We have kept a record of any response received.

References

[1] C. Zhang and P. Nie, "Application Value of Total Knee Arthroplasty plus Platelet-Rich Plasma Therapy in Traumatic Arthritis of the Knee," *Computational and Mathematical Methods in Medicine*, vol. 2022, Article ID 5483101, 6 pages, 2022.

Hindawi
Computational and Mathematical Methods in Medicine
Volume 2023, Article ID 9807415, 1 page
https://doi.org/10.1155/2023/9807415

Retraction

Retracted: Effect of Nursing Outcome-Oriented Intervention on Airway Management in Elderly Long-Term Bedridden Patients

Computational and Mathematical Methods in Medicine

Received 12 December 2023; Accepted 12 December 2023; Published 13 December 2023

This article has been retracted by Hindawi, as publisher, following an investigation undertaken by the publisher [1]. This investigation has uncovered evidence of systematic manipulation of the publication and peer-review process. We cannot, therefore, vouch for the reliability or integrity of this article.

Please note that this notice is intended solely to alert readers that the peer-review process of this article has been compromised.

Wiley and Hindawi regret that the usual quality checks did not identify these issues before publication and have since put additional measures in place to safeguard research integrity.

We wish to credit our Research Integrity and Research Publishing teams and anonymous and named external researchers and research integrity experts for contributing to this investigation.

The corresponding author, as the representative of all authors, has been given the opportunity to register their agreement or disagreement to this retraction. We have kept a record of any response received.

References

[1] W. Ding, F. Luo, P. Lin, Y. Tang, and Y. Liu, "Effect of Nursing Outcome-Oriented Intervention on Airway Management in Elderly Long-Term Bedridden Patients," *Computational and Mathematical Methods in Medicine*, vol. 2022, Article ID 9557330, 6 pages, 2022.

Hindawi
Computational and Mathematical Methods in Medicine
Volume 2023, Article ID 9806505, 1 page
https://doi.org/10.1155/2023/9806505

Retraction

Retracted: Berberine Inhibits Herpes Simplex Virus 1 Replication in HEK293T Cells

Computational and Mathematical Methods in Medicine

Received 12 December 2023; Accepted 12 December 2023; Published 13 December 2023

This article has been retracted by Hindawi, as publisher, following an investigation undertaken by the publisher [1]. This investigation has uncovered evidence of systematic manipulation of the publication and peer-review process. We cannot, therefore, vouch for the reliability or integrity of this article.

Please note that this notice is intended solely to alert readers that the peer-review process of this article has been compromised.

Wiley and Hindawi regret that the usual quality checks did not identify these issues before publication and have since put additional measures in place to safeguard research integrity.

We wish to credit our Research Integrity and Research Publishing teams and anonymous and named external researchers and research integrity experts for contributing to this investigation.

The corresponding author, as the representative of all authors, has been given the opportunity to register their agreement or disagreement to this retraction. We have kept a record of any response received.

References

[1] Y. Cui, L. Zhang, D. Hu, and Y. Yang, "Berberine Inhibits Herpes Simplex Virus 1 Replication in HEK293T Cells," *Computational and Mathematical Methods in Medicine*, vol. 2022, Article ID 7137401, 7 pages, 2022.

Hindawi
Computational and Mathematical Methods in Medicine
Volume 2023, Article ID 9805202, 1 page
https://doi.org/10.1155/2023/9805202

Retraction

Retracted: Effects of Nifedipine and Labetalol Combined with Magnesium Sulfate on Blood Pressure Control, Blood Coagulation Function, and Maternal and Infant Outcome in Patients with Pregnancy-Induced Hypertension

Computational and Mathematical Methods in Medicine

Received 12 December 2023; Accepted 12 December 2023; Published 13 December 2023

This article has been retracted by Hindawi, as publisher, following an investigation undertaken by the publisher [1]. This investigation has uncovered evidence of systematic manipulation of the publication and peer-review process. We cannot, therefore, vouch for the reliability or integrity of this article.

Please note that this notice is intended solely to alert readers that the peer-review process of this article has been compromised.

Wiley and Hindawi regret that the usual quality checks did not identify these issues before publication and have since put additional measures in place to safeguard research integrity.

We wish to credit our Research Integrity and Research Publishing teams and anonymous and named external researchers and research integrity experts for contributing to this investigation.

The corresponding author, as the representative of all authors, has been given the opportunity to register their agreement or disagreement to this retraction. We have kept a record of any response received.

References

[1] Y. Shao, S. Gu, and X. Zhang, "Effects of Nifedipine and Labetalol Combined with Magnesium Sulfate on Blood Pressure Control, Blood Coagulation Function, and Maternal and Infant Outcome in Patients with Pregnancy-Induced Hypertension," *Computational and Mathematical Methods in Medicine*, vol. 2022, Article ID 9317114, 8 pages, 2022.

Hindawi
Computational and Mathematical Methods in Medicine
Volume 2023, Article ID 9804870, 1 page
https://doi.org/10.1155/2023/9804870

Retraction

Retracted: A Preliminary Study on the Value of Intestinal Flora in Predicting Major Adverse Cardiovascular and Cerebrovascular Events in Patients with Refractory Hypertension

Computational and Mathematical Methods in Medicine

Received 12 December 2023; Accepted 12 December 2023; Published 13 December 2023

This article has been retracted by Hindawi, as publisher, following an investigation undertaken by the publisher [1]. This investigation has uncovered evidence of systematic manipulation of the publication and peer-review process. We cannot, therefore, vouch for the reliability or integrity of this article.

Please note that this notice is intended solely to alert readers that the peer-review process of this article has been compromised.

Wiley and Hindawi regret that the usual quality checks did not identify these issues before publication and have since put additional measures in place to safeguard research integrity.

We wish to credit our Research Integrity and Research Publishing teams and anonymous and named external researchers and research integrity experts for contributing to this investigation.

The corresponding author, as the representative of all authors, has been given the opportunity to register their agreement or disagreement to this retraction. We have kept a record of any response received.

References

[1] J. Jiao, Y. Zhang, P. Han, and S. Zhai, "A Preliminary Study on the Value of Intestinal Flora in Predicting Major Adverse Cardiovascular and Cerebrovascular Events in Patients with Refractory Hypertension," *Computational and Mathematical Methods in Medicine*, vol. 2022, Article ID 7723105, 7 pages, 2022.

Hindawi
Computational and Mathematical Methods in Medicine
Volume 2023, Article ID 9795457, 1 page
https://doi.org/10.1155/2023/9795457

Retraction

Retracted: Impact of Small Incision Reduction and Suture Linked with Functional Appliance of Sufferers with Irrecoverable TMJ Anterior Disc Displacement

Computational and Mathematical Methods in Medicine

Received 12 December 2023; Accepted 12 December 2023; Published 13 December 2023

This article has been retracted by Hindawi, as publisher, following an investigation undertaken by the publisher [1]. This investigation has uncovered evidence of systematic manipulation of the publication and peer-review process. We cannot, therefore, vouch for the reliability or integrity of this article.

Please note that this notice is intended solely to alert readers that the peer-review process of this article has been compromised.

Wiley and Hindawi regret that the usual quality checks did not identify these issues before publication and have since put additional measures in place to safeguard research integrity.

We wish to credit our Research Integrity and Research Publishing teams and anonymous and named external researchers and research integrity experts for contributing to this investigation.

The corresponding author, as the representative of all authors, has been given the opportunity to register their agreement or disagreement to this retraction. We have kept a record of any response received.

References

[1] X. Wei, W. Yan, A. Sun, H. Wang, and W. Wang, "Impact of Small Incision Reduction and Suture Linked with Functional Appliance of Sufferers with Irrecoverable TMJ Anterior Disc Displacement," *Computational and Mathematical Methods in Medicine*, vol. 2022, Article ID 7196599, 6 pages, 2022.

Hindawi
Computational and Mathematical Methods in Medicine
Volume 2023, Article ID 9793878, 1 page
https://doi.org/10.1155/2023/9793878

Retraction

Retracted: Electroacupuncture Treats Myocardial Infarction by Influencing the Regulation of Substance P in the Neurovascular to Modulate PGI2/TXA2 Metabolic Homeostasis via PI3K/AKT Pathway: A Bioinformatics-Based Multiomics and Experimental Study

Computational and Mathematical Methods in Medicine

Received 12 December 2023; Accepted 12 December 2023; Published 13 December 2023

This article has been retracted by Hindawi, as publisher, following an investigation undertaken by the publisher [1]. This investigation has uncovered evidence of systematic manipulation of the publication and peer-review process. We cannot, therefore, vouch for the reliability or integrity of this article.

Please note that this notice is intended solely to alert readers that the peer-review process of this article has been compromised.

Wiley and Hindawi regret that the usual quality checks did not identify these issues before publication and have since put additional measures in place to safeguard research integrity.

We wish to credit our Research Integrity and Research Publishing teams and anonymous and named external researchers and research integrity experts for contributing to this investigation.

The corresponding author, as the representative of all authors, has been given the opportunity to register their agreement or disagreement to this retraction. We have kept a record of any response received.

References

[1] P. Zhang, Y. Wang, X. Xing et al., "Electroacupuncture Treats Myocardial Infarction by Influencing the Regulation of Substance P in the Neurovascular to Modulate PGI2/TXA2 Metabolic Homeostasis via PI3K/AKT Pathway: A Bioinformatics-Based Multiomics and Experimental Study," *Computational and Mathematical Methods in Medicine*, vol. 2022, Article ID 5367753, 15 pages, 2022.

Hindawi
Computational and Mathematical Methods in Medicine
Volume 2023, Article ID 9790315, 1 page
https://doi.org/10.1155/2023/9790315

Retraction

Retracted: Effects of Transcranial Magnetic Stimulation Combined with Computer-Aided Cognitive Training on Cognitive Function of Children with Cerebral Palsy and Dysgnosia

Computational and Mathematical Methods in Medicine

Received 12 December 2023; Accepted 12 December 2023; Published 13 December 2023

This article has been retracted by Hindawi, as publisher, following an investigation undertaken by the publisher [1]. This investigation has uncovered evidence of systematic manipulation of the publication and peer-review process. We cannot, therefore, vouch for the reliability or integrity of this article.

Please note that this notice is intended solely to alert readers that the peer-review process of this article has been compromised.

Wiley and Hindawi regret that the usual quality checks did not identify these issues before publication and have since put additional measures in place to safeguard research integrity.

We wish to credit our Research Integrity and Research Publishing teams and anonymous and named external researchers and research integrity experts for contributing to this investigation.

The corresponding author, as the representative of all authors, has been given the opportunity to register their agreement or disagreement to this retraction. We have kept a record of any response received.

References

[1] J. Chen, X. Yu, and G. Luo, "Effects of Transcranial Magnetic Stimulation Combined with Computer-Aided Cognitive Training on Cognitive Function of Children with Cerebral Palsy and Dysgnosia," *Computational and Mathematical Methods in Medicine*, vol. 2022, Article ID 5316992, 7 pages, 2022.

Hindawi
Computational and Mathematical Methods in Medicine
Volume 2023, Article ID 9789418, 1 page
https://doi.org/10.1155/2023/9789418

Retraction

Retracted: Effects of Thoracic Paravertebral Block on Postoperative Anxiety and Depression for Patients Undergoing Thoracoscopic Lung Cancer Radical Surgery

Computational and Mathematical Methods in Medicine

Received 12 December 2023; Accepted 12 December 2023; Published 13 December 2023

This article has been retracted by Hindawi, as publisher, following an investigation undertaken by the publisher [1]. This investigation has uncovered evidence of systematic manipulation of the publication and peer-review process. We cannot, therefore, vouch for the reliability or integrity of this article.

Please note that this notice is intended solely to alert readers that the peer-review process of this article has been compromised.

Wiley and Hindawi regret that the usual quality checks did not identify these issues before publication and have since put additional measures in place to safeguard research integrity.

We wish to credit our Research Integrity and Research Publishing teams and anonymous and named external researchers and research integrity experts for contributing to this investigation.

The corresponding author, as the representative of all authors, has been given the opportunity to register their agreement or disagreement to this retraction. We have kept a record of any response received.

References

[1] C. Geng, C. Tong, H. Li, S. Shi, J. Yu, and L. Huang, "Effects of Thoracic Paravertebral Block on Postoperative Anxiety and Depression for Patients Undergoing Thoracoscopic Lung Cancer Radical Surgery," *Computational and Mathematical Methods in Medicine*, vol. 2022, Article ID 7629012, 6 pages, 2022.

Hindawi
Computational and Mathematical Methods in Medicine
Volume 2023, Article ID 9786509, 1 page
https://doi.org/10.1155/2023/9786509

Retraction

Retracted: Effect of Parecoxib Sodium Combined with Dexmedetomidine on Analgesia and Postoperative Pain of Patients Undergoing Hysteromyomectomy

Computational and Mathematical Methods in Medicine

Received 12 December 2023; Accepted 12 December 2023; Published 13 December 2023

This article has been retracted by Hindawi, as publisher, following an investigation undertaken by the publisher [1]. This investigation has uncovered evidence of systematic manipulation of the publication and peer-review process. We cannot, therefore, vouch for the reliability or integrity of this article.

Please note that this notice is intended solely to alert readers that the peer-review process of this article has been compromised.

Wiley and Hindawi regret that the usual quality checks did not identify these issues before publication and have since put additional measures in place to safeguard research integrity.

We wish to credit our Research Integrity and Research Publishing teams and anonymous and named external researchers and research integrity experts for contributing to this investigation.

The corresponding author, as the representative of all authors, has been given the opportunity to register their agreement or disagreement to this retraction. We have kept a record of any response received.

References

[1] X. Wang, Y. Chen, Y. Zhao et al., "Effect of Parecoxib Sodium Combined with Dexmedetomidine on Analgesia and Postoperative Pain of Patients Undergoing Hysteromyomectomy," *Computational and Mathematical Methods in Medicine*, vol. 2022, Article ID 5123933, 7 pages, 2022.

Hindawi
Computational and Mathematical Methods in Medicine
Volume 2023, Article ID 9786485, 1 page
https://doi.org/10.1155/2023/9786485

Retraction

Retracted: Diagnostic Values of Advanced Glycation End Products and Homocysteine in Patients with Alzheimer's Disease and Sarcopenia

Computational and Mathematical Methods in Medicine

Received 12 December 2023; Accepted 12 December 2023; Published 13 December 2023

This article has been retracted by Hindawi, as publisher, following an investigation undertaken by the publisher [1]. This investigation has uncovered evidence of systematic manipulation of the publication and peer-review process. We cannot, therefore, vouch for the reliability or integrity of this article.

Please note that this notice is intended solely to alert readers that the peer-review process of this article has been compromised.

Wiley and Hindawi regret that the usual quality checks did not identify these issues before publication and have since put additional measures in place to safeguard research integrity.

We wish to credit our Research Integrity and Research Publishing teams and anonymous and named external researchers and research integrity experts for contributing to this investigation.

The corresponding author, as the representative of all authors, has been given the opportunity to register their agreement or disagreement to this retraction. We have kept a record of any response received.

References

[1] X. Zhang, Y. Meng, W. Zhang et al., "Diagnostic Values of Advanced Glycation End Products and Homocysteine in Patients with Alzheimer's Disease and Sarcopenia," *Computational and Mathematical Methods in Medicine*, vol. 2022, Article ID 8949048, 8 pages, 2022.

Hindawi
Computational and Mathematical Methods in Medicine
Volume 2023, Article ID 9783730, 1 page
https://doi.org/10.1155/2023/9783730

Retraction

Retracted: Outcome of Nursing Based on Health Belief United with Knowledge, Belief, and Practice Mode on Gastroscopy of Patients with Gastric Cancer

Computational and Mathematical Methods in Medicine

Received 12 December 2023; Accepted 12 December 2023; Published 13 December 2023

This article has been retracted by Hindawi, as publisher, following an investigation undertaken by the publisher [1]. This investigation has uncovered evidence of systematic manipulation of the publication and peer-review process. We cannot, therefore, vouch for the reliability or integrity of this article.

Please note that this notice is intended solely to alert readers that the peer-review process of this article has been compromised.

Wiley and Hindawi regret that the usual quality checks did not identify these issues before publication and have since put additional measures in place to safeguard research integrity.

We wish to credit our Research Integrity and Research Publishing teams and anonymous and named external researchers and research integrity experts for contributing to this investigation.

The corresponding author, as the representative of all authors, has been given the opportunity to register their agreement or disagreement to this retraction. We have kept a record of any response received.

References

[1] J. Yang, J. Yang, D. Guo, Q. Zhao, and Y. Chen, "Outcome of Nursing Based on Health Belief United with Knowledge, Belief, and Practice Mode on Gastroscopy of Patients with Gastric Cancer," *Computational and Mathematical Methods in Medicine*, vol. 2022, Article ID 9491454, 7 pages, 2022.

Hindawi
Computational and Mathematical Methods in Medicine
Volume 2023, Article ID 9783405, 1 page
https://doi.org/10.1155/2023/9783405

Retraction

Retracted: Influence of Optimal Management of Hyperglycemia and Intensive Nursing on Blood Glucose Control Level and Complications in Patients with Postoperative Cerebral Hemorrhage

Computational and Mathematical Methods in Medicine

Received 12 December 2023; Accepted 12 December 2023; Published 13 December 2023

This article has been retracted by Hindawi, as publisher, following an investigation undertaken by the publisher [1]. This investigation has uncovered evidence of systematic manipulation of the publication and peer-review process. We cannot, therefore, vouch for the reliability or integrity of this article.

Please note that this notice is intended solely to alert readers that the peer-review process of this article has been compromised.

Wiley and Hindawi regret that the usual quality checks did not identify these issues before publication and have since put additional measures in place to safeguard research integrity.

We wish to credit our Research Integrity and Research Publishing teams and anonymous and named external researchers and research integrity experts for contributing to this investigation.

The corresponding author, as the representative of all authors, has been given the opportunity to register their agreement or disagreement to this retraction. We have kept a record of any response received.

References

[1] D. Sun, L. Sun, and F. Su, "Influence of Optimal Management of Hyperglycemia and Intensive Nursing on Blood Glucose Control Level and Complications in Patients with Postoperative Cerebral Hemorrhage," *Computational and Mathematical Methods in Medicine*, vol. 2022, Article ID 8553539, 7 pages, 2022.

Hindawi
Computational and Mathematical Methods in Medicine
Volume 2023, Article ID 9780394, 1 page
https://doi.org/10.1155/2023/9780394

Retraction

Retracted: Hub Genes and Long Noncoding RNAs That Regulates It Associated with the Prognosis of Esophageal Squamous Cell Carcinoma Based on Bioinformatics Analysis

Computational and Mathematical Methods in Medicine

Received 12 December 2023; Accepted 12 December 2023; Published 13 December 2023

This article has been retracted by Hindawi, as publisher, following an investigation undertaken by the publisher [1]. This investigation has uncovered evidence of systematic manipulation of the publication and peer-review process. We cannot, therefore, vouch for the reliability or integrity of this article.

Please note that this notice is intended solely to alert readers that the peer-review process of this article has been compromised.

Wiley and Hindawi regret that the usual quality checks did not identify these issues before publication and have since put additional measures in place to safeguard research integrity.

We wish to credit our Research Integrity and Research Publishing teams and anonymous and named external researchers and research integrity experts for contributing to this investigation.

The corresponding author, as the representative of all authors, has been given the opportunity to register their agreement or disagreement to this retraction. We have kept a record of any response received.

References

[1] J. Lu, R. Li, M. Fang, and S. Ke, "Hub Genes and Long Noncoding RNAs That Regulates It Associated with the Prognosis of Esophageal Squamous Cell Carcinoma Based on Bioinformatics Analysis," *Computational and Mathematical Methods in Medicine*, vol. 2022, Article ID 6027058, 11 pages, 2022.

Hindawi
Computational and Mathematical Methods in Medicine
Volume 2023, Article ID 9769073, 1 page
https://doi.org/10.1155/2023/9769073

Retraction

Retracted: A Bioinformatic Approach Based on Systems Biology to Determine the Effects of SARS-CoV-2 Infection in Patients with Hypertrophic Cardiomyopathy

Computational and Mathematical Methods in Medicine

Received 12 December 2023; Accepted 12 December 2023; Published 13 December 2023

This article has been retracted by Hindawi, as publisher, following an investigation undertaken by the publisher [1]. This investigation has uncovered evidence of systematic manipulation of the publication and peer-review process. We cannot, therefore, vouch for the reliability or integrity of this article.

Please note that this notice is intended solely to alert readers that the peer-review process of this article has been compromised.

Wiley and Hindawi regret that the usual quality checks did not identify these issues before publication and have since put additional measures in place to safeguard research integrity.

We wish to credit our Research Integrity and Research Publishing teams and anonymous and named external researchers and research integrity experts for contributing to this investigation.

The corresponding author, as the representative of all authors, has been given the opportunity to register their agreement or disagreement to this retraction. We have kept a record of any response received.

References

[1] X. Han, F. Wang, P. Yang et al., "A Bioinformatic Approach Based on Systems Biology to Determine the Effects of SARS-CoV-2 Infection in Patients with Hypertrophic Cardiomyopathy," *Computational and Mathematical Methods in Medicine*, vol. 2022, Article ID 5337380, 13 pages, 2022.

Hindawi
Computational and Mathematical Methods in Medicine
Volume 2023, Article ID 9760762, 1 page
https://doi.org/10.1155/2023/9760762

Retraction

Retracted: Detection and Correlation Analysis of Serum Uric Acid in Patients with Thyroid-Associated Ophthalmopathy

Computational and Mathematical Methods in Medicine

Received 12 December 2023; Accepted 12 December 2023; Published 13 December 2023

This article has been retracted by Hindawi, as publisher, following an investigation undertaken by the publisher [1]. This investigation has uncovered evidence of systematic manipulation of the publication and peer-review process. We cannot, therefore, vouch for the reliability or integrity of this article.

Please note that this notice is intended solely to alert readers that the peer-review process of this article has been compromised.

Wiley and Hindawi regret that the usual quality checks did not identify these issues before publication and have since put additional measures in place to safeguard research integrity.

We wish to credit our Research Integrity and Research Publishing teams and anonymous and named external researchers and research integrity experts for contributing to this investigation.

The corresponding author, as the representative of all authors, has been given the opportunity to register their agreement or disagreement to this retraction. We have kept a record of any response received.

References

[1] J. Zhou, X. Yu, Y. Lou, J. Bao, Y. Xia, and L. Zhu, "Detection and Correlation Analysis of Serum Uric Acid in Patients with Thyroid-Associated Ophthalmopathy," *Computational and Mathematical Methods in Medicine*, vol. 2022, Article ID 8406834, 6 pages, 2022.

Hindawi
Computational and Mathematical Methods in Medicine
Volume 2023, Article ID 9758345, 1 page
https://doi.org/10.1155/2023/9758345

Retraction

Retracted: Analysis of Data on Fludarabine, Cyclophosphamide, and Rituximab Chemoimmunotherapy for Chronic Lymphocytic Leukemia Shows High Patient Heterogeneity and the Need for More Consideration of Individualized Treatment

Computational and Mathematical Methods in Medicine

Received 12 December 2023; Accepted 12 December 2023; Published 13 December 2023

This article has been retracted by Hindawi, as publisher, following an investigation undertaken by the publisher [1]. This investigation has uncovered evidence of systematic manipulation of the publication and peer-review process. We cannot, therefore, vouch for the reliability or integrity of this article.

Please note that this notice is intended solely to alert readers that the peer-review process of this article has been compromised.

Wiley and Hindawi regret that the usual quality checks did not identify these issues before publication and have since put additional measures in place to safeguard research integrity.

We wish to credit our Research Integrity and Research Publishing teams and anonymous and named external researchers and research integrity experts for contributing to this investigation.

The corresponding author, as the representative of all authors, has been given the opportunity to register their agreement or disagreement to this retraction. We have kept a record of any response received.

References

[1] X. Xu, Y. Zhao, H. Ye et al., "Analysis of Data on Fludarabine, Cyclophosphamide, and Rituximab Chemoimmunotherapy for Chronic Lymphocytic Leukemia Shows High Patient Heterogeneity and the Need for More Consideration of Individualized Treatment," *Computational and Mathematical Methods in Medicine*, vol. 2022, Article ID 7451395, 21 pages, 2022.

Hindawi
Computational and Mathematical Methods in Medicine
Volume 2023, Article ID 9757648, 1 page
https://doi.org/10.1155/2023/9757648

Retraction

Retracted: Comparison of Effectiveness as well as Advantages and Disadvantages of Different Dimensions of Hysterosalpingo-Contrast Sonography for Diagnosis of Lesions Associated with Female Infertility

Computational and Mathematical Methods in Medicine

Received 12 December 2023; Accepted 12 December 2023; Published 13 December 2023

This article has been retracted by Hindawi, as publisher, following an investigation undertaken by the publisher [1]. This investigation has uncovered evidence of systematic manipulation of the publication and peer-review process. We cannot, therefore, vouch for the reliability or integrity of this article.

Please note that this notice is intended solely to alert readers that the peer-review process of this article has been compromised.

Wiley and Hindawi regret that the usual quality checks did not identify these issues before publication and have since put additional measures in place to safeguard research integrity.

We wish to credit our Research Integrity and Research Publishing teams and anonymous and named external researchers and research integrity experts for contributing to this investigation.

The corresponding author, as the representative of all authors, has been given the opportunity to register their agreement or disagreement to this retraction. We have kept a record of any response received.

References

[1] R. Pei, "Comparison of Effectiveness as well as Advantages and Disadvantages of Different Dimensions of Hysterosalpingo-Contrast Sonography for Diagnosis of Lesions Associated with Female Infertility," *Computational and Mathematical Methods in Medicine*, vol. 2022, Article ID 7508880, 7 pages, 2022.

Hindawi
Computational and Mathematical Methods in Medicine
Volume 2023, Article ID 9878617, 1 page
https://doi.org/10.1155/2023/9878617

Retraction

Retracted: Study on the Clinical Value of Noninvasive Prenatal Testing in Screening the Chromosomal Abnormalities of the Fetus in the Elderly Pregnant Women

Computational and Mathematical Methods in Medicine

Received 5 December 2023; Accepted 5 December 2023; Published 6 December 2023

This article has been retracted by Hindawi, as publisher, following an investigation undertaken by the publisher [1]. This investigation has uncovered evidence of systematic manipulation of the publication and peer-review process. We cannot, therefore, vouch for the reliability or integrity of this article.

Please note that this notice is intended solely to alert readers that the peer-review process of this article has been compromised.

Wiley and Hindawi regret that the usual quality checks did not identify these issues before publication and have since put additional measures in place to safeguard research integrity.

We wish to credit our Research Integrity and Research Publishing teams and anonymous and named external researchers and research integrity experts for contributing to this investigation.

The corresponding author, as the representative of all authors, has been given the opportunity to register their agreement or disagreement to this retraction. We have kept a record of any response received.

References

[1] Z. Gu, M. Du, T. Xu, and C. Jin, "Study on the Clinical Value of Noninvasive Prenatal Testing in Screening the Chromosomal Abnormalities of the Fetus in the Elderly Pregnant Women," *Computational and Mathematical Methods in Medicine*, vol. 2022, Article ID 2977128, 7 pages, 2022.

Hindawi
Computational and Mathematical Methods in Medicine
Volume 2023, Article ID 9878450, 1 page
https://doi.org/10.1155/2023/9878450

Retraction

Retracted: Effect of Enteral and Parenteral Nutrition Support on Pulmonary Function in Elderly Patients with Chronic Obstructive Pulmonary Disease Complicated by Respiratory Failure

Computational and Mathematical Methods in Medicine

Received 5 December 2023; Accepted 5 December 2023; Published 6 December 2023

This article has been retracted by Hindawi, as publisher, following an investigation undertaken by the publisher [1]. This investigation has uncovered evidence of systematic manipulation of the publication and peer-review process. We cannot, therefore, vouch for the reliability or integrity of this article.

Please note that this notice is intended solely to alert readers that the peer-review process of this article has been compromised.

Wiley and Hindawi regret that the usual quality checks did not identify these issues before publication and have since put additional measures in place to safeguard research integrity.

We wish to credit our Research Integrity and Research Publishing teams and anonymous and named external researchers and research integrity experts for contributing to this investigation.

The corresponding author, as the representative of all authors, has been given the opportunity to register their agreement or disagreement to this retraction. We have kept a record of any response received.

References

[1] L. Wang, W. Rui, S. Chen, Y. Li, and M. Ren, "Effect of Enteral and Parenteral Nutrition Support on Pulmonary Function in Elderly Patients with Chronic Obstructive Pulmonary Disease Complicated by Respiratory Failure," *Computational and Mathematical Methods in Medicine*, vol. 2022, Article ID 4743070, 8 pages, 2022.

Hindawi
Computational and Mathematical Methods in Medicine
Volume 2023, Article ID 9863871, 1 page
https://doi.org/10.1155/2023/9863871

Retraction

Retracted: Influences of Antithrombotic Elastic Socks Combined with Air Pressure in Reducing Lower Extremity Deep Venous Thrombosis for Patients Undergoing Cardiothoracic Surgery

Computational and Mathematical Methods in Medicine

Received 5 December 2023; Accepted 5 December 2023; Published 6 December 2023

This article has been retracted by Hindawi, as publisher, following an investigation undertaken by the publisher [1]. This investigation has uncovered evidence of systematic manipulation of the publication and peer-review process. We cannot, therefore, vouch for the reliability or integrity of this article.

Please note that this notice is intended solely to alert readers that the peer-review process of this article has been compromised.

Wiley and Hindawi regret that the usual quality checks did not identify these issues before publication and have since put additional measures in place to safeguard research integrity.

We wish to credit our Research Integrity and Research Publishing teams and anonymous and named external researchers and research integrity experts for contributing to this investigation.

The corresponding author, as the representative of all authors, has been given the opportunity to register their agreement or disagreement to this retraction. We have kept a record of any response received.

References

[1] W. Fu, Q. Zhang, X. Sun, and Y. Gu, "Influences of Antithrombotic Elastic Socks Combined with Air Pressure in Reducing Lower Extremity Deep Venous Thrombosis for Patients Undergoing Cardiothoracic Surgery," *Computational and Mathematical Methods in Medicine*, vol. 2022, Article ID 1338214, 6 pages, 2022.

Hindawi
Computational and Mathematical Methods in Medicine
Volume 2023, Article ID 9860406, 1 page
https://doi.org/10.1155/2023/9860406

Retraction

Retracted: The Significance of Implementing Bilevel Positive Airway Pressure under Cluster Nursing in Improving the Survival Possibility of Patients with Severe Pulmonary Infection Complicated by Respiratory Failure

Computational and Mathematical Methods in Medicine

Received 5 December 2023; Accepted 5 December 2023; Published 6 December 2023

This article has been retracted by Hindawi, as publisher, following an investigation undertaken by the publisher [1]. This investigation has uncovered evidence of systematic manipulation of the publication and peer-review process. We cannot, therefore, vouch for the reliability or integrity of this article.

Please note that this notice is intended solely to alert readers that the peer-review process of this article has been compromised.

Wiley and Hindawi regret that the usual quality checks did not identify these issues before publication and have since put additional measures in place to safeguard research integrity.

We wish to credit our Research Integrity and Research Publishing teams and anonymous and named external researchers and research integrity experts for contributing to this investigation.

The corresponding author, as the representative of all authors, has been given the opportunity to register their agreement or disagreement to this retraction. We have kept a record of any response received.

References

[1] X. Fang and H. Yang, "The Significance of Implementing Bilevel Positive Airway Pressure under Cluster Nursing in Improving the Survival Possibility of Patients with Severe Pulmonary Infection Complicated by Respiratory Failure," *Computational and Mathematical Methods in Medicine*, vol. 2022, Article ID 2324797, 8 pages, 2022.

Hindawi
Computational and Mathematical Methods in Medicine
Volume 2023, Article ID 9854393, 1 page
https://doi.org/10.1155/2023/9854393

Retraction

Retracted: MDH1 and MDH2 Promote Cell Viability of Primary AT2 Cells by Increasing Glucose Uptake

Computational and Mathematical Methods in Medicine

Received 5 December 2023; Accepted 5 December 2023; Published 6 December 2023

This article has been retracted by Hindawi, as publisher, following an investigation undertaken by the publisher [1]. This investigation has uncovered evidence of systematic manipulation of the publication and peer-review process. We cannot, therefore, vouch for the reliability or integrity of this article.

Please note that this notice is intended solely to alert readers that the peer-review process of this article has been compromised.

Wiley and Hindawi regret that the usual quality checks did not identify these issues before publication and have since put additional measures in place to safeguard research integrity.

We wish to credit our Research Integrity and Research Publishing teams and anonymous and named external researchers and research integrity experts for contributing to this investigation.

The corresponding author, as the representative of all authors, has been given the opportunity to register their agreement or disagreement to this retraction. We have kept a record of any response received.

References

[1] M. Hu, J. Yang, Y. Xu, and J. Liu, "MDH1 and MDH2 Promote Cell Viability of Primary AT2 Cells by Increasing Glucose Uptake," *Computational and Mathematical Methods in Medicine*, vol. 2022, Article ID 2023500, 15 pages, 2022.

Hindawi
Computational and Mathematical Methods in Medicine
Volume 2023, Article ID 9852615, 1 page
https://doi.org/10.1155/2023/9852615

Retraction

Retracted: Acupuncture Enhances Gastrointestinal Motility and Improves Autonomic Nervous Function in Patients with Septic Gastrointestinal Dysfunction

Computational and Mathematical Methods in Medicine

Received 5 December 2023; Accepted 5 December 2023; Published 6 December 2023

This article has been retracted by Hindawi, as publisher, following an investigation undertaken by the publisher [1]. This investigation has uncovered evidence of systematic manipulation of the publication and peer-review process. We cannot, therefore, vouch for the reliability or integrity of this article.

Please note that this notice is intended solely to alert readers that the peer-review process of this article has been compromised.

Wiley and Hindawi regret that the usual quality checks did not identify these issues before publication and have since put additional measures in place to safeguard research integrity.

We wish to credit our Research Integrity and Research Publishing teams and anonymous and named external researchers and research integrity experts for contributing to this investigation.

The corresponding author, as the representative of all authors, has been given the opportunity to register their agreement or disagreement to this retraction. We have kept a record of any response received.

References

[1] L. Ban, Y. Pu, H. Huang, B. You, W. Chen, and Y. Wang, "Acupuncture Enhances Gastrointestinal Motility and Improves Autonomic Nervous Function in Patients with Septic Gastrointestinal Dysfunction," *Computational and Mathematical Methods in Medicine*, vol. 2022, Article ID 1653290, 8 pages, 2022.

Hindawi
Computational and Mathematical Methods in Medicine
Volume 2023, Article ID 9758487, 1 page
https://doi.org/10.1155/2023/9758487

Retraction

Retracted: Identification of Molecular Targets and Underlying Mechanisms of Xiaoji Recipe against Pancreatic Cancer Based on Network Pharmacology

Computational and Mathematical Methods in Medicine

Received 5 December 2023; Accepted 5 December 2023; Published 6 December 2023

This article has been retracted by Hindawi, as publisher, following an investigation undertaken by the publisher [1]. This investigation has uncovered evidence of systematic manipulation of the publication and peer-review process. We cannot, therefore, vouch for the reliability or integrity of this article.

Please note that this notice is intended solely to alert readers that the peer-review process of this article has been compromised.

Wiley and Hindawi regret that the usual quality checks did not identify these issues before publication and have since put additional measures in place to safeguard research integrity.

We wish to credit our Research Integrity and Research Publishing teams and anonymous and named external researchers and research integrity experts for contributing to this investigation.

The corresponding author, as the representative of all authors, has been given the opportunity to register their agreement or disagreement to this retraction. We have kept a record of any response received.

References

[1] C. Xia, D. Chen, G. Wang et al., "Identification of Molecular Targets and Underlying Mechanisms of Xiaoji Recipe against Pancreatic Cancer Based on Network Pharmacology," *Computational and Mathematical Methods in Medicine*, vol. 2022, Article ID 4640849, 17 pages, 2022.

Hindawi
Computational and Mathematical Methods in Medicine
Volume 2023, Article ID 9850396, 1 page
https://doi.org/10.1155/2023/9850396

Retraction

Retracted: The Relationship between Angiotensin–Neprilysin Treatment, Echocardiographic Parameters, and NT-proBNP Levels in HFpEF Patients with Acute Decompensated Heart Failure

Computational and Mathematical Methods in Medicine

Received 5 December 2023; Accepted 5 December 2023; Published 6 December 2023

This article has been retracted by Hindawi, as publisher, following an investigation undertaken by the publisher [1]. This investigation has uncovered evidence of systematic manipulation of the publication and peer-review process. We cannot, therefore, vouch for the reliability or integrity of this article.

Please note that this notice is intended solely to alert readers that the peer-review process of this article has been compromised.

Wiley and Hindawi regret that the usual quality checks did not identify these issues before publication and have since put additional measures in place to safeguard research integrity.

We wish to credit our Research Integrity and Research Publishing teams and anonymous and named external researchers and research integrity experts for contributing to this investigation.

The corresponding author, as the representative of all authors, has been given the opportunity to register their agreement or disagreement to this retraction. We have kept a record of any response received.

References

[1] X. Zhang, S. Yang, and Z. Xu, "The Relationship between Angiotensin–Neprilysin Treatment, Echocardiographic Parameters, and NT-proBNP Levels in HFpEF Patients with Acute Decompensated Heart Failure," *Computational and Mathematical Methods in Medicine*, vol. 2022, Article ID 4298644, 6 pages, 2022.

Hindawi
Computational and Mathematical Methods in Medicine
Volume 2023, Article ID 9847256, 1 page
https://doi.org/10.1155/2023/9847256

Retraction

Retracted: Cognitive Function and Vitamin D Status in the Chinese Hemodialysis Patients

Computational and Mathematical Methods in Medicine

Received 5 December 2023; Accepted 5 December 2023; Published 6 December 2023

This article has been retracted by Hindawi, as publisher, following an investigation undertaken by the publisher [1]. This investigation has uncovered evidence of systematic manipulation of the publication and peer-review process. We cannot, therefore, vouch for the reliability or integrity of this article.

Please note that this notice is intended solely to alert readers that the peer-review process of this article has been compromised.

Wiley and Hindawi regret that the usual quality checks did not identify these issues before publication and have since put additional measures in place to safeguard research integrity.

We wish to credit our Research Integrity and Research Publishing teams and anonymous and named external researchers and research integrity experts for contributing to this investigation.

The corresponding author, as the representative of all authors, has been given the opportunity to register their agreement or disagreement to this retraction. We have kept a record of any response received.

References

[1] J. Zhang, J. Hu, R. Zhou, and Y. Xu, "Cognitive Function and Vitamin D Status in the Chinese Hemodialysis Patients," *Computational and Mathematical Methods in Medicine*, vol. 2022, Article ID 2175020, 6 pages, 2022.

Hindawi
Computational and Mathematical Methods in Medicine
Volume 2023, Article ID 9847198, 1 page
https://doi.org/10.1155/2023/9847198

Retraction

Retracted: The Value of CT Perfusion Parameters and Apparent Diffusion Coefficient Value of Magnetic Resonance Diffusion Weighted Imaging in Diagnosis of Hepatocellular Carcinoma

Computational and Mathematical Methods in Medicine

Received 5 December 2023; Accepted 5 December 2023; Published 6 December 2023

This article has been retracted by Hindawi, as publisher, following an investigation undertaken by the publisher [1]. This investigation has uncovered evidence of systematic manipulation of the publication and peer-review process. We cannot, therefore, vouch for the reliability or integrity of this article.

Please note that this notice is intended solely to alert readers that the peer-review process of this article has been compromised.

Wiley and Hindawi regret that the usual quality checks did not identify these issues before publication and have since put additional measures in place to safeguard research integrity.

We wish to credit our Research Integrity and Research Publishing teams and anonymous and named external researchers and research integrity experts for contributing to this investigation.

The corresponding author, as the representative of all authors, has been given the opportunity to register their agreement or disagreement to this retraction. We have kept a record of any response received.

References

[1] K. Li and B. Wang, "The Value of CT Perfusion Parameters and Apparent Diffusion Coefficient Value of Magnetic Resonance Diffusion Weighted Imaging in Diagnosis of Hepatocellular Carcinoma," *Computational and Mathematical Methods in Medicine*, vol. 2022, Article ID 2771869, 7 pages, 2022.

Hindawi
Computational and Mathematical Methods in Medicine
Volume 2023, Article ID 9847091, 1 page
https://doi.org/10.1155/2023/9847091

Retraction

Retracted: Long Noncoding RNA LINC00473 Ameliorates Depression-Like Behaviors in Female Mice by Acting as a Molecular Sponge to Regulate miR-497-5p/BDNF Axis

Computational and Mathematical Methods in Medicine

Received 5 December 2023; Accepted 5 December 2023; Published 6 December 2023

This article has been retracted by Hindawi, as publisher, following an investigation undertaken by the publisher [1]. This investigation has uncovered evidence of systematic manipulation of the publication and peer-review process. We cannot, therefore, vouch for the reliability or integrity of this article.

Please note that this notice is intended solely to alert readers that the peer-review process of this article has been compromised.

Wiley and Hindawi regret that the usual quality checks did not identify these issues before publication and have since put additional measures in place to safeguard research integrity.

We wish to credit our Research Integrity and Research Publishing teams and anonymous and named external researchers and research integrity experts for contributing to this investigation.

The corresponding author, as the representative of all authors, has been given the opportunity to register their agreement or disagreement to this retraction. We have kept a record of any response received.

References

[1] B. Li, H. Zhao, and J. Sun, "Long Noncoding RNA LINC00473 Ameliorates Depression-Like Behaviors in Female Mice by Acting as a Molecular Sponge to Regulate miR-497-5p/BDNF Axis," *Computational and Mathematical Methods in Medicine*, vol. 2022, Article ID 4244425, 12 pages, 2022.

Hindawi
Computational and Mathematical Methods in Medicine
Volume 2023, Article ID 9843413, 1 page
https://doi.org/10.1155/2023/9843413

Retraction

Retracted: Microarray and Bioinformatics Analysis of Differential Gene and lncRNA Expression during Erythropoietin Treatment of Acute Spinal Cord Injury in Rats

Computational and Mathematical Methods in Medicine

Received 5 December 2023; Accepted 5 December 2023; Published 6 December 2023

This article has been retracted by Hindawi, as publisher, following an investigation undertaken by the publisher [1]. This investigation has uncovered evidence of systematic manipulation of the publication and peer-review process. We cannot, therefore, vouch for the reliability or integrity of this article.

Please note that this notice is intended solely to alert readers that the peer-review process of this article has been compromised.

Wiley and Hindawi regret that the usual quality checks did not identify these issues before publication and have since put additional measures in place to safeguard research integrity.

We wish to credit our Research Integrity and Research Publishing teams and anonymous and named external researchers and research integrity experts for contributing to this investigation.

The corresponding author, as the representative of all authors, has been given the opportunity to register their agreement or disagreement to this retraction. We have kept a record of any response received.

References

[1] H. He, H. Huang, P. Hu, and Z. Chen, "Microarray and Bioinformatics Analysis of Differential Gene and lncRNA Expression during Erythropoietin Treatment of Acute Spinal Cord Injury in Rats," *Computational and Mathematical Methods in Medicine*, vol. 2022, Article ID 4121910, 13 pages, 2022.

Hindawi
Computational and Mathematical Methods in Medicine
Volume 2023, Article ID 9841057, 1 page
https://doi.org/10.1155/2023/9841057

Retraction

Retracted: Stretching Training Rehabilitation Has Potential to Alleviate Ankylosing Spondylitis in Mice by Inactivating the Wnt/β-Catenin Pathway

Computational and Mathematical Methods in Medicine

Received 5 December 2023; Accepted 5 December 2023; Published 6 December 2023

This article has been retracted by Hindawi, as publisher, following an investigation undertaken by the publisher [1]. This investigation has uncovered evidence of systematic manipulation of the publication and peer-review process. We cannot, therefore, vouch for the reliability or integrity of this article.

Please note that this notice is intended solely to alert readers that the peer-review process of this article has been compromised.

Wiley and Hindawi regret that the usual quality checks did not identify these issues before publication and have since put additional measures in place to safeguard research integrity.

We wish to credit our Research Integrity and Research Publishing teams and anonymous and named external researchers and research integrity experts for contributing to this investigation.

The corresponding author, as the representative of all authors, has been given the opportunity to register their agreement or disagreement to this retraction. We have kept a record of any response received.

References

[1] Y. Xie, X. Li, Q. Zhang, F. Guo, and Y. Wang, "Stretching Training Rehabilitation Has Potential to Alleviate Ankylosing Spondylitis in Mice by Inactivating the Wnt/β-Catenin Pathway," *Computational and Mathematical Methods in Medicine*, vol. 2022, Article ID 3932504, 10 pages, 2022.

Hindawi
Computational and Mathematical Methods in Medicine
Volume 2023, Article ID 9838096, 1 page
https://doi.org/10.1155/2023/9838096

Retraction

Retracted: Identification of Prognostic Signature of Necroptosis-Related lncRNAs and Molecular Subtypes in Glioma

Computational and Mathematical Methods in Medicine

Received 5 December 2023; Accepted 5 December 2023; Published 6 December 2023

This article has been retracted by Hindawi, as publisher, following an investigation undertaken by the publisher [1]. This investigation has uncovered evidence of systematic manipulation of the publication and peer-review process. We cannot, therefore, vouch for the reliability or integrity of this article.

Please note that this notice is intended solely to alert readers that the peer-review process of this article has been compromised.

Wiley and Hindawi regret that the usual quality checks did not identify these issues before publication and have since put additional measures in place to safeguard research integrity.

We wish to credit our Research Integrity and Research Publishing teams and anonymous and named external researchers and research integrity experts for contributing to this investigation.

The corresponding author, as the representative of all authors, has been given the opportunity to register their agreement or disagreement to this retraction. We have kept a record of any response received.

References

[1] G. Zhang, R. Chen, L. Zhu et al., "Identification of Prognostic Signature of Necroptosis-Related lncRNAs and Molecular Subtypes in Glioma," *Computational and Mathematical Methods in Medicine*, vol. 2022, Article ID 3440586, 21 pages, 2022.

Hindawi
Computational and Mathematical Methods in Medicine
Volume 2023, Article ID 9837874, 1 page
https://doi.org/10.1155/2023/9837874

Retraction

Retracted: Diagnostic Value of IGFBP-2 in Predicting Preeclampsia before 20 Weeks of Pregnancy: A Prospective Nested Case-Control Study

Computational and Mathematical Methods in Medicine

Received 5 December 2023; Accepted 5 December 2023; Published 6 December 2023

This article has been retracted by Hindawi, as publisher, following an investigation undertaken by the publisher [1]. This investigation has uncovered evidence of systematic manipulation of the publication and peer-review process. We cannot, therefore, vouch for the reliability or integrity of this article.

Please note that this notice is intended solely to alert readers that the peer-review process of this article has been compromised.

Wiley and Hindawi regret that the usual quality checks did not identify these issues before publication and have since put additional measures in place to safeguard research integrity.

We wish to credit our Research Integrity and Research Publishing teams and anonymous and named external researchers and research integrity experts for contributing to this investigation.

The corresponding author, as the representative of all authors, has been given the opportunity to register their agreement or disagreement to this retraction. We have kept a record of any response received.

References

[1] F. Gao, J. Yin, Y. Long et al., "Diagnostic Value of IGFBP-2 in Predicting Preeclampsia before 20 Weeks of Pregnancy: A Prospective Nested Case-Control Study," *Computational and Mathematical Methods in Medicine*, vol. 2022, Article ID 5075569, 8 pages, 2022.

Hindawi
Computational and Mathematical Methods in Medicine
Volume 2023, Article ID 9831659, 1 page
https://doi.org/10.1155/2023/9831659

Retraction

Retracted: Adverse Influences of Nonstrabismic Amblyopia on Quality of Life of Teenagers in China

Computational and Mathematical Methods in Medicine

Received 5 December 2023; Accepted 5 December 2023; Published 6 December 2023

This article has been retracted by Hindawi, as publisher, following an investigation undertaken by the publisher [1]. This investigation has uncovered evidence of systematic manipulation of the publication and peer-review process. We cannot, therefore, vouch for the reliability or integrity of this article.

Please note that this notice is intended solely to alert readers that the peer-review process of this article has been compromised.

Wiley and Hindawi regret that the usual quality checks did not identify these issues before publication and have since put additional measures in place to safeguard research integrity.

We wish to credit our Research Integrity and Research Publishing teams and anonymous and named external researchers and research integrity experts for contributing to this investigation.

The corresponding author, as the representative of all authors, has been given the opportunity to register their agreement or disagreement to this retraction. We have kept a record of any response received.

References

[1] Y. Wang and H. Wang, "Adverse Influences of Nonstrabismic Amblyopia on Quality of Life of Teenagers in China," *Computational and Mathematical Methods in Medicine*, vol. 2022, Article ID 2621991, 6 pages, 2022.

Hindawi
Computational and Mathematical Methods in Medicine
Volume 2023, Article ID 9829453, 1 page
https://doi.org/10.1155/2023/9829453

Retraction

Retracted: Effects of Peripherally Inserted Central Catheter (PICC) Catheterization Nursing on Bloodstream Infection in Peripheral Central Venous Catheters in Lung Cancer: A Single-Center, Retrospective Study

Computational and Mathematical Methods in Medicine

Received 5 December 2023; Accepted 5 December 2023; Published 6 December 2023

This article has been retracted by Hindawi, as publisher, following an investigation undertaken by the publisher [1]. This investigation has uncovered evidence of systematic manipulation of the publication and peer-review process. We cannot, therefore, vouch for the reliability or integrity of this article.

Please note that this notice is intended solely to alert readers that the peer-review process of this article has been compromised.

Wiley and Hindawi regret that the usual quality checks did not identify these issues before publication and have since put additional measures in place to safeguard research integrity.

We wish to credit our Research Integrity and Research Publishing teams and anonymous and named external researchers and research integrity experts for contributing to this investigation.

The corresponding author, as the representative of all authors, has been given the opportunity to register their agreement or disagreement to this retraction. We have kept a record of any response received.

References

[1] Q. Hu, Y. Su, and L. Yan, "Effects of Peripherally Inserted Central Catheter (PICC) Catheterization Nursing on Bloodstream Infection in Peripheral Central Venous Catheters in Lung Cancer: A Single-Center, Retrospective Study," *Computational and Mathematical Methods in Medicine*, vol. 2022, Article ID 2791464, 7 pages, 2022.

Hindawi
Computational and Mathematical Methods in Medicine
Volume 2023, Article ID 9823815, 1 page
https://doi.org/10.1155/2023/9823815

Retraction

Retracted: Mining of Potential Biomarkers and Pathway in Valvular Atrial Fibrillation (VAF) via Systematic Screening of Gene Coexpression Network

Computational and Mathematical Methods in Medicine

Received 5 December 2023; Accepted 5 December 2023; Published 6 December 2023

This article has been retracted by Hindawi, as publisher, following an investigation undertaken by the publisher [1]. This investigation has uncovered evidence of systematic manipulation of the publication and peer-review process. We cannot, therefore, vouch for the reliability or integrity of this article.

Please note that this notice is intended solely to alert readers that the peer-review process of this article has been compromised.

Wiley and Hindawi regret that the usual quality checks did not identify these issues before publication and have since put additional measures in place to safeguard research integrity.

We wish to credit our Research Integrity and Research Publishing teams and anonymous and named external researchers and research integrity experts for contributing to this investigation.

The corresponding author, as the representative of all authors, has been given the opportunity to register their agreement or disagreement to this retraction. We have kept a record of any response received.

References

[1] F. Zou, T. Chen, X. Xiang, C. Peng, S. Huang, and S. Ma, "Mining of Potential Biomarkers and Pathway in Valvular Atrial Fibrillation (VAF) via Systematic Screening of Gene Coexpression Network," *Computational and Mathematical Methods in Medicine*, vol. 2022, Article ID 3645402, 21 pages, 2022.

Hindawi
Computational and Mathematical Methods in Medicine
Volume 2023, Article ID 9820687, 1 page
https://doi.org/10.1155/2023/9820687

Retraction

Retracted: Downregulation of miR-146a-5p Promotes Acute Pancreatitis through Activating the TLR9/NLRP3 Signaling Pathway by Targeting TRAF6 In Vitro Rat Model

Computational and Mathematical Methods in Medicine

Received 5 December 2023; Accepted 5 December 2023; Published 6 December 2023

This article has been retracted by Hindawi, as publisher, following an investigation undertaken by the publisher [1]. This investigation has uncovered evidence of systematic manipulation of the publication and peer-review process. We cannot, therefore, vouch for the reliability or integrity of this article.

Please note that this notice is intended solely to alert readers that the peer-review process of this article has been compromised.

Wiley and Hindawi regret that the usual quality checks did not identify these issues before publication and have since put additional measures in place to safeguard research integrity.

We wish to credit our Research Integrity and Research Publishing teams and anonymous and named external researchers and research integrity experts for contributing to this investigation.

The corresponding author, as the representative of all authors, has been given the opportunity to register their agreement or disagreement to this retraction. We have kept a record of any response received.

References

[1] D. Deng, Z. Su, B. Wei, J. Zhou, H. Yang, and Z. Liang, "Downregulation of miR-146a-5p Promotes Acute Pancreatitis through Activating the TLR9/NLRP3 Signaling Pathway by Targeting TRAF6 In Vitro Rat Model," *Computational and Mathematical Methods in Medicine*, vol. 2022, Article ID 1747470, 11 pages, 2022.

Hindawi
Computational and Mathematical Methods in Medicine
Volume 2023, Article ID 9819283, 1 page
https://doi.org/10.1155/2023/9819283

Retraction

Retracted: Effects of Hypoxia-Inducible Factor 1 (HIF-1) Signaling Pathway on Acute Ischemic Stroke

Computational and Mathematical Methods in Medicine

Received 5 December 2023; Accepted 5 December 2023; Published 6 December 2023

This article has been retracted by Hindawi, as publisher, following an investigation undertaken by the publisher [1]. This investigation has uncovered evidence of systematic manipulation of the publication and peer-review process. We cannot, therefore, vouch for the reliability or integrity of this article.

Please note that this notice is intended solely to alert readers that the peer-review process of this article has been compromised.

Wiley and Hindawi regret that the usual quality checks did not identify these issues before publication and have since put additional measures in place to safeguard research integrity.

We wish to credit our Research Integrity and Research Publishing teams and anonymous and named external researchers and research integrity experts for contributing to this investigation.

The corresponding author, as the representative of all authors, has been given the opportunity to register their agreement or disagreement to this retraction. We have kept a record of any response received.

References

[1] G. Li, L. Tao, and H. Wu, "Effects of Hypoxia-Inducible Factor 1 (HIF-1) Signaling Pathway on Acute Ischemic Stroke," *Computational and Mathematical Methods in Medicine*, vol. 2022, Article ID 1860925, 8 pages, 2022.

Hindawi
Computational and Mathematical Methods in Medicine
Volume 2023, Article ID 9806902, 1 page
https://doi.org/10.1155/2023/9806902

Retraction

Retracted: Comparison of Efficacy and Psychology of Breast-Conserving Surgery and Modified Radical Mastectomy on Patients with Early Breast Cancer under Graded Nursing

Computational and Mathematical Methods in Medicine

Received 5 December 2023; Accepted 5 December 2023; Published 6 December 2023

This article has been retracted by Hindawi, as publisher, following an investigation undertaken by the publisher [1]. This investigation has uncovered evidence of systematic manipulation of the publication and peer-review process. We cannot, therefore, vouch for the reliability or integrity of this article.

Please note that this notice is intended solely to alert readers that the peer-review process of this article has been compromised.

Wiley and Hindawi regret that the usual quality checks did not identify these issues before publication and have since put additional measures in place to safeguard research integrity.

We wish to credit our Research Integrity and Research Publishing teams and anonymous and named external researchers and research integrity experts for contributing to this investigation.

The corresponding author, as the representative of all authors, has been given the opportunity to register their agreement or disagreement to this retraction. We have kept a record of any response received.

References

[1] T. Ren, J. Wu, L. Qian, J. Liu, and K. Ni, "Comparison of Efficacy and Psychology of Breast-Conserving Surgery and Modified Radical Mastectomy on Patients with Early Breast Cancer under Graded Nursing," *Computational and Mathematical Methods in Medicine*, vol. 2022, Article ID 4491573, 7 pages, 2022.

Hindawi
Computational and Mathematical Methods in Medicine
Volume 2023, Article ID 9806791, 1 page
https://doi.org/10.1155/2023/9806791

Retraction

Retracted: GINS2 Is Downregulated in Peripheral Blood of Patients with Intervertebral Disk Degeneration and Promotes Proliferation and Migration of Nucleus Pulposus Cells

Computational and Mathematical Methods in Medicine

Received 5 December 2023; Accepted 5 December 2023; Published 6 December 2023

This article has been retracted by Hindawi, as publisher, following an investigation undertaken by the publisher [1]. This investigation has uncovered evidence of systematic manipulation of the publication and peer-review process. We cannot, therefore, vouch for the reliability or integrity of this article.

Please note that this notice is intended solely to alert readers that the peer-review process of this article has been compromised.

Wiley and Hindawi regret that the usual quality checks did not identify these issues before publication and have since put additional measures in place to safeguard research integrity.

We wish to credit our Research Integrity and Research Publishing teams and anonymous and named external researchers and research integrity experts for contributing to this investigation.

The corresponding author, as the representative of all authors, has been given the opportunity to register their agreement or disagreement to this retraction. We have kept a record of any response received.

References

[1] H. Jiang, H. Sun, J. Dai, C. Zhang, and X. Tang, "GINS2 Is Downregulated in Peripheral Blood of Patients with Intervertebral Disk Degeneration and Promotes Proliferation and Migration of Nucleus Pulposus Cells," *Computational and Mathematical Methods in Medicine*, vol. 2022, Article ID 1986348, 13 pages, 2022.

Hindawi
Computational and Mathematical Methods in Medicine
Volume 2023, Article ID 9804692, 1 page
https://doi.org/10.1155/2023/9804692

Retraction

Retracted: Influences of Airway Obstruction Caused by Adenoid Hypertrophy on Growth and Development of Craniomaxillofacial Structure and Respiratory Function in Children

Computational and Mathematical Methods in Medicine

Received 5 December 2023; Accepted 5 December 2023; Published 6 December 2023

This article has been retracted by Hindawi, as publisher, following an investigation undertaken by the publisher [1]. This investigation has uncovered evidence of systematic manipulation of the publication and peer-review process. We cannot, therefore, vouch for the reliability or integrity of this article.

Please note that this notice is intended solely to alert readers that the peer-review process of this article has been compromised.

Wiley and Hindawi regret that the usual quality checks did not identify these issues before publication and have since put additional measures in place to safeguard research integrity.

We wish to credit our Research Integrity and Research Publishing teams and anonymous and named external researchers and research integrity experts for contributing to this investigation.

The corresponding author, as the representative of all authors, has been given the opportunity to register their agreement or disagreement to this retraction. We have kept a record of any response received.

References

[1] H. Li, H. Wang, H. Hao, H. An, and H. Geng, "Influences of Airway Obstruction Caused by Adenoid Hypertrophy on Growth and Development of Craniomaxillofacial Structure and Respiratory Function in Children," *Computational and Mathematical Methods in Medicine*, vol. 2022, Article ID 5096406, 7 pages, 2022.

Hindawi
Computational and Mathematical Methods in Medicine
Volume 2023, Article ID 9803037, 1 page
https://doi.org/10.1155/2023/9803037

Retraction

Retracted: Mechanisms of Banxia Xiexin Decoction Underlying Chronic Atrophic Gastritis via Network Pharmacology, Molecular Docking, and Molecular Dynamics Simulations

Computational and Mathematical Methods in Medicine

Received 5 December 2023; Accepted 5 December 2023; Published 6 December 2023

This article has been retracted by Hindawi, as publisher, following an investigation undertaken by the publisher [1]. This investigation has uncovered evidence of systematic manipulation of the publication and peer-review process. We cannot, therefore, vouch for the reliability or integrity of this article.

Please note that this notice is intended solely to alert readers that the peer-review process of this article has been compromised.

Wiley and Hindawi regret that the usual quality checks did not identify these issues before publication and have since put additional measures in place to safeguard research integrity.

We wish to credit our Research Integrity and Research Publishing teams and anonymous and named external researchers and research integrity experts for contributing to this investigation.

The corresponding author, as the representative of all authors, has been given the opportunity to register their agreement or disagreement to this retraction. We have kept a record of any response received.

References

[1] C. Chang, W. Feng, M. Sun, X. Yu, and Z. Sun, "Mechanisms of Banxia Xiexin Decoction Underlying Chronic Atrophic Gastritis via Network Pharmacology, Molecular Docking, and Molecular Dynamics Simulations," *Computational and Mathematical Methods in Medicine*, vol. 2022, Article ID 4237040, 13 pages, 2022.

Hindawi
Computational and Mathematical Methods in Medicine
Volume 2023, Article ID 9796430, 1 page
https://doi.org/10.1155/2023/9796430

Retraction

Retracted: Multislice Computed Tomography Angiography Imaging Diagnosis of Lower Extremity Arteriosclerosis in Patients with Hypertension and Its Correlation with the Level of High-Sensitivity C-Reactive Protein

Computational and Mathematical Methods in Medicine

Received 5 December 2023; Accepted 5 December 2023; Published 6 December 2023

This article has been retracted by Hindawi, as publisher, following an investigation undertaken by the publisher [1]. This investigation has uncovered evidence of systematic manipulation of the publication and peer-review process. We cannot, therefore, vouch for the reliability or integrity of this article.

Please note that this notice is intended solely to alert readers that the peer-review process of this article has been compromised.

Wiley and Hindawi regret that the usual quality checks did not identify these issues before publication and have since put additional measures in place to safeguard research integrity.

We wish to credit our Research Integrity and Research Publishing teams and anonymous and named external researchers and research integrity experts for contributing to this investigation.

The corresponding author, as the representative of all authors, has been given the opportunity to register their agreement or disagreement to this retraction. We have kept a record of any response received.

References

[1] J. Huo, Z. Wu, H. Jiang, and H. Zhang, "Multislice Computed Tomography Angiography Imaging Diagnosis of Lower Extremity Arteriosclerosis in Patients with Hypertension and Its Correlation with the Level of High-Sensitivity C-Reactive Protein," *Computational and Mathematical Methods in Medicine*, vol. 2022, Article ID 1768208, 8 pages, 2022.

Hindawi
Computational and Mathematical Methods in Medicine
Volume 2023, Article ID 9790685, 1 page
https://doi.org/10.1155/2023/9790685

Retraction

Retracted: To Study the Effect of Individualized Nursing Model Based on MDT Concept on Limb Function Recovery and Quality of Life in Patients with Breast Cancer

Computational and Mathematical Methods in Medicine

Received 5 December 2023; Accepted 5 December 2023; Published 6 December 2023

This article has been retracted by Hindawi, as publisher, following an investigation undertaken by the publisher [1]. This investigation has uncovered evidence of systematic manipulation of the publication and peer-review process. We cannot, therefore, vouch for the reliability or integrity of this article.

Please note that this notice is intended solely to alert readers that the peer-review process of this article has been compromised.

Wiley and Hindawi regret that the usual quality checks did not identify these issues before publication and have since put additional measures in place to safeguard research integrity.

We wish to credit our Research Integrity and Research Publishing teams and anonymous and named external researchers and research integrity experts for contributing to this investigation.

The corresponding author, as the representative of all authors, has been given the opportunity to register their agreement or disagreement to this retraction. We have kept a record of any response received.

References

[1] Y. Chen, F. Luo, and G. Shi, "To Study the Effect of Individualized Nursing Model Based on MDT Concept on Limb Function Recovery and Quality of Life in Patients with Breast Cancer," *Computational and Mathematical Methods in Medicine*, vol. 2022, Article ID 1032503, 6 pages, 2022.

Hindawi
Computational and Mathematical Methods in Medicine
Volume 2023, Article ID 9783851, 1 page
https://doi.org/10.1155/2023/9783851

Retraction

Retracted: Study on the Effect of Bushen Zhuanggu Tablet Combined with Conventional Regimen on Bone Mineral Density Improvement, Functional Recovery and Fracture Risk Prevention in Patients with Postmenopausal Osteoporosis

Computational and Mathematical Methods in Medicine

Received 5 December 2023; Accepted 5 December 2023; Published 6 December 2023

This article has been retracted by Hindawi, as publisher, following an investigation undertaken by the publisher [1]. This investigation has uncovered evidence of systematic manipulation of the publication and peer-review process. We cannot, therefore, vouch for the reliability or integrity of this article.

Please note that this notice is intended solely to alert readers that the peer-review process of this article has been compromised.

Wiley and Hindawi regret that the usual quality checks did not identify these issues before publication and have since put additional measures in place to safeguard research integrity.

We wish to credit our Research Integrity and Research Publishing teams and anonymous and named external researchers and research integrity experts for contributing to this investigation.

The corresponding author, as the representative of all authors, has been given the opportunity to register their agreement or disagreement to this retraction. We have kept a record of any response received.

References

[1] T. Chen, G. Li, and Y. Xu, "Study on the Effect of Bushen Zhuanggu Tablet Combined with Conventional Regimen on Bone Mineral Density Improvement, Functional Recovery and Fracture Risk Prevention in Patients with Postmenopausal Osteoporosis," *Computational and Mathematical Methods in Medicine*, vol. 2023, Article ID 4846392, 9 pages, 2023.

Hindawi
Computational and Mathematical Methods in Medicine
Volume 2023, Article ID 9780897, 1 page
https://doi.org/10.1155/2023/9780897

Retraction

Retracted: Diagnostic Value of CT Window Technique for Primary Omentum Infarction

Computational and Mathematical Methods in Medicine

Received 5 December 2023; Accepted 5 December 2023; Published 6 December 2023

This article has been retracted by Hindawi, as publisher, following an investigation undertaken by the publisher [1]. This investigation has uncovered evidence of systematic manipulation of the publication and peer-review process. We cannot, therefore, vouch for the reliability or integrity of this article.

Please note that this notice is intended solely to alert readers that the peer-review process of this article has been compromised.

Wiley and Hindawi regret that the usual quality checks did not identify these issues before publication and have since put additional measures in place to safeguard research integrity.

We wish to credit our Research Integrity and Research Publishing teams and anonymous and named external researchers and research integrity experts for contributing to this investigation.

The corresponding author, as the representative of all authors, has been given the opportunity to register their agreement or disagreement to this retraction. We have kept a record of any response received.

References

[1] Y. Du, Y. Chen, C.-h. Li et al., "Diagnostic Value of CT Window Technique for Primary Omentum Infarction," *Computational and Mathematical Methods in Medicine*, vol. 2022, Article ID 4173738, 6 pages, 2022.

Hindawi
Computational and Mathematical Methods in Medicine
Volume 2023, Article ID 9769373, 1 page
https://doi.org/10.1155/2023/9769373

Retraction

Retracted: Clinical Value of Contrast-Enhanced Ultrasound in Breast Cancer Diagnosis

Computational and Mathematical Methods in Medicine

Received 5 December 2023; Accepted 5 December 2023; Published 6 December 2023

This article has been retracted by Hindawi, as publisher, following an investigation undertaken by the publisher [1]. This investigation has uncovered evidence of systematic manipulation of the publication and peer-review process. We cannot, therefore, vouch for the reliability or integrity of this article.

Please note that this notice is intended solely to alert readers that the peer-review process of this article has been compromised.

Wiley and Hindawi regret that the usual quality checks did not identify these issues before publication and have since put additional measures in place to safeguard research integrity.

We wish to credit our Research Integrity and Research Publishing teams and anonymous and named external researchers and research integrity experts for contributing to this investigation.

The corresponding author, as the representative of all authors, has been given the opportunity to register their agreement or disagreement to this retraction. We have kept a record of any response received.

References

[1] Y. Yuan, M. Xu, Y. Ren, L. He, J. Chen, and L. Sun, "Clinical Value of Contrast-Enhanced Ultrasound in Breast Cancer Diagnosis," *Computational and Mathematical Methods in Medicine*, vol. 2022, Article ID 2017026, 6 pages, 2022.

Hindawi
Computational and Mathematical Methods in Medicine
Volume 2023, Article ID 9815867, 1 page
https://doi.org/10.1155/2023/9815867

Retraction

Retracted: Study on Strength and Quality Training of Youth Basketball Players

Computational and Mathematical Methods in Medicine

Received 26 September 2023; Accepted 26 September 2023; Published 27 September 2023

This article has been retracted by Hindawi following an investigation undertaken by the publisher [1]. This investigation has uncovered evidence of one or more of the following indicators of systematic manipulation of the publication process:

(1) Discrepancies in scope

(2) Discrepancies in the description of the research reported

(3) Discrepancies between the availability of data and the research described

(4) Inappropriate citations

(5) Incoherent, meaningless and/or irrelevant content included in the article

(6) Peer-review manipulation

The presence of these indicators undermines our confidence in the integrity of the article's content and we cannot, therefore, vouch for its reliability. Please note that this notice is intended solely to alert readers that the content of this article is unreliable. We have not investigated whether authors were aware of or involved in the systematic manipulation of the publication process.

In addition, our investigation has also shown that one or more of the following human-subject reporting requirements has not been met in this article: ethical approval by an Institutional Review Board (IRB) committee or equivalent, patient/participant consent to participate, and/or agreement to publish patient/participant details (where relevant).

Wiley and Hindawi regrets that the usual quality checks did not identify these issues before publication and have since put additional measures in place to safeguard research integrity.

We wish to credit our own Research Integrity and Research Publishing teams and anonymous and named external researchers and research integrity experts for contributing to this investigation.

The corresponding author, as the representative of all authors, has been given the opportunity to register their agreement or disagreement to this retraction. We have kept a record of any response received.

References

[1] Q. Meng, "Study on Strength and Quality Training of Youth Basketball Players," *Computational and Mathematical Methods in Medicine*, vol. 2022, Article ID 4676968, 11 pages, 2022.

Hindawi
Computational and Mathematical Methods in Medicine
Volume 2023, Article ID 9897161, 1 page
https://doi.org/10.1155/2023/9897161

Retraction

Retracted: Investigation and Countermeasures on Mental Health Status of Applied Fresh Graduates from the Perspective of Psychological Capital

Computational and Mathematical Methods in Medicine

Received 1 August 2023; Accepted 1 August 2023; Published 2 August 2023

This article has been retracted by Hindawi following an investigation undertaken by the publisher [1]. This investigation has uncovered evidence of one or more of the following indicators of systematic manipulation of the publication process:

(1) Discrepancies in scope

(2) Discrepancies in the description of the research reported

(3) Discrepancies between the availability of data and the research described

(4) Inappropriate citations

(5) Incoherent, meaningless and/or irrelevant content included in the article

(6) Peer-review manipulation

The presence of these indicators undermines our confidence in the integrity of the article's content and we cannot, therefore, vouch for its reliability. Please note that this notice is intended solely to alert readers that the content of this article is unreliable. We have not investigated whether authors were aware of or involved in the systematic manipulation of the publication process.

Wiley and Hindawi regrets that the usual quality checks did not identify these issues before publication and have since put additional measures in place to safeguard research integrity.

We wish to credit our own Research Integrity and Research Publishing teams and anonymous and named external researchers and research integrity experts for contributing to this investigation.

The corresponding author, as the representative of all authors, has been given the opportunity to register their agreement or disagreement to this retraction. We have kept a record of any response received.

References

[1] Y. Zeng, "Investigation and Countermeasures on Mental Health Status of Applied Fresh Graduates from the Perspective of Psychological Capital," *Computational and Mathematical Methods in Medicine*, vol. 2022, Article ID 5352958, 10 pages, 2022.

Hindawi
Computational and Mathematical Methods in Medicine
Volume 2023, Article ID 9869456, 1 page
https://doi.org/10.1155/2023/9869456

Retraction

Retracted: Management of Patients with Cervicofacial Edema and Paresthesia during Perioperative Period of Transoral Endoscopic Thyroidectomy

Computational and Mathematical Methods in Medicine

Received 1 August 2023; Accepted 1 August 2023; Published 2 August 2023

This article has been retracted by Hindawi following an investigation undertaken by the publisher [1]. This investigation has uncovered evidence of one or more of the following indicators of systematic manipulation of the publication process:

(1) Discrepancies in scope

(2) Discrepancies in the description of the research reported

(3) Discrepancies between the availability of data and the research described

(4) Inappropriate citations

(5) Incoherent, meaningless and/or irrelevant content included in the article

(6) Peer-review manipulation

The presence of these indicators undermines our confidence in the integrity of the article's content and we cannot, therefore, vouch for its reliability. Please note that this notice is intended solely to alert readers that the content of this article is unreliable. We have not investigated whether authors were aware of or involved in the systematic manipulation of the publication process.

Wiley and Hindawi regrets that the usual quality checks did not identify these issues before publication and have since put additional measures in place to safeguard research integrity.

We wish to credit our own Research Integrity and Research Publishing teams and anonymous and named external researchers and research integrity experts for contributing to this investigation.

The corresponding author, as the representative of all authors, has been given the opportunity to register their agreement or disagreement to this retraction. We have kept a record of any response received.

References

[1] X. Yang, J. G. Zhao, M. Liu, S. Wang, and L. Wang, "Management of Patients with Cervicofacial Edema and Paresthesia during Perioperative Period of Transoral Endoscopic Thyroidectomy," *Computational and Mathematical Methods in Medicine*, vol. 2022, Article ID 4775264, 9 pages, 2022.

Hindawi
Computational and Mathematical Methods in Medicine
Volume 2023, Article ID 9834256, 1 page
https://doi.org/10.1155/2023/9834256

Retraction

Retracted: Individualized Management of Quality of Care in Orthopedic Nurses Based on Sensitive Indicators

Computational and Mathematical Methods in Medicine

Received 1 August 2023; Accepted 1 August 2023; Published 2 August 2023

This article has been retracted by Hindawi following an investigation undertaken by the publisher [1]. This investigation has uncovered evidence of one or more of the following indicators of systematic manipulation of the publication process:

(1) Discrepancies in scope

(2) Discrepancies in the description of the research reported

(3) Discrepancies between the availability of data and the research described

(4) Inappropriate citations

(5) Incoherent, meaningless and/or irrelevant content included in the article

(6) Peer-review manipulation

The presence of these indicators undermines our confidence in the integrity of the article's content and we cannot, therefore, vouch for its reliability. Please note that this notice is intended solely to alert readers that the content of this article is unreliable. We have not investigated whether authors were aware of or involved in the systematic manipulation of the publication process.

In addition, our investigation has also shown that one or more of the following human-subject reporting requirements has not been met in this article: ethical approval by an Institutional Review Board (IRB) committee or equivalent, patient/participant consent to participate, and/or agreement to publish patient/participant details (where relevant).

Wiley and Hindawi regrets that the usual quality checks did not identify these issues before publication and have since put additional measures in place to safeguard research integrity.

We wish to credit our own Research Integrity and Research Publishing teams and anonymous and named external researchers and research integrity experts for contributing to this investigation.

The corresponding author, as the representative of all authors, has been given the opportunity to register their agreement or disagreement to this retraction. We have kept a record of any response received.

References

[1] W. Zhang, X. Huang, and T. Huang, "Individualized Management of Quality of Care in Orthopedic Nurses Based on Sensitive Indicators," *Computational and Mathematical Methods in Medicine*, vol. 2023, Article ID 1950220, 8 pages, 2023.

Hindawi
Computational and Mathematical Methods in Medicine
Volume 2023, Article ID 9805943, 1 page
https://doi.org/10.1155/2023/9805943

Retraction

Retracted: Study on the Effect of Self-Made Lifei Dingchuan Decoction Combined with Western Medicine on Cough Variant Asthma

Computational and Mathematical Methods in Medicine

Received 1 August 2023; Accepted 1 August 2023; Published 2 August 2023

This article has been retracted by Hindawi following an investigation undertaken by the publisher [1]. This investigation has uncovered evidence of one or more of the following indicators of systematic manipulation of the publication process:

(1) Discrepancies in scope

(2) Discrepancies in the description of the research reported

(3) Discrepancies between the availability of data and the research described

(4) Inappropriate citations

(5) Incoherent, meaningless and/or irrelevant content included in the article

(6) Peer-review manipulation

The presence of these indicators undermines our confidence in the integrity of the article's content and we cannot, therefore, vouch for its reliability. Please note that this notice is intended solely to alert readers that the content of this article is unreliable. We have not investigated whether authors were aware of or involved in the systematic manipulation of the publication process.

Wiley and Hindawi regrets that the usual quality checks did not identify these issues before publication and have since put additional measures in place to safeguard research integrity.

We wish to credit our own Research Integrity and Research Publishing teams and anonymous and named external researchers and research integrity experts for contributing to this investigation.

The corresponding author, as the representative of all authors, has been given the opportunity to register their agreement or disagreement to this retraction. We have kept a record of any response received.

References

[1] J. Li, Z. Huang, K. Li, X. Jian, and B. Liang, "Study on the Effect of Self-Made Lifei Dingchuan Decoction Combined with Western Medicine on Cough Variant Asthma," *Computational and Mathematical Methods in Medicine*, vol. 2022, Article ID 9803552, 8 pages, 2022.

Hindawi
Computational and Mathematical Methods in Medicine
Volume 2023, Article ID 9783851, 1 page
https://doi.org/10.1155/2023/9783851

Retraction

Retracted: Study on the Effect of Bushen Zhuanggu Tablet Combined with Conventional Regimen on Bone Mineral Density Improvement, Functional Recovery and Fracture Risk Prevention in Patients with Postmenopausal Osteoporosis

Computational and Mathematical Methods in Medicine

Received 5 December 2023; Accepted 5 December 2023; Published 6 December 2023

This article has been retracted by Hindawi, as publisher, following an investigation undertaken by the publisher [1]. This investigation has uncovered evidence of systematic manipulation of the publication and peer-review process. We cannot, therefore, vouch for the reliability or integrity of this article.

Please note that this notice is intended solely to alert readers that the peer-review process of this article has been compromised.

Wiley and Hindawi regret that the usual quality checks did not identify these issues before publication and have since put additional measures in place to safeguard research integrity.

We wish to credit our Research Integrity and Research Publishing teams and anonymous and named external researchers and research integrity experts for contributing to this investigation.

The corresponding author, as the representative of all authors, has been given the opportunity to register their agreement or disagreement to this retraction. We have kept a record of any response received.

References

[1] T. Chen, G. Li, and Y. Xu, "Study on the Effect of Bushen Zhuanggu Tablet Combined with Conventional Regimen on Bone Mineral Density Improvement, Functional Recovery and Fracture Risk Prevention in Patients with Postmenopausal Osteoporosis," *Computational and Mathematical Methods in Medicine*, vol. 2023, Article ID 4846392, 9 pages, 2023.

Hindawi
Computational and Mathematical Methods in Medicine
Volume 2023, Article ID 4846392, 9 pages
https://doi.org/10.1155/2023/4846392

Research Article

Study on the Effect of Bushen Zhuanggu Tablet Combined with Conventional Regimen on Bone Mineral Density Improvement, Functional Recovery and Fracture Risk Prevention in Patients with Postmenopausal Osteoporosis

Tianliang Chen,[1,2] **Guilan Li**,[3] **and Yongtao Xu**[2]

[1]*The Second Clinical Medical College of Guangzhou University of Chinese Medicine, China*
[2]*Department of Orthopedics, Gaozhou Hospital of Traditional Chinese Medicine, China*
[3]*Department of Encephalopathy, Gaozhou Hospital of Traditional Chinese Medicine, China*

Correspondence should be addressed to Tianliang Chen; 631301040104@mails.cqjtu.edu.cn

Received 8 August 2022; Revised 16 August 2022; Accepted 17 September 2022; Published 7 July 2023

Academic Editor: Min Tang

Objective. This case-control study was to explore the effect of Bushen Zhuanggu tablet combined with routine regimen on bone mineral density (BMD) improvement, functional recovery, and fracture prevention in postmenopausal osteoporosis (PMOP) patients. *Methods.* 180 postmenopausal osteoporosis patients were randomly selected from communities A, B, and C cohorts as research subjects from January to May 2021. The study subjects were divided into three groups. The groups were in a 1 : 1 ratio according to the principles of nonrandomised, concurrent controlled trials, and methods. There were 60 participants in each group (group A, group B, and group C). Group A was treated with Bushen Zhuanggu tablet for antiosteoporosis + basic treatment (calcium supplement and vitamin D). Group C was given Bushen Zhuanggu tablet for antiosteoporosis intervention. Group B was given basic treatment (calcium supplement and vitamin D supplementation) as a control group. The follow-up time was 6 months after treatment. Finally, we compare the differences in calcium and phosphorus metabolism indexes, BMD, bone metabolism indexes, upper and lower limb muscle strength, and quality of life scores. *Results.* Group A, B, and C's effective rate was 98.33%, 80.00%, and 93.33%, respectively. The group A's effective rate was significantly higher than that in group B and C, and the difference was statistically significant ($P < 0.05$). After 6 months intervention, the levels of serum Ca^{2+}, serum phosphorus (P), serum creatinine (Cr), and parathyroid hormone (PTH) in 3 groups decreased. Ca, P, Scr, and PTH levels in group A were the lowest among study groups, and the difference was statistically significant ($P < 0.05$). The increase in the BMD of lumbar spine, the left femoral neck, and Ward's triangle area of the three groups were observed with the highest data in group A. After 6 months of treatment, the levels of serum N-terminal propeptide of type I procollagen, PINP, and serum osteocalcin (OC) increased, while the levels of β-cross-linked C-terminal telopeptide of type I collagen (β-CTX) and alkaline phosphatase (ALP) decreased in the three groups. The improvement of all bone metabolic indexes in group A was significantly better than that in B and C groups, and the difference was statistically significant ($P < 0.05$). The enhanced upper limb muscle strength and the shorter standing-walking timing test (TUGT) time were observed after 6 months of treatment. The improvement effect of upper and lower limb muscle strength in group A was significantly better than that in B and C groups, and the difference was statistically significant ($P < 0.05$). There were significant differences in physiological function, life function, general health status, physical pain, mental state, emotional function, vitality, and social function among the three groups after 6 months treatment, and the difference was statistically significant ($P < 0.05$). The score of quality of life in group A was higher than that in B and C groups, and the difference was statistically significant ($P < 0.05$). *Conclusion.* Bushen Zhuanggu tablet combined with conventional therapy is effective in the postmenopausal osteoporosis treatment, which effectively increase the BMD, regulate calcium and phosphorus metabolism, promote the recovery of limb function, prevent the recurrence of fracture, and improve the patients' quality of life. This treatment scheme is worth popularizing.

1. Introduction

Osteoporosis (OP) has a high incidence in the elderly, especially in postmenopausal women. Osteoporosis is called "silent killer" because of its long incubation period and no obvious symptoms in the early stage. According to statistics, by 2019, the global incidence of osteoporosis has exceeded 200 million, and an average of 20 fractures per minute is caused by osteoporosis [1, 2]. Osteoporosis can occur in all age groups, among which postmenopausal women and elderly men have the highest incidence. Postmenopausal osteoporosis (PMOP), which accounts for the largest proportion, belongs to primary osteoporosis type I [3]. According to the survey, the prevalence rate of osteoporosis in women aged 40-50 in China is 4.3% [4, 5]; women over 50 is 32.1%; women over 65 is 51.6%. The prevalence rate in rural areas is slightly higher comparing with the one in urban areas. Postmenopausal osteoporosis has aroused the public attention and gradually become a significant health issue in our country.

Recent studies have shown that women lose bone mass rapidly during the 5-10 years after menopause with an annual loss rate of about 1.5% to 2.5% [6, 7]. Age, living environment, eating habits, and other diseases and other factors can lead to the occurrence of PMOP. The decline of ovarian function and the decrease of estrogen level are the main reasons. The current antiosteoporosis treatment in Western medicine is based on drugs, supplemented by physiotherapy. Because of its clear mechanism and definite curative effect, drug therapy has become one of the most commonly used drugs in osteoporosis treatment in clinic, mainly including the following categories [8, 9]. Postmenopausal osteoporosis is similar to "bone impotence," "bone fetish," "bone withering," and other diseases in TCM, among which the syndrome of "bone impotence" is the most similar. In TCM theory, the disease is located in the lumbar spine muscles and bones. Its origin lies in the kidney. Generally speaking, the pathogenesis is the deficiency of kidney, liver, and spleen (blood stasis and qi stagnation). The basic drugs include vitamin D and calcium supplements. In addition, bone resorption inhibitors include bisphosphates, calcitonin, estrogen, selective estrogen receptor modulators, and RANKL inhibitors. Bone formation enhancer mainly refers to thyroid hormone analogues. Other mechanism drugs also include active vitamin D and its analogues, vitamin K2 drugs, and strontium salts. The guidelines recommend that when selecting antiosteoporotic drugs in clinic, we should choose broad-spectrum antiosteoporotic drugs such as zoledronic acid, alendronate, and risedronate. However, there are more and more kinds of clinical antiosteoporosis drugs, along with the long-term use of antiosteoporosis drugs and the increase in the number of clinical cases. The continuous emergence of adverse reactions of drugs has also attracted more and more attention. And Western medicine treatment of osteoporosis has a high price, poor tolerance of some patients, adverse reactions and poor long-term efficacy, and other factors, making poor compliance. TCM has relatively few side effects. Basic theories, experimental explorations and clinical studies on the osteoporosis prevention and treatment in Chinese medicine are increasing day by day. Oral drug treatment is the first choice for patients with low BMD but no/low risk of fracture. For those patients with osteoporosis who cannot tolerate oral medication, who have contraindications to oral medication, or who have poor compliance, treatment with injectable, such as zoledronic acid, should be administered once a year [10, 11].

The use of evidence-based and comprehensive treatment can effectively relieve the patients' clinical symptoms. Some scholars have found that the effective components of kidney-tonifying herbs can promote bone formation and inhibit bone resorption. Under normal circumstances, the processes of bone formation are coupled and cooperated with bone resorption. In the case of osteoporosis, bone resorption is greater than bone formation, resulting in bone mass loss. Chinese medicine has unique advantages in the treatment of osteoporosis. However, there are few such scientific studies in clinic, and its application effect remains to be further confirmed [12]. It is necessary to demonstrate the clinical efficacy of TCM therapy in the postmenopausal osteoporosis treatment through scientific research, which can lay a theoretical foundation and thus promote the application of TCM therapy.

2. Materials and Methods

2.1. General Information. 180 randomly selected postmenopausal osteoporosis patients from communities A, B, and C from January to May 2021. Subjects were divided into group A ($n = 60$), group B ($n = 60$), and group C ($n = 60$) in a 1 : 1 ratio according to the measured BMD and the principles and methods of nonrandomised simultaneous controlled trials. Group A was treated with Bushen Zhuanggu tablets for antiosteoporosis + basic treatment (calcium supplementation and vitamin D) for intervention treatment. Group C was treated with Bushen Zhuanggu tablet for antiosteoporosis intervention. Group B was given basic treatment (calcium supplementation and vitamin D supplementation) as the control group. The follow-up time was 6 months after treatment. Group A was aged from 52 to 80 years with an average age of (68.37 ± 7.41) years. Menopause lasted for 1 to 5 years, with average of (2.57 ± 0.51) years. Body mass index (BMI) was 18.76~30.12 kg/m^2 with average BMI (24.89 ± 2.37) kg/m^2. Group B was aged from 51 to 79 years, with an average age of (67.34 ± 7.68) years. Menopause lasted from 1 to 6 years with an average of (2.92 ± 0.83) years. BMI ranged from BMI 18.47~29.82 kg/m^2 with an average BMI of (24.37 ± 2.14) kg/m^2. Group C was aged from 51 to 79 years, with an average age of (67.34 ± 7.68) years. The time of menopause ranged from 1 to 6 years with the average time of menopause 2.92 ± 0.83 years. The BMI of group C patients was 18.47~29.82 kg/m^2 and average BMI was 24.37 ± 2.14 kg/m^2 with P value over 0.05, which means there were no significant differences among three groups. This study was approved by the Medical Ethics Council of our hospital. All patients signed the informed consent form for the trial.

Selection criteria is as follows: (1) the selected cases were all diagnosed with postmenopausal osteoporosis, which met

the diagnostic criteria in the "Guidelines for Primary Osteoporosis Primary Care (Practical Edition 2019)" formulated in 2011 [13]; (2) the patients had no cognition, language, and intellectual dysfunction, with basic reading and writing skills; (3) all postmenopausal women with T value <-2.5; (4) the patients agreed to be followed up for 12 months, who were able to accept and answer telephone follow-up; (5) the patient's clinical data were complete.

Exclusion criteria is as follows: (1) premenopausal osteoporosis (no premenopausal osteoporosis: the patient reported no symptoms related to osteoporosis before menopause, no osteoporosis was found in physical examination, and the BMD test showed that $T > -1.0$. The course of osteoporosis was shorter than the time of menopause); (2) patients with secondary osteoporosis caused by other diseases; (3) those who refused to participate in the trial; (4) those who have recently taken drugs such as glucocorticoids, sex hormones, bisphosphonates, vitamin D, fluoride, and calcium that affect bone metabolism; (5) patients with chronic or severe organ diseases. (6) The individual with severe insufficiency and malignant tumor in either heart, liver, or renal.

2.2. Methods. Experimental group A was treated with Bushen Zhuanggu tablet for antiosteoporosis + basic treatment (calcium supplement and vitamin D) for intervention. Group C was given Bushen Zhuanggu tablet for antiosteoporosis for intervention. Group B was given basic treatment (supplemented with calcium and vitamin D) as a control group. Three groups were given health education, including fall prevention and daily life adjustment. Basic treatment content was oral calcium carbonate D3 (Caerqi, Wyeth Pharmaceutical Co., Ltd.) 600 mg/d, active vitamin D (Luo Gaiquan, Roche company) 0.5 μg/d, oral medication for 6 months. Usage of Bushen Zhuanggu tablets is as follows: 3 tablets/time, 3 times/day orally, the drug formula is Bushen Zhuanggu tablets (*Epimedium*, Drynaria, *Rehmannia glutinosa*, *Cornus*, dodder, astragalus, Chinese yam, all angelica, *Panax notoginseng*, danshen, etc.), the prescription has been proved by long-term clinical verification that it has a good effect on improving the clinical symptoms of osteoporosis patients.

2.3. Observation Index

2.3.1. Clinical Curative Effect. The therapeutic effects of the three groups were evaluated after treatment, and the specific evaluation criteria were referred to the relevant literature [14]. Markedly, effective was indicated the clinical symptoms of the patient basically disappeared, and the bone mineral density (BMD) level increased by more than 0.05 g cm^2. Effective was indicated the clinical symptoms of the patient improved, the BMD level increased, but the increase level was lower than 0.05 g cm^2. Ineffective was indicated the patient's clinical symptoms did not improve or even worsened, and BMD did not increase or decrease. The total effective rate of treatment = (markedly effective + effective) number of cases/total number of cases × 100%.

2.3.2. Muscle Strength Measurement. We carried out the muscle strength measurement before and 6 months after the treatment. The upper limb muscle strength test (two-hand grip strength test): the grip strength test used the electronic grip strength meter (Xiangshan CAMRY, model EH101); the resolution: 0.1KGF; the allowable error: 0.5KGF. Before the test begins, the subject was checked for grip strength disorders. The grip distance was adjusted, and the machine was switched on. The subject held the grip strength meter with the palm of the hand facing inwards and the display facing outwards, with the body upright, feet naturally apart, and arms naturally down, and then grasped as hard as they could. After one practice, the test began. The maximum grip strength of both hands was measured twice, and the average grip strength of two times was taken. After 3 and 6 months of treatment, the standing-walking timing test (TUGT) was performed. The subjects sat on a chair with high 45 cm height, stood up, walked in a straight line of 3 m, and then returned to the seat to sit down. The assessor recorded the time spent on each standing and walking test.

2.3.3. BMD Measurement. BMD was measured before and after treatment. Dual energy X-ray absorptiometry (HOLOGIC, Wi, USA) was used to detect the anterior and posterior lumbar vertebrae (L1 ~ L4), left femoral neck (Neck), and Wards triangle of each subject, expressed by BMD (g/cm^2). The accuracy of the instrument was 1%, and the repeated measurement error was 1%. In order to reduce the error, all testing operations were completed by the same person. Every day, the instrument was checked with the module provided by the manufacturer, and the test was carried out only after meeting the quality control requirements. The standard for judging bone mass was T score: when $T > -1.0$, it meant normal bone mass; when it was (−1.0, −2.5), it meant osteopenia; when $T < -2.5$, it meant osteoporosis [15].

2.3.4. Related Biochemical Indexes of Osteoporosis. The biochemical indexes related to osteoporosis were detected before treatment and 6 months after treatment. (1) Bone metabolic indexes are as follows: procollagen N-terminal propeptide of serum type I (PINP), serum osteocalcin (OC), collagen cross-linked carboxyl terminal peptide type I (β-CTX), and alkaline phosphatase (ALP). (2) Calcium and phosphorus metabolic indexes are as follows: serum calcium (Ca2+), serum phosphorus (P), serum creatinine (Cr), and Parathyroid Hormone (PTH).

Fasting peripheral blood 7 ml (including anticoagulant blood vessel 1 ml and procoagulant blood vessel 3 ml) was collected from each subject. The subjects were required to draw elbow venous blood from 8 to 10:00 am with empty stomach. The blood samples were collected on that day by Guangzhou Jinyu testing Technology Co., Ltd. Samples that were not sent on the same day (but ensured that they could be sent on the same day) must be stored in a refrigerator at 4°C within 6 hours. If the sample could not be sent for examination on the same day, the blood collection unit would be responsible for centrifuging and collecting serum (4-5 ml) and freezing it in the refrigerator at −20°C until it was submitted for examination. PINP and β-CTX were detected by o-cresolphthalein complex ketone method. OC was detected by radioimmunoassay. ALP and PTH were detected by

enzyme-linked immunosorbent assay. Ca^{2+}, P, and Cr were detected by RocheCobas8000 biochemical analyzer.

2.3.5. Quality of Life Assessment. The patients' life quality index were recorded before and six months after the intervention. At the same time, the data generated were evaluated by concise health scale (SF-36) [16]. The total score was 100.

2.3.6. Incidence of Refracture. Statistics were made on the number of new fractures in the two groups at 3 months, 6 months, and 12 months after treatment.

2.4. Statistical Analysis. SPSS23.0 statistical software was adopted to process the data. The measurement data were presented as $(\bar{x} \pm s)$. The group design T-test was adopted for the comparison and the analysis of variance was adopted for the comparison between multiple groups. Dunnett's test was adopted for comparison with the control group. The counting data were presented in the number of cases and the percentage, χ^2 test was adopted for comparison between groups, and bilateral test was employed for all statistical tests.

3. Results

3.1. The Therapeutic Effects among Different Groups. In group A, 36 cases were effective, 23 cases showed effect, and 1 case was ineffective, and the effective rate was 98.33%. The data in group B accordingly was 23, 25, and 12, with the effective rate of 80.0%. The data in group C was 30, 26, and 4, with the effective rate of 93.33%. As a result, the effective rate of group A was significantly higher, and the difference was statistically significant ($P < 0.05$, Figure 1).

3.2. Metabolic Indexes of Calcium and Phosphorus. Before treatment, there were no significant differences in the levels of Ca, P, Scr, and PTH in all study groups ($P > 0.05$). After the treatment of 6 months, figure in the 3 groups all decreased. The levels of Ca, P, Scr, and PTH in group A were lower than other groups, and the difference was statistically significant, as showed in Table 1.

3.3. Bone Mineral Density Contrast. Before treatment, there were no significant differences in the lumbar anteroposterior BMD, left femoral neck, and Ward's triangle BMD in each group with P value over 0.05. After treatment of 6 months, the lumbar spine anteroposterior BMD, left lateral femoral neck, and Ward's triangle BMD were all increased in the three groups, and the difference was statistically significant ($P < 0.05$). All results were shown in Table 2.

3.4. Comparison of Bone Metabolic Indexes. Before treatment, there were no significant differences in the levels of PINP, β-CTX, ALP, and OC among the three groups ($P > 0.05$). After treatment, the levels of PINP and OC in the three groups increased, while the levels of β-CTX and ALP decreased. Compared between groups, the improvement of various bone metabolism indexes in group A was significantly better than that in group B and C, and the difference was statistically significant ($P < 0.05$, Table 3).

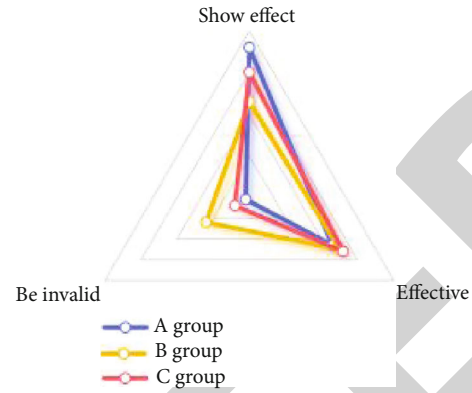

Figure 1: The therapeutic effects among different groups.

3.5. Comparison of Upper Limb Muscle Strength and TUGT. Before treatment, there was no significant difference in upper limb muscle strength and TUGT in different study groups ($P > 0.05$). The muscle strength of the upper limbs of the three groups was enhanced, and the TUGT was shortened after treatment. The improvement effect of the muscle strength of the upper limbs and the lower limbs of the group A was significantly better than that of the group B and C, and the difference was statistically significant($P < 0.05$, Table 4).

3.6. Comparison of Quality-of-Life Scores. No significant difference in quality-of-life scores were observed among the three groups before treatment ($P > 0.05$). There were statistical differences in the scores of physiological function, life function, general health status, physical pain, mental state, emotional function, vitality, and social function among the three groups after 6 months of intervention. In addition, the quality of life score of group A was higher than that of group B and C, and the difference was statistically significant ($P < 0.05$, Tables 5 and 6).

3.7. Comparison of New Bone Fracture Rate. In group A, the number of new fractures after 3, 6, and 12 months was 0, 1, and 3, respectively. In group B, the number of new fractures after 3, 6, and 12 months was 3, 7, and 14, respectively. The number of new fractures in group C was 2, 5, and 9, respectively, after 3, 6, and 12 months of treatment. The incidence of fracture in group A was lower than that in group B and C at each time point, and the difference was statistically significant ($P < 0.05$, Figure 2).

4. Discussion

Osteoporosis (OP) is a common systemic bone disease. OP characterized by decreased bone mass and bone microstructure, Meanwhile, there were increased bone brittleness in the OP patients, which will finally lead to the prone to fracture. The incidence of osteoporosis in the elderly is relatively high. Once a hip fracture occurs, it will directly lead to an increase in disability and mortality in the elderly [17]. According to statistics from the American Osteoporosis Foundation (NOF) in 2018, between 1.5 and 2 million of the 10 million

Table 1: Calcium and phosphorus metabolism indexes in three groups of patients [$\bar{x} \pm s$].

Group	N	Ca (mmol/L)		P (μmol/L)		Scr (mmol/L)		PTH (pg/mL)	
		Before treatment	Treatment for 6 months	Before treatment	Treatment for 6 months	Before treatment	Treatment for 6 months	Before treatment	Treatment for 6 months
A group	60	2.08 ± 0.23	1.73 ± 0.36^{a}	2.73 ± 0.56	1.98 ± 0.14^{a}	94.23 ± 24.67	78.32 ± 13.02^{a}	521.83 ± 57.08	435.08 ± 45.26^{a}
B group	60	1.98 ± 0.31	2.06 ± 0.46	2.57 ± 0.39	2.41 ± 0.18	94.06 ± 25.02	90.29 ± 12.68^{c}	518.32 ± 48.67	488.93 ± 41.47^{c}
C group	60	2.03 ± 0.27	1.87 ± 0.38^{b}	2.61 ± 0.48	2.25 ± 0.17^{b}	93.87 ± 23.28	84.51 ± 15.13^{b}	506.21 ± 53.72	477.92 ± 46.35^{b}
F		2.028	10.169	1.793	105.093	0.003	11.534	1.420	24.624
P		>0.05	<0.05	>0.05	<0.05	>0.05	<0.05	>0.05	<0.05

Note: the comparison of group A, B, and C ($P < 0.05$) before and after treatment.

Table 2: Bone mineral density in three groups [$\bar{x} \pm s$, g/cm^2].

Group	N	Lumbar vertebra orthopedic position(L_1~L_4)		Neck of left lateral femur		Ward's triangle area	
		Before treatment	Treatment for 6 months	Before treatment	Treatment for 6 months	Before treatment	Treatment for 6 months
A group	60	0.71 ± 0.23	0.92 ± 0.12^{a}	0.63 ± 0.14	0.82 ± 0.07^{a}	0.76 ± 0.18	0.89 ± 0.11^{a}
B group	60	0.72 ± 0.21	0.77 ± 0.09	0.61 ± 0.18	0.64 ± 0.05	0.69 ± 0.17	0.71 ± 0.12
C group	60	0.69 ± 0.18	0.87 ± 0.16^{c}	0.59 ± 0.15	0.71 ± 0.08^{c}	0.72 ± 0.21	0.78 ± 0.08
F		0.325	21.830	0.966	107.391	2.106	45.046
P		>0.05	<0.05	>0.05	<0.05	>0.05	<0.05

Note: the comparison of group A, B, and C ($P < 0.05$) before and after treatment.

Table 3: Bone metabolic indexes between the two groups [$\bar{x} \pm s$].

Group	N	PINP (ng/mL)		β-CTX (ng/mL)		ALP (U/L)		OC (ng/mL)	
		Before treatment	Treatment for 6 months	Before treatment	Treatment for 6 months	Before treatment	Treatment for 6 months	Before treatment	Treatment for 6 months
A group	60	43.95 ± 11.63	61.47 ± 12.26^{a}	0.66 ± 0.13	0.43 ± 0.08^{a}	99.41 ± 12.88	71.62 ± 12.08^{a}	5.62 ± 1.03	9.87 ± 1.83^{a}
B group	60	45.02 ± 11.71	48.72 ± 13.04	0.62 ± 0.11	0.59 ± 0.03^{b}	99.21 ± 12.67	86.54 ± 12.51^{b}	5.72 ± 1.13	6.05 ± 1.22
C group	60	44.71 ± 12.08	54.33 ± 11.48^{c}	0.61 ± 0.14	0.52 ± 0.06^{c}	98.56 ± 13.34	76.63 ± 11.71^{c}	5.34 ± 1.18	7.26 ± 1.47^{c}
F		0.130	10.838	16.257	106.239	0.070	23.609	1.872	98.033
P		>0.05	<0.05	>0.05	<0.05	>0.05	<0.05	>0.05	<0.05

Note: the comparison of group A, B, and C ($P < 0.05$) before and after treatment.

Table 4: Upper limb muscle strength and TUGT between the two groups [$\bar{x} \pm s$].

Group	N	Upper body strength (kg)		TUGT (s)	
		Before treatment	Treatment for 6 months	Before treatment	Treatment for 6 months
A group	60	18.32 ± 2.47	27.64 ± 1.13^{a}	10.45 ± 1.46	7.44 ± 1.03^{a}
B group	60	18.11 ± 2.82	20.06 ± 1.15^{b}	10.66 ± 1.42	9.04 ± 1.26^{b}
C group	60	17.74 ± 3.05	22.34 ± 1.14^{c}	10.52 ± 1.29	8.57 ± 1.14^{c}
F		0.665	698.216	0.354	30.836
P		>0.05	<0.05	>0.05	<0.05

Note: the comparison of group A, B, and C($P < 0.05$) before and after treatment.

Americans currently were suffering from osteoporosis develop osteoporotic fractures each year [18]. 1/8 of men over the age of 50 have osteoporotic fractures. Thoracic vertebral compression fracture is a common type of osteoporotic fracture, which can cause a variety of complications, including back pain, chest tightness and hunchback, resulting in limited lung function. Compression fractures of the lumbar spine can cause bloating and abdominal pain, constipation, and loss of appetite. These illnesses make older people in relative financial difficulty more vulnerable to psychological symptoms, such as depression and loss of self-esteem [19, 20].

Table 5: Quality of life scores among the three groups before treatment ($\bar{x} \pm s$, points).

Group	N	Physiological function	Physiological function	Somatic pain	General state of health	Mentality	Social function	Emotional function	Vitality
A group	60	61.12 ± 5.22	62.25 ± 5.36	61.47 ± 5.27	62.23 ± 5.10	61.17 ± 4.49	61.15 ± 4.48	60.88 ± 4.50	60.28 ± 5.77
B group	60	61.38 ± 5.37	62.31 ± 5.44	61.12 ± 5.10	62.98 ± 5.24	61.08 ± 4.42	61.09 ± 4.45	60.22 ± 4.45	61.03 ± 5.63
C group	60	61.00 ± 5.20	62.98 ± 5.60	60.99 ± 5.18	62.04 ± 5.02	61.01 ± 4.39	60.89 ± 4.42	60.34 ± 4.69	60.86 ± 5.60
F		0.082	0.330	0.138	0.565	0.007	0.056	0.359	0.289
P		>0.05	>0.05	>0.05	>0.05	>0.05	>0.05	>0.05	>0.05

Osteoporosis has become a common disease in the middle-aged and elderly population. Its incidence has increased significantly. A more effective prevention and treatment measure is urgently needed to improve the clinical prognosis of such patients. Osteoporotic fractures will bring a heavy burden to society and economy. Clinical data have suggested that patients disabled by osteoporosis-related diseases have longer hospital stays than patients with other chronic diseases, which will lead to a dramatic increase in the medical costs of osteoporosis-related diseases [21]. Epidemiological data showed that in 2017, there were 3.24 million elderly patients with osteoporosis-related fractures in China, including 450,000 hip fractures, 1.31 million vertebral fractures, and 960,000 other osteoporotic fractures [22]. It is estimated that by 2050, there will be 5.99 million patients with osteoporotic fractures in China. According to the meta-analysis of Rizzoli, the overall prevalence of osteoporosis among people over 60 years old in my country is 36% (49% in women and 23% in men) [23].

Bushen Zhuanggu tablet is based on the theory of "kidney governing bone and marrow." It is treated by nourishing the liver and kidneys, tonifying the qi and invigorating the blood, and forming prescriptions (*Eucommia ulmoides*, Herba Epimedii, Radix Scutellariae, Draconis, Radix *Angelicae sinensis*, *Codonopsis pilosula*, Radix Astragali, Dilong, etc.). At present, estrogen, calcium, bone formation enhancers, and bone resorption inhibitors are commonly used to treat PMOP. Although the targeted treatment of these drugs has significant clinical advantages, they pay too much attention to the local and ignore the overall concept, which is easy to cause complications of other systems [24]. The evidence showed that TCM could also effectively improve BMD, relieve bone pain and other symptoms. TCM has the advantages of rich resources, ideal efficacy, and little side effects, which provides a broad market for the treatment of PMOP [25]. The medicine is guided by the basic theory of Chinese medicine and combined with the clinical characteristics of osteoarthritis pain, clinical experience is constantly summarized and improved. In clinical practice, the medicine is mostly used for the back and leg pain caused by osteoporosis and osteoarthritis. However, its exact efficacy in postmenopausal osteoporosis treatment has not been revealed.

Our study demonstrated that in group A, the effective rate was 98.33%; in group B, the effective rate was 80.00%; and in group C,the treatment effective rate was 93.33%. The treatment effective rate of group A was the highest among different study groups. This suggested that no matter Bushen Zhuanggu tablet was used alone or Bushen Zhuanggu tablet was combined with conventional regimen, the clinical effect was more significant than that of conventional regimen. This is closely related to the prescription of Bushen Zhuanggu tablet. *Angelica sinensis* in the prescription can tonify the liver and kidney. Moreover, it can activate blood circulation and remove blood stasis. All kinds of medicines are combined, giving consideration to both exterior and interior, tonifying the kidney and filling essence, promoting blood circulation, promoting arthralgia, and dredging collaterals [26]. Bushen Zhuanggu tablet has a good curative effect in the treatment of PMOP, mainly because it can start from the etiology and pathology, improve the patient's condition, cure both the symptoms and the root causes, and have good short-term and long-term effects.

The results of this study showed that after 6 months of treatment, the levels of Ca, P, Scr, and PTH in the three groups decreased. The levels of Ca, P, Scr, and PTH in group A were lower than those in other groups. After intervention, the lumbar spine anteroposterior BMD, the left lateral femoral neck, and Ward's triangle bone mineral density were all increased in the three groups. Among them, group A was higher than B and C groups. After 6 months' treatment, the levels of PINP and OC in the three groups were increased, while the levels of β-CTX and ALP were decreased. BMD and bone quality indicates the bone strength. Others includes bone turnover, bone mineralization, and microfracture, in which bone turnover is the decisive factor of bone strength and can affect the formation of bone quality. On the other hand, the process of bone turnover is reflected by bone metabolic markers, which indirectly reflects osteoclasts activity. Bone metabolic markers are the products of the decomposition and synthesis of bone tissue itself, referred to as bone markers. BALP and β-CTX is the marker of bone formation and bone resorption, respectively. Bone metabolic markers can dynamically monitor the changes of bone formation and bone resorption after medication, which is helpful to judge the bone turnover rate and evaluate the curative effect [27, 28]. The improvement of various bone metabolism indexes in group A was significantly better than that in group B and C. This indicated that the adjuvant therapy of Bushen Zhuanggu tablet combined with conventional treatment could significantly improve the calcium and phosphorus metabolism and bone metabolism of the patients. The main reason is that the application of Bushen Zhuanggu tablet can improve the bone strength and bone quality of the patients.

Table 6: Quality of life scores among the three groups after treatment ($\bar{x} \pm s$, points).

Group	N	Physiological function	Physiological function	Somatic pain	General state of health	Mentality	Social function	Emotional function	Vitality
A group	60	77.38 ± 5.41^{a}	76.42 ± 6.01^{a}	76.23 ± 6.18^{a}	75.98 ± 4.63^{a}	73.82 ± 5.41^{a}	78.89 ± 4.62^{a}	81.56 ± 3.47^{a}	71.16 ± 5.42^{a}
B group	60	68.46 ± 4.87^{b}	63.41 ± 5.62^{b}	66.71 ± 6.02^{b}	65.32 ± 5.12^{b}	64.45 ± 5.61^{b}	70.03 ± 3.87^{b}	73.23 ± 3.15^{b}	64.28 ± 4.72^{b}
C group	60	72.25 ± 5.02^{c}	71.89 ± 5.37^{c}	72.01 ± 5.07^{c}	71.29 ± 5.07^{c}	70.02 ± 5.16^{c}	75.42 ± 4.26^{c}	78.55 ± 3.37^{c}	67.81 ± 5.24^{c}
F		46.139	81.320	40.902	70.044	45.760	65.868	96.114	26.903
P		<0.05	<0.05	<0.05	<0.05	<0.05	<0.05	<0.05	<0.05

Note: the comparison of group A, B, and C ($P < 0.05$) before and after treatment.

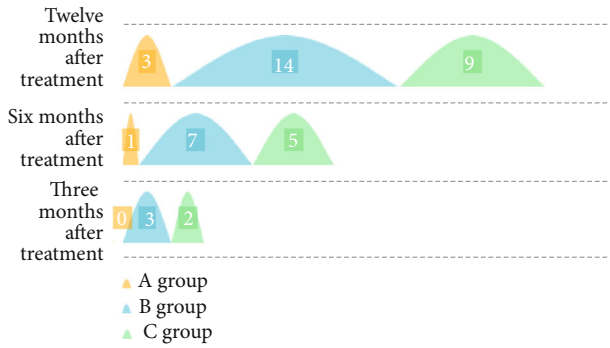

Figure 2: Comparison of new bone fracture rate among different groups.

The improvement effect of muscle strength in group A was significantly better than other groups. This showed that Bushen Zhuanggu tablet combined with routine treatment could significantly promote the limb function in patients with POMP. The main reason is that Bushen Zhuanggu tablet can improve patients' calcium and phosphorus metabolism, bone metabolism, BMD, and other physiological indexes. The improvement of these indexes is closely related to the improvement of muscle strength and the recovery of limb function, which will form a series of positive chain reactions. Modern medical research shows that there is a significant correlation between bone mass loss and muscle weakness [29, 30]. The improvement of muscle strength also contributes to the improvement of bone strength. The maximum load of weight-bearing bones after birth determines most of their strength. These loads come from muscle strength, so muscle strength can greatly affect the strength of our weight-bearing bones. When muscle exerts stress on bone, it will play a positive role in bone growth, remodeling, and maintenance of bone morphology to improve the strength of local bone under stress. Therefore, improving bone strength and increasing muscle strength is the key to reduce the fracture risk due to falls. The results illustrated that, the upper limb muscle strength of the three groups increased and TUGT shortened after 6 months of intervention. In addition, this study also found that there were significant differences in physiological function, life function, general health status, physical pain, mental state, emotional function, vitality, and social function scores among the three groups. The score of quality of life in group A was higher than that in B and C groups. Compared between groups, the incidence of fracture in group A was lower than that in group B and C at each time point. It is suggested that Bushen Zhuanggu tablet combined with conventional therapy can significantly improve the prognosis of patients with POMP and has a good preventive effect on the occurrence of fracture. The improvement in the quality of life of the patients is mainly due to the progressive improvement of their physical functions, their return to a normal life, their gradual integration into society, and a marked improvement in their physical and mental state. The decrease in the incidence of fracture is mainly due to the improvement of physiological indexes such as BMD, bone metabolism, and muscle strength, which can greatly reduce the risk of fracture. This study has some limitations; the sample size of this study is small, it belongs to a single-center study, and there is a certain deviation. There are patients' own factors and other confounding factors that may interfere with the accuracy of this study. In future research, we will carry out multicenter, large sample prospective studies, or we can draw more valuable conclusions.

To sum up, Bushen Zhuanggu tablet combined with conventional scheme is effective in the treatment of postmenopausal osteoporosis, which can significantly improve the BMD of patients, promote the recovery of limb function, and effectively prevent the occurrence of fracture. Bushen Zhuanggu tablet combined with conventional scheme is worthy of clinical promotion.

Data Availability

The datasets used and analyzed during the current study are available from the corresponding author upon reasonable request.

Conflicts of Interest

The authors declare that they have no conflicts of interest.

Acknowledgments

This project is supported by Maoming Science and Technology Planning Project (Project No. 2020KJZX008), Project name: To study the clinical efficacy of Bushen Zhuanggu tablets in the prevention and treatment of osteoporosis based on Bushen Zhuanggu method.

References

[1] R. M. Arceo-Mendoza and P. M. Camacho, "Postmenopausal osteoporosis: latest guidelines," *Endocrinology and Metabolism Clinics of North America*, vol. 50, no. 2, pp. 167–178, 2021.

[2] L. Baihui, T. Xiaoning, C. Jinlin, L. Jing, and C. Yan, "Research progress on the mechanism of kidney-tonifying herbs compound prescription in the treatment of postmenopausal osteoporosis," *Guide to traditional Chinese medicine*, vol. 27, no. 12, pp. 119–122, 2021.

[3] S. Zhang, X. Huang, X. Zhao et al., "Effect of exercise on bone mineral density among patients with osteoporosis and osteopenia: A systematic review and network meta-analysis," *Journal of Clinical Nursing*, vol. 31, no. 15-16, pp. 2100–2111, 2022.

[4] J. A. Kanis, C. Cooper, R. Rizzoli, J. Y. Reginster, and Scientific Advisory Board of the European Society for Clinical and Economic Aspects of Osteoporosis (ESCEO) and the Committees of Scientific Advisors and National Societies of the International Osteoporosis Foundation (IOF), "European guidance for the diagnosis and management of osteoporosis in postmenopausal women," *Osteoporosis International*, vol. 30, no. 1, pp. 3–44, 2019.

[5] Z. Guanping, W. Xiaoming, W. Xuan, W. Jinsheng, and L. Yuan, "Epidemiological investigation and related factors of osteoporosis in 6258 postmenopausal women," *Jiangxi traditional Chinese medicine*, vol. 52, no. 12, pp. 23–25, 2021.

[6] J. He, S. Xu, B. Zhang et al., "Gut microbiota and metabolite alterations associated with reduced bone mineral density or

Hindawi
Computational and Mathematical Methods in Medicine
Volume 2023, Article ID 9837890, 1 page
https://doi.org/10.1155/2023/9837890

Retraction

Retracted: Effect of Dapagliflozin on Clinical Outcome after Drug-Eluting Stent Implantation in Elderly T2DM Patients: A Real-World Study

Computational and Mathematical Methods in Medicine

Received 12 December 2023; Accepted 12 December 2023; Published 13 December 2023

This article has been retracted by Hindawi, as publisher, following an investigation undertaken by the publisher [1]. This investigation has uncovered evidence of systematic manipulation of the publication and peer-review process. We cannot, therefore, vouch for the reliability or integrity of this article.

Please note that this notice is intended solely to alert readers that the peer-review process of this article has been compromised.

Wiley and Hindawi regret that the usual quality checks did not identify these issues before publication and have since put additional measures in place to safeguard research integrity.

We wish to credit our Research Integrity and Research Publishing teams and anonymous and named external researchers and research integrity experts for contributing to this investigation.

The corresponding author, as the representative of all authors, has been given the opportunity to register their agreement or disagreement to this retraction. We have kept a record of any response received.

References

[1] Y. Lin, F. Zhou, X. Wang, Y. Guo, and W. Chen, "Effect of Dapagliflozin on Clinical Outcome after Drug-Eluting Stent Implantation in Elderly T2DM Patients: A Real-World Study," *Computational and Mathematical Methods in Medicine*, vol. 2023, Article ID 8441396, 5 pages, 2023.

Hindawi
Computational and Mathematical Methods in Medicine
Volume 2023, Article ID 8441396, 5 pages
https://doi.org/10.1155/2023/8441396

Research Article

Effect of Dapagliflozin on Clinical Outcome after Drug-Eluting Stent Implantation in Elderly T2DM Patients: A Real-World Study

Yuan Lin,[1] Fang Zhou,[2] Xihu Wang,[2] Yaju Guo,[1] and Weiguo Chen[2]

[1]*Department of Endocrinology, The Second Affiliated Hospital of Xi'an Medical University, Xi'an, 710038 Shaanxi, China*
[2]*Department of Cardiology, The Second Affiliated Hospital of Xi'an Medical University, Xi'an, 710038 Shaanxi, China*

Correspondence should be addressed to Fang Zhou; zhoufang202206@163.com

Received 22 July 2022; Revised 7 September 2022; Accepted 20 September 2022; Published 7 July 2023

Academic Editor: Min Tang

Objective. To investigate the effect of dapagliflozin therapy on the clinical outcome of drug-eluting stent (DES) implantation in elderly patients with type 2 diabetes mellitus (T2DM). *Methods*. We retrospectively studied the real-world data of patients with coronary heart disease who received DES implantation in our hospital from May 2019 to May 2021. Baseline general data and laboratory results of patients were collected. All patients were followed up for two years after PCI, and the follow-up endpoints included in-stent restenosis, major adverse cardiovascular events (MACE), revascularization, rehospitalization, and all-cause mortality. *Results*. Compared with those before treatment, body mass index, systolic blood pressure, diastolic blood pressure, TG, TC, LDL-C, FBG, and HbA1c were decreased in both groups after treatment, while HDL-C was increased after treatment ($P < 0.05$). There were significant differences in BMI, systolic blood pressure, diastolic blood pressure, FBG, and HbA1c between the two groups before and after treatment. At the end of follow-up, the incidence of in-stent restenosis and MACE in the dapagliflozin group was lower than that in the nondapagliflozin group. K-M curve analysis showed a significant difference in in-stent restenosis and MACE after DES implantation between the dapagliflozin group and the nondapagliflozin group (logrank$\chi^2 = 5.093$, 4.524; $P = 0.024$, 0.033). *Conclusion*. In accurate clinical data, dapagliflozin could significantly improve the postoperative BMI, blood pressure, and blood glucose outcome of patients with T2DM complicated with coronary heart disease and positively impact in-stent restenosis and MACE.

1. Introduction

Epidemiological surveys show that the global prevalence of diabetes is as high as 9.3% and is expected to rise to 10.2% by 2030. Diabetes is a significant public health problem that has burdened the global economy and medical resources [1, 2]. The combination of cardiovascular disease or cardiovascular complications is an essential inducement for poor prognosis of diabetic patients. Studies [3, 4] show that the risk of congestive heart failure and concomitant heart failure is significantly increased in diabetic patients, and the incidence of concomitant two-vessel and three-vessel coronary artery lesions is also significantly higher than that of nondiabetic patients. Diabetes mellitus is also a direct factor affecting the short-term and long-term poor prognosis of almost all patients with cardiovascular diseases. The causes may be closely related to cardiac microangiopathy, cardiomyopathy, and cardiovascular autonomic neuropathy associated with diabetes mellitus [5, 6]. Sodium-glucose cotransporter 2 (SGLT2) inhibitors are a new type of oral hypoglycemic drug [7]. As a low-affinity, high-capacity transporter, SGLT2 is widely distributed in the proximal convoluted tubules of the kidney and can transport sodium and glucose molecules by coupling, inhibiting gluconeogenesis and increasing insulin secretion, thereby lowering blood glucose [8, 9]. In recent years, studies [10, 11] have found that SGLT2 inhibitors not only improve blood glucose and reduce blood lipid, body weight, and blood pressure in patients with type 2 diabetes (T2DM) but also have a protective effect on the cardiovascular system. The mechanism may be related to the theory of myocardial energy, volume regulation, sodium-hydrogen exchange, and reducing myocardial fibrosis. For patients with T2DM complicated by cardiovascular disease, the advent of eluting drug stents (DES) has dramatically reduced

the risk of in-stent restenosis, stent thrombosis, and revascularization failure after percutaneous coronary intervention (PCI) in patients with metal stents and has a direct impact on the long-term prognosis of patients [12, 13]. However, there is currently insufficient evidence-based medical evidence on the effect of SGLT2 inhibitors on improving the clinical outcome of DES implantation in T2DM patients. This study conducted a retrospective analysis based on real-world clinical data to discuss and report this issue in depth.

2. Methods

2.1. Research Subjects. T2DM patients complicated with coronary heart disease who received DES implantation from May 2019 to May 2021 in the Department of Cardiology of our hospital were selected as subjects. Inclusion criteria are as follows: (1) meeting the relevant diagnostic criteria for T2DM and coronary heart disease [14, 15]; (2) at least one DES was implanted, and the operation was successful; (3) postoperative review data were complete; and (4) age >60 years old. Exclusion criteria are as follows: (1) patients with abnormal mental states unable to cooperate with the study; (2) complicated with severe liver, kidney, and heart dysfunction; (3) patients with a history of SGLT2 inhibitor use; (4) previous history of stent implantation or balloon dilation; (5) previous history of heart failure and myocardial infarction; and (6) postoperative review was not completed. Patients were divided into the dapagliflozin group ($n = 131$) and the nondapagliflozin group ($n = 106$) according to whether they took dapagliflozin or not. The study design followed the Declaration of Helsinki and was approved by the hospital's medical ethics committee.

2.2. Treatment Methods. All patients were treated with a standardized PCI strategy. Under lidocaine local anesthesia, the puncture sheath was inserted into the radial or femoral artery using the Seldinger method, and 3000 IU heparin and 200 μg nitroglycerin were given. Judkins method was used for body position projection, and the interventional physician judged the responsible blood vessel and the vascular status quo. PCI was performed after patients or their family members signed informed consent, and stent dilation surface and adhesion degree were evaluated. All patients received dual antiplatelet therapy for more than 12 months after PCI.

2.3. Data Collection. All patient data were obtained from our hospital's follow-up database, and patients' baseline clinical data were obtained through electronic medical records and archived paper medical records. After collecting and processing the original data of the patients, all the enrolled patients were coded twice after their personal information was hidden. Two physicians performed relevant data entry and verification, and cardiology and imaging physicians were invited to review the results.

The following data of the patients were collected: (1) baseline general data, including gender, age, body mass index (BMI), hypertension, dyslipidemia, smoking, drinking, systolic blood pressure, diastolic blood pressure, type of coronary heart disease, number of lesions, number of stents implanted, the total length of stents implanted, the minimum diameter of stents, and insulin use; (2) laboratory indicators, including triglyceride (TC), total cholesterol (TG), high-density lipoprotein cholesterol (HDL-C), low-density lipoprotein cholesterol (LDL-C), fasting blood glucose (FBG), glycosylated hemoglobin (HbA1c), and glomerular filtration rate (eGFR); and (3) clinical outcomes, all patients were followed up for two years after PCI. The follow-up endpoints included in-stent restenosis, major adverse cardiovascular events (MACE), revascularization, rehospitalization, and all-cause mortality.

2.4. Statistical Analysis. The collected experimental data were analyzed using SPSS 21.0. The measurement data in the experimental data that conformed to the normal distribution were expressed by $\bar{x} \pm s$, and the Independent Samples t-test was used for comparison. The count data were expressed as the number of cases or rate, and the χ^2 test or Fisher's exact method was used for comparison. Cox proportional hazards model was used to evaluate the effect of dapagliflozin on prognosis during follow-up, and hazard ratio (HR) and 95% confidence interval (95% CI) were calculated. Kaplan-Meier survival curve was used to observe and compare the clinical outcomes between the two groups, and the Log-rank method was used to compare the differences. All statistical tests were conducted by bilateral test, and $P < 0.05$ was considered statistically significant.

3. Results

3.1. Comparison of General Baseline Data between the Two Groups. There were no significant differences in gender, age, hypertension, dyslipidemia, smoking, drinking, type of coronary heart disease, number of lesions, number of stents implanted, the total length of stent implanted, the minimum diameter of the stent, and insulin use between the dapagliflozin group and the nondapagliflozin group ($P > 0.05$), and it was comparable, as shown in Table 1.

3.2. Comparison of Changes in Laboratory Indexes before and after Treatment between the Two Groups. There were no significant differences in BMI, systolic blood pressure, diastolic blood pressure, TG, TC, HDL-C, LDL-C, FBG, and HbA1c between the two groups before treatment ($P > 0.05$). The BMI, systolic blood pressure, diastolic blood pressure, TG, TC, LDL-C, FBG, and HbA1c in the two groups decreased after treatment, while HDL-C increased with statistical significance (with statistical significance $P < 0.05$). The differences in BMI, systolic blood pressure, diastolic blood pressure, FBG, and HbA1c before and after treatment were significantly different between the two groups ($P < 0.05$), while there was no significant difference in the differences in TG, TC, HDL-C, and LDL-C before and after treatment between the two groups ($P > 0.05$), as shown in Table 2.

3.3. Comparison of Postoperative Follow-Up Results between the Two Groups. By the end of follow-up, the incidence of in-stent restenosis and MACE in the dapagliflozin group was lower than that in the nondapagliflozin group, with

Table 1: Comparison of general baseline data between the two groups.

Item	Dapagliflozin group ($n = 131$)	Nondapagliflozin group ($n = 106$)	t/χ^2 value	P value
Gender (male/female)	71/60	60/46	0.137	0.711
Age (years)	67.86 ± 7.15	68.34 ± 7.63	0.499	0.619
Concomitant hypertension (cases)	36	35	0.856	0.355
Concomitant dyslipidemia (cases)	26	20	0.036	0.850
Smoking (cases)	18	15	0.008	0.928
Drinking (cases)	16	11	0.196	0.658
Type of coronary heart disease (unstable angina/acute myocardial infarction/other)	61/33/37	60/30/16	5.900	0.052
Number of lesions (single vessel/multiple vessels)	10/121	10/96	0.246	0.620
Number of stents implanted	3.13 ± 0.86	2.97 ± 0.80	1.469	0.143
The total length of stent implanted (mm)	62.53 ± 10.85	58.34 ± 11.86	1.482	0.140
Minimum diameter of the stent (mm)	2.66 ± 0.43	2.73 ± 0.40	1.285	0.200
Insulin use (cases)	51	48	0.972	0.324

Table 2: Comparison of changes in laboratory indexes before and after treatment between the two groups.

Index	Dapagliflozin group ($n = 131$)			Nondapagliflozin group ($n = 106$)		
	Before treatment	After treatment	Difference	Before treatment	After treatment	Difference
BMI (kg/m^2)	25.34 ± 2.10	23.16 ± 1.56^{ab}	2.18 ± 0.38^{c}	25.66 ± 2.26	24.93 ± 1.90	0.73 ± 0.16
Systolic blood pressure (mmHg)	130.39 ± 22.10	119.30 ± 15.39^{ab}	11.09 ± 3.20^{c}	131.86 ± 21.86	125.63 ± 20.19	6.23 ± 2.10
Diastolic blood pressure (mmHg)	81.13 ± 7.53	69.43 ± 7.83^{ab}	11.70 ± 2.64^{c}	81.30 ± 7.55	75.62 ± 7.60	5.67 ± 2.26
TG (mmol/L)	1.80 ± 0.66	1.61 ± 0.43^{a}	0.19 ± 0.10	1.83 ± 0.61	1.63 ± 0.40	0.20 ± 0.10
TC (mmol/L)	3.20 ± 0.67	2.86 ± 0.60^{a}	0.34 ± 0.18	3.25 ± 0.68	2.86 ± 0.53	0.39 ± 0.20
HDL-C (mmol/L)	0.97 ± 0.20	1.21 ± 0.26^{a}	0.24 ± 0.13	0.95 ± 0.22	1.22 ± 0.20	0.27 ± 0.15
LDL-C (mmol/L)	2.22 ± 0.65	1.93 ± 0.60^{a}	0.29 ± 0.20	2.19 ± 0.60	1.90 ± 0.56	0.29 ± 0.21
FBG (mmol/L)	7.18 ± 1.65	5.61 ± 1.64^{ab}	1.57 ± 0.40^{c}	7.09 ± 1.60	6.25 ± 1.68	0.84 ± 0.31
HbA1c	7.86 ± 1.64	6.53 ± 1.26^{ab}	1.33 ± 0.42^{c}	7.53 ± 1.50	6.88 ± 1.20	0.65 ± 0.39

Note: ^{a}represents $P < 0.05$ when compared between before and after treatment within the group, ^{b}represents $P < 0.05$ when compared between the two groups after treatment, and ^{c}represents $P < 0.05$ when compared the differences before/after treatment between the two groups.

Table 3: Comparison of postoperative follow-up results between the two groups (n/%).

Clinical outcomes	Dapagliflozin group ($n = 131$)	Nondapagliflozin group ($n = 106$)	P value	Adjusted HR (95% CI)
In-stent restenosis	16 (12.21)	28 (26.42)	0.005	0.533 (0.353~0.656)
MACE	6 (4.58)	15 (14.15)	0.010	0.739 (0.531~0.990)
Revascularization	7 (5.34)	7 (6.60)	0.267	0.916 (0.867~1.216)
Rehospitalization	5 (3.82)	6 (5.66)	0.547	0.934 (0.880~1.233)
All-cause death	2 (1.53)	1 (0.97)	1.000	1.034 (0.993~1.315)

statistically significant differences ($P < 0.05$). At the same time, there were no statistically significant differences in revascularization, rehospitalization, and all-cause mortality between the two groups ($P > 0.05$), as shown in Table 3.

3.4. K-M Curve Analysis. The K-M curve analysis results showed a statistically significant difference in in-stent restenosis and MACE after DES implantation in elderly T2DM patients between the dapagliflozin group and nondapagliflozin group (logrank $\chi^2 = 5.093$, 4.524; $P = 0.024$, 0.033), as shown in Figure 1.

4. Discussion

Currently, STLT2 inhibitors listed in China include dapagliflozin, canagliflozin, and empagliflozin, among which dapagliflozin is the most widely used [16, 17]. SGLT2 inhibitors, as a new type of hypoglycemic agent, not only have a good effect on blood glucose control but also have significant benefits on cardiovascular disease, cerebrovascular disease, body weight, blood pressure, blood lipid, kidney function, and other indicators [18, 19]. This study compared the effect of dapagliflozin treatment on the laboratory indicators of

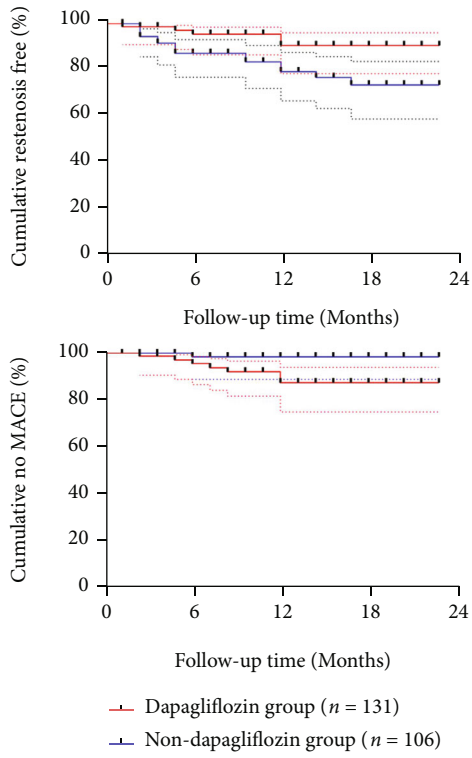

Figure 1: K-M curve analysis of the effect of dapagliflozin on the follow-up outcomes after DES implantation in elderly T2DM patients.

patients. The differences in BMI, systolic blood pressure, diastolic blood pressure, FBG, and HbA1c before and after treatment were significantly different between the two groups ($P < 0.05$), while there was no significant difference in the differences in TG, TC, HDL-C, and LDL-C before and after treatment between the two groups. This result shows that dapagliflozin treatment has obvious clinical benefits in BMI, lowering blood pressure, and controlling blood sugar, but there is no apparent advantage in blood lipids. In previous foreign studies [20, 21], some scholars found that dapagliflozin treatment can reduce systolic blood pressure by 11.9 mmHg, which is close to the results of this study. The production of adipokines is a common mechanism of cardiovascular disease and insulin resistance, and ectopic fat deposition in the perivascular and epicardium significantly affects the paracrine process of myocardial adipokines [22]. SGLT2 inhibitors can affect proinflammatory and anti-inflammatory adipokines, reduce visceral fat, subcutaneous fat, and total fat and positively affect lipid indexes [23]. However, there was no significant difference in the benefit of blood lipid changes between the two groups in this study, and its mechanism needs to be further explored.

In terms of improving clinical outcomes, this study showed that the incidence of in-stent restenosis and MACE in the dapagliflozin group was significantly lower than in the nondapagliflozin group. At the same time, there was no difference in revascularization, rehospitalization, and all-cause mortality between the two groups, and further, K-M curve analysis also showed the same results. In previous studies [24, 25], there are differences in the improvement of clinical outcomes of patients with dapagliflozin. The results of some scholars' research have shown that dapagliflozin can significantly reduce the incidence of all-cause mortality, rehospitalization, and cardiac death. However, this result was not reflected in this study, so the difference in results among different studies may be related to the difference in baseline data, treatment plan, race, and other factors of the enrolled subjects [26, 27]. In diabetic patients with coronary heart disease, cardiac insufficiency can lead to the overloading of the heart. Traditional diuretics can reduce cardiac volume load while aggravating insufficient blood volume circulation, while dapagliflozin can improve interstitial edema without affecting arterial perfusion [28]. In previous in vivo and in vitro studies, dapagliflozin can improve the vascular endothelial function of patients and reduce the endometrial hyperplasia of stents, which may be one of the reasons for the lower incidence of stent restenosis [29, 30].

As a retrospective real-world study, this study showed that dapagliflozin treatment could significantly improve postoperative BMI, blood pressure, and blood glucose outcomes in patients with T2DM complicated with coronary heart disease in real-world clinical data and had a positive effect on in-stent restenosis and MACE. However, this study has certain limitations. For example, this study is a single-center study, and it is difficult to control the main clinical variables of patients, which may cause certain selection biases. This study only evaluated the benefits of BMI, blood pressure, blood glucose, and blood lipids and had less evaluation of other possible benefits. It is necessary to expand the sample size and follow-up time further to improve and supplement the conclusions.

Data Availability

The labeled dataset used to support the findings of this study are available from the corresponding author upon request.

Conflicts of Interest

The authors declare no competing interests.

Acknowledgments

This research was supported by the Key R&D Projects of Science and Technology Department of Shaanxi Province-General Projects (No.2018SF-114 and No. 2019JM-136) and the Hospital Natural Science Project (No.2019KY0106).

References

[1] L. F. Li, L. L. Ding, Z. L. Zhan, and M. Qiu, "Meta-analysis on the safety and cardiorenal efficacy of SGLT2 inhibitors in patients without T2DM," *Frontiers in Cardiovascular Medicine*, vol. 8, article 690529, 2021.

[2] J. I. Malone and B. C. Hansen, "Does obesity cause type 2 diabetes mellitus (T2DM)? Or is it the opposite?," *Pediatric Diabetes*, vol. 20, no. 1, pp. 5–9, 2019.

[3] A. Hoseini, G. Namazi, A. Farrokhian et al., "The effects of resveratrol on metabolic status in patients with type 2 diabetes

Hindawi
Computational and Mathematical Methods in Medicine
Volume 2023, Article ID 9868969, 1 page
https://doi.org/10.1155/2023/9868969

Retraction

Retracted: Perioperative Effect of Single-Port Thoracoscopic Segmentectomy and Three-Port Thoracoscopic Segmentectomy in the Treatment of Early Non-Small-Cell Lung Cancer

Computational and Mathematical Methods in Medicine

Received 12 December 2023; Accepted 12 December 2023; Published 13 December 2023

This article has been retracted by Hindawi, as publisher, following an investigation undertaken by the publisher [1]. This investigation has uncovered evidence of systematic manipulation of the publication and peer-review process. We cannot, therefore, vouch for the reliability or integrity of this article.

Please note that this notice is intended solely to alert readers that the peer-review process of this article has been compromised.

Wiley and Hindawi regret that the usual quality checks did not identify these issues before publication and have since put additional measures in place to safeguard research integrity.

We wish to credit our Research Integrity and Research Publishing teams and anonymous and named external researchers and research integrity experts for contributing to this investigation.

The corresponding author, as the representative of all authors, has been given the opportunity to register their agreement or disagreement to this retraction. We have kept a record of any response received.

References

[1] C. Zhang, D. Jiang, C. Luo, D. Yuan, and G. Shang, "Perioperative Effect of Single-Port Thoracoscopic Segmentectomy and Three-Port Thoracoscopic Segmentectomy in the Treatment of Early Non-Small-Cell Lung Cancer," *Computational and Mathematical Methods in Medicine*, vol. 2023, Article ID 7550317, 6 pages, 2023.

Hindawi
Computational and Mathematical Methods in Medicine
Volume 2023, Article ID 7550317, 6 pages
https://doi.org/10.1155/2023/7550317

Research Article

Perioperative Effect of Single-Port Thoracoscopic Segmentectomy and Three-Port Thoracoscopic Segmentectomy in the Treatment of Early Non-Small-Cell Lung Cancer

Cong Zhang,[1] Dexiong Jiang,[1] Cuilian Luo,[2] Dongdong Yuan,[1] and Guansheng Shang[1]

[1]*Department of Thoracic Surgery, Chengdu Seventh People's Hospital, Chengdu, 610200 Sichuan, China*
[2]*Department of Oncology, Chengdu Seventh People's Hospital, Chengdu, 610200 Sichuan, China*

Correspondence should be addressed to Guansheng Shang; sgs0804@163.com

Received 26 July 2022; Revised 19 September 2022; Accepted 27 September 2022; Published 23 February 2023

Academic Editor: Min Tang

Background. Clinically, there were few reports on single-hole thoracoscopic segmental resection in non-small-cell lung cancer (NSCLC), and no report on the comparison of single-hole and three-hole thoracoscopic segmental resection. Hence, the purpose of the study was to explore the perioperative role of single-port thoracoscopic segmentectomy and three-port thoracoscopic segmentectomy for early-stage NSCLC. *Methods*. The clinical data of 80 patients with early-stage NSCLC who were treated in our hospital from January 2021 to June 2022 were selected as the retrospective research subjects and divided into a comparison/research group with 40 cases in each group according to different surgical methods. Among them, the comparison group was received three-port thoracoscopic segmentectomy, and the research group was received single-port thoracoscopic segmentectomy. The surgical indicators, immune and tumor marker levels, as well as prognostic complications between two groups were compared. *Results*. There was no remarkable diversity between the two groups in terms of operation time and the number of lymph nodes dissected during the operation ($P > 0.05$). The surgical blood loss in research group was lower than comparison group ($P < 0.05$). After treatment, the levels of CYFRA21-1, CA125, as well as VGEF in the research group were markedly lower than comparison group ($P < 0.05$). The differences in CD^{4+}, CD^{3+}, and CD^{4+}/CD^{8+} after treatment were prominent, and the research group was higher than comparison group ($P < 0.05$). There was no statistical difference in postoperative complications between the two groups ($P > 0.05$). *Conclusions*. Single-hole thoracoscopic lobectomy has obvious advantages in the treatment of NSCLC, which can reduce intraoperative bleeding, enhance the recovery of patients' immune function, and promote postoperative recovery.

1. Introduction

Non-small-cell lung cancer (NSCLC) is a relatively common clinical malignant tumor of the respiratory system. The incidence rate accounts for about 80% of all lung cancer patients. The mortality rate of patients after diagnosis is high, and it increases year by year with the passage of time [1]. Surgery, as a common method for the treatment of NSCLC, has gradually transitioned from traditional thoracoscopic lobectomy to segmentectomy after years of technological development [2]. At present, three-port thoracoscopy was commonly used in clinical treatment of patients with NSCLC, but there were still shortcomings such as obvious postoperative pain and thoracic movement disorders [3]. In recent years, single-port thoracoscopic segmentectomy, which was characterized by smaller chest wall incisions and more preservation of lung tissue, had been selectively applied in the surgical treatment of patients with NSCLC, especially for peripheral stage I lung cancer. It has been proved that its short-term clinical efficacy was basically the same as that of the three-hole method [3]. However, there were few reports on the single-hole method at present and comparative studies between single hole and three hole.

In the field of segmentectomy for early-stage NSCLC, the more traditional surgical method is the three-port method, including the observation port, the main operating port,

and the auxiliary operating port [4, 5]. Although this traditional surgical method had become more and more mature, but massive scholars have found that there were some defects in three-port thoracoscopic surgery, such as numbness or dyskinesia at the distal end of the chest wall, and pain in the auxiliary operating port of the back [6, 7]. So, the single-port thoracoscopic technique came into being, and it was also a major breakthrough in the minimally invasive technique of thoracic surgery in recent years [8]. Single-port thoracoscopic surgery usually chose the fourth or fifth intercostal space between the anterior axillary line and the midaxillary line as the only surgical incision, which was more suitable for the operation angle during the operation. The characteristic of single-port thoracoscope was that various surgical instruments and endoscopic lenses needed to be placed in the same incision, and the operating angle of view was closer to that of open surgery under direct vision, so the relative visual error was small [9].

Hence, the study aimed to seek the perioperative role of single-port thoracoscopic segmentectomy and three-port thoracoscopic segmentectomy for early-stage NSCLC, supplying a fresh direction for clinical treatment of NSCLC.

2. Material and Methods

2.1. Research Object. The clinical data of 80 patients with early-stage NSCLC who were treated in our hospital from January 2021 to June 2022 were selected as the retrospective research subjects and divided into a comparison/research group with 40 cases in each group according to different surgical methods. Diagnostic criteria were referred to Chinese Medical Association Lung Cancer Clinical Diagnosis and Treatment Guidelines [10].

2.2. Inclusion and Exclusion Criteria. Inclusion criteria are as follows: (1) chest high resolution CT (HRCT) showed that the tumor diameter was 2 cm or less, the solid component was less than 50%, and the intraoperative rapid freezing and postoperative pathological diagnosis were NSCLC; (2) cranio-thoracic T, radioactive radionuclide whole-body bone scintigraphy, abdominal color Doppler ultrasound, and other related examinations confirm that the tumor had no distant metastasis; (3) the tumors were all single lesions, and the resection margins of lung tissue were more than 2 cm away from the lesion edge; (4) The general condition of the patient was good, and the patient could tolerate segmentectomy under general anesthesia.

Exclusion criteria are as follows: (1) history of thoracic trauma, or a history of preoperative radiotherapy and chemotherapy; (2) combined with other malignant tumors; (3) central lung cancer or peripheral lung cancer with multiple lesions; (4) patients with underlying diseases such as severe diabetes and hypertension.

2.3. Surgical Methods. After admission, the patients in the two groups were inquired about the medical history in detail, carried out a general physical examination, assessed the patient's condition and general physical condition, and improved the relevant preoperative examinations. Preoperative related examinations included blood routine, liver and kidney function, blood type identification, blood coagulation routine, and electrolyte routine as well as routine before blood transfusion. Auxiliary examinations included head CT, chest CT, abdominal ultrasound, cardiac ultrasound, pulmonary function, electrocardiogram, and radionuclide system bone imaging. After the contraindications for surgery were excluded, the surgical treatment was performed. The patients' family members were interviewed before surgery, and the patients' cases were randomly divided into the comparison/research group according to the surgery method. The two groups of patients were operated by the same medical team, and they were placed in a 90-degree lying position on the unaffected side, with a pillow under the armpit to increase the width of the intercostal space. The anesthesia method was general anesthesia with double-lumen tracheal intubation. During the operation, the affected lung was kept collapsed, and the contralateral lung was ventilated with one lung. Among them, the research group usually chose the fourth or fifth intercostal space of the anterior axillary line, which was determined according to the interlobar fissure, the hilum of the lung, and the location of the lesion. In comparison group, an incision of about 1.5 cm in length was made at the 7th or 8th intercostal space of the midaxillary line, and the trocar was placed as the observation hole, and the 3rd or 4th intercostal space between the anterior axillary line and the midaxillary line was selected as the main operation hole. The size of the incision was 3-4 cm, a soft incision protective sleeve was placed in the incision, and an incision of about 1.5 cm in length between the 7th or 8th intercostal space of the posterior axillary line was selected as the auxiliary operation hole. Both groups underwent segmentectomy and hilar and mediastinal lymph node dissection.

2.4. Outcome Measures

(1) Perioperative indexes of the two groups (observation of intraoperative blood loss, operation time, and number of lymph node dissection). (2) Determination of tumor markers: after treatment, 5 ml of fasting elbow vein blood was drawn from the patient, the supernatant was centrifuged, and CYFRA21-1, CA125, as well as VGEF levels were measured by radioimmunoassay. (3) Immune function: after centrifugation of the above patients' serum, CD^{4+}, CD^{3+}, and CD^{4+}/CD^{8+} were measured via flow cytometry (American BD company, FACS Vantage type). (4) Adverse reaction determination: record the occurrence of complications of the two groups of patients during treatment

2.5. Statistical Analysis. All data were discussed using SPSS 28.0 The measurement data were expressed via $x \pm s$, and the intergroup data were tested by independent t test; χ^2 test was adopted for counting data. $P < 0.05$, significant difference.

Table 1: Comparison of general data between the two groups [n, ($\bar{x} \pm s$)].

Group	Gender (men/women)	Average age (age)	Tumor diameter (cm)	Pathological type	
				Adenocarcinoma	Squamous cell carcinoma
Comparison group (40)	28/12	56.87 ± 6.39	1.88 ± 0.23	33	7
Research group (40)	29/11	56.69 ± 6.23	1.89 ± 0.28	32	8
χ^2 / t	0.061	0.023	0.074	0.065	0.346
P	0.805	0.731	0.941	0.799	0.556

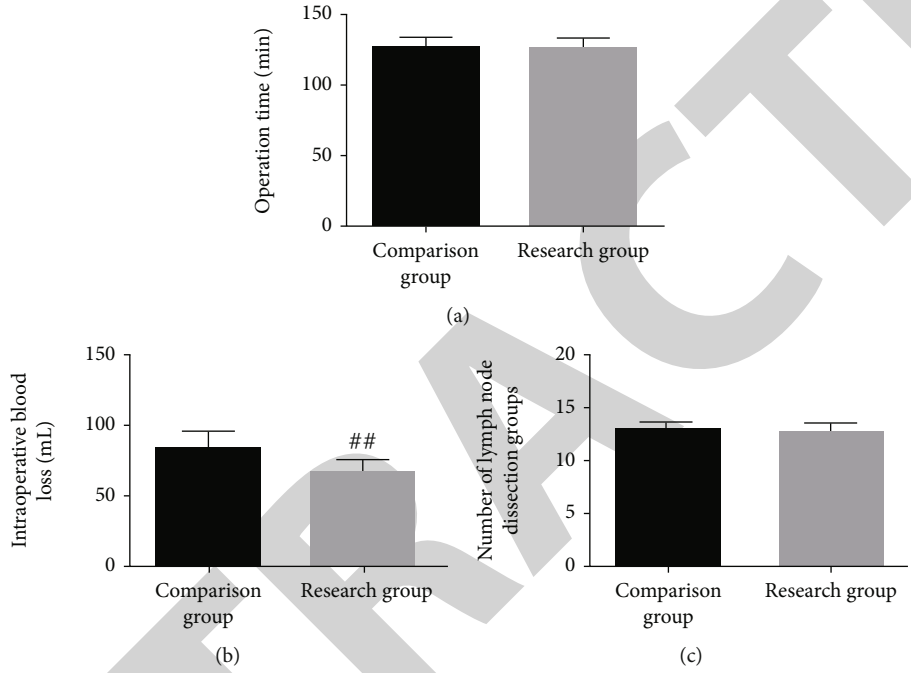

Figure 1: Comparison of operation time, intraoperative blood loss, and number of lymph node dissection groups. (a) Operation time; (b) Intraoperative blood loss. (c) Number of lymph node dissection groups. $^{\#\#}P < 0.01$ vs. comparison group.

3. Results

3.1. General Data Comparison. The gender, average age, tumor diameter, pathological type, and other general data of the two groups of patients were compared by t test and chi-squared test, and there was no significant difference ($P > 0.05$). See Table 1.

3.2. Perioperative Improvement. There was no statistical difference between the two groups in terms of operative time and the number of lymph node dissection groups ($P > 0.05$). Patients in research group had lower surgical bleeding than comparison group, and this difference was statistically significant ($P < 0.05$). See Figure 1.

3.3. Comparison of Tumor Marker Levels. There was no significant difference in the levels of tumor markers between the two groups before treatment. After treatment, the levels of CYFRA21-1, CA125, and VGEF in the research group were significantly lower than comparison group, and the difference was significant ($P < 0.05$). See Figure 2.

3.4. Immune Level Comparison. There was no significant diversity in the immune level between the two groups before treatment ($P > 0.05$), while the differences in CD^{4+}, CD^{3+}, and CD^{4+}/CD^{8+} after treatment were significant, and the research group was higher than comparison group ($P < 0.05$). See Figure 3.

3.5. Prognostic Complications. There was 1 case of postoperative pleural effusion and 1 case of postoperative air leakage in the study group, and 1 case of postoperative pulmonary infection in the control group. There was no statistical diversity in postoperative complications between the two groups ($P > 0.05$).

4. Discussion

NSCLC has become one of the most serious malignant tumors threatening human health in China. In addition, the physiological function of most patients declines, and the organs and tissues of various systems are aging, so the requirements for surgery are higher [11, 12]. The surgical treatment principle of NSCLC was to completely remove

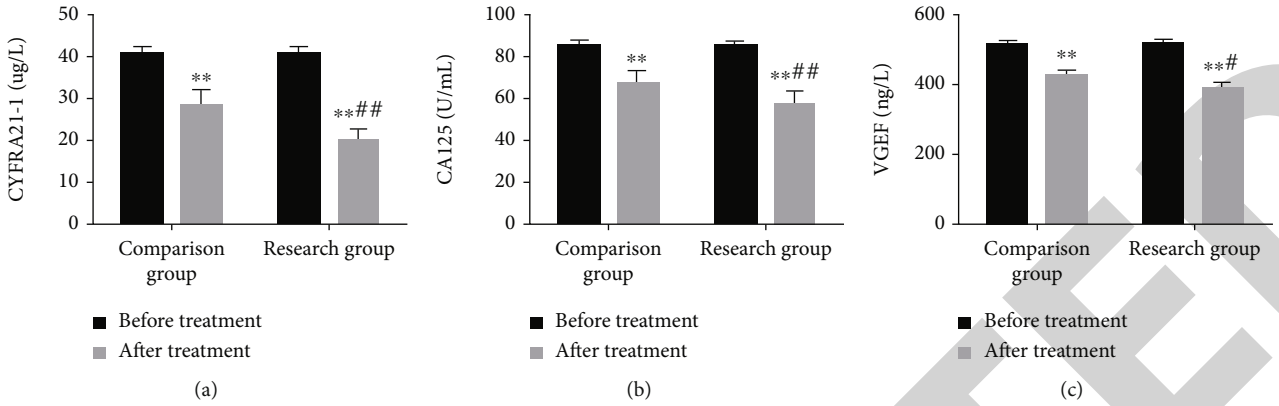

Figure 2: Comparison of tumor marker levels between two groups of patients. (a) CYFRA21-1; (b) CA125; (c) VGEF. $^{**}P < 0.01$ vs. before treatment, $^{\#/\#\#}P < 0.05/0.01$ vs. after comparison group.

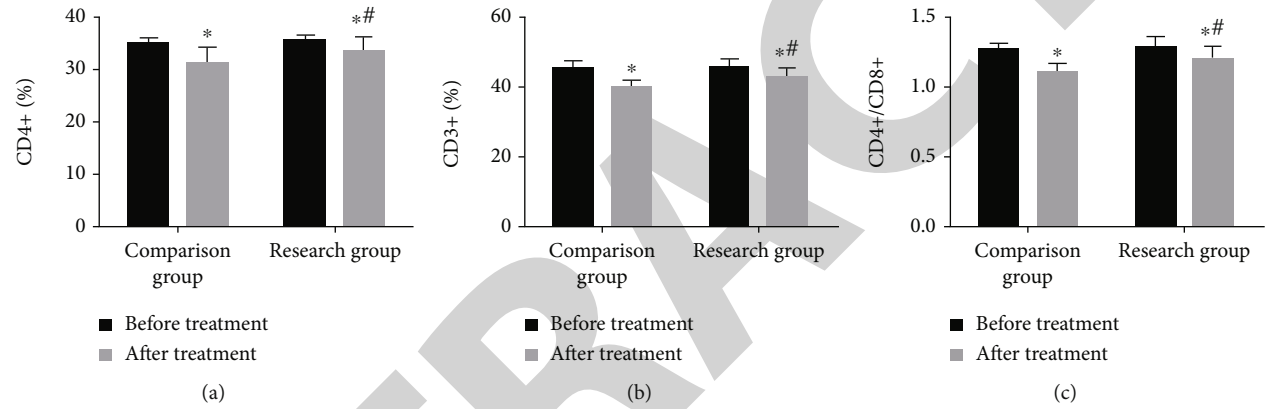

Figure 3: Comparison of immune levels. (a) CD^{4+}; (b) CD^{3+}; (c) CD^{4+}/CD^{8+}. $^{*}P < 0.05$ vs. before treatment, $^{\#}P < 0.05$ vs. after comparison group.

the tumor as far as possible and retain the healthy lung tissue as far as possible and perform corresponding lobectomy and systematic hilar and mediastinal lymph node dissection. Studies have found that for early-stage lung cancer with a diameter of less than 2 cm, segmentectomy had a similar long-term effect as lobectomy and preserves the patient's lung function to the greatest extent, while reducing related complications after lung resection [13]. Clinically, three-hole thoracoscopic lobectomy could remove the focus and gave play to the therapeutic effect [14]. In recent years, the technology of single-port thoracoscopic lobectomy had gradually matured, and many explorations have also confirmed the feasibility of single-port thoracoscopic segmentectomy [15]. In terms of operation time, postoperative extubation time, and complication rate, single-port thoracoscopic surgery is safe and reliable [16]. In addition, due to the incision was in an intercostal space, postoperative pain, chest wall paresthesia, and other discomforts were significantly reduced compared with traditional surgery [17]. On the premise that minimally invasive surgery was safe and feasible, the minimally invasive advantages of single-port thoracoscopy were more prominent, and the related lung function was protected [18]. The clinical application advantage of single-hole thoracoscopic lobectomy had become the focus of minimally invasive thoracic surgery [19].

The results of this study indicated that there was no remarkable diversity between the two groups in terms of operation time and the number of lymph nodes dissected during the operation. The surgical blood loss in research group was lower than in comparison group. The results indicated that single-hole thoracoscopic lobectomy had certain advantages in terms of surgical blood loss, which implied that single-hole thoracoscopic lobectomy, on the one hand, could select an operation hole between fourth, or fifth ribs according to the upper, middle, and lower lobe lesions, which could effectively reduce the number of incisions, reduce body trauma, reduce drainage flow, and shorten drainage time. On the other hand, when thoracoscopic accesses to the body, it was not easy to damage blood vessels, which could reduce bleeding [20].

Clinical imaging indicators are commonly used to evaluate the prognosis of patients, but imaging examination will be affected by the surrounding tissue, boundary, and volume of the lesion, and the requirements for imaging physicians and equipment are relatively high [21]. In addition, even if there is no progress in imaging results, the level of tumor

markers may continue to rise [22]. Tumor markers usually exist in the blood, and their levels in host cells will also show certain changes. Because of the advantages of fast and simple detection, it has a good indication for the patient's condition development and efficacy evaluation [23]. VEGF is affirmed to participate in NSCLC angiogenesis and metastasis [24]. CYFRA21-1 is a soluble fragment of cytokeratin, which could be released into the blood, which has a high diagnostic value for patients with NSCLC [25]. Its detection level can be used to reflect the short-term efficacy of tumor treatment [26]. The results of this study exhibited that the improvement of the above tumor markers in the patients in the research group was less than comparison group, suggesting that the single-port thoracoscopic segmentectomy might reduce the generation of tumor markers and improve the prognosis of NSCLC.

T lymphocytes have the function of immune regulation and can produce a better stable effect on the immune internal environment of the body [27]. Among them, CD^{8+} can effectively reflect inhibitory T cells, CD^{3+} is a marker of mature T cells, and CD^{4+} can represent helper T cells. Compared with normal people, the level of T cell differentiation antigens such as CD^{3+}, CD^{4+}, and CD^{4+}/CD^{8+} in cancer population is significantly lower [28]. Thus, the above indicators could effectively evaluate the level of autoimmunity [29]. The results of this study exhibited that the improvement of CD^{3+}, CD^{4+}, and CD^{4+}/CD^{8+} in the research group after treatment was better than comparison group. This might be because single-port thoracoscopic segmentectomy could activate the immune response of the body, promote cell apoptosis, and to some extent, promote the killing function of new lymphocytes, so it could enhance the body immunity and improve the prognosis [30]. Furthermore, the outcomes discovered that the incidence of postoperative complications in research and comparison group was roughly similar, and there was no prominent diversity, indicating that single-port thoracoscopic segmentectomy possessed high safety and excellent clinical effect in the early treatment of NSCLC. In addition, this study should further explore the lung function, overall survival rate, and progression free survival rate of NSCLC patients via a single-port thoracoscopic segmentectomy to estimate the prognosis.

To sum up, single-hole thoracoscopic segmental resection could decrease intraoperative bleeding, reduce the level of serum tumor markers, and ameliorate immune function. Its clinical effect was superior to three-hole thoracoscopic segmental resection, which possessed certain clinical application value.

Data Availability

No data were used to support this study.

Conflicts of Interest

The authors declare that they have no conflicts of interest.

Authors' Contributions

These authors (Cong Zhang, Dexiong Jiang, and Cuilian Luo) contribute to this work equally.

References

[1] Y. Gao, A. Abulimiti, D. He, A. Ran, and D. Luo, "Comparison of single- and triple-port VATS for lung cancer: a meta-analysis," *Open Medicine*, vol. 16, no. 1, pp. 1228–1239, 2021.

[2] C. G. Hu, K. Zheng, G. H. Liu et al., "Effectiveness and postoperative pain level of single-port versus two-port thoracoscopic lobectomy for lung cancer: a retrospective cohort study," *General Thoracic and Cardiovascular Surgery*, vol. 69, no. 2, pp. 318–325, 2021.

[3] C. Y. Wu, Y. Y. Chen, C. C. Chang et al., "Single-port thoracoscopic anatomic resection for chronic inflammatory lung disease," *BMC Surgery*, vol. 21, no. 1, p. 244, 2021.

[4] Y. Wang, Z. Wang, and F. Yao, "The safety and feasibility of three-dimension single-port video-assisted thoracoscopic surgery for the treatment of early-stage lung cancer," *Journal of Thoracic Disease*, vol. 12, no. 12, pp. 7257–7265, 2020.

[5] K. Hirai, S. Takeuchi, and J. Usuda, "Single-port video-assisted thoracic surgery for early lung cancer: initial experience in Japan," *Journal of Thoracic Disease*, vol. 8, Supplement 3, pp. S344–S350, 2016.

[6] Y. Yao, Q. Hua, S. Liu, Z. Yang, H. Shen, and W. Gao, "Efficacy of multi-groove silicone drains in single-port video-assisted thoracoscopic lung cancer surgery and their effect on C-reactive protein: a single-center experience," *Journal of Thoracic Disease*, vol. 13, no. 12, pp. 6885–6896, 2021.

[7] P. K. Hsu, W. C. Lin, Y. C. Chang et al., "Multiinstitutional analysis of single-port video-assisted thoracoscopic anatomical resection for primary lung cancer," *The Annals of Thoracic Surgery*, vol. 99, no. 5, pp. 1739–1744, 2015.

[8] W. Yang, G. Zhang, S. Pan et al., "Comparison of the perioperative efficacy between single-port and two-port video-assisted thoracoscopic surgery anatomical lung resection for non-small cell lung cancer: a systematic review and meta-analysis," *Journal of Thoracic Disease*, vol. 11, no. 7, pp. 2763–2773, 2019.

[9] C. Li, M. Xu, G. Xu, R. Xiong, H. Wu, and M. Xie, "A comparative study of acute and chronic pain between single port and triple port video-assisted thoracic surgery for lung cancer," *Zhongguo Fei Ai Za Zhi*, vol. 21, no. 4, pp. 279–284, 2018.

[10] Y. Shen, H. Wang, M. Feng, Y. Xi, L. Tan, and Q. Wang, "Single- versus multiple-port thoracoscopic lobectomy for lung cancer: a propensity-matched study," *European Journal of Cardio-Thoracic Surgery*, vol. 49, Supplement 1, pp. i48–i53, 2016.

[11] Z. Liu, R. Yang, and F. Shao, "Comparison of postoperative pain and recovery between single-port and two-port thoracoscopic lobectomy for lung cancer," *The Thoracic and Cardiovascular Surgeon*, vol. 67, no. 2, pp. 142–146, 2019.

[12] J. M. Borro, F. Regueiro, S. Pértega, M. Constenla, and S. Pita, "Comparative study of survival following videothoracoscopic lobectomy procedures for lung cancer: single- versus multiple-port approaches," *Archivos de Bronconeumología*, vol. 53, no. 4, pp. 199–205, 2017.

[13] C. S. Ng, H. K. Kim, R. H. Wong, A. P. Yim, T. S. Mok, and Y. H. Choi, "Single-port video-assisted thoracoscopic major lung resections: experience with 150 consecutive cases," *The*

Hindawi
Computational and Mathematical Methods in Medicine
Volume 2023, Article ID 9865637, 1 page
https://doi.org/10.1155/2023/9865637

Retraction

Retracted: A Systematic Review and Meta-Analysis of Influences of Chronic Kidney Disease on Patients after Percutaneous Coronary Intervention for Chronic Total Occlusions

Computational and Mathematical Methods in Medicine

Received 12 December 2023; Accepted 12 December 2023; Published 13 December 2023

This article has been retracted by Hindawi, as publisher, following an investigation undertaken by the publisher [1]. This investigation has uncovered evidence of systematic manipulation of the publication and peer-review process. We cannot, therefore, vouch for the reliability or integrity of this article.

Please note that this notice is intended solely to alert readers that the peer-review process of this article has been compromised.

Wiley and Hindawi regret that the usual quality checks did not identify these issues before publication and have since put additional measures in place to safeguard research integrity.

We wish to credit our Research Integrity and Research Publishing teams and anonymous and named external researchers and research integrity experts for contributing to this investigation.

The corresponding author, as the representative of all authors, has been given the opportunity to register their agreement or disagreement to this retraction. We have kept a record of any response received.

References

[1] W. Wu, M. Gao, and X. Wu, "A Systematic Review and Meta-Analysis of Influences of Chronic Kidney Disease on Patients after Percutaneous Coronary Intervention for Chronic Total Occlusions," *Computational and Mathematical Methods in Medicine*, vol. 2023, Article ID 9450752, 10 pages, 2023.

Hindawi
Computational and Mathematical Methods in Medicine
Volume 2023, Article ID 9450752, 10 pages
https://doi.org/10.1155/2023/9450752

Review Article

A Systematic Review and Meta-Analysis of Influences of Chronic Kidney Disease on Patients after Percutaneous Coronary Intervention for Chronic Total Occlusions

Weifei Wu, Menghan Gao, and Xu Wu

Department of Nephrology, Huzhou Central Hospital, Affiliated Central Hospital Huzhou University, No. 1558, Sanhuan North Road, Wuxing District, Huzhou, Zhejiang 313000, China

Correspondence should be addressed to Weifei Wu; 13738244255@163.com

Received 11 August 2022; Revised 28 September 2022; Accepted 6 October 2022; Published 22 February 2023

Academic Editor: Min Tang

Objective. Chronic kidney disease (CKD) is a clinical collective term for kidney disease with glomerular filtration rate (GFR) < 60 mL/min for more than three months due to various factors and is usually associated with coronary heart disease and is also an independent risk factor for coronary heart disease. This study is aimed at systematically reviewing the influence of CKD on the outcomes of patients after percutaneous coronary intervention (PCI) for chronic total occlusions (CTOs). *Methods.* The Cochrane Library, PubMed, Embase, China biomedical literature database (SinoMed), China National Knowledge Infrastructure, and Wanfang database were searched for case-control studies on the influence of CKD on outcomes after PCI for CTOs. After screening the literature, extracting data, and evaluating the quality of literature, RevMan 5.3 software was used for meta-analysis. *Results.* There were 11 articles with a total of 558,440 patients included. Meta-analysis results indicated that left ventricular ejection fraction (LVEF) level, diabetes, smoking, hypertension, coronary artery bypass grafting, angiotensin converting enzyme inhibitor (ACEI)/angiotensin receptor blocker (ARB), β-blockers, age, and renal insufficiency were the factors affecting outcomes after PCI for CTOs [risk ratio and 95% confidence interval were: 0.88 (0.86, 0.90), 0.96 (0.95, 0.96), 0.76 (0.59, 0.98), 1.39 (0.89, 2.16), 0.73 (0.38, 1.40), 0.24 (0.02, 3.9), 0.78 (0.77, 0.79), 0.81 (0.80, 0.82), and 1.50 (0.47, 4.79)]. *Conclusion.* LVEF level, diabetes, smoking, hypertension, coronary artery bypass grafting, ACEI/ARB, β-blockers, age, renal insufficiency, etc. are important risk factors for outcomes after PCI for CTOs. Controlling these risk factors is of great significance for the prevention, treatment, and prognosis of CKD.

1. Introduction

Chronic kidney disease (CKD), a clinical collective term for kidney disease with glomerular filtration rate (GFR) < 60 mL/min for more than three months due to various factors, is usually associated with coronary heart disease and is also an independent risk factor for coronary heart disease [1]. Chronic kidney disease (CKD) is recognized as an irreversible reduction of functional nephrons and leads to an increased risk of various pathological conditions; additionally, CKD patients have impaired immunity against bacteria and viruses [2]. It has been revealed that GFR decline is an independent predictive factor for coronary artery lesions and adverse cardiovascular events [3]. CKD has become a chronic disease that seriously threatens human health, bringing a huge economic burden to the country, society, and family.

Percutaneous coronary intervention (PCI) has been recognized by the medical community at home and abroad as an effective method for the treatment of coronary heart diseases [4]. PCI relieves symptoms of chronic ischemic heart disease patients resistant to optimal medical therapy and alters natural history of acute coronary syndromes [5]. According to the data reported by the National Health and Family Planning Commission online, an average of 426.82 patients per million population in China underwent PCI treatment, and the average number of implanted stents remained at about 1.5 [6]. In an existing system, a virtual

reality- (VR-) based surgery simulation system is presented for personalized PCI; in addition, the simulation system can directly take patient-specific clinical data as input and generate virtual 3D intervention scenarios [7]. However, PCI angina also negatively impacts 20-40% of patients and imposes a high burden on the healthcare system [8].

Chronic total occlusion (CTO) refers to lesions in which the coronary arteries are completely occluded, and the occlusion time exceeds 3 months. It is a common type of coronary heart disease, accounting for approximately half of the total number of coronary heart diseases. With the rapid development of PCI, more and more CTO patients have received PCI and achieved perfect recanalization. However, a study has revealed that CTO patients are usually older and are often complicated with diabetes mellitus, multivessel disease, lower left ventricular ejection fraction, and poor basal renal function [9]. At present, the meta-analysis of the influence of CKD on outcomes after PCI for CTOs is still rare in China, and the research cases are relatively scattered and lack quantitative statistics. To the best of our knowledge, seldom systematic review has attempted to analyze evidence on the subject in question, and no meta-analysis has been conducted in the literature to present pooled evidence on the outcomes after PCI for CTOs in the elderly [10]. Therefore, this study systematically evaluated the influencing factors affecting outcomes after PCI for CTOs, in order to provide an evidence-based insight for clinical early nursing intervention.

2. Materials and Methods

2.1. Literature Inclusion Criteria. Literatures involving patients diagnosed with coronary heart disease and accompanied by CKD were included. The influence of CKD risk factors on outcomes after PCI for CTOs served as exposure factors. Case-control studies in Chinese and English from 2010 to 2020 were included for meta-analysis. Exclusion criteria were listed as follows: (1) duplicates, (2) reviews, (3) full text is unavailable, and (4) inconsistency with the theme. Literatures adjudged to be eligible were identified using the preferred reporting items for systematic reviews and meta-analysis algorithm.

2.2. Literature Retrieval Strategy. The Cochrane Library, PubMed, Embase, China biomedical literature database (SinoMed), China National Knowledge Infrastructure (CNKI), and Wanfang database were searched online. The English search terms were "chronic kidney disease", "percutaneous coronary intervention", "chronic total occlusion", "CKD", "PCI", and "CTO". The related original documents were retrieved in each database by connecting the search terms with Boolean logic operators, and the related documents needed for this study were determined by analyzing the titles, abstracts, keywords, subject headings, and references of the documents.

2.3. Literature Screening and Data Extraction. According to the inclusion and exclusion criteria established by the meta-analysis, two researchers read through the abstracts of the selected literature to exclude literatures that did not meet the research conditions, and then the two researchers jointly extracted the research data and other relevant information, which were checked by another three independent researchers. If there was a disagreement, it would be resolved through a three-party consultation, and the opinions of the tutor and the tutor group would be listened.

2.4. Evaluation of Literature Quality. The Newcastle-Ottawa scale [11] was used to assess the quality of literatures, including comparability and outcomes. The full score of the scale was 9 points, of which comparability was counted as 2 points, and the remaining items were 1 point. Evaluation results >6 points were regarded as high-quality studies.

2.5. Statistical Analysis. Meta-analysis of the collected data was performed using RevMan 5.3 software. The final-effects indicators were measured by mean ± standard deviation (mean ± SD). The heterogeneity of the included papers was identified using both the statistical method and the forest plots, with P value of the Chi-squared and I^2 as heterogeneity measures. I^2 ranged from 0 to 100%. $I^2 = 0$ indicated that there was no heterogeneity, while higher I^2 indicated greater heterogeneity. The threshold of P values was 0.1, and I^2 was distinguished by 50%. If $P \geq 0.1$ and $I^2 \leq 50\%$, it indicated no statistical heterogeneity or small heterogeneity among the study results, and a fixed-effects model could be used for meta-analysis; if $P < 0.1$ and $I^2 > 50\%$, it indicated statistical heterogeneity among the study results, and a random-effects model could be used for meta-analysis. All count data were pooled as risk ratio (RR), and 95% confidence intervals (CI) were reported. $P < 0.05$ was considered statistically significant.

By making a funnel plot to evaluate whether the included studies had publication bias, simple scatter plot was made with the effect measure (RR) as the abscissa, and the standard error of the effect measure [SE (logRR)] as the ordinate. If the funnel graph in the funnel plot was symmetrical on both sides, it meant that there was no publication bias, otherwise, there was publication bias.

3. Results

3.1. Literature Retrieval Results. A total of 2610 related literatures were obtained through preliminary database search, including 387 in Cochrane Library, 588 in PubMed, 689 in Embase, 358 in SinoMed, 387 in CNKI, and 201 in Wanfang. There were 1864 remaining articles after using NoteExpress software to remove the duplicates. After reading the titles and abstracts, 654 reviews, 39 unavailable literatures, and 689 literatures inconsistent with the theme were excluded. After searching and reading the full text, 471 articles were further excluded, and 11 articles were finally included, involving 558,440 patients.

3.2. Basic Characteristics and Methodological Quality Evaluation of Included Studies. The basic characteristics and methodological quality evaluation of the included studies are shown in Table 1 and Table 2.

Table 1: Basic information of included studies.

Author	Year of publication	Number of cases/*N*		LVEF <40%/*N*		Type 2 diabetes/*N*		Smoking/*N*		Hypertension/*N*		Hyperlipidemia/*N*		Coronary artery bypass grafting/*N*		ACEI/ARB/*N*		*β*-blockers/*N*		Death/*N*		eGFR/mL·min^{-1}		Age >75 years/*N*		Renal insufficiency/*N*	
		S	C	S	C	S	C	S	C	S	C	S	C	S	C	S	C	S	C	S	C	S	C	S	C	S	C
Jiang et al. [12]	2010	35	393			12	77			20	193									12	1							
Bufe et al. [13]	2010	250	250																							67	21
Pu et al. [14]	2011	289	305																							25	18
Laufer-Perl et al. [15]	2014	878	471																								
Yang et al. [16]	2015	35	265	7	60	22	194	24	175	16	98	31	228	1	7	32	241	26	225	3	0	83.39 ± 44.00	76.33 ± 22.41	7	54		
Zheng and Cai [17]	2018	78	429																			88.9 ± 27.9	117.1 ± 45.7				
Azzalini et al. [18]	2018	214	878	115	278	100	301	38	288	179	628	157	657	41	115					2	1	43.0 ± 14.6	91.8 ± 20.8				
Naganuma et al. [19]	2018	555	908			268	412	81	153	491	734	363	693									31 ± 20	81 ± 17				
Faridi et al. [20]	2019	456402	94340	44423	10479	181793	39416	86778	18869	392034	82896			84803	21529			280131	63277	1826	377			189313	43937	34	13
Malik et al. [21]	2020	225	732			120	268	21	104											0	0	44.2 ± 14.5	87.3 ± 19.1				
Charalambous et al. [22]	2020	254	254			127	103	47	57	235	231	221	231	57	51	118	237			9	3						

Note: S indicates the study group while C indicates the control group.

Table 2: Evaluation of literature quality.

Authors	(1)	(2)	(3)	(4)	(5)	(6)	(7)	(8)	Total scores
Jiang et al. [12]	1	1	1	1	1	0	1	0	6
Bufe et al. [13]	1	1	1	1	1	1	1	1	8
Pu et al. [14]	1	1	1	1	1	1	1	1	8
Laufer-Perl et al. [15]	1	1	1	1	1	1	0	1	7
Yang et al. [16]	1	1	1	1	1	1	1	0	7
Zheng and Cai [17]	1	1	0	1	1	0	1	1	6
Azzalini et al. [18]	1	1	1	1	1	1	1	1	8
Naganuma et al. [19]	1	1	1	1	1	0	1	1	7
Faridi et al. [20]	1	1	1	1	1	1	1	1	8
Malik et al. [21]	1	1	1	1	1	1	1	1	8
Charalambous et al. [22]	1	1	1	1	1	1	1	1	8

3.3. Meta-Analysis Results

3.3.1. LVEF <40%. Three studies demonstrated the influence of LVEF <40% on outcomes after PCI for CTOs, with data heterogeneity ($I^2 = 97\%$), using a random-effects model. The number of cases with LVEF <40% included in the three studies was 44,545 (CKD group) and 10,817 (non-CKD group), respectively. The analysis results showed that the CKD group was higher than the non-CKD group [RR = 0.88, 95% CI (0.86, 0.90), $P < 0.00001$], and the difference was statistically significant (Figure 1).

3.3.2. Type 2 Diabetes. Seven studies demonstrated the influence of type 2 diabetes on outcomes after PCI for CTOs, with data heterogeneity ($I^2 = 90\%$), using a random-effects model. The number of cases with type 2 diabetes included in the seven studies was 182,442 (CKD group) and 40,771 (non-CKD group), respectively. The analysis results showed that the CKD group was higher than the non-CKD group [RR = 0.96, 95% CI (0.95, 0.96), $P < 0.00001$], and the difference was statistically significant (Figure 2).

3.3.3. Smoking. Six studies demonstrated the influence of smoking on outcomes after PCI for CTOs, with data heterogeneity ($I^2 = 74\%$), using a random-effects model. The number of cases with smoking included in the six studies was 86,989 (CKD group) and 19,646 (non-CKD group), respectively. The analysis results showed that the CKD group was higher than the non-CKD group [RR = 0.76, 95% CI (0.59, 0.98), $P = 0.03$], and the difference was statistically significant (Figure 3).

3.3.4. Hypertension. Six studies demonstrated the influence of hypertension on outcomes after PCI for CTOs, with data heterogeneity ($I^2 = 90\%$), using a random-effects model. The number of cases with hypertension included in the six studies was 392,975 (CKD group) and 84,780 (non-CKD group), respectively. The analysis results showed that the CKD group was higher than the non-CKD group [RR = 1.39, 95% CI (0.89, 2.16), $P = 0.14$], and the difference was not statistically significant (Figure 4).

3.3.5. Hyperlipidemia. Four studies demonstrated the influence of hyperlipidemia on outcomes after PCI for CTOs, with data heterogeneity ($I^2 = 66\%$), using a random-effects model. The number of cases with hyperlipidemia included in the four studies was 772 (CKD group) and 1809 (non-CKD group), respectively. The analysis results showed that the CKD group was lower than the non-CKD group [RR = −0.07, 95% CI (-0.10, -0.03), $P < 0.00001$], and the difference was statistically significant (Figure 5).

3.3.6. Coronary Artery Bypass Grafting. Four studies demonstrated the influence of coronary artery bypass grafting on outcomes after PCI for CTOs, with data heterogeneity ($I^2 = 92\%$), using a random-effects model. The number of cases with coronary artery bypass grafting included in the four studies was 84,896 (CKD group) and 21,769 (non-CKD group), respectively. The analysis results showed that the CKD group was higher than the non-CKD group [$RR = 0.73$, 95% CI (0.38, 1.40), $P = 0.35$], and the difference was not statistically significant (Figure 6).

3.3.7. ACEI/ARB. Two studies demonstrated the influence of ACEI/ARB on outcomes after PCI for CTOs, with data heterogeneity ($I^2 = 94\%$), using a random-effects model. The number of cases with ACEI/ARB included in the two studies was 150 (CKD group) and 478 (non-CKD group), respectively. The analysis results showed that the CKD group was higher than the non-CKD group [$RR = 0.24$, 95% CI (0.02, 3.9), $P = 0.32$], and the difference was not statistically significant (Figure 7).

3.3.8. β-Blockers. Two studies demonstrated the influence of β-blockers on outcomes after PCI for CTOs, without data heterogeneity ($I^2 = 0\%$), using a fixed-effects model. The number of cases with β-blockers in the two studies was 280,157 (CKD group) and 63,502 (non-CKD group), respectively. The analysis results showed that the CKD group was higher than the non-CKD group [RR = 0.78, 95% CI (0.77, 0.79), $P < 0.00001$], and the difference was statistically significant (Figure 8).

3.3.9. Death. Five studies demonstrated the mortality after PCI for CTOs, with data heterogeneity ($I^2 = 89\%$), using a random-effects model. The number of deaths included in

Study or subgroup	Experimental Events	Experimental Total	Control Events	Control Total	Weight	Risk ratio M-H, fixed, 95% CI	Year
Yang 2015	7	35	60	265	0.1%	0.88 [0.44, 1.78]	2015
Azzalini 2018	115	214	278	878	0.6%	1.70 [1.45, 1.99]	2018
Faridi 2019	44423	456403	10479	94340	99.3%	0.88 [0.86, 0.89]	2019
Total (95% CI)		**456651**		**95483**	**100.0%**	**0.88 [0.86, 0.90]**	
Total events	44545		10817				

Heterogeneity: chi² = 66.57, df = 2 ($P < 0.00001$); $I^2 = 97\%$
Test for overall effect: Z = 12.40 ($P < 0.00001$)

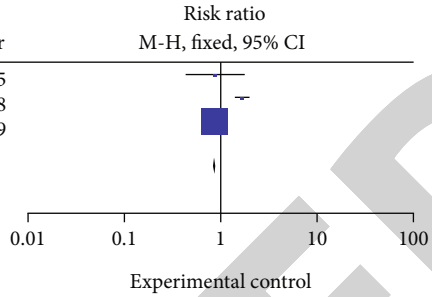

Figure 1: Forest plot of meta-analysis of LVEF on outcomes after PCI for CTOs.

Study or subgroup	Experimental Events	Experimental Total	Control Events	Control Total	Weight	Risk ratio M-H, fixed, 95% CI	Year
Jiang 2010	12	35	77	393	0.0%	1.75 [1.06, 2.89]	2010
Yang 2015	22	35	194	265	0.1%	0.86 [0.66, 1.12]	2015
Azzalini 2018	110	214	301	878	0.2%	1.36 [1.15, 1.62]	2018
Naganuma 2018	268	555	412	908	0.5%	1.06 [0.95, 1.19]	2018
Faridi 2019	181793	456402	39416	94340	98.9%	0.95 [0.95, 0.96]	2019
Charalambous 2020	127	254	103	254	0.2%	1.23 [1.02, 1.50]	2020
Malik 2020	120	225	268	732	0.2%	1.46 [1.25, 1.70]	2020
Total (95% CI)		**457720**		**97770**	**100.0%**	**0.96 [0.95, 0.96]**	
Total events	182442		40771				

Heterogeneity: chi² = 61.98, df = 6 ($P < 0.00001$); $I^2 = 90\%$
Test for overall effect: Z = 10.63 ($P < 0.00001$)

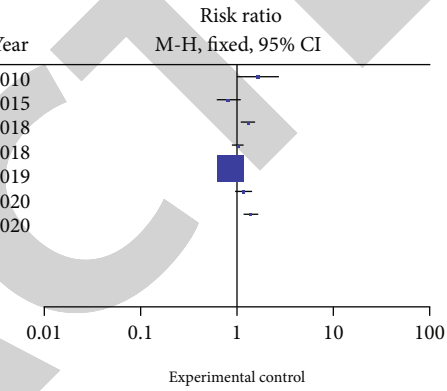

Figure 2: Forest plot of meta-analysis of type 2 diabetes on outcomes after PCI for CTOs.

Study or subgroup	Experimental Events	Experimental Total	Control Events	Control Total	Weight	Odds ratio M-H, random, 95% CI	Year
Yang 2015	24	35	175	265	7.9%	1.12 [0.53, 2.39]	2015
Azzalini 2018	38	214	288	878	16.9%	0.44 [0.30, 0.65]	2018
Naganuma 2018	81	555	153	908	19.8%	0.84 [0.63, 1.13]	2018
Faridi 2019	86778	456402	18869	94340	26.9%	0.94 [0.92, 0.96]	2019
Malik 2020	21	225	104	732	13.3%	0.62 [0.38, 1.02]	2020
Charalambous 2020	47	254	57	254	15.1%	0.78 [0.51, 1.21]	2020
Total (95% CI)		**457685**		**97377**	**100.0%**	**0.76 [0.59, 0.98]**	
Total events	86989		19646				

Heterogeneity: tau² = 0.06; chi² = 19.22 df = 5 ($P = 0.002$); $I^2 = 74\%$
Test for overall effect: Z = 2.15 ($P = 0.03$)

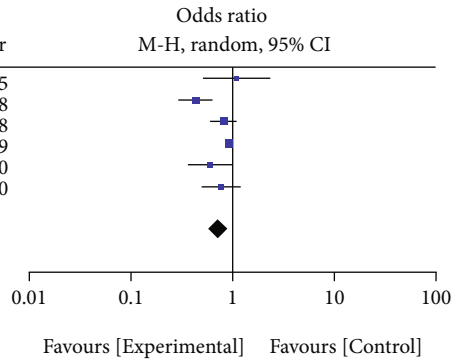

Figure 3: Forest plot of meta-analysis of smoking on outcomes after PCI for CTOs.

Study or subgroup	Experimental Events	Experimental Total	Control Events	Control Total	Weight	Odds ratio M-H, random, 95% CI	Year
Jiang 2010	20	35	193	393	13.8%	1.38 [0.69, 2.78]	2010
Yang 2015	16	35	98	265	13.6%	1.44 [0.71, 2.92]	2015
Azzalini 2018	491	555	734	908	19.0%	0.82 [1.34, 2.48]	2018
Naganuma 2018	179	214	628	878	18.0%	2.04 [1.38, 3.01]	2018
Faridi 2019	392034	456402	82896	94340	20.9%	0.84 [0.82, 0.86]	2019
Charalambous 2020	235	254	231	254	14.6%	1.23 [0.65, 2.32]	2020
Total (95% CI)		**457495**		**97038**	**100.0%**	**1.39 [0.89, 2.16]**	
Total events	392975		84780				

Heterogeneity: tau² = 0.24; chi² = 48.72, df = 5 ($P < 0.00001$); $I^2 = 90\%$
Test for overall effect: Z = 1.46 ($P = 0.14$)

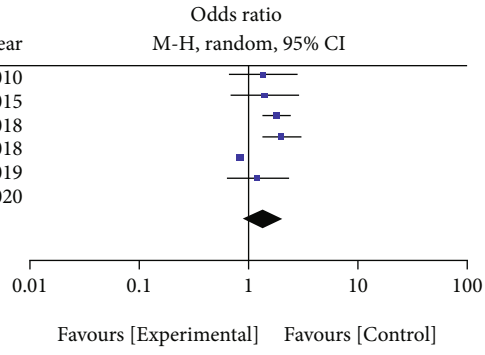

Figure 4: Forest plot of meta-analysis of hypertension on outcomes after PCI for CTOs.

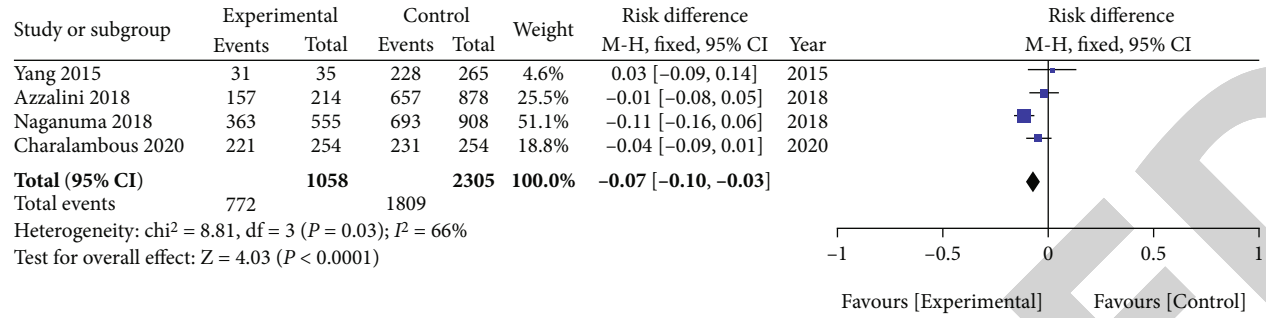

Figure 5: Forest plot of meta-analysis of hyperlipidemia on outcomes after PCI for CTOs.

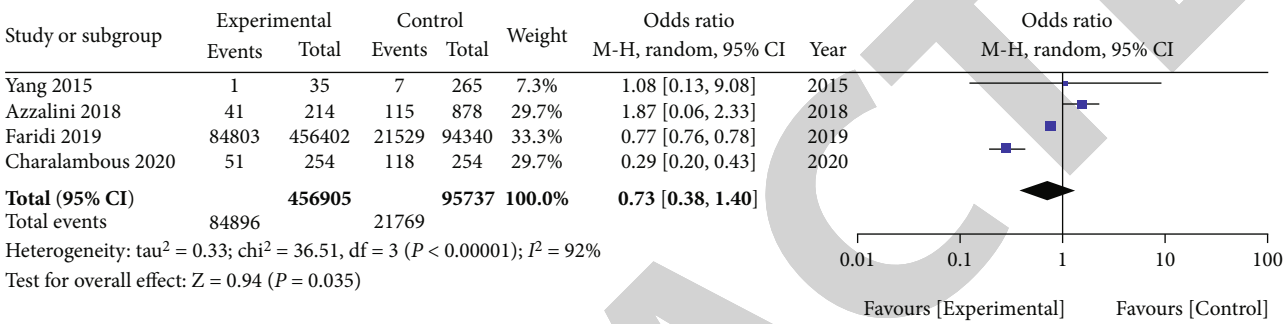

Figure 6: Forest plot of meta-analysis of coronary artery bypass grafting on outcomes after PCI for CTOs.

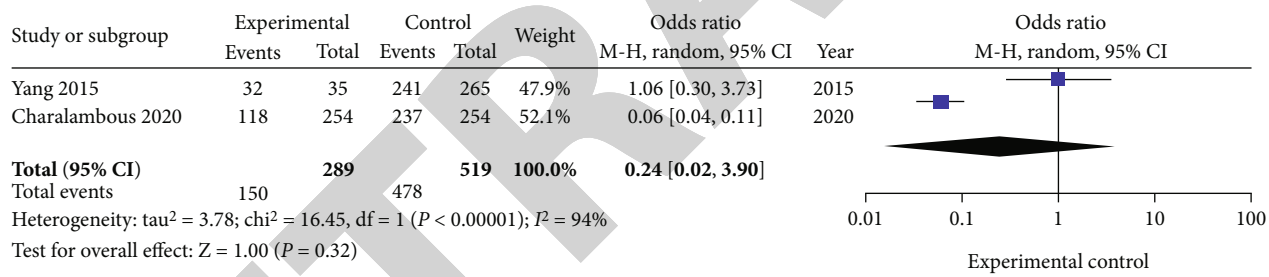

Figure 7: Forest plot of meta-analysis of ACEI/ARB on outcomes after PCI for CTOs.

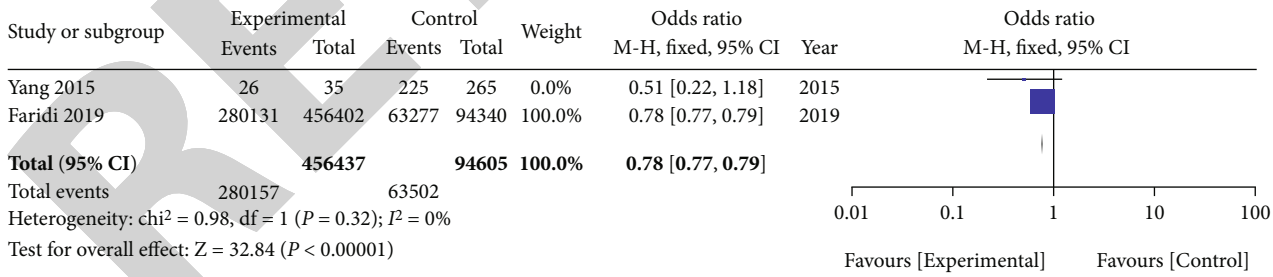

Figure 8: Forest plot of meta-analysis of β-blockers on outcomes after PCI for CTOs.

the five studies was 1852 (CKD group) and 382 (non-CKD group). The analysis results showed that the CKD group was higher than the non-CKD group [RR = 9.93, 95% CI (1.39, 70.67), $P = 0.02$], and the difference was statistically significant (Figure 9).

3.3.10. eGFR. Five studies demonstrated the influence of eGFR on outcomes after PCI for CTOs, with data heterogeneity ($I^2 = 96\%$), using a random-effects model. The analysis results showed that the CKD group was lower than the non-CKD group [RR = −37.25, 95% CI (-44.43, -30.08), $P < 0.00001$], and the difference was statistically significant (Figure 10).

3.3.11. Age >75 Years. Two studies demonstrated the influence of age on outcomes after PCI for CTOs, without data heterogeneity ($I^2 = 0\%$), using a fixed-effects model. The number of cases with age >75 years included in the two

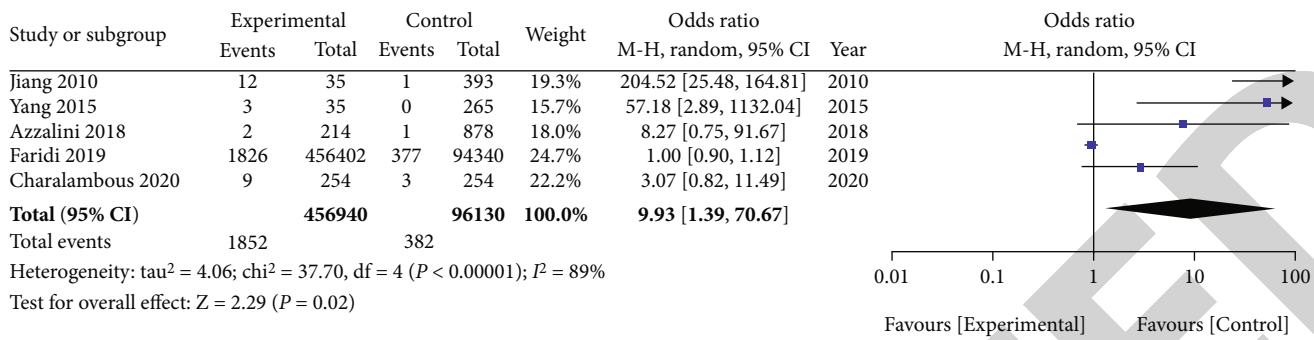

Figure 9: Forest plot of meta-analysis of death on outcomes after PCI for CTOs.

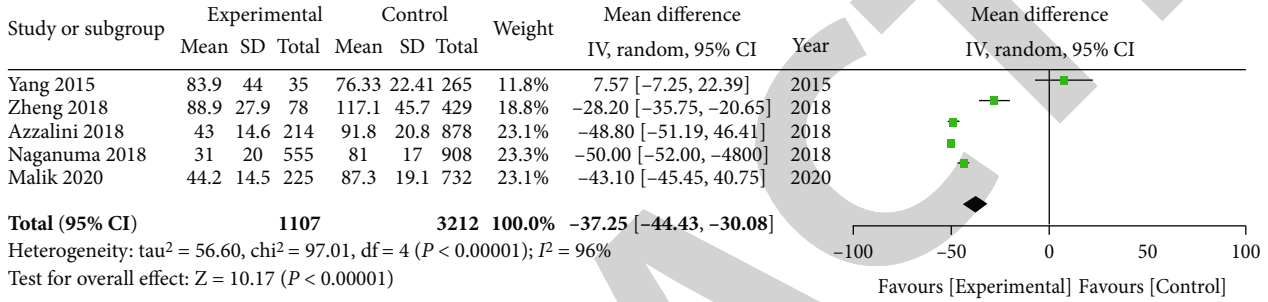

Figure 10: Forest plot of meta-analysis of eGFR on outcomes after PCI for CTOs.

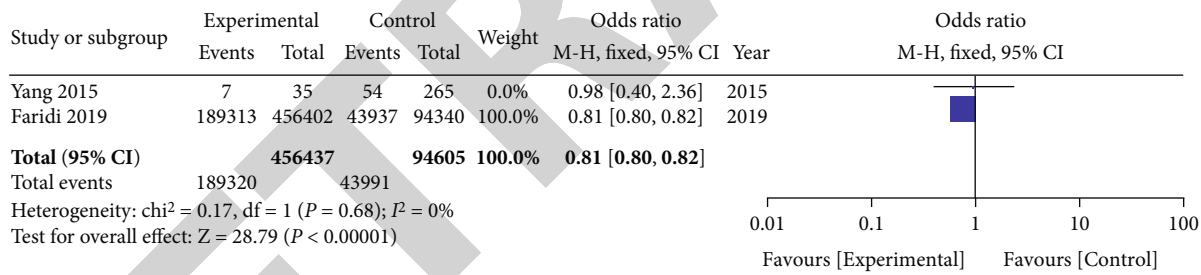

Figure 11: Forest plot of meta-analysis of age on outcomes after PCI for CTOs.

studies was 189,320 (CKD group) and 43,991 (non-CKD group), respectively. The analysis results showed that the CKD group was higher than the non-CKD group [RR = 0.81, 95% CI (0.80, 0.82), $P < 0.00001$], and the difference was statistically significant (Figure 11).

3.3.12. Renal Insufficiency. Three studies demonstrated the influence of renal insufficiency on outcomes after PCI for CTOs, with data heterogeneity ($I^2 = 91\%$), using a random-effects model. The number of cases with renal insufficiency included in the three studies was 126 (CKD group) and 52 (non-CKD group), respectively. The analysis results showed that the CKD group was higher than the non-CKD group [RR = 1.50, 95% CI (0.47, 4.79), $P = 0.5$], and the difference was not statistically significant (Figure 12).

3.4. Publication Bias Analysis. Publication bias analysis was performed on the included studies. The results showed that the funnel plot presented an inverted triangle pattern, and the results were less biased, and the results were credible (Figure 13).

4. Discussion

A total of 11 literatures were included in this study, of which 9 articles with a NOS scale score of ≥7 were of high quality, including 8 articles in English and 10 articles in Chinese. All literatures demonstrated that a controlled study was conducted, the experimental group was a CKD group, and the control group was a non-CKD group. The indicators included in the studies were concentrated, and the influence of various risk factors of CKD on outcomes after PCI for

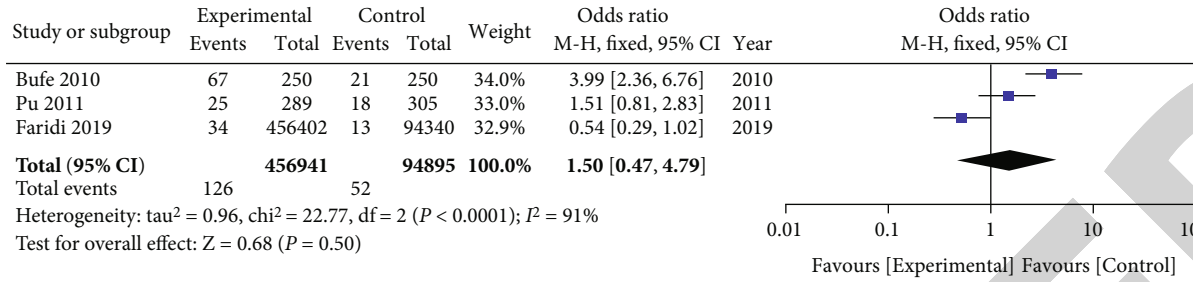

Figure 12: Forest plot of meta-analysis of renal insufficiency on outcomes after PCI for CTOs.

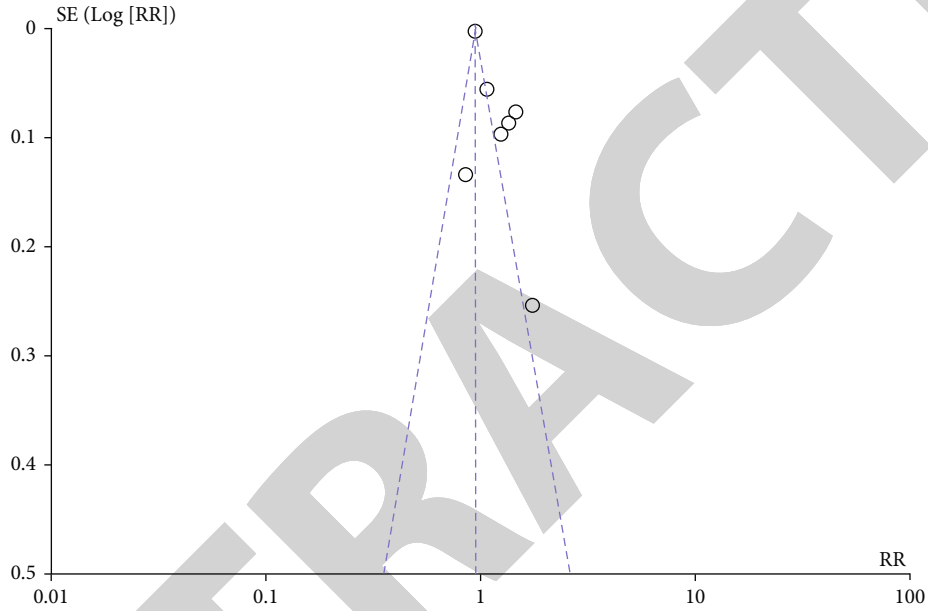

Figure 13: Funnel plot.

CTOs was analyzed to different degrees. The bias of the results was small, and the results of the studies were credible, which can be used for clinical reference.

CKD is one of the important causes of iatrogenic kidney damage [23]. Once it occurs, it will seriously affect the prognosis of patients. In 2004, Mehran et al. made a systematic scoring for chronic risk factors, and the final model for scoring included multiple factors of age >75 years, diabetes mellitus, chronic congestive heart failure, perioperative hypotension, anemia and chronic renal insufficiency, and elective use of intra-aortic balloon pump (IABP) implantation [24]. However, with the development of interventional techniques, more and more CTO patients can achieve ideal revascularization through interventions [25]. The pathophysiological mechanism of chronic disease is not yet fully understood, and the possible mechanisms include renal vasoconstriction and direct nephrotoxicity of oxidative stress [26]. Previously, the incidence of CKD in general population was about 1%-11% [27], and the incidence of CKD in different populations may vary considerably. In high-risk patients complicated with renal insufficiency, the incidence of CKD significantly increased [28]. CTO patients undergoing PCI may be a high-risk population of CKD, and the proportion of patients complicated with renal insufficiency is high. The meta-analysis results of this study demonstrated that renal insufficiency is one of the most important factors for outcomes after PCI for CTOs, with positive correlations. There have been previous studies on the incidence of CKD after PCI in CTO patients [29]. The results of literature studies have demonstrated that smoking after PCI can significantly reduce the long-term efficacy of antithrombotic therapy and increase the incidence of cardiovascular and cerebrovascular events, which may be related to the reduction of platelet activation of antithrombotic drugs by smoking [30]. The meta-analysis results of this study demonstrated that smoking is one of the most important factors for outcomes after PCI for CTOs, with positive correlations. A study has revealed that renal insufficiency is related to left ventricular remodeling, and there is a synergistic effect between the two, which will greatly increase the morbidity and mortality of coronary heart disease patients [31]. The meta-analysis results of this study also demonstrated that LVEF level, diabetes, hypertension, coronary artery bypass grafting, ACEI/ARB, β-blockers, and age were the most important factors for outcomes after PCI for CTOs, with positive correlations. Therefore, for CKD patients,

attention should be paid to the monitoring and control of blood pressure, LVEF level, age, and renal function testing, so that blood pressure can be controlled at the corresponding level, in order to improve the in-hospital prognosis of patients after PCI. At the same time, attention should be paid to whether the patients have diabetes, whether the patients smoke, and whether the patients take β-blockers, so as to effectively improve the prognosis of patients after PCI.

Our systemic review may provide theoretical reference for clinical treatments and research. Limitations of this meta-analysis need to be stated. At present, there are few studies on CKD in CTO-PCI. The sample size was small, the included trials had certain geographical limitations, and there was the possibility of publication bias; the studies evaluated the results using trial data, so baseline characteristics of different trials cannot be assessed. Thus, more randomized controlled trials with high quality, multifocus and large sample remained to be performed to further prove the conclusions.

5. Conclusion

With the acceleration of population aging and urbanization in China, people's living standards and lifestyles have undergone great changes, resulting in more and more factors affecting the cure of coronary heart disease. CKD also has a greater impact on the prognosis of coronary heart disease patients. At present, PCI has become an important treatment method for coronary heart disease. There are many influencing factors of coronary heart disease, and the prognosis of coronary heart disease patients complicated with CKD is also affected by the interaction of multiple factors. LVEF level, diabetes, smoking, hypertension, coronary artery bypass grafting, ACEI/ARB, β-blockers, age, and renal insufficiency are important risk factors for outcomes after PCI for CTOs. Controlling these risk factors is of great significance for the prevention, treatment, and prognosis of coronary heart disease.

Data Availability

All data generated or used during the study appear in the submitted article.

Conflicts of Interest

The authors declared that no conflicts of interest exist in this study.

Acknowledgments

This study was supported by the Innovative Talent Support Program of the Zhejiang Provincial Department of Health (No. 2020RC035).

References

[1] Z. Tian and M. Liang, "Renal metabolism and hypertension," *Nature Communications*, vol. 12, no. 1, p. 963, 2021.

[2] M. Kitamura, Y. Mochizuki, Y. Miyata et al., "Pathological characteristics of periodontal disease in patients with chronic kidney disease and kidney transplantation," *International Journal of Molecular Sciences*, vol. 20, no. 14, p. 3413, 2019.

[3] M. S. Khan, G. L. Bakris, M. Packer et al., "Kidney function assessment and endpoint ascertainment in clinical trials," *European Heart Journal*, vol. 43, no. 14, pp. 1379–1400, 2022.

[4] M. M. N. Meah, T. Joseph, W. Y. Ding et al., "Primary percutaneous coronary intervention in nonagenarians: is it worthwhile?," *BMC Cardiovascular Disorders*, vol. 21, no. 1, p. 30, 2021.

[5] F. Giannini, L. Candilio, S. Mitomo et al., "A practical approach to the management of complications during percutaneous coronary intervention," *JACC. Cardiovascular Interventions*, vol. 11, no. 18, pp. 1797–1810, 2018.

[6] X. F. Gao, Z. M. Wang, F. Wang et al., "Intravascular ultrasound guidance reduces cardiac death and coronary revascularization in patients undergoing drug-eluting stent implantation: results from a meta-analysis of 9 randomized trials and 4724 patients," *The International Journal of Cardiovascular Imaging*, vol. 35, no. 2, pp. 239–247, 2019.

[7] S. Li, J. Cui, A. Hao, S. Zhang, and Q. Zhao, "Design and evaluation of personalized percutaneous coronary intervention surgery simulation system," *IEEE Transactions on Visualization and Computer Graphics*, vol. 27, no. 11, pp. 4150–4160, 2021.

[8] J. B. Cruz Rodriguez and S. Kar, "Management of angina post percutaneous coronary intervention," *Current Cardiology Reports*, vol. 22, no. 2, p. 7, 2020.

[9] L. Azzalini, D. Karmpaliotis, R. Santiago et al., "Contemporary issues in chronic total occlusion percutaneous coronary intervention," *JACC. Cardiovascular Interventions*, vol. 15, no. 1, pp. 1–21, 2022.

[10] C. Cui and Z. Sheng, "Outcomes of percutaneous coronary intervention for chronic total occlusions in the elderly: a systematic review and meta-analysis," *Clinical Cardiology*, vol. 44, no. 1, pp. 27–35, 2021.

[11] S. Bylund, L. B. von Kobyletzki, M. Svalstedt, and Å. Svensson, "Prevalence and incidence of atopic dermatitis: a systematic review," *Acta Dermato-Venereologica*, vol. 100, no. 12, article adv00160, 2020.

[12] H. T. Jiang, Y. P. Sun, C. B. Yu, and X. K. Yan, "Clinical analysis of contrast-induced nephropathy after coronary intervention," *China Journal of Misdiagnosis*, vol. 10, no. 10, pp. 2238-2239, 2010.

[13] A. Bufe, J. Wolfertz, W. Dinh et al., "Gender-based differences in long-term outcome after ST-elevation myocardial infarction in patients treated with percutaneous coronary intervention," *Journal of Women's Health*, vol. 19, no. 3, pp. 471–475, 2010.

[14] J. Pu, P. Shan, S. Ding et al., "Gender differences in epicardial and tissue-level reperfusion in patients undergoing primary angioplasty for acute myocardial infarction," *Atherosclerosis*, vol. 215, no. 1, pp. 203–208, 2011.

[15] M. Laufer-Perl, Y. Shacham, S. Letourneau-Shesaf et al., "Gender-related mortality and in-hospital complications following ST-segment elevation myocardial infarction: data from a primary percutaneous coronary intervention cohort," *Clinical Cardiology*, vol. 38, no. 3, pp. 145–149, 2015.

[16] Y. Yang, N. Tan, Y. T. He, Y. Liu, and Y. H. Liu, "Risk factors of contrast-induced nephropathy in patients with chronic total occlusion who underwent percutaneous coronary

Hindawi
Computational and Mathematical Methods in Medicine
Volume 2023, Article ID 9834256, 1 page
https://doi.org/10.1155/2023/9834256

Retraction

Retracted: Individualized Management of Quality of Care in Orthopedic Nurses Based on Sensitive Indicators

Computational and Mathematical Methods in Medicine

Received 1 August 2023; Accepted 1 August 2023; Published 2 August 2023

This article has been retracted by Hindawi following an investigation undertaken by the publisher [1]. This investigation has uncovered evidence of one or more of the following indicators of systematic manipulation of the publication process:

(1) Discrepancies in scope

(2) Discrepancies in the description of the research reported

(3) Discrepancies between the availability of data and the research described

(4) Inappropriate citations

(5) Incoherent, meaningless and/or irrelevant content included in the article

(6) Peer-review manipulation

The presence of these indicators undermines our confidence in the integrity of the article's content and we cannot, therefore, vouch for its reliability. Please note that this notice is intended solely to alert readers that the content of this article is unreliable. We have not investigated whether authors were aware of or involved in the systematic manipulation of the publication process.

In addition, our investigation has also shown that one or more of the following human-subject reporting requirements has not been met in this article: ethical approval by an Institutional Review Board (IRB) committee or equivalent, patient/participant consent to participate, and/or agreement to publish patient/participant details (where relevant).

Wiley and Hindawi regrets that the usual quality checks did not identify these issues before publication and have since put additional measures in place to safeguard research integrity.

We wish to credit our own Research Integrity and Research Publishing teams and anonymous and named external researchers and research integrity experts for contributing to this investigation.

The corresponding author, as the representative of all authors, has been given the opportunity to register their agreement or disagreement to this retraction. We have kept a record of any response received.

References

[1] W. Zhang, X. Huang, and T. Huang, "Individualized Management of Quality of Care in Orthopedic Nurses Based on Sensitive Indicators," *Computational and Mathematical Methods in Medicine*, vol. 2023, Article ID 1950220, 8 pages, 2023.

Hindawi
Computational and Mathematical Methods in Medicine
Volume 2023, Article ID 1950220, 8 pages
https://doi.org/10.1155/2023/1950220

Research Article

Individualized Management of Quality of Care in Orthopedic Nurses Based on Sensitive Indicators

Weiling Zhang, Xiaomin Huang, and Tianwen Huang

The First Affiliated Hospital, Sun Yat-sen University, China

Correspondence should be addressed to Tianwen Huang; huangtw@mail.sysu.edu.cn

Received 25 August 2022; Revised 7 September 2022; Accepted 28 September 2022; Published 20 February 2023

Academic Editor: Min Tang

Background. Sensitive indicators of nursing quality focus on the core elements of nursing quality management. Nursing-sensitive quality indicators will play an increasingly important role in the macro and micro management of nursing quality in my country. *Objective*. This study were aimed at formulating the sensitive index management of orthopedic nursing quality based on individual nurses for improvement of the quality of orthopedic nursing. *Methods*. Based on the previous literature, the existing challenges in the early application of the orthopedic nursing quality evaluation index were summarized. Moreover, the management system of the orthopedic nursing quality-sensitive index based on individual nurses was devised and implemented, including monitoring the structure and result indices of individual nurses on duty and sampling the process indicators of patients managed by individual nurses. At the quarter-end, the data analysis was performed and fed back to determine the key points of the changes in the quality of specialized nursing affecting the individual, and the PDCA method was utilized for persistent improvement. The changes of sensitive indices of orthopedic nursing quality before (July-December 2018) and 6 months after implementation (July-December 2019) were compared. *Results*. There were significant differences in other indices (accuracy of limb blood circulation assessment/accuracy of pain assessment/postural care pass rate/accuracy of rehabilitation behavioral training/satisfaction of discharged patients) ($P < 0.05$). *Conclusion*. The formulation of an individual-based orthopedic nursing quality-sensitive index management system modifies the traditional quality management model, improves the specialized nursing level, contributes to the accurate core competence training of specialized nursing, and improves the quality of specialized nursing of individual nurses. Consequently, there is an overall improvement in the specialized nursing quality of the department, and fine management is attained.

1. Introduction

The sensitive indicators of nursing quality are nursing guidelines, regulations, procedures and methods formulated according to the content, characteristics, processes, management requirements of nursing work, and the characteristics and needs of nursing staff. Sensitive indicators of nursing quality are also yardsticks for measuring nursing work. The establishment of a systematic, scientific, and advanced nursing standardization system is conducive to improving the quality of nursing and nursing management and promoting the development of nursing disciplines and the training of nursing talents. On the basis of the above standards, each hospital formulates basic nursing quality standards, critically ill patient nursing quality standards, nursing documentation quality standards, and other standards but lacks specialist nursing quality standards. In the field of orthopedic nursing, domestic and foreign countries only focus on the evaluation of certain orthopedic diseases or individual nursing problems and lack comprehensive and overall orthopedic nursing quality standards. Sensitive indicators of nursing quality focus on the core elements of nursing quality management, and nursing-sensitive quality indicators will play an increasingly important role in the macro-

and micromanagement of nursing quality in my country. Quantitatively identify nursing practices that are most relevant to patient outcomes in an effort to improve patient safety and quality of care [1, 2]. The indicator management process includes data collection, quality control, data processing, and analysis, identifying key points of changes in nursing quality, selecting implementation measures, and improving program evaluation [3, 4].

Previously, indicator management was based on the integrity level of wards, departments, and hospitals [5–8]; however, the individualized management of nursing quality based on evaluation indicators has not yet been reported. At an early stage, the research team designed 10 sensitive indicators of orthopaedic care quality [9]. The application process mainly includes the following: based on the challenges of data collation, data processing, and analysis at the ward level, the determination of the focus of complete change in nursing quality, and the relatively common selection of implementation measures and improvement projects; giving full play to the enthusiasm of nurses, leading to passive inspection and improvement is challenging; comparing quality differences among nurses is challenging and not conducive to performance appraisal. Considering the above challenges, we implemented individualized management of the nursing quality of orthopaedic nurses based on sensitive indicators and achieved satisfactory results. The research team constructed 10 sensitive indicators of orthopaedic nursing quality in the previous research. During the application process, it was found that there is no corresponding standard, which is likely to cause different scales of evaluators, lack of homogeneity, and insufficient conversion into specific nursing behaviors, in order to establish an intrinsic link between indicators and standards to drive continuous improvement in the quality of specialist care.

2. Objects and Methods

2.1. Objects. The Department of Orthopedics of our hospital is a national key construction discipline, integrating trauma, joint, and spine surgeries, bone oncology, microsurgery, sports medicine, and other specialized disease treatment disciplines. Seventy-seven orthopedic nurses were included as the study participants, with the age ranging from 22 to 42 (29.69, 5.34) years; title: one deputy chief nurse (1.30%), 13 chief nurses (16.88%), 51 nurse practitioner (66.23%), and 12 nurses (15.58%); working years: 29 (37.66%) with <5 years, 30 (38.96%) with 5– 10 years, seven (9.09%) with 11– 15 years, and 11 (14.29%) with >15 years; and posts: 19 nursing team leaders or specialized nurses (24.68%), 22 senior nurses (28.57%), and 36 junior nurses (46.75%).

The following are the inclusion criteria: (i) clinical practical nurses registered with the Provincial Health Commission, (ii) clinical practical nurses registered with the Provincial Health Commission, (iii) clinical practical nurses registered with the Provincial Health Commission, with at least orthopaedic nursing work (1 year). The following are the exclusion criteria: (i) nursing managers (head nurses), nurses without a nursing practice certificate were excluded; (ii) working in orthopaedics for <1 year, with long-term leave; and (iii) sick leave, maternity leave; or studying abroad for more than 15 days (nurse).

2.2. Methods

2.2.1. Establishment of Sensitive Indicators of Orthopedic Nursing Quality. In 2018, based on the previous research and practices of 48 orthopedic nursing quality evaluation indicators [10], the research team summarized the existing problems, searched domestic and foreign literature, and using the Delphi method formulated 10 orthopedic nursing quality sensitive indicators, such as limb blood circulation evaluation accuracy, posture nursing qualification rate, rehabilitation behavior training accuracy, and deep vein thrombosis incidence rate. The expert authority coefficient of two rounds of expert inquiry was 0.902. The results obtained were credible, with positive coefficients of 0.96 and 1.00. After two rounds of expert consultation, the coefficient of variation was 0–0.27, and the coefficient of coordination was 0.36–0.68 ($P < 0.05$). Structural indicators (include 1.1 as shown in Table 1) were collected by daily registration, process indicators (2.1–2.4) by field assessment, and result indicators (3.1–3.4) by clinical data statistics (chart review) or satisfaction survey. Each index defines its connotation, evaluation elements, and calculation formula, as shown in Table 1. The evaluation criteria of specialized nursing quality were established, such as limb blood circulation, nerve function, axis turnover operation, plaster fixation patient care operation, spinal cord injury patient handling standards, and various auxiliary equipment use standards according to the indicators.

2.2.2. Implementation of Personalized Management of Orthopedic Nurses' Nursing Quality Based

(1) Establishment of a Specialist Nursing Quality Control Group. In January 2019, a specialist nursing quality control group was established. The group members comprised the department nursing director, district nursing director, and specialist nurses, with a total of 10 members. The inclusion criteria for team members were bachelor degree or above; rigorous scientific fact-finding attitude; rich nursing expertise, strong thinking, and judgment; experience in nursing quality evaluation; 10 or more years of experience in orthopedic nursing or management; and intermediate level or above. The responsibilities of the team members include organizing core competency training based on sensitive indicators and performing individual nursing quality personalized management (data collection, quality control, data processing and analysis, data feedback, and improvement project evaluation) for individual nurses based on sensitive indicators.

(2) Core Competency Training Based on Sensitive Indicators. The core competency training of orthopedic nurses includes the theoretical knowledge and practical skills related to sensitive indicators which are included as important elements of clinical practice competency. From January to March 2019, pretraining on personalized management of nursing quality of orthopedic nurses is organized and implemented. Content

Table 1: Orthopedic nursing quality sensitive indicators.

Secondary indicators	Connotation of indicators and evaluation elements	Calculation formula
1.1 Nurse-patient ratio	The ratio between the number of nursing staff and the number of patients	The sum of the number of patients per shift per day/the sum of the number of charge nurses per shift per day during the statistical cycle
2.1 Accuracy of limb blood circulation assessment	Local or affected limb tissue temperature, skin color, capillary filling response, swelling, and arterial pulsation with correct content, frequency, method, and timing	Number of patients assessed accurately/total number of patients sampled
2.2 Accuracy of neurological function assessment	Sensory, muscle strength, motor, reflex, and autonomic function in the spinal cord, peripheral innervated areas with the correct content, frequency, method, and timing	
2.3 Accuracy of pain assessment	Accurate pain assessment tools include pain time, location, degree, nature, duration, resting and active pain, concomitant symptoms, and the impact of pain on daily life, sleep, psychology, and functional activities, pain level after pharmacological analgesia	
2.4 Postural care pass rate	Appropriate postural pillows; necessary protective measures; correct and safe postural transfer; patients master the purpose, method, and precautions of functional or therapeutic position and transfer	Number of patients with accurate postural care/total number of patients sampled
2.5 Accuracy of rehabilitation training	Work with the physician to develop an individualized exercise program, include a method, amount, frequency, and time of exercise from preoperative to the post-discharge phase; appropriate assistive devices; patients exercise appropriately and progressively	Number of patients with accurate rehabilitation training/total number of patients sampled
3.1 Incidence of external fixation complications	Include compartment syndrome, instrument-related pressure injury, ineffective traction, skeletal traction displacement, and traction needle crossing infection	Number of patients with external fixation complications/person-days of patients with internal fixation in the statistical cycle
3.2 Incidence of deep vein thrombosis	Diagnosed by color Doppler ultrasound	Number of patients with deep vein thrombosis/number of patient days in the statistical cycle
3.3 Incidence of respiratory obstruction in high-risk patients	High-risk patients: cervical spine injury, advanced age (70 years), infants and children, anterior cervical spine surgery, and patients who underwent a tracheotomy.	Number of high-risk patients with respiratory obstruction/number of patient-days of high-risk patients in the statistical cycle
3.4 Discharge patient satisfaction	Satisfaction with the pain control, discharge notification, and services	Uniform assessment form: the patient satisfaction questionnaire (third-party survey is conducted by hospitals with conditions)

of the training included overview and interpretation of orthopedic nursing quality sensitive indicators, the connotation of indicators theoretical knowledge, nursing processes, and standards and application of orthopedic nursing quality sensitive indicators for nursing quality management; methods of training and assessment: theoretical lectures, case teaching, operation demonstrations, business visits, objective structured clinical examinations, skill training, and assessment; training hours: 120 h/person.

(3) The Specialist Nursing Quality Control Team Performing Individualized Monitoring and Improvement of Indicators. Individualized monitoring of structural indicators (nurse-patient ratio) and some outcome indicators (incidence of external fixation complications, deep vein thrombosis, and respiratory obstruction in high-risk patients) are conducted, that is, monitoring the nurse-patient ratio and outcome indicators during the shift of the responsible nurse. Patients who were under the charge nurse's supervision throughout the hospital stay were monitored for outcome indicators (patient satisfaction at discharge). To investigate satisfaction, the hospital's revised "Patient Satisfaction Questionnaire" was distributed at the time of discharge, which included patient satisfaction with the medical environment, quality of care, professional skills of nurses, and service attitude of nurses. The survey forms were placed in the satisfaction survey box by patients or family members to reduce human interference factors. The process indicators including accuracy of blood circulation assessment in limbs, the accuracy of neurological function assessment, the accuracy of pain assessment, the passing rate of postural care, and accuracy of rehabilitation behavior training of the patients under the charge of this responsible nurse were sampled, and record forms were filled out. Moreover, members of the quality

control team served as quality inspectors, and each nurse was continuously sampled for each indicator five times/quarter, and the total number of times each nurse sampled for the five indicators was 25 per quarter. The quality of the nurses' process of implementing specialized care was assessed to determine if the content was comprehensive, the method was correct, and the results were consistent with the quality inspector's evaluation. When the two evaluation results were inconsistent, another quality inspector made a judgment, and if necessary, the competent professor of the patient was asked to implement the evaluation and provide guidance.

Quarterly data entry of quality evaluation was performed to establish a database of sensitive indicators of orthopedic nursing quality based on individual nurses. At the end of each quarter, the quality management team analyzed the above data by calculating each nurse's indicator value, comparing the growth rate of each nurse's indicator value to the previous quarter, comparing the difference in indicator values between nurses at the same level of position, comparing the difference between each nurse's indicator value and the indicator target value for nurses in the same level of position, and providing feedback to the individual nurse on the results of the analysis and the individual finding the impact of individual specialty nursing The results of the analysis are fed back to the individual nurse, and the individual identifies priorities for continuous improvement that affect individual specialty care changes. Simultaneously, targeted training is provided at the ward and unit level for nurses with large differences in indicator values and fluctuating indicator values, and specialty nursing core competency training is implemented based on individual nurses. For example, the pain assessment accuracy of a nurse's patients was the lowest among the process indicators and lower than the pain assessment accuracy of nurses in the same level of positions. The individual detected that the reasons affecting his low pain assessment accuracy were his lack of mastery of the use of different pain assessment scales, subjective judgment during pain assessment, and lack of timely assessment after implementing pain interventions. The individual proposed improvement measures, including changing the concept of pain, believing in the patient's chief complaint, learning relevant knowledge, and writing a case report on pain assessment in conjunction with the case; asking the district nurse manager or pain specialist nurse for bedside guidance; and self-evaluating the accuracy of pain assessment and comparing it with the evaluation results of the QI officer.

2.2.3. Statistical Analysis. Statistical analysis was performed using SPSS 20.0 software to compare changes in orthopedic nursing quality sensitivity indicators before implementation (July-December 2018) and 6 months after implementation (July-December 2019). Percentages were used for descriptive analysis and the χ_2 test was used to compare the differences between the two groups with a test level of $\alpha = 0.05$. The types of diseases in which nurses performed care before and after implementation included extremity fractures, multiple injuries, pelvic fractures, brachial plexus injuries, hand trauma, osteoarthritis of the knee, femoral head necrosis, femoral neck fractures, femoral trochanter fractures, knee ligament injuries, knee meniscal injuries, lumbar disc herniation, cervical spondylosis, scoliosis, spinal cord injury, spinal fracture, extremity bone tumor, and sacral tumor. The differences in patients' sex, age, diagnosis, surgery, and condition classification were comparable and not statistically significant ($P > 0.05$). The results of the discharge patient satisfaction survey were selected for statistical analysis from the questionnaires completed by patients who had implemented the process index evaluation.

3. Results

There was no significant difference in the nurse-patient ratio of nurses in charge of the same post before and after the intervention ($P > 0.05$). The incidence of external fixation complications in high-risk patients was 0.65%, the incidence of deep vein thrombosis was 0.52%, and the incidence of respiratory obstruction was 0.13%. In high-risk patients, the incidence of deep vein thrombosis was 0.13% and the incidence of respiratory obstruction was 0. Comparing the process indicators of nurse management at different levels with the results of patient discharge satisfaction, all indicators except the accuracy rate of neurological function assessment of patients in the nursing management of level 3 and the satisfaction rate of discharged patients from nursing group leaders or specialist nurses have statistics difference in science ($P < 0.05$). See Tables 2–4.

4. Discussion

With the gradual formation of a consensus on the concept of "evidence-led improvement to replace evidence-based management," nursing-sensitive quality indicators will play an increasingly important role in the macro- and micromanagement of nursing quality in my country [11]. In recent years, researches on nursing-sensitive quality indicators have appeared one after another in my country, but the application of indicators is single, and most of them are based on the three-level quality control of nursing department-department-department and head nurse [12–15]. Individuals "do not know what the challenge is, do not know if the problem is related to the individual, do not know what my quality level is" and a series of confusions [16]. According to the epistemology of Marxism, the internal cause is the basis of change, the external cause is the condition of the change, and the external cause works through the internal cause [17]. Quality is prepared by individual nurses, and continuous improvement of quality is a process of active learning and improvement, rather than a process of passive improvement by individual nurses [18]. The results show that the index management based on individual nurses can timely feedback the quality level of nurses to individual nurses, making the quality evaluation more scientific and accurate; based on the index evaluation of individual nurses, the index results of all nurses in a certain period of time are summarized to form the overall quality [19]. At the

Table 2: Comparison of orthopedic nursing quality sensitive index values of primary charge nurses before and after implementation.

Group	Group Total sampled visits	Accuracy of limb blood circulation assessment (%)		Accuracy of neurological function assessment (%)		Accuracy of pain assessment (%)		Postural care pass rate (%)		Accuracy of rehabilitation behavioral training (%)		Discharge patient satisfaction (%)	
		The accurate number of persons	%	The accurate number of persons	%	The accurate number of persons	%	Qualified number of persons	%	The accurate number of persons	%	Number of persons satisfied	%
Pre-implementation	360	333	92.50	332	92.22	339	94.17	341	94.72	335	93.06	342	95.00
Post-implementation	360	346	96.11	336	93.33	353	98.06	352	97.78	348	96.59	352	97.78
χ_2		4.37		0.33		7.28		4.66		4.82		3.99	
P		0.04		0.57		0.01		0.03		0.03		0.04	

Table 3: Senior charge nurses before and after implementation Comparison of orthopedic care quality sensitivity index values.

Group	Total sampled visits	Accuracy of limb blood circulation assessment (%)		Accuracy of neurological function assessment (%)		Accuracy of pain assessment (%)		Postural care pass rate (%)		Accuracy of rehabilitation behavioral training (%)		Satisfaction of discharged patients (%)	
		The accurate number of persons	%	The accurate number of persons	%	The accurate number of persons	%	Qualified number of persons	%	The accurate number of persons	%	Satisfied number of persons	%
Preimplementation	220	209	95.00	205	93.18	210	95.45	208	94.55	206	93.64	211	95.91
Postimplementation	220	218	99.09	207	94.09	218	99.09	217	98.64	217	98.64	217	98.64
χ_2		5.07		0.15		4.2		4.42		4.46		2.14	
P		0.02		0.7		0.04		0.04		0.04		0.14	

Table 4: Comparison of orthopedic quality of care sensitivity index values for nursing team leaders and specialist nurses before and after implementation.

Group	Total sampled visits	Accuracy of limb blood circulation assessment (%)		Accuracy of neurological function assessment (%)		Accuracy of pain assessment (%)		Postural care pass rate (%)		Accuracy of rehabilitation behavioral training (%)		Satisfaction of discharged patients (%)	
		The accurate number of persons	%	The accurate number of persons	%	The accurate number of persons	%	Qualified number of persons	%	The accurate number of persons	%	Satisfied number of persons	%
Preimplementation	190	182	95.79	184	96.84	179	94.21	181	95.26	180	94.74	186	97.89
Postimplementation	190	189	99.47	187	98.42	188	98.95	189	99.47	188	98.95	189	99.47
χ_2		4.1		0.46		5.1		5.03		5.99		0.81	
P		0.04		0.50		0.02		0.03		0.01		0.37	

$P < 0.05$; when frequencies were less than 5, a continuity-corrected chi-square was used for testing.

professional level, it avoids the quality deviation that may have been caused by unreasonable quality monitoring in the past, and truly reflects the overall results [20]. This avoids the quality deviation that may be caused by unreasonable quality monitoring in the past, truly reflects the overall quality level, and is conducive to continuous quality improvement at the professional level.

Our study found no statistically significant difference in the proportion of nurses and patients in the same post before and after the intervention. The incidence of external

fixation complications in high-risk patients was 0.65%, the incidence of deep vein thrombosis was 0.52%, and the incidence of respiratory obstruction was 0.13%. In high-risk patients, the incidence of deep vein thrombosis was 0.13% and the incidence of respiratory obstruction was 0. The reason for the analysis is as follows: Because of the relatively stable nurse-to-patient ratio, the level of professional care in the department is reflected in the difference between the quality of the process and the outcome [21]. The evaluation of the professional nursing level before implementation is based on the overall professional level, from which it is found that the quality level of a certain nurse at a certain point in time is often fragmented and one-sided; after implementation, it can be comprehensive from individual nurses to the entire nurse system, reflecting the level of professional nursing [22]. Sensitive indicators of orthopaedic nursing quality, such as the accuracy rate of limb blood circulation assessment, the accuracy rate of neurological function assessment, the qualified rate of posture nursing, and the accuracy rate of rehabilitation behavior training, involve the whole process of orthopaedic specialist nursing, and have complex, diverse, and variable characteristics. There were no statistically significant differences in the accuracy of neurological assessments among nurse-managed patients across the three levels of positions, indicating the challenges of accurate neurological assessments and the lack of accurate identification of high-risk patients with preexisting or potential neurological impairments by nurses. [23]. Preexisting nerve injury usually occurs by cutting, pulling, and pinching; underlying nerve injury usually occurs as a result of hematoma compression, displacement of internal fixation, and complications of therapeutic procedures [24]. Nurses are often unable to actively observe and predict conditions, resulting in failed assessments. Thus, the goal of accurate assessment can be achieved by actively seeking clues, inquiring and making judgments, enhancing medical and nursing communication, and familiarizing with the cause of injury, surgery, and condition by responsible nurses [25]. The results show that continuous quality monitoring based on individual nurses can standardize nursing behavior and improve nurse compliance, thereby improving efficiency and quality [26]. To sum up, the value of sensitive indicators of orthopaedic nursing quality has gradually increased from primary and senior supervisor nurses to nursing team leaders and specialist nurses, and the level of qualifications, experience, knowledge, and skills has been continuously improved. Match workload, patient condition and nursing needs, and nurses' specialist care level [27]. This will further improve the quality of specialist care by ensuring that nurses provide higher quality care for Charlinger and critically ill patients.

Our study found that when comparing the process indicators of nurse management at different levels with patient discharge satisfaction outcomes, all patients except for the accuracy of neurological function assessment and patient satisfaction at discharge from nursing group leaders or specialist nurses in level 3 nursing management All indicators were statistically different. The reasons for the analysis are as follows: the assessment and management of nursing quality should be based on professional standards of nursing [28]. Nursing professional standards are an important part of the core competency training of nursing professions. Research shows that the training and evaluation of core competence of orthopaedic specialist nursing mainly includes theoretical knowledge, professional lethality, and comprehensive practical skills. The training mostly adopts group lectures, operation demonstrations, business visits, and difficult case discussions. This is training and assessment implemented from the holistic level of the orthopaedic education profession, which is a common clinical approach [29–32]. With the development of holistic nursing, responsible nursing, high-quality nursing, and evidence-based nursing, as well as the arrival of the era of precision medicine, the precise training of core competencies in specialist nursing is particularly urgent. The positioning of our precision training is that the training needs of nurses come from the evaluation of quality indicators. The quality inspectors monitor individual nurses with the accurate implementation of nursing professional standards as the yardstick. When the quality deviates from the standard, they immediately supervise and repeat the training to realize the core ability of accurate professional nursing. At the same time, the core competitive training of precision specialist nursing develops with the professional development. Nursing professional standards and corresponding operating procedures should be formulated and revised in a timely manner, professional core skills should be improved, nurses should be clearly instructed, and targeted training should be carried out [33]. After the completion of the design of the valve blood circulation observation ruler, the operation procedure of the flap blood circulation assessment was revised in time. After intensive training, the head nurse tested the nurse's mastery degree when assessing the accuracy of the limb blood circulation assessment, and immediately found a problem.

Based on individual nurses, this study implemented the management of sensitive indicators of orthopaedic nursing quality, and further explored the application value of sensitive indicators of specialized nursing quality. Facts have proved that both managers and individual nurses can accurately find the weak links in nursing according to the changes in the indicator data, thereby improving the professional nursing quality of individual nurses, thereby improving the overall professional nursing quality of the department, and achieving refinement. This study was limited to the orthopaedic ward in our hospital, and future research may include a multicenter study to further improve the management of sensitive indicators of orthopaedic care quality based on individual nurse practice.

Data Availability

No data were used to support this study.

Conflicts of Interest

The authors declare that they have no conflicts of interest.

References

[1] S. Burston, W. Chaboyer, and B. Gillespie, "Nurse-sensitive indicators suitable to reflect nursing care quality: a review and discussion of issues," *Journal of Clinical Nursing*, vol. 23, no. 13-14, pp. 1785–1795, 2014.

[2] R. M. Gallagher and P. A. Rowell, "Claiming the future of nursing through nursing-sensitive quality indicators," *Nursing Administration Quarterly*, vol. 27, no. 4, pp. 273–284, 2003.

[3] Z. Li, S. Cheng, L. Lv, S. Xy, and X. H. Liu, "The application of nursing-sensitive quality indicators in evaluating nursing efficacy," *La Clinica Terapeutica*, vol. 165, no. 5, p. e342-5, 2014.

[4] A. Chen, X. Jiang, F. Lian, J. Wu, X. Weng, and W. Li, "Application and Effectiveness of Big Data and Artificial Intelligence in the Construction of Nursing Sensitivity Quality Indicators," *Journal of Healthcare Engineering*, vol. 2021, Article ID 2087876, 2021.

[5] M. C. Callanan, B. Jarrett, C. R. Bragdon et al., "The John Charnley Award: risk factors for cup malpositioning: quality improvement through a joint registry at a tertiary hospital," *Clinical Orthopaedics and Related Research®*, vol. 469, no. 2, pp. 319–329, 2011.

[6] J. D. Baker, "Nursing research, quality improvement, and evidence-based practice: the key to perioperative nursing practice," *AORN journal*, vol. 1, no. 105, pp. 3–5, 2017.

[7] C. Fengju, Y. Chunzi, and L. Mei, "Establishment and application of quality indicators for cancer pain management based on information technology platform," *Journal of Nursing*, vol. 35, no. 24, pp. 12–14, 2020.

[8] S. M. Davies, J. Geppert, M. McClellan, K. M. McDonald, P. S. Romano, and K. G. Shojania, *Refinement of the HCUP Quality Indicators Rockville*, Agency for Healthcare Research and Quality, MD, 2001.

[9] J. F. Timsit, J. Baleine, L. Bernard et al., "Expert consensus-based clinical practice guidelines management of intravascular catheters in the intensive care unit," *Annals of Intensive Care*, vol. 10, no. 1, pp. 1–26, 2020.

[10] V. P. Nichols, F. Toye, S. Eldabe, H. K. Sandhu, M. Underwood, and K. Seers, "Experiences of people taking opioid medication for chronic non-malignant pain: a qualitative evidence synthesis using meta-ethnography," *BMJ open*, vol. 10, no. 2, p. e032988, 2020.

[11] W. Li, Y. Wen, Y. Du et al., "Development and clinical application of nursing-sensitive indicators for midline catheterization care using evidence-based methods," *Annals of Palliative Medicine*, vol. 10, no. 1, pp. 425–433, 2021.

[12] "40th International Symposium on Intensive Care & Emergency Medicine 2021," *Critical Care*, vol. 25, Supplement 1, p. 383, 2021.

[13] H. Jin, A. Chalkidou, M. Hawkins et al., "Cost-effectiveness analysis of stereotactic ablative body radiation therapy compared with surgery and radiofrequency ablation in two patient cohorts: metastatic liver cancer and hepatocellular carcinoma," *Clinical Oncology*, vol. 33, no. 3, pp. e143–e154, 2021.

[14] P. Cai, Y. Q. Yang, and Y. H. Chen, "Construction of sensitive indicators of nursing quality in rehabilitation departments," *Nursing Research*, vol. 34, no. 2, pp. 343–346, 2020.

[15] G. Juan and L. Guohong, "Construction of nursing-sensitive quality indicators in hematology," *Journal of PLA Nursing*, vol. 36, no. 10, pp. 9–12, 2019.

[16] L. Akhu-Zaheya, R. Al-Maaitah, and H. S. Bany, "Quality of nursing documentation: paper-based health records versus electronic-based health records," *Journal of Clinical Nursing*, vol. 27, no. 3-4, pp. e578–e589, 2018.

[17] K. O. Pei-Ying, H. O. Chen-Shie, and L. I. A. O. Pei-Hung, "The impact of a multilevel interactive nursing quality control and audit application on nursing quality management," *BMC Nursing*, vol. 20, no. 1, p. 243, 2021.

[18] P. S. Moldskred, A. K. Snibsøer, and B. Espehaug, "Improving the quality of nursing documentation at a residential care home: a clinical audit," *BMC Nursing*, vol. 20, no. 1, p. 103, 2021.

[19] G. Gardner, A. Gardner, and J. O'Connell, "Using the Donabedian framework to examine the quality and safety of nursing service innovation," *Journal of Clinical Nursing*, vol. 23, no. 1-2, pp. 145–155, 2014.

[20] K. Stewart, O. Doody, M. Bailey, and S. Moran, "Improving the quality of nursing documentation in a palliative care setting: a quality improvement initiative," *International Journal of Palliative Nursing*, vol. 23, no. 12, pp. 577–585, 2017.

[21] N. Wang, P. Yu, and D. Hailey, "The quality of paper-based versus electronic nursing care plan in Australian aged care homes: a documentation audit study," *International Journal of Medical Informatics*, vol. 84, no. 8, pp. 561–569, 2015.

[22] S. Poortaghi, M. Salsali, A. Ebadi, Z. Rahnavard, and F. Maleki, "Findings from a nursing care audit based on the nursing process: a descriptive study," *Nursing and Midwifery Studies*, vol. 4, no. 3, article e30181, 2015.

[23] M. K. D. Skaggs, J. F. Daniels, A. J. Hodge, and V. L. DeCamp, "Using the evidence-based practice service nursing bundle to increase patient satisfaction," *Journal of Emergency Nursing*, vol. 44, no. 1, pp. 37–45, 2018.

[24] V. Mac Donald, A. B. Maher, H. Mainz et al., "Developing and testing an international audit of nursing quality indicators for older adults with fragility hip fracture," *Orthopaedic Nursing*, vol. 37, no. 2, pp. 115–121, 2018.

[25] N. Wang, D. Hailey, and P. Yu, "Quality of nursing documentation and approaches to its evaluation: a mixed-method systematic review," *Journal of Advanced Nursing*, vol. 67, no. 9, pp. 1858–1875, 2011.

[26] M. Whalen, B. Maliszewski, H. Gardner, and S. Smyth, "Audit and feedback: an evidence-based practice literature review of nursing report cards," *Worldviews on Evidence-Based Nursing*, vol. 18, no. 3, pp. 170–179, 2021.

[27] A. Gandhi, H. Yu, and D. C. Grabowski, "High nursing staff turnover in nursing homes offers important quality information," *Health Affairs*, vol. 40, no. 3, pp. 384–391, 2021.

[28] Z. Shiyu and Y. Jiaohua, "Progress of research on quality sensitivity indicators in specialized nursing care," *Nursing Research*, vol. 33, no. 8, pp. 1342–1346, 2019.

[29] G. Hongyan and X. Hong, "Implications of the nursing quality evaluation system in the United States for nursing quality management in China," *China Nursing Management*, vol. 14, no. 5, pp. 459–462, 2014.

[30] L. Chunmei, S. Caiping, Z. Yumei, and J. Ren, "Construction of core competency evaluation index system for orthopaedic specialist nurses," *Chongqing Medicine*, vol. 44, no. 33, pp. 4686–4689, 2015.

[31] R. Wilson, C. M. Godfrey, K. Sears, J. Medves, A. Ross-White, and N. Lambert, "Exploring conceptual and theoretical

Hindawi
Computational and Mathematical Methods in Medicine
Volume 2023, Article ID 9895475, 1 page
https://doi.org/10.1155/2023/9895475

Retraction

Retracted: Analysis of Efflux Pump System and Other Drug Resistance Related Gene Mutations in Tigecycline-Resistant *Acinetobacter baumannii*

Computational and Mathematical Methods in Medicine

Received 12 December 2023; Accepted 12 December 2023; Published 13 December 2023

This article has been retracted by Hindawi, as publisher, following an investigation undertaken by the publisher [1]. This investigation has uncovered evidence of systematic manipulation of the publication and peer-review process. We cannot, therefore, vouch for the reliability or integrity of this article.

Please note that this notice is intended solely to alert readers that the peer-review process of this article has been compromised.

Wiley and Hindawi regret that the usual quality checks did not identify these issues before publication and have since put additional measures in place to safeguard research integrity.

We wish to credit our Research Integrity and Research Publishing teams and anonymous and named external researchers and research integrity experts for contributing to this investigation.

The corresponding author, as the representative of all authors, has been given the opportunity to register their agreement or disagreement to this retraction. We have kept a record of any response received.

References

[1] W. Zheng, Y. Huang, W. Wu, J. Zhu, and T. Zhang, "Analysis of Efflux Pump System and Other Drug Resistance Related Gene Mutations in Tigecycline-Resistant *Acinetobacter baumannii*," *Computational and Mathematical Methods in Medicine*, vol. 2023, Article ID 8611542, 12 pages, 2023.

Hindawi
Computational and Mathematical Methods in Medicine
Volume 2023, Article ID 8611542, 12 pages
https://doi.org/10.1155/2023/8611542

Research Article

Analysis of Efflux Pump System and Other Drug Resistance Related Gene Mutations in Tigecycline-Resistant *Acinetobacter baumannii*

Wenzheng Zheng, Yubo Huang, Wenbin Wu, Jiaxin Zhu, and Tiantuo Zhang

Department of Pulmonary and Critical Care Medicine, the Third Affiliated Hospital of Sun Yat-Sen University, Sun Yat-Sen University, and Institute of Respiratory Diseases, Guangzhou 510000, China

Correspondence should be addressed to Tiantuo Zhang; zhttuo@mail.sysu.edu.cn

Received 11 August 2022; Revised 26 August 2022; Accepted 12 September 2022; Published 17 February 2023

Academic Editor: Min Tang

Background. The isolation of tigecycline-resistant *Acinetobacter baumannii* in recent years has brought great difficulties to clinical prevention and treatment. *Purpose*. To explore the effect of efflux pump system and other resistance related gene mutations on tigecycline resistance in *Acinetobacter baumannii*. *Methods*. Fluorescence quantitative PCR was used to detect the expression levels of major efflux pump genes (*adeB*, *adeJ*, and *adeG*) in extensive drug-resistant *Acinetobacter baumannii*. The minimum inhibitory concentration (MIC) of tigecycline was detected by the broth microdilution testing and efflux pump inhibition experiment to assess the role of efflux pump in tigecycline resistance of *Acinetobacter baumannii*. Efflux pump regulatory genes (*adeR* and *adeS*) and tigecycline resistance related genes (*rpsJ*, *trm*, and *plsC*) were amplified by PCR and sequenced. By sequence alignment, tigecycline sensitive and tigecycline-insensitive *Acinetobacter baumannii* were compared with standard strains to analyze the presence of mutations in these genes. *Results*. The relative expression of *adeB* in the tigecycline-insensitive *Acinetobacter baumannii* was significantly higher than that in the tigecycline sensitive *Acinetobacter baumannii* (114.70 (89.53-157.43) vs 86.12 (27.23-129.34), $P = 0.025$). When efflux pump inhibitor carbonyl cyanide 3-chlorophenylhydrazone (CCCP) was added, the percentage of tigecycline-insensitive *Acinetobacter baumannii* with tigecycline MIC decreased was significantly higher than that of tigecycline-sensitive *Acinetobacter baumannii* (10/13 (76.9%) vs 26/59 (44.1%)), $P = 0.032$); the relative expression of *adeB* in the MIC decreased group was significantly higher than that in the MIC unchanged group (110.29 (63.62-147.15) vs 50.06 (26.10-122.59), $P = 0.02$); The relative expression levels of efflux pumps *adeG* and *adeJ* did not increase significantly, and there was no significant difference between these groups. One *adeR* point mutation (Gly232Ala) and eight *adeS* point mutations (Ala97Thr, Leu105Phe, Leu172Pro, Arg195Gln, Gln203Leu, Tyr303Phe, Lys315Asn, Gly319Ser) were newly detected. Consistent mutations in *trm* and *plsC* genes were detected in both tigecycline-insensitive and tigecycline-sensitive *Acinetobacter baumannii*, but no mutation in *rpsJ* gene was detected in them. *Conclusion*. Tigecycline-insensitive *Acinetobacter baumannii* efflux pump *adeABC* overexpression was an important mechanism for tigecycline resistance, and the mutations of efflux pump regulator genes (*adeR* and *adeS*) are responsible for *adeABC* overexpression. The effect of *trm*, *plsC*, and *rpsJ* gene mutations on the development of tigecycline resistance in *Acinetobacter baumannii* remains controversial.

1. Introduction

Acinetobacter baumannii (AB) is a nonmotile, oxidase-negative, nonfermenting sugar Gram-negative bacillus [1]. It is highly environmentally adaptable and can survive up to 5 months on dry solid surfaces due to biological properties such as low nutrient requirements, ability to survive in most temperature and pH environments, high resistance to disinfectants, and ease of biofilm formation on nonliving surfaces [2]. At the same time, its intrinsic resistance and its ability to rapidly upregulate endogenous resistance mechanisms or actively acquire exogenous resistance genes allow it to evolve

relatively quickly into a multiresistant bacterium with resistance to multiple antibiotics [3]. As a result, *Acinetobacter baumannii* is widely present in health care settings and difficult to eradicate. Extensive drug-resistant *Acinetobacter baumannii* (XDR AB) refers to insusceptibility to all classes of antimicrobial drugs except colistin and tigecycline [4, 5], and several studies have shown that drug-resistant *Acinetobacter baumannii* infections have been shown to have a high mortality rate, especially for carbapenem-resistant *Acinetobacter baumannii* (CRAB) infections, which can range from 35% to 61% [6–11]. Tigecycline (TGC) is currently regarded as an effective drug against CRAB or XDR-AB [12, 13], however, with the gradual application of tigecycline in clinical practice, tigecycline resistant *Acinetobacter baumannii* also emerged in recent years [14–16].

The mechanism of tigecycline resistance production by *Acinetobacter baumannii* is a hot topic of current interest, and existing studies suggest that overexpression of the efflux pump system plays a major role in multidrug resistant bacteria [17–19]. Closely related to *Acinetobacter baumannii* tigecycline is the RND family, which contains three major systems: *adeABC*, *adeFGH*, and *adeIJK* [20]. However, the degree of correlation between overexpression of each system and tigecycline resistance levels may vary, and whether the efflux pump system can play an important role in altering tigecycline resistance levels in clinical strains in which multiple resistance mechanisms may coexist, which issues are still controversial [21–23]. Meanwhile, it has been reported that the variation of *adeRS* two-component system changed the sensitivity of *Acinetobacter baumannii* to tigecycline by regulating the expression of efflux pump system [24, 25]. Moreover, recent studies have identified mutations in tigecycline drug target genes or membrane permeability-related genes in some strains without efflux pump overexpression, such as *trm*, *plsC*, and *rpsJ* genes [26–28], and the prevalence of these resistance genes in clinical drug-resistant strains has been less studied so far. Therefore, we explored the role of the above mechanisms in tigecycline-resistant *Acinetobacter baumannii* in our hospital.

2. Materials and Methods

2.1. Sources of Strains and Reagents. Seventy-two strains of extensive drug-resistant *Acinetobacter baumannii* isolated from the sputum of patients in the Third Affiliated Hospital of Sun Yat-Sen University from April 2014 to September 2017 were collected for tigecycline resistance mechanism study. The reagents used in our study were as follows: M-H broth dry powder (MUELLER-HINTON BROTH); OXOID, UK, carbonyl cyanide 3-chlorophenylhydrazone (CCCP); Sigma-Aldrich, USA, tigecycline dry powder (standard); Dalian Meilun Biological, China, magnesium chloride anhydrous; Shanghai Maclean, China, calcium chloride anhydrous; Shanghai Maclean, China, diethyl pyrocarbonate (DEPC); Sigma-Aldrich, USA, RNAiso Plus; TaKaRa, Dalian, China, LightCycler 480 SYBR Green I Master; Roche, Switzerland, Transcriptor cDNA Synth. Kit 1: Roche, Switzerland, Isopropanol; Guangzhou Chemical Reagent Factory, China, Chloroform; Guangzhou Chemical Reagent Factory, China, Anhydrous Ethanol; Guangzhou Chemical Reagent Factory, China, Dimethyl Sulfoxide (DMSO); Guangzhou Chemical Reagent Factory, China; Lysozyme; Sigma-Aldrich, USA; M-H Agarase; Sigma-Aldrich, USA. Aldrich; M-H agar dry powder (MUELLER-HINTON AGAR); OXOID, UK; 250 bp DNA Ladder (Dye Plus); and Baobao Bioengineering (Dalian) Co.

Table 1: Sequence list of fluorescent quantitative PCR primers.

Gene name	Primer name	Primer sequence(5′-3′)
rpoB	*rpoB*-F	TCCGCACGTAAAGTAGGAAC
	rpoB-R	ATGCCGCCTGAAAAAGTAAC
adeB	*adeB*-F	CTTGCATTTACGTGTGGTGT
	adeB-R	GCTTTTCTACTGCACCCAAA
adeG	*adeG*-F	GTGTAGTGCCACTGGTTACT
	adeG-R	ATGTGGGCTAGCTAACGGC
adeJ	*adeJ*-F	GGTCATTAATATCTTTGGC
	adeJ-R	GGTACGAATACCGCTGTCA

2.2. Drug Susceptibility Test (Broth Microdilution Method) and Efflux Pump Inhibition Test. The drug susceptibility test adopts the broth microdilution method, referring to the M07-A9 aerobic bacteria dilution method antibacterial drug susceptibility test standard (ninth edition) issued by the CLSI in the United States in 2012 [29]. The efflux pump inhibition test is the drug sensitivity test of TGC combined with CCCP efflux pump inhibitor (10ug/ml). The breakpoint of tigecycline sensitivity is based on the FDA standard: MIC≤2ug/ml is sensitive and MIC≥8ug/ml is resistant. *Escherichia coli* ATCC25922 were used as the drug-susceptible quality control bacteria, and *Acinetobacter baumannii* standard strain ATCC17978 was used as the control bacteria.

2.3. RNA Extraction and cDNA Synthesis. Extraction of bacterial total RNA was referred to the recommended steps of TaKaRa's RNAiso Plus (No. 9108/9109) and cDNA synthesis (reverse transcription) was performed according to the steps recommended by Transcriptor cDNA Synth. Kit 1 (No. 04 897 030 001).

2.4. Real-Time PCR. The standard strain of *Acinetobacter baumannii* ATCC17978 was used the control strain, and the mRNA expression of the *rpoB* reference gene of each target strain and the three efflux pump systems *adeB*, *adeG*, and *adeJ* of the RND family were detected, and the relative expression of these three efflux pump genes was calculated. Specific steps were as follows:

Synthesis of primer sequences: The primer sequences of target genes *adeB*, *adeG*, *adeJ*, and *rpoB* internal reference genes are shown in Table 1, and the synthesis was commissioned by BGI (Beijing Liuhe) Co.Ltd.

Reaction system and conditions: Follow the steps recommended by LightCycler 480 SYBR Green I Master.

Result data processing: Both the amplification curve and the dissolution curve were single-peak curves, indicating that

Table 2: List of primer sequences for each target gene.

Gene name	Primer name	Primer sequence(5′-3′)
adeR	*adeR*-F	GTTAAGGCAATAAAAAGTTGCTT
	adeR-R	TGGAGTAAGTGTGGAGAAATACG
adeS	*adeS*-F	CTTGGTTAGGTTAGATATGGCATT
	adeS-R	GGCGTGGGATATAGGCTAGATAA
plsC	*plsC*-F	CTAGGATCCTACCAGCCATTTGTTCGC
	plsC-R	TTGGTCGACCACGGTGATATTTCGTTTGC
trm	*Trm*-F	AAGGATCCACTTTATATGAGTCACC
	Trm-R	ATAACTGGATCCATCCACTCACCTT
rpsJ	*rpsJ*-F	ACCCAAAGCGATCTGAACATCAACAC
	rpsJ-R	ATGTCTAACCAGAGAATTCGTATCCGTCTTAAGTC

the product amplification repeatability and specificity were good, and the qualified test data was collected for calculation. mRNA relative expression $(RE) = 2^{-\triangle\triangle}Ct$, where $^{\triangle\triangle}Ct$ = (Ct Target-Ct *rpoB*) target strain-(Ct Target - Ct *rpoB*) control strain.

2.5. Detection of Efflux Pump Regulator Gene adeRS and Drug Resistance Related Genes plsC, Trm and rpsJ. Preparation of bacterial genomic DNA template is as follows: scrape a ring of fresh monoclonal bacteria cultured on LB agar medium overnight, resuspend in sterilized water, place in a 100°C water bath for 10 min, and collect the supernatant by centrifugation as the strain genomic DNA template.

Synthesis of primer sequences is as follows: the primer sequences of regulatory genes *adeR*, *adeS*, and drug resistance-related genes *plsC*, *trm*, and *rpsJ* are shown in Table 2, and the synthesis was commissioned by BGI (Beijing Liuhe) Co.Ltd.

The target gene amplification was performed in the Applied Biosystems PCR system (Veriti Thermal Cycler) with Golden DNA polymerase (Golden Easy PCR System KT221, TIANGEN BIOTECH (BEIJING), China).

The amplification conditions of the regulated genes *adeR* and *adeS* are shown as follows. The amplification conditions included 35 cycles of amplification under the following conditions: initial denaturation at 94°C for 5 min, denaturation at 94°C for 30 s, annealed at 54°C for 30 s, extend at 72°C for 2 min, and a final extension at 72°C for 5 min.

The amplification conditions of drug resistance-related genes *plsC*, *trm*, and *rpsJ* were shown as follows. Amplification was carried out with the following thermal cycling conditions: 5 min at 94°C and 35 cycles of amplification consisting of 30 s at 94°C, 30 s at 58/56/54°C (for *plsC*/*trm*/*rpsJ*, respectively), and 1 min at 72°C, with 5 min at 72°C for the final extension.

2.6. PCR Product Electrophoresis and Gel Imaging. Recovery, purification, and sequencing of PCR products by electrophoresis and gel cutting, BGI (Beijing Liuhe) Co., Ltd. was entrusted to carry out electrophoresis, gel cutting, recovery, and purification of PCR products, and the Sanger method was used for two-way detection and splicing.

Gene sequence alignment submitted the spliced gene sequence fragments to the PubMed website for BLAST alignment and annotated the unknown sequence fragments. Using the *adeR*, *adeS*, *plsC*, *trm*, and *rpsJ* genes in the complete genome of *Acinetobacter baumannii* standard strain ATCC17978 (NZ_CP018664.1) as the reference sequence, Bioedit and SnapGene software were used to perform multiple sequence alignment, translation, and mutation type of each spliced sequence identification.

2.7. Statistical Methods. The database was established using SPSS version 21.0 software package and statistical processing was performed. Normally distributed measurement data were described as mean ± standard deviation ($\bar{x} \pm SD$), and comparisons were made using independent samples *t*-test; nonnormally distributed measurement data were described as median (25% quantile~75% quantile); and described and compared using rank sum test. $P < 0.05$ difference was statistically significant. Graphs were drawn using GraphPad Prism 7.

3. Results

3.1. Drug Susceptibility Test and Efflux Pump Inhibition Test. The distribution of tigecycline MIC of 72 extensive drug-resistant *Acinetobacter baumannii* strains was shown in Figure 1, and the range of MIC was distributed between 16-0.5 ug/ml. According to the FDA tigecycline susceptibility criteria (MIC≥8 ug/ml as resistant, MIC≤2 ug/ml as sensitive), these *Acinetobacter baumannii* were divided into two groups: tigecycline sensitive extensive drug-resistant *Acinetobacter baumannii* (TS-XDR AB) group, which tigecycline MIC was less than or equal to 2 ug/ml, and tigecycline insensitive extensive drug-resistant *Acinetobacter baumannii* (TIS-XDR AB) group, which tigecycline MIC was greater than 2ug/ml. Among them, there were 59 strains (81.9%) in TS-XDR AB group and 13 strains (18.1%) in TIS-XDR AB group. The number of MIC 2 and 1 strains was relatively high, with 24 (33.3%) and 28 (38.9%) strains, respectively. This part of the results showed that this TIS-XDR AB accounted for only a small proportion of XDR AB, but they could indeed be isolated from clinical patients, and even

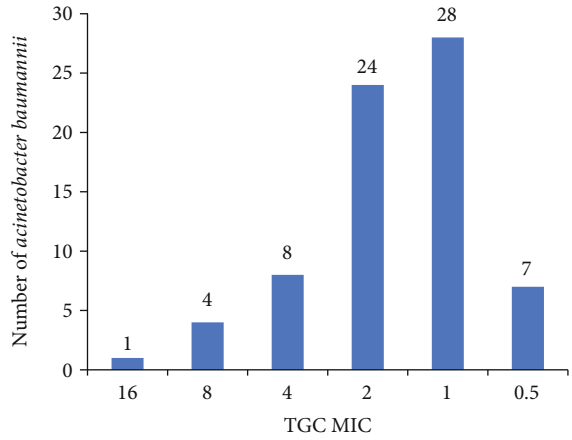

Figure 1: Distribution of tigecycline (TGC) MIC of 72 extensive drug-resistant *Acinetobacter baumannii* strains.

individual TIS-XDR AB developed high levels of resistance to tigecycline.

When the efflux pump inhibitor CCCP was added, the statistics of the MIC decreased of tigecycline in *Acinetobacter baumannii* were shown in Table 3 and Figure 2. Among them, the tigecycline MIC of 36 strains decreased by 2-8 times, accounting for 50%, 26 strains (44.1%) were TS-XDR AB, and 10 strains (76.9%) were TIS-XDR AB. The proportion of TIS-XDR AB with tigecycline MIC decreased was higher than that in TS-XDR AB group, which was statistically significant ($P = 0.032$). That is, the tigecycline MIC decreased of the TIS-XDR AB group was inhibited by the efflux pump was significantly higher than the TS-XDR AB group. The tigecycline MIC decreased by more than 2 times, which significantly affected by CCCP, including 6 strains, accounting for about 8.3%, of which 4 strains were TIS-XDR AB, and 2 strains were TIS-XDR AB. This part of the results showed that efflux pump inhibitors play a more important role in reducing tigecycline sensitivity in TIS-XDR AB than in TS-XDR AB.

3.2. Analysis of the Relative Expression of Efflux Pump System Detected by Real-Time Quantitative PCR. The relative expression (RE) of three main efflux pump genes was different between the TS-XDR AB group and the TIS-XDR AB group. Statistical analysis, the results are shown in Figure 3.

There is a significant difference in the relative expression of *adeB* gene between these two groups ($P = 0.025$). The relative expression of *adeB* in the TIS-XDR AB group is significantly higher than that in the TS-XDR AB group. However, there was no significant difference in the relative expression of *adeG* and *adeJ* genes between these two groups. This part of the results showed that *adeB* was significantly overexpressed in TIS-XDR AB compared with TS-XDR AB.

3.3. Analysis of the Relationship between the Relative Expression of the Efflux Pump System and the Decrease in Tigecycline Sensitivity. Grouping according to the efflux pump inhibition experiment, the RE of three major efflux pump genes was statistically analyzed between the tigecycline MIC decreased group and the tigecycline MIC no changed group, and the results were shown in Figure 4.

Table 3: TGC MIC decreased of *Acinetobacter baumannii* altered by CCCP.

	XDR AB	TS-XDR AB	TIS-XDR AB	*P*
Total number	72	59	13	
Number of TGC MIC decreased	36	26	10(76.9%)	
Rate of TGC MIC decreased	50%	44.1%	76.9%	0.032*

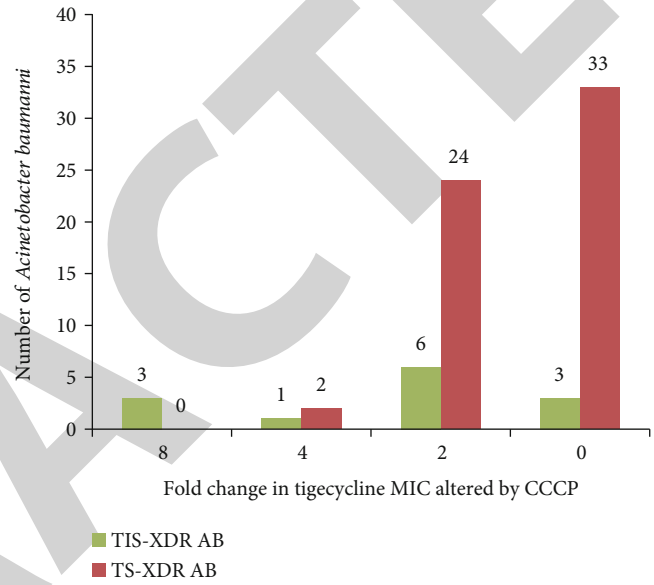

Figure 2: Distribution of fold change in tigecycline MIC of *Acinetobacter baumannii* altered by CCCP (carbonyl cyanide 3-chlorophenylhydrazone).

It can be seen that there was a significant difference in the RE of *adeB* gene between these two groups; that is, the RE of *adeB* in the tigecycline MIC decreased group is significantly higher than that in the tigecycline MIC no changed group. However, there was no significant difference in the RE of *adeG* and *adeJ* genes between these two groups. This part of the results showed that the overexpression of *adeB* was closely related to the reduction of tigecycline resistance in XDR AB by efflux pump inhibitors.

3.4. Amplification and Sequence Alignment of Efflux Pump Regulator Genes adeR and adeS and Drug Resistance-Related Genes plsC, Trm and rpsJ. The efflux pump regulation genes (*adeR* and *adeS*) and tigecycline resistance related genes (*plsC*, *trm*, and *rpsJ*) of 13 tigecycline insensitive extensive drug-resistant *Acinetobacter baumannii* were detected, and 4 tigecycline sensitive extensive drug-resistant *Acinetobacter baumannii* were used as controls. The tigecycline MIC of these *Acinetobacter baumannii* were shown in Tables 4.

The expected amplified fragments of *adeR* and *adeS* genes are about 800 bp and 1200 bp, and most strains can amplify the corresponding specific target fragments. The

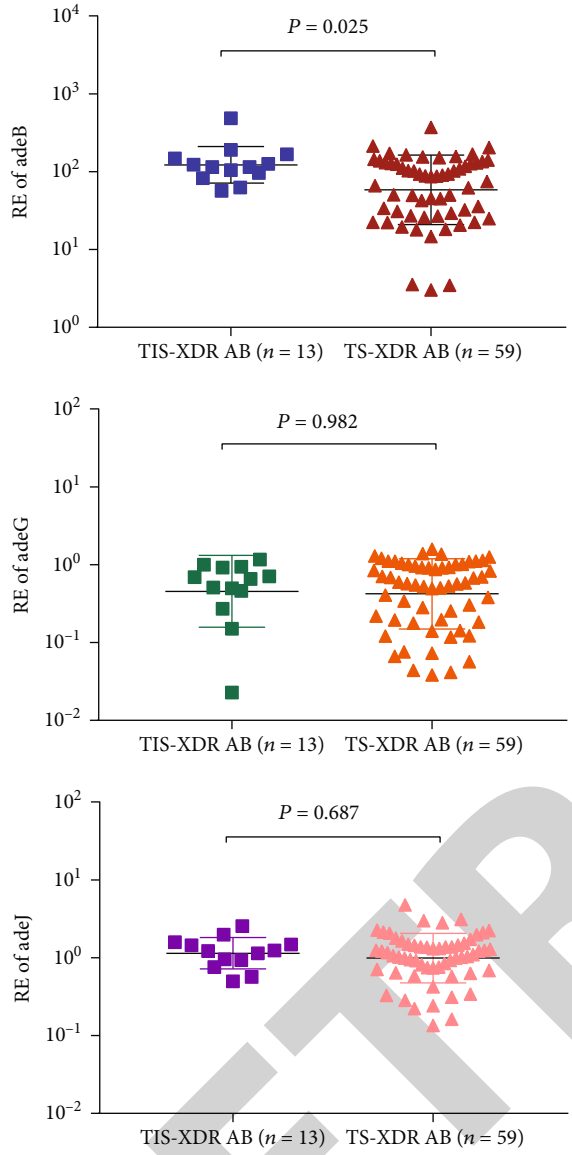

Figure 3: Relative expressions (RE) of efflux pump genes (*adeB*, *adeG*, and *adeJ*) of *Acinetobacter baumannii*. TIS-XDR AB: tigecycline insensitive extensive drug-resistant *Acinetobacter baumannii*; TS-XDR AB: tigecycline sensitive extensive drug-resistant *Acinetobacter baumannii*.

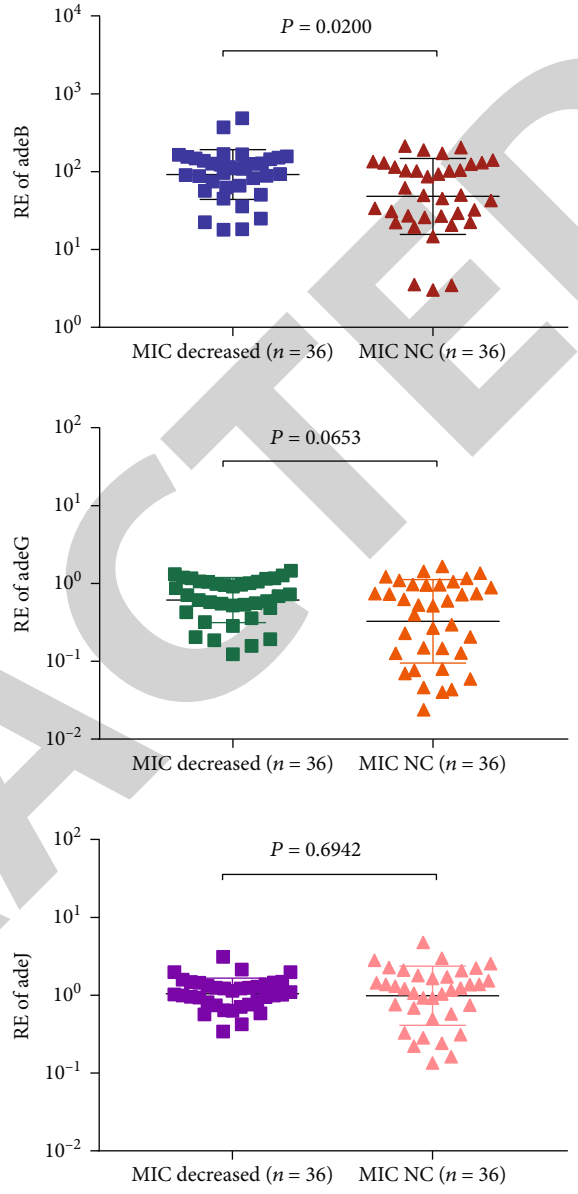

Figure 4: Relative expressions (RE) of efflux pump genes (*adeB*, *adeG*, and *adeJ*) of *Acinetobacter baumannii*. MIC decreased: the tigecycline MIC decreased group; MIC NC: the tigecycline MIC no changed group.

electropherogram of some strains were shown in Figure 5. Among them, the target fragments of the *adeS* gene amplified by the four strains 587, 576, 579, and 594 were significantly larger than expected, and the bands were about 2500 bp in Figure 5(b), suggesting that these genes may have inserted sequences.

The expected amplified fragments of *plsC*, *trm*, and *rpsJ* genes are about 1400 bp, 1200 bp, and 300 bp, and each strain can amplify the corresponding specific purpose fragment, the electropherogram of PCR products of some strains were shown in Figure 6.

These 17 extensive drug-resistant *Acinetobacter baumannii* have detected mutations in *adeR* and *adeS* genes, including substitution, insertion mutation, and deletion mutations. The nonsynonymous mutations of each strain were shown in Table 5. It can be seen in the table that there were 5-6 missense mutations in the *adeS* gene of each strain, but only 2-3 missense mutations in *adeR*. Among them, the *adeR* of 511S, 576, and 594 strains had single-base insertions at different sites (Insert652A, Insert718G, Insert32C) resulting in nonsense mutation which is the early appearance of termination codons (229 Stop, 246 Stop, 13 Stop). The translationally synthesized peptide chain was shortened. In addition, the insertion sequence ISAba1 appeared at the 3′ end of the *adeS* of strains 576, 579, 587, and 594, which would affect the transcription of downstream genes. This part of the results showed that several nonsynonymous mutations were detected in *adeR* and *adeS* genes.

Table 4: TGC MIC of 17 extensive drug-resistant *Acinetobacter baumannii*.

Strain number	498	502	507	511R	517	528	579	583	587	588	591	594
TGC MIC (μg/ml)	4	4	4	16	8	8	8	8	4	4	4	4
Strain number	511S	524	576	590S								
TGC MIC (μg/ml)	0.5	1	1	0.25								

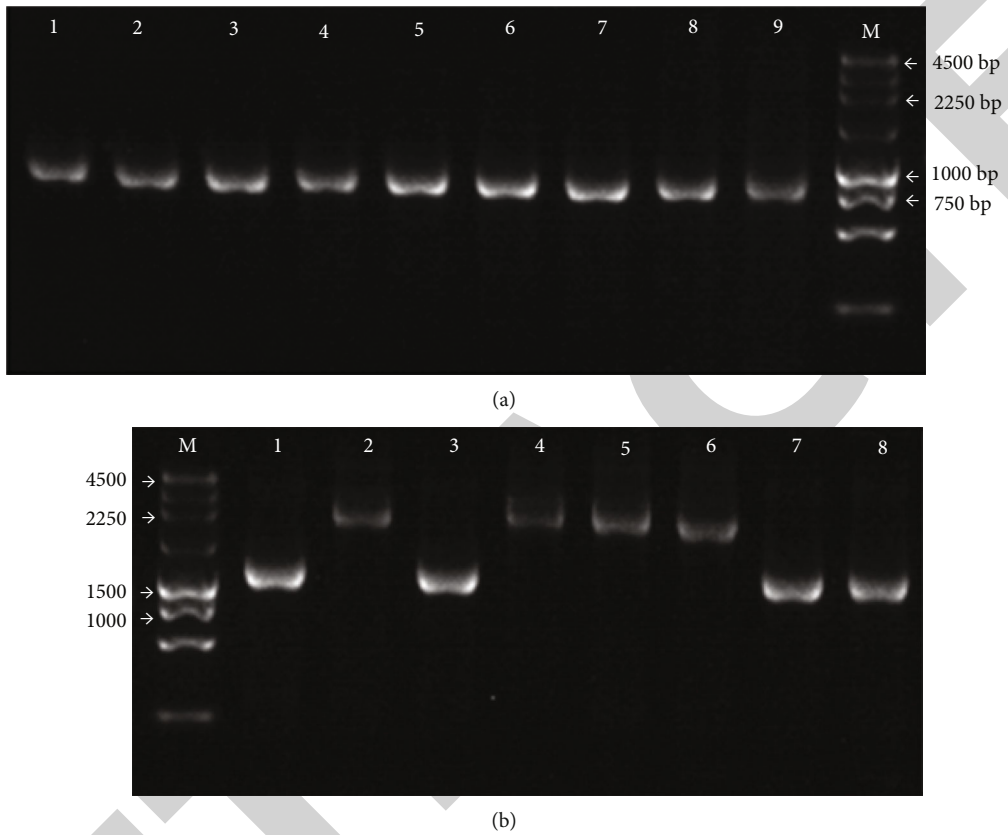

Figure 5: Electropherogram of efflux pump regulation genes *adeR* and *adeS* of *Acinetobacter baumannii* ((a) *adeR* gene, 1-9 were 583, 587, 588, 594, 576, 579, 590S, 591, ATCC17978; (b) *adeS* gene, 1-9 were 583, 587, 588, 594, 576, 579, 590S, 591, respectively, of which 587, 594, 576, 579 target fragments were about 2500 bp, larger than expected fragments, suggesting that there may be an insertion sequence.).

These 17 extensive drug-resistant *Acinetobacter baumannii* were found to contain mutations in *plsC*, *trm* genes, including substitution, insertion mutation, and deletion mutation. The nonsynonymous mutations of each strain were shown in Table 5. No mutation was found in the *rpsJ*. There was a missense mutation (CAA592AAA) and a terminator codon mutation (TAA925AAA) in the *plsC* gene. There were insertions or deletions bases at different sites (Insert29A, Deletion51A, Deletion267A) in the *trm* gene, resulting in nonsense mutation which is the early appearance of termination codons (16 Stop, 37 Stop, 92 Stop), and the peptide chain synthesized by translation of the gene was shortened. This part of the results showed that nonsynonymous mutations were detected in both *plsC* and *trm* but not in *rpsJ*.

4. Discussion

The efflux pump mechanism is an important mechanism for the resistance of *Acinetobacter baumannii* tigecycline. The RND family is the first reported and widely recognized efflux pump family, including *AdeABC*, *AdeFGH*, and *AdeIJK*. Among them, overexpression of *adeABC* efflux pump system plays the largest role in drug resistance [30–32]. Efflux pump inhibitors restore sensitivity to the drug by inhibiting the active efflux of the *Acinetobacter baumannii* efflux pump.

In this study, the relative expression levels of the multidrug transporter genes *adeB*, *adeG*, and *adeJ* in the efflux pump systems *adeABC*, *adeFGH*, and *adeIJK* of 72 XDR-Aba strains were detected, and it was found that the relative expression levels of *adeB* were significantly increased. Moreover, the relative expression of TIS group was significantly higher than that of TS-XDR group, suggesting that overexpression of *adeB* was closely related to tigecycline resistance in *Acinetobacter baumannii*, and overexpression of *adeB* was the main factor reducing the sensitivity of tigecycline in *Acinetobacter baumannii*. While the relative expression of *adeG* and *adeJ* did not increase significantly, and there was no significant difference between the two groups, suggesting that the expression

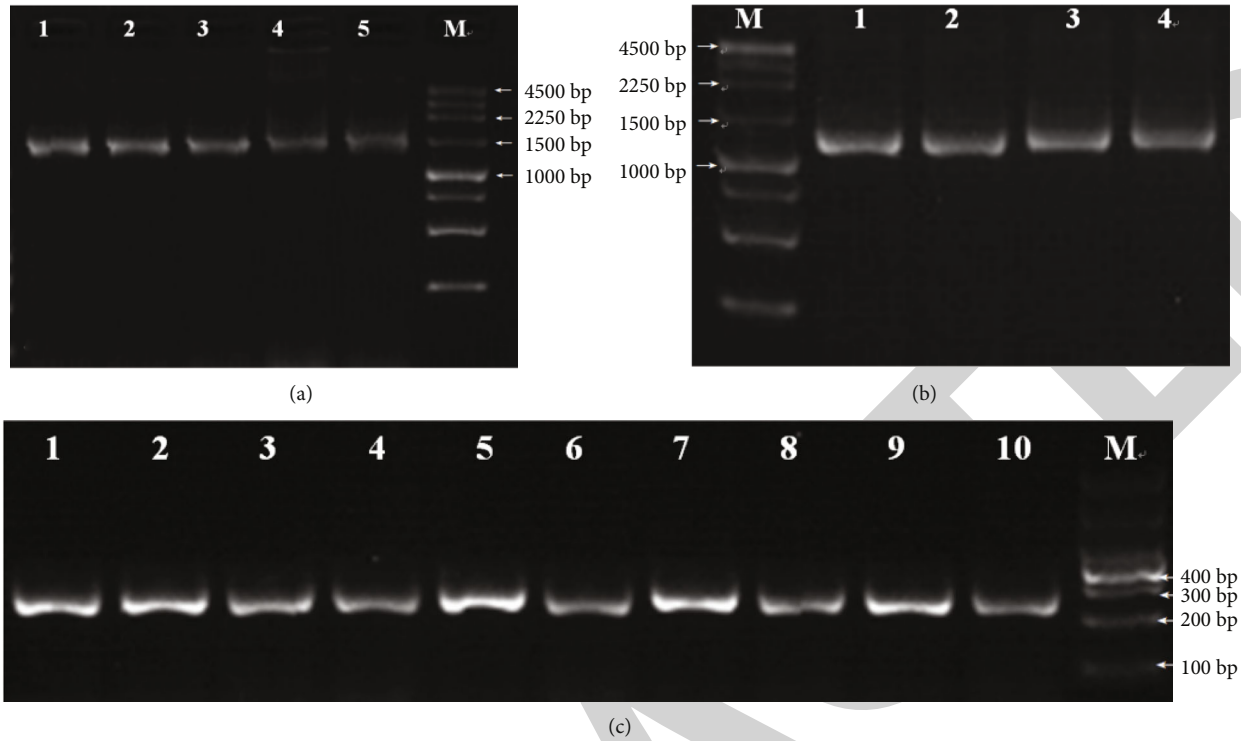

Figure 6: Electropherogram of tigecycline resistance-related genes *plsC*, *trm*, and *rpsJ* in *Acinetobacter baumannii* ((a) *plsC* gene, 1-5 were511R, 528, 579, 591, ATCC17978; (b) *trm* gene, 1-4 were498, 502, 507, 512, respectively; (c) *rpsJ* gene, 1-10 were 498, 502, 507, 512, 517, 536, 583, 587, 588, 594, respectively).

of these two efflux pump systems is not closely related to the tigecycline resistance of *Acinetobacter baumannii*, and their overexpression is not a cause of reduced tigecycline susceptibility in *Acinetobacter baumannii*. These results are consistent with other reports [21, 33, 34].

The efflux pump inhibition test also confirmed the above inference that after the addition of CCCP, the relative expression of *adeB* in the tigecycline MIC decreased group is significantly higher than that in the tigecycline MIC no changed group, suggesting that overexpression of *adeB* is closely related to the decreased tigecycline sensitivity induced by the inhibition of efflux pump, and overexpression of *adeB* is the main factor that efflux pump inhibitors reduce the tigecycline sensitivity of clinical *Acinetobacter baumannii*. While the relative expression of *adeG* and *adeJ* did not increase significantly, and there was no significant difference between the two groups, suggesting that the expression of these two efflux pump systems is not closely related to the decrease of tigecycline sensitivity due to the inhibition of efflux pumps, and their overexpression is not the reason that efflux pump inhibitors reduce tigecycline sensitivity in *Acinetobacter baumannii*. 50% (36 strains) of the strains showed a 2-8 fold decrease in MIC, suggesting that the active efflux of the efflux pump can increase the tigecycline MIC of most strains. However, only 8.3% (6 strains) of the strains had a greater than 2-fold decrease in MIC, of which 4 were non-susceptible strains, and the proportion of non-susceptible strains was 30.8% (4/13 strains), suggesting that the role of the efflux pump in affecting tigecycline MIC is limited. It is possible that multiple resistance mechanisms may combine to influence the sensitivity of tigecycline. In conclusion, although the efflux pump mechanism may play a limited role, the efflux pump system adeABC was widely present in *Acinetobacter baumannii* [35, 36], which is a fundamental factor for increasing the level of tigecycline resistance, and is even more critical in the resistance mechanism of a small number of strains.

Overexpression of the *adeABC* efflux pump system is regulated by the two-component regulatory gene *adeRS*, and mutations in either the *adeR* or *adeS* genes may lead to *adeABC* expression [37–39]. *adeB* expression was significantly increased in all 13 tigecycline-insensitive strains, and detection of *adeR* and *adeS* genes in these strains revealed by comparison that they had 2-7 nonsynonymous mutations. The *adeS* gene was more prone to mutations than the *adeR* gene, a phenomenon in agreement with the studies of Montana S et al. [40] and Hammerstrom Troy G et al. [41], suggesting that *adeS* has a higher degree of genetic variation and plays a more active role in the regulation of *adeABC* overexpression. Four nonsynonymous point mutations (Val120Ile, Ala136Val, Gly232Ala, Asp20Asn) and one insertional mutation (Insert32C) were found in *adeR* gene, and 12 nonsynonymous point mutations (Ala94Val, Ala97Thr, Leu105Phe, Leu172Pro, Gly186Val Arg195Gln, Gln203Leu, Asn268His, Tyr303Phe, Lys315Asn, Gly319Ser, Val348Ile) and one insertional mutation (ISAba1 inserted at the end of *adeS*) were found in *adeS* gene. In addition to three *adeR* point mutations (Val120Ile, Ala136Val,

Table 5: Base changes of non-synonymous mutations in *adeRS*, *plsC*, *trm*, and *rpsJ* genes of each strain and their corresponding amino acid changes.

Strain number	*adeR*	*adeS*	*plsC*	*Trm*	*rpsJ*
498	GTC358ATC(Val120Ile); GCA407GTA(Ala136Val); GGC695GCC(Gly232Ala)	CTT515CCT(Leu172Pro); GGT557GTT(Gly186Val); AAT802CAT(Asn268His); TAT908TTT(Tyr303Phe); GTT1042ATT(Val348Ile)	CAA592AAA(Gln198Lys); TAA925AAA(Stop309Lys)	Deletion51A(CAA51CAG; Gln17Gln) 37 Stop	None
502	GTC358ATC(Val120Ile); GCA407GTA(Ala136Val); GGC695GCC(Gly232Ala)	CTT515CCT(Leu172Pro); GGT557GTT(Gly186Val); AAT802CAT(Asn268His); TAT908TTT(Tyr303Phe); GTT1042ATT(Val348Ile)	CAA592AAA(Gln198Lys); TAA925AAA(Stop309Lys)	Deletion51A(CAA51CAG; Gln17Gln) 37 Stop	None
507	GTC358ATC(Val120Ile); GCA407GTA(Ala136Val); GGC695GCC(Gly232Ala)	CTT515CCT(Leu172Pro); GGT557GTT(Gly186Val); AAT802CAT(Asn268His); TAT908TTT(Tyr303Phe); GTT1042ATT(Val348Ile)	CAA592AAA(Gln198Lys); TAA925AAA(Stop309Lys)	Deletion267A(ATA267ATG; Ile89Met) 92 Stop	None
511S	GAT58AAT(Asp20Asn); GTC358ATC(Val120Ile); GCA407GTA(Ala136Val); Insert652A(CTG652ACT; Leu218Thr) 229 Stop	CTC313TTC(Leu105Phe); CTT515CCT(Leu172Pro); GGT557GTT(Gly186Val); AAT802CAT(Asn268His); TAT908TTT(Tyr303Phe); GTT1042ATT(Val348Ile)	CAA592AAA(Gln198Lys); TAA925AAA(Stop309Lys)	ATT88CAT(Asn30His); Deletion267A(ATA267ATG; Ile89Met) 92 Stop	None
511R	GAT58AAT(Asp20Asn); GTC358ATC(Val120Ile); GCA407GTA(Ala136Val)	CTC313TTC(Leu105Phe); CTT515CCT(Leu172Pro); GGT557GTT(Gly186Val); AAT802CAT(Asn268His); TAT908TTT(Tyr303Phe); GTT1042ATT(Val348Ile)	CAA592AAA(Gln198Lys); TAA925AAA(Stop309Lys)	Deletion51A(CAA51CAG; Gln17Gln) 37 Stop	None
512	GTC358ATC(Val120Ile); GCA407GTA(Ala136Val)	CTT515CCT(Leu172Pro); GGT557GTT(Gly186Val); CAG608CTG(Gln203Leu); AAT802CAT(Asn268His); TAT908TTT(Tyr303Phe); GTT1042ATT(Val348Ile)	CAA592AAA(Gln198Lys); TAA925AAA(Stop309Lys)	Deletion267A(ATA267ATG; Ile89Met) 92 Stop	None
517	GAT58AAT(Asp20Asn); GTC358ATC(Val120Ile); GCA407GTA(Ala136Val)	CTC313TTC(Leu105Phe); CTT515CCT(Leu172Pro); GGT557GTT(Gly186Val); AAT802CAT(Asn268His); TAT908TTT(Tyr303Phe); GTT1042ATT(Val348Ile)	CAA592AAA(Gln198Lys); TAA925AAA(Stop309Lys)	Insert29A(GTG29GAT; Val10Asp) 16 Stop	None
524	GTC358ATC(Val120Ile); GCA407GTA(Ala136Val)	CTT515CCT(Leu172Pro); GGT557GTT(Gly186Val); AAT802CAT(Asn268His); TAT908TTT(Tyr303Phe); GTT1042ATT(Val348Ile)	CAA592AAA(Gln198Lys); TAA925AAA(Stop309Lys)	Deletion267A(ATA267ATG; Ile89Met) 92 Stop	None
528	GTC358ATC(Val120Ile); GCA407GTA(Ala136Val)	GCC281GTC(Ala94Val); CTT515CCT(Leu172Pro); GGT557GTT(Gly186Val); AAT802CAT(Asn268His); TAT908TTT(Tyr303Phe); GTT1042ATT(Val348Ile)	CAA592AAA(Gln198Lys); TAA925AAA(Stop309Lys)	Deletion51A(CAA51CAG; Gln17Gln) 37 Stop	None
576	GTC358ATC(Val120Ile); GCA407GTA(Ala136Val); Insert718G(CCC718GCC; Pro240Ala) 246 Stop	CTT515CCT(Leu172Pro); GGT557GTT(Gly186Val); AAT802CAT(Asn268His); TAT908TTT(Tyr303Phe); GTT1042ATT(Val348Ile); ISAba1	ACT55CCT(Thr19Pro); CAA592AAA(Gln198Lys); TAA925AAA(Stop309Lys)	Deletion267A(ATA267ATG; Ile89Met) 92 Stop	None
579	GTC358ATC(Val120Ile); GCA407GTA(Ala136Val)	CTT515CCT(Leu172Pro); GGT557GTT(Gly186Val); AAT802CAT(Asn268His); TAT908TTT(Tyr303Phe); AAA945AAT(Lys315Asn); GTT1042ATT(Val348Ile); ISAba1	CAA592AAA(Gln198Lys); TAA925AAA(Stop309Lys)	Deletion267A(ATA267ATG; Ile89Met) 92 Stop	None

Table 5: Continued.

Strain number	*adeR*	*adeS*	*plsC*	*Trm*	*rpsJ*
583	GTC358ATC(Val120Ile); GCA407GTA(Ala136Val)	GCA289ACA(Ala97Thr); CTT515CCT(Leu172Pro); GGT557GTT(Gly186Val); AAT802CAT(Asn268His); TAT908TTT(Tyr303Phe); GTT1042ATT(Val348Ile)	CAA592AAA(Gln198Lys); TAA925AAA(Stop309Lys)	Deletion267A(ATA267ATG; Ile89Met) 92 Stop	None
587	GTC358ATC(Val120Ile); GCA407GTA(Ala136Val)	CTT515CCT(Leu172Pro); GGT557GTT(Gly186Val); CGG584CAG(Arg195Gln); AAT802CAT(Asn268His); TAT908TTT(Tyr303Phe); GTT1042ATT(Val348Ile); ISAba1	CAA592AAA(Gln198Lys); TAA925AAA(Stop309Lys)	Deletion267A(ATA267ATG; Ile89Met) 92 Stop	None
588	GTC358ATC(Val120Ile); GCA407GTA(Ala136Val)	GCA289ACA(Ala97Thr); CTT515CCT(Leu172Pro); GGT557GTT(Gly186Val); AAT802CAT(Asn268His); TAT908TTT(Tyr303Phe); GTT1042ATT(Val348Ile)	CAA592AAA(Gln198Lys); TAA925AAA(Stop309Lys)	Deletion51A(CAA51CAG; Gln17Gln) 37 Stop	None
590S	GTC358ATC(Val120Ile); GCA407GTA(Ala136Val)	CTT515CCT(Leu172Pro); GGT557GTT(Gly186Val); AAT802CAT(Asn268His); TAT908TTT(Tyr303Phe); GGC955AGC(Gly319Ser); GTT1042ATT(Val348Ile); ACC1048GCC(Thr350Ala)	CAA592AAA(Gln198Lys); TAA925AAA(Stop309Lys)	Deletion267A(ATA267ATG; Ile89Met) 92 Stop	None
591	GTC358ATC(Val120Ile); GCA407GTA(Ala136Val)	CTT515CCT(Leu172Pro); GGT557GTT(Gly186Val); AAT802CAT(Asn268His); TAT908TTT(Tyr303Phe); GGC955AGC(Gly319Ser); GTT1042ATT(Val348Ile)	CAA592AAA(Gln198Lys); TAA925AAA(Stop309Lys)	GAG135GAC(Glu45Asp); Deletion267A(ATA267ATG; Ile89Met) 92 Stop	None
594	Insert32C(CAA32CCA; Gln11Pro) 13 Stop	CTT515CCT(Leu172Pro); GGT557GTT(Gly186Val); CGG584CAG(Arg195Gln); AAT802CAT(Asn268His); TAT908TTT(Tyr303Phe); GTT1042ATT(Val348Ile); ISAba1	CAA592AAA(Gln198Lys); TAA925AAA(Stop309Lys)	Deletion267A(ATA267ATG; Ile89Met) 92 Stop	None

Asp20Asn) and four *adeS* point mutations (Ala94Val, Gly186Val, Asn268His, Val348Ile) and the insertion of ISAba1 mutation in *adeS* were reported to be associated with *adeABC* overexpression in previous studies [21, 36, 42, 43]; the remaining one *adeR* point mutation (Gly232Ala) and eight *adeS* point mutations (Ala97Thr, Leu105Phe, Leu172-Pro, Arg195Gln, Gln203Leu, Tyr303Phe, Lys315Asn, Gly319Ser) were newly detected in this study, and these mutations may lead to elevated expression of *adeABC*, but their specific effects remain to be experimentally verified. In addition to the efflux pump mechanism, some studies in recent years have also reported that mutations in the *trm*, *rpsJ* and *plsC* genes lead to increased tigecycline resistance [26–28]. Therefore, this study detected the sequences of these genes in 13 tigecycline-insensitive strains and 4 tigecycline-sensitive strains, to understand the resistance mechanism of tigecycline-insensitive *Acinetobacter baumannii* in our hospital. *Trm* gene detection found that 17 strains all had single base deletions or insertions (Insert29A, Deletion51A, Deletion267A) at different sites, resulting in nonsense mutation which is the early appearance of stop codons (16 Stop, 37 Stop, 92 Stop) and shortened synthesis. However, 4 of them were tigecycline-sensitive strains with MICs ranging from 0.25 to 1 ug/ml, so it was speculated that *trm* deletion could not significantly improve the resistance of *Acinetobacter baumannii* to tigecycline. This result is different from previous reports that the study compared the whole gene sequence of the tigecycline-insensitive mutant strain and its parental strain by genome sequencing, and found that the *trm* deletion mutation was the only difference between the two. It is speculated that the *trm* gene deletion leads to the decrease of tigecycline sensitivity. Chen Q et al. [27] also found a 35 bp nucleotide deletion in the *trm* gene of the drug-resistant mutant strain by genome sequencing. The wild-type *trm* gene complementation experiment restored the mutant strain's sensitivity to tigecycline, confirming that the *trm* gene mutation is one of the mechanisms of tigecycline resistance in *Acinetobacter baumannii*. Based on the above findings, we believe that *trm* gene deletion leads to tigecycline resistance is still controversial, and more studies are needed to clarify. *plsC* gene detection found that non-synonymous point mutations (Gln198Lys) and terminator codon mutations (Stop309Lys) were also present in tigecycline-sensitive *Acinetobacter baumannii*, suggesting that these mutations could not lead to tigecycline resistance. Although the study by Li X et al. [28] confirmed that the frameshift mutation of the *plsC* gene caused the synthetic shortened peptide chain leading to tigecycline resistance, this study did not detect the *plsC* gene deletion mutation. Therefore, the *plsC* gene deletion mutation is not the cause of the tigecycline resistance in *Acinetobacter baumannii* in our hospital. The *rpsJ* gene detection found that 13 strains did not find any mutation points, indicating that the gene is not related to tigecycline resistance in these strains.

In summary, our study revealed that the expression of *adeABC* efflux pump in extensive drug-resistant *Acinetobacter baumannii* was significantly increased, and the increase was more significant in tigecycline insensitive strains. The overexpression of *adeABC* was closely related to tigecycline resistance, and the mechanism of efflux pump was the cause of tigecycline resistance. It is a common and important mechanism, but only this mechanism has a limited impact, and most strains may have multiple resistance mechanisms that eventually lead to an increase of tigecycline resistance. *AdeABC* overexpression is the result of *adeRS* gene mutation, 1 *adeR* and 8 *adeS* point mutations have not been reported in previous studies, and the relationship between these mutant genes and *adeABC* overexpression remains to be explored. *trm*, *plsC*, and *rpsJ* genes have nothing to do with the resistance of *Acinetobacter baumannii* tigecycline in our hospital. The effect of *trm*, *plsC*, and *rpsJ* gene mutations on the development of tigecycline resistance in *Acinetobacter baumannii* remains unclear. Besides the pump mechanism, there might be other resistance mechanisms.

Data Availability

The datasets during the current study are available from the corresponding author on reasonable request.

Conflicts of Interest

The authors declare that they have no conflicts of interest.

Acknowledgments

This research was supported by the National Natural Science Foundation of China (Grant numbers: 82170014).

References

[1] A. Howard, M. O'Donoghue, A. Feeney, and R. D. Sleator, "*Acinetobacter baumannii*: an emerging opportunistic pathogen," *Virulence*, vol. 3, no. 3, pp. 243–250, 2012.

[2] H. W. Lee, Y. M. Koh, J. Kim et al., "Capacity of multidrug-resistant clinical isolates of *Acinetobacter baumannii* to form biofilm and adhere to epithelial cell surfaces," *Clinical Microbiology and Infection*, vol. 14, no. 1, pp. 49–54, 2008.

[3] S. J. Nigro and R. M. Hall, "Antibiotic resistance islands in A320 (RUH134), the reference strain for *Acinetobacter baumannii* global clone 2," *Journal of Antimicrobial Chemotherapy*, vol. 67, no. 2, pp. 335–338, 2012.

[4] C. Baiyi, H. Lixian, H. Bijie et al., "Expert consensus on diagnosis, treatment and prevention of Acinetobacter baumannii infection in China," *Chinese Journal of Medicine*, vol. 92, no. 2, pp. 76–85, 2012.

[5] A. P. Magiorakos, A. Srinivasan, R. B. Carey et al., "Multidrug-resistant, extensively drug-resistant and pandrug-resistant bacteria: an international expert proposal for interim standard definitions for acquired resistance," *Clinical Microbiology and Infection*, vol. 18, no. 3, pp. 268–281, 2012.

[6] L. S. Munoz-Price and R. A. Weinstein, "*Acinetobacter* infection," *The New England Journal of Medicine*, vol. 358, no. 12, pp. 1271–1281, 2008.

[7] H. Chang, Y. Chen, M. Lin et al., "Mortality risk factors in patients with *Acinetobacter baumannii* ventilator- associated pneumonia," *Journal of the Formosan Medical Association*, vol. 110, no. 9, pp. 564–571, 2011.

[8] H. Aydemir, G. Celebi, N. Piskin et al., "Mortality attributable to carbapenem-resistant nosocomial *Acinetobacter baumannii*

infections in a Turkish university hospital," *Japanese Journal of Infectious Diseases*, vol. 65, no. 1, pp. 66–71, 2012.

[9] S. T. Huang, M. C. Chiang, S. C. Kuo et al., "Risk factors and clinical outcomes of patients with carbapenem-resistant *Acinetobacter baumannii* bacteremia," *Journal of Microbiology, Immunology, and Infection*, vol. 45, no. 5, pp. 356–362, 2012.

[10] Y. Zheng, Y. Wan, L. Zhou et al., "Risk factors and mortality of patients with nosocomial carbapenem-resistant *Acinetobacter baumannii* pneumonia," *American Journal of Infection Control*, vol. 41, no. 7, pp. e59–e63, 2013.

[11] E. V. Lemos, F. P. de la Hoz, T. R. Einarson et al., "Carbapenem resistance and mortality in patients with *Acinetobacter baumannii* infection: systematic review and meta-analysis," *Clinical Microbiology and Infection*, vol. 20, no. 5, pp. 416–423, 2014.

[12] L. R. Peterson, "A review of tigecycline – the first glycylcycline," *International Journal of Antimicrobial Agents*, vol. 32, pp. S215–S222, 2008.

[13] K. B. Waites, L. B. Duffy, and M. J. Dowzicky, "Antimicrobial susceptibility among pathogens collected from hospitalized patients in the United States and in vitro activity of tigecycline, a new glycylcycline antimicrobial," *Antimicrobial Agents and Chemotherapy*, vol. 50, no. 10, pp. 3479–3484, 2006.

[14] R. E. Mendes, D. J. Farrell, H. S. Sader, and R. N. Jones, "Comprehensive assessment of tigecycline activity tested against a worldwide collection of *Acinetobacter* spp. (2005 -2009)," *Diagnostic Microbiology and Infectious Disease*, vol. 68, no. 3, pp. 307–311, 2010.

[15] M. W. Olson, A. Ruzin, E. Feyfant, T. S. Rush III, J. O'Connell, and P. A. Bradford, "Functional, biophysical, and structural bases for antibacterial activity of tigecycline," *Antimicrobial Agents and Chemotherapy*, vol. 50, no. 6, pp. 2156–2166, 2006.

[16] S. L. Da and S. H. Nunes, "Tigecycline: a review of properties, applications, and analytical methods," *Therapeutic Drug Monitoring*, vol. 32, no. 3, pp. 282–288, 2010.

[17] Y. Sun, Y. Cai, X. Liu, N. Bai, B. Liang, and R. Wang, "The emergence of clinical resistance to tigecycline," *International Journal of Antimicrobial Agents*, vol. 41, no. 2, pp. 110–116, 2013.

[18] C. Rumbo, E. Gato, M. López et al., "Contribution of efflux pumps, Porins, and β-lactamases to multidrug resistance in clinical isolates of *Acinetobacter baumannii*," *Antimicrobial Agents and Chemotherapy*, vol. 57, no. 11, pp. 5247–5257, 2013.

[19] J. M. Blair, G. E. Richmond, and L. J. Piddock, "Multidrug efflux pumps in gram-negative bacteria and their role in antibiotic resistance," *Future Microbiology*, vol. 9, no. 10, pp. 1165–1177, 2014.

[20] E. J. Yoon, Y. Nait Chabane, S. Goussard et al., "Contribution of resistance-nodulation-cell division efflux systems to antibiotic resistance and biofilm formation in Acinetobacter baumannii," *MBio*, vol. 6, no. 2, 2015.

[21] H. Li, X. Wang, Y. Zhang et al., "The role of RND efflux pump and global regulators in tigecycline resistance in clinicalAcinetobacter baumanniiisolates," *Future Microbiology*, vol. 10, no. 3, pp. 337–346, 2015.

[22] Y. Yuhan, Y. Ziyun, Z. Yongbo, L. Fuqiang, and Z. Qinghua, "Over expression of AdeABC and AcrAB-TolC efflux systems confers tigecycline resistance in clinical isolates of *Acinetobacter baumannii* and *Klebsiella pneumoniae*," *Revista da Sociedade Brasileira de Medicina Tropical*, vol. 49, no. 2, pp. 165–171, 2016.

[23] L. Damier-Piolle, S. Magnet, S. Brémont, T. Lambert, and P. Courvalin, "AdeIJK, a resistance-nodulation-cell division pump effluxing multiple antibiotics in *Acinetobacter baumannii*," *Antimicrobial Agents and Chemotherapy*, vol. 52, no. 2, pp. 557–562, 2008.

[24] T. Chang, B. Huang, J. Sun et al., "AdeR protein regulates *adeABC* expression by binding to a direct-repeat motif in the intercistronic spacer," *Microbiological Research*, vol. 183, pp. 60–67, 2016.

[25] G. E. Richmond, L. P. Evans, M. J. Anderson et al., "The *Acinetobacter baumannii* two-component system *AdeRS* regulates genes required for multidrug efflux, biofilm formation, and virulence in a strain-specific manner," *MBio*, vol. 7, no. 2, pp. e416–e430, 2016.

[26] K. Beabout, T. G. Hammerstrom, A. M. Perez et al., "The ribosomal S10 protein is a general target for decreased tigecycline susceptibility," *Antimicrobial Agents and Chemotherapy*, vol. 59, no. 9, pp. 5561–5566, 2015.

[27] Q. Chen, X. Li, H. Zhou et al., "Decreased susceptibility to tigecycline in Acinetobacter baumannii mediated by a mutation in trm encoding SAM-dependent methyltransferase," *Journal of Antimicrobial Chemotherapy*, vol. 69, no. 1, pp. 72–76, 2014.

[28] X. Li, L. Liu, J. Ji et al., "Tigecycline resistance in *Acinetobacter baumannii* mediated by frameshift mutation in plsC, encoding 1-acyl-sn-glycerol-3-phosphate acyltransferase," *European Journal of Clinical Microbiology & Infectious Diseases*, vol. 34, no. 3, pp. 625–631, 2015.

[29] CLSI, *Methods for dilution antimicrobial susceptibility tests for bacteria that grow aerobically; aprroved standard - ninth edition. CLSI document M07-A9*, Clinical and Laboratory Standards Institute, Wayne, PA, 2012.

[30] A. Y. Peleg, J. Adams, and D. L. Paterson, "Tigecycline efflux as a mechanism for nonsusceptibility *in Acinetobacter baumannii*," *Antimicrobial Agents and Chemotherapy*, vol. 51, no. 6, pp. 2065–2069, 2007.

[31] S. Coyne, P. Courvalin, and B. Périchon, "Efflux-mediated antibiotic resistance in Acinetobacterspp," *Antimicrobial Agents and Chemotherapy*, vol. 55, no. 3, pp. 947–953, 2011.

[32] X. Li, P. Plésiat, and H. Nikaido, "The challenge of efflux-mediated antibiotic resistance in gram-negative bacteria," *Clinical Microbiology Reviews*, vol. 28, no. 2, pp. 337–418, 2015.

[33] M. Lin, Y. Lin, C. Tu, and C. Y. Lan, "Distribution of different efflux pump genes in clinical isolates of multidrug- resistant *Acinetobacter baumannii* and their correlation with antimicrobial resistance," *Journal of Microbiology, Immunology and Infection*, vol. 50, no. 2, pp. 224–231, 2017.

[34] A. Ruzin, F. W. Immermann, and P. A. Bradford, "RT-PCR and statistical analyses of adeABC expression in clinical isolates of *Acinetobacter calcoaceticus-Acinetobacter baumannii* complex," *Microbial Drug Resistance*, vol. 16, no. 2, pp. 87–89, 2010.

[35] W. Jia, C. Li, H. Zhang, G. Li, X. Liu, and J. Wei, "Prevalence of genes of *OXA-23* Carbapenemase and *AdeABC* efflux pump associated with multidrug resistance of *Acinetobacter baumannii* isolates in the ICU of a Comprehensive Hospital of Northwestern China," *International Journal of Environmental Research and Public Health*, vol. 12, no. 8, pp. 10079–10092, 2015.

[36] S. Pagdepanichkit, C. Tribuddharat, and R. Chuanchuen, "Distribution and expression of the Ade multidrug efflux systems in Acinetobacter baumanniiclinical isolates," *Canadian Journal of Microbiology*, vol. 62, no. 9, pp. 794–801, 2016.

Hindawi
Computational and Mathematical Methods in Medicine
Volume 2023, Article ID 9835206, 1 page
https://doi.org/10.1155/2023/9835206

Retraction

Retracted: An Eight-mRNA Prognostic Model to Predict Survival in Hepatic Cellular Cancer

Computational and Mathematical Methods in Medicine

Received 12 December 2023; Accepted 12 December 2023; Published 13 December 2023

This article has been retracted by Hindawi, as publisher, following an investigation undertaken by the publisher [1]. This investigation has uncovered evidence of systematic manipulation of the publication and peer-review process. We cannot, therefore, vouch for the reliability or integrity of this article.

Please note that this notice is intended solely to alert readers that the peer-review process of this article has been compromised.

Wiley and Hindawi regret that the usual quality checks did not identify these issues before publication and have since put additional measures in place to safeguard research integrity.

We wish to credit our Research Integrity and Research Publishing teams and anonymous and named external researchers and research integrity experts for contributing to this investigation.

The corresponding author, as the representative of all authors, has been given the opportunity to register their agreement or disagreement to this retraction. We have kept a record of any response received.

References

[1] D. Xia, X. Liao, and H. Zhang, "An Eight-mRNA Prognostic Model to Predict Survival in Hepatic Cellular Cancer," *Computational and Mathematical Methods in Medicine*, vol. 2023, Article ID 7278231, 7 pages, 2023.

Hindawi
Computational and Mathematical Methods in Medicine
Volume 2023, Article ID 7278231, 7 pages
https://doi.org/10.1155/2023/7278231

Research Article

An Eight-mRNA Prognostic Model to Predict Survival in Hepatic Cellular Cancer

Dong Xia, Xuebin Liao, and Huamao Zhang

General Surgery Ward 1, Dujiangyan People's Hospital, Dujiangyan, Chengdu, 611830 Sichuan, China

Correspondence should be addressed to Huamao Zhang; zhanghuamao987@fjmu.edu.cn

Received 3 August 2022; Revised 22 September 2022; Accepted 12 October 2022; Published 4 February 2023

Academic Editor: Min Tang

Background. Transcriptional dysregulation plays a critical role in the onset and development of malignant tumors. Employing gene dysregulation to forecast the change of tumors is valuable for cancer diagnosis. However, the prognostic prediction for HCC using combined gene models remains insufficient. *Methods*. The expression profiles of GSE103512 and TCGA-LIHC were downloaded. Gene Ontology (Go) was used to evaluate the overlapping differential genes (DEG) in TCGA and GSE103512. The core genes in the critical module most significantly related to HCC were obtained by WGCNA. Eight genes most significantly related to HCC and OS were identified by reweighted coexpression network analysis and Cox regression. *Results*. We selected eight genes, FZEB1, CDK1, RAD54L, COL1A2, ATP1B3, CASP8, USP39, and HOXB7. Moreover, we constructed an eight-gene model and forecasted the prognosis of HCC. ROC curve of the eight-mRNA prognostic model was screened out (AUC = 0.635), suggesting that this model exhibited a good prediction performance. Survival analysis showed that the survival rate of patients in the high-risk group was significantly lower than that in the low-risk group. *Conclusion*. The eight-mRNAs model might forecast the OS of HCC patients and advance remedial decision-making.

1. Introduction

Hepatocellular carcinoma (HCC) is the world's fifth most common malignant tumor, with more than 700000 new cancer cases worldwide every year [1, 2]. Although the primary prevention strategy, early screening and diagnosis, and more advanced treatment technologies have been applied, the overall incidence rate and mortality of HCC continue to rise [3]. The occurrence and development of HCC are regulated by multiple mechanisms and participated by multiple molecules [4, 5]. Despite the advancement of diagnostic and medicinal approaches, the forecast of HCC is relatively poor due to the elevated recurrence ratio [6]. Therefore, it is urgent to identify prognostic biomarkers, observe high-risk patients with poor prognoses, and prevent a recurrence.

With the rapid development of genomics, such as genes, proteins, metabolism, and in-depth research on tumor biology, hundreds of biomarkers with prognostic value have been identified [7]. There is an urgent need to analyze prognostic markers of hepatocellular carcinoma to guide clinical treatment strategies. Gene interaction networks provide the possibility of systematic analysis [8]. Previous studies have shown that gene interaction networks might be used to explore the potential internal relationship between functional gene clusters (functional modules) and prognostic factors [9]. The gene coexpression network could be constructed by weighted gene coexpression network analysis (WGCNA). The key modules might be used to explore tumor mechanisms, predict the survival rate of patients, and establish new diagnostic or therapeutic diagnostic strategies [10, 11]. WGCNA provides a functional interpretation tool for systems biology and has been applied in breast cancer, endometrial cancer, and other tumors [12].

To improve the accuracy of prognostic markers, a coexpression network was constructed with the integration of the protein interaction (PPI) data. In addition, it is well established that crucial genes have essential functions in disease development and tend to show consistent expression variations in patients. Therefore, selecting crucial genes as predictors to build a prognosis model could enhance the stability of the model and improve the biological correlation between the identified genes and disease.

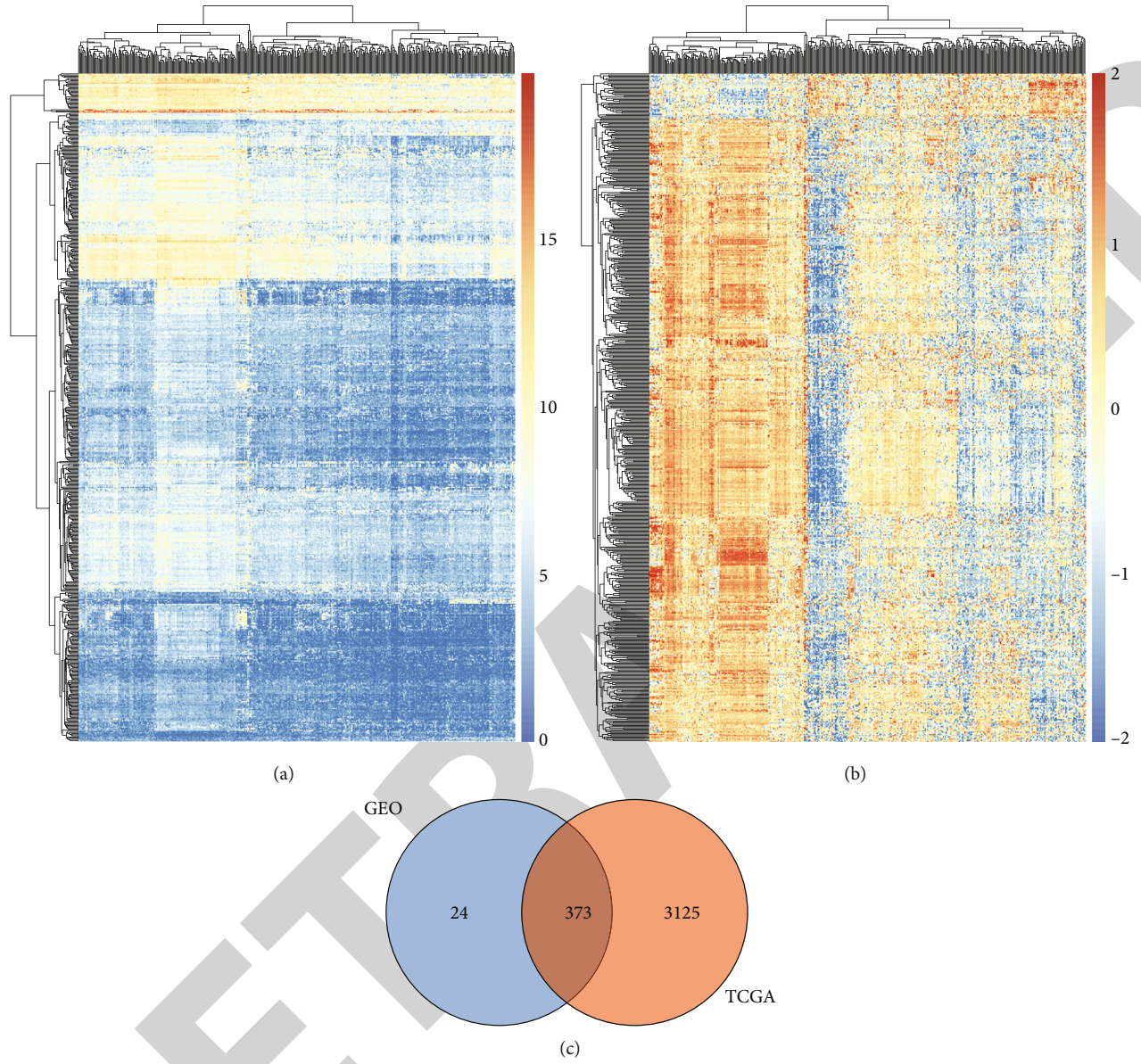

Figure 1: (a) A heat map showed the DEGs from the GSE103512 dataset. (b) A heat map showed the DEGs from the TCGA. (c) A Venn diagram showed the common DEGs by the intersection of TCGA and GSE103512. A total of 83 upregulated and 76 downregulated were identified.

2. Methods

2.1. Data Collection. The research data of patients are downloaded from the Cancer Genome Atlas (TCGA) liver hepatocellular carcinoma (LIHC) cohort and gene expression omnibus (GEO) GSE103512 dataset, which contains experimental and clinical data. The transcriptome sequencing data and clinical information of HCC patients were downloaded from this database, and the encoded gene expression was normalized.

2.2. Screening of Differentially Expressed Genes. R Studio was used to screen the differentially expressed genes (DEGs) with the "edger" package. The heat map was drawn for the DEGs. The false discovery rate (FDR) value of each gene was calculated by the BH method, and the fold change (FC) of gene expression level in HCC and adjacent tissues was calculated. The screening criteria are as follows: FDR < 0.05 and $|\log^2 FC| > 1$. $\log^2 FC > 1$ indicated that the gene expression was upregulated, and $\log^2 FC < -1$ indicated that the expression was downregulated.

2.3. Screening of Prognosis-Related Genes. Cox regression analysis screened genes related to overall survival (OS). For each gene, according to its expression value, the patients were divided into a high-expression group and a low-expression group for univariate regression analysis. The regression analysis was carried out by R software, and $P < 0.05$ was considered statistically significant.

2.4. Identification of the HCC Modules. The "WGCNA" package in R Studio was used to identify the modules. The

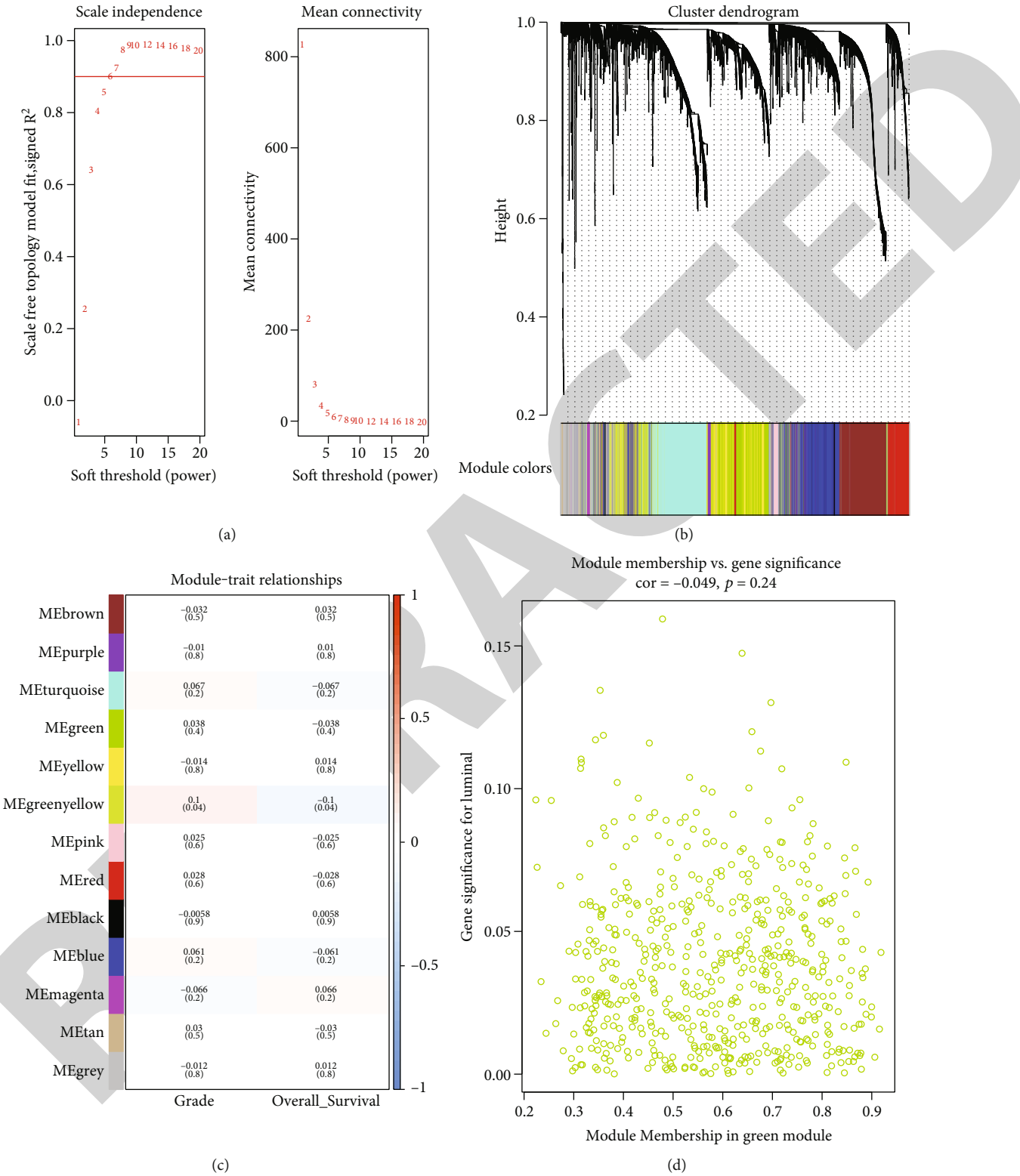

Figure 2: (a) The power value for the contiguity matrix in WGCNA. (b) The cluster dendrogram of mRNAs in GSE103512. (c) The association between modules and the clinical characters. (d) The scatter diagram of GS and MM in the green yellow module showed the correlation between OS genes.

"goodsamplegenes()" function was used to check whether there were abnormal genes in the data and selected an appropriate threshold to eliminate outliers. Draw a gene feature heat clustering diagram, and complete the construction of the coexpression network and the selection of modules. Choose the β value to calculate the adjacency matrix.

Construct a clustering tree to select modules, set the minimum capacity and cutting height of modules, and merge modules with high similarity. The prognosis module is identified by associating the module data with the characteristic clinical data. Scatter plots of gene significance (GS) and module membership (mm) were drawn in the prognosis module to clarify the importance of genes in the module.

2.5. Constructing PPI Network and Screening Hub Gene. The String database (http://string-db.org/) was used to build the PPI network. Input the filtered DEGs into the String database, and construct the PPI network matched with the total score > 0.3. The connectivity of protein nodes was calculated using the Cytohubba plug-in. Genes with high connectivity were regarded as hub genes.

2.6. Construction of Coexpression Network of Prognostic Genes. The weighted gene coexpression network analysis method is used to construct the HCC prognosis network. According to the topological overlap matrix, hierarchical clustering divides the network and identifies the modules in the network. The Benjamin-Hochberg method is used to correct the correlation coefficient P value of gene pairs in the module, and the gene pairs with $P < 0.05$ are selected to construct the module network.

2.7. Construction and Evaluation of the Eight-mRNA Prognostic Model. The "glmnet()" package in R Studio was used to construct and evaluate the eight-mRNA prognostic model. Draw the ROC curve of the model, and calculate the AUC to evaluate the prediction efficiency of the model. The high- and low-risk groups of HCC prognosis were divided by the median of the model risk score. The survival curve of the model was drawn by the Kaplan Meier method, and a log-rank test tested the survival difference to evaluate the ability of the model to distinguish the high and low risk of gastric cancer prognosis. If $P < 0.05$, the difference is statistically significant.

3. Results

3.1. Identification of DEGs. A total of 89 normal hepatic samples and 101 HCC samples were identified from the GSE103512 dataset. We obtained 197 downregulated DEGs and 200 upregulated DEGs in the GSE103512 dataset (Figure 1(a)). Furthermore, 1856 downregulated DEGs and 1642 upregulated DEGs were obtained from the TCGA dataset (Figure 1(b)). A total of 177 upregulated and 196 downregulated common DEGs were identified by the intersection of the two datasets (Figure 1(c)).

3.2. Identification of the Critical Module by WGCNA. Employing the WGCNA, the common DEGs were assessed for coexpression network analysis. The power of $\beta = 6$ and scale-free $R^2 = 0.89$ were chosen to construct a clustering tree, and a total of 13 modules were identified ultimately (Figure 2(a)). As shown in Figure 2(b), the ME of the green yellow module was the most significant gene module among the 13 modules. Furthermore, the ME in the green yellow module exhibited an advanced connection to overall survival

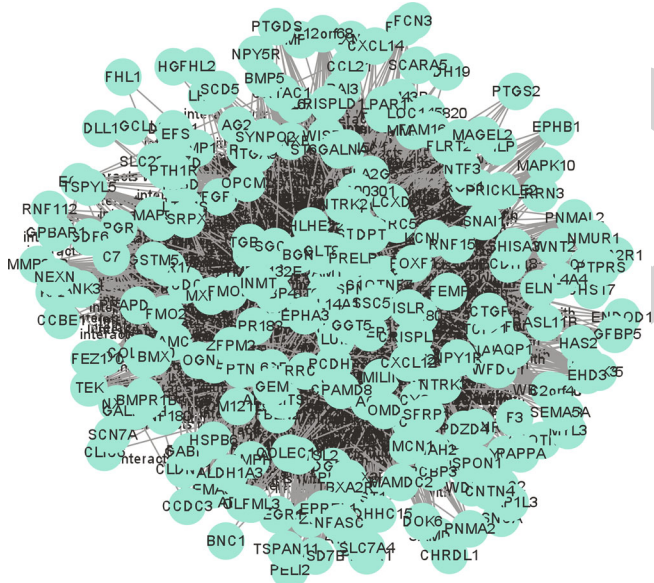

Figure 3: The PPI network was constructed for the green yellow module.

than other modules (Figure 2(c)). The scatter diagram of GS and MM in the green yellow module suggested that the genes in the green yellow module were highly correlated with the overall survival (Figure 2(d), $P < 0.05$). Consequently, we selected this green yellow module as the key module for further investigation.

3.3. Construction of PPI Network. For the green yellow module, the protein interaction data of module genes are used for reweighting. The PPI network containing 754 module genes was constructed using the String database. We obtained the reweighted coexpression network for the prognosis module, which contained 78 nodes and 503 edges. We next analyzed the topological characteristics of the reweighted module network and observed that the reweighted coexpression network could be defined as the small world network. Its small world index is 2.033. The genes with a weight greater than 0.3 in the reweighted coexpression network were selected, and the weight network diagram was depicted using Cytoscape software (Figure 3).

3.4. Go Enrichment Analysis. We performed the Go enrichment to obtain the enriched Go terms involved in the reweighted coexpression network. A total of 843 enriched Go terms were identified with FDR < 0.05. The FDR value less than 1×10^{-10} in the biological process is shown in Table 1. As shown in Table 1, the DEGs in the reweighted coexpression network were enriched in the ER-associated ubiquitin-dependent protein catabolic process, regulation of cell proliferation, endoplasmic reticulum lumen, and regulation of apoptotic process pathways.

3.5. Eight Genes Correlated with the OS of HCC Patients. Next, we calculate the score of each gene in the reweighted coexpression network and rank the genes according to the

Table 1: Go enrichment analysis for reweighted coexpression network.

GO:0000152~nuclear ubiquitin ligase complex	Number of alleles	FDR
GO:0043231~intracellular membrane-bounded organelle	35	$2.93E-13$
GO:0010008~endosome membrane	46	$2.95E-12$
GO:0019898~extrinsic component of membrane	37	$1.45E-16$
GO:0042405~nuclear inclusion body	59	$3.49E-12$
GO:0005740~mitochondrial envelope	27	$3.97E-12$
GO:0016020~membrane	44	$6.21E-12$
GO:0005788~endoplasmic reticulum lumen	61	$6.35E-14$
GO:0000800~lateral element	53	$3.03E-24$
GO:0051092~positive regulation of NF-kappaB transcription factor activity	23	$2.77E-11$
GO:0043123~positive regulation of I-kappaB kinase/NF-kappaB signaling	35	$4.42E-12$
GO:0045922~negative regulation of the fatty acid metabolic process	41	$1.45E-12$
GO:0042981~regulation of apoptotic process	55	$5.22E-14$
GO:0042127~regulation of cell proliferation	76	$6.58E-11$
GO:0030433~ER-associated ubiquitin-dependent protein catabolic process	80	$4.48E-13$
GO:0008152~metabolic process	25	$5.33E-14$
GO:0010803~regulation of tumor necrosis factor-mediated signaling pathway	54	$4.32E-14$
GO:0008625~extrinsic apoptotic signaling pathway via death domain receptors	37	$2.47E-13$
GO:0097190~apoptotic signaling pathway	55	$3.88E-13$

Table 2: The eight prognostic genes and their prognostic model.

	HR	95% CI	logrank *P*	Cox *P*	AUC
ZEB1	0.86	0.74~0.95	0.022	0.043	0.69
CDK1	0.67	0.47~0.81	0.013	0.002	0.65
RAD54L	0.77	0.62~0.94	0.004	0.013	0.66
COL1A2	0.88	0.70~0.92	0.035	0.008	0.68
ATP1B3	0.79	0.53~0.68	0.001	0.016	0.65
CASP8	0.65	0.79~0.97	0.047	0.009	0.64
USP39	0.72	0.86~0.88	0.007	0.037	0.68
HOXB7	0.81	0.84~0.94	0.035	0.020	0.69

score. The top eight genes with the highest scores were selected to test their prediction performance. Among the top eight genes, four (USP39, ATP1B3, CASP8, and RAD54L) have been validated to play crucial roles in the progression of HCC and are closely related to the prognosis of HCC. According to the score ranking, a prognostic model was established for the top eight candidate prognostic markers. The prognostic model was constructed by a linear combination of the expression values of these eight prognostic biomarkers and the regression coefficients obtained from Cox regression analysis (Table 2).

$$\begin{aligned}\text{Riskscore} = {} & (-0.145894 \times E_{\text{CSTF2}}) + (-0.43876 \times E_{\text{CDK1}}) \\ & + (-0.14688 + E_{\text{RAD54L}}) + (-0.125743 + E_{\text{COL1A2}}) \\ & + (-0.325682 \times E_{\text{ATP1B3}}) + (-0.35801 \times E_{\text{CASP8}}) \\ & + (-0.6859 \times E_{\text{USP39}}) + (-0.259056 \times E_{\text{HOXB7}}).\end{aligned} \quad (1)$$

3.6. Evaluation of the Eight-mRNA Prognostic Model. The ROC curve of the eight-mRNA prognostic model was screened out (AUC = 0.635), suggesting that this model exhibited an excellent prediction performance (Figure 4). Survival analysis showed that the survival rate of patients in the high-risk group was significantly lower than that in the low-risk group (log-rank = 0.0055, Figure 5).

4. Discussion

HCC is one of the malignant tumors with a high mortality rate in China [13]. Although significant progress has been made in immunotherapy and targeted therapy, the prognosis of patients with advanced HCC is still poor [14]. Bioinformatics analysis could identify the abnormally expressed genes under pathological conditions and assist in selecting novel and more accurate diagnostic and prognostic biomarkers [15]. Based on the application and development of computer technology and artificial intelligence in medical biology, bioinformatics analysis has become necessary for studying molecular markers related to disease phenotype [16]. In this study, we analyzed biological information to identify eight mRNAs correlated with the OS of HCC patients and establish a survival prognosis risk scoring model. The ROC curve of the eight-mRNA prognostic model exhibited an excellent prediction performance of HCC outcome. Kaplan Meier analysis showed that the survival time of patients in the high-risk group was lower than that of patients in the low-risk group.

As an advanced algorithm in bioinformatics analysis, weighted gene coexpression network analysis makes the calculation results more accurate by establishing a scale-free

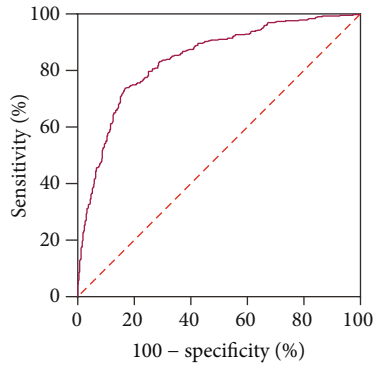

Figure 4: The ROC curve of the eight-mRNA prognostic model was depicted.

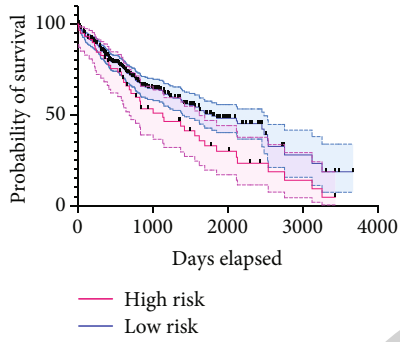

Figure 5: Survival analysis showed the survival rate of patients.

network and has been widely used in the study of tumor subtypes and prognostic markers [17]. This study constructed a coexpression network of HCC prognostic genes and identified the network modules. The prognostic module was reweighted using the PPI network data of module genes. The small world index of our reweighted module network obtained is 2.033, which is in line with the characteristics of a small world network. These findings suggested that the nodes in our reweighted module network were highly clustered.

Next, we analyzed the highly clustered nodes in the reweighted module network and identified the topological importance of nodes by scoring. We selected eight genes correlated with the OS of HCC patients with the highest scores. Among the top eight genes with the highest scores, USP39, ATP1B3, AHSA1, and RAD54L have essential functions in HCC cell proliferation and tumor growth, indicating that topologically essential genes play critical roles in HCC forecasting. Zinc-finger E-box-binding homeobox 1 (ZEB1) is a critical inducer of epithelial-to-mesenchymal transition (EMT) to stimulate cancer progression. However, the effect of ZEB1 on HCC development remains insufficient [18, 19]. Caspase 8 (CASP8) is an essential protease in the apoptosis pathway of the death receptor [20]. After being recruited and activated by death signals, CASP8 might activate its downstream effector protease to induce apoptosis. The role of CASP 8 is, however, unclear.

In brief, this study integrated microarray data from GEO and TCGA to identify critical genes. WGCNA combined Cox regression analysis was used to screen out genes of HCC prognosis. Eight critical genes related to the pathogenesis and progression of HCC were identified. These genes might play crucial roles in the cell cycle and abnormal behavior of HCC, indicating that these genes have great potential in the treatment and prognosis of HCC. In addition, we performed survival analysis and established a Cox proportional hazards model to identify prognostic biomarkers. A genetic marker of 8 genes was constructed to predict the overall survival rate. These results will provide a reference for a further study of the pathogenesis and drug treatment of HCC.

Data Availability

The labeled dataset used to support the findings of this study is available from the corresponding author upon request.

Conflicts of Interest

The authors declare no competing interests.

Authors' Contributions

Dong Xia and Xuebin Liao contribute equally to this work and share first authorship.

References

[1] A. Rizzo, "The evolving landscape of systemic treatment for advanced hepatocellular carcinoma and biliary tract cancer," *Cancer Treatment and Research Communications*, vol. 27, article 100360, 2021.

[2] Z. Song, Q. Xiao, Z. Shi, G. Yu, and D. K. Jiang, "Caspase polymorphisms and prognosis of hepatocellular carcinoma," *PLoS One*, vol. 12, no. 4, article e0176802, pp. 220–224, 2017.

[3] A. Bort, B. Sánchez, I. D. Miguel, P. Mateos-Gómez, and I. Diaz-Laviada, "Dysregulated lipid metabolism in hepatocellular carcinoma cancer stem cells," *Molecular Biology Reports*, vol. 47, no. 4, pp. 2635–2647, 2020.

[4] C. Wang, C. Shang, X. Gai, T. Song, and X. Zheng, "Sulfatase 2-induced cancer-associated fibroblasts promote hepatocellular carcinoma progression via inhibition of apoptosis and induction of epithelial-to-mesenchymal transition," *Frontiers in Cell and Development Biology*, vol. 9, article 631931, 2021.

[5] Z. D. Hu, Y. Jiang, H. M. Sun, J. W. Wang, and J. Yan, "KIF11 promotes proliferation of hepatocellular carcinoma among patients with liver cancers," *BioMed Research International*, vol. 2021, Article ID 2676745, 8 pages, 2021.

[6] Y. Huang, W. Luo, S. Chen et al., "Association of a Novel DOCK2 Mutation-Related Gene Signature With Immune in Hepatocellular Carcinoma," *Frontiers in Genetics*, vol. 13, article 872224, 2022.

[7] D. R. Velez Edwards, R. Romero, J. P. Kusanovic et al., "Polymorphisms in maternal and fetal genes encoding for proteins involved in extracellular matrix metabolism alter the risk for small-for-gestational-age," *The Journal of Maternal-Fetal & Neonatal Medicine*, vol. 24, no. 2, pp. 362–380, 2011.

[8] S. Noori, N. Al-A'Araji, and E. Al-Shamery, "Identifying protein complexes from protein–protein interaction networks based on the gene expression profile and core-attachment

Hindawi
Computational and Mathematical Methods in Medicine
Volume 2023, Article ID 9821497, 1 page
https://doi.org/10.1155/2023/9821497

Retraction

Retracted: Role of GLI1 in Hypoxia-Driven Endometrial Stromal Cell Migration and Invasion in Endometriosis

Computational and Mathematical Methods in Medicine

Received 12 December 2023; Accepted 12 December 2023; Published 13 December 2023

This article has been retracted by Hindawi, as publisher, following an investigation undertaken by the publisher [1]. This investigation has uncovered evidence of systematic manipulation of the publication and peer-review process. We cannot, therefore, vouch for the reliability or integrity of this article.

Please note that this notice is intended solely to alert readers that the peer-review process of this article has been compromised.

Wiley and Hindawi regret that the usual quality checks did not identify these issues before publication and have since put additional measures in place to safeguard research integrity.

We wish to credit our Research Integrity and Research Publishing teams and anonymous and named external researchers and research integrity experts for contributing to this investigation.

The corresponding author, as the representative of all authors, has been given the opportunity to register their agreement or disagreement to this retraction. We have kept a record of any response received.

References

[1] L. Wang, J. Liang, S. Bi et al., "Role of GLI1 in Hypoxia-Driven Endometrial Stromal Cell Migration and Invasion in Endometriosis," *Computational and Mathematical Methods in Medicine*, vol. 2022, Article ID 6890790, 9 pages, 2022.

Hindawi
Computational and Mathematical Methods in Medicine
Volume 2022, Article ID 6890790, 9 pages
https://doi.org/10.1155/2022/6890790

Research Article

Role of GLI1 in Hypoxia-Driven Endometrial Stromal Cell Migration and Invasion in Endometriosis

Lili Wang,[1] Jiaxin Liang,[2] Siyi Bi,[3] Yixuan Li,[3] Wei Zhang,[3] Wang Xiwen,[3] Yi Liu,[2] and Hengwei Liu[3]

[1]*Department of Obstetrics and Gynecology, Wuhan Fourth Hospital, Puai Hospital, Tongji Medical College, Huazhong University of Science and Technology, Wuhan, China*
[2]*Department of Obstetrics and Gynecology, Union Hospital, Tongji Medical College, Huazhong University of Science and Technology, Wuhan 430022, China*
[3]*Department of Obstetrics and Gynecology, Zhongnan Hospital of Wuhan University, Wuhan University, Wuhan 430071, China*

Correspondence should be addressed to Hengwei Liu; hw.liu@whu.edu.cn

Received 16 August 2022; Revised 4 September 2022; Accepted 3 October 2022; Published 15 October 2022

Academic Editor: Min Tang

Endometriosis (EMs) is a benign disease with the characteristics of invasion and migration, and its pathogenesis is related to hypoxia. The abnormal activation of glioma-associated oncogene homolog 1 (GLI1) plays an important role in the metastasis of multiple types of tumors. However, it is not clear whether GLI1 regulates the migration and invasion of endometrial stromal cells under hypoxic condition. Therefore, we use comprehensive analysis to explore the effects of hypoxic on GLI1 expression and their regulation on the pathogenesis of EMs. In this study, from immunohistochemistry, RT-qPCR, and western blot analysis, we discovered that the expression of hypoxia-induced factor-1α (HIF-1α) and GLI1 was significantly increased in eutopic and ectopic endometrium of patients with EMs. In human primary eutopic endometrial stromal cells (ESCs), hypoxia can increase the expression of HIF-1α and GLI1 in a time-dependent manner. And hypoxia could promote GLI1 expression in a HIF-1α-dependent manner. Moreover, data from transwell assays manifested that the migration and invasion ability of ESCs was significantly enhanced under hypoxia, and this effect could be reversed by silencing GLI1. Furthermore, the expression of MMP2 and MMP9 was also increased under hypoxia, while silencing GLI1 could reverse this event. In summary, our research verified that GLI1, which activated by hypoxia, may contribute to the migration and invasion of ESCs through the upregulation of MMP2 and MMP9 and can be a novel therapeutic target in EMs.

1. Introduction

Endometriosis (EMs) is defined as the presence of endometrial tissue (glandular epithelium or stromal cells) outside the uterine cavity, concurrent adhesion, invasion, and growth. According to statistics, EMs affect 6% to 10% of reproductive-age women. It is the main cause of pelvic pain and infertility in women of productive age and seriously interferes with women's reproductive health [1, 2]. Numerous theories have been put forward for the pathogenesis of EMs, including retrograde menstruation, coelomic metaplasia, lymphatic and venous dissemination theory, and immune defense deficiency theory [3]. The most widely accepted theory, retrograde menstruation theory, refers to endometrial fragments retrograde into the pelvis through the fallopian tube during the menstrual cycle, then implant in the abdominal organs, resulting in chronic inflammation and adhesion [4, 5]. However, there are still defects in this explanation, and so far, there is no one theory that can fully explain the pathogenesis of EMs.

Hypoxia is not only a critical factor involved in a variety of pathophysiological processes but also an important microenvironment for the pathogenesis of EMs [6, 7]. According to retrograde menstruation theory, the blood supply was lost, and the hypoxia environment appeared after the endometrium fell off. Retrograded endometrial fragments in the pelvic may undergo certain changes under this microenvironment to combat the scarcity of nutrients and

the accumulation of stress. Studies have shown that pelvic hypoxia could affect the occurrence and development of EMs by regulating the synthesis and response of estrogen [8, 9], angiogenesis [10], and epigenetic [11].

The Hedgehog signaling pathway is highly conserved in the process of biological evolution, while glioma-associated oncogene 1 (GLI1) is the core downstream transcription factor of this signaling pathway [12]. Abnormal activation of GLI1 leads to increased transcription of target genes, which regulates a variety of cellular biological processes, including proliferation, apoptosis, migration, and invasion [13–15]. At present, higher expression of the GLI1 gene has been observed in multiple malignant tumors, including hepatocellular carcinoma [16] and pancreatic cancer [17]. It plays an important role in tumor invasion and metastasis. Although EMs are regarded as a benign disease, ectopic endometrial cells show malignant biological characteristics and have a stronger ability of invasion, migration, and abnormal proliferation compared with normal types [18]. Previous study [19] has demonstrated that GLI1 was elevated in eutopic endometrium of EMs; however, whether GLI1 may play a critical role under hypoxic environments in the development of EMs is still poorly understood.

In the present study, we aimed to clarify the relationship between the GLI1 gene and the pathogenesis of EMs and also to determine the role of GLI1 in the invasion of EMs mediated by hypoxia. This study provides novel theoretical basis and treatment strategy for the pathogenesis of EMs.

2. Materials and Methods

2.1. Patients and Tissue Collection. The patients were recruited from the Department of Obstetrics and Gynecology, Union Hospital, Tongji Medical College, Huazhong University of Science and Technology between June 2017 and October 2018. The normal endometrial tissues of 30 healthy women with infertility due to male factors, ectopic endometrium tissues, and corresponding eutopic endometrial tissues of 30 patients with ovarian endometriosis were collected. According to the standard of the American Society of Reproductive Medicine (ASRM), it is classified as stage I-IV EMs [20]. The ectopic endometrial tissue was separated by laparoscopy, and the corresponding eutopic endometrial tissue was separated by hysteroscopy. All specimens were collected during the proliferative phase of the normal menstrual cycle. The tissue samples were collected using the Nowak's curette just before the surgical procedure, and transported to the laboratory for research use. This study was approved by the Ethics Committee of Tongji Medical College of Huazhong University of Science and Technology (IORG No: IORG0003571), and all the above patients signed informed consent. All fresh specimens were frozen and stored in liquid nitrogen to further extract protein and RNA. The clinical data about the patients are reported in Supplemental Table 1.

2.2. Human Primary Eutopic Endometrial Stromal Cells (ESCs) Isolation and Cell Culture Conditions. Isolation of primary eutopic endometrial stromal cells from eutopic endometrium of infertile patients with EMs. The collected fresh tissue was placed on ice, washed with precooled PBS, and shredded to 1 mm^3 size tissue homogenate. Type II collagenase (0.1%, Sigma Aldrich, MO, USA) was added to digest for 60 min at 37°C. The tissue homogenate was filtered through aseptic 400 μm and 100 μm sieves, respectively, to remove undigested tissue and epithelial cells. The supernatant was discarded after 1000 rpm/min centrifugation for 5 min. Then the red blood cell lysate reagent (Beyotime, Shanghai, China) was added and mixed well to make it fully cleaved. After 1000 rpm/min centrifugation for 5 min, supernatant was discarded and cells were suspended with 2 ml DMEM/F12 medium containing 10%FBS (Gibco, CA, USA) and cultured at 37°C.

2.3. Immunohistochemistry Staining. The paraffin-embedded fresh tissue specimen was stained by immunohistochemical staining according to the standard procedure. Soak the sample in 3% hydrogen peroxide solution at room temperature and incubate with the primary antibody overnight at 4°C. The secondary antibody labeled with biotin was incubated at room temperature for 2 hours and washed with PBS 3 times, incubated with diaminobenzidine (DAB) and hematoxylin, and observed and photographed under the microscope. The primary antibody used included the following: anti-HIF1α (Affinity, AF1009, 1 : 100) and anti-GLI1 (Abcam, ab217326, 1 : 100). The immunostaining score of HIF-1α and GLI1 protein in endometrial tissues is presented in Supplemental Table 4.

2.4. RNA Extraction and Quantitative Real-Time Polymerase Chain Reaction (qRT-PCR). The qRT-PCR assay was performed according to our previous study [21]. The total RNA of ESCs was collected by TRIzol reagent (Vazyme Biotech, Nanjing, China), and the RNA was reverse transcribed into cDNA by HiScrip II QRT SuperMix (Vazyme Biotech, Nanjing, China). The expression level of mRNA was calculated by the method of $2^{-\Delta\Delta Ct}$. The primer sequences used for real-time RT-PCR are presented in in Supplemental Table 2.

2.5. Western Blot. The total proteins of ESCs were collected by radioimmunoprecipitation assay buffer (RIPA) (Beyotime Biotechnology, China) and quantified by bicinchoninic acid assays (Beyotime, Shanghai, China). The protein samples were denatured after incubation at 95°C for 10 minutes. Target proteins were separated by 12% SDS-PAGE and transferred to a polyvinylidene fluoride membrane, sealed with 5% skim milk at room temperature for 1 hour, incubated overnight with the primary antibody, and then soaked with the secondary antibody. The primary antibody used included the following: anti-HIF-1α (Affinity, AF1009, 1 : 1000), anti-GLI1 (Abcam, ab217326, 1 : 1000), anti-MMP2 (Affinity, AF5330, 1 : 1000), anti-MMP9 (Affinity, AF5228, 1 : 1000), anti-GAPDH (ProteinTech, 10494-1-AP, 1 : 20000). The commercial sources and characteristics of antibodies used are summarized in Supplemental Table 3.

2.6. Cell Transfection. For adenoviral transduction, ESCs in the logarithmic phase were digested and inoculated on a 6-

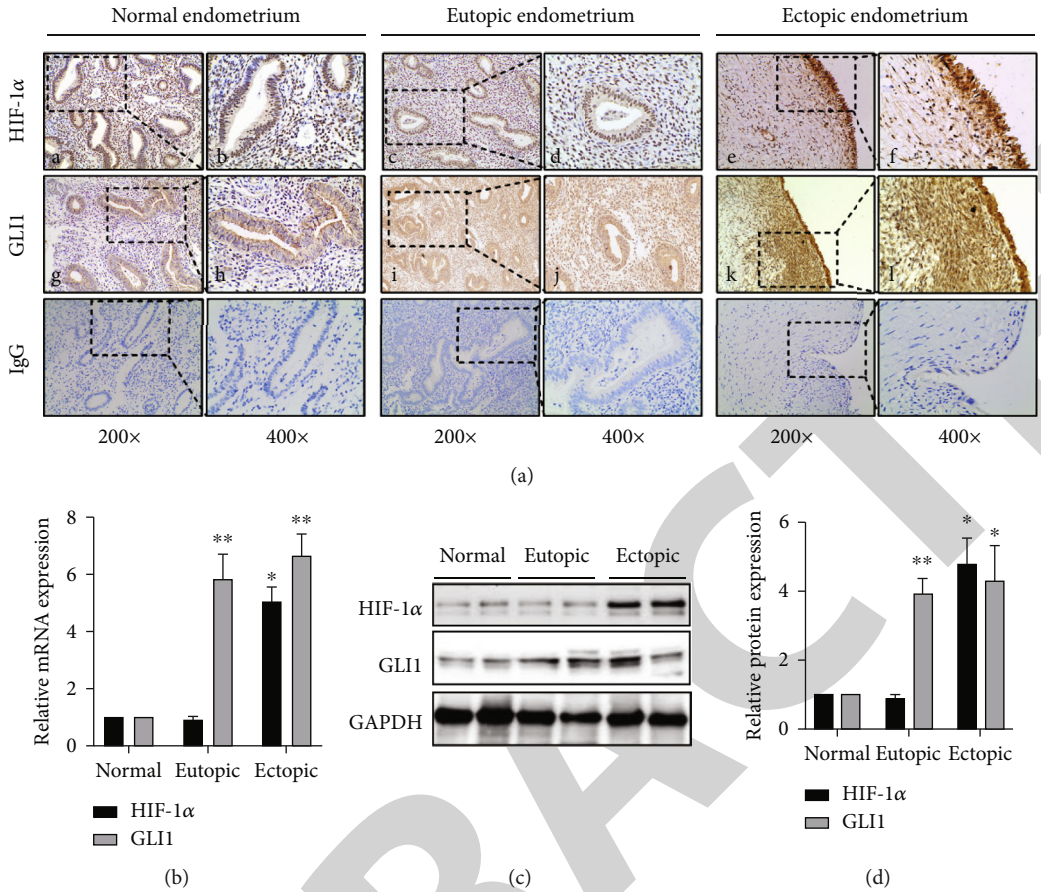

FIGURE 1: Differential expression of GLI1 and HIF-1α in normal, eutopic and ectopic endometrial tissues. (a) Immunohistochemistry assay was performed to confirm the expression and localization of HIF-1α and GLI1 protein in normal proliferative endometrium (A, B, G, and H), eutopic endometrium (C, D, I, and J), and ectopic endometrium (E, F, K, and L). The images were observed under 200 times and 400 times visual field. (b) The relative expression levels of GLI1 and HIF-1α in eutopic ($n = 40$) and ectopic ($n = 40$) endometrial specimens from patients with ovarian endometriosis (EMs) and normal endometrial ($n = 40$) specimens were measured by (b) qRT-PCR and (c, d) western blot. Statistical analysis was conducted by the Kruskal–Wallis test. The data are presented as the mean ± SD of three independent experiments. $^{*}P < 0.05$, $^{**}P < 0.005$ by one-way ANOVA.

well plate according to 5×10^4/ml. When the cell density reached 50-60%, the cells were ready to be transfected. Before infection, the medium was replaced by 1 ml fresh complete medium. The control shRNA adenovirus vector and GLI1 shRNA adenovirus vector (multiplicity of infection (MOI) = 50) were added, respectively. After cultured for 24 hours, fresh complete medium was replaced to continue the culture for another 24 hours, and the fluorescence expression of GFP was detected under the fluorescence (IX51, Olympus, Tokyo, Japan) inverted microscope. If the fluorescence rate in the visual field was more than 80%, the follow-up experiment could be carried out.

For siRNA transient transfection, 50 nmol/l siRNA-HIF-1α was transfected into ESCs by using Lipofectamine 2000 Reagent (Thermo Scientific, Waltham, MA, USA) and OPTI-MEM (Invitrogen, USA) according to the manufacturer's protocol. All the RNA oligoribonucleotides were purchased from RiboBio (RiboBio, Guangzhou, China). The primer sequences used for siRNA analyses are presented in in Supplemental Table 2.

2.7. Transwell Migration and Invasion Assays. The migration and invasive ability of ESCs was evaluated by transwell assay. For invasion assay, the superior chamber was precoated with 50 μl of Matrigel (2 mg/ml) (Becton, Dickinson and Company) and incubated at 37°C for at least 4 h. Then cells were resuspended with serum-free DMEM/F12 medium after digestion, and the cell concentration was adjusted to 1×10^6 cells/ml after counting. The 200 μl cell suspension was added to the upper surface of the chambers. 500 μl complete medium containing 10% FBS was added into the lower chamber. After being incubated at 37°C for 24 hours, the chamber was taken out. The chamber was cleaned with PBS, fixed with paraformaldehyde and stained with 0.1% crystal violet, and observed under the microscope (Nikon Eclipse TE2000U inverted microscope with a CCD camera).

2.8. Statistical Analysis. The experimental results in this study were repeated three times independently, and the GraphPad Prism8.0 software was used to analyze. The data that passed normality test were determined by applying

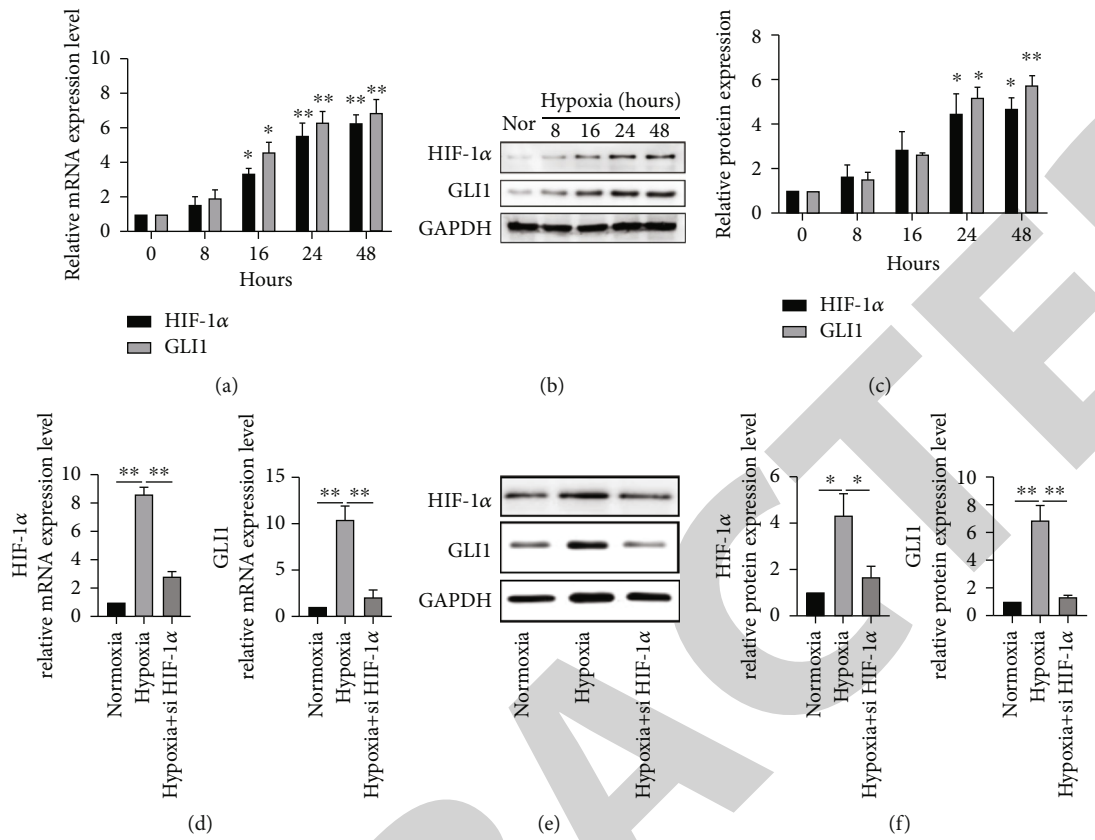

Figure 2: Hypoxia promotes GLI1 expression of the ESCs in a HIF-1α-dependent manner. (a) GLI1 and HIF-1α expression in ESCs was detected by qRT-PCR following treatment with hypoxia at a series of time points (0, 8, 16, 24, and 48 hours). (b, c) GLI1 and HIF-1α protein expression in ESCs was determined following treatment with hypoxia at indicated time points (0, 8, 16, 24, and 48 hours). (d–f) ESCs were transfected with HIF-1α-specific siRNA in the presence of hypoxia, and then the expression of GLI1 and HIF-1α mRNA and protein was measured by qRT-PCR and western blot. The data are presented as the mean ± SD of three independent experiments. $^{*}P < 0.05$, $^{**}P < 0.005$ by one-way ANOVA.

Student's t test and one-way analysis of variance followed by Tukey's post hoc test among more than two groups. For all statistical tests, $P < 0.05$ was considered significant.

3. Results

3.1. Expressions of GLI1 and HIF-1α in Ovarian Endometriosis. Immunohistochemical was used to determine the expression of HIF-1α and GLI1 in normal endometrium and eutopic and ectopic endometrium of EMs. The results showed that HIF-1α was located in both the cytoplasm and nucleus of glandular epithelial cells and stromal cells in endometrial tissue. Compared with normal endometrium, the expression of HIF-1α in ectopic endometrium was remarkably increased, but there was no significant difference in eutopic endometrium (Figure 1(a) (A–F)). Strong GLI1 expression was observed in the cytoplasm of glandular epithelial cells in normal endometrium, while it is mainly located in the nucleus in eutopic and ectopic endometrium of EMs (Figure 1(a) (G–I)). Besides, it was also observed that a significant increase in the expression of GLI1 in eutopic and ectopic endometrium of patients with EMs when compared with normal endometrium (Figure 1(a) (G–I)). To further compare the expression of GLI1 and HIF-1α in ovarian endometriosis, qRT-PCR and western blot assays were also performed. The results showed that the mRNA and protein expression of GLI1 in eutopic and ectopic endometrium of patients with EMs was significantly higher than those in normal proliferative endometrium (Figures 1(b)–1(d)). As for HIF-1α, the expression level of mRNA and protein was also significantly increased in ectopic tissues, but no significant change was observed between eutopic and normal endometrium (Figures 1(b)–1(d)). These results indicated that these two genes may both play an important role in the development of EMs. However, whether there was a connection between HIF-1α and GLI1 remained unknown.

3.2. Hypoxia Promotes GLI1 Expression of the ESCs in a HIF-1α-Dependent Manner. To clarify whether the expression of GLI1 and HIF-1α was associated with hypoxia, we performed qRT-PCR and western blot assays for isolated eutopic endometrial stromal cells (ESCs) under hypoxia treatment. As shown in Figures 2(a)–2(c), RT-PCR and western blot results indicated that a time-dependent increase in both HIF-1α and GLI1 mRNA and protein expression were observed. Furthermore, we also knockdown the expression of HIF-1α by specific siRNA under hypoxia condition to investigate the role of HIF-1α in hypoxia induced GLI1 activation. The results

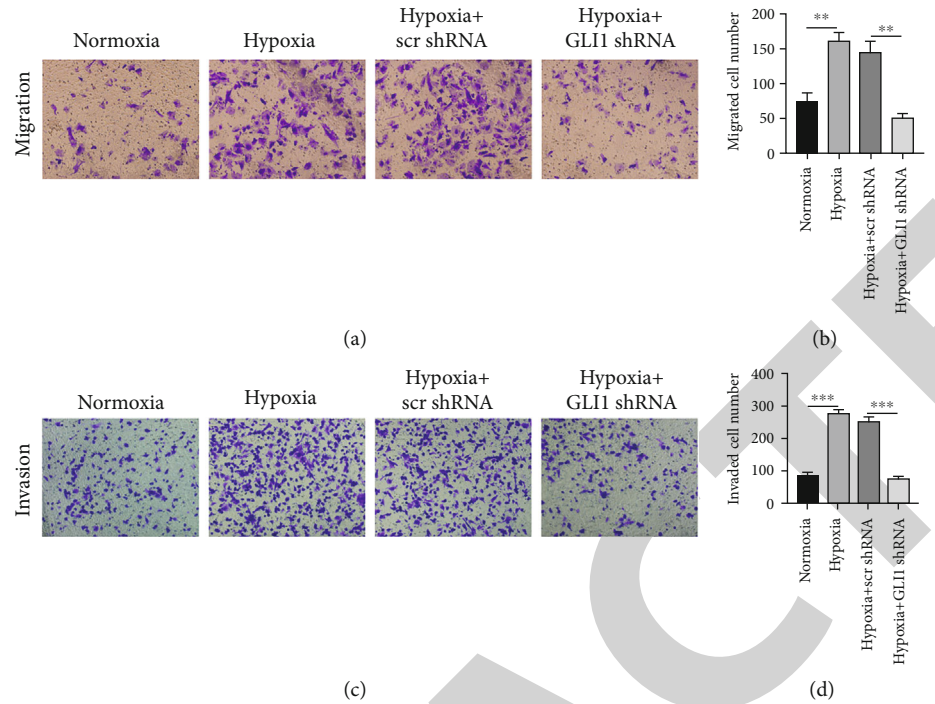

Figure 3: Inhibition of GLI1 attenuates the migration and invasion capacities of ESCs. (a, b) Transwell assays showed the migration capacities of ESCs infected with scramble shRNA and GLI1 shRNA. (c, d) Transwell assays showed the invasion capacities of ESCs infected with scramble shRNA and GLI1 shRNA. All images were taken at ×200 magnification. The data are presented as the mean ± SD of three independent experiments. $^{*}P < 0.05$, $^{**}P < 0.005$, $^{***}P < 0.001$ by one-way ANOVA.

suggested that compared with ESCs cultured under hypoxia condition, decreased expression of HIF-1α and Beclin1 and GLI1 was observed in ESCs transfected with HIF-1α siRNA under hypoxia condition (Figures 2(d)–2(f)). These suggest that GLI1 activation under hypoxic condition was dependent on the status of HIF-1α.

3.3. Hypoxia Promotes Invasion of Endometrial Stromal Cells in a GLI1-Dependent Manner. To investigate the biological function of GLI1 under hypoxia condition, we constructed an empty adenovirus and GLI1 shRNA recombinant adenovirus vectors. Transwell migration and invasion assays showed that the invasive ability of cells was significantly enhanced under hypoxia when compared with the normoxic group, while silencing the GLI1 gene can effectively reverse this effect (Figures 3(a)–3(d)). These evidences indicated that the enhanced invasion of eutopic endometrial stromal cells in EMs mediated by hypoxia was depended on GLI1 expression.

3.4. GLI1 Contributed to EMs Invasion through Upregulation of MMP2 and MMP9. Given the importance of matrix metalloproteinases family genes (MMPs) in the process of cell migration and invasion, we focused on the effects of GLI1 on the expression of MMP2 and MMP9 under hypoxia. It was shown that the mRNA and protein expression of GLI1, MMP2, and MMP9 was markedly higher under hypoxia when compared with normoxia (Figures 4(a)–4(c)). To further determine its internal relationship, we silenced GLI1 under hypoxia and sought to clarify whether the upregulation of MMP2 and MMP9 under hypoxia could be attributed to GLI1. The results of qRT-PCR and western blot assays showed that both MMP2 and MMP9 diminished after GLI1 silencing under hypoxic conditions (Figures 4(a)–4(c)). Collectively, the findings suggested that the ability of GLI1 to promote invasion under hypoxia may be realized by MMP2 and MMP9.

4. Discussion

Endometriosis is an estrogen-dependent chronic gynecological disease. The pelvic pain, infertility, and increase in the risk of epithelial ovarian cancer caused by EMs triggered a serious physical, mental, and financial burden on women. Up to now, there is still no typical conclusion on the specific pathogenesis of EMs [22]. The lack of detailed knowledge about this disorder also leads to barren and ineffective treatments. Despite receiving drug or surgical treatment, EMs patients still face a high risk of recurrence and long-term drug side effects [23]. Therefore, it is of great clinical significance to explore the molecular mechanism of the occurrence and development of endometriosis and to find specific sites to achieve the targeted therapy of EMs.

Hypoxia is a usual phenomenon, and it is one of the most common features in the solid tumor microenvironment. Hypoxia has been widely reported to be related to the invasive phenotype of tumors, including cell proliferation, angiogenesis, and drug resistance, [24–28]. Extensive studies have confirmed that the effect of hypoxia on tumor invasion is achieved through the transcriptional activation

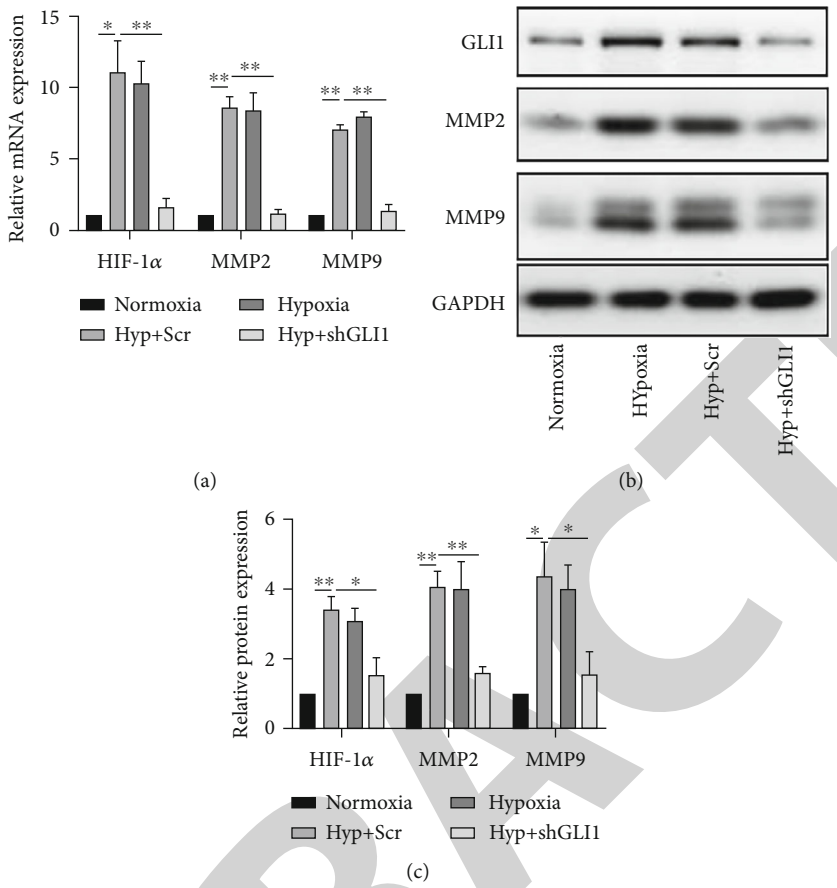

Figure 4: GLI1 contributed to EMs invasion through upregulation of MMP2 and MMP9. (a, b) GLI1, MMP2, and MMP9 mRNA and protein expression was determined by qRT-PCR and western blot in ESCs treated with normoxia, hypoxia, hypoxia + scramble shRNA, and hypoxia + GLI1 shRNA. The data are presented as the mean ± SD of three independent experiments. $^{*}P < 0.05$, $^{**}P < 0.005$, $^{***}P < 0.001$ by one-way ANOVA.

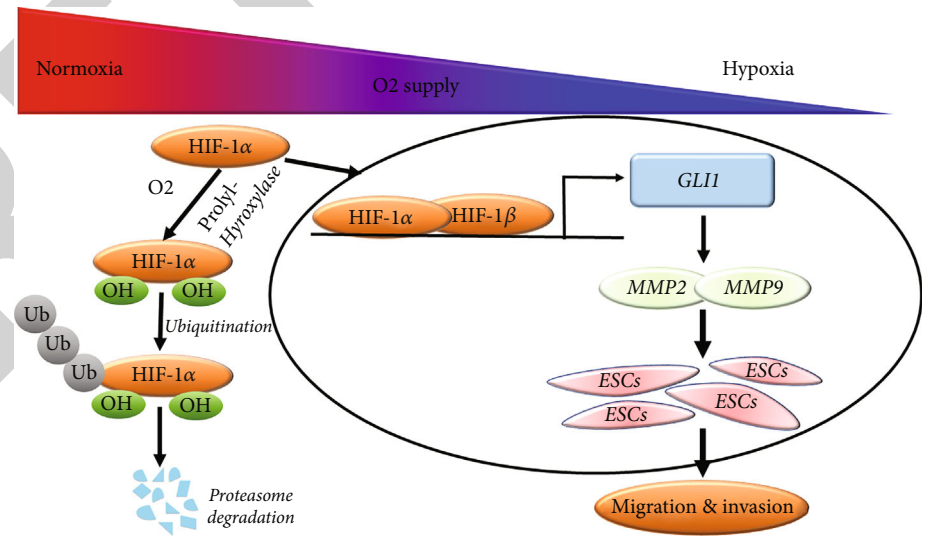

Figure 5: A brief schematic diagram depicting how hypoxia promote migration and invasion by regulating GLI1 mediated MMP2 and MMP9 expression in human eutopic endometrial stromal cells (ESCs).

of different genes by hypoxia-induced factor [29–31]. Although it is not a tumor, EMs also shows many malignant features similar to tumors, such as strong invasion and migration [18, 32, 33]. In this study, we found that the expression of HIF-1α was increased in ectopic lesions of patients with EMs. After continuous hypoxia stimulation of eutopic endometrial stromal cells, HIF-1α elevated in a time-dependent manner. Hypoxia-induced factor-1α (HIF-1α) is the main factor in cell response to hypoxia stress. Under hypoxia conditions, HIF-1α forms dimer with HIF-1β and together regulates downstream by interaction with hypoxia response element (HRE) [34]. The augment expression of HIF-1α in ectopic lesions suggests that hypoxia plays an essential role in the occurrence and development of EMs.

Similarly, besides HIF-1α, we found that the expression of GLI1 increased in ectopic lesions and also showed upregulated expression in a time-dependent manner to hypoxia. Moreover, hypoxia could upregulate GLI1 through HIF-1α activation. GLI1 is at the terminal end of the highly conserved Hedgehog signaling (Hh) pathway. When GLI1 is released, it can trans into the nucleus to regulate gene transcription as a transcription factor [35]. Abnormal activation of the Hh pathway can lead to various biological events such as cancer stem cell self-renewal, growth, invasion, and migration [36–39]. As the terminal molecule of the Hh signaling pathway, the occurrence of these malignant events is closely related to GLI1. Therefore, we speculate that the high expression of GLI1 in patients with EMs may be the culprit of downstream malignant events. We found that the enhancement of hypoxia-induced migration and invasion abilities in eutopic endometrial stromal cells was attenuated after silencing of GLI1 gene. These findings prove that the highly expressed GLI1 can contribute to hypoxia-induced invasion enhancement in EMs.

As a transcription factor, GLI1 functions mainly by regulating the expression of downstream genes. We speculate that GLI1 may affect cell migration and invasion by regulating matrix metallopeptidases (MMPs). MMPs have been found to degrade extracellular matrix and basement membrane [40]. It is frequently found in malignant tumors and is closely related to invasion and migration [41–43]. Li et al. [44] found that programmed cell death 4 (PDCD4) can attenuate the expression of THE NF-κB/MMP2/MMP9 signaling pathway, thus attenuating the migration and invasion potentiality of human endometrial stromal cells. This suggests that MMPs may play a role in the migration and invasion of EMs. It was found that the expression of MMP2 and MMP9 was significantly augmented under hypoxia, and this event could be reversed by silencing of GLI1. This indicates that GLI1 could regulate migration and invasion of endometrial stromal cell through MMP2 and MMP9.

However, our current study has some limitations. Firstly, only proliferative phase endometrium was analyzed, and the sample size was relatively small, which may reduce the interpretable power of the data. Therefore, large sample size from an entire menstrual cycle should be studied in our future research. Second, the exact molecular regulatory mechanisms underlying GLI1 mediated MMP2/9 upregulation in human endometrial stromal cells remains to be elucidated. Last but not least, only late-stage ovarian endometriosis sample was used, and the results may provide little insight into peritoneal and deep infiltrating lesions. Therefore, future research is needed to pay more attention into these questions.

In conclusion, we have first uncovered a novel link between hypoxia microenvironment and GLI1 in the pathogenesis of endometriosis. Our results presented that GLI1 has a significant higher expression in ovarian endometriosis and is correlated with elevated expression of HIF-1α. We further demonstrate that hypoxia can induce the expression of GLI1 in ECS cell, which then promotes cell migration and invasion through the MMP2/9 pathway (Figure 5). Overall, the HIF1α-GLI1-MMPs axis will be a potential therapeutic in ovarian endometriosis.

Data Availability

The datasets generated during and/or analyzed during this study are available from the corresponding author on reasonable request.

Ethical Approval

This study was approved by the Ethics Committee of Tongji Medical College of Huazhong University of Science and Technology (IORG No: IORG0003571), and all the above patients signed informed consent.

Conflicts of Interest

The authors declare no competing interests.

Authors' Contributions

Lili Wang and Jiaxin Liang completed the experiments and data collection and were a major contributor in writing the manuscript. Yi Liu contributed to clinical sample collection. Hengwei Liu performed the immunohistochemistry and molecular biology examination of the study. Siyi Bi and Yixuan Li contributed to data collection and data analysis. Hengwei Liu guided the overall design of the subject. Wei Zhang and Xiwen Wang reviewed and polished the manuscript. All authors read and approved the final manuscript. Lili Wang and Jiaxin Liang contributed equally to this work.

Acknowledgments

This work was supported by grants from the National Natural Science Foundation of China (no. 82001524 to Hengwei Liu; no. 8197061339 to Yi Liu), the Natural Science Foundation of Hubei Province (no. 2020CFB310 to Hengwei Liu), the Fundamental Research Fund for the Central Universities (no. 2042020kf0154 to Hengwei Liu), the Zhongnan Hospital of Wuhan University Science, Technology and Innovation Cultivating Fund (no. znpy2019077 to Hengwei Liu), the Program of Excellent Doctoral (Postdoctoral) of Zhongnan Hospital of Wuhan University (no. ZNYB2019009 to Hengwei Liu). We would like to thank all patients who agreed to participate in this study and all colleagues who helped with this research.

Supplementary Materials

Table S1: clinical characteristics of patients. Table S2: primer sequences used for real-time RT-PCR and siRNA analyse. Table S3: commercial sources and characteristics of antibodies used. Table S4: immunostaining score of HIF-1α and GLI1 protein in normal endometrium, eutopic endometrium and ectopic endometrium of endometriosis. *(Supplementary Materials)*

References

[1] L. C. Giudice, "Clinical practice. Endometriosis," *The New England Journal of Medicine*, vol. 362, no. 25, pp. 2389–2398, 2010.

[2] H. Chen, F. Malentacchi, M. Fambrini, A. H. Harrath, H. Huang, and F. Petraglia, "Epigenetics of estrogen and progesterone receptors in endometriosis," *Reproductive Sciences*, vol. 27, no. 11, pp. 1967–1974, 2020.

[3] P. T. K. Saunders and A. W. Horne, "Endometriosis: etiology, pathobiology, and therapeutic prospects," *Cell*, vol. 184, no. 11, pp. 2807–2824, 2021.

[4] J. Halme, M. G. Hammond, J. F. Hulka, S. G. Raj, and L. M. Talbert, "Retrograde menstruation in healthy women and in patients with endometriosis," *Obstetrics and Gynecology*, vol. 64, no. 2, pp. 151–154, 1984.

[5] J. A. Sampson, "Metastatic or embolic endometriosis, due to the menstrual dissemination of endometrial tissue into the venous circulation," *The American Journal of Pathology*, vol. 3, no. 2, pp. 93–110.43, 1927.

[6] M. H. Wu, K. Y. Hsiao, and S. J. Tsai, "Hypoxia: the force of endometriosis," *The Journal of Obstetrics and Gynaecology Research*, vol. 45, no. 3, pp. 532–541, 2019.

[7] I. Filippi, P. Carrarelli, S. Luisi et al., "Different expression of hypoxic and angiogenic factors in human endometriotic lesions," *Reproductive Sciences*, vol. 23, no. 4, pp. 492–497, 2016.

[8] M. H. Wu, C. W. Lu, F. M. Chang, and S. J. Tsai, "Estrogen receptor expression affected by hypoxia inducible factor-1α in stromal cells from patients with endometriosis," *Taiwanese Journal of Obstetrics & Gynecology*, vol. 51, no. 1, pp. 50–54, 2012.

[9] A. G. Recchia, E. M. De Francesco, A. Vivacqua et al., "The G Protein-coupled Receptor 30 Is Up-regulated by Hypoxia-inducible Factor-1α (HIF-1α) in Breast Cancer Cells and Cardiomyocytes," *Journal of Biological Chemistry*, vol. 286, no. 12, pp. 10773–10782, 2011.

[10] J. L. Fu, K. Y. Hsiao, H. C. Lee et al., "Suppression of COUP-TFII upregulates angiogenin and promotes angiogenesis in endometriosis," *Human Reproduction*, vol. 33, no. 8, pp. 1517–1527, 2018.

[11] K. Y. Hsiao, M. H. Wu, N. Chang et al., "Coordination of AUF1 and miR-148a destabilizes DNA methyltransferase 1 mRNA under hypoxia in endometriosis," *Molecular Human Reproduction*, vol. 21, no. 12, pp. 894–904, 2015.

[12] J. Briscoe and P. P. Thérond, "The mechanisms of Hedgehog signalling and its roles in development and disease," *Nature Reviews. Molecular Cell Biology*, vol. 14, no. 7, pp. 416–429, 2013.

[13] S. Inaguma, K. Kasai, and H. Ikeda, "GLI1 facilitates the migration and invasion of pancreatic cancer cells through MUC5AC-mediated attenuation of E-cadherin," *Oncogene*, vol. 30, no. 6, pp. 714–723, 2011.

[14] A. Merchant, G. Joseph, Q. Wang, S. Brennan, and W. Matsui, "Gli1 regulates the proliferation and differentiation of HSCs and myeloid progenitors," *Blood*, vol. 115, no. 12, pp. 2391–2396, 2010.

[15] J. Astorga and P. Carlsson, "Hedgehog induction of murine vasculogenesis is mediated by Foxf1 and Bmp4," *Development*, vol. 134, no. 20, pp. 3753–3761, 2007.

[16] H. Y. Kim, H. K. Cho, S. P. Hong, and J. Cheong, "Hepatitis B virus X protein stimulates the Hedgehog-Gli activation through protein stabilization and nuclear localization of Gli1 in liver cancer cells," *Cancer Letters*, vol. 309, no. 2, pp. 176–184, 2011.

[17] J. Guo, J. Gao, Z. Li et al., "Adenovirus vector-mediated Gli1 siRNA induces growth inhibition and apoptosis in human pancreatic cancer with Smo-dependent or Smo-independent Hh pathway activation *in vitro* and *in vivo*," *Cancer Letters*, vol. 339, no. 2, pp. 185–194, 2013.

[18] M. S. Anglesio, N. Papadopoulos, A. Ayhan et al., "Cancer-associated mutations in endometriosis without cancer," *The New England Journal of Medicine*, vol. 376, no. 19, pp. 1835–1848, 2017.

[19] H. Liu, W. Zhang, L. Wang et al., "GLI1 is increased in ovarian endometriosis and regulates migration, invasion and proliferation of human endometrial stromal cells in endometriosis," *Annals of Translational Medicine*, vol. 7, no. 22, p. 663, 2019.

[20] M. Canis, J. G. Donnez, D. S. Guzick et al., "Revised American Society for Reproductive Medicine classification of endometriosis: 1996," *Fertility and Sterility*, vol. 67, no. 5, pp. 817–821, 1997.

[21] H. Liu, Y. Du, Z. Zhang et al., "Autophagy contributes to hypoxia-induced epithelial to mesenchymal transition of endometrial epithelial cells in endometriosis," *Biology of Reproduction*, vol. 99, no. 5, pp. 968–981, 2018.

[22] H. S. Taylor, A. M. Kotlyar, and V. A. Flores, "Endometriosis is a chronic systemic disease: clinical challenges and novel innovations," *Lancet*, vol. 397, no. 10276, pp. 839–852, 2021.

[23] P. Vercellini, P. Viganò, E. Somigliana, and L. Fedele, "Endometriosis: pathogenesis and treatment," *Nature Reviews. Endocrinology*, vol. 10, no. 5, pp. 261–275, 2014.

[24] B. Zhang, Y. L. Li, J. L. Zhao et al., "Hypoxia-inducible factor-1 promotes cancer progression through activating AKT/cyclin D1 signaling pathway in osteosarcoma," *Biomedicine & Pharmacotherapy*, vol. 105, pp. 1–9, 2018.

[25] M. Hockel, K. Schlenger, B. Aral, M. Mitze, U. Schaffer, and P. Vaupel, "Association between tumor hypoxia and malignant progression in advanced cancer of the uterine cervix," *Cancer Research*, vol. 56, no. 19, pp. 4509–4515, 1996.

[26] Q. Chang, I. Jurisica, T. Do, and D. W. Hedley, "Hypoxia predicts aggressive growth and spontaneous metastasis formation from orthotopically grown primary xenografts of human pancreatic cancer," *Cancer Research*, vol. 71, no. 8, pp. 3110–3120, 2011.

[27] A. M. Baker, T. R. Cox, D. Bird et al., "The role of lysyl oxidase in SRC-dependent proliferation and metastasis of colorectal cancer," *Journal of the National Cancer Institute*, vol. 103, no. 5, pp. 407–424, 2011.

[28] H. E. Barker, J. Chang, T. R. Cox et al., "LOXL2-mediated matrix remodeling in metastasis and mammary gland involution," *Cancer Research*, vol. 71, no. 5, pp. 1561–1572, 2011.

Hindawi
Computational and Mathematical Methods in Medicine
Volume 2023, Article ID 9819283, 1 page
https://doi.org/10.1155/2023/9819283

Retraction

Retracted: Effects of Hypoxia-Inducible Factor 1 (HIF-1) Signaling Pathway on Acute Ischemic Stroke

Computational and Mathematical Methods in Medicine

Received 5 December 2023; Accepted 5 December 2023; Published 6 December 2023

This article has been retracted by Hindawi, as publisher, following an investigation undertaken by the publisher [1]. This investigation has uncovered evidence of systematic manipulation of the publication and peer-review process. We cannot, therefore, vouch for the reliability or integrity of this article.

Please note that this notice is intended solely to alert readers that the peer-review process of this article has been compromised.

Wiley and Hindawi regret that the usual quality checks did not identify these issues before publication and have since put additional measures in place to safeguard research integrity.

We wish to credit our Research Integrity and Research Publishing teams and anonymous and named external researchers and research integrity experts for contributing to this investigation.

The corresponding author, as the representative of all authors, has been given the opportunity to register their agreement or disagreement to this retraction. We have kept a record of any response received.

References

[1] G. Li, L. Tao, and H. Wu, "Effects of Hypoxia-Inducible Factor 1 (HIF-1) Signaling Pathway on Acute Ischemic Stroke," *Computational and Mathematical Methods in Medicine*, vol. 2022, Article ID 1860925, 8 pages, 2022.

Hindawi
Computational and Mathematical Methods in Medicine
Volume 2022, Article ID 1860925, 8 pages
https://doi.org/10.1155/2022/1860925

Research Article

Effects of Hypoxia-Inducible Factor 1 (HIF-1) Signaling Pathway on Acute Ischemic Stroke

Guoliang Li,[1] Liang Tao,[2] and Hui Wu[3]

[1]*Department of Neurosurgery, People's Hospital of Dongxihu District, Wuhan, Hubei 430040, China*
[2]*Department of Neurosurgery, Wuhan Third Hospital, Tongren Hospital of Wuhan University, China*
[3]*Department of Traditional Chinese Medicine, Wuhan NO.1 Hospital, 215 Zhongshan Avenue, Qiaokou District, Wuhan, China*

Correspondence should be addressed to Hui Wu; 2016122569@jou.edu.cn

Received 10 July 2022; Revised 9 August 2022; Accepted 5 September 2022; Published 14 October 2022

Academic Editor: Min Tang

Background. Epidemiological surveys show that a large number of cerebrovascular diseases occur in China every year, and among these cerebrovascular diseases, ischemic diseases are predominant. Ischemia leads to irreversible degenerative necrosis of a large number of brain neurons and severe neurological deficits. *Aims*. This study is aimed at exploring the mechanism of the major regulatory effect of hypoxia-inducible factor 1 (HIF-1) pathway on proangiogenesis and providing new ideas for the treatment of ischemic stroke. *Materials and Methods*. The rats were randomly divided into normal and ischemic control groups, and the ischemic control group was subjected to the middle cerebral artery occlusion (MCAO) cerebral ischemia model by the wire embolization method, and the rats were executed in batches at 6 h, 1 d, and 3 d after ischemia-reperfusion, and the brain tissue specimens were taken for examination to investigate the effect of hypoxia-inducible factor 1 (HIF-l) signaling pathway on acute ischemic stroke. *Results*. At 3 d, the number of VEGFR2 positive cells increased significantly, and there was a significant difference compared with the control group ($P < 0.05$). At 3 d, the number of HIF-1α-positive cells increased significantly, and there was a significant difference compared with the control group ($P < 0.05$). The number of Hes1+factor VIII positive cells in the ischemic cortex increased significantly on the 1st and 3rd day, and there was a significant difference compared with the control group ($P < 0.05$). The expression of Hes1 protein was significantly lower than the normal level after 6 h of ischemia, and the protein expression was significantly increased at 1 d and 3 d after ischemia ($P < 0.05$). *Conclusion*. By detecting the expression changes of Hesl+factor VII in the ischemic area, the results show that ischemia and hypoxia activate the HIF-1, making the HIF-l the main regulatory pathway in the process of angiogenesis after ischemia.

1. Introduction

With the in-depth study of the pathophysiology of cerebral ischemic area, it is recognized that there is a penumbra after ischemia, that is, the relative ischemic area around the ischemic core area [1]. In the penumbra area, due to incomplete ischemia due to the supply of collateral circulation, a large number of neurons only undergo reversible degeneration. This reversible degeneration provides an opportunity to rescue as many neurons as possible in future treatments [2]. If the formation of new blood vessels in the ischemic area can be promoted to restore local blood flow as soon as possible, it is not only beneficial to rescue reversibly degenerated neurons but also provides a good microenvironment for the survival, proliferation, and functional remodeling of neural stem cells in the subsequent functional repair. Treatment of stroke can minimize neurological deficits and improve prognosis [3]. Clinical research data show that the prognosis of patients with high-density of new capillaries in the area of cerebral ischemia injury is significantly better than that of patients with low-density, so it can effectively promote the formation of local blood vessels in the ischemic area as soon as possible to restore the blood reperfusion of ischemic brain tissue. The treatment of blood stroke is of great significance [4].

Neovascularization refers to the process of sprouting and forming new functional blood vessels on the basis of the original vascular network, which can be seen in many

pathological and physiological processes [5]. In the process of neovascularization, the expression and synergistic effect of numerous vascular growth factors are required, the most important of which is vascular endothelial growth factor (VEGF) [6]. VEGF is one of the target genes directly regulated by HIF-1, and the two are closely related to the process of angiogenesis after ischemia. In ischemic brain tissue, both are expressed on neurons with the same expression phase [7]. HIF-1 is a transcription factor discovered during erythropoietin gene expression studies in hepatocytes and transgenic animals [8, 9]. So far, more than 100 target genes have been found to directly act on HIF-1, which are involved in the processes of angiogenesis, apoptosis, cell proliferation, and energy metabolism. Hypoxia activates HIF-1 in ischemic stroke and induces HIF-1 related processes. Target genes are transcribed and produce corresponding biological effects [10]. Animal models of ischemia have confirmed that HIF-1 protein can promote the formation of new blood vessels. Even after the removal of the oxygen-dependent degradation region, HIF-1 protein can still activate its downstream target genes to generate a large number of vascular tissues [11]. After hypoxia, HIF-1 not only affects the expression of angiopoietin, platelet growth factor, etc., but also directly acts on downstream target genes such as VEGF to participate in angiogenesis, making it a core regulator of angiogenesis after hypoxia [12]. Further study of its mechanism is that HIF-1 binds to the VEGF site under hypoxic conditions to enhance the expression of VEGF promoter, significantly increase the transcriptional activity of VEGF, and promote angiogenesis [13]. It can be seen that HIF-1 plays an indispensable role in the regulation of VEGF during angiogenesis under hypoxia.

2. Material and Methods

2.1. Research Object. Twenty clean-grade adult (9 weeks) male Sprague-Dawley (SD) rats weighing 250-280 g were selected, and the experimental rats were randomly divided into sham-operated, 6 h, 1 d, and 3 d postischemic groups, with 5 SD rats in each group. The rats with cerebral ischemia were executed at the corresponding time points of 6 h, 1 d, and 3 d after cerebral ischemia-reperfusion, respectively. The rats in the sham-operated group only did the same surgical operation without treating the carotid artery, and the rest treatments were the same for both.

Sterilization: The glass instruments used were soaked in sulfuric acid and potassium dichromate cleaning solution for 24h, then washed thoroughly, then rinsed with triple distilled water, dried in the oven at 60°C, and then sterilized by dry heat at 160°C for 2 h; the plastic equipment used were cleaned, rinsed with triple distilled water, dried at 60°C, and then autoclaved at 120°C; all metal surgical instruments were sterilized by immersion in glutaraldehyde.

De-RNAse Treatment: EP tubes, gun tips, and other disposable supplies were treated with 0.1% DEPC water overnight, dried, and then autoclaved at 120°C; reagents were prepared in newly opened bottles or DEPC water; metal, glass, and other supplies were sterilized by dry baking at 250 C for 4 h.

2.2. Experimental Animal Inclusion Criteria. The following signs were observed after awakening from anesthesia in the MCAO model, and those who showed the following signs indicated the success of the model: Horner's sign on the right side and neurological deficit on the left limb and neurological function score according to the Zea Longa 5-point scale: 0: normal, no symptoms of neurological damage; 1: unable to fully extend the contralateral front paw; 2: turn to the left when walking; 3: lean to the opposite side when walking; 4: unable to walk spontaneously, loss of consciousness. Animal models were included if they scored 1 – 3.

2.3. Methods. Ischemic Injury Model. The focal ischemic injury model of middle cerebral artery embolism was made by referring to the modified Longa and Nagasawa method. The brief steps are as follows: weigh 250-280 g of SD rats, rats were sacrificed intramuscularly at 2 mg/kg xylazine plus 10 mg/kg ketamine, and inject pentobarbital at the same time. Limbs and head were fixed supine on the operating table. Cut off the neck hair, sterilize the skin, make a longitudinal incision in the middle of the neck, and cut the skin to expose the right common carotid artery, internal carotid artery, and external carotid artery. Under the operating microscope, the anterior superficial and deep fascia of the neck was incised to expose the anterior trachea muscle group, which was separated to the depth between the angle formed by the anterior tracheal muscle group and the right sternocleidomastoid muscle. Next step is free the common carotid artery, internal carotid artery, and external carotid artery (be careful not to damage adjacent important nerves and branches) and ligate the proximal common carotid artery and the distal external carotid artery with silk thread, and the internal carotid artery is temporarily blocked by arterial clips. A V-shaped incision was made in the proximal wall of the external carotid artery, and a self-made 4-0 thread plug (about 3 cm in length, with a smooth sphere with a diameter of 0.3 mm at the tip) was inserted into the ordinary carotid artery through the incision first. The next step is insert a 4-0 wire plug (about 0.3 mm in diameter) into the common carotid artery through the incision, then completely incise the external carotid artery, tie the reserved wire on the external carotid artery A, and make sure that the wire plug is not too large when inserted resistance. After that, loosen the arterial clamp, slightly return the bolt at the bifurcation of the common carotid artery, and slide it into the internal carotid artery A. The next steps is slowly enter the middle cerebral artery without resistance, then block the blood supply of the middle cerebral artery, and then stop the insertion when the elastic resistance is felt, and the insertion length is about 18 ± 0.5 m from the bifurcation of the common carotid artery; after that, fix the bolt and apply a simple bandage incision. After blocking the blood supply of the middle cerebral artery for 2 hours, the neurological function of the awake rats was scored, and the rats were anesthetized again. And the rats were anesthetized again for internal carotid artery reperfusion. The cervical incision was sutured and returned to the cage. Rats in the sham operation group only had free blood vessels, and other

treatments were the same as those in the operation group. The rectal temperature of SD rats was maintained between 36.5-37.0°C throughout the surgery. SD rats in each group were sacrificed, and the ischemic cortical brain tissue was preserved. The procedure was as follows: rats were sacrificed intramuscularly at 2 mg/kg xylazine plus 10 mg/kg ketamine, and the heart was perfused with 500 ml of sterile saline to isolate intact brain tissue. After that, place the brain tissue at 20°C for 30 min. Approximately 100 mg of each brain tissue was excised with a deribonuclease-treated razor blade from the affected cortical area before and after the bregma and divided into two deribonuclease-treated 1.5 ml EP tubes and stored in a refrigerator at 80°C.

5 frozen sections of each brain tissue were randomly selected from each experimental group at each time point, and the expression of VEGFR2 in the ischemic cortical area was detected by immunohistochemical staining, and the specific steps were the same as those for HIF-1α immunofluorescence staining and briefly described as follows: rabbit anti-rat VEGFR2 antibody (1 : 100) was added to the brain tissue sections in 60 ul drops, completely covering the brain tissue, at 4°C. The sections were wet boxed overnight, and FITC-labeled goat anti-rabbit IgG (1 : 200) 60 ul was added dropwise on the next day, and the reaction was performed at 37°C for 50 min, protected from light. Glycerol-sealed slices were observed under fluorescence microscope and photographed.

2.3.1. Result Determination: the cytoplasm cytosol of VEGFR2-positive cells showed green fluorescence under fluorescence microscope. Counting: 5 nonoverlapping fields of view were randomly selected in the ischemic cortical area of each section at ×400 cell counting, and the average number of positive cells in each field of view was taken for each brain tissue.

2.3.2. Detection of HIF-1. 5 frozen sections of each brain tissue were randomly selected from each experimental group at each time point, and the expression of Hs1 and microvessel density in vascular endothelial cells in ischemic cortex was detected by double immunohistofluorescence staining with HIF-1+factor VIII. The specific steps are the same as HIF-1α factor immunofluorescence staining: mix mouse anti-rat Hes1 antibody and rabbit anti-rat factor VVII antibody in 0.01 M PBS, so that the final concentration of both antibodies is 1 : 100, take 60ul of the mixture and add on brain tissue sections, react at 4°C for 24 hours; mix TRITC-labeled bovine anti-rabbit IgG and FITC-labeled goat anti-mouse IgG in 0.01MPBS, so that the final concentration of the two antibodies is 1 : 200, take and mix Add 60 ul of the solution to the brain tissue section and react at 37°C for 50 minutes in the dark, and add 50 ul of 1% DAPI solution dropwise and react in the dark for 5 min at room temperature. After mounting with 50% glycerol, observe and take pictures under a fluorescence microscope. The results showed that the cytoplasm of vascular endothelial cells showed red fluorescence under the fluorescence microscope, the cytoplasm of Hs1-positive cells showed green fluorescence, and the nuclei of all cells showed blue fluorescence after DAPI staining. *Counting:* 5 nonoverlapping visual fields were randomly selected in the ischemic cortex of each slice to count Hes1-positive vascular endothelial cells, and the average number of Hs1-positive endothelial cells in each visual field of each brain tissue was taken.

2.4. Statistical Analysis. All statistical data in this study were entered into Excel software by the first author and the corresponding author, respectively, and the statistical processing software was SPSS25.0 for calculation. The mean ± standard deviation ($\bar{x}\pm s$) was used to represent the measured value of the measurement data and compared with the analysis of variance between groups. Count data were expressed as a percentage (%) and compared with χ^2 analysis. Repeated measures analysis of variance between groups was used to measure the measurement expressed as mean ± standard deviation ($\bar{x} \pm s$). Count data expressed as a percentage (%) were tested by χ^2. Included data that did not conform to a normal distribution were described by M (QR), using the Mann–Whitney test. All statistical tests were two-sided probability tests, and the statistical significance was $P < 0.05$.

3. Results

3.1. Expression of HIF-1. There was only a small increase in the number of HIF-1α positive cells in the cortical area after 6 h and 1 d of cerebral ischemia-reperfusion, and the difference in the number of HIF-1 positive cells after 6 h and 1 d was not statistically significant compared with the control group ($P > 0.05$); however, by 3 d, there was a significant increase in the number of HIF-1α positive cells, which was statistically significant compared with the control group ($P < 0.05$). See Figure 1.

3.2. Expression of VEGFR2. The number of VEGFR2-positive cells in cortical areas increased in a few after 6 h and 1 d of cerebral ischemia-reperfusion, and the difference between the number of VEGFR2-positive cells after 6 h and 1 d compared with the control group was not statistically significant ($P > 0.05$); however, by 3 d, the number of VEGFR2-positive cells increased significantly, and there was a statistically significant difference compared with the control group ($P < 0.05$). See Figure 2.

3.3. Changes in Microvessel Density. After 6 hours of cerebral ischemia-reperfusion, the number of Hes1+factor VIII positive cells in the ischemic cortex was lower than normal, and there was a statistical difference between the control group and the 6 h group by t-test ($P < 0.05$). After 1 d and 3 d ischemic cortex the number of Hes1+factor VIII positive cells in the area increased significantly, compared with the control group, there was a significant difference ($P < 0.05$). See Figure 3.

3.4. Test Results. The expression of HIF-1α protein in ischemic cortex was changed at 6 h, 1 d, and 3 d. The expression of HIF-1 was almost the same as normal after 6 h of ischemia. The expression of HIF-1α protein increased significantly after 1 d and 3 d of ischemia, but the expression of HIF-1α was significantly increased after 1 d and 3 d of

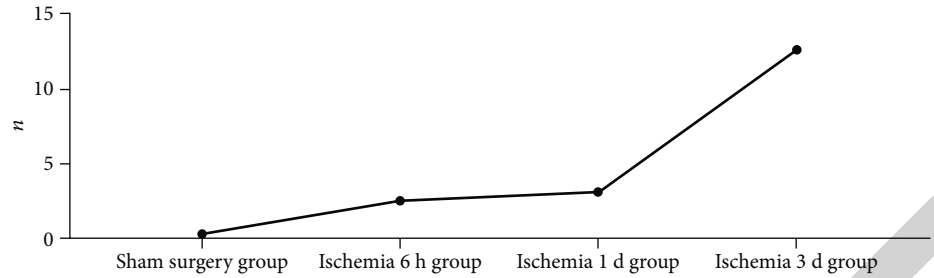

Figure 1: The number of HIF-1α positive cells. All HIF-1 expression data in this study were entered by the author into Excel software, and the statistical processing software was calculated by SPSS25.0, expressed as mean ± standard deviation, and found by independent samples t -test. In the brain the number of HIF-1α positive cells in the cortex increased only slightly after 6 h and 1 d after ischemia-reperfusion, and the number of HIF-1α positive cells after 6 h and 1 d was not significantly different from the control group ($P > 0.05$). The number of HIF-1α positive cells increased significantly when compared with the control group, and the difference was statistically significant ($P < 0.05$).

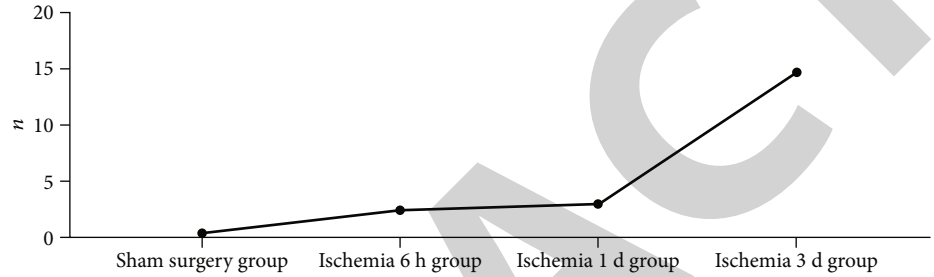

Figure 2: Expression of VEGFR2. All HIF-1 expression data in this study were entered by the author into Excel software, and the statistical processing software was calculated by SPSS25.0, expressed as mean ± standard deviation, and found by independent samples t-test. The number of VEGFR2-positive cells in the cortex increased slightly after 6 h and 1 d of perfusion. There was no significant difference in the number of VEGFR2-positive cells after 6 h and 1d compared with the control group ($P > 0.05$). However, the number of VEGFR2-positive cells increased significantly at 3 d. Compared with the control group, there was a significant difference with statistical significance ($P < 0.05$).

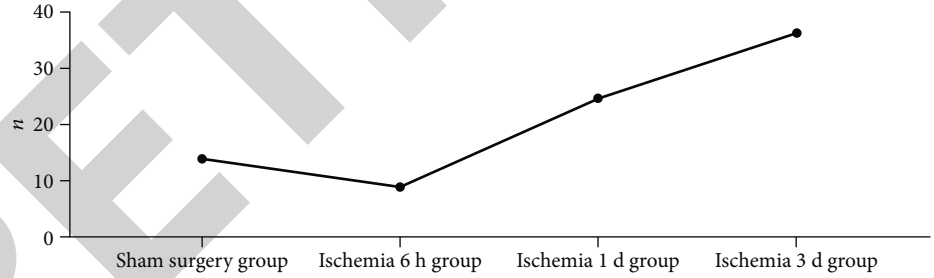

Figure 3: Changes in microvessel density. All changes in microvessel density in this study were entered by the author into excel software, and the statistical processing software was calculated by SPSS25.0, expressed as mean ± standard deviation, and found by independent samples t-test. The number of Hes1+factor VIII positive cells in the ischemic cortex after 6 hours of perfusion was lower than normal, and there was a statistically significant difference between the control group and the 6 h group by t-test ($P < 0.05$). The number of factor-positive cells increased significantly, and there was a significant difference compared with the control group, with statistical significance ($P < 0.05$).

ischemia. The expression of notch1 protein gradually increased in the cerebral cortex at 6 h, 1 d, and 3 d after ischemia and reached a peak at 3 d, while the expression of Hes1 protein first decreased and then increased. After 6 h of ischemia, the Hes1 protein expression was significantly lower than the normal level, and then the protein expression increased significantly at 1 d and 3 d. See Figure 4.

4. Discussion

There is still little progress in the treatment of ischemic stroke, which is still based on symptomatic, neurotrophic, thrombolytic, and anticoagulant treatments with poor prognosis and many residual complications [14]. With the deepening of the understanding of the pathophysiology of the ischemic zone of brain tissue, the concept of cerebral

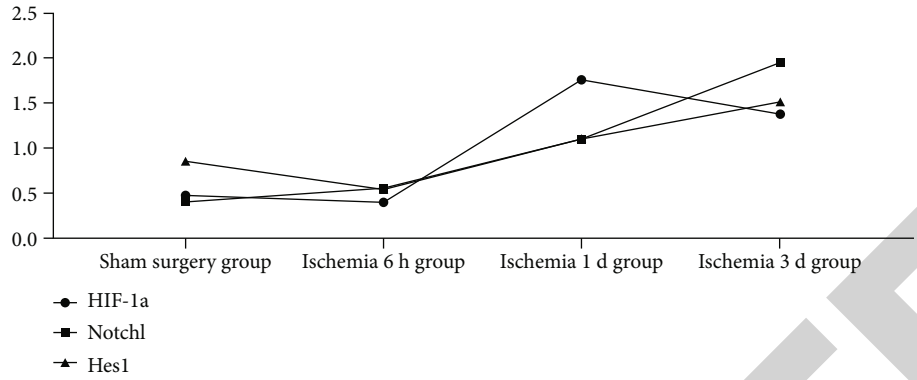

Figure 4: Changes in microvessel density. All changes in this study were entered by the author into Excel software, and the statistical processing software was calculated using SPSS 25.0, expressed as mean ± standard deviation, independent sample t-test. The expression of notch1 protein in the cerebral cortex at 6 h, 1 d, and 3 d after ischemia showed a gradual increasing trend, reaching a peak at 3 d, while the expression of Hes1 protein showed a process of first decreasing and then increasing. At 6 h after ischemia, the expression of Hes1 protein was significantly lower than the normal level, and the protein expression level increased significantly at 1 d and 3 d.

ischemic semidark zone was proposed, and people turned to advocate early restoration of blood flow to save the dying cells in the semidark zone and improve the prognosis of treatment [15]. Newly generated microvessels not only provide blood supply to the ischemic zone but also induce the release of various trophic factors, which are beneficial for neurological recovery. It has been observed in clinical practice that the higher the number of microvessels in the brain tissue of ischemic stroke patients, the longer their poststroke survival time [16]. VEGF is an early and well established vascular growth factor that has been widely used in ischemic diseases, and previous studies have demonstrated that the administration of exogenous vascular growth factor stimulates neurological recovery in ischemic areas. The study of other VEGF-related factors and signaling pathways has further improved the understanding of the process of angiogenesis and provided new ideas for the treatment of ischemic stroke [19].

Both subunits have a base helix loop helix and PAS structure and belong to the bHLH-PAS family [20]. The subunits are located in the cytoplasm, and their concentration levels are correlated with low oxygen concentration levels, while the B subunit is a constructive expression, independent of oxygen concentration, mainly related to maintaining HIF structural stability and dimerization activity conformational shift [21]. Hypoxia-induced production of HIF-1 on neovascularization is currently recognized by the following mechanisms of action: preparation for angiogenesis by synthesizing vasodilation and upregulation of VEGFE and ligand expression to increase vascular permeability [22]. Upregulation of metalloprotein hydrolase activity and degradation of the extracellular matrix provide an environment for cell survival [23]. HIF-1 acts on VEGF to induce migration and proliferation of vascular endothelial cells, binds angiopoietin, and promotes vascular sprout formation [24]. Through the action of VEGF, angiopoietin and integrin, single vessel bud lumen anastomoses with each other forms a vascular network and finally acts on stromal cells through platelet-derived growth factor and angiopoietin 1 to wrap around the neovascularization to form mature vessels [25]. Through the above mechanism of action, it makes HIF-1 a central regulator of posthypoxia vascular neogenesis. α is the active regulatory unit of HIF-1, which includes two important structural domains: the oxygen-dependent degradation structural domain, which regulates the stabilizing effect of HIF under oxygen concentration [26] and the two transcriptional activation structural domains, one each at the N- and C-termini. C-TAD regulates gene transcriptional activity, while N-TAD is the domain of action that forms heterodimers with HIF-1α and binds DNA cis-response elements [27]. Three sequence homology a-subunits have been identified: HIF-1α, HIF-2α, and HIF-3α. Hypoxia is the predominant HIF-1 expression apoptotic factor, and hypoxia-activated HIF-1α binds to HIF-1β, translocates into the nucleus, cross-links to hypoxic response elements in the regulatory region of target genes, and induces gene expression [28]. Under normoxic conditions HIF-lα is hydroxylated by prolyl hydroxylase and acetylated by acetyltransferase, and the hydroxylated and acetylated HIF-1α is then bound to the Von Hippel-Lindau (pVHL) protein and degraded by ubiquitination [29]. Also because the asparagine hydroxylation of HIF-1α affects its binding to the hypoxic response element of the target gene enhancer thereby inhibiting the transcription of downstream target genes, and more than 100 target genes have been found to be directly acted upon by hypoxia-inducible factors, which are involved in processes such as angiogenesis, cell regulation, cell proliferation, and energy metabolism [30]. Due to the importance of VEGF for neovascularization, the relationship between HIF and VEGF after hypoxia has been extensively studied in-depth [31]. In a neonatal mouse model of MCA 1.5 h, it was found that the positive expression of HIF-1 increased after 4 h of ischemia, peaked at 6 h, and started to decrease after 24 h, mainly expressed on neurons, while it was observed that VEGF mRNA appeared to be expressed in brain tissue after 2-4 h, declined after 6 h, and returned to normal levels at 24 h, while the site and temporal phase of VEGF protein expression were the same as those of HIF-1α [32]. In a model of cerebral ischemia caused by cardiac arrest, a significant increase in HIF-1 was detected after 1 h

of reperfusion, and VEGF mRNA and VEGF protein increased at 12-46 h and 24-46 h and persisted until 7 d later, respectively [33]. Rapid expression of HIF-1 was also observed early in mice reischemic after hypoxic preconditioning, while its downstream gene products EPO and VEGF were also abundantly expressed after 6 h [34]. Some studies for the expression of HIF-1 after cerebral ischemia have suggested in the literature that the increase in its expression is induced by postischemic hypoxia [35]. The peak of HIF-1α expression after ischemia was observed at 3 d, while some scholars observed the peak of HIF-lα expression after low pressure cerebral ischemia at 48-96 h. Our experiment also observed an increase in HIF-1 expression after cerebral ischemia, and the results were basically similar to the literature [36]. The expression of HIF-1α increased after 6 h of ischemia-reperfusion, and the number of positive cells reached a peak at 3 d after ischemia. We observed that HIF-1α protein expression increased significantly on day 1 and day 3, but the peak appeared on day 1. The expression of VEGFR2 positive cells was also observed in a gradual increase, with the strongest expression at 3 d. For the peak of HIF-1 expression after ischemia, there are various scenarios appearing among different literature, for the delayed peak of HIF-1α expression after simple cerebral ischemia; this phenomenon has not been clearly explained in the literature, which may be related to a combination of factors such as induction of HIF-1 by rehypoxia after ischemic tolerance and induction of HIF-1α expression by inflammatory factors in response to tissue inflammation after ischemia [37]. Postischemic hypoxia HIF-1 exerts a regulatory effect on VEGF and affects angiogenesis [38]. With the in-depth study, it has been recognized that the apoptotic mechanism of HIF-1 on VEGF expression is as follows: activation of HIF-1 into the nucleus directly binds to HRE to activate VEGF genes and induce transcription [39]. HIF-1 upregulates the transcription of VEGFR1, and HIF-1 acts on specific sites of VEGF mRNA and increases its stability to ensure VEGF expression [40].

We learned from the results of this study by detecting the changes in the expression of Hesl+factor VII in the ischemic area, the results show that ischemia and hypoxia activate the HIF-1 signaling pathway, and with the increase of HIF-1 expression, it can effectively promote the formation of new blood vessels. The same point between the study and previous studies is that cerebral ischemia and hypoxia induce HIF-1α production, comprehensively regulate the upregulation of VEGF expression, bind VEGF to VEGFR2, and activate Notch signaling pathway through intercellular stimulatory signals. The relationship between Notch signaling pathway molecules and VEGFR interaction is that they work together to promote the formation of new blood vessels. There is no divergent field for the time being. The novelty of this study is that by detecting the changes of HIF-1α in the ischemic cerebral cortex, it starts the main process of angiogenesis by regulating the corresponding downstream target genes and has an important effect on angiogenesis after ischemia. By detecting the changes of Hes1+VIII factor expression in the ischemic area, the HIF-1-VEGF-Notch signaling pathway becomes the main regulatory pathway in the process of angiogenesis after ischemia.

In summary, by detecting changes in Hesl+VII factor expression in ischemic areas, the results indicate that ischemia and hypoxia activate the HIF-l, and with the increase in HIF-1 expression, the proliferation of vascular endothelial cells is increased, effectively contributing to neovascularization and making the HIF-1 a major regulatory pathway in the process of postischemic vascular neogenesis.

Data Availability

No data were used to support this study.

Conflicts of Interest

The authors declare that they have no conflicts of interest.

Authors' Contributions

Guoliang Li designed and performed the experiments. Liang Tao provided support for data analysis and writing the manuscript, and Hui Wu provided the supervision, resources, discussion, design, and peer review process. All the authors have seen and approved the manuscript. Guoliang Li and Liang Tao are co-first authors, and both authors contributed equally to the work.

References

[1] F. A. Montellano, K. Ungethüm, L. Ramiro et al., "Role of blood-based biomarkers in ischemic stroke prognosis: a systematic review," *Stroke*, vol. 52, no. 2, pp. 543–551, 2021.

[2] T. Tao, M. Liu, M. Chen et al., "Natural medicine in neuroprotection for ischemic stroke: challenges and prospective," *Pharmacology & Therapeutics*, vol. 216, article 107695, 2020.

[3] Y. Zhou, J. Liao, Z. Mei, X. Liu, and J. Ge, "Insight into crosstalk between ferroptosis and necroptosis: novel therapeutics in ischemic stroke," *Oxidative Medicine and Cellular Longevity*, vol. 2021, Article ID 9991001, 19 pages, 2021.

[4] A. Ajoolabady, S. Wang, G. Kroemer et al., "Targeting autophagy in ischemic stroke: from molecular mechanisms to clinical therapeutics," *Pharmacology & Therapeutics*, vol. 225, article 107848, 2021.

[5] P. Jolugbo and R. A. S. Ariëns, "Thrombus composition and efficacy of thrombolysis and thrombectomy in acute ischemic stroke," *Stroke*, vol. 52, no. 3, pp. 1131–1142, 2021.

[6] D. Zhang, F. L. Lv, and G. H. Wang, "Effects of HIF-1α on diabetic retinopathy angiogenesis and VEGF expression," *European Review for Medical and Pharmacological Sciences*, vol. 22, no. 16, pp. 5071–5076, 2018.

[7] A. Zimna and M. Kurpisz, "Hypoxia-inducible factor-1 in physiological and pathophysiological angiogenesis: applications and therapies," *BioMed Research International*, vol. 2015, Article ID 549412, 13 pages, 2015.

[8] F. Şimşek, Ü. Işık, E. Aktepe, F. Kılıç, F. B. Şirin, and M. Bozkurt, "Comparison of serum VEGF, IGF-1, and HIF-1α levels in children with autism spectrum disorder and healthy controls," *Journal of Autism and Developmental Disorders*, vol. 51, no. 10, pp. 3564–3574, 2021.

[9] R. C. de Mattos, I. D. S. Guimarães, L. S. Thiago, and A. C. de Melo, "Evaluation of HIF-1α and VEGF-A expression in

radiation-induced cystitis: A case-control study," *International Brazilian Journal of Urology*, vol. 47, no. 2, pp. 295–305, 2021.

[10] S. Han, J. Huh, W. Kim, S. Jeong, D. S. Min, and Y. Jung, "Phospholipase D activates HIF-1-VEGF pathway via phosphatidic acid," *Experimental & Molecular Medicine*, vol. 46, no. 12, p. e126, 2014.

[11] S. B. Choi, J. B. Park, T. J. Song, and S. Y. Choi, "Molecular mechanism of HIF-1-independent VEGF expression in a hepatocellular carcinoma cell line," *International Journal of Molecular Medicine*, vol. 28, no. 3, pp. 449–454, 2011.

[12] F. Plastino, N. A. Pesce, and H. André, "MicroRNAs and the HIF/VEGF axis in ocular neovascular diseases," *Acta Ophthalmologica*, vol. 99, no. 8, pp. e1255–e1262, 2021.

[13] H. Liu, X. Ren, and C. Ma, "Effect of berberine on angiogenesis and HIF-1α/VEGF signal transduction pathway in rats with cerebral ischemia-reperfusion injury," *Journal of the College of Physicians and Surgeons–Pakistan*, vol. 28, no. 10, pp. 753–757, 2018.

[14] C. D. Maida, R. L. Norrito, M. Daidone, A. Tuttolomondo, and A. Pinto, "Neuroinflammatory mechanisms in ischemic stroke: focus on cardioembolic stroke, background, and therapeutic approaches," *International Journal of Molecular Sciences*, vol. 21, no. 18, p. 6454, 2020.

[15] S. Zhang, J. Zhang, C. Wang et al., "COVID-19 and ischemic stroke: mechanisms of hypercoagulability (Review)," *International Journal of Molecular Medicine*, vol. 47, no. 3, p. 21, 2021.

[16] X. T. Su, L. Wang, S. M. Ma et al., "Mechanisms of acupuncture in the regulation of oxidative stress in treating ischemic stroke," *Oxidative Medicine and Cellular Longevity*, vol. 2020, Article ID 7875396, 15 pages, 2020.

[17] S. Paul and E. Candelario-Jalil, "Emerging neuroprotective strategies for the treatment of ischemic stroke: an overview of clinical and preclinical studies," *Experimental Neurology*, vol. 335, article 113518, 2021.

[18] M. Sakai, N. Takahashi, H. Ikeda et al., "Design, synthesis, and target identification of new hypoxia-inducible factor 1 (HIF-1) inhibitors containing 1-alkyl-1 _H_ -pyrazole-3-carboxamide moiety," *Bioorganic & Medicinal Chemistry*, vol. 46, p. 116375, 2021, Epub 2021 Aug 30.

[19] A. M. Basavaraju, N. Shivanna, C. Yadavalli, P. K. Garlapati, and A. K. Raghavan, "Ameliorative effect of Ananas comosus on cobalt chloride-induced hypoxia in Caco2 cells via HIF-1α, GLUT 1, VEGF, ANG and FGF," *Biological Trace Element Research*, vol. 199, no. 4, pp. 1345–1355, 2021.

[20] Y. K. Choi, "A positive circuit of VEGF increases Glut-1 expression by increasing HIF-1α gene expression in human retinal endothelial cells," *Archives of Pharmacal Research*, vol. 40, no. 12, pp. 1433–1442, 2017.

[21] Y. Wang, Y. D. Zhu, Q. Gui, X. D. Wang, and Y. X. Zhu, "Glucagon-induced angiogenesis and tumor growth through the HIF-1-VEGF-dependent pathway in hyperglycemic nude mice," *Genetics and Molecular Research*, vol. 13, no. 3, pp. 7173–7183, 2014.

[22] R. B. Reis, A. A. Rodrigues Junior, R. N. Feres, and V. F. Muglia, "Editorial comment: evaluation of HIF-1α and VEGF-A expression in radiation-induced cystitis: a case-control study," *International Brazilian Journal of Urology*, vol. 47, no. 2, pp. 306-307, 2021.

[23] S. Cascio, A. D'Andrea, R. Ferla et al., "miR-20b modulates VEGF expression by targeting HIF-1α and STAT3 in MCF-7 breast cancer cells," *Journal of Cellular Physiology*, vol. 224, no. 1, pp. 242–249, 2010.

[24] P. Zhang, Y. Wang, Y. Hui et al., "Inhibition of VEGF expression by targeting HIF-1 alpha with small interference RNA in human RPE cells," *Ophthalmologica*, vol. 221, no. 6, pp. 411–417, 2007, PMID: 17947829.

[25] D. Medici and B. R. Olsen, "Rapamycin inhibits proliferation of hemangioma endothelial cells by reducing HIF-1-dependent expression of VEGF," *PLoS One*, vol. 7, no. 8, article e42913, 2012.

[26] M. L. Lemus-Varela, M. E. Flores-Soto, R. Cervantes-Munguía et al., "Expression of HIF-1α, VEGF and EPO in peripheral blood from patients with two cardiac abnormalities associated with hypoxia," *Clinical Biochemistry*, vol. 43, no. 3, pp. 234–239, 2010.

[27] R. Amato, F. Pisani, E. Laudadio et al., "HIF-1-dependent induction of β3 adrenoceptor: evidence from the mouse retina," *Cell*, vol. 11, no. 8, p. 1271, 2022.

[28] M. Kobayashi, A. Morinibu, S. Koyasu, Y. Goto, M. Hiraoka, and H. Harada, "A circadian clock gene, PER2, activates HIF-1 as an effector molecule for recruitment of HIF-1α to promoter regions of its downstream genes," *The FEBS Journal*, vol. 284, no. 22, pp. 3804–3816, 2017.

[29] M. C. Chen, W. L. Hsu, P. A. Hwang, and T. C. Chou, "Low molecular weight fucoidan inhibits tumor angiogenesis through downregulation of HIF-1/VEGF signaling under hypoxia," *Marine Drugs*, vol. 13, no. 7, pp. 4436–4451, 2015.

[30] G. E. Görtz, M. Horstmann, B. Aniol et al., "Hypoxia-dependent HIF-1 activation impacts on tissue remodeling in Graves' ophthalmopathy-implications for smoking," *The Journal of Clinical Endocrinology and Metabolism*, vol. 101, no. 12, pp. 4834–4842, 2016.

[31] M. Dai, P. Cui, M. Yu, J. Han, H. Li, and R. Xiu, "Melatonin modulates the expression of VEGF and HIF-1α induced by CoCl2 in cultured cancer cells," *Journal of Pineal Research*, vol. 44, no. 2, pp. 121–126, 2008.

[32] P. Farhadi, R. Yarani, S. Kiani, and K. Mansouri, "Perfluorocarbon as an adjuvant for tumor anti-angiogenic therapy: relevance to hypoxia and HIF-1," *Medical Hypotheses*, vol. 146, article 110357, 2021.

[33] Y. Wang and Q. Hua, "Clinical significance of HIF-1 alpha, VEGF and VEGF-C expression in papillary thyroid carcinoma," *Lin Chung Er Bi Yan Hou Tou Jing Wai Ke Za Zhi*, vol. 21, no. 5, pp. 204–206, 2007, 208.

[34] J. Yan, Z. Zhang, and H. Shi, "HIF-1 is involved in high glucose-induced paracellular permeability of brain endothelial cells," *Cellular and Molecular Life Sciences*, vol. 69, no. 1, pp. 115–128, 2012.

[35] D. Trisciuoglio, C. Gabellini, M. Desideri et al., "Involvement of BH4 domain of bcl-2 in the regulation of HIF-1-mediated VEGF expression in hypoxic tumor cells," *Cell Death and Differentiation*, vol. 18, no. 6, pp. 1024–1035, 2011.

[36] C. Y. Cheng, T. Y. Ho, C. Y. Hsiang et al., "Angelica sinensisExerts Angiogenic and anti-apoptotic effects against cerebral ischemia-reperfusion injury by activating p38MAPK/HIF-1α/VEGF-A signaling in rats," *The American Journal of Chinese Medicine*, vol. 45, no. 8, pp. 1683–1708, 2017.

[37] W. J. Piotrowski, J. Kiszałkiewicz, D. Pastuszak-Lewandoska et al., "Expression of HIF-1A/VEGF/ING-4 axis in pulmonary sarcoidosis," *Advances in Experimental Medicine and Biology*, vol. 866, pp. 61–69, 2015.

Hindawi
Computational and Mathematical Methods in Medicine
Volume 2023, Article ID 9786509, 1 page
https://doi.org/10.1155/2023/9786509

Retraction

Retracted: Effect of Parecoxib Sodium Combined with Dexmedetomidine on Analgesia and Postoperative Pain of Patients Undergoing Hysteromyomectomy

Computational and Mathematical Methods in Medicine

Received 12 December 2023; Accepted 12 December 2023; Published 13 December 2023

This article has been retracted by Hindawi, as publisher, following an investigation undertaken by the publisher [1]. This investigation has uncovered evidence of systematic manipulation of the publication and peer-review process. We cannot, therefore, vouch for the reliability or integrity of this article.

Please note that this notice is intended solely to alert readers that the peer-review process of this article has been compromised.

Wiley and Hindawi regret that the usual quality checks did not identify these issues before publication and have since put additional measures in place to safeguard research integrity.

We wish to credit our Research Integrity and Research Publishing teams and anonymous and named external researchers and research integrity experts for contributing to this investigation.

The corresponding author, as the representative of all authors, has been given the opportunity to register their agreement or disagreement to this retraction. We have kept a record of any response received.

References

[1] X. Wang, Y. Chen, Y. Zhao et al., "Effect of Parecoxib Sodium Combined with Dexmedetomidine on Analgesia and Postoperative Pain of Patients Undergoing Hysteromyomectomy," *Computational and Mathematical Methods in Medicine*, vol. 2022, Article ID 5123933, 7 pages, 2022.

Hindawi
Computational and Mathematical Methods in Medicine
Volume 2022, Article ID 5123933, 7 pages
https://doi.org/10.1155/2022/5123933

Research Article

Effect of Parecoxib Sodium Combined with Dexmedetomidine on Analgesia and Postoperative Pain of Patients Undergoing Hysteromyomectomy

Xiaowei Wang, Yongxue Chen, Yonglei Zhao, Zhigang Wang, Lu Zhao, Junde Hou, and Fei Liu

Department of Anesthesia, Handan Central Hospital, China

Correspondence should be addressed to Fei Liu; hdlf2021@163.com

Received 27 July 2022; Revised 16 August 2022; Accepted 15 September 2022; Published 14 October 2022

Academic Editor: Min Tang

Background. Propofol combined with remifentanil is the most common anesthesia method in laparoscopic hysteromyomectomy. However, whether the combination of the two is helpful to patients undergoing hysteromyomectomy still requires unclear. *Objective*. To determine the effect of parecoxib sodium combined with dexmedetomidine on analgesia and postoperative pain of patients undergoing hysteromyomectomy. *Methods*. Altogether, 72 patients receiving hysteromyomectomy in our hospital from February 2017 to March 2019 were enrolled. Among them, 35 patients treated with parecoxib sodium were assigned to the control group, while the rest 37 patients treated with parecoxib sodium combined with dexmedetomidine were assigned to the research group. The following items of the two groups were evaluated: visual analog scale (VAS) score, mechanical pain threshold (MPT), Riker sedation-agitation scale (RSAS) score, and expression of serum cortisol and melatonin. *Results*. At 12 and 24 h after operation, the VAS score of the research group was lower than that of the control group ($P < 0.05$), and at 6, 12, and 24 h after operation, the MPT of the research group was notably higher than that of the control group ($P < 0.05$). In addition, at 10 min after extubation, the research group got notably lower RSAS score than the control group ($P < 0.05$). Before extubation and at 20 min after extubation, the research group showed notably higher melatonin expression and notably lower serum cortisol expression than the control group (both $P < 0.05$). *Conclusion*. Parecoxib sodium combined with dexmedetomidine can effectively control the postoperative pain of patients undergoing hysteromyomectomy, reduce the incidence of agitation, and effectively control serum cortisol and melatonin in them.

1. Introduction

Hysteromyoma is the most common benign tumors of female genitalia, with a global incidence of about 34.8% [1]. It mostly occurs in middle-aged and elderly people [2]. According to the statistical results obtained by Pritts et al., there were about 1.1 million new patients with hysteromyoma worldwide in 2015 [3]. One study by Carranza-Mamane et al. [4] has pointed out that the incidence of hysteromyoma is increasing annually, and more and more young people suffer from it. It is estimated that over 10 million patients will suffer from hysteromyoma worldwide by 2050 [5]. Hysteromyoma has always been a clinical research hotspot due to its high incidence. The main symptoms of patients with uterine fibroids are increased menstruation, prolonged menstruation, increased vaginal secretions or vaginal discharge, compression symptoms (such as frequent urination, constipation), etc. As hysteromyoma has no obvious characteristics in the early stage, patients with this disease often do not have significant clinical manifestations, which leads them to miss the best treatment opportunity [6]. Therefore, the clinically reported incidence of uterine fibroids is much lower than the actual incidence of uterine fibroids. As the disease progresses, if the disease cannot be controlled in time, it will not only endanger women's physical health and induce the consequences of hysterectomy, but also affect their psychological state along with the disease. The current treatment of uterine fibroids can be roughly divided into: follow-up observation, drug treatment, surgical treatment,

minimally noninvasive treatment, minimally noninvasive surgical treatment including high intensity focused ultrasound (HIFU), and uterine artery embolization. Currently, operation is the most effective treatment for hysteromyoma [7]. As laparoscopic technique develops and comes into use, there is an efficient and minimally invasive method for hysteromyoma, and patients suffer significantly less surgical trauma and have higher acceptance toward surgery [8].

Propofol combined with remifentanil is the most common anesthesia method in laparoscopic hysteromyomectomy. Targeted continuous pumping can control the depth of anesthesia, with the advantages of taking effect quickly and contributing to fast recovery [9, 10]. Patients may suffer from different degrees of hyperalgesia during recovery and are likely to have agitation, which will greatly compromise their postoperative recovery, so it is necessary to use analgesic and sedative drugs [11]. According to studies by Hadi et al. and Lenz et al., parecoxib sodium and dexmedetomidine can effectively alleviate patients' hyperalgesia and agitation during recovery [12, 13]. However, whether the combination of the two is helpful to patients undergoing hysteromyomectomy still requires further study.

Therefore, this study explored the effect of parecoxib sodium combined with dexmedetomidine on analgesia and postoperative pain of patients undergoing hysteromyomectomy, with the goal of providing reference for future clinical practice.

2. Materials and Methods

2.1. Clinical Data. Altogether, 72 patients receiving hysteromyomectomy in our hospital from February 2017 to March 2019 were enrolled. Among them, 35 patients (mean age of 32.5 ± 6.8 years) treated with parecoxib sodium were assigned to the control group, while the rest 37 patients (mean age of 32.7 ± 6.4 years) treated with parecoxib sodium combined with dexmedetomidine were assigned to the research group. This study was carried out with permission from the Ethics Committee of our hospital.

2.2. Inclusion and Exclusion Criteria. The inclusion criteria of the study are as follows: patients clinically diagnosed as hysteromyoma based on abdominal ultrasonography, patients whose myoma location and size were determined, patients ≥20 years old, patients with detailed general clinical data, and those who or whose immediate families signed informed consent forms.

The exclusion criteria of the study are as follows: patients with severe comorbid cognitive or mental disorders, patients who dropped out from the study halfway, patients with comorbid malignant tumor, severe organ dysfunction, infectious diseases, coagulation dysfunction or hypertension, patients unable to cooperate with the evaluation of perioperative pain and other indicators, and patients with contraindications to sedative and analgesic drugs including propofol, remifentanil, parecoxib sodium, and dexmedetomidine.

2.3. Anesthesia Methods. Before operation, each patient was required to fast for food and liquids and injected with penehyclidine hydrochloride (0.5 mg) and phenobarbital sodium (0.1 g) to promote his/her muscle relaxation and reduce his/her gland secretion. The patient' airway was evaluated to understand if he/she had difficult airway, and his/her vital signs including respiration, heart rate, and blood pressure were monitored. Anesthesia induction: each patient was injected intravenously with propofol (2 m/kg) and midazolam (0.06 mg/kg) and also injected intravenously with 15 μg sufentanil for analgesia. In addition, rocuronium (0.15 mg/kg) was adopted as muscle relaxant for each patient. For patients operated on for a long time, the muscle relaxant was added intermittently during the operation. After anesthesia induction, each patient was given tracheal intubation, and remifentanil and propofol were pumped into the patient through a micro pump. At the end, the patient was injected intramuscularly with atropine and neostigmine, and the inserted trachea was pulled out when the patient was able to breathe spontaneously. For patients in the control group, 40 mg parecoxib sodium (Pfizer Inc., State Food and Drug Administration (SFDA) approval number: J20080045) was injected intravenously before pneumoperitoneum was established. For patients in the research group, 0.5 μg/kg dexmedetomidine (Guorui Pharmaceutical Co., Ltd., Sichuan, SFDA: 20110097) was injected based on treatment for the control group.

2.4. Enzyme Linked Immunosorbent Assay (ELISA) Determination. Fasting venous peripheral blood (4 mL) was sampled from each patient before and after treatment and let to stand at room temperature for 30 min, followed by 10-min centrifugation at 3000 rpm/min to obtain the upper serum. The obtained serum was subpackaged by enzyme-free EP tubes. Some samples were adopted for experiment, and the rest were stored at -80°C. ELISA kits were purchased from Beijing North Biotechnology Co., Ltd., and all steps were carried out strictly according to the kit instructions.

2.5. Scoring Criteria. The visual analog scale (VAS) was adopted to evaluate the postoperative pain of each patient [14]. The scale has a full score of 10 points, and a higher score indicates more serious pain and worse pain control effect. The Von Frey Kit was adopted to measure the mechanical pain threshold (MPT) of each patient at different time points as follows: the fiber tip of the detection tool was made to vertically contact with the skin 2 cm around the incision, and the fiber tip was bent for 2 s. The fiber size was increased gradually from 0.4 g, and the increase was stopped when the patient felt tingling pain. The final intensity value (Xf) was recorded. MPT = Xf × maximum likelihood estimation value × logarithmic value of intensity distance. In addition, the Riker sedation-agitation scale (RSAS) was adopted to score the agitation of each patient after recovery. The scoring rules were as follows: 1 point if the patient could not be awaken, and he/she only responded slightly to malignant stimulation, or even had no response; 2 points if the patient was in sedation, responding to physical stimulation, but unable to respond and communicate with instructions; 3 points if the patient was in sedation and drowsiness, could be awaken by mild stimulation, could obey simple instructions, and fall asleep quickly; 4 points if

Table 1: Comparison of clinical data between control group and observation group [n(%)].

	The research group ($n = 37$)	The control group ($n = 35$)	χ^2 or t	P value
Age (Y)	32.7 ± 6.4	32.5 ± 6.8	0.055	0.956
Hypertension history				
Yes	11 (29.73)	12 (34.29)	0.172	0.679
No	26 (70.27)	23 (65.71)		
BMI	22.05 ± 1.24	22.02 ± 1.17	0.106	0.916
Smoking history				
Yes	15 (40.56)	14 (40.00)	0.002	0.963
No	22 (59.46)	21 (60.00)		
Drinking history				
Yes	18 (48.65)	17 (48.57)	0.007	0.995
No	19 (51.35)	18 (51.43)		
Place of residence				
Urban area	23 (62.16)	25 (71.43)	0.695	0.405
Rural area	14 (37.84)	10 (28.57)		
Dietary favor				
Light	12 (32.43)	11 (31.43)	0.008	0.927
Spicy	25 (67.57)	24 (68.57)		
Exercise habit				
Yes	23 (62.16)	20 (57.14)	0.188	0.664
No	14 (37.84)	15 (42.86)		
Course of disease (week)	4.74 ± 1.04	4.92 ± 0.86	0.798	0.427

the patient was quiet, could be awaken easily, and could obey instructions; 5 points if the patient was restless and anxious and could be made to recover to a quiet state under promotion of medical staff; 6 points if the patient was in a relatively serious agitation and required repeated persuasion and even protective restriction by medical staff; 7 points if the patient was in a threatening agitation, he/she attacked on medical staff, and cooperation with him/her was difficult to achieve. Riker score ≥ 5 points was defined as agitation.

2.6. Outcome Measures. Primary outcome measures are as follows: VAS score, MPT, and RSAS score of each patient were evaluated.

Secondary outcome measures are as follows: the expression of serum cortisol and melatonin in each patient was determined.

2.7. Statistical Analyses. In this study, the collected data were analyzed statistically using SPSS20.0 (IBM Corp, Armonk, NY, USA) and visualized into required figures using GraphPad 7. Data distribution was analyzed using the Kolmogorov-Smirnov (K-S) test, and data in normal distribution were expressed as the mean ± standard deviation (Mean ± SD). Intergroup comparison was carried out using the independent-samples t test and introgroup comparison was carried out using the paired t test. Enumeration data were expressed as the rate (%), analyzed using the chi-square test, and expressed as χ^2. $P < 0.05$ indicates a notable difference.

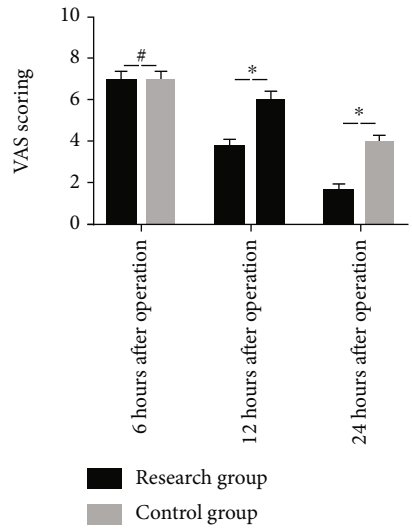

Figure 1: VAS scores of patients at different time points. At 12 and 24 h after operation, the VAS score of the research group was greatly lower than that of the control group. Note: $^*P < 0.05$ vs. research group.

3. Results

3.1. Clinical Data. There was no remarkable difference between the research group and the control group in clinical data including age, hypertension history, body mass index (BMI), smoking history, drinking history, place of residence,

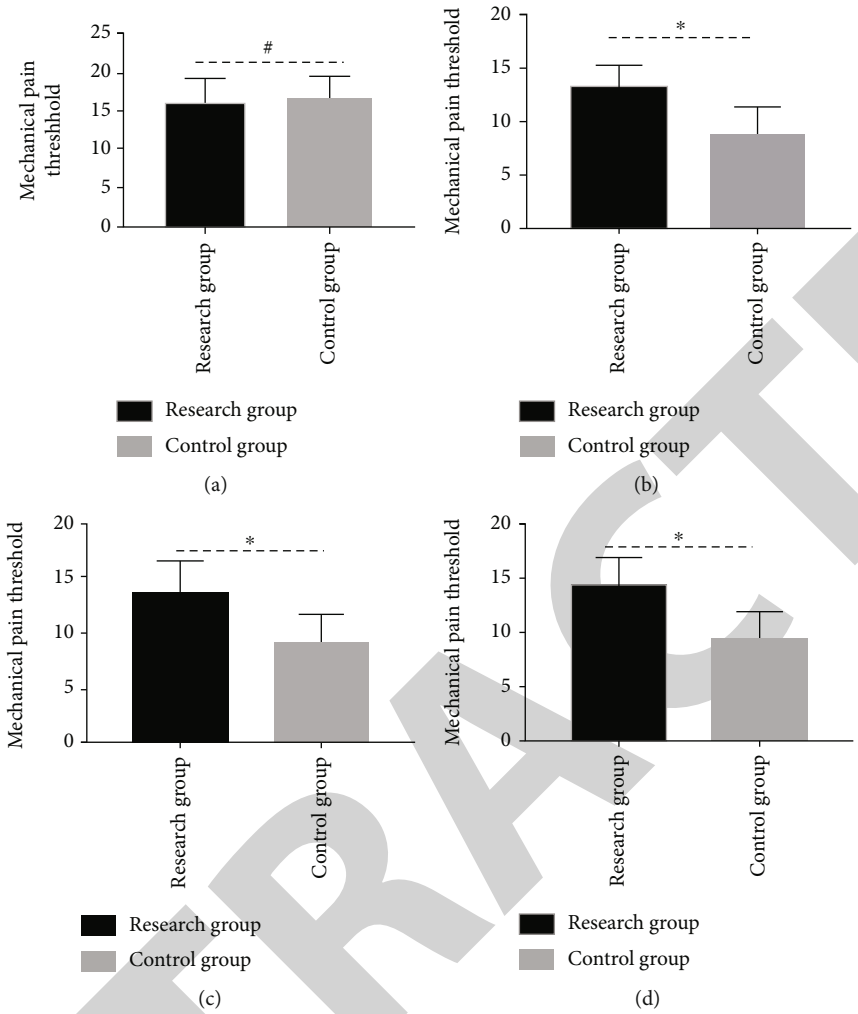

Figure 2: Comparison of mechanical pain threshold between the two groups. (a) Comparison of mechanical pain threshold between the two groups before anesthesia induction. (b) Comparison of mechanical pain threshold between the two groups at 6 h after operation. (c) Comparison of mechanical pain threshold between the two groups at 12 h after operation. (d) Comparison of mechanical pain threshold between the two groups at 24 h after operation. Note: $^{*}P < 0.05$ vs. research group.

dietary favor, exercise habit, and course of disease, so they were comparable (all $P > 0.05$). Table 1.

3.2. VAS Score. No notable difference was found between the two groups in VAS score at 6 h after operation ($P > 0.05$), while at 12 and 24 h after operation, the VAS score of the research group was greatly lower than that of the control group ($P < 0.05$) as shown in Figure 1.

3.3. MPT of Patients. Before anesthesia induction, no notable difference was found between the two groups in MPT ($P > 0.05$), while at 6, 12, and 24 h after operation, the research group showed notably higher MPT than the control group ($P < 0.05$) as shown in Figure 2.

3.4. RSAS Score. There was no notable difference in RSAS score between the two groups at extubation ($P > 0.05$), while the score of the research group was notably lower than that of the control group at 10 min after extubation ($P < 0.05$) as shown in Figure 3.

3.5. Expression of Melatonin. According to the determination results of melatonin, the two groups were not notably different in the expression before anesthesia induction ($P > 0.05$), while before extubation and at 20 min after extubation, the research group showed notably higher melatonin expression than the control group ($P < 0.05$) as shown in Figure 4.

3.6. Expression of Serum Cortisol. According to the determination results of serum cortisol, the two groups were not notably different in the expression of serum cortisol before anesthesia induction ($P > 0.05$), while before extubation and at 20 min after extubation, the research group showed notably lower cortisol expression than the control group ($P < 0.05$) as shown in Figure 5.

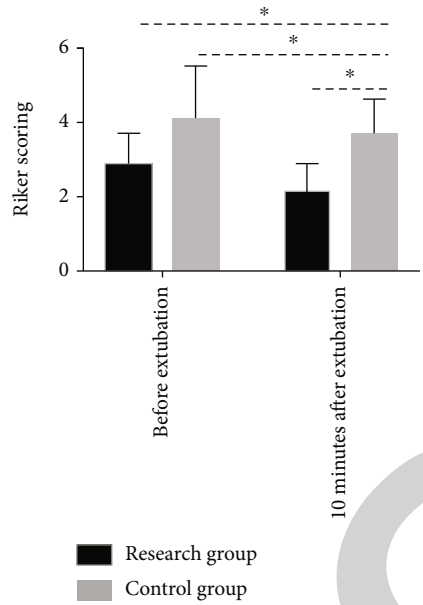

Figure 3: RSAS score of patients. The RSAS score of the research group was notably lower than that of the control group at 10 min after extubation ($P < 0.05$). Note: $^*P < 0.05$ vs. research group.

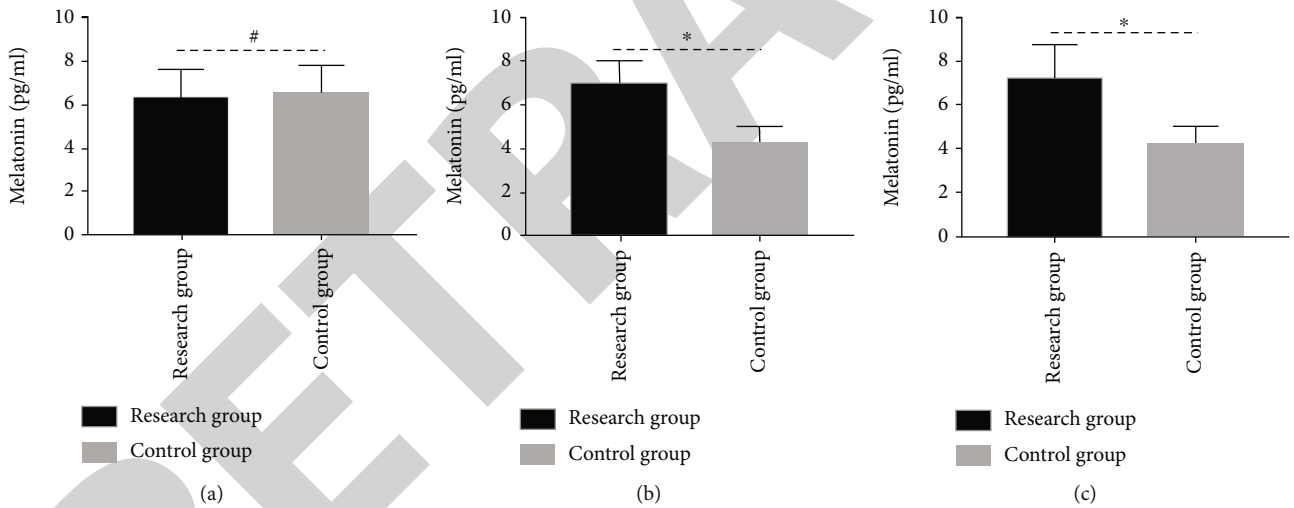

Figure 4: Expression of melatonin. (a) Comparison of melatonin expression between the two groups before anesthesia induction. (b) Comparison of melatonin expression between the two groups before extubation. (c) Comparison of melatonin expression between the two groups at 20 min after extubation. Note: $^*P < 0.05$ vs. research group.

4. Discussion

Hysteromyoma is the tumor with the highest incidence in female genitalia, and its pathogenesis has always been a hot clinical research topic. However, there is a lack of clear research on the pathogenesis of hysteromyoma at home and abroad. As modern medical technology advances, gene theory has been gradually verified to be closely related to many tumor diseases [15, 16]. The activation of oncogenes and inactivation of tumor suppressor genes and mismatch repair genes are the basis of tumorigenesis and development. The overexpression of some oncogenes is caused by gene amplification. Moreover, oncogenes may gain selective growth advantages and produce resistance to chemotherapy drugs, which are all factors affecting the prognosis of patients with tumor [17, 18].

In this study, we compared VAS score and RSAS score between the two groups, finding that combination of 0.5 μg/kg dexmedetomidine and 40 mg parecoxib sodium can effectively relieve postoperative pain and allergy and reduce postoperative agitation of patients receiving laparoscopic hysteromyomectomy under general anesthesia of propofol and remifentanil. The occurrence of hyperalgesia is related to the increased sensitivity of spinal dorsal horn neurons. After anesthesia and operation, the postsynaptic potential mediated by N-methyl-D-aspartate receptor

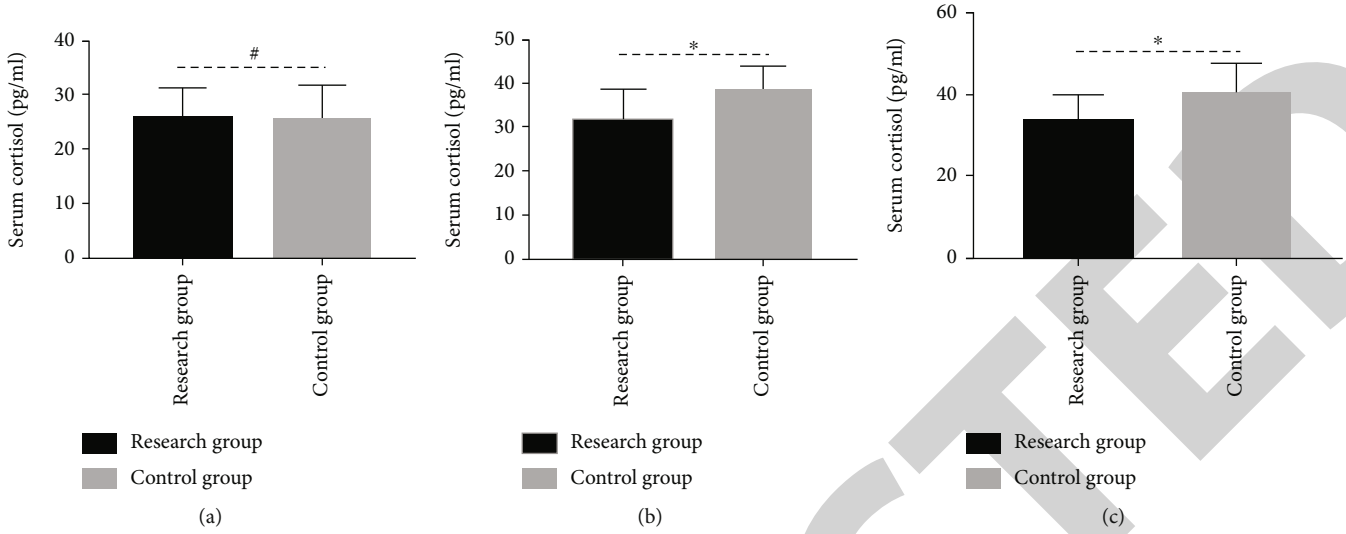

Figure 5: Expression of serum cortisol. (a) Comparison of serum cortisol expression between the two groups before anesthesia induction. (b) Comparison of serum cortisol expression between the two groups before extubation. (c) Comparison of serum cortisol expression between the two groups at 20 min after extubation. Note: $^*P < 0.05$ vs. research group.

increases, while the threshold of action potential decreases. Dexmedetomidine exerts antagonistic effect on N-methyl-D-aspartate receptor, thus inhibiting hyperalgesia. Its inhibitory effect on postoperative hyperalgesia in patients receiving general surgery has also been widely recognized [19, 20]. Parecoxib sodium is a novel COX-2 inhibitor which has been put into clinical use in recent years. It metabolizes into valdecoxib after entering blood and exerts the inhibition of COX-2 activity in peripheral and central nervous system [21]. Some studies have shown that patients undergoing laparoscopic hysteromyomectomy have different degrees of pain hypersensitivity, and the auxiliary use of dexmedetomidine before pneumoperitoneum can significantly ameliorate the reduction of MPT. Both dexmedetomidine and parecoxib sodium can strongly relieve postoperative pain hypersensitivity. The combination of them has better inhibitory effect on pain hypersensitivity at 24 h after operation, and the efficacy difference may be related to the mechanism of drug action [22]. We analyzed the expression of serum cortisol and melatonin in the two groups, finding that before anesthesia induction, the two groups were not greatly different in the expression of them, while before extubation and at 20 min after extubation, the research group showed notably higher melatonin expression and notably lower serum cortisol expression than the control group. Postoperative agitation of patients receiving general anesthesia is mainly manifested as excitement and disorientation. Its mechanism is not completely clear at present, and it may be related to surgical trauma, massive blood loss, postoperative pain, and catheter indwelling. Improper handling may bring about serious complications and may be even life-threatening [23]. Agitation after recovery may be linked to the change of nervous system excitability. Melatonin is a crucial hormone regulating the excitability, but surgery, trauma, and other factors may lead to a decrease in melatonin secretion, inhibiting central excitement and inducting agitation during the recovery period [24].

Through the above study, we have preliminarily verified that parecoxib sodium combined with dexmedetomidine can alleviate agitation, hyperalgesia and postoperative pain in patients undergoing hysteromyomectomy. However, the study still has some limitations. The drug dose is relatively single and the sample size is small. Therefore, we hope to include more samples and increase drug dosage in future research to make our study more comprehensive and supplement our research results.

To sum up, parecoxib sodium combined with dexmedetomidine can effectively control the postoperative pain of patients undergoing hysteromyomectomy and reduce their agitation, which provides reference for future clinical practice.

Data Availability

The datasets used and analyzed during the current study are available from the corresponding author upon reasonable request.

Conflicts of Interest

The authors declare that they have no conflicts of interest.

Authors' Contributions

Xiaowei Wang and Junde Hou contributed equally to this work and share first authorship.

References

[1] J. Donnez, R. Hudecek, O. Donnez et al., "Efficacy and safety of repeated use of ulipristal acetate in uterine fibroids," *Fertility and Sterility*, vol. 103, no. 2, pp. 519–527.e3, 2015.

[2] E. A. Stewart, "Uterine fibroids," *New England Journal of Medicine*, vol. 372, no. 17, pp. 1646–1655, 2015.

[3] E. A. Pritts, D. J. Vanness, J. S. Berek et al., "The prevalence of occult leiomyosarcoma at surgery for presumed uterine

Hindawi
Computational and Mathematical Methods in Medicine
Volume 2023, Article ID 9806505, 1 page
https://doi.org/10.1155/2023/9806505

Retraction

Retracted: Berberine Inhibits Herpes Simplex Virus 1 Replication in HEK293T Cells

Computational and Mathematical Methods in Medicine

Received 12 December 2023; Accepted 12 December 2023; Published 13 December 2023

This article has been retracted by Hindawi, as publisher, following an investigation undertaken by the publisher [1]. This investigation has uncovered evidence of systematic manipulation of the publication and peer-review process. We cannot, therefore, vouch for the reliability or integrity of this article.

Please note that this notice is intended solely to alert readers that the peer-review process of this article has been compromised.

Wiley and Hindawi regret that the usual quality checks did not identify these issues before publication and have since put additional measures in place to safeguard research integrity.

We wish to credit our Research Integrity and Research Publishing teams and anonymous and named external researchers and research integrity experts for contributing to this investigation.

The corresponding author, as the representative of all authors, has been given the opportunity to register their agreement or disagreement to this retraction. We have kept a record of any response received.

References

[1] Y. Cui, L. Zhang, D. Hu, and Y. Yang, "Berberine Inhibits Herpes Simplex Virus 1 Replication in HEK293T Cells," *Computational and Mathematical Methods in Medicine*, vol. 2022, Article ID 7137401, 7 pages, 2022.

Hindawi
Computational and Mathematical Methods in Medicine
Volume 2022, Article ID 7137401, 7 pages
https://doi.org/10.1155/2022/7137401

Research Article

Berberine Inhibits Herpes Simplex Virus 1 Replication in HEK293T Cells

Yujuan Cui,[1,2] Liangjun Zhang,[2] Dandong Hu,[1,2,3] and Yingli Yang[1]

[1]*School of Life Science, Northwest Normal University, Lanzhou, Gansu 730070, China*
[2]*Beijing Yanqing Center for Diseases Prevention and Control, Beijing 102100, China*
[3]*Beijing Yanqing Market Supervision Inspection and Testing Monitoring Center, Beijing 102100, China*

Correspondence should be addressed to Yingli Yang; 1450940233@xs.hnit.edu.cn

Received 23 August 2022; Accepted 29 September 2022; Published 14 October 2022

Academic Editor: Min Tang

Berberine exhibits polytrophic medicinal roles in various diseases and is safe and effective. However, its role and the underlying mechanism in the replication of herpes simplex virus 1 (HSV-1) remain unreported. This research aimed to determine the functional mechanisms of berberine on HSV-1 infection. We determined the CC50 ($405.11 \pm 15.67\ \mu$M) and IC50 ($45.6 \pm 6.84\ \mu$M) of berberine on HEK293T cells infected with HSV-1. Berberine inhibited the transcription and translation of HSV-1 activity-related genes (gD, ICP-4, ICP-5, and ICP-8) in HSV-1-infected HEK293T cells dose-dependently. Berberine also inhibited the phosphorylation of MAPK proteins (JNK and p38) and inflammatory responses induced by HSV-1 infection in HEK293T cells dose-dependently. In conclusion, berberine attenuates HSV-1 replication through its activity, infective ability, and inflammatory response. Our research indicated that berberine may be a candidate drug for HSV-1 infection.

1. Introduction

Herpes simplex virus (HSV) is a virus with double-stranded DNA under an envelope structure. HSV usually infects the body through the mucous membranes, skin, nerve tissue, and other related lesions. It has two serum subsets, HSV-1 and HSV-2. Infection with HSV-1 mainly leads to pharyngitis, cold sores, and keratitis and in severe cases will cause sporadic encephalitis and other dangerous diseases. HSV-2 mainly invades through damaged skin and mucous membranes to cause genital herpes [1]. Immediate early gene (α gene), early gene (β gene), and late gene (γ gene) express after HSV-1-infected host cells [2]. Infection cell protein (ICP4) expression peaks 2~4 hours after infection. The expression of the β gene requires activation of α gene products [3]. ICP5 and ICP8 can regulate viral DNA replication and participate in γ gene transcription [4]. Glycoprotein D (gD) is a late protein encoded by the γ gene peaking 12~15 hours after infection, which is the main component of the virus envelope and helps the virus to absorb and enter the host cell [5]. All these indicators can be used to evaluate the activity of HSV-1. Berberine is an alkaloid in the protoberberine group that existed in Berberidaceae, Papaveraceae, and Ranunculaceae [6].

Berberine shows polytrophic medicinal effects, including anti-inflammatory [7], antibacterial, and antifungal [8]. Berberine acts on a series of signaling pathways to improve diabetes [9–11]. Several *in vitro* studies have found that berberine diminishes the proliferation, migration, and metastasis of cancer cells and accelerates apoptosis [11–13]. It has been found that berberine promotes apoptosis by activating ROS-related signals, such as the JNK/p38 signaling pathway. ROS can activate JNK/p38 that block antiapoptotic protein Bcl-XL expression to release cytochrome C and stimulate caspases [14]. Recently, berberine shows antiviral properties against influenza A virus (IAV) [15], respiratory syncytial virus (RSV) [16], chikungunya virus (CHIKV) [17], enterovirus 71 (EV71, [18], human papillomavirus (HPV) [19], and herpes simplex 55 virus (HSV) [20], but its roles in HSV-1 infection is still unknown.

Here, we aimed to explore the antiviral and anti-inflammatory impact of berberine in HSV-1-infected

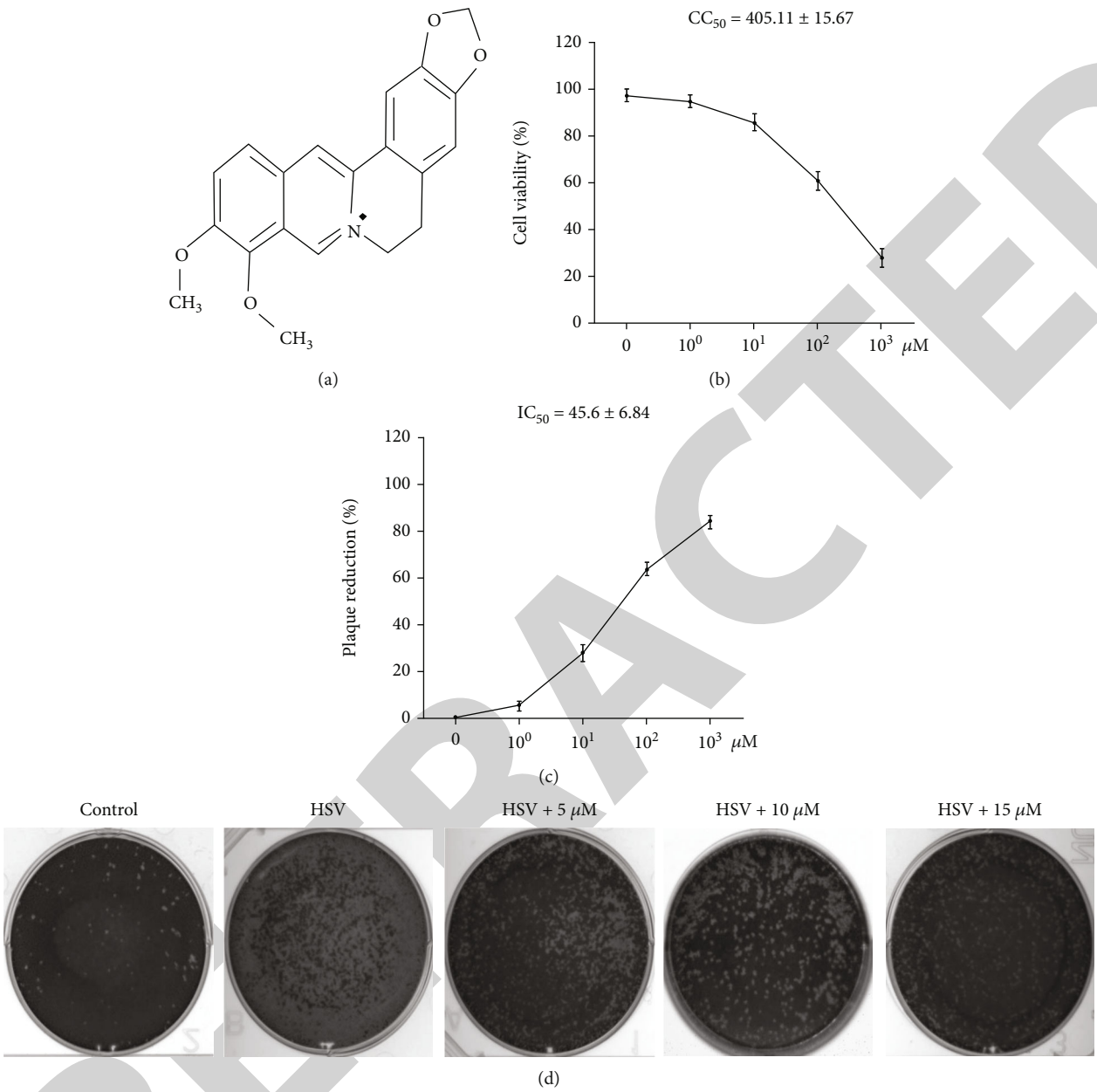

Figure 1: Berberine antagonizes HSV-1 infection in HEK293T cells. (a) Berberine chemical structure. (b) CCK-8 assay was performed to explore berberine CC_{50} in HEK293T cells. (c) Plaque reduction assay was carried out to explore berberine IC_{50} in HEK293T cells. (d) Plaque reduction assay was performed to assess the effect of berberine on HSV-1 plaque formation in HEK293T cells. All data are presented as the means ± SD.

HEK293T cells. It was reported that berberine can dose-dependently reduce the activity of HSV-1 and HSV-1-induced secretion of inflammatory factors and the phosphorylation of p38 and JNK.

2. Material and Methods

2.1. Material

2.1.1. Cells. HEK293T cells were obtained from Fudan University (Shanghai, China) and kept in DMEM (Roche, Basel, Switzerland) plus 1% antibiotics and 10% FBS (Solarbio, Beijing, China) under a humid incubator containing 5% CO_2 at 37°C.

2.1.2. Drugs and Cell Treatments. Berberine was purchased from Solarbio (Beijing, China, purity ≥98%). HEK293T cells were grouped: control group, cells were untreated; HSV group, infected with 200 pfu/well HSV; HSV+5 μM group, treated with 5 μM berberine and 200 pfu/well HSV; HSV +10 μM group, treated with 10 μM berberine and 200 pfu/well HSV; HSV+15 μM group, treated with 15 μM berberine and 200 pfu/well HSV. Following 24-h culture, HEK293T

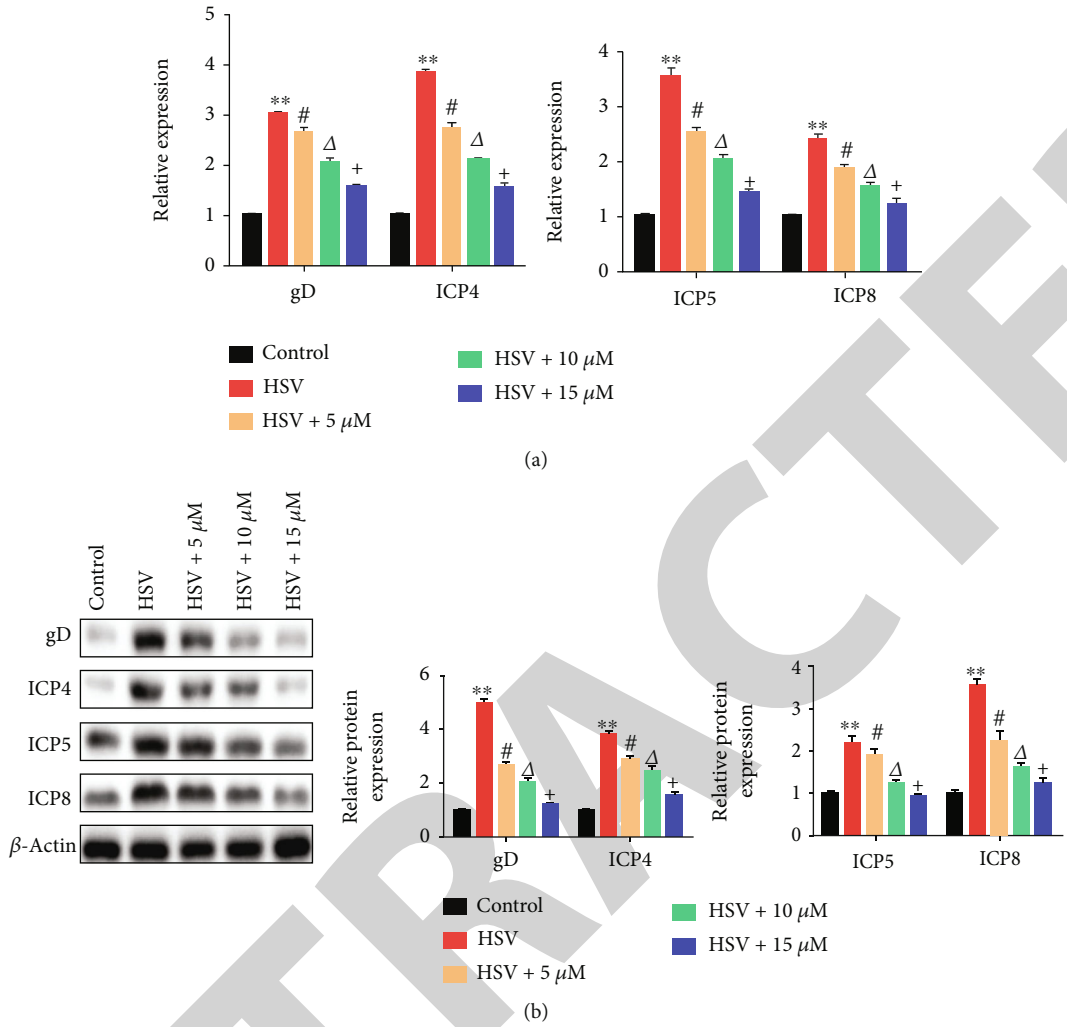

Figure 2: Berberine decreases HSV-1 activity in HEK293T cells. (a) RT-qPCR was performed to assess the mRNA levels of HSV-1-related genes, including gD, ICP4, ICP5, and ICP8. (b) Western blot was performed to measure the protein levels of gD, ICP4, ICP5, and ICP8. All data are presented as the means ± SD. $^{**}P < 0.01$ *vs.* control group, $^{\#}P < 0.05$ *vs.* HSV group, $^{\Delta}P < 0.05$ *vs.* HSV+5 μM group, and $^{+}P < 0.05$ *vs.* HSV+10 μM group.

cells were applied to plaque reduction assay, RT-qPCR, western blot, and ELISA.

3. Methods

3.1. Cytotoxicity Assay. The cytotoxicity of berberine on HEK293T cells was determined based on the CCK-8 assay [21]. The minimum berberine concentration required to produce a toxic effect on 50% of HEK293T cells (CC_{50}) was calculated by regression analysis of the dose-response curve.

3.2. Plaque Reduction Assay. The anti-HSV-1 ability of berberine was evaluated [21] (Jung et al., 2011). In detail, HEK293T cells (1×10^5/well) were cultured in a 24-well plate and treated with a corresponding dose of HSV-1 or berberine for 24 h. DMEM was added with 1% methylcellulose solution and 2% FCS (Solarbio, Beijing, China). Then, HEK293T cells were cultured under 5% CO_2 at 37°C for 72 h. Monolayer cells were fixed and stained with 1% crystal violet, and formative plaques were counted. Finally, the minimum berberine concentration required to inhibit the 50% cytopathic effect (IC_{50}) was calculated by regression analysis of the dose-response curve. The selectivity index (SI) was calculated by CC_{50}/IC_{50}.

3.3. RT-qPCR. RNA was isolated using TRIzol (Takara, Liaoning, China), and cDNA was obtained with M-MLV Reverse Transcriptase (RNase H) kit (Takara, Liaoning, China). RT-qPCR was performed according to the previous report [22].

3.4. ELISA. Following treatment with corresponding doses of HSV-1 or berberine for 24 h, 1 mL of extraction solution (Beyotime, Nanjing, China) was used to lyse HEK293T cells. Subsequently, the levels of inflammatory factors in the supernatant were determined with ELISA kits (Roche, Basel, Switzerland).

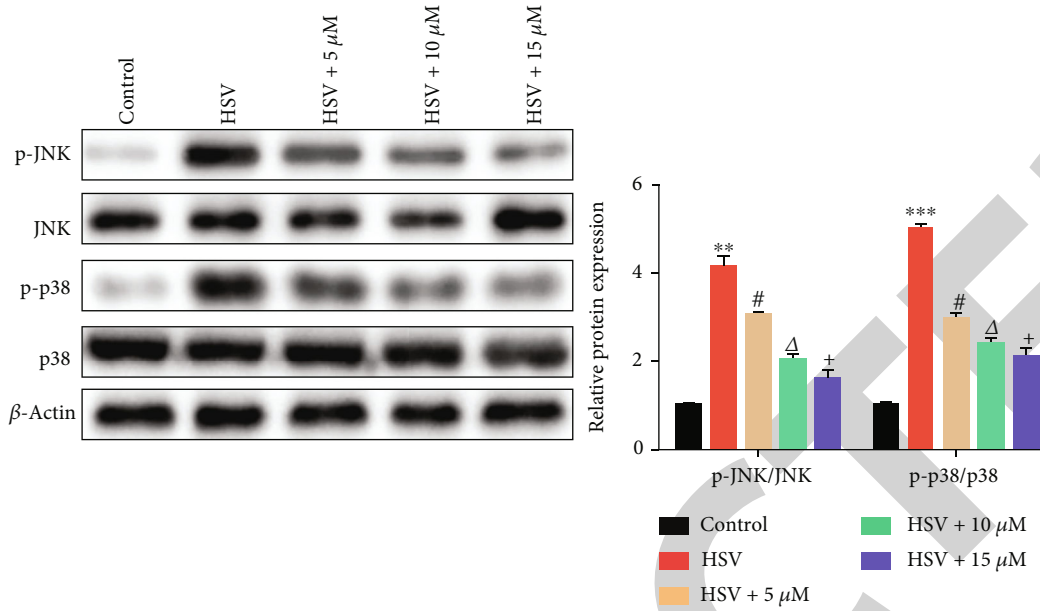

Figure 3: Berberine inhibits JNK and p38 activation induced by HSV-1 infection. Western blot was performed to assess the protein levels of p-JNK, JNK, p-p38, p38, and β-actin in HEK293T cells. All data are presented as the means ± SD. $^{**}P < 0.01$ and $^{***}P < 0.001$ *vs.* control group, $^{\#}P < 0.05$ *vs.* HSV group, $^{\Delta}P < 0.05$ *vs.* HSV+5 μM group, and $^{+}P < 0.05$ *vs.* HSV+10 μM group.

3.5. Western Blot. Proteins were obtained using Cell Lysis Buffer (Beyotime, Nanjing, China). Western blot was executed based on the previous description [23]. The primary antibodies were ordered from Roche (Basel, Switzerland 1 : 1000) and goat-anti-rabbit IgG secondary antibody was the secondary antibody (Santa Cruz, San Francisco, USA, 1 : 2000). OD was quantified by Image J (Image J Inc.).

3.6. Statistical Analysis. Data were presented as the mean ± SD of three independent experiments and processed by GraphPad 5.0 (GraphPad Software, Inc.). Student's *t*-test or one-way ANOVA plus Tukey post hoc tests were conducted. $P < 0.05$ indicated statistical significance.

4. Results

4.1. Berberine Antagonizes HSV-1 Infection in HEK293T Cells. Berberine's chemical structure formula was analyzed (Figure 1(a)), and CCK-8 assay was conducted to explore berberine cytotoxicity on HEK293T cells. The CC_{50} of berberine on HEK293T cells was calculated to be 405.11 ± 15.67 μM, according to the regression analysis of the dose-response curve generated by CCK-8 assay (Figure 1(b)). In Figure 1(c), the IC_{50} of berberine on HEK293T cell infected with HSV-1 was 45.6 ± 6.84 μM based on plaque reduction assay. The decrease in HSV-1 plaque formation caused by the increase in berberine concentration was dose-related, indicating that berberine could inhibit HSV-1 infection of HEK293T cells. The selective index (SI) was 7.43-10.86 (in Figure 1(d)).

4.2. Berberine Decreases HSV-1 Activity in HEK293T Cells. To further analyze the effects of berberine on HSV-1 activity in HEK293T cells, RT-qPCR and western blot analyses were followed to assess the levels of HSV-1 infection-related genes, including g D, ICP-4, ICP-5, and ICP-8. RT-qPCR manifested that HSV-1 upregulated the transcription of the four HSV-1 infection-related genes, relative to the control group ($P < 0.01$), while berberine antagonized this upregulation effect dose-dependently compared with the HSV group (Figure 2(a); $P < 0.05$). Consistently, HSV infection promoted g D, ICP-4, ICP-5, and ICP-8 protein expression, whereas berberine antagonized this promotion dose-dependently (Figure 2(b); $P < 0.05$). Taken together, berberine deceased HSV-1 activity in HEK293T cells.

4.3. Berberine Inhibits JNK and p38 Activation Induced by HSV-1 Infection. It has been revealed that HSV-1 activated the MAPK pathway [24, 25]. To further explore the effect of HSV-1 on the MAPK pathway, the phosphorylation levels of MAPK-related proteins (JNK and p38) in HEK293T cells were assessed. Results showed that HSV-1 infection upregulates the phosphorylation levels of JNK ($P < 0.01$) and p38 ($P < 0.001$) proteins. Besides, further investigation indicated that berberine inhibited the HSV-1 infection-induced phosphorylation levels of JNK and p38 in HEK293T cells dose-dependently ($P < 0.05$; Figure 3). Collectively, berberine inhibited JNK and p38 activation in HSV-1-treated HEK293T cells.

4.4. Berberine Decreases Inflammatory Responses Induced by HSV-1 Infection. HSV-1 triggers inflammatory responses, such as gingival stomatitis, cold sores, keratitis, and meningitis [26, 27]. To investigate the effect of berberine on inflammatory responses caused by HSV-1, RT-qPCR and ELISA were conducted. Our results showed that HSV-1 infection upregulated the mRNA and secretion levels of cytokines ($P < 0.05$) and berberine dose-dependently

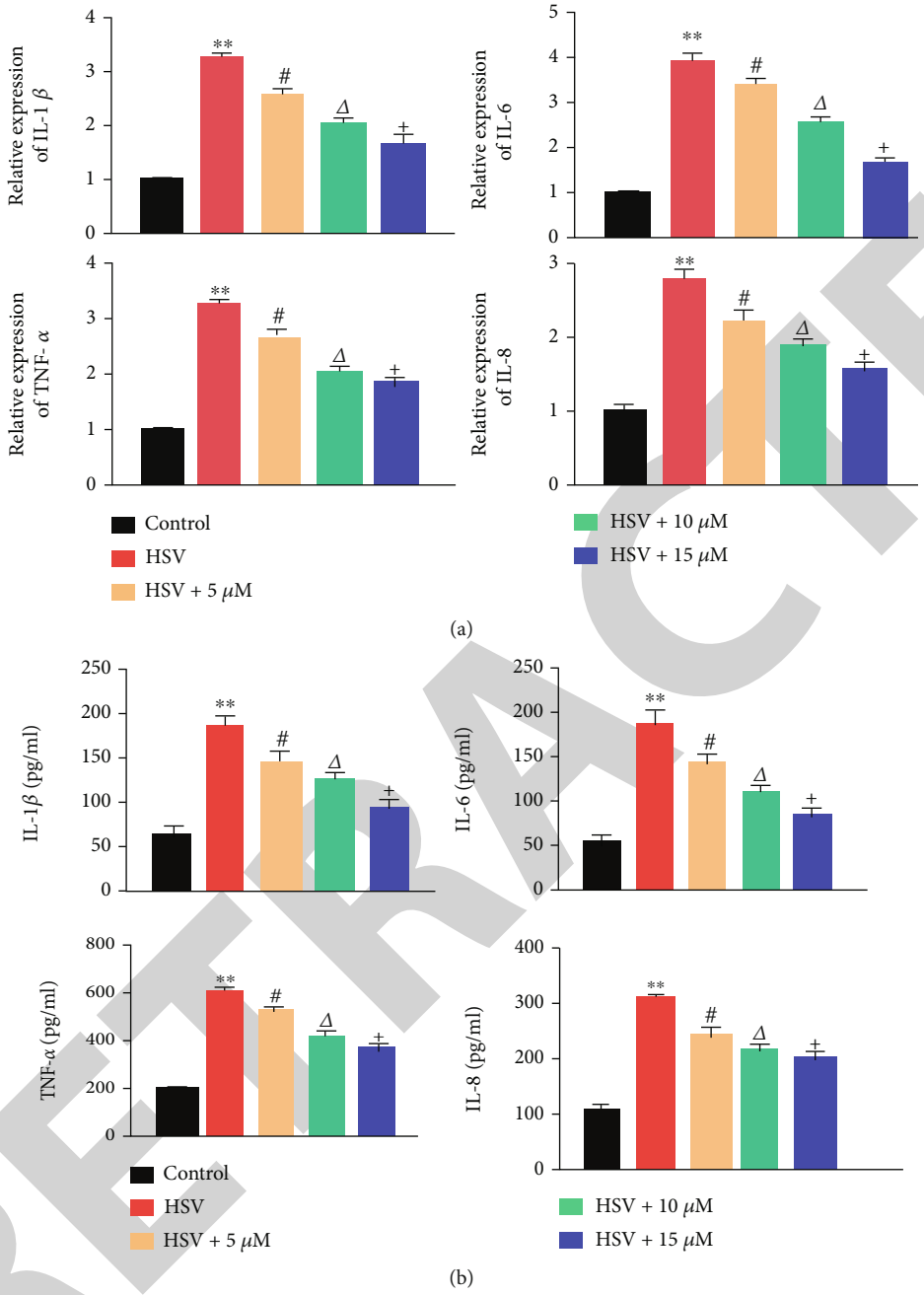

Figure 4: Berberine decreases inflammatory response induced by HSV-1 infection. (a) RT-qPCR analysis was performed to assess the mRNA levels of inflammatory cytokines, including IL-1β, IL-6, TNF-α, and IL-8 in HEK293T cells. (b) ELISA assay was carried out to assay IL-1β, IL-6, TNF-α, and IL-8 expression in HEK293T cell supernatant. All data are presented as the means ± SD. $^{**}P < 0.01$ and $^{***}P < 0.001$ *vs.* control group, $^{\#}P < 0.05$ *vs.* HSV group, $^{\Delta}P < 0.05$ vs. HSV+5 μM group, and $^{+}P < 0.05$ vs. HSV+10 μM group.

downregulated their levels triggered by HSV-1 infection ($P < 0.05$; Figures 4(a) and 4(b)). Taken together, berberine inhibited inflammatory responses induced by HSV-1 infection in HEK293T cells.

5. Discussion

Herpesviruses develop latency or cause oral and genital herpes, conjunctivitis, eczema herpeticum, and other diseases in 90% of the population. Herpesvirus also disturbs AIDS treatment under HIV infection [28]. It is important to seek drug candidates against HSV-1. Here, it was proved that berberine antagonized HSV-1 activity, inflammatory responses, and MAPK pathway activation in HEK293T cells which may contribute to the inhibition of HSV-1.

Berberine is cytotoxic to mast cells, rat hepatocytes, and Vero cells [17, 29, 30]. Cytotoxicity is a factor that must be considered in seeking a candidate for HSV-1 treatment. A study showed that berberine exerted an anticancer impact against HeLa cells with CC_{50} of 12.08 μg/mL whereas

exhibited low toxicity (CC_{50}: 71.14 μg/mL) on normal Vero cells [31]. Chin et al. found that the CC_{50} of berberine extracted from *Coptis chinensis* on Vero cells was 392.5 μM, the IC_{50} was 66.49 μM, and the SI was 5.9 [32]. Our results found that berberine could effectively inhibit HSV-1 activity (IC_{50}: $45.6 \pm 6.84\,\mu$M) in HEK293T cells and was with low toxicity (CC_{50}: $405.11 \pm 15.67\,\mu$M). The SI was 7.43-10.86, indicating berberine is a relatively safe and effective candidate for HSV-1 inhibition *in vitro*.

Our study found that HSV-1 infection upregulates the phosphorylation levels of JNK and p38 proteins, which was similar to other's reports. MAPK pathway activation was stimulated by HSV-1 infection [24, 25]. Berberine was illustrated to reduce the phosphorylation levels of JNK and p38 MAPK under CVB3 infection [33]. Zeng et al. illuminated the mechanism of berberine weakened host components JNK-MAPK, ERK-MAPK, and p38-MAPK activation [34]. Li et al. found that berberine retarded IL-33-stimulated cytokine production in RPMCs [29]. It has been demonstrated that the levels of ROS-related factors were boosted under IL-1β treatment and pretreatment of berberine exhibited inhibitory roles. Besides, the decrease in inflammatory responses indicated that berberine diminished the HSV-1 infection-caused inflammation.

In conclusion, our study showed that berberine inhibited HSV-1 replication by downregulation of HSV-1 activity, inflammatory responses, and MAPK pathway activation in HEK293T cells. Berberine may be a potential candidate for the treatment of HSV-1 infection.

Data Availability

The data supporting the manuscript's conclusions will be made available to any qualified researcher without reservation.

Conflicts of Interest

There are no conflicts of interest to declare.

References

[1] A. J. Debono, S. J. Mistry, J. Xie et al., "The synthesis and biological evaluation of multifunctionalised derivatives of noscapine as cytotoxic agents," *ChemMedChem*, vol. 9, no. 2, pp. 399–410, 2014.

[2] J. L. Coleman and D. Shukla, "Recent advances in vaccine development for herpes simplex virus types I and II," *Human Vaccines & Immunotherapeutics*, vol. 9, no. 4, pp. 729–735, 2013.

[3] D. Chen, A. Su, Y. Fu et al., "Harmine blocks herpes simplex virus infection through downregulating cellular NF-κB and MAPK pathways induced by oxidative stress," *Antiviral Research*, vol. 123, pp. 27–38, 2015.

[4] K. F. Bryant, Z. Yan, D. H. Dreyfus, and D. M. Knipe, "Identification of a divalent metal cation binding site in herpes simplex virus 1 (HSV-1) ICP8 required for HSV replication," *Journal of Virology*, vol. 86, no. 12, pp. 6825–6834, 2012.

[5] R. I. Montgomery, M. S. Warner, B. J. Lum, and P. G. Spear, "Herpes simplex virus-1 entry into cells mediated by a novel member of the TNF/NGF receptor family," *Cell*, vol. 87, no. 3, pp. 427–436, 1996.

[6] H. Mortazavi, B. Nikfar, S. A. Esmaeili et al., "Potential cytotoxic and anti-metastatic effects of berberine on gynaecological cancers with drug-associated resistance," *European Journal of Medicinal Chemistry*, vol. 187, article 111951, 2020.

[7] E. Küpeli, M. Koşar, E. Yeşilada, K. Hüsnü, and C. Başer, "A comparative study on the anti-inflammatory, antinociceptive and antipyretic effects of isoquinoline alkaloids from the roots of Turkish *Berberis* species," *Life Sciences*, vol. 72, no. 6, pp. 645–657, 2002.

[8] A. H. Amin, T. V. Subbaiah, and K. M. Abbasi, "Berberine sulfate: antimicrobial activity, bioassay, and mode of action," *Canadian Journal of Microbiology*, vol. 15, no. 9, pp. 1067–1076, 1969.

[9] Q. Chen, R. Mo, N. Wu et al., "Berberine ameliorates diabetes-associated cognitive decline through modulation of aberrant inflammation response and insulin signaling pathway in DM rats," *Frontiers in Pharmacology*, vol. 8, p. 334, 2017.

[10] L. Zhu, J. Han, R. Yuan, L. Xue, and W. Pang, "Berberine ameliorates diabetic nephropathy by inhibiting TLR4/NF-κB pathway," *Biological Research*, vol. 51, no. 1, p. 9, 2018.

[11] X. Zhang, L. Gu, J. Li et al., "Degradation of MDM2 by the interaction between berberine and DAXX leads to potent apoptosis in MDM2-overexpressing cancer cells," *Cancer Research*, vol. 70, no. 23, pp. 9895–9904, 2010.

[12] J. Li, L. Gu, H. Zhang et al., "Berberine represses *DAXX* gene transcription and induces cancer cell apoptosis," *Laboratory Investigation; A Journal of Technical Methods and Pathology*, vol. 93, no. 3, pp. 354–364, 2013.

[13] Y. Wang and S. Zhang, "Berberine suppresses growth and metastasis of endometrial cancer cells via miR-101/COX-2," *Biomedicine & Pharmacotherapy = Biomedecine & Pharmacotherapie*, vol. 103, pp. 1287–1293, 2018.

[14] Y. H. Kang, E. Lee, M. K. Choi et al., "Role of reactive oxygen species in the induction of apoptosis by alpha-tocopheryl succinate," *International Journal of Cancer*, vol. 112, no. 3, pp. 385–392, 2004.

[15] Y. Wu, J. Q. Li, Y. J. Kim, J. Wu, Q. Wang, and Y. Hao, "In vivo and in vitro antiviral effects of berberine on influenza virus," *Chinese Journal of Integrative Medicine*, vol. 17, no. 6, pp. 444–452, 2011.

[16] H. B. Shin, M. S. Choi, C. M. Yi, J. Lee, N. J. Kim, and K. S. Inn, "Inhibition of respiratory syncytial virus replication and virus-induced p38 kinase activity by berberine," *International Immunopharmacology*, vol. 27, no. 1, pp. 65–68, 2015.

[17] F. S. Varghese, B. Thaa, S. N. Amrun et al., "The antiviral alkaloid berberine reduces chikungunya virus-induced mitogen-activated protein kinase signaling," *Journal of Virology*, vol. 90, no. 21, pp. 9743–9757, 2016.

[18] H. Wang, K. Li, L. Ma et al., "Berberine inhibits enterovirus 71 replication by downregulating the MEK/ERK signaling pathway and autophagy," *Virology Journal*, vol. 14, no. 1, p. 2, 2017.

[19] S. Mahata, A. C. Bharti, S. Shukla, A. Tyagi, S. A. Husain, and B. C. Das, "Berberine modulates AP-1 activity to suppress HPV transcription and downstream signaling to induce growth arrest and apoptosis in cervical cancer cells," *Molecular Cancer*, vol. 10, no. 1, p. 39, 2011.

[20] S. Song, M. Qiu, Y. Chu et al., "Downregulation of cellular c-Jun N-terminal protein kinase and NF-κB activation by berberine may result in inhibition of herpes simplex virus

Hindawi
Computational and Mathematical Methods in Medicine
Volume 2023, Article ID 9820687, 1 page
https://doi.org/10.1155/2023/9820687

Retraction

Retracted: Downregulation of miR-146a-5p Promotes Acute Pancreatitis through Activating the TLR9/NLRP3 Signaling Pathway by Targeting TRAF6 In Vitro Rat Model

Computational and Mathematical Methods in Medicine

Received 5 December 2023; Accepted 5 December 2023; Published 6 December 2023

This article has been retracted by Hindawi, as publisher, following an investigation undertaken by the publisher [1]. This investigation has uncovered evidence of systematic manipulation of the publication and peer-review process. We cannot, therefore, vouch for the reliability or integrity of this article.

Please note that this notice is intended solely to alert readers that the peer-review process of this article has been compromised.

Wiley and Hindawi regret that the usual quality checks did not identify these issues before publication and have since put additional measures in place to safeguard research integrity.

We wish to credit our Research Integrity and Research Publishing teams and anonymous and named external researchers and research integrity experts for contributing to this investigation.

The corresponding author, as the representative of all authors, has been given the opportunity to register their agreement or disagreement to this retraction. We have kept a record of any response received.

References

[1] D. Deng, Z. Su, B. Wei, J. Zhou, H. Yang, and Z. Liang, "Downregulation of miR-146a-5p Promotes Acute Pancreatitis through Activating the TLR9/NLRP3 Signaling Pathway by Targeting TRAF6 In Vitro Rat Model," *Computational and Mathematical Methods in Medicine*, vol. 2022, Article ID 1747470, 11 pages, 2022.

Hindawi
Computational and Mathematical Methods in Medicine
Volume 2022, Article ID 1747470, 11 pages
https://doi.org/10.1155/2022/1747470

Research Article

Downregulation of miR-146a-5p Promotes Acute Pancreatitis through Activating the TLR9/NLRP3 Signaling Pathway by Targeting TRAF6 In Vitro Rat Model

Dehai Deng, Zhou Su, Biwei Wei, Jie Zhou, Huiying Yang, and Zhihai Liang

Department of Gastroenterology, The First Affiliated Hospital of Guangxi Medical University, Nanning, China

Correspondence should be addressed to Zhihai Liang; ahhai@163.com

Received 23 August 2022; Revised 9 September 2022; Accepted 19 September 2022; Published 14 October 2022

Academic Editor: Min Tang

Acute pancreatitis (AP) is mainly caused by acinar cells releasing various inflammatory factors, causing inflammatory storms and leading to severe pancreatitis. Detection methods and treatment targets for pancreatitis are lacking, raising the urgency of identifying diagnostic markers and therapeutic targets for AP. MicroRNAs (miRNAs) have recently been identified as molecular markers for various biological processes such as tumors, immunity, and metabolism, and the involvement of miRNAs in inflammatory responses has been increasingly studied. To explore the role of miRNAs in AP is the primary objective of this study. By using qPCR on our cerulein-induced pancreatitis cell model, it is worth noting that the change of miR-146a-5p expression in inflammation-related miRNAs in AP was predominant. Next, ELISA, CCK8, and flow cytometry were used to inspect the impact of miR-146a-5p on pancreatitis. BiBiServ bioinformatics anticipated binding ability of miR-146a-5p and 3′-untranslated region (3′UTR) of TNF receptor-associated factor 6 (TRAF6), and the dual-luciferase assay verified the combination of the two. TRAF6 knockdown verified the effect of TRAF6 on the progression of pancreatitis. Finally, rescue experiments verified the capability of miR-146a-5p and TRAF6 interaction on the Toll-like receptor 9 (TLR9)/NOD-like receptor protein 3 (NLRP3) signaling pathway and cell function. The expression of miR-146a-5p decreased in cerulein-induced AR42J pancreatic acinar cells. Functional experiments verified that miR-146a-5p facilitated the proliferation of AR42J pancreatic acinar cells and inhibited their apoptosis. Bioinformatic predictions and dual-luciferase experiments verified the actual binding efficiency between miR-146a-5p and 3′UTR of TRAF6. Our study confirmed that knockdown of TRAF6 restrained the progression of pancreatitis, and knockdown of TRAF6 rescued pancreatitis caused by miR-146a-5p downregulation by the TLR9/NLRP3 signaling pathway. Therefore, downregulation of miR-146a-5p in the induced pancreatitis cell model promotes the progression of pancreatitis via the TLR9/TRAF6/NLRP3 signaling pathway. There is potential for miR-146a-5p to serve as a diagnostic marker and therapeutic nucleic acid drug for AP.

1. Introduction

Acute pancreatitis (AP) is a common acute abdominal condition in gastroenterology. It is characterized by rapid onset, severe illness, and rapid change. If not actively treated, it can be life-threatening [1]. Pancreatitis is mainly diagnosed by detecting serum amylase and lipase. However, this diagnosis is often missed, especially if the patient has this triglyceride [2]. Therefore, there is an urgent need to identify more accurate pancreatitis-related molecular markers.

Recently, continuously increasing researches have expounded that microRNAs (miRNAs) play important roles in acinar cell damage and inflammation [3]. Hu et al. found that microRNA-19b (miR-19b) mimic inhibited the survival rate of AR42J cells and increased their expression in AP tissues [4]. Zhang et al. showed that miR-216a activates phosphoinositide-3-kinase (PI3K)/AKT signaling via the target phosphatase-and-tensin homolog to cause pancreatic tissue damage and inflammation [5]. By constructing an miR-21 knockout mouse model, Ma et al. proved that

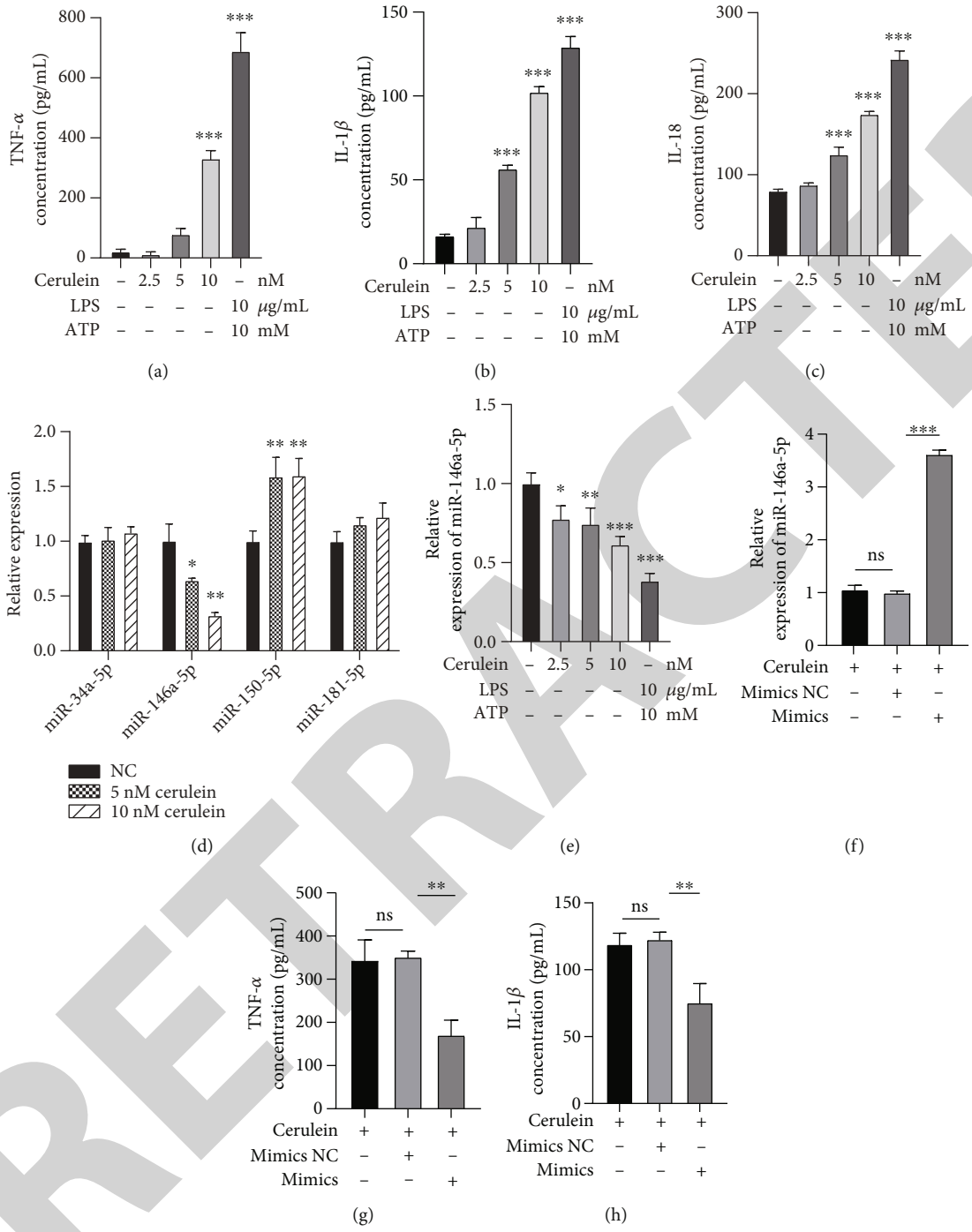

Figure 1: Continued.

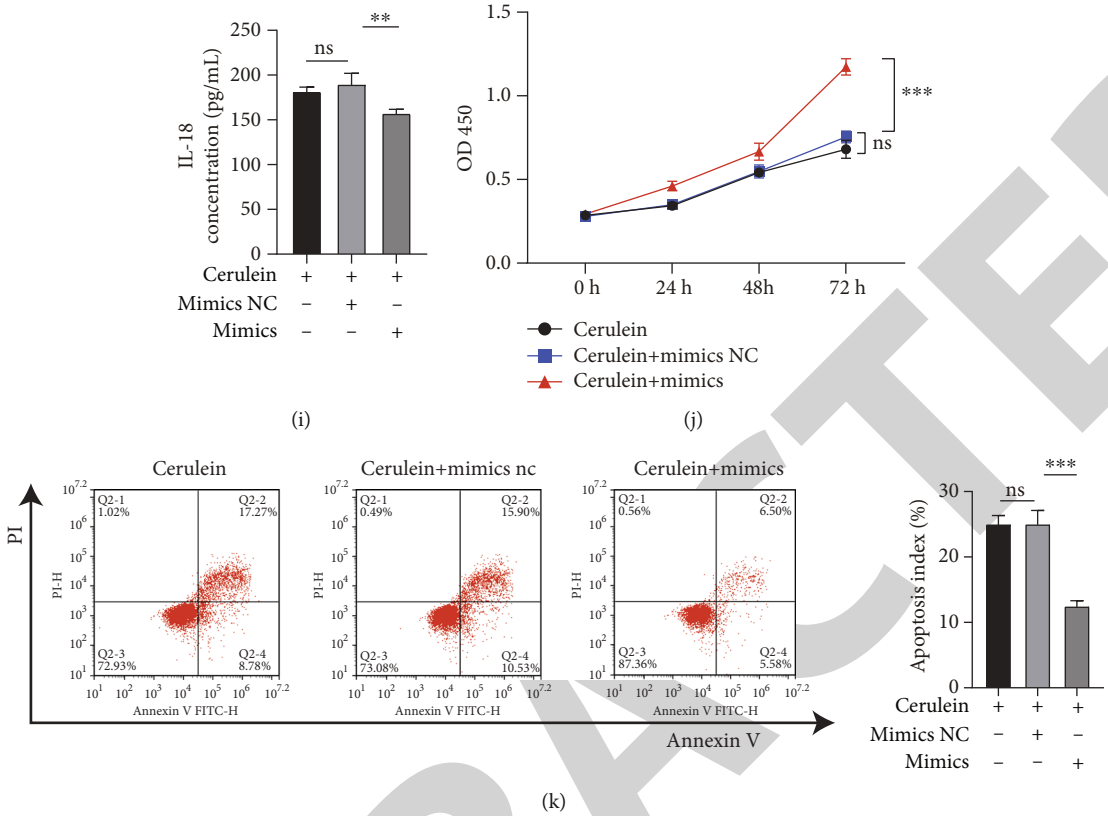

Figure 1: miR-146a-5p is highly expressed in cerulein-induced pancreatitis. (a–c) After treating AR42J cells with 0, 2.5, 5, and 10 nM cerulein, ELISA detected the levels of inflammatory factors in the culture medium, with 10 μg/mL LPS and 10 mM ATP as positive controls. (d, e) The expression of inflammation-related miRNAs in AR42J cells with 10 nM cerulein was detected by RT-qPCR, with 10 μg/mL LPS and 10 mM ATP as positive controls. (f) RT-qPCR was used for disclosing the expression of miR-146a-5p in cerulein-induced AR42J cells with miR-146a-5p mimics or mimics nc. (g–i) ELISA detected the expression of inflammatory factors in the culture medium of cerulein-induced AR42J cells. (j) CCK8 detected the proliferation of cerulein-induced AR42J cells. (k) Flow cytometry (FCM) assay detected the apoptosis of cerulein-induced AR42J cells. $^{*}p < 0.05$, $^{**}p < 0.01$, and $^{***}p < 0.001$. The experiments were repeated three times, the statistical test was a two-tailed test, and errors bars in the figures represent standard deviation (SD).

miR-21 deletion repressed pancreatic injury and inflammation [6].

TNF receptor-associated factor 6 (TRAF6) belongs to the TNF receptor-associated factor family. It can activate the NF-κB signaling pathway and is also an E3 ligase. Therefore, TRAF6 as a signal pathway regulator refer to miscellaneous biological processes such as ubiquitination, autophagy, and inflammation [7, 8]. Ellipticine can treat acute pancreatitis by inhibiting the expression of TRAF6 [9]. It is well known that lipopolysaccharide (LPS) can bind to the TLR4 receptor on the cell membrane, recruiting myeloid differentiation factor 88 (MyD88) and TRAF6, activating a series of signaling pathways, and including inflammation [10].

Inflammasomes are a type of macromolecular complex in cells, mainly composed of the NLR protein family, associated speck-like protein containing a CARD (ASC), and downstream protein caspase-1 [11]. NLRP3 inflammasome refers to various inflammatory bowel diseases, inflammatory nephropathy, and autoimmune diseases [12–14]. Hoque et al. found that the NLRP3 inflammasome is highly correlated with the occurrence of AP [15]. At the same time, many studies have shown that TRAF6 regulates the activity of NLRP3 inflammasome to regulate neuroinflammation, gouty arthritis, and other inflammatory responses [16–18]. However, the relationship between TRAF6 and NLRP3 inflammasome in pancreatitis has not yet been studied.

In light of the existing state of knowledge, the present study elucidated that miR-146a-5p regulates the NLRP3 signaling pathway through the target TRAF6 to stimulate the development of pancreatitis.

2. Materials and Methods

2.1. Cell Culture and Transfection. AR42J rat acinar cells (purchased from ATCC) and 293T cell lines (from own laboratory) were preserved in DMEM medium, and AR42J pancreatic cells were treated with 0 nM, 2.5 nM, 5 nM, and 10 nM cerulein (Solarbio, C6660) to construct a pancreatitis model. 50 nM of miR-146a-5p mimic or inhibitor and si-TRAF6 were transfected into AR42J acinar cells using Lipofectamine 2000 (Invitrogen). See Supplementary Table I for RNA sequence. 293T cells were used for the dual-luciferase experiments.

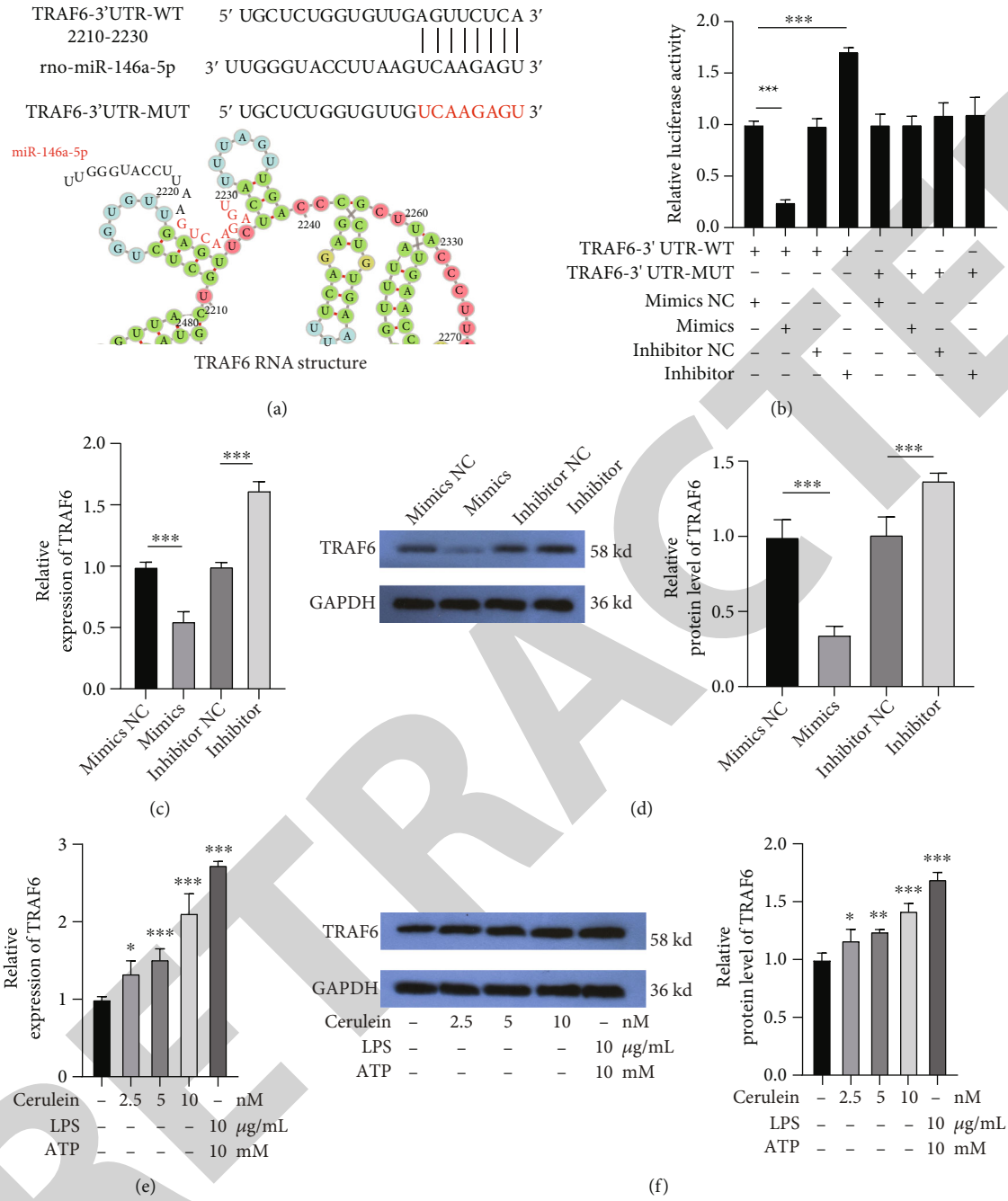

Figure 2: miR-146a-5p targets TRAF6. (a) miR-146a-5p and TRAF6-3′UTR binding site as indicated by prediction software BiBiServ and RNAfold. (b) Dual-luciferase detection of miR-146a-5p and TRAF6-3′UTR binding. (c, d) qPCR and WB detection of the expression of TRAF6 after adding miR-146a-5p mimics. Band analysis software is ImageJ (version 1.8.0_172). (e, f) qPCR and WB inspection of the expression of TRAF6 in AR42J cells treated with 0, 2.5, 5, and 10 nM cerulein. Band analysis software is ImageJ (version 1.8.0_172). $^{*}p < 0.05$, $^{**}p < 0.01$, and $^{***}p < 0.001$. The experiments were repeated three times, the statistical test was a two-tailed test, and errors bars in the figures represent standard deviation (SD).

2.2. Enzyme-Linked Immunosorbent Assay (ELISA). The standard protein and supernatant were added to the coated ELISA plates. Perform corresponding operations according to the ELISA kit and the 450 nm reading recorded with an enzyme-linked immunoassay. The detection indicators are TNF-α (Beyotime, PT518), IL-1β (Thermo, BMS224-2), and IL-18 (Abcam, ab215539).

2.3. RT-qPCR. The total RNA of cerulein-treated AR42J acinar cells was extracted with TRIzol reagent. The extracted RNA was reverse-transcribed into cDNA using Random Primer (hexadeoxyribonucleotide mix: pd(N)6; Takara Bio, Japan). PCR experiments were carried out under the following conditions: 95°C for 10 min, 55°C for 2 min, 72°C for 2 min, followed by 40 cycles of 95°C for 15 s and 60°C for

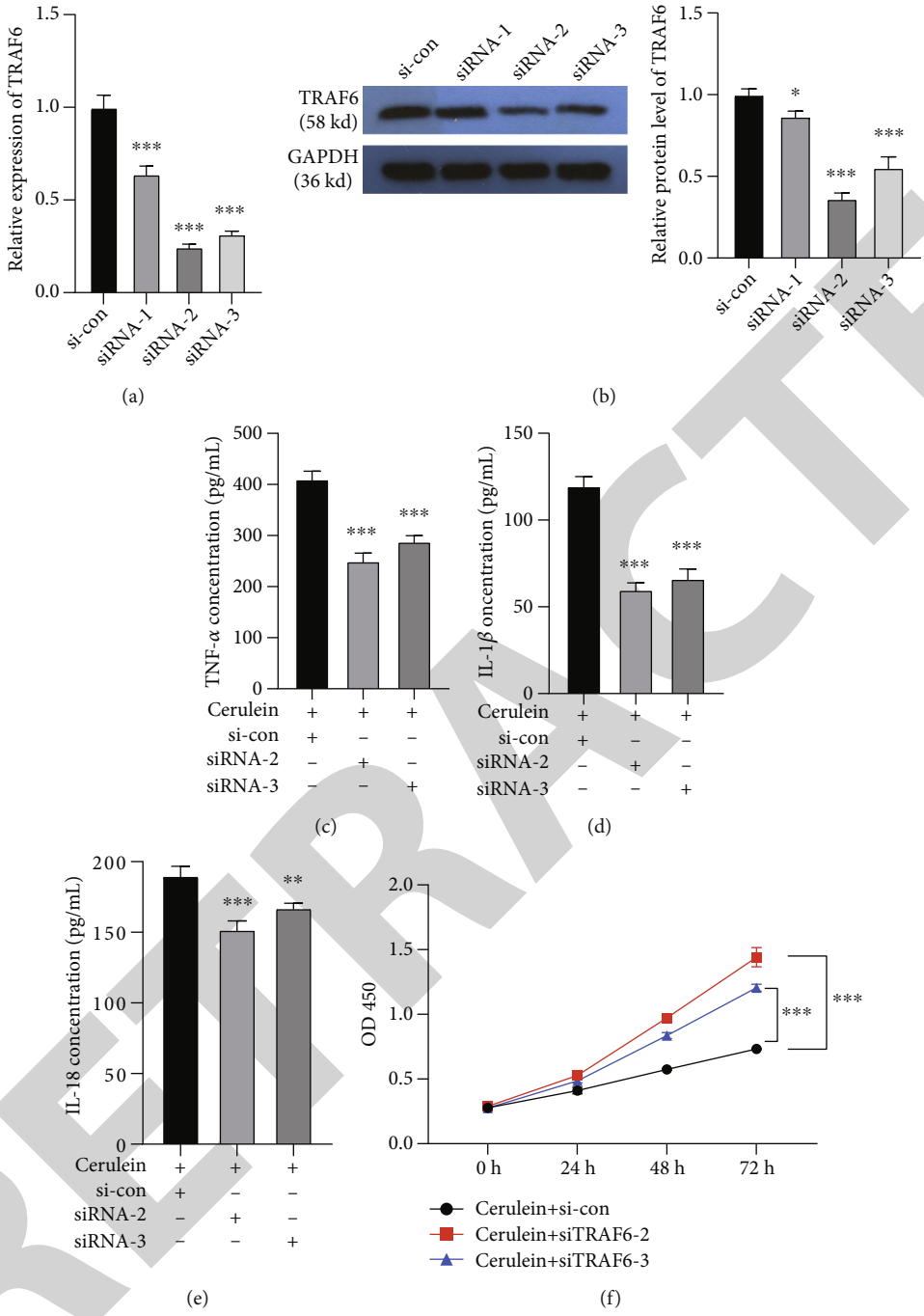

Figure 3: Continued.

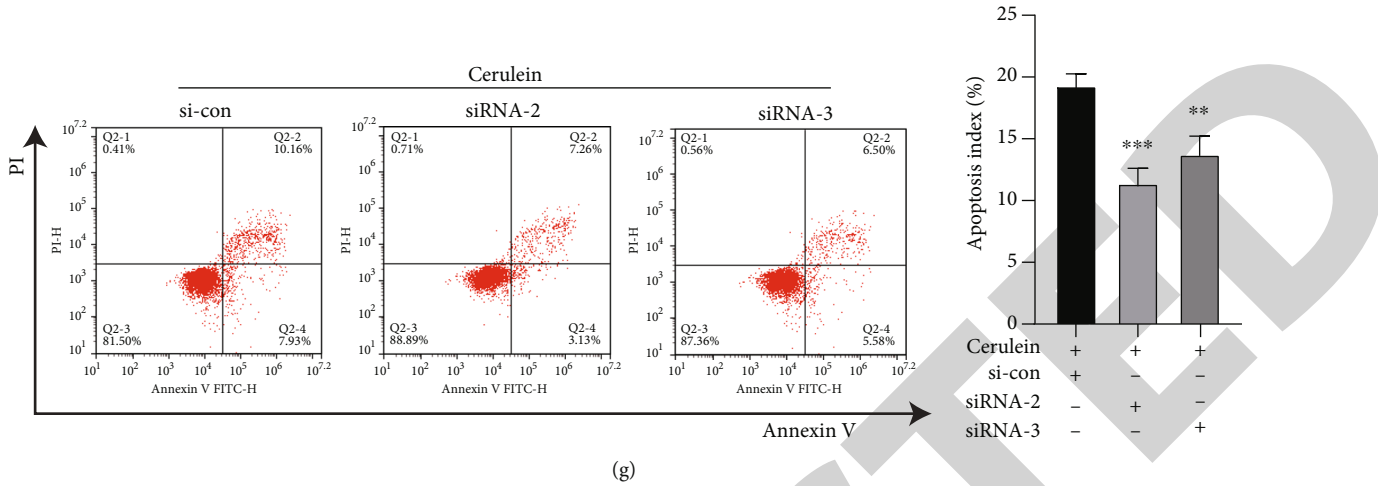

(g)

Figure 3: Knockdown of TRAF6 inhibits the development of pancreatitis. (a) 24 h after transfection of TRAF6-siRNA, qPCR detects the knockdown efficiency of siRNA on TRAF6 in 10 nM cerulein-induced AR42J cells. (b) 48 h after transfection of TRAF6-siRNA, WB detected the knockdown efficiency of siRNA on TRAF6 in 10 nM cerulein-induced AR42J cells. Band analysis software is ImageJ (version 1.8.0_172). (c–e) The levels of inflammatory factors in the culture medium were detected by ELISA in 10 nM cerulein-induced AR42J cells. (f) CCK8 detected the effect of TRAF6 knockdown on cell proliferation in 10 nM cerulein-induced AR42J cells. (g) FCM detected the influence of TRAF6 knockdown on cell death in 10 nM cerulein-induced AR42J cells. $^{*}p < 0.05$, $^{**}p < 0.01$, and $^{***}p < 0.001$. The experiments were repeated three times, the statistical test was a two-tailed test, and errors bars in the figures represent standard deviation (SD).

1 min. See Supplementary Table II for PCR primer. The expression levels of TRAF6 and microRNA were calculated using the $2^{-\Delta\Delta Ct}$ method. GAPDH and 18sRNA are internal controls for mRNA and microRNAs, respectively.

2.4. Western Blotting (WB). According to the instructions, cerulein-treated AR42J acinar cells with RIPA buffer (Beyotime) and 30 μg denatured proteins were subjected to detect protein expression. Membrane with protein attached was incubated with primary antibodies against TRAF6 (1:1000, AB137452, Abcam), TLR9 (1 : 200, ab134368, Abcam), NLRP3 (1 : 1000, ab260017, Abcam), caspase-1 (1 : 1000, ab179515, Abcam), ASC (1 : 1000, ab283684, Abcam), and GSDMD (1 : 1000, ab210070, Abcam). The loading control was GAPDH (1 : 10 000, ab181602, Abcam). Band analysis software is ImageJ (version 1.8.0_172).

2.5. Dual-Luciferase Assay. The TRAF6-3′UTR sequence (WT) and the TRAF6-3′UTR mutant sequence (MUT) were subcloned into the psiCHECK2 vector (Synbio Technologies). psiCHECK2-TRAF6-WT or psiCHECK2-TRAF6-MUT and miR-146a-5p mimics or control (mimics NC) was cotransfected to 293T cells with Lipofectamine 2000 (Invitrogen). After 48 h, the dual-luciferase reporter kit (Promega, A6002) was used on handling transfected cells. Firefly fluorescence and *Renilla* fluorescence values were estimated with a microplate reader (Varioskan LUX, Thermo).

2.6. Cell Proliferation Rate Assays. 10 μL Cell Counting Kit-8 regent (Beyotime, C0038) was added to 5×10^3 cells per well at 0, 24, 48, and 72 h. Cells were collected, centrifuged at a low speed (JIDI-5R, Guangzhou JiDi Instrument Co., Ltd., China). The optical density was measured with an enzyme-labeled instrument (Thermo Fisher Scientific) at 450 nm.

2.7. Cell Apoptosis Assay. According to the procedure of Annexin V-FITC Apoptosis Detection Kit (Beyotime, C1062S). FITC Annexin V (5 μL) was added to cells (10^6 cells/mL) for incubation, followed by the addition of propidium iodide (5 μL). The experiment was conducted under incubation conditions—dark, 15 min, and 23 ± 2°C. Apoptosis was assessed by flow cytometry (FCM; BD Biosciences).

2.8. Statistical Analysis. Data are expressed as the mean ± standard deviation. Where there were more than two groups of data, statistical analysis was performed using one-way analysis of variance (ANOVA) and Dunnett's post hoc test, and Student's *t*-test was used to analyze the means of two groups. All experiments were repeated three times.

3. Results

3.1. miR-146a-5p Is Highly Expressed in Cerulein-Induced Pancreatitis. In order to find microRNAs associated with acute pancreatitis, first, AR42J acinar cells were dealt with 0, 2.5, 5, and 10 nM cerulein to construct a cerulein-induced pancreatitis model. 10 μg/mL LPS and 10 mM ATP were positive controls. IL-1β, IL-18, and TNF-α inflammatory factors were raised in the AR42J acinar cells with the concentration of cerulein (Figures 1(a)–1(c)). And the expression of miR-146-5p had the most significant reduction in cerulein-induced pancreatitis in inflammation-related miRNAs—miR-34a-5p, miR-146a-5p, miR-150-5p, and miR-181b-5p (Figures 1(d) and 1(e)).

3.2. miR-146a-5p Suppresses the Development of Pancreatitis. To explore the effect of miR-146a-5p on the progression of pancreatitis, we transfected mimics NC and miR-146a-5p mimics into AR42J acinar cells treated with 10 nM cerulein.

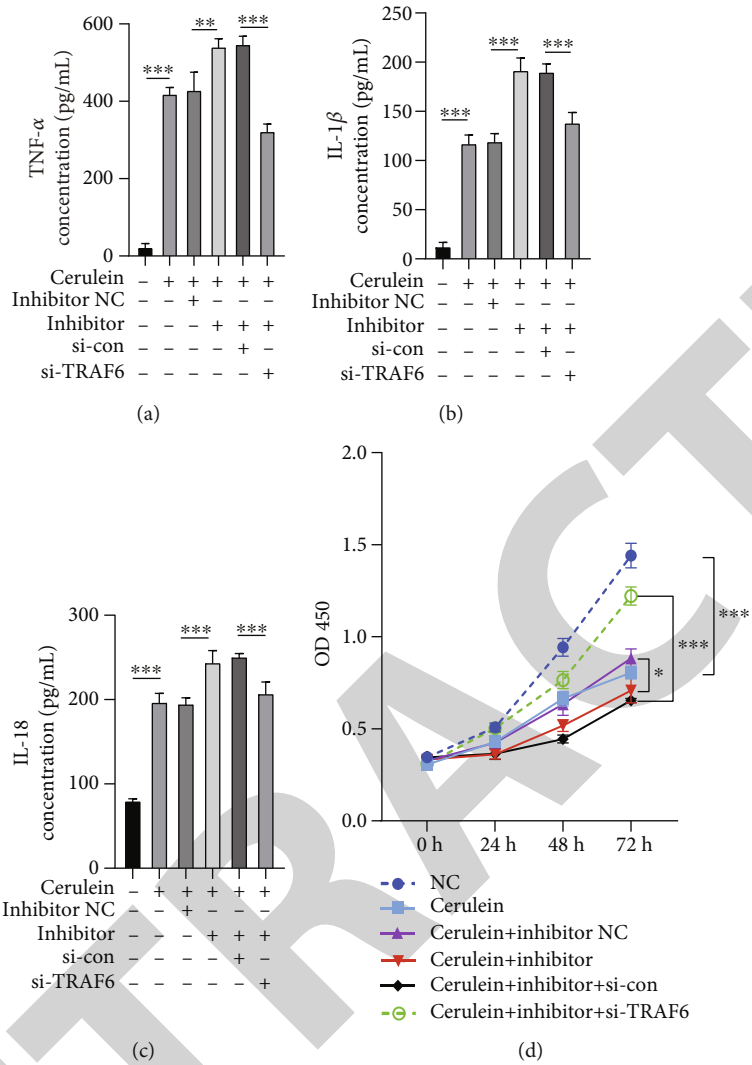

Figure 4: Continued.

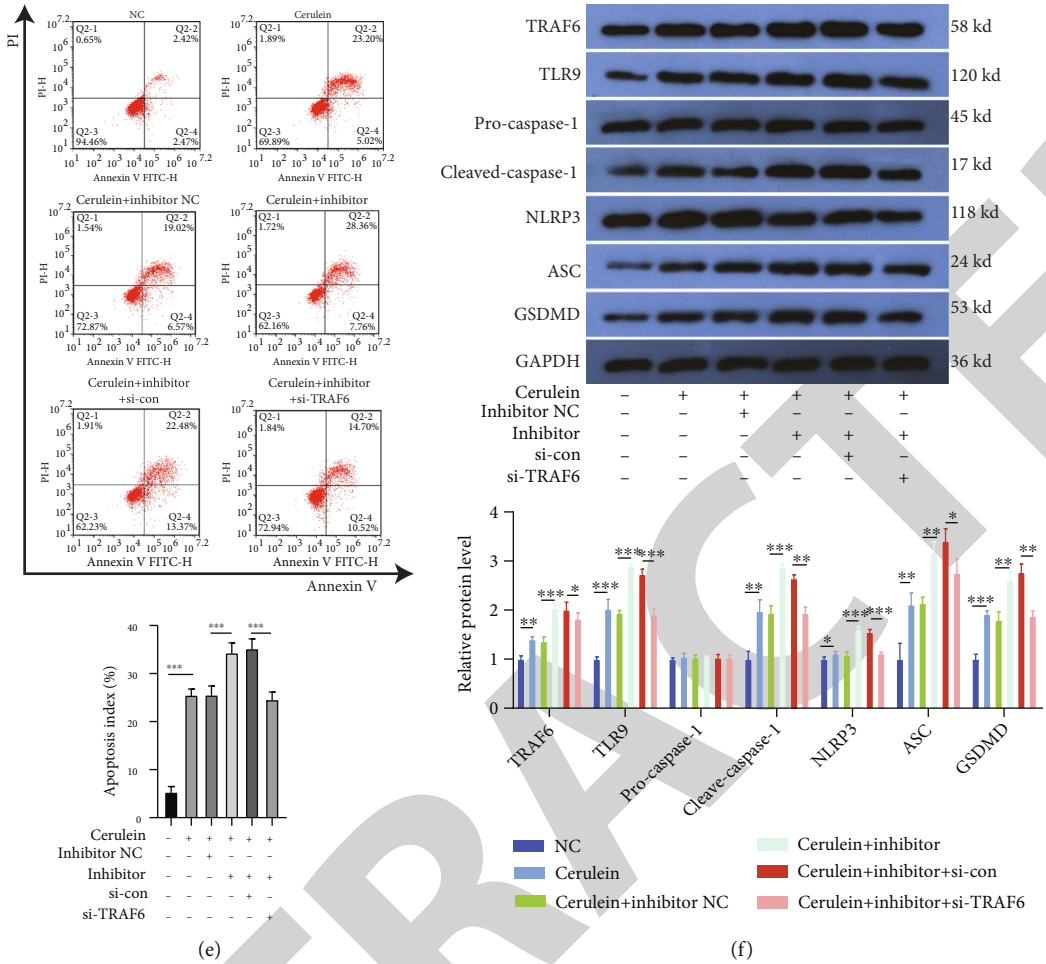

Figure 4: miR-146a-5p downregulation promotes the progression of pancreatitis via the TLR9/TRAF6/NLRP3 signaling pathway. (a–c) ELISA detected the levels of inflammatory factors in the culture medium. (d) The CCK8 assay detected proliferation. (e) FCM detected cell death. (f) Western blot detected the levels of TRAF6, TLR9, ASC, NLRP3, pro-caspase-1, cleaved-caspase-1 and GSDMD. Band analysis software is ImageJ (version 1.8.0_172). $^{*}p < 0.05$, $^{**}p < 0.01$, and $^{***}p < 0.001$. The experiments were repeated three times, the statistical test was a two-tailed test, and errors bars in the figures represent standard deviation (SD).

After the addition of the mimics, the expression of miR-146a-5p was obviously exaltation (Figure 1(f)). miR-146a-5p overexpression inhibited the expression of IL-1β, IL-18, and TNF-α inflammatory factors in cerulein-treated AR42J acinar cells (Figures 1(g)–1(i)). Upregulated miR-146a-5p boosted the proliferation of AR42J acinar cells treated with cerulein (Figure 1(j)). Moreover, the results of FCM presented that miR-146a-5p overexpression curbed apoptosis in cerulein-treated AR42J acinar cells (Figure 1(k)). In summary, miR-146a-5p restrained the development of pancreatitis.

3.3. The miR-146a-5p miRNA Targets TRAF6. Next, we needed to study the mechanism by which miR-146a-5p inhibits pancreatitis. It is known that the mechanism of LPS-induced acute inflammation is mainly through the activation of the inflammatory pathway by TRAF6 protein to release inflammatory factors [19]. Therefore, we supposed that TRAF6 was activated in cerulein-induced pancreatitis. The BiBiServ biological analysis software results exhibited miR-146a-5p binding to the TRAF6 protein 3′UTR, and RNAfold software predicted the secondary structure of the miR-146a-5p binding TRAF6 (Figure 2(a)). Dual-luciferase experiment certified the binding site of miR-146a-5p to TRAF6 3′UTR (Figure 2(b)). The results of qPCR and WB presented that miR-146a-5p can effectively subside the expression of TRAF6, and miR-146a-5p inhibitor can significantly increase the expression of TRAF6 (Figures 2(c) and 2(d)). At the same time, we tested the expression of TRAF6 in the cerulein induction model, and the results showed that TRAF6 increased with an increase in treatment concentration (Figures 2(e) and 2(f)), which was negatively correlated with the previous expression of miR-146a-5p.

3.4. TRAF6 Knockdown Inhibits the Development of Pancreatitis. To verify that TRAF6 knockdown can inhibit the development of pancreatitis, we designed three siRNAs and transfected them into cerulein-induced AR42J acinar cells. qPCR and WB detection results showed three siRNAs had knockdown effects on TRAF6, and the knockdown effects of siRNA2 and siRNA3 were more significant (Figures 3(a) and 3(b)). Therefore, we chose siRNA2 and siRNA3 for the follow-up experiments. ELISA

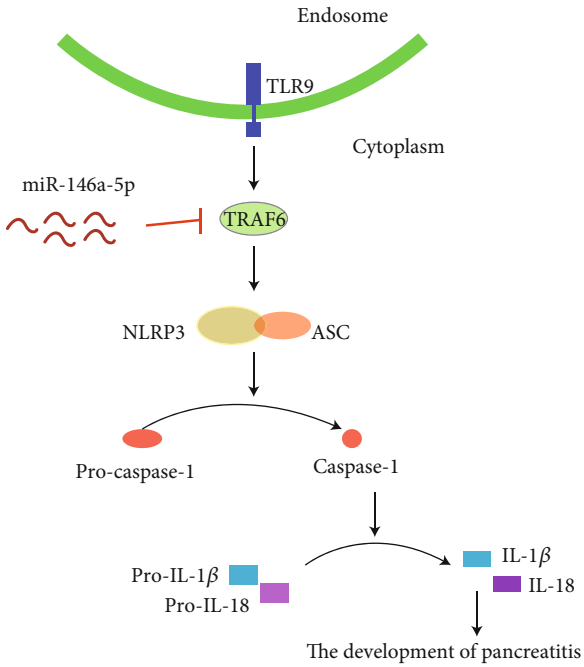

Figure 5: Cartoon illustration of miR-146a-5p regulating acute pancreatitis.

results showed that TRAF6 knockdown inhibited the expression of IL-1β, IL-18, and TNF-α inflammatory factors in AR42J acinar cells induced by cerulein (Figures 3(c)–3(e)). The results of CCK8 showed that TRAF6 knockdown could promote the proliferation of cerulein-induced AR42J acinar cells (Figure 3(f)). The results of apoptosis experiments exhibited that knockdown of TRAF6 inhibited the apoptosis of AR42J acinar cells induced by cerulein (Figure 3(g)). In summary, TRAF6 knockdown inhibited the development of pancreatitis.

3.5. Downregulation of miR-146a-5p Promotes the Progression of Pancreatitis via the TLR9/TRAF6/NLRP3 Signaling Pathway. To confirm that TRAF6 advanced the progression of pancreatitis, we designed a rescue experiment. In the AR42J acinar cells induced by cerulein, the miR-146a-5p antagonist was transfected, and TRAF6 was knocked down on this basis. The function of the miR-146a-5p/TRAF6 axis on apoptosis was verified by ELISA, CCK8, and cell apoptosis experiments. Knockdown of TRAF6 restored that miR-146a-5p suppressed the release of IL-1β, IL-18, and TNF-α inflammatory factor in AR42J acinar cells with cerulein (Figures 4(a)–4(e)). Therefore, we deduced that miR-146a-5p downregulation could accelerate the progression of pancreatitis through the target TRAF6. Furthermore, we wanted to identify the signaling pathway by which miR-146a-5p/TRAF6 regulates pancreatitis. Hoque et al. found that acute pancreatitis and pancreatic acinar cell death are related to TLR9 and NLRP3 inflammasomes [15]. Therefore, in the rescue experiment, we used WB to detect the expression of the TLR9 and NLRP3 inflammasome-associated proteins (NLRP3, ASC, GSDMD, pro-caspase-1, and cleaved-caspase-1). Knockdown of TRAF6 restored the miR-146a-5p inhibitor to the NLRP3 signaling pathway in cerulein-induced AR42J acinar cells (Figure 4(f)). Our observations therefore confirmed that the missing miR-146a-5p pushed the progression of pancreatitis via the TLR9/TRAF6/NLRP3 signaling pathway (Figure 5(a)).

4. Discussion

AP is characterized by the destruction of acinar cells, which contributes to the release of several inflammatory factors [20]. Inflammatory cells are then recruited to the pancreas, activating digestive proteases prematurely and triggering a systemic inflammatory response and, potentially, life-threatening multiple organ failure [13]. Pancreatic acinar cell damage may be caused by the programmed death of acinar cells, including apoptosis, autophagy, pyroptosis, and necrosis [20–22]. Pyroptosis is highly related to the inflammatory response. Therefore, pancreatic acinar cell pyroptosis may be a key factor in the pathogenesis of AP.

In our study, we first constructed a model of cerulein-induced acinar cell pyroptosis. The upregulated expression of TNF-α, IL-18, and IL-1β indicated that cerulein successfully induced acinar cell pyroptosis. Given that microRNAs are involved in multiple inflammations as a regulator, we selected 4 miRNAs related to pancreatitis and relatively conservative sequences based on literature reports—comprising miR-34a-5p, miR-146a-5p, miR-150-5p, and miR-181b-5p, which were induced by cerulein detection in AR42J cells [23, 24]. miR-146a-5p is obviously repressing in the pancreatitis group, and subsequent functional experiments have testified that miR-146a-5p can inhibit the progression of pancreatitis. This is consistent with our results. Stem cell-derived exosomal miR-146a-5p reduces microglial-mediated neuroinflammation via suppression of the IRAK1/TRAF6 signaling pathway after ischemic stroke [25].

The function of miRNA is to pair the target mRNA-3′ UTR through base complementation and form a silencing to degrade mRNA [26]. Bioinformatics is a reliable method for candidate gene analysis. Wenjie et al. utilized computer algorithms to discover that sensory ion channels TRPC3 and TRPC7 could be the potential therapeutic targets in pancreatic cancer [27]. So, we used biological analysis prediction software, BiBiServ, to predict that miR-146a-5p can bind to TRAF6 and that miR-146a-5p can significantly downregulate the expression of TRAF6. At the same time, we utilized RNAfold software to predict the secondary structure of TRAF6 mRNA and illustrated the binding sites of miR-146a-5p and TRAF6 in the structure. Furthermore, we confirmed that downregulation of TRAF6 can inhibit the progression of pancreatitis. Similarly, Chen et al. also unearthed that TRAF6 expedites the development of pancreatitis [28]. Xing et al. confirmed that TRAF6 can mediate the initiation of the NLRP3 inflammasome [18]. Sensory ion channels TRPC3 and TRPC7 could be the potential

therapeutic targets in pancreatic cancer and TRPC3 might be involved in dysregulating mitochondrial functions during pancreatic adenocarcinoma genesis.

Studies have shown that acinar cell apoptosis does not lead to pancreatitis, whereas acinar cell pyroptosis or necrosis can induce pancreatitis [29, 30]. Our results also show that the process of cerulein-induced pancreatitis mainly activates the NLRP3 inflammasome, cleaves caspase-1, activates GSDMD, and leads to the development of pancreatitis. Gao et al. confirmed that the activation of NLRP3 inflammasome and GSDMD in acinar cells triggers acute pancreatitis and systemic inflammation [31]. Our rescue experiment testified that miR-146a-5p downregulation can activate the further exacerbation of pancreatitis and activate the NLRP3 signaling pathway through the target TRAF6. Other studies have also confirmed that downregulation of TRAF6 by miR-146a-5p regulates pyroptosis and autophagy [17, 32, 33]. Therefore, miR-146a-5p may become a nucleic acid drug for inhibiting acute pancreatitis, which requires us to further conduct animal experiments and clinical trials.

Meanwhile, our study also revealed that the expression of TLR9 was upregulated in cerulein-induced pancreatitis. Zhao et al. also found that TLR9 can activate the NLRP3 inflammasome in mice with allergic airway inflammation [34]. However, how TLR9 and inflammasomes are activated in AP requires further study.

Abbreviations

AP:	Acute pancreatitis
TRAF6:	TNF receptor-associated factor 6
NLRP3:	NOD-like receptor protein 3
TLR:	Toll-like receptor
UTR:	Untranslated region
LPS:	Lipopolysaccharide
ASC:	Associated speck-like protein containing a CARD
GSDMD:	Gasdermin D
FBS:	Fetal bovine serum
MEM:	Minimum essential medium
miRNA:	MicroRNA
SDS-PAGE:	Sodium dodecyl sulfate polyacrylamide gel electrophoresis
GEO:	Gene Expression Omnibus
siRNA:	Small interfering RNA
NC:	Negative control
FCM:	Flow cytometry.

Data Availability

The data used to support the findings of this study are included within the article.

Conflicts of Interest

The authors declare that they have no competing interests.

Authors' Contributions

Liang Zhihai conceived and designed the study and developed the methodology. Deng Dehai, Su Zhou, Wei Biwei, Zhou Jie and Yang Huiying performed experiments and collected the data. Liang Zhihai wrote the original draft of the manuscript. All authors read and approved the final manuscript. Deng Dehai and Su Zhou contributed to the work equally and should be regarded as co-first authors.

Acknowledgments

This study was supported by the National Natural Science Foundation of China (No. 81960126) and the Nanning Qingxiu District Science and Technology Project (No. 2019026).

Supplementary Materials

Supplementary Table I: the sequence of siRNAs targeting TRAF6 and miR-146a-5p mimics/inhibitor. Supplementary Table II: the primer sequences used to analyze the expression of various RNAs and miRNAs. *(Supplementary Materials)*

References

[1] T. Tran and N. Lee, "Recurrent hypertriglyceridemic pancreatitis (HTGP); and the use of insulin drip as treatment," *The Journal of the Louisiana State Medical Society: Official Organ of the Louisiana State Medical Society*, vol. 169, no. 2, pp. 55-56, 2017.

[2] M. Dinda, C. Quirt, W. Mackillop, and M. Singer, "Freeze fracturing properties of native and heat-adapted Chinese hamster ovary (CHO) cells," *Biochemistry and Cell Biology*, vol. 67, pp. 473–476, 1989.

[3] Y. Yang, Q. Huang, C. Luo et al., "MicroRNAs in acute pancreatitis: From pathogenesis to novel diagnosis and therapy," *Journal of cellular physiology*, vol. 235, pp. 1948–1961, 2020.

[4] M. X. Hu, H. W. Zhang, Q. Fu et al., "Functional role of MicroRNA-19b in acinar cell necrosis in acute necrotizing pancreatitis," *Journal of Huazhong University of Science and Technology [Medical Sciences]*, vol. 36, pp. 221–225, 2016.

[5] J. Zhang, X. Ning, W. Cui, M. Bi, D. Zhang, and J. Zhang, "Transforming growth factor (TGF)-beta-induced microRNA-216a promotes acute pancreatitis via Akt and TGF-beta pathway in mice," *Digestive diseases and sciences*, vol. 60, pp. 127–135, 2015.

[6] X. Ma, D. J. Conklin, F. Li et al., "The oncogenic microRNA miR-21 promotes regulated necrosis in mice," *Nature communications*, vol. 6, p. 7151, 2015.

[7] Y. Min, M. J. Kim, S. Lee, E. Chun, and K. Y. Lee, "Inhibition of TRAF6 ubiquitin-ligase activity by PRDX1 leads to inhibition of NFKB activation and autophagy activation," *Autophagy*, vol. 14, no. 8, pp. 1347–1358, 2018.

[8] S. Akira, K. Takeda, and T. Kaisho, "Toll-like receptors: critical proteins linking innate and acquired immunity," *Nature Immunology*, vol. 2, no. 8, pp. 675–680, 2001.

[9] X. Li, C. Ye, M. Mulati, L. Sun, and F. Qian, "Ellipticine blocks synergistic effects of IL-17A and TNF-alpha in epithelial cells

Hindawi
Computational and Mathematical Methods in Medicine
Volume 2023, Article ID 9805202, 1 page
https://doi.org/10.1155/2023/9805202

Retraction

Retracted: Effects of Nifedipine and Labetalol Combined with Magnesium Sulfate on Blood Pressure Control, Blood Coagulation Function, and Maternal and Infant Outcome in Patients with Pregnancy-Induced Hypertension

Computational and Mathematical Methods in Medicine

Received 12 December 2023; Accepted 12 December 2023; Published 13 December 2023

This article has been retracted by Hindawi, as publisher, following an investigation undertaken by the publisher [1]. This investigation has uncovered evidence of systematic manipulation of the publication and peer-review process. We cannot, therefore, vouch for the reliability or integrity of this article.

Please note that this notice is intended solely to alert readers that the peer-review process of this article has been compromised.

Wiley and Hindawi regret that the usual quality checks did not identify these issues before publication and have since put additional measures in place to safeguard research integrity.

We wish to credit our Research Integrity and Research Publishing teams and anonymous and named external researchers and research integrity experts for contributing to this investigation.

The corresponding author, as the representative of all authors, has been given the opportunity to register their agreement or disagreement to this retraction. We have kept a record of any response received.

References

[1] Y. Shao, S. Gu, and X. Zhang, "Effects of Nifedipine and Labetalol Combined with Magnesium Sulfate on Blood Pressure Control, Blood Coagulation Function, and Maternal and Infant Outcome in Patients with Pregnancy-Induced Hypertension," *Computational and Mathematical Methods in Medicine*, vol. 2022, Article ID 9317114, 8 pages, 2022.

Hindawi
Computational and Mathematical Methods in Medicine
Volume 2022, Article ID 9317114, 8 pages
https://doi.org/10.1155/2022/9317114

Research Article

Effects of Nifedipine and Labetalol Combined with Magnesium Sulfate on Blood Pressure Control, Blood Coagulation Function, and Maternal and Infant Outcome in Patients with Pregnancy-Induced Hypertension

Yuping Shao, Siyi Gu, and Xiaoping Zhang

Department of Obstetrics and Gynecology, Qingpu Branch of Zhongshan Hospital Affiliated to Fudan University, Shanghai 201700, China

Correspondence should be addressed to Xiaoping Zhang; 15040340301@xs.hnit.edu.cn

Received 3 August 2022; Revised 11 August 2022; Accepted 27 August 2022; Published 13 October 2022

Academic Editor: Min Tang

Objective. The purpose is to investigate the influence of nifedipine, labetalol, and magnesium sulfate on blood pressure control, blood coagulation, and maternal and infant outcome in those suffering from pregnancy-induced hypertension (PIH). *Methods*. From January 2019 to April 2021, 100 participants with PIH in our center were randomly assigned to a control group and a research group. As a control, nifedipine combined with magnesium sulfate was administered. Nifedipine, labetalol, and magnesium sulfate were administered to the research group. The curative effect, blood pressure level, blood coagulation function, vascular endothelial function, and pregnancy comparisons were made between the two groups. *Results*. Based on the results of the study, the effective rate totaled 92.00%, while as for the control group, it was 80.0%, which indicates that there was a statistically significant difference between the effective rates of the research group and that of the control group, and the difference was statistically significant ($P < 0.05$). Blood pressure and blood coagulation function did not differ significantly between the two groups before treatment, and the difference was not statistically significant ($P > 0.05$). After treatment, both groups experienced a significant drop in systolic and diastolic blood pressure. After treatment, a higher PT index was found in the research group than in the control group. Likewise, the Fbg, D-D, and PLT were lower compared to those in the control group, and the difference was statistically significant ($P < 0.05$). Neither group had significantly different vascular endothelial function before treatment, and the difference was not statistically significant ($P > 0.05$). After treatment, the ET-1 of the two groups decreased, and the level of NO increased. There was a lower ET-1 in the research group than in the control group as well as a higher NO level in the research group than in the control group, and the difference was statistically significant ($P < 0.05$). Compared with the pregnancy outcome, in comparison to the controls, the research group had a higher vaginal delivery rate. Significantly, fewer cases of fetal distress, intrauterine asphyxia, and placental abruption were reported in the research group than in the control group, and the difference was statistically significant ($P < 0.05$). *Conclusion*. Nifedipine, in combination with magnesium sulfate and labetalol, is effective at treating PIH, reducing blood pressure, improving blood coagulation, preventing cardiovascular events and vascular endothelial function, and further improve the pregnancy outcome.

1. Introduction

With the improvement of living standards, the weight of many pregnant women has increased excessively during pregnancy. Annually, the number of hypertensive disorders complicating pregnancy (HDCP) increases due to the lack of regular antenatal examinations and uneven distribution of medical resources [1, 2]. HDCP can be divided into gestational hypertension, preeclampsia-eclampsia, and eclampsia if blood pressure rises after 20 weeks of pregnancy. If hypertension persists until 12 weeks after delivery, it can be divided into some categories: high blood pressure with preeclampsia and chronic hypertension during pregnancy. The survey shows that the global incidence of pregnancy induced

hypertension is as high as 8%; the incidence of preeclampsia is 7% [3, 4]. According to statistics, the incidence of (HDSP) in China is 5% to 12%. The World Health Organization (WHO) has released statistics that about 50, 000 women around the world die of epilepsy and its complications every year [5]. The risk is higher in less developed regions such as Asia and Africa, where the case fatality rate of patients with pregnancy induced hypertension (PIH) is about 10%. In less developed areas, the case fatality rate of PIHin Latin America is about 25% [6]. Therefore, as a global disease, PIH has attracted widespread attention because of its serious threat to maternal and infant safety.

Fetal growth restriction may occur when β-blockers are used during early pregnancy. The side effects of the drug are scalp tingling and vomiting. Nifedipine was often chosen as calcium channel blockers because it can effectively inhibit calcium influx, dilate blood vessels, and relax smooth muscle. Clinical use of nifedipine can prevent threatened preterm labor. Importantly the side effects on pregnant women are relatively small because of the long antihypertensive stable duration and the small effect on the circulatory system. The main drugs of PIH treatment commonly used in clinic are magnesium sulfate, which has the effects of sedation, spasmolysis, and antihypertensive. But due to the single use of drugs, it is difficult to achieve the ideal therapeutic effect [7]. Labetalol, a commonly used α-receptor and β-receptor blocker, could act directly on the blood vessels of the human body, reducing the patient's blood pressure by dilating the blood vessels. While the cardiac output and pulse output will not change during the treatment.

During the treatment, side effects such as palpitation and headache may occur after taking nifedipine. At present, it is considered that nifedipine and labetalol have good therapeutic effect onPIH. Placental blood flow rarely changes, effectively prevent blood pressure from falling too much, having the effect of increasing prostacyclin level, antiplatelet aggregation, and promoting fetal lung maturation. It is often recommended for patients with moderate and severe PIH. Labetalol's advantage lies in the effective control of blood pressure in pregnant women. While the placenta is not affected by drugs, which can have a satisfactory effect on the perinatal final maternal and infant outcome [8, 9]. Labetalol, as a first-line drug for reducing blood pressure in PIH, is mainly due to its mild effect on lowering blood pressure and does not affect placental blood flow, which will not lead to symptoms such as low blood pressure and rapid heart rate [10, 11]. Therefore, the present study outlines the clinical effectiveness of nifedipine and magnesium sulfate combined with labetalol in PIH, to guide clinical decision making in the selection of a better treatment plan.

2. Materials and Methods

2.1. General Information. Our hospital treated 100 patients with pregnancy-induced hypertension from January 2019 to April 2021, and the study focused on their outcomes. A random sampling of patients was taken into account to divide them into the study and control groups. The control group was treated with Adalat combined with magnesium sulfate, and the research group was treated with the combination of Adalat, labetone, and magnesium sulfate. An average age of (32.56 ± 3.42) years was found in the control group, which ranged from 20 to 44 years old; a 24-year-old was the youngest participant in the study, followed by an average of 34 years old, and a 44-year-old was the oldest. There was no significant difference in the general data between the two groups, and the difference was not statistically significant ($P > 0.05$). Patients signed informed consent, and the study was approved by the Medical Ethics Association of the hospital where it was conducted.

2.2. Inclusion Criteria. (i) It accords with the diagnostic manifestation of pregnancy-induced hypertension in western medicine, specifically referring to the diagnostic guidelines of HDCP and the 9th edition of Obstetrics and Gynecology [12, 13]; (ii) all patients are singleton pregnancy, and the fetus and various indexes are normal after related imaging examination; (iii) the patients have no hypertension, diabetes, and abnormal blood coagulation in the past years; (iv) the clinical data of the patients in this study are complete

2.3. Exclusion Criteria. (i) This study involved patients who are allergic to certain drugs; (ii) patients with other major organ diseases and/or neuropsychiatric diseases; (iii) patients having hematological tumors or other blood system diseases; (iv) patients with insufficient clinical data or withdrawal; (v) patients with severe injuries to liver, kidney, and other organs

2.4. Methods. After admission, all patients were given routine diet education guidance, close monitoring of blood pressure. Medical officers assist patients to complete the relevant examinations. Medical staff should carefully record the blood pressure control of patients, instruct patients to maintain a light diet, emphasize dietary taboos and matters needing attention in life, supervise the use of drugs, and strengthen the observation of adverse drug reactions.

Drug regimen for patients in the control group: magnesium sulfate injection (Anyang Kyushu Pharmaceutical Co., Ltd., national drug standard H41023035, specification: 10 ml:2.5 g), 20 ml was mixed with 100 m1 5% glucose injection (Jiangsu Shenlong Pharmaceutical Co., Ltd., national medicine standard word H32024365, specification: 100 ml/bag), intravenous drip for 0.5 h, and then 60 ml magnesium sulfate injection combined with 1000 m1 5% glucose injection was mixed with intravenous drip for maintenance treatment. At the same time, patients were given oral nifedipine tablets (Guangdong South China Pharmaceutical Group Co., Ltd., Chinese medicine H44023986, specification: 10 mg $\times$ 100 s) 3 times a day, 10 mg each time.

The patients in the research group were given oral labetalol hydrochloride tablets (Zhengzhou Kaili Pharmaceutical Co., Ltd., Chinese medicine H41024906, specification: 50 mg $\times$ 20 tablets $\times$ 2 plates) 3 times a day, 100 mg each time. For the following two weeks of treatment, both groups were evaluated for clinical efficacy.

2.5. Observation Index

2.5.1. Evaluation of Curative Effect [13]. Effective: (i) as a result of the treatment, the systolic blood pressure was below 140 mmHg; the diastolic blood pressure was below 90 mmHg, and the urine protein <0.3 g/24 h, $90\% > N \geq 66.67\%$. (ii) systolic blood pressure 140~150 mmHg, diastolic blood pressure 90~100 mmHg, and urinary protein <1.0 g/24 h, $66.7\% > N \geq 33.3\%$ after 7 days of treatment.

Ineffective: (iii) after 7 days of treatment, the systolic blood pressure fluctuated in 150~160 mmHg, and diastolic blood pressure 100~110 mmHg, albuminuria ≥ 1 g, 24 h, $N < 33.3\%$. Total effective rate = (number of effective cases + effective cases)/total number of cases × 100%.

2.5.2. Blood Coagulation Index and Vascular Endothelial Function. Prothrombin time (PT) and fibrinogen (Fbg) were detected before treatment and 2 weeks after treatment (CA-7000 automatic blood coagulation analyzer). The D-dimer (D-dimer) (enzyme-linked immunosorbent assay), platelet count (PLT), endothelin-1 (ET-1), and nitric oxide (NO) were detected.

2.5.3. Blood Pressure Level and Pregnancy Outcome. Researchers recorded both groups' blood pressure levels before and after treatments. At the same time, the pregnancy outcomes of the two groups were recorded (vaginal delivery, fetal distress, intrauterine asphyxia, placental abruption).

2.6. Statistical Analysis. SPSS23.0 statistical software was adopted to process the data. The measurement data were presented as $(\bar{x} \pm s)$. The group design t-test was adopted for the comparison, and the analysis of variance was adopted for the comparison between multiple groups. Dunnett's test was adopted for comparison with the control group. The counting data were presented in the number of cases and the percentage, χ^2 test was adopted for comparison between groups, and bilateral test was employed for all statistical tests.

3. Results

3.1. Comparative Study of Curative Effects. There were no patients who quit the study. In the research group, a 92.00% success rate was achieved in 31 cases whose effectiveness was marked; 15 cases whose effectiveness was marked, and four cases whose effectiveness was ineffective. The comparison group had 28 cases that were significantly effective, 12 cases that were effective, and 10 cases that were ineffective, with an efficacy rate of 80%. Studies conducted in the research group had a higher efficacy rate than in the control group, and the difference was statistically significant ($P < 0.05$). Figure 1 shows all the results of the data analysis.

3.2. Blood Pressure Level Comparison. A comparison of blood pressure levels between the two groups before and 2 weeks after treatment did not reveal any significant differences, and the difference was not statistically significant ($P > 0.05$). Systolic and diastolic blood pressure decreased significantly after treatment in both groups. Significantly, in the research group, both systolic and diastolic blood pressures were higher than those in the control group, with the difference being statistically significant, and the difference was statistically significant ($P < 0.05$). The data results are summarized in Table 1.

3.3. Comparison of Blood Coagulation Function Indexes. Neither group had significantly different indexes of blood coagulation before treatment, and the difference was not statistically significant ($P > 0.05$). A significant increase in PT indexes was observed in the research group after treatment, and the Fbg, D-D, and PLT were significantly lower than those in the control group. Differences between them were statistically significant, and the difference was statistically significant ($P < 0.05$). All the data results are shown in Table 2.

3.4. Comparison of Vascular Endothelial Function. Prior to treatment, there were no significant differences in vascular endothelial function between the two groups, and the difference was not statistically significant ($P > 0.05$). After treatment, the level of ET-1 of the two groups decreased, and the level of NO increased. Compared to the control group, the research group's ET-1 was lower, and its level of NO was higher than the control group's; the difference was statistically significant ($P < 0.05$). The results of the data analysis are presented in Table 3.

3.5. Comparison of Pregnancy Outcome. Compared with the pregnancy outcome, it was more common for women in the research group to give birth via vaginal delivery than in the control group, and the incidences of fetal distress, intrauterine asphyxia, and placental abruption in the research group were lower than those in the control group, and the difference was statistically significant ($P < 0.05$). All the data results are shown in Figure 2.

4. Discussion

HDCP is a kind of disease which coexists with hypertension and pregnancy, in addition to preeclampsia and gestational hypertension, chronic hypertension related to preeclampsia, eclampsia, and chronic hypertension complicating pregnancy are also among its complications. The main clinical manifestations are urinary protein, elevated blood pressure, and limb edema, which could lead to a series of consequences, such as fetal growth retardation, placental abruption, preterm delivery, fetal death, and postpartum hemorrhage. In severe cases, serious complications including heart failure, convulsion, liver failure, coma, and renal failure may occur [14]. Among the causes of maternal death, HDCP ranked second [15]. Preeclampsia is defined as follows: after 20 weeks of pregnancy, expecting mothers without history of hypertension find that their blood pressure has increased
(-
systolic blood pressure ≥ 140 mmHg and/or diastolic blood pressure ≥ 90 mmHg), accompanied by changes in urinary protein or pathological changes in the vital organ system, or placental-fetal lesions, accounting for about 3.9% of all

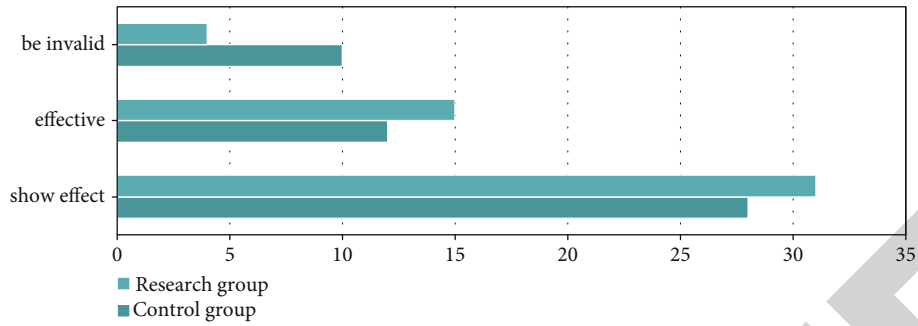

Figure 1: Comparison of curative effect between the two groups.

Table 1: Comparison of blood pressure between the two groups.

Grouping	N	Systolic blood pressure		Diastolic pressure	
		Before treatment	After treatment	Before treatment	After treatment
Control group	50	164.83 ± 14.95	134.39 ± 12.44	99.94 ± 7.53	83.19 ± 5.86
Research group	50	165.39 ± 15.44	120.39 ± 9.83	99.91 ± 7.55	78.39 ± 5.64
t value		0.184	6.243	0.019	4.173
P value		>0.05	<0.05	>0.05	<0.05

Table 2: Comparison of coagulation function indexes between the two groups.

Grouping	N	PT (s)		Fbg (g/L)		D-D (mg/L)		PLT ($x10^9$/L)	
		Before treatment	After treatment	Before treatment	After treatment	Before treatment	After treatment	Before treatment	After Treatment
Control group	50	8.01 ± 1.05	10.93 ± 1.22	7.68 ± 1.34	5.49 ± 1.21	1.52 ± 0.36	1.29 ± 0.31	52.23 ± 24.05	39.94 ± 23.11
Research group	50	7.99 ± 1.04	12.48 ± 1.21	7.71 ± 1.36	4.12 ± 0.66	1.55 ± 0.40	0.73 ± 0.36	52.97 ± 24.11	18.49 ± 9.31
t value		0.096	6.378	0.111	7.028	0.394	8.335	0.154	6.087
P value		0.924	<0.05	0.912	<0.05	0.694	<0.05	0.878	<0.05

Table 3: Comparison of vascular endothelial function between the two groups.

Grouping	N	ET-1 (ng/L)		NO (Mol/L)	
		Before treatment	After treatment	Before treatment	After treatment
Control group	50	69.96 ± 3.45	57.76 ± 3.64	40.64 ± 3.23	70.56 ± 4.64
Research group	50	69.42 ± 2.64	39.91 ± 2.95	40.65 ± 3.18	50.85 ± 3.44
t value		0.878	26.939	0.015	24.128
P value		>0.05	<0.05	>0.05	<0.05

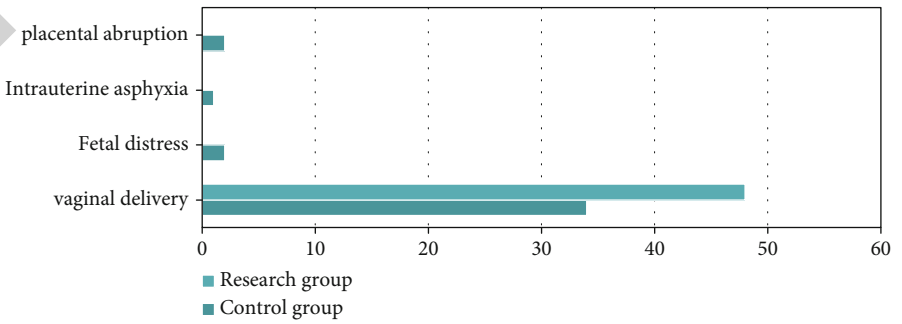

Figure 2: Comparison of pregnancy outcomes between the two groups.

pregnancies [16]. The present study outlines the clinical effectiveness of nifedipine and magnesium sulfate combined with labetalol in PIH, to guide clinical decision making in the selection of a better treatment plan.

The present study outlines the clinical effectiveness of nifedipine and magnesium sulfate combined with labetalol in PIH, to guide clinical decision making in the selection of a better treatment plan. With the development of modern medical technology and the deepening of clinical research on preeclampsia, the methods to control the development of preeclampsia have also made considerable progress, effectively reducing neonatal mortality and maternal prenatal complications [17, 18]. There is no complete understanding of the etiology and pathogenesis of pregnancy-induced hypertension. In the past ten years, the theory of "placental superficial implantation", as a theory to explain HDCP, has been gradually accepted by most scholars [19]. Current studies have confirmed that the erosion function of trophoblasts in early pregnancy decreases, which leads to the shallow implantation of placenta into the endometrium and triggers the occurrence of PIH. Similar to allogeneic transplantation during pregnancy, embryonic trophoblast cells need to erode into the decidua of the mother's uterus, invade the spiral artery, and then replace the arterial endothelial cells to establish an interactive circulation between the fetus and the mother, which can provide necessary nutritional support for the development of the embryo. In normal pregnancy, the diameter of placental villi decreased significantly with the increase of the diameter of spiral arterioles between decidua and uterus. This physiological change increases the total area of gas exchange between mother and fetus, which is beneficial to the normal growth and development of fetus. If there are abnormalities in this process, the erosion ability of extravillous trophoblasts is impaired; the uterine spiral artery is not eroded enough by trophoblasts, and the erosion range is reduced [20].

Clinical studies have found that PIH has many effects on pregnant women, fetuses, and newborns. Some scholars have suggested that it may be related to the occurrence of some neonatal diseases, such as septicemia, infection, retinopathy, intracranial hemorrhage, and so on. It will also be affected in the aspects of hormone system, blood cytology, blood glucose and blood lipid metabolism, nervous system development as well as long-term intelligence, physical strength, psychology, and quality of life. The uterine spiral artery has not experienced the changes of normal pregnancy, but still maintains the sensitivity to vasoconstrictive substances and relatively narrow diameter. This will lead to shallow placenta implantation than normal pregnancy, decreased blood perfusion, and a series of clinical symptoms of HDCP [21]. The increase of blood pressure after pregnancy will lead to the damage of vascular endothelium and the release of endogenous vasodilator factor, vasodilator factor, and NO. Under the influence of prostacyclin (PGIa), it increases the synthesis of thromboxane A (TXA), which induces the imbalance of the ratio of vasoconstrictor factor to vasodilator factor, leading to a further increase in blood pressure. There are corresponding pathological changes in each target organ, which affect the quality of life of pregnant women and the life safety of mothers and infants [22–24]. An important pathological feature of hypertension during pregnancy is systemic arterial spasm; the result of which is an increase in peripheral resistance and blood pressure, the decrease of blood flow through placenta and placental function compared with normal pregnancy, and the enhancement of vascular permeability. Blood viscosity increased in a state of hypercoagulability, followed by intravascular coagulation and microvascular thrombosis.

When using drugs to control blood pressure in HDCP, methyldopa, and labetalol combined with nifedipine should be considered firstly [25]. Due to the different physical types, receptors, and pharmacological mechanisms of medicine in pregnant women, it is not possible to determine that labetalol hydrochloride can play a better effect on each body in the group. Limited by the scope of the trial, we rule out not only the existence of other kinds of augmentation drugs but also the good history of the treatment of PIH. The preferred drug for controlling blood pressure in HDCP is α-adrenergic agonist methyldopa. Its pharmacological effect is to stimulate the α-receptor and inhibit the peripheral sympathetic nerve. Its curative effect has been confirmed, and its side effects are drowsiness, constipation, dry mouth, and bradycardia. Unfortunately, this drug is not used in our market [26]. Labetalol hydrochloride tablets have the advantages of long-term tolerance and safety to both mother and fetus. As a salicylamide derivative, its chemical structure can effectively select α and β-adrenergic receptors [27]. There are mainly α receptors in peripheral resistance vessels and volume vessels, which can dilate the above vessels after blocking α receptors. The coronary blood flow increased significantly; the myocardial oxygen consumption was reduced, and the cardiac load was reduced. The clinical effect is quick, and it does not reduce blood pressure to too low and does not affect the blood perfusion of placenta, brain, uterus, kidney, and fetus. β-adrenoceptor mainly acts on the atrioventricular junction. Blocking β-receptor can prolong the conduction time of myocardial bioelectric signals in this area, thus reduce the heart rate and myocardial oxygen consumption. It slows down the heart rate and lowers blood pressure at the same time [28]. The heart rate of patients will not decrease indefinitely after slowing down to a certain extent, and then tend to stabilize by themselves. According to the clinical pharmacological study [29], labetalol hydrochloride tablets also have the functions of reducing platelet consumption, inhibiting platelet aggregation, and promoting fetal lung maturation. But there are inevitable limitations.

Magnesium sulfate can also dilate vascular smooth muscle and dilate spastic peripheral blood vessels as a preventative measure and treatment for eclampsia. It can play a role immediately after intravenous injection lasting for 30 min and renal excretion. However, during the treatment of magnesium sulfate, the knee reflex and respiration of the patients should be observed, and the urine volume should be $\geq$25 mL/h. In addition, the dose and flow velocity should be controlled according to the patient's signs. Nifedipine can inhibit Ca^{2+} inflow, relax vascular smooth muscle, dilate coronary artery, and increase coronary blood flow, thus lowering blood pressure. Low-dose coronary artery dilatation

does not affect blood pressure, so it is a better antianginal drug [30]. In the treatment of PIH, magnesium sulfate is first of all recommended, which can inhibit the activity of central nervous system and conduct a reduction in the release of acetylcholine from motor nerve-muscle junctions and a relaxation of muscle contractions. As an antihypertensive drug, there are no adverse reactions such as water and sodium retention and edema that are common in general vasodilators. The effect of sublingual administration is faster than that of oral administration. The antihypertensive effect appeared after 10 minutes of spray administration; the effect was the most significant after 1 hour, and the blood pressure increased after about 3 hours (some can last for 11 hours). Intravenous injection within 10 minutes can reduce blood pressure by 21%-26% [31]. Nifedipine is a dihydropyridine calcium channel blocker, which can dilate vascular smooth muscle and improve peripheral vasospasm. Magnesium sulfate combined with nifedipine can better relax peripheral vascular smooth muscle, reduce vascular resistance, and improve uterine artery blood flow. Vascular endothelium injury can release a large number of vasoactive substances, which participate in the regulation of vascular tension, smooth muscle cell proliferation, vascular wall inflammation, and so on [32].

The combined application of labetalol, nifedipine, and magnesium sulfate can effectively improve blood circulation and reduce the damage of hypertension to heart, kidney, and other target organs, thus improving the internal environment [33, 34]. It is consistent with the results of Uwizeyimana et al. [35] and Houehanou et al. [36]. Most of the patients with PIH are in hypercoagulable state. Nifedipine combined with magnesium sulfate and labetalol can dilate blood vessels and reduce blood pressure [37]. Compared with the control group, the research group's total efficacy rate was significantly higher, as were the levels of systolic blood pressure and diastolic blood pressure. It is suggested that labetalol can block both α-receptor and β-receptor, effectively expand blood volume and reduce cardiac preload by blocking α-receptor, and can reduce myocardial oxygen consumption and increase cardiac output by blocking β-adrenoceptor. Results revealed that PT levels in the research group rose, whereas FBG levels and Dmurd levels declined. There was a higher degree of improvement in the PIH group than in the control group, indicating that nifedipine alone or in combination with magnesium sulfate and labetalol could reduce hypercoagulability. ET-1, an endogenous injury factor produced in pathological state can produce the metabolite A2, promote the release of calcium ions from the calcium library, and increase the production of free radicals. NO is a vasodilating factor, which can maintain vascular endothelial function and regulate blood pressure [38, 39]. Both groups experienced a decrease in ET-1 levels as well as an increase in NO levels after treatment, indicating that nifedipine with magnesium sulfate and labetalol can relieve these side effects. The reason may be that nifedipine combined with magnesium sulfate and labetalol can downregulate the expression of endothelin and improve endothelial dysfunction. Nifedipine combined with magnesium sulfate and labetalol can regulate peroxide injury and reduce the release of free radicals to prevent vascular endothelial damage [40, 41]. There are some limitations in this study. First, the sample size of this study is not large, and it is a single-center study, so bias is inevitable. In future research, we will carry out multicenter and large-sample prospective studies, or more valuable conclusions can be drawn.

In conclusion, PIH can be effectively treated with nifedipine, magnesium sulfate, and labetalol, which can effectively reduce blood pressure, improve blood coagulation and vascular endothelial function, and further improve the pregnancy outcome.

Data Availability

The datasets used and analyzed during the current study are available from the corresponding author upon reasonable request.

Conflicts of Interest

The authors declare that they have no conflicts of interest.

References

[1] N. B. Allen and S. S. Khan, "Blood pressure trajectories across the life course," *American Journal of Hypertension*, vol. 34, no. 3, pp. 234–241, 2021.

[2] K. R. Roell, Q. E. Harmon, K. Klungsøyr, A. E. Bauer, P. Magnus, and S. M. Engel, "Clustering longitudinal blood pressure trajectories to examine heterogeneity in outcomes among preeclampsia cases and controls," *Hypertension*, vol. 77, no. 6, pp. 2034–2044, 2021.

[3] Y. Zhang, Z. Meng, Z. Li, L. Wang, S. Qiu, and C. Xu, "A pregnant woman with congenital hepatic fibrosis delivers a healthy neonate," *Liver International*, vol. 41, no. 1, pp. 128–132, 2021.

[4] S. Guruvare and C. Ram, "Target blood pressure goals for treating hypertension in pregnancy," *Hypertension Journal*, vol. 6, no. 4, pp. 4–7, 2020.

[5] A. Lyndon, R. J. Baer, C. L. Gay, A. M. el Ayadi, H. C. Lee, and L. Jelliffe-Pawlowski, "A population-based study to identify the prevalence and correlates of the dual burden of severe maternal morbidity and preterm birth in California," *The Journal of Maternal-Fetal & Neonatal Medicine*, vol. 34, no. 8, pp. 1198–1206, 2021.

[6] K. R. Ghosh, S. Akhter, A. K. Das, N. Naher, S. R. Paul, and B. Islam, "Outcome of labetalol and methyldopa as oral antihypertensive agent in the treatment of pregnancy induced hypertension," *Mediscope*, vol. 8, no. 1, pp. 19–26, 2021.

[7] J. S. Deshpande, D. P. Sundrani, A. S. Sahay, S. A. Gupte, and S. R. Joshi, "Unravelling the potential of angiogenic factors for the early prediction of preeclampsia," *Hypertension*, vol. 44, no. 7, pp. 756–769, 2021.

[8] E. Armenia and M. Vornovitsky, "Hypertension in pregnancy," *Hypertension Journal*, vol. 6, no. 1, pp. 28-29, 2020.

[9] W. Kawarazaki and T. Fujita, "Kidney and epigenetic mechanisms of salt-sensitive hypertension," *Nature Reviews. Nephrology*, vol. 17, no. 5, pp. 350–363, 2021.

[10] W. Chen, H. Li, Q. Zhou, and J. Xue, "Effect of hypertension on prognosis in patients with pregnancy-related acute kidney injury: a retrospective, propensity score-matched cohort

study," *Yi xue ban = Journal of Central South University. Medical sciences*, vol. 45, no. 7, pp. 797–803, 2020.

[11] C. S. M. Ruano, C. Apicella, S. Jacques et al., "Alternative splicing in normal and pathological human placentas is correlated to genetic variants," *Human Genetics*, vol. 140, no. 5, pp. 827–848, 2021.

[12] Y. Zi and Z. Weiyuan, "Interpretation of guidelines for diagnosis and treatment of hypertensive disorder complicating pregnancy (2015)," *Chinese Journal of practical Gynecology and Obstetrics*, vol. 31, no. 10, pp. 886–893, 2015.

[13] M. A. Jafar, S. Rauf, and D. Daud, "Profile of minimal and non-minimal change nephrotic syndrome in children: a cross-sectional study," *Green Medical Journal*, vol. 2, no. 2, pp. 39–48, 2020.

[14] V. Giardini, S. Allievi, C. Fornari et al., "Management of pregnancy blood pressure increase in the emergency room: role of PlGF-based biochemical markers and relative economic impact," *The Journal of Maternal-Fetal & Neonatal Medicine*, vol. 34, no. 7, pp. 1083–1090, 2021.

[15] M. O. Alese, J. Moodley, and T. Naicker, "Preeclampsia and HELLP syndrome, the role of the liver," *The Journal of Maternal-Fetal & Neonatal Medicine*, vol. 34, no. 1, pp. 117–123, 2021.

[16] S. Hayakawa, S. Komine-Aizawa, K. Takada, T. Kimura, and H. Yamada, "Anti-SARS-CoV-2 vaccination strategy for pregnant women in Japan," *The Journal of Obstetrics and Gynaecology Research*, vol. 47, no. 6, pp. 1958–1964, 2021.

[17] A. Premkumar, N. K. Ayala, C. H. Miller, W. A. Grobman, and E. S. Miller, "Postpartum NSAID use and adverse outcomes among women with hypertensive disorders of pregnancy: a systematic review and meta-analysis," *American Journal of Perinatology*, vol. 38, no. 1, pp. 1–9, 2021.

[18] M. K. Maducolil, S. Al-Obaidly, T. Olukade, H. Salama, M. AlQubaisi, and H. Al Rifai, "Maternal characteristics and pregnancy outcomes of women with chronic hypertension: a population-based study," *Journal of Perinatal Medicine*, vol. 48, no. 2, pp. 139–143, 2020.

[19] R. Kalra, S. Jindal, S. P. Dave, S. Bansal, and B. M. Loya, "Severe hypertension complicating pregnancy, pheochromocytoma: a rare case report," *Indian Journal of Obstetrics and Gynecology Research*, vol. 7, no. 1, pp. 129–132, 2020.

[20] C. Golla, M. Banadakoppa, J. Espinoza, and C. Yallampalli, "873: Is hypertension during pregnancy a risk factor for SGA at all gestational ages?," *American Journal of Obstetrics and Gynecology*, vol. 222, no. 1, pp. S545–S546, 2020.

[21] G. K. Davis, A. Henry, C. Arnott, and M. A. Brown, "The long-term cardiovascular impact of hypertension in pregnancy – A missed opportunity," *Obstetrics and Gynecology*, vol. 61, no. 3, pp. 474–477, 2021.

[22] N. O. Enaruna, "VP50.25: Predicting pregnancy and long-term risk of hypertension with uterine artery Doppler and flow-mediated dilation of the brachial artery in Nigerian women," *Ultrasound in Obstetrics and Gynecology*, vol. 56, no. S1, pp. 291–291, 2020.

[23] M. Vestgaard, B. Ásbjörnsdóttir, L. Ringholm et al., "White coat hypertension in early pregnancy in women with pre-existing diabetes: prevalence and pregnancy outcomes," *Diabetologia: Clinical and Experimental Diabetes and Metabolism = Organ of the European Association for the Study of Diabetes (EASD)*, vol. 62, no. 12, pp. 2188–2199, 2019.

[24] J. Hu, M. Danielli, R. C. Thomas et al., "COVID-19: women with diabetes and hypertension during pregnancy," *British Journal of Midwifery*, vol. 28, no. 11, pp. 800-801, 2020.

[25] M. Medubayeva, L. Latypova, A. Kerimkulova et al., "Peculiarities of pregnancy course and delivery outcomes in women with various forms of arterial hypertension," *Georgian Medical News*, vol. 300, pp. 26–32, 2020.

[26] M. C. Tolcher, K. A. Fox, H. Sangi-Haghpeykar, S. Clark, and M. A. Belfort, "22: intravenous labetalol versus oral nifedipine for acute hypertension in pregnancy: effects on cerebral perfusion pressure," *American Journal of Obstetrics and Gynecology*, vol. 222, no. 1, pp. S20–S21, 2020.

[27] A. Birukov, F. Herse, J. H. Nielsen et al., "Blood pressure and angiogenic markers in pregnancy," *Hypertension*, vol. 76, no. 3, pp. 901–909, 2020.

[28] S. A. Fatima, J. M. Latha, N. Vani, and S. H. Fatima, "A comparative study of serum lipids and lipoprotein- a levels of women with pregnancy induced hypertension (PIH) and normotensive pregnant women," *International Journal of Clinical Biochemistry and Research*, vol. 7, no. 4, pp. 488–496, 2021.

[29] J. N. Martin and J. M. Tucker, "Adverse maternal consequences associated with prolonged acute-onset severe systolic hypertension during pregnancy & early postpartum: pitfalls in practice & lessons learned," *Open Journal of Obstetrics and Gynecology*, vol. 11, no. 5, pp. 626–635, 2021.

[30] W. Ballard, B. Dixon, C. A. McEvoy, and A. K. Verma, "Pulmonary arterial hypertension in pregnancy," *Cardiology Clinics*, vol. 39, no. 1, pp. 109–118, 2021.

[31] P. Chamnan and P. Wuttikonsammakit, "First trimester risk factors of pregnancy associated hypertension in Sanpasitthiprasong hospital," *Thai Journal of Obstetrics and Gynaecology*, vol. 26, no. 1, pp. 26–39, 2021.

[32] F. Bakouei, M. A. Delavar, S. Mashayekh-Amiri, S. Esmailzadeh, and Z. Taheri, "Efficacy of n-3 fatty acids supplementation on the prevention of pregnancy induced-hypertension or preeclampsia: a systematic review and meta-analysis," *Taiwanese Journal of Obstetrics and Gynecology*, vol. 59, no. 1, pp. 8–15, 2020.

[33] S. Lal, R. Sahai, A. Nidhi, and R. Ranjan, "Comparative study of oral nifedipine versus intravenous labetalol in severe hypertension in pregnancy: a randomized controlled study," *Indian Journal of Obstetrics and Gynecology Research*, vol. 7, no. 1, pp. 75–80, 2020.

[34] A. H. Affinati and R. J. Auchus, "Endocrine causes of hypertension in pregnancy," *Gland Surgery*, vol. 9, no. 1, pp. 69–79, 2020.

[35] P. Uwizeyimana, E. Musabyemariya, O. Tengera, and A. Collins, "Neonatal outcomes from mothers with hypertension disorders of pregnancy: a retrospective study at a referral hospital in Rwanda," *Rwanda Journal of Medicine and Health Sciences*, vol. 3, no. 2, pp. 193–203, 2020.

[36] Y. C. Houehanou, S. A. Amidou, D. Sonou et al., "Prevalence of hypertension during pregnancy in Benin: results from STEPS survey in 2015," *Journal of Epidemiology*, vol. 11, no. 3, pp. 284–292, 2021.

[37] F. Ramzan, S. Qadir, S. G. Zarin, F. Tahir, and S. Malik, "Role of labetalol in control of hypertension during pregnancy," *Pakistan Journal of Medical and Health Sciences*, vol. 15, no. 5, pp. 1061–1063, 2021.

[38] A. Sampaio, G. Norte, M. J. Campos, A. Raimundo, C. Carreira, and R. Órfão, "Anaesthetic management of

Hindawi
Computational and Mathematical Methods in Medicine
Volume 2023, Article ID 9843748, 1 page
https://doi.org/10.1155/2023/9843748

Retraction

Retracted: Relationship between Severity of Lumbar Spinal Stenosis and Ligamentum Flavum Hypertrophy and Serum Inflammatory Factors

Computational and Mathematical Methods in Medicine

Received 12 December 2023; Accepted 12 December 2023; Published 13 December 2023

This article has been retracted by Hindawi, as publisher, following an investigation undertaken by the publisher [1]. This investigation has uncovered evidence of systematic manipulation of the publication and peer-review process. We cannot, therefore, vouch for the reliability or integrity of this article.

Please note that this notice is intended solely to alert readers that the peer-review process of this article has been compromised.

Wiley and Hindawi regret that the usual quality checks did not identify these issues before publication and have since put additional measures in place to safeguard research integrity.

We wish to credit our Research Integrity and Research Publishing teams and anonymous and named external researchers and research integrity experts for contributing to this investigation.

The corresponding author, as the representative of all authors, has been given the opportunity to register their agreement or disagreement to this retraction. We have kept a record of any response received.

References

[1] N. He, W. Qi, Y. Zhao, and X. Wang, "Relationship between Severity of Lumbar Spinal Stenosis and Ligamentum Flavum Hypertrophy and Serum Inflammatory Factors," *Computational and Mathematical Methods in Medicine*, vol. 2022, Article ID 8799240, 7 pages, 2022.

Hindawi
Computational and Mathematical Methods in Medicine
Volume 2022, Article ID 8799240, 7 pages
https://doi.org/10.1155/2022/8799240

Research Article

Relationship between Severity of Lumbar Spinal Stenosis and Ligamentum Flavum Hypertrophy and Serum Inflammatory Factors

Nina He, Wenbin Qi, Yongli Zhao, and Xiaojun Wang

Department of Rehabilitation Physiotherapy, Shandong University Qilu Hospital (Qingdao), Qingdao, Shandong 266000, China

Correspondence should be addressed to Xiaojun Wang; wxj403498608@163.com

Received 27 July 2022; Revised 18 August 2022; Accepted 3 September 2022; Published 12 October 2022

Academic Editor: Min Tang

Objective. This study is aimed at investigating the correlation between lumbar spinal stenosis (LSS) severity, ligamentum flavum hypertrophy, and the upregulation of inflammatory markers. *Methods*. From March 2019 and May 2022, eighty-five inpatients with LSS were enlisted as the study's research group, while sixty-five patients hospitalized for lumbar intervertebral disc herniation over the same time period served as the study's control group. Moreover, mild, moderate, and severe subgroups of patients were created within the research population based on their LSS severity. The ligamentum flavum thickness and the positive expression rates of TNF-α, TGF-β1, and IL-1α were compared between the study group and the control group. The levels of TNF-α, TGF-β1, and IL-1α that were found to be positively expressed were compared between the mild, moderate, and severe groups. Patients with LSS had their ligamentum flavum thickness and their positive expression rates of TNF-α, TGF-β1, and IL-1α analyzed using Spearman correlation analysis. We evaluated the diagnostic utility of the positive expression rates of IL-α1, TGF-β1, and TNF-α and ligamentum flavum thickness in distinguishing the severity of LSS using a receiver operating characteristic (ROC) curve. *Results*. The rates of both lower limb pain (40.00%) and intermittent claudication (80.00%) in the LSS group were higher than those in the lumbar disc herniation group (15.38%, 12.31%), with statistical significance ($P < 0.05$). However, no substantial disparity was observed in left lower limb pain, right lower limb pain, low back pain, lower limb sensation, muscle strength, and reflex abnormalities between the two groups ($P > 0.05$). Positive expressions of TGF-β1, TNF-α, and IL-1α and thicker ligamentum flavum were more prevalent in the LSS group than in the lumbar intervertebral disc herniation group. All indexes were significantly ($P < 0.05$) higher in the moderate stenosis group than in the severe stenosis group. Additionally, the thickness of the ligamentum flavum and the positive expression rates of TNF-α, TGF-β1, and IL-1α were higher in the mild and moderate stenosis groups than in the severe stenosis group. The expression levels of TNF-α, TGF-β1, and IL-1α were favorably linked with ligamentum flavum thickness ($P < 0.05$). ROC curve analysis showed that the thickness of ligamentum flavum, the expression of IL-1α, the expression of TGF-β1, and the expression of TNF-α could effectively diagnose mild, moderate, and severe LSS ($P < 0.05$). *Conclusion*. Ligamentum flavum hypertrophy and positive expression rates of IL-1α, TGF-β1, and TNF-α are closely linked to LSS, which can effectively identify mild, moderate, and severe LSS.

1. Introduction

Lumbar spinal stenosis (LSS) can cause lumbago and leg pain or lower extremity motor dysfunction in middle-aged and elderly people. The pathogenesis is mainly intervertebral disc bulge, protrusion or degenerative calcification, vertebral joint hyperplasia and ossification, ligamentum flavum hypertrophy, and calcification, which can lead to stenosis of the spinal canal, lateral recess, nerve root canal, or foramina, thus causing a series of symptoms such as compression of cauda equina nerve, blood vessels, and nerve roots in the dural sac or inflammatory reactions [1, 2]. Anatomically, there are three distinct forms of LSS: lateral foraminal, recess, and central canal stenosis. Degeneration of the facet joints, ligamentum flavum and intervertebral disc are the primary anatomical factors in central stenosis. The

Table 1: Comparison of clinical symptoms and signs between the two groups [n (%)].

Group	Left lower extremity pain	Right lower extremity pain	Both lower extremity pain	Low back pain	Lower extremity sensation, muscle strength, and reflex abnormalities	Intermittent claudication
LSS group ($n = 85$)	24 (28.24)	27 (31.76)	34 (40.00)	68 (80.00)	78 (91.76)	68 (80.00)
Lumbar disc herniation group ($n = 65$)	23 (35.38)	23 (35.38)	10 (15.38)	55 (84.62)	62 (95.38)	8 (12.31)
χ^2 value	0.875	0.217	10.767	0.532	0.776	67.524
P value	0.350	0.641	0.001	0.466	0.378	<0.001

degeneration of the intervertebral disc often has a high degree of loss, and the hypertrophic ligamentum flavum can form space behind both sides of the spinal canal, further aggravating the central stenosis [3–5]. Lateral recess stenosis is mostly caused by the proliferation of osteophytes on the medial side of the superior articular process, which is related to disc herniation and inflammatory response of the articular process. Foraminal stenosis is caused by osteophytes above the articular process and is associated with disc degeneration. Various inflammatory factors and increased load stress can lead to ligamentum flavum injury, and the repair process is accompanied by ligament fibrosis and collagen fiber hyperplasia, resulting in ligamentum flavum hypertrophy [6–8]. The goal of this research was to examine the connection between degenerative hypertrophy of the ligamentum flavum and the development of LSS and an inflammatory response, so as to further improve the prevention, diagnosis, and treatment of LSS and provide theoretical support for clinical treatment of LSS.

2. Materials and Methods

2.1. General Information. The selection included 85 LSS patients who received care at our facility between March 2019 and May 2022, and 65 patients with lumbar intervertebral disc herniation who were hospitalized during the same period were selected. There were 51 men and 34 females in the LSS group, with ages ranging from 40 to 75 (56.96 ± 7.05 years) and disease durations averaging 29.22 $\pm$ 9.46 months (range = 10 to 55). There were 40 men and 25 females in the lumbar disc herniation cohort; the age range was from 42 to 72 years old, with a mean age of 55.97 ± 7.38 years; the duration of disease was from 6 to 45 months, with a mean of 30.74 ± 8.01 months. Overall, there was comparable difference between the two groups' data ($P > 0.05$). Eventually, MRI and CT scans were performed on every patient. Patients with LSS were categorized into those with mild stenosis (23 cases), moderate stenosis (45 cases), and severe stenosis (17 cases), depending on the number of stenotic segments in their arteries. The hospital's ethics board gave its stamp of approval to this research. Inclusion criteria include ① patients diagnosed with LSS or lumbar disc herniation by imaging examination, ② central stenosis, ③ complete lumbar spine imaging data, and ④ all patients who voluntarily participated in this study. Exclusion criteria include ① those who have suffered a spinal fracture or spinal cord damage, ② patients with developmental lumbar spinal stenosis, ③ patients complicated with spinal tumor, spinal deformity, and other spinal diseases, ④ patients with osteoarticular tuberculosis, osteomyelitis, and severe senile osteoporosis, and ⑤ patients with severe organ dysfunction.

2.2. Methods. ① Thickness measurement of ligamentum flavum: all patients underwent CT scanning at different lesion segments (L3/L4, L4/L5, and L5/S1). The oblique diameter of the spinal canal was measured and compared to the thickness of the ligamentum flavum of both joint capsules to determine the disc height ratio at the superior vertebral arch notch. ② Lamina ligamentum flavum was removed during posterior spinal canal and lateral recess decompression, rinsed in 0.9% sodium chloride solution, fixed in 4.0% paraformaldehyde, embedded in paraffin, and cut into 5-8 pieces for immunohistochemistry staining. Immunohistochemical staining sections of transforming growth factor- (TGF-) β1, tumor necrosis factor- (TNF-) α, and interleukin- (IL-) 1α in the two groups were observed with Olympus light microscope (Japan) by two-person double-blind method. The sections of each group were placed under the same intensity light, and 5 visual fields were randomly selected from each section under a high-power microscope (×40). Judgment of immunohistochemical results: if there were brown or dark brown particles in the cytoplasm or membrane of the ligamentum flavum tissue and the staining intensity was higher than the background nonspecific staining, the cells were considered positive. If the nucleus was stained blue and there was no brown-yellow reactant in the membrane or cytoplasm, the cells were considered negative. Five complete and nonoverlapping high magnification fields were selected at the tissue edge of ligamentum flavum in each section, and the expression rate of positive cells in each field was measured. The average expression rate of 5 fields was taken as the final measurement value. Positive cell expression rate: 0 indicates no expression (-); <25% indicates slight expression (+); ≥25% indicates obvious expression (++). The expression degree and positive expression rate of three inflammatory factors including TGF-β1, TNF-α, and IL-1α in the ligamentum flavum of the two groups were compared.

Table 2: Comparison of ligamentum flavum thickness and TGF-β1, TNF-α, and IL-1α positive expression rate between the two groups ($\bar{x} \pm s$).

Group	Ligamentum flavum thickness (mm)	IL-1α (%)	TGF-β1 (%)	TNF-α (%)
LSS group ($n = 85$)	5.55 ± 1.51	90.66 ± 8.31	75.14 ± 9.03	45.37 ± 7.15
Lumbar disc herniation group ($n = 65$)	2.51 ± 0.70	12.97 ± 3.78	46.20 ± 6.02	8.53 ± 3.03
t value	16.408	76.528	23.488	42.776
P value	<0.001	<0.001	<0.001	<0.001

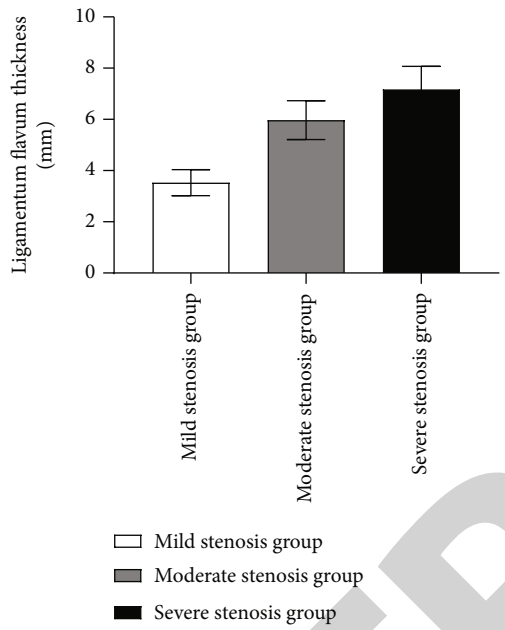

Figure 1: Comparison of ligamentum flavum thickness among three subgroups.

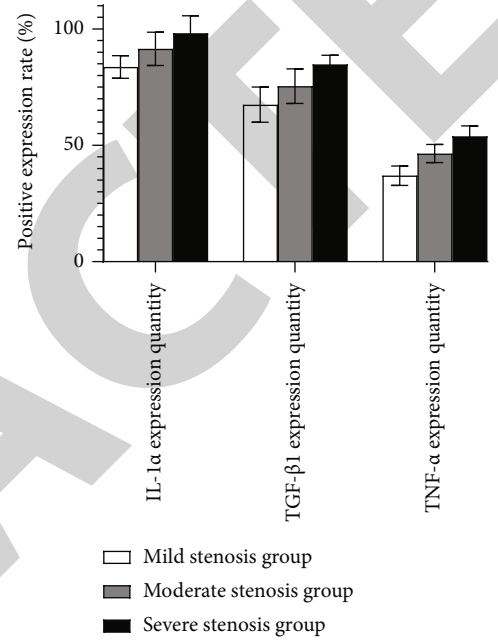

Figure 2: Comparison of positive expression rates of TNF-α, TGF-β1, and IL-1α among three subgroups.

2.3. Observation Indicators. The indicators are as follows: ① comparison of ligamentum flavum thickness and expression quantity of TGF-β1, TNF-α, and IL-1α between the LSS group and the lumbar disc herniation group; ② comparison of ligamentum flavum thickness and expression quantity of TGF-β1, TNF-α, and IL-1α in mild, moderate, and severe stenosis groups; ③ correlation analysis between the severity of LSS and the expression quantity of TGF-β1, TNF-α, and IL-1α and the ligamentum flavum thickness; ④ the ROC curve analysis of TGF-β1, TNF-α, and IL-1α and ligamentum flavum thickness in differentiating the severity of LSS.

2.4. Statistical Methods. Data for this study were entered into an Excel spreadsheet by two researchers working independently of one another and then analyzed and processed using SPSS 24.0. In this study, we used a mean ± SD ($x \pm s$) format for our measurement data. When the data follows a normal distribution with consistent variance, the t-test is used. n and % were utilized to characterize the count data, and the chi-square test was performed to compare the two groups. All were two-sided tests. The relationship between the thickness of the ligamentum flavum and the levels of TGF-β1, TNF-α, and IL-1α in individuals with LSS was examined using Spearman correlation analysis. $P < 0.05$ was regarded as a statistically significant difference when analyzing the diagnostic value of ligamentum flavum thickness and the positive expression rates of TGF-β1, TNF-α, and IL-1α in determining the degree of LSS using the receiver operating characteristic (ROC) curve.

3. Results

3.1. The Signs and Clinical Symptom Comparison between the Two Groups. Both lower extremity pain (40.00%) and intermittent claudication (80.00%) were more prevalent in the LSS group than in the lumbar disc herniation group, with a statistically significant difference ($P < 0.05$) between the two groups. Left lower extremity pain, right lower extremity pain, low back pain, lower extremity sensation, muscle strength, and reflex abnormalities were all similar across the two groups ($P > 0.05$). See Table 1.

3.2. Comparison of Ligamentum Flavum Thickness and Positive Expression Rates of TGF-β1, TNF-α, and IL-1α between the Two Groups. The ligamentum flavum thickness in the LSS group was greater than that in the lumbar

Table 3: Comparison of ligamentum flavum thickness and positive expression rates of TNF-α, TGF-β1, and IL-1α among three subgroups ($\bar{x} \pm s$).

Group	Ligamentum flavum thickness (mm)	IL-1α (%)	TGF-β1 (%)	TNF-α (%)
Mild stenosis group ($n = 23$)	3.53 ± 0.51	83.63 ± 4.87	67.45 ± 7.54	36.95 ± 4.19
Moderate stenosis group ($n = 45$)	5.97 ± 0.76^{a}	91.43 ± 7.16^{a}	75.42 ± 7.41^{a}	46.47 ± 3.91^{a}
Severe stenosis group ($n = 17$)	7.17 ± 0.90^{ab}	98.13 ± 7.53^{ab}	84.77 ± 3.96^{ab}	53.85 ± 4.49^{ab}
F value	135.287	23.500	30.770	86.277
P value	<0.001	<0.001	<0.001	<0.001

Note: $^{a}P < 0.05$ when compared with the mild stenosis group; $^{b}P < 0.05$ when compared with the moderate stenosis group.

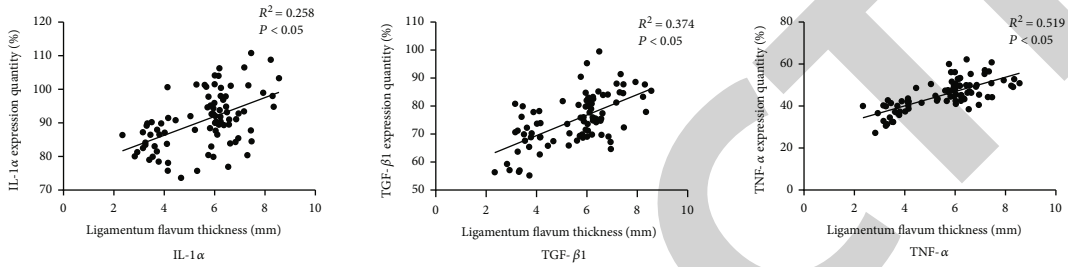

Figure 3: Correlation between ligamentum flavum thickness and expression quantity of IL-1α, TGF-β1, and TNF-α.

Table 4: ROC curve analysis of expression quantity of IL-1α, TGF-β1, and TNF-α and ligamentum flavum thickness in differentiating mild to moderate LSS.

	AUC	P value	Cut-off value	95% CI
Ligamentum flavum thickness	0.986	<0.001	4.67	0.968-1.000
IL-1α expression quantity	0.825	<0.001	89.18	0.729-0.921
TGF-β1expression quantity	0.765	<0.001	73.93	0.646-0.884
TNF-α expression quantity	0.976	<0.001	42.14	0.947-1.000

Table 5: ROC curve analysis of expression quantity of IL-1α, TGF-β1, and TNF-α and ligamentum flavum thickness in differentiating moderate to severe LSS.

	AUC	P value	Cut-off value	95% CI
Ligamentum flavum thickness	0.835	<0.001	6.62	0.716-0.955
IL-1α expression quantity	0.742	0.003	94.66	0.598-0.887
TGF-β1 expression quantity	0.890	<0.001	80.89	0.809-0.971
TNF-α expression quantity	0.891	<0.001	50.55	0.807-0.975

intervertebral disc herniation group. There was a statistically significant ($P < 0.05$) increase in the TGF-β1, TNF-α, and IL-1α positive expression when compared to the group with lumbar intervertebral disc herniation (Table 2).

3.3. Comparison of Ligamentum Flavum Thickness and TGF-β1, TNF-α, and IL-1α Positive Expression Rate among Three Subgroups. There were significant differences in the ligamentum flavum thickness and the TGF-β1, TNF-α, and IL-1α positive expression among the three subgroups ($P < 0.05$). There were statistically significant ($P < 0.05$) increases in ligamentum flavum thickness, TGF-β1, TNF-α, and IL-1α positive expression, and each index in the moderate stenosis group compared to the severe stenosis group, as shown in Figures 1 and 2 and Table 3.

3.4. Correlation Analysis between Ligamentum Flavum Thickness and TGF-β1, TNF-α, and IL-1α Expression. The ligamentum flavum thickness was positively correlated with the expressions of IL-1α, TGF-β1, and TNF-α ($P < 0.05$). See Figure 3.

3.5. ROC Curve Analysis of Expression Quantity of TNF-α, TGF-β1, and IL-1α and Ligamentum Flavum Thickness in Differentiating the Severity of LSS. ROC curve analysis showed that the ligamentum flavum thickness and TGF-

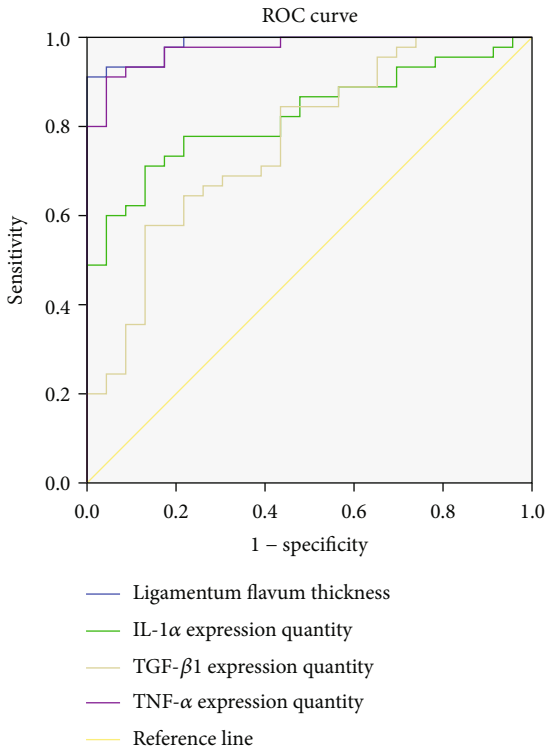

Figure 4: ROC curve analysis of IL-1α, TGF-β1, and TNF-α expression quantity and ligamentum flavum thickness in differentiating mild to moderate LSS.

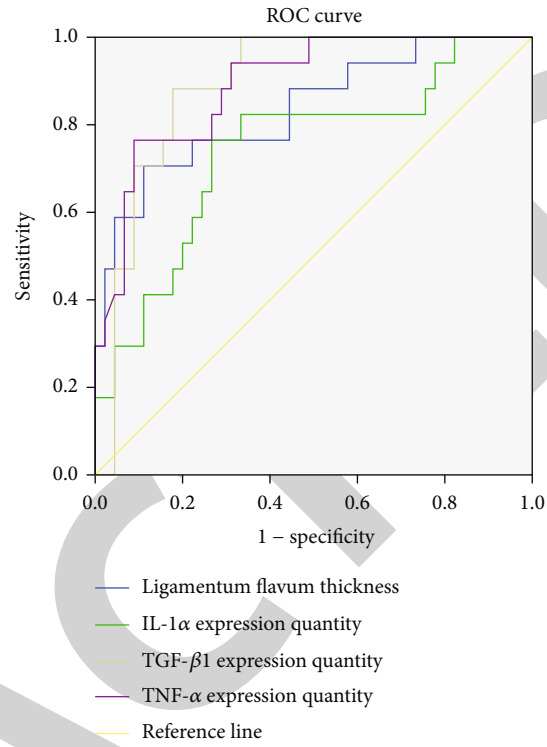

Figure 5: ROC curve analysis of IL-1α, TGF-β1, and TNF-α expression quantity and ligamentum flavum thickness in differentiating moderate to severe LSS.

β1, TNF-α, and IL-1α expression could effectively diagnose mild, moderate, and severe LSS ($P < 0.05$). The AUC values of ligamentum flavum thickness and expression quantity of TNF-α, TGF-β1, and IL-1α in the identification of mild to moderate LSS were 0.986, 0.825, 0.765, and 0.976, respectively, and the cut-off values were 4.67, 89.18, 73.93, and 42.14, respectively. The AUC values of ligamentum flavum thickness and expression quantity of TNF-α, TGF-β1, and IL-1α in the identification of moderate to severe LSS were 0.835, 0.742, 0.890, and 0.891, and the cut-off values were 6.62, 94.66, 80.89, and 50.55, respectively. See Tables 4 and Tables 5 and Figures 4 and 5.

4. Discussion

Hypertrophy and ligamentum flavum hypertrophy may cause a narrowing of the spinal canal (coronal diameter), as well as hyperplasia and cohesiveness of the bilateral facet joints and the superior facet joints, all of which increase the chances of LSS [9–11]. Patients with mild LSS should be treated with rest, drugs, and relevant symptomatic treatment. Patients with severe LSS accompanied by intractable pain and ineffective nonsurgical treatment should be treated with surgery. The degenerated and herniated intervertebral discs and facet joints act on the ligamentum flavum by releasing inflammatory factors, causing ligamentum flavum hypertrophy [12, 13]. IL-1α can promote the formation of inflammation and cause pain. IL-1α is a predisposed factor for the thickening and ossification of ligamentum flavum, which can affect ligamentum flavum by stimulating nerves, degrading collagen, and mediating cycloxygenase-2 metalloproteinase inhibitors. The positive expression rate of IL-1α in the LSS group was substantially greater than that in the control group in this research, which may be related to chronic mechanical effects and increased pain in patients with LSS, and pain is caused by stimulation of nerve fibers. The ligamentum flavum was thicker and fibrotic in the LSS group, with fibroblasts serving as the predominant cell type, so the positive expression of IL-1α was increased. According to relevant studies, IL-1α is highly expressed in the intervertebral disc and lumbar facet joint and patients with lumbar stenosis tend to have a more active ligamentum flavum, and this activity is positively connected with lumbar region and leg pain [14, 15]. Hypertrophy of the ligamentum flavum in the lumbar spine causes a loss of elasticity and an increase in collagen fibers [16, 17]. It has been suggested that TGF-β1 is closely related to fibroblast proliferation [18, 19]. TGF-β1 can change the growth characteristics of fibrocytes and reduce the contact inhibition effect in the process of fibrocyte growth. It can not only promote cell proliferation but also promote the synthesis of extracellular matrix. Since TGF-β1 can cause a variety of tissue hypertrophy, which is closely related to a variety of fibrotic diseases, the mechanism of TGF-β1 promoting ligament flavum hypertrophy lies in inducing fibroblast differentiation into myofibroblasts, which can promote the fibrosis of ligament flavum tissue by

promoting the production of type I and III collagen [20]. Therefore, the main role of TGF-β1 in inducing ligamentum flavum hypertrophy is to promote the proliferation and differentiation of fibroblasts and the formation of collagen fibers. TNF-α mainly affects the metabolism of collagen fibers in the ligamentum flavum matrix. TNF-α is an inflammatory factor secreted by macrophages, which is an initiating factor of inflammatory cascade reaction and can reflect the severity of inflammation [21, 22]. According to relevant studies, TNF-α content is closely related to the effect of macrophage migration inhibitory factor (MIF), which is an upstream factor of TNF-α and can promote the expression of TNF-α in fibroblasts and stroma. In addition, MIF can indirectly promote the expression of TNF-α by inhibiting the migration of macrophages [23, 24]. In addition, ligamentum flavum hypertrophy may be caused by TNF-α due to its ability to stimulate the production of downstream metalloproteinases through positive feedback. Ligamentum flavum has both type I and type III collagen fibers. Hypertrophy of the ligamentum flavum is associated with TNF-α because TNF-α may increase the production of type III collagen.

In this study, in patients with LSS, the ligamentum flavum was thicker than in those with lumbar disc herniation, and the LSS group also had higher levels of TGF-β1, TNF-α, and IL-1α positive expression. Each indicator was greater in the moderate stenosis group than the severe stenosis group, and the differences between the groups were statistically significant ($P < 0.05$). Positive expression rates of TNF-α, TGF-β1, and IL-1α increased with increasing stenosis severity, and the findings demonstrated that these cytokines were strongly expressed in the LSS group. The degree of LSS was correlated with an increase in ligamentum flavum thickness, which was considerably greater in the LSS group than in the lumbar disc herniation group. Clinical studies have shown that corticosteroids and nonsteroidal analgesic and anti-inflammatory drug COX-2 inhibitors can relieve clinical symptoms by inhibiting inflammatory response, and patients with LSS often have ligamentum flavum hypertrophy. In this work, we found that LSS was closely linked with the TGF-β1, TNF-α, and IL-1α positive expression rate as assessed by Spearman's correlation analysis ($P < 0.05$). Previous research has shown that TNF-α and IL-1α are both substantially expressed in the intervertebral discs, lumbar facet joints, and ligamentum flavum of individuals with LSS and that this expression is connected with neurological dysfunction and lumbar and leg pain [25, 26]. IL-1α can enhance the synthesis of pain mediators prostaglandin and 5-hydroxytryptamine. Prostaglandin E2 is an important transmitter of inflammatory response, which can enhance the sensitivity of nerve terminal receptors, thus enhancing the pain effect. IL-1α induces nerve root pain through mediating other inflammatory mediators, eventually leading to lumbar and leg pain. TNF-α can induce inflammatory reactions such as endoneurial edema, decreased blood flow, intravascular coagulation, and medulla decomposition, which can play a role in the regulation of nerve root sensitivity and cause lumbar and leg pain. Lumbar and leg pain is the main symptom of LSS, which can also explain that the expression of inflammatory factors increases with the degree of LSS.

ROC curve analysis results of this study showed that the thickness of ligamentum flavum and the expression quantity of TNF-α, TGF-β1, and IL-1α could effectively diagnose mild, moderate, and severe LSS ($P < 0.05$). The AUC values of ligamentum flavum thickness and expression quantity of TNF-α, TGF-β1, and IL-1α in identifying mild to moderate LSS were 0.986, 0.825, 0.765, and 0.976, respectively, and the cut-off values were 4.67, 89.18, 73.93, and 42.14, respectively. The AUC values of ligamentum flavum thickness and expression quantity of IL-1α, TGF-β1, and TNF-α in identifying moderate to severe LSS were 0.835, 0.742, 0.890, and 0.891, respectively, and the cut-off values were 6.62, 94.66, 80.89, and 50.55, respectively. For patients with mild LSS, rest, medication, and relevant symptomatic treatment are required, while surgery may be required for patients with moderate and severe LSS. Early identification of patients after admission is beneficial to quickly determine the treatment plan, and appropriate treatment plan can promote the rational utilization of medical resources and improve the prognosis of patients, suggesting that the thickness of ligamentum flavum can be measured in patients with LSS after admission. In this study, the TGF-β1, TNF-α, and IL-1α positive expression rate was determined by postoperative immunohistochemistry, which can reveal the expression patterns of inflammatory factors in patients with LSS.

In conclusion, the severity of LSS is closely correlated with ligamentum flavum hypertrophy and the expression quantity of TNF-α, TGF-β1, and IL-1α. Ligamentum flavum hypertrophy and the TGF-β1, TNF-α, and IL-1α positive expression rate can effectively distinguish the LSS severity.

Data Availability

The labeled dataset used to support the findings of this study is available from the corresponding author upon request.

Conflicts of Interest

The authors declare no competing interests.

References

[1] M. Arabmotlagh, R. M. Sellei, J. M. Vinas-Rios, and M. Rauschmann, "Klassifikation und diagnostik der lumbalen spinalkanalstenose," *Der Orthopäde*, vol. 48, no. 10, pp. 816–823, 2019.

[2] M. K. L. Lai, P. W. H. Cheung, and J. P. Y. Cheung, "A systematic review of developmental lumbar spinal stenosis," *European Spine Journal*, vol. 29, no. 9, pp. 2173–2187, 2020.

[3] Y. Liu, Y. Qi, D. M. Diaty et al., "Retraction note: Treatment for lumbar spinal stenosis secondary to ligamentum flavum hypertrophy using percutaneous endoscopy through interlaminar approach: a retrospective study," *Journal of Orthopaedic Surgery and Research*, vol. 16, no. 1, p. 443, 2021.

[4] H. Takeda, S. Nagai, D. Ikeda, S. Kaneko, T. Tsuji, and N. Fujita, "Collagen profiling of ligamentum flavum in patients with lumbar spinal canal stenosis," *Journal of Orthopaedic Science*, vol. 26, no. 4, pp. 560–565, 2021.

[5] T. Yamada, M. Horikawa, T. Sato et al., "Hypertrophy of the ligamentum flavum in lumbar spinal canal stenosis is

Hindawi
Computational and Mathematical Methods in Medicine
Volume 2023, Article ID 9832018, 1 page
https://doi.org/10.1155/2023/9832018

Retraction

Retracted: Efficacy of Xiyanping in the Treatment of Elderly Patients with Chronic Obstructive Pulmonary Disease and Its Effect on the Expression of GDF-15 and HIF-1α in Serum

Computational and Mathematical Methods in Medicine

Received 12 December 2023; Accepted 12 December 2023; Published 13 December 2023

This article has been retracted by Hindawi, as publisher, following an investigation undertaken by the publisher [1]. This investigation has uncovered evidence of systematic manipulation of the publication and peer-review process. We cannot, therefore, vouch for the reliability or integrity of this article.

Please note that this notice is intended solely to alert readers that the peer-review process of this article has been compromised.

Wiley and Hindawi regret that the usual quality checks did not identify these issues before publication and have since put additional measures in place to safeguard research integrity.

We wish to credit our Research Integrity and Research Publishing teams and anonymous and named external researchers and research integrity experts for contributing to this investigation.

The corresponding author, as the representative of all authors, has been given the opportunity to register their agreement or disagreement to this retraction. We have kept a record of any response received.

References

[1] J. X. Wang, Y. Zhang, S. F. Wang, J. Li, and P. C. Li, "Efficacy of Xiyanping in the Treatment of Elderly Patients with Chronic Obstructive Pulmonary Disease and Its Effect on the Expression of GDF-15 and HIF-1α in Serum," *Computational and Mathematical Methods in Medicine*, vol. 2022, Article ID 6193110, 8 pages, 2022.

Hindawi
Computational and Mathematical Methods in Medicine
Volume 2022, Article ID 6193110, 8 pages
https://doi.org/10.1155/2022/6193110

Research Article

Efficacy of Xiyanping in the Treatment of Elderly Patients with Chronic Obstructive Pulmonary Disease and Its Effect on the Expression of GDF-15 and HIF-1α in Serum

Jun Xia Wang,[1] Ying Zhang ,[2] Shu Fang Wang,[3] Juan Li,[4] and Peng Cheng Li[3]

[1]*Pharmacy Department of Shijiazhuang Eighth Hospital, China*
[2]*Department of Anesthesiology, Shijiazhuang Eighth Hospital, China*
[3]*Department of Internal Medicine of Tang County Hospital of Traditional Chinese Medicine, China*
[4]*Department of Internal Medicine, Langfang Hospital of Traditional Chinese Medicine, China*

Correspondence should be addressed to Ying Zhang; zy15303119869@163.com

Received 15 August 2022; Revised 24 August 2022; Accepted 17 September 2022; Published 12 October 2022

Academic Editor: Min Tang

Background. COPD is a chronic respiratory disease with a long course and recurrent characteristics. According to relevant statistics, the global incidence of COPD is more than 30%, which seriously affects the life of patients and endangers their health. *Objective*. To observe the curative effect of Xiyanping in elderly patients with COPD and its influence on the expressions of growth differentiation GDF-15 and HIF-1α in serum. *Methods*. From August 2019 to December 2021, 86 elderly patients with acute exacerbation of COPD were admitted to our hospital. As the research objects, they were divided into the control group ($n = 43$) and the observation group ($n = 43$) randomly. The control group received the conventional treatment, while the observation group got Xiyanping on the basis of the control group. The differences in the duration of antibiotic use, expectoration, hospital stays, adverse reactions and serum-related factors, blood routine, pulmonary function, airway hyperreactivity index, COPD assessment test (CAT) score, and Borg score were made a comparison between them. *Results*. On the 3rd and 7th days after being treated, the sputum excretion in them was higher than before, but on the 3rd day of treatment, the sputum excretion in the observation group was higher than that in the control group, while on the 7th day of treatment, the sputum excretion was lower than that in the control group with statistically significant differences ($P < 0.05$). Before treatment, the serum-related factors and blood routine indexes between them were similar ($P > 0.05$). After treatment, GDF-15, HIF-1α, CXCL12, TNF-α, IL-8, TGF-β, WBC, and NEU in them were significantly lower than before, and the values in the observation group were significantly lower than those in the control group with statistically significant differences ($P < 0.05$). There was no difference in the related indexes of pulmonary function and airway hyperreactivity between them before treatment. After being treated, FEV1, FVC, and FEV1/FVC in them were significantly higher than those before treatment. The airway resistance and lung compliance of the two groups at exhalation and inspiration were significantly lower than before, and the values in the observation group were significantly lower than those in the control group ($P < 0.05$). There was no difference in CAT and Borg scores between them before treatment. After treatment, the CAT score and Borg score of these patients were significantly lower than those before treatment, and the value of the observation group was significantly lower than that of the control group ($P < 0.05$). The duration of antibiotic use and length of stay in the observation group were significantly shorter than those of the control group, while the incidence of adverse reactions was not statistically significantly different compared with the control group ($P > 0.05$). *Conclusion*. Xiyanping can improve pulmonary function of elderly patients with acute exacerbation of COPD, reduce the response of airway hyperreactivity, and promote the excretion of sputum.

1. Introduction

Chronic obstructive pulmonary disease (COPD) in the elderly is a common clinical respiratory disease, featured by incompletely reversible airflow limitation, and the disease develops in a progressive way [1]. As a risk factor for acute exacerbation of COPD, infection can aggravate cough, increase sputum volume, and result in dyspnea [2, 3]. Infection control is a key measure in the treatment of acute exacerbation of elderly COPD. At present, antibiotics are generally used in clinical treatment, but the long-term application of antibiotics can cause drug-resistant strains, leading to flora imbalance and fungal infection [4].

According to the theory of traditional Chinese medicine, COPD belongs to "lung distension," "asthmatic cough," and phlegm blockages in lung collateral, accompanied by exogenous pathogenic qi, causing the stasis of heat-phlegm [4]. Xiyanping is a traditional Chinese medicine injection extracted and refined from Andrographis paniculata with antibacterial, antiviral, and other pharmacological effects, and it is widely used in infectious diseases such as bronchitis, tonsillitis, and bacterial diseases [5]. However, the studies on the efficacy of Xiyanping in COPD were few. The study is aimed at observing the influence of Xiyanping in elderly patients with COPD and its effect on the expression of GDF-15 and HIF-1α in serum. The report is as follows.

1.1. Core Tips. In this study, we found that Xiyanping could improve the pulmonary function of elderly patients with acute exacerbation of COPD, reduce the response of airway hyperreactivity, and promote the excretion of sputum, which might be related to the regulation of GDF-15 and HIF-1α-related factors.

2. Data and Methods

2.1. General Information. This study has been approved by the ethics committee. Diagnostic criteria in line with the standard of Chronic Obstructive Pulmonary Disease Diagnosis and Treatment Guidelines (2013 revision) [6] include (1) patients with COPD clinical symptoms, (2) patients who have a contact history of risk factors (including environmental factors and host factors), (3) FEV1/FVC that achieved 60%–80% after using a bronchodilator, and (4) chest X-ray/CT examination that showed increased lung texture, increased chest diameter, and increased lung field transparency.

Acute exacerbation of COPD was in line with the standard of AECOPD Diagnosis and Treatment of Chinese Expert Consensus (2017 update) [7]: (1) continuous deterioration of respiratory symptoms and (2) it is necessary to change the drug treatment plan.

2.2. Case Selection. Inclusion criteria include (1) meeting the criteria for acute exacerbation of COPD, (2) ages from 60 to 85 years without gender restriction, (3) excluding the related symptoms caused by tuberculosis and bronchiectasis, (4) patients and their families who agreed to join this study, and (5) complete clinical data.

Exclusion criteria include (1) in situ or metastatic lung cancer; (2) with previous history of pulmonary resection; (3) patients with defects in immune function; (4) bedridden or mobility-impaired patients; (5) patients with severe heart, liver, or kidney dysfunction; and (6) mental diseases.

2.3. Collection of Cases. From August 2019 to December 2021, 86 elderly patients with acute exacerbation of COPD admitted to our hospital were confirmed with the inclusion and exclusion criteria and were selected as the research subjects. As the research objects, they were divided into the control group ($n = 43$) and the observation group ($n = 43$) randomly. After the statistical test, it was found that the general information of them was balanced.

2.4. Method. The control group was given conventional treatment, including oxygen therapy, ambroxol phlegm, β2 receptor agonist bronchodilator, inhaled corticosteroids anti-inflammatory, broad-spectrum antibiotics, and other comprehensive treatment.

Based on the control group, the observation group was treated with Xiyanping injection (produced by China Jiangxi Qingfeng Pharmaceutical Co., Ltd., specification: 5 mL: 125 mg, SEDA approval number Z20026249). A total of 250 mg Xiyanping was added into 0.9% sodium chloride injection 250 mL for intravenous drip, one time per day. The two groups were evaluated after 14 days of treatment.

2.5. Detection Method. Before and after treatment, 10 mL of fasting venous blood samples was taken from patients with an empty stomach and divided into two vacuum blood vessels. One was detected by the Shenzhen Mairui five classification blood cell analyzer to test the blood routine for recording the levels of white blood cell count (WBC) and neutrophil ratio (NEU). The other one was centrifuged within 1 hour after blood collection with the rotating speed of 3500 r/min for 10 minutes. The serum was taken to detect GDF-15, HIF-1α, CXCL12, TNF-α, IL-8, and TGF-β by ELISA. The kits were all products of Shanghai Enzyme-Linked Biotechnology Co., Ltd., and the instrument was the Shenzhen Mairui RT-96A microplate reader.

Before and after treatment, CHEST GRAPHHI-10 Jester pulmonary function instrument was used to detect forced expiratory volume in the first second (FEV1) and forced vital capacity (FVC) and calculate FEV1/FVC in them. The BUXCO FinePointe RC lung compliance measurement system was used to detect airway resistance and lung compliance during exhalation and inspiration of airway hyperreactivity-related indexes in two groups.

2.6. Scoring Standard. Chronic obstructive pulmonary assessment test (CAT) score [8]: the evaluation is mainly aimed at the influence of patients' health and daily life with a total of eight items for the range from 0 to 40. The high or low score indicated that the influence of disease on health and daily life was large or small.

Borg score [9]: the degree of dyspnea was mainly evaluated, including blood oxygen saturation, heart rate, blood pressure, and respiratory frequency from the range of 0 to 10. The scores indicated the degree of dyspnea.

2.7. Statistical Method. Professional SPSS19.0 software was used for data processing; GDF-15, HIF-1α, lung function indicators, and other data which were in accordance with normal distribution should be described by $\bar{\chi} \pm s$; the t-test was used for comparison, count data was described by n (%), and the χ^2 test was used for comparison, with statistical significance ($P < 0.05$).

3. Results

3.1. Differences in General Data between Two Groups. The process of the disease, the severity of illness, complications and smoking, age, and other general information were compared between the two groups, and there was no statistical difference ($P > 0.05$) (see Table 1).

3.2. Comparison of Sputum Excretion between Two Groups. There was nothing different in sputum excretion between them before treatment. On the 3rd and 7th days after being treated, the sputum excretion in them was higher than before, but on the 3rd day of treatment, the sputum excretion in the observation group was higher than that in the control group, while on the 7th day of treatment, the sputum excretion was lower than that in the control group with a statistically significant difference ($P < 0.05$) (see Table 2 and Figure 1).

3.3. Difference in Serum-Related Factors such as GDF-15 and HIF-1α between Two Groups. There was no difference in serum-related factors such as GDF-15 and HIF-1α between them before treatment. After treatment, GDF-15, HIF-1α, CXCL12, TNF-α, IL-8, and TGF-β in them were significantly lower than before, and the values in the observation group were significantly lower than those in the control group with a statistically significant difference ($P < 0.05$) (see Table 3).

3.4. Difference in Blood Routine Indexes between Two Groups. There was nothing different in blood routine indexes between them before treatment. After treatment, WBC and NEU in them were significantly lower than before, and values in the observation group were significantly lower than those in the control group (see Table 4).

3.5. Difference in Pulmonary Function Indexes between Two Groups. There was nothing different in pulmonary function indexes between them before treatment. After treatment, FEV1, FVC, and FEV1/FVC in them were significantly higher than before, and the values in the observation group were significantly higher than those in the control group with statistically significant differences ($P < 0.05$) (see Table 5).

3.6. Differences in Airway Hyperreactivity Indicators between the Two Groups. There was nothing different in the related indexes of airway hyperreactivity between them before treatment. After being treated, airway resistance and lung compliance of them at exhalation and inspiration were significantly lower than before, and the values in the observation group were significantly lower than those in the control group with a statistically significant difference ($P < 0.05$) (see Table 6).

3.7. Differences in CAT and Borg Scores between the Two Groups. There was nothing different in the CAT score and Borg score between them before treatment. After being treated, the CAT score and Borg score of them were significantly lower than before, and the value of the observation group was significantly lower than that of the control group with a statistically significant difference ($P < 0.05$) (see Table 7).

3.8. Differences in Duration of Antibiotic Use, Hospital Stays, and Adverse Reactions between the Two Groups. The duration of antibiotic use and hospital stays in the observation group were significantly shorter than those of the control group, while compared with the control group, there were no significant differences in the incidence of adverse reactions ($P > 0.05$) (see Table 8).

4. Discussion

An epidemiological survey shows that COPD ranks the sixth leading reason for death among the world's population and ranks 3rd among the causes of death from diseases in China. At present, there are about 100 million COPD patients in China, including about 30 million patients over 60 years old [10]. When they suffered from cold, infection, and inhalation of harmful gases, the symptoms would aggravate. In severe cases, respiratory failure and even death can occur [11]. At present, the routine treatment of western medicine for acute exacerbation of COPD can alleviate the clinical symptoms to some extent. However, the drug resistance of antibiotics makes the lower respiratory tract infection of a considerable number of patients unable to be effectively controlled; thus, it is difficult to achieve the ideal therapeutic effect [12].

According to the theory of traditional Chinese medicine, pathogenic qi which causes diseases invades the lung. The improper treatment leads to retention of pathogenic qi, and accumulation of phlegm and blood stasis damages healthy qi. Once the body is attacked by pathogenic qi, the sputum and blood stasis in the body will be invoked to aggravate cough and asthma. The therapeutic doctrine is heat-clearing and detoxifying, resolving phlegm, and relieving cough [13]. Xiyanping is a traditional Chinese medicine injection, and its active component is andrographolide sulfonate which was prepared by sulfonation of the extract from Andrographis paniculata leaves. The in vitro antibacterial experiments showed that it had obvious inhibitory effects on adenovirus, influenza virus, respiratory syncytial virus, and pathogenic microorganisms such as Staphylococcus aureus, Streptococcus, pneumococcal bacteria, and Escherichia coli. It is currently widely used in the treatment of respiratory and intestinal infectious diseases [14, 15].

In this study, it was found that the sputum excretion of the patients treated with Xiyanping adjuvant therapy was higher than that of the patients with conventional treatment 3 days later, while on the 7th day of treatment, the sputum

Table 1: Differences in general information between the two groups.

Normal information	Control group ($n = 43$)	Observation group ($n = 43$)	χ^2 or t	P
Gender (n (%))			0.191	0.662
Male	24 (55.81)	26 (60.47)		
Female	19 (44.19)	17 (39.53)		
Age ($\bar{\chi} \pm s$)	68.96 ± 5.77	69.21 ± 5.23	0.211	0.834
BMI ($\bar{\chi} \pm s$) (kg/m^2)	22.33 ± 2.16	21.98 ± 2.24	0.738	0.463
Severity of illness (n (%))			0.508	0.476
Moderate	32 (74.42)	29 (67.44)		
Severe	11 (25.58)	14 (32.56)		
COPD course of disease ($\bar{\chi} \pm s$) (year)	10.25 ± 3.11	10.08 ± 2.98	0.259	0.796
Smoking status (n (%))			0.426	0.808
None	24 (55.81)	21 (48.84)		
Quit smoking	8 (18.60)	9 (20.93)		
Smoking	11 (25.58)	13 (30.23)		
Concomitant disease (n (%))				
Hypertension	17 (39.53)	20 (46.51)	0.427	0.514
Diabetes	15 (34.88)	12 (27.91)	0.486	0.486
Coronary heart disease	12 (27.91)	16 (37.21)	0.847	0.357
Hyperlipidemia	18 (41.86)	17 (39.53)	0.048	0.826

Table 2: Comparison of expectoration between the two groups.

Group	n	Expectoration ($\bar{\chi} \pm s$) (mL)		
		Before therapy	Treatment 3 d	Treatment 7 d
Control group	43	28.65 ± 7.46	74.11 ± 12.41*	86.32 ± 14.79*
Observation group	43	27.91 ± 8.03	105.45 ± 15.63*	34.55 ± 9.45*
t		0.443	10.297	19.342
P		0.659	<0.001	<0.001

Compared with before treatment, *$P < 0.05$.

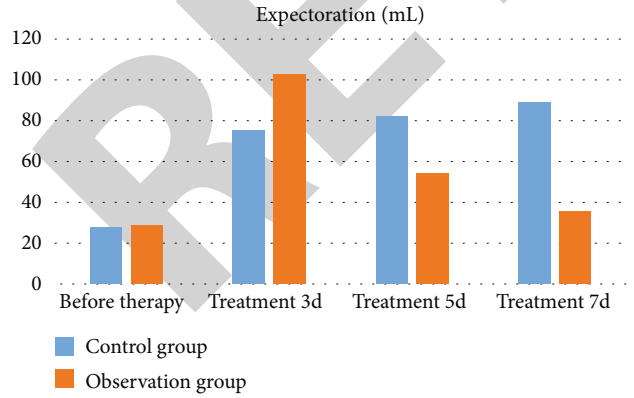

Figure 1: Comparison of sputum excretion between the two groups. Before therapy, they were similar in the two groups. On the 3rd day after treatment, the sputum excretion of the observation group was higher than that of the control group. On the 7th day after treatment, the sputum excretion of the observation group was lower than that of the control group.

excretion was lower than that in the control group. The CAT score and Borg score were lower than those of conventional treatment, and the duration of antibiotic use and hospital stays in the observation group were significantly shorter than those of the control group, while the incidence of adverse reactions in the two groups was similar. These results suggest that Xiyanping can not only better promote sputum excretion in elderly patients with acute exacerbation of COPD, reduce the symptom of dyspnea, accelerate the recovery process, and decrease the application of antibiotics but also not increase the risk of adverse reactions. Pulmonary function and airway responsiveness are clinical indicators for judging the severity and prognosis of COPD. In this study, it was found that FEV1, FVC, and FEV1/FVC of patients with Xiyanping adjuvant therapy after treatment were higher than those with conventional therapy, and their airway resistance and lung compliance during exhalation and inspiration were lower than those of patients with conventional therapy, suggesting that Xiyanping was conducive to improve lung function and reduce airway hyperreactivity

Table 3: Differences in serum-related factors such as GDF-15 and HIF-1α between them ($\bar{\chi} \pm s$).

Group	n	GDF-15 (μg/L)		HIF-1α (ng/L)		CXCL12 (ng/L)	
		Before	After	Before	After	Before	After
Control group	43	2.85 ± 0.49	1.65 ± 0.38*	30.58 ± 8.99	18.11 ± 6.43*	314.52 ± 74.96	274.63 ± 54.14*
Observation group	43	2.79 ± 0.55	1.21 ± 0.27*	29.97 ± 9.07	11.42 ± 4.45*	305.88 ± 79.11	213.52 ± 43.63*
t		0.534	6.190	0.313	5.610	0.520	5.763
P		0.595	<0.001	0.755	<0.001	0.605	<0.001
Group	n	TNF-α (μg/L)		IL-8 (μg/L)		TGF-β (ng/mL)	
		Before	After	Before	After	Before	After
Control group	43	4.15 ± 0.58	3.21 ± 0.52*	104.52 ± 27.65	38.56 ± 12.41*	71.56 ± 24.41	52.05 ± 17.79*
Observation group	43	4.06 ± 0.61	2.55 ± 0.43*	101.78 ± 31.64	21.35 ± 8.25*	68.96 ± 25.56	41.31 ± 14.66*
t		0.701	6.414	0.428	7.573	0.482	3.055
P		0.485	<0.001	0.670	<0.001	0.631	0.003

Compared with before treatment, *$P < 0.05$.

Table 4: Differences in blood routine indexes between the two groups ($\bar{\chi} \pm s$).

Group	n	WBC ($\times 10^9$/L)		NEU (%)	
		Before	After	Before	After
Control group	43	12.23 ± 2.89	8.87 ± 1.97*	87.45 ± 8.63	76.64 ± 6.49*
Observation group	43	12.31 ± 2.57	7.18 ± 1.54*	85.97 ± 8.44	69.85 ± 5.14*
t		0.136	4.432	0.804	5.378
P		0.892	<0.001	0.424	<0.001

Compared with before treatment, *$P < 0.05$.

Table 5: Differences in pulmonary function indexes between the two groups ($\bar{\chi} \pm s$).

Group	n	FEV1 (L)		FVC (L)		FEV1/FVC (%)	
		Before	After	Before	After	Before	After
Control group	43	1.21 ± 0.49	1.68 ± 0.52*	2.04 ± 0.59	2.46 ± 0.61*	53.25 ± 8.47	66.56 ± 7.56*
Observation group	43	1.23 ± 0.43	2.19 ± 0.61*	2.11 ± 0.58	2.89 ± 0.64*	55.04 ± 8.29	75.48 ± 6.04*
t		0.201	4.172	0.555	3.189	0.990	6.045
P		0.841	<0.001	0.580	0.002	0.325	<0.001

Compared with before treatment, *$P < 0.05$.

Table 6: Differences in airway hyperreactivity indicators between the two groups ($\bar{\chi} \pm s$).

Group	n	Airway resistance during exhalation (cm H_2O/(L·s))		Airway resistance during inspiration (cm H_2O/(L·s))		Lung compliance (mL/cm H_2O)	
		Before	After	Before	After	Before	After
Control group	43	1.87 ± 0.74	1.42 ± 0.51*	1.81 ± 0.89	1.54 ± 0.41*	174.25 ± 45.36	135.26 ± 31.05*
Observation group	43	1.89 ± 0.69	1.21 ± 0.43*	1.86 ± 0.82	1.28 ± 0.37*	169.85 ± 48.14	108.57 ± 24.96*
t		0.130	2.064	0.271	3.087	0.436	4.393
P		0.897	0.042	0.787	0.003	0.664	<0.001

Compared with before treatment, *$P < 0.05$.

in elderly patients with acute exacerbation of COPD. By introducing hydrophilic groups into the structure of andrographolide to enhance its antibacterial activity, Xiyanping prevents the proliferation and replication of viruses and bacteria by preventing protein from wrapping DNA fragments of pathogenic microorganisms and inhibits prostaglandin synthesis, protects lysosome membrane, reduces capillary permeability, and improves cellular immune function [16,

Table 7: Differences in CAT scores and Borg scores between the two groups (($\bar{\chi} \pm s$), fraction).

Group	n	CAT score		Borg score	
		Before	After	Before	After
Control group	43	17.05 ± 5.94	11.89 ± 2.16*	8.87 ± 2.07	6.13 ± 1.88*
Observation group	43	16.53 ± 6.17	9.23 ± 2.07*	8.95 ± 2.13	4.57 ± 1.29*
t		0.398	5.830	0.177	4.487
P		0.692	<0.001	0.860	<0.001

Compared with before treatment, *$P < 0.05$.

Table 8: Differences in duration of antibiotic use, length of stay, and adverse reactions between the two groups.

Group	n	Antibiotic use time ($\bar{\chi} \pm s$) (d)	Hospital stay ($\bar{\chi} \pm s$) (d)	Adverse reactions (n (%))			
				Rash	Diarrhea	Irritable	Total
Control group	43	8.47 ± 1.89	13.07 ± 2.57	1 (2.33)	2 (4.65)	0 (0.00)	3 (6.98)
Observation group	43	6.35 ± 1.41	9.84 ± 1.93	2 (4.65)	1 (2.33)	1 (2.33)	4 (9.30)
t or χ^2		5.896	6.590				0.156
P		<0.001	<0.001				0.693

17]. In addition, Xiyanping also has an antagonistic effect on endotoxin. It can block LPS-mediated systemic inflammatory response and produce a good synergistic effect when combined with antibiotics [18, 19]. The lung ventilation function can be improved and airway hyperreactivity can be reduced when infection and inflammation are effectively controlled [20].

Local and systemic inflammatory response is an important pathological change in patients with acute exacerbation of COPD. WBC and NEU are immune cells of the body, which are highly expressed after infection and play their own anti-infection role [20–22]. GDF-15 is a stress response protein, which is mostly secreted by macrophages and adipocytes after activation to participate in physiological and pathological processes such as growing development and inflammatory reactions [23–25]. HIF-1α is a transcription factor regulating cells under hypoxic conditions, which can activate downstream inflammatory pathways and aggravate inflammatory injury of the respiratory tract [26]. CXCL12 is a member of the chemokine protein family, which forms a complex with the receptor and participates in the inflammatory response process [27, 28]. TNF-α is a proinflammatory factor synthesized by activated mononuclear macrophages, which can not only cause direct inflammatory injury in lung tissue but also promote the synthesis of other proinflammatory factors, such as IL-8, resulting in worsening tissue damage [29–31]. TGF-β can regulate cell growth and differentiation, inhibit immune cell differentiation and proliferation, and promote fibroblasts to release proinflammatory factors such as IL-6 [32–34]. In the study, it was found that the level of inflammatory indexes in the patients treated with Xiyanping adjuvant therapy was significantly lower than that in the patients treated with conventional therapy, suggesting that Xiyanping could regulate GDF-15 and HIF-1α to other inflammatory-related factors and reduce the inflammatory response of the body, which was one of the important mechanisms in the treatment of acute exacerbation of COPD in the elderly by detecting the above inflammatory indexes.

There were some limitations of this study. The sample size was limited. And this study was conducted in only one hospital. Thus, the results need to be confirmed by a multicenter randomized controlled study with a large cohort.

In summary, Xiyanping could improve the pulmonary function of elderly patients with acute exacerbation of COPD, reduce the response of airway hyperreactivity, and promote the excretion of sputum.

Data Availability

The datasets used and analyzed during the current study are available from the corresponding author upon reasonable request.

Conflicts of Interest

The authors declare that they have no conflicts of interest.

Authors' Contributions

Jun Xia Wang and Ying Zhang did the same work as the co-first author. Jun Xia Wang and Ying Zhang have contributed equally to this work and share the first authorship.

Acknowledgments

The study was funded by the Project of Hebei Administration of Traditional Chinese Medicine, No.: 2020292.

References

[1] A. Kichloo, M. Aljadah, N. Vipparla, and F. Wani, "Optimal glucocorticoid dose and the effects on mortality, length of stay,

and readmission rates in patients diagnosed with acute exacerbation of chronic obstructive pulmonary disease (AECOPD)," *Journal of Investigative Medicine*, vol. 67, no. 8, pp. 1161–1164, 2019.

[2] J. G. Lin, J. Lyu, M. H. Sun, X. Liao, and Y. M. Xie, "Systematic review and meta-analysis of shenfu injection on treating acute exacerbation of chronic obstructive pulmonary disease," *World Journal of Traditional Chinese Medicine*, vol. 6, no. 3, pp. 276–283, 2020.

[3] A. Singanayagam, S. L. Loo, M. Calderazzo et al., "Antiviral immunity is impaired in COPD patients with frequent exacerbations," *American Journal of Physiology*, vol. 317, no. 6, pp. L893–L903, 2019.

[4] W. Yd, Z. Li, and L. Fs, "Study on the distribution of TCM constitution in patients with stable chronic obstructive pulmonary disease," *World Chinese medicine*, vol. 16, no. 23, pp. 3532–3538, 2021.

[5] Q. Zhao, W. Lq, Z. Xq, Y. Zh, S. Sl, and Z. Xiong, "The efficacy of Xiyanping combined with levofloxacin in the treatment of lower respiratory tract bacterial infection in acute exacerbation of COPD," *Hainan Medical*, vol. 30, no. 18, pp. 2412–2414, 2019.

[6] Chronic obstructive pulmonary disease group, respiratory disease branch of Chinese Medical Association, *Guidelines for the Diagnosis and Treatment of Chronic Obstructive Pulmonary Disease (2013 Revision)*, vol. 6, no. 5, 2013General practice clinical and education, 2013.

[7] Expert group on diagnosis and treatment of acute exacerbation of chronic obstructive pulmonary disease (AECOPD), "Chinese expert consensus on the diagnosis and treatment of acute exacerbation of chronic obstructive pulmonary disease (AECOPD) (updated in 2017)," *International Journal of Respiratory Medicine*, vol. 37, no. 14, pp. 1041–1057, 2017.

[8] T. Yh and F. Gh, "The application of chronic obstructive pulmonary disease assessment test in the efficacy evaluation of patients with acute exacerbation," *Chinese Journal of Tuberculosis and Respiratory*, vol. 37, no. 1, pp. 56-57, 2014.

[9] Z. Xn and Y. Ly, "Evaluation of mechanical ventilation in patients with acute exacerbation of chronic obstructive pulmonary disease by four grades," *International Journal of Respiratory Medicine*, vol. 39, no. 16, pp. 1226–1230, 2019.

[10] M. I. Abas, M. Z. Zubir, M. F. Ishak et al., "Patients characteristics and outcomes analysis of COPD readmissions in a teaching Hospital in Kuala Lumpur, Malaysia," *International medical journal IMJ*, vol. 27, no. 6, pp. 705–708, 2020.

[11] A. Salari-Moghaddam, A. Milajerdi, B. Larijani, and A. Esmaillzadeh, "Processed red meat intake and risk of COPD: a systematic review and dose- response meta-analysis of prospective cohort studies," *Clinical Nutrition*, vol. 38, no. 3, pp. 1109–1116, 2019.

[12] Y. Aydemir, Ö. Aydemir, A. Şengül et al., "Comparison of oxidant/antioxidant balance in COPD and non-COPD smokers," *Journal of Critical Care*, vol. 48, no. 6, pp. 566–569, 2019.

[13] Z. Yw, S. Cl, L. Wei, and W. Zw, "Study on the mechanism of promoting the improvement of COPD in remission stage and airway mucosal tissue repair based on TCM comprehensive treatment mode," *Laboratory medicine and clinical*, vol. 18, no. 7, pp. 897–900, 2021.

[14] Z. Bh, L. Zheng, H. Shao, and Y. Lp, "Rapid health technology assessment of Xiyanping injection in the treatment of respiratory diseases in children," *Evaluation and aAnalysis of dDrug uUse in Chinese Hospitals*, vol. 22, no. 2, pp. 208–212, 2022.

[15] L. Zl, "Effect of Xiyanping combined with high flow humidified oxygen inhalation on inflammatory mediators and pulmonary function in patients with acute respiratory failure," *Chinese medicine and clinical*, vol. 21, no. 2, pp. 223–227, 2021.

[16] S. Soisuwan, V. Teeranachaideekul, A. Wongrakpanich, P. Langguth, and V. B. Junyaprasert, "Impact of uncharged and charged stabilizers on *in vitro* drug performances of clarithromycin nanocrystals," *European Journal of Pharmaceutics and Biopharmaceutics*, vol. 137, no. 7, pp. 68–76, 2019.

[17] C. M. Lee, E. H. Jung, J. Y. Byeon et al., "Effects of steady-state clarithromycin on the pharmacokinetics of zolpidem in healthy subjects," *Archives of Pharmacal Research*, vol. 42, no. 12, pp. 1101–1106, 2019.

[18] X. Sy, W. Li, Z. Hx, P. Pw, M. Ey, and W. Bo, "Clinical application analysis of Xiyanping aerosol inhalation in the treatment of infantile pneumonia," *Chinese Journal of Clinical Pharmacology*, vol. 37, no. 12, pp. 1596–1598,1602, 2021.

[19] N. Don, X. Dh, Y. Gh, R. Ning, and L. Xx, "Effect and mechanism of Xiyanping injection on serum inflammatory factors and whole blood bitterness receptor levels in patients with ARDS," *Journal of Guizhou Medical University*, vol. 46, no. 12, pp. 1433–1437,1451, 2021.

[20] S. Y. Lee, S. S. Cho, C. S. Bae, M. S. Bae, and D. H. Park, "Socheongryongtang suppresses COPD-related changes in the pulmonary system through both cytokines and chemokines in a LPS COPD model," *Pharmaceutical Biology*, vol. 58, no. 1, pp. 538–544, 2020.

[21] S. Gao, Y. Duan, J. Chen, and J. Wang, "Evaluation of blood markers at admission for predicting community acquired pneumonia in chronic obstructive pulmonary disease," *COPD:Journal of Chronic Obstructive Pulmonary Disease*, vol. 18, no. 5, pp. 557–566, 2021.

[22] J. Huang, T. Zeng, Y. Tian et al., "Clinical significance of high-mobility group box-1 (HMGB1) in subjects with type 2 diabetes mellitus (T2DM) combined with chronic obstructive pulmonary disease (COPD)," *Journal of clinical laboratory analysis*, vol. 33, no. 6, pp. 910–915, 2019.

[23] K. Larissi, M. Politou, A. Margeli et al., "The growth differentiation factor-15 (GDF-15) levels are increased in patients with compound heterozygous sickle cell and beta-thalassemia (HbS/β^{thal}), correlate with markers of hemolysis, iron burden, coagulation, endothelial dysfunction and pulmonary hypertension," *Blood cells, molecules and diseases*, vol. 77, no. 7, pp. 137–141, 2019.

[24] L. Fang, F. Li, and C. Gu, "GDF-15: a multifunctional modulator and potential therapeutic target in cancer," *Current Pharmaceutical Design*, vol. 25, no. 6, pp. 654–662, 2019.

[25] S. D. Kriechbaum, C. B. Wiedenroth, K. Peters et al., "Galectin-3, GDF-15, and sST2 for the assessment of disease severity and therapy response in patients suffering from inoperable chronic thromboembolic pulmonary hypertension," *Biomarkers*, vol. 25, no. 7, pp. 578–586, 2020.

[26] L. Lin, J. Sun, D. Wu et al., "MicroRNA-186 is associated with hypoxia-inducible factor-1α expression in chronic obstructive pulmonary disease," *Molecular Genetics & Genomic Medicine*, vol. 7, no. 3, pp. e531–e685, 2019.

[27] S. N. Rathnayake, F. A. Hoesein, C. J. Galban et al., "Gene expression profiling of bronchial brushes is associated with the level of emphysema measured by computed tomography-based parametric response mapping," *American Journal of Physiology-Lung Cellular and Molecular Physiology*, vol. 318, no. 6, pp. L1222–L1228, 2020.

Hindawi
Computational and Mathematical Methods in Medicine
Volume 2023, Article ID 9807415, 1 page
https://doi.org/10.1155/2023/9807415

Retraction

Retracted: Effect of Nursing Outcome-Oriented Intervention on Airway Management in Elderly Long-Term Bedridden Patients

Computational and Mathematical Methods in Medicine

Received 12 December 2023; Accepted 12 December 2023; Published 13 December 2023

This article has been retracted by Hindawi, as publisher, following an investigation undertaken by the publisher [1]. This investigation has uncovered evidence of systematic manipulation of the publication and peer-review process. We cannot, therefore, vouch for the reliability or integrity of this article.

Please note that this notice is intended solely to alert readers that the peer-review process of this article has been compromised.

Wiley and Hindawi regret that the usual quality checks did not identify these issues before publication and have since put additional measures in place to safeguard research integrity.

We wish to credit our Research Integrity and Research Publishing teams and anonymous and named external researchers and research integrity experts for contributing to this investigation.

The corresponding author, as the representative of all authors, has been given the opportunity to register their agreement or disagreement to this retraction. We have kept a record of any response received.

References

[1] W. Ding, F. Luo, P. Lin, Y. Tang, and Y. Liu, "Effect of Nursing Outcome-Oriented Intervention on Airway Management in Elderly Long-Term Bedridden Patients," *Computational and Mathematical Methods in Medicine*, vol. 2022, Article ID 9557330, 6 pages, 2022.

Hindawi
Computational and Mathematical Methods in Medicine
Volume 2022, Article ID 9557330, 6 pages
https://doi.org/10.1155/2022/9557330

Research Article

Effect of Nursing Outcome-Oriented Intervention on Airway Management in Elderly Long-Term Bedridden Patients

Weiwei Ding,[1] Fei Luo,[2] Pingping Lin,[3] Yu Tang,[4] and Ying Liu[1]

[1]*Department of Neurosurgery, Yantai Affiliated Hospital of Binzhou Medical University, Yantai, Shandong 264100, China*
[2]*Department of Gastrointestinal Surgery, Yantai Affiliated Hospital of Binzhou Medical University, Yantai, Shandong 264100, China*
[3]*Department of Obstetrics, Yantai Affiliated Hospital of Binzhou Medical University, Yantai, Shandong 264100, China*
[4]*College of Basic Medicine, Binzhou Medical University, Yantai, Shandong 264000, China*

Correspondence should be addressed to Ying Liu; mupingliuying@163.com

Received 25 July 2022; Revised 2 September 2022; Accepted 12 September 2022; Published 11 October 2022

Academic Editor: Min Tang

Objective. This study intended to explore the nursing outcome-oriented intervention's effect on airway management in elderly long-term bedridden patients. *Methods*. A total of 120 cases of elderly long-term bedridden patients admitted to our hospital from May 2018 to June 2020 were enrolled and randomly divided into the observation group ($n = 60$) and control group ($n = 60$). The control group received the routine nursing intervention, while the observation group received the nursing outcome-oriented intervention. Forced expiratory volume (FEV1), forced vital capacity (FVC), and maximal voluntary ventilation (MVV) in the first second were compared between the two groups before and after the intervention. The pulmonary infection of the two groups was observed. Total protein, hemoglobin, albumin, and cholesterol levels were compared between the two groups. Hamilton Anxiety Scale (HAMA) and Hamilton Depression Scale (HAMD) were used to evaluate the two groups' psychological status before and after the intervention. The Generic Quality of Life Inventory-74 (GQOLI-74) assessed the two groups' quality of life. *Results*. After the intervention, the levels of FEV1, FVC, and MVV; total protein, hemoglobin, albumin, and cholesterol; and scores of physical function, psychological function, social function, and material life function in the observation group were higher than those in the control group. Pulmonary infection, secondary infection, the infection rate is more than 3%, HAMA, and HAMD scores, and the incidence of pressure ulcers, aspiration, constipation, and the falling bed was lower than those in the control group, with statistical significance (all $P < 0.05$). *Conclusion*. Nursing outcome-oriented intervention can effectively improve lung function, pulmonary infection, nutritional status, negative mood, and quality of life of long-term bedridden elderly patients.

1. Introduction

Older adults often need to stay in bed for a long time because of a weak physique or chronic diseases, but the long-term bedridden states can cause complications such as pulmonary infection and pressure sores, which seriously affect the quality of life of patients. Without professional nursing care, these elderly patients generally develop hypostatic pneumonia after long-term bed rest; moreover, reduced or lost function of humidification and heating of upper respiratory mucosa of elderly patients can result in difficult expectoration of astringent or sticky sputum, swallowing reflex, and hypesthesia of laryngeal mucosa, causing aspiration. The establishment of an artificial airway is designed to improve the respiratory function of patients, alleviate respiratory disorders, and assist in the clearance of respiratory secretions. Improper nursing of the artificial airway will significantly reduce its use and therapeutic effect, increase the risk of related adverse reactions, and even endanger patients' lives. Therefore, effective airway management based on the physical condition and psychological characteristics of the elderly is of great importance. Although conventional nursing intervention can help patients reduce stress reactions to a certain extent, it follows

the established model for the patient taking care of them. The end of nursing means that the patient ends after the care intervention. It can measure whether the nursing method is effective and help the nursing staff make clinical decisions; that is, nursing staff can improve and implement the existing and potential patient problems during the treatment process. Nursing outcome-oriented nursing intervention differs from conventional nursing based on the patient's physical and psychological states. In nursing outcome-oriented nursing intervention, the nursing outcome should be selected first, followed by nursing with the outcome as the target, improving nursing efficiency and patients' prognosis and quality of life [1–4].

This study was aimed at investigating the effect of the nursing outcome-oriented intervention on airway management in elderly patients with long-term bedridden conditions.

2. Material and Methods

2.1. General Data. One hundred twenty elderly long-term bedridden patients admitted to our hospital from May 2018 to June 2020 were recruited and randomly divided into the observation and control groups, with 60 cases in each group. In the observation group, there were 38 males and 22 females. The age ranged from 65 to 88 years, with an average age of 75.53 ± 5.94. The bed stay ranged from 1 to 16 months, with an average of 9.85 ± 2.43 months. The following are the primary disease types: cerebral hemorrhage in 24 cases, cerebral infarction in 32 cases, and lower limb fracture in 4 cases. In the control group, there were 42 males and 18 females. The age was from 65 to 88 years, with an average age of 74.78 ± 4.39 years. The average bed stay ranged from 1 to 15 months, with an average of 9.17 ± 3.14 months. The following are the primary disease types: cerebral hemorrhage in 27 cases, cerebral infarction in 28 cases, and lower limb fracture in 5 cases. The general data of the two groups were comparable (all $P > 0.05$). This study was approved by the hospital ethics committee.

2.2. Inclusion Criteria. The following are the inclusion criteria: (1) clear clinical diagnosis, (2) stay in bed ≥ 1 month, (3) complete clinical data, and (4) voluntary participation.

2.3. Exclusion Criteria. The following are the exclusion criteria: (1) Patients with mental diseases or consciousness disorders; (2) patients with severe deterioration of the primary disease; (3) patients with severe immune dysfunction; (4) patients with congenital heart disease, liver and kidney insufficiency, coagulation dysfunction, and malignant tumor diseases; (5) patients with severe respiratory tract infection and pressure ulcers at the time of admission; and (6) patients with insufficient nursing compliance.

2.4. Grouping

2.4.1. Control Group. The control group was given routine nursing. After admission, patients and their families received conventional health education. Patients were told the precautions, including diet, during bed rest treatment, and given routine airway management, routine massage nursing, and routine psychological counseling. During the stay in bed, nurses observed patients' airway status to observe whether there was a lung infection, patted patients' back to help maintain normal respiratory function, and instructed the family members to carry out relevant training. The patient's symptoms were closely watched, and discomfort should be reported to the doctor in time.

2.4.2. Observation Group. The observation group received the nursing outcome-oriented intervention, and the nursing goals were set according to nursing outcomes. The evaluation indexes of nursing outcomes include physical health, functional health, psychological and social health, perceived health, knowledge and behavior, family health, and community health. In this study, they can be summarized into three areas: (1) improving patients' bad moods; (2) improving patients' airway function—(a) body posture management, (b) cough and expectoration, (c) airway humidification, and (d) respiratory function training; and (3) improving the quality of life of patients—(a) nutrition support, (b) prevention of falling into bed, (c) prevention of venous thrombosis, and (d) prevention of constipation.

2.5. Observation Targets. The following are the observation targets:

(1) Pulmonary function indices: forced expiratory volume in the first second (FEV1), forced vital capacity (FVC), and maximal voluntary ventilation (MVV) were compared between the two groups before and after the intervention.

(2) Whether the patient has a pulmonary infection

(3) Nutritional state: before and after the intervention, the fasting venous blood was taken from patients in the morning to detect the total protein, hemoglobin, albumin, and cholesterol levels in both groups.

(4) Mental state: Hamilton Anxiety Scale (HAMA) [5] and Hamilton Depression Scale (HAMD) [6] were used to evaluate the two groups' psychological status before and after the intervention. HAMA includes 14 entries and can be graded as five levels: no anxiety (0~7 points), suspected anxiety (8~14 points), anxiety (15~21 points), moderate anxiety (22~29 points), and severe anxiety (≥30 points). HAMD includes 24 entries and can be graded as three levels: no depression (0~8 points), mild to moderate depression (21~35 points), and severe depression (≥36 points).

(5) Whether the patient has any adverse reactions

(6) Quality of life: Generic Quality of Life Inventory-74 (GQOLI-74) [7] was used to evaluate the quality of life of the two groups before and after the intervention, consisting of 64 items in 4 dimensions. The maximum score for each dimension is 80, and the higher the score, the better the quality of life.

2.6. Statistical Approaches. All data in this study were input into an Excel table by two people without communication

Table 1: Comparison of lung function between the two groups ($\bar{x} \pm s$).

Group	FEV1 (%)		FVC (%)		MVV (L/min)	
	Before intervention	After intervention	Before intervention	After intervention	Before intervention	After intervention
Observation group ($n = 60$)	37.34 ± 4.05	48.78 ± 4.43[a]	62.01 ± 5.31	68.77 ± 5.98[a]	78.39 ± 4.36	85.07 ± 6.45[a]
Control group (n =60)	37.27 ± 3.63	41.99 ± 3.51[a]	60.53 ± 4.53	63.18 ± 5.21[a]	78.31 ± 5.27	79.63 ± 6.17[a]
t value	0.107	9.298	1.646	5.450	0.096	4.719
P value	0.915	<0.001	0.102	<0.001	0.924	<0.001

Compared with the same group before the intervention, [a]$P < 0.05$.

Table 2: Comparison of pulmonary infection between the two groups [cases (%)].

Group	Pulmonary infection	Secondary infection	More than 3%	Ventilator use
Observation group ($n = 60$)	29 (48.33)	20 (33.33)	14 (23.33)	3 (5.00)
Control group ($n = 60$)	50 (83.33)	42 (70.00)	36 (60.00)	7 (11.67)
χ^2 value	16.338	16.151	16.594	1.745
P value	<0.001	<0.001	<0.001	0.186

Table 3: Comparison of nutritional status between the two groups ($\bar{x} \pm s$).

Group	Total protein (g/l)		Hemoglobin (g/l)		Albumin (g/l)		Cholesterol (mmol/l)	
	Before intervention	After intervention	Before intervention	After intervention	Before intervention	After intervention	Before intervention	After intervention
Observation group ($n = 60$)	51.95 ± 7.22	58.52 ± 5.25[a]	103.23 ± 16.51	109.55 ± 9.04[a]	178.34 ± 40.91	213.22 ± 58.52[a]	3.12 ± 0.98	4.07 ± 0.87[a]
Control group ($n = 60$)	53.29 ± 5.26	55.51 ± 5.44[a]	103.44 ± 11.34	104.80 ± 13.63[a]	176.12 ± 55.38	179.42 ± 48.34[a]	3.35 ± 0.86	3.34 ± 1.17
t value	1.164	3.076	0.083	2.251	0.250	3.449	1.396	3.849
P value	0.247	0.003	0.934	0.027	0.803	0.001	0.165	<0.001

Compared with the same group before the intervention, [a]$P < 0.05$.

and analyzed by statistical software SPSS24.0. Measurement data were expressed as the mean ± SD and tested by a t-test when they were in line with normal distribution and had equal variance. Counting data were described by n and %, and the chi-square test was used to compare groups. All tests were two-sided, and $P < 0.05$ was considered statistically significant.

3. Results

3.1. Comparison of Lung Function between the Two Groups. Before the intervention, no significant differences between the two groups were seen in FEV1, FVC, and MVV levels (all $P > 0.05$). After the intervention, the levels of FEV1, FVC, and MVV in both groups were increased, and the improvement degree of each indicator in the observation group was greater than that in the control group ($P > 0.05$) (Table 1).

3.2. Comparison of Pulmonary Infection between the Two Groups. The pulmonary infection, secondary infection, and infection rate of more than 3% in the observation group were significantly lower than in the control group (all $P < 0.05$, Table 2).

3.3. Comparison of Nutritional Status between the Two Groups. Before the intervention, no significant differences between the two groups were observed in total protein, hemoglobin, albumin, and cholesterol levels (all $P > 0.05$). After the intervention, the levels of total protein, hemoglobin, and albumin in both groups increased, and the levels of total protein, hemoglobin, albumin, and cholesterol in the observation group were significantly higher than those in the control group (all $P < 0.05$) (Table 3).

3.4. Comparison of Psychological States between the Two Groups. Before the intervention, the two groups had no significant differences in HAMA and HAMD scores ($P > 0.05$). After the intervention, HAMA and HAMD scores were decreased in both groups, and the observation group was lower than the control group, with statistical significance (both $P < 0.05$) (Table 4).

3.5. Comparison of Adverse Events between the Two Groups. The incidence of pressure sores, aspiration, constipation, and falling bed in the observation group was significantly

Table 4: Comparison of psychological states between the two groups ($\bar{x} \pm s$).

Group	HAMA score		HAMD score	
	Before intervention	After intervention	Before intervention	After intervention
Observation group ($n = 60$)	18.52 ± 1.90	11.53 ± 1.02[a]	16.75 ± 1.60	9.70 ± 0.96[a]
Control group ($n = 60$)	18.23 ± 1.76	16.75 ± 1.63[a]	17.15 ± 1.45	14.42 ± 1.00[a]
t value	0.847	21.013	1.435	26.378
P value	0.398	<0.001	0.154	<0.001

Compared with the same group before the intervention, [a]$P < 0.05$.

Table 5: Comparison of adverse events between the two groups [cases (%)].

Group	Pressure sores	Aspiration	Constipation	Falling bed
Observation group ($n = 60$)	6 (10.00)	10 (16.67)	17 (28.33)	4 (6.67)
Control group ($n = 60$)	32 (53.33)	42 (70.00)	45 (75.00)	19 (31.67)
χ^2 value	26.033	34.751	26.162	12.102
P value	<0.001	<0.001	<0.001	<0.001

Table 6: Comparison of quality of life between the two groups ($x \pm s$, points).

Group	Physical function		Mental function		Social function		The function of material life	
	Before intervention	After intervention	Before intervention	After intervention	Before intervention	After intervention	Before intervention	After intervention
Observation group ($n = 60$)	45.70 ± 4.39	51.27 ± 7.62[a]	46.07 ± 4.72	70.38 ± 6.71[a]	45.90 ± 4.81	65.83 ± 5.70[a]	49.52 ± 4.85	68.25 ± 6.09[a]
Control group ($n = 60$)	46.47 ± 5.13	47.42 ± 5.81	47.62 ± 4.61	54.97 ± 6.88[a]	46.52 ± 4.51	57.80 ± 5.99[a]	51.12 ± 6.06	62.60 ± 6.47[a]
t value	0.879	3.112	1.820	12.423	0.724	7.527	1.597	4.926
P value	0.381	0.002	0.071	<0.001	0.470	<0.001	0.113	<0.001

Compared with the same group before the intervention, [a]$P < 0.05$.

lower than in the control group, and the differences were statistically (all $P < 0.05$, Table 5).

3.6. Comparison of Quality of Life between the Two Groups. Before the intervention, no significant differences were seen in scores of physical, psychological, social, and material life function scores between the two groups (all $P > 0.05$). After the intervention, the scores of psychological function, social function, and material life function increased in both groups, and the scores of these indices of the observation group were higher than those of the control group, with statistical significance (all $P < 0.05$) (Table 6).

4. Discussion

With the progress of population aging, the demand for hospital treatment and nursing of elderly patients is rising gradually. The common diseases of elderly patients, such as cardiovascular and cerebrovascular diseases, chronic diseases, and fractures, need long-term bed treatment, which can cause various complications [8–10]. For elderly patients with poor physical reserve ability, even a short time in bed may adversely affect the body. The circulatory, respiratory, digestive, skin, and other aspects of elderly long-term bedridden patients can vary. Moreover, patients who stay in bed for a long time are unable to carry out necessary social communication, and long-term loneliness can affect the psychological state of patients, resulting in anxiety and depression over time, further affecting the prognosis of patients. Swallowing reflexes and hypesthesia of laryngeal mucosa may also lead to aspiration and lung infection, so attention should be paid to airway management in long-term bedridden elderly patients [11, 12]. In this study, the observation group received nursing outcome-oriented nursing, while the control group received routine nursing. The results showed that the levels of FEV1, FVC, and MVV in the observation group were higher than those in the control group. FEV1 is the volume of air exhaled in the first second of exhalation. FVC is the maximum volume of air a person can exhale, and FEV1 and FVC are often used as pulmonary function indicators in clinical practice [13, 14]. The levels of FEV1 and FVC in ordinary people are about 83%. Too high or too low levels indicate abnormalities. MVV is the maximum volume, and its value is related to factors such as airway patency and respiratory muscle strength [15]. In the present study, the improvement degree of FEV1, FVC, and MVV levels in the observation group was more remarkable than that in the control group, proving that the effect of nursing outcome-oriented nursing on lung function improvement of the long-term bedridden elderly patients is better than that of conventional nursing. Nursing outcome-oriented nursing outcomes were summarized into three areas: improving

patients' negative mood, improving patients' airway function, and improving patients' quality of life. Then, targeted nursing was carried out based on the nursing outcomes. The improvement of lung function in the observation group may be related to respiratory function training in improving patients' airway function. In this study, the pulmonary infection, secondary infection, and ≥3 infection rate in the observation group were all lower than those in the control group, indicating that nursing outcome-oriented nursing intervention had a better effect than conventional nursing in reducing the pulmonary infection rate in the elderly long-term bedridden patients. In the nursing intervention guided by nursing results, posture management, cough expectoration, and airway humidification can effectively promote patients to cough up phlegm. Difficulty in expectoration can easily lead to pulmonary infection, so promoting expectoration is conducive to reducing the incidence of pulmonary infection.

Comparisons of the nutritional status after intervention showed that the levels of nutritional indicators such as total protein, hemoglobin, albumin, and cholesterol in the observation group were higher than those in the control group, indicating that nursing outcome-oriented nursing intervention can effectively improve the nutritional status of patients. Chronic bedridden patients may be accompanied by dysphagia, leading to malnutrition and insufficient nutritional intake, affecting patient outcomes. Therefore, proper nutritional support is beneficial to reducing complications and promoting patients' recovery. Improving patients' quality of life in nursing outcome-oriented nursing intervention includes nutritional support for elderly patients, and in vitro nutritional support for patients with eating difficulties can ensure adequate nutrition during hospitalization. In this study, HAMA and HAMD scores of the observation group were lower than those of the control group after the intervention, indicating that nursing outcome-oriented nursing intervention had a better effect on improving patients' bad moods than conventional nursing. Previous studies have shown that a bad mood can affect the recovery of patients [16–18]. In the present study, a nursing outcome-oriented nursing intervention is aimed at improving patients' adverse emotional outcomes. The downbeat mood of the long-term bedridden elderly patients was effectively improved by encouraging them with words and creating a good atmosphere in the wards. Previous studies have demonstrated that long-term bed rest can cause multiple complications, such as pressure sores and constipation [19, 20]. Elderly patients are also prone to falling beds. Elderly patients have poor physical function, and falling into bed can lead to severe consequences. In the present study, the incidence of pressure sores, aspiration, constipation, and falling bed in the observation group was lower than that in the control group, indicating that nursing outcome-oriented nursing intervention can effectively reduce the incidence of adverse events in long-term bedridden elderly patients. The nursing outcome-oriented nursing intervention is aimed at "improving patients' quality of life." Based on the characteristics of long-term bed rest, nursing interventions targeted to prevent falling bed, venous thrombosis, and constipation were given. In addition, airway management was also conducive to preventing aspiration, effectively reducing adverse events. After the intervention, the scores of physical, psychological, social, and material life functions of the observation group were higher than those of the control group, indicating that nursing outcome-oriented nursing intervention can effectively improve patients' quality of life. The part of "improving patients' quality of life" in the nursing outcome-oriented nursing intervention, nutritional support, and prevention of adverse events was provided to patients, effectively improving the nutritional status of patients and reducing the occurrence of adverse events.

In conclusion, nursing outcome-oriented intervention can effectively improve the lung function and nutritional status of long-term bedridden elderly patients, relieve their negative mood, improve their quality of life, and reduce the occurrence of adverse events such as infection and complications, showing clinical application value.

Data Availability

The labeled dataset used to support the findings of this study is available from the corresponding author upon request.

Conflicts of Interest

The authors declare no competing interests.

Acknowledgments

This study was supported by the Yantai Bureau of Science and Technology, Construction and Application of Respiratory Care Program for Bedridden Patients Based on Nursing Outcome (No. 2020YD076).

References

[1] J. Li, X. Wu, Z. Li et al., "Nursing resources and major immobility complications among bedridden patients: a multicenter descriptive study in China," *Journal of Nursing Management*, vol. 27, no. 5, pp. 930–938, 2019.

[2] J. Guo, C. Gao, H. Xin et al., "The application of "upper-body yoga" in elderly patients with acute hip fracture: a prospective, randomized, and single-blind study," *Journal of Orthopaedic Surgery and Research*, vol. 14, no. 1, p. 250, 2019.

[3] H. Liu, D. Zhu, J. Cao et al., "The effects of a standardized nursing intervention model on immobile patients with stroke: a multicenter study in China," *European Journal of Cardiovascular Nursing*, vol. 18, no. 8, pp. 753–763, 2019.

[4] J. Cao, T. Wang, Z. Li et al., "Factors associated with death in bedridden patients in China: a longitudinal study," *PLoS One*, vol. 15, no. 1, article e0228423, 2020.

[5] E. Thompson, "Hamilton Rating Scale for Anxiety (HAM-A)," *Occupational Medicine (London)*, vol. 65, no. 7, p. 601, 2015.

[6] M. Hamilton, "A rating scale for depression," *Journal of Neurology, Neurosurgery, and Psychiatry*, vol. 23, no. 1, pp. 56–62, 1960.

[7] L. Lingjiang and Y. Desen, "Comprehensive assessment questionnaire for quality of life," *Clinical Metadata*, vol. 24, no. 9, pp. 763–763, 2009.

Hindawi
Computational and Mathematical Methods in Medicine
Volume 2023, Article ID 9826193, 1 page
https://doi.org/10.1155/2023/9826193

Retraction

Retracted: Investigation of the Clinical Effect of New Shoulder Joint Abduction Frame in Humeral Fracture Patients after Arthroscopic Shoulder Surgery

Computational and Mathematical Methods in Medicine

Received 12 December 2023; Accepted 12 December 2023; Published 13 December 2023

This article has been retracted by Hindawi, as publisher, following an investigation undertaken by the publisher [1]. This investigation has uncovered evidence of systematic manipulation of the publication and peer-review process. We cannot, therefore, vouch for the reliability or integrity of this article.

Please note that this notice is intended solely to alert readers that the peer-review process of this article has been compromised.

Wiley and Hindawi regret that the usual quality checks did not identify these issues before publication and have since put additional measures in place to safeguard research integrity.

We wish to credit our Research Integrity and Research Publishing teams and anonymous and named external researchers and research integrity experts for contributing to this investigation.

The corresponding author, as the representative of all authors, has been given the opportunity to register their agreement or disagreement to this retraction. We have kept a record of any response received.

References

[1] G. Yu, M. Yu, S. Liu, H. Xue, and Y. Sun, "Investigation of the Clinical Effect of New Shoulder Joint Abduction Frame in Humeral Fracture Patients after Arthroscopic Shoulder Surgery," *Computational and Mathematical Methods in Medicine*, vol. 2022, Article ID 8764155, 7 pages, 2022.

Hindawi
Computational and Mathematical Methods in Medicine
Volume 2022, Article ID 8764155, 7 pages
https://doi.org/10.1155/2022/8764155

Research Article

Investigation of the Clinical Effect of New Shoulder Joint Abduction Frame in Humeral Fracture Patients after Arthroscopic Shoulder Surgery

Guiyang Yu, Meining Yu, Shan Liu, Hui Xue, and Yuehua Sun

Second Central Hospital of Baoding, Zhuozhou 072750, China

Correspondence should be addressed to Hui Xue; xuehui126@163.com and Yuehua Sun; sunyuehua163163163@163.com

Received 22 July 2022; Revised 8 August 2022; Accepted 29 August 2022; Published 11 October 2022

Academic Editor: Min Tang

Objective. This work is organized to analyze the clinical effects of new shoulder joint abduction frame on the bone metabolic markers, shoulder joint function, and visual analogue scale (VAS) of humeral fracture patients undergoing arthroscopic surgery. *Methods*. 118 patients with humeral fracture who planned to undergo shoulder surgery in our hospital from November 2018 to June 2021 were selected as the study objects and were divided into two groups according to the random number method, with 59 patients in each group. The patients in the two groups were subjected to arthroscopic shoulder surgery. New shoulder joint abduction frame was used for shoulder joint fixation in the abduction frame group, and sling was used for shoulder joint fixation in the sling group after surgery. The duration of fixation was 4-6 weeks. Finally, the prognostic indicators, complications, and serum bone metabolism levels in 4 and 6 weeks after surgery, shoulder joint function (Neer score), VAS score before surgery and after 3 and 6 months of surgery, and excellent or good rate of shoulder joint activity after 6 months of surgery were compared between the two groups. *Results*. The postoperative fracture healing time and start time of shoulder joint training were shorter, and the humeral varus angle and femur height loss were smaller in the abduction frame group than in the sling group ($P < 0.05$). There was no significant difference in the total incidence of complications between the two groups (3.39% and 13.56%, respectively) ($P > 0.05$). After 4 or 6 weeks of surgery, the levels of serum osteoprotegerin (OPG) and carboxyterminal propeptide of type I procollagen (PICP) were increased but the levels of tartrate-resistant acid phosphatase-5B (TRAP-5B) were decreased in the two groups with more significant differences in the abduction frame group ($P < 0.05$). After 6 months of follow-up, 2 cases were lost to follow-up in the abduction frame group and 3 cases in the sling group. Neer scores were increased, while VAS scores were decreased in the two groups in the third or sixth months after surgery with significant differences in the abduction frame group ($P < 0.05$). The excellent or good rate of shoulder joint activity was 94.74% (54/57) in the abduction frame group, significantly higher than that in the sling group (80.36%; 45/56) ($P < 0.05$). *Conclusion*. The fixation effect of new shoulder joint abduction frame is significant after arthroscopic surgery, and patients can carry out functional training as early as possible, which is helpful to promote fracture healing, relieve pain, and restore shoulder joint function with high safety.

1. Introduction

Humeral fracture is a common type of fracture, accounting for 4%~5% of total body fractures, mostly caused by violence [1, 2]. With the development of transportation industry and construction industry, the incidence of humeral fracture gradually increased. Operation is the main treatment for type iii-iv humeral fractures. The previous treatment method is mainly based on traditional open reduction and internal fixation, which can restore the fracture plane and improve the function of shoulder joint. However, this treatment method can lead to large trauma and slow postoperative recovery, which can affect the quality of fracture healing [3, 4]. In recent years, with the development of minimally invasive concept, arthroscopic shoulder surgery has been gradually applied in the treatment of upper limb joints, and its light trauma and accurate reduction of joint plane are conducive to postoperative recovery [5]. Because humeral fracture patients need to be fixed for a period

Table 1: Comparison of baseline data between the two groups ((±s)/n(%)).

Baseline data	Abduction frame group ($n = 59$)	Sling group ($n = 59$)	$t/\chi^2/u$	P
Gender			2.248	0.134
Male	39 (66.10)	31 (52.54)		
Female	20 (33.90)	28 (47.46)		
Age (year)	59 ~ 70 (64.62 ± 2.44)	60 ~ 71 (65.03 ± 2.27)	0.954	0.367
BMI (kg/m^2)	19.3 ~ 26.8 (23.15 ± 1.65)	19.6 ~ 27.1 (23.52 ± 1.58)	1.244	0.216
Location of injury			0.960	0.619
Left	29 (49.15)	35 (59.32)		
Right	30 (50.85)	24 (40.68)		
Risk factors			1.142	0.767
Traffic accident	32 (54.24)	30 (50.85)		
Fall from height	13 (22.03)	14 (23.73)		
Fall injury	10 (16.95)	8 (13.56)		
Other	4 (6.78)	7 (11.86)		
Time from injury to surgery (d)	1 ~ 7 (3.85 ± 1.22)	1 ~ 6 (3.74 ± 1.03)	0.529	0.598
Shoulder joint history			0.778	0.378
Yes	8 (13.56)	5 (8.47)		
No	51 (86.44)	54 (91.53)		

of time after surgery, it is difficult to perform functional exercise in the early stage when sling fixation is used, which may affect the functional recovery of shoulder joint [6]. However, the shoulder joint abduction frame can avoid the defects caused by conventional sling fixation, showing a good application prospect in the rehabilitation of humeral fracture patients. Thus, 118 patients with humeral fracture hospitalized in our hospital were selected for the present study, aiming to reveal the clinical advantages of joint abduction frame in shoulder arthroscopic surgery. The contents are reported as follows.

2. Materials and Methods

2.1. Clinical Patients. A total of 118 patients with humeral fracture who planned to undergo shoulder surgery in our hospital from November 2018 to June 2021 were selected for the study, and these patients were divided into two groups (59 cases per group) based on the random number method. As shown in Table 1, there were no significant differences between the two groups in gender, age, body mass index (BMI), location of injury, risk factors, time from injury to surgery, and medical history of shoulder joint ($P > 0.05$).

2.2. Inclusion and Exclusion Criteria. Inclusion criteria: (i) patients with a clear history of trauma. (ii) Patients had Neer type iii-iv humeral fracture indicated by X-ray, computed tomography (CT), or magnetic resonance imaging (MRI) with fracture displacement >0.5 cm [7]. (iii) Patients who could normally communicate and had stable vital signs and clear consciousness. (iv) Patients who met the surgical indications and completed plate internal fixation. (v) Patients who signed the written informed consent.

Exclusion criteria: (i) Patients with abnormal organ function and coagulation function. (ii) Patients with coinfection of systemic diseases. (iii) Patients with a prior history of upper limb surgery. (iv) Patients with pathological fracture. (v) Patients with contraindications of abduction frame fixation and sling fixation after shoulder joint surgery. (vi) Patients with osteoporosis or degenerative arthritis.

2.3. Method

2.3.1. Operation Method. All patients were subjected to plate internal fixation, and the detailed method was shown as follows. The patient received brachial plexus anesthesia. An incision was made in front and below the acromion, and the deltoid muscle was dissected longitudinally to expose the broken end of fracture. The fractured end was reset through shoulder arthroscopy and fixed with Kirschner wire. Then, plates were inserted and fixed using Kirschner wire. The proximal end of the plate did not exceed the upper edge of the greater tuberculum. The screw hole was exposed at the distal end of 1.5 cm of the plates. The screws were inserted and tightened and then Kirschner wire was taken out after the determination of satisfaction of fracture reduction and plate fitting. The shoulder joint was passively moved to confirm the effective fixation of the fractured end. The surgical area was cleaned, drainage tube was placed, and the incision was sutured. Patients in the control group received sling fixation, and the detailed methods were shown as follows. On the 1st day after surgery, the forearm, elbow, and upper arm were covered with the "body pocket" of the sling, bending the elbow at 90degrees. The sling was knotted and tightened from the chest to the back neck and fixed for 4-6 weeks. Patients in the study group were fixed using new shoulder joint abduction frame. When the pain of the patients was alleviated (about 4 days after surgery), the affected limb was fixed using abduction frame. According to the stability

Table 2: Postoperative recovery of the two groups (±*s*).

Group	Number	Postoperative shoulder training start time (weeks)	Fracture healing time (weeks)	Humeral varus angle (°)	Femur height loss (mm)
Abduction frame group	59	4.05 ± 0.48	11.95 ± 1.15	0.85 ± 0.19	1.47 ± 0.41
Sling group	59	4.84 ± 0.52	12.88 ± 1.43	1.47 ± 0.25	2.59 ± 0.44
t value		8.575	3.893	15.166	14.304
P value		<0.001	<0.001	<0.001	<0.001

Table 3: Complications *n* (%) of the two groups.

Group	Number of cases	Muscle atrophy	Shoulder stiffness	Muscle atrophy	Nonunion of fracture	Total incidence
Abduction frame group	59	0 (0.00)	1 (1.69)	0 (0.00)	1 (1.69)	2 (3.39)
Sling group	59	1 (1.69)	3 (5.08)	1 (1.69)	1 (1.69)	7 (11.86)
χ^2 value						1.925
P value						0.165

and comfort of the affected limb, the abduction frame was maintained at about 50°. Then, the abduction frame was adjusted to 90° according to the growth situation of the affected shoulder and fixed for 4-6 weeks. Anti-infection treatment was given to all patients after surgery. One day after surgery, wrist joint and fist clenching training were performed. One week after surgery, elbow training was conducted. Five weeks after surgery, X-ray reexamination was carried out according to the doctor's advice, and shoulder functional training was carried out according to the reexamination results.

2.3.2. Detection Method. 5 mL venous blood was collected from patients and centrifuged and stored at 4°C for the following study. Then, the levels of tartrate-resistant acid phosphatase-5B (Trap-5B), osteoprotegerin (OPG), carboxyterminal propeptide of type I procollagen (PICP) were analyzed according to the guidebooks of commercial kits (Bioscience, Tanjian, China) using chemiluminescence immunoanalyzer (IMMULITE 2000 Xpi; Siemens, Beijing, China).

2.3.3. Observational Indexes

(i) Comparison of prognostic indexes including fracture healing time, postoperative shoulder training start time, femur height loss, and humeral varus angle between the two groups

(ii) Comparison of complications including muscle atrophy, tissue adhesion, fracture nonunion, and shoulder joint stiffness in the two groups

(iii) The levels of bone metabolism indexes (OPG, PICP, and TRAP-5B) were compared between the two groups before operation and in the fourth and sixth weeks after operation

(iv) Comparison of shoulder joint function and pain degree between the two groups before operation and in the third and sixth months after operation. Neer scale (Neer) [8] was used to evaluate shoulder joint function, including pain, function, anatomical function, and range of motion. The full score was 100, and the higher score indicated the better the shoulder joint function. Visual analogue scale (VAS) was used to assess the degree of pain [9]. The full score was 10, and the higher score indicated the more severe pain

(v) Neer score was used to evaluate the excellent or good rate of shoulder joint activity between the two groups after 6 months of operation. Poor is <70 points, average is 70-79 points, good is 80-90 points, and excellent is >90 points. Excellent or good rate = (excellent cases + good cases)/total number of cases × 100%

2.4. Statistical Analysis. All data were analyzed using SPSS 22.0 software. Variables data were shown as means ± standard deviations and were compared using *t* test. $P < 0.05$ indicated statistical significance.

3. Results

3.1. Postoperative Recovery. As shown in Table 2, shoulder training start time and fracture healing time were shorter, and the humeral varus angle and femur height loss were smaller in the abduction frame group than in the sling group ($P < 0.05$).

3.2. Complication. As presented in Table 3, there was no significant difference in the total incidence of complications between the abduction frame group (3.39%) and the sling group (13.56%) ($P > 0.05$).

3.3. The Levels of Serum Bone Metabolism. As shown in Table 4, there was no significant difference in the serum levels of OPG, PTCP, and TRAP-5b between the two groups before operation. But the serum levels of OPG and PTCP were higher

Table 4: Serum levels of bone metabolism indexes in two groups (±*s*).

Group	Number	OPG (pg/mL)			PICP (ng/mL)			TRAP-5b (U/L)		
		Preoperative	4 weeks after surgery	6 weeks after surgery	Preoperative	4 weeks after surgery	6 weeks after surgery	Preoperative	4 weeks after surgery	6 weeks after surgery
Abduction frame group	59	114.53 ± 11.35	147.62 ± 12.73[a]	168.47 ± 13.25[a]	51.41 ± 4.67	71.48 ± 5.54[a]	93.37 ± 6.42[a]	4.07 ± 0.73	1.82 ± 0.41[a]	0.76 ± 0.22[a]
Sling group	59	117.42 ± 12.47	135.69 ± 12.55[a]	154.59 ± 12.13[a]	52.44 ± 4.59	62.39 ± 5.51[a]	78.54 ± 5.73[a]	3.96 ± 0.69	2.44 ± 0.52[a]	1.53 ± 0.27[a]
t value		1.317	5.126	5.935	1.212	8.936	13.238	0.841	7.192	16.982
P value		0.191	<0.001	<0.001	0.228	<0.001	<0.001	0.402	<0.001	<0.001

Note: [a]$P < 0.05$, compared with preoperative group.

Table 5: Neer and VAS scores of the two groups (±*s*, points).

Group	Number of cases	Neer score Preoperative	Neer score 3 months after surgery	Neer score 6 months after surgery	VAS score Preoperative	VAS score 3 months after surgery	VAS score 6 months after surgery
Abduction frame group	59	53.59 ± 3.59	68.72 ± 5.15[a]	87.44 ± 6.75[a]	7.12 ± 1.13	1.89 ± 0.53	0.95 ± 0.21[a]
Sling group	59	54.12 ± 3.27	62.59 ± 4.53[a]	75.52 ± 7.43[a]	6.95 ± 1.27	2.77 ± 0.62	1.24 ± 0.26[a]
t value		0.838	6.865	8.929	0.768	8.287	6.528
P value		0.404	<0.001	<0.001	0.444	<0.001	<0.001

Note: during the 6-month follow-up, 2 cases were lost to follow-up in the abduction frame group, and 3 cases in the suspension group; [a]$P < 0.05$, compared with preoperative group.

Table 6: The excellent or good rate of shoulder joint movement in the two groups *n* (%).

Group	Number of cases	Poor	General	Good	Excellent	Total efficiency
Abduction frame group	57	0 (0.00)	3 (5.26)	25 (43.86)	29 (50.88)	54 (94.74)
Sling group	56	2 (3.57)	9 (16.07)	24 (42.86)	21 (37.50)	45 (80.36)
χ^2 value						5.381
P value						0.020

in the fourth or sixth weeks after operation than before operation with higher in the abduction frame group ($P < 0.05$). On the contrary, the serum level of TRAP-5b was lower in the fourth or sixth weeks after operation than before operation with lower in the abduction frame group ($P < 0.05$).

3.4. Neer and VAS Scores. As illustrated in Table 5, there was no significant difference in Neer and VAS scores in the two groups before operation. But Neer score was higher in the third or sixth months after operation in the two groups with higher in the abduction frame group ($P < 0.05$). VAS score was lower in the third or sixth months after operation in the two groups with lower in the abduction frame group ($P < 0.05$).

3.5. Excellent or Good Rate of Shoulder Joint Activity. The excellent or good rate of shoulder joint activity in the abduction frame group (94.74%; 54/57) was significantly higher than that in the sling group (80.36%; 45/56) ($P < 0.05$). The results were presented in Table 6.

4. Discussion

Humerus is prone to fracture by violence, which can cause shoulder joint mobility disorder. The upper limb is widely used and thus higher requirements are needed in the treatment of humerus fracture [10]. The treatment principle of humeral fracture is to restore the anatomical plane of the joint, maintain the stability of the fracture, ensure the blood circulation of the humerus, and carry out functional training as early as possible [11]. Traditional open reduction and internal fixation have large incision scar, severe soft tissue separation, and high risk of complications. Shoulder arthroscopy surgery, as a minimally invasive technique, has a smaller incision and can reduce tissue damage. Moreover, shoulder arthroscopy can clear the surgical field and is convenient for the detection of fracture end and cartilage damage. In addition, shoulder arthroscopy can timely remove free cartilage and improve the accuracy of fracture end reduction. Previous studies have suggested that the treatment of humeral fracture by arthroscopy of shoulder is significantly effective [12, 13].

In addition to surgical treatment, early functional training for fracture patients is an important method, but joints need to be fixed for a period of time after internal fixation surgery. As reported [14, 15], after fixation surgery, the muscle contraction function is greatly reduced, which can cause muscle stiffness, tissue adhesion, muscle atrophy, etc., affecting the recovery of joint function. Sling fixation is a common fixation method. Although the fixation effect can be achieved, some studies have pointed out that this fixation method can make the affected limb in a sagging state, which can lead to muscle atrophy and articular capsulitis, resulting in shoulder joint mobility disorder [16]. Shoulder joint abduction frame is a new upper limb fixation tool, which is mainly used for conservative fracture treatment and postoperative fracture fixation clinically at present. It can stabilize joints, enable patients to carry out functional training of affected limbs as soon as possible, and reduce the risk of loss of abductor angle and fracture displacement. In the present work, we found that the fracture healing time and start time of shoulder joint training were shorter, and the humeral varus angle and femur height loss were smaller in the abduction frame group than in the sling group after surgery, which suggested that the application of new shoulder joint abduction frame after shoulder arthroscopy can enable patients to carry out functional training early, which is conducive to fracture healing and reduces the risk of humeral varus angle and femur height loss. But there was no significant difference in the total incidence of complications in the two groups, which might be related to the small number of samples included in this study. Moreover, Neer scores and the excellent or good rate of shoulder joint activity were higher in the study group than in the control group. Our data indicated that the new shoulder joint abduction frame had

significant advantages in restoring the function of the shoulder joint and alleviating the pain of patients with fracture after surgery, which might be associated with the early exercise of patients.

OPG is a soluble protein synthesized and secreted by osteoblast cell lines, which is a key coupling cell in the process of bone formation. This protein can not only reflect the activity of osteoblasts but also inhibit the activity of osteoclasts and prevent bone loss [17]. PICP can reflect the synthesis rate of type I collagen and indirectly reflect the activity of bone cells and bone formation, which is conducive to the evaluation of postoperative rehabilitation of patients [17, 18]. TRAP-5b is a glycoprotein secreted by activated macrophages, osteoclasts, and dendritic cells. Serum TRAP-5b can be used as an indicator to evaluate osteoclast activity, and its high level indicates the enhancement of osteoclast activity, which can reduce bone strength and affect the quality of bone healing [19]. Our results showed that the serum levels of OPG and PTCP were higher in the fourth or sixth weeks after operation than before operation with higher levels in the abduction frame group. The serum level of TRAP-5b was lower in the fourth or sixth weeks after operation than before operation with a lower level in the abduction frame group. Our findings suggested that new shoulder joint abduction frame after arthroscopic shoulder surgery could reduce the activity of osteoclasts and improve the activity of osteoblasts, providing a suitable microenvironment for fracture healing. The reason may be that the shoulder abduction frame makes the affected limb relax and create conditions for the early training of patients. Moreover, it can improve blood circulation and promote postoperative swelling, thus providing an environment for bone metabolism.

Taken together, the use of new shoulder joint abduction frame after arthroscopic shoulder surgery enables patients to carry out functional training as early as possible, promote fracture healing, and help to relieve postoperative pain, finally restoring the affected shoulder joint function.

Data Availability

The labeled dataset used to support the findings of this study are available from the corresponding author upon request.

Conflicts of Interest

The authors declare no competing interests.

Authors' Contributions

Guiyang Yu and Yuanyuan Yao are co-first authors of this manuscript.

References

[1] O. Jo, P. Borbas, F. Grubhofer et al., "Prosthesis designs and tuberosity fixation techniques in reverse total shoulder arthroplasty: influence on tuberosity healing in proximal humerus fractures," *Journal of Clinical Medicine*, vol. 10, no. 18, p. 4146, 2021.

[2] N. C. Harvey, A. Odén, E. Orwoll et al., "Measures of physical performance and muscle strength as predictors of fracture risk independent of FRAX, falls, and aBMD: a meta-analysis of the osteoporotic fractures in men (MrOS) study," *Journal of Bone and Mineral Research*, vol. 33, no. 12, pp. 2150–2157, 2018.

[3] L. Howard, R. Berdusco, F. Momoli et al., "Open reduction internal fixation vs non-operative management in proximal humerus fractures: a prospective, randomized controlled trial protocol," *BMC Musculoskeletal Disorders*, vol. 19, no. 1, p. 299, 2018.

[4] N. K. Pandya, "Adolescent clavicle fractures: is there a role for open reduction and internal fixation," *Current Reviews in Musculoskeletal Medicine*, vol. 12, no. 2, pp. 228–232, 2019.

[5] D. Camus, P. Domos, E. Berard, J. Toulemonde, P. Mansat, and N. Bonnevialle, "Isolated arthroscopic Bankart repair vs. Bankart repair with "remplissage" for anterior shoulder instability with engaging Hill-Sachs lesion: a meta-analysis," *Orthopaedics & Traumatology, Surgery & Research*, vol. 104, no. 6, pp. 803–809, 2018.

[6] D. A. Houck, M. J. Kraeutler, E. C. McCarty, and J. T. Bravman, "Fixed- versus adjustable-loop femoral cortical suspension devices for anterior cruciate ligament reconstruction: a systematic review and meta-analysis of biomechanical studies," *Orthopaedic Journal of Sports Medicine*, vol. 6, no. 10, p. 232596711880176, 2018.

[7] L. Li, T. Y. Li, P. Jiang et al., "Clavicle hook plate versus distal clavicle locking plate for Neer type II distal clavicle fractures," *Journal of Orthopaedic Surgery and Research*, vol. 14, no. 1, p. 472, 2019.

[8] L. Xie, Y. Zhang, C. Chen, W. Zheng, H. Chen, and L. Cai, "Deltoid-split approach versus deltopectoral approach for proximal humerus fractures: a systematic review and meta-analysis," *Orthopaedics & Traumatology, Surgery & Research*, vol. 105, no. 2, pp. 307–316, 2019.

[9] Y. T. Sung and J. S. Wu, "The visual analogue scale for rating, ranking and paired-comparison (VAS-RRP): a new technique for psychological measurement," *Behavior Research Methods*, vol. 50, no. 4, pp. 1694–1715, 2018.

[10] T. R. Liebs, I. Rompen, S. M. Berger, and K. Ziebarth, "Health-related quality of life after conservatively and surgically-treated paediatric proximal humeral fractures," *Journal of Children's Orthopaedics*, vol. 15, no. 3, pp. 204–214, 2021.

[11] H. Ömeroğlu, "Basic principles of fracture treatment in children," *Eklem Hastalıkları ve Cerrahisi*, vol. 29, no. 1, pp. 52–57, 2018.

[12] E. A. White, M. R. Skalski, D. B. Patel et al., "Isolated greater tuberosity fractures of the proximal humerus: anatomy, injury patterns, multimodality imaging, and approach to management," *Emergency Radiology*, vol. 25, no. 3, pp. 235–246, 2018.

[13] M. C. Liebensteiner, I. Khosravi, M. T. Hirschmann, P. R. Heuberer, M. Saffarini, and M. Thaler, "It is not 'business as usual' for orthopaedic surgeons in May 2020- the Austrian-German-Swiss experience," *Journal of Experimental Orthopaedics*, vol. 7, no. 1, p. 61, 2020.

[14] X. Shi, H. Liu, R. Xing et al., "Effect of intramedullary nail and locking plate in the treatment of proximal humerus fracture: an update systematic review and meta-analysis," *Journal of Orthopaedic Surgery and Research*, vol. 14, no. 1, p. 285, 2019.

[15] M. Kloub, K. Holub, J. Urban, P. Látal, M. Peml, and M. Křivohlávek, "Intramedullary nailing of displaced four-part fractures of the proximal humerus," *Injury*, vol. 50, no. 11, pp. 1978–1985, 2019.

Hindawi
Computational and Mathematical Methods in Medicine
Volume 2023, Article ID 9780897, 1 page
https://doi.org/10.1155/2023/9780897

Retraction

Retracted: Diagnostic Value of CT Window Technique for Primary Omentum Infarction

Computational and Mathematical Methods in Medicine

Received 5 December 2023; Accepted 5 December 2023; Published 6 December 2023

This article has been retracted by Hindawi, as publisher, following an investigation undertaken by the publisher [1]. This investigation has uncovered evidence of systematic manipulation of the publication and peer-review process. We cannot, therefore, vouch for the reliability or integrity of this article.

Please note that this notice is intended solely to alert readers that the peer-review process of this article has been compromised.

Wiley and Hindawi regret that the usual quality checks did not identify these issues before publication and have since put additional measures in place to safeguard research integrity.

We wish to credit our Research Integrity and Research Publishing teams and anonymous and named external researchers and research integrity experts for contributing to this investigation.

The corresponding author, as the representative of all authors, has been given the opportunity to register their agreement or disagreement to this retraction. We have kept a record of any response received.

References

[1] Y. Du, Y. Chen, C.-h. Li et al., "Diagnostic Value of CT Window Technique for Primary Omentum Infarction," *Computational and Mathematical Methods in Medicine*, vol. 2022, Article ID 4173738, 6 pages, 2022.

Hindawi
Computational and Mathematical Methods in Medicine
Volume 2022, Article ID 4173738, 6 pages
https://doi.org/10.1155/2022/4173738

Research Article

Diagnostic Value of CT Window Technique for Primary Omentum Infarction

Yue Du, Yan Chen, Cai-hong Li, Bi Zhou, Jin-liang Wu, Liang-rui Gu, and Kai Yang

Department of Radiology, Shanghai Sixth People's Hospital Affiliated to Shanghai Jiao Tong University School of Medicine, No. 222, West Huanhu 3 Road, 201306 Shanghai, China

Correspondence should be addressed to Kai Yang; 631302050123@mails.cqjtu.edu.cn

Received 10 August 2022; Accepted 17 September 2022; Published 11 October 2022

Academic Editor: Min Tang

Objective. The diagnostic value of CT window width technique in primary omentum infarction was evaluated by this study. *Methods.* The abdominal CT data of 32 patients with clinically diagnosed abdominal omentum infarction were retrospectively selected and analyzed. The fixed window position was 50 HU, and the window width was 135 HU, 250 HU (abdomen), 350 HU (mediastinum), and 500 HU, respectively. The detection rate of lesions was analyzed and compared. *Results.* Window widths of 135 HU, 250 HU (abdomen), 350 HU (mediastinum), and 500 HU have a detection rate of 12.5% (4 cases), 62.5% (20 cases), 100% (32 cases), 100% (32 cases) for abdominal omental lesions, respectively. However, 500 HU showed worse abdominal bowel and parenchymal organs than 350 HU. *Conclusion.* According to the comprehensive image quality, the ideal window width for diagnosis of primary omentum infarction is 350HU (mediastinal) window width.

1. Introduction

According to the etiology, it is divided into primary and secondary omental infarction [1, 2]. Among them, secondary omental infarction is more common, including abdominal trauma, retinal torsion, adhesion, and other abdominal organ lesions and other main causes [3, 4]. Primary omental infarction is an acute vascular injury on the omentum that is rare and of unknown etiology [5, 6]. Primary tumors of the omentum are very rare and there have been no systematic literature review. No chapters on primary diseases and tumors of the omentum are mentioned in classical surgery. This article reviews the types, clinical features, and imaging features of primary omental tumors so as to improve physicians' understanding of primary omental tumors. Abdominal CT window width technique was used to diagnose parenchymal organs and intestines [7]. Because the omentum is fat density, it is black in the conventional abdominal window width technique, which often leads to missed diagnosis of omental lesions. Searching the literature on epiploic appendagitis [8] [9], the authors suggest that the general abdominal window width is unclear for some cases, and even individual cases are not displayed. On the basis of appropriate adjustment of the window width, the cases that are missed can be clearly observed. The omentum is a common site of metastasis of ovarian cancer [10] [11], stomach [12, 13], and colon cancer [14, 15], and is also a prone site of granulomatous inflammation, including tuberculosis infection and fibrosis. However, no CT window width technique has been found in the literature for the diagnosis of primary greater omental infarction. Therefore, this paper discusses the diagnostic value of CT window width technology in primary omental infarction so as to improve the detection rate and diagnosis rate of CT and avoid missed diagnosis.

2. Materials and Methods

2.1. Materials. Retrospective analysis included 32 patients with primary omental infarction diagnosed by abdominal pain in our hospital from March 2017 to February 2022. Among the 32 cases, 28 males and 4 female, aged 21-95 years, the average age of 39 ± 17 years. Lesion location: 14 cases of descending colon, 12 cases of sigmoid colon, and 6

cases of ascending colon. No injury and recent-operation history, due to short-term abdominal pain as the main symptoms of the diagnosis, abdominal pain lasted about 1-3 days. There was no nausea, vomiting, diarrhea, and fever. Only 6 patients showed a slight increase in inflammatory markers such as white blood cells, neutrophil counts, and C-reactive protein in laboratory tests. All the 32 cases disappeared after clinically conservative treatment of symptoms.

2.2. Methods

2.2.1. CT Scan and Diagnosis. Scanning using Aquilion/TSX-101A spiral CT machine, parameters were as follows: 120KV/154 mA, layer thickness according to need to use 5.0/1.0 mm, pitch is 1, because they are acute abdomen treatment, so only 1 case performed an enhanced CT examination. Three senior professional doctors, proficient in abdominal imaging diagnosis, diagnosed and analyzed the abdominal CT images of 32 patients with window width 135HU, 250HU, 350HU, 500HU, and window level fixed to 50HU.

2.2.2. Statistical Analysis. Statistical analysis was performed using the SPSS20.0 software package, the measurement data were expressed as mean ± standard deviation ($\bar{x} \pm S$), the diagnostic rate of primary greater omental infarction was analyzed by one-way ANOVA with different window width. When comparing the two groups, Duncan's test was used, with P less than 0.05 denoted as statistically significant difference.

3. Results

Clinicians' understanding can be improved by understanding the types of common and rare omental tumors. The differential diagnosis of intraperitoneal tumor and omental tumor depends on the imaging and pathological features of soft tissue sarcoma. Combining the relationship between tumor and adjacent organs and carefully judging the source of tumor blood supply can enable doctors to make more perfect treatment decisions. Table 1 reports the respective diagnosis rates and comprehensive analysis results. 32 cases of CT showed different degrees of lamellae high density shadows around the intestine, 22 of which showed a small extent of plaque blur shadow, 8 cases showed a little blurred shadow, 2 cases showed a high-density pie-shaped shadow and calcification in the side of the intestine. 3 cases underwent abdominal enhanced CT examination and the lesion no enhancement. The displaying rates of images is low with 135 and 250HU window width, and some are not even displayed. As shown in Table 1, lesions were clearly visible in all 16 cases at 350 HU and 500HU window widths. There were significant differences in the diagnostic rates of 135HU, 250HU, and 350HU (500HU) window width techniques for primary omental infarction ($P > 0.05$), and there was no significant difference between 350HU and 500HU. Typical image data are shown in Figure 1. After metastasis, the distal omentum is congested, edema, thrombosis, and even necrosis due to blood supply disturbance, forming purple mass which is also slightly hard. There were many bloody exudates in the abdominal cavity. Toxic substances produced by omental necrosis can cause systemic toxemia. If coinfected, bacteria can return along the omental vein, causing portal phlebitis.

4. Discussion

4.1. Etiology and Predilection Site. Clinical and imaging doctors should pay attention to the clinical research of rare tumors, accumulate experience, understand the occurrence, development rules and characteristics of omental tumors, improve the accuracy of clinical diagnosis, timely treat patients, and make treatment more standardized and comprehensive. Primary omental infarction is rare, and it is an unexplained retinal acute vascular disease [16] [17]. Due to venous filling or abnormal venous return, omental weight causes vascular endothelial injury, and increased intra-abdominal pressure and anatomical variation of omental vein can also cause omental vein thrombosis, which is recognized by most experts and scholars [17, 18]. This disease is more common in well-nourished males and is related to obesity. There were 28 males and 4 females in this group, which is similar to literature [19, 20]. According to previous studies, lesions mainly occur on the right side of the omentum, accounting for about 90% of all cases. There was more fat deposition in the right part of the omentum, and the right part was longer, more active, and easier to distort. Vascular variability in the right omentum also increases the likelihood of venous thrombosis [9, 17–19]. However, 26 cases were located in the lower left abdomen, and only 6 cases in the right lower abdomen in our cases, contrary to the reported in the literature [19]. We analyzed the reason may be due to the randomness of the collected data, resulting in a difference result. The right abdomen has the presence of gallbladder, appendix, and other organs, often causing acute cholecystitis, appendicitis, etc., and the clinical symptoms of primary omental infarction are very similar to acute appendicitis and cholecystitis [20]. CT examination can provide multiplanar reconstruction to describe the anatomical location and origin of the mass as well as the relationship between the mass and adjacent organs and vascular system. MRI can complement the tissue features of CT well and has a high contrast resolution for intraperitoneal soft tissue sarcoma, which is helpful to assess local invasion, but its practicality for overall staging is poor. Identification of unidentified distant metastases can be facilitated by combining positron emission tomography and CT imaging. Clinicians first suspect acute cholecystitis or acute appendicitis when a patient presents right-sided abdominal pain. After general conservative anti-inflammatory treatment, most of them recovered, so abdominal CT examination was not performed. There are relatively few organs in the left abdomen, and when the patient presents symptoms such as abdominal pain, CT scan is first performed to further determine the cause [21]. Therefore, left omental infarction is more common than right omental infarction.

4.2. Pathophysiology. After the necrotic omentum is reset, a large number of toxins can return into human blood

Table 1: Diagnostic rate of different CT window widths for primary omentum infarction. The different letters 135HU, 250HU, and 350HU indicate a significant difference of $P < 0.05$.

Window width	135HU	250HU	350HU	500HU
Deputy chief physician A	18.75% (6/32)	62.5% (20/32)	100% (32)	100% (32)
Deputy chief physician B	6.25% (2/32)	50% (16/32)	100% (32)	100% (32)
Deputy chief physician C	12.5% (4/32)	75% (24/32)	100%(32)	100% (32)
Comprehensive result	12.5% ± 5.1%	62.5% ± 10.21%	100% ± 0%	100% ± 0%

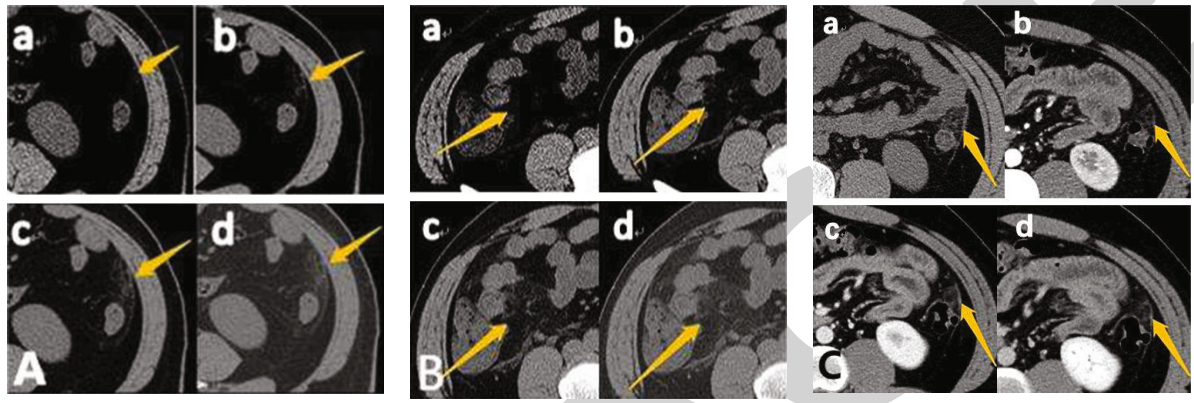

(a) (b) (c)

Figure 1: (A) Female, 30-year-old, primary omental infarction: 1 day of pain in the left lower quadrant of the patient, (a-d) the window width being 135HU, 250HU, 350HU, and 500HU, respectively. (a) There is no obvious abnormal performance. (b) A little blurry shadow around the descending colon. (c and d) The small piece of high-density shadow near the descending colon, and the surrounding fat gap is cloudy. (B) Male, 54 years old, primary omental infarction: 2 days of right lower quadrant pain, (a-d) the window widths 135HU, 250HU, 350HU, 500HU, respectively; no obvious abnormalities in (a and b), (c and d) image can clearly show a large flake blur shadow around the ascending colon, accompanied by turbidity around the fat gap. (C) Female, 22 years old, primary omental infarction: the patient's left lower quadrant pain for 2 days, the image of the window width of 350HU and the changes after the enhancement. (a) Adjacent descending colon shown the density increased, the peripheral fat gap was blurred. (b-d) Were the arterial phase, the venous phase, and the delayed phase shown the lesions no enhancement.

through the vein of the omentum, aggravating the toxic symptoms such as postoperative high fever. Therefore, it is not suitable to reset the necrotic omentum before resection. Laparoscopic resection of the greater omentum with torsion necrosis, using ultrasonic scalpel or electrocoagulation, electric hook separation, and silk thread ligation, in order to prevent too much ligated tissue or insufficient ligation and postoperative bleeding of the stump. Although laparoscopic surgery requires certain surgical skills, compared with traditional open surgery, the trauma is small and the recovery is fast. All patients in this group were discharged after surgery and were followed up for half a year without discomfort. Ultrasound-guided percutaneous biopsy has been a common diagnostic method for intraperitoneal lesions, such as liver, kidney, pancreas, and other solid organs, but it is not often used in peritoneal and omental lesions. Most diagnoses are based on fine needle aspiration cytology, with low diagnostic rate and poor accuracy. Only a few diagnoses are based on small samples of histopathology. However, ultrasound-guided percutaneous biopsy is easy to be carried out in the outpatient department, with little damage, good safety, no serious complications, and high diagnostic accuracy. In the early stage, local omental vein thrombosis, adipose tissue congestion, and occasionally a small amount of bleeding can be seen. In the middle stage, the lesions developed further, and the inflammatory cells infiltrated in the local omental adipose tissue. In the late stage, inflammatory exudate, necrotic tissue lysis and absorption, infarction omental adipose tissue fibrosis, hyperplastic changes, and small punctured calcification can be seen. The infarcted omentum is shaped "pie-like", often accompanied by exudative changes. When the spread is wide, it can be extended to adjacent tissues and parietal peritoneum, and adhesion occurs but generally does not cause thickening of the intestinal wall [22, 23]. Accurate imaging of omental lesions under ultrasound is the primary premise of biopsy. The omentum has a relatively fixed position in front of the small intestine. Abnormal thickness and hardness, front and side free were shown in ultrasound results. No intestinal peristalsis, no intestinal gas hyperecho, and easy to find lesions. The formation of a hard mass in the infarct area can be found during the operation, which is red or purple-black with hard texture.

4.3. Diagnosis. Primary omental infarction is a diagnosis of exclusion, which can be diagnosed according to the following [24–26]: (1) the duration of abdominal pain is short, mostly 1-3 days, but the signs of local peritonitis are obvious, and the general condition is good, except for trauma, recent surgical history, other organ diseases in the abdominal

cavity, etc. (2) CT manifested as a pie-like or flaky high-density shadow and blurred shadow around the intestine. (3) Diagnostic abdominal puncture can draw bloody liquid, amylase normal or elevated is not obvious. (4) Laparoscopy or surgery can be seen if the local large omentum becomes black and manifested as irregular pie-shaped necrotic tissue. The 16 cases collected in this paper were diagnosed as primary omental infarction based on the above-mentioned (1)-(3) diagnostic criteria, and were also cured by symptomatic conservative treatment. Because of acute abdomen, most of them did not undergo enhanced CT examination. After the recommendation, one patient underwent enhanced CT examination, and the lesion did not change. Primary omental torsion is a torsion of the omentum without any disease. The cause is unknown and may be related to abnormal omental anatomy. Violent activity, sudden change of position, gastrointestinal peristalsis after overeating, changes in intra-abdominal pressure are also causes of torsion.

The omentum is a double membrane made up of peritoneum and adipose tissue, which includes blood vessels, nerves, lymphatics, and connective tissue. The omentum is connected with the greater curvature of the stomach and the transverse colon, covering the abdominal organs in a skirt shape. When infection, tumor, or other pathological changes occur in the abdominal cavity, the omentum needs to be formed by wrapping and adhesion to limit the spread of the disease. The omentum consists of fat pads and special tissue entities called macula. Microscopically, the macula is an aggregate of white blood cells, mainly macrophages and lymphocytes. The omentum is a thin structure containing a large number of adipose tissue and macrophages, which is represented as fat density on CT [22]. Early or mild omental infarction shows only a small amount of fat layer opacity around the colon on CT image. Further development can be manifested as flaky or pie-like high-density shading [17]. The lesion did not change after enhancement. Calcification of the omentum was observed in the late infarct.

The CT window technique includes window width and window level. Increasing the window width increases the range of tissue density that can be observed, but the image contrast is reduced; while the window width reduction results in the opposite result, and the low-density portion of the tissue is not displayed [27–30].

There are three theories about the occurrence of omental teratoma: (1) during embryonic development, the migrated germ cells are captured by the omentum, and the primary teratoma of the omentum comes from the displaced germ cells; (2) ovarian teratoma in normal position fell off due to torsion or rupture, and it was implanted with omentum; and (3) there is extra ovarian tissue in omentum. The observation range of the conventional abdominal window width (135HU) is small, when the tissue around the organ such as omentum and mesentery is not ideally displayed. When the window width is appropriately increased to 350HU and 500HU, the changes of omentum tissue can be clearly displayed. In our group, the lesion display effect is poor and easy to miss diagnosis with 135HU and 250HU window width, and there is no case of missed diagnosis with 350HU and 500HU window width. The window width of 350HU showed clear changes in the parenchymal organs, the intestines, and the wall of the colon wall, and the window width of 500HU showed poor performance. Therefore, the use of window width 350HU as the ideal window width for the diagnosis of primary omental infarction and reduce misdiagnosis and missed diagnosis. The etiology of omental torsion can be divided into primary and secondary. Secondary omental torsion is a common peritonitis or postoperative spinal cord adhesion that causes torsion during exercise. The contents of the inguinal hernia are omentum, which is attached to the hernia sac and forms torsion in the process of autonomic reinnervation of the hernia. Cysts or tumors on the omentum make the free margin of the omentum asymmetric and easy to twist.

5. Conclusions

Mesenteric and omental lipomas are rare benign solid tumors. Omental lipoma grows slowly, is liquid, soft in texture, and does not infiltrate the surrounding organs. Lipomatous lesions, which occur primarily in children and adolescents, can easily be mistaken for normal omental fat. Whether patients develop different nonspecific symptoms will be determined by the size and location of the tumor. Omental lipomas are usually asymptomatic or have progressive abdominal distension, anorexia, abdominal pain, constipation, abdominal distension, and weight loss. The clinical symptoms of primary omental infarction lack specificity. In addition to the need to distinguish it from other acute abdomen, the rational application of CT window width technique is also very important. The best image performance can be obtained by appropriate retinal tissue window width technology, which can significantly reduce the missed diagnosis rate of primary omental infarction, provide help for clinical diagnosis and selection of reasonable treatment plan, and avoid delayed disease and unnecessary surgery. Preoperative diagnosis can be made according to imaging characteristics. Omental lipomas often appear as a polyechoic mass with an envelope on ultrasonography. Liposarcoma can be distinguished from lipoma by heterologous echogenicity on B-ultrasound, tumor size, or abundant Doppler flow signals. Omental lipoma can be misdiagnosed as normal mesenteric fat. Based on the above reasons, 350HU window width is considered to be the ideal window width for diagnosing primary omental infarction and reducing misdiagnosis and missed diagnosis. However, in daily work, conventional window width is required for diagnosis, which is mainly supplemented by special window width.

Data Availability

The datasets used and analyzed during the current study are available from the corresponding author upon reasonable request.

Conflicts of Interest

The authors declare no conflicts of interest.

Authors' Contributions

Yan Chen, Cai-hong Li, and Kai Yang conceived the project and designed the entire article. Bi Zhou helped collect image data. Jin-liang Wu and Liang-rui Gu performed image evaluation. All authors read and approved the final version of the manuscript.

Acknowledgments

This work was supported by Shanghai Municipal Health and Family Planning Commission (no. 201640191).

References

[1] I. Al-Bader, A. Al-Said Ali, K. Al-Sharraf, and A. Behbehani, "Primary omental torsion: two case reports," *Medical Principles and Practice*, vol. 16, no. 2, pp. 158–160, 2007.

[2] R. M. Cervellione, F. S. Camoglio, S. Bianchi et al., "Secondary omental torsion in children: report of two cases and review of the literature," *Pediatric Surgery International*, vol. 18, no. 2-3, pp. 184–186, 2002.

[3] S. Singh, M. Rowe, G. Hopkins, and A. Dahiya, "The way to a man's heart is through his stomach? A unique case report of transient constrictive pericarditis secondary to infarction of herniated omentum following bariatric surgery," *European Heart Journal-Case Reports*, vol. 6, no. 6, p. ytac205, 2022.

[4] A. Hollerweger, T. Rettenbacher, P. Macheiner, and N. Gritzmann, "Die spontane Fettgewebsnekrose von Omentum majus und appendices epiploicae: Klinisches Bild, Ultraschall- und CT-Befunde," *RöFo-Fortschritte auf dem Gebiet der Röntgenstrahlen und der bildgebenden Verfahren*, vol. 165, no. 12, pp. 529–534, 1996.

[5] A. Nubi, W. McBride, and G. Stringel, "Primary omental infarct: conservative vs operative management in the era of ultrasound, computerized tomography, and laparoscopy," *Journal of Pediatric Surgery*, vol. 44, no. 5, pp. 953–956, 2009.

[6] P. K. Sasmal, O. Tantia, N. Patle, and S. Khanna, "Omental torsion and infarction: a diagnostic dilemma and its laparoscopic management," *Journal of Laparoendoscopic & Advanced Surgical Techniques. Part A*, vol. 20, no. 3, pp. 225–229, 2010.

[7] L. Xu, X. D. Zhang, C. Zeng, and H. F. Yang, "Analysis of missed diagnosis of gastric lipomas by CT," *Current Medical Imaging*, vol. 17, no. 7, pp. 911–915, 2021.

[8] X. Yu, "Study of CT Manifestations of 13 Cases with Parotid Adenolymphomas," *Journal of Chinese Oncology*, vol. 6, pp. 515–517, 2016.

[9] W. Yong, D. Zhenhai, H. Dongjin, Y. Jianchun, Z. Weidong, and X. Yue, "CT findings and differential diagnosis of primary enterocolitis," *Journal of Radiology*, vol. 28, no. 2, pp. 181–183, 2013.

[10] K. M. Nieman, H. A. Kenny, C. V. Penicka et al., "Adipocytes promote ovarian cancer metastasis and provide energy for rapid tumor growth," *Nature Medicine*, vol. 17, no. 11, pp. 1498–1503, 2011.

[11] A. Etzerodt, M. Moulin, T. K. Doktor et al., "Tissue-resident macrophages in omentum promote metastatic spread of ovarian cancer," *The Journal of Experimental Medicine*, vol. 217, no. 4, article e20191869, 2020.

[12] M. Chen, F. Q. He, M. S. Liao, C. Yang, and X. D. Chen, "Gastrectomy with omentum preservation versus gastrectomy with omentectomy for locally advanced gastric cancer: a systematic review and meta-analysis," *International Journal of Surgery*, vol. 96, p. 106176, 2021.

[13] J. Pan, Z. Fan, Z. Wang et al., "CD36 mediates palmitate acid-induced metastasis of gastric cancer via AKT/GSK-3β/β-catenin pathway," *Journal of Experimental & Clinical Cancer Research*, vol. 38, no. 1, p. 52, 2019.

[14] L. Havrlentova, H. Faistova, M. Mazur, D. Ziak, and S. Polak, "Comparative analysis of human omental milky spots between the patients with colon cancer and the control group," *Bratislavské Lekárske Listy*, vol. 118, no. 10, pp. 580–584, 2017.

[15] S. Toom and Y. Xu, "Rapid development of omentum metastasis following stereotactic body radiotherapy (Sbrt) to para-aortic lymph nodes from colon cancer," *Journal of Gastrointestinal Cancer*, vol. 49, no. 2, pp. 190–194, 2018.

[16] R. Cianci, A. Filippone, R. Basilico, and M. L. Storto, "Idiopathic segmental infarction of the greater omentum diagnosed by unenhanced multidetector-row CT and treated successfully by laparoscopy," *Emergency Radiology*, vol. 15, no. 1, pp. 51–56, 2008.

[17] X. Zhu, Z. Huang, H. Shao, and S. Xuezheng, "Diagnosis and treatment of idiopathic segmental omental infarction," *General Practice Clinical and Educational*, vol. 13, no. 5, pp. 554-555, 2015.

[18] J. Chen, Y. Wang, and Z. Wang, "Diagnosis and treatment of idiopathic greater omental segmental infarction," *Journal of Henan Medical College*, vol. 28, no. 3, pp. 176–178, 2016.

[19] G. Mavridis, E. Livaditi, N. Baltogiannis, E. Vasiliadou, and G. Christopoulos-Geroulanos, "Primary omental torsion in children: ten-year experience," *Pediatric Surgery International*, vol. 23, no. 9, pp. 883–883, 2007.

[20] Z. Pogorelić, J. Katić, K. Gudelj, I. Mrklić, K. Vilović, and Z. Perko, "Unusual cause of acute abdomen in a child – torsion of greater omentum: report of two cases," *Scottish Medical Journal*, vol. 60, no. 3, pp. e1–e4, 2015.

[21] W. Duan and J. Bai, "The value of multi-plane spiral CT reconstruction in the diagnosis of acute appendicitis," *Chinese Journal of Practical Diagnosis and Therapy*, vol. 30, no. 3, pp. 296–298, 2016.

[22] J. Zhao and R. Bai, "Clinical and CT findings of abdominal fat necrosis," *International Journal of Medical Radiology*, vol. 36, no. 6, pp. 538–540, 2013.

[23] R. Iannaccone, F. Piacentini, T. Murakami et al., "Hepatocellular carcinoma in patients with nonalcoholic fatty liver disease: helical CT and MR imaging findings with clinical-pathologic comparison," *Radiology*, vol. 243, no. 2, pp. 422–430, 2007.

[24] H. Zhou, B. Shen, W. Xiao, and H. Xinzhong, "Laparoscopic diagnosis and treatment of 9 cases of idiopathic segmental omental infarction," *Chinese Journal of Integrated Traditional and Western Medicine*, vol. 18, no. 1, pp. 91-92, 2012.

[25] B. K. P. Gou and H. N. Koong, "Non-operative management of idiopathic segmental infarction of the greater omentum successfully diagnosed by computed tomography," *Journal of Gastroenterology and Hepatology*, vol. 21, no. 10, pp. 1638-1639, 2006.

[26] F. Li, G. Liu, F. Liu, and Z. Zuyan, "Diagnostic value of acute mesenteric ischemia by dual-source CT angiography," *Chinese Journal of Practical Diagnosis and Therapy*, vol. 28, no. 1, pp. 35-36, 2014.

[27] Z. Wang, Q. Qu, K. Cai, and T. Xu, "CT image examination based on virtual reality analysis in clinical diagnosis of

Hindawi
Computational and Mathematical Methods in Medicine
Volume 2023, Article ID 9841057, 1 page
https://doi.org/10.1155/2023/9841057

Retraction

Retracted: Stretching Training Rehabilitation Has Potential to Alleviate Ankylosing Spondylitis in Mice by Inactivating the Wnt/β-Catenin Pathway

Computational and Mathematical Methods in Medicine

Received 5 December 2023; Accepted 5 December 2023; Published 6 December 2023

This article has been retracted by Hindawi, as publisher, following an investigation undertaken by the publisher [1]. This investigation has uncovered evidence of systematic manipulation of the publication and peer-review process. We cannot, therefore, vouch for the reliability or integrity of this article.

Please note that this notice is intended solely to alert readers that the peer-review process of this article has been compromised.

Wiley and Hindawi regret that the usual quality checks did not identify these issues before publication and have since put additional measures in place to safeguard research integrity.

We wish to credit our Research Integrity and Research Publishing teams and anonymous and named external researchers and research integrity experts for contributing to this investigation.

The corresponding author, as the representative of all authors, has been given the opportunity to register their agreement or disagreement to this retraction. We have kept a record of any response received.

References

[1] Y. Xie, X. Li, Q. Zhang, F. Guo, and Y. Wang, "Stretching Training Rehabilitation Has Potential to Alleviate Ankylosing Spondylitis in Mice by Inactivating the Wnt/β-Catenin Pathway," *Computational and Mathematical Methods in Medicine*, vol. 2022, Article ID 3932504, 10 pages, 2022.

Hindawi
Computational and Mathematical Methods in Medicine
Volume 2022, Article ID 3932504, 10 pages
https://doi.org/10.1155/2022/3932504

Research Article

Stretching Training Rehabilitation Has Potential to Alleviate Ankylosing Spondylitis in Mice by Inactivating the Wnt/β-Catenin Pathway

Yu Xie,[1] Xiang Li,[2] Qiuchi Zhang,[3] Feng Guo,[1] and Yue Wang[1]

[1]*Affiliated Hospital of Nanjing University of Chinese Medicine (Rheumatology Department, Jiangsu Province Hospital of Chinese Medicine), Nanjing 210029, China*
[2]*Nanjing University of Chinese Medicine, Nanjing 210046, China*
[3]*Affiliated Hospital of Nanjing University of Chinese Medicine (Neurology Department, Jiangsu Province Hospital of Chinese Medicine), Nanjing 210029, China*

Correspondence should be addressed to Yue Wang; wangyuephd20@126.com

Received 6 September 2022; Revised 21 September 2022; Accepted 26 September 2022; Published 7 October 2022

Academic Editor: Min Tang

Ankylosing spondylitis (AS) is a chronic inflammatory disease characterized by invasion of the joints of the central axis that involves soft tissues and joints surrounding the spine. Stretching training rehabilitation (STR) has been widely applied for the treatment of AS. The Wnt/β-catenin signalling pathway is closely related to AS. In this study, we aimed to explore the potential molecular mechanisms underlying the protective effect of STR on AS both *in vitro* and *in vivo*. Male DBA/1 mice were employed to establish an AS animal model. Hematoxylin-eosin staining showed that STR reversed pathological damages in bone tissues and the total antioxidant capacity of AS mice and increased the antioxidant capacity by upregulating superoxide dismutase and malondialdehyde expression in DBA/1 mice. The MTT, RT-qPCR, and Western blotting results further indicated that STR improved the survival rate of cells by downregulating the expression of target genes in the Wnt/β-catenin pathway and by inhibiting cell inflammation and apoptosis. In conclusion, our findings indicated that STR treatment might be an effective therapeutical strategy for AS.

1. Introduction

Ankylosing spondylitis (AS) is a prototypical disease of spinal arthritis (SpA) [1]. It is a chronic inflammatory disease characterized by invasion of the joints of the central axis that involves soft tissues and joints surrounding the spine [2, 3]. The main clinical manifestations are trunk pain and joint swelling and pain at the early stage of the disease, and the main manifestations of the disease are stiffness of the spine and joints [4]. Currently, the pathogenic mechanism for AS is not completely clear. Moreover, an effective cure is unavailable, which has a serious effect on patients' health and daily life, and thus, it is called "undead cancer" [5]. The main goal of AS treatment is to control inflammation as early as possible to improve function and reduce deformity. Various ligaments of the human body will be opened during the stretching process, heating and sweating will occur through physical activity, and then, the whole body will be adjusted to the best state, which is convenient for larger and more intense exercises [6, 7]. Stretching is a common method used in flexibility training. Through good stretching, the joints and muscles of the body will become more flexible, which may effectively improve the stiffness of the limbs and improve the flexibility of the body [8, 9]. A radical cure has not been developed for AS. Appropriate intervention measures are used to control symptoms, restore and maintain physiological functions, delay disease progression, reduce the disability rate, and improve quality of life which are the main goals of treatment and care [10]. Studies conducted abroad have confirmed that stretching training improves the physical activity of patients, delays spinal sclerosis, and promotes

disease recovery [11]. This study observes the therapeutic effect of stretching exercise prescriptions on patients with AS and the specific mechanism of disease treatment.

Recent studies have shown that the Wnt/β-catenin signalling pathway is closely related to AS [12]. Wnt/β-catenin proteins bind to receptors located on the cell membrane and activate intracellular signalling pathways through autocrine or paracrine mechanisms, resulting in modulation of the expression of target genes [13]. The Wnt/β-catenin signalling pathway has been conformed to regulate cell proliferation, differentiation, inflammation, and apoptosis in different human diseases and cancers [14].

In this study, DBA/1 mice were used to experimentally verify the regulatory effect of stretching exercise on Wnt/β-catenin activity, inflammation, and cell apoptosis. We found that stretching exercise improved the antioxidant capacity of AS mice. We extracted synovial cells from the ankle joint of mice and added pathway inhibitors and agonists to explore the effect of stretching exercise on Wnt/β-catenin activity and cell proliferation. Our results indicated that stretching exercise might be an effective therapeutical strategy for AS.

2. Materials and Methods

2.1. Animals and Groups. Fifty male DBA/1 mice (Vital River, Beijing, China) of SPF grade aged 26 weeks, with an average body weight of 21.7 ± 1.4 g, were used. The culture room temperature was set to 22–25°C with a humidity of 50-70%, and animals were provided free access to food and drinking water. Fifty DBA/1 mice were randomly divided into five groups with 10 mice in each group: (1) the normal mouse group (normal group), (2) the unprocessed AS model mouse group (model group), (3) AS model mice receiving routine nursing care+pressure-relief stretch (positive control group), (4) AS model mice treated with routine nursing care +pressure-relief stretch+simulated stretching training (stretching exercise group), and (5) normal mice undergoing stretching exercise. The model group and the normal group were raised normally every day [15]. Stretching exercise was performed as described. The mouse was gently stretched in the direction of the lower limbs to fully stretch the mouse. Two sessions were performed per day, and each session included 10 stretches in 5 d/week for 12 weeks. In addition, the pressure-relief stretch was largely mimicking the actions of the stretching exercise procedure. However, the mouse was never stretched in the direction of the lower limbs in order to avoid any pressures induced by the stretching motion.

2.2. Hematoxylin-Eosin (HE) Staining. Mice were anaesthetized and then sacrificed by dislocation of the cervical vertebra. Ten minutes after confirming the death of mice, the heart of each mouse was sequentially cardiac perfused with 10 mL each of 1x PBS and 4% paraformaldehyde via the vena cava. Then, the bone tissue was removed and placed in a 30% sucrose solution overnight. After the tissue sunk to the bottom, it was embedded at -80°C. Continuous coronal sections were cut using a freezing slicer (Thermo Fisher Scientific, Waltham, MA, USA). Sections were fixed with 70%, 80%, and 90% alcohol for 5 s, stained with hematoxylin for 15 s, incubated with 1% hydrochloric acid alcohol for 5 s and 0.5% ammonia for 10 s, and stained with eosin for 5 s. Next, sections were washed with 1x PBS, dehydrated with 70%, 80%, and 90% alcohol for 5 s, and sealed with neutral gum. The final stained sections were observed under a microscope (Nikon, Tokyo, Japan) [16].

2.3. Total Antioxidant Status (TAS) Determination. Serum samples were prepared using a standard venous blood sampling protocol. Blood in mice was collected through the tail vein (0.1 mL/mouse) after anaesthesia. After centrifugation at 3,000 × g for 10 min at 4°C, the serum was obtained then transferred to a clean tube, followed by storage at −80°C until use. The FRAP chemical colorimetry assay was chosen. The serum samples were analysed using the total antioxidant status (TAS) test kit (Sigma-Aldrich, Saint Louis, MO, USA) for the TAS determination. The operation steps are described below: (1) Preparation: place the required specimens and reagents at room temperature (18-25°C) and allow them to slowly rewarm. (2) The test wavelength of the automatic biochemical analyser (HITACHI 7600-210) was set to 580-605 nm. (3) A blank control was prepared. After calibration (2.18 mmol/L) and quality control (1.47 mmol/L), the quality control range ($x \pm s$) was 1.46 ± 0.14 mmol/L, and the quality control result was 1.41 mmol/L. Thus, both calibration and quality control were appropriate for the assay. (4) Serum samples from each group of mice were loaded into the sample rack, and their TAS levels were measured [17, 18].

2.4. Superoxide Dismutase (SOD) Assay. Serum samples were prepared using a standard venous blood sampling protocol. Blood in mice was collected through the tail vein (0.1 mL/mouse) after anaesthesia. After centrifugation at 3,000 × g for 10 min at 4°C, the serum was obtained then transferred to a clean tube, followed by storage at −80°C until use. In an alkaline environment, pyrogallol produces its own oxidation color reaction. The intensity of the color reaction caused by self-oxidation is high or low, depending on the concentration of superoxide anion radicals released during the reaction. Therefore, a high concentration of superoxide anion radicals is released during the reaction, and vice versa, a low concentration of superoxide anion radicals. Briefly, 4.5 mL of Tris-HCl-EDTA buffer, pH 8.2, was placed in a 10 mL colorimetric tube, incubated at 25°C for 10 min, and then added to 10 mL of a 45 mmol/L pyrogallol solution at 25°C. The optical density value was measured at a wavelength of 325 nm once every 30 s for a total of 4 min to obtain the autooxidation rate of pyrogallol in OD_A/min. At the same time, a blank test was performed with 10 mmol/L hydrochloric acid. For this analysis, 4.5 mL of the Tris-HCl-EDTA buffer solution, pH 8.2, was placed in a 10 mL colorimetric tube and incubated at 25°C for 10 min. Ten milliliters of sample solution at 25°C was mixed quickly with the buffer, and the density value was measured at a 325 nm wavelength at 30 s and 4 min. The rate of change in the optical density value was reported as OD_B/min. SOD activity (U/mL) $= [(OD_A\text{-}OD_B)/OD_A] \times 100\% \div 50\% \times V_1 \div V_2 \times n$. Here, V_1 is the total volume of the reaction solution (mL), V_2 is the measured sample volume (mL), n is the sample diluent

multiple, OD_A is the autooxidation rate of pyrogallol, and OD_B is the change rate of the sample optical density value [19].

2.5. Malondialdehyde (MDA) Assay. Serum samples were prepared using a standard venous blood sampling protocol. Blood in mice was collected through the tail vein (0.1 mL/mouse) after anaesthesia. After centrifugation at 3,000 × g for 10 min at 4°C, the serum was obtained then transferred to a clean tube, followed by storage at −80°C until use. Malondialdehyde (MDA) was heated with thiobarbituric acid (TBA) under acidic conditions (100°C, 20-60 min) to produce pink substances, and the maximum absorption peak at 535 nm was recorded to calculate the amount of lipid peroxidation. Briefly, 0.4 mL of the test solution was added to 3.6 mL of lecithin solution; then, 0.4 mL of $FeSO_4$ solution was added to catalyse the oxidation reaction, mixed, and placed in a constant temperature water bath shaker at 37°C in the dark for 1 h, followed by the addition of 1 mL of trichloroacetic acid solution. Next, 1 mL of TBA was added, shaken well, boiled in a water bath for 15 min, cooled quickly, and centrifuged at 5000 r/min for 10 min, and the supernatant was collected, and the absorbance Ax was measured at 535 nm. The blank tube contained distilled water instead of the sample to be tested, the operation method was the same as that of quality control, and the absorbance A0 of the blank tube was measured. Three parallel measurements were performed [19].

2.6. Synovial Tissue Extraction and Cell Culture. Synovial tissues were minced from mice in four different groups (normal, normal+stretching exercise, model, and model+stretching exercise) with ophthalmic scissors, digested with type I collagenase (1 mg/mL), and digested in a 37°C, 5% CO_2 cell incubator for 2 to 4 h. The sample was filtered using a 100 μm pore size filter and a large and small cell strainer and then centrifuged to pellet the cells. DMEM (Invitrogen, Carlsbad, CA, USA) containing 10% FBS (Invitrogen) was used to resuspend the cells and transferred to a cell culture flask for culture; the medium was changed every 2 to 4 days. The cell morphology and growth of the primary and post-passage cells were observed. When the cells reached passages 3-4, they were digested to prepare a single cell suspension with a density of 1×10^5 cells/mL. Additionally, LiCl (10 mmol/L; Sigma-Aldrich) or IWR (10 mmol/L; Sigma-Aldrich) was added to cells of the model or model+stretching exercise groups [20].

2.7. 3-(4,5)-Dimethylthiahiazo(-z-y1)-3,5-di-phenytetrazoliumromide (MTT) Assay. Three replicate wells in each group were prepared; 100 μL of medium was added to each well and incubated overnight. The MTT reagent (Beyotime, Shanghai, China) was added to each well and incubated for 4 h in the dark; the culture solution was discarded, DMSO solution was added and shaken for 10 min, and finally, the absorbance was measured at 570 nm using a microplate reader (Molecular Devices, USA) [21]. All experiments were performed in biological triplicates, and data are representative of three independent experiments.

2.8. RT-qPCR Analysis. Total RNA was isolated from bone tissues and synovial cells of mice in each group using the TRIzol reagent (Invitrogen) and converted cDNAs using the OneScript Reverse Transcriptase OneScript cDNA Synthesis Kit (Abcam, Cambridge, MA, USA). Twenty-five microliters of Dream Taq PCR Master Mix (Abcam), 1.5 μL of forward and reverse primers (Ribobio, Guangzhou, China), 2 μL of cDNAs, and 20 μL of nuclease-free water were included in the amplification reaction mixture (50 μL), and the PCR conditions were as follows: 95°C (2 min, one cycle); 35 cycles of 95°C (30 s), 58°C (30 s), and 72°C (1 min) (21) [15]; and a final cycle of 72°C (10 min). The mouse β-actin gene was used as an internal control. The following primer sequences were used: β-catenin, F: 5′-CCACTCCAGGAATGAAGG-3′, R: 5′-AGCAGTCTCATTCCAAGC-3′; TNF-α, F: 5′-ATAAGAGCAAGGCAGTGGAG-3′, R: 5′-TCCAGCAGACTCAATACACA-3′; IL-17, F: 5′-AGCCAGAGTCCTTCAGAGAG-3′, R: 5′-TCCTTAGCCACTCCTTCTGT-3′; Bcl-2, F: 5′-CTGGTGGACAACATCGC-3′, R: 5′-GGAG-AAATCAAACAGAGGC-3′; and β-actin, F: 5′-TCACCATCTTCCAGGAGCGAG-3′, R: 5′-TGTCGCTGTTGAAGTCAGAG-3′. All experiments were performed in biological triplicates ($n = 6$), and data are representative of three independent experiments. The relative transcript abundances ($2^{-\Delta\Delta CT}$) were calculated based on the equation $2^{-\Delta CT}$ ($\Delta CT = CT_{\text{target gene}} - CT_{\beta\text{-actin}}$). The differences were determined using unpaired Student's t-test for comparisons between different groups. A P value of <0.05 was regarded as statistically significant.

2.9. Western Blot Assay. Western blotting was used to detect the relative protein expression. After extracting the total protein from the bone tissue, 10-25 μL was added to each well for sodium dodecyl sulphate-polyacrylamide gel electrophoresis (SDS-PAGE) (60 V, when the distance migrated by bromophenol blue was approximately 1 cm from the bottom of the separation gel, stop electrophoresis) followed by wet transfer to polyvinylidene fluoride (PVDF) membranes (Millipore, Billerica, MA, USA) at 120 mA (2-3 h). The membrane was blocked with a solution containing 5% skim milk powder at room temperature for 1 h and rinsed with TBST 3 times. The membrane was incubated with antibodies against β-catenin (Abcam, ab32572, 1 : 5000), TNF-α (Abcam, ab183218, 1 : 1000), IL-17 (Abcam, ab79056, 1 : 2000), and β-actin (Abcam, ab8227, 1 : 1000) at 4°C overnight, rinsed with TBST 3 times, incubated with the secondary antibody (Abcam, ab6721, 1 : 2000) in the dark at room temperature for 2 h, and rinsed with TBST 3 times in the dark. Bands were visualized with electrochemiluminescence (ECL) (Pierce, Rockford, IL, USA), and analysed by ImageJ (v1.8.0; National Institutes of Health) [22, 23].

2.10. Statistical Analysis. Statistical analyses were performed using GraphPad Prism software (version 7.0). Data are presented as the means ± SD (standard deviations). Differences and comparisons between multiple groups were analysed using one-way ANOVA followed by a post hoc test (Tukey's test). $P < 0.05$ indicated a significant difference.

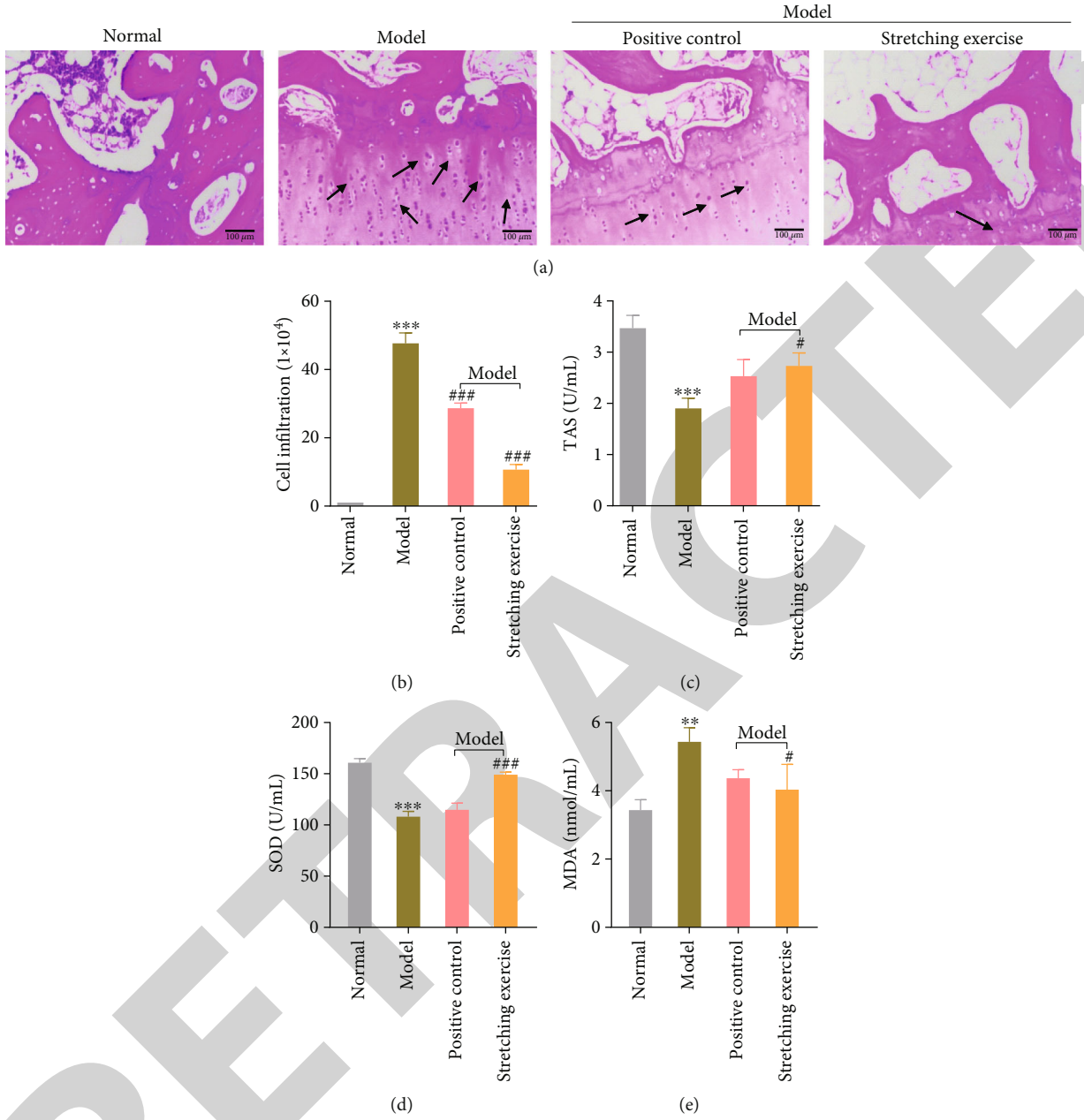

Figure 1: Effect of stretching exercise on pathological changes in the Achilles tendon of each group of AS mice. Forty DBA/1 mice were randomly divided into four groups ($n = 10$/group): the normal mouse group (namely, normal group), unprocessed AS model mouse group (namely, model group), AS model mice receiving routine nursing care+pressure-relief stretch used as a control group (namely, positive control group), and AS model mice treated with routine nursing care+pressure-relief stretch+simulated stretching training (namely, stretching exercise group). (a) Pathological observation of the Achilles tendon using H&E staining method to detect osteogenesis. Arrows (in black) indicate the locations of the infiltration of inflammatory cells, fibroblasts, and cartilage and bone formation. Bar: 100 μm. (b) Cell infiltration in different groups was detected. (c–e) The effect of stretching exercise on the antioxidant capacity of AS mice. The serum TAS (c), SOD (d), and MDA (e) levels were determined and compared between different groups of DBA/1 mice. Data are representative of three independent experiments. Data are presented as means ± SD. Comparisons between multiple groups were analysed using one-way ANOVA followed by a post hoc test (Tukey's test). $^{**}P < 0.01$ and $^{***}P < 0.001$ vs. control; $^{\#}P < 0.05$ and $^{\#\#\#}P < 0.001$ vs. model.

3. Results

3.1. Stretching Exercise Reverses the Pathological Damage to Bone Tissues in AS Mice. The Achilles tendon showed no infiltration of inflammatory cells and fibroblasts and a normal morphological structure in the normal group. The model group presented varying degrees of cartilage and bone formation, inflammatory cells, and fibroblast-like infiltration of attachment points. The mice in the stretching exercise group had small Achilles tendon tissues that more frequently

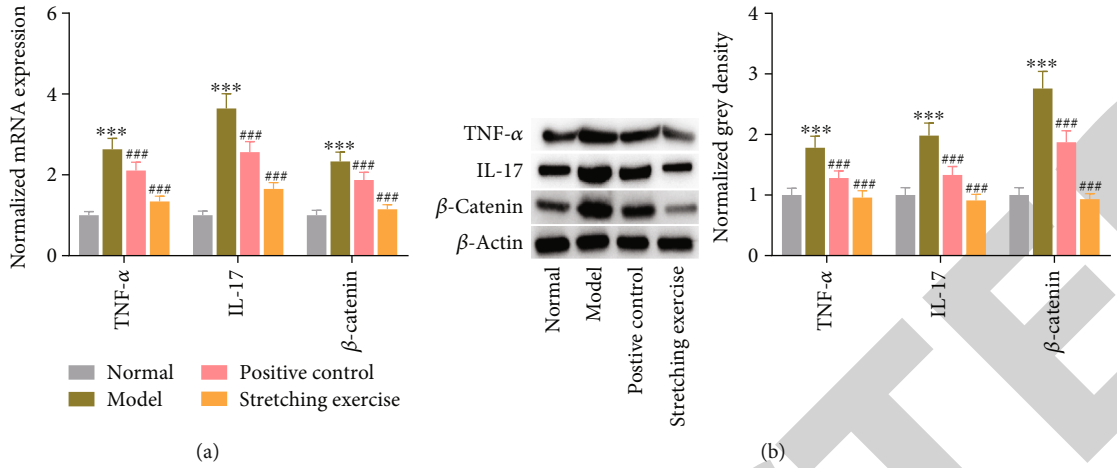

(a) (b)

FIGURE 2: Stretching exercise downregulates the expression of β-catenin and inflammatory factors in AS mice. (a) TNF-α, β-catenin, and IL-17 mRNA expression levels were detected using RT-qPCR. (b) Protein expression levels were detected using Western blot assays. Mouse β-actin was used as an internal reference. Data are representative of three independent experiments. Data are presented as means ± SD. Differences and comparisons between multiple groups were analysed using one-way ANOVA followed by a post hoc test (Tukey's test). $^{***}P < 0.001$ vs. control; $^{###}P < 0.001$ vs. model.

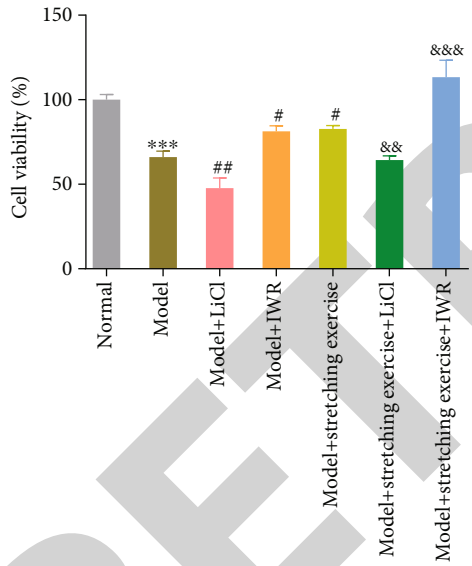

FIGURE 3: The effect of stretching exercise treatment on the survival rate of synovial cells was determined using the MTT assay. Synovial cells were extracted from the ankle joint tissues of mice (normal, model, and model+stretching exercise). Cells in the model and model+stretching exercise groups were treated with LiCl or IWR. All experiments were performed in triplicates, and data are representative of three independent experiments. Data are presented as means ± SD. Differences and comparisons between multiple groups were analysed using one-way ANOVA followed by a post hoc test (Tukey's test). $^{***}P < 0.001$ vs. control; $^{#}P < 0.05$ and $^{##}P < 0.01$ vs. model; $^{&&}P < 0.01$ and $^{&&&}P < 0.001$ vs. model+stretching exercise.

contained scattered infiltrating lymphocytes, and cartilage and bone formation were rare (Figures 1(a) and 1(b)). Therefore, the therapeutic effect on the stretching exercise group was better than that on the normal group. These results indicate that stretching exercise reverses pathological injuries in an AS mouse model.

3.2. Stretching Exercise Increases the Antioxidant TAS of AS Mice by Upregulating SOD Expression and Inhibiting MDA Expression. We examined the antioxidant effect of stretching exercise on mice with AS and found a significantly lower serum level of the antioxidant TAS in model mice than in normal mice, while mice in the stretching exercise group had significantly increased TAS levels (Figure 1(c)). Based on these results, stretching exercise improves the antioxidant capacity of AS mice. We further measured the serum SOD and MDA levels in each group of mice to verify the effect of stretching exercise on the antioxidant capacity of AS mice. The serum level of the antioxidant SOD was significantly decreased in the model group when compared with the normal mice (Figure 1(d)). However, after stretching exercise treatment, AS mice exhibited a significant increase in SOD levels compared with the model group (Figure 1(d)). The MDA levels were also determined in mice of each group. Serum levels of the MDA in mice from the model group were significantly higher than those in healthy subjects (Figure 1(e)). However, stretching exercise treatment significantly decreased MDA levels in AS model mice (Figure 1(e)).

3.3. Stretching Exercise Downregulates the Wnt/β-Catenin Signalling Pathway in AS Mice and Inhibits the Expression of Inflammatory Factors. Total RNA and proteins were extracted from mouse plasma samples, and the relative mRNA expression levels of inflammation-related factors were detected using RT-qPCR. As shown in Figure 2(a), compared with the normal group, the expression levels of TNF-α and IL-17 in the model group were increased significantly and were then significantly reduced after stretching exercise. Meanwhile, the expression level of the β-catenin mRNA in the model group was significantly higher than that

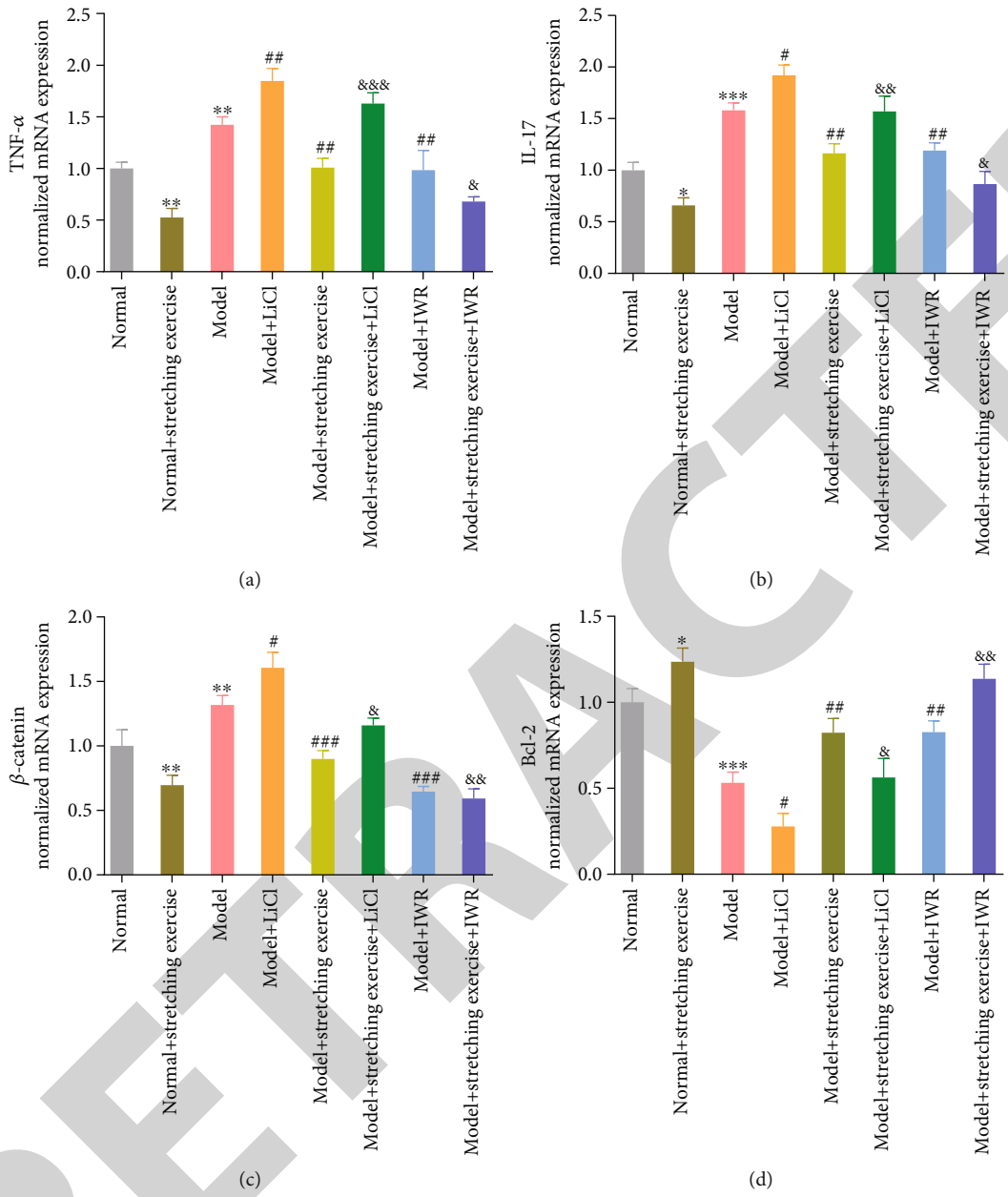

Figure 4: Expression of target genes in the Wnt/β-catenin signalling pathway. Total RNA was extracted from synovial cells from mice in four groups (normal, normal+stretching exercise, model, and model+stretching exercise). Cells in the model and model+stretching exercise groups were treated with LiCl or IWR. (a) TNF-α, (b) IL-17, (c) β-catenin, and (d) Bcl-2 mRNA expression levels were determined using RT-qPCR. The β-actin mRNA was used as an internal reference. All experiments were performed in triplicates, and data are representative of three independent experiments. Data are presented as means ± SD. Differences and comparisons between multiple groups were analysed using one-way ANOVA followed by a post hoc test (Tukey's test). $^{*}P < 0.05$, $^{**}P < 0.01$, and $^{***}P < 0.001$ vs. control; $^{\#}P < 0.05$, $^{\#\#}P < 0.01$, and $^{\#\#\#}P < 0.001$ vs. model; $^{\&}P < 0.05$, $^{\&\&}P < 0.01$, and $^{\&\&\&}P < 0.001$ vs. model+stretching exercise.

in the control group, while β-catenin expression in the stretching exercise group was significantly decreased. The relative protein levels were detected using Western blot assays (Figure 2(b)). Compared with the normal control group, the levels of inflammation-related factors TNF-α, IL-17, and β-catenin were significantly elevated in the model group, while stretching exercise reduced their levels.

3.4. Stretching Exercise Improves the Viability of Synovial Cells. We extracted synovial cells from the ankle joint tissues of mice from three groups (normal, model, and model +stretching exercise) and added LiCl (agonist of the canonical Wnt signalling) and IWR (inhibitor of the canonical Wnt signalling) to the cells of the model group and the model+stretching exercise group to study the mechanism underlying the therapeutic effect of stretching exercise on

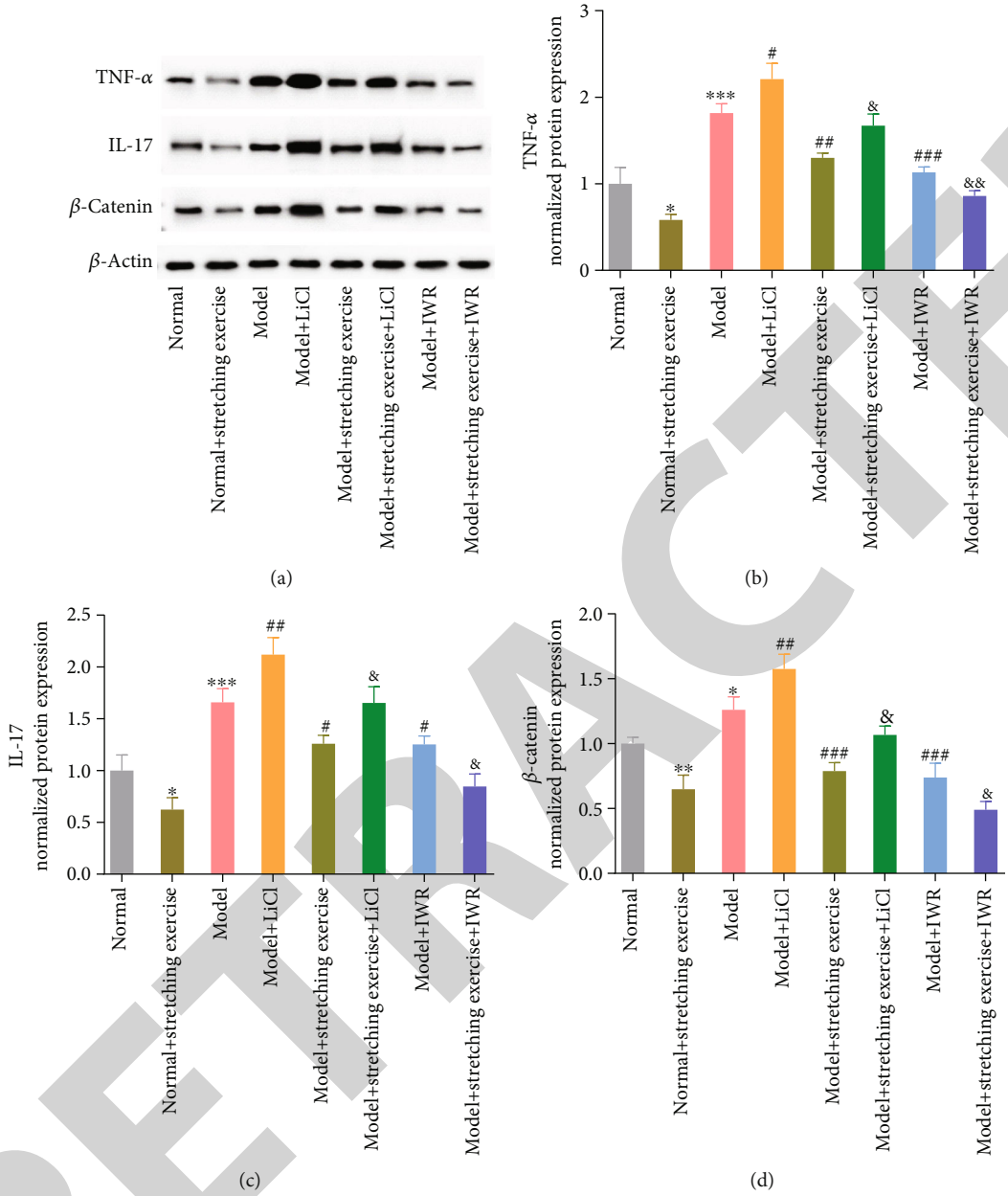

Figure 5: Western blot assay of the levels of target proteins involved in the Wnt/β-catenin signalling pathway: (a) TNF-α, IL-17, and β-catenin protein bands. (b) TNF-α, (c) IL-17, and (d) β-catenin quantified protein expression levels. The β-actin protein was used as an internal reference. Total protein was extracted from synovial cells from mice in four groups (normal, normal+stretching exercise, model, and model+stretching exercise). Cells in the model and model+stretching exercise groups were treated with LiCl or IWR. All experiments were performed in triplicates, and data are representative of three independent experiments. Data are presented as means ± SD. Differences and comparisons between multiple groups were analysed using one-way ANOVA followed by a post hoc test (Tukey's test). $^{*}P < 0.05$, $^{**}P < 0.01$, and $^{***}P < 0.001$ vs. control; $^{\#}P < 0.05$, $^{\#\#}P < 0.01$, and $^{\#\#\#}P < 0.001$ vs. model; $^{\&}P < 0.05$ and $^{\&\&}P < 0.01$ vs. model+stretching exercise.

AS. MTT results showed that cell in the model group has lower viability than that in the normal group. LiCl decreased cell viability while IWR or stretching exercise increased cell viability. Stretching simulation reversed the effect of LiCl and aggravated the effect of IWR on cell viability (Figure 3).

3.5. Stretching Exercise Shows Anti-inflammatory Effect and Inhibits Cell Apoptosis by Blocking the Wnt/β-Catenin Signalling Pathway. We extracted synovial cells from the ankle joint tissues of mice from four groups (normal, normal+stretching exercise, model, and model+stretching exercise) and added LiCl and IWR to the cells of the model group and the model+stretching exercise group. The RT-qPCR results revealed that cells in the model group showed increased TNF-α, IL-17, and β-catenin mRNA expression. Stretching exercise decreased TNF-α, IL-17, and β-catenin mRNA levels in both normal synovial cells and model cells. LiCl increased TNF-α, IL-17, and β-catenin mRNA

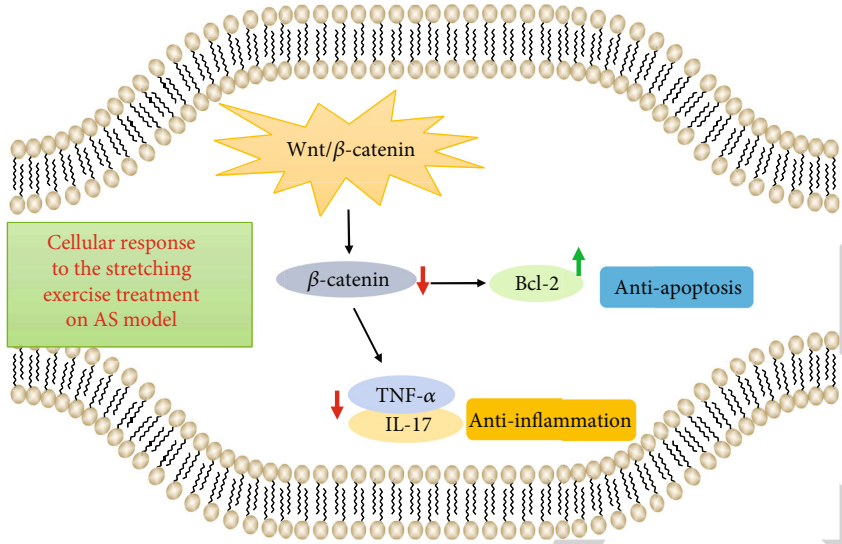

Figure 6: Summary of the cellular response and potential molecular mechanism of stretching training treatment on AS model. Stretching training treatment improved the viability of synovial cells *in vitro* and downregulated the expression of target genes in the Wnt/β-catenin signalling pathway, inhibited inflammation and cell apoptosis, and relieved pathological damages in bone tissue in DBA/1 mice of AS.

expression while IWR decreased TNF-α, IL-17, and β-catenin mRNA expression in model cells. Stretching exercise rescued the effects of LiCl and aggravated the effects of IWR on TNF-α, IL-17, and β-catenin mRNA expression in model cells (Figures 4(a)–4(c)). Figure 4(d) revealed that cells in the model group showed decreased Bcl-2 mRNA expression. Stretching exercise increased Bcl-2 mRNA in both normal synovial cells and model cells. LiCl decreased Bcl-2 mRNA expression while IWR increased Bcl-2 mRNA expression in model cells. The stretching exercise rescued the effects of LiCl and aggravated the effects of IWR on Bcl-2 mRNA expression in model cells. Western blotting was further conducted to reveal the protein levels of TNF-α, IL-17, and β-catenin, and the results were the same as the RT-qPCR results (Figures 5(a)–5(d)). These results indicated that stretching training shows an anti-inflammatory effect and inhibits cell apoptosis by blocking the Wnt/β-catenin signalling pathway.

4. Discussion

AS is a systemic disease that is mainly caused by chronic inflammation of the joints [24, 25]. Its incidence is mostly related to specific genetic factors, endocrine disorders, autoimmune function, and the external environment [26]. The cause of the disease has not been elucidated. Currently, clinicians generally believe that early and timely treatment and effective control of disease progression are particularly important for patients [26]. Stretching training is important for fitness exercises because it relieves fatigue symptoms, accelerates the rate of lactic acid decomposition in the body after exercise, and fully stretches muscle tissue [27, 28], along with reducing the incidence of sports injuries, preventing blood stasis, and ensuring the safety of sports while enhancing the body's ability in all aspects [29]. The body should not feel pain during stretching training [30]. Usually, when the body feels comfortable, a sufficient approach is to ensure that the muscles have a certain degree of tension. Studies have shown that stretching training exerts a good therapeutic effect on AS [31, 32].

In this paper, DBA/1 mice were used as a focus for follow-up research to verify the specific mechanism by which stretching training inhibits inflammation and apoptosis through the Wnt/β-catenin signalling pathway. AS is a type of rheumatism characterized by chronic inflammation of the axial joint and may involve the internal organs and other tissues [33]. TNF-α, IL-6, IL-8, and IL-17 have been identified to be overexpressed in AS patients [34]. Furthermore, in AS patients, neutrophils are activated so that reactive oxygen species are generated, resulting in oxidative stress [35]. Naringin represses AS progression via inhibiting inflammation and oxidative stress in mice [36]. We found that stretching training effectively improves the antioxidant capacity of AS mice and effectively alleviates inflammation associated with AS. It reduces the pathological damage of AS and downregulates TNF-α, IL-17, and β-catenin expression. The Wnt pathway has been confirmed to be closely associated with AS development [37]. For example, miR-148a-3p facilitates osteogenic differentiation of fibroblasts in AS by activating the Wnt pathway and targeting DKK1 [38]. miR-22-3p by M2 macrophage-derived extracellular vesicles facilitates the development of AS through the Wnt/β-catenin pathway [39]. We subsequently extracted synovial cells from DBA/1 mice and treated some cells with Wnt/β-catenin inhibitor or agonist. Compared with the model group, the expression of the TNF-α, IL-17, and β-catenin was increased by LiCl and decreased by IWR. Stretching exercise rescued the effects of LiCl and aggravated the effects of IWR on TNF-α, IL-17, and β-catenin expression. Expression of antiapoptotic factor Bcl-2 showed the opposite trend under the same treatment. These results indicated that the therapeutical effect of stretching exercise on AS is mediated

by the Wnt/β-catenin axis. Stretching exercise inhibits cell inflammation and apoptosis through blocking the Wnt/β-catenin signalling pathway.

Based on this study, stretching exercise could significantly improve the antioxidant capacity of AS mice by increasing the serum level of TAS, SOD, and MDA *in vivo*. This provides an interesting point worthy of discussion and further investigation. Many diseases, such as cardiovascular diseases, neurodegenerative disease, cancer, diabetes, atherosclerosis, inflammatory diseases, and premature aging, are all related to oxidative stress [40]. However, there is little information available on the potential indicators for the application of stretching exercise in the treatment of oxidative stress-related diseases, and few mechanisms have been excavated. Therefore, our results might enlighten the research and clinical treatment of oxidative stress-induced bone-related diseases and have a certain significance of reference for other oxidative stress-induced diseases.

In summary, we experimentally verified the regulatory effect of stretching exercise on Wnt/β-catenin signalling and its inhibition of inflammation and the occurrence of apoptosis. Stretching exercise improves the antioxidant capacity of AS mice by regulating Wnt/β-catenin signalling (Figure 6). Our results indicated that stretching exercise might be an effective therapeutical strategy for AS treatment, although further clinical evidence is needed.

Data Availability

Data analysed in the current study are available from the corresponding author on reasonable request.

Ethical Approval

All experiments were approved by the Ethics Committee of Jiangsu Province Hospital of Chinese Medicine. The experiments in this study were performed in full compliance with government policy and the Declaration of Helsinki. The contents of this study are in full compliance with government policy and the Declaration of Helsinki.

Conflicts of Interest

The authors declare that they have no competing interests.

Authors' Contributions

Yu Xie, Xiang Li, and Qiuchi Zhang contribute equally to this work.

Acknowledgments

This work was supported by the National Natural Science Foundation of China (No. 81973769).

References

[1] D. Bond, "Ankylosing spondylitis: diagnosis and management," *Nursing Standard*, vol. 28, no. 16, pp. 52–59, 2013.

[2] A. Danve, "Thoracic manifestations of ankylosing spondylitis, inflammatory bowel disease, and relapsing polychondritis," *Clinics in Chest Medicine*, vol. 40, no. 3, pp. 599–608, 2019.

[3] E. S. Rodríguez-López, V. E. Garnacho-Garnacho, J. Guodemar-Pérez, P. García-Fernández, and M. Ruiz-López, "One year of Pilates training for ankylosing spondylitis: a pilot study," *Journal of Alternative and Complementary Medicine*, vol. 25, no. 10, pp. 1054–1061, 2019.

[4] A. El Maghraoui, "Extra-articular manifestations of ankylosing spondylitis: prevalence, characteristics and therapeutic implications," *European Journal of Internal Medicine*, vol. 22, no. 6, pp. 554–560, 2011.

[5] E. B. Gouveia, D. Elmann, and M. S. Morales, "Ankylosing spondylitis and uveitis: overview," *Revista Brasileira de Reumatologia*, vol. 52, no. 5, pp. 742–756, 2012.

[6] S. Freitas, J. Vaz, P. Bruno, R. Andrade, and P. Mil-Homens, "Stretching effects: high-intensity & moderate-duration vs low-intensity & long-duration," *International Journal of Sports Medicine*, vol. 37, no. 3, pp. 239–244, 2016.

[7] A. D. Kay, J. Dixon, L. D. Bligh, and A. J. Blazevich, "The external validity of a novel contract-relax stretching technique on knee flexor range of motion," *Scandinavian Journal of Medicine & Science in Sports*, vol. 30, no. 1, pp. 74–82, 2020.

[8] A. Assumpcao, L. A. Matsutani, S. L. Yuan et al., "Muscle stretching exercises and resistance training in fibromyalgia: which is better? A three-arm randomized controlled trial," *European Journal of Physical and Rehabilitation Medicine*, vol. 54, no. 5, pp. 663–670, 2018.

[9] R. M. Ruivo, P. Pezarat-Correia, and A. I. Carita, "Effects of a resistance and stretching training program on forward head and protracted shoulder posture in adolescents," *Journal of Manipulative and Physiological Therapeutics*, vol. 40, no. 1, pp. 1–10, 2017.

[10] D. Sharan and J. S. Rajkumar, "Physiotherapy for ankylosing spondylitis: systematic review and a proposed rehabilitation protocol," *Current Rheumatology Reviews*, vol. 13, no. 2, pp. 121–125, 2017.

[11] J. R. Millner, J. S. Barron, K. M. Beinke et al., "Exercise for ankylosing spondylitis: an evidence-based consensus statement," *Seminars in Arthritis and Rheumatism*, vol. 45, no. 4, pp. 411–427, 2016.

[12] R. Liu, X. Zhang, G. Jiang et al., "Gene-gene interaction and association of Wnt/& beta; -catenin signalling pathway gene polymorphisms with ankylosing spondylitis susceptibility in the Chinese Han population," *Autoimmunity*, vol. 52, no. 7-8, pp. 281–288, 2019.

[13] J. Liu, Q. Xiao, J. Xiao et al., "Wnt/β-catenin signalling: function, biological mechanisms, and therapeutic opportunities," *Signal Transduction and Targeted Therapy*, vol. 7, no. 1, p. 3, 2022.

[14] G. Colozza and B. K. Koo, "Wnt/β-catenin signaling: structure, assembly and endocytosis of the signalosome," *Development, Growth & Differentiation*, vol. 63, no. 3, pp. 199–218, 2021.

[15] Y. Lin, X. Liang, Y. Yao, H. Xiao, Y. Shi, and J. Yang, "Osthole attenuates APP-induced Alzheimer's disease through up-regulating miRNA-101a-3p," *Life Sciences*, vol. 225, pp. 117–131, 2019.

[16] T. Le Zou, H. F. Wang, T. Ren et al., "Osthole inhibits the progression of human gallbladder cancer cells through JAK/STAT3 signal pathway both In Vitro and In Vivo," *Anti-Cancer Drugs*, vol. 30, no. 10, pp. 1022–1030, 2019.

Hindawi
Computational and Mathematical Methods in Medicine
Volume 2023, Article ID 9878450, 1 page
https://doi.org/10.1155/2023/9878450

Retraction

Retracted: Effect of Enteral and Parenteral Nutrition Support on Pulmonary Function in Elderly Patients with Chronic Obstructive Pulmonary Disease Complicated by Respiratory Failure

Computational and Mathematical Methods in Medicine

Received 5 December 2023; Accepted 5 December 2023; Published 6 December 2023

This article has been retracted by Hindawi, as publisher, following an investigation undertaken by the publisher [1]. This investigation has uncovered evidence of systematic manipulation of the publication and peer-review process. We cannot, therefore, vouch for the reliability or integrity of this article.

Please note that this notice is intended solely to alert readers that the peer-review process of this article has been compromised.

Wiley and Hindawi regret that the usual quality checks did not identify these issues before publication and have since put additional measures in place to safeguard research integrity.

We wish to credit our Research Integrity and Research Publishing teams and anonymous and named external researchers and research integrity experts for contributing to this investigation.

The corresponding author, as the representative of all authors, has been given the opportunity to register their agreement or disagreement to this retraction. We have kept a record of any response received.

References

[1] L. Wang, W. Rui, S. Chen, Y. Li, and M. Ren, "Effect of Enteral and Parenteral Nutrition Support on Pulmonary Function in Elderly Patients with Chronic Obstructive Pulmonary Disease Complicated by Respiratory Failure," *Computational and Mathematical Methods in Medicine*, vol. 2022, Article ID 4743070, 8 pages, 2022.

Hindawi
Computational and Mathematical Methods in Medicine
Volume 2022, Article ID 4743070, 8 pages
https://doi.org/10.1155/2022/4743070

Research Article

Effect of Enteral and Parenteral Nutrition Support on Pulmonary Function in Elderly Patients with Chronic Obstructive Pulmonary Disease Complicated by Respiratory Failure

Liangge Wang,[1] **Wenxiu Rui**,[1] **Si Chen**,[2] **Yazhou Li**,[2] **and Minhuan Ren**[3]

[1]*Department of Rehabilitation Medicine, Nanjing Mingzhou Rehabilitation Hospital, Nanjing, Jiangsu 210000, China*
[2]*Department of Respiratory Medicine, Affiliated Taikang Xianlin Drum Tower Hospital, Medical School of Nanjing University, Nanjing, Jiangsu 210000, China*
[3]*Department of Internal Medicine, Nanjing Sports Institute Sports Rehabilitation Hospital, Nanjing, 210000 Jiangsu, China*

Correspondence should be addressed to Liangge Wang; 18014840168@163.com

Received 30 July 2022; Accepted 8 September 2022; Published 5 October 2022

Academic Editor: Min Tang

Objective. To investigate the effect of enteral and parenteral nutrition support (EPNS) on pulmonary function in elderly patients with chronic obstructive pulmonary disease (COPD) complicated by respiratory failure (RF). *Methods*. A total of 127 patients who underwent treatment for elderly patients with COPD complicated by RF in our hospital from February 2020 to May 2022 were collected for a retrospective analysis. There were 41 patients with enteral nutrition support (group A), 46 with parenteral nutrition support (group B), and 40 with EPNS (group C). The levels of serum albumin (ALB), prealbumin (PA), serum hemoglobin (Hb), and serum transferrin (TRF) were measured before and after nutritional support in the three groups, and the changes in pulmonary function of patients were compared. The changes in the levels of inflammatory factors and markers of oxidative stress (OS) in serum were also detected, and the incidence of adverse reactions and length of stay (LOS) were counted. *Results*. ALB, PA, Hb, and TRF levels were increased in all 3 groups after nutritional support, with the highest in group C ($P < 0.05$). Similarly, lung function was improved in all 3 groups and inflammatory factor levels and OS were suppressed, also most dramatically in group C ($P < 0.05$). There was no difference in the incidence of adverse reactions among the 3 groups, and the LOS in group C was shorter than those in groups A and B ($P < 0.05$). *Conclusion*. EPNS can effectively improve the lung function of patients with COPD combined with RF and reduce the inflammation and OS damage. It can effectively improve the therapeutic effect of patients and has great application prospects in the treatment of COPD combined with RH in the future.

1. Introduction

Chronic obstructive pulmonary disease (COPD) is a chronic inflammation of the airways caused by a variety of causes, including long-term smoking, exposure to harmful gases, and harmful particles [1]. It occurs in middle-aged and elderly people; according to the survey statistics, the global incidence of COPD over 40 years old has been as high as 9% to 10% [2]. Long-term cough, sputum, and gradual onset of wheezing after activity, shortness of breath, and decreased activity tolerance are the main clinical manifestations of COPD in the elderly, with the development of the disease, different degrees of neurological symptoms (such as insomnia, irritability, and coma), and circulatory system disorders (such as skin congestion and increased blood pressure) [3]. In most patients, COPD is often combined with other diseases with remarkable clinical symptoms, among which respiratory failure (RF) is a common complication of COPD in the elderly, increasing the disability and mortality rates of COPD and causing greater suffering and harm to the elderly [4]. At present, COPD combined with RF patients need to take antibiotics, oxygen therapy, mechanical ventilation, and other comprehensive treatment; the long treatment cycle is easy to lead to intestinal flora disorders, causing

digestion and absorption disorders; on the one hand, it affects the effect of treatment but also may cause more damage to their body [5, 6].

Nutritional support can provide COPD patients with energy and nutrients required for body metabolism and help improve patients' immune function and is a key measure to reduce nutritional loss and malnutrition in elderly patients with COPD complicated by RF [7, 8]. A review of the data revealed that enteral and parenteral nutrition support (EPNS) is a new model clinically, combining the advantages of enteral nutrition support and parenteral nutrition support, which can provide more reliable treatment coverage for patients [9]. However, the literature on research related to EPNS in elderly COPD complicated by RF is still relatively scarce and lacks reliable references.

We believe that the use of EPNS can provide patients with COPD complicated with RF a better nutritional status, thereby enhancing clinical treatment effects and improving patient outcomes. Therefore, to provide a reliable theoretical basis for the future clinical treatment of COPD with RF in the elderly, this study will analyze the application of EPNS.

2. Materials and Methods

2.1. Study Area. The study was carried out from February 2020 to July 2022.

2.2. Research Object. A total of 127 patients who underwent treatment for elderly patients with COPD complicated by RF in our hospital from February 2020 to May 2022 were collected for a retrospective analysis. There were 41 patients with enteral nutrition support (group A), 46 with parenteral nutrition support (group B), and 40 with EPNS (group C). This study was approved by the medical ethics committee.

2.3. Exclusion and Inclusion Criteria. The inclusion criteria are as follows: patients diagnosed with COPD complicated by RF [10] by our hospital; patients with complete medical records, age > 65 years, patients which agreed to cooperate and participate in our medical staff arrangements, patients which might receive parenteral and enteral nutrition support, and patients or their immediate family members having signed an informed consent form. The exclusion criteria are as follows: patients with other malignancies, patients with multiple chronic diseases, patients with other cardiovascular diseases, patients with organ dysfunction, patients with drug allergies, patients with mental illness or physical disability who cannot take care of themselves, and patients who were transferred to another hospital.

2.4. Treatment Methods. All three groups of patients were admitted to the hospital to receive uniform conventional treatment, such as anti-infection, sputumification, antispasmodic and asthma, correction of water-electrolyte disorders, and maintenance of acid-base balance. Group A received enteral nutrition support on this basis with enteral nutrition suspension (enteral nutritional suspension (TPF)) 500 mL (1.5 kcal/mL), purchased from NUTRICIA (Wuxi). A feeding tube was implanted into the upper portion of the stomach, duodenum, or jejunum before connection, with an energy density of 1 Kcal/mL. The initial rate should be slow, with a normal rate of 100 to 125 mL/h, and the dose adjusted according to the condition of patients. Patients' gastrointestinal tolerance and timely intervention were assessed regularly. Group B received parenteral nutrition support based on conventional treatment, using a central venous puncture cannula, prepared from sugar, fat, amino acids, electrolytes, vitamins, trace elements, phosphorus preparations, sodium heparin, insulin, and ranitidine preparations, with a pump rate of 50–80 mL/h and a total volume of 700–1500 mL/d. Group C received EPNS based on conventional treatment. Firstly, patients were given enteral nutritional support to supplement the set standard energy value and the shortage was completed by parenteral nutritional support until the energy supplementation standard was fully satisfied and then stopped.

2.5. Testing Indexes

(1) Changes in nutritional parameters [11] before and after nutritional support in three groups of patients, including serum albumin (ALB), prealbumin (PA) levels (fully automated biochemical analyzer), serum hemoglobin (Hb) levels (fully automated hematocrit analyzer), and serum transferrin (TRF) levels (ARRAY 360 special protein analyzer)

(2) Changes in pulmonary function parameters [12] before and after nutritional support in the three groups, including left ventricular ejection fraction (LVEF) (cardiac ultrasound), forced expiratory volume in the first second (FEV1), forced expiratory volume in 1 second percentage (FEV1%) predicted (FEV1%pred), and forced expiratory volume in 1 second (FEV1) and forced vital capacity (FVC) (FEV1/FVC) (FGC-A spirometer)

(3) Changes in inflammatory factors, including serum tumor necrosis factor α (TNF-α), high-sensitive C-reactive protein (hs-CRP), calcitoninogen (PCT), and interleukin 10 (IL-10) levels (enzyme-linked immunosorbent assay), before and after nutritional support in the three groups of patients

(4) Oxidative stress indicators [13], including superoxide dismutase (SOD) and malondialdehyde (MDA) (enzyme-linked immunosorbent assay)

(5) Incidence of complications during treatment in the three groups of patients (incidence = number of complications/total number × 100%)

(6) LOS in the three groups of patients

2.6. Statistical Methods. The data were statistically analyzed via SPSS 23.0 statistical software. The counting data were expressed as the rate, and the measurement data were represented as mean ± standard deviation. The counting data were assessed through chi square, and one-way ANOVA and LSD post hoc tests were used for comparison between

Table 1: Comparison of three groups of baseline data.

Group	n	Age	Sex (male/female)	Course of disease (years)	Comorbidities (hypertension/diabetes)	Nationality (Han/minority)
Group A	41	69.9 ± 3.5	23 (56.1)/18 (43.9)	6.7 ± 1.4	10 (24.4)/9 (21.6)	37 (90.2)/4 (9.8)
Group B	46	70.0 ± 3.9	25 (54.3)/21 (45.7)	6.3 ± 1.0	11 (23.9)/8 (17.4)	41 (89.1)/5 (10.9)
Group C	40	70.8 ± 3.1	19 (47.5)/21 (52.5)	6.2 ± 1.2	9 (22.5)/7 (17.5)	36 (90.0)/4 (10.0)
χ^2/F		0.796	0.674	1.985	0.492	0.034
P		0.454	0.614	0.142	0.974	0.984

multiple groups. Differences were considered statistically remarkable at $P < 0.05$.

3. Results

3.1. Summary of Results. ALB, PA, Hb, and TRF levels were increased in all 3 groups after nutritional support, with the highest in group C ($P < 0.05$). Inflammatory factor levels and OS were suppressed, also most dramatically in group C ($P < 0.05$). The LOS in group C was shorter than those in groups A and B ($P < 0.05$).

3.2. Comparison of Three Groups of Baseline Data. Baseline data were collected and collated from patients in groups A, B, and C. Statistical analysis was performed to compare the age, gender, course of disease, number of hypertension/diabetes comorbidities, and nationality of patients in the three groups. It manifested that all three groups saw no statistically obvious differences ($P > 0.05$, Table 1), suggesting that patients were comparable.

3.3. Changes in Nutritional Indexes before and after Nutritional Support in Three Groups. There was no difference in ALB, PA, Hb, and TRF levels among the three groups before nutritional support ($P > 0.05$); ALB was higher in group C (39.27 ± 1.98 g/L) than in group B (34.08 ± 2.21 g/L) after nutritional support, while ALB was higher in group B than in group A ($P < 0.05$, Figure 1(a)). PA levels increased in all three groups after nutritional support, and the level in group C (266.21 ± 35.78 mg/L) was higher than those in the other two groups ($P < 0.05$, Figure 1(b)). The Hb levels of the three groups were the same as the above, and the level in group C (122.84 ± 5.47 g/L) was higher than that in group B (114.11 ± 5.96 g/L) versus group A (103.36 ± 6.77 g/L) after nutritional support ($P < 0.05$, Figure 1(c)). Finally, the TRF test revealed that group C was also higher than groups B and A after nutritional support ($P < 0.05$, Figure 1(d)).

3.4. Changes in Pulmonary Function Indexes before and after Nutritional Support in Three Groups. There was no difference in pulmonary function indexes between the three groups before nutritional support ($P > 0.05$), and they all increased after nutritional support ($P < 0.05$). LVEF, FEV1, EEV1, and FEV1/FVC were 52.75 ± 1.74%, 2.13 ± 0.46%, 70.13 ± 5.25%, and 73.48 ± 7.80%, respectively, higher in group C than in the other two groups after nutritional support ($P < 0.05$), whereas there was no difference between groups A and B ($P > 0.05$, Figures 2(a)–2(d)).

3.5. Changes in Inflammatory Factors before Nutritional Support in Three Groups. Similarly, there was no difference in inflammatory factor levels in all 3 groups before nutritional support ($P > 0.05$) and TNF-α was 92.29 ± 8.24 ng/L in group C after nutritional support, which was higher than those in groups A and B ($P < 0.05$, Figure 3(a)). And hs-CRP in group C was 6.08 ± 1.15 mg/L, again the lowest of the 3 groups ($P < 0.05$, Figure 3(b)). PCT was also higher in groups A and B than in group C when the 3 groups were compared ($P < 0.05$, Figure 3(c)), while the IL-10 levels in the 3 groups revealed that group C was lower than groups A and B ($P < 0.05$, Figure 3(d)). TNF-α, hs-CRP, PCT, and IL-10 were lower in all 3 groups after nutritional support than before nutritional support ($P < 0.05$).

3.6. Comparison of Oxidative Stress Response before and after Nutritional Support in Three Groups. SOD were 40.61 ± 16.53 U/mL, 41.23 ± 17.39 U/mL, and 57.06 ± 14.72 U/mL in groups A, B, and C, respectively, after nutritional support, which was higher than before nutritional support, with the highest in group C ($P < 0.05$, Figure 4(a)), while MDA was 5.84 ± 1.55 μmol/L, 5.90 ± 1.51 μmol/L, and 5.16 ± 1.16 μmol/L in the 3 groups after nutritional support, all of which were lower than before support, with group C being the lowest ($P < 0.05$, Figure 4(b)).

3.7. Incidence of Adverse Reactions during Treatment in the Three Groups of Patients. During the treatment period, the incidence of adverse reactions was 9.76% in group A, 21.74% in group B, and 12.50% in group C. There was no statistically marked difference in the incidence of adverse reactions among the three groups ($P > 0.05$, Table 2).

3.8. Comparison of LOS between the Three Groups. Statistically, the LOS was 13.83 ± 2.07 d in group A, 13.70 ± 1.82 d in group B, and 10.13 ± 1.71 d in group C. Statistical analysis denoted no difference in LOS between patients in groups A and B ($P > 0.05$), while it was lower with group C than with groups A and B ($P < 0.05$, Figure 5).

4. Discussion

COPD is one of the diseases with high morbidity and mortality worldwide, and its mortality rate is even higher than that of some malignant diseases [14, 15]. For COPD patients

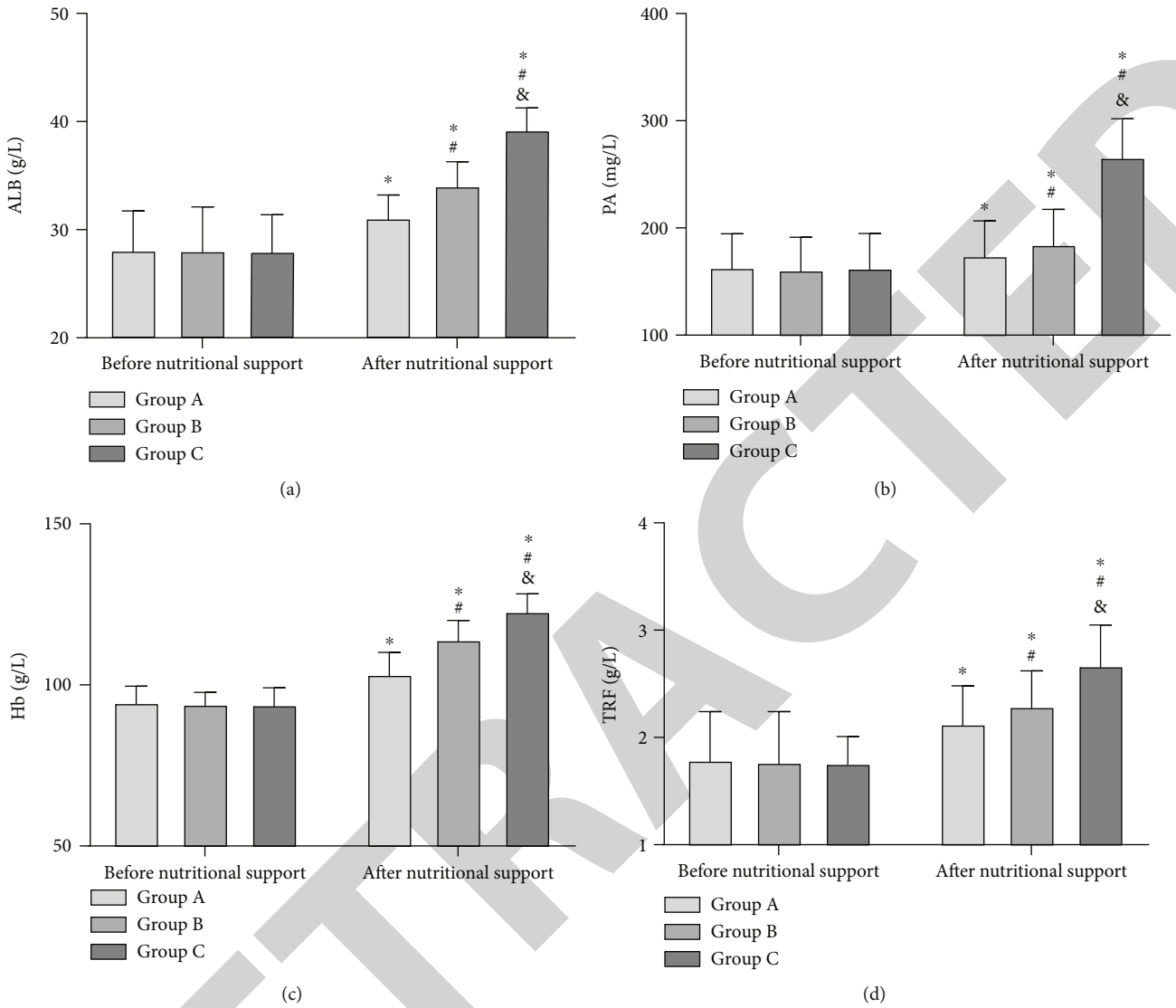

Figure 1: Changes in nutritional indexes before and after nutritional support in three groups. (a) Changes in ALB before and after nutritional support in three groups. (b) Changes in PA before and after nutritional support in three groups. (c) Changes in Hb before and after nutritional support in three groups. (d) Changes in TRF before and after nutritional support in three groups. *Comparison with the same group before treatment ($^{*}P < 0.05$); $^{\#}$comparison with group A after the treatment ($^{\#}P < 0.05$); $^{\&}$comparison with group B after the treatment ($^{\&}P < 0.05$).

with concomitant RF, the progression is more aggressive and the prognostic mortality is further increased [16]. How to effectively relieve patients' clinical symptoms and improve their prognosis has become a hot spot and a difficult task in modern clinical work. The use of nutritional support in COPD is gradually gaining clinical attention. At present, the effectiveness of conventional enteral and parenteral nutrition support in COPD has been verified several times but there is room for further improvement in both. For example, Singer found that enteral nutrition support can help reduce systemic inflammatory response in intensive care unit (ICU) patients but long-term use will lead to the decline of organ function [17]. Senkal et al. stated that parenteral nutrition support is suitable for long-term use after gastrointestinal surgery, but the incidence of complications and adverse reactions in patients has a certain trend of increasing [18]. EPNS, a nutritional support regimen that combines the advantages of enteral and parenteral nutritional support, has achieved remarkable results in the treatment of diseases such as pneumonia [19, 20]. If the application effect on patients with COPD complicated with RF can be confirmed, it will effectively improve the therapeutic effect of COPD complicated with RF and improve the prognosis of patients, which has extremely important clinical significance.

ALB, TF, PA, and Hb, as nutrients in the human body, have multiple processes involved in substance synthesis, maintenance of osmolality, and promotion of erythrocyte maturation and protein metabolism [21–23]. In contrast, ALB, TF, PA, and Hb were effectively elevated in patients with COPD combined with RF under the three nutritional support regimens of enteral, parenteral, and EPNS, with

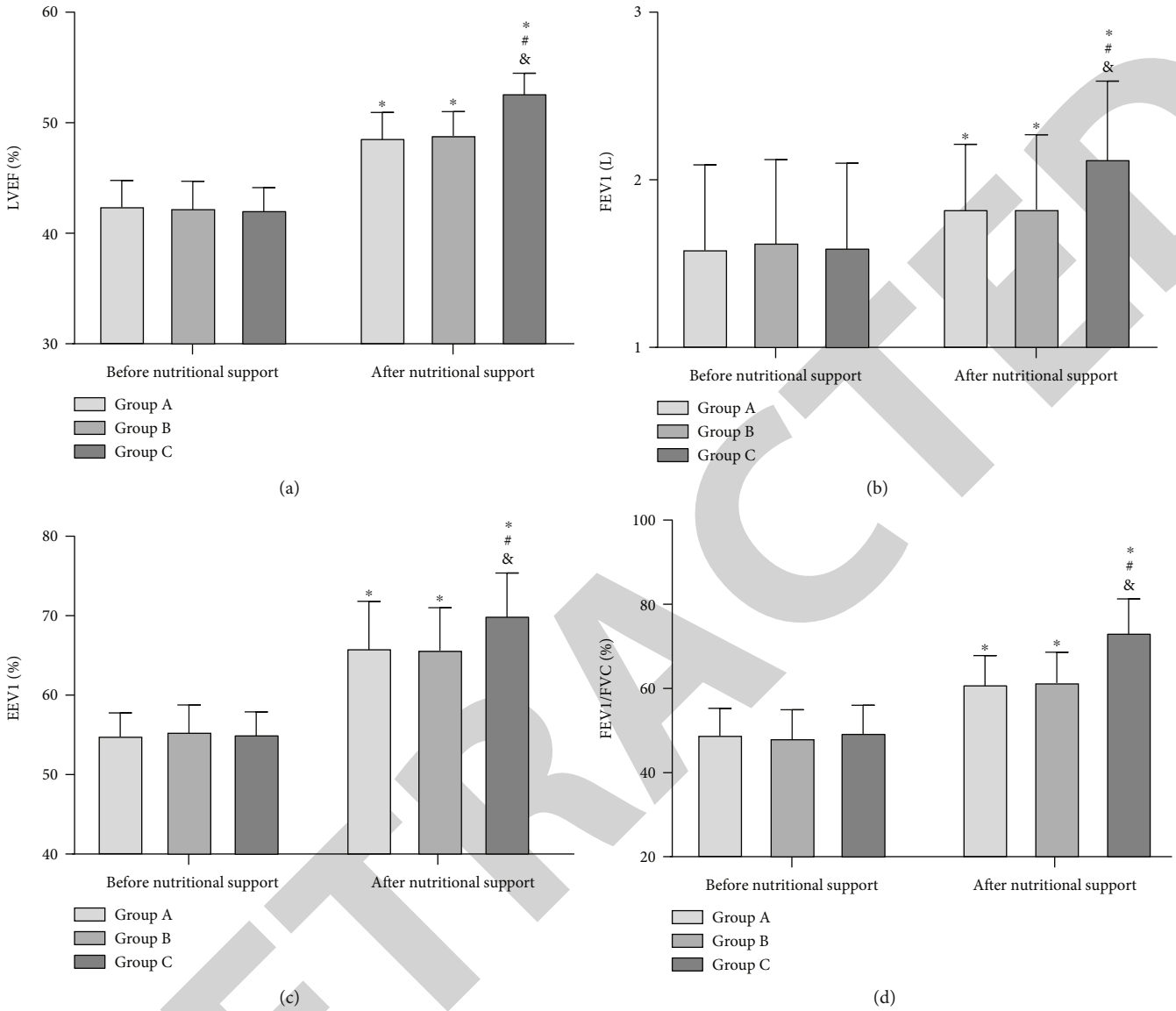

Figure 2: Changes in pulmonary function indexes before and after nutritional support in three groups. (a) Changes in LVEF before and after nutritional support in three groups. (b) Changes in FEV1 before and after nutritional support in three groups. (c) Changes in EEV1 before and after nutritional support in three groups. (d) Changes in FEV1/FVC before and after nutritional support in three groups. * Comparison with the same group before treatment ($^{*}P < 0.05$); # comparison with group A after the treatment ($^{\#}P < 0.05$); & comparison with group B after the treatment ($^{\&}P < 0.05$).

the most remarkable tips in group C patients using EPNS, which is also consistent with the results of previous studies [24] and can confirm the value of EPNS in COPD. It is well known that enteral nutrition support is supplemented by oral and nasal feeding into the gastrointestinal tract for digestion and absorption, which effectively protects the function of the gastrointestinal tract, reduces the occurrence of systemic inflammatory reactions and multiorgan failure, and enables COPD patients to get offline as much as possible [25]. However, there are problems of intolerance and underfeeding, which make it difficult to rapidly improve the nutritional status of patients with AECOPD [26]. Parenteral nutrition support is supplemented through blood circulation; although it provides more adequate nutrients, it increases the intestinal burden of patients and is less safe [27]. EPNS combines the advantages of both nutritional support regimens, giving the organism sufficient nutritional supply based on safeguarding the function of the gastrointestinal tract [28]. Thus, the nutritional status of patients is more markedly improved. In addition, because of the severity of symptoms in patients with COPD combined with RF, mechanical ventilation is often required and invasive procedures are accompanied by severe stress and immune damage [29]. Therefore, patients' pulmonary function, inflammation, and stress injury are also worthy of clinical attention. In this study, we saw an increase in pulmonary function and a decrease in inflammation and OS in all three groups after treatment, again most significantly in group C, further

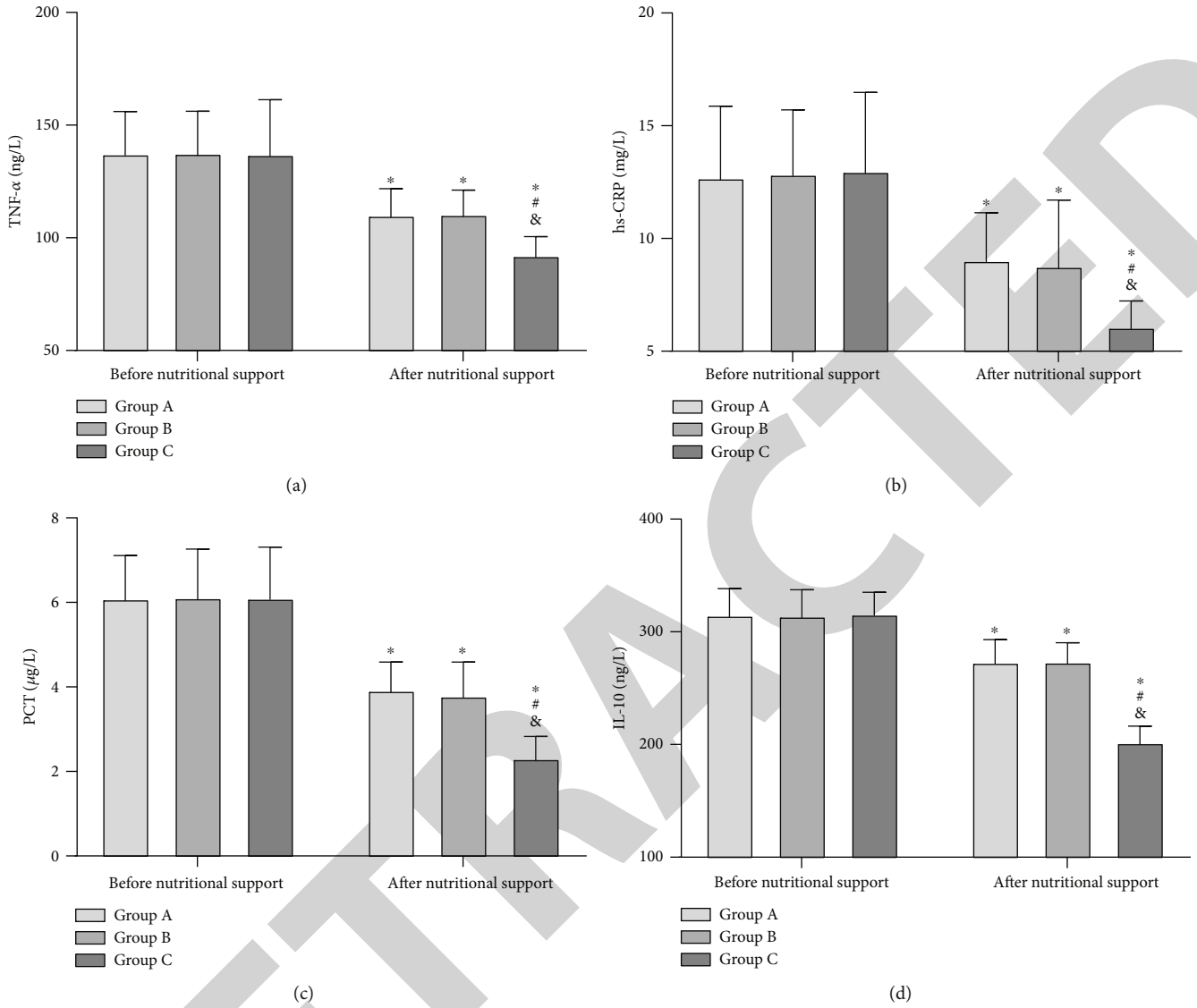

Figure 3: Changes in inflammatory factors before nutritional support in three groups. (a) Changes in TNF-α before and after nutritional support in three groups. (b) Changes in hs-CRP before and after nutritional support in three groups. (c) Changes in PCT before and after nutritional support in three groups. (d) Changes in IL-10 before and after nutritional support in three groups. *Comparison with the same group before treatment ($^{*}P < 0.05$); $^{\#}$comparison with group A after the treatment ($^{\#}P < 0.05$); $^{\&}$comparison with group B after the treatment ($^{\&}P < 0.05$).

demonstrating the excellent results of EPNS application. It has been noted in previous studies that EPNS leads to an increase in nutrients in patients, the recovery of the body's immune system, and the enhancement of their immunity [30]. In COPD patients, the use of EPNS is also more effective in improving ventilation and reducing ventilator dependence, thus improving patients' recovery more comprehensively. The difference in adverse effects was seen when comparing the three groups of patients, which also indicates that EPNS has a high-safety profile and can be promoted in COPD patients. Nevertheless, this may also be a statistical calculation chance due to the small number of cases included in this study, which requires our subsequent validation and analysis. Finally, the LOS of patients in group C was reduced, which also once again verified that EPNS could not only improve patients' recovery but also shorten their recovery period and provide a more reliable prognosis. In previous studies, we found that the application of EPNS has an excellent effect on improving the prognosis and quality of life of patients. This is because EPNS helps to promote the recovery of various body functions in patients and can create a good environment for the normal functioning of organ functions [31, 32]. For COPD with the possibility of recurrent attacks, the use of EPNS may also reduce the prognosis of patients with disease recurrence, which is also of great significance for COPD.

The prognosis of the three groups of patients cannot be assessed at this time, because we did not perform a prognostic follow-up. In addition, in studies about enteral nutrition support, the change of intestinal flora of patients is also a

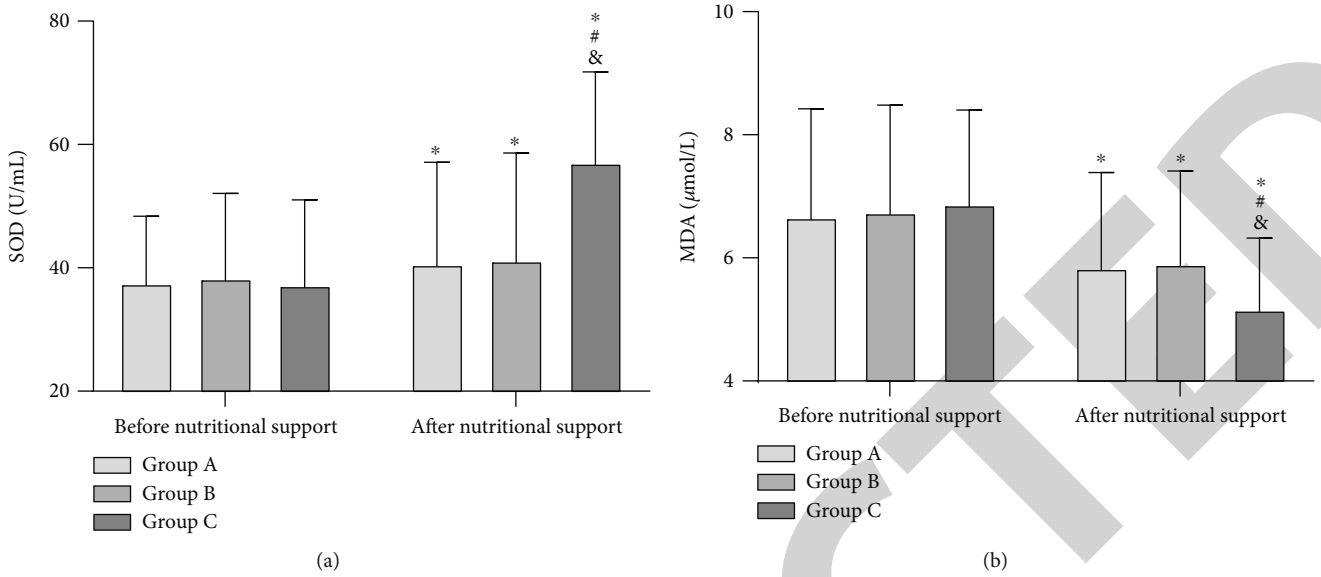

Figure 4: Comparison of oxidative stress response before and after nutritional support in three groups. (a) Changes in SOD before and after nutritional support in three groups. (b) Changes in MDA before and after nutritional support in three groups. *Comparison with the same group before treatment ($^{*}P < 0.05$); #comparison with group A after the treatment ($^{\#}P < 0.05$); &comparison with group B after the treatment ($^{\&}P < 0.05$).

Table 2: Incidence of adverse reactions during treatment in the three groups of patients.

Group	n	Bloating	Diarrhea	Metabolic complications	Infectious complications	Incidence of adverse reactions
Group A	41	1 (2.44)	1 (2.44)	2 (4.88)	0 (0.00)	9.76
Group B	46	3 (6.52)	2 (4.35)	3 (6.52)	2 (4.35)	21.74
Group C	40	2 (5.00)	2 (5.00)	1 (2.50)	0 (0.00)	12.50
χ^2						2.725
P						0.256

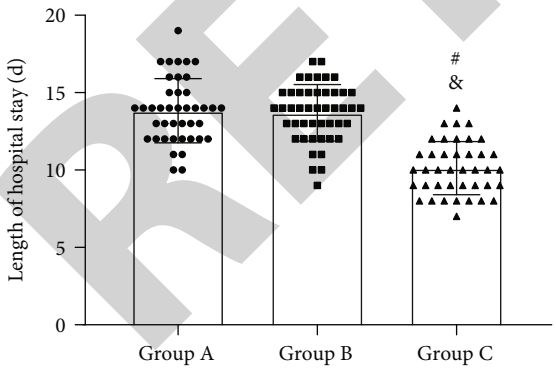

Figure 5: Comparison of LOS between the three groups. #Comparison with group A after the treatment ($^{\#}P < 0.05$); &comparison with group B after the treatment ($^{\&}P < 0.05$).

focus of attention and the analysis of intestinal flora examination was not performed, which also needs to be confirmed by our experiments as soon as possible. Besides, we still need to expand the number of cases in the study population to obtain more representative results for clinical reference.

5. Conclusion

EPNS can effectively improve the lung function of patients with COPD combined with RF, reduce the inflammation and OS damage, and provide a more reliable prognosis for patients. Hence, it is worth popularizing.

Data Availability

The datasets used and/or analyzed during the current study are available from the corresponding author upon reasonable request.

Conflicts of Interest

The authors declare that they have no conflicts of interest.

References

[1] K. F. Rabe and H. Watz, "Chronic obstructive pulmonary disease," *Lancet*, vol. 389, no. 10082, pp. 1931–1940, 2017.

[2] W. W. Labaki and S. R. Rosenberg, "Chronic obstructive pulmonary disease," *Annals of Internal Medicine*, vol. 173, no. 3, pp. ITC17–ITC32, 2020.

Hindawi
Computational and Mathematical Methods in Medicine
Volume 2023, Article ID 9864257, 1 page
https://doi.org/10.1155/2023/9864257

Retraction

Retracted: Time to First Dressing Change after Peripherally Inserted Central Venous Catheter (PICC) Insertion in Breast Cancer Patients

Computational and Mathematical Methods in Medicine

Received 12 December 2023; Accepted 12 December 2023; Published 13 December 2023

This article has been retracted by Hindawi, as publisher, following an investigation undertaken by the publisher [1]. This investigation has uncovered evidence of systematic manipulation of the publication and peer-review process. We cannot, therefore, vouch for the reliability or integrity of this article.

Please note that this notice is intended solely to alert readers that the peer-review process of this article has been compromised.

Wiley and Hindawi regret that the usual quality checks did not identify these issues before publication and have since put additional measures in place to safeguard research integrity.

We wish to credit our Research Integrity and Research Publishing teams and anonymous and named external researchers and research integrity experts for contributing to this investigation.

The corresponding author, as the representative of all authors, has been given the opportunity to register their agreement or disagreement to this retraction. We have kept a record of any response received.

References

[1] Y. Zeng, W. Li, X. Li, and L. Ma, "Time to First Dressing Change after Peripherally Inserted Central Venous Catheter (PICC) Insertion in Breast Cancer Patients," *Computational and Mathematical Methods in Medicine*, vol. 2022, Article ID 9380796, 8 pages, 2022.

Hindawi
Computational and Mathematical Methods in Medicine
Volume 2022, Article ID 9380796, 8 pages
https://doi.org/10.1155/2022/9380796

Research Article

Time to First Dressing Change after Peripherally Inserted Central Venous Catheter (PICC) Insertion in Breast Cancer Patients

Yinghua Zeng, Wenji Li, Xiaojin Li, and Lanlan Ma

Department of Breast, Southern Hospital, Southern Medical University, 6th Floor, Digestive Building, No. 1838, Guangzhou Avenue North, Baiyun District, Guangzhou, Guangdong, China

Correspondence should be addressed to Lanlan Ma; 2016122614@jou.edu.cn

Received 28 July 2022; Revised 5 August 2022; Accepted 5 September 2022; Published 3 October 2022

Academic Editor: Min Tang

Background. Peripherally inserted central catheter (PICC) is the most commonly used infusion route for chemotherapy in Chinese breast cancer patients because of its convenience, ease of operation, and many maintenance sites. *Objective*. The objective of this study is to investigate the effect of the first dressing change time on the healing of puncture site and the economic and psychological impact in patients with breast cancer after PICC insertion. *Methods*. From April 2020 to October 2020, 120 patients with PICC intubation after breast cancer surgery were selected as the research objects and divided into test group and the control group with 60 cases in each group according to the random number table method. The time of the first dressing change in the control group was routinely performed within 24 hours after PICC catheter placement, while the first dressing change in test group was performed at 48 hours after catheter placement. The effect of the first dressing change time after PICC catheterization on patients after breast cancer surgery was compared between the two groups. *Results*. There were significant differences between the two groups in the degree of pain after the first dressing change, the degree of oozing at the puncture site within 1 week, the duration of oozing, and the frequency of maintenance within 3 weeks, cost, depression, and anxiety ($P < 0.05$). *Conclusion*. The first dressing change 48 hours after PICC cauterization in patients after breast cancer surgery reduces significantly puncture site bleeding, reduces the frequency of dressing change, and benefits the physical and mental health of patients.

1. Introduction

Chemotherapy is one of the main treatment methods for breast cancer patients, but long-term chemotherapy has certain damage and stimulation to the blood vessels of patients. Peripherally inserted central catheter (PICC) is the most popular breast cancer surgery in China due to its convenience, ease of operation, and many maintenance sites. The most common route of infusion for patients after chemotherapy is PICC [1]. China's "Infusion Therapy Nursing Practice Guidelines and Implementation Rules" proposes that the puncture dressing should be changed for the first time within 24 hours after PICC catheterization [2]. However, in clinical observation, it was found that patients with breast cancer after PICC intubation often experienced different degrees of blood oozing at the puncture site for several consecutive days after 24 hours of dressing change [3]. The patient complained of pain at the puncture port and bleeding from the puncture port during the first dressing change. Frequent dressing changes also increase the patient's economic [4] and psychological stress [5, 6].

Some studies have shown that prolonging the first dressing change time of PICC in patients with hematological tumors can reduce the occurrence of bleeding at the puncture point [7]. However, the current research on the time of the first PICC dressing change has not done in-depth research on the effects of pain, psychology, and other aspects of patients. Breast cancer patients are mostly women, with low tolerance to pain, and their psychological state is easily affected by multiple factors [8], and is prone to depression, anxiety, and other emotions [9–11]. In order to improve the overall comfort of breast cancer patients undergoing chemotherapy after PICC intubation, we changed the time of the first dressing change after PICC intubation to explore its clinical, psychological, and economic effects on patients after PICC intubation.

2. Material and Methods

2.1. Research Object. Patients with postoperative breast cancer who were to undergo PICC placement from April 2020 to October 2020 in the breast department of a large comprehensive tertiary care hospital in Guangzhou, Guangdong Province, were selected for the study, and PICC placement under ultrasound guidance was performed by the same nurse. Inclusion criteria: (1) Patients with postoperative chemotherapy for breast cancer; (2) Age ≧18 years; (3) The patient agrees and cooperates with PICC; (4) The upper limb on the placement side meets the placement conditions; (5) Has basic cognitive ability and communication skills. Exclusion criteria are as follows: (1) postoperative bilateral breast cancer; (2) history of psychological disorders; (3) advanced postoperative metastasis; and (4) preoperative neoadjuvant therapy has been performed. Finally, 120 patients were obtained for the study. All study subjects were numbered according to the order of tube placement and divided into 60 cases each in the control group and test group in a 1 : 1 ratio.

2.2. Methods

2.2.1. Insertion Methods and Management. (1) Piercing nurse qualification: more than 10 years in PICC placement practice. (2) PICC: uniform manufacturer, using the 4Fr catheter made by Bard, USA. (3) Puncture site: postoperative healthy upper limb, placement vessel with your vein as the first choice, followed by the median elbow vein and brachial vein. Avoid the damaged skin vessels, and choose 4~8 cm above the elbow for puncture. (4) The procedure of tube placement: B ultrasound-guided puncture was performed using the Seldinger technique, and hemostasis was achieved with sterile gauze during tube placement. The weight of the blooded gauze was measured with an electronic scale, and the weight difference between it and the same size of dry gauze was calculated and recorded as bleeding volume. The puncture port was compressed with a 10 cm ×10 cm sterile gauze block folded in 8 layers to stop bleeding, plus IV3000 sterile transparent dressing for fixation. (5) Confirmation of catheter position: After successful placement, press the puncture site for 30 min, and go to the radiology department to take an orthopantomogram of the chest to determine the position of the catheter tip. The tip of the catheter was located in the lower 1/3 of the superior vena cava, indicating successful catheter placement. (6) Postoperative maintenance: The first changing medical dressings were performed by a trained and qualified nurse within 24-h catheter placement in the control group, while the first changing medical dressings were performed within 24-h catheter placement in the test group. Patients in both groups should be continuously observed for 3 weeks after the first changing medical dressings. If there was no bleeding from the puncture port, loosening of the patch, or discomfort of the rash at the patch, the dressing was changed once a week. Once bleeding from the puncture port is detected, the dressing should be changed at any time until the bleeding stops.

2.3. Observation Indicator. 1) Degree of bleeding at the puncture site: (i) No bleeding: no bleeding after placement; mild bleeding: a small amount of bleeding can be seen in the dressing at the puncture site after the patient is active; (ii) moderate bleeding: a small or moderate bleeding can be seen at the puncture site when lying still , but not beyond the catheter wall; (iii) Severe bleeding: massive bleeding at the puncture site can be seen along the PICC catheter wall [12]. 2) Duration of bleeding at the puncture site: (i) Grade 0: a small amount of bleeding was seen 24 hours after the dressing was placed, but no fresh blood was seen; (ii) Grade I: bleeding at the puncture site continued for 2-3 days; (iii) Grade II: bleeding at the puncture site for 4-5 days; (iv) Grade III: bleeding at the puncture site for 6 days or more [13]. Patients were assessed for pain at the puncture site at the time of the first dressing change. (4) Generalized Anxiety Disorder Questionnaire (GAD-7): This scale was developed by American scholars Pulitzer et al. [14] and Chineseized by Qu Shan and Shengli [15] and is a concise and effective anxiety self-assessment tool. The scale contains a total of 7 entries and is used to understand the patient's emotional state in the past 2 weeks. The scale is rated on a 4-point Likert scale, with 0 being "not at all," 1 being "occasionally for a few days," 2 being "often," and 3 being "Every day." The total score ranges from 0 to 21. The Bernbach's alpha coefficient was 0.898, and the retest reliability was 0.856. Patient Health Questionnaire Depression Scale (PHQ-9): this scale, developed by Williams et al. [16] and tested for reliability in Chinese version by Xu Yong et al. [17], is an important tool used to assess depression and contains a total of 9 items to evaluate the subjects' emotional state in the past 2 weeks. The scale was scored on a 4-point Likert scale, with scores ranging from 0 to 3 representing "not at all" to "every day." The total score of the scale ranged from 0 to 27. The Cronbach's alpha coefficient was 0.833, and the retest reliability was 0.801.

2.4. Statistical Analysis. SPSS 26.0 software was used for data analysis in this study, and the measurement data were expressed as mean standard deviation, and the count data were expressed as frequency and percentage. The *t*-test was used for measurement data between two groups (age, number of punctures, number of transfers, and bleeding volume); chi-square analysis was used for count data between two groups (occupation, marital status, side of placement, vascular, platelet abnormalities, and chemotherapy regimen); Wilton rank sum test was used for grade data between two groups (education, monthly income, and TNM stage); anxiety and depression scores of the same patient before and after PICC placement paired *t*-test were used for changes in anxiety and depression scores before and after PICC placement in the same patient. $P < 0.05$ was considered statistically significant.

3. Results

3.1. Comparison of General Data between Two Groups. A total of 60 cases in the control group and the test group were included in this study. The age of the control group was (45.329.0) years old, and the age of the test group was (48.489.10) years old; there was no significant difference in

Table 1: Table of general patient information [$-x \pm s$, n(%)].

Variables	Control group ($n = 60$)	Test group ($n = 60$)	P
Age (years)	45.32 ± 9.07	48.48 ± 9.10	0.059
Education level			
Illiterate	1 (1.7)	2 (3.3)	
Elementary school	14 (23.3)	12 (20.0)	
Junior high school	23 (38.3)	21 (35.0)	0.983
High school/junior college	9 (15.0)	17 (28.3)	
College and above	13 (21.7)	8 (13.3)	
Profession			
Unemployed	18 (30.0)	17 (28.3)	
Self-employed	9 (15.0)	5 (8.3)	
Business unit	7 (11.7)	3 (5.0)	0.240
Staff	20 (33.3)	26 (43.3)	
Retire	6 (10.0)	9 (15.0)	
Monthly income			
<2,000	20 (33.3)	17 (28.3)	
2,000-4,000	28 (46.7)	21 (35.0)	0.165
4,000-8,000	5 (8.3)	18 (30.0)	
>8,000	6 (10.0)	4 (6.7)	
Marriage			
Married	52 (86.7)	57 (95.0)	
Unmarried	6 (10.0)	1 (1.7)	0.128
Widowed/divorced	2 (3.3)	2 (3.3)	
Placement side			
Left	29 (48.3)	30 (50.0)	0.856
Right	31 (51.7)	30 (50.0)	
Blood vessel			
Expensive	56 (93.3)	54 (90.0)	0.511
Brachial vein	4 (6.7)	6 (10.0)	
Number of punctures	1.18 (0.54)	1.13 (0.39)	0.560
Tube times	1.26 (0.70)	1.08 (0.38)	0.093
Bleeding volume (g)	0.76 (0.40)	0.81 (0.30)	0.408
Chemotherapy			
TE	5 (8.3)	2 (3.3)	
TC	1 (1.7)	1 (1.7)	0.345
EC-T	53 (88.3)	56 (93.3)	
Other	1 (1.7)	1 (1.7)	
TNM staging			
0	0 (0.0)	3 (5.0)	
1	4 (6.7)	1 (1.7)	0.631
2	39 (65.0)	36 (60.0)	
3	17 (28.3)	20 (33.3)	

Note: TE is anthracycline combined with taxman; TC is organophosphate combined with taxman; EC-T is anthracycline combined with organophosphate followed by taxman; others are anthracycline combined with taxman followed by platinum.

education, occupation, monthly income, and marriage between the two groups; 30 (50%) cases of left upper limb cauterization in the test group. There were 30 (50%) cases of right upper extremity cauterization. 29 (48.3%) cases of left upper extremity cauterization, and 31 (51.7%) cases of right upper extremity cauterization in the control group. There were no significant differences in the anterior platelet abnormalities and blood loss during cauterization; there

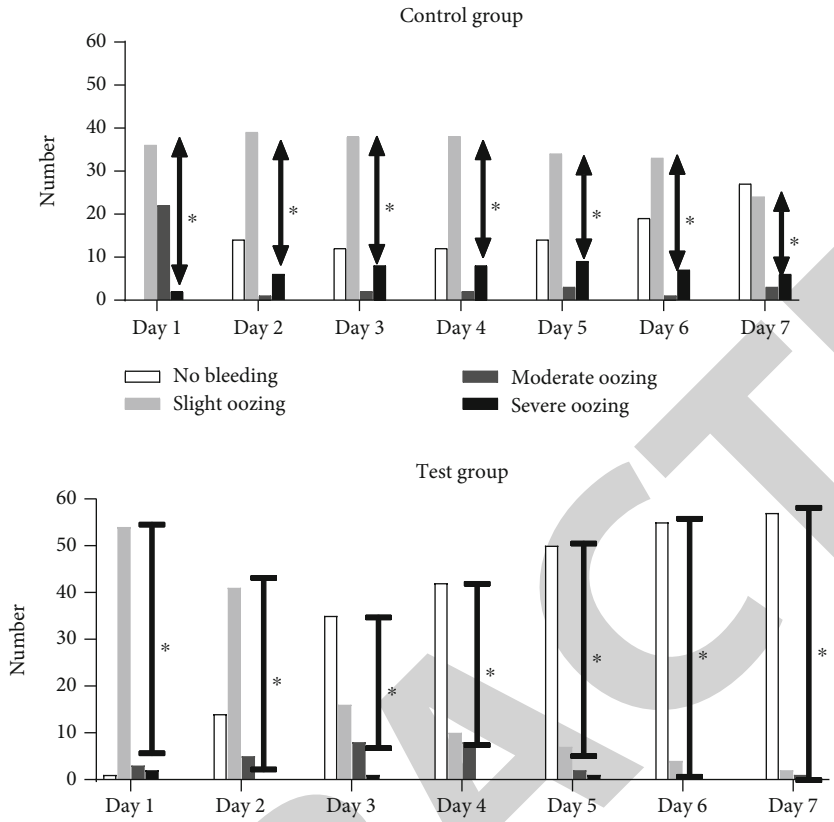

Figure 1: Comparison of the degree of bleeding at the puncture port within 1 week after catheter placement between the two groups. In our study, SPSS26.00 statistical software was used for statistical analysis and comparison of the degree of bleeding at the puncture port within 1 week after catheter placement between the two groups. Measurement data expressed as mean ± standard deviation using repeated measures analysis of variance showed that the bleeding at the puncture site was assessed and graded daily for 1 week after catheter placement in both groups. Within 1 week after catheter placement, there was a statistically significant difference between the control group and the experimental group in the degree of blood oozing at the puncture point every day ($^*P < 0.05$). The patients in the test group generally had less bleeding at the puncture site, and the proportion of patients without bleeding after cauterization was higher over time, and the difference was statistically significant ($^*P < 0.05$).

were no significant differences in disease stages and chemotherapy regimens between the two groups (see Table 1).

3.2. Comparison of Blood Oozing after PICC Incubation between Two Groups of Patients. The bleeding at the puncture site was assessed and graded daily for 1 week after catheter placement in both groups. Within 1 week after catheter placement, there was a statistically significant difference between the control group and the experimental group in the degree of blood oozing at the puncture point every day ($P < 0.05$). The patients in the test group generally had less bleeding at the puncture site, and the proportion of patients without bleeding after cauterization was higher over time, and the difference was statistically significant ($P < 0.05$) (see Figure 1).

3.3. The Duration of Bleeding at the Puncture Site and the Pain Score. In the control group, 21.7% of the patients in the control group were grade II, and 65.0% were in grade III; 28.3% of the patients in the test group were in grade II, and 5.0% were grade III. There was a statistically significant difference between the two groups in the classification of the duration of bleeding at the puncture point ($P < 0.05$). The pain score of the first dressing change in the control group was 3.28 ± 1.08 points, and the score in the test group was 1.56 ± 0.65 points (see Figure 2).

3.4. Comparison of Anxiety and Depression Scores between the Two Groups of Patients before and after Incubation. The paired t-test was used to compare the changes in the anxiety and depression scores of the two groups of patients before and after intubation. It can be seen that the anxiety and depression levels of the patients were reduced after intubation, and the difference was statistically significant ($P < 0.05$); among them, the two scores of the patients in the experimental group decreased more significantly after intubation, and the difference was statistically significant ($P < 0.05$). In the control group, there was no significant difference in anxiety scores before and after intubation ($P > 0.05$). However, the depression score was slightly increased, and the difference was statistically significant ($P < 0.05$) (see Figure 3).

3.5. Comparison of Maintenance Frequency and Maintenance Cost between Two Groups of Patients within 3 Weeks. The

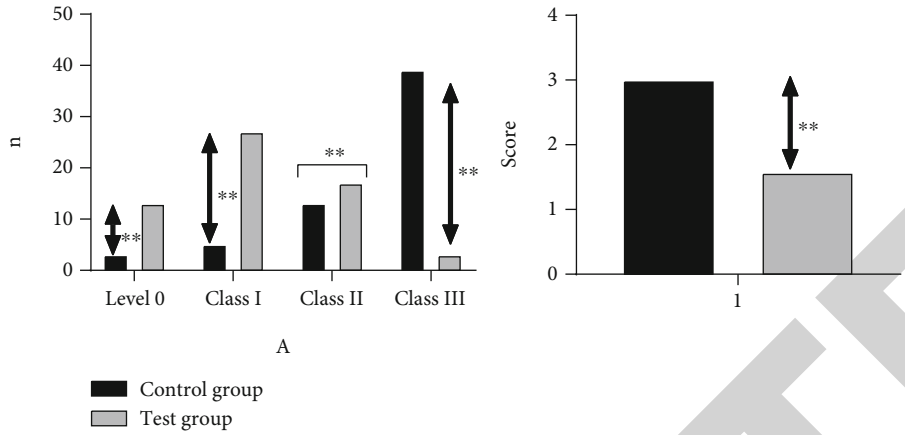

Figure 2: Puncture site oozing duration and pain score. In our study, SPSS26.00 statistical software was used for statistical analysis and puncture site oozing duration and pain score. Measurement data expressed as mean ± standard deviation using repeated measures analysis of variance showed that 21.7% of the patients in the control group were grade II, and 65.0% were grade III; 28.3% of the patients in the test group were grade II, and 5.0% were grade III. There was a statistically significant difference between the two groups in the classification of the duration of bleeding at the puncture point ($^{**}P < 0.05$). The pain score of the first dressing change in the control group was 3.28 ± 1.08 points, and the score in the test group was 1.56 ± 0.65 points. Academic differences ($^{**}P < 0.05$).

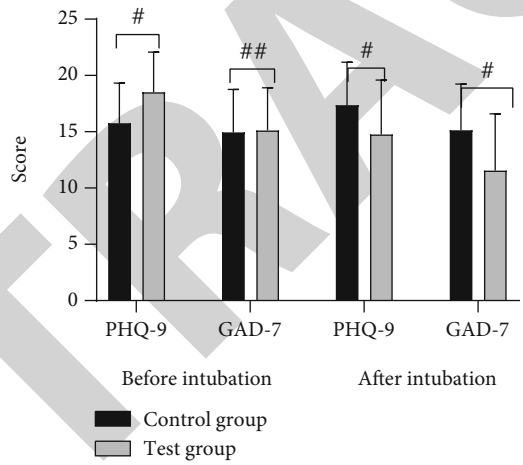

Figure 3: Comparison of anxiety and depression scores between the two groups of patients before and after incubation. In our study, SPSS26.00 statistical software was used for statistical analysis and comparison of anxiety and depression scores between the two groups of patients before and after incubation. Measurement data expressed as mean ± standard deviation using repeated measures analysis of variance showed that the changes in anxiety and depression scores of the two groups of patients before and after incubation were compared using paired *t*-test, as shown. The paired *t*-test was used to compare the changes in the anxiety and depression scores of the two groups of patients before and after intubation. It can be seen that the anxiety and depression levels of the patients were reduced after intubation, and the difference was statistically significant. Significant ($\#P < 0.05$); among them, the two scores of the patients in the experimental group decreased more significantly after intubation, and the difference was statistically significant ($\#P < 0.05$). In the control group, there was no significant difference in anxiety scores before and after intubation ($\#\#P > 0.05$). However, the depression score was slightly increased, and the difference was statistically significant ($\#P < 0.05$).

maintenance frequency and maintenance cost within 3 weeks were compared between the two groups, and the independent samples *t*-test was used for comparison. The maintenance frequency in the control group was higher than that in the experimental group, and the difference was statistically significant ($P < 0.05$). The maintenance cost in the control group was higher than that in the experimental group within 3 weeks, and the difference was statistically significant ($P < 0.05$) (see Table 2).

4. Discussion

4.1. Effect on Bleeding from the Puncture Site. Some investigators have shown through a study of patients with PICC placement in liver disease that changing medication at an interval of 3 days after placement can reduce the occurrence of local blood seepage [18]. The results of Chen Min et al. showed that the first change of medication 48 hours after PICC placement in patients with hematologic tumors was

Table 2: Comparison of maintenance frequency and maintenance cost of two groups of patients within 3 weeks.

Variable	Control group ($n = 60$)	Test group ($n = 60$)	P
Maintenance frequency	4.80 (1.30)	3.57 (0.85)	<0.001
Maintenance cost (yuan)	443.05 (138.23)	349.25 (86.38)	<0.001

effective in reducing the bleeding from the puncture site; the study by Ma Yujun et al. [19] compared the bleeding from the puncture site at different times after the first change of medication after placement and showed that prolonging the first change after placement was beneficial in reducing divisional bleeding. The results of Figure 2 show that the degree of bleeding at 48 hours after drug exchange in postoperative breast cancer patients after placement was generally on the mild side, and the percentage of patients who did not bleed after placement was higher over time, which is consistent with the findings of Chen Min and Ma Yujun et al. The first dressing change 48 h after PICC placement in postoperative breast cancer patients is in accordance with the guideline recommendation of 48-h change of gauze dressing [20], which can promote healing of the puncture site and reduce blood leakage from the puncture opening. The rationale is that (i) the 48-h period is still in the period of bacterial multiplication inhibition, while the prolongation of the closure time is more conducive to the repair of fiber glass and granulation tissue, and (ii) it can avoid premature destruction of the blood clot leading to re-injury of the puncture site, which can affect wound healing.

4.2. Effect on Patient Pain. This study shows that the pain score of patients who changed the dressing of the puncture port 24 h after the placement was significantly higher than that of the 48-h group. The frequent stimulation of antiseptic solution during changing medical dressings will also increase the pain of patients [21]. Therefore, extending the time of the first dressing change for patients with PICC placement after breast cancer surgery can provide longer time for the healing of the puncture port, avoid the stimulation of the wound that has not yet healed by the disinfectant solution, and reduce the pain of patients.

4.3. Psychological Impact. The diagnosis and treatment of breast cancer have a strong negative impact on patients' psychological health, triggering various negative psychological reactions such as stress, depression, and anxiety [22]. For breast cancer patients who have just undergone surgery [23], they are psychologically vulnerable, both from having a physical disability after surgery [24] and from the fear of about to start chemotherapy [25]. It has been shown that the majority of patients have anxiety after PICC placement [26], and in this study, it was found that the change in anxiety and depression scores in the control group after PICC placement in breast cancer patients generally increased by 2-3 points compared to the test group. The reasons for this may be due to the lack of knowledge about PICC placement and the restriction of limb movement on the side of the placement, which put the patients in a state of tension and anxiety, and the leakage of blood from the puncture port after placement, which further increased the depression and anxiety of the patients. Therefore, the first changing medical dressings 48 hours after PICC placement in postoperative breast cancer patients can reduce patients' depression and anxiety, which is of great significance to improve the physical and mental health of postoperative breast cancer patients. Therefore, it is especially important to take effective measures to alleviate the adverse psychological symptoms of patients after incubation. For example, ①introduce the purpose and precautions of incubation to patients before PICC placement, and at the same time, distribute graphic and easy-to-understand publicity materials to enhance the effect of education. ②Respect the patient, understand the patient's psychological state patiently before placement, and give support and encouragement. ③During incubation, pay attention to the patient's feelings, and relieve the patient's tension by chatting with the patient or playing relaxing music. ④Continue to follow up the patient after the placement of the tube, find out the complications, and deal with them in time to relieve their discomfort that may occur during the period with the tube. ⑤Social support: Care for the patient, the patient is given the necessary life care by the family during the period with the tube. Teach patients and their families how to care for them at home during PICC placement, encourage them to participate in the management of PICC catheters, and help patients gain confidence.

4.4. Economic Impact. The puncture site should be kept dry and free of blood and fluid after PICC placement. Patients in the control group were changed 24 hours after catheter placement, which led to repeated bleeding at the puncture site after the change because the puncture site had not yet healed and was stimulated by the disinfectant solution during the change. To avoid puncture site infection, the puncture site dressing had to be changed again, so the frequency of maintenance and maintenance costs was higher in the control group patients than in test group. PICC placement operators should standardize the placement process and provide comprehensive and effective health education to patients. Patients and their families should be instructed to continuously observe the puncture site to avoid adverse reactions after placement and to reduce the number and cost of additional hospital admissions for maintenance.

Shortcomings of this study: Pain and bleeding after PICC catheter placement may be related to a variety of factors. This study focused on the effect of the time of the first changing medical dressings after PICC catheter placement and failed to take into account the weight and coagulation of the enrolled patients, and this study was conducted in only one hospital with a small sample size; therefore, it needs to be tested continuously in clinical practice.

PICC catheters provide a safe and effective route to chemotherapy for oncology patients in breast units, but PICC placement requires blade dilation at the puncture port, which inevitably increases injury, and bleeding from the puncture port often occurs after placement [27], and extending the time to the first PICC changing medical dressings is important for postoperative breast cancer patients [28]. The results of this study show that the first changing medical dressings 48 hours after PICC placement in postoperative breast cancer patients can reduce the degree and duration of blood oozing from the puncture port [29].

In conclusion, the first dressing change 48 hours after PICC catheter placement in postoperative breast cancer patients can reduce bleeding at the puncture site, relieve pain, and relieve the patients' depression and anxiety. At the same time, it can also reduce the frequency of dressing changes, reduce the economic burden of patients, and improve the quality of life of patients.

Data Availability

All data used to support the findings of this study are included in the article.

Conflicts of Interest

The authors declare that they have no conflicts of interest.

Authors' Contributions

Yinghua Zeng and Wenji Li are co-first authors.

Acknowledgments

This study has been supported by the Guangdong Nursing Association Nursing Research Project (gdhlxueh2019zx022).

References

[1] L. A. Gorski, "The 2016 infusion therapy standards of practice," *Home Healthcare Now*, vol. 35, no. 1, pp. 10–18, 2017.

[2] S. Stock, R. Tebest, C. Samel et al., "Implementation of an innovative hands-on training to improve adherence to hygiene rules: A feasibility Study," *Nurse Educ Today*, vol. 36, p. 411, 2016.

[3] Q. Fang and H. Yuqing, "Cause analysis and nursing countermeasures of common complications after PICC incubation in cancer chemotherapy patients," *Electronic Journal of Practical Clinical Nursing*, vol. 3, no. 4, pp. 141–146, 2018.

[4] Y. Mengdong, "Research and effect observation of improved compression method in reducing blood leakage in patients with hematological tumors," *Modern Hospital*, vol. 13, no. 10, pp. 67–69, 2013.

[5] J P. Li, W W. Jiangg, W K. Bi et al.et al., "Feasibility analysis of external application of Xiao-Shuan-San in preventing PICC-related thrombosis," *Complement Ther Med*, vol. 52 article 102448., 2020.

[6] Z. Xiaoqin, "The effect of high-quality nursing intervention on the psychological state of PICC incubation in breast cancer patients," *Electronic Journal of Practical Clinical Nursing*, vol. 4, no. 11, pp. 36-37, 2019.

[7] E. Johansson, F. Hammarskjöld, D. Lundberg, M H. Arnlind et al., "Advantages and disadvantages of peripherally inserted central venous catheters (PICC) compared to other central venous lines: a systematic review of the literature," *Acta Oncol*, vol. 52, no. 5, p. 892, 2013.

[8] Z. Fan, M. Xin, and Y. Ping, "Research on resilience and influencing factors of breast cancer patients," *Chinese Journal of Nursing*, vol. 50, no. 9, pp. 1087–1090, 2015.

[9] P. E. Bidstrup, J. Christensen, B G. Mertz, N. Rottmann, S O. Dalton, and C. Johansen, "Trajectories of distress, anxiety, and depression among women with breast cancer: looking beyond the mean," *Acta Oncologica*, vol. 54, no. 5, pp. 789–796, 2015.

[10] C. Miaskowski, C. Elboim, S M. Paul et al., "Polymorphisms in tumor necrosis factor-α are associated with higher anxiety levels in women after breast cancer surgery," *Clinical Breast Cancer*, vol. 16, no. 1, pp. 63–71.e3, 2016.

[11] C. Tojal and R. Costa, "Depressive symptoms and mental adjustment in women with breast cancer," *Psychooncology*, vol. 24, no. 9, pp. 1060–1065, 2015.

[12] L. Xuehua and J. Lian, "Factors and preventive measures of bleeding at the puncture point of indwelling PICC tube in chemotherapy patients," *Chinese Journal of Medical Practice*, vol. 4, no. 1, 2005.

[13] C. Si, F. Yun, and C. Lanyan, "Study on the effect of three ways to prevent puncture point bleeding in patients with PICC," *China Journal of Practical Nursing*, vol. 32, no. 21, pp. 1639–1641, 2016.

[14] R. L. Pulitzer, K. Kroenke, J. B. Williams, and B. Löwe, "A brief measure for assessing generalized anxiety disorder: the GAD-7," *Archives of Internal Medicine*, vol. 166, no. 10, pp. 1092–1097, 2006.

[15] Q. Shan and Shengli, "A diagnostic test of the generalized anxiety scale for generalized anxiety disorder screening in the outpatient department of general hospital psychology," *Chinese Journal of Mental Health*, vol. 29, no. 12, pp. 939–944, 2015.

[16] R. L. Pulitzer, K. Kroenke, and J. B. Williams, "Validation and utility of a self-report version of PRIME-MD: the PHQ primary care study. Primary care evaluation of mental disorders. Patient health questionnaire," *JAMA*, vol. 282, no. 18, pp. 1737–1744, 1999.

[17] M. Alizadeh-Khoei, F. Sharifi, M E. Akbari, R. Fadayevatan, and M. Haghi, "Iranian Brief Pain Inventory: Validation and Application in Elderly People With Cancer Pain," *J Pain Symptom Manage*, vol. 54, no. 4, pp. 563–569, 2017.

[18] C. Acun, A. Baker, L S. Brown, K A. Iglesia, J. Sisman et al., "Peripherally inserted central cathether migration in neonates: Incidence, timing and risk factors," *J Neonatal Perinatal Med*, vol. 14, no. 3, pp. 411–417, 2021.

[19] J. Wasiak, H. Cleland, F. Campbell, A. Spinks et al., "Dressings for superficial and partial thickness burns," *Cochrane Database Syst Rev*, vol. 2013 article CD002106., no. 3, pp. 451–454, 2013.

[20] "2021 Infusion Therapy Standards of Practice Updates," *J Infus Nurs*, vol. 44, no. 4, pp. 189-190, 2021.

[21] I. Ozono, S. Sakamoto, T. Okazaki, J. Oshita, D. Ishii, and K. Kurisu, "Management of post-puncture bleeding after neurointerventional procedures performed with a large-bore sheath introducer," *J Clin Neurosci*, vol. 74, pp. 61–64, 2020.

Hindawi
Computational and Mathematical Methods in Medicine
Volume 2023, Article ID 9783730, 1 page
https://doi.org/10.1155/2023/9783730

Retraction

Retracted: Outcome of Nursing Based on Health Belief United with Knowledge, Belief, and Practice Mode on Gastroscopy of Patients with Gastric Cancer

Computational and Mathematical Methods in Medicine

Received 12 December 2023; Accepted 12 December 2023; Published 13 December 2023

This article has been retracted by Hindawi, as publisher, following an investigation undertaken by the publisher [1]. This investigation has uncovered evidence of systematic manipulation of the publication and peer-review process. We cannot, therefore, vouch for the reliability or integrity of this article.

Please note that this notice is intended solely to alert readers that the peer-review process of this article has been compromised.

Wiley and Hindawi regret that the usual quality checks did not identify these issues before publication and have since put additional measures in place to safeguard research integrity.

We wish to credit our Research Integrity and Research Publishing teams and anonymous and named external researchers and research integrity experts for contributing to this investigation.

The corresponding author, as the representative of all authors, has been given the opportunity to register their agreement or disagreement to this retraction. We have kept a record of any response received.

References

[1] J. Yang, J. Yang, D. Guo, Q. Zhao, and Y. Chen, "Outcome of Nursing Based on Health Belief United with Knowledge, Belief, and Practice Mode on Gastroscopy of Patients with Gastric Cancer," *Computational and Mathematical Methods in Medicine*, vol. 2022, Article ID 9491454, 7 pages, 2022.

Hindawi
Computational and Mathematical Methods in Medicine
Volume 2022, Article ID 9491454, 7 pages
https://doi.org/10.1155/2022/9491454

Research Article

Outcome of Nursing Based on Health Belief United with Knowledge, Belief, and Practice Mode on Gastroscopy of Patients with Gastric Cancer

Junna Yang,[1] Jing Yang,[2] Dongmei Guo,[3] Qingchao Zhao,[1] and Yang Chen[4]

[1]*Department of Endoscopy, The Number Two Hospital of Baoding, Baoding, Hebei 071000, China*
[2]*Digestive Endoscopy Department, Hebei Province Chinese Medicine Hospital, No. 389 Zhongshan East Road, Shijiazhuang, Hebei 050011, China*
[3]*Department of Nursing, The Number Two Hospital of Baoding, Baoding, Hebei 071000, China*
[4]*Nuclear Magnetic Resonance Room, The Number Two Hospital of Baoding, Baoding, Hebei 071000, China*

Correspondence should be addressed to Jing Yang; 20211533@stu.hebmu.edu.cn

Received 18 August 2022; Revised 29 August 2022; Accepted 21 September 2022; Published 3 October 2022

Academic Editor: Min Tang

Aim. If gastric cancer can be detected through early screening, and scientific and reasonable intervention methods can be selected in time, the condition can be effectively controlled. Routine nursing has been unable to obtain satisfactory results, and the effect on improving the compliance of the examiner is not outstanding. The research aims to estimate the outcome of nursing based on health belief combined with knowledge, belief, and practice on gastroscopy in patients with gastric cancer. *Methods*. 126 patients with clinically diagnosed gastric cancer in the Number Two Hospital of Baoding from May 2020 to May 2022 were randomly divided into belief guidance group and mode group, with 63 instances each. The mode group was intervened via the mode of knowledge, belief, and practice, and the belief guidance group was intervened via the nursing based on health belief on the basis of the mode group. Before and after the nursing, the health belief, examination compliance, inappropriateness, and negative emotion in different time periods were contrasted between the two groups. *Results*. After the nursing, the scores of health belief scale in the belief guidance group were enhanced than those in the mode group; the compliance rate of the belief guidance group was markedly enhanced than that of the mode group, and the inappropriateness during the insertion and examination was lower than that of the mode group; the scores of self-rating anxiety scale (SAS) and self-rating depression scale (SDS) in the two groups preinsertion and postnursing were markedly lower than those in the mode group. *Conclusion*. Nursing based on health belief guidance united with knowledge, belief, and practice mode nursing can advance the health belief and compliance of gastroscopy in patients with gastric cancer, reduce discomfort, and effectively advance the negative emotions of patients. It is worthy of clinical application.

1. Introduction

Clinical studies have found that gastric ulcer, gastric polyp, atrophic gastritis, and partial gastrectomy are all high-risk groups of gastric cancer and may be caused by irregular diet and bad living habits. If diagnosed as soon as possible and provided with effective treatment in time, the survival rate of high-risk groups can be effectively prolonged. Therefore, the clinic gradually attaches importance to the screening and prevention of gastric cancer [1, 2]. Early screening and diagnosis of gastric cancer are conducive to illness treatment, and gastroscopy is an important means to advance the diagnostic accuracy. However, it is an invasive operation, and a little carelessness may cause more adverse reactions, so it is a high-risk group. The low compliance of cooperative examination directly hinders the development of early gastric cancer screening [3, 4]. Therefore, how to advance the compliance of gastric cancer patients with gastroscopy is an urgent problem. Nursing based on health belief can advance patients' health awareness, help to alleviate patients'

psychological resistance, and achieve good results in the nursing application of patients [5]. The knowledge, belief, and practice mode includes three processes of acquiring knowledge, generating beliefs, and forming behaviors. It is a nursing mode to change patients' health-related behaviors [6, 7]. The purpose of this study is to estimate the outcome of nursing of health belief-based nursing united with knowledge, belief, and practice mode in patients with gastric cancer, and to provide a basis for the diversity of nursing methods of gastroscopy in patients with gastric cancer.

2. General Information

2.1. Data and Methods. 126 patients with clinically diagnosed gastric cancer in the Number Two Hospital of Baoding from May 2020 to May 2022 were selected as the study subjects. During the study period, there were no instances in the two groups. Inclusion criteria: (a) first gastroscopy; (b) all were aware of the study and voluntarily participated; (c) the instance data of all patients are complete. Exclusion criteria: (a) patients united with infectious illnesses; (b) gastrointestinal bleeding; (c) communication barrier; (4) patients with serious cardiovascular illness and immune system illness. The patients were randomly divided into belief guidance group and mode group, 63 instances each. The gender, age, education level, adverse life history, and chronic gastritis history of the two groups were similar ($P > 0.05$), and the comparability was strong, as shown in Table 1. The mode group utilized the mode of knowledge, belief, and practice. The specific methods were as follows: (a) before the examination, the patient should be informed of the necessity of the examination, and then explained the examination steps and precautions to the patient. For instance, when the gastroscope entered the oral cavity, the tongue should not rub against the mirror. When the gastroscope was in the throat, the swallowing action should be performed. When the gastroscope entered the esophagus, the patient should exhale with the nasal inhalation mouth; (b) in the course of examination, instructed patients to maintain proper posture, put on braces, and patted patients on the back, encouraged patients, and paid attention to gentle language and positive attitude; (c) after the examination, took off the braces and handed the paper towels to the patients to clean their faces, and reassured the patients again. At the same time, the patients were instructed not to eat or drink water within 4 hours after the examination and to eat warm and liquid food within 24 hours.

The belief guidance group carried out nursing based on health belief guidance on the basis of the mode group. The specific methods were as follows: (a) established a health belief group, including the head nurse and the nurse. Under the leadership of the head nurse, the group held a meeting to jointly formulate the nursing content and the gastric cancer related knowledge questionnaire; (b) carried out health lectures and explained the prevention and treatment of gastric cancer, gastroscopy, adverse reactions, etc. To patients in plain language, pictures or videos actively corrected the patients' incorrect diet and lifestyle and popularized the influence of diet and lifestyle on illnesses; (c) organized patients to visit the hospital environment and inspection equipment to eliminate the fear of patients; (d) kept in touch with patients via phone or Wechat, urged them to maintain good living habits, gave encouragement, and advanced their confidence in treatment. After the examination, assessed the patients' knowledge of gastroscopy and gastric cancer through Wechat questioning and corrected the patients who had wrong ideas in time; (e) nursing before gastroscopy; (f) nursing after gastroscopy.

2.2. Observation Indicators

2.2.1. Health Belief Evaluation. Before and after the nursing, the patients' health beliefs were assessed with the health beliefs scale, which included five dimensions such as barriers, severity, benefits, susceptibility, and self-efficacy. The full score of each dimension was 20 points. The higher the score, the higher the patients' health beliefs in this dimension [8].

2.2.2. Inspection Compliance and Inappropriate Evaluation. The patient's active cooperation during the examination was counted, and the compliance rate was calculated. After completing the examination, the patients were asked to recall the pain during the insertion and examination, and the pain degree was assessed via visual analog scoring method, with a score of 0-10. The higher the score, the stronger the pain degree and the lower the comfort [9].

2.2.3. Negative Emotion Evaluation. Before the nursing, before the insertion and after the nursing, the patients' negative emotions were assessed via self-rating anxiety scale(-SAS) and self-rating depression scale (SDS). Each of the two scales had 20 items, and each item counted 0-4 points. After the rough score of the scale was accumulated, multiplied it via 1.25 to take an integer as the standard score of the scale. The full score was 100 points. The lower the score, the lighter the patient's negative emotional symptoms [10, 11].

2.3. Statistical Methods. The data in this paper were estimated via SPSS 21.0 statistical software. The patient's gender, compliance, and other counting data were revealed via the rate (%). The chi-squared test was utilized for the diversity between groups. The patient's health belief scale score, inappropriateness score, and other measuring data were revealed via the mean ± standard deviation ($\bar{x} \pm s$), which conformed to the normal distribution. The independent sample t-test was utilized for the diversity between groups, and the paired sample t-test was utilized for the diversity within groups; $P < 0.05$ was statistically significant.

3. Results

3.1. Diversity of Health Belief Scale Scores between the Two Groups before and after Nursing. After the nursing, the scores of all dimensions of the health belief scale in the two groups increased, and the scores of the belief guidance group were markedly enhanced than those of the mode group ($P < 0.05$), concluding obstacle ($t = 2.834$, $P = 0.005$),

Table 1: Diversity of two groups of general data.

	Belief guidance group ($n = 63$)	Mode group ($n = 63$)	t / χ^2 / Z value	P value
Gender [n (%)]				
Male	31 (49.21)	30 (47.62)	0.032	0.859
Female	32 (50.79)	33 (52.38)		
Age (years)				
Education level [n (%)]	57.34 ± 7.81	58.38 ± 6.93		
Primary school	18 (28.57)	17 (26.98)	0.144	0.930
Junior high school	20 (31.75)	22 (34.92)		
High school and above	25 (39.68)	24 (38.10)		
Adverse life history [n (%)]				
Yes	43 (68.25)	45 (71.43)	0.151	0.698
No	20 (31.75)	18 (28.57)		
History of chronic gastritis [n (%)]				
Yes	39 (53.42)	41 (65.08)	1.896	0.168
No	24 (46.58)	22 (34.92)		

seriousness ($t = 3.603$, $P < 0.001$), benefit ($t = 5.920$, $P < 0.001$), susceptibility ($t = 5.410$, $P < 0.001$), and self-efficacy ($t = 5.241$, $P < 0.001$), as shown in Table 2.

3.2. Diversity of Compliance and Inappropriateness between the Two Groups. The compliance rate of the belief guidance group was markedly enhanced than that of the mode group ($t = 5.020$, $P = 0.025$), and the inappropriate insertion of endoscopy ($t = 4.039$, $P < 0.001$) and the inappropriateness of examination were markedly lower than those of the mode group ($t = 4.832$, $P < 0.001$), as shown in Table 3.

3.3. Diversity of Negative Emotions between the Two Groups in Different Time Periods. The scores of SAS and SDS in both groups decreased markedly before inserting the gastroscope and after nursing, and the SAS and SDS scores in the belief guidance group were markedly lower than those in the mode group before inserting the gastroscope ($t = 5.358$, $P < 0.001$) and after nursing ($t = 4.305$, $P < 0.001$). As shown in Table 4.

4. Discussion

Gastroscopy plays an important role in gastric cancer screening, illness progress monitoring, and illness severity judgment [12–15]. Whereas, patients are often nervous and even afraid before the examination, resulting in low examination cooperation and inaccurate examination results, thus delaying the condition [16–19]. The causes of bad mood can be summarized as follows: (a) gastroscopy is an invasive examination, and patients who do not know much about it think that the operation will damage the throat and esophagus and are unwilling to cooperate with the examination; (b) in the process of examination, patients are prone to cough, nausea, and vomiting due to physical stimulation of gastroscope; (c) patients lack relevant knowledge about the monitoring of gastric cancer, the importance of gastroscopy, and the operation procedure of gastroscopy, especially for the first time. Therefore, during the nursing of gastroscopy, attention should be paid to the health guidance and emotional guidance of patients [20–24]. In this study, the mode group adopted the mode of knowledge, belief, and behavior nursing, which mainly applied the acquisition of knowledge, belief, and practice before the gastroscopy and process of gastroscopy and examination. Via explaining the examination steps and matters needing attention to the patients before the gastroscopy, let the patients acquire knowledge and beliefs, guide the patients to operate correctly and give encouragement during the examination, and promote the formation of correct behavior [25–27]. The belief guidance group united with nursing guided via health beliefs; in addition to knowledge, belief, and practice mode nursing, another health belief group was established to strengthen patients' health beliefs through health lectures, Wechat, or telephone communication for a period of time before gastroscopy, so as to relieve nervousness, anxiety, and fear. The results corroborated that the scores of all dimensions of the health belief scale in the belief guidance group were markedly enhanced than those in the mode group, and the compliance rate and comfort in the belief guidance group were better than those in the mode group. It is implied that nursing based on health belief guidance plays an effective role in improving patients' disorder, severity, benefit, susceptibility, and self-efficacy, and the improvement of patients' overall health belief is beneficial to advance patients' coordination. Make the patient take the initiative to accept the examination and reduce the pain and discomfort caused via improper cooperation [28–30]. The scores of SAS and SDS in the belief guidance group before and after gastroscopy were markedly lower than those in the mode group, implying that nursing based on health belief guidance can effectively alleviate patients' negative emotions such as anxiety and depression. This is because health belief guidance makes patients have relevant knowledge reserve before examination, is well aware of the importance of gastroscopy, and has certain psychological expectations for examination,

Table 2: Diversity of health belief scale scores between the two groups before and after nursing ($\bar{x} \pm s$).

Group	Obstacle		Seriousness		Benefit		Susceptibility		Self-efficacy	
	Before nursing	After nursing	Before nursing	After nursing	Before nursing	After nursing	Before nursing	After nursing	Before nursing	After nursing
Belief guidance group ($n = 63$)	9.21 ± 2.12	13.22 ± 3.16*	8.16 ± 2.09	13.09 ± 3.47*	7.45 ± 1.24	13.87 ± 3.24*	8.28 ± 1.93	15.68 ± 4.01*	9.04 ± 2.42	15.19 ± 4.56*
Mode group ($n = 63$)	9.25 ± 2.06	11.56 ± 3.41*	8.25 ± 2.02	10.99 ± 3.06*	7.54 ± 1.32	10.79 ± 2.56*	8.54 ± 1.95	12.11 ± 3.37*	9.10 ± 2.54	11.43 ± 3.41*
t value	0.107	2.834	0.246	3.603	0.394	5.920	0.752	5.410	0.136	5.241
P value	0.915	0.005	0.806	< 0.001	0.694	< 0.001	0.453	< 0.001	0.892	< 0.001

Note: Contrasted to the same group before nursing, * $P < 0.05$.

Table 3: Diversity of inspection compliance and inappropriateness between the two groups (n, %/ $\bar{x} \pm s$).

Group	Compliance rate [n (%)]	The gastroscope insertion was not appropriate ($\bar{x} \pm s$, scores)	Inappropriate in the process of inspection ($\bar{x} \pm s$, scores)
Belief guidance group ($n = 63$)	58 (92.06)	2.76 ± 0.65	2.57 ± 0.55
Mode group ($n = 63$)	49 (77.78)	3.19 ± 0.54	3.07 ± 0.61
χ^2 value/t value	5.020	4.039	4.832
P value	0.025	< 0.001	< 0.001

Table 4: Diversity of negative emotions between the two groups in different time periods ($\bar{x} \pm s$).

Belief guidance group ($n = 63$)	SAS			SDS		
	Before nursing	Before inserting the gastroscope	After nursing	Before nursing	Before inserting the gastroscope	After nursing
Belief guidance group ($n = 63$)	62.67 ± 6.42	50.74 ± 5.66*	43.29 ± 5.17*	61.23 ± 5.93	49.76 ± 5.62*	42.13 ± 4.83*
Mode group ($n = 63$)	61.98 ± 6.36	56.12 ± 5.61*	47.21 ± 5.05*	60.81 ± 6.02	55.21 ± 4.87*	46.49 ± 4.77*
t value	0.606	5.358	4.305	0.395	5.817	5.098
P value	0.546	< 0.001	< 0.001	0.694	< 0.001	< 0.001

Note: Contrasted to the same group before nursing, * $P < 0.05$.

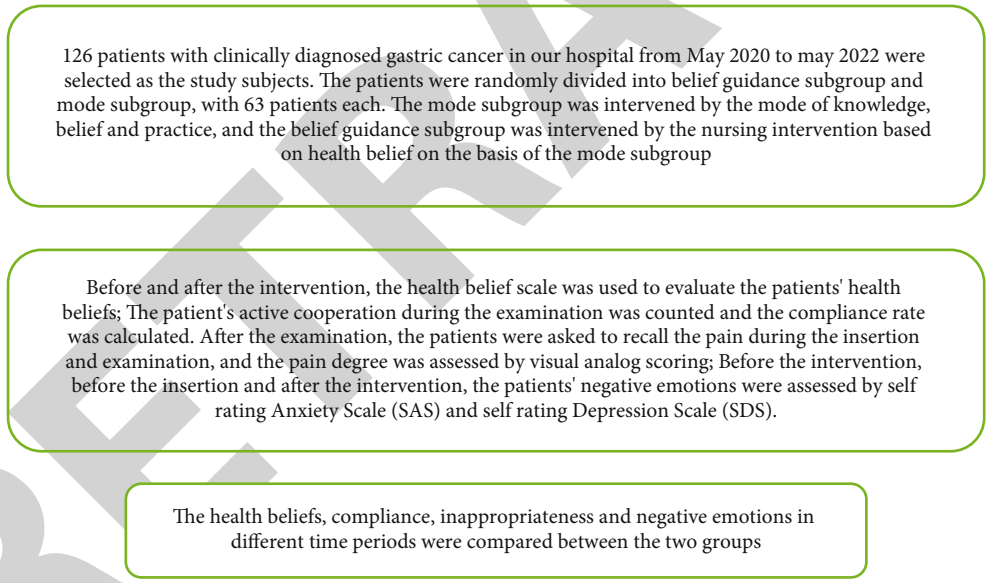

Figure 1: Outcome of nursing based on health belief united with knowledge, belief, and practice mode on gastroscopy of patients with gastric cancer.

so the negative emotion before insertion is obviously alleviated. In the process of examination, patients with high degree of fit, advanced comfort, and after the completion of the examination, once again strengthen patients' health awareness and correct patients' misconceptions, so the improvement of patients' negative emotion after the completion of nursing is also relatively good.

All in all, on the basis of nursing based on knowledge, belief, and practice mode, nursing based on health belief guidance in patients with gastric cancer before and after gastroscopy can effectively advance patients' health beliefs and cultivate patients' health behavior, so as to advance patients' examination compatibility, reduce discomfort, and alleviate patients' negative emotions before and after treatment (Figure 1). Whereas, the number of instances in this study is small, and the observation time is short, which still needs to be further verified via multicenter and large sample size studies. However, the number of studies included in this study is small, and the search for relevant factors is not comprehensive. In the follow-up study, it is necessary to increase the number of studies and multicenter samples for further in-depth research.

Data Availability

The datasets used and analyzed during the current study are available from the corresponding author upon reasonable request.

Conflicts of Interest

The authors declare that they have no conflicts of interest.

Acknowledgments

This study was supported by the Baoding Science and Technology Planning Project (No. 2041ZF015).

References

[1] H. Yoon and N. Kim, "Diagnosis and management of high risk group for gastric cancer," *Gut Liver*, vol. 9, no. 1, pp. 5–17, 2015.

[2] S. Abi Doumeth, H. Bou Daher, A. El Mokahal, A. Tawil, and A. I. Sharara, "Prevalence and characteristics of post-gastroscopy gastric cancer: a retrospective study from an academic medical center," *Arab Journal of Gastroenterology*, vol. 22, no. 3, pp. 193–198, 2021.

[3] S. Pérez Romero, A. de Las, F. Parras et al., "Quality indicators in gastroscopy. Gastroscopy procedure," *Revista Española de Enfermedades Digestivas*, vol. 111, no. 9, pp. 699–709, 2019.

[4] D. Libânio and M. Dinis-Ribeiro, "Gastroscopy and gastric cancer-related mortality: time to change recommendations regarding screening?," *Gastrointestinal Endoscopy*, vol. 87, no. 1, pp. 128–130, 2018.

[5] B. Cengiz, Z. Bahar, and A. E. Canda, "The effects of patient care results of applied nursing intervention to individuals with stoma according to the health belief model," *Cancer Nursing*, vol. 43, no. 2, pp. E87–E96, 2020.

[6] B. Qu, Q. Hou, X. Men, X. Zhai, T. Jiang, and R. Wang, "Research and application of KABP nursing model in cardiac rehabilitation of patients with acute myocardial infarction after PCI," *American Journal of Translational Research*, vol. 13, no. 4, pp. 3022–3033, 2021.

[7] A. Babington-Ashaye, S. Diop, A. Geissbuhler, and P. D. Moerloose, "Unravelling the knowledge, beliefs, behaviours and concerns of Persons with Haemophilia and their carriers in Senegal," *Haemophilia*, vol. 26, no. 5, pp. 840–846, 2020.

[8] G. Q. Liu, "Effect of nursing intervention based on health belief guidance on compliance of gastroscopy in high-risk population of gastric cancer," *J Qilu Nurs*, vol. 27, no. 11, pp. 71–74, 2021.

[9] B. Yu, P. J. Hazlewood, X. Yin et al., "Effect of electroacupuncture on discomfort during gastroscopy: a study protocol for a randomized controlled trial," *Trials*, vol. 23, no. 1, p. 364, 2022.

[10] W. W. Zung, "A rating instrument for anxiety disorders," *Psychosomatics*, vol. 12, no. 6, pp. 371–379, 1971.

[11] W. W. Zung, "A self-rating depression scale," *A Self-rating depression scale Archives of General Psychiatry*, vol. 12, no. 1, pp. 63–70, 1965.

[12] W. K. Leung, H. J. Ho, J. T. Lin, M. S. Wu, and C. Y. Wu, "Prior gastroscopy and mortality in patients with gastric cancer: a matched retrospective cohort study," *Gastrointestinal Endoscopy*, vol. 87, no. 1, pp. 119–127.e3, 2018.

[13] F. Prinz, A. Ebigbo, A. Probst, and H. Messmann, "Gastric cancer- endoscopic treatment of early lesions, the west learns from the east," *Best Practice & Research. Clinical Gastroenterology*, vol. 50-51, article 101739, 2021.

[14] T. Gotoda, N. Uedo, S. Yoshinaga et al., "Basic principles and practice of gastric cancer screening using high- definition white-light gastroscopy: eyes can only see what the brain knows," *Digestive Endoscopy*, vol. 28, pp. 2–15, 2016.

[15] Y. Mao, Q. Zhao, S. Yin, X. Ding, and H. Wang, "Genome-wide expression profiling and bioinformatics analysis of deregulated genes in human gastric cancer tissue after gastroscopy," *Asia-Pacific Journal of Clinical Oncology*, vol. 14, no. 2, pp. e29–e36, 2018.

[16] S. H. Park, H. J. Lee, J. H. Park et al., "Clinical significance of intra-operative gastroscopy for tumor localization in totally laparoscopic partial gastrectomy," *Journal of Gastrointestinal Surgery*, vol. 25, no. 5, pp. 1134–1146, 2021.

[17] H. Huang, Y. Rong, M. Wang et al., "Analysis of gastroscopy results among healthy people undergoing a medical checkup: a retrospective study," *BMC Gastroenterology*, vol. 20, no. 1, p. 412, 2020.

[18] L. Xia, S. Sun, and W. Dai, "Deep learning-based ultrasound combined with gastroscope for the diagnosis and nursing of upper gastrointestinal submucous lesions," *Computational and Mathematical Methods in Medicine*, vol. 2022, Article ID 1607099, 9 pages, 2022.

[19] S. Cam, "The efficacy of a simple single-paged visual illustration on anxiety during pediatric gastroscopy: a randomized clinical trial," *Acta Gastroenterologica Belgica*, vol. 83, no. 4, pp. 533–539, 2020.

[20] F. Men, L. Wei, B. Liu et al., "Comparison of the safety of the application of painless gastroscopy and ordinary gastroscopy in chronic hypertension patients combined with early gastric cancer," *Oncology Letters*, vol. 15, no. 3, pp. 3558–3561, 2018.

[21] L. Hao, X. Hu, B. Zhu, W. Li, X. Huang, and F. Kang, "Clinical observation of the combined use of propofol and etomidate in painless gastroscopy," *Medicine (Baltimore)*, vol. 99, no. 45, article e23061, 2020.

[22] Y. Y. Liu, Y. Q. Liu, and M. A. Petrini, "Effect of information of patients' coping style on pregastroscopy anxiety," *Gastroenterology Nursing*, vol. 41, no. 1, pp. 47–58, 2018.

[23] D. Lu, J. H. Wang, C. Lu et al., "Alleviating pregastroscopy anxiety using mobile social media application," *Frontiers in Medicine*, vol. 9, article 855892, 2022.

[24] J. M. Chen, D. D. Li, Y. S. Chen et al., "The effectiveness of electro-acupuncture combined with dyclonine hydrochloride in relieving the side effects of gastroscopy: a controlled trial," *Annals of Palliative Medicine*, vol. 10, no. 3, pp. 2958–2970, 2021.

[25] J. Wang, L. Chen, M. Yu, and J. He, "Impact of knowledge, attitude, and practice (KAP)-based rehabilitation education on the KAP of patients with intervertebral disc herniation," *Palliative Medicine*, vol. 9, no. 2, pp. 388–393, 2020.

[26] X. C. Xiao, "Effect of knowledge-attitude-practice model in nursing of patients undergoing gastroscopy," *Tod Nur*, vol. 26, no. 6, pp. 163–165, 2019.

[27] Y. Dong, H. Gao, Z. Jin et al., "Application of a knowledge, attitude, belief, and practice model in pain management of patients with acute traumatic fractures and alcohol dependence," *Pain Research & Management*, vol. 2022, article 8110896, 7 pages, 2022.

Hindawi
Computational and Mathematical Methods in Medicine
Volume 2023, Article ID 9758345, 1 page
https://doi.org/10.1155/2023/9758345

Retraction

Retracted: Analysis of Data on Fludarabine, Cyclophosphamide, and Rituximab Chemoimmunotherapy for Chronic Lymphocytic Leukemia Shows High Patient Heterogeneity and the Need for More Consideration of Individualized Treatment

Computational and Mathematical Methods in Medicine

Received 12 December 2023; Accepted 12 December 2023; Published 13 December 2023

This article has been retracted by Hindawi, as publisher, following an investigation undertaken by the publisher [1]. This investigation has uncovered evidence of systematic manipulation of the publication and peer-review process. We cannot, therefore, vouch for the reliability or integrity of this article.

Please note that this notice is intended solely to alert readers that the peer-review process of this article has been compromised.

Wiley and Hindawi regret that the usual quality checks did not identify these issues before publication and have since put additional measures in place to safeguard research integrity.

We wish to credit our Research Integrity and Research Publishing teams and anonymous and named external researchers and research integrity experts for contributing to this investigation.

The corresponding author, as the representative of all authors, has been given the opportunity to register their agreement or disagreement to this retraction. We have kept a record of any response received.

References

[1] X. Xu, Y. Zhao, H. Ye et al., "Analysis of Data on Fludarabine, Cyclophosphamide, and Rituximab Chemoimmunotherapy for Chronic Lymphocytic Leukemia Shows High Patient Heterogeneity and the Need for More Consideration of Individualized Treatment," *Computational and Mathematical Methods in Medicine*, vol. 2022, Article ID 7451395, 21 pages, 2022.

Hindawi
Computational and Mathematical Methods in Medicine
Volume 2022, Article ID 7451395, 21 pages
https://doi.org/10.1155/2022/7451395

Research Article

Analysis of Data on Fludarabine, Cyclophosphamide, and Rituximab Chemoimmunotherapy for Chronic Lymphocytic Leukemia Shows High Patient Heterogeneity and the Need for More Consideration of Individualized Treatment

Xiaoli Xu, Ying Zhao, Haiyan Ye, Yonglei Qi, Wenning Xu, Yiwen Ling, and Shaojiang Yang

Department of Hematology, First People's Hospital of Foshan, Foshan, China

Correspondence should be addressed to Ying Zhao; zhaoying@fsyyy.com

Received 28 July 2022; Revised 11 August 2022; Accepted 8 September 2022; Published 3 October 2022

Academic Editor: Min Tang

Object. In this study, bioinformatics analysis of differentially expressed genes (DEGs) and signaling pathway activities in different progression stages of chronic lymphocytic leukemia (CLL) and pre- and post-chemoimmunotherapy (CIT) treatment was performed. This may provide novel ideas for molecular diagnosis and individualized treatment strategies for CLL patients. *Methods*. Data from single-cell RNA sequencing (RNA-seq) of CLL patients were obtained from the Gene Expression Omnibus database. The R package was utilized to analyze the data, and the relation of results was predicted via the GeneMANIA website. The information of 7 samples covered three stages: observation stage, pretreatment by CIT with rituximab, fludarabine, and cyclophosphamide (pre-CIT), and post-CIT. The differentially expressed genes (DEGs) were identified, and functional enrichment analyses were performed. B cell subpopulations and pseudotime trajectories analysis was conducted. *Results*. A total of 70,659 DEGs were identified. Each patient's DEGs presented their own characteristics, with low similarity. Therefore, it is difficult to identify potential hub genes. Similarly, pathway enrichment analysis showed significant tumor heterogeneity among CLL patients. Analysis of relapsed post-CIT compared to the observation stage suggested that the *TP53* pathway should be taken seriously as it is closely related to treatment strategy and patient prognosis. *Conclusions*. Tumor heterogeneity may be a more common manifestation of CLL. Individualized treatment should be considered for CLL. *TP53* abnormality and its regulatory factors should still be the focus of CLL diagnosis and treatment.

1. Introduction

Chronic lymphocytic leukemia (CLL) is one of the most common adult leukemia in the world. The incidence of CLL is estimated to be more than 4-6 per 100,000 population annually in developed countries, and the ratio of men to women is about 2 : 1 [1, 2]. Although the median age at diagnosis is 72 years, 10% of CLL patients are younger than 55 years [3]. Diagnosis as early as possible may help improve patient prognosis. Currently, clinical diagnostic criteria are based on the number and morphology of monoclonal B lymphocytes. The number of monoclonal B lymphocytes is over 5 x 10/L in the peripheral blood [3]. Meanwhile, the characteristic of most leukemia cells found in the blood smear is small and mature-appearing lymphocytes. The cells present a narrow border of cytoplasm, a dense nucleus lacking discernible nucleoli and partially aggregated chromatin [3]. In terms of cellular molecules, several B cell surface antigens are coexpressed, such as CD19, CD20, and together with CD5, CD23, CD43, and CD200 [4]. Although it can be clearly diagnosed as CLL based on the clinical diagnostic criteria and markers of the cell surface, there is indeed still a great deal of uncertainty in the progression and prognosis of the tumor. It has been identified that CLL presents an

inherited genetic susceptibility, the family members of CLL patients with 6-9 folds increased risk [3]. This has led to the exploration of the deeper molecular mechanisms characterizing CLL in order to achieve precise diagnosis and treatment.

In general practice, treatment of CLL relies on the Rai and Binet staging systems and the presence of symptoms [5, 6]. Most patients of early-stage (Rai 0; Binet A) present with asymptomatic and should be monitored without therapy, that is the observation stage. Patients with advanced (Rai III and IV; Binet B, and C) symptomatic disease and rapidly progressive lymphocytosis usually need to be treated and could benefit from treatment [1, 3, 7]. Chemoimmunotherapy (CIT) using the anti-CD20 monoclonal antibody rituximab and fludarabine plus cyclophosphamide (FCR) has become the standard treatment for most CLL patients [1]. However, recent developments in the diagnosis and treatment of CLL have emphasized individualized treatment strategies. It is recommended that the therapy decision is based on the integration of the factors related to the neoplasm and the factors related to the patient [2]. Treatment of CLL patients should take into account their disease subsets, treatment tolerance factors such as age, comorbidities, and genetic factors such as *TP53* mutation/deletion [2]. Therefore, in addition to consideration of different clinical stages, the patient's chromosomal or genetic abnormalities should also be referred to. The implementation of appropriate anticancer treatment on this basis may help improve prognosis. However, the molecular pathological mechanism of CLL is complex and has individual characteristics. Even an excellent model needs frequent updating and tailoring to a particular population of CLL patients to sustain its predictive effectiveness [8]. This requires extensive in-depth molecular mechanistic exploration work, including research methods and strategies.

With the development of next-generation sequencing technology, bioinformatics analysis brings a more comprehensive and novel perspective to decode life mysteries, detect pathogens, and improve quality of life [9]. Whole-genome and -exome sequencing has contributed to the characterization of the mutational spectrum of the disease. Sequencing analysis studies on CLL are gradually being reported. A previous study of RNA-sequencing (RNA-seq) in different subpopulations of normal B lymphocytes and CLL cells has shown differential expression of transcriptional elements, including genes of protein-coding, noncoding RNAs, and pseudogenes [10]. Differentially expressed genes (DEGs) between B cells and CLL specimens were revealed [10, 11]. In addition, there were studies around small noncoding RNAs (sncRNAs), subtype-specific epigenome signatures, and transcription regulatory networks of CLL [12, 13]. In the area of drug tolerance, Landau et al. suggested that the frequently observed clonal shifts during the early treatment period of CLL, heralded the emergence of drug-resistant clones [14]. However, few studies have been reported on bioinformatics analysis of CLL treatment and relapse in recent years.

This research has explored the genetic characteristics and differences in signaling pathway activity among CLL patients and pre- and post-CIT treatment based on data analysis. The initial goal was to uncover genes and signaling pathways that may play a critical role in CLL treatment and prognosis. However, the findings suggested that the heterogeneity among patients with CLL and at different stages of the disease was evident. When considering genetic abnormalities that are closely related to CLL, such as the *TP53* pathway, individualized patient care should also be taken into account.

2. Materials and Methods

2.1. Data. Single-cell RNA sequencing data of GSE165087 were obtained from Gene Expression Omnibus (GEO) datasets (https://www.ncbi.nlm.nih.gov/geo/query/acc.cgi?acc=GSE165087). The information of patient 1, patient 2, and patient 3 was chosen, including 10 samples that cover three stages. They are observation (OB) (CLL 1_1.1, CLL 1_1.2), pretreatment by CIT with fludarabine, cyclophosphamide and rituximab (pre-CIT) (CLL 1_3.1, CLL 1_3.2, CLL 2_1, CLL 3_1), and post-treatment by CIT (post-CIT) (CLL 1_5.1, CLL 1_5.2, CLL 2_2, CLL 3_2). We combined the two technical repetitions into one to optimize the structure. As a consequence, we reorganized 7 samples (CLL 1-1, CLL 1-2, CLL 1-3, CLL 2-1, CLL 2-2, CLL 3-1, and CLL 3-2) to further analyze. The analysis process of this study is shown in Figure 1.

2.2. Quality Control, Dimensionality Reduction, and Data Integration. The single-cell RNA-seq data were imported into the Scater package (version 1.14.6) [15]. The median absolute deviation (MAD) was used to judge the unique molecular identifiers (UMI) and feature count outliers. We used the function of Outlier to remove cells with a log-library size of more than 3 MADs (the median log-library size) and cells with a mitochondrial gene expression ratio greater than 20% which usually corresponds to dead or injured cells. To eliminate differences in gene expression between cells based on count data, the global scaling normalization method LogNormalize was applied to standardize the measurement of the characteristic expression for each cell with the total expression. And then 2000 genes with high variation were extracted by the VST method, based on a large coefficient of variation. After integrating multiple samples with the function of IntegrateData, we scaled the data by linear transformations to ensure each gene was given the same weight with a mean of 0 and a variance of 1. For the sake of reducing the computational burden and the noise in the data, principal component analysis (PCA) was used for preliminary dimensionality reduction. We used the Seurat package (version 3.1.4) function of FindNeighbors and FindClusters to cluster the cells [16]. The clustering data were projected into low-dimensional space via uniform manifold approximation and projection (UMAP), a nonlinear dimension reduction technique retaining the original topological structure.

2.3. Cell Annotation and Ratio Calculation. Following obtaining 8 stable cell subpopulations from cluster analysis,

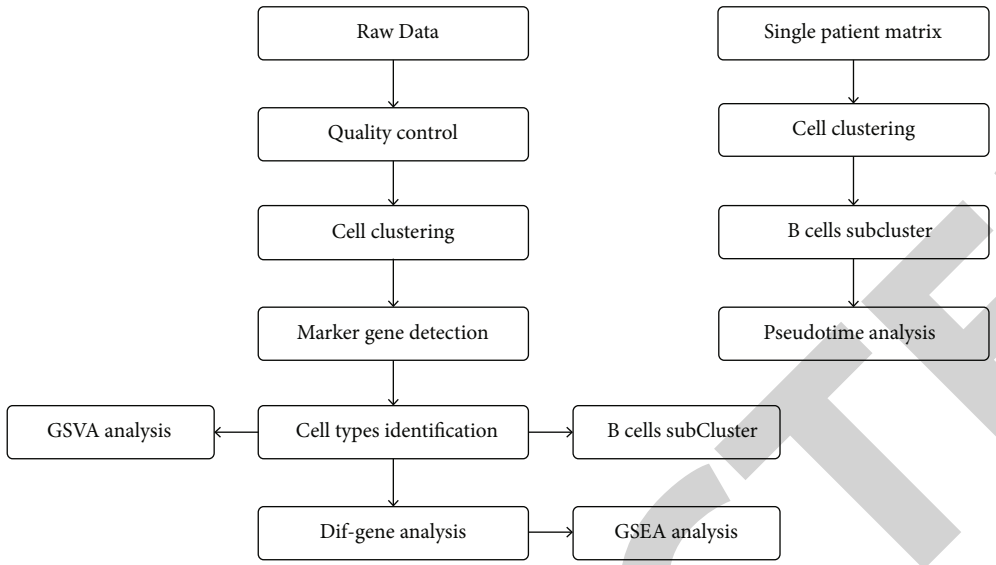

Figure 1: The analysis process.

we used the function of the FindAllMarkers Wilcoxon rank-sum test to determine the multiple gene differences between the cell group and other groups with the average value of avg_logFC. Database PanglaoDB and CellMarker provided marker genes in different cell types and the SingleR algorithm [17] assisted the verification of identified cell types by calculating the Spearman correlation between the expression profile of each cell and that of each reference sample so that the 6 types of cell subpopulations were determined. In the present study, we analyzed B cells.

2.4. Variance Analysis and Pathway Enrichment. The gene expression variance evaluation of B cells was conducted by R package, which was compared in each group via Kruskal-Wallis Test. Gene Set Enrichment Analysis (GSEA) was implemented in the Fgsea package (version 1.12.0) to determine pathways [18]. Sequencing was performed according to LogFC of rank-sum test difference analysis as the sorted gene list. Further GSEA analysis was performed via the Kyoto Encyclopedia of Genes and Genomes (KEGG) gene set. Gene Set Variation Analysis (GSVA) package (version 1.34.0) [19] and the subsequent analysis described by MSigDB databases were driven to pathways of Geno Ontology (GO) annotation, hallmarker terms, and KEGG. As a footnote, GO and KEGG analyses were used to estimate the functions of DEGs, concluding with the biological process (BP), cell composition (CC), and molecular function (MF), which were analyzed by Fisher's test. $P < 0.05$ was regarded as statistically significant.

2.5. Gene Association Network. We chose differentially expressed genes interested and differentially enrichen pathway interested and performed the latent relation among them via GeneMANIA (http://genemania.org/), including physical interactions, coexpression, colocalization, genetic interaction, and pathway.

2.6. B Cell Subpopulations Clustering. To explore the pathways and functions involved in each subpopulation of B cells, gene enrichment analysis was performed for each subpopulation. Rank-sum test was used to compare the differences in gene expression levels of B cell subsets.

2.7. B Cell Pseudotime Trajectories Analysis. Pseudotime trajectories analysis refers to the construction of cell lineage development based on the changes in gene expression levels of different cell subpopulations over time which is a virtual time sequence according to the track of transformation and succession from cell to cell. Monocle uses an algorithm to learn the sequence of changes in gene expression that each cell must undergo as part of a dynamic biological process. Once it understands the overall trajectory of changes in gene expression, Monocle can place each cell in the right place within the trajectory. Monocle relies on a machine-learning technique called reverse graph embedding to construct single-cell trajectories. We used Monocle 2 package (v2.8.0) [20] to analyze cell state transitions and then we put the top 100 differentially expressed genes in the Seurat package to establish the pseudotime trajectories. The B cells state conducted origin of the pseudotime as orderCells. The abnormal gene expression profiles were set to root_state argument, and then we invoked orderCells, DDRTree reducing dimensions, and the plot_cell_trajectory plotting the minimum spanning tree. The top 100 differentially expressed genes of B cells were calculated by the function differential GeneTest. We performed genes meeting the thresholds with mean_expression ≥ 0.5 and dispersion_empirical $\geq 1 *$ dispersion_ fit to present cells in pseudotime order.

2.8. Gene Variance Pseudotime Trajectories. Genes with similar trends were grouped into two categories. In one group, the expression was from low to high. We set the low state at the beginning of differentiation, and it decreased gradually

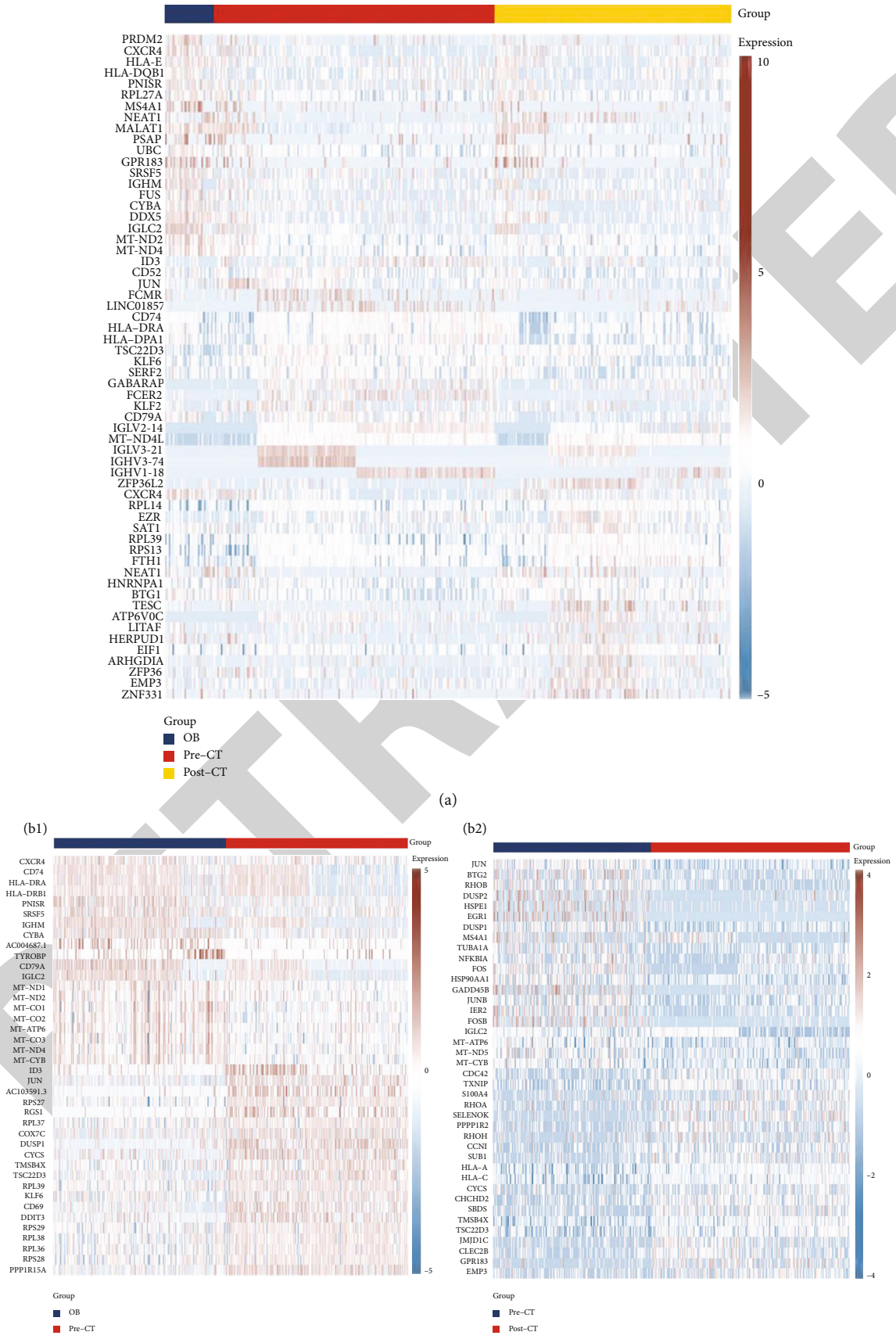

Figure 2: Continued.

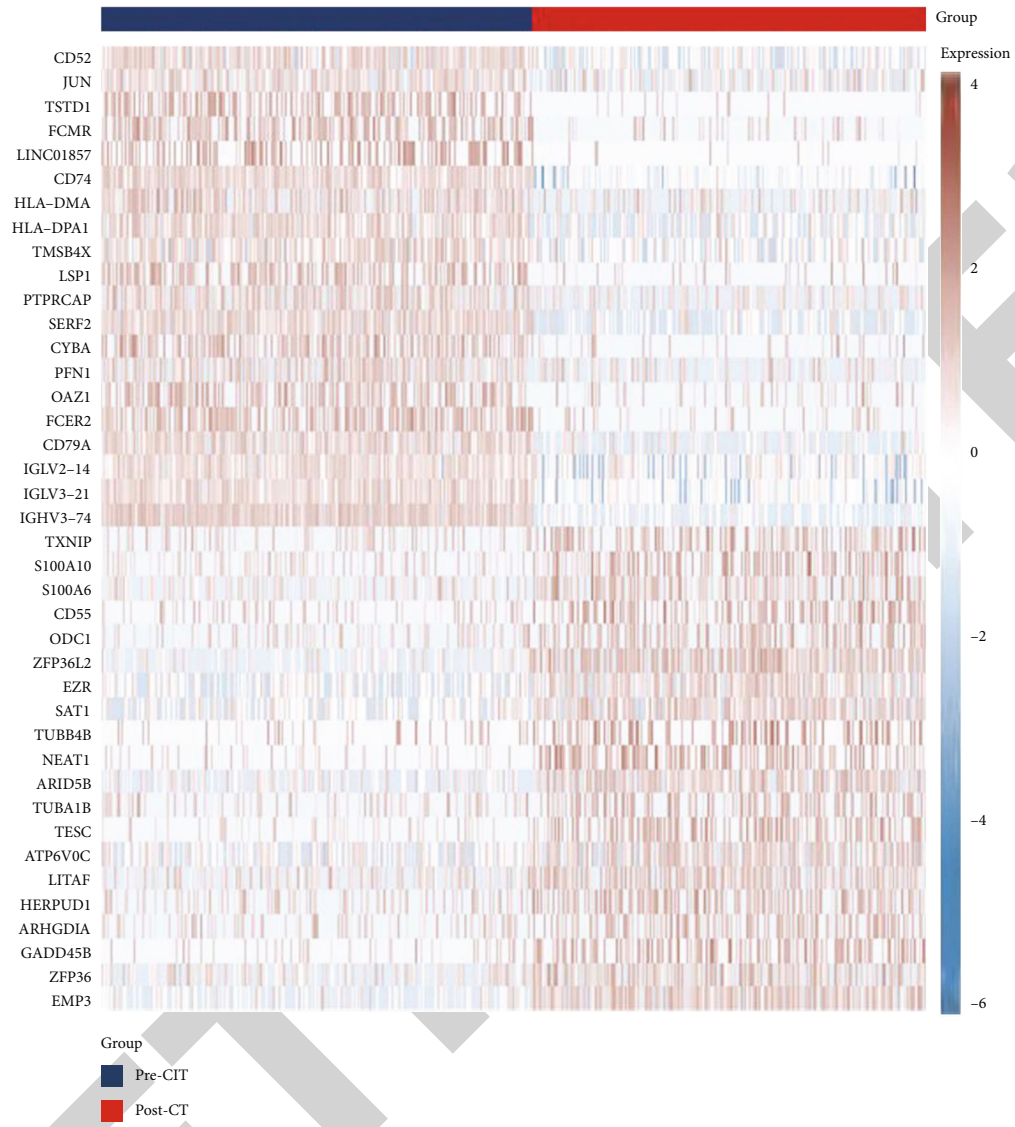

(c)

Figure 2: Continued.

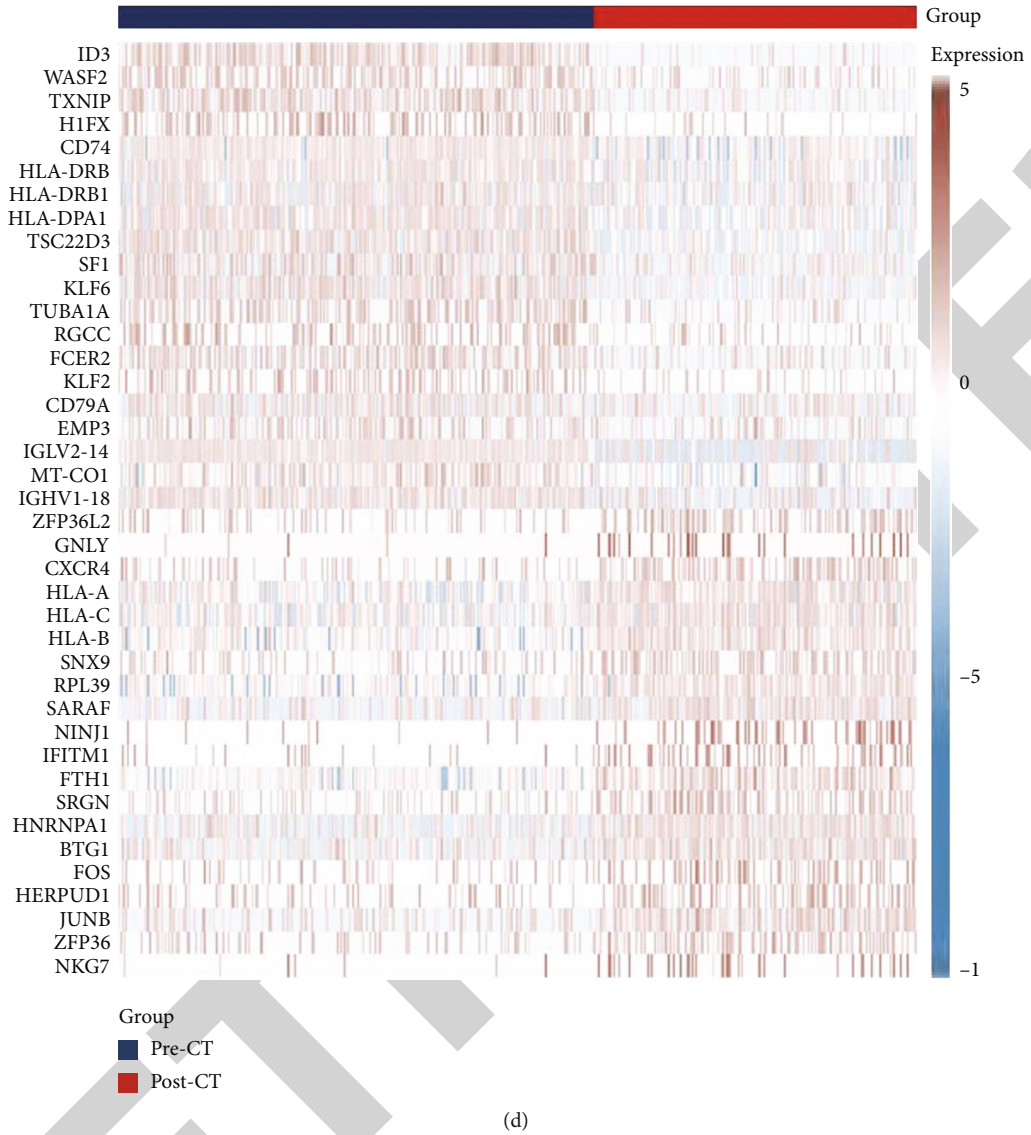

(d)

Figure 2: DEGs in B lymphocytes of CLL patients. (a) The top 20 genes with the largest expression in each group. (b) The DEGs of patient 1, compared between observation stage and post-CIT. (c) The DEGs of patient 1, compared between pre-CIT and post-CIT. (d, e) The DEGs of patient 2 and 3, compared between pre-CIT and post-CIT.

with the increase of pseudotime. In the other group, the expression level was high at the beginning of differentiation and decreased gradually with the increase of pseudotime.

2.9. Statistical Analysis. All statistical analyses were carried out via the R package (http://www.r-project.org). A two-sided paired or unpaired Student's *t*-test and unpaired Wilcoxon rank-sum test were used for indication. $P < 0.05$ was considered to manifest statistical significance.

3. Results

3.1. Identification of DEGs in B Lymphocytes of CLL Patients. In the present study, 7 data series which covered 3 stages were analyzed. A total of 70,659 DEGs were identified. In order to screen the representative DEGs between pre-CIT and relapsed post-CIT in CLL patients, we took the top 20 genes with the largest expression in each group to draw a heat map according to logFC, as shown in (Figure 2(a)). However, the DEGs of patients lack commonalities, and each patient appeared to present his/her own characteristics (Figures 2(b)–2(d)). None of the high expression genes coincide among the three patients when comparing pre-CIT with relapsed post-CIT. There was only one gene, *JUN* (Jun proto-oncogene, AP-1 transcription factor subunit), with high expression in both patient 1 and 2, while other 5 genes including *CD47*, *HLA-DPA1*, *FCER2*, *CD79A*, and *IGLV2-14* were highly expressed in both patient 2 and 3 in the compared pre-CIT with post-CIT. But most encoded proteins of these genes were B cell antigen or involved in immune response, which did not reveal the underlying pathological mechanism of CLL very well. Similarly, none of the high

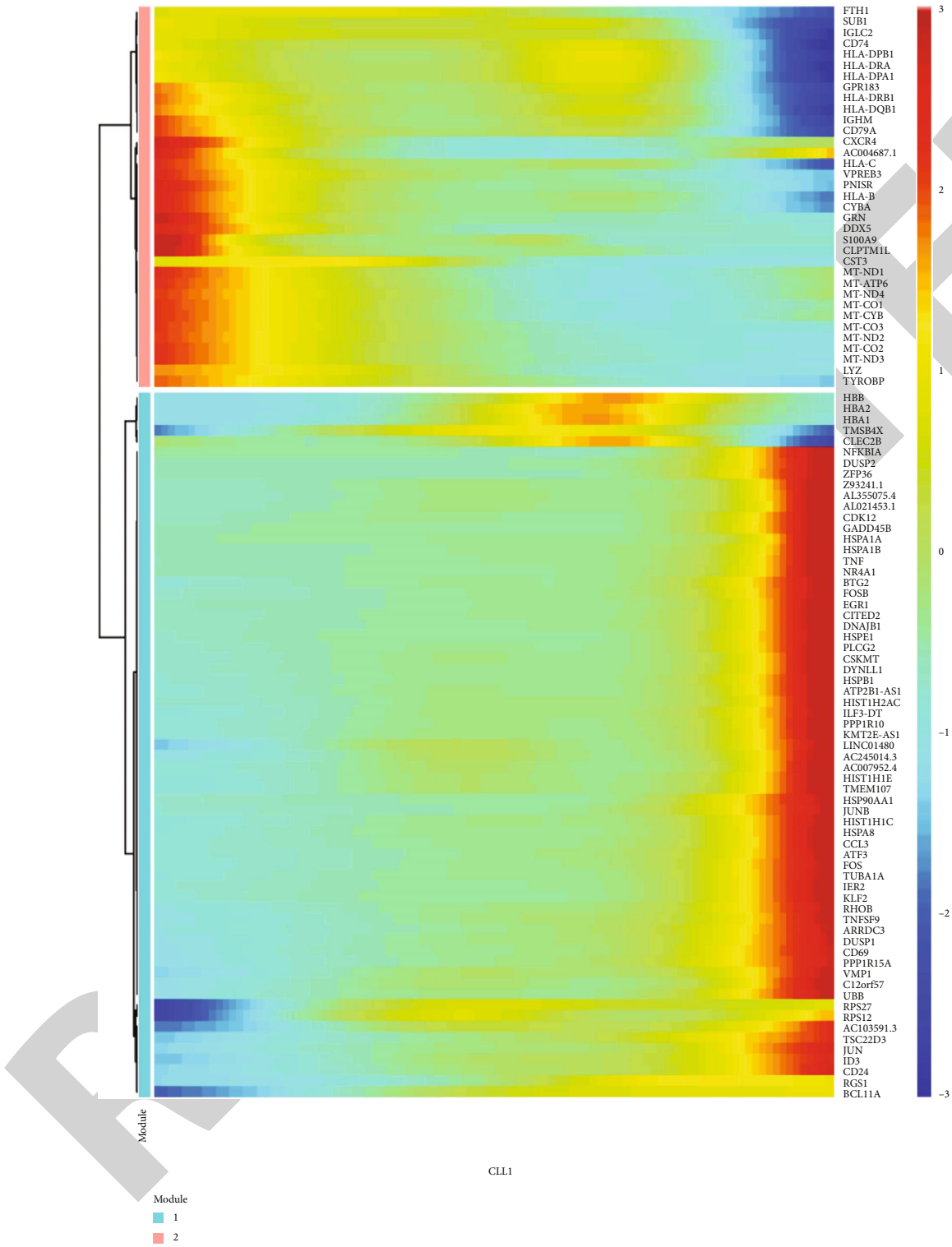

(a)

Figure 3: Continued.

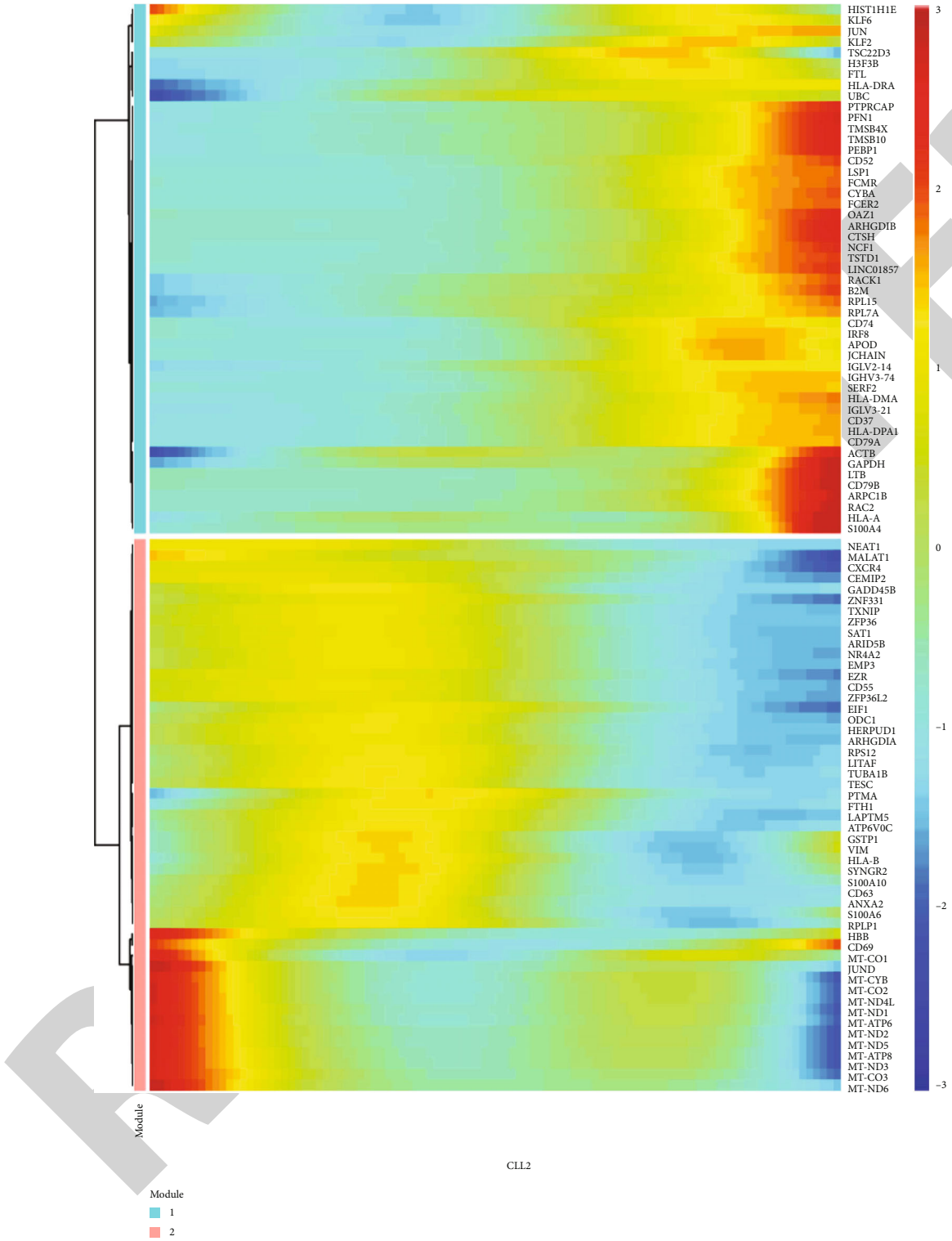

(b)

Figure 3: Continued.

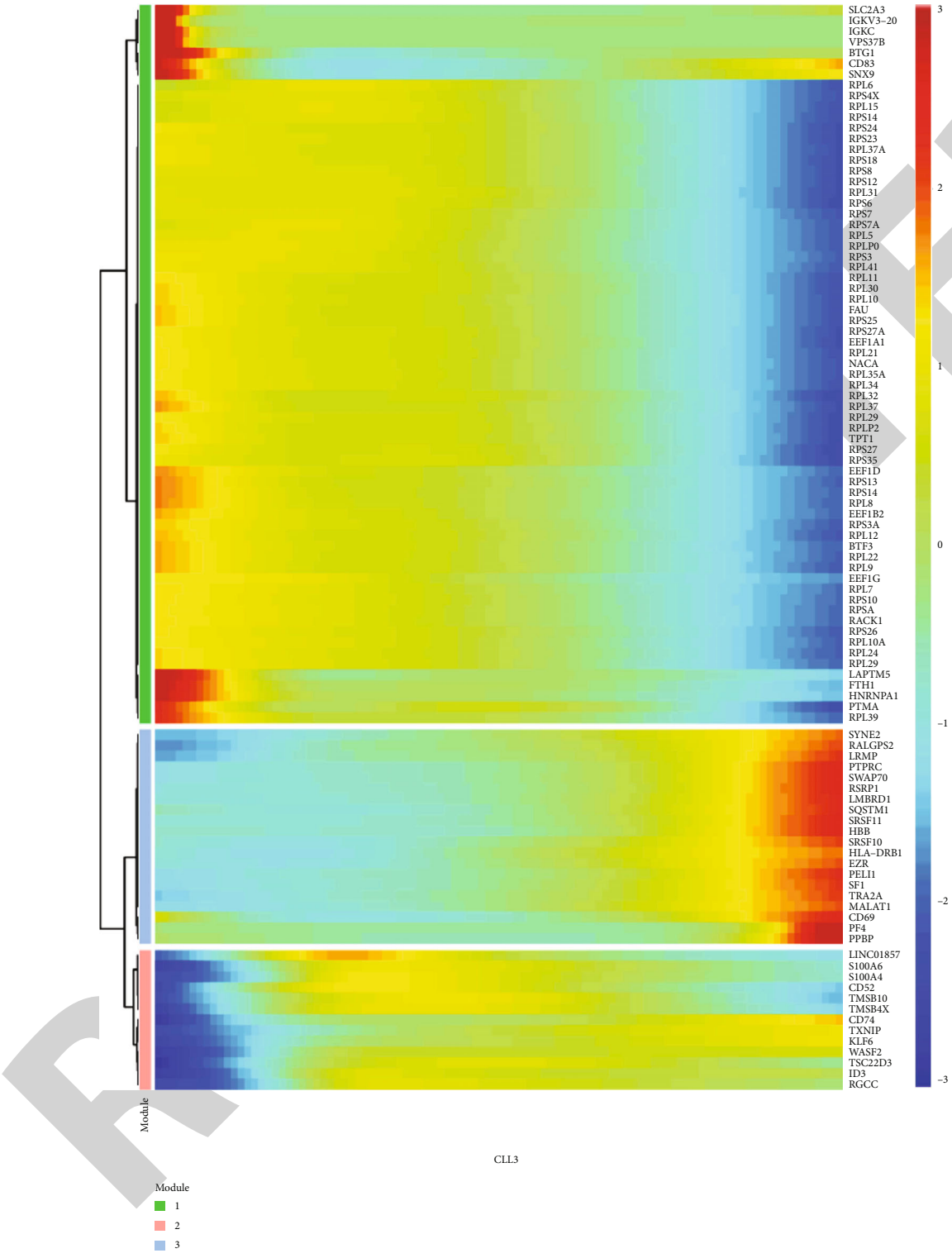

(c)

Figure 3: The top 100 DEGs pseudotime heat map of the three CLL patients.

expression genes coincide among the three patients compared relapsed post-CIT with pre-CIT. In the relapsed post-CIT, there were 2 genes, *TXNIP* and *EMP3*, presented high expression in both patient 1 and 2. 2 genes, *HLA-A* and *HLA-C*, presented high expression in both patient 1 and 3. And 3 genes, *ZFP36L2*, *HERPUD1*, and *ZFP36*, presented high expression in both patient 2 and 3. In addition to this, 17-19 of the 20 DEGs were not the same among patients, even the expression trends of some genes were reversed in different patients. Therefore, the results

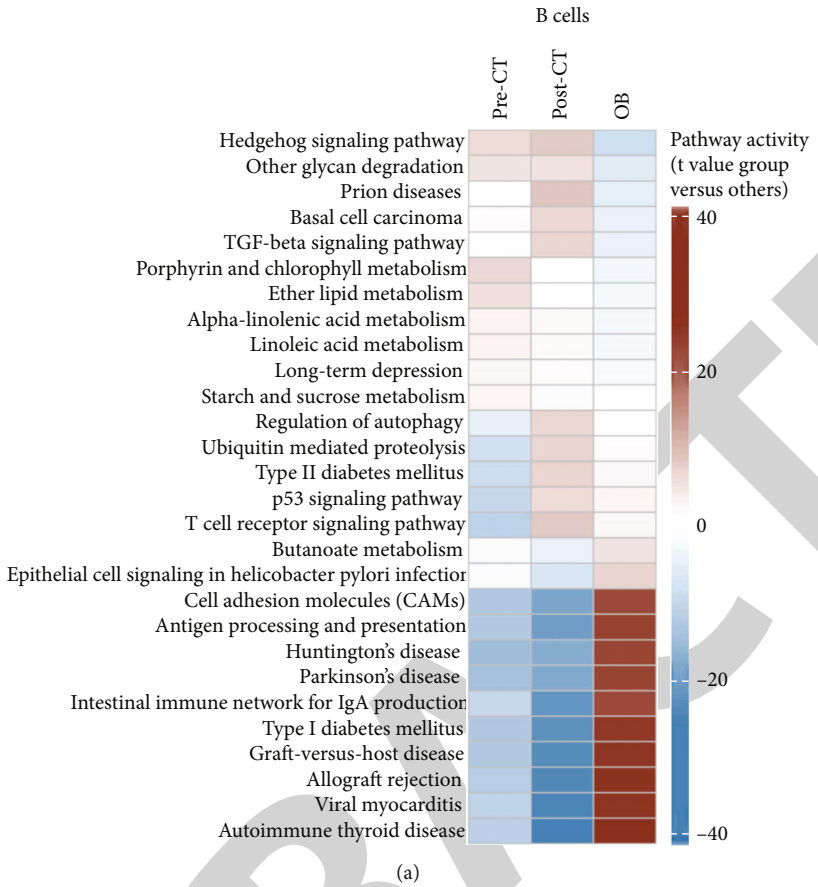

(a)

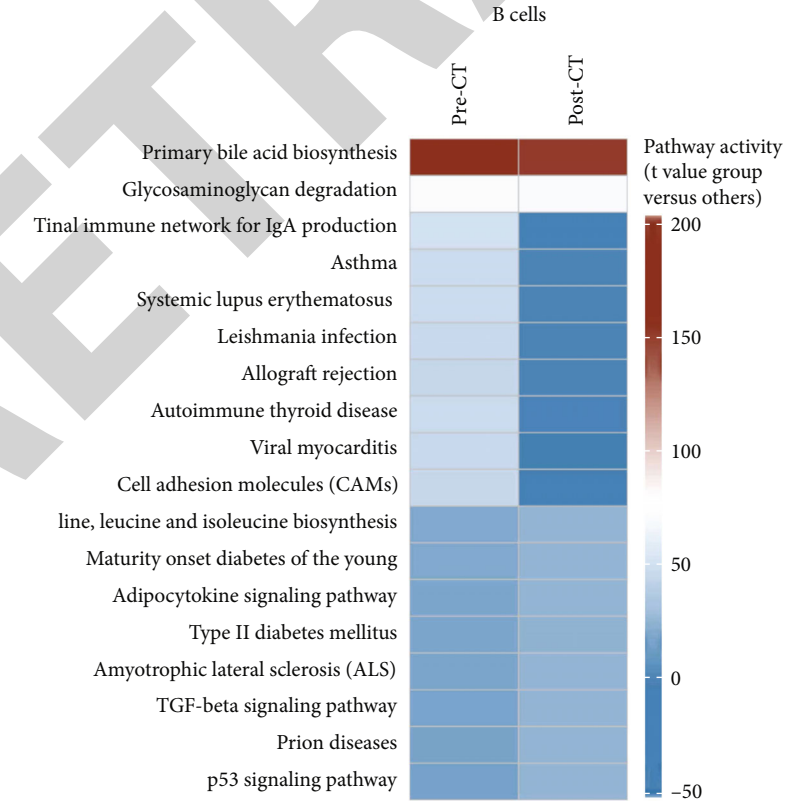

(b)

Figure 4: Continued.

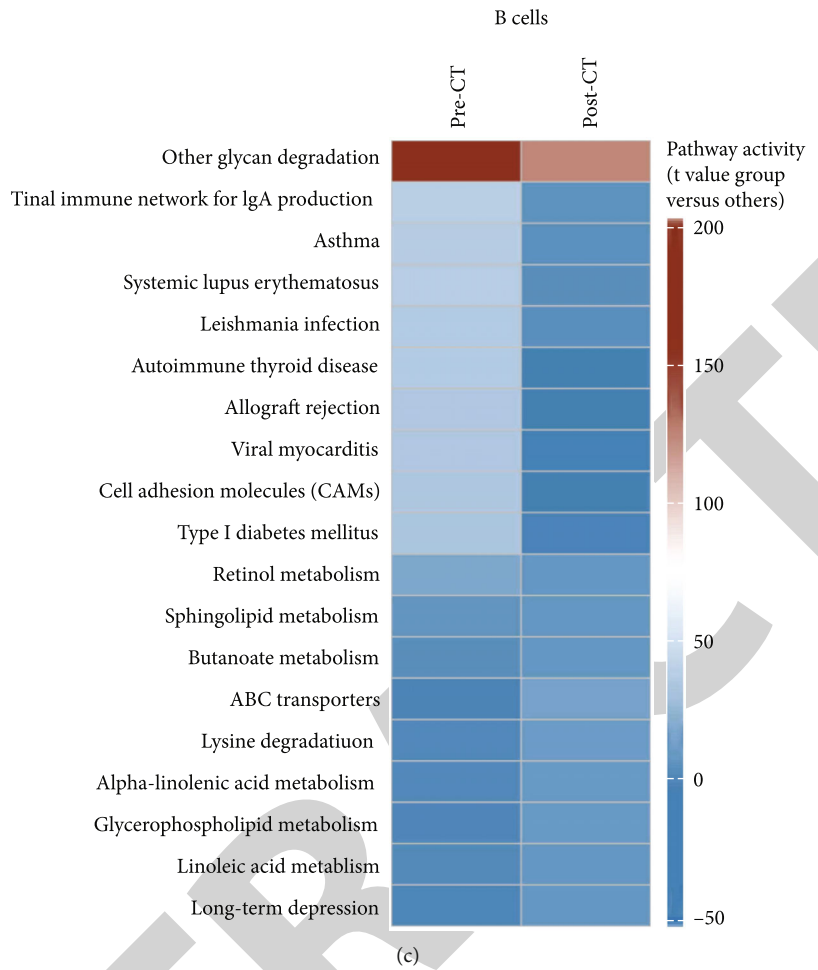

Figure 4: Pathway enrichment analyses of the common DEGs of CLL patients. (a) Patient 1, (b) patient 2, and (c) patient 3.

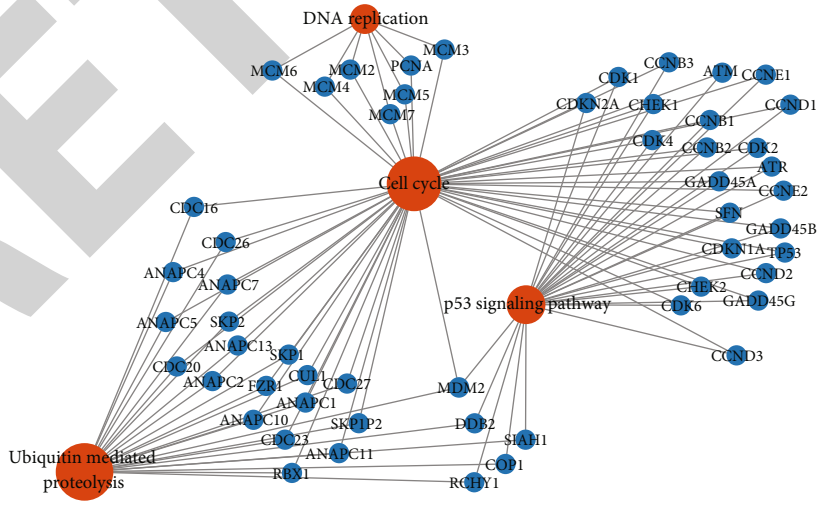

Figure 5: Pathway network.

suggested that the DEGs of relapsed post-CIT presented significant heterogeneity among CLL patients.

The top 100 DEGs of each CLL patient were selected for pseudotime analysis and genes with similar trends were grouped together. The heat maps show clusters of genes with the same expression pattern (Figures 3(a)–3(c)). Similarly, the results also showed that the DEGs of pseudotime were heterogeneous among patients.

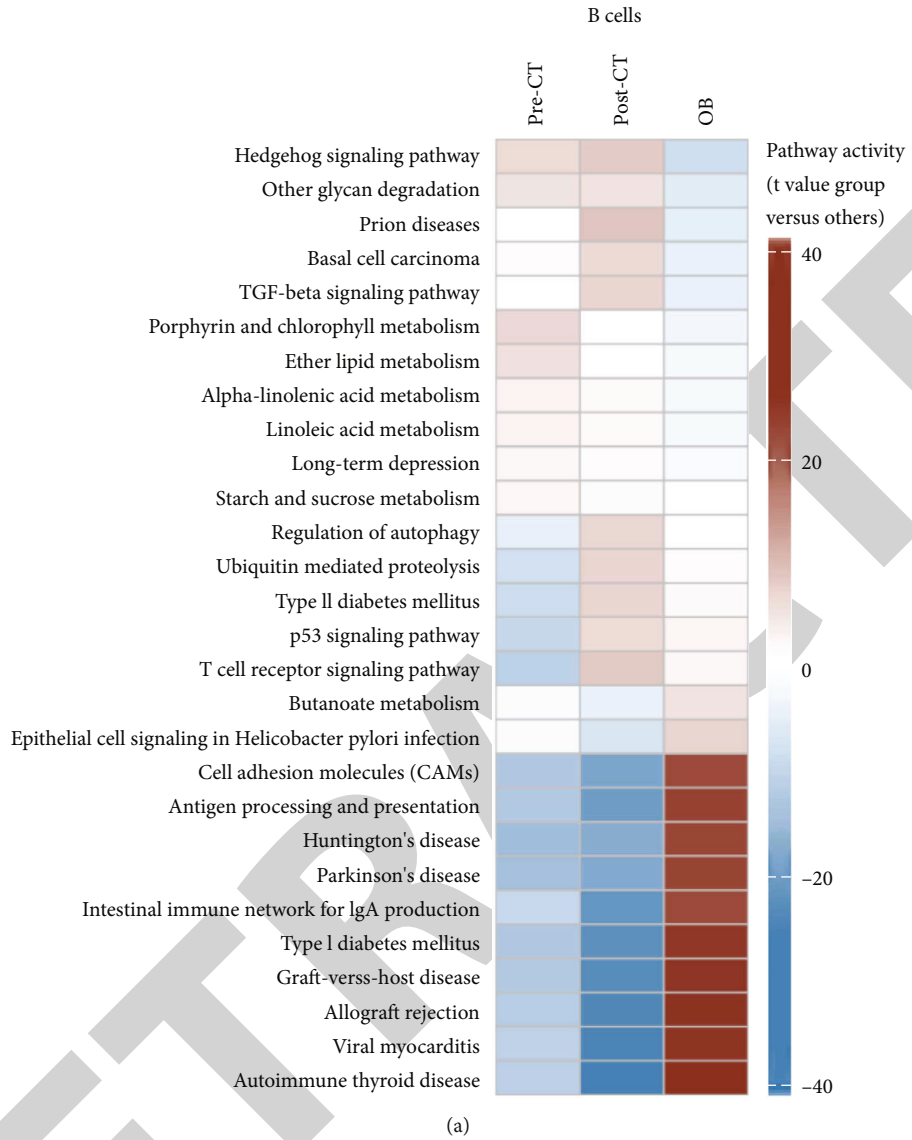

(a)

Figure 6: Continued.

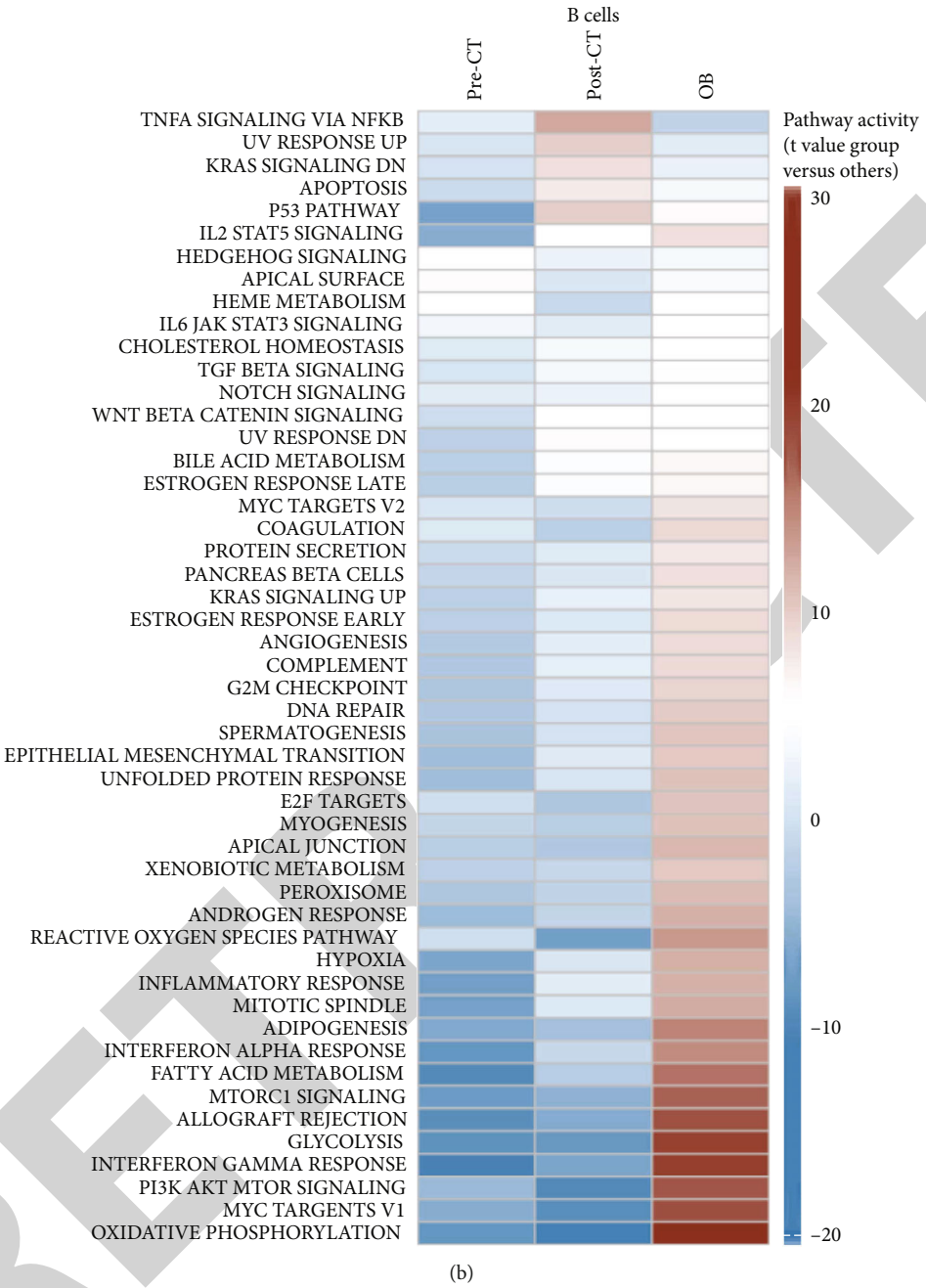

(b)

Figure 6: Continued.

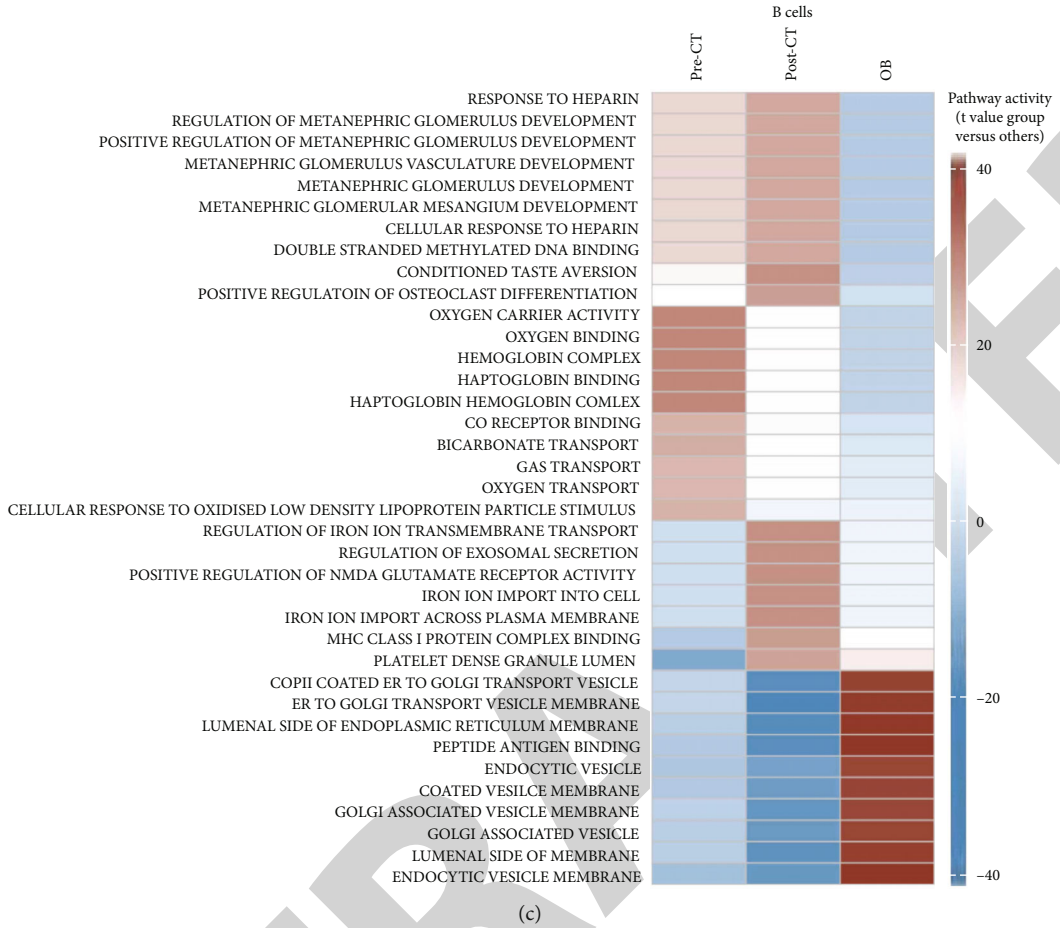

(c)

Figure 6: KEGG, Hallmark, and GO pathway enrichment analyses of patient 1. (a) KEGG, (b) Hallmark, and (c) GO.

3.2. Pathway Enrichment Analyses of the Common DEGs of CLL Patients. To further explore the potential role of signaling pathways in the disease mechanism of CLL, we conducted pathway enrichment analysis across different stages of each patient according to DEGs. However, we found significant differences among CLL patients, suggesting significant heterogeneity (Figure 4). There were 5 pathways with the most significant differences of patient 1 which were the regulation of autophagy, ubiquitin-mediated proteolysis, and *TP53* signaling pathway, etc. (Figure 4(a)). Pathways with significant differences between pre-CIT and post-CIT in patient 2 were related to energy metabolism, these were glycosaminoglycan degradation, immune disorders, and the *TP53* signaling pathway, *etc.* (Figure 4(b)). Although it was somewhat similar between patient 3 and patient 2, more than half of the differential pathways were not consistent (Figure 3(c)). This result probably suggested that changes in energy metabolism and immune factors may affect the therapeutic efficacy of CLL, thereby affecting disease progression. However, there were individual differences in signaling pathway characteristics of different patients. No convincing molecular mechanism for CLL disease progression can be deduced yet from the results of the current pathway enrichment analysis. To further search for target pathways, we narrowed the scope and drew a network map of several major pathways that may be involved in CLL pathophysiology and their closely related genes for further analysis of potential targets (Figure 5). Among these, the *TP53* pathway and ubiquitin-mediated proteolysis pathway were closely related to the cell cycle process through multigene groups. This suggested that classical signaling pathways such as *TP53* may still be the main therapeutic entry point.

3.3. KEGG, Hallmark, and GO Pathway Enrichment Analyses of Patient 1. Heterogeneity of DEGs and pathways among patients suggested that it was better to perform individual analyses independently. To uncover the molecular metabolic characteristics of stability and progression of CLL, we further analyzed the differences between the observation stage and relapsed post-CIT in patient 1 (Figure 6). As shown in the KEGG graph analyzed by GSVA (Figure 6(a)), pathways with significantly increased activity in relapsed post-CIT compared to the observation stage were the *TP53* signaling pathway, ubiquitin-mediated proteolysis, immune abnormality, etc. (Figure 4(a)). Pathways with decreased activity were TGF-beta signaling pathway, other glycan degradation, hedgehog signaling pathway, etc. (Figure 6(a)). Hallmarks is a gene set related to tumor

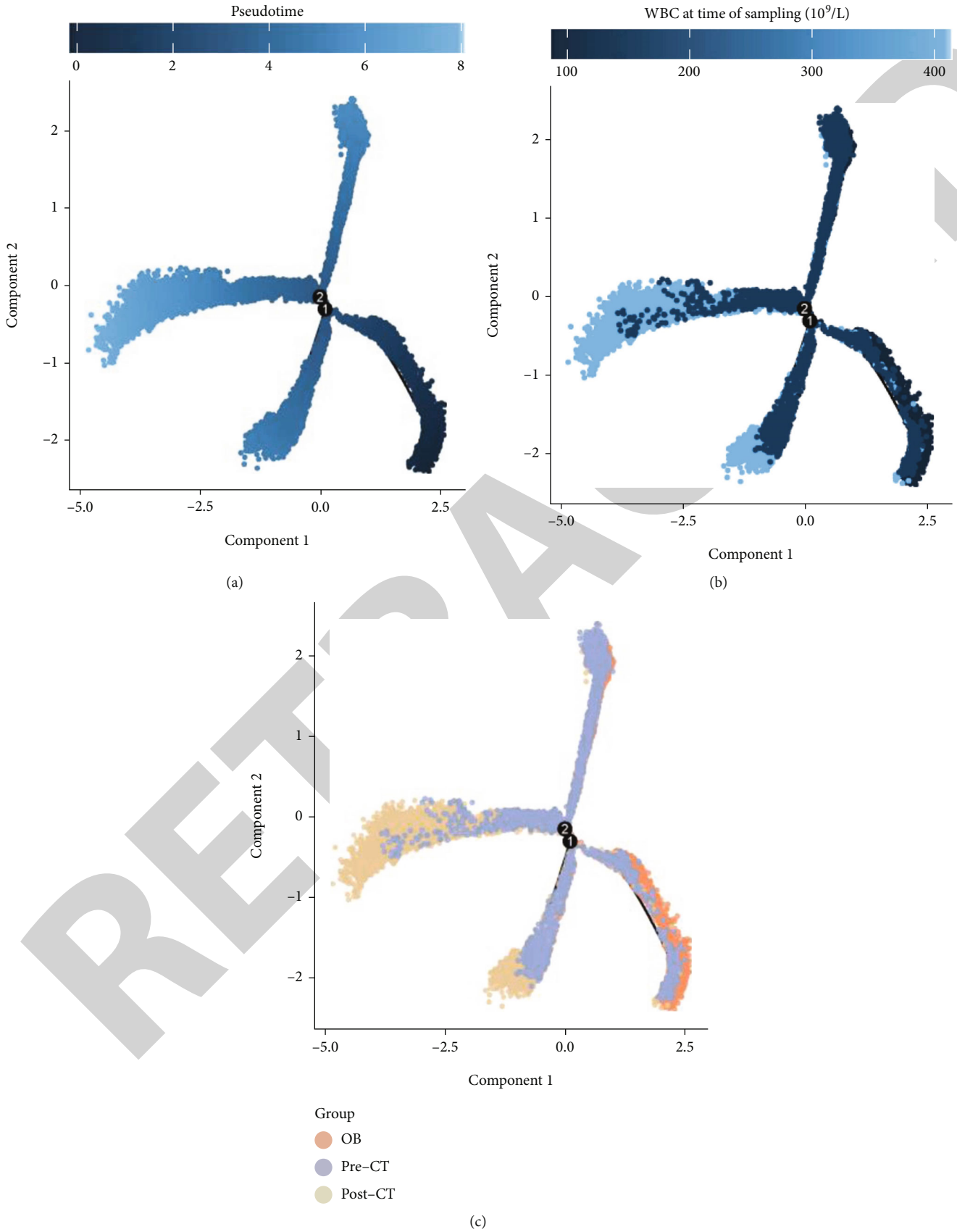

Figure 7: Continued.

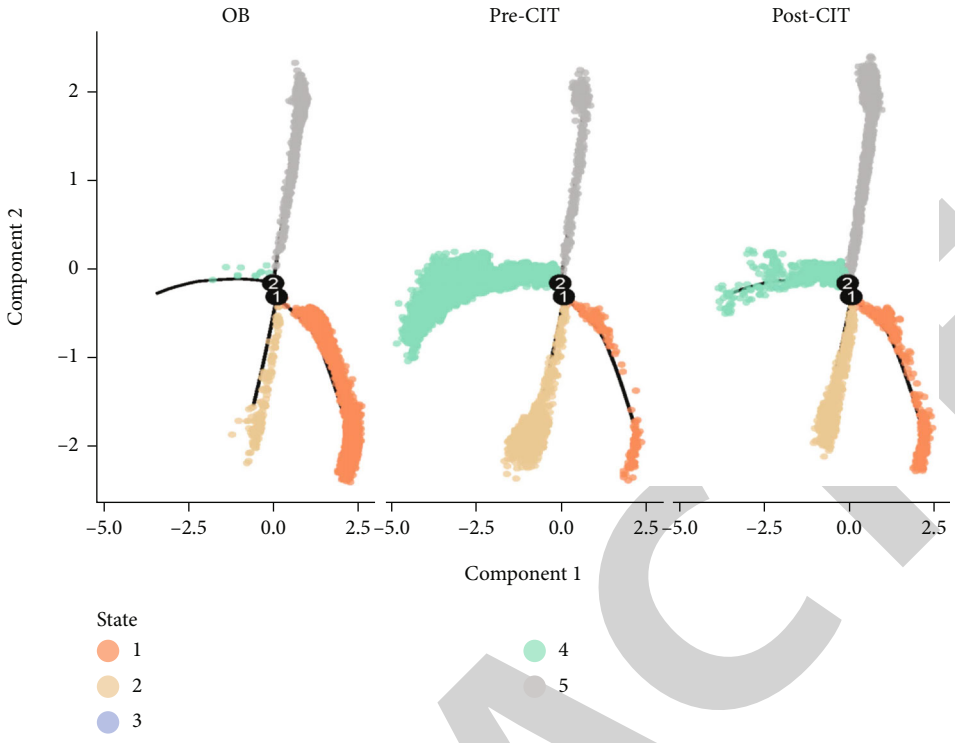

(d)

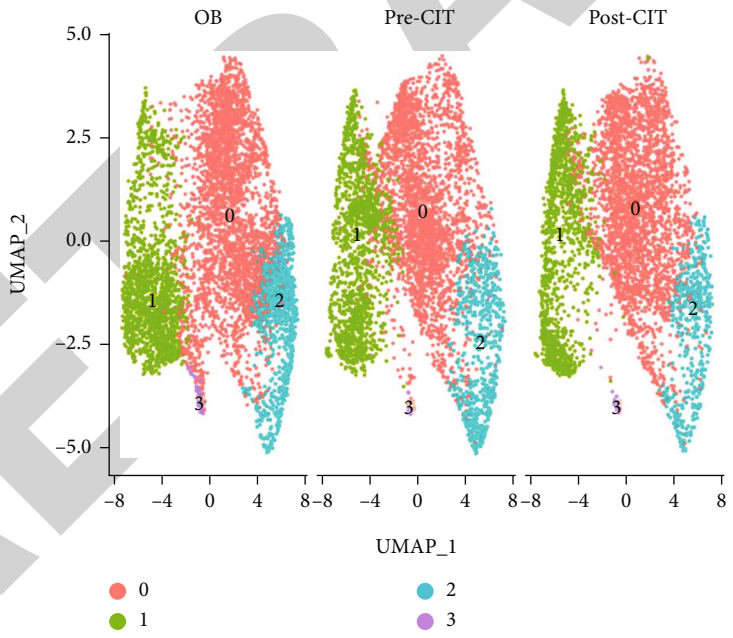

(e)

Figure 7: Continued.

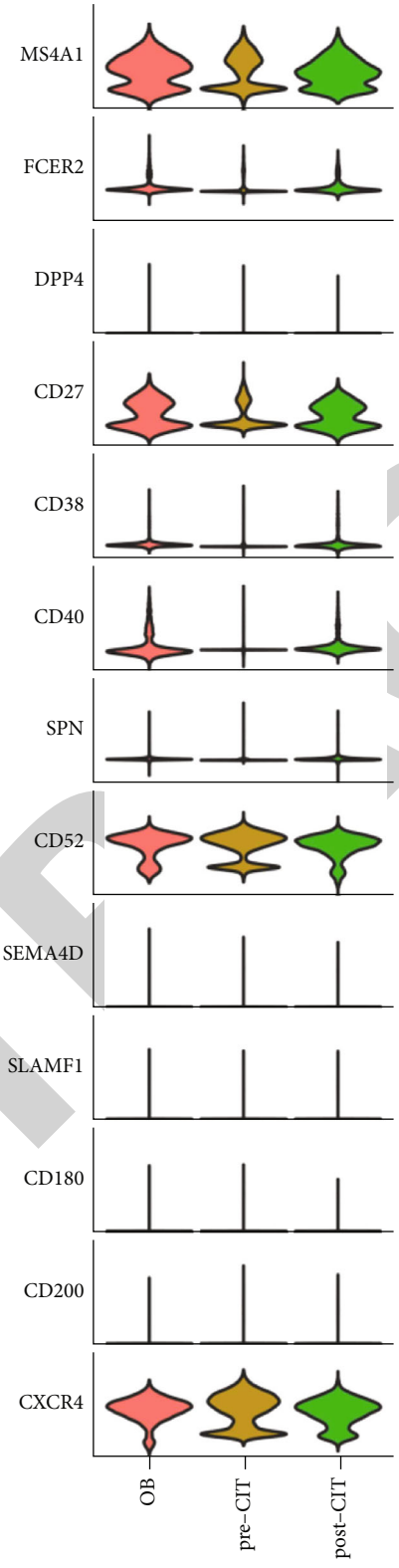

(f)

Figure 7: B cell pseudotime trajectories and DEGs of subpopulations of patient 1. (a) The colors of B cells lineage development darkened with the pseudotime developing. (b) The colors of B cells lineage development darkened with the WBC increasing.(c) The B cell pseudotime trajectories were distinguished to 3 stages of CLL. (d) The B cell pseudotime trajectories of each stage of CLL. (e) The UMAPs showed the distribution of B cell subpopulation of each stage in CLL. (f) The violin plots present little expressed difference of different B cell markers in the 3 stages.

growth and metastasis dissemination, which helps to define the character of malignancies. Results of hallmark showed that pathways with significantly increased activity were the *TP53* signaling pathway, TNFα signaling via NFkB, apoptosis, etc. (Figure 6(b)). Pathways with decreased activity were energy metabolism and oxidative regulation, etc. (Figure 6(b)). There were a small number of resemblances between the observation stage and post-CIT containing the *TP53* pathway, which was in accordance with the result of KEGG. During the observation stage, the activity of the *TP53* pathway stayed low and started negative growth at the stage of pre-CIT and reversing to positive growth when post-CIT (Figure 6(b)). However, the results of GO showed that the organelle structure and function may vary at different stages of CLL progression (Figure 6(c)). These pathway enrichment analysis results from different focuses suggested that there were significant differences in the activities of pathways in the observation stage and the relapsed post-CIT, especially the *TP53* signaling pathway and energy metabolism pathway, which were closely related to malignant tumors.

3.4. B Cell Pseudotime Trajectories and DEGs of Subpopulations of Patient 1. The B cells lineage development was constructed as a pseudotime tree trajectory (Figure 7(a)), in which dots represented cells and cells with a similar situation were clustered together. We sorted out clusters of different stages of CLL in patient 1 (Figure 7(b)) and separated each state of the 3 stages (Figure 7(c)). The B cell pseudotime trajectories showed the virtual developmental model of the post-CIT was different from the observation stage. To better understand how treatment with CIT impacted B cells of CLL patients, we presented B cell subpopulations of each stage of patient 1 (Figure 7(d)). Although the B cell subpopulation clusters of different stages did not present significant differences, there was no similarity in DEGs between different B cell subpopulations and stages of B cells (Figures 7(e) and 7(f)). This suggested that subpopulations of B cells in the same patient also exhibited heterogeneity as CLL progresses.

4. Discussion

Exploring the pathological mechanism of CLL contributes to the update of its treatment strategy, but only a limited number of its pathogenesis and risk factors have been identified until now. There is still a long way to go to build accurate prognostic prediction models for CLL that can be effectively translated into the clinic [8]. CLL is one of the strongest inherited predispositions of hematological malignancies [1, 21, 22]. Intricate genetic factors bring challenges to the exploration of molecular mechanisms of CLL. Microarray technology such as RNA-seq may help us understand the significant differences in the molecular mechanisms between pre-CIT and post-CIT of CLL. However, the results of the present study showed significant heterogeneity among the patients and different stages of CLL. Furthermore, we focused on the differences between the steady stage of observation of CLL and the relapse after CIT treatment. Several well-known signaling pathways and genes such as *TP53* may be the potential target associated with disease progression and treatment. Individualized treatment strategies should be increasingly applicable to CLL patients.

Cancer is a disease which is dynamic and generally becomes more heterogeneous during the evolution course, which provides the fuel for resistance to treatment [23]. Tumor heterogeneity can be broadly divided into intertumoral and intratumoral heterogeneity. A recent study showed that around 95.1% of informative samples of cancer (2,658 cancer samples contained 38 cancer types) presented evidence of distinct subclonal expansions and frequent branching relationships between each other [24]. This indicated that tumor heterogeneity is pervasive. Single-cell RNA-seq analysis results of the present study showed significant differences in gene expression traits and active pathways among CLL patients, including pre-CIT and post-CIT, showing heterogeneity. Moreover, all these patients relapsed after CIT, and at the same time, heterogeneity predicts challenges for subsequent treatment and prognosis. Research on cancer brings us awareness that it is not a fixed course when cancer develops and progresses, maybe as an integrated destabilization of key cellular processes [23]. Cancer is dynamic and continues to evolve, which might ultimately generate a bulk tumor which is molecularly heterogeneous, the differential sensitivity levels to anticancer therapies are shown by distinct molecular signatures [23]. This probably pointed out one of the main reasons for the treatment bottleneck of cancer, including CLL, especially when it progresses from observation stage to relapsed post-CIT as this study showed. Previous studies of whole-exome sequencing of more than 1,000 CLL specimens and whole-genome sequencing of 200 CLL patients have revealed the presence of 0.9 mutations per megabase and a load of 10-30 nonsilent events per patient [14, 25–28]. Additionally, CLL is genetically heterogeneous, containing multiple clonal and subclonal populations [25]. The treatment tolerance and the abundance and identity of the selected subclones with their evolution were affected by the interactions of these subclones along with their response to internal or external constraint [25, 26, 28]. With exposure to sequential treatment, the genomic complexity of a tumor generally increases. Clonal evolution arises more frequently in tumors receiving CIT [28]. Although tumor heterogeneity poses challenges for treatment and prognosis, studying heterogeneity has fueled a shift in the treatment paradigm towards the use of personalized or genotype-guided approaches. Evidence has indicated that heterogeneity can predict resistance to both chemotherapies and targeted therapy and can inform prognostication, therefore, the assessment of tumor heterogeneity is essential for the development of effective treatment [23, 25, 29].

Although realizing that CLL is highly heterogeneous, the present study compared DEGs and signaling pathway activity between the observation stage and relapsed post-CIT of CLL to unearth potential factors which may affect CLL progression and treatment tolerance. Results showed that several well-known signaling pathways presented significant differences between CLL stabilization and progression, such as the *TP53* pathway. A previous study had identified that *TP53* aberrations predict an aggressive disease course and refractoriness to CIT [1]. Results of a randomized prospective

trial (followed-up of 52.8 months) showed that *TP53* mutations in 8.5% of CLL patients and none of the patients with *TP53* mutation achieved a complete response [30]. A meta-analysis of an international consortium created an international prognostic index for CLL that integrated the major prognostic parameters [31]. *TP53* status (no abnormalities vs. del [17p] or *TP53* mutation or both) is one of the 5 independent prognostic factors [31]. *TP53* mutation was the strongest prognostic marker regarding progression-free survival (PFS) according to the multivariate analysis [30]. The median PFS and overall survival (OS) of patients with *TP53* mutation were significantly decreased compared with patients without *TP53* mutation. The prognostic implication of *TP53* dysregulation is related to its association with resistance to DNA damaging agents and a decreased time to first treatment and unfavorable OS [32–34]. Accordingly, *TP53* inactivation is one of a major determinants of therapeutic decisions [25]. Patients with a *TP53* mutation or del (17p) are in a high-risk category and should be treated with targeted agents [35]. An allogeneic hematopoietic stem cell transplantation (SCT) may be considered in relapsing patients with *TP53* mutations or del (17p), or patients that are refractory to inhibitor therapy [35]. However, some patients do not have suitable access to SCT. It is still recommended that the presence of del17p and *TP53* disruptions should be tested for patients of treatment-naive requiring therapy [25]. If these lesions are present, even at the subclonal, treatment of genotoxic drugs (alkylating agents, anthracyclines, or purine analogues) should not be performed, for a poor response to genetic lesions will hamper DNA repair [26, 36, 37]. An earlier study had shown that the median PFS of CLL patients with *TP53* abnormalities treated using FCR or other CIT combinations was less than 18 months [34]. Thus, ibrutinib and venetoclax are recommended for patients with *TP53* mutations upfront treatment, for the estimated median PFS of more than 30 months [38–40]. For CLL patients with relapsed or refractory after CIT treatment, targeted therapies may be the best option [25]. Results of a recent clinical trial showed that the 5-year PFS rate of patients receiving ibrutinib was 92% in treatment-naive patients and 44% in relapsed or refractory patients, the median PFS was 51 months in heavily pretreated patients receiving ibrutinib [41]. Taking this into account, the combination of venetoclax and rituximab was approved in 2018 by the FDA, and it is an option worth considering for the treatment of relapsed or refractory CLL [42]. Although these studies have brought new insights into CLL, new breakthroughs are still needed in individualized treatment and prognosis. The signaling pathways and their regulators related to CLL progression still need to be further studied to bring novel ideas for individualized treatment decisions.

The present study still has certain limitations. The limited number of samples for different stages of CLL and CIT treatment may cause bias in the analysis of existing data. This study has not yet conducted experimental verification of the current inferences and hypothesis, especially key gene expression and signaling pathways. The new discoveries and viewpoints of the results of this study need to be proved by future experiments.

5. Conclusion

In conclusion, tumor heterogeneity may be a more common manifestation of CLL. Given this, in-depth diagnosis and individualized treatment strategies may be required for CLL management. Among these, *TP53* abnormality and its regulatory factors should still be the focus of CLL diagnosis and treatment.

Data Availability

The data used to support the findings of this study are included within the article.

Disclosure

In accordance with Taylor & Francis policy and my ethical obligation as a researcher, I am reporting that this paper has no actual or potential conflict of interest including any financial, personal, or other relationships with other people or organizations that could inappropriately influence or be perceived to influence their work.

Conflicts of Interest

The authors declare that they have no conflicts of interest.

Authors' Contributions

Xiaoli Xu and Ying Zhao contributed to this work equally as co-first authors.

Acknowledgments

This study was supported by Foshan Medical Science Technology Project Management (NO. 2020001005372), the Research Fund of Guangdong Province for Medical Science (NO. A2018528), and National Key Research and Development Program of China (NO. 2018YFC2002500). We would like to acknowledge the technical support given by the GuangZhou ExoDiag Biomedical Tech Co., Ltd. and Guangzhou Gencoding Lab.

References

[1] M. Hallek, T. D. Shanafelt, and B. Eichhorst, "Chronic lymphocytic leukaemia," *The Lancet*, vol. 391, no. 10129, pp. 1524–1537, 2018.

[2] B. Jakšić, V. Pejša, S. Ostojić-Kolonić et al., "Guidelines for diagnosis and treatment of chronic lymphocytic leukemia. Krohem B-Cll 2017," *Acta Clinica Croatica*, vol. 57, no. 1, pp. 190–215, 2018.

[3] B. Eichhorst, T. Robak, E. Montserrat et al., "Chronic lymphocytic leukaemia: ESMO clinical practice guidelines for diagnosis, treatment and follow-up," *Annals of Oncology*, vol. 32, no. 1, pp. 23–33, 2021.

[4] A. C. Rawstron, K. A. Kreuzer, A. Soosapilla et al., "Reproducible diagnosis of chronic lymphocytic leukemia by flow cytometry: an European research initiative on CLL (ERIC) & European Society for Clinical Cell Analysis (ESCCA)

Harmonisation project," *Cytometry Part B, Clinical Cytometry*, vol. 94, no. 1, pp. 121–128, 2018.

[5] K. R. Rai, A. Sawitsky, E. P. Cronkite, A. D. Chanana, R. N. Levy, and B. S. Pasternack, "Clinical staging of chronic lymphocytic leukemia," *Blood*, vol. 46, no. 2, pp. 219–234, 1975.

[6] J. L. Binet, A. Auquier, G. Dighiero et al., "A new prognostic classification of chronic lymphocytic leukemia derived from a multivariate survival analysis," *Cancer*, vol. 48, no. 1, pp. 198–206, 1981.

[7] M. Hallek, B. D. Cheson, D. Catovsky et al., "Guidelines for the diagnosis and treatment of chronic lymphocytic leukemia: a report from the International Workshop on Chronic Lymphocytic Leukemia updating the National Cancer Institute-Working Group 1996 guidelines," *Blood*, vol. 111, no. 12, pp. 5446–5456, 2008.

[8] S. Molica, "Chronic lymphocytic leukemia prognostic models in real life: still a long way off," *Expert Review of Hematology*, vol. 14, no. 2, pp. 137–141, 2021.

[9] L. Liu, Y. Li, S. Li et al., "Comparison of next-generation sequencing systems," *Journal of Biomedicine & Biotechnology*, vol. 2012, Article ID 251364, 2012.

[10] P. G. Ferreira, P. Jares, D. Rico et al., "Transcriptome characterization by RNA sequencing identifies a major molecular and clinical subdivision in chronic lymphocytic leukemia," *Genome Research*, vol. 24, no. 2, pp. 212–226, 2014.

[11] W. Liao, G. Jordaan, P. Nham, R. T. Phan, M. Pelegrini, and S. Sharma, "Gene expression and splicing alterations analyzed by high throughput RNA sequencing of chronic lymphocytic leukemia specimens," *BMC Cancer*, vol. 15, no. 1, p. 714, 2015.

[12] A. F. Rendeiro, C. Schmidl, J. C. Strefford et al., "Chromatin accessibility maps of chronic lymphocytic leukaemia identify subtype-specific epigenome signatures and transcription regulatory networks," *Nature Communications*, vol. 7, no. 1, article 11938, 2016.

[13] G. Kaur, V. Ruhela, L. Rani et al., "RNA-Seq profiling of deregulated miRs in CLL and their impact on clinical outcome," *Blood Cancer Journal*, vol. 10, no. 1, p. 6, 2020.

[14] D. A. Landau, C. Sun, D. Rosebrock et al., "The evolutionary landscape of chronic lymphocytic leukemia treated with ibrutinib targeted therapy," *Nature Communications*, vol. 8, no. 1, article 2185, 2017.

[15] D. J. McCarthy, K. R. Campbell, A. T. Lun, and Q. F. Wills, "Scater: pre-processing, quality control, normalization and visualization of single-cell RNA-seq data in R," *Bioinformatics*, vol. 33, no. 8, pp. 1179–1186, 2017.

[16] T. Stuart, A. Butler, P. Hoffman et al., "Comprehensive integration of single-cell data," *Cell*, vol. 177, pp. 1888–1902.e21, 2019.

[17] D. Aran, A. P. Looney, L. Liu et al., "Reference-based analysis of lung single-cell sequencing reveals a transitional profibrotic macrophage," *Nature Immunology*, vol. 20, no. 2, pp. 163–172, 2019.

[18] A. Sergushichev, "An algorithm for fast preranked gene set enrichment analysis using cumulative statistic calculation," p. 060012, 2016, https://www.biorxiv.org/content/10.1101/060012v1.

[19] S. Hanzelmann, R. Castelo, and J. Guinney, "GSVA: gene set variation analysis for microarray and RNA-seq data," *BMC Bioinformatics*, vol. 14, no. 1, p. 7, 2013.

[20] C. Trapnell, D. Cacchiarelli, J. Grimsby et al., "The dynamics and regulators of cell fate decisions are revealed by pseudotemporal ordering of single cells," *Nature Biotechnology*, vol. 32, no. 4, pp. 381–386, 2014.

[21] J. R. Cerhan and S. L. Slager, "Familial predisposition and genetic risk factors for lymphoma," *Blood*, vol. 126, no. 20, pp. 2265–2273, 2015.

[22] H. Yan, S. Tian, G. Kleinstern et al., "Chronic lymphocytic leukemia (CLL) risk is mediated by multiple enhancer variants within CLL risk loci," *Human Molecular Genetics*, vol. 29, no. 16, pp. 2761–2774, 2020.

[23] I. Dagogo-Jack and A. T. Shaw, "Tumour heterogeneity and resistance to cancer therapies," *Nature Reviews Clinical Oncology*, vol. 15, no. 2, pp. 81–94, 2018.

[24] S. C. Dentro, I. Leshchiner, K. Haase et al., "Characterizing genetic intra-tumor heterogeneity across 2,658 human cancer genomes," *Cell*, vol. 184, no. 8, pp. 2239–2254.e39, 2021.

[25] F. Bosch and R. Dalla-Favera, "Chronic lymphocytic leukaemia: from genetics to treatment," *Nature Reviews Clinical Oncology*, vol. 16, no. 11, pp. 684–701, 2019.

[26] D. A. Landau, S. L. Carter, P. Stojanov et al., "Evolution and impact of subclonal mutations in chronic lymphocytic leukemia," *Cell*, vol. 152, no. 4, pp. 714–726, 2013.

[27] X. S. Puente, M. Pinyol, V. Quesada et al., "Whole-genome sequencing identifies recurrent mutations in chronic lymphocytic leukaemia," *Nature*, vol. 475, no. 7354, pp. 101–105, 2011.

[28] D. A. Landau, E. Tausch, A. N. Taylor-Weiner et al., "Mutations driving CLL and their evolution in progression and relapse," *Nature*, vol. 526, no. 7574, pp. 525–530, 2015.

[29] E. J. Jordan, H. R. Kim, M. E. Arcila et al., "Prospective comprehensive molecular characterization of lung adenocarcinomas for efficient patient matching to approved and emerging therapies," *Cancer Discovery*, vol. 7, no. 6, pp. 596–609, 2017.

[30] T. Zenz, B. Eichhorst, R. Busch et al., "TP53 mutation and survival in chronic lymphocytic leukemia," *Journal of Clinical Oncology: Official Journal of the American Society of Clinical Oncology*, vol. 28, no. 29, pp. 4473–4479, 2010.

[31] International CLL-IPI Working Group, "An international prognostic index for patients with chronic lymphocytic leukaemia (CLL-IPI): a meta-analysis of individual patient data," *The Lancet Oncology*, vol. 17, no. 6, pp. 779–790, 2016.

[32] D. Rossi, S. Rasi, V. Spina et al., "Integrated mutational and cytogenetic analysis identifies new prognostic subgroups in chronic lymphocytic leukemia," *Blood*, vol. 121, no. 8, pp. 1403–1412, 2013.

[33] H. Döhner, S. Stilgenbauer, A. Benner et al., "Genomic aberrations and survival in chronic lymphocytic leukemia," *New England Journal of Medicine*, vol. 343, no. 26, pp. 1910–1916, 2000.

[34] T. Zenz, A. Kröber, K. Scherer et al., "Monoallelic TP53 inactivation is associated with poor prognosis in chronic lymphocytic leukemia: results from a detailed genetic characterization with long-term follow-up," *Blood*, vol. 112, no. 8, pp. 3322–3329, 2008.

[35] M. Hallek, "Chronic lymphocytic leukemia: 2020 update on diagnosis, risk stratification and treatment," *American Journal of Hematology*, vol. 94, no. 11, pp. 1266–1287, 2019.

[36] F. Nadeu, G. Clot, J. Delgado et al., "Clinical impact of the subclonal architecture and mutational complexity in chronic lymphocytic leukemia," *Leukemia*, vol. 32, no. 3, pp. 645–653, 2018.

Hindawi
Computational and Mathematical Methods in Medicine
Volume 2023, Article ID 9823815, 1 page
https://doi.org/10.1155/2023/9823815

Retraction

Retracted: Mining of Potential Biomarkers and Pathway in Valvular Atrial Fibrillation (VAF) via Systematic Screening of Gene Coexpression Network

Computational and Mathematical Methods in Medicine

Received 5 December 2023; Accepted 5 December 2023; Published 6 December 2023

This article has been retracted by Hindawi, as publisher, following an investigation undertaken by the publisher [1]. This investigation has uncovered evidence of systematic manipulation of the publication and peer-review process. We cannot, therefore, vouch for the reliability or integrity of this article.

Please note that this notice is intended solely to alert readers that the peer-review process of this article has been compromised.

Wiley and Hindawi regret that the usual quality checks did not identify these issues before publication and have since put additional measures in place to safeguard research integrity.

We wish to credit our Research Integrity and Research Publishing teams and anonymous and named external researchers and research integrity experts for contributing to this investigation.

The corresponding author, as the representative of all authors, has been given the opportunity to register their agreement or disagreement to this retraction. We have kept a record of any response received.

References

[1] F. Zou, T. Chen, X. Xiang, C. Peng, S. Huang, and S. Ma, "Mining of Potential Biomarkers and Pathway in Valvular Atrial Fibrillation (VAF) via Systematic Screening of Gene Coexpression Network," *Computational and Mathematical Methods in Medicine*, vol. 2022, Article ID 3645402, 21 pages, 2022.

Hindawi
Computational and Mathematical Methods in Medicine
Volume 2022, Article ID 3645402, 21 pages
https://doi.org/10.1155/2022/3645402

Research Article

Mining of Potential Biomarkers and Pathway in Valvular Atrial Fibrillation (VAF) via Systematic Screening of Gene Coexpression Network

Fan Zou[1], **Tiantian Chen**[1], **Xiuying Xiang**[2], **Chengjiang Peng**[1], **Shuai Huang**[1] and **Shaohong Ma**[1]

[1]*Department of Cardiovascular Surgery, The Third Affiliated Hospital of Sun Yat-sen University, No. 600, Tianhe Road, Tianhe District, Guangzhou City, Guangdong Province, China*
[2]*Department of Hematopathology, The First Affiliated Hospital of Jinan University, Tianhe District, Guangzhou City, Guangdong Province, China*

Correspondence should be addressed to Shaohong Ma; mashh6@mail.sysu.edu.cn

Received 24 August 2022; Revised 6 September 2022; Accepted 19 September 2022; Published 3 October 2022

Academic Editor: Min Tang

Purpose. We apply the bioinformatics method to excavate the potential genes and therapeutic targets associated with valvular atrial fibrillation (VAF). *Methods*. The downloaded gene expression files from the gene expression omnibus (GEO) included patients with primary severe mitral regurgitation complicated with sinus or atrial fibrillation rhythm. Subsequently, the differential gene expression in left and right atrium was analyzed by R software. Additionally, weighted correlation network analysis (WGCNA), principal component analysis (PCA), and linear model for microarray data (LIMMA) algorithm were used to determine hub genes. Then, Metascape database, DAVID database, and STRING database were used to annotate and visualize the gene ontology (GO) analysis, KEGG pathway enrichment analysis, and PPI network analysis of differentially expressed genes (DEGs). Finally, the TFs and miRNAs were predicted by using online tools, such as PASTAA and miRDB. *Results*. 20,484 differentially expressed genes related to atrial fibrillation were obtained through the analysis of left and right atrial tissue samples of GSE115574 gene chip, and 1,009 were with statistical significance, including 45 upregulated genes and 964 downregulated genes. And the hub genes implicated in AF of NPC2, ODC1, SNAP29, LAPTM5, ST8SIA5, and FCGR3B were screened. Finally, the main regulators of targeted candidate biomarkers and microRNAs, EIF5A2, HIF1A, ZIC2, ELF1, and STAT2, were found in this study. *Conclusion*. These hub genes, NPC2, ODC1, SNAP29, LAPTM5, ST8SIA5, and FCGR3B, are important for the development of VAF, and their enrichment pathways and TFs elucidate the involved molecular mechanisms and assist in the validation of drug targets.

1. Background

Atrial fibrillation (AF) is the most common sustained arrhythmia, and actual epidemiological data are often underestimated. According to research, in China, the prevalence and incidence of atrial fibrillation show increasing epidemiological characteristics with age, and the total prevalence of the population can reach 0.77%, and those over 80 years old can reach over 10 years old [1]. With the development of my country's economy and the aging of the population, the number of patients with atrial fibrillation has increased rapidly, and the number of patients with atrial fibrillation is expected to increase exponentially in the next 10 years [2]. Embolism and heart failure are common complications of atrial fibrillation, and the mortality rate is more than twice that of the general population [3]. Due to the numerous pathogenic factors of atrial fibrillation, it is difficult to prevent and treat clinically, which is still one of the problems in cardiovascular.

Valve disease is one of the common causes of atrial fibrillation in cardiovascular surgery, including macrovascular disease, congenital heart disease, and coronary artery disease [4]. Valvular atrial fibrillation was first proposed in the 2012

Table 1: Top 5 up- and downregulated genes of chip GSE115574.

Gene ID	logFC	AveExpr	t	P Value	Adj.P.Val	B
RGS6	0.516701	4.290465	9.958301	$2.64E-14$	$2.27E-12$	22.2945
OTOGL	1.275203	5.172998	7.768166	$1.26E-10$	$2.37E-09$	13.94223
KIAA0753	0.551188	5.603697	7.504565	$3.53E-10$	$5.69E-09$	12.92274
PCDHGA10	0.936869	4.489173	7.259196	$9.26E-10$	$1.28E-08$	11.97422
LOC100506813	0.653479	5.248975	6.776567	$6.13E-09$	$6.37E-08$	10.11424
FCGR3B	-1.26104	3.645921	-24.147	$1.66E-32$	$3.41E-28$	62.87675
CTNS	-0.61385	4.013762	-17.8101	$1.44E-25$	$1.11E-21$	47.67246
SLC35E1	-0.60841	5.726716	-17.7658	$1.63E-25$	$1.11E-21$	47.55132
TIFAB	-0.74335	3.823311	-17.3504	$5.35E-25$	$2.74E-21$	46.40393
ARHGAP22	-0.61343	3.371978	-16.8357	$2.39E-24$	$9.80E-21$	44.95354

ESC updated guidelines, in which atrial fibrillation is divided into "valvular atrial fibrillation (VAF)" and "nonvalvular atrial fibrillation (NVAF)", VAF is defined as valvular heart disease atrial fibrillation and atrial fibrillation, fibrillation after valve replacement [5]. Common complications of atrial fibrillation include heart failure and embolism. The study found that the incidence of heart failure caused by atrial fibrillation is 3.4 times that of normal people, while the incidence of embolism caused by atrial fibrillation is about 5% per year, which is 7 times that of normal people [6]. Cerebral embolism is the most common and most dangerous complication of atrial fibrillation. Studies have shown that the incidence of stroke caused by atrial fibrillation is 20% per year. The stroke caused by NVAF is 7 times that of normal people, while the stroke caused by VAF is up to 17 times that of normal people [7]. According to the survey, the incidence of valvular atrial fibrillation is as high as 70%, and the mortality and disability rate caused by heart failure and cerebral embolism are higher in cardiac surgery complicated with atrial fibrillation. Valvular atrial fibrillation seriously affects the hospitalization time and survival time of patients, seriously reduces the quality of life of patients, and also brings serious economic burden to family members. However, current treatments have not achieved satisfactory results [8]. In view of its high incidence and serious impact on human health and safety, exploring the diagnosis and treatment of valvular atrial fibrillation is one of the research hotspots in the cardiovascular field in recent years.

At present, the treatment of atrial fibrillation is generally divided into drug therapy and nondrug therapy. Drug therapy mainly includes ventricular rate control, anticoagulation therapy to prevent thromboembolism, and antiarrhythmic therapy to restore and maintain sinus rhythm. Long-term drug therapy has a high recurrence rate, which leads to new-onset arrhythmias, and also brings many disadvantages to patients, such as poor tolerance, bleeding risk caused by anticoagulant drugs, and poor efficacy. In interventional therapy, radiofrequency ablation has become one of the most important methods for the treatment of valvular atrial fibrillation. However, there are still some deficiencies in radiofrequency ablation for atrial fibrillation, the recurrence rate is still high, up to 40%, and with the extension of follow-up time, the recurrence rate is still on the rise [9–11]. Therefore, the key to solving the problem lies in elucidating the molecular mechanism of the occurrence and maintenance of valvular atrial fibrillation. Whether there are key regulatory factors in the process has not been reported.

However, the genetic variants currently defined combine to explain only a small fraction of the incidence of atrial fibrillation. On the one hand, many studies have focused on serum and animal experiments to explore the relationship between atrial fibrillation and mechanisms or biomarkers, but there are fewer reports on atrial tissue directly affecting atrial fibrillation, especially in patients with valvular atrial fibrillation. On the other hand, these results suggest that genetic variants isolated from individual samples cannot be broadly applied to the general population. Hub genes identified from differential expression analysis may lose statistical power in protein-protein interaction networks due to mutual functional regulation. Due to the high standard of genetic selection, some key genes may have been lost. Based on the above notes, we will use multiple algorithms, including LIMMA, WGCN, PCA, and gene functional analysis of microarray data, to obtain key genes and gene regulatory networks for valvular atrial fibrillation. These will help us better understand the molecular mechanism of atrial fibrillation and the interaction of the complex gene environment and provide a theoretical basis for the diagnosis and treatment of atrial fibrillation.

2. Materials and Methods

2.1. Materials. We downloaded these data from the Public Resource Database GEO (http://www.ncbi.nlm.nih.gov/geo/) and generated expression profiling arrays using Affymetrix Human Genome U133 Plus 2 GPL570 (HG-U133_Plus_2). The retrieval involved the following process: (1) collecting datasets searched with the keywords "atrial fibrillation" and "valvular disease". (2) Select "Homo sapiens" as the specimen source and "Expression profiling by high throughput sequencing" as the study type. (3) The gene chip data is selected as "Affymetrix Human Genome" on the test

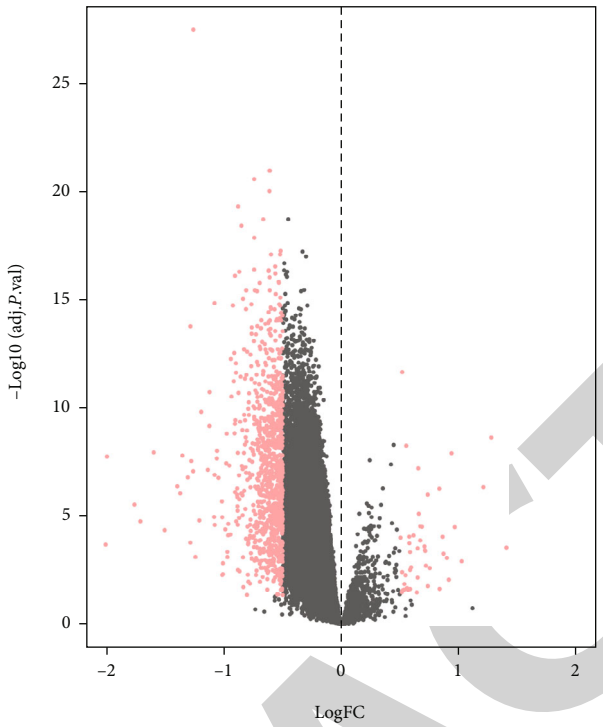

(a)

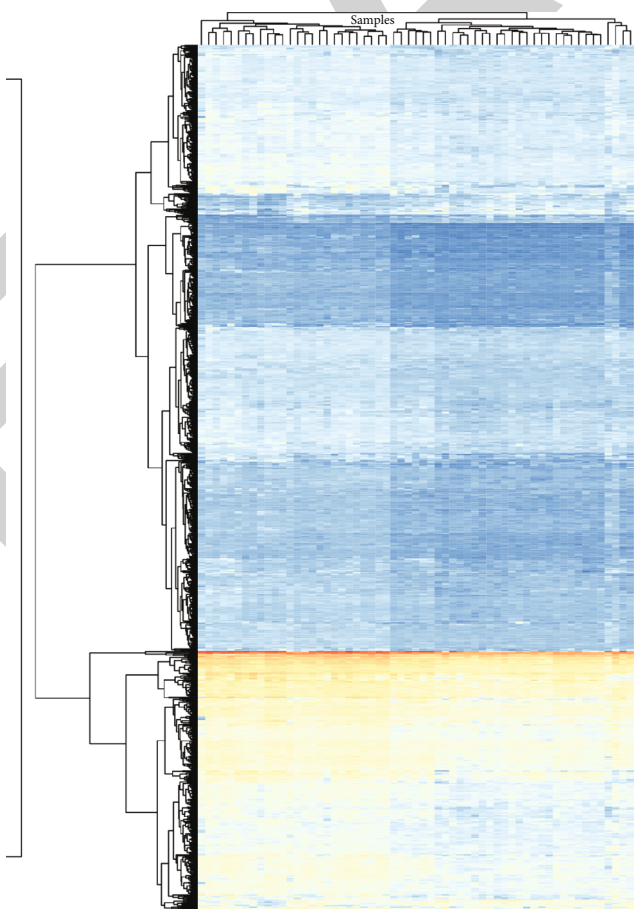

(b)

Figure 1: Continued.

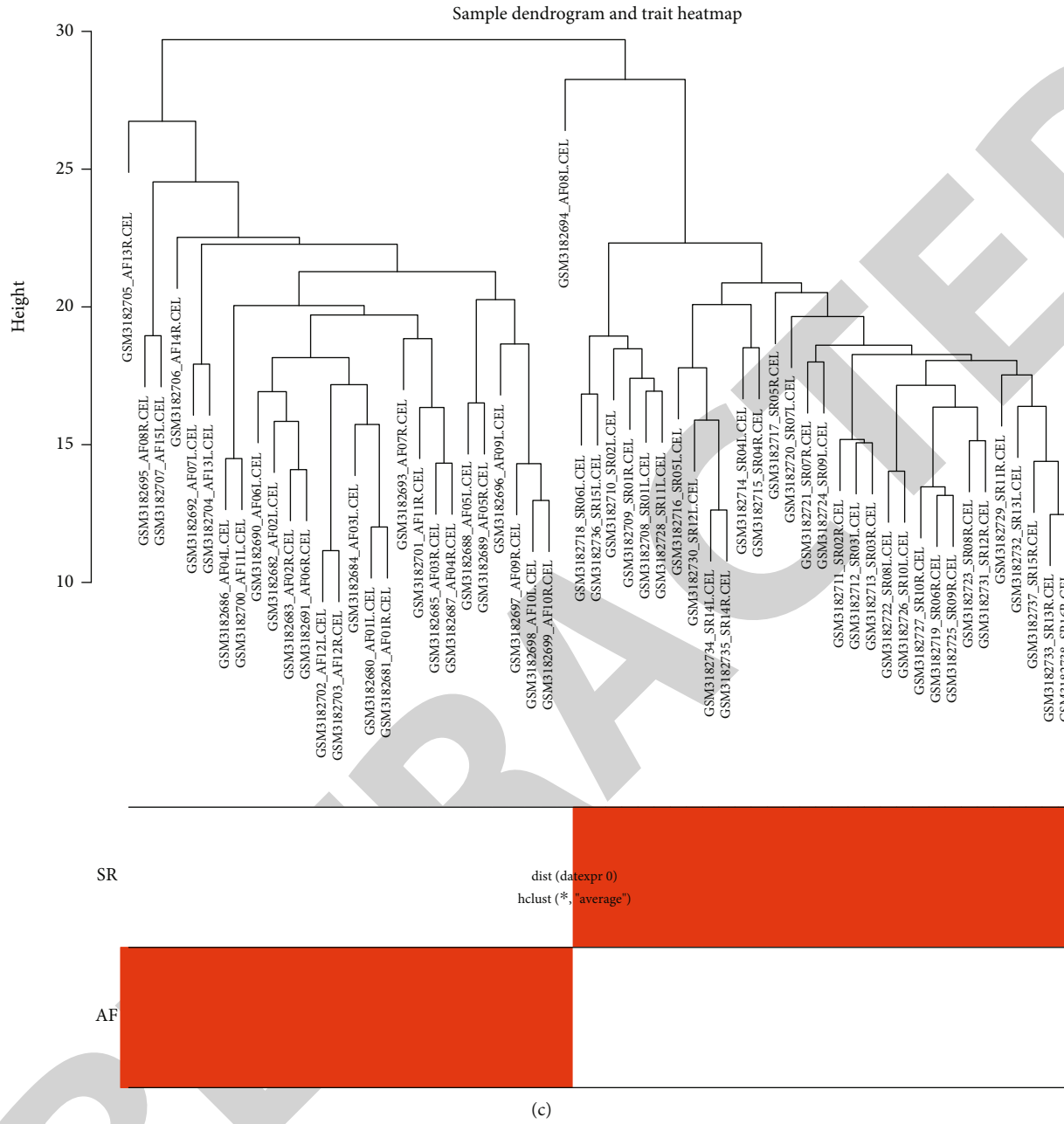

Figure 1: Differential expression genes (DEGs). (a) Volcano map, *Y*-axis represents *P* value, *X*-axis represents multiple changes, each point represents a gene, and red and black represent up-down genes; (b) heat map of differentially expressed genes; and (c) sample name map.

platform. The GSE115574 dataset was published on September 4, 2019, from surgically resected left and right atrial tissue from 30 patients with severe chronic mitral regurgitation, including 15 with preoperative atrial fibrillation and 15 with preoperative sinus. In this study, patients with persistent atrial fibrillation lasted more than 6 months. Patients with sinus rhythm had no clinical evidence of atrial fibrillation and no history of any antiarrhythmic drugs.

2.2. Data Processing. Using the "ComBat" function of the SVA package, the study is aimed at eliminating bias from the high-throughput data from different microarrays. The aim of bioinformatics is to analyze all of the raw data from microarrays, including background correction, quantile normalization, and probe summarization values [12]. The study also used some advanced algorithms, such as robust multiarray average for background-adjusted, normalized, and log-transformed probe expression values; the *t*-test in the "LIMMA" package to identify differentially expressed genes (DEGs); and the Benjamini–Hochberg method that aims at adjusting *P* values [13]. DEGs are gene expression values with $|\log 2FC| > 1$ and *P* value <0.05. The aim of selecting coannotated genes (a total of 20,484 genes) in GPL570 platform was to illuminate further coexpression network analysis.

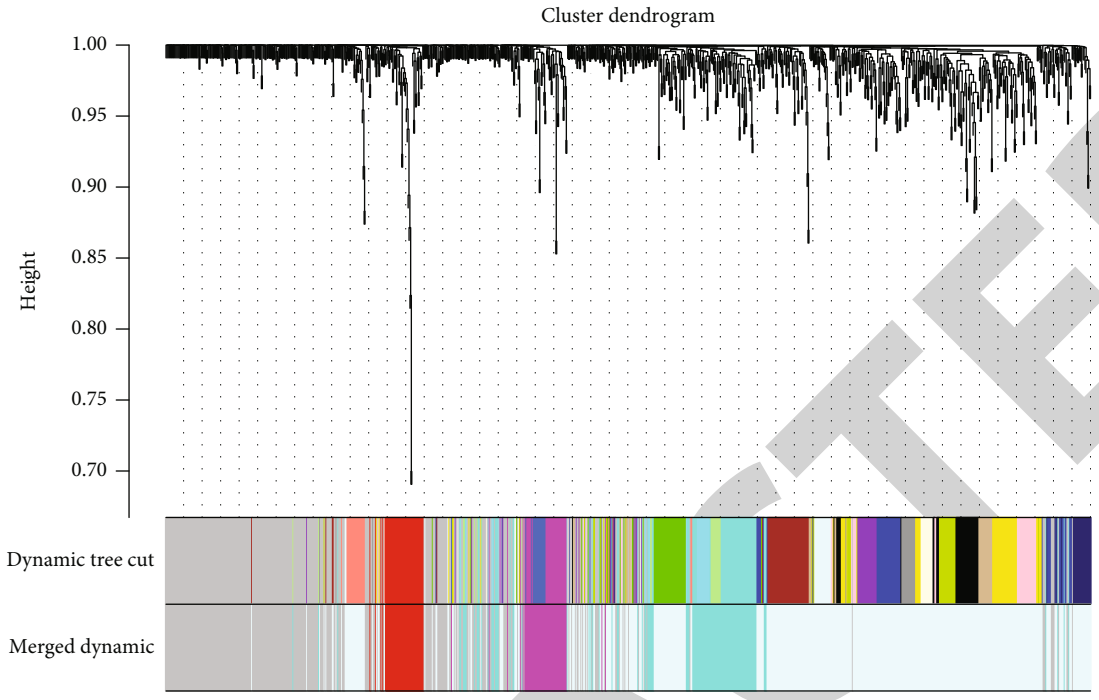

(a)

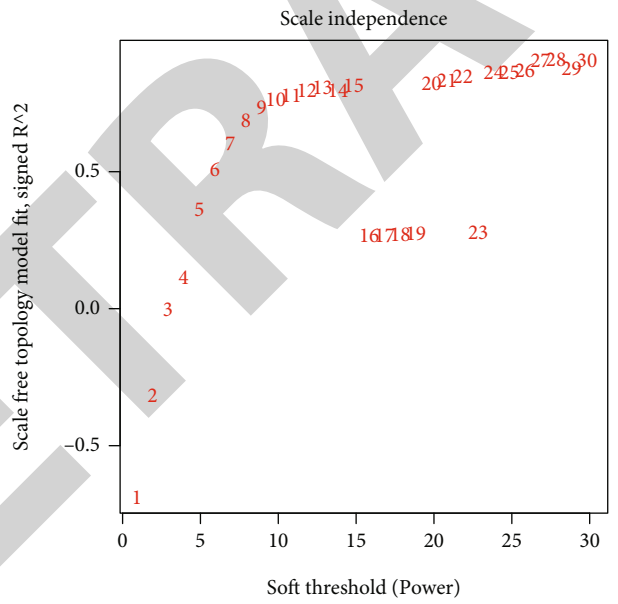

(b)

Figure 2: Continued.

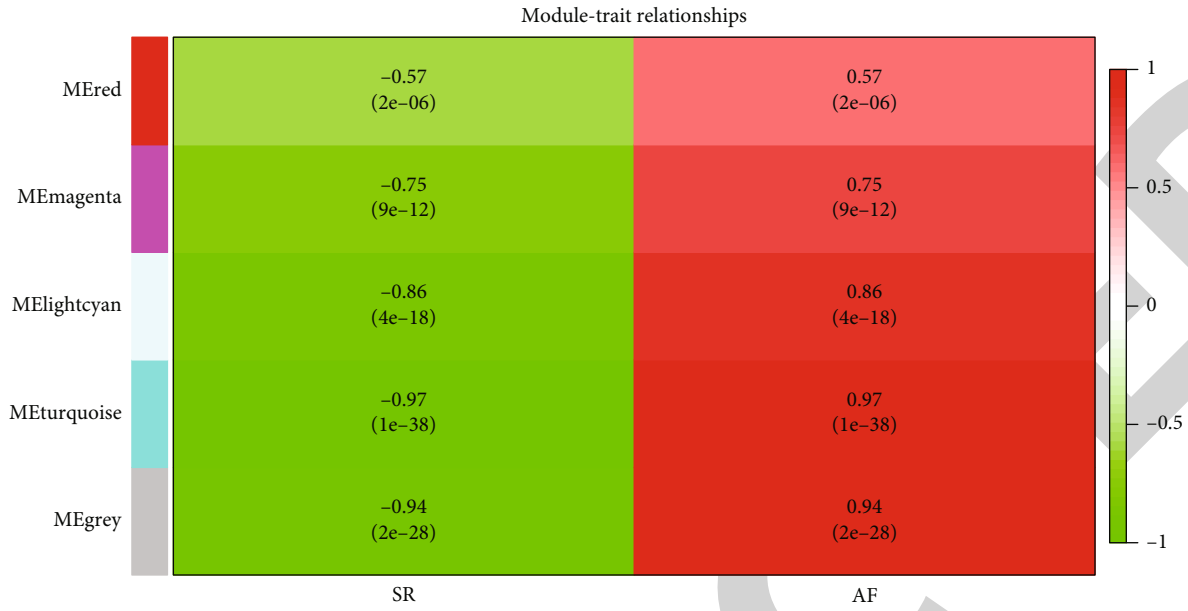

(c)

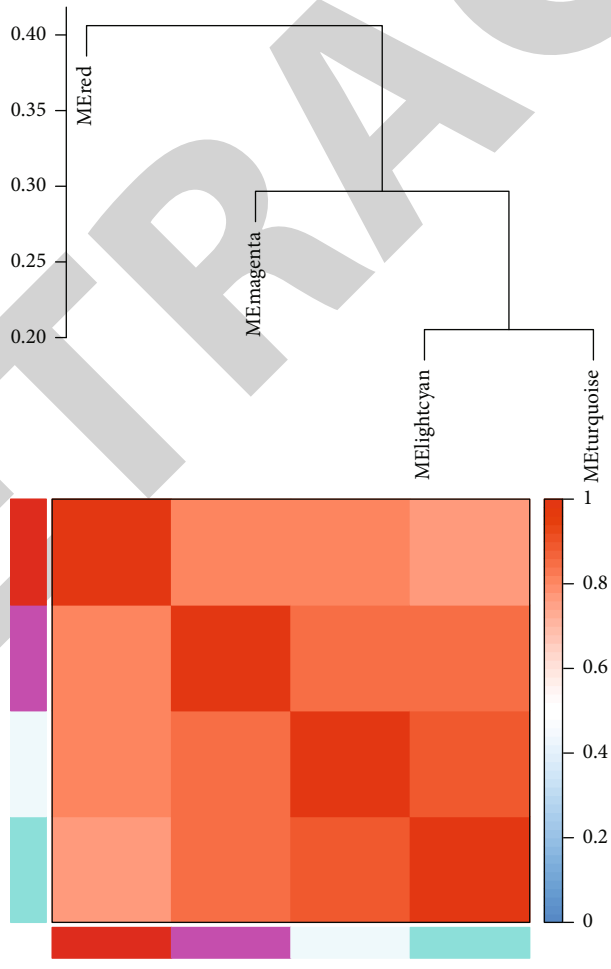

(d)

Figure 2: Continued.

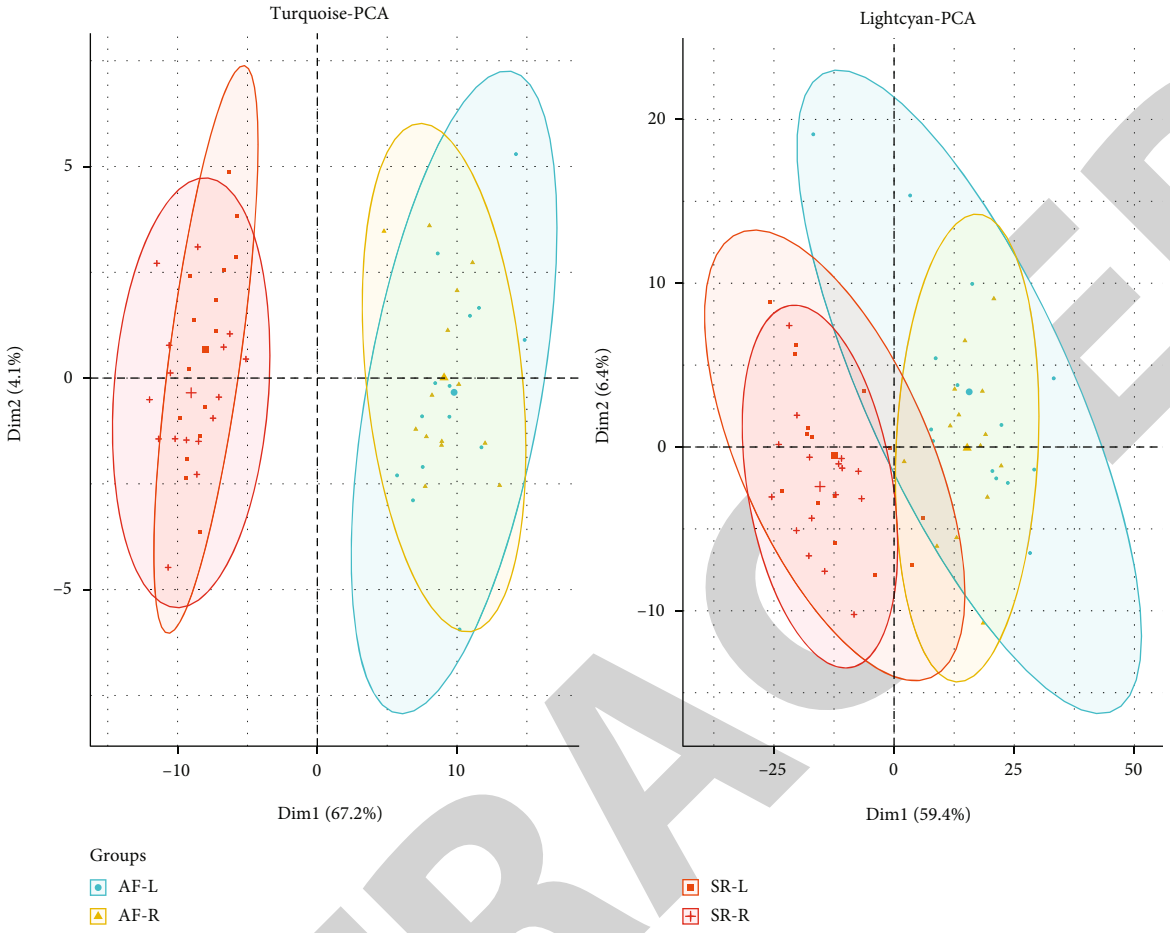

(e)

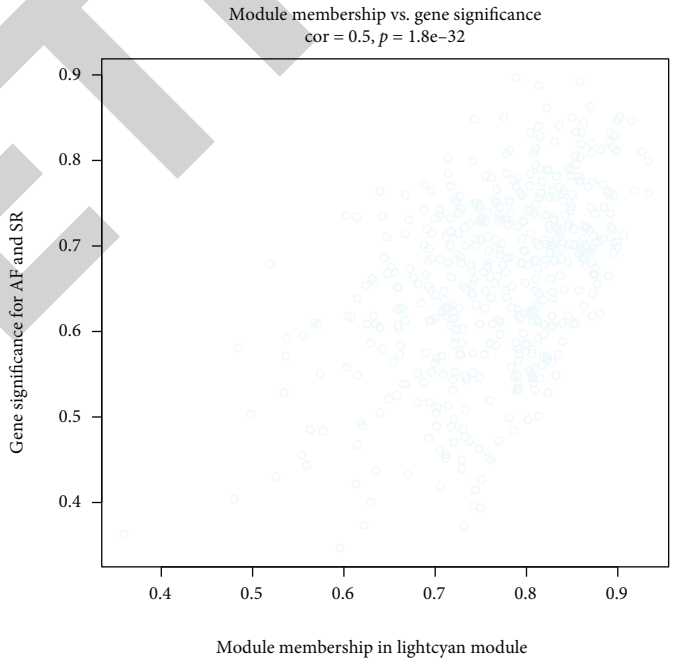

(f)

Figure 2: Continued.

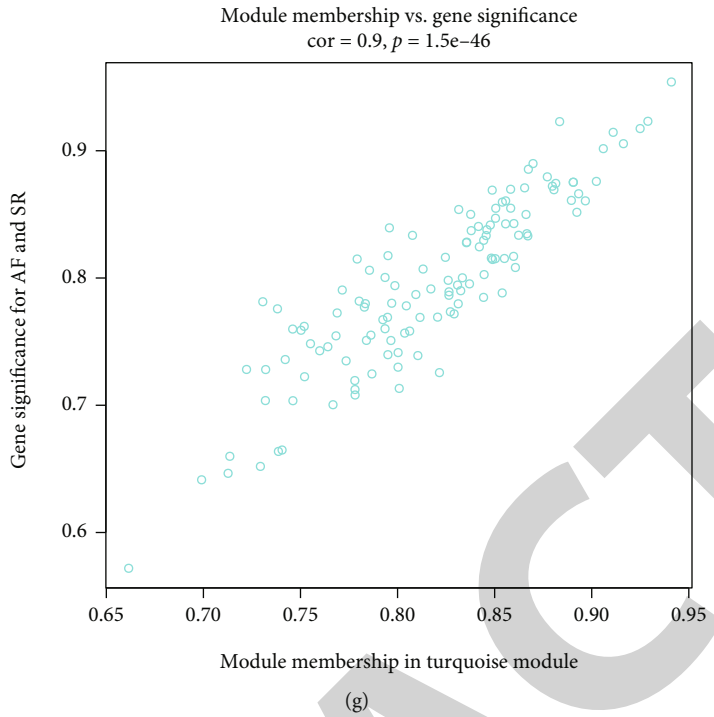

(g)

Figure 2: Construction of weighted gene coexpression network (WGCN) and gene module analysis for patients with atrial fibrillation and sinus rhythm accompanied by severe mitral regurgitation: (a) gene coexpression module diagram based on dynamic branching method; (b) value of module dependency of dynamic branch cutting method (when power value is 12, independent area rises to 0.8); (c) the relationship between gene coexpression module and clinical traits. Red represents positive correlation and green represents negative correlation. (d) Connectivity of characteristic genes, with the decrease of red, the positive correlation is weaker. (e) Principal component analysis (PCA) of the two key modules, MElightcyan and MEturquoise. MEturquoise first principal component: 67.2%, second principal component: 4.1%; MElightcyan first principal component: 59.4%, second principal component: 6.4%; genetic significance (GS), module membership (MM), and activity analysis of key modules related to atrial fibrillation in (f) and (g).

2.3. Weighted Gene Coexpression Network (WGCN) Construction and Module Detection. The coexpression network analysis has functions which integrate other informations and avoid information missing. Another system-level insight is better than other approaches, so as to give WGCNA an edge. Therefore, a system-level analysis based on WGCNA is used in the study. The WGCN was constructed using the WGCN package in RStudio. All analyses were conducted using RStudio [14].

The functional enrichment of differentially expressed genes related to atrial fibrillation was analyzed by online public database, Metascape database (http://metascape.org/gp/index.html), and database for annotation, visualization, and integrated discovery bioinformatics resources database (DAVID, http://david.abcc.ncifcrf.gov/). The analysis involved the following processes: (1) the purpose of this project is to obtain gene annotations, visualize bioinformatics resources, and integrate them, DAVID database was used to carry out gene ontology (GO) analysis on differentially expressed genes, and GO entries with P value less than 0.05 were considered to be significantly enriched [15]. (2) Downloaded from Metascape, the Kyoto Encyclopedia of Genes and Genomes (KEGG) pathway, and adjusted P value <0.05 and enrichment score > 1.0 was considered to indicate a statistically significant difference [16].

2.4. Construction of Protein-Protein Interaction (PPI) Network and Screening of Key Genes. Protein-protein interaction network is a complex interaction and communication network between two or more proteins. The network can take place in many biological processes, including gene expression, molecular transport, signal transduction, and catalytic metabolic reactions. It can also be used to predict the interaction between related genes and their proteins and has certain significance for studying the molecular mechanism and drug targets in the occurrence and development of diseases. Therefore, we utilize the STRING database (V10.5; http://string-db.org) and Cytoscape software (V3.5.1; http://cytoscape.org/) to construct PPI network of differentially expressed genes enriched in key KEGG pathway, such as biological metabolic processes, autophagy, ion conversion, and immune inflammatory processes and to visualize and annotate. The cut-off criteria were set to: $P <$ 0.05 and enrichment score > 1.0, that is, the elimination of no correlation or weak action of the protein [17]. We obtain the key modules and core genes in PPI network using the MCODE plugin of Cytoscape software.

2.5. Prediction of Transcription Factors and microRNAs of Key Genes. The transcription factors of key genes are predicted by using the iRegulon plugin of the Cytoscape

Table 2: The KEGG network pathway terms of key modules.

Modules	Description	Gene	Log*P*
MElightcyan	mTOR signaling pathway	ATP6V1B2, CHUK, PRKAA2, MAP2K1, RPS6KA2, RPS6KA3, etc.	-5.10575
	Fc epsilon RI signaling pathway	GFPT1, HEXB, HK1, etc.	-4.82544
	Autophagy-animal	PRKAA2, SNAP29, SH3GLB1, etc.	-3.22867
	Proteasome	PSMC4, PSMD7, PSMD8,etc.	-2.80551
	Lysosome	ATP6AP1, HEXB, LAPTM5, etc.	-2.58718
	Natural killer cell-mediated cytotoxicity	ARAF, FCER1G, IFNGR2, ITGB2, etc.	-2.41921
	Insulin signaling pathway	ARAF, HK1, PRKAA2, etc.	-2.34109
MEturquoise	Glycosaminoglycan biosynthesis, heparan sulfate backbone	EXT1, EXT2	-2.28058
	SNARE interactions in vesicular transport	STX4, SNAP29, YKT6	-2.19845
	Natural killer cell-mediated cytotoxicity	FCGR3B, ITGAL, HCST	-2.70881
	Glycosaminoglycan biosynthesis, heparan sulfate backbone	EXTL3	-1.73339
	O-glycan biosynthesis, mucin type core	GALNT10	-1.30872
	Lysosome	CTNS, CTSV	-1.65612
	Staphylococcus aureus infection	C2, FCGR3B, ITGAL	-3.80614

software, and the parameters are set as follows: the minimum value of gene homology is 0.05; maximum FDR for motif similarity is 0.001; and the normalized enrichment score (NES) is greater than 5. Finally, using online tools from miRDB (http://mirdb.org/) was applied to predict interactions between miRNAs and co-DEGs involved in AF. Therefore, the regulatory factors with high NSE values and microRNAs were used as regulatory networks to participate in the development of atrial fibrillation.

3. Results

3.1. Identification of Differentially Expressed Genes (DEGs). The AF and SR patients without additional treatment from GSE115574 (GPL570) datasets were used in all the samples for further analysis, including 15 cases of preoperative atrial fibrillation and 15 cases of preoperative sinus. We identified 54,675 probes corresponding to 20,484 genes in GSE115574 datasets and GPL570 platform. There were 1,009 DEGs with statistical significance, including 45 upregulated genes and 964 downregulated genes. The first five genes of up- and downregulated genes are shown in Table 1. The heat map and the volcano plot for the DEGs are illustrated in Figure 1.

3.2. Construct Coexpression Network and Gene Module. We obtained 6 clusters (MElightcyan, MEgrey, MEmagenta, MEred, MEturquoise, and MEyellow; Figure 2(a)) in the 59 samples with 1009 gene variables after sample cluster analysis and samples that did not get lost in the analyses. The WGCN analysis involved the following processes: (1) when the standard parameter was set to 10 (power valve), the scale independence rose to 0.8 and the mean relation was higher in Figure 2(b). (2) We obtained the two key models, MElightcyan: VAF Pearson valve = 0.97, $P = 1e - 38$; SR Pearson valve = −0.97, $P = 1e - 38$ and MEturquoise: VAF Pearson valve = 0.86, $P = 4e - 18$; SR Pearson valve = −0.86, $P = 4e - 18$ (Figure 2(c)). (3) The heat map suggested no significant difference in module genes. The interaction analysis of coexpression modules showed a significant independence (Figure 2(d)). (4) We found the three clusters in different modules of the connectivity of eigen-genes, and the study illuminates obvious connectivity among the eigen-genes of different modules within the same cluster showed, whereas there was no difference among different clusters' modules in Figure 2(d). (5) Differentially expressed genes in the MElightcyan and MEturquoise modules are shown in Table 2. On other hand, as to VAF, we also found the significant difference of the MEgreen and MEbrown module genes in response to AF and SR in two-dimensional PCA results (Figure 2(e)). Figures 2(f) and 2(g) show the gene significance (GS) analysis results about a significant difference between the genes and the characteristic of AF, *P* values are far less than 0.05.

3.3. Functional GO Terms and Pathway Enrichment Analyses. Further functional enrichment analysis was carried out on DEGs of the MElightcyan and MEturquoise key modules, including gene ontology (GO) analysis and KEGG pathway enrichment analysis. Regarding GO terms enrichment, the MElightcyan module was mainly enriched in GO biological process (BP): cell protein modification process, intracellular signal transduction process, proteasome-mediated ubiquitin-dependent protein degradation process, negative regulation of classical Wnt signaling pathway, stimulating c-type lectin receptor signaling pathway, and other common processes such as enrichment. Cellular components: cytoplasm, extracellular matrix, cell membrane, Golgi body, endoplasmic reticulum, mitochondria, etc. Molecular function: protein binding, ATP energy binding, transmembrane transport, same protein binding point, ubiquitin protein transferase activity, protein activation, etc. These results are shown in Figure 3(a). Genes in the MEturquoise module were predominantly enriched in BP: vesicle secretion, cell localization, membrane tissue generation,

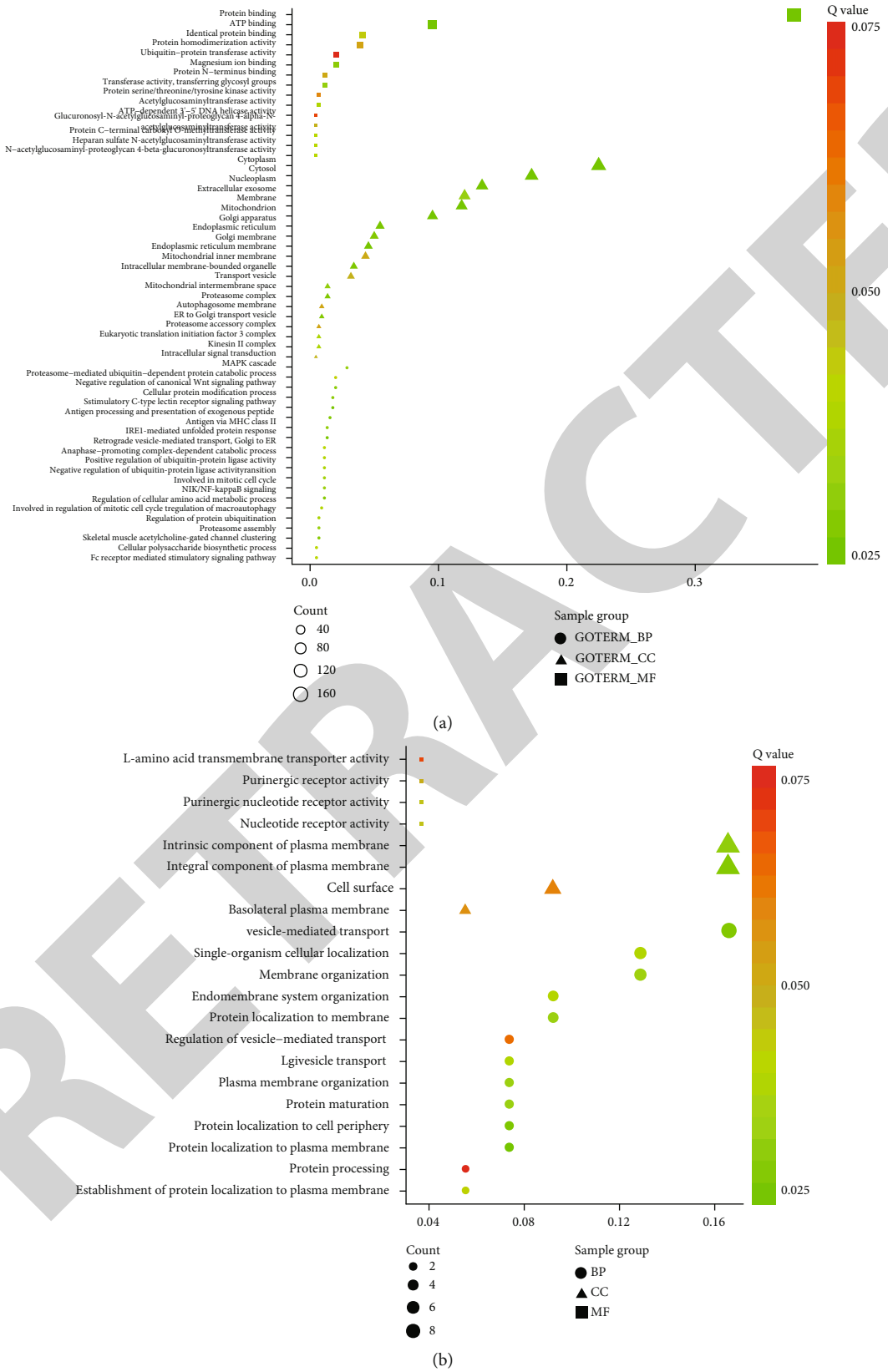

Figure 3: Key module DEGs gene ontology (GO) analysis. (a, b) GO analysis of DAVID database MElightcyan and MEturquoise module gene, dot size represents the number of genes contained, dot color represents Q value.

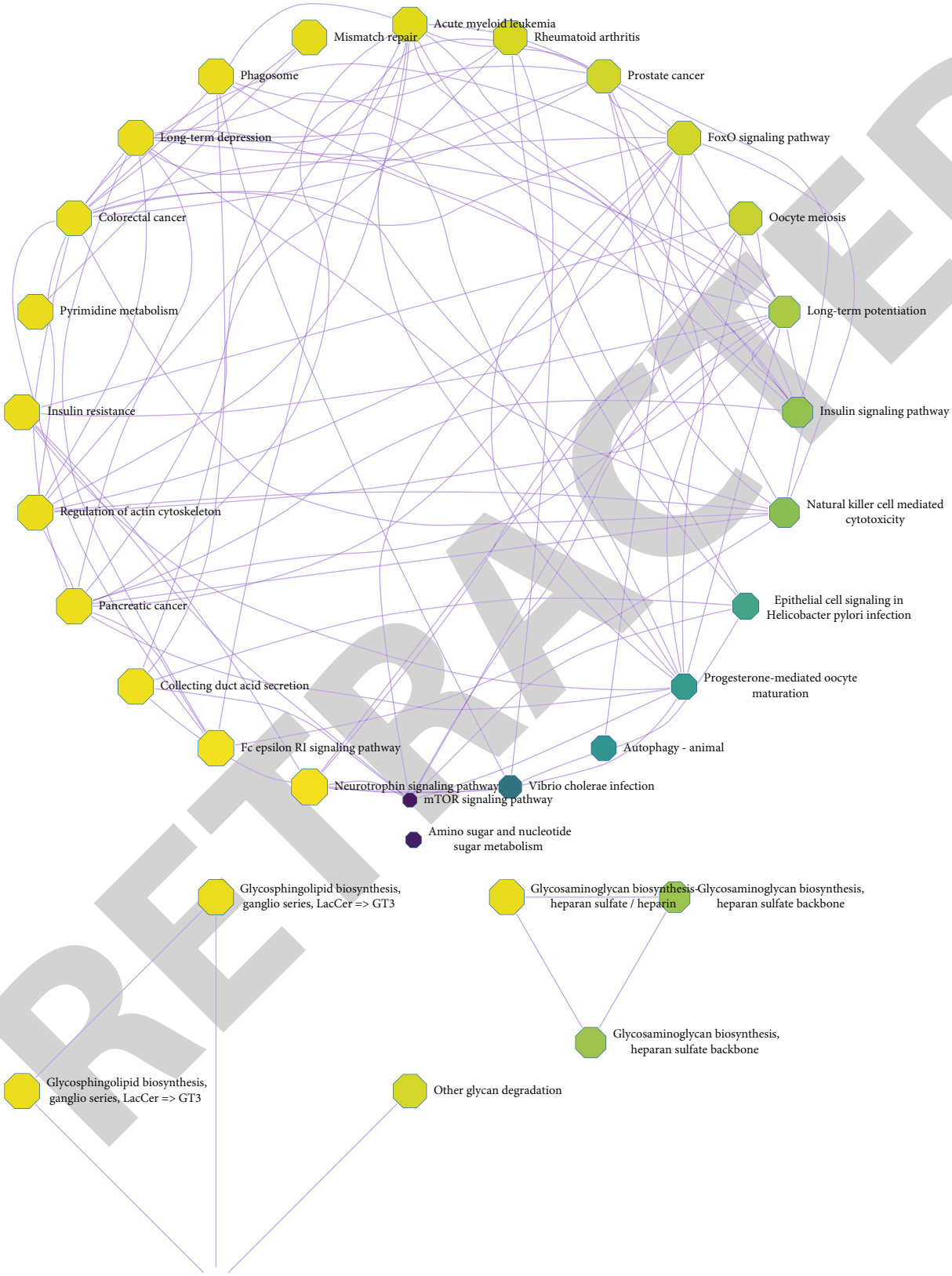

(a)

Figure 4: Continued.

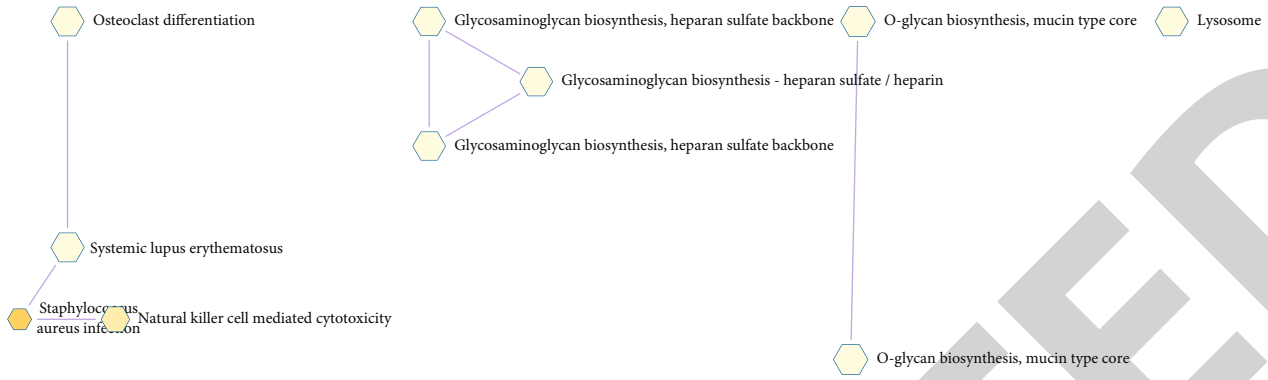

(b)

Figure 4: The KEGG analysis of the key module DEGs: (a, b) the enrichment analysis in the Metascape database, the circle size represents the size of the Log*P* value, and the color represents the enrichment fraction.

membrane protein localization, etc. In terms of cellular components, genes are mainly enriched in membrane components, including plasma membrane and extracellular membrane. In terms of MF, it is mainly concentrated in the activity of energy receptor and amino acid transmembrane transporter. These results are illustrated in Figure 3(b).

KEGG pathway analysis data appeared in Figure 4 is downloaded to the Metascape database. The results suggested that the MElightcyan module genes were significantly enriched in the interaction of vesicular transport, classical mTOR signaling pathway, FOXO signaling pathway, biosynthesis, and metabolism. MEturquoise module DEGs are enriched in natural killer cell-mediated cytotoxicity, cytoskeleton synthesis, and inflammatory response pathways.

3.4. Construction of Protein-Protein Interaction (PPI) Network and Screening of DEGs. Additionally, Table 3 illustrates a part of the visible pathway that is tightly correlated with atrial structural remodeling and electrical remodeling from the KEGG pathway network. After submitting the genes enriched in cancer-correlated pathways to the STRING database, PPI network were obtained for the MElightcyan and MEturquoise modules, respectively, with a confidence threshold greater than 0.4 in Figure 5(a). We subsequently conducted a module analysis. When a "score > 3" was defined as the cut-off criterion in MCODE, 5 clusters of modules (Module 1, Module 2, Module 3, Module 4, and Module 5) were identified from the PPI network visualized by STRING in the MElightcyan modules (Figures 5(b)–5(f)), and Figure 5(g) shows the functional modules of the MEturquoise modules. Furthermore, the MCODE analysis showed the 6 seed genes of each cluster, these were ST8SIA5, ODC1, LAPTM5, NPC2, SNAP29, and FCGR3B. Thus, they are likely to be novel therapeutic target genes or biomarkers.

3.5. Identification of Hub Gene Involving in VAF. What's more, the gene expression levels in clinical traits and left or right atrial tissues were compared based on GEO database. Consequently, the gene differential expression level with regrading to hub genes was constructed. We also found a statistical difference in the gene expression levels of these genes between VAF and SR, while no statistical difference between right and left atrial tissues in Figure 6. Subsequently, expression levels of the six hub genes show a significant difference in expression level between VAF and SR, respectively. Figure 7 appeared all the $P < 0.05$.

Table 3: TFs of top five enrichment fractions.

TF	NES	Target	Motif
EIF5A2	12.134	4	2
HIF1A	8.032	6	91
ZIC2	7.489	6	4
ELF1	7.474	2	7
STAT2	6.947	5	6

3.6. Investigating Transcription Factors (TFs) and microRNAs of Hub Genes. To extend our findings, we predicted the TFs and found that EIF5A2, HIF1A, ZIC2, ELF1, and STAT2 as the master regulators of the hub genes are involved in VAF. The results are illustrated in Table 4 and Figure 8. Finally, prediction analysis using miRDB and TargetScan bioinformatic tools identified the selected miRNAs targeting each hub co-DEG involved in AF and these data appear. These data enable us to understand how predicted miRNAs are related to AF progress and maintain.

4. Discussion

Currently, the pathogenesis of atrial fibrillation is still unclear, but atrial electrical remodeling and atrial structural remodeling are considered as important pathological mechanisms for the occurrence and maintenance of atrial fibrillation. Due to the reversibility of electrical remodeling and the irreversibility of structural remodeling, it is of vital significance to study atrial structural remodeling for the occurrence, development, diagnosis, and treatment of AF [18, 19]. Atrial fibrosis is not only the characteristic manifestation of atrial structural remodeling but also the primary prerequisite for the occurrence and maintenance of atrial

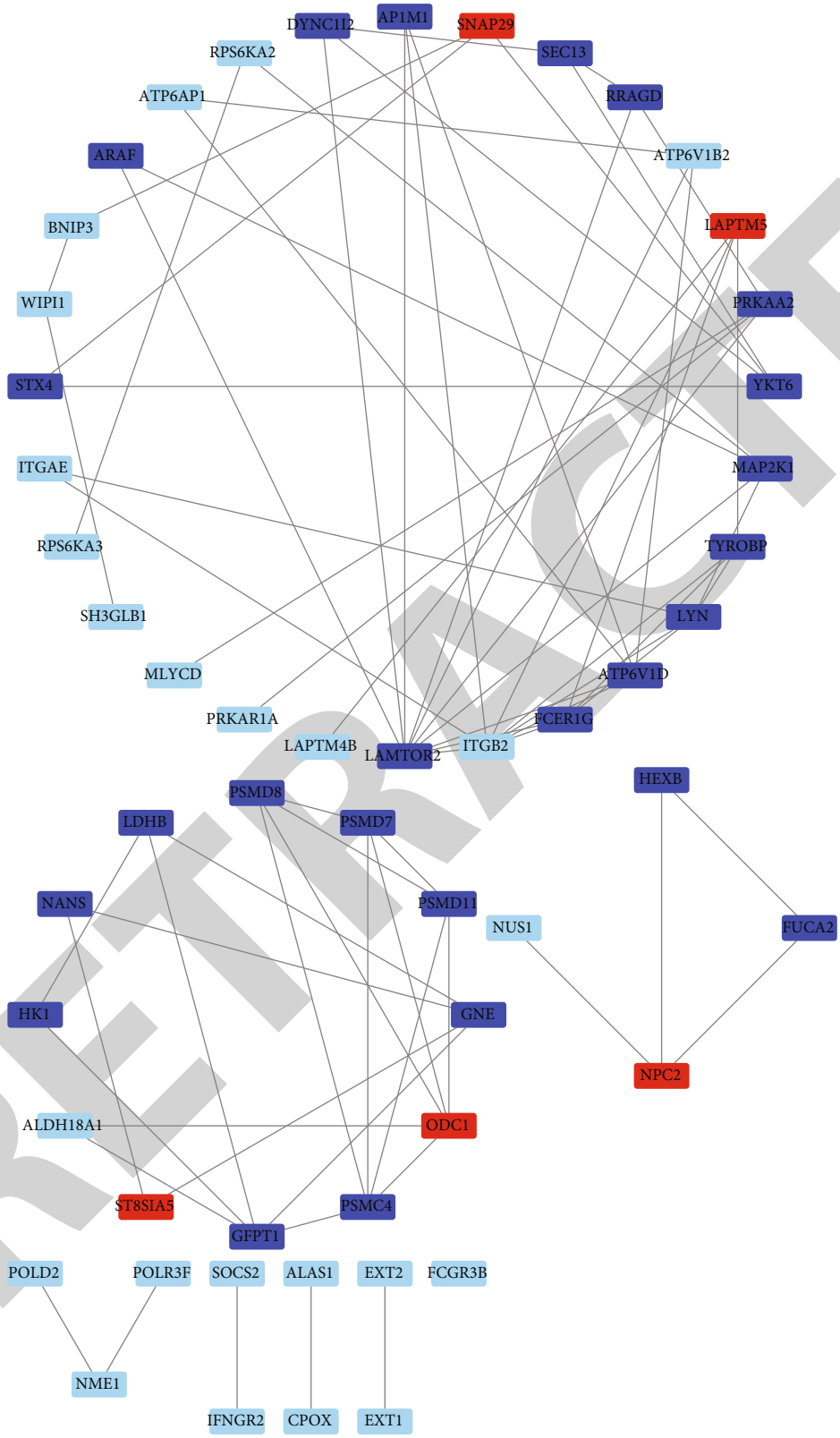

(a)

Figure 5: Continued.

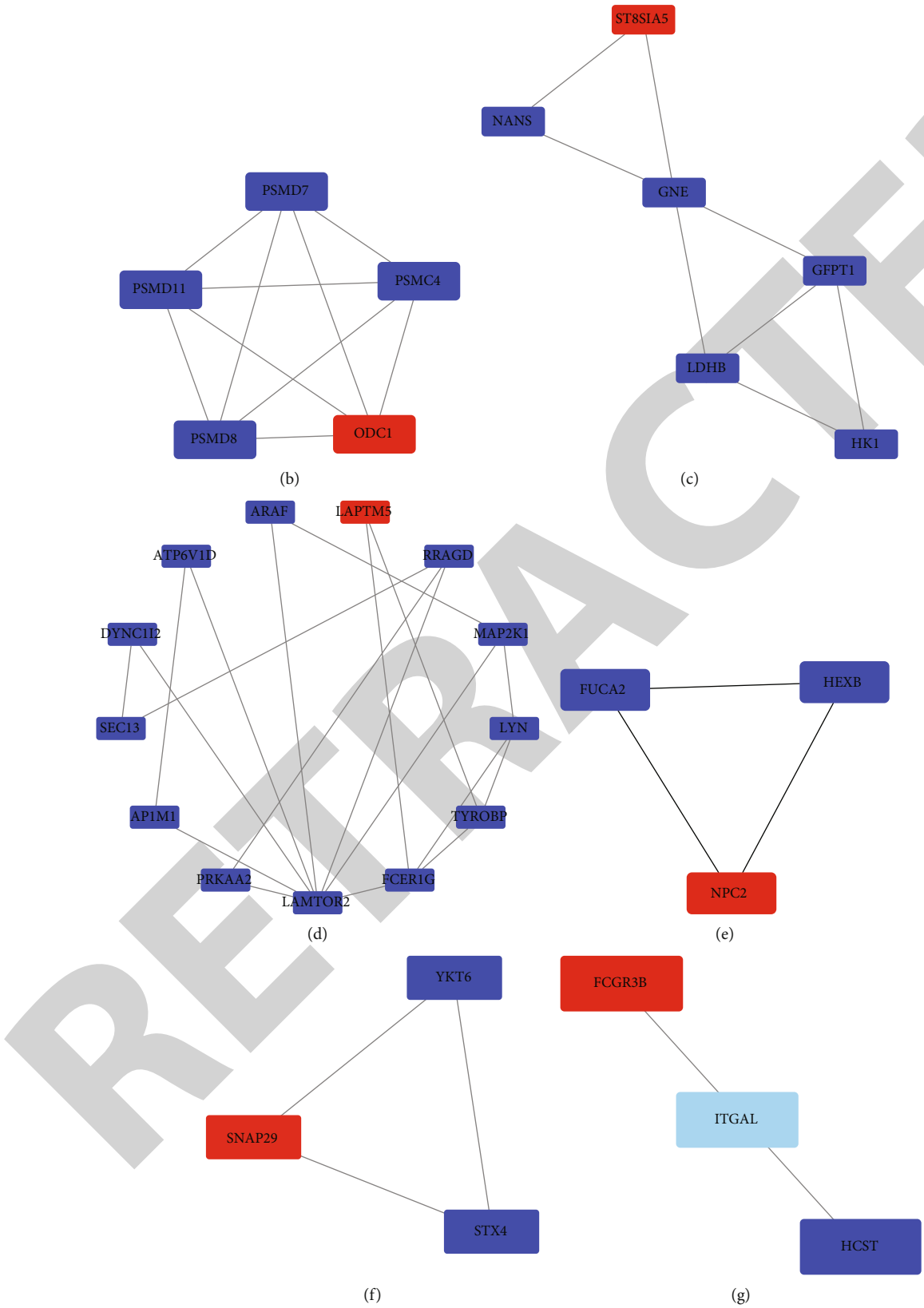

Figure 5: DEGs protein-protein interaction network map and key gene screening maps. (a) and (h) represent the PPI of DEGs in which the MElightcyan and MEturquoise modules related to pathways of atrial remodeling and fibrosis, such as energy metabolism, biosynthesis, ion channels, cytoskeleton, and vesicle secretion. (b)–(g) represent modules 1~5 obtained by MCODE plugin analysis of the DEGs protein interaction network of the MElightcyan, in which red represents the central node, namely, the key gene of the corresponding module.

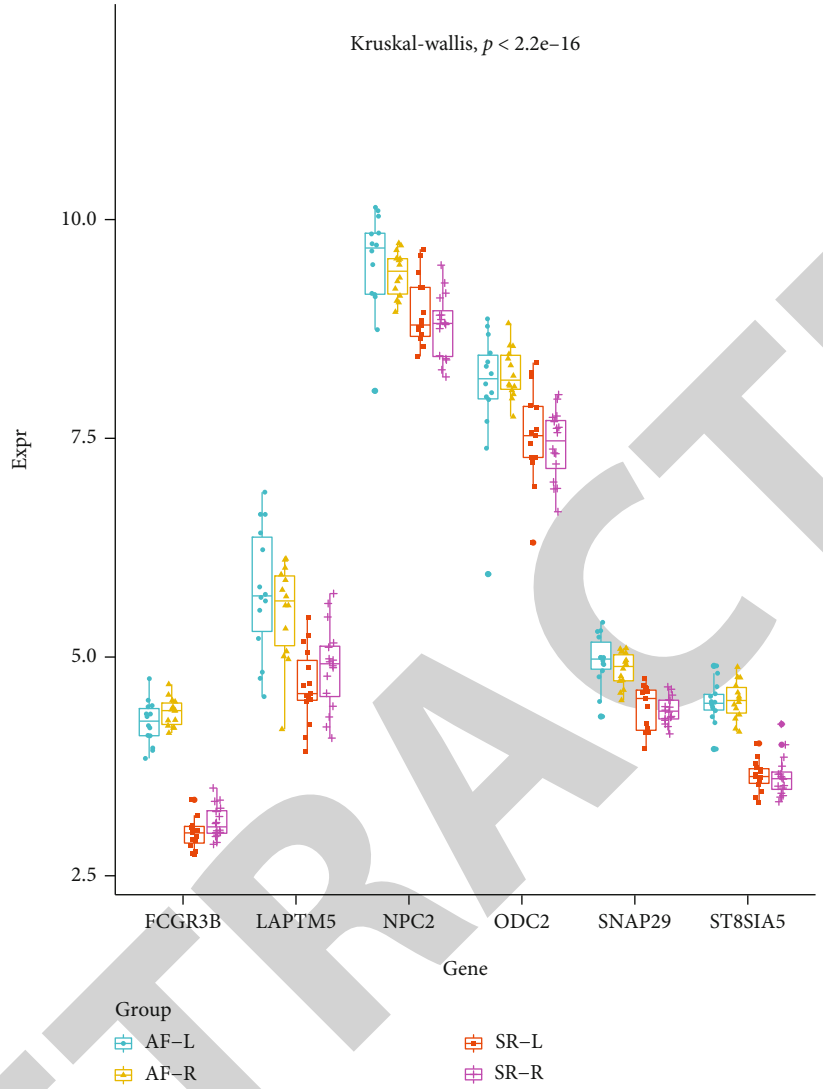

Figure 6: Box plot diagram of hub gene expression in atrial fibrillation and sinus patients and left and right atrial tissues.

fibrillation. Therefore, the molecular mechanism of atrial fibrosis may be a potential target for the treatment of AF [20]. The present study suggests that these mechanisms may be involved in the process of atrial fibrosis leading to atrial fibrillation, including renin-angiotensin-aldosterone system (RAAS), transforming growth factor-β1 (TGF-β1), oxidative stress and inflammation, calcium overload, MMPs, and microRNA.

Some research teams have found that RAAS system plays an important role in atrial electrical remodeling and structural remodeling, participating in various arrhythmia and atrial fibrosis processes [21]. Under physiological conditions, the core factor of RAAS is Ang-II, which physiologically can contract blood vessels, raise hypertension, and increase cardiac afterload, thus leading to cardiac structural remodeling. Xiao et al. found that Ang-II can cause obvious atrial enlargement and atrial fibrosis in mice and finally cause AF [22]. Savelieva et al. and Girmatsion et al. also found that in animal experiments, RAAS inhibitor inhibition can not only inhibit atrial remodeling and fibrosis but also delay the occurrence of atrial fibrillation; in clinical trials, angiotensin inhibitor can also reduce the incidence of new AF [23, 52]. Some studies have further found that atrial fibrosis can be caused by increasing Ang-II expression via stimulating angiotensin type 1 receptor (AT1R) and TGF-β1, thus leading to atrial fibrillation [24]. Transforming growth factor-β1 is secreted by cardiac fibroblasts and then differentiated into active fibroblasts. Atrial fibrosis is closely related to active fibroblasts. Therefore, a large number of studies show that transforming growth factor-β1 plays an important role in the occurrence and development of AF. Studies have found that the transforming growth factor-β1 is secreted not only by fibroblasts but also by macrophages, and the transforming growth factor-β1 can increase cell adhesion factor, which can lead to myocardial fibrosis and cardiac structural remodeling [25]. Verheule et al. found in mouse model that the stimulation of TGF-β1 can cause atrial fibrillation [26]. Studies have further found that the TGF-β1 can participate in Smad signaling pathway by regulating the expression of TGF-β1 activated kinase and TGF-

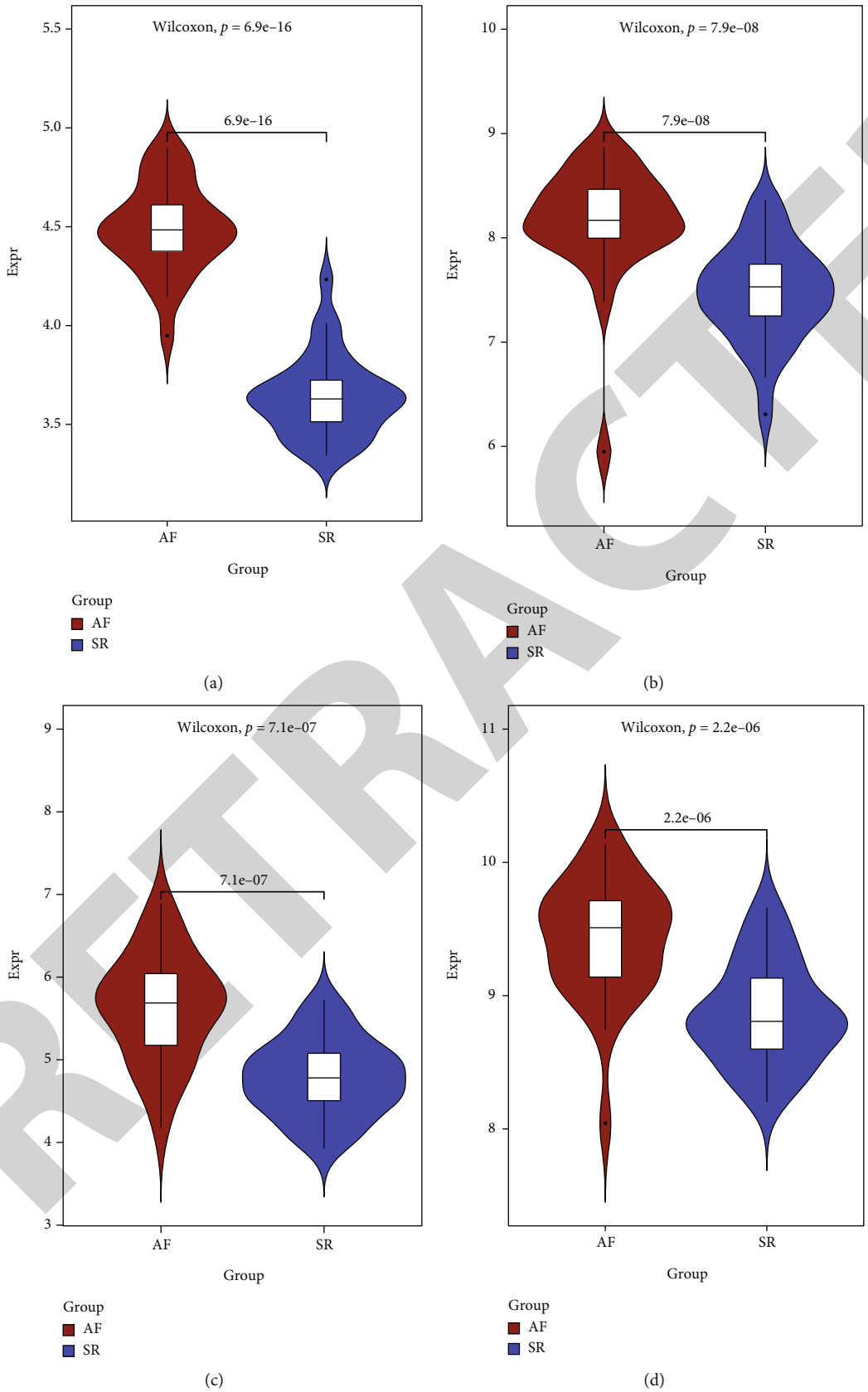

Figure 7: Continued.

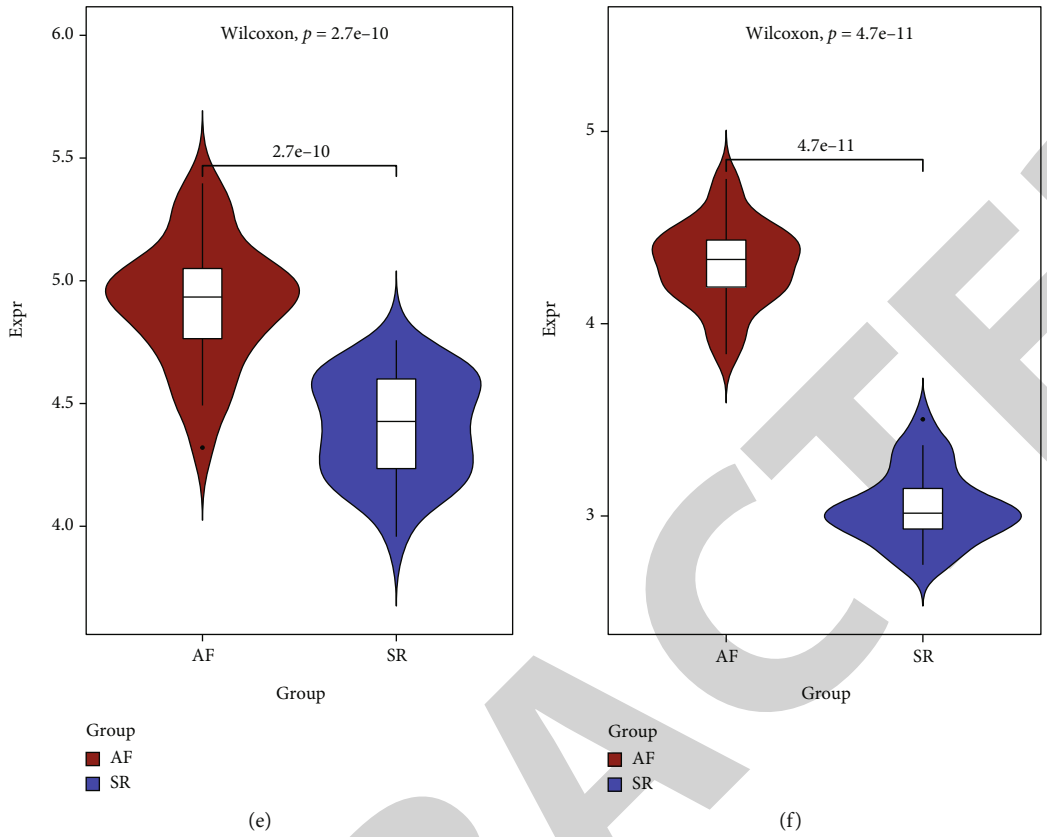

Figure 7: The violin plot diagram of hub gene expression level between atrial fibrillation and sinus rhythm patients: (a)–(f) represent the differences in the expression levels of the six hub genes, ST8SIA5 ($P = 6.9e - 16$), ODC1 ($P = 7.9e - 08$), LAPTM5 ($P = 7.1e - 07$), NPC2 ($P = 2.2e - 06$), SNAP29 ($P = 2.7e - 10$), and FCGR3B ($P = 4.7e - 11$), in patients with atrial fibrillation and sinus diseases, with P values less than 0.05, which are of significant statistical significance.

β1-fibroblast protein kinase C-alpha (PKC-alpha) pathway by regulating the expression of alpha-SMA to affect atrial fibrosis and structural remodeling and lead to AF [27, 28]. Oxidative stress and inflammatory response pathway can also lead to atrial fibrosis, which in turn leads to atrial fibrillation. Some people believe that reactive oxygen species lead to atrial fibrosis and atrial fibrillation by stimulating the expression of MMPs to make fibroblast proliferation [29]. Some also believe that reactive oxygen species cause atrial fibrosis by affecting energy proteins such as nicotinamide adenine dinucleotide phosphate (NADPH) oxidase [30]. And Colman et al. found that there were a large number of inflammatory cell infiltration in fibrotic and necrotic cardiomyocytes in the atrial tissue of patients with persistent atrial fibrillation, such as Ang-II, tumor necrosis factor-α (TNF-α), interleukin- (proinflammatory cytokines and hormone release IL-) 6 and IL-8 [31].What's more, it is found that the incidence of atrial fibrillation increases with the increase of C-reactive protein, indicating that C-reactive protein can be used as an independent risk factor for atrial fibrillation [32]. On the one hand, ion channels can affect cardiac contraction by affecting cardiac electrical activity; on the other hand, it can also cause atrial fibrosis and maintain arrhythmias by delayed triggering of myocardial depolarization through a variety of pathways, such as the expression of neutral protease calpain, the activation of RyR receptors, and the opening and closing of transient receptor potential channels [33, 34]. Regarding matrix metalloproteinases (MMP), it is a family of zinc-dependent proteolytic enzymes that affect extracellular matrix, including gelatinase, collagenase, and matrix enzyme, while extracellular matrix plays an important role in the treatment of atrial fibrosis. Studies have found that tissue inhibitors of metalloproteinases (TIMPs) can affect the expression level of metalloproteinases. Now it is mainly found that metalloproteinase-2 and metalloproteinase-9 are closely related to atrial fibrosis and atrial fibrillation [35].

To this end, the research team used the GO and KEGG pathways of atrial fibrosis and atrial remodeling related to atrial fibrillation as the modules for screening candidate genes, such as ion channels, protein and membrane biosynthesis, biological metabolism, energy metabolism, and other pathways. Then the candidate genes were screened by STRING online database and Cystoscape software, and six key genes were obtained, namely, ST8SIA5, ODC1, LAPTM5, NPC2, SNAP29, and FCGR3B.

α-2, 8-sialyltransferase 5 (ST8SIA5) mediates the transfer of sialic acid through the α-2pyrine 8-chain. Sialic acids have been reported to be involved in a variety of biological processes, including cell-cell adhesion, immune defense, tumor cell metastasis, and inflammation [36]. These

Table 4: Functional analysis and microRNA prediction of hub genes.

Hub gene	MicroRNAs		Functional	*P* value
ST8SIA5	miR-218-5p miR-203a-3p.1	KEGG	Glycosphingolipid biosynthesis, ganglio series, LacCer = > GT3	0.019
	miR-218-5p miR-4295 miR-3666 miR-301a-3p	GO	Golgi apparatus Golgi membrane	0.0004 0.0001
ODC1	miR-188-5p miR-6866-3p miR-133a-3p miR-3184-5p	KEGG	Polyamine biosynthesis, arginine = > ornithine = > putrescine	0.014
		GO	Cytoplasm Cytosol	2.0 E-06 0.0001
LAPTM5	Hsa-miR-330-3p Hsa-miR-6766-3p Hsa-miR-219a-5p Hsa-miR-4782-3p	KEGG	Lysosome mTOR signaling pathway	0.019 0.05
		GO	Membrane Proteasome accessory complex	0.00007 0.006
NPC2	Hsa-miR-23c Hsa-miR-23a-3p Hsa-miR-130a-5p Hsa-miR-23b-3p	KEGG	Lysosome Amino sugar and nucleotide sugar metabolism	0.0258 0.04
		GO	Endoplasmic reticulum Extracellular exosome	0.049 0.0107
SNAP29	miR-338-3p miR-124-3p Hsa-miR-222-3p Hsa-miR-221-3p	KEGG	SNARE interactions in vesicular transport Autophagy-animal	0.024 0.03
		GO	Golgi membrane Autophagosome membrane	4.69E-4 0.0045
FCGR3B	Hsa-miR-6893-3p Hsa-miR-370-3p	KEGG	Natural killer cell mediated cytotoxicity Staphylococcus aureus infection	0.027 0.038

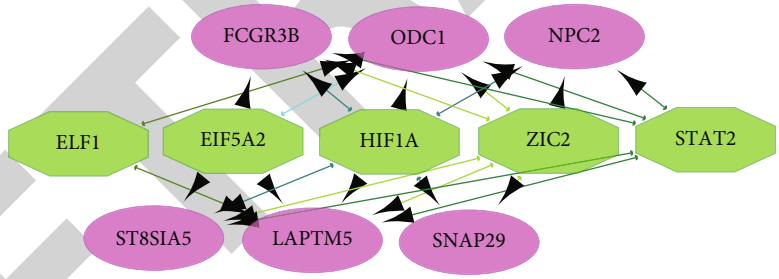

Figure 8: Prediction of transcription factors of hub gene: green indicates the top five transcription factors with the highest standard enrichment score, red indicates the hub gene, and arrows indicate the degree of association between TFs and hub gene.

biological processes also participate in the occurrence and development of atrial fibrosis and atrial remodeling. According to some researches, ST8SIA4 can promote the proliferation, migration, and invasion of thyroid cancer cells by activating PI3K-AKT-mTOR signaling pathway [37]. Sialyltransferase can also catalyze the transfer of sialic acid to proteins and lipids and participates in the synthesis of oligosaccharide core structures [38]. Natural sialylation is very important for the function of therapeutic proteins because it affects the physical, chemical, and immunogenicity of glycoproteins, and more importantly, it affects the properties of extracellular matrix to lead to atrial fibrosis.

Lysosomal-associated protein transmembrane 5 (LAPTM5) [39], Niemann-Pick C2 protein (NPC2) [40], and synaptosomal-associated protein 29 (SNAP29) [41] have the most characteristics of autophagy. Autophagy is a dynamic process regulated by multiple genes and molecular signals. The formation of autophagosomes, the transport of autophagy substrates to lysosomes and the degradation of autophagosomes in lysosomes are called autophagy energy fluxes. Autophagy is an important metabolic pathway to maintain homeostasis in eukaryotic cells under starvation, inflammation, and hypoxia/reoxygenation injury. Autolytic corpuscles mainly eliminate aging organelles and misfolded proteins and provide energy for cells. Autophagy is maintained at a low level in normal myocardium [42]. However, myocardial energy metabolism is disturbed, including myocardial injury caused by atrial fibrillation, and autophagy may be overactivated or inhibited [43]. Low-level autophagy is an important method to maintain cardiomyocyte homeostasis, that is, any form of myocardial injury will lead to cardiomyocyte autophagy. And excessive activation or

inhibition of autophagy will lead to myocardial injury. Therefore, LAPTM5, NPC2, and SNAP29 may lead to atrial remodeling through myocardial injury caused by autophagy.

In addition, some studies have found that LAPTMs can act on the fibroblasts of type IV mucoliposomal disease and cause the disease. The analysis of fibroblasts of type IV mucin liposome disease shows that there are a large number of vacuolar structures, including a large number of mucopolysaccharides and lipids. Changes in the composition of extracellular matrix can lead to fibrosis [44]. LAPTMs may also cause changes in myocardial extracellular matrix components and lead to atrial fibrosis. In addition, the study also found that the structure and function of LAPTMs family is similar to mucin 1, which is known as transient receptor potential superfamily. This is an inward rectifier channel, and the change of its activity will affect the plasma levels of calcium, sodium, and magnesium ions [45]. It has also been found that injection of overexpressed NPC2 into mice through adeno-associated virus serotype 9 can lead to the accumulation of fibroblasts, and it has also been found that NPC can affect Purkinje cells, and which are also involved in cardiac electrophysiological activities [46]. More importantly, the main function of NPC is to affect the transport of cholesterol and low density lipoprotein, so it plays an important role in cardiovascular disease [47].

Ornithine decarboxylase 1 (ODC1) is mainly involved in the metabolism of polyamines, which regulates cell proliferation and differentiation. Some studies have shown that ODC1 can participate in inflammatory response after macrophage stimulation [48]. This is consistent with the presence of a large number of inflammatory cells around the myocardium in patients with atrial fibrillation, which indicates that ODC1 may participate in atrial fibrosis through inflammatory reaction and lead to atrial fibrillation. FCGR3B is a gene encoding FC-γ receptor 3B, which is mainly involved in immune regulation, inflammation, and cytotoxicity. Some studies have found that FCGR3B can lead to pulmonary fibrosis through proinflammatory and fibrogenic processes, including tumor necrosis factor-α, transforming growth factor-β, MCP-1, and IL-8 [49]. Although there are no reports about the direct relationship between FCGR3B and atrial fibrillation, the mechanism of atrial fibrosis in atrial fibrillation mentioned above is consistent with the mechanism of pulmonary fibrosis caused by FCGR3B, so FCGR3B may be a potential biomarker for the maintenance of atrial fibrillation.

In this study, not only six key genes were screened but also the regulatory factors of key genes, TFs and microRNAs, were predicted. Widely found across species, microRNA (miRNA, miR) is a highly conserved noncoding RNA that is composed of 19~26 nucleotides [50]. Because miRNA can regulate the expression of nearly 1/3 of all protein coding genes in the human genome, it has become an important area of research in a variety of cardiovascular disease, including atrial fibrillation. The gene that contains the miRNA coding sequence is called the miRNA host gene (HG). Because miRNA originates from posttranscriptional splicing of its host gene and may affect its host gene's expression due to their innate complementary sequences, there is crosstalk between a miRNA and its host gene. Therefore, the studies of miRNA and its host gene may provide a theoretical basis for revealing the mechanism of AF [51]. Some studies have found that microRNA-1 k affects the level of IK-1 by regulating Kir-2. It is well known that the upregulation of IK-1, which is responsible for the inward-rectifier potassium channel, is one of the important mechanisms for maintaining atrial fibrillation [52]. Meanwhile, the expression levels of miR-21 and miR-29 also confirmed that they were involved in the maintenance of atrial fibrillation [53, 54]. To this end, we also use an online database to predict the microRNAs of the six hub genes in Table 4. Finally, our results also found that the main regulatory factors of EIF5A2, HIF1A, ZIC2, ELF1, and STAT2, which target key genes, were significantly associated with valvular atrial fibrillation.

In summary, through bioinformatics, we found that autophagy, energy metabolism, ion channel, oxidative stress, and inflammatory reaction may play important roles in the occurrence and maintenance of atrial fibrillation through a variety of physiological or pathophysiological processes. Based on network regulation, we also revealed potential therapeutic targets for VAF. We also obtained six hub gene markers involved in the occurrence and maintenance of atrial fibrillation, which were statistically significant, including ST8SIA5, ODC1, LAPTM5, NPC2, SNAP29, and FCGR3B. Most of these genes are related to lysosomal autophagy, which provides new insights into the molecular mechanism of occurrence and development of atrial fibrillation. Finally, our results also confirmed that the main regulatory factors, EIF5A2, HIF1A, ZIC2, ELF1, and STAT2, are significantly associated with the occurrence and maintenance of atrial fibrillation through targeting candidate genes. Of course, microRNAs corresponding to candidate genes are also predicted, which may also be potential markers of valvular atrial fibrillation.

5. Limitation

There are still some limitations in our research. First of all, our results are based on microarray analysis of gene expression values, and then protein network construction is carried out. However, this is not directly equivalent to protein expression, so the biomarker in this study should be gene, not protein. What's more, it should be verified in vitro, in vivo, and clinical trials, rather than just limited to network prediction.

6. Conclusions

The results found that these hub genes, NPC2, ODC1, SNAP29, LAPTM5, ST8SIA5, and FCGR3B, play a key role in the development and maintenance of VAF, and their enrichment pathways and TFs elucidate the involved molecular mechanisms and assist in the validation of drug targets.

Conflicts of Interest

The authors declare that they have no conflict of interest.

Authors' Contributions

Fan Zou and Tiantian Chen are co-first authors.

Acknowledgments

This study was funded by the Natural Science Foundation Project of Guangdong Basic and Applied Basic Research Fund (Grant No.2019A1515010969).

References

[1] J. D. Roberts and M. H. Gollob, "Impact of genetic discoveries on the classification of lone atrial fibrillation," *Journal of the American College of Cardiology*, vol. 55, no. 8, pp. 705–712, 2010.

[2] A. Majeed, K. Moser, and K. Carroll, "Trends in the prevalence and management of atrial fibrillation in general practice in England and Wales, 1994-1998: analysis of data from the general practice research database," *Heart*, vol. 86, no. 3, pp. 284–288, 2001.

[3] D. Dobrev, L. Carlsson, and S. Nattel, "Novel molecular targets for atrial fibrillation therapy," *Nature Reviews. Drug Discovery*, vol. 11, no. 4, pp. 275–291, 2012.

[4] J. Oldgren, J. S. Healey, M. Ezekowitz et al., "Variations in cause and management of atrial fibrillation in a prospective registry of 15,400 emergency department patients in 46 countries: the RE-LY atrial fibrillation registry," *Circulation*, vol. 129, no. 15, pp. 1568–1576, 2014.

[5] A. J. Camm, G. Y. Lip, R. De Caterina et al., "2012 focused update of the ESC guidelines for the management of atrial fibrillation: an update of the 2010 ESC guidelines for the management of atrial fibrillation. Developed with the special contribution of the European heart rhythm association," *European Heart Journal*, vol. 33, no. 21, pp. 2719–2747, 2012.

[6] Z. Zhou and D. Hu, "An epidemiological study on the prevalence of atrial fibrillation in the Chinese population of mainland China," *Journal of Epidemiology*, vol. 18, no. 5, pp. 209–216, 2008.

[7] J. Y. Kim, S. J. Lee, J. H. Kim, C. M. Choi, S. R. Yoon, and K. I. Jung, "Effects of atrial fibrillation on the outcome of the rehabilitation in patients with cerebral infarction," *Annals of Rehabilitation Medicine*, vol. 38, no. 6, pp. 766–774, 2014.

[8] E. J. Benjamin, D. Levy, S. M. Vaziri, R. B. D'Agostino, A. J. Belanger, and P. A. Wolf, "Independent risk factors for atrial fibrillation in a population-based cohort. The Framingham Heart Study," *The Framingham Heart Study. JAMA*, vol. 271, no. 11, pp. 840–844, 1994.

[9] A. Kourliouros, I. Savelieva, A. Kiotsekoglou, M. Jahangiri, and J. Camm, "Current concepts in the pathogenesis of atrial fibrillation," *American Heart Journal*, vol. 157, no. 2, pp. 243–252, 2009.

[10] A. Boldt, U. Wetzel, J. Lauschke et al., "Fibrosis in left atrial tissue of patients with atrial fibrillation with and without underlying mitral valve disease," *Heart (British Cardiac Society)*, vol. 90, pp. 400–405, 2004.

[11] C. R. Mitchell and M. K. Das, "Paroxysmal lone atrial fibrillation is associated with an abnormal atrial substrate: characterizing the "second factor"," *Journal of Atrial Fibrillation*, vol. 2, p. 202, 2009.

[12] R. A. Irizarry, B. Hobbs, F. Collin et al., "Exploration, normalization, and summaries of high density oligonucleotide array probe level data," *Biostatistics (Oxford, England)*, vol. 4, pp. 249–264, 2003.

[13] M. E. Ritchie, B. Phipson, D. I. Wu et al., "Limma powers differential expression analyses for RNA-sequencing and microarray studies," *Nucleic Acids Research*, vol. 43, article e47, 2015.

[14] P. Langfelder and S. Horvath, "WGCNA: an R package for weighted correlation network analysis," *BMC Bioinformatics*, vol. 9, no. 1, p. 559, 2008.

[15] D. W. Huang, B. T. Sherman, Q. Tan et al., "DAVID bioinformatics resources: expanded annotation database and novel algorithms to better extract biology from large gene lists," *Nucleic Acids Research*, vol. 35, Supplement_2, pp. W169–W175, 2007.

[16] Y. Zhou, B. Zhou, L. Pache et al., "Metascape provides a biologist-oriented resource for the analysis of systems-level datasets," *Nature Communications*, vol. 10, p. 1523, 2019.

[17] D. Szklarczyk, J. H. Morris, H. Cook et al., "The STRING database in 2017: quality-controlled protein-protein association networks, made broadly accessible," *Nucleic Acids Research*, vol. 45, pp. D362–D368, 2017.

[18] C. S. Lin and C. H. Pan, "Regulatory mechanisms of atrial fibrotic remodeling in atrial fibrillation," *Cellular and Molecular Life Sciences: CMLS*, vol. 65, no. 10, pp. 1489–1508, 2008.

[19] T. Krogh-Madsen, G. W. Abbott, and D. J. Christini, "Effects of electrical and structural remodeling on atrial fibrillation maintenance: a simulation study," *PLoS Computational Biology*, vol. 8, no. 2, article e1002390, 2012.

[20] S. Levy and P. Sbragia, "Remodelling in atrial fibrillation," *Archives des Maladies du Coeur et des Vaisseaux*, vol. 98, no. 4, pp. 308–312, 2005.

[21] B. Burstein and S. Nattel, "Atrial fibrosis: mechanisms and clinical relevance in atrial fibrillation," *Journal of the American College of Cardiology*, vol. 51, no. 8, pp. 802–809, 2008.

[22] H. D. Xiao, S. Fuchs, D. J. Campbell et al., "Mice with cardiac-restricted angiotensin-converting enzyme (ACE) have atrial enlargement, cardiac arrhythmia, and sudden death," *The American Journal of Pathology*, vol. 165, pp. 1019–1032, 2004.

[23] I. Savelieva, N. Kakouros, A. Kourliouros, and A. J. Camm, "Upstream therapies for management of atrial fibrillation: review of clinical evidence and implications for European Society of Cardiology guidelines. Part I: primary prevention," *Part I: primary prevention. Europace*, vol. 13, no. 3, pp. 308–328, 2011.

[24] X. He, X. Gao, L. Peng et al., "Atrial fibrillation induces myocardial fibrosis through angiotensin II type 1 receptor-specific Arkadia-mediated downregulation of Smad7," *Circulation Research*, vol. 108, pp. 164–175, 2011.

[25] P. J. Lijnen, V. V. Petrov, and R. H. Fagard, "Induction of cardiac fibrosis by transforming growth factor- β_1," *Molecular Genetics and Metabolism*, vol. 71, no. 1-2, pp. 418–435, 2000.

[26] S. Verheule, T. Sato, T. Everett et al., "Increased vulnerability to atrial fibrillation in transgenic mice with selective atrial fibrosis caused by overexpression of TGF-β1," *Circulation Research*, vol. 94, no. 11, pp. 1458–1465, 2004.

[27] B. Qiao, S. R. Padilla, and P. D. Benya, "Transforming growth factor (TGF)-β-activated kinase 1 mimics and mediates TGF-β-induced stimulation of type II collagen synthesis in chondrocytes independent of _Col2a1_ transcription and Smad3 signaling∗," *The Journal of Biological Chemistry*, vol. 280, no. 17, pp. 17562–17571, 2005.

Hindawi
Computational and Mathematical Methods in Medicine
Volume 2023, Article ID 9849304, 1 page
https://doi.org/10.1155/2023/9849304

Retraction

Retracted: circKMT2E Protect Retina from Early Diabetic Retinopathy through SIRT1 Signaling Pathway via Sponging miR-204-5p

Computational and Mathematical Methods in Medicine

Received 12 December 2023; Accepted 12 December 2023; Published 13 December 2023

This article has been retracted by Hindawi, as publisher, following an investigation undertaken by the publisher [1]. This investigation has uncovered evidence of systematic manipulation of the publication and peer-review process. We cannot, therefore, vouch for the reliability or integrity of this article.

Please note that this notice is intended solely to alert readers that the peer-review process of this article has been compromised.

Wiley and Hindawi regret that the usual quality checks did not identify these issues before publication and have since put additional measures in place to safeguard research integrity.

We wish to credit our Research Integrity and Research Publishing teams and anonymous and named external researchers and research integrity experts for contributing to this investigation.

The corresponding author, as the representative of all authors, has been given the opportunity to register their agreement or disagreement to this retraction. We have kept a record of any response received.

References

[1] J. Shi and L. Li, "circKMT2E Protect Retina from Early Diabetic Retinopathy through SIRT1 Signaling Pathway via Sponging miR-204-5p," *Computational and Mathematical Methods in Medicine*, vol. 2022, Article ID 7188193, 12 pages, 2022.

Hindawi
Computational and Mathematical Methods in Medicine
Volume 2022, Article ID 7188193, 12 pages
https://doi.org/10.1155/2022/7188193

Research Article

circKMT2E Protect Retina from Early Diabetic Retinopathy through SIRT1 Signaling Pathway via Sponging miR-204-5p

Jilai Shi and Li Li

Department of Endocrinology, The Affiliated Hospital of Shandong University of Traditional Chinese Medicine, Jinan, Shandong 250014, China

Correspondence should be addressed to Li Li; bangtang1234@126.com

Received 6 July 2022; Revised 4 August 2022; Accepted 23 August 2022; Published 30 September 2022

Academic Editor: Min Tang

Objective. To explore the changes of circRNAs in the retina of diabetic patients without diabetic retinopathy (DR) to screen latent protective factor. *Methods*. The sequencing data of the retina from three diabetic donors that possess no noticeable pathological feature of the retina at ultimate eye inspection and three healthy donative samples were involved in this study. Herein, we carried out bioinformatics analysis to disclose the expression pattern and characteristics of circRNAs on the basis of Gene Ontology as well as KEGG pathway analyses. Then, sequencing data were applied to infer the interaction between selected circRNAs and miR-204-5p. The potential miRNA response elements for the annotated circRNAs and their target gene were speculated using TargetScan as well as miRanda. *Results*. RNA sequencing detected 28,978 alternative circRNAs. Thereinto, 1063 were expressed with significant difference. circKMT2E was upregulated more than two folds in alloxan-induced diabetic retinal tissues compared with normal retinal tissues, exhibiting an expression trend opposite to miR-204-5p. Bioinformatics analysis showed that circKMT2E have four seed sequences on hsa-miR-204-5p. Thus, circKMT2E was speculated to have function on the basis of sponging miR-204-5p in order to participate in the pathogenetic process of DR. Besides, miR-204-5p was speculated to be able to bind SIRT1, which can interact with its target proteins, and adjusts various cell functions including cellular inflammatory responses, proliferation, as well as apoptosis. *Conclusion*. The upregulation of circKMT2E in the early stage of DR may be involved in its pathogenesis and may activate the SIRT1 signaling pathway to protect the retina by the sponge function to miR-204-5p.

1. Introduction

Diabetes mellitus (DM) as a kind of noncommunicable chronic metabolic disease has prevailed worldwide [1, 2]. The complications of DM affect nearly every tissue of the human body; among all affected tissue, diabetic retinopathy (DR) refers to the frequent microvascular complication that accompanies DM. DR currently is deemed as one of the most common causes of blindness especially in working-aged people [2, 3]. Most studies organized for western populations have found a DR prevalence of more than 30% in individuals of similar age and duration of disease [1].

In the wake of the quick progress of high-throughput sequencing approaches, the function of circular RNAs (circRNAs), which take part in significant processes in diverse diseases, has been increasingly focused on [4–7]. circRNAs, dissimilar to linear RNAs, could take shape in a closed annulus structure presenting better steadiness as well as more specific peculiarities [8–11]. circRNAs, which are normally expressed according to the stage-specific manner as well as tissue-specific pattern, can participate in a series of physiological as well as pathological processes [12–14]. circRNAs contain microRNA (miRNA) response elements, by which circRNAs could adjust the expression of their target genes

[15]. circRNAs, as a type of noncoding RNAs with modulatory capacity, can weaken the impact of miRNAs on the basis of silencing miRNA via sponge function, which is related to the posttranscriptional management of genes [15, 16].

On basis of the combination of bioinformatics analysis and basic experiment, the networks of gene modulatory among mRNAs, circRNAs, and miRNAs reported by a few previous studies have offered us more profound knowledge of the process of pathology and development for the retina. Therein, miR-204, a miRNA widely expressed in the lung, kidney, eye, mammary gland, skin, as well as melanocytes, executes significant functions during both functional maintenance and retinal development [17]. miR-204, a type of enriched miRNAs in eyes, owns the most prominent expression in the ocular tissue, such as the retina, lens, and ciliary body. Therefore, the extensive expression of miR-204 implies that it could adjust several vital cellular activities for ocular tissue [18–20]. Mao et al. found that the expression levels of miR-204-5p were significantly augmented in the retina from diabetic rats; besides, miR-204-5p additionally endorses the development process of DR on the basis of downregulating the microtubule-linked protein 1 light chain 3 to inhibit autophagy [21]. However, Yang et al. found that high glucose can downregulate miR-204 in ARPE19 cells [22].

During the initial progress of DR, vascular pathology, for instance, areas of vascular nonperfusion, microaneurysms, and decreased retinal blood flow, appears [3, 23]. Reduced blood flow of the retina, to some extent, manifests inchoately, not only in humans with DM but also in animal models with DM [23, 24]. Altered accommodation of inner retinal vascular is normally deemed as an accommodation forerunner to the occurrence of grievous vascular pathology in DR [25]. The controversial capacity of miR-204 in the pathogenetic process of DR may suggest that miR-204 participates in the early protective effect but terminal disablement.

In this study, to ascertain the function of miR-204 in early diabetic retina as well as to reveal the early latent pathogenetic process of DR, in-depth sequencing data from postmortem human retinal tissue including three diabetic donors without DR and three healthy donors were enrolled. Mainly based on bioinformatics analysis, we found that the upregulation of circKMT2E in the early stage of diabetic retinal feedback may be involved in the pathogenesis of DM that activates the SIRT1 signaling pathway to protect the retina by the sponge function to miR-204-5p.

2. Methods

2.1. In-Depth Sequencing Data. The in-depth transcriptomic data of both healthy and diabetic donors (with no evident visual injury or obvious pathology of the retina at the ultimate ocular inspection) were downloaded from the NCBI BioProject database with accession numbers PRJNA672929 and PRJEB10043 using "prefetch" order in Linux with the NCBI SRA Toolkit. After stratified sampling, three healthy subjects and three diabetic subjects were signed up in this investigation. The retinal samples from a postmortem human were acquired via the Iowa Lions Eye Bank (Coralville, Iowa, USA) in which samples were safeguarded within 6 h postmortem [26]. For the option of donors, Becker et al. [26] did not enlist donors who possess a confirmed medical history of Hepatitis B or C and HIV. Besides, donated ocular samples that were provided with neurodegenerative diseases were also excluded.

2.2. Differential Gene Expression Analysis. Sequencing reads with satisfying quality were matched to the online reference genome or transcriptome with the aid of STAR software (v2.5.1b) [27]. All identified circRNAs on the basis of DCC software were then annotated with the aid of the circBase database as well as Circ2Traits. circRNAs that possess significant differential appearance between the above-mentioned two groups were recognized based on t-test. The p value was corrected using the Benjamini and Hochberg method [28]. Fold change ≥ 2.0 as well as p value ≤ 0.05 were used for filtering circRNAs with differential expression.

2.3. Enrichment Analyses on Basis of GO and KEGG. Enrichment analyses on the basis of GO (http://www.geneontology.org) as well as KEGG (http://www.genome.jp/kegg) were implemented on the host genes of circRNAs with differential expression. GO is a methodic and organized database in order to depict both genes and its product. It not only covered molecular function but also revealed biological processes as well as cell component. With the help of the pathway analysis from KEGG, the signaling pathways that contain circRNAs as well as their biological functions can be inferred. The relevant p value was computed on the basis of Fisher's exact test, with a suggested threshold value at 0.05.

2.4. Early DR-Related Candidate circRNA Analysis. The abundance of circRNAs was calculated by Ballgown and computed by Fragments Per Kilobase of exon model per Million mapped fragments (FPKM). The threshold value of FPKM in each group was 0.5, which mean the circRNA would be deemed as expressing in this group if FPKM $>$ 0.5. For the circRNA expression, Student's t-test was applied on the basis of GraphPad Prism 8.0 to compute the significance for differences.

2.5. Interaction Network Analysis of circRNA, miRNA, and Target Gene. The underlying miRNA reaction elements for the annotated circRNAs and target gene were predicted using custom-written software on the basis of both TargetScan and miRanda (Cloud-seq Biotech, Shanghai, China). CircPrimer1.2 (http://www.bioinf.com.cn/) and UCSC genome browser were used to annotate the arrangement of circKMT2E and its positions on parental genes, respectively. circMir1.0 software, on the basis of miRanda 2010 (http://www.microRNA.org/microRNA/getDownloads.do) and RNAhybrid-2.1.2 (https://bibiserv.cebitec.uni-bielefeld.de/rnahybrid/), was applied to annotate putative bundling situations of miR-204-5p on circKMT2E transcripts.

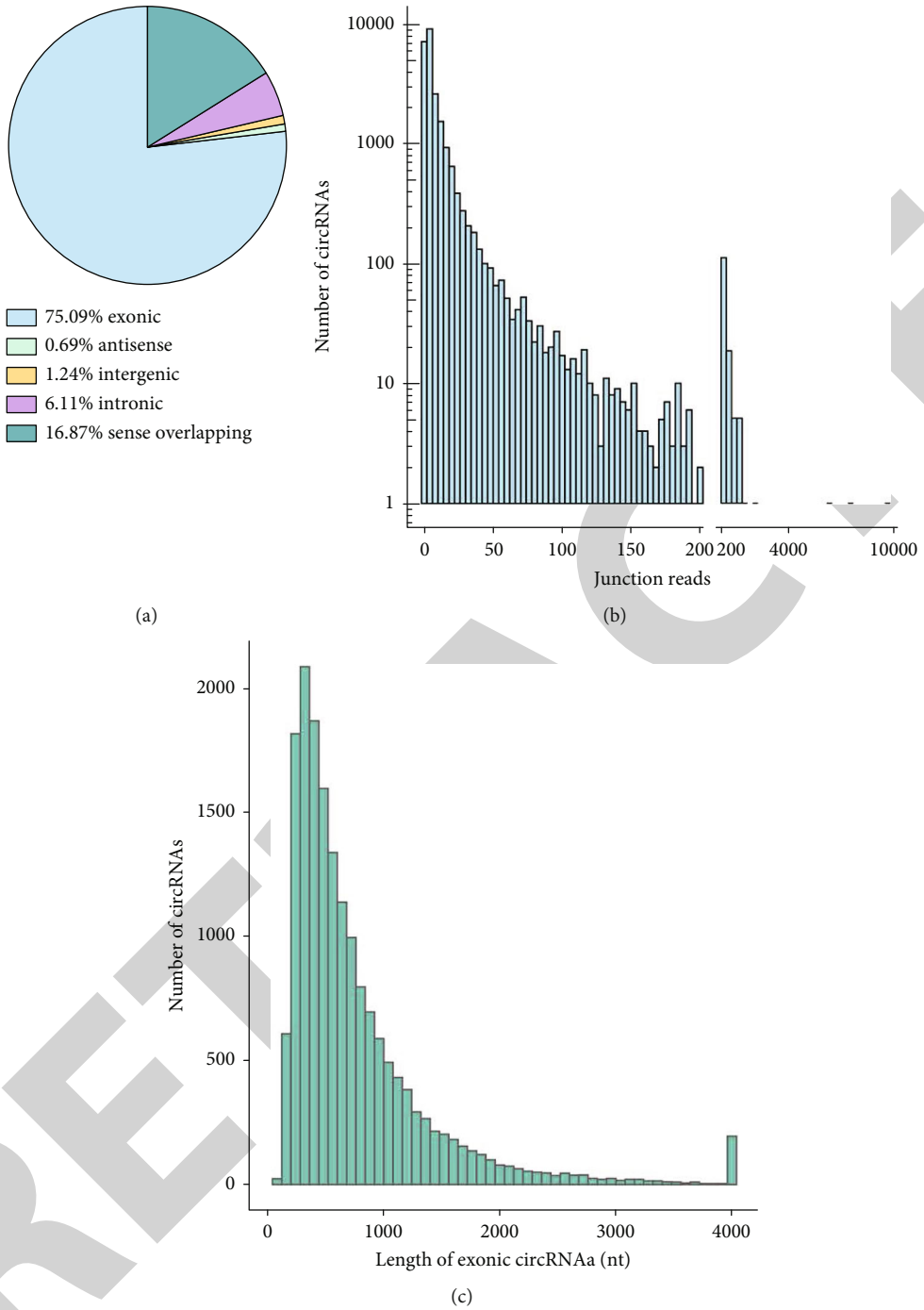

Figure 1: Overall result of RNA sequencing. (a) The genomic location of circRNAs. (b) The amount of circRNAs as well as their junction reads discerned in DR as well as normal tissues. (c) The length distribution of exonic circRNAs.

3. Results

3.1. Overall Result of RNA Sequencing. We identified the expression level of numerous circRNAs existing in retinal tissues on the basis of the samples donated from the diabetic subjects with no conspicuous visual damage or observable pathology at ultimate ocular detection as well as the retinal tissues from control healthy donors using the high-throughput sequencing. Under the sequencing, a total of 28,978 circRNAs were perceived in human retinal tissues, of which 10,970 circRNAs were observed for the first time as newfound circRNAs, while 18,008 circRNAs were already included in the circBase. (Figure 1(b)). According to the functional explanation in this study, which refers to the genome of these annotated circRNAs, 75.09% of these circRNAs were situated in protein-coding exons, while 0.69%, 1.24%, 6.11%, and 16.87% of them belonged to introns, intergenic, antisense, and sense overlapping regions, respectively (Figure 1(a)). The median size of exonic circRNAs was distributed at 556 nt (Figure 1(c)).

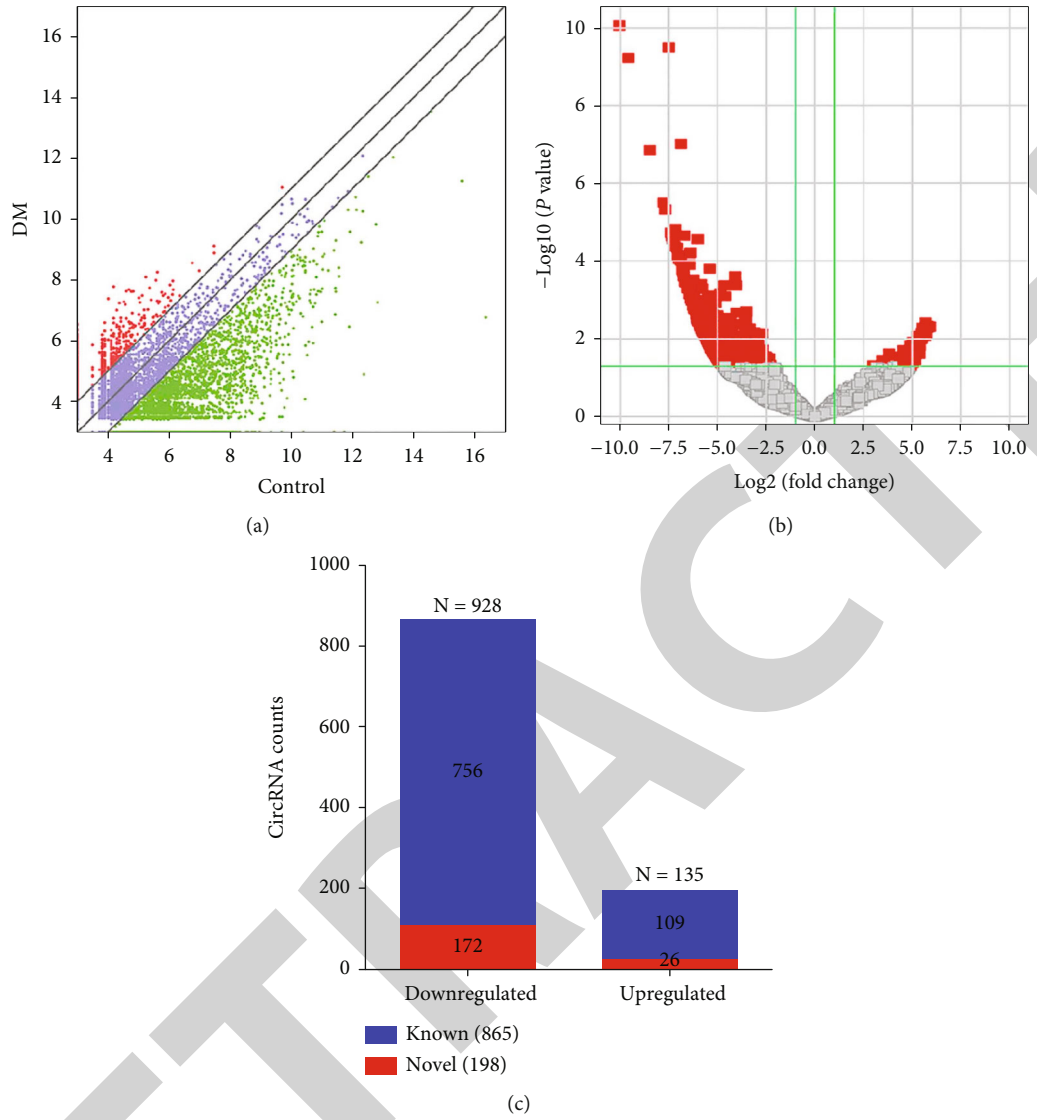

Figure 2: Continued.

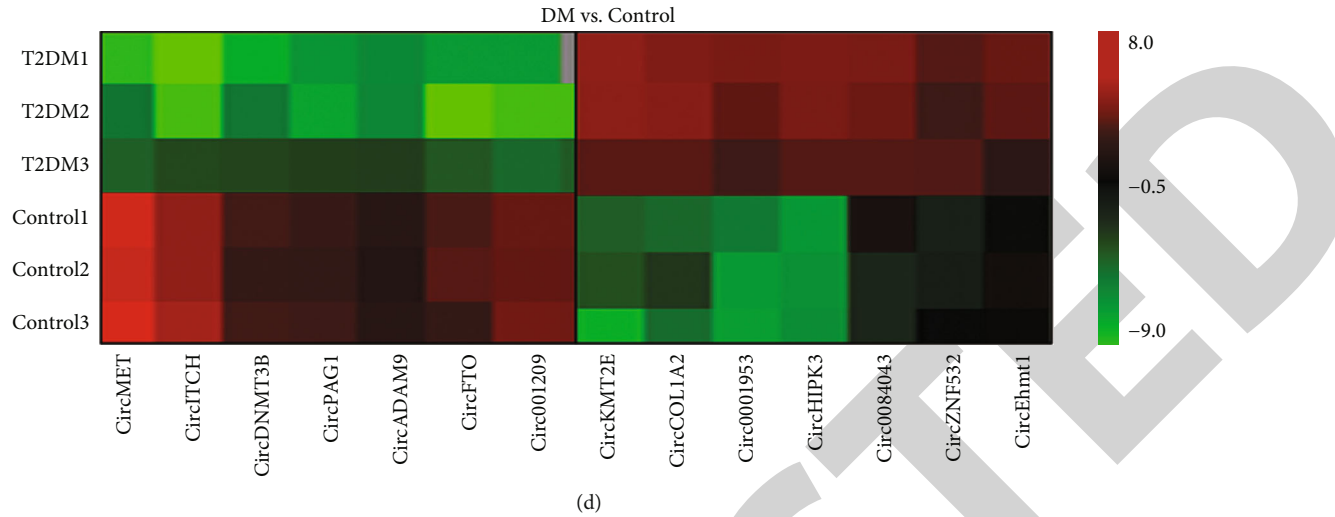

(d)

Figure 2: Differential expression of circRNAs in diabetic retinopathy tissues. (a) The scatter plot of circRNA expression of the retinal tissues from diabetes mellitus (DM) and control groups. The middle black line indicates that the DM and normal control groups present no significant difference. circRNAs beyond the top black line or under the bottom black line signpost >2-fold alterations. The red spots disclose augmented circRNAs, and the green spots reveal diminished circRNAs in the DR group in contrast to the control group (fold change ≥ 2.0). (b) The volcano plot of the circRNAs with remarkable differential expression between two groups. The vertical green lines represent 2.0-fold (log2 scaled) augmented and diminished changes. The horizontal green line refers to a p value of 0.05 (−log10 scaled). The red spots represent circRNAs with remarkable differential expression (fold change ≥ 2.0, $p \leq 0.05$). (c) A number of 1063 circRNAs are significantly differentially expressed with ≥2-fold changes ($p \leq 0.05$) in the DM group in contrast to the control group. There are 142 significantly upregulated circRNAs and 921 significantly downregulated circRNAs, including 198 novel circRNAs (red). (d) A number of 1063 circRNAs were probed to having a significant changed expression between two groups, and 14 circRNAs that presented more than 5-fold difference were delivered in this figure. The circRNAs with high expression were red-colored, while circRNAs with low expression were green-colored.

3.2. Expression Pattern and Characteristics of circRNAs in Retinal Tissues in Type 2 Diabetes Patients without Diabetic Retinopathy. Differentially expressed circRNAs between above-mentioned two groups are exhibited on the basis of a scatter plot (Figure 2(a)). As shown in the volcano plot ($p \leq 0.05$ as well as fold change ≥ 2.0), the number of 1063 circRNAs was disclosed to present significant differential expression between the above-mentioned two groups, of which 142 circRNAs were increased and 921 circRNAs were decreased in the DM group in contrast with the control group (Figure 2(b)). Among screened circRNAs with differential expression, 198 circRNAs were detected as novel circRNAs, and 865 circRNAs were already included in the circBase (Figure 2(c)). Besides, a total of 14 circRNAs were revealed to present more than 5-fold differential expression, including circMET, circITCH, circDNMT3B, circPAG1, circADAM9, circFTO, circ001209, circKMT2E, circCOL1A2, circ0001953, circHIPK3, circ0084043, circZNF532, and circEhmt1 (Figure 2(d)).

3.3. Distribution of the circRNAs with Differential Expression. Among 1063 differentially expressed circRNAs, 1056 were derived from 805 unique genes, while the host genes of 7 circRNAs cannot be ascertained. 81.49% of the 805 genes generated only one circRNA, 11.80% of these genes generated two different circRNAs, and 6.71% of these genes generated more than two circRNAs (Figure 3(a)). In addition, these circRNAs differentially distributed throughout all of human chromosomes (Figures 3(b) and 3(c)).

3.4. Gene Ontology and KEGG Pathway Analyses of Differentially Expressed circRNAs. In the process of bioinformatics analysis, to annotate the capacity of the target genes of all circRNAs that were differentially expressed, Gene Ontology analysis was applied. The top ten enriched functional entries of cellular components, biological processes, and molecular functions are shown in Figure 4. The most enriched biological process was intracellular metabolic, organelle organization as well as cell protein metabolic process (Figure 4(a)). Of the cellular components, the genes were closely related to the intracellular part, intracellular organelle, cytoplasm, and catalytic complex (Figure 4(b)). For the molecular functions, the largest proportion of top genes was referred to as binding and protein binding (Figure 4(c)). To further understand the correlation between these top genes and the pathogenesis of the early DR, we employed pathway analysis based on KEGG. The top ten strikingly enriched KEGG pathways are shown in Figure 4(d).

3.5. The Latent Connection between miR-204-5p and circRNA. Due to the specific significance of miR-204 in the biology of the retina [17, 22], in this study, what circRNAs the predicted miRNA targets were identified on the basis of miRNA target prediction software—TargetScan. A total of 240 circRNAs were inferred to possess miR-204-5p response elements. By comparing these circRNAs with the differentially expressed genes in DM retina, our research team discovered that 206 (85.83%, 206/240) circRNAs were expressed with significant difference in the DM group,

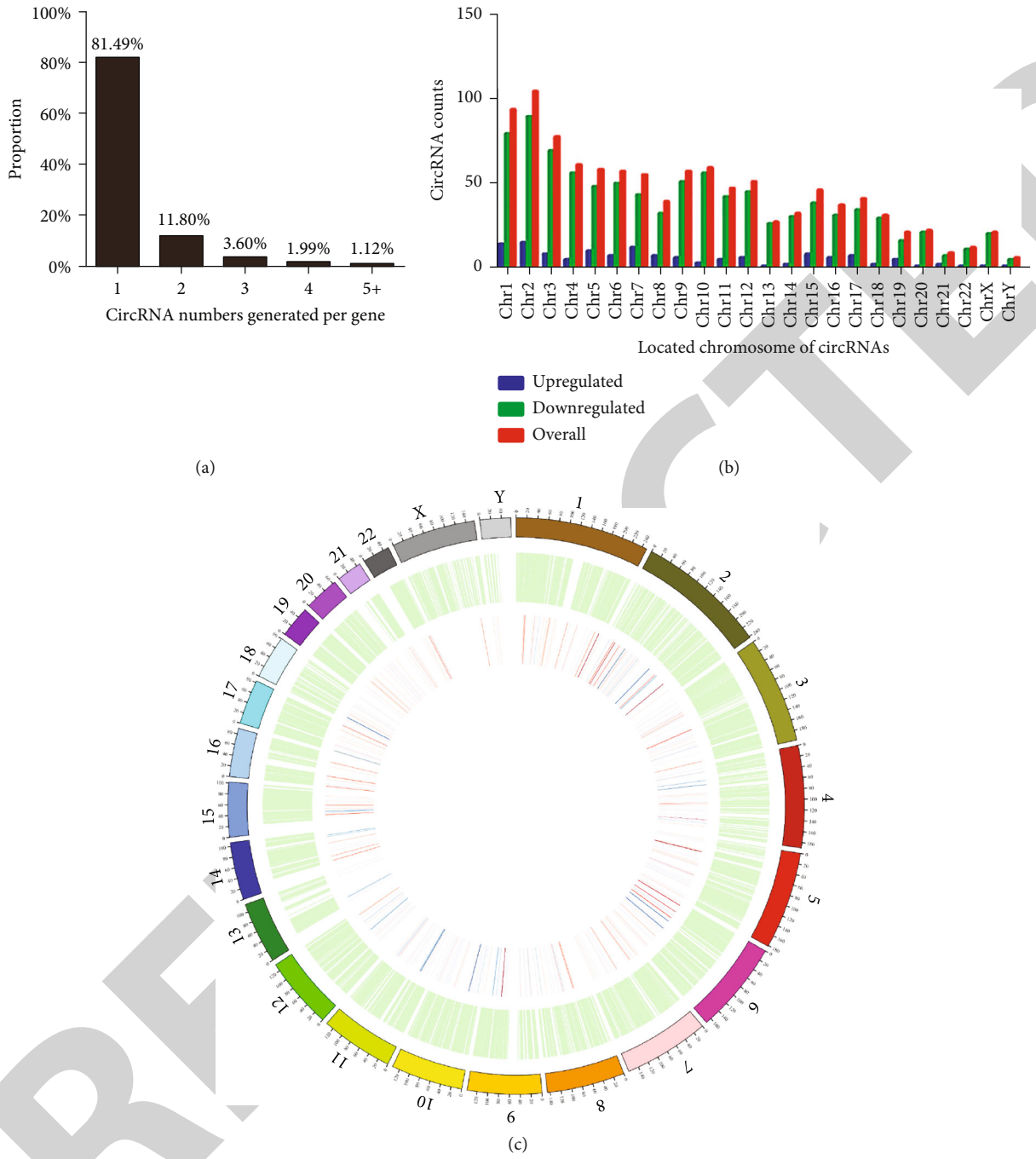

Figure 3: Distribution of the differentially expressed circRNAs. (a) Analysis of circRNAs and their host genes shows most genes (81.49%) generating only one circRNA. (b) Chromosomal distribution of the differentially expressed circRNAs. (c) Chromosomal distribution of screened circRNAs in the human chromosomes. The farthest outer layer discloses the situation of the circRNAs. From the outside to the inside, the inner circles disclosed the expression distribution of all circRNAs in diabetic as well as normal samples.

including 18 (7.5%, 18/240) upregulated and 188 (78.33%, 188/240) downregulated circRNAs (Figure 5(a)). That is, the alteration of the miR-204-5p-related circRNAs seems to be associated with the pathogenesis of DM.

The predicted mutual combination of miRNA and circRNA was ranked according to pairing structure scores computed by miRanda algorithms, with the result revealing that hsa-miR-204-5p had a high score for upregulating circRNA circKMT2E and downregulating circRNA circPAG1. Hence, circKMT2E and circPAG1 were further used for the FPKM analysis. These two circRNAs both showed the same expression patterns with the sequencing results (Figure 5(b)). circKMT2E is upregulated significantly (FC = 4.449, $p = 0.047$), while circPAG1 is downregulated significantly (FC = 0.413, $p = 0.021$), in the DM group in contrast to the healthy control.

Besides, circKMT2E, derived from Exon4-Exon15 of transcript KMT2E of Chromosome 7 (q22.3) (Figures 6(a)

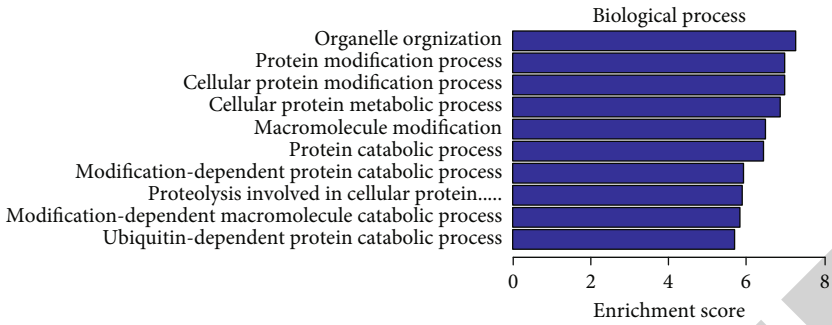

(a)

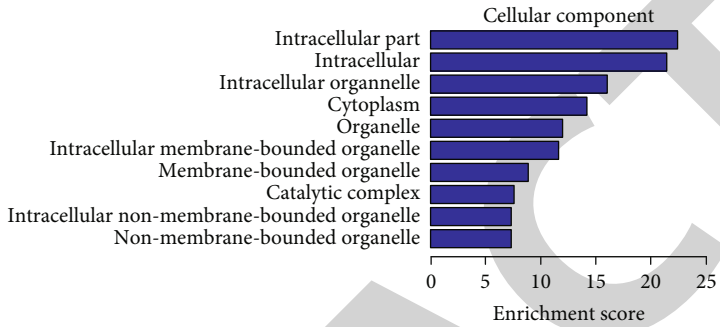

(b)

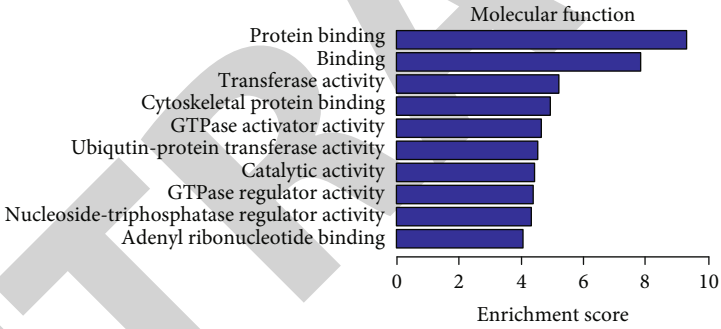

(c)

Figure 4: Continued.

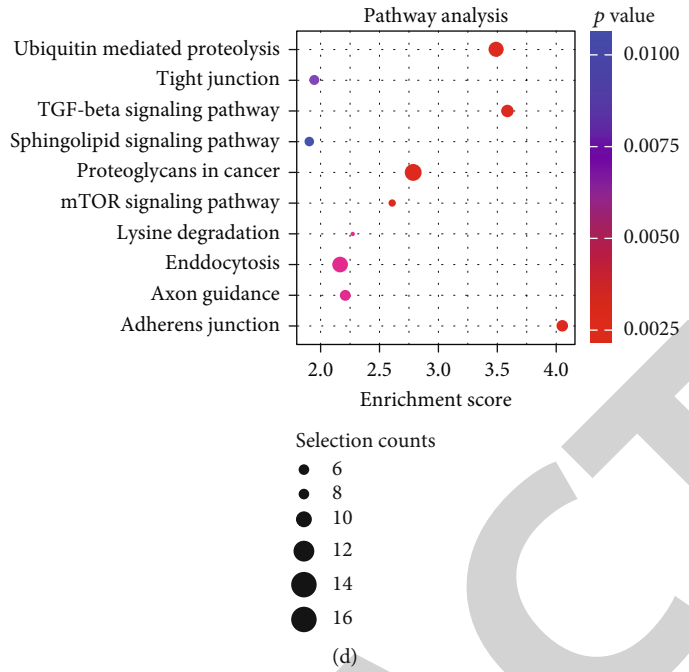

Figure 4: Gene ontology analysis as well as Kyoto Encyclopedia of Genes and Genomes analysis of the host genes of circRNAs with differential expression. GO analysis annotates differentially expressed circRNAs through three aspects, including (a) biological process, (b) cellular components, and (c) molecular function. The bar plots show the top ten improvement score values of the expressive enrichment terms. (d) The top ten relevant pathways are identified for the differentially expressed circRNAs. The enrichment score value of displayed Pathway ID equals "–log10 (p value)." The dot plot discloses the top ten enrichment score (–log10 (p value)) values of the expressive enrichment pathway.

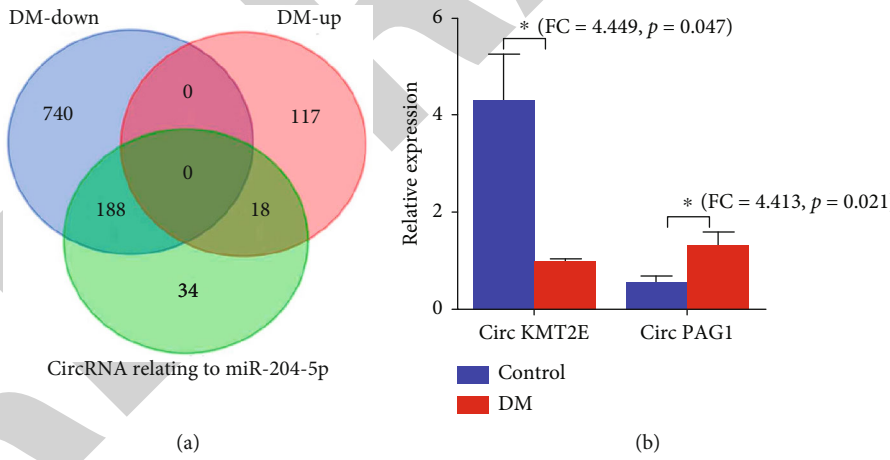

Figure 5: Screening the miR-204-5p binding circRNAs and validating their expression pattern by FPKM analysis. (a) An overlapping number of miR-204-5p binding circRNAs and differentially expressed circRNAs in DM and control retina (DM-up: upregulated circRNAs in diabetic retinopathy; DM-down: downregulated circRNAs in diabetic retinopathy). (b) Validation of circRNA expression by FPKM analysis. Bars represent mean ± SEM ($^*p < 0.05$; DM: diabetic cataract; FC: fold change). $^*p < 0.05$.

and 6(b)), was significantly upregulated in DM retina and exhibiting an opposite expression pattern to miR-204-5p. Bioinformatics prediction revealed that circKMT2E having four matched sequences could combine with miR-204-5p (Figures 6(c) and 6(d)). Further analysis of TargetScan revealed that miR-204-5p could combine with SIRT1. Briefly, circKMT2E seems can activate the SIRT1 signaling pathway by the sponge function to miR-204-5p.

4. Discussion

circRNAs and miRNAs, which have dynamic and tissue- and cell-type-specific expression patterns, attract many researches to focus on their potential function, especially on their roles in the pathogenesis of diseases and the possibility to serve as fresh therapeutic targets for DR treatment [29]. Currently, most general studies show that circRNA

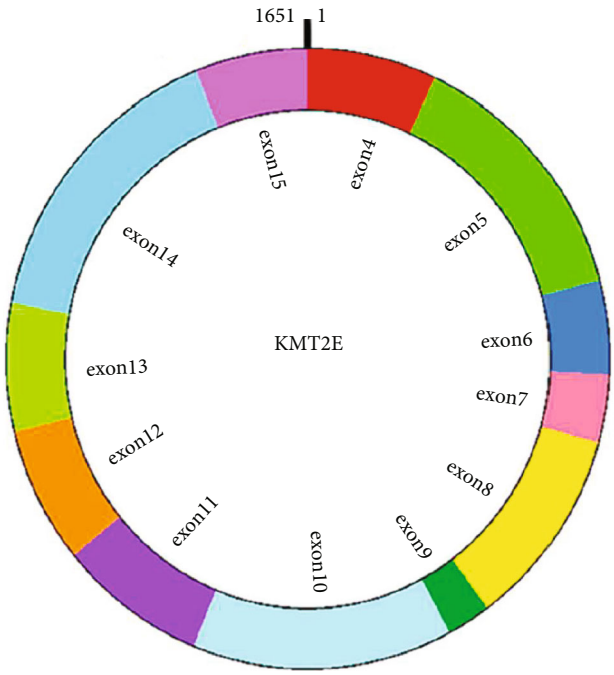

(a)

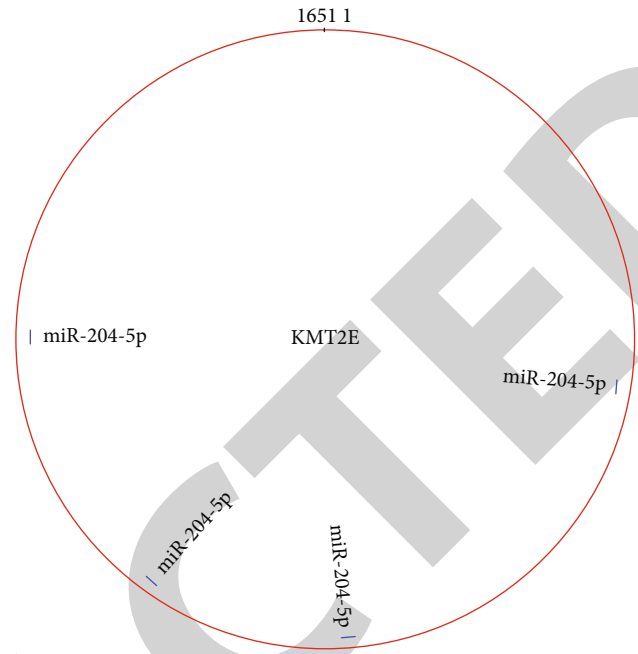

(b)

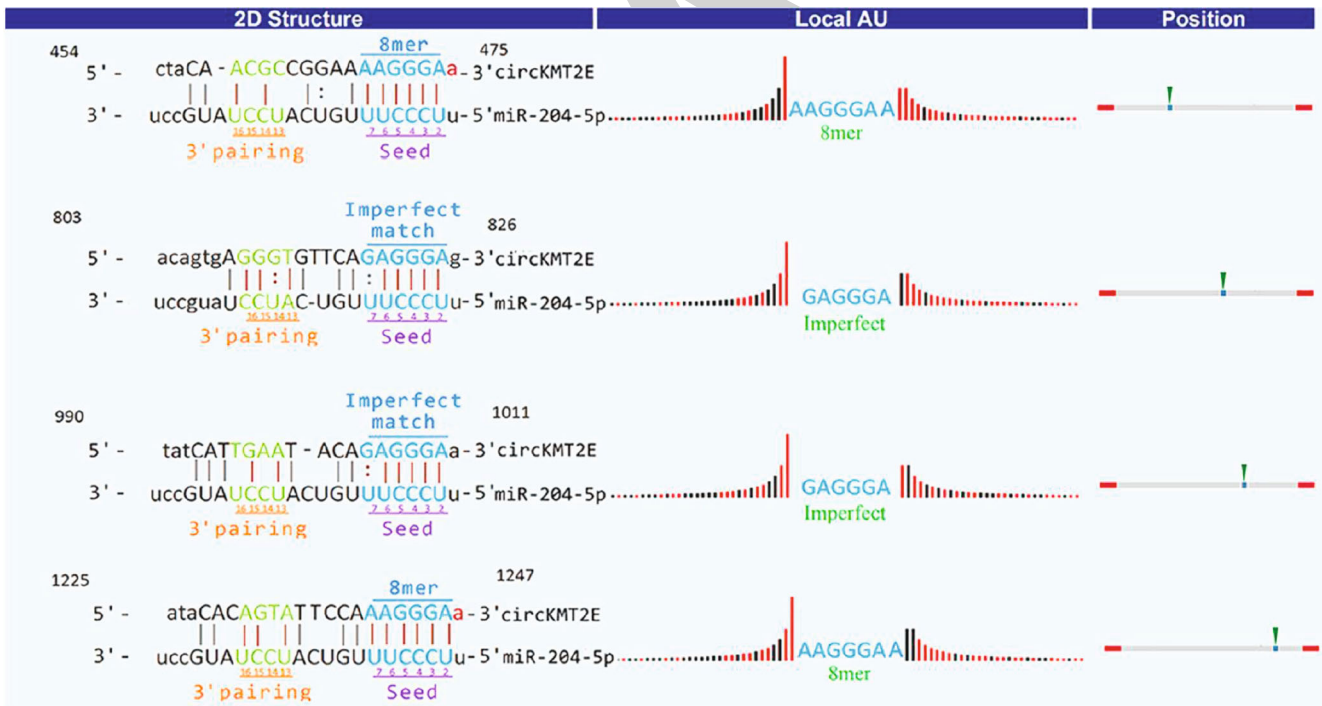

(c)

SIRT1 3' UTR 5' -UUGGAAUGUUAAUGUAAAGGGAA-3'
|||||||
mmu-miR-204-5p 3'-UCCGUAUCCUACUGUUUCCCUU-5'

(d)

Figure 6: It seems circKMT2E can activate the SIRT1 signaling pathway by the sponge function to miR-204-5p. (a) The structure of circKMT2E located between the fourth and fifteenth exons of the KMT2E gene. (b) The assumed binding sites of miR-204-5p on circKMT2E. (c) Detailed annotation of the predicted binding site sequence between circKMT2E and miR-204-5p. The "2D Structure" column displays the combining sequence of circKMT2E and miR-204-5p. The "Local AU" shows the upstream and downstream of 30 nucleotides of the seed sequence. The "Position" column exhibits the possible situation of miRNA response elements on circRNA sequence. (d) miR-204-5p possesses binding site for SIRT1.

can frequently act as the "sponges" of correlative miRNA and decrease the inhibiting effect of miRNAs toward target gene expression [28, 30]. In this study, compared with the control group, 14 different circRNAs in retinal samples from diabetic donors who do not possess conspicuous ocular impairment or obvious pathology of the retina at the last eye exam were revealed to present significant alteration and may participate in the early pathological feedback of DR. Some of this circRNAs have been confirmed by systematic research; for example, Zhu et al. [31] found that downregulation of circDMNT3B was conducive to the vascular dysfunction of DR on basis of targeting miR-20b-5p and BAMBI (a type 1 TGFβ receptor antagonist), and Shan et al. [32] found that circZNF532 adjusts diabetes-induced retinal pericyte deterioration as well as vascular dysfunction.

It was reported by Qi et al. [21] as well as Yang et al. [22] that miR-204 may be significative in the pathogenesis of DR; however, both the capacity of miR-204 in the early phase of DR and its upstream mechanism are remain sealed. Thus, we launched this study by focusing on miR-204. Based on RNA-seq and FPKM analysis as well as a previous study of miR-204-5p, we further focused on circKMT2E, which is derived from the fourth to fifteenth exons of the annotated KMT2E gene region. circKMT2E was significantly upregulated in diabetic donors without DR and showed a conflicting expression pattern to miR-204-5p. Bioinformatics analysis further revealed that circKMT2E possesses four seed sequences that can be matched with hsa-miR-204-5p. Thus, we deduced that circKMT2E, to some extent, may be a potential controller in the early pathological process of diabetic retina and be associated with the miR-204-5p sponge function. Same as the previous study conducted by Lv et al. [33] that focused on islet β-cells, our bioinformatics analysis showed that human miR-204-5p can bind SIRT1.

KMT2E is usually related to neurodevelopmental diseases, such as autism spectrum disorder, mental retardation, macrosomia, neurodevelopmental disorders, and epilepsy [34, 35]. Thus, since the retina contains abundant neuronal quantity and separate neuronal types [36], the circKMT2E seems to broadly benefit diabetic retina. Besides, miR-204 was also previously described to have various regulatory functions such as serving as an autophagy- and apoptosis-related controlling factor in various diseases. Besides, Yan et al. reported that the ischemia reperfusion injury of the spinal cord can be protected on the basis of the inhibition of miR-204, which is possible with the aid of promoting autophagy and antiapoptosis [37]. Jian et al. disclosed that miR-204 protected cardiomyocytes by adjusting autophagy through regulating LC3-II protein during hypoxia reoxygenation, and Cheng et al. [38] found that endogenous miR-204 can protect the kidney against chronic injury in hypertension and diabetes. That is, miR-204 can present diverse function for different tissues. In addition, Qi et al. found that miR-204-5p was presented as considerably augmented in the retina tissue collected from diabetic rats and further found that miR-204-5p can promote DR development [21]. However, Yang et al. found that high glucose can downregulate miR-204 in ARPE19 cells, which is a kind of human retinal pigment epithelial cell line [22]. It seems that miR-204-5p has both a stage- and a tissue-specific manner.

SIRT1, a constituent of the silent information regulator 2 family, is a Class III histone deacetylase, which interplays with target proteins, and adjusts many cellular progresses, for example, cellular apoptosis, proliferation, and inflammatory responses [33, 39]. Generally, Sirt1 is mainly a histone deacetylase predominately localized in the nucleus, and its activity relies on cellular NAD availability [39]. Functionally, SIRT1 could deacetylate a series of histones, for example, H3 and H4, and more than 50 transcription factors and DNA repair proteins, for example, NF-κB [40]. It is expressed throughout the retina and is currently deemed as a guardian of the development of DR. In addition, the associative ability of miR-204-5p to SIRT1 was confirmed by a previous study [41]. Thus, in the early stage of diabetic retinal feedback, the upregulation of circKMT2E may be involved in the pathogenesis of DM on the basis of activating the SIRT1 signaling pathway to protect the retina by the sponge function to miR-204-5p, just as the augment of Sirt1 is also defensive against diverse ocular diseases such as cataract, retinal degeneration, as well as optic neuritis [39, 42].

Therefore, this study substantially appended to previous studies by finding that, in the early stage of diabetic retinal reaction, circKMT2E can seemingly activate the SIRT1 signaling pathway to defend the retina based on its sponge function to miR-204-5p. Besides, this study illustrated the controversial capacity of miR-204-5p in early diabetic retina. However, this study possesses several limitations. First, the direct binding abilities of circKMT2E and miR-204-5p were not substantiated by dual-luciferase reporter assay. Second, the transfection experiment of the retinal cell was not included in this study. Third, which factor makes miR-204-5p lose efficacy and induce DR was not ascertained. Although our study found that the differentially expressed circRNAs were involved in the pathologic process of DR and offered an innovative target for the therapy of DR, the exact mechanisms need further validation.

5. Conclusion

In the present study, our research team scrutinized the circRNAs that possess differential expression in the retina from diabetic donors who did not possess ocular damage or retinal alteration of pathology and preliminarily discussed the relation between miR-204-5p and related circRNAs during the early diabetic retina. The upregulation of circKMT2E in the early stage of diabetic retinal feedback may be involved in the pathogenesis of DM that activates the SIRT1 signaling pathway to protect retina by the sponge function to miR-204-5p.

Data Availability

The labeled dataset used to support the findings of this study are available from the corresponding author upon request.

Conflicts of Interest

The authors declare no competing interests.

References

[1] R. Unnikrishnan, R. M. Anjana, and V. Mohan, "Diabetes mellitus and its complications in India," *Nature Reviews Endocrinology*, vol. 12, no. 6, pp. 357–370, 2016.

[2] A. M. Schmidt, "Highlighting diabetes mellitus: the epidemic continues," *Arteriosclerosis, Thrombosis, and Vascular Biology*, vol. 38, no. 1, pp. e1–e8, 2018.

[3] N. Cheung, P. Mitchell, and T. Y. Wong, "Diabetic retinopathy," *The Lancet*, vol. 376, no. 9735, pp. 124–136, 2010.

[4] B. Han, J. Chao, and H. Yao, "Circular RNA and its mechanisms in disease: from the bench to the clinic," *Pharmacology & Therapeutics*, vol. 187, pp. 31–44, 2018.

[5] U. Dube, J. L. del-Aguila, Z. Li et al., "An atlas of cortical circular RNA expression in Alzheimer disease brains demonstrates clinical and pathological associations," *Nature Neuroscience*, vol. 22, no. 11, pp. 1903–1912, 2019.

[6] V. N. S. Garikipati, S. K. Verma, Z. Cheng et al., "Circular RNA CircFndc3b modulates cardiac repair after myocardial infarction via FUS/VEGF-A axis," *Nature Communications*, vol. 10, no. 1, article 4317, 2019.

[7] S. L. Mehta, R. J. Dempsey, and R. Vemuganti, "Role of circular RNAs in brain development and CNS diseases," *Progress in Neurobiology*, vol. 186, article 101746, 2020.

[8] S. P. Barrett and J. Salzman, "Circular RNAs: analysis, expression and potential functions," *Development*, vol. 143, no. 11, pp. 1838–1847, 2016.

[9] L. L. Chen and L. Yang, "Regulation of circRNA biogenesis," *RNA Biology*, vol. 12, no. 4, pp. 381–388, 2015.

[10] W. R. Jeck, J. A. Sorrentino, K. Wang et al., "Circular RNAs are abundant, conserved, and associated with ALU repeats," *RNA*, vol. 19, no. 2, pp. 141–157, 2013.

[11] H. Suzuki, Y. Zuo, J. Wang, M. Q. Zhang, A. Malhotra, and A. Mayeda, "Characterization of RNase R-digested cellular RNA source that consists of lariat and circular RNAs from pre-mRNA splicing," *Nucleic Acids Research*, vol. 34, no. 8, pp. e63–e63, 2006.

[12] J. Salzman, R. E. Chen, M. N. Olsen, P. L. Wang, and P. O. Brown, "Cell-type specific features of circular RNA expression," *PLoS Genetics*, vol. 9, no. 9, article e1003777, 2013.

[13] J. U. Guo, V. Agarwal, H. Guo, and D. P. Bartel, "Expanded identification and characterization of mammalian circular RNAs," *Genome Biology*, vol. 15, no. 7, p. 409, 2014.

[14] A. Rybak-Wolf, C. Stottmeister, P. Glažar et al., "Circular RNAs in the mammalian brain are highly abundant, conserved, and dynamically expressed," *Molecular Cell*, vol. 58, no. 5, pp. 870–885, 2015.

[15] Y. Tay, J. Rinn, and P. P. Pandolfi, "The multilayered complexity of ceRNA crosstalk and competition," *Nature*, vol. 505, no. 7483, pp. 344–352, 2014.

[16] Y. Hu, Y. Zhao, C. Shi et al., "A circular RNA from APC inhibits the proliferation of diffuse large B-cell lymphoma by inactivating Wnt/β-catenin signaling via interacting with TET1 and miR-888," *Aging*, vol. 11, no. 19, pp. 8068–8084, 2019.

[17] A. Bereimipour, H. Najafi, E. S. Mirsane, S. Moradi, and L. Satarian, "Roles of miR-204 in retinal development and maintenance," *Experimental Cell Research*, vol. 406, no. 1, article 112737, 2021.

[18] M. Karali, I. Peluso, V. Marigo, and S. Banfi, "Identification and characterization of microRNAs expressed in the mouse eye," *Investigative Ophthalmology & Visual Science*, vol. 48, no. 2, pp. 509–515, 2007.

[19] S. Xu, P. D. Witmer, S. Lumayag, B. Kovacs, and D. Valle, "MicroRNA (miRNA) transcriptome of mouse retina and identification of a sensory organ-specific miRNA cluster," *Journal of Biological Chemistry*, vol. 282, no. 34, pp. 25053–25066, 2007.

[20] M. Drewry, I. Helwa, R. R. Allingham, M. A. Hauser, and Y. Liu, "miRNA profile in three different normal human ocular tissues by miRNA-Seq," *Investigative Ophthalmology & Visual Science*, vol. 57, no. 8, pp. 3731–3739, 2016.

[21] F. Qi, X. Jiang, T. Tong, H. Chang, and R.-X. Li, "miR-204 inhibits inflammation and cell apoptosis in retinopathy rats with diabetic retinopathy by regulating Bcl-2 and SIRT1 expressions," *European Review for Medical and Pharmacological Sciences*, vol. 24, no. 12, pp. 6486–6493, 2020.

[22] Y. Yang, J. Zhou, W. H. Li, Z. X. Zhou, and X. B. Xia, "lncRNA NEAT1 regulated diabetic retinal epithelial-mesenchymal transition through regulating miR-204/SOX4 axis," *PeerJ*, vol. 9, article e11817, 2021.

[23] S. A. Mills, A. I. Jobling, M. A. Dixon et al., "Fractalkine-induced microglial vasoregulation occurs within the retina and is altered early in diabetic retinopathy," *Proceedings of the National Academy of Sciences of the United States of America*, vol. 118, no. 51, 2021.

[24] A. C. Clermont and S. E. Bursell, "Retinal blood flow in diabetes," *Microcirculation*, vol. 14, no. 1, pp. 49–61, 2007.

[25] C. Y. Cheung, M. K. Ikram, R. Klein, and T. Y. Wong, "The clinical implications of recent studies on the structure and function of the retinal microvasculature in diabetes," *Diabetologia*, vol. 58, no. 5, pp. 871–885, 2015.

[26] K. Becker, H. Klein, E. Simon et al., "In-depth transcriptomic analysis of human retina reveals molecular mechanisms underlying diabetic retinopathy," *Scientific Reports*, vol. 11, no. 1, article 10494, 2021.

[27] A. Dobin, C. A. Davis, F. Schlesinger et al., "STAR: ultrafast universal RNA-seq aligner," *Bioinformatics*, vol. 29, no. 1, pp. 15–21, 2013.

[28] C. Fan, X. Liu, W. Li et al., "Circular RNA circ KMT2E is upregulated in diabetic cataract lenses and is associated with miR-204-5p sponge function," *Gene*, vol. 710, pp. 170–177, 2019.

[29] H. R. Zhou and H. Y. Kuang, "Circular RNAs: novel target of diabetic retinopathy," *Reviews in Endocrine & Metabolic Disorders*, vol. 22, no. 2, pp. 205–216, 2021.

[30] S. Liang, S. Dou, W. Li, and Y. Huang, "Profiling of circular RNAs in age-related cataract reveals circZNF292 as an antioxidant by sponging miR-23b-3p," *Aging*, vol. 12, no. 17, pp. 17271–17287, 2020.

[31] K. Zhu, X. Hu, H. Chen et al., "Downregulation of circRNA DMNT3B contributes to diabetic retinal vascular dysfunction through targeting miR-20b-5p and BAMBI," *eBioMedicine*, vol. 49, pp. 341–353, 2019.

[32] K. Shan, C. Liu, B. H. Liu et al., "Circular noncoding RNA HIPK3 mediates retinal vascular dysfunction in diabetes mellitus," *Circulation*, vol. 136, no. 17, pp. 1629–1642, 2017.

[33] X. Lv, Y. Zhao, X. Yang et al., "Berberine potentiates insulin secretion and prevents β-cell dysfunction through the miR-

Hindawi
Computational and Mathematical Methods in Medicine
Volume 2023, Article ID 9897854, 1 page
https://doi.org/10.1155/2023/9897854

Retraction

Retracted: Correlation of Serum M-CSF, CER, and TIMP-1 Levels with Liver Fibrosis in Viral Hepatitis

Computational and Mathematical Methods in Medicine

Received 12 December 2023; Accepted 12 December 2023; Published 13 December 2023

This article has been retracted by Hindawi, as publisher, following an investigation undertaken by the publisher [1]. This investigation has uncovered evidence of systematic manipulation of the publication and peer-review process. We cannot, therefore, vouch for the reliability or integrity of this article.

Please note that this notice is intended solely to alert readers that the peer-review process of this article has been compromised.

Wiley and Hindawi regret that the usual quality checks did not identify these issues before publication and have since put additional measures in place to safeguard research integrity.

We wish to credit our Research Integrity and Research Publishing teams and anonymous and named external researchers and research integrity experts for contributing to this investigation.

The corresponding author, as the representative of all authors, has been given the opportunity to register their agreement or disagreement to this retraction. We have kept a record of any response received.

References

[1] H. Yao, X. Yang, M. Yan et al., "Correlation of Serum M-CSF, CER, and TIMP-1 Levels with Liver Fibrosis in Viral Hepatitis," *Computational and Mathematical Methods in Medicine*, vol. 2022, Article ID 6736225, 8 pages, 2022.

Hindawi
Computational and Mathematical Methods in Medicine
Volume 2022, Article ID 6736225, 8 pages
https://doi.org/10.1155/2022/6736225

Research Article

Correlation of Serum M-CSF, CER, and TIMP-1 Levels with Liver Fibrosis in Viral Hepatitis

Hairong Yao,[1] Xuan Yang,[2] Man Yan,[3] Xueqin Fang,[2] Yange Wang,[2] Hong Qi,[2] and Li Sun[2]

[1]*Department of Cardiology, Xi'an No.3 Hospital, The Affiliated Hospital of Northwest University, Xi'an, Shaanxi 710018, China*
[2]*Department of Infection, Xi'an No.3 Hospital, The Affiliated Hospital of Northwest University, Xi'an, Shaanxi 710018, China*
[3]*Department of Hepatobiliary, Xi'an No.3 Hospital, The Affiliated Hospital of Northwest University, Xi'an, Shaanxi 710018, China*

Correspondence should be addressed to Li Sun; sl13892886616@163.com

Received 19 July 2022; Revised 25 August 2022; Accepted 1 September 2022; Published 30 September 2022

Academic Editor: Min Tang

Objective. This research is aimed at investigating the relationship between liver fibrosis in viral hepatitis and macrophage colony-stimulating factor (M-CSF), tissue inhibitor of matrix metalloproteinase (TIMP-1), and ceruloplasmin (CER) in serum level. *Methods*. Patients were randomly selected among those admitted to our hospital, and 60 healthy volunteers were chosen to serve as control participants. The levels of serum M-CSF, CER, and TIMP-1 were compared. According to the severity of their liver fibrosis, patients with CHB were separated into four groups: S1, S2, S3, and S4. Serum levels of M-CSF, CER, and TIMP-1 were correlated with liver fibrosis and hepatitis markers, and the diagnostic usefulness of the three indices was assessed with liver cirrhosis patients. *Results*. Increases in M-CSF and TIMP-1 in the CHB group but decreases in CER were statistically significant ($P < 0.05$). Serum levels of M-CSF, CER, TIMP-1, HA, PC-III, C-IV, and LN differed significantly across the four study groups ($P < 0.05$). Over time, as liver fibrosis worsened, we observed a progressive uptick in M-CSF, TIMP-1, LN, HA, C-IV, and PC-III levels and a progressive downtick in CER levels, with significant ($P < 0.05$) differences between the groups. There was a significant positive correlation between liver fibrosis and serum M-CSF, PC-III, TIMP-1, HA, LN, and C-IV levels in the CHB group ($P < 0.05$) and a significant negative correlation between serum CER and these same factors ($P < 0.05$). The AUC of 0.956 for diagnosing the S4 stage was greater than that of 0.857, 0.851, and 0.817 for M-CSF, CER, and TIMP-1, respectively. *Conclusions*. In CHB patients, the liver fibrosis degree is associated with the M-CSF, CER, and TIMP-1 levels, and the combined clinical detection of these three markers has better diagnostic significance.

1. Introduction

The liver is crucial to functioning several vital processes, including metabolism, immunity, coagulation, and many more. Long-term infection with the hepatitis B virus (HBV) is the primary cause of chronic hepatitis B (CHB) fibrosis, a multisystem chronic liver disease. However, HBV is not easy to clear, the patient's liver function inflammation is apparent, and it may progress to liver cirrhosis, which has become a significant public health problem. Proactive and efficient therapeutic approaches will slow the advancement of liver fibrosis to cirrhosis [1, 2]. Liver biopsy, an invasive procedure with limited clinical applicability, is still the gold standard for diagnosing liver fibrosis, and the biochemical and serological indicators are convenient and economical, which is a hotspot of current research [3].

Macrophage colony-stimulating factor (M-CSF) is composed of fibroblasts, activated macrophages, endometrial epithelial secretory cells, bone marrow stromal cells, vitamin D-activated osteoblasts, and activated vascular endothelial cells. Hepatic inflammatory responses are partly mediated by serum M-CSF, which has a role in the pathophysiology of hepatic fibrosis [4] by attracting and aggregating hepatic stellate cells. Ceruloplasmin (CER) is primarily metabolized in the liver. CER is a serum glycoprotein with 6 copper atoms per molecule, which is mainly synthesized in the liver.

When liver function is damaged, especially liver failure, the level of CER in serum often decreases significantly. The primary function of CER is to combine with serum-free copper to complete the transport and metabolism process. Abnormal liver function will lead to abnormal serum CER levels, resulting in a series of cell and organ toxicity after copper deposition [5]. Excessive accumulation of extracellular matrix (ECM) in the liver is linked to liver fibrosis, and the ECM metabolism is related to matrix metal proteases (MMPs) and tissue inhibitors of metal proteases (TIMPs) [6]. Studies have shown that only TIMP-1 and TIMP-2 exist in the liver, while the specificity and sensitivity of TIMP-1 are superior to TIMP-2 in liver fibrosis diagnosis [7]. Studies have shown that TIMP-1 plays a role in the progression of liver fibrosis by degrading and transforming epithelial cells into mesenchymal cells [8]. Based on these findings, this research is aimed at offering a reference for clinical diagnosis of liver fibrosis progression by analyzing the blood levels of M-CSF, CER, and TIMP-1 in HBV-infected CHB patients. The report is as follows.

2. Materials and Methods

2.1. Research Subjects. From March 2017 to March 2020, a total of 115 CHB patients admitted to our hospital were selected. Following were the criteria for inclusion: (1) the pathological diagnosis of the liver biopsy was based on the Protocol for Prevention and Treatment of Viral Hepatitis [9], and the diagnostic criteria were following the Guidelines for Prevention and Treatment of Chronic Hepatitis B (2019 edition) [10]. (2) Hepatitis B surface antigen test was positive, and HBV infection history was longer than six months. (3) There were no contraindications to liver puncture. (5) Complete clinical data. Exclusion criteria are as follows: (1) abnormal liver function brought on by autoimmune liver disease, fatty liver, other viral hepatitis, and alcohol-related liver disease; (2) accompanied by malignant tumor; (3) patients with heart, kidney, and other serious diseases; (4) patients with blood system diseases; (5) patients with a previous history of liver surgery; (6) pregnant and lactation women; and (7) patients are taking anti-inflammatory, antifibrotic, immune-regulating drugs before enrollment. Liver fibrosis was divided into four stages: S1 was mild fibrosis, with 32 cases; S2 was moderate fibrosis, with 28 cases; S3 was advanced liver fibrosis, with 30 cases; and S4 was liver cirrhosis, with 25 cases. Sixty healthy volunteers were chosen as a control group for the same period. The Medical Ethics Review Board provided its approval for this investigation.

2.2. Observation Indicators. (1) General data collection is as follows: weight, height, gender, systolic blood pressure (SBP), diastolic blood pressure (DBP), and age of the CHB group and the healthy group were collected. The changes in SBP and DBP of the subjects were measured by a sphygmomanometer. Body Mass Index (BMI) = weight/height^2 (international unit kg/m^2). (2) After enrolling patients, 3 mL of fasting venous blood was obtained, and the upper serum was collected by centrifugation. This allowed us to measure the serum levels of M-CSF, CER, and TIMP-1. Enzyme-linked immunoadsorption (ELISA) was used to measure M-CSF and TIMP-1 in the serum. The kits were purchased from Rapid Bio Company, USA. The serum CER level was detected by the immunoturbidimetric method, and the instrument was an IMMAGE 800 automatic specific protein analysis system produced by Beckman Company in the United States, and supporting reagents were used. (3) Comparison of serum liver fibrosis indexes in the CHB group is as follows: After the patients were enrolled, 3 mL of fasting venous blood was taken, and the upper serum was collected by centrifugation. Enzymatic chemiluminescence immunoassay was used to detect type IV collagen (C-IV), laminin (LN) levels, hyaluronic acid (HA), and type III procollagen (PC-III); the kits were purchased from Roche Germany.

2.3. Statistical Analysis. For the statistical analysis, we utilized SPSS 20.0. t-test was employed on measurement data represented as $x \pm s$. The rate (%) was calculated from the count data, and a χ^2 test was performed. The association between serum levels of M-CSF, CER, and TIMP-1 and HA, PC-III, C-IV, and LN was analyzed using Pearson's correlation analysis. Serum M-CSF, CER, and TIMP-1 levels were analyzed in connection to liver fibrosis severity using Spearman's correlation. Using a ROC curve, we compared the diagnostic accuracy of serum M-CSF, CER, and TIMP-1 for the S4 stage; a difference at the $P < 0.05$ was considered significant.

3. Results

3.1. Comparison of General Data between CHB Group and Healthy Group. Table 1 shows no statistically significant differences between the CHB group and the healthy group concerning gender, age, body mass index, systolic blood pressure, or diastolic blood pressure ($P > 0.05$).

3.2. Comparison of Serum M-CSF, CER, and TIMP-1 Levels between CHB Group and Healthy Group. Table 2 shows that compared to the healthy controls, the CHB group had significantly higher serum M-CSF and TIMP-1 levels and significantly lower CER levels. These differences were statistically significant ($P < 0.05$).

3.3. Comparison of Serum M-CSF, CER, and TIMP-1 Levels in CHB Patients with Different Degrees of Liver Fibrosis. The levels of serum M-CSF, CER, and TIMP-1 varied significantly across the S1, S2, S3, and S4 groups ($P < 0.05$). As liver fibrosis progressed, the blood levels of M-CSF, TIMP-1, and CER changed over time, with statistically significant variations across all groups ($P < 0.05$), as indicated in Table 3.

3.4. Changes in Serological Markers of Liver Fibrosis in CHB Patients. Serum C-IV, LN, PC-III, and HA levels varied across the S1, S2, S3, and S4 groups in a statistically significant way ($P < 0.05$). The blood levels of HA, PC-III, C-IV, and LN steadily increased as liver fibrosis progressed, and statistically significant differences existed between all groups ($P < 0.05$), as shown in Table 4.

Table 1: Comparison of general data between the two groups.

Group	Number of cases	Gender (male/female, cases)	Age (years)	BMI (kg/m^2)	SBP (mmHg)	DBP (mmHg)
CHB group	115	69/46	46.57 ± 7.85	25.43 ± 4.61	127.87 ± 7.49	78.42 ± 6.37
Healthy group	60	31/29	46.32 ± 7.49	24.89 ± 4.97	128.20 ± 8.71	77.80 ± 6.78
t/χ^2		1.118	0.203	0.716	0.261	0.598
P		0.290	0.839	0.475	0.794	0.551

Table 2: Comparison of serum M-CSF, CER, and TIMP-1 levels between the CHB group and healthy group.

Group	Number of cases	M-CSF (pg/mL)	CER (g/L)	TIMP-1 (μg/L)
CHB group	115	241.83 ± 64.80	0.24 ± 0.08	175.15 ± 37.79
Healthy group	60	140.01 ± 42.28	0.30 ± 0.05	127.01 ± 22.95
t		11.003	5.291	9.030
P		<0.001	<0.001	<0.001

Table 3: Comparison of serum M-CSF, CER, and TIMP-1 levels in CHB patients with different degrees of liver fibrosis.

Group	Number of cases	M-CSF (pg/mL)	CER (g/L)	TIMP-1 (μg/L)
S1 group	32	181.12 ± 36.82	0.31 ± 0.11	143.68 ± 23.09
S2 group	28	227.26 ± 52.17①	0.25 ± 0.05①	162.02 ± 21.63①
S3 group	30	266.93 ± 43.08①②	0.22 ± 0.04①②	189.41 ± 23.40①②
S4 group	25	305.72 ± 50.14①②③	0.18 ± 0.02①②③	213.03 ± 39.57①②③
F		39.443	19.299	35.152
P		<0.001	<0.001	<0.001

Note: ① indicated $P < 0.05$ when compared with the S1 group; ② indicated $P < 0.05$ when compared with the S2 group, $P < 0.05$; ③ indicated $P < 0.05$ when compared with the S3 group.

Table 4: Changes in serological markers of liver fibrosis in CHB patients.

Group	Number of cases	HA (ng/mL)	PC-III (μg/mL)	C-IV (μg/mL)	LN (ng/mL)
S1 group	32	77.09 ± 18.27	102.71 ± 23.02	83.73 ± 16.20	94.62 ± 17.43
S2 group	28	172.58 ± 22.54①	121.56 ± 21.64①	111.47 ± 21.82①	135.09 ± 18.72①
S3 group	30	363.26 ± 30.62①②	202.48 ± 31.50①②	172.65 ± 25.41①②	154.66 ± 25.89①②
S4 group	25	562.97 ± 41.75①②③	252.79 ± 27.16①②③	207.22 ± 34.75①②③	225.55 ± 31.34①②③
F		1399.680	216.987	138.553	153.927
P		<0.001	<0.001	<0.001	<0.001

Note: ① indicated $P < 0.05$ when compared with the S1 group; ② indicated $P < 0.05$ when compared with the S2 group, $P < 0.05$; ③ when compared to the S3 group, $P < 0.05$.

3.5. Correlation of Changes in Serum M-CSF, CER, and TIMP-1 Levels with Liver Fibrosis, HA, PC-III, C-IV, and LN. The serum M-CSF and TIMP-1 in the CHB group were positively connected with hepatitis A, B, C, and IV, liver fibrosis, and liver nodules severity ($P < 0.05$), respectively, as shown in Table 5 and Figures 1–4.

3.6. Analysis of the Diagnostic Value of Serum M-CSF, CER, and TIMP-1 Levels for the S4 Stage. ROC curve was used for analysis. The AUC of the three indicators combined to diagnose the S4 stage was 0.956, which was higher than the 0.857, 0.851, and 0.817 of using M-CSF, CER, and TIMP-1 for diagnosis alone, respectively, as shown in Figure 5 and Table 6.

4. Discussion

Liver cirrhosis is the outcome of liver fibrosis, a degenerative condition familiar to many types of viral hepatitis. A critical step in the development is the hepatic stellate cell (HSC)

Table 5: Correlation of changes in serum M-CSF, CER, and TIMP-1 levels with the degree of liver fibrosis, HA, PC-III, C-IV, and LN.

Correlative factors	The degree of liver fibrosis		HA (ng/mL)		PC-III (μg/mL)		C-IV (μg/mL)		LN (ng/mL)	
	r	*P*	*r*	*P*	*r*	*P*	*r*	*P*	*r*	*P*
M-CSF	0.727	<0.001	0.691	<0.001	0.626	<0.001	0.651	<0.001	0.606	<0.001
CER	-0.606	<0.001	-0.515	<0.001	-0.482	<0.001	-0.525	<0.001	-0.479	<0.001
TIMP-1	0.685	<0.001	0.679	<0.001	0.652	<0.001	0.551	<0.001	0.628	<0.001

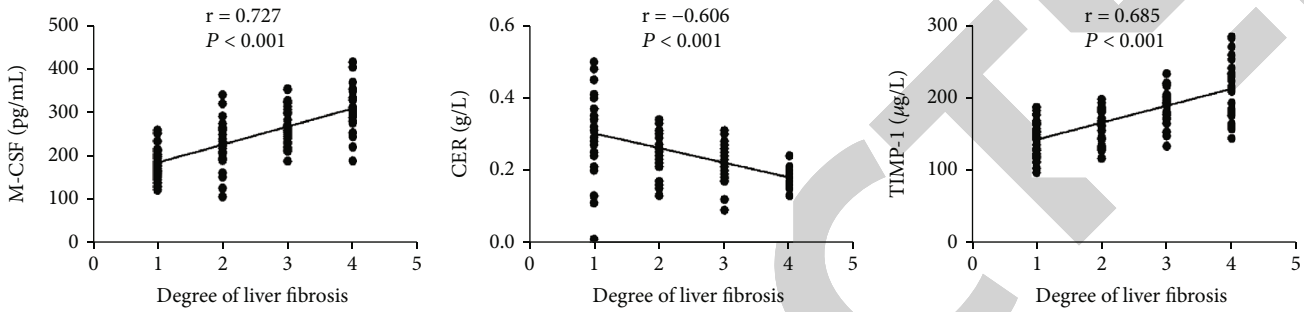

Figure 1: Correlation of changes in serum M-CSF, CER, and TIMP-1 levels and liver fibrosis degree.

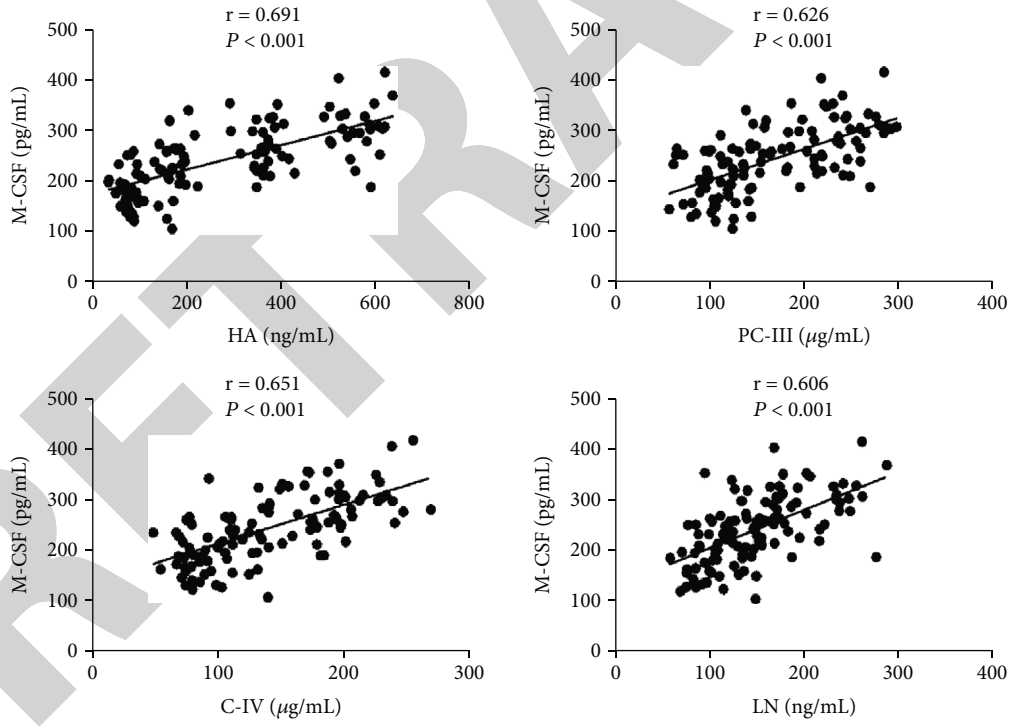

Figure 2: Correlation of serum M-CSF levels with HA, LN, C-IV, and PC-III levels.

activation. Liver fibrosis develops when activated HSCs deposit their ECM-laden extracellular matrix into liver tissues, causing a shift in the matrix's constituent proteins [11]. Since liver fibrosis is reversible, early detection of the severity of the condition is crucial to developing an effective treatment strategy and improving the prognosis [12]. HA, PC-III, C-IV, and LN are essential indicators of liver fibrosis. Liver fibrosis is connected with the amount of extracellular matrix present, and HA is a critical component of the extracellular matrix [13]. LN is a noncollagenous structural glycoprotein deposited in a large amount in the space of hepatic sinusoidal endothelial cells during liver fibrosis; C-IV is the main component of the hepatic interstitial basement membrane and forms the basement membrane along the hepatic

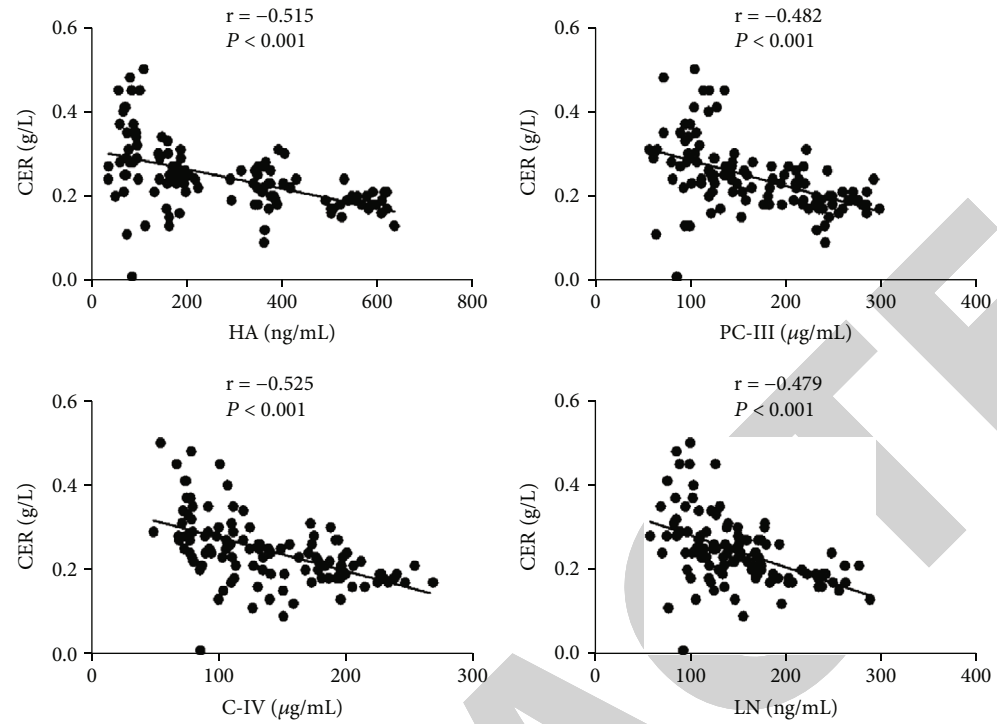

Figure 3: Correlation of CER serum levels with C-IV, PC-III, HA, and LN levels.

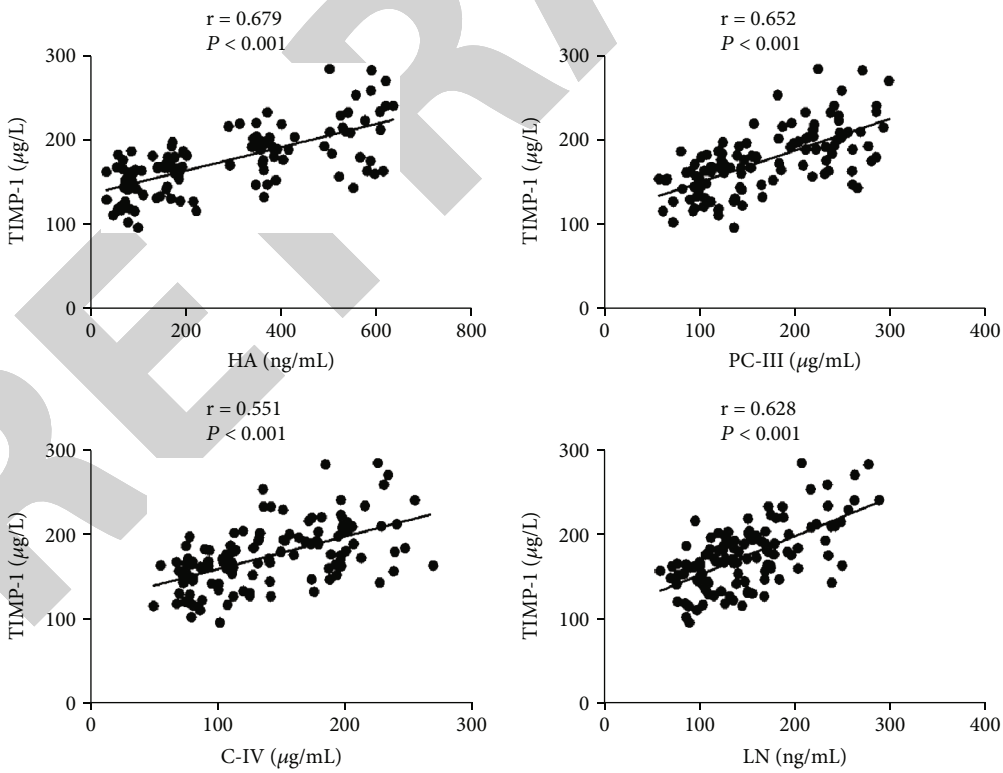

Figure 4: Correlation of serum TIMP-1 levels with C-IV, PC-III, HA, and LN levels.

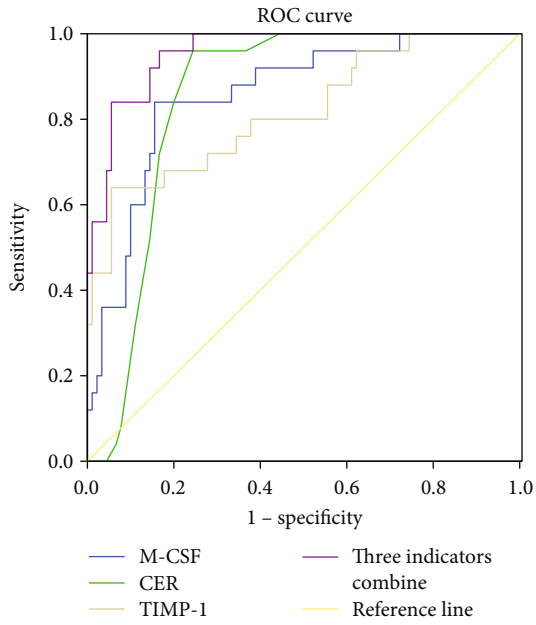

Figure 5: ROC curve analysis of serum M-CSF, CER, and TIMP-1 levels for the diagnosis of the S4 stage.

sinusoidal wall together with LN. The liver fibrosis degree is closely related to C-IV and LN [14]. PC-III is mainly degraded by type III procollagen and released into the blood, effectively reflecting collagen production levels [15]. In this study, significant differences were seen between the patients' S1, S2, S3, and S4 in terms of serum HA, PC-III, C-IV, and LN levels. Serum levels of HA, PC-III, C-IV, and LN increased as liver fibrosis progressed, showing that HA, PC-III, C-IV, and LN levels were connected to the degree of liver fibrosis in patients. Moreover, this finding has vital clinical guiding importance.

M-CSF is a cytokine produced by activated macrophages, endometrial epithelial secretory cells, osteoblasts, and other cells. By adhering to its receptors, it can control the proliferation and differentiation of mononuclear macrophage cells, which is crucial for physiological processes such as bone metabolism, mammary gland development, and ovarian ovulation; it can also be used as a proinflammatory cytokine to participate in inflammatory and immune responses and to participate in the pathological process of liver fibrosis [16, 17]. In this study, CHB had a greater serum M-CSF level than the healthy group. Between the S1, S2, S3, and S4 patient groups, there were considerable changes in the serum M-CSF levels, and the M-CSF rose dramatically as liver fibrosis progressed. The degree of liver fibrosis, HA, PC-III, C-IV, and LN levels were all positively linked with serum M-CSF levels, indicating a possible connection between the two. ROC curve analysis was used to determine the AUC of serum M-CSF for the diagnosis of the S4 stage, and it was determined to be 0.857, indicating that M-CSF can be used as a serological indicator for clinical diagnosis of liver cirrhosis. The reasons may be the following aspects: (1) M-CSF can regulate the expression of chemokines and receptors in monocytes and macrophages so that the inflammatory response of the liver continues. (2) The increased expression of M-CSF can regulate the production of MMP, aggravate the deposition of collagen fibers, and increase inflammatory cells infiltration in the liver. (3) M-CSF may prevent NK cells from producing and secreting antifibrotic factor (interferon), thereby reducing the apoptosis of HSC and indirectly promoting the progression of liver cirrhosis [18, 19].

CER is a single-chain $\alpha 2$ globulin with oxidase, mainly synthesized and secreted by the liver. When hepatocytes are immune-damaged by HBV replication in the body, the synthesis of CER will be reduced [20]. Studies have shown that [21] individuals with nonalcoholic fatty liver disease who have the CER gene mutation also have more severe liver fibrosis. Hyperferritinemia and increased hepatic iron storage have been linked to CER gene mutations in these patients. In this study, CHB had a lower serum CER level than the healthy group. Between the patient groups S1, S2, S3, and S4, the serum CER levels varied significantly, and the CER decreased significantly with the aggravation of liver fibrosis degrees. The serum CER levels were negatively correlated with C-IV, PC-III, LN liver fibrosis degree, and HA levels. According to ROC analysis, serum CER may be utilized as a sensitive biomarker for the diagnosis of liver cirrhosis, with an AUC of 0.851 for the diagnosis of the S4 stage. Tan et al. [22] have shown that in patients with CHB, CER levels correlated with the liver fibrosis degree, which was of great value in diagnosing CHB cirrhosis. Kang et al. [23] showed that patients with HBV infection have a negative correlation between CER and liver fibrosis. Significant fibrosis, advanced fibrosis, and liver cirrhosis were all predicted by CER with AUCs of 0.774, 0.812, and 0.853, respectively, which were similar to the results of this study.

TIMP-1 was firstly isolated from the skeletal muscle of rabbits. The encoding gene is located in the P11 region of the X chromosome and is secreted by HSCs. The TIMP levels were proportional to the number of activated HSCs [24]. There was a correlation between TIMP-1 levels and liver fibrosis severity and cirrhosis in patients with CHB [25]. According to a study by Medeiros et al. [26], patients with chronic hepatitis C who were treated with direct-acting antiviral therapy had significantly lower levels of MMP-9/TIMP-1, suggesting that this complex may be a valuable biomarker for active fibrosis that can determine the extent of liver fibrosis in patients following viral clearance. Serum TIMP-1 levels in CHB were greater than those in the control group. Significant variations in blood TIMP-1 levels were seen between the S1, S2, S3, and S4 groups of individuals. In a positive correlation with liver fibrosis, HA, PC-III, C-IV, and LN severity, TIMP-1 seemed to be linked to fibrosis progression. The area under the curve (AUC) for TIMP-1 in the diagnosis of the S4 stage was 0.817, according to ROC curve analysis, while the AUC of the combination of the three indicators was 0.956, which were all higher than the single indicator, suggesting that the combined diagnostic value of M-CSF, CER, and TIMP-1 was higher than using a single indicator for prediction. It primarily results from the fact that TIMP-1 can bind to all MMPs, except for MMP-14 and MMP-19, which may block the action of MMP-1,

Table 6: A diagnostic value analysis of serum M-CSF, CER, and TIMP-1 levels for the S4 stage.

	AUC	P value	Cutoff value	Sensitivity	Specificity	95% CI
M-CSF	0.857#	<0.001	272.71 pg/mL	84.00	84.44	0.777~0.937
CER	0.851#	<0.001	0.21 g/L	96.00	75.56	0.782~0.919
TIMP-1	0.817#	<0.001	204.38 μg/L	64.00	94.40	0.715~0.919
Combined	0.956	<0.001	—	96.00	83.33	0.922~0.991

Note: Compared with the prediction value by combined indicators, $^{\#}P < 0.05$.

slow down the breakdown of ECM, and encourage the development of liver fibrosis [27]. Researchers have found that [28] cucurbitaside protects liver tissue and slows the progression of liver fibrosis in a mouse model. This protective effect might be due to cucurbitaside's ability to inhibit lipid peroxidation and collagen synthesis by reducing the expression of Col-I, TIMP-1, TIMP -2 mRNA, and MMP-2 TGF-1 proteins. Of course, this research still has certain shortcomings. This research only includes a small number of patients, and their inclusion may have been predetermined. An active investigation on the levels of M-CSF, CER, and TIMP-1 in CHB patients does not exist simultaneously. The evolution of these markers after therapy is not looked into. Future research will combine many locations to increase the number of samples used, enhancing the depth and precision of this investigation.

In conclusion, liver fibrosis is associated with M-CSF, CER, and TIMP-1 levels in CHB patients. The diagnostic significance of the clinical combination detection of these three indications is higher, which aids in clinical prevention and treatment.

Data Availability

The labeled dataset used to support the findings of this study are available from the corresponding author upon request.

Conflicts of Interest

The author declares no competing interests.

Acknowledgments

This research was supported by Planned Project of Shaanxi Provincial Department of Science and Technology: General Project—Social Development Field (Project No.: s2018-yf-ybsf-0217).

References

[1] T. Inoue and Y. Tanaka, "Novel biomarkers for the management of chronic hepatitis B," *Clinical and Molecular Hepatology*, vol. 26, no. 3, pp. 261–279, 2020.

[2] A. Koffas, M. Kumar, U. S. Gill, A. Jindal, P. T. F. Kennedy, and S. K. Sarin, "Chronic hepatitis B: the demise of the 'inactive carrier' phase," *Hepatology International*, vol. 15, no. 2, pp. 290–300, 2021.

[3] Y. Sun, X. Wu, J. Zhou et al., "Persistent low level of hepatitis B virus promotes fibrosis progression during therapy," *Clinical Gastroenterology and Hepatology*, vol. 18, no. 11, pp. 2582–2591.e6, 2020.

[4] A. Tan-Garcia, F. Lai, J. P. Sheng Yeong et al., "Liver fibrosis and CD206$^+$ macrophage accumulation are suppressed by anti-GM-CSF therapy," *JHEP Reports*, vol. 2, no. 1, article 100062, 2020.

[5] E. A. El-Rayah, P. J. Twomey, E. M. Wallace, and P. A. McCormick, "Both α-1-antitrypsin Z phenotypes and low caeruloplasmin levels are over-represented in alcohol and nonalcoholic fatty liver disease cirrhotic patients undergoing liver transplant in Ireland," *European Journal of Gastroenterology & Hepatology*, vol. 30, no. 4, pp. 364–367, 2018.

[6] C. Lefeuvre, M. Roux, S. Blanchard et al., "Analysis of hepatic fibrosis markers in the serum of chronic hepatitis B patients according to basal core promoter/precore mutants," *Scientific Reports*, vol. 12, no. 1, p. 10261, 2022.

[7] X. M. Li, J. H. Peng, Z. L. Sun et al., "Chinese medicine CGA formula ameliorates DMN-induced liver fibrosis in rats via inhibiting MMP2/9, TIMP1/2 and the TGF-β/Smad signaling pathways," *Acta Pharmacologica Sinica*, vol. 37, no. 6, pp. 783–793, 2016.

[8] Z. Guixian, L. Musong, W. Yuanyuan, Q. Wei, and C. Hui, "Effects of Yinchenhao decoction on caspase-12 pathway and TIMP-1 and Smad 2 in hepatic fibrosis rats," *Laboratory Animal Science*, vol. 37, no. 2, pp. 47–52, 2020.

[9] Chinese Medical Association Infectious Diseases and Parasitic Diseases Branch, Chinese Medical Association Hepatology Branch, "Prevention and treatment of viral hepatitis," *Chinese Journal of Infectious Diseases*, vol. 19, no. 1, pp. 56–62, 2001.

[10] Chinese Society of Hepatology, Chinese Society of Gastroenterology, Chinese Society of Infectious Diseases, "Consensus on the diagnosis and treatment of liver fibrosis (2019)," *Chinese Journal of Hepatology*, vol. 27, no. 9, pp. 657–667, 2019.

[11] Z. Q. Zhang, B. S. Shi, W. Lu, D. P. Liu, D. Huang, and Y. L. Feng, "HBcrAg y HBcAb cuantitativos versus HBsAg y ADN del VHB en la prediccion de los niveles de fibrosis hepatica de los pacientes con hepatitis B cronica," *Gastroenterología y Hepatología*, vol. 43, no. 9, pp. 526–536, 2020.

[12] Q. Y. Yao, Y. D. Feng, P. Han, F. Yang, and G. Q. Song, "Hepatic microenvironment underlies fibrosis in chronic hepatitis B patients," *World Journal of Gastroenterology*, vol. 26, no. 27, pp. 3917–3928, 2020.

[13] Z. Zhipin, Q. Le, N. Runan et al., "The effect of three-leaf fragrant tea on the NLRP3/Caspase-1/GSDMD signaling pathway in CCl4-induced liver fibrosis rats," *Chinese Medicine Pharmacology and Clinical*, vol. 37, no. 4, pp. 96–101, 2021.

[14] G. Lijie, Y. Sun, and Z. Shaohua, "Effects of oxymatrine on serum inflammatory cytokine levels and liver fibrosis indicators in patients with chronic hepatitis B," *Shandong Medicine*, vol. 61, no. 17, pp. 65–67, 2021.

Hindawi
Computational and Mathematical Methods in Medicine
Volume 2023, Article ID 9817359, 1 page
https://doi.org/10.1155/2023/9817359

Retraction

Retracted: Comparison of the Effects of Laparoscopic Surgery and Traditional Open Surgery on Stone Clearance, Laboratory Indexes and Life Quality in Patients with Renal Calculi

Computational and Mathematical Methods in Medicine

Received 12 December 2023; Accepted 12 December 2023; Published 13 December 2023

This article has been retracted by Hindawi, as publisher, following an investigation undertaken by the publisher [1]. This investigation has uncovered evidence of systematic manipulation of the publication and peer-review process. We cannot, therefore, vouch for the reliability or integrity of this article.

Please note that this notice is intended solely to alert readers that the peer-review process of this article has been compromised.

Wiley and Hindawi regret that the usual quality checks did not identify these issues before publication and have since put additional measures in place to safeguard research integrity.

We wish to credit our Research Integrity and Research Publishing teams and anonymous and named external researchers and research integrity experts for contributing to this investigation.

The corresponding author, as the representative of all authors, has been given the opportunity to register their agreement or disagreement to this retraction. We have kept a record of any response received.

References

[1] Q. Ai, D. Tang, Y. Li, Y. Huang, and J. Yang, "Comparison of the Effects of Laparoscopic Surgery and Traditional Open Surgery on Stone Clearance, Laboratory Indexes and Life Quality in Patients with Renal Calculi," *Computational and Mathematical Methods in Medicine*, vol. 2022, Article ID 8211389, 9 pages, 2022.

Hindawi
Computational and Mathematical Methods in Medicine
Volume 2022, Article ID 8211389, 9 pages
https://doi.org/10.1155/2022/8211389

Research Article

Comparison of the Effects of Laparoscopic Surgery and Traditional Open Surgery on Stone Clearance, Laboratory Indexes and Life Quality in Patients with Renal Calculi

Qian Ai,[1] Dong Tang,[1] Yongfa Li,[1] Yingjie Huang,[2] and Junxian Yang [1]

[1]*Department of Urology, Wuhan Puren Hospital, No. 1 Benxi street, Qingshan District, Wuhan City, Hubei Province 430081, China*
[2]*Tianyou Hospital Affiliated to Wuhan University of Science and Technology, 430064, China*

Correspondence should be addressed to Junxian Yang; 1533210862@xzyz.edu.cn

Received 29 July 2022; Revised 11 August 2022; Accepted 15 September 2022; Published 29 September 2022

Academic Editor: Min Tang

Objective. A case-control study was conducted to determine the effectiveness of laparoscopic surgery and traditional open surgery on stone clearance, laboratory indexes, and life quality in patients with renal calculi. *Methods*. During March 2017 to March 2022, 272 patients with complex renal calculi (CRC) cured in our hospital were assigned into control group ($n = 136$) and research group ($n = 136$) arbitrarily. The former accepted traditional open surgery, while the latter accepted laparoscopic surgery. The operation time, intraoperative blood loss, hospital stay, and time of getting out of bed were compared. The degree of postoperative incision pain was assessed by visual analogue scale (VAS). The life quality was assessed by the Comprehensive Assessment Questionnaire-74 (GQOL-74). The indexes of renal function and urine metabolism were measured. Then, the postoperative stone clearance rate and complications were calculated. *Results*. Operation time, blood loss intraoperatively, time out of bed, and hospitalization were all remarkably reduced in the research group, and the difference was statistically significant ($P < 0.05$). The complete stone clearance rates in study and control cohorts were 75.73% and 63.24%, respectively. The VAS scores were lessened after the operation. Compared with the two groups, the VAS scores of the research group were remarkably lower at 1 to 2 weeks and 1 and 3 months after the operation, and the difference was statistically significant ($P < 0.05$). One week after operation, the levels of β 2-microglobulin (β 2-MG), N-acetyl-β-glucosaminidase (NAG), and renal injury molecule-1 (kidney injury molecule-1, Kim-1) in the research group were remarkably lower. The levels of urinary β 2-MG, NAG, and KIM-1 in the research group were remarkably lower, and the difference was statistically significant ($P < 0.05$). One week after operation, the levels of urinary oxalic acid, uric acid, and urinary calcium lessened averagely. The levels of urinary oxalic acid, uric acid, and urinary calcium in the research group were lower, and the difference was statistically significant ($P < 0.05$). The quality-of-life scores were compared. One week after the operation, the scores of physical function, psychological function, social function, and material function were all augmented, and the difference was statistically significant ($P < 0.05$). The incidence of complications was 9.56% and 2.21%, respectively. The incidence of complications in the research group was lower, and the difference was statistically significant ($P < 0.05$). *Conclusion*. Laparoscopic surgery is successful when treating CRC, which is superior to invasive surgery in postoperative complications, stone clearance rate, improvement of postoperative renal function, and life quality. It is one of the ideal treatment methods for CRC. However, the role of open surgery when treating CRC cannot be ignored. This needs to be further confirmed by large samples of randomized controlled trials.

1. Introduction

Urinary calculi are a kind of global disease, which is also one of the most common urological diseases in China. In 1983, it had risen to 86%, and its new incidence was still rising in recent years [1, 2].

Among the main causes of renal stone disease is the abnormal accumulation of crystal substances such as uric

acid and oxalic acid in the kidney of the patient. When the accumulation of kidney stones is small, patients can expel them from the body by drinking a lot of water. However, patients are usually unable to detect them effectively in the early stage of the disease. They often wait until the accumulation of kidney stones is too large, and the patients feel obviously uncomfortable [3, 4]. The main incidence group of kidney stone is young and middle-aged male [5]. However, the incidence of kidney stone in male group is much higher than that in female group [6, 7]. For this kind of patients, the stones in the body are mainly removed by operation, while the patients with complex kidney stones are mostly treated by open surgery.

In recent 30 years, with the clinical application of extracorporeal shock wave lithotripsy (ESWL) and percutaneous nephrolithotripsy (PCNL), great changes have taken place when treating renal calculi. Surgery has been remarkably reduced. In spite of this, complex renal stones remain a difficult challenge. Some literature has reported in the world have confirmed that these minimally invasive techniques can still cause varying degrees of renal function damage and have a very high stone residual rate [8]. Surgical treatment is still needed for those cases whose ESWL treatment fails but PCNL and ureteroscopy are not suitable for treatment [9]. Based on the above reality, many scholars have been trying to use laparoscopy to treat upper urinary tract calculi to replace the traditional open surgery to achieve a safe, effective, less pain, and rapid recovery of minimally invasive purpose. Minimally invasive decompressive surgical techniques have excellent results in preserving renal function in management of EPN. The presence of risk factors may not always be associated with high mortality if the patients are treated aggressively in the initial phase of management with minimally invasive techniques. Extracorporeal shock wave is a procedure to break up stones inside the urinary tract, bile ducts, or pancreatic duct with a series of shock waves generated by a machine. The shock waves enter the body and are targeted using an X-ray. Surgery has become the preferred treatment modality for patients with large renal calculi. The technique provides excellent stone clearance, but complication rates are higher than those of minimally invasive techniques, such as ureteroscopy and shock wave lithotripsy. Surgery is still needed for those cases whose ESWL treatment fails, but PCNL and ureteroscopy are not suitable for treatment. Since the 1990s, many scholars at home and abroad began to try to use laparoscopy to treat CRC to replace the traditional open surgery to achieve safe, effective, less pain, and rapid recovery of minimally invasive.

At present, laparoscopic surgery is often used in the clinical treatment of CRC. Although traditional open surgery is less and less, its therapeutic value cannot be ignored. There is no conclusion as to whether this kind of patients should choose traditional open surgery or laparoscopic surgery. At present, the research on the treatment of complex stones by traditional open surgery and laparoscopic surgery mainly would focus on the removal of renal stones and postoperative complications, while neglecting the comparison of patients' life quality. This study was conducted to determine the effectiveness of laparoscopic surgery and traditional open surgery on stone clearance, laboratory indexes, and life quality in patients with renal calculi.

2. Patients and Methods

2.1. General Information. During March 2017 to March 2022, 272 patients with CRC cured in our hospital were arbitrarily assigned into control group ($n = 136$) and research group ($n = 136$). The former accepted traditional open surgery, while the latter accepted laparoscopic surgery. The control group consisted of patients with ages ranging from 21 to 69, with an average age of 45.83 ± 4.23 years. The control cohort included 73 men and 63 women, and the course of disease ranged from 6 months to 13 years (mean 6.43 ± 1.42) years. Stone distribution was that left 70 cases and right 66 cases. Stone diameter was 2.79 ± 0.61 cm. Stone types were staghorn in 44 cases, complete cast in 40 cases, and incomplete cast in 52 cases. Patients in the research group ranged in age from 27 to 70 years old with an average age of 46.21 ± 4.46. There were 75 men and 61 women, and the course of disease ranged from 7 months to 12 years with an average of (6.32 ± 1.19) years. 67 stones were located on the left side, and 69 stones were located on the right side. The stone diameter is $(2.81 \pm 0.63$ cm). 47 cases were staghorn stones, 39 cases were completely calcified stones, and 50 cases were incompletely calcified stones. General patient data did not show any statistical significance ($P > 0.05$). This study was permitted by the Medical Ethics Council of our hospital, and all patients signed the informed consent form for the trial.

Diagnostic criteria of CRC: All the selected cases were diagnosed as CRC by B-ultrasound, CT, intravenous urography, and hematuria routine examination. The specific diagnostic criteria referred to the guidelines to diagnose and treat urinary calculi [10].

Selection criteria are as follows: (1) all the patients were diagnosed with CRC; (2) there were no cognitive, language, or intellectual impairments, and the patients' basic reading and writing skills were intact, aged ≥18 years old; (3) the clinical data, medical history, and examination records of the patients were perfect; (4) the patients agreed to receive continuous postoperative follow-up and be able to accept and answer telephone follow-up; and (5) in accordance with the indication of operation and anesthesia. Anesthesia indications were absence of lumbar disease and systemic infection. Surgical indications are as follows: stone diameter ≥1.0 cm; stone diameter less than 1 cm, but accompanied by obvious obstruction, hydronephrosis, renal insufficiency, infection caused by stone, and could not be controlled by drugs; and after more than 3 months of conservative treatment, the effect was still not obvious. The above indicators only needed to meet one item to determine the existence of surgical indications.

Exclusion criteria are as follows: (1) patients with serious heart, liver, renal insufficiency, and malignant tumors; (2) patients with coagulation dysfunction; (3) those who refused to participate in the test; (4) patients with renal dysfunction and severe hydronephrosis, urethral or ureteral

malformations, and organic urinary tract obstruction; (5) patients with basic diseases affecting the operation; (6) patients with mental diseases; and (7) those who were treated with anticoagulants for a long time.

2.2. Treatment Methods

2.2.1. Preoperative Preparation. The day before operation, patients were instructed to undergo general examination, including blood biochemistry, blood lipids, blood glucose, blood coagulation, electrocardiogram, chest plain film, and blood type. Patients over 60 years old were examined by preoperative pulmonary function and cardiac color ultrasound, those with respiratory diseases were examined before operation, and those with cardiovascular diseases were examined by cardiac color ultrasound. Before operation, urinary tract infection was controlled by antibiotics. The day before the operation, the patients were told to eat a small residue diet and given a slow bay agent to empty the intestines. Gastric tube was placed before operation, and gastrointestinal decompression was performed. Catheter was placed to avoid bladder expansion.

2.2.2. Treatment Methods. The control group received traditional invasive surgery. The open lithotripsy was divided into intrarenal sinus pyelolithotomy and pyelolithotomy. The intrarenal sinus pyelolithotomy and surgical incision were made between the 11 intercostals to dissociate the kidney and dissociate along the ureter to the renal hilum until the renal pelvis was found. The research group was treated with laparoscopic nephrolithotomy, including laparoscopic pyelolithotomy, laparoscopic pyelolithotomy, laparoscopic pyelolithotomy, and laparoscopic partial nephrectomy.

(1) Laparoscopic pyelolithotomy or intrarenal sinus pyelolithotomy. Under general anesthesia, all patients were positioned on their contralateral side with an indwelling catheter and lying 90 degrees. To establish pneumoperitoneum, trocar was performed at the umbilical margin or the lateral margin of the rectus abdominis muscle, the anterior line of the umbilical axilla, and the costal edge of the middle line of the clavicle, respectively. The lateral peritoneum and perirenal fascia were opened. During this procedure, the inferior pole of the kidney was exposed, and the renal pelvis and even the renal sinus were separated. After the location of the stone was found, the renal pelvis was longitudinally cut or extended to the intrarenal sinus. The renal pelvis incision was enlarged, and the stone was removed. The renal pelvis and calyx were washed out, and no stone was flushed out. The 4-0 absorbable line of Dmur J tube was placed to suture the renal pelvis incision (the intrarenal pelvis was not sutured), and the perirenal drainage tube was placed to end the operation

(2) Laparoscopic pyelolithoplasty and lithotomy. The operation was performed under general anesthesia, and routine indwelling catheterization was performed before operation. The patient took 90° recumbent position on the healthy side and established pneumoperitoneum. 10-mm and 5-mm cannula needles of diameter were put at the umbilical margin, the anterior axillary line, and the midline of the clavicle. According to the need of the operation, one subcostal incision of the posterior axillary line was added, and the 5-mm trocar was placed. The narrow segments of the UPJ were resected after the kidney, and renal pelvis and ureter were exposed. The ureter was longitudinally opened to 0.5 cm-0.8 cm. The dilated renal pelvis was trimmed, and the calculi in the renal pelvis and calyceal were removed.

The renal pelvis and ureteral incision were closed end-to-end with interrupted sutures of 5-0 or 4-0 absorbable thread. The incision was then restored, and the double J tube with guidewire was put into the peritoneal cavity, the ureter was inserted downwards, and the guidewire is removed. The upper end of the double J-tube was fed into the renal pelvis, and the anterior incision was then interrupted with sutures. The modified renal pelvis incision was sutured continuously with 5-0 or 4-0 absorbable thread, the wound was washed, the perirenal drainage tube was placed, and the operation was ended.

(3) Laparoscopic partial nephrectomy and lithotomy. The patient received general anesthesia, routine indwelling catheterization before operation, and 90-degree healthy lateral position. 10-mm and 5-mm cannulas of diameter were put at the umbilical margin, the anterior axillary line, and the midline of the clavicle. If necessary, the 5 mm cannula was used to expose the kidney. In addition, 1 cm-diameter cannula with a diameter of 1 cm was worn at the posterior lower part of the endoscopic cannula to place a noninvasive intestinal forceps that controlled the renal pedicle vessels. During the operation, the lateral peritoneum and perirenal fascia were opened. The renal pedicle and the middle and inferior pole of the kidney were dissociated and exposed to fully control the renal pedicle and facilitate the removal of the inferior pole of the kidney and the treatment of the wound. The specimen bag and suture equipment were prepared. The wound was sutured with 2-0 absorbable line\ "8\" or continuous suture to stop bleeding. When the blocking time of renal pedicle reached 25 min, the renal pedicle forceps were opened about 1 min~2 min (in 2 cases of renal ischemia 25 min, only the forceps were opened once, and only the forceps were opened without removing the renal pedicle clamp), and then reclamped to control the renal pedicle to continue to deal with the wound. After the wound was closed, an attempt was made to open the renal infarct noninvasive bowel clamp. If there was bleeding, suture the bleeding site with the word "8\" to stop the bleeding. If the operative field was not clear, the renal pedicle could be reclamped to control the renal pedicle and then suture to stop the bleeding. When there was no bleeding in the incision, the renal pedicle noninvasive intestinal clamp was removed. The operation was finished by releasing the skin tube around the kidney.

2.3. Observation Index

2.3.1. Operation Related Index. In addition to intraoperative blood loss, operating time, postoperative hospital stays, time spent out of bed, and stone clearance rate, we calculated postoperative complications. Amount of blood lost intraoperatively is the amount of blood lost during the surgery.

Table 1: The surgical indexes between the two groups $[\bar{x} \pm s]$.

Grouping	N	Operation time (min)	Intraoperative bleeding volume (mL)	Time to get out of bed (d)	Hospitalization time (d)
Control group	136	153.38 ± 12.45	253.18 ± 14.22	3.25 ± 0.64	12.46 ± 2.63
Research group	136	121.42 ± 10.53	97.25 ± 10.08	1.67 ± 0.28	7.52 ± 1.17
t value		22.858	104.327	26.376	20.104
P value		<0.05	<0.05	<0.05	<0.05

Stone clearance rate = (the number of cases meeting the stone clearance criteria/the total number of cases in this group) × 100%. Approximately one month after their operations, each patient was followed up. The number of complications like urinary fistula, incision infection, bleeding, ureteral injury, renal function injury, and other complications were statistically compared. The incidence of complications = (sum of all kinds of complications/total number of cases in this group) × 100%. The operation time was the difference between patients going in and out of the operating room. Postoperative hospital stay referred to the time from the completion of the operation to the discharge of the patient. The time to get out of bed referred to the time it takes from the end of the operation to the first time to get out of bed. The stone clearance rate was recorded and analyzed when the patient was discharged [11].

2.3.2. VAS Scoring. VAS score was employed to measure the pain degree before and after operation, and the full score was 10. The specific evaluation criteria were as follows: 0: no pain; <3: mild pain, bearable; 4-6: pain and affect sleep; and 7-10: strong pain, unbearable, and affecting life. The patients were evaluated before treatment, 1 to 2 weeks, and 1 and 3 months after operation.

2.3.3. Renal Function and Urinary Metabolic Index. The second 4-7 mL of morning urine was obtained before and 1 week after operation. The levels of β 2-MG, NAG, and Kim-1 were analyzed by enzyme-linked immunosorbent assay (Elisa) on Beckman BS-460. Urinary metabolic indexes, including urinary oxalic acid, uric acid, and urinary calcium, were measured by automatic analyzer.

2.3.4. Life Quality Score. The life quality of the patients was evaluated with the life technician GQOL-74 [12] before and 1 week after operation. The scale involved four aspects, including physical, psychological, social, and material function.

2.4. Statistical Analysis. IBMSPSS24.0 software was applied for statistical analysis. The measurement data were expressed by mean ± standard deviation. The counting data were expressed by frequency or rate. *T*-test was used when measurement data obey normal distribution, and rank sum test was used when it did not obey normal distribution. $\chi 2$ test was used to compare the classified counting data. Repeated measurement data were analyzed by repeated measurement analysis of variance. The main effect test results were used when there was no interaction, and simple effect analysis was carried out when there was interaction. $P <$ 0.05 indicated that the difference between groups is statistically significant.

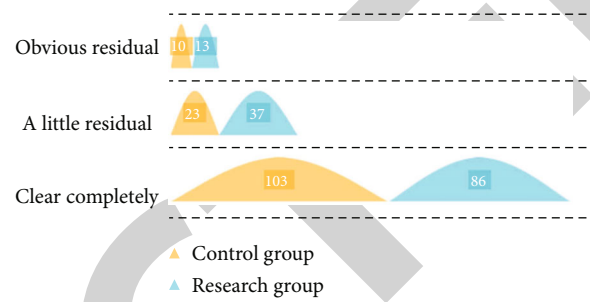

Figure 1: Stone clearance rate between the two groups.

3. Results

3.1. Surgical Indexes. Operation time, blood loss intraoperatively, time out of bed, and hospitalization are all remarkably reduced in the research group, and the difference is statistically significant ($P < 0.05$), as indicated in Table 1.

3.2. Stone Clearance Rate. In the comparison of stone clearance rate, 103 cases were completely removed, 23 cases were slightly residual, and 10 cases were obvious residual. The complete stone clearance rate was 75.73% in the research group. While 86 cases, 37 cases and 13 cases in the control group were completely removed. The complete stone clearance rate was 63.24%. Compared between groups, the complete stone clearance rate in the research group is higher, and the difference is statistically significant ($P < 0.05$), as indicated in Figure 1.

3.3. VAS Score Comparison. Repeated measures analysis of variance found that there exhibited a statistically remarkable difference in the VAS score ($P < 0.05$). There exhibited remarkable difference among different time points ($P < 0.05$). There exhibited remarkable difference in × time interaction, and the difference was statistically significant ($P < 0.05$). After treatment, the VAS scores were lessened. VAS scores of the research group are remarkably lower at 1 to 2 weeks and 1 and 3 months after the operation, and the difference is statistically significant ($P < 0.05$), as indicated in Table 2.

3.4. The Renal Function Indexes. One week after the operation, the levels of β 2-MG, NAG, and KIM-1 were lessened. Compared with the two groups, the levels of which in the urine of the research group are remarkably lower one week

Table 2: The postoperative VAS scores between the two groups [$\bar{x}\pm s$, points].

Grouping	N	Before treatment	One week after operation	2 weeks after operation	One month after operation	Three months after operation
Control group	136	6.42 ± 2.17	4.72 ± 1.91	3.14 ± 0.42	1.08 ± 0.14	0.92 ± 0.14
Research group	136	6.33 ± 2.06	3.42 ± 1.23	1.83 ± 0.87	0.89 ± 0.03	0.33 ± 0.06
Intergroup (F/P)				39.662/0.000		
Time (F/P)				51.846/0.000		
Intergroup × time (F/P)				60.091/0.000		

Table 3: The urinary β 2-MG, NAG, and KIM-1 levels between the two groups after operation [$\bar{x} \pm s$].

Grouping	N	β 2-MG (mg/L)		NAG (IU/L)		KIM-1 (ng)	
		Before operation	One week after operation	Before operation	One week after operation	Before operation	One week after operation
Control group	136	0.45 ± 0.18	0.36 ± 0.07[a]	9.06 ± 1.83	7.28 ± 1.63[a]	91.24 ± 9.53	84.83 ± 8.27[a]
Research group	136	0.48 ± 0.15	0.21 ± 0.05[b]	9.22 ± 1.76	5.84 ± 1.66[b]	90.09 ± 9.41	77.63 ± 7.84[b]
t value		1.493	20.335	0.735	7.218	1.001	7.368
P value		>0.05	<0.05	>0.05	<0.05	>0.05	<0.05

Note: The comparison between the control group before and after operation, [a]$P < 0.05$. The comparison of preoperative and postoperative in the research group, [b]$P < 0.05$.

Table 4: The urine metabolism between the two groups [$\bar{x} \pm s$].

Grouping	N	Urinary oxalic acid (mmol/L)		Uric acid (mmol/L)		Urinary calcium (mmol/L)	
		Before operation	One week after operation	Before operation	One week after operation	Before operation	One week after operation
Control group	136	5.82 ± 0.38	3.62 ± 0.23	0.71 ± 0.23	0.49 ± 0.01	6.36 ± 1.83	4.19 ± 0.83
Research group	136	5.77 ± 0.35	2.68 ± 0.17	0.78 ± 0.29	0.27 ± 0.03	6.73 ± 1.65	3.06 ± 0.45
t value		0.129	38.328	2.206	81.132	1.751	13.958
P value		>0.05	<0.05	>0.05	<0.05	>0.05	<0.05

Note: The comparison between the control group before and after operation, [a]$P < 0.05$. The comparison of preoperative and postoperative in the research group, [b]$P < 0.05$.

after the operation, and the difference is statistically significant ($P < 0.05$), as indicated in Table 3.

3.5. The Urine Metabolism. One week after operation, the levels of urinary oxalic acid, uric acid, and urinary calcium lessened averagely. Compared with the control group, the levels of urinary oxalic acid, uric acid, and calcium in the research group are remarkably lower, and the difference is statistically significant ($P < 0.05$), as indicated in Table 4.

3.6. The Quality-of-Life Scores between the Two Groups. One week after the operation, the physical, psychological, function, and material function scores were augmented. Compared with the two groups, the physical, psychological, social, and material function scores of the research group are higher, and the difference is statistically significant ($P < 0.05$), as indicated in Table 5.

3.7. The Incidence of Postoperative Complications. In the control group, there were 5 cases of urinary fistula, 1 case of incision infection, 3 cases of bleeding, 1 case of ureteral injury, and 3 cases of renal function injury. The incidence of complications was 9.56%. In the research group, urinary fistula, incision infection, and renal function injury occurred in 1 case, and the incidence rate of postoperative complications was 2.21%. The incidence of complications in the research group is lower, and the difference is statistically significant ($P < 0.05$), as indicated in Figure 2.

4. Discussion

The treatment of complex kidney stones is still a difficult problem at present. PCNL is considered to be the best choice to treat these stones [13]. However, not all cases are suitable for PCNL treatment [14, 15]. At the same time, complications such as massive hemorrhage, severe injury, and intrarenal infection after PCNL treatment still limit the application of PCNL [16]. Nowadays, the pathogenesis of renal calculi is not fully understood, which may be relevant to heredity, metabolism, infection, environment, diet, anatomy, and drugs. Among them, complex renal stones refer to stones whose diameter is longer than 2.5 cm, staghorn calculi, multiple stones, and difficult to remove stones due to abnormal renal function or anatomy [16–18]. Because this operation is required high experience and skills of

Table 5: The quality-of-life scores between the two groups [$\overline{x}\pm s$, points].

Grouping	N	Somatic function		Psychological function		Social function		Material function	
		Before operation	One week after operation	Before operation	One week after operation	Before operation	One week after operation	Before operation	One week after operation
Control group	136	51.89 ± 10.36	63.66 ± 10.45[a]	52.56 ± 12.48	65.23 ± 15.48[a]	63.57 ± 8.15	79.83 ± 3.56[a]	57.83 ± 8.46	81.37 ± 18.79[a]
Research group	136	52.34 ± 11.37	78.89 ± 16.23[b]	52.36 ± 12.44	79.35 ± 15.41[b]	61.93 ± 8.43	71.03 ± 12.15[b]	58.61 ± 7.46	66.84 ± 4.83[b]
t value		0.341	9.201	0.132	7.539	1.631	7.176	0.806	8.734
P value		>0.05	<0.05	>0.05	<0.05	>0.05	<0.05	>0.05	<0.05

Note: The comparison between the control group before and after operation, [a]$P < 0.05$. The comparison of preoperative and postoperative in the research group, [b]$P < 0.05$.

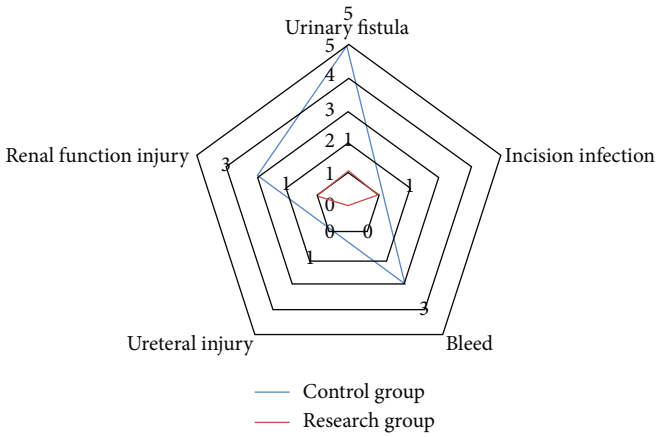

Figure 2: Comparison of postoperative complications between the two groups.

laparoscopic surgery, many urologists prefer ESWL, PCNL, and traditional open surgery to treat CRC [19]. Laparoscopic surgery, however, is more readily apparent when compared with traditional open surgery in minimally invasive surgery.

We showed that laparoscopic surgery spent less time, less blood loss, and faster postoperative recovery than traditional open surgery, which fully confirmed the safety of laparoscopic surgery in this study. The application of laparoscopic surgery can also effectively reduce the postoperative stone residual rate and improve the stone clearance rate in patients with CRC, which can prove that the operation has a remarkable clinical efficacy and safety to treat CRC. In this study, the VAS scores of patients with laparoscopic surgery at 1 to 2 weeks and 1 and 3 months after operation were lower than those with traditional open surgery. It was mainly because laparoscopic surgery was a minimally invasive operation with small incision, less damage to normal tissue, and lower risk of various complications; the postoperative recovery was faster; and the pain symptoms of patients were milder. This study was conducted to determine the effectiveness of laparoscopic surgery and traditional open surgery on stone clearance, laboratory indexes, and life quality in patients with renal calculi.

The common clinical complex renal stones are staghorn calculi and intrapelvic cast stones [20]. For single branch staghorn calculi of extrarenal renal pelvis or complete intrapelvic cast stones, laparoscopic pyelolithotomy can be performed successfully. However, for intrarenal pyelolithiasis, staghorn calculi with multiple branches growing into different calyceal and multiple calyceal stones with secondary infundibulum stenosis or calyceal diverticulum, it is much more complicated, and laparoscopic pyelolithotomy alone may not be successful. Currently, intrarenal sinus peotomy or partial renal parenchyma incision becomes necessary [21, 22].

It was very important for the smooth removal of staghorn stones, because this approach can make it easier for us to separate to the funnel part. For staghorn stones with multiple branches, only the shorter branch of the lower calyx was delivered out of the renal pelvis, and the longer branch of the upper calyx was successfully removed. The experience of Rhudd AR is worth using for reference. In our study, most laparoscopic pyelolithotomy was performed through laparoscopic pyelolithotomy (including intrarenal sinus pyelolithotomy). For laparoscopic pyelolithotomy, good exposure is the key to successful operation, while transabdominal approach is easier to expose the kidney and separate renal pelvis 137, so transabdominal approach is used in our study. During the operation, the middle and inferior pole of the kidney should be freed as much as possible, and the inferior pole of the kidney should be raised or gauze padded into the inferior pole of the kidney to expose the kidney. Blunt or sharp separation can be chosen when separating the renal pelvis, but it must be noted that the action of separation should be patient and skillful. Sometimes, due to the serious adhesion of the surrounding tissue, separation will be very difficult and easy to bleed, which requires more patience and meticulous, and the selection of electrocoagulation hook separation will help to separate, especially when separating the renal pelvis in the renal sinus. According to the experience of Radfar MH et al. electrocoagulation hook was selected to separate. The direction of separation was more precise and accurate, and small vascular bleeding affecting the visual field of operation can also be found immediately. Moreover, electrocoagulation can be used to stop bleeding [23]. When cutting and removing stones, the incision should be above the stones, and the incision should be large enough to facilitate the removal of stones, especially upward as far as possible into the renal sinus. However, it should not go beyond the junction of the renal pelvis and ureter so that the ureter was not torn during subsequent examination of the calyces and the removal of the stone. Loosening and removing stones was also a very patient and skillful task, especially for more branched staghorn stones. YanQ et al. introduced that when loosening and peeling off stones [24], we should start from the right side of the stones [24].

β 2-MG can moderate small molecule globulin, can reflect the degree of glomerular injury, and has high specificity and sensitivity [25]. KIM-1 was highly expressed in hypoxic renal tissue, and its level was relevant with the degree of renal tubular injury positively [26]. NAG is a marker of lysosomes, which is very abundant in renal tubular epithelial cells. When the glomerular filtration membrane is damaged, NAG can enter the urine, causing the level of urinary NAG to increase. This research showed that compared with traditional surgical treatment, laparoscopic treatment could reduce the damage of renal tissue in patients with renal calculi to some extent and protect renal function. The analysis of the reason was that laparoscopic surgery can decide the specific location, size, shape, and number of stones on the premise of avoiding great trauma caused by traditional laparotomy and remove the stone thoroughly and effectively. At the same time, ultrasonic knife resection of adhesive tissue can effectively stop bleeding and further reduce the amount of bleeding during operation. The laparoscopy has three-dimensional visual effect, which can enlarge the image. For larger stones or incarcerated stones, we can choose the clamp method to remove the stones according to the actual situation. It is beneficial to the thorough removal of stones and reduce the occurrence of residual stones. During the

period of renal stone lithotripsy, in order to ensure that the surgical field is clearly visible, a large amount of water needs to be irrigated through the working channel. However, the water perfusion pressure is higher than the physiological pressure in the renal pelvis, and it is simple to cause urinary reflux in the renal pelvis and damage renal tissue.

Laparoscopic surgery is difficult to operate, which requires higher hardware equipment. In addition, the cost of hospitalization is higher than that of open surgery, which limits the wide development of laparoscopic surgery. After the removal of urinary calculi, the urinary tract was unobstructed, hydronephrosis was gradually relieved, and the life quality and anxiety were improved. This study was also indicated that laparoscopic surgery was better than traditional surgery in these three aspects. The reason may be that long-term surgical posture has an adverse effect on the comfort of patients, which may affect the late recovery of patients [27]. In addition, laparoscopic surgery has fewer complications than traditional surgery, which is also one of the reasons for the high life quality of patients. Minimally invasive decompression surgery techniques have been shown to be effective in preserving renal function in EPN. The presence of risk factors is not necessarily associated with high mortality if the patient is treated aggressively with minimally invasive techniques in the initial stages of management. Extracorporeal shock wave is a procedure in which a series of shock waves generated by a machine is used to break up the urinary tract. The shock waves enter the body and are located using X-rays. The procedure has become the treatment of choice for patients with large kidney stones. The technique provides good stone removal but has a higher complication rate than minimally invasive techniques such as ureteroscopy and shock wave lithotripsy. This study still has some shortcomings. Firstly, the quality of this study is limited due to the small sample size we included in the study. Secondly, this research is a single-center study, and our findings are subject to some degree of bias. Therefore, our results may differ from those of large-scale multicenter studies from other academic institutes. This research is still clinically significant, and further in-depth investigations will be carried out in the future.

To sum up, laparoscopic surgery has a higher application value in patients with renal stone diseases, with remarkable advantages such as less trauma, high safety, high stone clearance rate, and protection of renal function, which can remarkably enhance the postoperative life quality of patients.

Data Availability

The datasets used and analyzed during the current study are available from the corresponding author upon reasonable request.

Conflicts of Interest

The authors declare that they have no conflicts of interest.

References

[1] G. Abedi and M. Monga, "Flexible ureteroscopy for treatment of upper urinary tract calculus," *Journal of Endourology*, vol. 35, no. S2, pp. S-56–S-61, 2021.

[2] A. Kanashiro and O. Angerri, "Urinary pH relevance on urolithiasis management," *Archivos Españoles de Urología*, vol. 74, no. 1, pp. 102–111, 2021.

[3] C. Thongprayoon, A. E. Krambeck, and A. D. Rule, "Determining the true burden of kidney stone disease," *Nature Reviews. Nephrology*, vol. 16, no. 12, pp. 736–746, 2020.

[4] A. Sharma, I. Kumar, K. Verma, B. Thakur, and N. Thakur, "Preliminary phytochemical screening of Persicaria sagittata: future prospective for kidney stone," *Research Journal of Pharmacy and Technology*, vol. 14, no. 8, pp. 4367–4370, 2021.

[5] P. Peerapen and V. Thongboonkerd, "Kidney stone proteomics: an update and perspectives," *Expert Review of Proteomics*, vol. 18, no. 7, pp. 557–569, 2021.

[6] C. Haritha, D. Ramya, R. Naveen, S. V. Prasanna, and P. Salomi, "A comprehensive review on bergenia ligulata (paashanbheda) and its role in the treatment of kidney stone formation," *International Journal of Research in Ayurveda and Pharmacy*, vol. 12, no. 4, pp. 94–99, 2021.

[7] M. B. Moor, N. A. Dhayat, S. Schietzel, M. Grössl, B. Vogt, and D. G. Fuster, "Urinary tetrahydroaldosterone is associated with circulating FGF23 in kidney stone formers," *Urolithiasis*, vol. 50, no. 3, pp. 333–340, 2022.

[8] M. H. Radfar, M. Dadpour, N. Simforoosh et al., "Laparoscopic pyelolithotomy in patients with previous ipsilateral renal stone surgery," *Urologia*, vol. 88, no. 1, pp. 41–45, 2021.

[9] R. Molina Escudero, J. A. Herranz Yagüe, L. Crespo Martínez, and B. Á. Páez, "Laparoscopic management of horseshoe kidney stones," *Archivos Españoles de Urología*, vol. 73, no. 9, pp. 856–859, 2020.

[10] C. Xingfa, "Interpretation of guidelines for diagnosis and treatment of urinary calculi," *Journal of Modern Urology*, vol. 15, no. 6, pp. 408–410, 2010.

[11] P. Hong, Z. Li, D. Zhu et al., "A simple modification for the usage of flexible cystoscope in modified laparoscopic pyeloplasty for ureteropelvic junction obstruction with renal calculi: A flexible guiding tube," *Urologia Internationalis*, vol. 102, no. 3, pp. 262–268, 2019.

[12] P. V. Glybochko, Y. G. Alyaev, A. M. Pshikhachev et al., "The potential of endovideosurgical technologies for simultaneous ipsilateral presentation of a kidney tumor and kidney stone," *Urologiia*, vol. 3, pp. 70–75, 2016.

[13] W. Xuebin, M. Qingli, L. Boshi, W. Delong, and J. Bin, "Analysis of the clinical effect and effect on renal function of percutaneous nephroscopic EMS lithotripsy in patients with CRC," *Modern Drug Application in China*, vol. 15, no. 18, pp. 87–89, 2021.

[14] F. Weihong, Z. Bin, and X. Xiaorong, "Clinical analysis of percutaneous nephrolithotripsy combined with anterograde and retrograde ureteroscopy when treating CRC," *Massage and Rehabilitation Medicine*, vol. 12, no. 18, pp. 52–54, 2021.

[15] Y. Liu, W. Zhu, and G. Zeng, "Percutaneous nephrolithotomy with suction: is this the future?," *Current Opinion in Urology*, vol. 31, no. 2, pp. 95–101, 2021.

[16] M. Ç. Çakici, F. Keser, R. G. Atis, and A. Yildirim, "Mini-percutaneous nephrolithotomy in a child with multiple urogenital

Hindawi
Computational and Mathematical Methods in Medicine
Volume 2023, Article ID 9878617, 1 page
https://doi.org/10.1155/2023/9878617

Retraction

Retracted: Study on the Clinical Value of Noninvasive Prenatal Testing in Screening the Chromosomal Abnormalities of the Fetus in the Elderly Pregnant Women

Computational and Mathematical Methods in Medicine

Received 5 December 2023; Accepted 5 December 2023; Published 6 December 2023

This article has been retracted by Hindawi, as publisher, following an investigation undertaken by the publisher [1]. This investigation has uncovered evidence of systematic manipulation of the publication and peer-review process. We cannot, therefore, vouch for the reliability or integrity of this article.

Please note that this notice is intended solely to alert readers that the peer-review process of this article has been compromised.

Wiley and Hindawi regret that the usual quality checks did not identify these issues before publication and have since put additional measures in place to safeguard research integrity.

We wish to credit our Research Integrity and Research Publishing teams and anonymous and named external researchers and research integrity experts for contributing to this investigation.

The corresponding author, as the representative of all authors, has been given the opportunity to register their agreement or disagreement to this retraction. We have kept a record of any response received.

References

[1] Z. Gu, M. Du, T. Xu, and C. Jin, "Study on the Clinical Value of Noninvasive Prenatal Testing in Screening the Chromosomal Abnormalities of the Fetus in the Elderly Pregnant Women," *Computational and Mathematical Methods in Medicine*, vol. 2022, Article ID 2977128, 7 pages, 2022.

Hindawi
Computational and Mathematical Methods in Medicine
Volume 2022, Article ID 2977128, 7 pages
https://doi.org/10.1155/2022/2977128

Research Article

Study on the Clinical Value of Noninvasive Prenatal Testing in Screening the Chromosomal Abnormalities of the Fetus in the Elderly Pregnant Women

Zhiping Gu, Mengmeng Du, Tianhui Xu, and Chunyan Jin

Department of Medical Genetics and Prenatal Diagnosis, Taizhou People's Hospital, Taizhou, 225300 Jiangsu, China

Correspondence should be addressed to Chunyan Jin; gta5857@126.com

Received 16 August 2022; Revised 27 August 2022; Accepted 30 August 2022; Published 28 September 2022

Academic Editor: Min Tang

Introduction. To explore the clinical value of noninvasive prenatal testing (NIPT) in screening the chromosomal abnormalities of the fetus in the elderly pregnant women. *Materials and Methods*. Between January 2020 and December 2021, 1949 elderly pregnant women underwent NIPT in our hospital. At the same time, 236 elderly pregnant women received invasive prenatal diagnosis, and the pregnancy outcomes were followed-up. *Results*. When NIPT was used for prenatal screening of fetal chromosomal aneuploidy, its diagnostic coincidence rate for trisomy 21 was the highest, with a coincidence rate of 90.00%, and the diagnostic coincidence rate for other chromosomal abnormalities was the lowest, only 22.22%. The sensitivity, specificity, positive predictive rate, and negative predictive rate for T21 by NIPT were 100%, 99.97%, 94.28%, and 100%; for T18 were 100%, 99.92%, 72.22%, and 100%, respectively; and for T13 were 100%, 99.95%, 50%, and 100%, respectively. Patients with high risks according to NIPT results further received invasive prenatal diagnosis, and 18 cases were excluded from the follow-up. For the remaining 1933 cases in the NIPT group, there was an incidence of 2.28% of adverse pregnancy outcomes. For the remaining 234 cases in the Amniocentesis group, there was an incidence of 1.28% of adverse pregnancy outcomes. There was no significant difference between the two groups ($P > 0.05$). The diagnostic rate of fetal chromosomal abnormalities in pregnant women under 40 years old was about 0.39-0.79%; however, the risk for people over 40 is relatively high at 1.32-4.44%. *Conclusion*. The noninvasive prenatal screening of fetal DNA in the second trimester of pregnancy for elderly pregnant women has high application value in the prediction of pregnancy outcome. The high risk of pregnancy can be determined by detecting trisomy 21, 18, and 13 syndromes, and the probability of adverse pregnancy outcome increases.

1. Introduction

With the continuous development and progress of society, great changes have taken place in people's ideas. The number of late marriage and late childbirth groups is increasing. In addition, the country has fully opened the second and third child policy, which has led to an increase in the number of elderly pregnant women in China, showing an upward trend [1]. The risk of pregnancy and delivery of older pregnant women is relatively high. The probability of adverse pregnancy outcomes is relatively high. Abortion, stillbirth, and fetal malformation account for a large proportion. For example, trisomy 21, 18, and 13 syndromes are common fetal chromosomal abnormalities. The fetus is prone to physical structure deformity or nerve damage after delivery, which has a great impact on the newborn family and economic burden [2]. Therefore, it is very necessary to do a good job in the screening of fetal malformations and chromosomal abnormalities in the second trimester of pregnancy for older pregnant women. It can accurately screen fetal malformations, which is of great significance for the prediction of adverse pregnancy [3]. At present, the gold standard to screen fetal chromosomal abnormalities in clinical practice is invasive prenatal diagnosis, that is, amniocentesis diagnosis [4]. However, this diagnostic method is traumatic, and will increase the probability of abortion in elderly pregnant women. At the same time, it has the risk of amniotic fluid infection. The diagnostic application has certain limitations

[5]. In recent years, many studies have shown [6–8] that there is a certain amount of free fetal DNA in the peripheral blood of pregnant women in the second trimester of pregnancy, so the noninvasive screening of fetal DNA in the second trimester of pregnancy was born. Noninvasive prenatal testing (NIPT) has been reported to have high sensitivity and specificity for detecting common chromosomal aneuploidies (trisomies 21, 18, and 13), with low false positive and false negative rates [9]. Moreover, clinical experiments have indicated that NIPT has a good detection effect in both high-risk and low-risk populations of serological screening, and the detection efficiency is much higher than that of serological screening [10]. In some cases, it can replace amniocentesis, and the detection rate and diagnostic coincidence rate of fetal chromosomal abnormalities are higher.

In this study, we investigated the clinical value of NIPT in screening the chromosomal abnormalities of the fetus in the elderly pregnant women.

2. Materials and Methods

2.1. General Clinical Data. A total of 1949 elderly pregnant women who received NIPT in our hospital from January 2020 to December 2021 were enrolled in this study. According to the informed consent and NIPT results, 236 elderly pregnant women directly received amniotic fluid prenatal diagnosis at the same time, and the pregnancy outcomes were followed-up. The expected age of the study subjects was between 35 and 50 years old, and the average age of pregnant women was 39.48 ± 3.83 years old. The gestational weeks of NIPT ranged from 12 to 28 weeks, with an average of 16.18 ± 1.05 weeks.

Inclusion criteria: (1) the elderly pregnant women refer to the pregnant women whose actual age is ≥35 at the expected delivery date; (2) all pregnant women included in the study were required to complete pregnancy outcome follow-up.

Exclusion criteria: (1) pregnant women with previous history of induced labor or delivery of fetus with abnormal chromosome, or pregnant women with history of unexplained abortion, stillbirth, abnormal fetus, and neonatal death; (2) pregnant women with definite chromosomal abnormalities or who have given birth to children with monogenic genetic diseases or genetic metabolic diseases; (3) pregnant women who have given birth to children with congenital heart disease, open spina bifida, anencephaly, and other abnormalities; (4) having a family genetic history or having a history of marriage between close relatives within three generations; (5) pregnant women who had suffered from severe infectious diseases in the early stage of pregnancy; (6) fetal ultrasound showed multiple soft index abnormalities; (7) gestational weeks <12 weeks or >22 weeks; (8) pregnant women with malignant tumors; (9) receiving allogeneic blood transfusion, transplantation surgery, allogeneic cell therapy, and so on within one year; (10) other conditions that the physician felt significantly affected the accuracy of the results.

2.2. Methods. For pregnant women who meet the inclusion and exclusion criteria, amniotic fluid prenatal diagnosis is recommended when the NIPT indicated the positive results of chromosomal abnormalities. According to the principle of statistics, the detection rate of fetal chromosomal aneuploidy between NIPT and amniocentesis groups was counted.

2.3. NIPT Detection. The pregnant women have signed informed consent before NIPT testing. 5 ml of maternal peripheral blood samples were selected and temporarily stored in a refrigerator at 4°C. Samples will be excluded if hemolyzed or stored for more than 8 hours before plasma separation. Blood specimens were processed as follows: centrifugation at 4°C, 1600 g for 10 min, and plasma was carefully collected and distributed into 2.0 ml Eppendorf tubes. The plasma was centrifuged again at 16000 g at 4°C for another 10 min. The upper layer of plasma was carefully divided into 2.0 ml new Eppendorf tubes, each containing approximately 600 ml of plasma, stored in a refrigerator at -80°C. Repeated freezing and thawing of plasma should be avoided before the experiment. DNA extraction, library construction, and sequencing were performed using Nucleic Acid Extraction Kit (BGI, Shenzhen, China) on BGIseq-500 sequencing platform (BGI). Fetal chromosome aneuploidies (T21, T18, and T13) detection kit (Combinatorial Probe-Anchor Synthesis Sequencing Method) (BGI) was used for library construction. Sequencing was performed using Universal Reaction Kit for Sequencing (Combinatorial Probe-Anchor Synthesis Sequencing Method) (BGI). Z-score set the range of -3 and 3 as the threshold to evaluate the risk of chromosomal aneuploidies. $Z = 3$ was considered as the cut-off value, and the sample was classified as high-risk of chromosomal abnormalities when $|Z| > 3$, Z between -3 and 3 represented the sample was classified as low risk [11].

2.4. Amniotic Fluid Puncture Test. The amniocentesis procedure was as follows: Pregnant women with indications should have B-ultrasound first to determine the placenta position and fetal condition, so as to avoid accidental injury to the placenta. If there is no B-mode ultrasound, palpation can be used to find the part of the floating fetal body with large cystic sex and easy to touch, and the placenta can also be avoided. After selecting the needle entry point, the skin was disinfected, disinfection towel was spread, local anesthesia was given, and the waist needle with the needle center was used to pierce the selected point vertically; when the needle passed through the abdominal wall and uterine wall, it was disinfected twice, and the needle core was removed. 2 ml of amniotic fluid was aspirated with a 2 ml syringe and discarded. This section of amniotic fluid may contain maternal cells. Then, 20 ml of amniotic fluid was aspirated with a 20 ml empty needle, which was placed in two disinfection tubes and capped. Take out the needle, cover with sterilized gauze, compress for 2-3 minutes, and the pregnant woman stayed in bed for 2 hours. The amniotic fluid was centrifuged for 5-10 minutes, the above clear liquid was used for biochemical test, and the sediment was used for cell culture or DNA extraction. Amniotic fluid cells were cultured

in a 5% carbon dioxide incubator at 37°C. When the results of NIPT indicated that trisomy 21, 18, and 13 were at high risk or indicative of abnormal chromosome number, G-banding chromosome karyotype analysis + chromosome microarray analysis (CMA) were performed in amniotic fluid cell culture; If NIPT results suspect that there may be other chromosomal abnormalities or gene level microdeletions and microduplications, amniotic fluid cell culture G-banding chromosome karyotype analysis + gene chip detection shall be given to make a definite diagnosis.

2.5. Follow-Up. The pregnancy outcomes of all pregnant women were followed-up, except those with abnormal results in prenatal diagnosis and induced labor including outpatient, telephone, and Internet follow-ups.

Follow-up contents: (1) Pregnant women who have low-risk NIPT results or who refuse to undergo prenatal diagnosis despite high-risk NIPT results should follow-up, whether there are structural or soft index abnormalities in B-ultrasound results after NIPT. (2) Whether peripheral blood chromosome examination is performed after delivery, or whether induced labor tissue microarray is performed for induced labor. (3) Whether the appearance of induced labor fetus or newborn is normal. (4) Whether the weight of the newborn is normal. (5) At the same time, it is judged according to whether the newborn's appearance and physical and intellectual development are abnormal. The follow-up was completed in 2-6 months after termination of pregnancy.

2.6. Statistical Analysis. SPSS (version 22.0) software was used for statistical processing of all data in this study. The sensitivity, specificity, and positive predictive rate of NIPT were evaluated. The coincidence between the chromosome aneuploidy in NIPT and prenatal diagnosis of amniotic fluid was compared. Chi-square test was used to analyze data conforming to normal distribution. The difference was statistically significant when $P < 0.05$.

3. Results

3.1. Test Results of Each Group. A total of 1949 subjects were included in the study. The number of positive women who underwent NIPT test was 42, and the positive rate was 2.15%. Further amniotic fluid puncture test identified 10 cases of T21, 4 cases of T18, 0 case of T13, 7 cases of sex chromosome aneuploidy, 9 cases of other chromosome aneuploidy, and 12 cases of chromosome copy number variation. In the amniocentesis group, 236 cases of elderly pregnant women directly received amniotic fluid puncture test. The results confirmed 9 cases of T21, 1 case of T18, 3 cases of sex chromosome abnormality, 2 cases of other chromosome aneuploidy, and 3 cases of chromosome copy number variation. The positive cases were 18, and the positive rate was 0.92%. When NIPT was used for prenatal screening of fetal chromosomal aneuploidy, its diagnostic coincidence rate for trisomy 21 was the highest (90.00%), and the diagnostic coincidence rate for other chromosomal aneuploidy was the lowest (22.22%), as shown in Table 1.

3.2. Invasive Diagnosis Results for CNV. Among the 236 cases that received amniotic fluid puncture test, the results indicated that there was 1 pathogenic case and 1 likely pathogenic case, as shown in Table 2.

3.3. Pregnancy Outcome Follow-Up. According to the prenatal diagnosis results, 16 pregnant women in the NIPT group and 2 pregnant women in the amniocentesis group chose to induce labor, and these participants were excluded from our follow-up. For the remaining 1933 cases in the NIPT group, the follow-up results showed that there were 35 abortions, 3 stillbirth, and 6 fetal malformations, a total of 44 adverse pregnancy outcomes with an incidence of 2.28%. For the remaining 234 cases in the amniocentesis group, there were 2 abortions, 0 stillbirth, and 1 fetal malformations with 1.28% adverse pregnancy outcomes. There was no significant difference between the two groups, $P > 0.05$, as shown in Table 3.

3.4. Screening Efficiency of NIPT for Common Fetal Chromosomal Aneuploidy and Other Chromosomal Abnormalities. The sensitivity, specificity, positive predictive rate, and negative predictive rate of trisomy 21 screened by NIPT were 100%, 99.97%, 94.28%, and 100%, respectively. The sensitivity, specificity, positive predictive rate, and negative predictive rate of trisomy 18 were 100%, 99.92%, 72.22%, and 100%, respectively, and the sensitivity, specificity, positive predictive rate, and negative predictive rate of trisomy 13 were 100%, 99.95%, 50%, and 100%, respectively, as shown in Table 4.

3.5. Relationship between Maternal Age and Fetal Chromosome Abnormality. A total of 1949 elderly pregnancies were included in this study and underwent NIPT. Among them, 42 cases received amniotic fluid prenatal diagnosis after NIPT test was positive, and 236 cases directly received invasive prenatal diagnosis. The results of fetal chromosomal abnormalities are listed in the following table according to the age of pregnant women, and the true positive rate of fetal chromosomal aneuploidy at all ages is calculated, as shown in Table 5. The diagnostic rate of fetal chromosomal abnormalities in pregnant women under 40 years old was about 0.39-0.79%; however, the risk for people over 40 is relatively high at 1.32-4.44%.

4. Discussion

Birth defects are one of the common diseases of newborns in China, and chromosomal abnormalities are one of the important causes of birth defects [12]. Among them, autosomal abnormalities can be manifested in different degrees of mental retardation, growth retardation, appearance, and organ deformity, and sex chromosome abnormalities can be manifested in gonadal hypoplasia, hermaphroditism, etc. At present, there is no effective treatment for these chromosomal abnormalities. We can only try to avoid the birth of such children through secondary prevention, especially children with trisomy 21 syndrome.

NIPT is a new noninvasive detection method. It uses a new generation of high-throughput sequencing technology

Table 1: Test results of each group.

Groups	T21	T18	T13	Sex chromosome aneuploidy	Other chromosome aneuploidy	Chromosome copy number variation	Total cases	Positive rate (%)
NIPT group	10	4	0	7	9	12	42	2.15%
Amniocentesis group	9	1	0	3	2	3	18	0.92%
Coincidence rate (%)	90.00	25.00	—	42.86	22.22	25	42.86	42.8%

Table 2: Invasive diagnosis results for CNV.

Maternal age	Gestational age	NPIT site	Invasive diagnosis	Pathogenesity
38	16	del 16p13.11-p12.3[b]	del 16p13.12-p12.3[b]	Pathogenic
42	17	Dup 22q11.21	Dup 22q11.21	Likely pathogenic

Table 3: Follow-up of pregnancy outcomes in patients with different risks.

Groups	N	Abortion	Stillbirth	Fetal malformation	Incidence of defects
NIPT group	1933	35	3	6	2.28%
Amniocentesis group	234	2	0	1	1.28%
χ^2				0.9724	
P				0.3241	

Table 4: Efficiency of NIPT in screening common fetal chromosomal aneuploidy and other chromosomal abnormalities.

	Sensitivity	Specificity	Positive predictive value	Negative predictive value
21-trisomy syndrome	100%	99.97%	94.28%	100%
18-trisomy syndrome	100%	99.92%	72.22%	100%
13-trisomy syndrome	100%	99.95%	50.00%	100%

Table 5: Analysis of chromosome screening in pregnant women of different age groups.

Age (years)		35	36	37	38	39	40	41	42	43	≧44	Total
N		782	257	262	183	126	98	76	68	52	45	1949
Diagnosis of chromosome abnormality	T21	2	1	0	1	1	1	1	1	0	1	9
	T18	0	0	1	0	0	0	0	0	0	0	1
	T13	0	0	0	0	0	0	0	0	0	0	0
	Sex chromosome abnormality	1	0	0	0	0	1	0	0	1	0	3
	Other exceptions	1	0	1	0	0	0	0	1	1	1	5
	Total	4	1	2	1	1	2	1	2	2	2	18
True positive rate (%)		0.51	0.39	0.76	0.54	0.79	2.04	1.32	2.94	3.85	4.44	0.92

to sequence fetal free DNA fragments in maternal peripheral blood, and then judge whether the fetus has abnormal chromosome aneuploidy. Ben et al. and Smid et al. had confirmed that cell-free fetal DNA (cffDNA) existed in the peripheral blood of pregnant women, and its metabolic law met the requirements of prenatal screening [13, 14], but the technology at that time could not achieve high-throughput detection. With the rapid development of high-throughput detection technology, NIPT was gradually used in clinical detection [15, 16]. At present, the superiority of NIPT technology has been widely recognized at home and abroad. Many clinical pilots have conducted large-scale data research on NIPT and found that the positive predictive value of NIPT for T21 is as high as 80~89%, and the positive predictive value of T18 is also greater than 60%, both of which are significantly higher than the positive predictive value of routine serological screening (T21 is 3.4%~4.2%, T18 is 8.3%). Moreover, the missed screening rates of T21

and T18 detected by NIPT were 0.3% and 0.2%, respectively, which were significantly lower than those of serological screening (3.6%~5.2% for T21 and 0.6% for T18) [17]. It can be seen that NIPT has absolute advantages over the traditional serological prenatal screening in the screening of T21 and T18. In addition, it has the characteristics of noninvasive operation, which effectively solves some problems existing in interventional prenatal diagnosis, and even in some aspects, it can replace prenatal diagnosis. It has been widely concerned by all walks of life and has gradually become a research hotspot [18].

Prenatal examination and prenatal diagnosis are the main measures used to eliminate fetal deformities and prevent birth defects. The traditional serological screening is mainly aimed at the common chromosomal diseases of the fetus (T21, T18). Although early screening can be carried out, the detection rate is low and the false positive rate is high. Even if the prenatal screening results of pregnant women are high-risk, there is only a 5% chance that the fetus can be diagnosed with chromosomal diseases [19]. The high risk of screening results will increase the mental and psychological burden of pregnant women and their families to a certain extent, and the low-positive detection rate makes many people feel lucky and give up prenatal diagnosis, which leads to the loss of the original significance of prenatal screening and the birth of children. In fact, this kind of missing screen occurs almost every year, causing lifelong regret. Conventional prenatal diagnosis methods (such as chorionic puncture, amniocentesis, amniotic fluid, umbilical vein puncture) require uterine puncture of pregnant women, which is traumatic and has the risk of fetal loss and infection. As a result, a considerable number of pregnant women are afraid of this method, so their compliance is reduced. In addition, whether the soft index of systematic ultrasound is abnormal or not, is often used to evaluate the risk that the fetus may be associated with chromosomal diseases [20]. However, due to the nonspecificity of these soft indices, their sensitivity is not high. Limited by this, ultrasound doctors must have many years of experience in prenatal diagnosis before they can find these abnormalities. However, there are certain differences in the current medical level in China, which limits its application to a certain extent [21].

The existing norms of prenatal screening and prenatal diagnosis in China require that pregnant women with serological screening results at critical risk can undergo NIPT, while older pregnant women with high-risk results or expected childbirth age ≥35 years old are still recommended to choose interventional prenatal diagnosis as the first choice [22]. However, with the continuous deterioration of the living environment and the increasing number of planned pregnancies, especially older pregnancies, after the liberalization of the two child policy, the proportion of high-risk and older pregnant women has doubled. However, the poor compliance caused by the fear of trauma of prenatal diagnosis among pregnant women and the shortage of medical resources have brought enormous pressure to prenatal diagnosis [23]. Therefore, this study intended to actively find a more optimized screening program in order to reduce the missed screening rate, reduce the number of cases requiring interventional prenatal diagnosis, and achieve the purpose of reducing the operation risk as much as possible.

In this study, 1949 pregnant women with high risk of prenatal screening or advanced age (NIPT group) required NIPT first. The results of NIPT showed high risk in 42 cases which received further invasive prenatal diagnosis, the results of NIPT were low-risk in 1907 cases, and no missed screening was found at present according to the pregnancy outcome. At the same time, 236 pregnant women received invasive prenatal diagnosis for further confirmation.

The elderly pregnant women included in the study first had NIPT, and then had further prenatal diagnosis when NIPT results were at high risk. Compared with the elderly pregnant women who had direct interventional prenatal diagnosis, there was a coincidence rate of 42.8% in fetal chromosomal abnormalities between the two methods. Similarly, according to Table 2, there was no significant difference between NPT test results and invasive test results of copy number variants (CNVs). CNVs are ubiquitous in the human genome, and CNVs-related diseases, including Digeorge syndrome (22Q11), CRIP-Du-Chat syndrome (5P-), and 1P36 deletion syndrome, have been documented [24]. Moreover, there is increasing evidence that CNV is associated with adverse pregnancy outcomes [25]. In our study, there is no significant difference in the detection rate of fetal chromosomal abnormalities between the screening of high-risk pregnant women and the direct interventional prenatal diagnosis. Therefore, we infer that if some elderly pregnant women refuse to directly carry out interventional prenatal diagnosis, they can be asked to choose NIPT first. If NIPT results are high-risk, then carry out interventional prenatal diagnosis, which should be equivalent to the detection rate of direct interventional prenatal diagnosis. At least, the probability of missing fetal chromosomal aneuploidy is very small. This approach can reduce a large part of the operation risk and also provide an alternative and relatively reliable way for pregnant women with surgical contraindications. Relieve the mental pressure of pregnant women and their families, improve compliance, reduce the risk of surgery, and reduce the work intensity of prenatal diagnosis practitioners. At present, the cost of NIPT is relatively high, which hinders its further promotion in clinical practice. Of course, as the government pays more attention to this cause and the cost of high-throughput sequencing is further reduced, this problem is expected to be solved. The wide application of NIPT is just around the corner. In addition, according to the data in Table 5, the diagnostic rate of fetal chromosomal abnormalities in pregnant women under the age of 40 was lower than 1%; however, the risk for people over 40 was relatively high, could be up to 4.44%. In order to prevent missed screening and reduce the chance of puncture surgery, different prenatal screening and prenatal diagnosis schemes can be adopted for elderly pregnant women in stages.

It should be noted that during the follow-up, a very small number of pregnant women were informed of the high risk of NIPT and directly terminated their pregnancy without further prenatal diagnosis. Therefore, normal fetuses may be abandoned. This should be related to the pregnant

women's insufficient understanding of the false positive of NIPT, leading to the wrong choice. In fact, at present, the diagnostic coincidence rate of NIPT for T21was the highest (90.00%), which was significantly higher than that of other groups (see Table 1). Therefore, NIPT can only be used as a high-precision screening and cannot replace prenatal diagnosis to detect all chromosomal abnormalities. There are still false positives. To the best of our knowledge, NIPT is a noninvasive prenatal screening technique for fetal aneuploidies. NIPS is based on high-throughput sequencing to detect cffDNA in maternal blood [26]. Therefore, the most likely reason for false positives is that fetal and fetal cffDNA accounts for insufficient proportion of total cffDNA. Therefore, pregnant women with positive NIPT results must undergo interventional prenatal diagnosis to determine whether the fetus has chromosome or gene-level abnormalities. With our in-depth study of NIPT, we hope that more pregnant women can correctly understand the relationship between NIPT and interventional prenatal diagnosis and make correct and scientific choices. This can also promote the benign and sustainable development of NIPT.

There are some shortcomings of this study. Firstly, there were some undiagnosed cases in the high-risk groups tested by NIPT. Moreover, because of the low incidence of trisomy 18 and trisomy 13, age-stratified studies could not be performed as in trisomy 21. Therefore, more studies with larger sample sizes are expected to be carried out in the future to provide more data support for optimizing prenatal screening and diagnosis strategies for elderly pregnant women.

In conclusion, the noninvasive prenatal screening of fetal DNA in the second trimester of pregnancy for older pregnant women has a high application value in the prediction of pregnancy outcomes. The high risk of pregnancy can be determined by detecting trisomy 21, 18, and 13, and the probability of adverse pregnancy outcomes increases. Therefore, noninvasive prenatal screening of fetal DNA in the second trimester of pregnancy should be popularized in clinical practice, so as to reduce the probability of adverse pregnancy outcomes in older pregnant women.

Data Availability

Data appears in the submitted article.

Ethical Approval

This study was approved by the Ethics Committee of our hospital.

Consent

The informed consent was signed by all patients and their family before treatment.

Conflicts of Interest

The authors report no conflicts of interest.

Acknowledgments

This work was supported by the Taizhou People's Hospital.

References

[1] D. W. Bianchi and R. W. K. Chiu, "Sequencing of circulating cell-free DNA during pregnancy," *The New England Journal of Medicine*, vol. 379, no. 5, pp. 464–473, 2018.

[2] D. Oepkes, G. C. Page-Christiaens, C. J. Bax et al., "Trial by Dutch laboratories for evaluation of non-invasive prenatal testing. Part I—clinical impact," *Prenatal Diagnosis*, vol. 36, no. 12, pp. 1083–1090, 2016.

[3] S. W. Li, A. N. Barrett, L. Gole et al., "The assessment of combined first trimester screening in women of advanced maternal age in an Asian cohort," *Singapore Medical Journal*, vol. 56, no. 1, pp. 47–52, 2015.

[4] P. Benn, H. Cuckle, and E. Pergament, "Non-invasive prenatal testing for aneuploidy: current status and future prospects," *Ultrasound in Obstetrics & Gynecology*, vol. 42, no. 1, pp. 15–33, 2013.

[5] M. A. Ferguson-Smith and J. R. Yates, "Maternal age specific rates for chromosome aberrations and factors influencing them: report of a collaborative European study on 52 965 amniocenteses," *Prenatal Diagnosis*, vol. 4 Spec No, no. 7, pp. 5–44, 1984.

[6] A. Tabor and Z. Alfirevic, "Update on procedure-related risks for prenatal diagnosis techniques," *Fetal Diagnosis and Therapy*, vol. 27, no. 1, pp. 1–7, 2010.

[7] L. L. Poon, T. N. Leung, T. K. Lau, and Y. M. D. Lo, "Presence of fetal RNA in maternal plasma," *Clinical Chemistry*, vol. 46, no. 11, pp. 1832–1834, 2000.

[8] E. K. Ng, N. B. Tsui, T. K. Lau et al., "mRNA of placental origin is readily detectable in maternal plasma," *Proceedings of the National Academy of Sciences of the United States of America*, vol. 100, no. 8, pp. 4748–4753, 2003.

[9] M. Badeau, C. Lindsay, J. Blais et al., "Genomics-based noninvasive prenatal testing for detection of fetal chromosomal aneuploidy in pregnant women," *Cochrane Database of Systematic Reviews*, vol. 11, article CD011767.7, 2017.

[10] E. Iwarsson, B. Jacobsson, J. Dagerhamn, T. Davidson, E. Bernabe, and A. M. Heibert, "Analysis of cell-free fetal DNA in maternal blood for detection of trisomy 21, 18 and 13 in a general pregnant population and in a high risk population - a systematic review and meta-analysis," *Acta Obstetricia et Gynecologica Scandinavica*, vol. 96, no. 1, pp. 7–18, 2017.

[11] S. Chen, T. K. Lau, C. Zhang et al., "A method for noninvasive detection of fetal large deletions/duplications by low coverage massively parallel sequencing," *Prenatal Diagnosis*, vol. 33, no. 6, pp. 584–590, 2013.

[12] Y. M. Lo, J. Zhang, T. N. Leung, T. K. Lau, A. M. Z. Chang, and N. M. Hjelm, "Rapid clearance of fetal DNA from maternal plasma," *American Journal of Human Genetics*, vol. 64, no. 1, pp. 218–224, 1999.

[13] P. A. Benn, J. F. Egan, M. Fang, and R. Smith-Bindman, "Changes in the utilization of prenatal diagnosis," *Obstetrics and Gynecology*, vol. 103, no. 6, pp. 1255–1260, 2004.

[14] M. Smid, S. Galbiati, A. Vassallo et al., "No evidence of fetal DNA persistence in maternal plasma after pregnancy," *Human Genetics*, vol. 112, no. 5-6, pp. 617-618, 2003.

Hindawi
Computational and Mathematical Methods in Medicine
Volume 2023, Article ID 9897161, 1 page
https://doi.org/10.1155/2023/9897161

Retraction

Retracted: Investigation and Countermeasures on Mental Health Status of Applied Fresh Graduates from the Perspective of Psychological Capital

Computational and Mathematical Methods in Medicine

Received 1 August 2023; Accepted 1 August 2023; Published 2 August 2023

This article has been retracted by Hindawi following an investigation undertaken by the publisher [1]. This investigation has uncovered evidence of one or more of the following indicators of systematic manipulation of the publication process:

(1) Discrepancies in scope

(2) Discrepancies in the description of the research reported

(3) Discrepancies between the availability of data and the research described

(4) Inappropriate citations

(5) Incoherent, meaningless and/or irrelevant content included in the article

(6) Peer-review manipulation

The presence of these indicators undermines our confidence in the integrity of the article's content and we cannot, therefore, vouch for its reliability. Please note that this notice is intended solely to alert readers that the content of this article is unreliable. We have not investigated whether authors were aware of or involved in the systematic manipulation of the publication process.

Wiley and Hindawi regrets that the usual quality checks did not identify these issues before publication and have since put additional measures in place to safeguard research integrity.

We wish to credit our own Research Integrity and Research Publishing teams and anonymous and named external researchers and research integrity experts for contributing to this investigation.

The corresponding author, as the representative of all authors, has been given the opportunity to register their agreement or disagreement to this retraction. We have kept a record of any response received.

References

[1] Y. Zeng, "Investigation and Countermeasures on Mental Health Status of Applied Fresh Graduates from the Perspective of Psychological Capital," *Computational and Mathematical Methods in Medicine*, vol. 2022, Article ID 5352958, 10 pages, 2022.

Hindawi
Computational and Mathematical Methods in Medicine
Volume 2022, Article ID 5352958, 10 pages
https://doi.org/10.1155/2022/5352958

Research Article

Investigation and Countermeasures on Mental Health Status of Applied Fresh Graduates from the Perspective of Psychological Capital

Yuanzhen Zeng

Mental Health Education and Consultation Center, Guangxi Agricultural Vocational and Technical University, Nanning, 530001 Guangxi, China

Correspondence should be addressed to Yuanzhen Zeng; 3180200242@caa.edu.cn

Received 28 July 2022; Revised 20 August 2022; Accepted 27 August 2022; Published 28 September 2022

Academic Editor: Min Tang

Based on the perspective of psychological capital, the mental health status of applied college graduates is analyzed, and the corresponding countermeasures are put forward. Questionnaires are issued to investigate the mental health status of fresh graduates. The BSSI score of male students (102.05 ± 2.01) is not significantly different from that of female students ($P > 0.05$). SCL-90 scores of male students include somatization (1.95 ± 0.01), compulsion (1.84 ± 0.15), interpersonal relationship (1.75 ± 0.14), depression (1.92 ± 0.08), anxiety (1.70 ± 0.10), hostility (7.25 ± 0.16), terror (1.35 ± 0.41), bigotry (1.29 ± 0.17), and psychosis (1.33 ± 0.64). There is no significant difference compared with those of female students ($P > 0.05$). SCL-90 scores of high stress graduates include somatization (2.00 ± 0.17), compulsion (2.30 ± 0.08), interpersonal relationship (1.61 ± 0.20), depression (1.87 ± 0.09), anxiety (1.80 ± 0.11), hostility (1.30 ± 0.20), terror (1.39 ± 0.14), paranoid (1.48 ± 0.10), and psychosis (1.50 ± 0.11). There is significant difference between forced and low pressure graduates ($P < 0.05$). There is no statistical significance in other items ($P > 0.05$). Colleges and universities need to work together with fresh graduates to deal with negative emotions and stress, so as to improve mental health and promote employment.

1. Introduction

The experts led by Luthans and others believed that psychological capital was "a positive psychological state displayed by individuals in the process of growth and development, specifically manifested as self-efficacy, optimism, hope and resilience." Psychological capital referred to in the research includes the following four dimensions.

Self-efficacy (Figure 1) refers to people's belief that they can complete a certain task or work behavior [1]. It involves not the skill itself, but the degree of confidence that one can use the skill to complete the behavior [2]. Self-efficacy is an individual's degree of self-determination and trust. It is a kind of belief. A person's self-efficacy is not related to his actual ability or skill but has a great influence on his behavior. People with a strong sense of self-efficacy are confident in dealing with problems when facing adverse situations. They are willing to accept challenges and make efforts in a strange and changing environment. They believe that they can change difficulties and are more likely to achieve goals. However, people with low self-efficacy lack confidence in themselves. They are more likely to retreat, be anxious, and be restless when facing pressure and difficulties and are prone to have escape psychology and avoidance behaviors, which are not conducive to achieving goals [3, 4].

Professor Selingman, an American psychologist, used attributive styles to distinguish optimism from pessimism [5]. In his opinion, optimism refers to that individuals make their own, lasting, and universal attributions to positive events while making external, temporary, and specific attributions related to the situation to negative events when interpreting the events that have occurred. In the face of difficulties, setbacks, and failures, optimistic people can regard misfortune or change as an opportunity and challenge. They

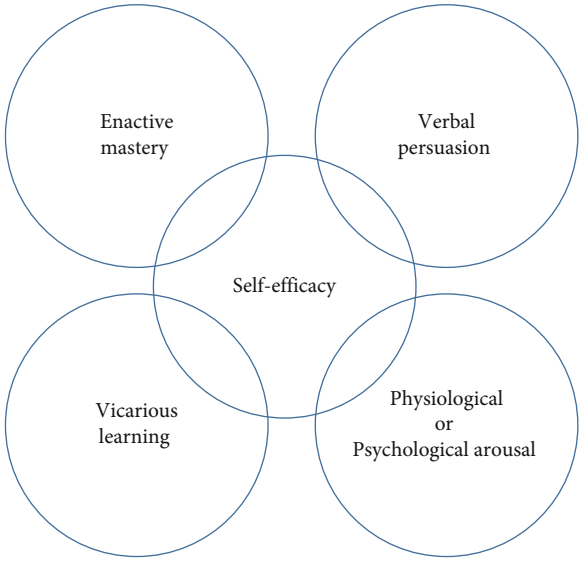

Figure 1: Self-efficacy.

can face with a positive attitude and see the potential of all kinds of opportunities. In the pursuit of difficult goals, optimistic people can persevere unremittingly. They have positive expectations for the future and keep making efforts, with a belief that they will eventually achieve success.

Kim, S. H. defined hope as a positive motivational state formed on the basis of the experience generated by the interaction between the motivation for success (the energy of targeted feedback) and the path (plan to achieve the goal). Hope is a positive state of individual motivation. A person who is hopeful about the future sets challenging goals based on the realities of himself and his environment and finds ways to achieve his personal goals through perseverance. Hopeful people take the initiative to set goals in life and try to solve problems effectively [6]. They have the ability of independent thinking and will achieve their goals through active rather than passive waiting and gradually achieve their goals through their own positive attitude, unremitting efforts, and various methods. The targeted feedback is shown in Figure 2.

Resilience refers to an individual's ability to persevere, maintain confidence, quickly recover from happiness, and find ways to achieve success when faced with difficulties or adversity. It is an important factor for an individual to overcome hardship, walk out of adversity, and march towards success. It is also known as resilience and mental resilience. People with high resilience can actively deal with difficult problems when they are in trouble, make themselves stronger and more flexible in failure and adversity, and quickly recover their psychological state and even reach a better state. In challenging positive events, individuals with high resilience can develop their potential abilities with extraordinary willpower to help individuals eventually get out of difficulties [7].

2. Literature Review

2.1. Psychological Capital. Improving psychological capital is beneficial to the career development of college students. College students are facing the transformation from students to social and professional people and facing a series of conflicts and contradictions from the society, family, and their own growth. Whether they can grow up healthily, the play of many abilities is affected by psychological capital. College students who have a strong sense of self-efficacy are strong, optimistic, and full of hope for the future and are better able to adapt to the society and the workplace [8]. On the contrary, it is prone to psychological problems and occupational maladjustment, which may lead to insurmountable obstacles and even a vicious circle in the future personal career development. If college students can have more psychological capital, possess optimistic and confident psychological quality, and be full of hope for the future, they can deal with various problems better in life. In this way, in the development of his or her career (Figure 3), he or she can "respond to all changes with the same changes," which will benefit him or her immensely [9].

Accumulating psychological capital is beneficial to cultivating innovative and entrepreneurial talents. In August 2012, the General Office of the Ministry of Education issued a document requiring entrepreneurship courses to be offered in regular colleges and universities across the country. The move is intended to promote the all-round development of college students and speed up the process of building China into a power of human resources. At present, China's entrepreneurship education is in its infancy, and many college students lack confidence, correct self-recognition, practical experience, and ability to solve practical problems. They are full of hope and confused about the future. In study and life, there is a lack of real role models and realistic goals to strive for. It is difficult to carry out innovation and entrepreneurship education in such student groups. Because of this, it is particularly important to develop the psychological capital of college students, and it is extremely urgent to carry out entrepreneurship education in colleges and universities. On the one hand, entrepreneurship education can awaken and excavate the psychological capital of college students. On the other hand, psychological capital of college students can be accumulated and improved (Figure 4) [10, 11].

Increasing psychological capital is helpful to improve the employability of college students. The rise of psychological capital theory provides a new perspective for improving the job-hunting competitiveness of college students [12]. With abundant psychological capital, college students are more likely to succeed in their first employment and become more comfortable in their future career development. Many college students cannot find a job because of their poor ability and low quality, and employability cannot meet the requirements of employers. Ability and personality become the focus of employers' investigation. Employers want applicants to have self-management ability, unity and cooperation ability, interpersonal communication ability, initiative learning ability, and creative problem-solving ability. Employers prefer candidates with positive attitude, confidence and thirst for knowledge, honest words and actions, and ability to work under pressure (Figure 5) [13]. The self-introduction, leaderless group discussion, psychological test, and other links in the process of interview and written examination all examine the ability and personality of college students from different angles.

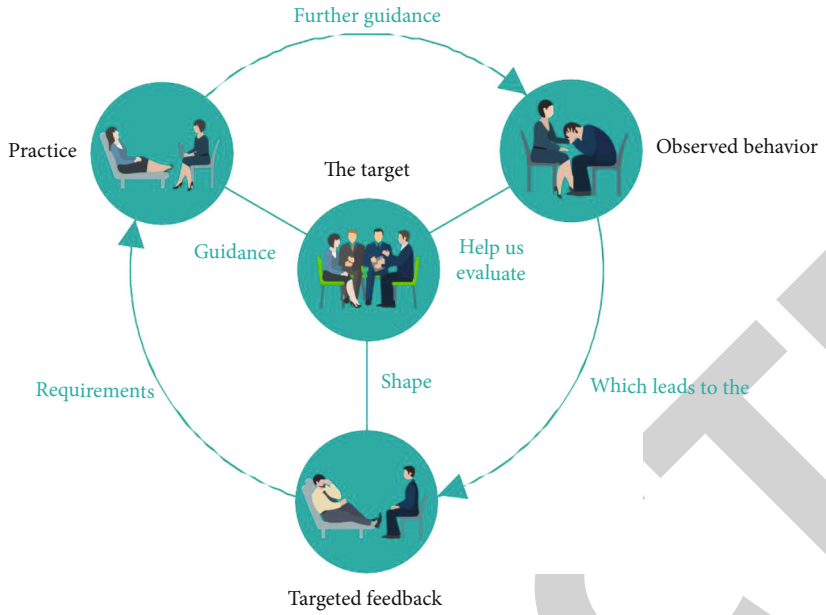

Figure 2: Targeted feedback.

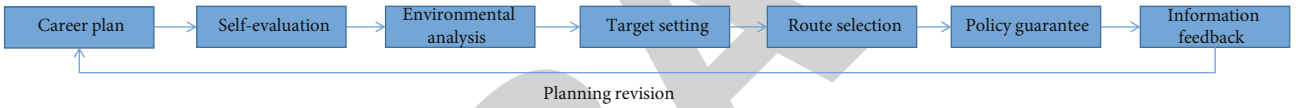

Figure 3: Career planning.

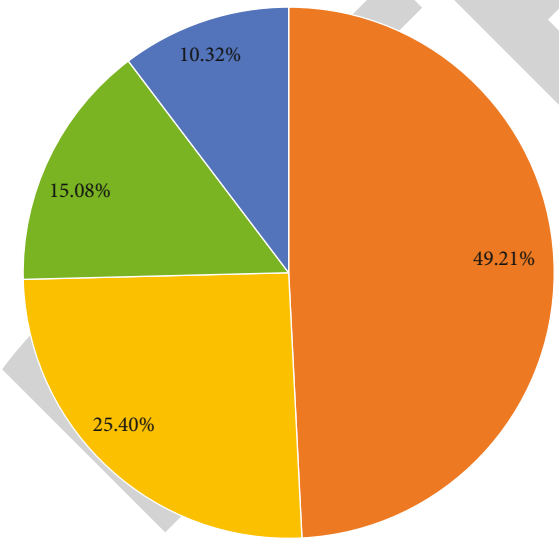

Figure 4: Causes of low psychological capital of college students.

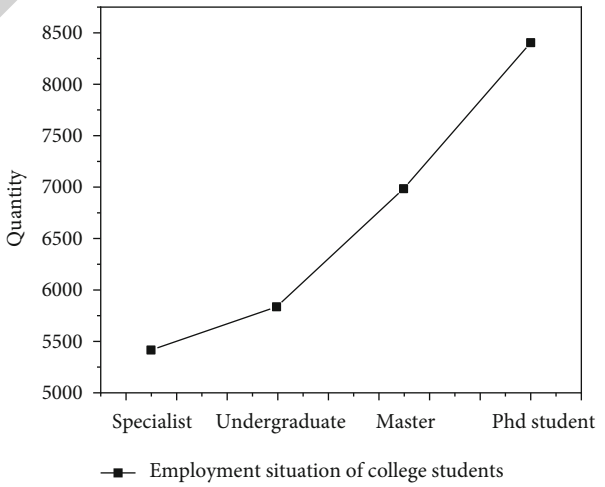

Figure 5: Employment of college students.

Paying attention to psychological capital is beneficial to realize its synergistic effect with human capital and social capital. In recent years, the joint effect of human capital, social capital, and psychological capital on college students' job hunting and personal career has attracted the attention of human resource managers in universities, college students, and enterprises. Human capital includes individual education, certificates, training experience, and knowledge experience. Social capital refers to the network of social relationships in which an individual is a member and can utilize

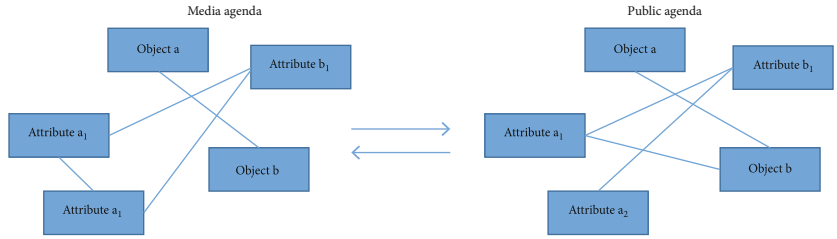

Figure 6: Social network.

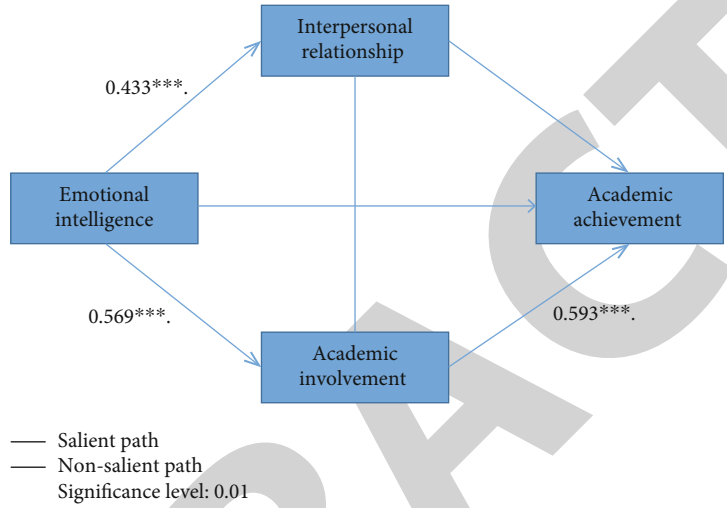

Figure 7: Intelligence of college students.

them. Psychological capital includes positive psychological qualities such as self-confidence, optimism, resilience, and hope. Three-dimensional capital is indispensable in the development of individual career. These three aspects transform and influence each other and finally make individuals obtain a perfect career. Some college students devote themselves to study only for scholarships and certificates, hardly taking part in any extracurricular activities. Some university student cadre, because of the work reason and organizing all kinds of activities, often play truant and fail frequently. Some college students are mediocre in academic performance and have no self-established social relationship network (Figure 6). They do not know how to turn to others for help when they encounter problems [14, 15].

2.2. Mental Health of College Students. Mental health is very important for a person. It means that a person's physiology, psychology, and society are in a harmonious state with each other. Its characteristics are as follows.

Normal intelligence (Figure 7): this is the most basic psychological condition for people's life, study, work, and labor [16].

Emotional stability and happiness: this is an important sign of mental health. It shows that a person's central nervous system is in relative balance, meaning that the body functions in harmony. A mentally healthy person's behavior is coordinated, his behavior is controlled by consciousness, his thought and behavior are coordinated, and he has the ability to control himself. If a person's behavior and thought contradict each other, his attention is not focused, his thoughts are confused, his language is fragmented, and his work is chaotic. Psychological adjustment should be carried out.

Good interpersonal relationship (Figure 8): living in society, one should be good at getting along with others, help others, and establish good interpersonal relationship. People's communication activities can reflect people's mental health state. Normal friendly communication between people is not only a necessary condition to maintain mental health but also an important method to obtain mental health [17].

Good adaptability: living in a complicated and changeable world, people will encounter a variety of environments and changes in their life. Therefore, a person should have good adaptability. No matter realistic how the environment has changed, one will be able to get used to the mental health. A person's mental health is not necessarily in every aspect of performance. As long as in life practice, he can correctly understand himself.

Sound will: will is a psychological process of choosing, deciding, and performing a purposeful activity. The one with sound will shows a higher level in the action of the consciousness, decisiveness, tenacity and self-control, and other aspects. Students with sound will have a conscious purpose in all kinds of activities. They can make timely decisions

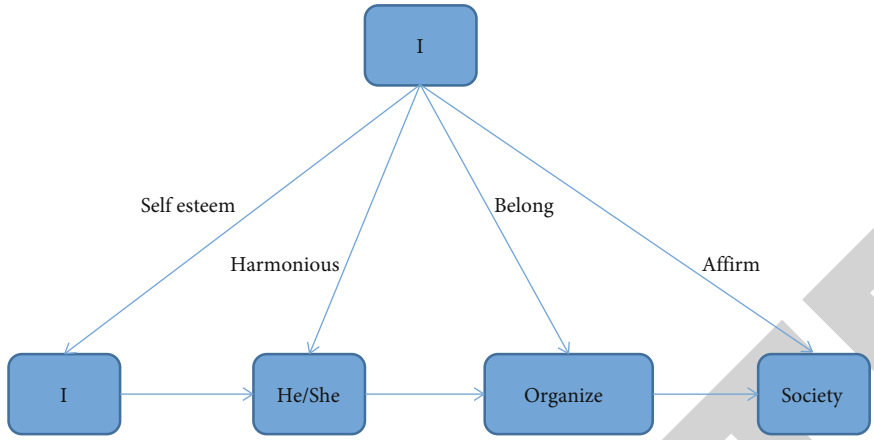

Figure 8: Harmonious interpersonal relationship.

and use a practical and prepared way to solve the problems encountered. In the face of difficulties and setbacks, they can take a reasonable way of reaction and can control emotions in action and words and deeds.

Complete personality (Figure 9) [18, 19]: personality refers to the sum total of the individual's relatively stable psychological characteristics. Perfect personality refers to a sound and unified personality, that is, what an individual thinks, says, and does is coordinated and consistent. One is the integrity and unity of all elements of personality structure, such as having correct self-consciousness, not producing self-identity mix, taking positive and enterprising outlook on life as the core of personality, and taking this as the center of their own, needs, goals, and actions together.

Correct self-evaluation: correct self-evaluation is the important condition of college students' mental health. College students perform self-observation, self-recognition, self-judgment, and self-assessment, so as to achieve self-knowledge and appropriately know themselves. They can accept themselves, with self-esteem, self-improvement, self-control, and moderate self-love. They can face up to the reality. With the reform of the cultural system and the proposal of the national slogan of "education for all," the number of new college students in our country is increasing. With the increasing number of college students, the mental health problems of college students are becoming more and more serious.

2.3. Psychology of Fresh Graduates. With the reform of China's economic structure and system, the problem of difficult employment of college students has become more prominent, and the psychological problems of college students have aroused widespread social concern. Since the expansion of college entrance examination in 1999 (Figure 10), college education has turned from elite education to mass education, with the enrollment growth rate of ordinary colleges and universities reaching 42%, the average annual growth rate of college enrollment reaching 30%, and the enrollment rate exceeding 60% [20].

College students are no longer popular. Employment pressure and emotional problems have become the main psychological problems of fresh graduates. On the one hand, colleges and universities need to take various measures to promote employment and, at the same time, need to carry out employment psychological counseling through multiple channels. Anxiety is the basic emotion developed by college students in the process of struggling with the changing situation and adapting to the survival. Moderate anxiety can fully mobilize the function of each organ and improve the reaction speed and alertness of individual brain. According to the survey, anxiety is the main psychological problem of fresh college students, who are worried about the changing environment and the transformation of social roles. Maintaining a moderate level of anxiety can create stress. Anxiety is a normal psychological reaction. This moderate psychological pressure, to some extent, is to urge themselves, which can stimulate college students' enterprising spirit, so as to participate in the employment competition more actively. It manifests itself as being self-motivated and enterprising. With graduation time is coming, the vast majority of students are anxious. They should learn to talk. Talking out is an important method in psychological counseling. If you feel anxious during the employment process, please try to talk to your classmates, friends, and family, and seek the help of a professional psychologist. For the college graduates' psychological counseling work, universities should pay attention to the emotional guidance, such as guiding students to understand and vent their own emotions. Setbacks are inevitable. Individuals should learn to motivate themselves and carry out positive self-suggestion, such as maintaining an optimistic and confident psychological state. They should reduce the negative impact of adverse psychological factors and maintain a healthy psychological state [21].

Blind following psychology refers to a psychological phenomenon in which individuals abandon their original ideas and opinions and adopt conformity due to the influence or pressure of group behavior in communication. It is a social psychological phenomenon prevalent in university campuses. The social causes of blind following are complex. College students lack the consciousness of making personal career planning. They are out of touch with the society and unable to fully understand the needs of the social industry. They lack in-depth professional learning, social practice

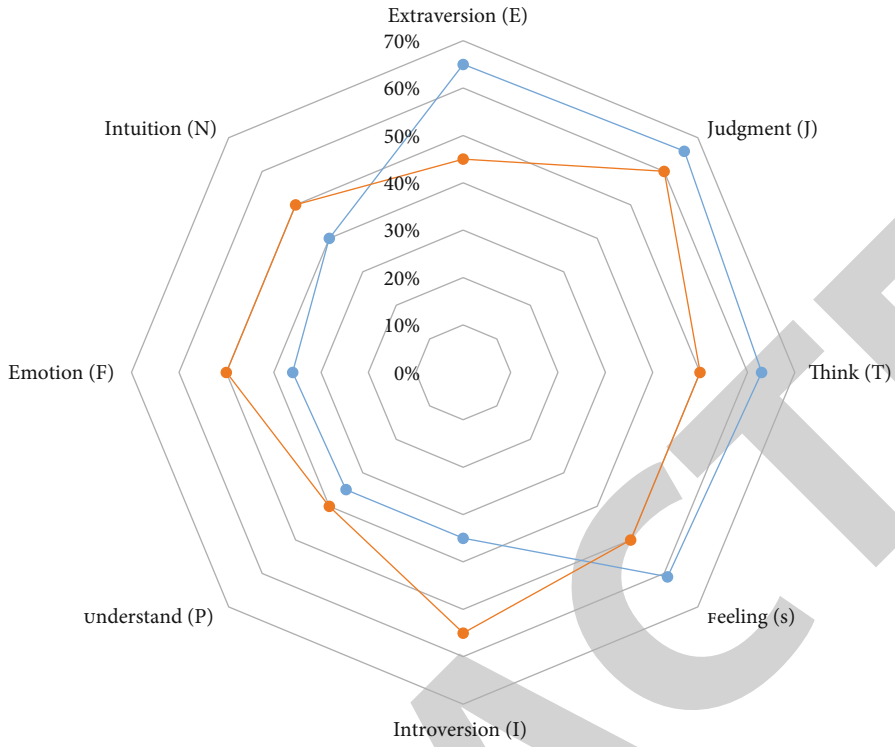

Figure 9: Classical personality composition.

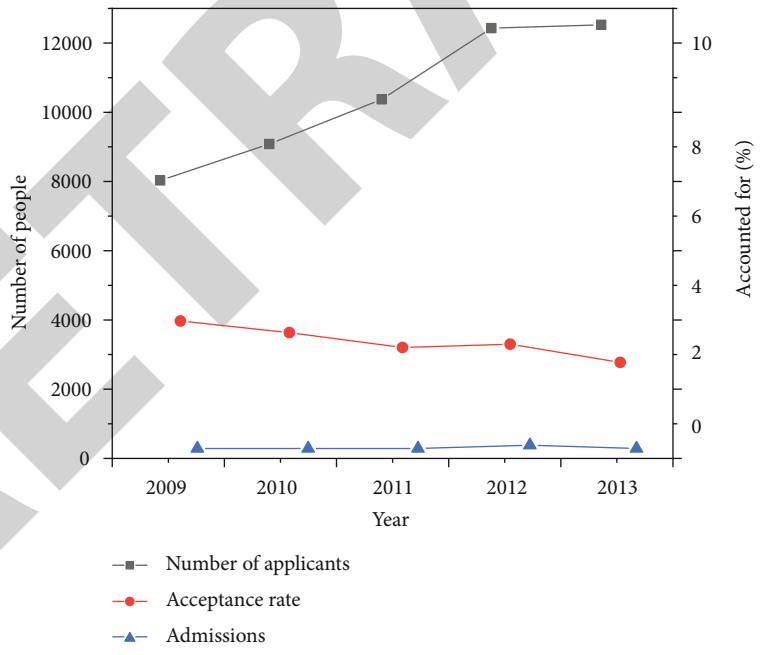

Figure 10: College entrance examination expansion.

experience, and decision-making ability. Therefore, under the influence of the herd mentality, when choosing a career, they tend to follow what others say and go with the flow, lack of a comprehensive analysis of their own ability, and lack of due decisiveness and persistence when making decisions. Blind following psychology not only hinders college students to play their own subjective initiative but also limits the potential of college students to play in a deeper level. They are easy to lose themselves and unable to overcome their own limitations to achieve greater achievements. To avoid the bind following psychology, fresh graduates need to be personalized when making career plans. That is, according to their own conditions and requirements, combined with professional development prospects and social development interests, a rational employment plan with personalized characteristics is formulated. They also need to

know their own interests, temperament, and personality. Rational thinking is conducive to the development of a full-life career. They should adjust career mentality and correct understanding of self. Self-development is very important [22].

3. Methods

3.1. Research Object. Under the premise of voluntary participation, a total of 359 medical students from 8 classes in a medical university were selected as the object of the questionnaire survey. Finally, 325 valid questionnaires were collected with a recovery rate of 90.53%. There were 143 male graduates aged 23-25 with an average age of 23.55 (SD, 0.70) years and 182 female graduates aged 23-24 with an average age of 23.19 (SD, 0.35) years. All the graduates involved in the survey have completed the undergraduate study and can be awarded the bachelor's degree according to the regulations of the university [23].

3.2. Survey Methods

(1) General investigation: a preliminary investigation and statistics were made on the gender, age, success of postgraduate entrance examination (admission notice shall prevail), and employment (employment agreement shall prevail) of the graduates who participated in the survey

(2) Beck Pressure Scale was used to measure the stress status of medical college graduates. Beck-Srivastava Stress Inventory (BSSI) consisted of 46 items, which could be used to investigate the stressors and stress intensity of graduates. In terms of pressure sources, 6 items were designed and the graduates were asked to rank the most common items such as economic pressure, love pressure, interpersonal relationship, family problems, academic problems, prospects, and employment, so as to determine the most important pressure sources faced by the graduates. In terms of stress intensity, 40 items were designed and each item was scored on a scale of 1-5, with 1 indicating "no pressure," 2 indicating "very light pressure," 3 indicating "moderate pressure," 4 indicating "excessive pressure," and 5 indicating "great pressure." Four factors closely related to stress intensity, including learning pressure (specifically associated with 10 items), economic pressure (specifically associated with 10 items), interpersonal relationship (specifically associated with 10 items), and clinical practice (specifically associated with 10 items), can be tested and scored. The scores of specific associated items of each factor were added to obtain the total score of the factor, and the total scores of the four factors were added to obtain the final BSSI score. According to the standards set by the original work, the detection criteria of graduates with great pressure are as follows.

$$\begin{gathered}\text{BSSI Factor score} \geq 3 \text{ score},\\ \text{BSSI Total score} \geq 72 \text{ score}\end{gathered} \tag{1}$$

Cronbach's a of BSSI was confirmed by using it in premedical students and domestic adolescents as follows.

$$\text{BSSI} = 0.82 \sim 0.90. \tag{2}$$

Therefore, it can accurately detect the pressure of graduates who participate in the survey.

Symptom Check List 90 (SCL-90), also known as the symptom self-rating scale, consists of 90 items. Each item is scored on a 1-5 scale, with 1 indicating "no symptoms," 2 indicating "very mild symptoms," 3 indicating "moderate symptoms," 4 indicating "severe symptoms," and 5 indicating "severe symptoms." Somatization (12 items of specific association), compulsion (10 items of specific association), interpersonal relationship (9 items of specific association), depression (13 items of specific association), anxiety (10 items of specific association), hostility (specific association six items), horror concrete association (7 items of specific association), paranoid (6 items of specific association), and psychosis (7 items of specific association) closely related to mental health factors are tested (another 7 items without specific factor, in as "other"). The total score of the associated items of each factor is added to obtain the total score of the factor, and the total score of the 10 factors is added to obtain the final SCL-90 score. The detection criteria for possible mental health problems are as follows.

$$\begin{gathered}\text{SCL} - 90\text{Total score} \geq 160\text{score},\\ \text{Positive factor number} \geq 43\text{item},\\ \text{The average of a single factor points} \geq 2\text{score}.\end{gathered} \tag{3}$$

Cronbach's α of SCL-90 in domestic medical students can reach 0.945, so it can accurately detect the mental health status of graduates involved in the survey.

(3) Quality control

The whole process of the survey was completed under the guidance of student management workers (counselors or deputy secretaries of the General Branch of the CPC, all with national psychological counseling teacher qualification). If the graduates who participated in the survey have any questions about the specific questions of the questionnaire, they are answered on the spot. Incomplete answers, difficult to identify after alteration, and $L \geq 7$ points in TABP questionnaire were excluded.

(4) Statistical treatment

All inputs were recorded by statistical professionals and processed by SPSS20.0 statistical analysis software. If the quantitative variables followed normal distribution, mean $\pm$ standard deviation ($X \pm \text{SD}$) was used to describe them; otherwise, median (interquartile spacing) was used to represent them. On the premise that the relevant quantitative

Table 1: Mental health status score.

Gender	Male students	Female students	P
BSSI score	102.05 ± 2.01	94.51 ± 1.05	<0.05

Table 2: Mental health status by gender.

SCL-90	Male students	Female students	P
Somatization	1.95 ± 0.01	1.94 ± 0.02	>0.05
Compulsion	1.84 ± 0.15	1.87 ± 0.09	>0.05
Interpersonal relationship	1.75 ± 0.14	1.74 ± 0.10	>0.05
Depression	1.92 ± 0.08	2.00 ± 0.10	>0.05
Anxiety	1.70 ± 0.10	1.71 ± 0.20	>0.05
Hostility	7.25 ± 0.16	7.31 ± 0.04	>0.05
Terror	1.35 ± 0.41	1.40 ± 0.02	>0.05
Paranoid	1.29 ± 0.17	1.30 ± 0.10	>0.05
Psychosis	1.33 ± 0.64	1.34 ± 0.58	>0.05

Table 3: Mental health status of different mental capital.

SCL-90	High pressure	Low pressure	P
Somatization	2.00 ± 0.17	1.99 ± 0.10	>0.05
Compulsion	2.30 ± 0.08	1.80 ± 0.11	<0.05
Interpersonal relationship	1.61 ± 0.20	1.60 ± 0.09	>0.05
Depression	1.87 ± 0.09	1.87 ± 0.15	>0.05
Anxiety	1.80 ± 0.11	1.74 ± 0.19	>0.05
Hostility	1.30 ± 0.20	1.31 ± 0.15	>0.05
Terror	1.39 ± 0.14	1.40 ± 0.13	>0.05
Paranoid	1.48 ± 0.10	1.45 ± 0.20	>0.05
Psychosis	1.50 ± 0.11	1.47 ± 0.12	>0.05

variables approximately conform to the normal distribution, multiple linear regression was used to analyze the specific factors affecting the mental health of medical college graduates. For the comparison of quantitative data between the two groups, t test was used if the variance was uniform; otherwise, rank sum test was used, and $P < 0.05$ was used as the criterion for statistically significant difference.

4. Results

4.1. Mental Health Status Score. The BSSI score of male students (102.05 ± 2.01) shows no statistical significance compared with that of female students ($P > 0.05$), as shown in Table 1.

4.2. Mental Health Status by Gender. SCL-90 scores of male students include somatization (1.95 ± 0.01), compulsion (1.84 ± 0.15), interpersonal relationship (1.75 ± 0.14), depression (1.92 ± 0.08), anxiety (1.70 ± 0.10), hostility (7.25 ± 0.16), terror (1.35 ± 0.41), bigotry (1.29 ± 0.17), and psychosis (1.33 ± 0.64) which had no significant difference compared with female students ($P > 0.05$). See Table 2.

4.3. Mental Health Status of Different Mental Capital. SCL-90 scores of high stress graduates include somatization (2.00 ± 0.17), compulsion (2.30 ± 0.08), interpersonal relationship (1.61 ± 0.20), depression (1.87 ± 0.09), anxiety (1.80 ± 0.11), hostility (1.30 ± 0.20), terror (1.39 ± 0.14), paranoid (1.48 ± 0.10), and psychosis (1.50 ± 0.11). There is significant difference between forced and low pressure graduates ($P < 0.05$). There is no statistical significance for other items ($P > 0.05$), as shown in Table 3.

5. Conclusions

Developing and accumulating psychological capital of college students is the bounden responsibility of universities and college students themselves. The psychological capital of college students can be fully explored only when universities and students make joint efforts to create a good

atmosphere and conditions and make full use of the environment and resources in all aspects.

5.1. Campus Environment. The school needs to create a harmonious and loose campus culture environment, improve the psychological quality of students, and cultivate the soil for the growth of college students' psychological capital. The campus culture can improve college students' sense of identity and belonging and encourage them to read, study, practice, and participate in various activities of enthusiasm, initiative, and creativity. Through a variety of promotions, management system, and evaluation system, colleges and universities should promote and encourage all students to participate in various campus culture activities and practice, so as to find and focus on a few college students with no practical experience. For this part of the students, the psychological capital is scarce. They are in urgent need to be provided psychological assistance. College mental health education and counseling center should intensify propaganda, build a set of mature psychological problem prevention and intervention mechanism through a variety of forms, and make college students actively seek counseling staff to help when meeting problems, so as to ensure that the college students' psychological problems can be found in time and more serious problems can be avoided.

5.2. Career Guidance. Colleges and universities should improve the employment guidance work, pay attention to the rich resources of college students, and improve the students' self-confidence. Colleges and universities should improve the employment guidance institutions, ensure that the division of labor is clear, enhance the service consciousness of staff, and highlight their professionalism. The employment guidance institutions of colleges and universities should maintain cooperation with professional talent assessment, intermediary agencies, and employers. The employment guidance should run through college students' career planning, job hunting guidance, entrepreneurship education, and follow-up investigation after entry. College students' own resources should be explored and utilized through the personal achievement stories, career interviews, and career experience reports, so as to encourage each other, experience success repeatedly, and enhance the sense of self-efficacy. Through students to tell about the positive qualities of self-confidence, sincerity, diligence, tenacity, optimism, and gratitude of people and things, multilevel model groups are established, so as to improve the value system of college students and enhance the confidence of college students to enter the society and employment.

5.3. Social Support. College students should be pleased with themselves, actively engage in practice, establish their own social support system, and develop and improve their psychological capital. Many college students cannot recognize their own advantages, nor can they face up to or even try to cover up their shortcomings. They are unable to accept and be pleased with themselves, and it is difficult to produce real confidence. Only when college students tolerate and accept everything about themselves, cherish the present, plan the future carefully, and believe that their imperfect selves can still create a wonderful life can they truly possess self-confidence. College students can accumulate experience, improve their knowledge structure, improve practical ability, and cultivate innovative spirit by actively participating in various extracurricular practical activities. Lack of social practice and work experience is an important reason for many college students' employment difficulties. A college student who actively participates in social practice shows maturity, self-confidence, optimism, and active communication and coordination skills. Therefore, when encountering various difficulties in life, study, and emotion, he or she can be more patient and actively try to solve problems. An effective social support system can give college students confidence and strength when they encounter setbacks, so that they can recover their courage and have a strong will and finally overcome difficulties and achieve success. The psychological capital stored by college students will extend to their future professional life and long-term life development. Therefore, colleges and universities should fully realize the importance of developing the psychological capital of college students, create a good campus environment, and provide necessary support for college students, so as to realize the educational function of the university. College students themselves should be deeply aware of the important role of psychological capital in promoting employability and career development and continue to accumulate their own positive psychological capital, improve their competitiveness, and take responsibility for their own development.

Data Availability

The labeled data set used to support the findings of this study is available from the corresponding author upon request.

Conflicts of Interest

The author declares that there are no conflicts of interest.

Acknowledgments

This work was supported by the 2020 Guangxi Higher Education Undergraduate Teaching Reform Project "research and practice of hybrid teaching mode of college students' mental health based on SPOC platform" (Project No. 2020JGA379).

References

[1] G. Dhiman, V. Kumar, A. Kaur, and A. Sharma, "Don: deep learning and optimization-based framework for detection of novel coronavirus disease using x-ray images," *Interdisciplinary Sciences Computational Life Sciences*, vol. 13, no. 2, pp. 260–272, 2021.

[2] P. Ajay, B. Nagaraj, and J. Jaya, "Bi-level energy optimization model in smart integrated engineering systems using WSN," *Energy Reports*, vol. 8, pp. 2490–2495, 2022.

[3] J. Liu, X. Liu, J. Chen, X. Li, T. Ma, and F. Zhong, "Investigation of ZrMnFe/sepiolite catalysts on toluene degradation in

Hindawi
Computational and Mathematical Methods in Medicine
Volume 2023, Article ID 9869456, 1 page
https://doi.org/10.1155/2023/9869456

Retraction

Retracted: Management of Patients with Cervicofacial Edema and Paresthesia during Perioperative Period of Transoral Endoscopic Thyroidectomy

Computational and Mathematical Methods in Medicine

Received 1 August 2023; Accepted 1 August 2023; Published 2 August 2023

This article has been retracted by Hindawi following an investigation undertaken by the publisher [1]. This investigation has uncovered evidence of one or more of the following indicators of systematic manipulation of the publication process:

(1) Discrepancies in scope

(2) Discrepancies in the description of the research reported

(3) Discrepancies between the availability of data and the research described

(4) Inappropriate citations

(5) Incoherent, meaningless and/or irrelevant content included in the article

(6) Peer-review manipulation

The presence of these indicators undermines our confidence in the integrity of the article's content and we cannot, therefore, vouch for its reliability. Please note that this notice is intended solely to alert readers that the content of this article is unreliable. We have not investigated whether authors were aware of or involved in the systematic manipulation of the publication process.

Wiley and Hindawi regrets that the usual quality checks did not identify these issues before publication and have since put additional measures in place to safeguard research integrity.

We wish to credit our own Research Integrity and Research Publishing teams and anonymous and named external researchers and research integrity experts for contributing to this investigation.

The corresponding author, as the representative of all authors, has been given the opportunity to register their agreement or disagreement to this retraction. We have kept a record of any response received.

References

[1] X. Yang, J. G. Zhao, M. Liu, S. Wang, and L. Wang, "Management of Patients with Cervicofacial Edema and Paresthesia during Perioperative Period of Transoral Endoscopic Thyroidectomy," *Computational and Mathematical Methods in Medicine*, vol. 2022, Article ID 4775264, 9 pages, 2022.

Hindawi
Computational and Mathematical Methods in Medicine
Volume 2022, Article ID 4775264, 9 pages
https://doi.org/10.1155/2022/4775264

Research Article

Management of Patients with Cervicofacial Edema and Paresthesia during Perioperative Period of Transoral Endoscopic Thyroidectomy

Xia Yang,[1] Jian Guo Zhao,[1] Mengting Liu,[1] Shan Wang,[1] and Li Wang[2]

[1]*Department of Thyroid and Breast Surgery, Wuhan Number 1 Hospital, Tongji Medical College, Huazhong University of Science and Technology, China*
[2]*Department of Nursing, Wuhan Number 1 Hospital, Tongji Medical College, Huazhong University of Science and Technology, China*

Correspondence should be addressed to Li Wang; 16011010321@stu.suse.edu.cn

Xia Yang and Jian Guo Zhao contributed equally to this work.

Received 3 August 2022; Revised 11 August 2022; Accepted 23 August 2022; Published 28 September 2022

Academic Editor: Min Tang

Objective. To analyze the clinical intervention effect of transoral endoscopic thyroidectomy on the neck and face during perioperative period. *Method*. From January 2019 to January 2020, 60 patients included in this study were randomly divided into observation group and control group according to the ratio of 1 : 1, with 30 cases in each group. Both groups underwent rapid surgical intervention during the perioperative period. The patients in the observation group received neck and face management. The degree of jaw swelling, the degree of facial microexpression completion, and the changes in jaw and neck sensation were compared between the two groups. *Results*. There was no significant difference in neck and face swelling, pain, facial microexpression, and feeling between the two groups before operation. Patients with facial I/II swelling degree in the observation group were significantly more than in the control group, and the patients with III swelling degree were less than in the control group. There was significant difference for facial swelling between the two groups in the three intervention periods after the operation, and the difference was statistically significant ($P < 0.05$). The scores of facial microexpression in the observation group were higher than those in the control group during the three postoperative intervention periods, with statistical significance ($P < 0.05$). There was no significant difference in the pain score of the first day after surgery between the two groups ($P = 0.298$). In the other two postoperative intervention periods, the pain score of the observation group was lower than that of the control group, with a statistically significant difference, and the difference was statistically significant ($P < 0.05$). The threshold of chin and neck sensory pressure in the two groups was statistically significant ($P < 0.05$) except that the "cheek in area 4" ($P = 0.290$). *Conclusion*. The results showed that these interventions, such as the elevation of bed after operation, 24-hour intermittent cryotherapy, ice cubes in mouth, and the "meter" functional training, have good clinical effects on the symptoms of facial swelling and abnormal sensation of neck and face. It can accelerate the speed of edema dissipation, improve the patients' postoperative comfort, and improve the satisfaction and quality of life of patients with the effect of surgery and beauty.

1. Introduction

The incidence of thyroid diseases has been increasing in recent years, and timely and good treatment is the key to alleviate adverse symptoms [1]. Traditional thyroid surgery is mature and safe, but it will have a great impact on the maxillofacial aesthetics of patients [2]. With the progress of medical technology, the deepening of ESAR, and improvement of patients' aesthetics requirements, the oral endoscopic thyroidectomy has developed rapidly due to its

advantages such as hidden scar, no wound on the body surface, and quick healing, which meets people's pursuit of minimally invasive effect and the aesthetics requirements, and has gradually become one of the routine operations in thyroid and breast surgery [2–4].

The corresponding complications of the new operation are different from other operations. Clinical practice found that oral endoscopic thyroidectomy compared with the traditions is prone to submandibular ecchymosis, mental nerve injury, facial muscle injury, and other complications affecting the lower lip and mandible motor sensory abnormalities. At present, reports of oral endoscopic thyroidectomy in China are gradually increasing, but there is little attention to the complications related to physical and psychological comfort caused by short-term decrease in facial beauty and paresthesia after surgery and no comprehensive clinical intervention measures. However, relevant studies [5] have shown that due to the particularity of the operation and physical structure of the surgical incision, postoperative tissue edema is prone to occur.

Therefore, it is urgent to strengthen the neck and face management of perioperative transoral endoscopic thyroid patients in order to reduce postoperative psychological pressure of patients, improve satisfaction with cosmetic effect and quality of life, and provide reference for later treatment. Reactive swelling is currently considered to be traumatic swelling caused by surgery, which usually occurs 2~3 days after surgery [6], resulting in facial swelling, pain, numbness, and so on. It is easy to cause anxiety and reduce the patients' satisfaction with cosmetic effect and quality of life. In recent years, our hospital has carried out more than 200 sets of oral thyroid surgery. The purpose of this study is to objectively evaluate the facial edema and skin sensation of patients after oral endoscopic thyroidectomy based on the Semmes-Weinstein test theory, combined with the related measuring instruments and evaluation tools, so as to provide clinical reference for the prevention and nursing of postoperative edema, pain, facial microexpression damage, and other complications. Now, the following report is made.

2. Materials and Methods

2.1. Patients. 60 patients were enrolled in our study from January 2019 to January 2020 and were randomized into observation group and control group in 1 : 1 ratio, with 30 cases in each group. Any public report related to the results of this study will not disclose the patient's personal identity, and the patient's personal data will be strictly confidential. All patients underwent thyroid function test, thyroid ultrasonography, enhanced thyroid CT, and other routine examinations during preoperative and hospitalization. The associated surgical risks were fully passaged to the patient, respecting the patient's autonomy. There was no significant difference between the two groups in age, gender, BMI, nature of lesion, tumor diameter, and weight of resected tumor ($P > 0.05$), and the results are shown in Table 1. The qualifications of surgeons and nurses in the two groups were the same. This study was in line with the Declaration of Helsinki. Informed consent was signed before the study, and patients voluntarily participated in this study.

Table 1: Patients' characteristics.

Variables	Observation group ($n = 30$)	Control group ($n = 30$)	P
Age (year)	39.10 ± 11.24	41.03 ± 7.93	0.445
Gender (n)			
Male	3	27	0.685
Female	4	26	
BMI (kg/m^2)	20.08 ± 1.75	20.34 ± 1.75	0.573
Nature of lesion (n)			
Benign	23	7	0.519
Malignant	25	5	
Tumor diameter (cm)	1.78 ± 0.42	1.69 ± 0.52	0.486
Weight of resected tumor (g)	18.92 ± 1.55	18.31 ± 2.04	0.195

2.2. Inclusion and Excluding Criteria. The surgical indications and contraindications of patients were referred to "Expert Consensus on Endoscopic Thyroidectomy Via Oral Vestibular Approach (2018)" [7]. Inclusion criteria are as follows: (1) benign thyroid tumor ≤ 5 cm; (2) ≤1 cm thyroid micropapillary carcinoma with no evidence of metastasis; (3) the lesion was unilateral tumor by thyroid ultrasonography; and (4) patients have the willingness for cosmetic surgery. Exclusion criteria are as follows: (1) history of jaw and neck surgery; (2) severe heart, brain, lung, kidney, and other diseases that affect the safety of surgery; (3) thyroid tumors are located in the upper pole of the thyroid; and (4) a history of severe cervical spondylosis.

2.3. Surgical Methods. All 60 patients used mouthwash to clean their mouths before operation, took the supine position with the neck hyperextension, and intubated the trachea through the mouth for general anesthesia. The cervical white line was incised, and the thyroid gland was exposed. Unilateral lobotomy with (or without) ipsilateral central lymph node dissection was performed, oral vestibular mucosa was sutured with absorbable suture [7], and the specimens were sent to the department of pathology for examination. During the operation, three incisions (1.5 cm, 5 mm, and 5 mm) were made through the oral vestibule, and the endoscope and instruments were placed from the oral vestibule to reach the thyroid region. The subcutaneous tissue was separated by ultrasonic scalpel, and the operation space was established.

2.4. Study Design

2.4.1. Fast Track Surgery. All patients were given clinical intervention of fast track surgery.

(1) Preoperative. (A) Comprehensive assessment of the patient's basic diseases and physical conditions was conducted. For example, patients with lung diseases or smokers

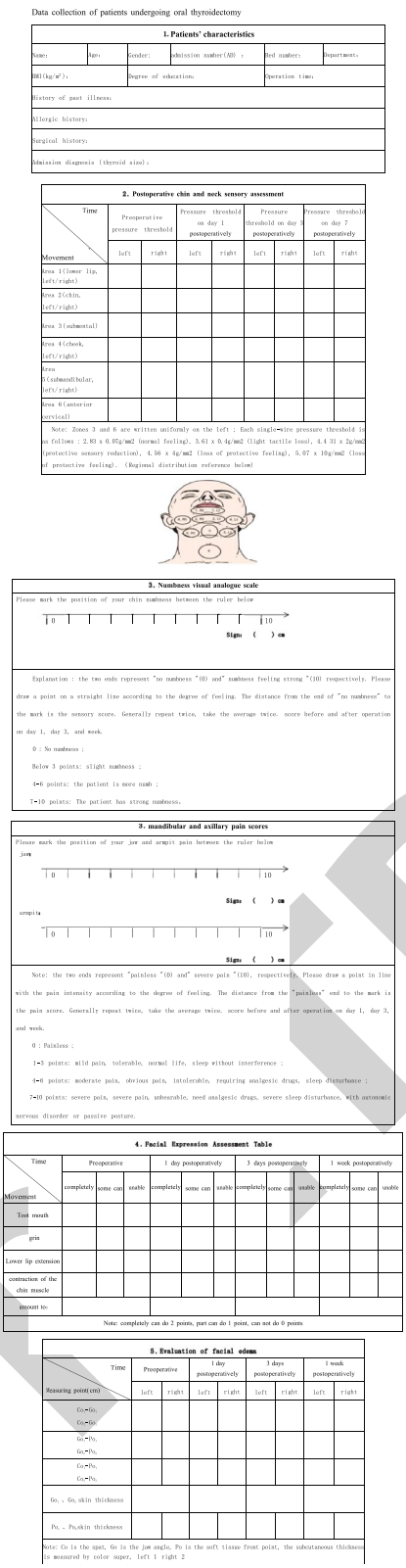
Data collection of patients undergoing oral thyroidectomy

1. Patients' characteristics

Name:	Date	Gender:	Admission number(AD) :	Bed number:	Department:
BMI(kg/m²):		Degree of education:		Operation time:	
History of past illness:					
Allergic history:					
Surgical history:					
Admission diagnosis (thyroid size):					

2. Postoperative chin and neck sensory assessment

Time / Movement	Preoperative pressure threshold		Pressure threshold on day 1 postoperatively		Pressure threshold on day 3 postoperatively		Pressure threshold on day 7 postoperatively	
	left	right	left	right	left	right	left	right
Area 1(lower lip, left/right)								
Area 2(chin, left/right)								
Area 3(submental)								
Area 4(cheek, left/right)								
Area 5(submandibular, left/right)								
Area 6(anterior cervical)								

Note: Zones 3 and 6 are written uniformly on the left ; Each single-wire pressure threshold is as follows : 2.83 x 0.07g/mm2 (normal feeling), 3.61 x 0.4g/mm2 (light tactile loss), 4.4 31 x 2g/mm2 (protective sensory reduction), 4.56 x 4g/mm2 (loss of protective feeling), 5.07 x 10g/mm2 (loss of protective feeling). (Regional distribution reference below)

3. Numbness visual analogue scale

Please mark the position of your chin numbness between the ruler below

0 ——— 10

Sign: ( ) cm

Explanation : the two ends represent "no numbness "(0) and" numbness feeling strong "(10) respectively. Please draw a point on a straight line according to the degree of feeling. The distance from the end of "no numbness" to the mark is the sensory score. Generally repeat twice, take the average twice. score before and after operation on day 1, day 3, and week.

0 : No numbness ;

Below 3 points: slight numbness ;

4-6 points: the patient is more numb ;

7-10 points: The patient has strong numbness.

3. mandibular and axillary pain scores

Please mark the position of your jaw and armpit pain between the ruler below

jaw

0 ——— 10

Sign: ( ) cm

armpits

0 ——— 10

Sign: ( ) cm

Note: the two ends represent "painless "(0) and" severe pain "(10), respectively. Please draw a point in line with the pain intensity according to the degree of feeling. The distance from the "painless" end to the mark is the pain score. Generally repeat twice, take the average twice. score before and after operation on day 1, day 3, and week.

0 : Painless ;

1-3 points: mild pain, tolerable, normal life, sleep without interference ;

4-6 points: moderate pain, obvious pain, intolerable, requiring analgesic drugs, sleep disturbance ;

7-10 points: severe pain, severe pain, unbearable, need analgesic drugs, severe sleep disturbance, with autonomic nervous disorder or passive posture.

4. Facial Expression Assessment Table

Time / Movement	Preoperative			1 day postoperatively			3 days postoperatively			1 week postoperatively		
	completely	some can	unable	completely	some can	unable	completely	some can	unable	completely	some can	unable
Close mouth												
grin												
Lower lip extension												
contraction of the chin muscle												
Amount to:												

Note: completely can do 2 points, part can do 1 point, can not do 0 points

5. Evaluation of facial edema

Time / Measuring point(cm)	Preoperative		1 day postoperatively		3 days postoperatively		1 week postoperatively	
	left	right	left	right	left	right	left	right
C_0-I_{O_1}								
C_0-I_{O_2}								
C_0-P_{O_1}								
C_0-P_{O_2}								
C_0-C_0 skin thickness								
P_{O_1}-P_{O_1} skin thickness								

Note: Co is the spot, Go is the jaw angle, Po is the soft tissue front point, the subcutaneous thickness is measured by color super, left 1 right 2

Figure 1: Data acquisition map.

should master effective method of coughing, and aerosol inhalation treatment should be performed when necessary. (B) Patients with hypertension and diabetes need to follow

Figure 2: Semmes-Weinstein sensory measurement.

the doctor's advice and regulate the disease with rational drug use and diet guidance. (C) According to the patient's individual situation, one-to-one health education was carried out to introduce the operating room environment, intraoperative cooperation methods, and relevant matters needing attention, and emphasizing the advantages and methods of the concept of ERAS. (D) The skin and oral were cleaned before surgery. Gargling with oral cleaning solution and rinsing three times a day were made by our hospital. Teeth were cleaned if necessary. (E) Oral administration of 5% glucose 100 ml from the morning of the operation day was done. (F) Starting from the day of admission, surgical posture training was performed, including neck relaxation exercise, neck hyperextension training, deep breathing, and balloon blowing training, so as to improve the tolerance of anesthesia and reduce the risk of anesthesia. (G) The patients' psychological changes were dynamically grasp, psychological counseling was timely conducted, and successful treatment cases were explained to patients, to improve their confidence and eliminate anxiety and fear.

(2) Intraoperative. (A) The patient's vital signs and the changes in the amount of access were closely observed. (B) Keep the temperature and humidity in the operating room appropriate to reduce the unavoidable exposure during the operation. (C) The operator should move gently and follow the principle of sterility.

(3) Postoperative. (A) After the operation, the patients returned to the ward and were properly placed. The patients who were not awake after anesthesia went to the pillow and lay on their back, with their head tilted to one side. Vital signs were monitored, and special attention was paid to breathing and wound conditions. The respiratory tract was kept unobstructed and low flow oxygen inhalation was given. (B) Pressure bandaging under jaw was applied on the1st day after operation to reduce local edema. If the swelling was alleviated, the time of the head cover could be reduced. (C) If necessary, aerosol inhalation should be performed as instructed by the doctor to reduce respiratory edema and prevent infection. (D) Instruct the patients to pay attention to the protection of the operation area during

Table 2: Comparison of swelling degree between two groups before and after intervention.

Group	n	Intervention time															
		Pre-op				Post-op 1 day				Post-op 3 days				Post-op 1 week			
		0	I	II	III	0	I	II	III	0	I	II	III	0	I	II	III
Observation group	30	30	0	0	0	0	4	20	6	0	11	18	1	6	23	1	0
Control group	30	30	0	0	0	0	0	21	9	0	6	20	4	0	21	9	0
Z		0				-6.140				-2.032				-3.492			
P		>0.05				<0.05				0.042				<0.05			

Abbreviations: Pre-op, preoperative; Post-op, postoperative.

Table 3: Comparison of VAS (pain) and facial microexpression score between the two groups.

Group	n	Visual analogue pain score (points, $\bar{x}\pm s$)				Facial microexpression score (points, $\bar{x}\pm s$)			
		Pre-op	Post-op 1 day	Post-op 3 days	Post-op 1 week	Pre-op	Post-op 1 day	Post-op 3 days	Post-op 1week
Observation group	30	0.00	5.17 ± 1.56	2.37 ± 1.07	1.50 ± 1.01	8.00	1.60 ± 0.81	3.00 ± 1.08	6.47 ± 0.97
Control group	30	0.00	5.57 ± 1.38	3.17 ± 0.75	2.67 ± 1.24	8.00	1.20 ± 0.61	2.03 ± 0.96	4.90 ± 1.37
t		NA	-1.051	-3.366	-3.996	NA	2.154	3.652	5.098
P		NA	0.298	0.001	<0.05	NA	0.036	0.001	<0.05

activities and coughing. (E) If there was no discomfort for 6 h after surgery, the patient could take a semireclining and prevent the neck violent activity. If the vital signs were stable and the anesthesia was fully awake, patients can drink a small amount of water. If there was no other discomfort, liquid diet could be given. After 24 hours of operation, you can gradually transition to semi liquid, soft food, and common food and gargle with mouthwash before and after eating. (F) After anesthesia, turning over and stretching of limbs can be carried out on the bed, and in the first day after operation, voice training can be carried out in the early stage.

(4) Discharge Guidance. Patients received discharge and dietary guidance [8], and outpatient follow-up was conducted one week after surgery.

2.4.2. Cervicofacial Interventions. The observation group was given cervicofacial interventions on the basis of the control group after operation:

(1) After the operation, the patient returned to the ward and was given ice compress on the operation site according to the doctor's advice. The cold treatment time was 24 hours, no more than 30 minutes each time. During this period, it should be applied after an interval of 30 minutes. The purpose is to make local vasoconstriction, reduce capillary permeability, and reduce local congestion and pain caused by tissue swelling oppressive nerve endings. It was wrapped in disposable sealing bags when putting ice, taken care to sanitize the isolation principle. During cryotherapy, the local skin condition and skin color of the patients should be observed to prevent frostbite. Check the ice bag for water leakage, listen to the complaints of the patients, and stop the cold treatment immediately if there is any abnormality

(2) At 2 h postoperatively, the patient's consciousness recovered and the bedside could be raised by 5-10° without discomfort. In the later stage, the patient's bedside should be raised step by step to maintain 30°, 60° of semidecumbent position, and 90° of the sitting position, so as to facilitate smooth incision drainage [9]

(3) After the patient is fully conscious (2 h postoperatively), the nurse wears film gloves to give an ice block to the patient to hold it in the mouth. The ice is a sphere with a radius of 1 cm and is placed at the front of the patient's tongue tip. One piece at a time was placed in the front of tongue tip and slowly swallowed in patients with conscious state if no discomfort, every 30 min to give a piece, within 6 h; the purpose was to reduce the patients with jaw tissue swelling and pain. If there were uncomfortable symptoms such as choking, let the patient's thumb web press the operation area to cough effectively

(4) Postoperative rehabilitation: at 3 days postoperatively, "meter" rehabilitation training could be started to prevent tissue scar contracture and promote blood circulation in the neck. Postoperative rehabilitation should be carried out gradually, and the actions should be slow and gentle. Avoid food of spicy and easy to plug teeth, and gargle with water after eating. Come to the hospital for reexamination one week after surgery

Table 4: Comparison of chin and neck sensation (pressure threshold) between the two groups.

Zones	Pre-op (g/mm^2, $\bar{x}\pm s$)		P	Post-op 1 day (g/mm^2, $\bar{x}\pm s$)		P	Post-op 3 days (g/mm^2, $\bar{x}\pm s$)		P	Post-op 1week (g/mm^2, $\bar{x}\pm s$)		P
	A ($n = 30$) A ($n = 30$)	B ($n = 30$) B ($n = 30$)		A ($n = 30$) A ($n = 30$)	B ($n = 30$) B ($n = 30$)		A ($n = 30$) A ($n = 30$)	B ($n = 30$) B ($n = 30$)		A ($n = 30$) A ($n = 30$)	B ($n = 30$) B ($n = 30$)	
1: lower lip												
Left	0.07 ± 0.00	0.07 ± 0.00		0.15 ± 0.43	0.61 ± 0.72	0.002	0.15 ± 0.14	0.27 ± 0.16	0.003	0.08 ± 0.60	0.16 ± 0.15	0.012
Right	0.07 ± 0.00	0.07 ± 0.00		0.23 ± 0.37	0.74 ± 0.79	0.003	0.15 ± 0.14	0.27 ± 0.16	0.003	0.08 ± 0.60	0.16 ± 0.15	0.012
2: chin												
Left	0.07 ± 0.00	0.07 ± 0.00		0.22 ± 0.37	0.67 ± 0.76	0.005	0.14 ± 0.13	0.24 ± 0.17	0.007	0.08 ± 0.60	0.15 ± 0.14	0.024
Right	0.07 ± 0.00	0.07 ± 0.00		0.22 ± 0.37	0.67 ± 0.76	0.005	0.14 ± 0.13	0.24 ± 0.17	0.007	0.08 ± 0.60	0.15 ± 0.14	0.024
3: below the chin	0.07 ± 0.00	0.07 ± 0.00		0.38 ± 0.57	0.75 ± 0.78	0.042	0.15 ± 1.14	0.28 ± 0.16	0.001	0.07 ± 0.00	0.14 ± 0.13	0.012
4: cheek			NA									
Left	0.07 ± 0.00	0.07 ± 0.00		0.20 ± 0.17	0.25 ± 0.17	0.290	0.11 ± 0.11	0.18 ± 0.16	0.069	0.10 ± 0.10	0.17 ± 0.15	0.055
Right	0.07 ± 0.00	0.07 ± 0.00		0.20 ± 0.17	0.25 ± 0.17	0.290	0.11 ± 0.11	0.18 ± 0.16	0.069	0.10 ± 0.10	0.17 ± 0.15	0.055
5: submandibular												
Left	0.07 ± 0.00	0.07 ± 0.00		0.25 ± 0.17	0.49 ± 0.62	0.044	0.13 ± 0.13	0.21 ± 0.17	0.024	0.07 ± 0.00	0.14 ± 0.13	0.013
Right	0.07 ± 0.00	0.07 ± 0.00		0.25 ± 0.17	0.50 ± 0.62	0.034	0.13 ± 0.13	0.21 ± 0.17	0.024	0.07 ± 0.00	0.14 ± 0.13	0.013
6: neck	0.07 ± 0.00	0.07 ± 0.00		0.29 ± 0.36	0.67 ± 0.67	0.050	0.14 ± 0.13	0.26 ± 0.17	0.003	0.08 ± 0.60	0.15 ± 0.14	0.027

Abbreviations: A: observation group; B: control group.

2.5. Evaluation Index

(1) The soft ruler with a standard scale was used to evaluate patients' facial swelling by the Perez-Gonzalez direct measurement color Doppler ultrasound

(2) VAS was used to evaluate patients' pain of the operation side. A self-made scale was used to evaluate to evaluate the facial microexpressions, including toot mouth, grin mouth, lower lip extension, and chin muscle contraction; VAS was used to evaluate the pain of the surgical site. Draw a 10 cm horizontal line on the paper, and the two ends indicated "painless" (0) and "severe pain" (10), respectively. According to the degree of feelings, the patient drew a point on the straight line which is consistent with the intensity of feeling, and the distance from the "painless" end to the mark is the feeling score. Generally, it was repeated twice, and the average value was taken. The scores were evaluated preoperatively, 1 day, 3 days, and 1 week after surgery

(3) Sensory changes in the chin and neck were assessed by the Semmes-Weinstein monofilament test. Chin and neck sensory evaluation [10]: the baseline nylon monofilament test of FEI company of the United States was used to objectively evaluate the sensation of 10 areas of chin, face, and neck: area 1 (lower lip, right, and left), zone 2 (chin, right and left), zone 3 (submental), zone 4 (cheek, right, and left), zone 5 (submandibular, right, and left), and zone 6 (grade VI). The basic nylon monofilament test box is designed to fully follow the Semmes-Weinstein test theory for fine tactile examination that can measure sensations from light touch to deep pressure. The strength represented by different specifications was as follows: $2.83 = 0.07\,g/mm^2$ (normal sensation), $3.61 = 0.4\,g/mm^2$ (hypotactile loss), $4.31 = 2\,g/mm^2$ (protective hypoesthesia), $4.56 = 4\,g/mm^2$ (protective loss of sensation), and $5.07 = 10\,g/mm^2$ (protective loss of sensation). The patient took the sitting position, closed his eyes, gently scratched the monofilament on the skin of the measured area, and recorded the pressure value of the lightest monofilament identified by the patient as the pressure threshold of the specified area. The measured values of the left and right areas are taken as the average

2.6. Data Collection and Analysis

2.6.1. Evaluation of Facial Edema. The patient was in the upright position, and the mouth angle (Co), mandibular angle (Go), and soft tissue premaxillary point (Po) were selected on both sides. The body surface distances of Co-Go, Co-Po, and Go-Po were measured with a soft ruler before surgery, on the first day, the third day, and one week after operation (the average values of the left and right sides were taken), and the percentage of facial swelling was calculated according to the formula: (the measured distance on the first day, the third day and one week postoperatively – the measured distance before surgery)/the measured distance before surgery × 100%. The subcutaneous thickness at Po and 2 cm beside Po point was measured by color ultrasound.

(1) Evaluation Criteria for Swelling [11]. 0 degree means appearance is basically normal and facial swelling percentage ≤ 3%; I degrees means mild swelling appearance and facial swelling percentage > 3%and ≤ 6%; II degrees means the appearance of moderate swelling and facial swelling percentage > 6%and ≤ 12%. III degrees means appearance of severe swelling, local skin, and facial swelling percentage > 12%.

(2) Facial Microexpression Evaluation. Self-made facial microexpression questionnaire was adopted, including pout, grin, lower lip extension, and chin muscle contraction. "Fully capable" was scored as "2," "partially capable" was scored as "1," and "not able" was scored as "0"; the facial microexpression scores of patients in four study periods were compared (Figures 1 and 2).

2.7. Statistical Analysis. The IBMSPSS24.0 software was applied for statistical analysis. The measurement data were expressed by mean ± standard deviation. The counting data were expressed by frequency or rate. t-test was used when measurement data obey normal distribution, and rank sum test was used when it did not obey normal distribution. χ^2 test was used to compare the classified counting data. Repeated measurement data were analyzed by repeated measurement analysis of variance. Main effect test results were used when there was no interaction, and simple effect analysis was carried out when there was interaction. $P < 0.05$ indicated that the difference between groups is statistically significant.

3. Results

(1) Comparison of the degree of swelling between the two groups showed that there was no significant difference before surgery ($P > 0.05$). After intervention, there were statistically significant differences in the degree of swelling on the first day, the third day, and the week after surgery, and the difference was statistically significant ($P < 0.05$); results are shown in Table 2

(2) Preoperative VAS and facial microexpression score of the two groups were all within the normal range and were not comparable ($P > 0.05$). The VAS of the two groups was not statistically significant except "the 1st day after surgery" ($P = 0.298$), and the other two postoperative intervention periods were statistically significant. The scores of facial microexpression in the observation group were all higher than those in the control group during the 3 postoperative

intervention periods, and the difference was statistically significant ($P < 0.05$), as shown in Table 3

(3) The preoperative pressure threshold values of chin and neck in the two groups were all within the normal sensory range and were not comparable. Postoperatively, except for the "cheek in area 4" data, which was not statistically significant ($P > 0.05$), and the difference was statistically significant ($P < 0.05$) at the time of postoperative intervention, which was statistically significant (see Table 4 for details)

4. Discussion

In this study, we found that the incision of patients undergoing endoscopic oral thyroidectomy was hidden, which brought some difficulties to the observation and nursing of postoperative incision swelling and bleeding. According to the anatomy of the mandible, oral vestibular incision may cause mental nerve injury and facial expression muscle injury, which has a certain impact on the motor and sensory function of the lower lip and mandible [12, 13]. It was reported that the lesions of the mental nerve were about 0.7%~33.3% [12, 14]. This study enrolled 60 patients with oral endoscopic thyroid surgery according to the standards of aspiration and drainage, to explore postoperative intervention measures, aimed at providing clinical reference value for patients with better recovery in the later stage.

This study was carried out for one year under the standard of admission and exclusion. Through setting up the control group and the observation group, and taking the corresponding clinical intervention, it was found that all patients in the study had swelling of mandible and neck, abnormal sensation, facial microexpression damage, and pain on the 1st day after operation, which may be caused by too much chin muscle transection during the central incision and chin muscle tearing caused by operation leverage [15]. The neck incision is hidden in the oral vestibule by oral endoscopic thyroidectomy to achieve the purpose of neck beauty and improve patients' satisfaction with the beauty effect. Our jaw and lower lip not only have the same aesthetic function as the neck skin but also have important social functions in daily life [15]. Serious swelling of patients in postoperative may lead to appearance of psychological disorder such as mouth restriction and self-image disorder, which may affect the work, life, and interpersonal communication, resulting in the decline of patients' quality of life. However, with the management of effective interventions and the extension of postoperative time, the degree of discomfort decline and recovery in the observation group was better than that in the observation group. Except for "VAS" and "cheek in the 4th zone" on the 1st day after operation, the other data of the two groups were statistically significant ($P < 0.05$), which may be related to the body stress reaction, surgical site, and incision.

Giving ice to patients after operation can effectively reduce the patient's oral temperature, the proliferation of oral bacteria, and mandibular edema. At the same time, melting ice water is slowly swallowed by patients, which is conducive to improving the comfort of patients. Therefore, keen observation and serious sense of responsibility are the keys to complete clinical work and reduce complications. Interval cryotherapy within 24 hours after surgery can slow down local blood flow, help blood clotting and control bleeding, and reduce pain caused by tissue swelling. Postoperative patients are prone to lower lip and jaw swelling, combined with high oral temperature and preoperative water prohibition. The proper and gradual elevation of the head of the bed and the cryotherapy can safely and effectively drain and accelerate the speed of facial edema dissipation, which is similar to the research results of Yuping et al. [9]. Meanwhile, according to the relevant results, it is safe to treat nerve injury by endoscopic thyroidectomy, which is the same as KYung [11].

Relevant data [16, 17] showed that continuous ice compress can reduce the sensitivity of local nerve endings and cells, thus increasing the pain threshold or shortening the pain time. Enwemeka et al. [18] found that ice compress therapy can reduce the temperature of tissue 2 cm below the skin and found that there is blood exchange between deep and shallow tissues, which explains that ice compress therapy can effectively reduce swelling and pain of local tissues. Swenson et al. [19] considered that the difference of the curative effect of ice compress lies in the difference of using method through applying ice compress to soft tissue trauma in the early stage of sports medicine. Although it is effective for patients to reduce swelling, if continuous ice compress method is adopted and ice compress medium is replaced, whether the speed of patients' swelling is faster than intermittent ice compress therapy needs further study [20–24].

Process and behavioral outcomes are just one way to measure impact. Results related to postoperative quality of life and patient satisfaction should be considered [25–29]. Similarly, the feedback and opinions of medical staff are equally important. These should be the themes of future research. The limitation of this study lies in the lack of follow-up of patients after discharge. In the next study, we should extend the study time and strengthen the intervention of patients' continuing care, so as to quantitatively evaluate the postoperative quality of life of patients. This study still has some shortcomings. Firstly, the quality of this study is limited due to the small sample size we included in the study. Secondly, this research is a single-center study and our findings are subject to some degree of bias. Therefore, our results may differ from those of large-scale multicenter studies from other academic institutes. This research is still clinically significant, and further in-depth investigations will be carried out in the future.

5. Conclusion

Intervention management of cervicofacial edema and paresthesia during perioperative period of oral endoscopic thyroidectomy can effectively reduce postoperative facial edema, accelerate the dissipation of swelling, improve

postoperative sensory comfort, and improve the satisfaction of patients with surgical effect and quality of life.

Data Availability

The datasets used and analyzed during the current study are available from the corresponding author upon reasonable request.

Conflicts of Interest

The authors declare that they have no conflicts of interest.

Authors' Contributions

Jian Guo Zhao and Xia Yang contributed equally to the article and share the first author.

Acknowledgments

This study was financially supported by the 2017 Wuhan Municipal Health Commission Medical Research Project Youth Project (WX17Q01).

References

[1] W. Gao, *Clinical Diagnosis and Treatment of Thyroid Nodules Coexisting with Other Solid Tumors*, Anhui Medical University, Hefei, 2017.

[2] D. A. Diniz, K. K. N. Gonçalves, C. C. G. Silva et al., "Complications associated with submental liposuction: a scoping review," *Medicina Oral, Patología Oral y Cirugía Bucal*, vol. 27, no. 3, pp. e257–e264, 2022.

[3] S. B. Zhan, X. W. Peng, and X. Zhou, "Clinical application of transoral vestibular endoscopic thyroidectomy," *Chinese Journal of Otorhinolaryngology-Skull Base Surgery*, vol. 24, no. 1, pp. 87–90, 2018.

[4] D. Q. Zhang, C. W. Wu, D. Inversini et al., "Lessons learned from a faulty transoral endoscopic thyroidectomy vestibular approach," *Surgical Laparoscopy, Endoscopy & Percutaneous Techniques*, vol. 28, no. 5, pp. e94–e99, 2018.

[5] Z. Litao, "Analysis and nursing care of complications after oral vestibular endoscopi-c thyroidectomy," *Journal of Guangzhou Medical University*, vol. 46, no. 2, pp. 107–112, 2018.

[6] G. B. Grossi, C. Maiorana, R. A. Garramone, A. Borgonovo, L. Creminelli, and F. Santoro, "Assessing postoperative discomfort after third molar surgery: a prospective study," *Oral and Maxillofacial Surgery*, vol. 65, no. 5, pp. 901–917, 2007.

[7] W. Ping, W. Guoyang, T. Wen, T. Wen, and F. Youben, "Oral vestibular approach to endoscopic thyroid surgery: a review," *China real With surg*, vol. 38, no. 10, pp. 1104–1107, 2018.

[8] Y. Wang and W. Xue, "Clinical application of rapid rehabilitation surgical nursing intervention in perioperative period of thyroid cancer," *Oncology Clinical and Rehabilitation*, vol. 27, no. 7, pp. 889–892, 2020.

[9] Y. Gao, L. Meifeng, C. Yu, and M. Zheng, "Journal of prevention and treatment for thyroid tumor surgery," *Chinese Journal of Nursing*, vol. 26, no. 26, pp. 3673–3676, 2010.

[10] K. Tae, D. W. Lee, H. S. Bang, Y. H. Ahn, J. H. Park, and D. S. Kim, "Sensory change in the chin and neck after transoral thyroidectomy: prospective study of mental nerve injury," *Head & Neck*, vol. 42, no. 11, pp. 3111–3117, 2020.

[11] M. Wang, *Effects of Different Cold Compressing Methods on Swelling and Pain after Mandibular Impacted Wisdom Teeth Extraction*, Fujian Medical University, 2016.

[12] X. W. Peng, Z. Li, H. Li et al., "The clinical application of mental nerve dissection in transoral endoscopic thyroidectomy via an oral vestibular approach," *Surgical Endoscopy*, vol. 34, no. 1, pp. 153–158, 2020.

[13] S. Celik, O. Makay, M. D. Yoruk et al., "A surgical and anatomo-histological study on trans-oral endoscopic thyroidectomy vestibular approach (TOETVA)," *Surgical Endoscopy*, vol. 34, no. 3, pp. 1088–1102, 2020.

[14] A. Anuwong, K. Ketwong, P. Jitpratoom, T. Sasanakietkul, and Q. Y. Duh, "Safety and outcomes of the transoral endoscopic thyroidectomy vestibular approach," *JAMA surgery*, vol. 153, no. 1, pp. 21–27, 2018.

[15] Z. Guibin, Z. Guojun, M. Chi et al., "Oral vestibular approach to endosco-pic thyroid surgery for papillary thyroid carcinoma," *Journal of Otolaryngology and Opht-halmology of Shandong University*, vol. 34, no. 3, pp. 58–62, 2020.

[16] Y. Guo, Q. Zheng, N. Lei, Z. Xiuying, and W. Xiaoying, "Effect of cold compress on analgesia after knee arthroscopy," *Chinese Journal of Nursing*, vol. 43, no. 9, pp. 786-787, 2008.

[17] F. Liuping, L. Xiaofang, and H. Fangzhen, "Comparison of the effect of differen-t ice compress modality after knee joint surgery," *Chinese Journal of Nursing*, vol. 5, no. 21, pp. 52-53, 2014.

[18] C. S. Enwemeka, C. H. Allen, P. A. Avila, J. A. Bina, J. Konrade, and S. Munns, "Soft tissue thermodynamics before, during, and after cold pack therapy," *Journal of the American Dental Association (1939)*, vol. 136, no. 6, pp. 774–778, 2005.

[19] C. Swenson, L. Sward, and J. Karlsson, "Cryotherapy in sports medicine," *Scandinavian journal of medicine & science in sports*, vol. 6, no. 4, pp. 193–200, 1996.

[20] P. Kendigelen, A. C. Tutuncu, G. Ashyralyyeva et al., "Laryngotracheal edema due to thermal injury: a complication after thyroidectomy in children," *Archivos Argentinos de Pediatría*, vol. 115, no. 1, pp. e31–e33, 2017.

[21] A. Kısaoğlu, B. Özoğul, M. N. Akçay et al., "Completion thyroidectomy in differentiated thyroid cancer: when to perform?," *Turkish Journal of Surgery/Ulusal cerrahi dergisi*, vol. 30, no. 1, pp. 18–21, 2014.

[22] L. Caulley, S. Johnson-Obaseki, L. Luo, and H. Javidnia, "Risk factors for postoperative complications in total thyroidectomy: a retrospective, risk-adjusted analysis from the National Surgical Quality Improvement Program," *Medicine (Baltimore)*, vol. 96, no. 5, article e5752, 2017.

[23] M. A. Gulcelik, L. Dogan, G. G. Akgul, E. H. Güven, and G. N. Ersöz, "Completion thyroidectomy: safer than thought," *Oncology research and treatment*, vol. 41, no. 6, pp. 386–390, 2018.

[24] I. S. Mamidi, S. Fassas, L. J. Pasick et al., "Adverse effects of chronic steroid use following thyroidectomy," *The Journal of Surgical Research*, vol. 267, pp. 17–24, 2021.

[25] D. Bawa, A. Alghamdi, H. Albishi et al., "Post-thyroidectomy complications in southwestern Saudi Arabia: a retrospective study of a 6-year period," *Annals of Saudi Medicine*, vol. 41, no. 6, pp. 369–375, 2021.

[26] G. M. Menderico Jr., A. L. Weissenberg, C. M. Borba, G. M. Sallani, and J. O. Poy, "Complications of transoral endoscopic

Hindawi
Computational and Mathematical Methods in Medicine
Volume 2023, Article ID 9837874, 1 page
https://doi.org/10.1155/2023/9837874

Retraction

Retracted: Diagnostic Value of IGFBP-2 in Predicting Preeclampsia before 20 Weeks of Pregnancy: A Prospective Nested Case-Control Study

Computational and Mathematical Methods in Medicine

Received 5 December 2023; Accepted 5 December 2023; Published 6 December 2023

This article has been retracted by Hindawi, as publisher, following an investigation undertaken by the publisher [1]. This investigation has uncovered evidence of systematic manipulation of the publication and peer-review process. We cannot, therefore, vouch for the reliability or integrity of this article.

Please note that this notice is intended solely to alert readers that the peer-review process of this article has been compromised.

Wiley and Hindawi regret that the usual quality checks did not identify these issues before publication and have since put additional measures in place to safeguard research integrity.

We wish to credit our Research Integrity and Research Publishing teams and anonymous and named external researchers and research integrity experts for contributing to this investigation.

The corresponding author, as the representative of all authors, has been given the opportunity to register their agreement or disagreement to this retraction. We have kept a record of any response received.

References

[1] F. Gao, J. Yin, Y. Long et al., "Diagnostic Value of IGFBP-2 in Predicting Preeclampsia before 20 Weeks of Pregnancy: A Prospective Nested Case-Control Study," *Computational and Mathematical Methods in Medicine*, vol. 2022, Article ID 5075569, 8 pages, 2022.

Hindawi
Computational and Mathematical Methods in Medicine
Volume 2022, Article ID 5075569, 8 pages
https://doi.org/10.1155/2022/5075569

Research Article

Diagnostic Value of IGFBP-2 in Predicting Preeclampsia before 20 Weeks of Pregnancy: A Prospective Nested Case-Control Study

Fei Gao,[1,2,3] **Jiaye Yin**,[3] **Yan Long**,[3] **Sufei Zhu**,[3] **Zhenting Huang**,[3] **Jielin Wang**,[3] **Hao Zheng**,[3] **Wen Wang**,[1,2] **and Lei Zheng**[1,2]

[1]*The First School of Clinical Medicine, Southern Medical University, Guangzhou 510515, China*
[2]*Laboratory Medicine Center, Nanfang Hospital, Southern Medical University, Guangzhou 510515, China*
[3]*Department of Laboratory, Guangzhou Women and Children's Medical Center, China*

Correspondence should be addressed to Wen Wang; wen.wang@qmul.ac.uk and Lei Zheng; nfyyzhenglei@smu.edu.cn

Received 24 August 2022; Revised 3 September 2022; Accepted 7 September 2022; Published 28 September 2022

Academic Editor: Min Tang

Backgroud. Preeclampsia (PE) is a critical type of hypertensive disorder of pregnancy, which seriously affects maternal and infant health. The etiology of PE is unclear, and there is no clear prediction model. In this study, new biomarkers were identified before 20 weeks of gestation to construct an early PE prediction model. *Purpose*. To identify novel biomarker insulin-like growth factor binding protein-2 (IGFBP-2) associated with preeclampsia (PE) before 20 weeks of gestation and to explore the predictive value of plasma IGFBP-2 in PE. *Methods*. A prospective nested case-control investigation involving 122 PE patients and 122 normal controls (NC) that were matched 1 : 1 in terms of age and week of pregnancy was carried out in Guangzhou Women and Children's Medical Center (Guangzhou, China, 2018030306) from April 2016 to December 2019. At 8 to 20 weeks, blood samples from the mother were taken. To calculate the correlations, univariate conditional logistic regression was employed. *Results*. Herein, 12 clinical indices were significantly different between the PE and NC groups (uric acid (UA), cystatin C (Cys C), aspartate aminotransferase (AST), glutamyl transpeptidase (γ-GT), total bilirubin (TB), prothrombin time (PT), red blood cell (RBC), hematocrit (HCT), red cell distribution width (RDW), platelets (PLT), mean platelet volume (MPV), and thrombocytocrit (PCT)). Compared with the NC group (36.79 ± 19.91 pg/mL), the expression level of IGFBP2 in the PE group (19.76 ± 19.40 pg/mL) before 20 weeks of pregnancy was significantly decreased ($P < 0.01$). Two high-risk factors were found to be significantly associated with PE independently of confounders: anemia 4.35 (2.20-8.45) ($P < 0.01$) and cesarean section history 8.25 (2.67-26.67) ($P < 0.01$). As a result of the univariate logistic regression analysis, the following three variables were included in the final logistic regression model.: $Y = -18.841 - 0.085 \times (\text{IGFBP-2}) + 0.630 \times (\text{RDW}) + 0.165 \times (\text{AST}) + 0.863 \times (\text{MPV})$. In comparison to IGFBP-2 alone as an independent predictor of PE (AUC = 0.897, 95% CI 0.830–0.964), the model's discriminatory power was considerably higher (AUC = 0.953, 95% CI 0.911–0.995). *Conclusion*. Plasma IGFBP-2 before 20 weeks of pregnancy combined with high-risk factors and routine blood indexes has a high early predictive value for PE.

1. Introduction

Preeclampsia (PE) is a critical type of hypertensive disorder in pregnancy, manifested as persistently high blood pressure and proteinuria after 20 weeks of pregnancy, with an incidence of 3%-8% [1]. PE inhibits fetal intrauterine growth and affects several organs (including the liver, kidneys, lungs, and heart) as well as the nervous system of pregnant women. It also causes mortality, premature birth, and other problems. The programmed structural and functional changes caused by PE injury during pregnancy also elevate the risk of cardiovascular diseases after childbirth. Early screening of women at risk for PE can reduce the risk of preterm birth and early-onset preeclampsia by preventive measures, such as the use of aspirin and calcium [2].

Except for pregnancy termination, currently, there is no effective treatment that might underlie the risk of premature delivery. In clinical treatment, it is usually faced with the

difficulty of deciding the maternal-fetal benefits [3–5]. Therefore, it is important to identify women who are at risk of PE in advance so that preventative and intervention strategies may be implemented. There are many biomarkers that have been suggested to predict PE. Presently, only a few effective clinical predictors have been identified for PE, resulting in a poor prognosis for the mother and perinatal infants and a sudden increase in the risk of death [6–8].

Several studies speculated that during the formation of PE placenta, extravillous trophoblast (EVT) suffers from decreased invasiveness and extravillous uterine spiral artery remodeling obstacle, resulting in shallow placenta implantation and poor placental vascular formation. In placental implantation, plasma proteins have a specific role as placental factors that induce endothelial dysfunction and a variety of other pathophysiological alterations linked to PE [9–11]. Due to the complexity and multifactorial nature of the disease, we employed antibody microarray technology to identify the crucial predictive proteins linked to PE.

Insulin-like growth factor binding protein 2 (IGFBP-2) belongs to the IGFBPs family, in which the content of IGFBP-2 is the second. IGFBP-2 was the first member found to be highly expressed in glioma, and it is associated with tumor differentiation, invasion, apoptosis, and angiogenesis [12, 13]. Placental microparticles may comprise fragments that are formed and released into the mother's blood circulation during pregnancy [14]. As a result, there is a lot of attention being paid to determining if there may be a difference in plasma IGFBP-2 levels between those with and without PE. The novel factor IGFBP-2 and previously known risk factors were incorporated in the current investigation to potentially increase the discriminatory performance of PE.

2. Methods

2.1. Study Design and Subjects. The research was based on an ongoing prospective study at the Guangzhou Women and Children's Medical Center (2018030306), Guangzhou, China, from April 2016 to December 2019. All subjects signed an informed consent, which was approved by the Ethics Committee of Guangzhou Women and Children's Medical Center. The samples were collected at enrollment, and the subjects followed up for up to 42 days postdelivery. Baseline demographic data and the mother's medical history and lifestyle information were collected.

In this nested case-control study, 5951 women were recruited during the discovery phase. PE occurred in 214 subjects, 122 of whom met all inclusion and exclusion criteria; the remaining patients were eliminated (Figure 1). These 122 PE-affected women were matched at a 1 : 1 ratio in terms of age, gestational week, and sample date to 122 controls who had uncomplicated pregnancies.

2.2. Diagnosis of PE

2.2.1. Inclusion Criteria for Case Group. According to the expert consensus PE [15] in Guidelines for The Diagnosis and Treatment of Gestational Hypertension (2020), PE was defined as hypertension (systolic blood pressure ≥ 140 mmHg and/or diastolic blood pressure ≥ 90 mmHg) and proteinuria (urinary protein quantification > 0.3 g/24 h, or random urinary protein quantification ≥ 2 +) emerging after 20 weeks of gestation. However, in the absence of proteinuria, hypertension should be accompanied by more than one of the following symptoms: (1) visual impairment, persistent headache, or other abnormalities of the central nervous system; (2) abnormal transaminase levels: elevated serum aspartate aminotransferase (AST) or alanine aminotransferase (ALT); (3) impaired renal function: urinary protein level > 2.0 g/24 h, or oliguria, or serum creatinine *level* > 106 μmol/L; (4) hypoproteinemia with ascites, pleural effusion, or pericardial effusion; (5) platelet count continued to decrease to 100×10^9 P/L; and (6) fetal growth restriction or oligohydramnios, intrauterine death, and placental abruption.

2.2.2. Case Group Exclusion Criteria. Patients with a history of hypertension, kidney disease, or other conditions causing elevated blood pressure prior to the 20th week of gestation were excluded. In addition, cases of primary lipid metabolism abnormalities, stillbirth, miscarriage, multiple pregnancies, fetal malformation, thyroid disease, gestational diabetes, and liver and kidney diseases were excluded [16].

2.2.3. Inclusion Criteria for Normal Pregnancy. The pregnant woman gave birth to one full-term live fetus without any abnormalities.

2.3. Sample Collection. Women between 8 and 20 weeks of their pregnancies had their peripheral venous blood samples drawn, which were centrifuged at 3500 × g for 10 min at room temperature, and then promptly kept at -80°C. A total of 507 proteins of interest were found using a RayBio Label-based Human Antibody Microarray (catalog # AAH-BLG-1; RayBiotech, Norcross, GA, USA). Assays were carried out as per the manufacturer's instructions. Because of the challenges in collecting early pregnancy plasma samples from women with PE, only IGFBP-2 levels were examined as they showed a high fold-change among the downregulated proteins in the protein microarray. IGFBP-2 is also essential in trophoblastic immune privilege and trophoblast invasion in the early stages of pregnancy. IGFBP-2 plasma concentrations were measured by ELISA kit (Bes11047H, BersinBio, Guangzhou, China).

2.4. Data Collection. On the basis of a literature review and clinical expertise, the potential risk factors were chosen. Medical records were used to collect the data. Sociodemographic characteristics (maternal age, gestational age, body mass index (BMI), ethnicity, and place of birth), pregnancy history, past medical history, family history (gestational diabetes mellitus and hypertension), and adverse perinatal outcomes (scar uterus, oligohydramnios, premature rupture of membranes, postpartum hemorrhage, premature delivery, and low birth weight) were the included variables. Routine blood indices (blood routine, coagulation function, liver function, and kidney function) before 20 weeks of gestation were collected and analyzed.

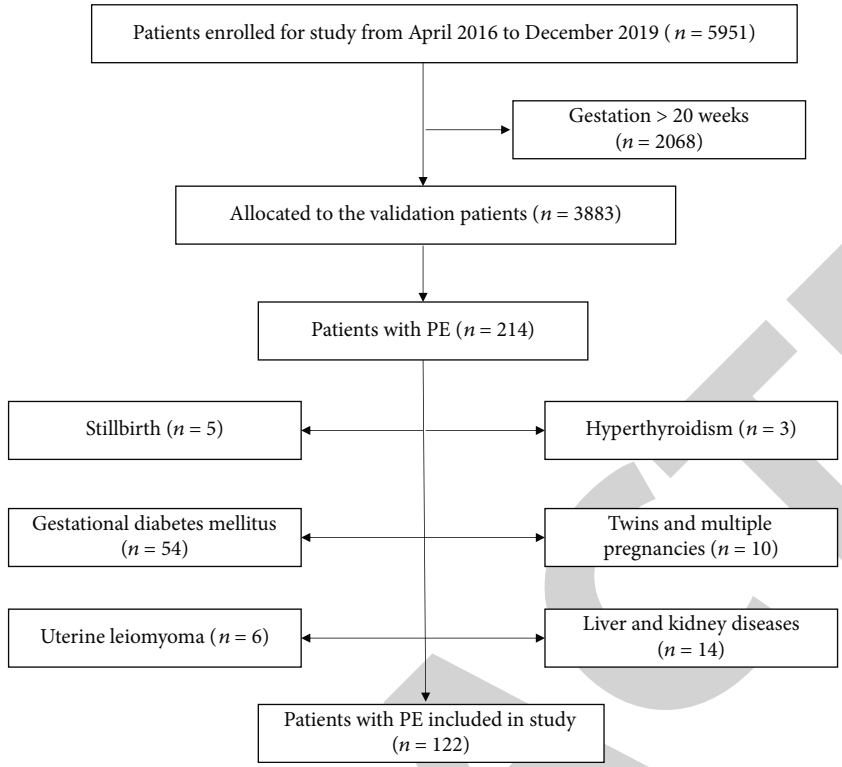

Figure 1: Flow diagram of study design.

2.5. Statistical Analysis. Data analysis was carried out using SPSS 26.0 software. The normal-distribution measurement results were expressed as mean ± standard deviation (SD), and an independent sample test was employed to compare the variables across groups. Median (interquartile spacing) (*M* (P25, P75)) was used for skewed distribution. Wilcoxon rank-sum test or Mann–Whitney *U* test was utilized to compare the variables across groups. For the correlation analyses, Spearman correlation analysis was utilized. Single factor analysis was used for screening significant risk factors, and multivariate logistic regression analysis was utilized for determining the prediction model of PE. The receiver operating characteristic (ROC) curve was drawn by using a stepwise logistic regression model to determine the sensitivity, specificity, negative/positive likelihood ratio, and other indicators, and the predictive value of indicators was evaluated by the area under the curve (AUC) value. $P < 0.05$ was taken as significant.

3. Results

3.1. Demographical Data. In total, 244 pregnant women, 122 of whom were in the PE group and 122 of whom were in the normal pregnancy group, were enrolled in this study. Before 20 weeks of gestation, the BMI level of the PE group was higher in comparison to that of the normal pregnancy group ($P < 0.05$); however, there were no significant differences detected in the race, nationality, age, and gestational age between the two groups ($P > 0.05$). The results were as follows: in the PE group, the changes in blood cell system, the red blood cell count, hematocrit, red blood cell distribution width, mean platelet volume and specific platelet volume, serum uric acid and cystatin C, serum aspartate aminotransferase, glutamyl transpeptidase, and total bilirubin levels in the liver function test, and prothrombin time were higher in comparison to those in the normal group ($P < 0.05$), while platelet count was lower than the normal group. No statistical difference was observed in the other items (Table 1).

3.2. Analysis of High-Risk Factors and Adverse Outcomes. Univariate analysis showed that history of anemia and cesarean section were statistically significant in the PE group ($P < 0.05$). The relative risk odds ratio (OR) (95% confidence interval (CI)) values of anemia and cesarean section history are 4.35 (2.20-8.45) and 8.25 (2.67-26.67), respectively. The probability of high risk of placenta accreta, scar uterus, oligohydramnios, abnormal placenta, and low birth weight in the PE group was remarkably higher in comparison to that in the normal pregnancy group ($P < 0.05$). The relative risk OR (95% CI) of high risk of placenta accreta, scar uterus, oligohydramnios, and placental abnormality in pregnancy was 2.33 (1.18-26.67), 9.71 (2.93-31.19), 25.16 (4.41-263.70), and 3.82 (1.28-10.89), respectively. And then, the relative risk OR (95% CI) of low birth weight was 49.08(8.21-505.90). On the other hand, there was no significant difference observed between the PE group and normal groups in pregnancy times and history of spontaneous abortion ($P > 0.05$) (Table 2).

3.3. Correlation between Plasma IGFBP-2 Expression Level and Routine Laboratory Indicators. The plasma IGFBP-2

Table 1: Clinical data of the PE group and control groups.

Variables	PE ($n = 122$)	NC ($n = 122$)	P
Han, n (%)	118 (96.72)	119 (97.54)	0.99
Guangdong nationality, n (%)	90 (73.77)	89 (72.95)	0.99
Age (years)	32.37 ± 4.82	32.48 ± 4.50	0.87
Gestational weeks	16.75 ± 2.56	17.18 ± 2.27	0.19
BMI (kg/m^2)	26.21 ± 5.17	24.83 ± 3.63	0.01
Renal function indexes			
UA (μmol/L)	271.0 (228.0, 310.5)	217.5 (191.0, 248.8))	<0.01
Cr (μmol/L)	43.0 (38.0, 46.0)	42.0 (37.0, 47.0)	0.73
Urea (mmol/L)	2.75 (2.19, 3.23)	2.82 (2.44, 3.38)	0.20
Cys C (mg/L)	0.59 (0.49, 0.71)	0.55 (0.45, 0.62)	<0.01
Liver function indexes			
ALT (U/L)	16.00 (11.00, 26.00)	16.00 (12.00, 26.25)	0.30
AST (U/L)	21.00 (18.00, 26.00)	17.00 (14.00, 21.00)	<0.01
γ-GT (U/L)	12.50 (10.00, 17.00)	11.00 (8.00, 14.00)	<0.01
TB (μmol/L)	8.90 (7.55, 10.95)	7.00 (5.80, 9.25)	<0.01
Blood coagulation indexes			
PT (s)	12.10 (11.70, 12.40)	11.80 (11.50, 12.30)	<0.01
APTT (s)	33.10 (31.20, 34.55)	32.40 (30.38, 34.83)	0.28
TT (s)	16.00 (15.45, 16.55)	15.80 (15.20, 16.30)	0.34
Fib (g/L)	4.69 ± 0.89	4.66 ± 0.70	0.82
Blood routine indexes			
RBC (10^{12}/L)	4.09 (3.77, 4.45)	3.85 (3.64, 4.11)	<0.01
HB (g/L)	119.9 ± 11.39	118.8 ± 9.70	0.36
HCT (%)	36.30 (34.00, 38.53)	35.00 (33.10, 36.70)	<0.01
RDW (%)	16.20 (14.53, 16.80)	13.05 (11.50, 15.00)	<0.01
PLT (10^9/L)	224.8 ± 51.15	253.0 ± 55.31	<0.01
MPV (fL)	10.75 (9.90, 11.40)	8.10 (7.70, 9.03)	<0.01
PCT (%)	0.24 ± 0.05	0.21 ± 0.05	<0.01

expression level before 20 weeks of pregnancy was detected by enzyme-linked immunosorbent assay (ELISA). A total of 100 pregnant women (50 in the NC group and 50 in the PE group) were detected before 20 weeks of pregnancy. As a result, before 20 weeks of pregnancy, the level of IGFBP-2 in the PE group (19.76 ± 19.40 pg/mL) was substantially lower in comparison to that in the normal group (32.59 ± 17.90 pg/mL) ($P < 0.01$) (Figure 2).

Spearman's correlation analysis was carried out to assess the expression level of plasma IGFBP-2 before 20 weeks of pregnancy in the PE group and routine laboratory indicators. The outcomes demonstrated that the plasma IGFBP-2 expression level before 20 weeks of pregnancy was negatively correlated with AST, RBC, RDW, and MPV ($r = -0.34$, -0.25, -0.31, -0.30; $P < 0.01$) in PE; however, there was no statistically significant correlation with other indicators (Table 3).

3.4. Efficacy of the Predictive Model. The statistically significant high-risk factors and clinical indicators were included in the regression analysis, and the stepwise logistic regression analysis was adopted. Finally, the regression analysis model was obtained: $Y = -18.841 - 0.085 \times (\text{IGF BP-2}) + 0.630 \times (\text{RDW}) + 0.165 \times (\text{AST}) + 0.863 \times (\text{MPV})$ (Table 4).

Using ROC analysis of IGFBP-2 levels, the discriminatory capacity of IGFBP-2 and the clinical factors related to PE were evaluated (Figure 3). Using IGFBP-2 as a single predictor, the AUC was 0.897 (95% CI 0.830–0.964) with 86.0% sensitivity and 84.0% specificity. Subsequently, the AUC increased to 0.953 (95% CI 0.911–0.995) with 94.0% sensitivity and 88.0% specificity when clinical factors for PE were entered into the logistic model based on the optimal cutoff point (Table 5).

4. Discussion

We found plasma IGFBP-2 levels before 20 weeks of gestation in this nested case-control research from a cohort of Chinese pregnant women to be prospectively linked to the risk of PE. In the Chinese population, the level of IGFBP-2 is predicted for 89.7% of PE cases. The combination of improved the detection rate of PE to 95.3%. The inclusion

Table 2: Analysis of high-risk factors and adverse outcomes between the NC group and PE groups.

	PE ($n = 122$)	NC ($n = 122$)	OR (95% CI)	P
High-risk factors				
Anemia, n (%)	44 (36.07)	14 (11.48)	4.35 (2.20-8.45)	<0.01
History of diabetes	0 (0)	0 (0)	N	N
History of hypertension	1 (0.8)	0 (0)	N	0.99
Gravidity = 1, n (%)	39 (31.97)	37 (30.33)	1.08 (0.63-1.85)	0.78
Gravidity ≥ 3, n (%)	49 (40.16)	39 (31.97)	1.43 (0.84-2.38)	0.18
History of preterm birth, n (%)	1 (0.8)	1 (0.8)	N	N
Spontaneous abortion ≥ 2, n (%)	11 (9.02)	7 (5.74)	1.63 (0.61-4.19)	0.33
Cesarean delivery, n (%)	21 (17.21)	3 (2.46)	8.25 (2.67-26.67)	<0.01
Stillbirths, n (%)	1 (0.8)	0 (0)	N	0.99
Adverse pregnancy and perinatal outcomes				
High risk of Down's screening, n (%)	30 (24.60)	15 (12.30)	2.33 (1.18-26.67)	0.01
Scar uterus, n (%)	24 (19.67)	3 (2.46)	9.71 (2.93-31.19)	<0.01
Oligohydramnios, n (%)	21 (17.21)	1 (0.8)	25.16 (4.41-263.70)	<0.01
Premature rupture of membranes, n (%)	25 (20.49)	15 (12.30)	1.84 (0.94-3.66)	0.08
Placenta abnormality, n (%)	14 (11.48)	4 (3.28)	3.82 (1.28-10.89)	0.03
Postpartum hemorrhage, n (%)	1 (0.8)	4 (3.28)	0.24 (0.02-1.51)	0.37
Preterm birth, n (%)	3 (2.46)	0 (0)	N	0.25
Fetal weight (<2500 g)	35 (28.69)	1 (0.8)	49.08 (8.21-505.90)	<0.01

N: defy calculation.

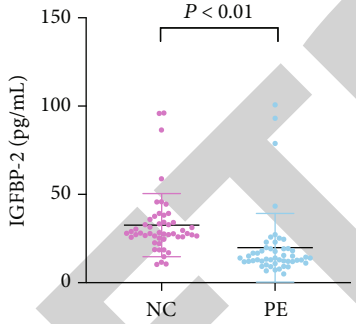

Figure 2: Comparison of IGFBP-2 levels between the PE group and NC groups.

of IGFBP-2 improved the PE prediction beyond conventional risk factors and clinical markers. To our knowledge, this is the first study to investigate the predictive value of IGFBP-2 on PE in the Chinese population, which provides a novel perspective for the prediction of PE.

Maternal markers, ultrasound markers, and biomarkers including PIGF, sFlt-1, and PAPP-A have all been employed for PE prediction [6–8]. Based on several studies on the early markers for PE recognition, several multiparameter algorithms have been developed. In summary, although a large number of markers and algorithms have been studied, a reliable PE prediction model has not been developed. Presently, there is no clinically significant screening test available for the prediction of PE development. The abnormal vascular remodeling of the spiral arteries in the uterus, resulting in superficial implantation of the placenta, might be the pathogenesis of PE. With the use of maternal trophoblast invasion factors like IGFBP-2, this condition can be used to predict PE. IGFBP-2 levels in the blood of pregnant women who later developed PE were shown to be lower in earlier studies. Recent studies consistently show that in early pregnancy (before 20 weeks gestation), the plasma level of IGFBP-2 in the PE group was substantially lower in comparison to that in the control group (Figure 2). In addition, IGFBP-2 can regulate the inflammatory response, apoptosis, differentiation invasion, and angiogenesis through multiple signaling pathways such as the Ras-MAPK pathway, PI-3K/AKT pathway, JNK pathway, P53, PTEN, and Wnt/β-catenin molecules [17–23]. In this study, it was found for the first time that the plasma IGFBP-2 level decreased before 20 weeks of pregnancy in the PE group, which inhibited the invasion of EVT and caused PE. Simultaneously, the expression level of IGFBP-2 was negatively correlated with AST, RBC, RDW, and MPV (Table 3).

Several studies reported that social, nutritional, blood, inflammation, immune, genetic, and other factors would affect the occurrence of PE [24, 25]. In this study, the red blood cell count, red blood cell distribution width, and prothrombin time in the PE group were higher in comparison to those in the normal group. Reportedly, the increase in RBC distribution width is due to the influence of inflammatory factors on RBC production and deformation ability [26, 27]. This study found that red blood cell count in the PE group increased significantly in early pregnancy, which might be due to the compensatory response caused by microcirculation ischemia and hypoxia in the body. An increased number of red blood cells in pregnant women,

Table 3: Correlation analysis between the plasma IGFBP-2 expression level and clinical index.

	r	P
UA (μmol/L)	-0.18	0.07
CysC (mg/L)	-0.05	0.62
AST (U/L)	-0.34	<0.01
γ-GT (U/L)	-0.13	0.18
TB (μmol/L)	-0.03	0.79
PT (s)	-0.13	0.19
RBC (10^{12}/L)	-0.25	<0.01
HCT (%)	-0.14	0.18
RDW (%)	-0.31	<0.01
PLT (10^9/L)	-0.11	0.25
MPV (fL)	-0.30	<0.01
PCT (%)	0.012	0.91

Table 4: Logistic regression analysis of risk factors for PE.

Risk factor	B	SE	Wald	P	OR (95% CI)
IGFBP-2	-0.085	0.034	6.141	0.013	0.918 (0.858, 0.982)
RDW	0.630	0.194	10.590	0.001	1.878 (1.285, 2.745)
AST	0.165	0.056	8.756	0.003	1.179 (1.057, 1.315)
MPV	0.863	0.234	13.566	0.001	2.371 (1.498, 3.753)

insufficient blood volume, and blood viscosity also lead to microthrombosis in PE pregnant women, thereby aggravating disorders related to blood circulation [28]. The liver and kidney function indicators (glutamyl transpeptidase, aspartate transferase, creatinine, and cystatin C) in the PE group were increased, which was consistent with the study by van der Tuuk et al. [29]. The pregnant women with PE had specific organ damage before they showed significant hypertension and proteinuria in the early pregnancy. Due to individual differences and the compensatory phase of organ damage, imaging and test indicators may still be within the normal range and not detected easily [30–33]. The combined assessment of risk factors and blood indicators in early pregnancy may play an important role in identifying high-risk groups for PE.

In the current study, anemia and cesarean section history were also found to be different between the PE and NC groups, consistent with previous studies. The highest relative risk in our study was the history of cesarean section. This procedure caused scar uterus, which was prone to dysplasia of the placental decidua, aggravating the symptoms of placental ischemia and hypoxia and leading to spasmodic contraction of small arteries and inducing PE. Placental tissue changes caused by anemia during pregnancy are characterized by dysregulation of the pregnancy-placental-fetal system and placental tissue ischemia in response to hypoxia [34]. PE can cause multiple complications and adverse pregnancy outcomes for both mothers and babies. In this study, the PE group had an increased risk of Down's syndrome, scar uterus, oligohydramnios, and placental abnormalities ($P < 0.05$). In addition, the proportion of low-birth-weight infants in the PE group was considerably higher in comparison to that in the NC group ($P < 0.01$).

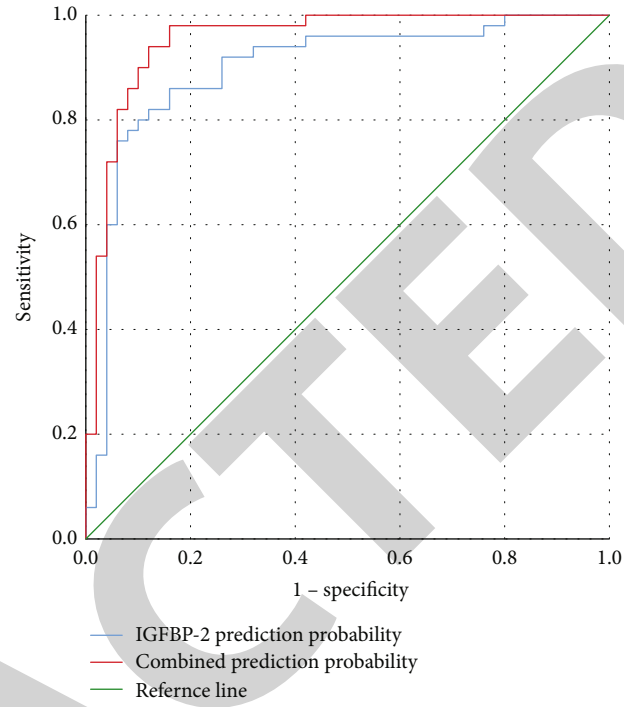

Figure 3: ROC curve of single and combined IGFBP-2 in predicting preeclampsia.

In addition, in the present study, when IGFBP-2 was incorporated into the logistic model as a novel factor, the AUC was 0.897 (95% CI 0.830–0.964) with 86.0% sensitivity and 84.0% specificity, and the model had a high discriminatory performance for PE (Table 5). This indicates that plasma IGFBP-2 before 20 weeks of pregnancy may have a predictive effect on PE. In comparison to the levels of angiogenic factors or placental hormones in the first trimester, our model has excellent discriminatory power.

According to a prospective study by Skråstad et al., the AUC for placental growth factor was 0.63 [35]. Abdelaziz et al. reported an AUC of 0.57 for soluble endoglin [36]. In a longitudinal study by Akolekar et al., the AUC values for placental protein 13 and pregnancy-associated plasma protein A were 0.82 and 0.87, respectively. According to the ROC curve, IGFBP-2 is a good biomarker for predicting the occurrence of preeclampsia in early pregnancy. In this study, the prediction and diagnosis rates of preeclampsia were improved to a certain extent by combining high-risk factors (anemia, cesarean section history), blood routine, coagulation routine, and liver and kidney function. The obtained logistic regression model combined with clinical risk factors prediction: $Y = -18.841 - 0.085 \times (\text{IGFBP-2}) + 0.630 \times (\text{RDW}) + 0.165 \times (\text{AST}) + 0.863 \times \text{MPV}$.

Nevertheless, the present study has some limitations. Although many pregnant women were enrolled in our cohort, the number of women who developed PE was insufficient, thus limiting the accuracy of our relative risk estimates. In addition, all women in our investigation were

Table 5: Evaluation of AUC and related parameters by IGFBP-2 and joint index.

Variable	AUC ± SD	*P*	(95% CI)
IGFBP-2 prediction probability	0.897 ± 0.034	<0.01	0.830-0.964
Combined prediction probability	0.953 ± 0.021	<0.01	0.911-0.995

from the same province, which might lead to a bias in the outcomes that should be validated by a prospective multicenter clinical study. Since the study's controls excluded participants who had abnormal results, there may have been a bias with overestimation of discriminatory power. Herein, we validated only IGFBP-2 levels because it showed the higher-fold change among the downregulated proteins in the protein microarray. To further enhance the discriminatory performance, we will substantiate the expression of the other 24 differentially expressed proteins in subsequent research.

In conclusion, plasma IGFBP-2 before 20 weeks of pregnancy combined with high-risk factors and routine blood indices has a high early predictive value for preeclampsia.

Data Availability

The data used to support the findings of this study are included within the article.

Ethical Approval

This study was approved by the Ethics Committee of Guangzhou Women and Children's Medical Center (2018030306).

Conflicts of Interest

The authors declare that they have no competing interests.

Authors' Contributions

(I) Conception and design were provided by Fei Gao and Yan Long. (II) Administrative support was provided by Wen Wang and Lei Zheng. (III) Provision of study materials or patients was done by Fei Gao and Jiaye Yin. (IV) Collection and assembly of data were done by Jielin Wang and Hao Zheng. (V) Data analysis and interpretation were done by Sufei Zhu and Zhenting Huang. (VI) Manuscript writing was done by all authors. (VII) Final approval of manuscript was done by all authors. Fei Gao and Jiaye Yin contributed equally to this work and share first authorship. Jiaye Yin is the co-first author of this article.

Acknowledgments

This study is supported by the internal research fund of the Guangzhou Women and Children's Medical Center (GWCMC2020-4-010).

References

[1] G. J. Burton, C. W. Redman, J. M. Roberts, and A. Moffett, "Pre-eclampsia: pathophysiology and clinical implications," *BMJ*, vol. 366, p. l2381, 2019.

[2] W. Kirsten, "Gestational hypertension and preeclampsia," *MCN: The American Journal of Maternal/Child Nursing*, vol. 44, no. 3, p. 170, 2019.

[3] L. C. Poon, A. Shennan, J. A. Hyett et al., "The International Federation of Gynecology and Obstetrics (FIGO) initiative on pre-eclampsia: a pragmatic guide for first-trimester screening and prevention," *International Journal of Gynaecology and Obstetrics: the Official Organ of the International Federation of Gynaecology and Obstetrics*, vol. 145, no. S1, pp. 1–33, 2019.

[4] L. C. Chappell, C. A. Cluver, J. Kingdom, and S. Tong, "Pre-eclampsia," *Lancet*, vol. 398, no. 10297, pp. 341–354, 2021.

[5] X. Chen, P. Li, M. Liu et al., "Gut dysbiosis induces the development of pre-eclampsia through bacterial translocation," *Gut*, vol. 69, no. 3, pp. 513–522, 2020.

[6] D. Wright, M. Y. Tan, N. O'Gorman et al., "Predictive performance of the competing risk model in screening for pre-eclampsia," *American Journal of Obstetrics and Gynecology*, vol. 220, no. 2, p. 199.e1, 2019.

[7] B. Serra, M. Mendoza, E. Scazzocchio et al., "A new model for screening for early-onset preeclampsia," *American Journal of Obstetrics and Gynecology*, vol. 222, no. 6, pp. 608.e1–608.e18, 2020.

[8] J. Hu, J. Gao, J. Liu et al., "Prospective evaluation of first-trimester screening strategy for preterm pre- eclampsia and its clinical applicability in China," *Ultrasound in Obstetrics & Gynecology*, vol. 58, no. 4, pp. 529–539, 2021.

[9] A. Filipek and E. Jurewicz, "Preeclampsia - a disease of pregnant women," *Postepy Biochemii*, vol. 64, no. 4, pp. 229–232, 2018.

[10] I. Tsakiridis, S. Giouleka, A. Arvanitaki et al., "Gestational hypertension and preeclampsia: an overview of national and international guidelines," *Obstetrical and Gynecological Survey*, vol. 76, no. 10, pp. 613–633, 2021.

[11] X. Su, Y. Liu, G. H. Li et al., "Associations of hypothyroxinemia with risk of preeclampsia–eclampsia and gestational hypertension," *Frontiers in Endocrinology*, vol. 12, p. 1452, 2021.

[12] S. Mehmet, *The insulin-like growth factor binding proteins (IGFBPs) and their role in the regulation of human chondrocyte growth*, Diss. King's College London (University of London), 2000.

[13] G. N. Fuller, C. H. Rhee, K. R. Hess et al., "Reactivation of insulin-like growth factor binding protein 2 expression in glioblastoma multiforme: a revelation by parallel gene expression profiling," *Cancer Research*, vol. 59, no. 17, pp. 4228–4232, 1999.

[14] B. Dane, C. Dane, M. Kiray, A. Cetin, M. Koldas, and M. Erginbas, "Correlation between first-trimester maternal serum markers, second-trimester uterine artery doppler

Hindawi
Computational and Mathematical Methods in Medicine
Volume 2023, Article ID 9769073, 1 page
https://doi.org/10.1155/2023/9769073

Retraction

Retracted: A Bioinformatic Approach Based on Systems Biology to Determine the Effects of SARS-CoV-2 Infection in Patients with Hypertrophic Cardiomyopathy

Computational and Mathematical Methods in Medicine

Received 12 December 2023; Accepted 12 December 2023; Published 13 December 2023

This article has been retracted by Hindawi, as publisher, following an investigation undertaken by the publisher [1]. This investigation has uncovered evidence of systematic manipulation of the publication and peer-review process. We cannot, therefore, vouch for the reliability or integrity of this article.

Please note that this notice is intended solely to alert readers that the peer-review process of this article has been compromised.

Wiley and Hindawi regret that the usual quality checks did not identify these issues before publication and have since put additional measures in place to safeguard research integrity.

We wish to credit our Research Integrity and Research Publishing teams and anonymous and named external researchers and research integrity experts for contributing to this investigation.

The corresponding author, as the representative of all authors, has been given the opportunity to register their agreement or disagreement to this retraction. We have kept a record of any response received.

References

[1] X. Han, F. Wang, P. Yang et al., "A Bioinformatic Approach Based on Systems Biology to Determine the Effects of SARS-CoV-2 Infection in Patients with Hypertrophic Cardiomyopathy," *Computational and Mathematical Methods in Medicine*, vol. 2022, Article ID 5337380, 13 pages, 2022.

Hindawi
Computational and Mathematical Methods in Medicine
Volume 2022, Article ID 5337380, 13 pages
https://doi.org/10.1155/2022/5337380

Research Article

A Bioinformatic Approach Based on Systems Biology to Determine the Effects of SARS-CoV-2 Infection in Patients with Hypertrophic Cardiomyopathy

Xiao Han,[1] **Fei Wang**,[2] **Ping Yang**,[3] **Bin Di**,[1] **Xiangdong Xu**,[1] **Chunya Zhang**,[1] **Man Yao**,[1] **Yaping Sun**,[1] **and Yangyi Lin**[4]

[1]*Department of Cardiology, Jiading District Central Hospital Affiliated Shanghai University of Medicine & Health Sciences, Shanghai, China*
[2]*Department of Emergency Medicine, Jiading District Central Hospital Affiliated Shanghai University of Medicine & Health Sciences, Shanghai, China*
[3]*Department of Pharmacy, Xinhua Hospital Affiliated to Shanghai Jiaotong University School of Medicine, Shanghai, China*
[4]*Department of Pulmonary Vascular Disease, State Key Laboratory of Cardiovascular Disease, Fuwai Hospital, National Center for Cardiovascular Diseases, Chinese Academy of Medical Sciences and Peking Union Medical College, Beijing, China*

Correspondence should be addressed to Ping Yang; yangping@xinhuamed.com.cn

Received 10 August 2022; Revised 26 August 2022; Accepted 1 September 2022; Published 27 September 2022

Academic Editor: Min Tang

Recently, severe acute respiratory syndrome coronavirus 2 (SARS-CoV-2), the causative agent of coronavirus disease 2019 (COVID-19), has infected millions of individuals worldwide. While COVID-19 generally affects the lungs, it also damages other organs, including those of the cardiovascular system. Hypertrophic cardiomyopathy (HCM) is a common genetic cardiovascular disorder. Studies have shown that HCM patients with COVID-19 have a higher mortality rate; however, the reason for this phenomenon is not yet elucidated. Herein, we conducted transcriptomic analyses to identify shared biomarkers between HCM and COVID-19 to bridge this knowledge gap. Differentially expressed genes (DEGs) were obtained using the Gene Expression Omnibus ribonucleic acid (RNA) sequencing datasets, GSE147507 and GSE89714, to identify shared pathways and potential drug candidates. We discovered 30 DEGs that were common between these two datasets. Using a combination of statistical and biological tools, protein-protein interactions were constructed in response to these findings to support hub genes and modules. We discovered that HCM is linked to COVID-19 progression based on a functional analysis under ontology terms. Based on the DEGs identified from the datasets, a coregulatory network of transcription factors, genes, proteins, and microRNAs was also discovered. Lastly, our research suggests that the potential drugs we identified might be helpful for COVID-19 therapy.

1. Introduction

It has been determined that severe acute respiratory syndrome coronavirus 2 (SARS-CoV-2), a novel member of the *Coronaviridae* family and the class of *Pisoniviricetes*, causes mild and severe respiratory diseases in humans [1–4]. Even though SARS-CoV-2 infections primarily affect the respiratory tract, they frequently cause heart injuries in patients with moderate to severe coronavirus disease 2019 (COVID-19), particularly in those with underlying cardiovascular diseases [5–7]. Furthermore, growing evidence demonstrates a link between COVID-19 and increased mortality from heart failure and cardiovascular diseases [8].

Hypertrophic cardiomyopathy (HCM) is one of the most prevalent inherited heart conditions associated with angiotensin-converting enzyme 2 (ACE2) deficiency in patients with heart failure [9, 10]. SARS-CoV-2 binds with ACE2 and accelerates its degradation, thereby decreasing its ability to counteract the activity of the renin-angiotensin system (RAS) protein [11]. Although the present

results suggested that ACE2 expression increased with ACE inhibitor treatment in HCM patients' tissues, they were not statistically significant [12]. Therefore, understanding the impact of SARS-CoV-2 infection in patients with HCM and developing therapeutic drugs that could decrease the odds of complications or death are essential. However, current efforts mainly focus on studying stress cardiomyopathies secondary to COVID-19, such as takotsubo cardiomyopathy [13, 14]. To date, no bioinformatic research on the impact of COVID-19 in patients with preexisting HCM at the molecular level has been reported.

Herein, to bridge the knowledge gap, the cooccurrence of HCM and COVID-19 was examined using two datasets, GSE89714 (HCM) and GSE147507 (COVID-19), obtained from the Gene Expression Omnibus (GEO) database. We identified the differentially expressed genes (DEGs) in each dataset and searched for DEGs shared by the two diseases. These common DEGs, designated as the primary experimental genes, were also used to identify various transcriptional regulators. Then, the hub genes were extracted from these common DEGs using the specific algorithm in the Cytoscape programme. Additionally, the hub genes were used to predict potential therapeutic drugs. Overall, we predicted four agents that could be potentially therapeutic for HCM patients with COVID-19.

2. Materials and Methods

2.1. Study Datasets. The National Center for Biotechnology Information (https://www.ncbi.nlm.nih.gov/geo/) and GEO databases were used to obtain the COVID-19 and HCM ribonucleic acid sequencing (RNA-seq) datasets [15]. The following criteria were used to assess the quality of the eligible datasets: (1) case-control study; (2) high-throughput sequencing for expression profiling; (3) comparable experimental and control or untreated conditions; (4) more than three samples in each group; and (5) complete raw and processed microarray data was available. The high-throughput Illumina NextSeq 500 RNA sequencing platform was used to obtain the transcriptional profiles of lung biopsy samples from patients with COVID-19 for the GSE147507 [16]. RNA-seq data from heart tissue samples of four participants without HCM and five participants with HCM are included in the GSE89714 dataset. The HiSeq 2000 platform was used for the sequencing experiment. The CuffLinks programme was employed to assess gene expression. Table 1 summarises the two datasets.

The cut-off criteria were set at $P < 0.05$ and $|\log FC| \geq 1.0$ to identify significant DEGs in each dataset using the DESEq2 R package. Jvenn online software was used to obtain the shared DEGs between GSE147507 and GSE89714 [17]. DEG expression was considered exclusive between the two datasets if statistically significant differences existed across different conditions [18].

2.2. Gene Ontology (GO) and Pathway Enrichment Analyses. Genome enrichment analysis helps determine the chromosome positions associated with various interrelated diseases [19]. We used an online tool, Enrichr (https://maayanlab.cloud/Enrichr/), to determine the possible molecular pathways and mechanisms involving the common DEGs. The shared pathways between HCM and COVID-19 were examined using four databases: BioCarta, WikiPathways, Reactome, and Kyoto Encyclopedia of Genes and Genomes (KEGG). A P value of < 0.05 was used as a standard metric in quantifying the top-ranked pathways.

2.3. Protein-Protein Interaction (PPI) Network Analysis. The interaction of different cellular proteins can indirectly reflect a protein's functions and roles. Understanding PPI networks can therefore shed light on how proteins function across the board in cellular machinery [20–23]. The shared DEGs were uploaded to the STRING database (https://string-db.org/) [21] to illustrate potential protein connections between HCM and COVID-19. The common DEG PPI network was created using a low confidence score of 0.15. The obtained PPI network was viewed using Cytoscape software (v.3.8.0).

2.4. Hub Gene Extraction and Submodule Analysis. Cytohubba, a validated Cytoscape plugin, ranks and extracts central or targeted elements based on numerous network features. Maximal clique centrality is a commonly used algorithm in Cytohubba for analysing networks from various perspectives [24, 25]. The top 10 hub genes in the obtained PPI network were identified using this method. Additionally, we classified the shortest paths between hub genes based on the calculations from Cytohubba.

2.5. Recognition of Transcription Factors (TFs) and MicroRNAs (miRNAs). A TF is a protein that binds to gene elements and regulates gene expression [26]. Candidate TFs that are topologically connected to mutual DEGs obtained from the JASPAR database were identified using the NetworkAnalyst platform, a popular web tool for the meta-analysis of gene expression data and viewing biological mechanisms, roles, and gene translation (https://www.networkanalyst.ca/) [27]. JASPAR provides open-access profiles of various TFs in six taxonomic groups [28]. In addition, TarBase and miRTarBase were used to analyse miRNA-targeted gene interactions to find miRNAs that potentially influence gene translation [29, 30]. These online tools can be used by researchers to filter high-degree miRNAs and identify the associated biochemical processes and characteristics to generate the most plausible hypothesis.

2.6. Prediction of Candidate Drugs. Predicting protein-drug interactions (PDIs) or identifying candidate drug molecules was a crucial aspect of this study. Enrichr was used to select potential drug molecules based on the identified DEGs in HCM and COVID-19 and the Drug Signatures database (DSigDB). Gene set libraries enabled by Enrichr allow users to study gene set enrichment at the genome-wide level [31]. Targeted drug substances connected to DEGs were identified using the DSigDB (https://maayanlab.cloud/Enrichr/) [32].

2.7. Gene and Disease Association Analysis. The DisGeNET database links various biomedical aspects of medical conditions with gene-disease relations. It focuses on our growing

Table 1: A description of the two datasets with their GEO information.

Disease name	GEO accession	GEO platform	Total DEG count	Upregulated DEG count	Downregulated DEG count
SARS-CoV-2	GSE147507	GPL18573	1781	1390	391
HCM	GSE89714	GPL11154	207	134	73

Abbreviations: GEO: Gene Expression Omnibus; DEGs: differentially expressed genes; SARS-CoV-2: severe acute respiratory syndrome coronavirus 2; HCM: hypertrophic cardiomyopathy.

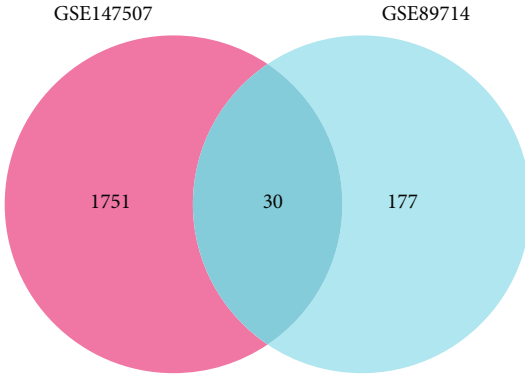

Figure 1: Ribonucleic acid sequencing datasets for hypertrophic cardiomyopathy (HCM) (GSE89714) and coronavirus disease 2019 (COVID-19) (GSE147507) were used in this study. The integrated analysis identified 30 differentially expressed genes shared between COVID-19 and HCM.

understanding of human genetic disorders (https://www.networkanalyst.ca/) [33]. We used this tool to determine various diseases related to the common DEGs and their chronic complications.

3. Results

3.1. Identification of DEGs and Common DEGs. Patients with COVID-19 exhibited a differential expression of 1,781 genes, including 1,390 upregulated and 391 downregulated genes after disease exposure. Similarly, various statistical analysis techniques were used to rank the DEGs identified for HCM. All DEGs were identified using a criterion of $P < 0.05$ and $|\log FC| \geq 1$. Using the Jvenn online platform, 30 common DEGs were identified between the two datasets (Figure 1). There was a close relationship between the two diseases as they shared several genes [34].

3.2. GO and Pathway Enrichment Analyses. Using Enrichr, GO and pathway enrichment analyses were performed. Table 2 summarises the top 10 GO terms in the biological processes, molecular functions, and cellular component categories. DEGs are listed in increasing order based on P value. Figure 2 summarises the linear comparison of the overall ontological analysis of each category. An organism's active pathways reveal how it responds to its inherent modifications. It illustrates the interaction between diseases through basic molecular processes [35]. We examined four global databases, KEGG, WikiPathways, Reactome, and BioCarta, to determine the most important pathways involving the DEGs common to HCM and COVID-19. Table 3 summarises the critical pathways identified based on the examined datasets. Pathway enrichment analysis was performed on the datasets (Figure 3). DEGs are listed in increasing order based on P value. A P value of < 0.05 was used to determine the top functional items and pathways.

3.3. Classification of Hub Proteins and Submodules. We predicted the interaction of DEGs by analysing the STRING PPI network using Cytoscape. The PPI network constructed using the common DEGs comprised 30 nodes and 124 edges (Figure 4). Additionally, most of the interconnected nodes in the PPI network were identified as hub genes. Using the Cytohubba plugin, the top 10 DEGs were considered hub genes. This gene list includes thrombospondin 2 (*THBS2*), biglycan (*BGN*), collagen type I alpha 2 chain (*COL1A2*), actin alpha 2 (*ACTA2*), myosin heavy chain 11 (*MYH11*), adipocyte enhancer-binding protein 1 (*AEBP1*), immunoglobulin superfamily containing leucine-rich repeat (*ISLR*), frizzled-related protein (*FRZB*), microfibril-associated protein 4 (*MFAP4*), and lysyl oxidase homolog 1 (*LOXL1*). These hub genes might be used as biomarkers to identify diseases and develop new therapeutic approaches. To comprehend the connections between the hub genes, we also constructed a submodule network using the Cytohubba plugin (Figure 5).

3.4. Determination of Regulatory Signatures. There is a network-based approach to identify the transcriptional changes, identify the regulatory TFs and miRNAs, and gain insights into the molecules that regulate hub proteins or common DEGs. Figure 6 illustrates the interactions between the regulatory TFs and DEGs. Figure 7 illustrates the interactions between miRNA regulators and DEGs. According to the analyses of the TF-gene and miRNA-gene interaction networks, 41 TFs and 19 posttranscriptional miRNA signatures regulated more than one DEG, proving that they actively competed with one another.

3.5. Prediction of Candidate Drugs. Understanding the factors responsible for receptor sensitivity requires an assessment of PDIs [36, 37]. We used Enrich to identify four potential drug molecules for HCM and COVID-19 provided by DSigDB. Based on the P value, the top four candidate compounds were extracted. Table 4 lists the most effective drugs identified.

3.6. Determination of Disease Association. Similarities in gene expression between the two conditions can be used to infer disease association and correlation [36, 37]. The first step toward developing therapeutic intervention strategies for diseases is identifying gene-disease relationships [38]. We found that degenerative polyarthritis, hyperkyphosis, and platyspondyly were highly correlated with the hub genes

Table 2: Gene ontology analysis of common differentially expressed genes between hypertrophic cardiomyopathy and coronavirus disease 2019.

Category	GO ID	Term	*P* values	Genes
GO biological process	GO:0006939	Smooth muscle contraction	1.10E-06	*ACTA2*, *EDNRA*, and *MYH11*
	GO:0014829	Vascular-associated smooth muscle contraction	6.06E-05	*ACTA2*, *EDNRA*
	GO:0048251	Elastic fiber assembly	6.06E-05	*MFAP4*, *MYH11*
	GO:0030198	Extracellular matrix organization	7.69E-05	*COL1A2*, *BGN*, *CYP1B1*, *TIMP1*, and *LOXL1*
	GO:0046466	Membrane lipid catabolic process	9.71E-05	*ENPP2*, *CYP1B1*
	GO:0042310	Vasoconstriction	0.000118625	*ACTA2*, *EDNRA*
	GO:0097435	Supramolecular fiber organization	0.000160702	*MFAP4*, *COL1A2*, *CYP1B1*, *MYH11*, and *LOXL1*
	GO:0030199	Collagen fibril organization	0.000317018	*COL1A2*, *CYP1B1*, and *LOXL1*
	GO:0085029	Extracellular matrix assembly	0.000588116	*MFAP4*, *MYH11*
	GO:0055013	Cardiac muscle cell development	0.000588116	*MYH11*, *MYLK3*
GO molecular function	GO:0005105	Type 1 fibroblast growth factor receptor binding	0.007478193	*FGF18*
	GO:0005111	Type 2 fibroblast growth factor receptor binding	0.007478193	*FGF18*
	GO:0004528	Phosphodiesterase I activity	0.007478193	*ENPP2*
	GO:0101020	Estrogen 16-alpha-hydroxylase activity	0.011939153	*CYP1B1*
	GO:0002020	Protease binding	0.013479908	*COL1A2*, *TIMP1*
	GO:0048407	Platelet-derived growth factor binding	0.016380734	*COL1A2*
	GO:0031432	Titin binding	0.019331061	*ANKRD1*
	GO:0008191	Metalloendopeptidase inhibitor activity	0.020803015	*TIMP1*
	GO:0042288	MHC class I protein binding	0.025206075	*TUBB4B*
	GO:0031690	Adrenergic receptor binding	0.025206075	*ARRDC3*
GO cellular component	GO:0062023	Collagen-containing extracellular matrix	6.41E-08	*MFAP4*, *COL1A2*, *ABI3BP*, *BGN*, *PLAT*, *AEBP1*, *THBS2*, and *LOXL1*
	GO:0031091	Platelet alpha granule	0.000327618	*ISLR*, *TIMP1*, and *THBS2*
	GO:0034774	Secretory granule lumen	0.001211585	*C3*, *ISLR*, *TIMP1*, and *TUBB4B*
	GO:0005775	Vacuolar lumen	0.001772031	*C3*, *BGN*, and *TUBB4B*
	GO:0031093	Platelet alpha granule lumen	0.004526565	*ISLR*, *TIMP1*
	GO:0071953	Elastic fiber	0.007478193	*MFAP4*
	GO:0035578	Azurophil granule lumen	0.008026254	*C3*, *TUBB4B*
	GO:0005788	Endoplasmic reticulum lumen	0.008747528	*C3*, *COL1A2*, and *TIMP1*
	GO:0001527	Microfibril	0.016380734	*MFAP4*
	GO:0005859	Muscle myosin complex	0.022272833	*MYH11*

of HCM and COVID-19 (Figure 8). These conditions are complex and multifactorial. Its pathophysiology is influenced by alterations in cell structure, barriers, and environmental factors.

4. Discussion

HCM is a common genetic cardiovascular disease that may lead to heart failure. SARS-CoV-2 also infected cardiac cells expressing ACE2, thereby advancing heart failure [39]. Individuals with cardiomyopathy are at high risk of SARS-CoV-2 infection. Herein, we identified molecular targets that could serve as COVID-19 biomarkers. Additionally, these markers might provide crucial details about how they contribute to diseases and conditions. In biomedicine and systems biology research, the expression profiling of high-throughput sequencing data is useful for identifying potential biomarkers [40]. Recently, RNA-seq, a new sequencing method, has significantly improved our ability to examine gene fusions, mutations/single nucleotide polymorphism posttranscriptional modifications, and differential gene expression analyses [41]. As advances in high-throughput sequencing technologies are made, it is becoming more challenging to cope with the increasing bioinformatics data

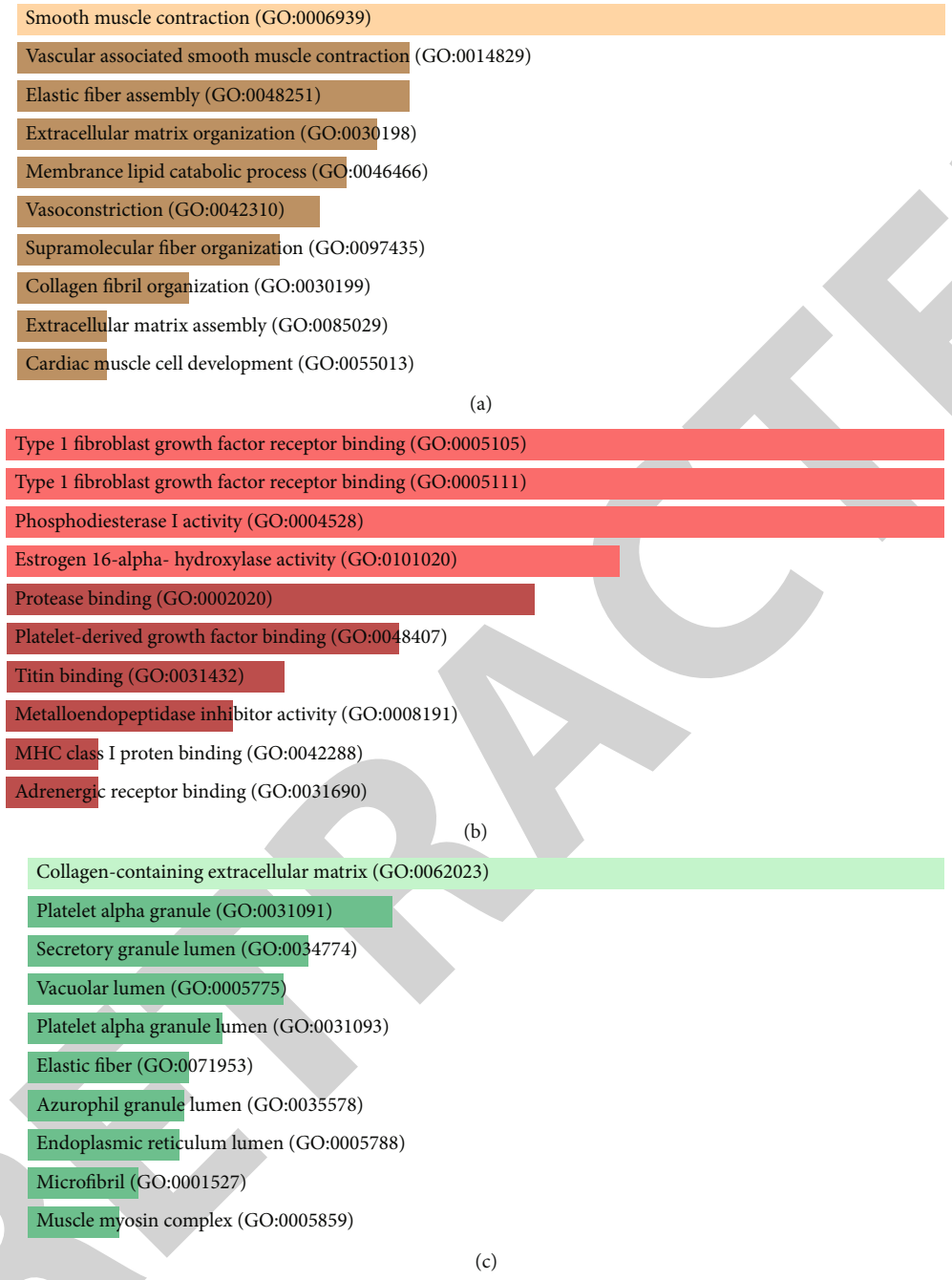

Figure 2: Gene ontology analysis of common differentially expressed genes shared between hypertrophic cardiomyopathy and coronavirus disease 2019 was performed using Enrichr. Terms were evaluated by categories: (a) biological processes, (b) molecular function, and (c) cellular components.

obtained using traditional biological methods. All these limitations may be solved by approaches with artificial intelligence [42].

In this study, our transcriptome analyses revealed that 30 DEGs share similar expression patterns between HCM and COVID-19. GO pathway analysis was performed to obtain insights into the biological significance of the common DEGs in disease progression The smooth muscle contraction pathway and vascular-associated smooth muscle contraction pathway were among the top GO terms identified for the biological process. There is a strong correlation between smooth muscle contraction and SARS-CoV-2 infection, according to several studies. Dysfunction endothelial cells prevent the release of adequate nitrogen oxide (NO), causing smooth muscle constriction [43] and reducing the cells' ability to neutralise reactive oxygen species and release NO [44, 45]. The top two GO pathways identified in the molecular function category are types 1 and 2 fibroblast growth factor (FGF) receptor binders. Cardiac hypertrophy in the postnatal period has been linked to the FGF family, and activating mutations in FGF receptor-1 have been shown to cause HCM [46]. The release of proinflammatory

Table 3: Pathway enrichment analysis of common differentially expressed genes between hypertrophic cardiomyopathy and coronavirus disease 2019.

Category	Pathways	*P* values	Genes
WikiPathways human	IL-18 signaling pathway WP4754	4.84E-05	*ACTA2*, *BTG2*, *COL1A2*, *TIMP1*, and *IER3*
	Endochondral ossification with skeletal dysplasias WP4808	0.000119283	*FRZB*, *FGF18*, and *PLAT*
	Endochondral ossification WP474	0.000119283	*FRZB*, *FGF18*, and *PLAT*
	miR-509-3p alteration of YAP1/ECM axis WP3967	0.000291693	*EDNRA*, *THBS2*
	miRNA targets in ECM and membrane receptors WP2911	0.000493146	*COL1A2*, *THBS2*
	Focal adhesion-PI3K-Akt-mTOR-signaling pathway WP3932	0.00103726	*COL1A2*, *FGF18*, *THBS2*, *FGF12*
	PI3K-Akt signaling pathway WP4172	0.001585899	*COL1A2*, *FGF18*, *THBS2*, and *FGF12*
	Focal adhesion WP306	0.003186561	*COL1A2*, *THBS2*, and *MYLK3*
	Complement and coagulation cascades WP558	0.003412595	*C3*, *PLAT*
	Genotoxicity pathway WP4286	0.004013249	*ACTA2*, *BTG2*
BioCarta	Inhibition of matrix metalloproteinases h reckPathway	0.011939153	*TIMP1*
	BTG family proteins and cell cycle regulation h btg2Pathway	0.013421829	*BTG2*
	Alternative complement pathway h alternativePathway	0.014902355	*C3*
	Lectin induced complement pathway h lectinPathway	0.019331061	*C3*
	Platelet amyloid precursor protein pathway h plateletAppPathway	0.020803015	*PLAT*
	Classical complement pathway h classicPathway	0.022272833	*C3*
	Fibrinolysis pathway h fibrinolysisPathway	0.022272833	*PLAT*
	Beta-arrestins in GPCR desensitization h bArrestinPathway	0.041187484	*EDNRA*
	Activation of cAMP-dependent protein kinase, PKA h gsPathway	0.042627715	*EDNRA*
	Role of Beta-arrestins in the activation and targeting of MAP kinases h barr-mapkPathway	0.044065855	*EDNRA*
KEGG 2019 human	Vascular smooth muscle contraction	4.48E-05	*ACTA2*, *EDNRA*, *MYH11*, and *MYLK3*
	Apelin signaling pathway	0.001114898	*ACTA2*, *PLAT*, and *MYLK3*
	Phagosome	0.001503079	*C3*, *THBS2*, and *TUBB4B*
	Focal adhesion	0.003324312	*COL1A2*, *THBS2*, and *MYLK3*
	Regulation of actin cytoskeleton	0.004174068	*FGF18*, *MYH11*, and *MYLK3*
	Calcium signaling pathway	0.005454596	*EDNRA*, *FGF18*, and *MYLK3*
	Complement and coagulation cascades	0.007187738	*C3*, *PLAT*
	ECM-receptor interaction	0.007685775	*COL1A2*,,*THBS2*
	Platelet activation	0.014809355	*COL1A2*, *MYLK3*
	PI3K-Akt signaling pathway	0.015674766	*COL1A2*, *FGF18*, and *THBS2*
Reactome	Extracellular matrix organization R-HSA-1474244	5.84E-05	*MFAP4*, *COL1A2*, *BGN*, *TIMP1*, and *LOXL1*
	Smooth muscle contraction R-HSA-445355	0.0011157	*ACTA2*, *MYH11*
	Elastic fiber formation R-HSA-1566948	0.001719859	*MFAP4*, *LOXL1*
	Signaling by PDGF R-HSA-186797	0.002034436	*FGF18*, *PLAT*, *THBS2*, and *IER3*
	Assembly of collagen fibrils and other multimeric structures R-HSA-2022090	0.002965286	*COL1A2*, *LOXL1*
	Muscle contraction R-HSA-397014	0.003096721	*ACTA2*, *MYH11*, and *FGF12*
	PI5P, PP2A, and IER3 regulate PI3K/AKT signaling R-HSA-6811558	0.006864228	*FGF18*, *IER3*
	Collagen formation R-HSA-1474290	0.007187738	*COL1A2*, *LOXL1*
	Diseases of glycosylation R-HSA-3781865	0.007685775	*BGN*, *THBS2*
	Negative regulation of the PI3K/AKT network R-HSA-199418	0.008026254	*FGF18*, *IER3*

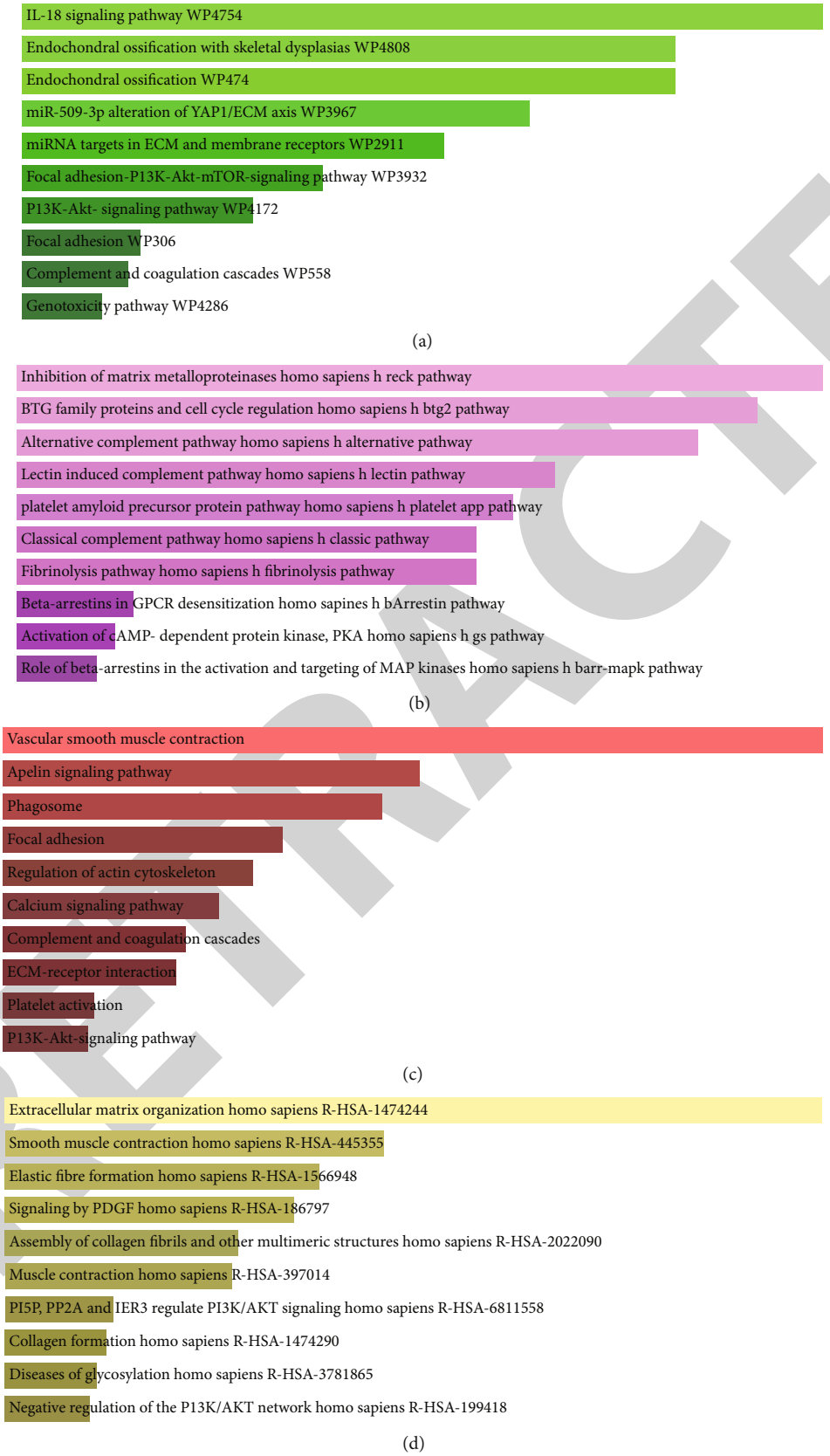

Figure 3: Pathway enrichment analysis of the common differentially expressed genes between hypertrophic cardiomyopathy and coronavirus disease 2019 was performed using Enrichr. Different databases were used in the analysis: (a) WikiPathways, (b) BioCarta, (c) Reactome, and (d) Kyoto Encyclopedia of Genes and Genomes 2019 human database.

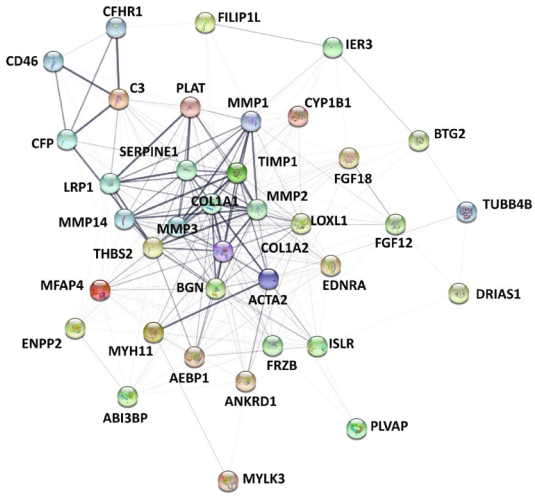

FIGURE 4: Protein-protein interaction (PPI) network of common differentially expressed genes (DEGs) between hypertrophic cardiomyopathy and coronavirus disease 2019. The circular nodes represent the DEGs, while the edges represent their interactions. The PPI network has 30 nodes and 124 edges.

cytokines, such as interleukin- (IL-) 9, IL-10, type 1 FGF, and type 2 FGF, was found in excessive and uncontrolled quantities in critically ill COVID-19 patients [47]. These cytokines are considered valuable biomarkers for evaluating disease progression and potential biological therapeutic targets currently being investigated. In the cellular component category, the top GO terms identified using the common DEGs were collagen-containing extracellular matrix (ECM) and platelet alpha granule. Similarly, the Reactome analysis of the DEGs was mainly enriched in ECM organization (R-HSA-1474244), smooth muscle contraction (R-HSA-445355), and elastic fiber formation (R-HSA-1566948). The ECM comprises fibrillar structures that are made of collagen. Cardiorespiratory disease has been linked to collagen dysfunction [48].

We developed a PPI network based on the identified DEGs to understand how proteins behave biologically and predict potential drug targets. Herein, we used the topological metric (i.e., degree) to identify hub proteins that could serve as COVID-19 potential drug targets or biomarkers and could be linked to various pathological and cellular mechanisms. Most of the top hub proteins identified are associated with HCM and COVID-19 risk factors. These diseases have been linked to ten hub-protein products, including THBS2, BGN, COL1A2, ACTA2, MYH11, AEBP1, ISLR, FRZB, MFAP4, and LOXL1. In this study, a cut-off parameter of 12 degrees was used to identify hub proteins. Cardiorespiratory diseases are significantly impacted by the THBS family of proteins. The effects of circular RNA knockdown on the growth, migration, and necrosis of lung cancer cells are reversed by the overexpression of *THBS2*, a miR-590-5 target [49]. Additionally, this gene was linked to adenovirus infection [50] and could function as one of COVID-19's possible therapeutic targets. Meanwhile, *THBS1* and *COL1A1* are genes involved in cardiac remodelling, a hallmark of cardiac hypertrophy [51]. Lastly, BGN ubiquitously exists in the intestinal ECM; thus, *BGN* could potentially serve as a therapeutic target for HCM patients with COVID-19.

Herein, the TF-gene and miRNA interactions were also analysed to identify potential transcriptional regulators of the common DEGs. TFs and miRNAs regulate gene expression and posttranscriptional RNA silencing, two processes that are crucial to understanding disease development. We discovered connections between the common DEGs, TFs, and miRNAs. The identified TFs, such as the GATA-binding factor 2, histone H4 TF, TF AP-2 alpha, nuclear factor kappa B subunit 1, *BGN*, and forkhead box C 1, were found to relate to diffident types of developmental and hereditary diseases. Moreover, most of the miRNAs involved in various cancer types (e.g., hsa-mir-29c-3p, hsa-mir-1-3p, and hsa-mir-128-3p) [52–54] and immunity disorders (e.g., hsa-mir-129-2-3p, hsa-mir-16-5p, hsa-mir-182-5p, hsa-mir-27b-3p, and hsa-mir-124-3p) [55–59], as well as TFs related to the corresponding genes, target major proteins to alter their role in disease progression. For example, hsa-mir-29c-3p, hsa-mir-1-3p, and hsa-mir-129-2-3p have been found to target THBS2 [52, 53, 55]. Four miRNAs that we predicted—hsa-mir-376a-5p, hsa-mir-30a-5p, hsa-mir-23b-3p, and hsa-mir-27a-5p—were found to be associated with various HCM-related genes [60–63]. Many of the miRNAs identified are linked to several cancer types, especially lung cancer.

The DEGs and their relation to various diseases were analysed using a gene-disease analysis. Our findings for COVID-19 revealed the involvement of several diseases, such as lung cancer, cardiovascular diseases, blood disorders, liver ailments, and blood coagulation disorders. According to some reviews, SARS-CoV-2 could exacerbate the pathological process of degenerative osteoarthritis. ACE2 expression, RAS imbalances, inflammation, and dysfunction at the molecular level have been suggested as the causative factors [64]. Based on the aforementioned reports, we speculate that systemic inflammation and ischaemia could aggravate cardiac injury in patients with HCM. Hence, anti-inflammatory therapy is particularly important for patients with COVID-19 and HCM.

Herein, we identified dasatinib, a tyrosine kinase inhibitor used for leukaemia. Previous reports predicted that dasatinib could inhibit the binding of SARS-CoV-2 spike protein to ACE2 [65]. However, dasatinib has not yet been previously reported as a treatment option for patients with HCM. By boosting the activation of the mammalian target of rapamycin complex 2, rapamycin, another drug candidate discovered, may be used to reduce inflammation in patients with heart disease [66]. Meanwhile, another drug, decitabine, could increase neoantigen expression to enhance T cell-mediated toxicity against glioblastoma [67]. Testosterone enanthate replacement therapy is commonly used in patients with low testosterone [68]. Additionally, testosterone administration helps suppress the inflammatory response [69] and modulates the immune response, which would be more significant in female patients. We witnessed the first case of corticosteroid and tocilizumab application in reversing the severely reduced left ventricular systolic

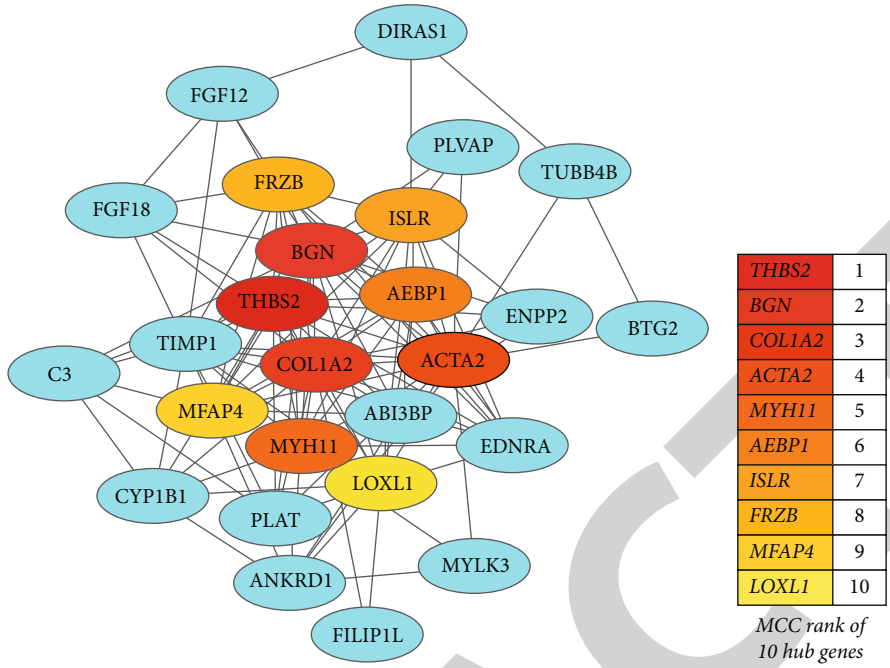

Figure 5: Determination of hub genes from the protein-protein interaction network using the latest maximal clique centrality procedure with the Cytohubba plugin in Cytoscape. The nodes highlighted in red or yellow represent the top 10 hub genes and their interactions with other molecules. There are 26 nodes and 119 edges in the network.

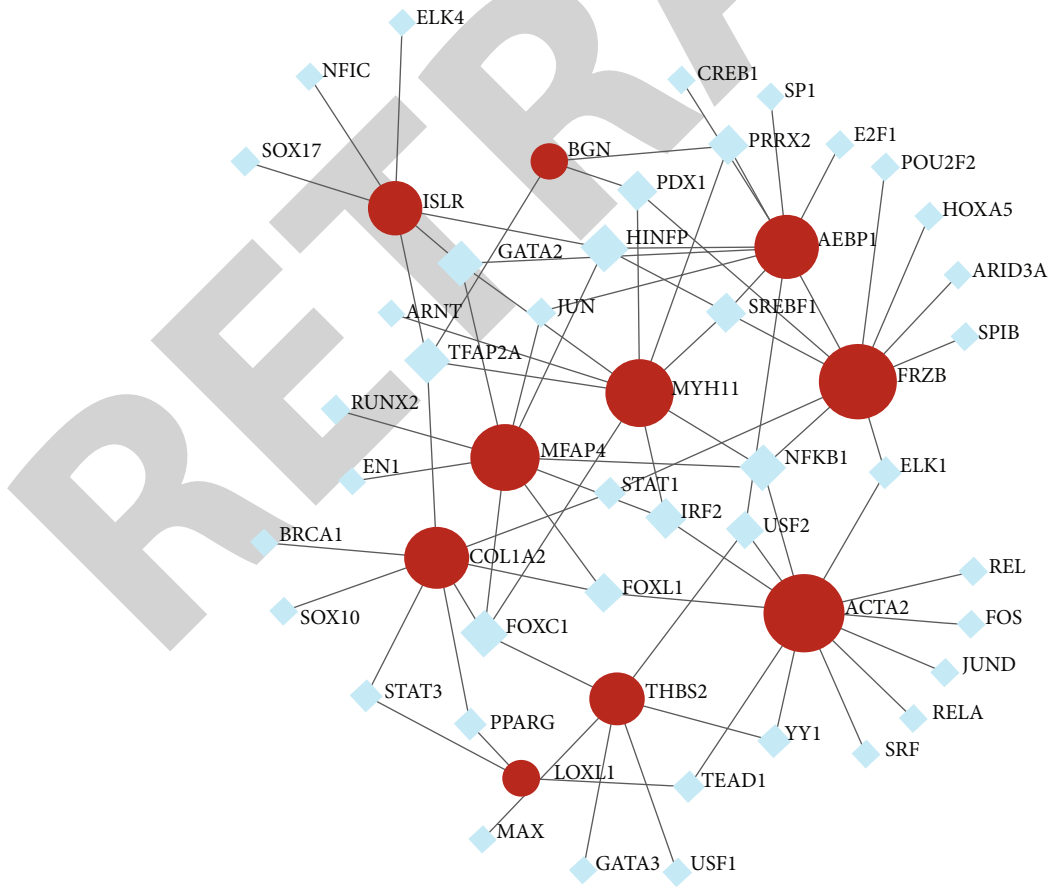

Figure 6: Differentially expressed gene-transcription factor (TF) regulatory interactions were constructed based on our analyses. The nodes in this diagram represent the TFs, while circular nodes are gene symbols that interact with the TFs.

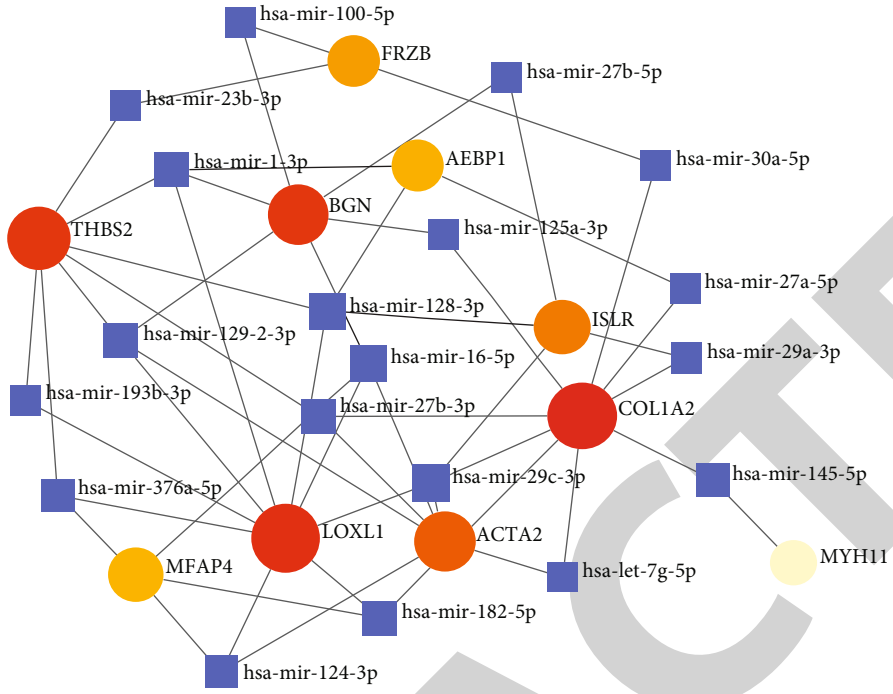

Figure 7: An interconnected network of differentially expressed genes and microRNAs (miRNAs). The circular node represents miRNAs, while the square nodes represent the interaction between genes and miRNAs.

Table 4: The candidate drugs for hypertrophic cardiomyopathy and coronavirus disease 2019.

Name	*P* value	Chemical formula	Structure
Dasatinib CTD 00004330	2.22E-06	$C_{22}H_{26}ClN_7O_2S$	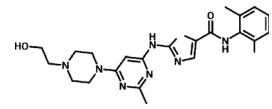
Rapamycin CTD 00007350	2.09E-04	$C_{51}H_{79}NO_{13}$	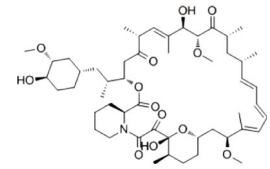
Decitabine CTD 00000750	0.001005467	$C_8H_{12}N_4O_4$	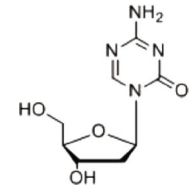
Testosterone enanthate CTD 00000155	0.001963753	$C_{26}H_{40}O_3$	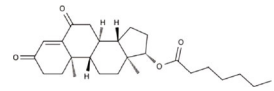

function due to myocardial depression caused by COVID-19 [70]. This partially demonstrates the clinical viability of our candidate drugs in patients with HCM and paves the way for future pharmaceutical studies. Although we could identify candidate drugs based on our bioinformatics analyses, the findings are also limited in that no experiments or further analytical validation were performed on the data obtained. These reasons could lead to unreliable and imprecise conclusions. Thus, further experiments or clinical trials are necessary to validate their effectiveness and safety.

5. Conclusions

As the COVID-19 vaccine becomes more widely used, more side effects are being reported [71]. Despite the ongoing

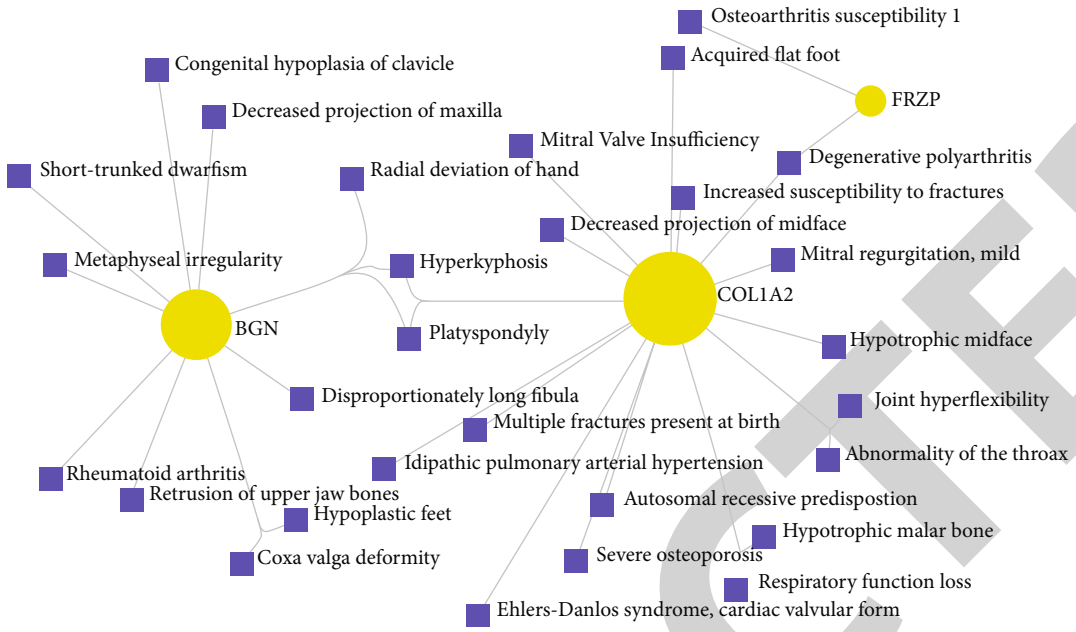

Figure 8: Figure showing the disease-gene association network. Circular nodes represent the gene symbols, and square nodes represent the disease.

development of numerous COVID-19 vaccines, mutant SARS-CoV-2 strains continue to appear. According to this study's bioinformatics analysis, the 10 most important genes that HCM and COVID-19 have in common are *THBS2*, *BGN*, *COL1A2*, *ACTA2*, *MYH11*, *AEBP1*, *ISLR*, *FRZB*, *MFAP4*, and *LOXL1*. Each of these hub genes is essential for various functional mutation developments. Therefore, we used transcriptomic analysis to identify shared pathways and molecular biomarkers between HCM and COVID-19, which could aid in COVID-19 vaccine development and the discovery of novel therapeutic targets.

Data Availability

The data used to support the findings of this study are included in the article.

Conflicts of Interest

The authors declare that they have no competing interests.

Authors' Contributions

Xiao Han and Fei Wang contributed equally to this work.

References

[1] Y. Y. Zheng, Y. T. Ma, J. Y. Zhang, and X. Xie, "COVID-19 and the cardiovascular system," *Nature Reviews Cardiology*, vol. 17, no. 5, pp. 259-260, 2020.

[2] V. C. C. Cheng, S. K. P. Lau, P. C. Y. Woo, and K. Y. Yuen, "Severe acute respiratory syndrome coronavirus as an agent of emerging and reemerging infection," *Clinical Microbiology Reviews*, vol. 20, no. 4, pp. 660–694, 2007.

[3] R. Lu, X. Zhao, J. Li et al., "Genomic characterisation and epidemiology of 2019 novel coronavirus: implications for virus origins and receptor binding," *Lancet*, vol. 395, no. 10224, pp. 565–574, 2020.

[4] A. Saghazadeh and N. Rezaei, "Immune-epidemiological parameters of the novel coronavirus -a perspective," *Expert Review of Clinical Immunology*, vol. 16, no. 5, pp. 465–470, 2020.

[5] C. Huang, Y. Wang, X. Li et al., "Clinical features of patients infected with 2019 novel coronavirus in Wuhan, China," *The Lancet*, vol. 395, no. 10223, pp. 497–506, 2020.

[6] E. Driggin, M. V. Madhavan, B. Bikdeli et al., "Cardiovascular considerations for patients, health care workers, and health systems during the COVID-19 pandemic," *Journal of the American College of Cardiology*, vol. 75, no. 18, pp. 2352–2371, 2020.

[7] A. Lala, K. W. Johnson, J. L. Januzzi et al., "Prevalence and impact of myocardial injury in patients hospitalized with COVID-19 infection," *Journal of the American College of Cardiology*, vol. 76, no. 5, pp. 533–546, 2020.

[8] A. Hessami and N. Rezaei, "Cardiovascular diseases burden in COVID-19," *The American Journal of Emergency Medicine*, vol. 50, p. 790, 2021.

[9] S. R. Ommen, S. Mital, M. A. Burke et al., "2020 AHA/ACC guideline for the diagnosis and treatment of patients with hypertrophic cardiomyopathy: a report of the American College of Cardiology/American Heart Association Joint Committee on Clinical Practice Guidelines," *The Journal of Thoracic and Cardiovascular Surgery*, vol. 162, no. 1, pp. e23–e106, 2021.

[10] N. Z. Cuervo and N. Grandvaux, "ACE2: evidence of role as entry receptor for SARS-CoV-2 and implications in comorbidities," *eLife Sciences*, vol. 9, 2020.

[11] D. Chen, X. Li, Q. Song et al., "Assessment of hypokalemia and clinical characteristics in patients with coronavirus disease

2019 in Wenzhou, China," *JAMA Network Open*, vol. 3, no. 6, p. e2011122, 2020, Published 2020 Jun 1.

[12] N. R. Tucker, M. Chaffin, K. C. Bedi Jr. et al., "Myocyte-specific upregulation of ACE2 in cardiovascular disease: implications for SARS-CoV-2-mediated myocarditis," *Circulation*, vol. 142, no. 7, pp. 708–710, 2020.

[13] A. Panchal, A. Kyvernitakis, and R. Biederman, "An interesting case of COVID-19 induced reversed takotsubo cardiomyopathy and insight on cardiac biomarkers," *Cureus*, vol. 12, no. 11, article e11296, 2020.

[14] R. Beshai and J. J. Lee, "Unusual case of takotsubo cardiomyopathy secondary to COVID-19 vaccine: case report and literature review," *Cureus*, vol. 14, no. 5, article e25398, 2022.

[15] T. Barrett, D. B. Troup, S. E. Wilhite et al., "NCBI GEO: archive for functional genomics data sets–10 years on," *Nucleic Acids Research*, vol. 39, no. Database, p. D1005, 2011.

[16] D. Blanco-Melo, B. E. Nilsson-Payant, W. C. Liu et al., "Imbalanced host response to SARS-CoV-2 drives development of COVID-19," *Cell*, vol. 181, no. 5, pp. 1036–1045.e9, 2020.

[17] P. Bardou, J. Mariette, F. Escudié, C. Djemiel, and C. Klopp, "jvenn: an interactive Venn diagram viewer," *BMC Bioinformatics*, vol. 15, no. 1, 2014.

[18] A. Anjum, S. Jaggi, E. Varghese, S. Lall, A. Bhowmik, and A. Rai, "Identification of differentially expressed genes in RNA-seq data of Arabidopsis thaliana: a compound distribution approach," *Journal of Computational Biology*, vol. 23, no. 4, pp. 239–247, 2016.

[19] A. Subramanian, P. Tamayo, V. K. Mootha et al., "Gene set enrichment analysis: a knowledge-based approach for interpreting genome-wide expression profiles," *Proceedings of the National Academy of Sciences of the United States of America*, vol. 102, no. 43, pp. 15545–15550, 2005.

[20] M. V. Kuleshov, M. R. Jones, A. D. Rouillard et al., "Enrichr: a comprehensive gene set enrichment analysis web server 2016 update," *Nucleic Acids Research*, vol. 44, no. W1, pp. W90–W97, 2016.

[21] D. Szklarczyk, A. L. Gable, D. Lyon et al., "STRING v11: protein-protein association networks with increased coverage, supporting functional discovery in genome-wide experimental datasets," *Nucleic Acids Research*, vol. 47, no. D1, pp. D607–D613, 2018.

[22] "Large-scale mapping of human protein–protein interactions by mass spectrometry," *Molecular Systems Biology*, vol. 3, no. 1, pp. 89–89, 2007.

[23] B. H. Asa and N. W. Stafford, "Kernel methods for predicting protein-protein interactions," *Bioinformatics*, vol. 21, Supplement 1, pp. i38–i46, 2005.

[24] P. Shannon, A. Markiel, O. Ozier et al., "Cytoscape: a software environment for integrated models of biomolecular interaction networks," *Genome Research*, vol. 13, no. 11, pp. 2498–2504, 2003.

[25] C. H. Chin, S. H. Chen, H. H. Wu, C. W. Ho, M. T. Ko, and C. Y. Lin, "cytoHubba: identifying hub objects and sub-networks from complex interactome," *BMC Systems Biology*, vol. 8, no. S4, p. S11, 2014.

[26] G. Caramori, K. Ito, and I. M. Adcock, "Transcription factors in asthma and COPD," *Idrugs the Investigational Drugs Journal*, vol. 7, no. 8, pp. 764–770, 2004.

[27] J. Xia, E. E. Gill, and R. E. W. Hancock, "NetworkAnalyst for statistical, visual and network-based meta-analysis of gene expression data," *Nature Protocols*, vol. 10, no. 6, pp. 823–844, 2015.

[28] A. Khan, O. Fornes, A. Stigliani et al., "JASPAR 2018: update of the open-access database of transcription factor binding profiles and its web framework," *Nucleic Acids Research*, vol. 46, no. D1, pp. D260–D266, 2018.

[29] P. Sethupathy, B. Corda, and A. G. Hatzigeorgiou, "TarBase: a comprehensive database of experimentally supported animal microRNA targets," *RNA*, vol. 12, no. 2, pp. 192–197, 2006.

[30] S. D. Hsu, F. M. Lin, W. Y. Wu et al., "miRTarBase: a database curates experimentally validated microRNA–target interactions," *Nucleic Acids Research*, vol. 39, suppl_1, pp. D163–D169, 2011.

[31] Z. Xie, A. Bailey, M. V. Kuleshov et al., "Gene set knowledge discovery with Enrichr," *Current Protocols*, vol. 1, no. 3, p. e90, 2021.

[32] M. Yoo, J. Shin, J. Kim et al., "DSigDB: Drug Signatures Database for Gene Set Analysis," *Bioinformatics*, vol. 31, no. 18, pp. 3069–3071, 2015.

[33] J. Piñero, À. Bravo, N. Queralt-Rosinach et al., "DisGeNET: a comprehensive platform integrating information on human disease-associated genes and variants," *Nucleic Acids Research*, vol. 45, no. D1, pp. D833–D839, 2017.

[34] M. Al-Mustanjid, S. H. Mahmud, M. R. Royel et al., "Detection of molecular signatures and pathways shared in inflammatory bowel disease and colorectal cancer: a bioinformatics and systems biology approach," *Genomics*, vol. 112, no. 5, pp. 3416–3426, 2020.

[35] U. Wittig and A. D. Beuckelaer, "Analysis and comparison of metabolic pathway databases," *Briefings in Bioinformatics*, vol. 2, no. 2, pp. 126–142, 2001.

[36] Z. Wu, F. Cheng, J. Li, W. Li, G. Liu, and Y. Tang, "SDTNBI: an integrated network and chemoinformatics tool for systematic prediction of drug-target interactions and drug repositioning," *Briefings in Bioinformatics*, vol. 18, no. 2, pp. 333–347, 2017.

[37] S. Mahmud, W. Chen, Y. Liu et al., "PreDTIs: prediction of drug–target interactions based on multiple feature information using gradient boosting framework with data balancing and feature selection techniques," *Briefings in Bioinformatics*, vol. 22, no. 5, 2021.

[38] M. A. Moni and P. Liò, "comoR: a software for disease comorbidity risk assessment," *Bioinformatics*, vol. 4, no. 1, p. 8, 2014.

[39] B. Siripanthong, S. Nazarian, D. Muser et al., "Recognizing COVID-19-related myocarditis: the possible pathophysiology and proposed guideline for diagnosis and management," *Heart Rhythm*, vol. 17, no. 9, pp. 1463–1471, 2020.

[40] M. R. Rahman, T. Islam, T. Zaman et al., "Identification of molecular signatures and pathways to identify novel therapeutic targets in Alzheimer's disease: insights from a systems biomedicine perspective," *Genomics*, vol. 112, no. 2, pp. 1290–1299, 2020.

[41] Z. Nain, H. K. Rana, P. Liò, S. M. Islam, M. A. Summers, and M. A. Moni, "Pathogenetic profiling of COVID-19 and SARS-like viruses," *Briefings in Bioinformatics*, vol. 22, no. 2, pp. 1175–1196, 2020.

[42] M. S. Khatun, W. Shoombuatong, M. M. Hasan, and H. Kurata, "Evolution of sequence-based bioinformatics tools for protein-protein interaction prediction," *Current Genomics*, vol. 21, no. 6, pp. 454–463, 2020.

[43] J. Pober and W. Sessa, "Evolving functions of endothelial cells in inflammation," *Nature Reviews. Immunology*, vol. 7, no. 10, pp. 803–815, 2007.

[44] S. Åkerström, V. Gunalan, C. T. Keng, Y. J. Tan, and A. Mirazimi, "Dual effect of nitric oxide on SARS-CoV

Hindawi
Computational and Mathematical Methods in Medicine
Volume 2023, Article ID 9760762, 1 page
https://doi.org/10.1155/2023/9760762

Retraction

Retracted: Detection and Correlation Analysis of Serum Uric Acid in Patients with Thyroid-Associated Ophthalmopathy

Computational and Mathematical Methods in Medicine

Received 12 December 2023; Accepted 12 December 2023; Published 13 December 2023

This article has been retracted by Hindawi, as publisher, following an investigation undertaken by the publisher [1]. This investigation has uncovered evidence of systematic manipulation of the publication and peer-review process. We cannot, therefore, vouch for the reliability or integrity of this article.

Please note that this notice is intended solely to alert readers that the peer-review process of this article has been compromised.

Wiley and Hindawi regret that the usual quality checks did not identify these issues before publication and have since put additional measures in place to safeguard research integrity.

We wish to credit our Research Integrity and Research Publishing teams and anonymous and named external researchers and research integrity experts for contributing to this investigation.

The corresponding author, as the representative of all authors, has been given the opportunity to register their agreement or disagreement to this retraction. We have kept a record of any response received.

References

[1] J. Zhou, X. Yu, Y. Lou, J. Bao, Y. Xia, and L. Zhu, "Detection and Correlation Analysis of Serum Uric Acid in Patients with Thyroid-Associated Ophthalmopathy," *Computational and Mathematical Methods in Medicine*, vol. 2022, Article ID 8406834, 6 pages, 2022.

Hindawi
Computational and Mathematical Methods in Medicine
Volume 2022, Article ID 8406834, 6 pages
https://doi.org/10.1155/2022/8406834

Research Article

Detection and Correlation Analysis of Serum Uric Acid in Patients with Thyroid-Associated Ophthalmopathy

Jingbo Zhou,[1] Xu Yu,[1] Yan Lou,[1] Jinjing Bao,[1] Yuequan Xia,[2] and Lin Zhu[3]

[1]*Department of Endocrinology, Affiliated Hospital of Nanjing University of Chinese Medicine, Nanjing 210029, China*
[2]*School of Graduate, Nanjing University of Chinese Medicine, Nanjing 210023, China*
[3]*Physical Examination Center, Affiliated Hospital of Nanjing University of Chinese Medicine, Nanjing 210029, China*

Correspondence should be addressed to Lin Zhu; zhulin5688@outlook.com

Received 12 August 2022; Revised 8 September 2022; Accepted 12 September 2022; Published 27 September 2022

Academic Editor: Min Tang

Purpose. To probe the property of serum uric acid in evaluating the activity of patients with thyroid-associated ophthalmopathy. *Methods*. A total of 443 patients with TAO admitted to our hospital from March 2016 to February 2021 were selected for the observation group. Simultaneously, 443 healthy subjects were selected for the control group. The observation group was divided into the active group ($n = 254$) and the inactive group ($n = 189$) according to the clinical activity score (CAS). Besides, the patients were divided into mild group ($n = 201$), moderate severe group ($n = 133$) and extremely severe group ($n = 109$) based on the severity of TAO. Serum uric acid, free triiodothyronine (FT3), free thyroid hormone (FT4), thyrotropin stimulating hormone (TSH) and glycosylated hemoglobin (HbA1c) levels were detected and analyzed in each group. *Results*. Serum UA, FT3, FT4, TSH and HbA1c in the active group were significantly enhanced than those in the other two groups ($P < 0.05$), and there was no significant difference between the inactive group and the control group ($P > 0.05$). In different disease severity groups, the serum UA level of patients in the active group was significantly promoted than that in the inactive group and control group ($P < 0.05$) and was decreased successively in extremely severe group, moderate severe group and mild group, with statistical significance ($P < 0.05$). Pearson's analysis showed that UA was positively correlated with FT3, FT4, and HbA1c ($r = 0.652, P = 0.031$; $r = 0.571, P = 0.042$; $r = 0.737, P = 0.024$), while was reversely correlated with TSH level ($r = -0.137, P = 0.262$). There was no correlation between UA and FT3, FT4, and HbA1c levels in the inactive group. UA detection showed the average sensitivity and specificity of TAO activity were 94.3% and 85.2%, respectively. There was no significant correlation between the severity of disease and serum UA in inactive patients ($P = 0.135$). There was a positive correlation between the severity of disease and serum UA in active patients ($P = 0.005$). *Conclusion*. UA may be used as a laboratory indicator for quantitative clinical diagnosis of thyroid-associated ophthalmopathy (TAO) and as a parameter for the presence of TAO activity.

1. Introduction

Thyroid-associated ophthalmopathy (TAO) belongs to one of the most common orbital diseases, with the highest morbidity in adults. It is generally considered to be an organ-specific autoimmune disease associated with thyroid dysfunction [1]. Its clinical manifestations are mainly eyeball protrusion, contracture of upper eyelid, diplopia, strabismus, optic nerve damage, and so on [2]. The course of TAO is divided into two stages: active phase and quiescent phase [3]. Due to the fact that different treatment methods need to be adopted at different stages of the disease, it is of great significance to evaluate the activity of eye disease for the selection of treatment methods and estimation of prognosis. At present, the evaluation of TAO activity is mainly based on the symptoms and signs of patients, as well as imaging examination, which is easily affected by subjective factors such as patients themselves and ophthalmologists' work experience [4]. Recently, the study of laboratory parameters on TAO activity has made some progress, and it has been reported that urinary glycosaminoglycan (uGAG) and serum uric acid (sUA) play important roles in the evaluation

of TAO activity [5, 6]. UA is the final product of the purine metabolism in the human body [7]. sUA levels indicate the balance between the metabolic breakdown of purine nucleotides and UA excretion [8]. sUA levels are considered an independent predictor for metabolic syndrome [9]. However, diverse reports have different conclusions, and the examination method is time-consuming, making it difficult to be routinely applied.

In this study, 443 patients with TAO treated in our hospital were carried on detecting the content of sUA, for the sake of exploring the role of sUA in the evaluation of activity of TAO patients.

2. Clinical Data and Methods

2.1. General Clinical Data. A total of 443 patients including 233 males and 210 females with TAO admitted to our hospital from March 2016 to February 2021 were selected as the observation group, and 443 healthy people including 225 males and 218 females were chosen as the control group during the same period. All patients obtained informed consent, and the research was reviewed and approved by the medical ethics committee of hospital. The following are the inclusion criteria: (1) The diagnostic criteria of TAO were met. (2) Informed consent was signed by both patients and their families and approved by the hospital's medical ethics committee. (3) There are no conscious disorders and mental disorders. (4) Thyroid function in all patients was within normal range. (5) The intraocular pressure of patients was within a normal range. The following are the exclusion criteria: (1) The presence of internal diseases affecting SUA levels, such as primary gout, malignant tumor, kidney disease, diabetes, and blood diseases; (2) age < 20 or >75 years old; (3) having autoimmune thyroiditis and secondary hyperthyroidism; and (4) pregnant and lactating women.

2.2. Methods

2.2.1. Blood Sample Collection. All subjects fasted for 12 h before blood collection, strictly controlled their diet for 1 week before blood collection, and did not eat food with great influence on blood lipid and uric acid. All subjects were collected 5 mL fasting venous blood in the morning after enrollment. Among them, patients in the observation group were added with methylimidazole or propylthiouracil, and their blood was collected again after thyroid function was normal. The blood samples were centrifuged at 3000 r/min for 10 min with an effective centrifugation radius of 6 cm. The serum was routinely separated and stored in a 20°C refrigerator for testing.

2.2.2. Measurements of Blood Glucose and Blood Lipid Levels. Fasting blood glucose (FBG), total cholesterol (TC), triglyceride (TG), high-density lipoprotein cholesterol (HDL-C), and low-density lipoprotein cholesterol (LDL-C) were assessed by the Hitachi 7600 automatic biochemical analyzer.

2.2.3. Determination of Thyroid Hormone and Blood Uric Acid Levels. Levels of serum free triiodothyronine (FT3), free thyroxine (FT4), thyrotropin stimulating hormone (TSH), and glycosylated hemoglobin (HbA1c) in both groups were detected by electrochemiluminescence immunoassay (Roche, Cobas E601). The serum uric acid levels of the two groups were determined by uric acid oxidase-peroxidase method.

2.2.4. TAO Subgroups. Patients in the observation group were divided into two groups according to the difference in clinical activity score (CAS) [10]. If CAS score reached 4, patients were selected in the active stage; otherwise, patients were in the inactive stage. Among which, 254 cases were in the active stage and 189 cases were in the inactive stage. Meanwhile, the patients were divided into the mild group ($n = 201$), the moderate severe group ($n = 133$), and the extremely severe group ($n = 109$) according to the severity of TAO. TAO has three levels of severity: mild, moderate-severe, and very severe (threatening vision). Based on one or more of the following: mild or sufficient interference with daily life, eyelid pullback ≥ 2 mm, soft tissue involvement, higher than normal, unstable or persistent diplopia ≥ 3 mm, corneal contact lubricant reaction, thyroid dysfunction optic neuropathy, and/or corneal rupture. After statistical analysis, there was no significant difference in age, gender and other general clinical data of each group, which was comparable.

2.3. Statistical Analysis. SPSS21.0 was used for data analysis. The assessment data of FBG, TC, TG, HDIL-C, LDL-C, FT3, FT4, TSH, and blood uric acid levels in the two groups were in line with normal distribution by a normality test and were described by $Z \pm S$. A group t-test was used for intergroup comparison, and a paired t-test was used for intragroup comparison. Correlation was analyzed by Pearson's correlation analysis. The test standard $\alpha = 0.05$; $P < 0.05$ was statistically significant.

3. Results

3.1. Comparison of UA, FT3, FT4, TSH, and HbA1c between the CAS Group and Control Group. As indicated in Figure 1, serum UA, FT3, FT4, TSH, and HbA1c in the active group were significantly elevated than those in the other two groups ($P < 0.05$), and there was no statistical significance between the inactive group and the control group ($P > 0.05$).

3.2. Comparison of UA Levels between Patients with Different Degree of Disease and CAS Stage and Control Group. As revealed in Table 1, in the groups of different severity of disease, serum UA level in the active patients was significantly promoted than that in the inactive patients and the control group ($P < 0.05$), and was decreased successively in the extremely severe group, the moderate severe group and the mild group, with statistical significance ($P < 0.05$).

3.3. Correlation between UA and FT3, FT4, TSH, and HbA1c in the CAS Group. As unveiled in Figure 2, Pearson's analysis uncovered that UA was positively correlated with FT3, FT4, and HbA1c ($r = 0.652, P = 0.031$; $r = 0.571, P = 0.042$; $r = 0.737, P = 0.024$), whereas was inversely correlated with TSH level ($r = -0.137, P = 0.262$). UA in the inactive group had no correlation with FT3, FT4, and HbA1c levels.

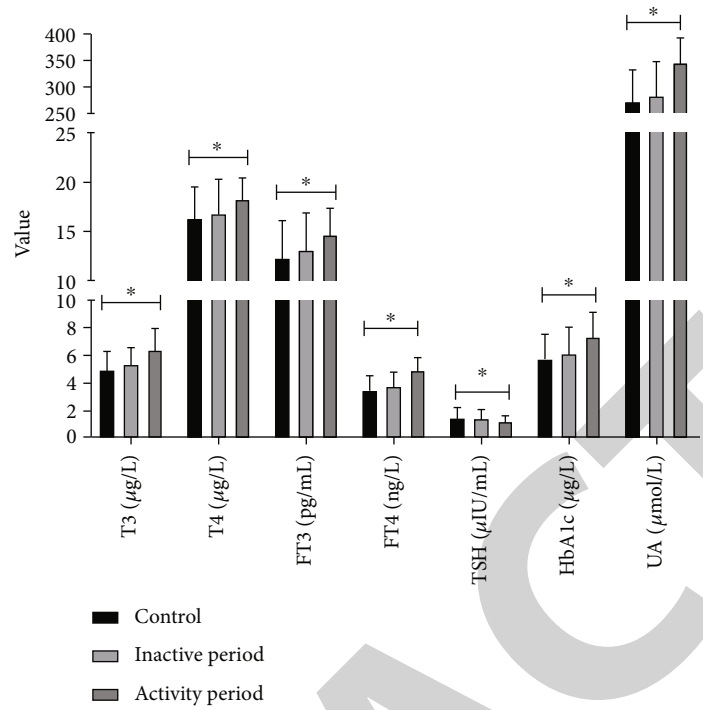

Figure 1: Comparison of UA, FT3, FT4, TSH, and HbA1c between the CAS group and control group.

Table 1: Comparison of UA levels between CAS stage patients with different disease severity and control group.

Groups	n	Inactive period	Active period
Control group	443	271.82 ± 60.45	
Mild group	201	279.46 ± 62.67	294.33 ± 65.33
Moderate severity group	133	302.21 ± 72.44	325.43 ± 71.55
Severity group	109	327.59 ± 68.48	372.25 ± 63.45

3.4. OC Curve Analysis of UA in TAO Patients. As shown in Figure 3, the area of UA under ROC curve in TAO patients was 0.941. The average sensitivity and specificity of UA were 94.3% and 85.2%, respectively. The activity of 443 patients with TAO matched the diagnosis of 402 cases.

3.5. Correlation Analysis between the Disease Severity of Active Period and UA. As demonstrated in Table 2, there was no significant correlation between the severity of disease and serum UA in inactive patients ($P = 0.135$). There was a positive correlation between the severity of disease and serum UA in active patients ($P = 0.005$).

4. Discussion

TAO is an autoimmune disease of which thyroid and orbital tissues produce common antigens leading to T cells and cytokine-mediated autoimmune reactions, characterized by infiltration of lymphocytes and plasma cells, stimulation of proliferation of orbital fibroblasts, and secretion of GAG accumulation in orbit, that is, secretory deposition and tissue edema (inflammatory active phase), and in the later stage, fibrogenesis (quiescent phase). Due to the accumulation of a large number of hydrophilic macromolecular substances, aminoglucosan results in extraocular muscle edema, thereby increasing the pressure behind the eye, and results in the eyeball protrusion of patients. Moreover, limited extraocular muscle activity due to edema causes a series of symptoms, such as diplopia, extraocular muscle contracture, corneal exposure, and eye movement disorders with eyelids unable to close [11–13].

TAO is a wasting disease. Patients in the active stage are in a high metabolic state for a long time and consume more adenosine triphosphate (ATP) than normal people, leading to the increased production of uric acid. It can be seen from the pathway of purine metabolism that ATP participates in the process of uric acid metabolism. ATP metabolism will form ADP or AMP. Under normal conditions, the rates of AMP synthesis and decomposition are similar, so that the daily uric acid production is constant. If the body occurs hypermetabolic states such as hyperthyroidism, ATP will be consumed in large quantities, resulting in the production of AMP and increased production of uric acid, thus causing inflammation in the body. As reported previously, the ocular deposition of GAG in TAO patients is mainly HA [14]. TAO patients not only have glycosaminoglycan deposition in orbital tissues but also have increased blood and uric acid levels. Therefore, serum UA was selected as the measurement index in this study. Recently, UA is closely associated with thyroid dysfunction [15]. In a recent cross-sectional study, UA has a positive correlation with thyroid nodules [16]. Moreover, various studies have found that the change

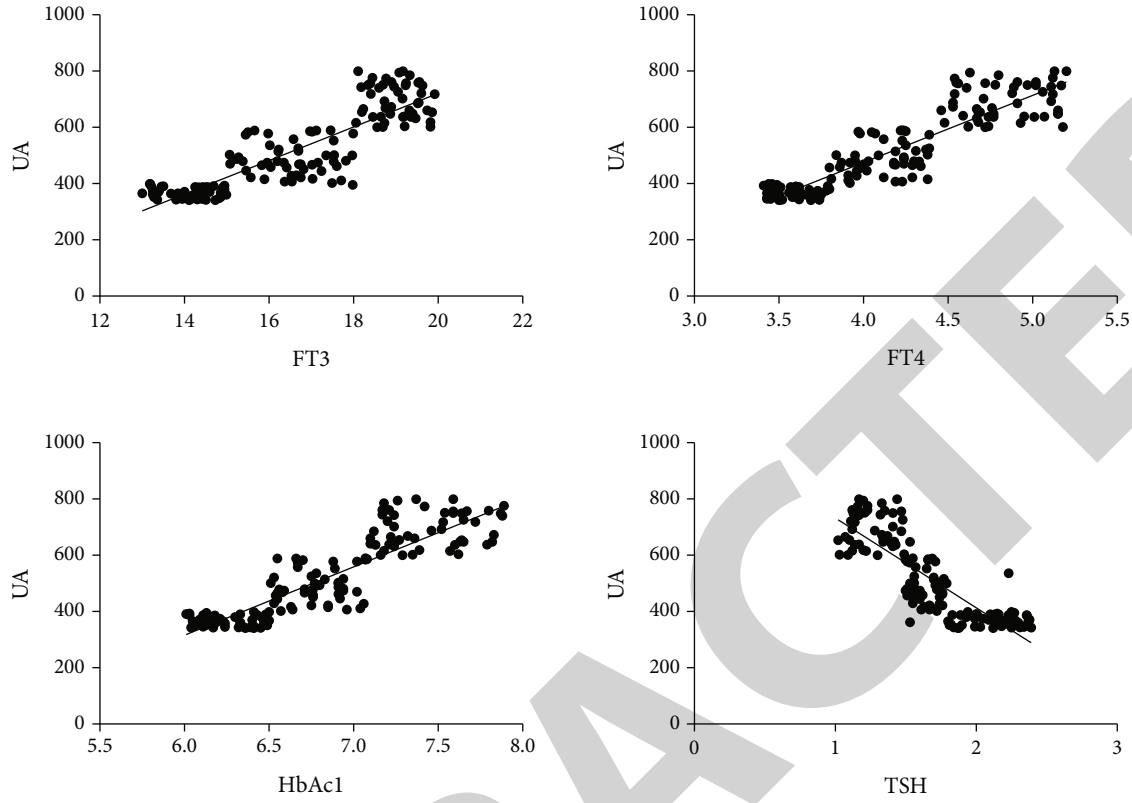

Figure 2: Correlation between UA and FT3, FT4, TSH, and HbA1c in CAS group.

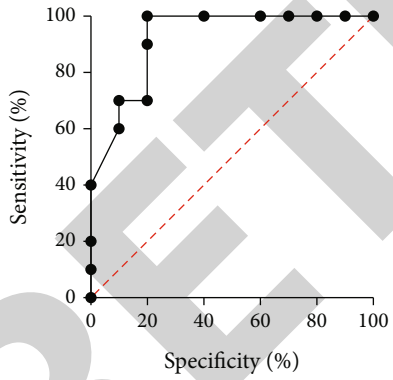

Figure 3: OC curve analysis of UA in TAO patients.

Table 2: Correlation analysis between the disease severity of active period and UA.

Project	UA	
	r	P
Inactive patient severity	0.102	0.135
Active patient severity	0.695	0.005

of serum uric acid level is related to the incidence and mortality of diabetes, cardiovascular diseases, renal diseases, and various clinical syndromes [17, 18]. Hyperuricemia is also an important component of metabolic syndrome [19, 20]. It has been reported that sUA in the TAO group is higher than that in healthy age- and sex-matched volunteers [21]. Consistently, the results in this research unmasked that the concentration of UA in the active TAO group was significantly enhanced than that in the static TAO group and the normal control group ($P < 0.05$), which was 2.38 times of that in the static TAO group and 2.80 times of that in the normal control group. Furthermore, there was no significant difference of serum UA concentration between the static TAO group and the normal control group ($P > 0.05$), which was in line with the existing research views [22, 23]. This indicated that patients in the active TAO group had inflammation in eyelid and thyroid, and UA production rate could be increased. However, serum UA expression of patients in the inactive TAO group was normal, which may be related to the fade of inflammatory cell infiltration during this period. This study also proved that in the groups of different severity of disease, serum UA level in the active patients was significantly increased than that in the control group and was decreased successively in the extremely severe group, the moderate severe group, and the mild group ($P < 0.05$). These results mirrored that the more severe condition of active TAO patients, the higher the serum UA expression level was. For active TAO patients, the degree of illness can affect the expression of UA. In this paper, correlation analysis suggested that there was a significant positive correlation between the severity of disease and serum UA expression in active patients ($P = 0.005$). As we know, FT3, FT4, and HbA1c are important indexes for assessing thyroid function

[24]. In our study, we found that UA in active patients was positively correlated with FT3, FT4, and HbA1c ($r = 0.652$, $P = 0.031$; $r = 0.571$, $P = 0.042$; $r = 0.737$, $P = 0.024$), while it was negatively correlated with TSH level ($r = -0.137$, $P = 0.262$). However, inactive patients had no such correlation ($P = 0.135$), and UA in the inactive group had no correlation with FT3, FT4, and HbA1c levels ($P > 0.05$), which was consistent with existing research views. This indicated that the UA level was increased with the aggravation of disease during active TAO period.

The two most basic indicators of diagnostic value are sensitivity and specificity. ROC curve can evaluate the efficiency of a test from these two aspects and directly reflect the area under the curve, which is convenient for comparison between different methods. The area under ROC curve is used to evaluate the accuracy of the diagnostic experiment. According to Swets criteria, the area below 0.5 indicates that the experiment has no diagnostic value, the area between 0.5 and 0.7 has a low accuracy, the area between 0.7 and 0.9 has a certain accuracy, and the area > 0.9 has a high accuracy. This paper showed that the area of UA under the ROC curve was 0.941, suggesting that all UA indicators had high diagnostic value.

This study has some limitations: the sample size of is small, and the current results can only draw preliminary conclusions. In the near future, the sample size should be expanded and the detailed group studies should be conducted to explore the dose-response relationship.

Above all, UA levels of patients in active TAO stage was obviously enhanced than that of motionless phase and the normal control group, and the difference was statistically significant, which showed that UA was involved in the pathological process of TAO patients. Besides, the serum UA level in TAO group was promoted with the increase of the severity of eye disease, which indicated that both of them were closely correlated with the incidence of TAO and were positively correlated with the severity of secretory ophthalmopathy. Our study suggested that UA could be used as a laboratory index for clinical diagnosis of TAO patients and a parameter for the activity of TAO and provided a basis for exploring the value of UA level and its changes in the clinical therapeutic effect and prognosis evaluation of TAO.

Data Availability

Original data included/analyzed in this study are available from the corresponding author under reasonable requests.

Conflicts of Interest

The authors declare that they have no conflicts of interest.

Acknowledgments

This work was supported by the Investigator-Initiated Clinical Study under grant number YJZ202222.

References

[1] E. J. Neag and T. J. Smith, "2021 update on thyroid-associated ophthalmopathy," *Journal of Endocrinological Investigation*, vol. 45, no. 2, pp. 235–259, 2022.

[2] D. Li and F. Sun, "Observations on the efficacy of two methods for the treatment of upper eyelid retraction in thyroid-associated ophthalmopathy," *BioMed Research International*, vol. 2021, Article ID 9514279, 6 pages, 2021.

[3] D. H. Verity and G. E. Rose, "Acute thyroid eye disease (TED): principles of medical and surgical management," *Eye*, vol. 27, no. 3, pp. 308–319, 2013.

[4] G. J. Kahaly, J. Hardt, F. Petrak, and U. T. Egle, "Psychosocial factors in subjects with thyroid-associated ophthalmopathy," *Thyroid*, vol. 12, no. 3, pp. 237–239, 2002.

[5] N. Giordano, C. Santacroce, G. Mattii, S. Geraci, A. Amendola, and C. Gennari, "Hyperuricemia and gout in thyroid endocrine disorders," *Clinical and Experimental Rheumatology*, vol. 19, no. 6, pp. 661–665, 2001.

[6] J. Zhang, Z. Meng, Q. Zhang et al., "Gender impact on the correlations between subclinical thyroid dysfunction and hyperuricemia in Chinese," *Clinical Rheumatology*, vol. 35, no. 1, pp. 143–149, 2016.

[7] W. Ma, C. Cui, S. Feng et al., "Serum uric acid and triglycerides in Chinese patients with newly diagnosed moyamoya disease: a cross-sectional study," *BioMed Research International*, vol. 2019, Article ID 9792412, 7 pages, 2019.

[8] L. Wang, T. Zhang, Y. Liu, F. Tang, and F. Xue, "Association of serum uric acid with metabolic syndrome and its components: a Mendelian randomization analysis," *BioMed Research International*, vol. 2020, Article ID 6238693, 7 pages, 2020.

[9] A. Masajtis-Zagajewska, J. Majer, and M. Nowicki, "Losartan and eprosartan induce a similar effect on the acute rise in serum uric acid concentration after an oral fructose load in patients with metabolic syndrome," *Journal of the Renin-Angiotensin-Aldosterone System*, vol. 2021, article 2214978, 7 pages, 2021.

[10] G. J. Kahaly, R. S. Douglas, R. J. Holt, S. Sile, and T. J. Smith, "Teprotumumab for patients with active thyroid eye disease: a pooled data analysis, subgroup analyses, and off-treatment follow-up results from two randomised, double-masked, placebo-controlled, multicentre trials," *The Lancet Diabetes and Endocrinology*, vol. 9, no. 6, pp. 360–372, 2021.

[11] Y. Ye, X. Gai, H. Xie, L. Jiao, and S. Zhang, "Association between serum free thyroxine (FT4) and uric acid levels in populations without overt thyroid dysfunction," *Annals of Clinical and Laboratory Science*, vol. 45, no. 1, pp. 49–53, 2015.

[12] T. J. Smith, G. J. Kahaly, D. G. Ezra et al., "Teprotumumab for thyroid-associated ophthalmopathy," *The New England Journal of Medicine*, vol. 376, no. 18, pp. 1748–1761, 2017.

[13] E. Şahlı and K. Gündüz, "Thyroid-associated ophthalmopathy," *Turkish journal of ophthalmology*, vol. 47, no. 2, pp. 94–105, 2017.

[14] T. J. Smith and J. Janssen, "Insulin-like growth factor-I receptor and thyroid-associated ophthalmopathy," *Endocrine Reviews*, vol. 40, no. 1, pp. 236–267, 2019.

[15] G. Desideri, R. Bocale, A. M. D'Amore et al., "Thyroid hormones modulate uric acid metabolism in patients with recent onset subclinical hypothyroidism by improving insulin sensitivity," *Internal and Emergency Medicine*, vol. 15, no. 1, pp. 67–71, 2020.

Hindawi
Computational and Mathematical Methods in Medicine
Volume 2023, Article ID 9847198, 1 page
https://doi.org/10.1155/2023/9847198

Retraction

Retracted: The Value of CT Perfusion Parameters and Apparent Diffusion Coefficient Value of Magnetic Resonance Diffusion Weighted Imaging in Diagnosis of Hepatocellular Carcinoma

Computational and Mathematical Methods in Medicine

Received 5 December 2023; Accepted 5 December 2023; Published 6 December 2023

This article has been retracted by Hindawi, as publisher, following an investigation undertaken by the publisher [1]. This investigation has uncovered evidence of systematic manipulation of the publication and peer-review process. We cannot, therefore, vouch for the reliability or integrity of this article.

Please note that this notice is intended solely to alert readers that the peer-review process of this article has been compromised.

Wiley and Hindawi regret that the usual quality checks did not identify these issues before publication and have since put additional measures in place to safeguard research integrity.

We wish to credit our Research Integrity and Research Publishing teams and anonymous and named external researchers and research integrity experts for contributing to this investigation.

The corresponding author, as the representative of all authors, has been given the opportunity to register their agreement or disagreement to this retraction. We have kept a record of any response received.

References

[1] K. Li and B. Wang, "The Value of CT Perfusion Parameters and Apparent Diffusion Coefficient Value of Magnetic Resonance Diffusion Weighted Imaging in Diagnosis of Hepatocellular Carcinoma," *Computational and Mathematical Methods in Medicine*, vol. 2022, Article ID 2771869, 7 pages, 2022.

Hindawi
Computational and Mathematical Methods in Medicine
Volume 2022, Article ID 2771869, 7 pages
https://doi.org/10.1155/2022/2771869

Research Article

The Value of CT Perfusion Parameters and Apparent Diffusion Coefficient Value of Magnetic Resonance Diffusion Weighted Imaging in Diagnosis of Hepatocellular Carcinoma

Kezhen Li[1] **and Baiping Wang**[2]

[1]*Medical Imaging Department, Wanning People's Hospital, 571500, China*
[2]*Department of Radiology, The Second Affiliated Hospital of Hainan Medical University, 570311, China*

Correspondence should be addressed to Baiping Wang; wangbp08@hainmc.edu.cn

Received 29 July 2022; Revised 16 August 2022; Accepted 31 August 2022; Published 27 September 2022

Academic Editor: Min Tang

Background. Hepatocellular carcinoma is one of the malignant tumors with the highest incidence in the world. According to the latest statistics of the National Cancer Center, the incidence of liver cancer ranks fifth in malignant tumors and its mortality rate ranks second in China, which seriously threatens people' s life and health. *Aim*. To investigate the value of CT perfusion parameters and apparent diffusion coefficient (ADC) of magnetic resonance imaging (MRI) diffusion weighted imaging (DWI) in the diagnosis of hepatocellular carcinoma. *Methods*. 43 patients with hepatocellular carcinoma and 40 patients with hepatic hemangioma treated in our hospital from August 2018 to August 2021 were selected for CT perfusion imaging and MRI examination. *Results*. The liver blood flow (BF), liver blood volume (BV), and hepatic artery perfusion (HAP) in the hepatocellular carcinoma group were (267.38 ± 35.59) ml/(min·100 g), (30.20 ± 8.82) ml/100 g, and (0.64 ± 0.10) ml/(min·ml), respectively, which were significantly higher than those in the hepatic hemangioma group ($p < 0.05$). The ADC value of hepatocellular carcinoma DWI sequence was $(1.20 \pm 0.17) \times 10^{-3}$ mm^2, which was significantly lower than that of hepatic hemangioma ($p < 0.05$). The area under ROC curve of BF, BV, HAP, and ADC values for hepatocellular carcinoma was 0.860, 0.754, 0.804, and 0.890, respectively. The area under ROC curve of the four groups was compared ($p > 0.05$). *Conclusion*. CT perfusion parameters BF, BV, HAP, and DWI sequence ADC values have certain application value in the diagnosis of hepatocellular carcinoma, and there is no significant difference between the diagnostic value of each parameter.

1. Introduction

Hepatocellular carcinoma is the most common malignant tumor in China, with the characteristics of occult onset and rapid progress [1, 2]. There is no special symptom in the early stage of liver cancer, and patients often present with pain in the liver area, anorexia, and dyspepsia. When there is a serious symptom, most patients have reached the advanced stage of cancer. At this time, retreatment can only prolong the survival time of patients and cannot cure the disease [3, 4]. Therefore, the early diagnosis of hepatocellular carcinoma is of great importance, and CT and magnetic resonance imaging (MRI) are commonly used [5, 6]. However, the soft tissue density resolution of CT is poor, and the detection rate and qualitative of lesions are also insufficient. Relevant studies have found that hepatocellular carcinoma can cause abnormal blood flow in the portal vein of the body. CT perfusion imaging can detect the above changes, so CT perfusion imaging has a certain diagnostic effect on hepatocellular carcinoma [7, 8]. Diffusion weighted imaging (DWI) of MRI can respond to the physiological and pathological characteristics of the body by means of the movement of water molecules in the tissue, and the most important indicator is the apparent diffusion coefficient (ADC) value [9, 10]. DWI provides a variety of analytical methods, such as DWI images, ADC maps, and ADC values, which can reflect the internal changes of malignant tumors at the

Table 1: Comparison of general data of patients with hepatocellular carcinoma and hepatic hemangioma.

Group	Cases	Male/female	Age (year)	Hypertension (%)	Diabetes (%)
Hepatocellular carcinoma	43	23/20	55.60 ± 7.82	13 (30.23)	11 (25.58)
Hepatic hemangioma	40	28/12	53.49 ± 8.43	12 (30.00)	10 (25.00)
t/χ^2		2.385	1.183	0.001	0.004
p		0.123	0.240	0.982	0.951

cellular and molecular levels, and has unparalleled advantages in noninvasive evaluation of early tumor efficacy [11, 12]. DWI is the best method for quantitative study of microvascular perfusion and diffusion in vivo and has been successfully applied to the central nervous system [13, 14]. DWI has been gradually used for the diagnosis of abdominal disease. In liver disease, it is mainly used for the identification of lesions and the judgment of benign and malignant lesions in the early stage [15, 16]. This study aims to explore the value of CT perfusion parameters and MRI-DWI ADC in the diagnosis of hepatocellular carcinoma.

Core tips: ADC value is the most important indicator in DWI of MRI. ADC value can quantitatively analyze the benign and malignant tumors. CT perfusion imaging has a certain diagnostic effect on hepatocellular carcinoma. This study attempts to combine CT perfusion parameters and ADC values of MRI-DWI to explore its role in the diagnosis of hepatocellular carcinoma, which has certain clinical significance.

2. Materials and Methods

2.1. General Information. 43 cases of hepatocellular carcinoma (HCC) and 40 cases of hepatic hemangioma treated in our hospital from August 2018 to August 2021 were selected as research subjects. Inclusion criteria: (1) All patients were confirmed by pathology. (2) Age>18 years. (3) CT and MRI examination in our hospital. (4) The clinical image data were preserved completely. (5) Informed consent has been obtained from patients and their families. Exclusion criteria: (1) A history of radiotherapy and chemotherapy before examination. (2) Patients with other systemic malignant tumors. (3) Patients who dropped out of the study. The general data of patients with hepatocellular carcinoma and hepatic hemangioma are compared in Table 1. This study has been approved by the Ethics Committee.

2.2. CT Perfusion Imaging. All patients underwent CT perfusion imaging. After fasting for 8 hours, the patients were assisted to take supine position with advanced feet and arms up. The sternal handle and the midpoint of the sisal process were positioned to guide the patients to carry out correct scanning breathing training. GE company 64-slice spiral CT machine was used for dynamic perfusion scanning. Scanning parameter settings: tube voltage is 120kV, tube current is 200mA, layer thickness is 1.0 mm, scanning pitch is 1.2 mm, scanning thickness is 5mm, the instrument with CT scan and enhanced scan function. Patients were given 800~1000 ml warm boiled water before examination. First of all, the upper abdomen was scanned horizontally. The larger tumor area was taken as the scanning center, and the similar layer near the lesion center was selected as the perfusion level. The scanning range was from the sternocleidomastoid to the iliac spin. The arterial phase (27 s), portal venous phase (66 s), and delayed phase (180 s) were scanned (Figure 1). The conventional CT scan was performed first, and then the CT enhanced scan mode was switched to obtain the duration and enhancement degree of the lesion, and the blood supply characteristics and internal structure of the lesion were analyzed. The contrast agent was iodixanol (BayerAGt, J20171008, Batch No. KT09T6p). The high-pressure syringe was used to inject at a rate of 4 ml/s at a dose of 1.5 ml/kg, and the scanning was delayed by 150–180 s. The data was transmitted to the SunUltraAW4 workstation. The software for processing the data was Perfusion3, and the corresponding time density curve was obtained by computer processing. After computer calculation, the blood flow (BF), blood volume (BV), hepatic arterial perfusion (HAP), and mean transit time (MTT) were obtained.

2.3. MRI Examination. The instrument used was SIGNA-CONTOUR015T MRI produced by GE Company in the United States. The patients have fasted within 4–6 h before examination, and all metal objects were removed. The coils used matched phased array coils and abdominal phased array coils. The field intensity was set to 45 mT/m, the thickness of the layer was set to 10 mm, and the layer spacing was 210 mm. The range was from the top of the diaphragm to the lower pole of the right kidney, and the respiratory gating was placed. T2 weighted imaging (T2WI), dual-echo T1 weighted imaging (T1WI), DWI, and ADC3 phase enhancement scanning were performed on the diaphragm on the abdominal transverse axis, breath holding on the transverse axis, free breathing transverse axis, and breath holding transverse axis, respectively (Figure 2). Gd-DTPA was used as the contrast agent. The injection volume was 0.1 ml/kg and the injection rate was 1.5 ml/s. The axial artery phase (26 s), portal vein phase (60s), and equilibrium phase (180 s) were scanned. Parameter settings are as follows: (1) T2WI: TR2200ms, average times 1, layer spacing 1 mm, layer thickness 5 mm, FOV 40 cm ×40 cm, matrix 252 × 213; (2) T1WI: TR3.6 ms, average times 1, layer spacing 1mm, layer thickness 5mm, FOV 40cm ×40 cm, matrix 252 × 213; (3) DWI: diffusion sensitive gradient field parameters (b value) were 0, 50, 400, 800 mm2/s, NSA1, layer spacing 1mm, layer thickness 5mm, FOV 40cm ×40 cm, matrix 252 × 213.

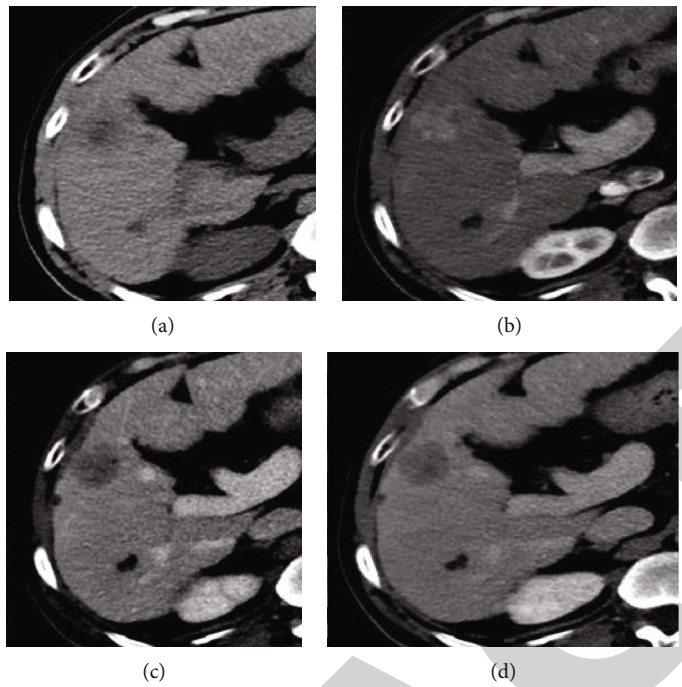

Figure 1: CT image of hepatocellular carcinoma. (a: plain scan period; b: arterial phase; c: portal venous phase; d: delayed phase).

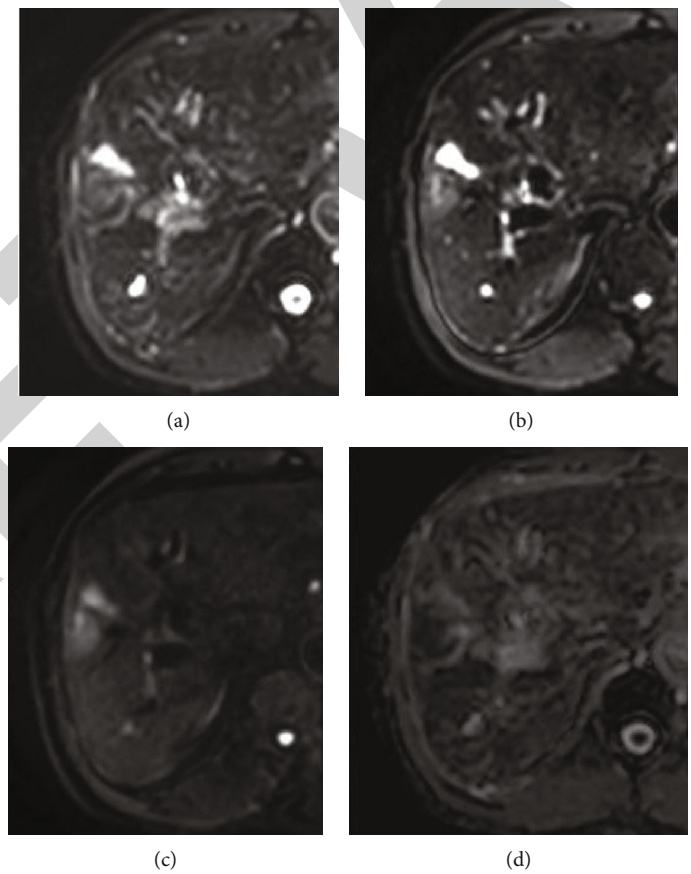

Figure 2: MRI image of hepatocellular carcinoma. (a: T2WI; b: T1WI; c: DWI; d: ADC).

2.4. Statistical Processing. SPSS22.0 software was used for data analysis. Age, ADC value, and other data were expressed as ($\chi \pm s$), and t test was used to analyze the difference between groups. Comparison of gender and other data using 2 tests; the diagnostic value was analyzed by receiver operating characteristic (ROC) curve. $p < 0.05$ was statistically significant.

Table 2: Comparison of CT perfusion parameters between hepatocellular carcinoma and hepatic hemangioma.

Group	Cases	BF [ml/(min·100 g)]	BV (ml/100 g)	HAP [ml/(min·ml)]	MTT (s)
Hepatocellular carcinoma	43	267.38 ± 35.59	30.20 ± 8.82	0.64 ± 0.10	11.78 ± 1.43
Hepatic hemangioma	40	190.92 ± 31.19	21.10 ± 9.10	0.44 ± 0.12	12.03 ± 1.56
t		10.376	4.625	8.270	-0.762
p		<0.001	<0.001	<0.001	0.448

Table 3: Comparison of CT perfusion parameters in patients with hepatocellular carcinoma of different gender and age.

Group	Cases	BF [ml/(min·100 g)]	BV (ml/100 g)	HAP [ml/(min·ml)]	MTT (s)
Sex					
Male	23	264.40 ± 39.12	28.83 ± 6.50	0.63 ± 0.12	11.73 ± 1.55
Female	20	270.12 ± 37.10	31.10 ± 7.43	0.66 ± 0.13	11.98 ± 1.62
t		-0.490	-1.069	-0.787	-0.517
p		0.627	0.291	0.436	0.608
Age					
<50 year	24	263.39 ± 40.40	28.95 ± 5.84	0.62 ± 0.14	11.80 ± 1.62
≥50 year	19	271.11 ± 38.83	30.92 ± 6.11	0.67 ± 0.16	12.01 ± 1.70
t		-0.633	-1.076	-1.092	-0.413
p		0.530	0.288	0.281	0.682
Hypertension					
Yes	13	265.59 ± 39.29	29.01 ± 6.10	0.64 ± 0.13	11.92 ± 1.72
No	30	270.02 ± 40.11	31.01 ± 5.28	0.66 ± 0.18	12.06 ± 1.80
t		-0.335	-1.089	-0.361	-0.237
p		0.740	0.283	0.720	0.814
Diabetes					
Yes	11	267.10 ± 40.10	29.88 ± 5.98	0.65 ± 0.14	11.97 ± 1.81
No	32	271.12 ± 41.17	30.82 ± 6.12	0.67 ± 0.16	12.12 ± 1.92
t		-0.281	-0.442	-0.368	-0.227
p		0.780	0.661	0.715	0.822

Table 4: Comparison of ADC values of DWI sequence between hepatocellular carcinoma and hepatic hemangioma.

Group	Cases	ADC ($\times 10^{-3}$ mm^2)	t	p
Hepatocellular carcinoma	43	1.20 ± 0.17	-12.526	<0.001
Hepatic hemangioma	40	1.63 ± 0.14		

Table 5: Comparison of ADC values of DWI sequence in patients with hepatocellular carcinoma of different gender and age.

Group	Cases	ADC ($\times 10^{-3}$ mm^2)	t	p
Sex				
Male	23	1.18 ± 0.12	-1.177	0.246
Female	20	1.22 ± 0.10		
Age				
<50 year	24	1.19 ± 0.11	-0.467	0.643
≥50 year	19	1.21 ± 0.17		
Hypertension				
Yes	13	1.20 ± 0.13	-0.777	0.441
No	30	1.23 ± 0.11		
Diabetes				
Yes	11	1.18 ± 0.14	-1.163	0.252
No	32	1.24 ± 0.15		

3. Results

3.1. Comparison of CT Perfusion Parameters between Hepatocellular Carcinoma and Hepatic Hemangioma. BF, BV, and HAP in hepatocellular carcinoma were significantly higher than those in hepatic hemangioma ($p < 0.05$) (see Table 2).

3.2. Comparison of CT Perfusion Parameters in Patients with Hepatocellular Carcinoma of Different Genders and Ages. The BF, BV, HAP, and MTT were compared between male and female patients with hepatocellular carcinoma, patients with hepatocellular carcinoma aged <50 years and ≥50 years, and patients with hepatocellular carcinoma with and without hypertension and diabetes mellitus (see Table 3).

Table 6: ROC curve parameters.

Index	Area under curve	p	Truncation value	Sensitivity (%)	Specificity (%)
BF	0.860	<0.001	240 ml/(min·100 g)	78.90	72.20
BV	0.754	<0.001	28.50 ml/100 g	70.40	69.00
HAP	0.804	<0.001	0.56 ml/(min·ml)	76.50	70.00
ADC	0.890	<0.001	1.30 ×10-3 mm2	84.50	78.80

3.3. Comparison of ADC Values of DWI Sequences between Hepatocellular Carcinoma and Hepatic Hemangioma. ADC value of hepatocellular carcinoma DWI sequence was significantly lower than that of hepatic hemangioma ($p < 0.05$) (see Table 4).

3.4. Comparison of ADC Values of DWI Sequences in Patients with Hepatocellular Carcinoma of Different Genders and Ages. DWI ADC values were compared between male and female patients with hepatocellular carcinoma, patients with hepatocellular carcinoma aged <50 years and ≥50 years, and patients with hepatocellular carcinoma with and without hypertension and diabetes mellitus (see Table 5).

3.5. Judgmental Value. The areas under ROC curves of BF, BV, HAP, and ADC values for HCC were 0.860, 0.754, 0.804, and 0.890, respectively, $p < 0.05$, and the areas under ROC curves of the four were compared ($p > 0.05$). The specific parameters are shown in Table 6 and Figure 3.

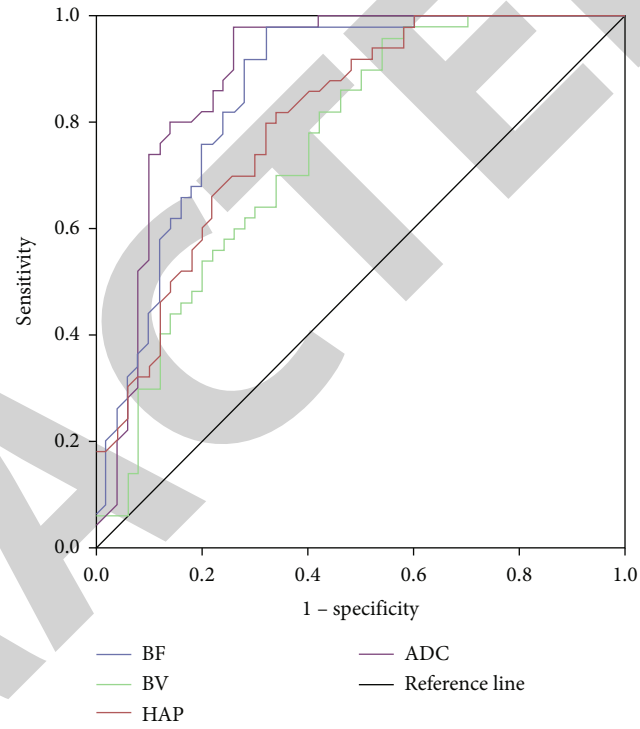

Figure 3: ROC curve analysis.

4. Discussion

Most people believe that the etiology of hepatocellular carcinoma is closely related to viral infection and environmental factors [17, 18] However, the initial symptoms are not obvious, bringing great difficulties to clinical diagnosis and treatment. Effective diagnosis is an important prerequisite for formulating treatment measures and evaluating curative effect. Therefore, it is particularly necessary to conduct timely, accurate, and effective examinations and study the patient 's disease-related indicators [19, 20].

According to relevant research reports [21, 22], the accuracy of CT examination of liver cancer is very high, and the diagnostic value of small lesions is also very high. Therefore, the clinical acceptance of CT examination is very high, and CT examination has become the most commonly used method for the diagnosis of primary liver cancer. At the same time, as the blood flow of malignant tumor patients is mostly obviously abnormal, CT perfusion imaging can clearly display the anatomical details of small lesions and hepatocellular carcinoma, and reflect the blood flow.

The results showed that there was no significant difference in BF, BV, HAP, and MTT between male and female patients with hepatocellular carcinoma and patients aged <50 and ≥50 years old. It suggested that different ages and genders did not affect factors such as liver blood flow. The results of this study showed that BF, BV, and HAP in HCC group were significantly higher than those in hepatic hemangioma group. After the patient developed into hepatocellular carcinoma, the blood perfusion status of the liver changed to a certain extent. With the malignant proliferation of cancer, the blood flow in the artery becomes larger, which leads to insufficient blood supply in the portal vein. Therefore, the judgment of the nature of the tumor can also be reflected by the supply of arterial blood. In the detection of new blood vessels in liver cancer cells, the flow rate is accelerated, resulting in a certain degree of damage to vascular endothelial cells. Due to the presence of different sizes of arteries and veins, arterial portal vein and other different ways and levels of direct entry into the tumor, BV, BF, and HAP increased.

The results of this study showed that there was no significant difference in ADC values of DWI sequences between male and female patients with hepatocellular carcinoma, age <50 years and age ≥50 years. After excluding the influence of age and gender on ADC, it was found that the ADC value of hepatocellular carcinoma DWI sequence was significantly lower than that of hepatic hemangioma. The reason is that although the dispersion of water molecules is different, the b0 image signal of hepatic hemangioma is still very high, so due to T2 transmission effect, their DWI shows high signal. It has been found in some studies [23, 24] that

DWI examination technology plays an increasingly important role in the identification of benign and malignant liver tumors. Due to a variety of components in tumor cells, intercellular space becomes smaller, and the diffusion of water molecules in malignant tumors is more difficult than that in normal cases, and the ADC value is also smaller than that in normal tissues. However, in the benign lesion of hemangioma, hepatic hemangioma is mainly composed of liquid components. The components in cells have little effect on the movement of water molecules, and the ADC value is larger than that of normal tissues. DWI sequence quantitatively analyzed the movement of water molecules in tissues by ADC values. DWI can detect the direction of cell permeability, capillary perfusion, and cell membrane permeability [25, 26].

MRI DWI can reflect the nature of the lesion at the histological level. For example, focal nodular hyperplasia contains normal phagocytotic hepatocytes, and the uptake of contrast agents in the process of hepatobiliary enhancement will present a slightly higher or equal signal, while hepatocellular carcinoma will not [27–29]. In normal liver cells, contrast agent uptake rate will reduce the majority of low signal, while there are still a few lesions showing high signal or equal signal. The results showed that there was no significant difference between the area under the ROC curve of liver cells and BF, BV, HAP, and ADC values. It is suggested that CT perfusion parameters BF, BV, HAP, and DWI sequence ADC values had certain value in the diagnosis of hepatocellular carcinoma and had certain application value. Although the number of cases is small, the increased specific value is not accurate, but the overall detection efficiency is certainly improved. The specific reason is that two imaging examinations can make up for each other' s shortcomings. Considering that the two methods can clearly show the solid part of the tumor and provide help for judgment, they can be used together.

There are few studies on DWI in differentiating hepatocellular carcinoma from hepatic hemangioma [30, 31]. According to this study, we found that the ADC value of DWI sequence could be used for the diagnosis of hepatocellular carcinoma, which had clinical reference significance. However, this study still has many limitations, such as the limited number of samples, which will affect statistical results. In addition, this study is limited to two types of tumors, which need to be further explored in the next study.

5. Conclusion

CT perfusion parameters BF, BV, HAP, and DWI sequence ADC values have certain application value in the diagnosis of hepatocellular carcinoma, and there is no significant difference between the diagnostic value of each parameter.

Data Availability

The datasets used and analyzed during the current study are available from the corresponding author upon reasonable request.

Conflicts of Interest

The authors declare that they have no conflicts of interest.

References

[1] M. Kim, T. W. Kang, D. I. Cha et al., "Identification of arterial hyperenhancement in CT and MRI in patients with hepatocellular carcinoma: value of unenhanced images," *Korean Journal of Radiology*, vol. 20, no. 2, pp. 236–245, 2019.

[2] European Association For The Study Of The Liver; European Organisation For Research And Treatment Of Cancer, "EASL-EORTC clinical practice guidelines: management of hepatocellular carcinoma," *European Journal of Cancer (Oxford, England: 1990)*, vol. 56, no. 4, pp. 908–943, 2012.

[3] R. Liu, L. L. Zhu, C. Y. Yu et al., "Quantitative evaluation of the compatibility effects of aidi injection on the treatment of hepatocellular carcinoma using targeted metabolomics: a new strategy on the mechanism study of an anticancer compound in traditional chinese medicine," *World Journal of Traditional Chinese Medicine*, vol. 7, no. 1, pp. 111–119, 2021.

[4] L. R. Roberts, C. B. Sirlin, F. Zaiem et al., "Imaging for the diagnosis of hepatocellular carcinoma: a systematic review and meta-analysis," *Hepatology*, vol. 67, no. 1, pp. 401–421, 2018.

[5] A. Y. Kim, D. H. Sinn, W. K. Jeong et al., "Hepatobiliary MRI as novel selection criteria in liver transplantation for hepatocellular carcinoma," *Journal of Hepatology*, vol. 68, no. 6, pp. 1144–1152, 2018.

[6] M. Wang, C. Wei, Z. Shi, and J. Zhu, "Study on the diagnosis of small hepatocellular carcinoma caused by hepatitis B cirrhosis via multi-slice spiral CT and MRI," *Oncology Letters*, vol. 15, no. 1, pp. 503–508, 2018.

[7] F. H. Yan, J. Z. Shen, R. C. Li et al., "Enhancement patterns of small hepatocellular carcinoma shown by dynamic MRI and CT," *Hepatobiliary & Pancreatic Diseases International*, vol. 1, no. 3, pp. 420–424, 2002.

[8] R. M. Perl, J. Portugall, C. Hinterleitner et al., "Differences between CT-perfusion and biphasic contrast-enhanced CT for detection and characterization of hepatocellular carcinoma: potential explanations for discrepant cases," *Anticancer Research*, vol. 41, no. 3, pp. 1451–1458, 2021.

[9] A. Nishie, T. Tajima, K. Ishigami et al., "Detection of hepatocellular carcinoma (HCC) using super paramagnetic iron oxide (SPIO)-enhanced MRI: added value of diffusion-weighted imaging (DWI)," *Journal of Magnetic Resonance Imaging*, vol. 31, no. 2, pp. 373–382, 2010.

[10] K. Huang, Z. Dong, H. Cai et al., "Imaging biomarkers for well and moderate hepatocellular carcinoma: preoperative magnetic resonance image and histopathological correlation," *BMC Cancer*, vol. 19, no. 1, p. 364, 2019.

[11] T. Shimizu, U. Motosugi, N. Komatsu et al., "MRI-based risk factors of hepatocellular carcinoma in patients with chronic liver disease: a prospective observational study," *Journal of Magnetic Resonance Imaging*, vol. 51, no. 2, pp. 389–396, 2020.

[12] F. C. Piskin, H. T. Balli, K. E. Erdoğan, S. Sozutok, and K. Aikimbaev, "Whole tumor volumetric ADC analysis: relationships with histopathological differentiation of hepatocellular carcinoma," *Abdominal Radiology*, vol. 46, no. 11, pp. 5180–5189, 2021.

[13] X. Ma, H. Ouyang, S. Wang et al., "Histogram analysis of apparent diffusion coefficient predicts response to

Hindawi
Computational and Mathematical Methods in Medicine
Volume 2023, Article ID 9795457, 1 page
https://doi.org/10.1155/2023/9795457

Retraction

Retracted: Impact of Small Incision Reduction and Suture Linked with Functional Appliance of Sufferers with Irrecoverable TMJ Anterior Disc Displacement

Computational and Mathematical Methods in Medicine

Received 12 December 2023; Accepted 12 December 2023; Published 13 December 2023

This article has been retracted by Hindawi, as publisher, following an investigation undertaken by the publisher [1]. This investigation has uncovered evidence of systematic manipulation of the publication and peer-review process. We cannot, therefore, vouch for the reliability or integrity of this article.

Please note that this notice is intended solely to alert readers that the peer-review process of this article has been compromised.

Wiley and Hindawi regret that the usual quality checks did not identify these issues before publication and have since put additional measures in place to safeguard research integrity.

We wish to credit our Research Integrity and Research Publishing teams and anonymous and named external researchers and research integrity experts for contributing to this investigation.

The corresponding author, as the representative of all authors, has been given the opportunity to register their agreement or disagreement to this retraction. We have kept a record of any response received.

References

[1] X. Wei, W. Yan, A. Sun, H. Wang, and W. Wang, "Impact of Small Incision Reduction and Suture Linked with Functional Appliance of Sufferers with Irrecoverable TMJ Anterior Disc Displacement," *Computational and Mathematical Methods in Medicine*, vol. 2022, Article ID 7196599, 6 pages, 2022.

Hindawi
Computational and Mathematical Methods in Medicine
Volume 2022, Article ID 7196599, 6 pages
https://doi.org/10.1155/2022/7196599

Research Article

Impact of Small Incision Reduction and Suture Linked with Functional Appliance of Sufferers with Irrecoverable TMJ Anterior Disc Displacement

Xiaotong Wei, Wei Yan, Anjun Sun, Hao Wang, and Wei Wang

Oral and Maxillofacial Surgery Department, Cangzhou Central Hospital, Hebei Province, Cangzhou City 061000, China

Correspondence should be addressed to Xiaotong Wei; 631301060102@mails.cqjtu.edu.cn

Received 26 July 2022; Revised 22 August 2022; Accepted 8 September 2022; Published 26 September 2022

Academic Editor: Min Tang

Background and Aim. Irrecoverable anterior disc displacement (ADD) of temporomandibular joint (TMJ) seriously affects the quality of life of patients. This research was aimed to explore the recovery effect of small incision reduction and suture on patients. *Methods*. 90 patients with irreducible ADD of TMJ treated from August 2020 to August 2021 were acquired in our hospital. They were randomly divided into control group and trial group randomly. There were 45 patients in each group. The sufferers in the control group were treated with oral drug therapy and small incision reduction and suture, while those in the trial group were treated with small incision reduction and suture linked with functional appliance. The pain score, dysfunction, joint function recovery, facial improvement, and clinical impacts of the two groups were contrasted. *Results*. Compared with that in the control group at 1 week, 4 weeks, and 6 months after therapy, the pain score in the trial group was markedly higher. After therapy, in the two groups, maximum vertical opening (MVO), left lateral excursion (LLE), and right lateral excursion (RLE) levels were markedly higher than those in the control group. The MRI score of the trial group was markedly higher than that of the control group at 1 week, 4 weeks, and 6 months after therapy, and the total effective rate of the trial group was markedly higher than that of the control group. *Conclusion*. The use of small incision reduction and suture linked with functional appliance in the therapy of sufferers with irreducible ADD of TMJ is beneficial to relieve pain, promote the recovery of body function, and contribute to the recovery of joint function.

1. Introduction

Anterior disc displacement (ADD) of temporomandibular joint (TMJ) is a common disease, and its pathogenesis is complicated, which is markedly related to environmental, genetic, and acquired genetic factors [1, 2]. ADD of TMJ refers to the obstruction of TMJ of the brain, which leads to the disorder of internal structure and the disorder of internal structure of TMJ, which seriously affects the life of sufferers [3, 4]. The occurrence of the disease is relatively sudden. With the continuous evolution of the ADD of the TMJ, there will be abnormal mouth opening, resulting in the obstruction of joint function, the damage of the joint strangulation, and the local pain in the joint area, which will seriously affect the quality of life of the sufferers [5, 6]. At present, clinical medical research has found that the irreducible ADD of the TMJ will cause local pain in the articular disc and maxillofacial region, which will seriously affect the patient's living ability, cause joint deformation and serious drop in joint height, and then lead to facial deformity, which will have a great impact on the patient. It occurs frequently in young people [7]. Conservative therapy for sufferers, the course of the disease cure cycle is long, and for those with severe symptoms, it will affect the appearance of sufferers [8, 9]. Therefore, we should find a more scientific and accurate therapy, so as to effectively improve the satisfaction of sufferers. Small incision reduction and suture can effectively reduce the pain of sufferers, thus effectively reduce the difficulty of operation, thus improve the clinical impact, promote the growth and repair of joints, and improve the healthy life and ability of sufferers. The recovery of neurological function plays a very important role [10–12]. This

study formulated the relevant therapy methods for the ADD of the TMJ and could explore the therapy methods of the sufferers with ADD of the TMJ. In this study, 90 sufferers with ADD of the TMJ admitted in our hospital from September 2019 to December 2021 were selected as the trial group, which were reported as follows.

2. Materials and Methods

2.1. General Information. 90 patients with irreducible ADD of the TMJ treated from August 2020 to August 2021 were acquired in our hospital. They were randomly divided into control group and trial group. There were 45 patients in each group. Among them, there were 20 males and 25 females in the trial group, the age was 35-60 years old, the average age was (46.36 ± 8.31) years, the height was 161-183 cm, the average height was (165.79 ± 5.78 cm), the weight 61 kg-81 kg, the average weight (67.61 ± 6.21) kg, and the body mass index 21-30 kg/m^2, the average body mass index (25.63 ± 2.23) kg/m^2. There were 23 males and 22 females in the control group, the age was 38-62 years old, the average height was (45.46 ± 10.01) years, the height was 162-182 cm, the average height was (164.46 ± 3.98 cm), the weight 63 kg-84 kg, the average weight was (66.46 ± 6.82) kg, and the body mass index was 21-34 kg/m^2, the average was (26.69 ± 2.35) kg/m^2. There was no noteworthy divergence in sex, age, and other general data ($P > 0.05$), which was comparable.

2.2. Inclusion and Exclusion Criteria. Inclusion criteria: the pain of TMJ lasted for more than 3 months; the pain site was mainly located in sufferers with ADD of the TMJ, which can be radiated above the joint; the main manifestation of pain was joint pain; the ADD of the TMJ could not be reduced; the medical records such as past history and medication history were complete; informed consent was signed. Exclusion criteria: ADD of the TMJ caused by various visceral diseases; ADD of the TMJ caused by deformity, tumor, fracture, or other trauma; pregnant and lactating women; long-term bedridden sufferers; disturbance of consciousness; complicated with dysfunction of the heart, kidney, lung, and other important organs.

2.3. Research Methods. The sufferers in the control group received routine therapy for ADD of the TMJ; they were treated with modified small incision surgery, and the subcutaneous tissue was cut into the subtemporal anterior membrane, cut the front of the vein, so as to cut the superficial layer of infratemporal membrane, resection along the vein. So as to protect the inferior middle temporal vein and the temporal branch of the nerve, injected normal saline into the articular cavity, so as to effectively protect the middle artery, exposed the joint capsule, added physiological saline into the supraarticular cavity, opened the attachment point of the joint disc from the inside, released the front part, reset the joint part, separated along the internal tendons, and reset the joint disc, so as to effectively improve the reduction function of the joint disc, put the suture out at the inside and outside, after it was introduced into the forearm of the external auditory canal, after threading the suture, the sutured part was sutured at the joint, and finally put the drainage tube into it, sewed the part tightly, and removed the suture after operation, so as to effectively improve the postoperative reexamination position of the sufferer and observe the recovery of the scar.

The sufferers in the trial group were treated with small incision reduction and suture linked with functional appliances. The sufferers were in the prone position, with a thin pillow on their abdomen, and its abdomen was covered with a thin pillow. Aligned the sufferer's jaw, performed the blade at the front, performed the operation at the midline, and used its forward extension reduction for correction, adjusted the activity every day, adjusted the grinding tool with the corrector, and the adjustment height was 1 mm. Configured it 24 hours a day. Adjusted the mold from front to back, and the mold adjustment height was 1 mm until the mold pressing part was effectively adjusted, the posterior teeth were adjusted with the help of the tube sleeve device, and the anterior jaw was effectively adjusted, removed the corresponding cannula and adjusted the jaw, the orthodontic apparatus was removed. Physical therapy was conducted, once a day, and lasted for 10 days.

2.4. Trial Indicators. (I) Pain score: visual analogue score (VAS) [13] was used to evaluate the pain degree of the two groups before therapy, 1 week, 4 weeks, and 6 months after therapy. The higher the score, the more severe the pain. (II) Mandibular movement: the standard of mandibular movement [10] was used to evaluate the painless maximum vertical opening (MVO), left lateral excursion (LLE), and right lateral excursion (RLE) before and after therapy. (III) Clinical curative impact evaluation: Excellent: after therapy, the low back pain disappeared, the movement was unimpeded, and the sufferers were able to work and live normally; Good: the pain almost disappeared, the activity was slightly limited, but had little impact on work and life; Fair: the symptoms were improved to a certain extent, but the pain existed, affecting work and life; Poor: the symptoms were not improved or even aggravated. Total efficiency rate = (Cases of good + Cases of fair)/Total cases. (IV) MRI index observation: before therapy, 1 week, 4 weeks, and 6 months after therapy, the sufferers in the two groups were observed with MRI, so as to effectively evaluate the position of their joint disc, and different therapy methods were used for sufferers with joint disc in different positions, so as to determine their MRI index and evaluate the postoperative repositioning

2.5. Statistical Processing. The data of this study were analyzed by SPSS22.0 statistical software. The trial indexes selected in the study were expressed by mean ± standard deviation ($\bar{x} \pm s$). Independent sample t-test was used for inter-group comparison, and paired sample t-test was used for intra-group comparison. $P < 0.05$ meant the difference was statistically significant.

Table 1: VAS pain score ($\bar{x} \pm s$, score).

Grouping	Instances	Before therapy	One week after therapy	4 weeks after therapy	6 months after therapy
Trial group	45	4.39 ± 1.17	$1.07 \pm 0.43^*$	$0.81 \pm 0.32^*$	$0.50 \pm 0.12^*$
Control group	45	4.54 ± 1.11	$1.40 \pm 0.52^*$	$1.12 \pm 0.47^*$	$0.72 \pm 0.26^*$
t value		0.624	3.281	3.657	5.154
P value		0.534	0.002	0.0004	<0.0001

Note: Contrasted with before therapy, $^*P < 0.05$.

Table 2: Mandibular condition of two groups of sufferers ($\bar{x} \pm s$, mm).

Grouping	MVO (mm)		LLE (mm)		RLE (mm)	
	Before therapy	After therapy	Before therapy	After therapy	Before therapy	After therapy
Trial group (n =45)	22.86 ± 5.28	$43.46 \pm 7.15^*$	7.59 ± 0.52	$8.36 \pm 0.42^*$	6.85 ± 1.12	$7.78 \pm 0.53^*$
Control group (n =45)	22.90 ± 5.54	$28.61 \pm 7.17^*$	7.56 ± 0.43	$7.89 \pm 0.34^*$	6.74 ± 1.29	$7.08 \pm 0.76^*$
t value	0.351	9.872	0.298	5.835	0.432	5.608
P value	0.972	0.001	0.766	<0.0001	0.667	<0.0001

Note: Contrasted with before therapy, $^*P < 0.05$.

Table 3: Clinical efficacy [n (%)].

Grouping	n	Excellent	Good	Fair	Poor	Total efficiency rate
Trial group	45	23 (51.11)	18 (40.00)	3 (6.67)	1 (2.22)	41 (91.11)
Control group	45	15 (33.33)	17 (37.78)	10 (22.22)	3 (6.67)	32 (71.11)
x^2 value						5.874
P value						0.015

Table 4: MRI scores ($\bar{x} \pm s$, score).

Grouping	Instances	Before therapy	One week after therapy	4 weeks after therapy	6 months after therapy
Trial group	45	36.45 ± 7.32	$27.30 \pm 7.65^*$	$26.51 \pm 6.85^*$	$27.31 \pm 7.56^*$
Control group	45	37.10 ± 6.81	$21.43 \pm 7.78^*$	$19.73 \pm 5.46^*$	$21.33 \pm 7.20^*$
t value		0.436	3.609	5.192	3.842
P value		0.664	<0.0001	<0.0001	<0.0001

Note: Contrasted with before therapy, $^*P < 0.05$.

3. Results

3.1. Contrasted the VAS Scores of the Two Groups. There was noteworthy divergence in the VAS score and the change trend of VAS score among the trial group and the control group ($P < 0.05$). Before therapy, there was no noteworthy divergence in VAS pain score between the two groups ($P > 0.05$). The VAS pain score of the trial group was markedly higher than that of the control group at 1 week, 4 weeks, and 6 months after therapy ($P > 0.05$), as shown in Table 1.

3.2. Comparison of Mandibular Conditions between the Two Groups. Before therapy, there was no noteworthy divergence in the levels of MVO, LLE, and RLE between the two groups ($P > 0.05$), but the levels of MVO, LLE, and RLE in the two groups strengthened markedly after therapy ($P < 0.05$), and the levels of MVO, LLE, and RLE in the trial group were markedly higher than those in the control group ($P < 0.05$), as shown in Table 2.

3.3. Clinical Efficacy. The total effective rate of sufferers in the trial group was 91.11%, which was markedly higher than that in the control group ($P < 0.05$), as shown in Table 3.

3.4. MRI Score. Before therapy, there was no noteworthy divergence in MRI score between the two groups ($P > 0.05$). The MRI score of the trial group was markedly higher than that of the control group 1 week, 4 weeks, and 6 months after therapy ($P < 0.05$), as shown in Table 4.

4. Discussion

As a common clinical disease, the etiology of ADD of the TMJ is complicated, and some sufferers have clear pathological causes and imaging manifestations, such as difficulty in mouth opening, serious abnormality in mouth opening, and pain in the joint area. However, the vast majority of patients have joint pain during the onset, which seriously affects the quality of life of patients [14, 15]. In the clinic,

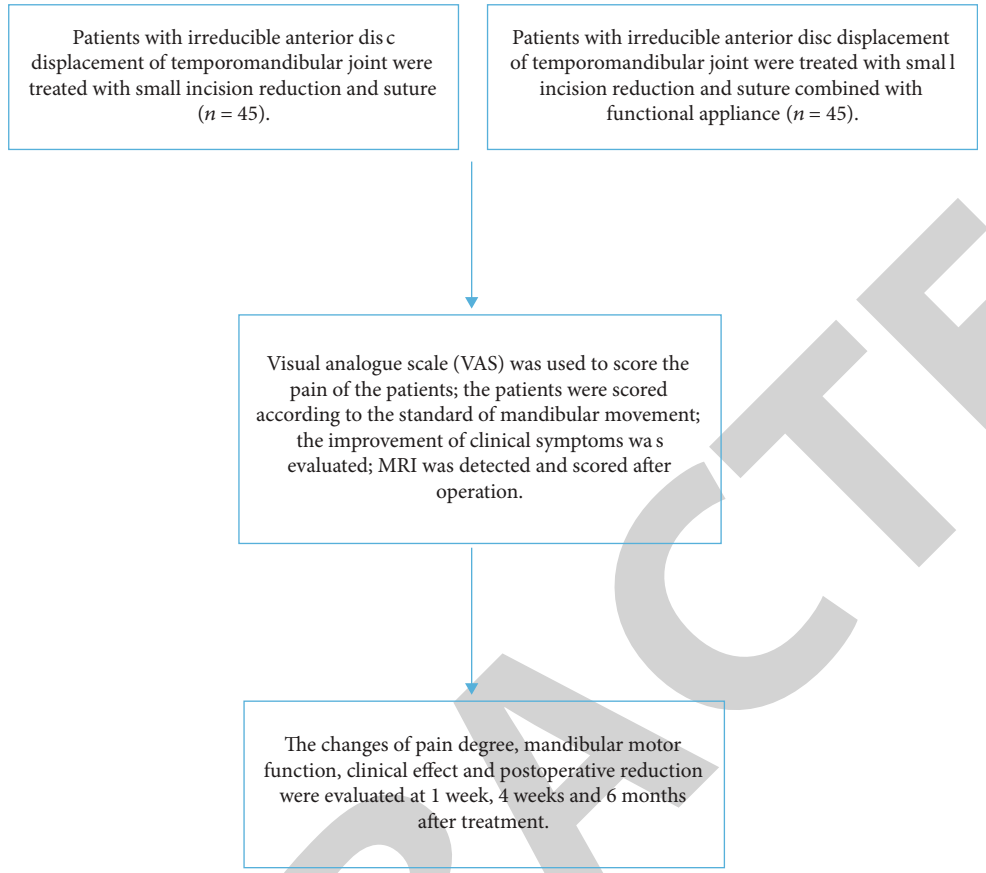

Figure 1: Abstract diagram.

ADD of the TMJ arthropathic pain is more common. The sufferer's articular disc can be restored due to long-term abnormal stress or other minor injuries. The failure of reduction of the articular disc will cause facial pain and dysfunction and cause serious damage to the articular disc. In addition, its facial deformities seriously affect the quality of life of the patients. At present, the therapy of ADD of the TMJ is often lack of pertinence, and the curative impact is poor, which brings serious problems to sufferers and their families [16–18]. At present, the clinical therapy of ADD of the TMJ is mainly small incision reduction and suture, which will bring some disadvantages and cannot be treated accurately. With the gradual development of medical technology, the improvement of small incision reduction and suture in the past therapy process, which can effectively treat the changes in the lower position of sufferers, has now made a major breakthrough and achieved noteworthy therapeutic impacts [19–22]. In the process of therapy with functional instruments, both its accuracy and feasibility can be well guaranteed, which provides a sufficient scientific basis for guiding the therapy of sufferers' mandibular joints, and can effectively solve sufferers' pain feelings [23].

In this study, the VAS pain score of the trial group was markedly higher than that of the control group at 1 week, 4 weeks, and 6 months after therapy; it showed that using small incision reduction and suture linked with functional appliance to treat sufferers with irreducible ADD of the TMJ could reduce the degree of pain and duration of pain, played a good role in promoting the prognosis of sufferers, and improved the quality of life of sufferers [24–26]. It was consistent with the study of small incision reduction and suture in the treatment of ADD of the TMJ, relieving pain and improving joint function by Xing et al. [27]. From the clinical efficacy of the two groups of sufferers, the total effective rate of the trial group was 91.11%, markedly higher than that of the control group, indicating that the therapy impact of small incision reduction and suture linked with functional appliance on sufferers with irreducible ADD of the TMJ was better, and the total effective rate of cure was higher. From the MRI scores of the two groups of sufferers, the MRI scores of sufferers with chronic low back pain in the trial group were markedly higher than those in the control group 1 week, 4 weeks, and 6 months after therapy. This was consistent with the higher effective rate of joint reduction compared with the reduction and suture of TMJ under small incision by He et al. confirmed [28]. These conclusions indicated that the therapy of sufferers with irreducible ADD of the TMJ with small incision reduction and suture linked with functional appliances could promote the recovery of sufferers' physical functions, reduce the recurrence of sufferers' conditions, and control the prognosis better.

To sum up, the therapy of sufferers with irreducible ADD of the TMJ with small incision reduction and suture linked with functional appliance is conducive to reducing

the degree of pain, improving the pain situation of sufferers, avoiding some postoperative complications, promoting the recovery of normal functions, and improving the quality of life of sufferers (Figure 1).

Data Availability

The datasets used and analyzed during the current study are available from the corresponding author upon reasonable request.

Conflicts of Interest

The authors declare that they have no conflicts of interest.

Acknowledgments

This study was supported by The Guiding Project of Cangzhou Key R&D Plan (204106135).

References

[1] D. Zuniawati, I. Indasah, and P. D. Kusumawati, "Analysis of risk factors that influence the lumbago event in hand-rolled clove cigarette workers at Margantara Jaya Cigarette Factories," *JOURNAL FOR QUALITY IN PUBLIC HEALTH*, vol. 4, no. 1, pp. 228–232, 2020.

[2] L. Cao, Q. Zhang, Y. Yuan et al., "CADASIL with clinical manifestations of lumbago, hunchback and Parkinson's syndrome," *Zhonghua yi xue yi chuan xue za zhi = Zhonghua yixue yichuanxue zazhi Chinese journal of medical genetics*, vol. 36, no. 9, pp. 922–925, 2019.

[3] T. Y. Tsai, C. L. Lee, and H. M. Chiou, "Therapy of intradural extramedullary myxopapillary ependymoma of lumbar spine: a rare case report and literature review," *Formosan Journal of Musculoskeletal Disorders*, vol. 10, no. 1, pp. 38–42, 2019.

[4] D. Roshini and A. Leo, "Motor control training in chronic low back pain," *Journal of Clinical and Diagnostic Research*, vol. 13, no. 4, pp. YC01–YC05, 2019.

[5] I. Urits, V. Cai, M. Aner et al., "post Dural puncture headache, managed with epidural blood patch, is associated with subsequent chronic low back pain in patients: a pilot study," *Current Pain and Headache Reports*, vol. 24, no. 1, pp. 1–4, 2020.

[6] Z. Wu, Y. Zhu, W. Xu, J. Liang, Y. Guan, and X. Xu, "Analysis of biomechanical properties of the lumbar extensor myofascia in elderly sufferers with chronic low back pain and that in healthy people," *Bio Med Research International*, vol. 2020, article 7649157, pp. 1–10, 2020.

[7] D. Soydan Çabuk, M. Etöz, İ. E. Akgün, S. Doğan, E. Öztürk, and A. Coşgunarslan, "The evaluation of lateral pterygoid signal intensity changes related to temporomandibular joint anterior disc displacement," *Oral Radiology*, vol. 37, no. 1, pp. 74–79, 2021.

[8] K. T. Woo, C. Choong-Meng, C. Lim et al., "Changes in primary glomerulonephritis in Singapore over four decades," *Clinical Nephrology*, vol. 91, no. 3, pp. 155–161, 2019.

[9] A. Chalkia, H. Gakiopoulou, I. Theohari, P. G. Foukas, D. Vassilopoulos, and D. Petras, "Transforming growth factor-β1/Smad signaling in glomerulonephritis and its association with progression to chronic kidney disease," *American Journal of Nephrology*, vol. 52, no. 8, pp. 653–665, 2021.

[10] R. Abdolahipour, A. Nowrouzi, M. B. Khalili, A. Meysamie, and S. Ardalani, "Aqueous Cichorium intybus L. seed extract may protect against acute palmitate-induced impairment in cultured human umbilical vein endothelial cells by adjusting the Akt/eNOS pathway, ROS: NO ratio and ET-1 concentration," *Journal of Diabetes and Metabolic Disorders*, vol. 19, no. 2, pp. 1045–1059, 2020.

[11] N. Yoshikawa, N. Ohashi, T. Tsuji et al., "Is dose adjustment of prednisolone required in patients with IgA nephropathy during rifampicin treatment for Mycobacterium avium complex lung disease?," *Therapeutic Drug Monitoring*, vol. 41, no. 4, pp. 546-547, 2019.

[12] L. Shi, J. Sheng, G. Chen et al., "Combining IL-2-based immunotherapy with commensal probiotics produces enhanced antitumor immune response and tumor clearance," *J Immuno Ther Cancer*, vol. 8, no. 2, pp. 1–14, 2020.

[13] J. A. Turner, E. Stephen-Victor, S. Wang et al., "Regulatory T cell-derived TGF-β1 controls multiple checkpoints governing allergy and autoimmunity," *Immunity*, vol. 53, no. 6, pp. 1331-1332, 2020.

[14] Y. Zheng, J. Zhang, and H. Fan, "Clinical observation of small incision combined with manipulative reduction and pinning internal fixation for Sanders IV type calcaneal fracture," *Journal of New Chinese Medicine*, vol. 23, 2017.

[15] L. I. Xi, C. Chen, X. Lin, and Y. Shi, "Therapy effect of calcaneus fracture with percutaneous reduction and Kirschner wire internal fixation linked with calcium sulfate bone grafting and small incision and reduction of the sacral sinus linked with calcium sulfate bone grafting," *Fujian Medical Journal*, vol. 35, 2018.

[16] F. Zeng, C. Chen, X. Chen, L. Zhang, and M. Liu, "Small incisions combined with negative-pressure wound therapy for treatment of protobothrops mucrosquamatus bite envenomation: a new treatment strategy," *Medical Science Monitor*, vol. 25, pp. 4495–4502, 2019.

[17] T. Umut, K. Alper, and S. Yves, "Dorsal preservation surgery: a novel modification for dorsal shaping and hump reduction," *Aesthetic Surgery Journal*, vol. 25, 2022.

[18] M. A. Plymale, D. L. Davenport, S. Walsh-Blackmore et al., "Costs and complications associated with infected mesh for ventral hernia repair," *Surgical Infections*, vol. 21, no. 4, pp. 344–349, 2020.

[19] C. C. Pitts, A. Almaguer, J. T. Wilson, J. H. Quade, and M. D. Johnson, "Radiographic and postoperative outcomes of plate versus screw constructs in open reduction and internal fixation of calcaneus fractures via the sinus tarsi," *Foot & Ankle International*, vol. 40, no. 8, pp. 929–935, 2019.

[20] Z. Wang, Y. Lu, K. Xiao et al., "Bimanual irrigation-aspiration for ectopia lentis and use of a small incision for 4-point scleral-sutured foldable intraocular lens and anterior vitrectomy in patients with Marfan syndrome," *Indian Journal of Ophthalmology*, vol. 67, no. 10, p. 1629, 2019.

[21] Y. H. Liu, X. B. Hu, X. M. Yang, Y. W. Wang, and M. Deng, "Comparing remifentanil and sufentanil in stress reduction during neurosurgery: a randomised controlled trial," *International Journal of Clinical Pharmacy*, vol. 42, no. 5, pp. 1326–1334, 2020.

[22] S. Domoto, K. Jujo, J. Yamaguchi et al., "Utility of the minimum-incision transsubclavian approach for transcatheter aortic valve replacement on clinical outcomes in patients with small vessel anatomy," *Journal of Cardiology*, vol. 78, no. 1, pp. 31–36, 2021.

Hindawi
Computational and Mathematical Methods in Medicine
Volume 2023, Article ID 9808951, 1 page
https://doi.org/10.1155/2023/9808951

Retraction

Retracted: Application Value of Total Knee Arthroplasty plus Platelet-Rich Plasma Therapy in Traumatic Arthritis of the Knee

Computational and Mathematical Methods in Medicine

Received 12 December 2023; Accepted 12 December 2023; Published 13 December 2023

This article has been retracted by Hindawi, as publisher, following an investigation undertaken by the publisher [1]. This investigation has uncovered evidence of systematic manipulation of the publication and peer-review process. We cannot, therefore, vouch for the reliability or integrity of this article.

Please note that this notice is intended solely to alert readers that the peer-review process of this article has been compromised.

Wiley and Hindawi regret that the usual quality checks did not identify these issues before publication and have since put additional measures in place to safeguard research integrity.

We wish to credit our Research Integrity and Research Publishing teams and anonymous and named external researchers and research integrity experts for contributing to this investigation.

The corresponding author, as the representative of all authors, has been given the opportunity to register their agreement or disagreement to this retraction. We have kept a record of any response received.

References

[1] C. Zhang and P. Nie, "Application Value of Total Knee Arthroplasty plus Platelet-Rich Plasma Therapy in Traumatic Arthritis of the Knee," *Computational and Mathematical Methods in Medicine*, vol. 2022, Article ID 5483101, 6 pages, 2022.

Hindawi
Computational and Mathematical Methods in Medicine
Volume 2022, Article ID 5483101, 6 pages
https://doi.org/10.1155/2022/5483101

Research Article

Application Value of Total Knee Arthroplasty plus Platelet-Rich Plasma Therapy in Traumatic Arthritis of the Knee

Canhong Zhang[1] **and Pengfei Nie**[2]

[1]*Department of Orthopedics, Quanzhou First Hospital Affiliated to Fujian Medical University, Quanzhou, 362000 Fujian, China*
[2]*Department of Orthopedics, Ningbo Beilun People's Hospital, Ningbo, 315800, Zhejiang, China*

Correspondence should be addressed to Canhong Zhang; zhangch1988@126.com

Received 24 June 2022; Revised 23 August 2022; Accepted 1 September 2022; Published 26 September 2022

Academic Editor: Min Tang

Purpose. This work is aimed at determining the application value of platelet-rich plasma (PRP) therapy plus total knee arthroplasty (TKA) in traumatic arthritis (TA) of the knee. *Methods*. A retrospective study was conducted on 78 cases of TA of the knee admitted between March 2021 and January 2022 to the Quanzhou First Hospital Affiliated to Fujian Medical University. Based on different treatment methods, 38 cases treated with TKA were assigned to the control group, and 40 cases intervened by PRP+TKA were included in the observation group. The operation time (OT), drainage volume (DV), total blood loss (TBL), incision inflammatory reaction rate, and grade A healing rate were recorded. Besides, preoperative and postoperative knee joint Hospital for Special Surgery (HSS) scores, knee joint pain assessed by visual analogue scale (VAS), knee joint range of motion (ROM), and bone metabolism parameters (osteocalcin (OST), total N-terminal propeptide of type I procollagen (tPINP), and β-isomerized C-terminal telopeptides (β-CTX)) were recorded. *Results*. The observation group showed reduced postoperative DV and TBL than the control group ($P < 0.05$). The two cohorts differed insignificantly in OT, incision inflammatory response rate, and grade A healing rate ($P > 0.05$). The observation group also had better improvement in the HSS score, pain VAS score, and knee ROM ($P < 0.05$). And higher postoperative OST and tPINP levels while lower β-CTX were determined in the observation group ($P < 0.05$). *Conclusions*. PRP+TKA can validly improve the levels of bone metabolism markers in patients with TA of the knee and promote their knee functional recovery, with favorable safety.

1. Introduction

As a prevalent joint inflammation, knee arthritis mainly results from various traumas, with 12% of all knee osteoarthritis (OA) cases attributed to sports, motor vehicle accidents, falls, or any other sources of physical trauma. Such traumas can damage ligaments, cartilage, and/or bones, thus altering the mechanics of joints [1]. Besides, there will be structural changes in fat pads, synovium, ligaments, and muscles, which is why knee arthritis is generally considered a whole-joint disease [2–5]. The prevalence of the disease has increased significantly and continues to rise over the past decades, becoming one of the leading causes of disability in elderly patients worldwide [6]. As the second largest common musculoskeletal disease after low back pain, knee arthritis poses a substantial economic burden every year [7, 8]. A large part of the economic burden comes from the time cost and the cost of aggressive surgical interventions used in previous treatments [9]. Therefore, it carried great clinical implications for exploring more effective and safe treatment strategies for patients with knee arthritis from the perspectives of surgical indicators, limb recovery status, and bone metabolism indicators.

As one of the most successful orthopedic procedures, total knee arthroplasty (TKA) is now widely used in a wide variety of primary and secondary OA [10], and the number of patients undergoing this procedure is increasing at an accelerating rate as the world's aging population increases [11, 12]. The operation can effectively relieve patients' pain and restore their mobility [13]. However, this technique is highly demanding, and improper operation can easily bring a series of postoperative complications to patients, even

causing death in serious cases [14, 15]. Given these limitations of the current orthopedic surgery, people's interest in platelet-rich plasma (PRP) has increased [16]. PRP is an autologous mixture produced by centrifugal separation of whole blood, and its therapeutic effects are usually attributed to the concentrated anabolic agent it contains [17, 18]. At present, PRP has been used clinically in many fields such as orthopedic surgery, gynecology, and orthopedics. However, there are few studies on the combined use of TKA and PRP in knee joint therapy [19]. Accordingly, this study discusses the influence of the combined treatment through a series of indexes such as bone metabolism parameters and limb recovery function, with the view of providing ideas and references for the clinical treatment of traumatic knee arthritis.

2. Methods

2.1. General Information. This research retrospectively collected the clinical data of 78 cases of traumatic knee arthritis who underwent TKA treatment in the Quanzhou First Hospital Affiliated to Fujian Medical University between March 2021 and January 2022. All patients volunteered to participate in this trial. They were assigned to either the observation group or the control group, depending on the differences in treatment methods. The control group ($n = 38$) was given TKA, and observation group ($n = 40$) underwent PRP and TKA. No statistical difference was observed between groups regarding general data, which was comparable ($P > 0.05$). Inclusion criteria are as follows: ① diagnosis of TA of the knee, ② presence of obvious clinical symptoms in the past month, with repeated swelling and pain of knee joint, and ③ degenerative changes of knee joint as indicated by imaging examination. Exclusion criteria are as follows: ① rheumatoid arthritis, systemic lupus erythematosus, and other rheumatic immune diseases; ② TKA intolerance due to severe heart and brain diseases or liver and kidney diseases; ③ history of TKA treatment; ④ hematological diseases such as leukemia, idiopathic thrombocytopenic purpura, deep vein thrombosis, or frequent use of anticoagulants that affects the coagulation system; and ⑤ women with reproductive or breastfeeding needs. The Ethics Committee of the Quanzhou First Hospital Affiliated to Fujian Medical University approved this study, and all subjects provided informed consent.

2.2. Methods. The control group received tourniquet hemostasis after combined spinal and epidural analgesia or lumbar anesthesia, with the pressure set at 250-280 mmHg. A skin incision was created in the anterior midline of the knee, and the joint capsule was opened and fully exposed via the medial parapatellar approach. The suprapatellar synovial bursa was completely released, and the patellar bone was moved outward to thoroughly expose the surgical focus of the patient. Next, the meniscus and anterior cruciate ligament were resected after proper protection of the patient's medial and lateral collateral ligaments, and the osteophytes at the focal site were thoroughly cleaned. Minimally invasive surgical instruments were then used to perform osteotomy at the joint of the patient with a hallux valgus angle of 5°-7° after the procedure. Then, the tibial articular surface was osteotomized with the extramedullary positioning system with a posterior slope of 3° to 5° after osteotomy, and the medial and lateral soft tissues and the posterior joint capsule were fully released. All patients were tested for total knee prosthesis. Following prosthesis installation, the tourniquet was released in time, and the drainage tube was placed after confirming that there was no bleeding, followed by joint cavity closure and layer-by-layer suture. All operations were performed by the same experienced and senior attending physician in our hospital. The observation group was additionally given PRP. Before the operation, 40 mL of venous blood was extracted, centrifuged twice (10 minutes each time) at 2000 r/min, and prepared using a PRP preparation box. A total of 6 mL PRP was obtained by the above standard procedure. After the prosthesis was installed, PRP was injected into the joint, followed by wound closure layer by layer, dressing, pressurizing, and tourniquet-loosening. Patient follow-up was conducted for 4 weeks, and PRP was injected twice at an interval of 2 weeks. All knee X-rays were collected for comparison before and after treatment.

2.3. Measurement Indicators

(1) Surgical indications

The surgical indications of two groups of patients were investigated and tested, and the relevant indexes were operation time (OT), drainage volume (DV), and total blood loss (TBL).

(2) Limb recovery

Patients' limb recovery was statistically analyzed. The related indexes were preoperative and postoperative knee joint Hospital for Special Surgery (HSS) scores, visual analogue scale (VAS) score for knee pain, and knee joint range of motion (ROM).

The HSS knee score has a full score of 100 points, including 30 points for pain, 22 points for function, 18 points for ROM, 10 points each for muscle strength, flexion deformity, and instability. Higher scores are associated with better knee joint function. The total score of VAS is 10, with 0, 1-3, 4-6, and 7-10 for no, mild, moderate, and severe pain, respectively. The score is in direct proportion to pain severity. The total score of ROM is 100, with the operating score and the theoretical score accounting for 80 and 20 points, respectively. The higher the score is, the better the knee joint ROM is.

(3) Bone metabolism markers

The bone metabolism markers of the two groups, including osteocalcin (OST), total N-terminal propeptide of type I procollagen (tPINP), and β-isomerized C-terminal telopeptides (β-CTX), were detected by an automatic chemiluminescence immunoanalyzer preoperatively and during postoperative follow-up.

Table 1: General data.

Classification	Observation group ($n = 40$)	Control group ($n = 38$)	t/χ^2	P
Sex			0.43	0.512
Male	24	20		
Female	16	18		
Age (years old)	42.13 ± 6.67	41.84 ± 4.96	0.22	0.809
BMI (kg/m^2)	24.03 ± 2.38	23.87 ± 2.93	0.27	0.792
Average income	3014.13 ± 28.34	3019.21 ± 31.40	0.75	0.455
Working status			1.01	0.314
On-the-job	30	32		
Laid-off/resigned	10	6		
Smoking			0.01	0.916
Yes	33	31		
No	7	7		
Drinking			1.03	0.311
Yes	35	30		
No	5	8		

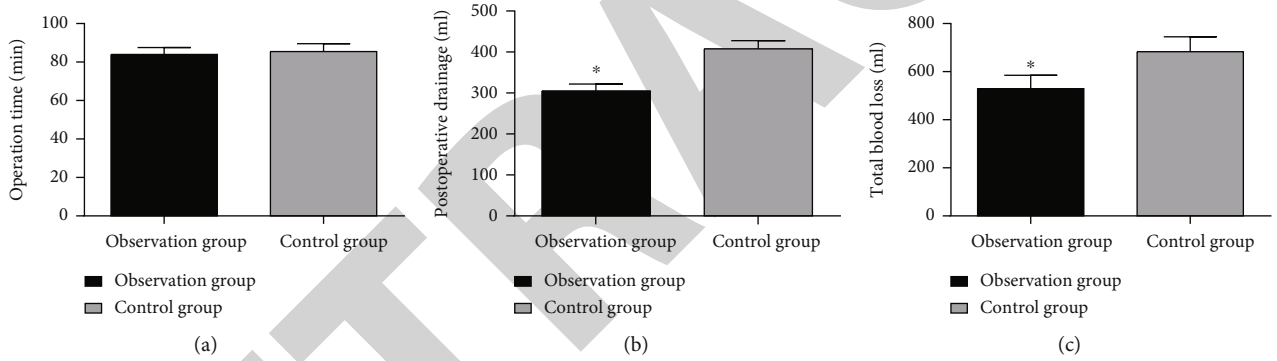

Figure 1: Surgical indications of two groups of patients. (a) Operation time of two groups. (b) Postoperative drainage volume of two groups. (c) Total blood loss of two groups. Note: *compared with the control group, $P < 0.05$.

(4) Incision inflammation rate

The degree of incision inflammation in two groups of patients was investigated and statistically analyzed. According to the presence of redness, swelling, heat and exudation, the inflammatory reaction was divided into four grades: none, mild, moderate, and severe.

(5) Healing status

The healing status of patients, which was divided into grade A healing (excellent healing), B (incision inflammation but no purulence), and C (purulent wound but healing after drainage and dressing change), was also investigated and counted.

2.4. Statistics and Methods. SPSS22.0 (Asia Analytics Formerly SPSS China) was used to comprehensively analyze data and GraphPad Prism 6 (GraphPad Software, San Diego, USA) to plot figures. Enumeration data (e.g., sex and working status) were analyzed by χ^2, while measuring data (age, body mass index (BMI), etc.) recorded as ($\bar{\chi} \pm S$) were tested with the t-test. $P < 0.05$ was used to indicate significance.

3. Results

3.1. General Data. The two cohorts of patients differed insignificantly in gender, age, BMI, and other general data ($P > 0.05$), see Table 1 for details.

3.2. Surgical Indications. The two groups showed similar OT ($P > 0.05$), but the postoperative DV and TBL were obviously lower in the observation group ($P < 0.05$), as displayed in Figure 1.

3.3. Limb Recovery. The preoperative HSS score, pain VAS score, and knee ROM were similar in the two groups ($P > 0.05$). Postoperatively, improvements in the above parameters were observed in both cohorts ($P < 0.05$). with

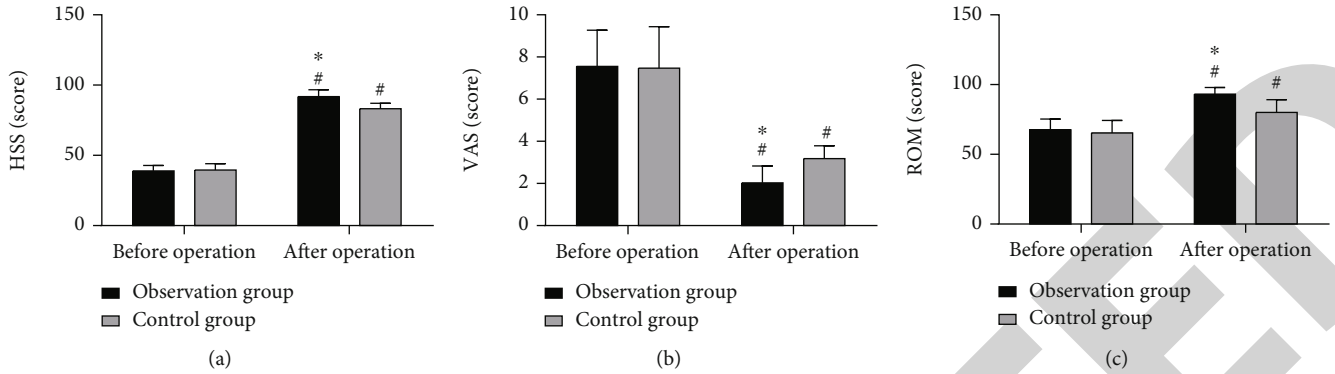

Figure 2: Limb recovery in two groups: (a) HSS scores before and after surgery in the two groups. (b) VAS scores before and after surgery. (c) Knee ROM scores before and after surgery. Note: # and * means $P < 0.05$ compared with the pretreatment level (within the group) and the control group, respectively. HSS: Hospital for Special Surgery; VAS: visual analogue scale; ROM, range of motion.

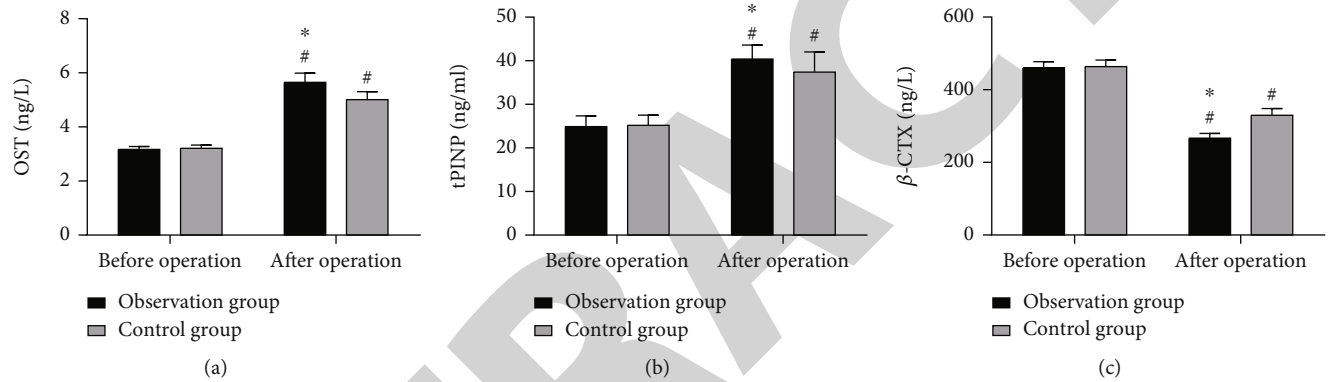

Figure 3: Bone metabolism markers: (a) OST levels before and after operation, (b) tPINP levels before and after operation, and (c) β-CTX levels before and after operation. Note: # and * means $P < 0.05$ compared with the pretreatment level (within the group) and the control group, respectively. OST: osteocalcin; tPINP: total N-terminal propeptide of type I procollagen; β-CTX: β-isomerized C-terminal telopeptides.

Table 2: Healing rate of two groups.

Classification	Observation group ($n = 40$)	Control group ($n = 38$)	χ^2	P
Grade A healing	38 (95.00)	35 (92.11)	0.27	0.602
Grade B healing	1 (2.50)	3 (7.89)	1.08	0.280
Grade C healing	1 (2.50)	0 (0.00)	0.96	0.327

Table 3: Incision inflammation rate.

Classification	Observation group ($n = 40$)	Control group ($n = 38$)	χ^2	P
Mild inflammation	1 (2.50)	2 (5.26)	—	—
Moderate inflammation	1 (2.50)	0 (0.00)	—	—
Severe inflammation	0 (0.00)	1 (2.63)	—	—
Inflammatory reaction rate (%)	2 (5.00)	3 (7.89)	0.27	0.602

more superior results in the observation group ($P < 0.05$). For details, please see Figure 2.

3.4. Bone Metabolism Markers. The preoperative OST, tPINP, and β-CTX showed no statistical differences between groups ($P > 0.05$). Postoperatively, OST and tPINP of both cohorts elevated notably and β-CTX reduced significantly, and compared with the control group, OST and tPINP were higher and β-CTX was lower in the observation group ($P < 0.05$) (Figure 3).

3.5. Grade A Healing Rate. The two groups were not statistically different in grade A, B, and C healing rates after treatment ($P > 0.05$) (Table 2).

3.6. Incision Inflammation Rate. The investigation revealed no statistical difference between groups in the incision inflammation rate ($P > 0.05$) (Table 3).

4. Conclusion

Arthritis is the most common joint disease, disabling 630 million people worldwide [20, 21]. Although all kinds of orthopedic surgeries, such as knee replacement, can effectively improve patients' symptoms, they can also easily lead to postoperative inflammation and negative emotions in patients that will hinder their recovery from the disease [22, 23]. In this part, we will discuss whether TKA combined with PRP can better treat patients with TA of the knee by combining the research results obtained.

First, limb function and healing rate of patients in the two groups were analyzed. Although both cohorts had good postoperative healing and recovered limb function, the observation group showed better recovery of limb function, indicating better recovery efficacy in patients who used combined therapy. Knee replacement surgery has seen significant progress in recent years, but patient outcomes remain poor despite improvements in surgical technique and prosthesis placement procedures. In fact, many patients not only have limited postoperative improvement in joint function but also experience postoperative pain and altered life quality [24]. In addition, studies have shown a relatively high incidence of complications in older patients undergoing this procedure [25]. Therefore, knee replacement alone can hardly ensure a good surgical outcome. PRP is a volume of the treated autologous peripheral blood, which has been used for more than 30 years in a variety of corresponding symptoms because of its platelet concentration above baseline [26]. And recently, it has been widely applied to treat musculoskeletal diseases, as its strong regenerative capacity can play a better role in recovering patients' limbs. At present, PRP therapy is a feasible treatment option with clinical benefits and gratifying results [27, 28]. Therefore, compared with the control group, the observation group made use of the advantages of the regenerative ability of PRP therapy, contributing to higher efficacy to better recover their limb function. As far as patients' surgical indications are concerned, the surgical indications of patients in the observation group are better than those in the control group because of better curative effects.

From the perspective of bone metabolism markers, higher postoperative OST and tPINP levels and lower β-CTX were determined in the observation group. As aforementioned, PRP therapy has a strong regenerative capacity and a favorable effect on the recovery of patients' limb function. OST and tPINP are specifically expressed in osteoblasts and are the most abundant noncollagen proteins in bones, which play an important role in bone formation [29, 30]. β-CTX, a degradation product of C-terminal peptide of type I collagen, is one of the most valuable markers for evaluating osteoclast activity and bone resorption. Increased levels of β-CTX indicate the decrease of bone density and the deterioration of bone quality [31]. Combined with the characteristics of PRP therapy mentioned above, it can be concluded that due to the use of PRP therapy in the observation group, the bone metabolism markers and limb function were better improved in patients from this group.

This study still shows limitations. This time, we failed to use indexes that can better reflect inflammation to evaluate the inflammatory response of patients. Nor have we investigated patient compliance during treatment or their postoperative psychological states. Future efforts will be devoted to addressing these limitations, so that the clinical treatment plan will become more perfect.

To sum up, PRP+TKA can effectively improve the levels of bone metabolism markers in patients with TA of the knee and promote knee functional recovery, with favorable safety.

Data Availability

The labeled datasets used to support the findings of this study are available from the corresponding author upon request.

Conflicts of Interest

The authors declare no competing interests.

Acknowledgments

The Startup Fund for scientific research, Fujian Medical University (Grant number: 2021QH1248) supported this study.

References

[1] B. A. Kornah, H. M. Safwat, S. K. Abdel-Hameed et al., "Managing of post-traumatic knee arthritis by total knee arthroplasty: case series of 15 patients and literature review," *Journal of Orthopaedic Surgery and Research*, vol. 14, no. 1, 2019.

[2] R. F. Loeser, S. R. Goldring, C. R. Scanzello, and M. B. Goldring, "Osteoarthritis: a disease of the joint as an organ," *Arthritis and Rheumatism*, vol. 64, no. 6, pp. 1697–1707, 2012.

[3] J. Martel-Pelletier, A. J. Barr, F. M. Cicuttini et al., "Osteoarthritis," *Nature Reviews Disease Primers*, vol. 2, pp. 1–18, 2016.

[4] T. E. Swingler, L. Niu, P. Smith et al., "The function of microRNAs in cartilage and osteoarthritis," *Clinical and Experimental Rheumatology*, vol. 37 Supplement 120, no. 5, pp. 40–47, 2019.

[5] D. C. Ilas, S. M. Churchman, D. McGonagle, and E. Jones, "Targeting subchondral bone mesenchymal stem cell activities for intrinsic joint repair in osteoarthritis," *Future Science OA*, vol. 3, no. 4, 2017.

[6] GBD, "Disease and injury incidence and prevalence collaborators global, regional, and national incidence, prevalence, and years lived with disability for 310 diseases and injuries, 1990–2015: a systematic analysis for the Global Burden of Disease Study 2015," *The Lancet*, vol. 2016, no. 388, pp. 1545–1602, 2015.

Hindawi
Computational and Mathematical Methods in Medicine
Volume 2023, Article ID 9879478, 1 page
https://doi.org/10.1155/2023/9879478

Retraction

Retracted: The Effect of Microwave Ablation Combined with Anti-PD-1 Monoclonal Antibody on T Cell Subsets and Long-Term Prognosis in Patients Suffering from Non-Small-Cell Lung Cancer

Computational and Mathematical Methods in Medicine

Received 12 December 2023; Accepted 12 December 2023; Published 13 December 2023

This article has been retracted by Hindawi, as publisher, following an investigation undertaken by the publisher [1]. This investigation has uncovered evidence of systematic manipulation of the publication and peer-review process. We cannot, therefore, vouch for the reliability or integrity of this article.

Please note that this notice is intended solely to alert readers that the peer-review process of this article has been compromised.

Wiley and Hindawi regret that the usual quality checks did not identify these issues before publication and have since put additional measures in place to safeguard research integrity.

We wish to credit our Research Integrity and Research Publishing teams and anonymous and named external researchers and research integrity experts for contributing to this investigation.

The corresponding author, as the representative of all authors, has been given the opportunity to register their agreement or disagreement to this retraction. We have kept a record of any response received.

References

[1] W. Yu, J. Sun, T. Wang, and Y. Du, "The Effect of Microwave Ablation Combined with Anti-PD-1 Monoclonal Antibody on T Cell Subsets and Long-Term Prognosis in Patients Suffering from Non-Small-Cell Lung Cancer," *Computational and Mathematical Methods in Medicine*, vol. 2022, Article ID 7095423, 7 pages, 2022.

Hindawi
Computational and Mathematical Methods in Medicine
Volume 2022, Article ID 7095423, 7 pages
https://doi.org/10.1155/2022/7095423

Research Article

The Effect of Microwave Ablation Combined with Anti-PD-1 Monoclonal Antibody on T Cell Subsets and Long-Term Prognosis in Patients Suffering from Non-Small-Cell Lung Cancer

Wenbo Yu,[1] Jiewei Sun,[2] Tao Wang,[2] and Yanan Du[3]

[1]*Department of Respiratory and Critical Care Medicine, Yantai Yuhuangding Hospital, Yantai, Shandong 264001, China*
[2]*Department of Interventional Therapy, Yantai Yuhuangding Hospital, Yantai, Shandong 264001, China*
[3]*Department of Nuclear Medicine, Yantai Yuhuangding Hospital, Yantai, Shandong 264001, China*

Correspondence should be addressed to Yanan Du; d15153590568@126.com

Received 19 July 2022; Revised 22 August 2022; Accepted 29 August 2022; Published 26 September 2022

Academic Editor: Min Tang

Objective. This research is aimed at studying the effect of microwave ablation combined with the antiprogrammed death- (PD-) 1 monoclonal antibody on T cell subsets and long-term prognosis in patients suffering from non-small-cell lung cancer (NSCLC). *Methods*. Employing the random number table technique, a total of 122 NSCLC patients who received treatment at our hospital between May 2015 and June 2019 were selected and assigned to the observation group and the control group, and each group comprised 61 patients ($n = 61$). While the control group received only anti-PD-1 monoclonal antibody treatment, the observation group received microwave ablation in combination with anti-PD-1 monoclonal antibody. The clinical efficacy was observed for both groups. The levels of T cell subsets (CD3+, CD4+, and CD8+), serum tumor markers (squamous cell carcinoma antigen (SCCA), cytokeratin Ig fragment (CYFRA21-1), and serum carcinoembryonic antigen (CEA)), nuclear factor kappa B (NF-κB), protease C (PKC), and mitogen-activated protein kinase (MAPK) mRNA expression between the two groups were compared. The frequency of adverse reactions was observed in both groups. The survival time of both the groups was recorded over the course of three years of follow-up. The Kaplan-Meier method was employed for analyzing the survival of both the control and the observation group. *Results*. The response rate (RR) of the observation group (80.33%) was considerably greater in comparison to that of the control group (62.30%) ($P < 0.05$). Following treatment, the observation group's levels of CD3+, CD4+, CD8+, SCCA, CyFRA21-1, and CEA and the mRNA expressions of NF-κB, PKC, and MAPK were superior to those of the control group, with statistical significances (all $P < 0.05$). Between the two groups, there was no significant difference in the occurrence of adverse reactions ($P > 0.05$). The observation group had greater 1-, 2-, and 3-year survival rates (57.38%, 39.34%, and 29.51%) than the control group (32.79%, 18.03%, and 8.20%), with statistically significant differences (all $P < 0.05$). *Conclusion*. Microwave ablation in combination with an anti-PD-1 monoclonal antibody could effectively improve the level of T cell subsets and serum tumor markers in NSCLC patients, resulting in a long-term prognosis of patients with good therapeutic effect and safety.

1. Introduction

Among malignant tumor diseases, lung cancer is highly prevalent in China. With the elevated aggravation of air pollution, the prevalence of lung cancer also increases globally. Non-small-cell lung cancer (NSCLC) is responsible for approximately 85% of cases of lung cancer, according to statistics [1, 2]. Most of the patients had been in the advanced stage when diagnosed and had lost the chance of treatment via surgery. Systemic chemotherapy was mostly used, but its effect in improving the survival time of the patients is not satisfying. According to the relevant studies, programmed death-1 (PD-1) can be used as an immune checkpoint to inhibit T cell immune function by inhibiting the dephosphorylation of tyrosine phosphatase SHP-2 in the downstream signaling pathway of T cell antigen receptor. When T cells are repeatedly stimulated by the tumor microenvironment and chronic infection antigen, PD-1 expression

level can be further promoted and T cell differentiation can be induced to enter the depletion state [3, 4]. Immunotherapy targeting immune checkpoint PD-1 and programmed death ligand-1 (PD-L1) inhibitors is a new treatment scheme for advanced lung cancer. PD-1 inhibitors such as pembrolizumab and nivolumab have achieved good clinical therapeutic effects [5, 6]. Immunotherapy is relatively safe compared with chemotherapy, but it may cause immune-related adverse reactions. In latest years, the clinical treatment of NSCLC has seen a significant increase in the use of percutaneous microwave curing therapy (PMCT). It has the benefits of good efficacy, high safety, and low trauma. Microwave heating can promote the coagulation and necrosis of tumor tissue, increase the permeability of cell membrane and nuclear membrane, and lead to the exposure of denatured and degraded single-stranded DNA complex, which is conducive to targeted treatment. Compared with traditional radiofrequency ablation, microwave ablation also has the advantage of ablating a large number of necrotic tissues in a short procedure time, which can better treat perivascular tissues and enlarge the ablation area [7]. This research sought to determine the impact of anti-PD-1 monoclonal antibody in combination with microwave ablation on the level of T cell subsets and the long-term prognosis of NSCLC.

2. Material and Methods

2.1. General Data. A total of 122 NSCLC patients who received treatment at our hospital between May 2015 and June 2019 were selected and assigned to the observation group and the control group by employing the random number table technique. Each group comprised 61 patients ($n = 61$). The observation group consisted of 22 females and 39 males. The average age was 59.67 ± 7.61 years, with ages ranging from 32 to 82. According to the histopathological classification of the patients, there were 37and 24 cases of adenocarcinoma and squamous cell carcinoma, respectively. TNM staging revealed that 13 patients were in stage I, 9 were in stage II, 16 were in stage III, and 23 were in stage IV. In 39 patients, the tumor was found in the right lung, while in 22 patients, it was found in the left lung. There were 26 patients who had tumors larger than 3 cm and 35 patients whose tumors were smaller than or equal to 3 cm. There were 25 females and 36 males in the control group. The mean age was 59.44 ± 7.63, with ages ranging from 30 to 83. As per the histopathological classification of the patients, there were 39 and 22 cases of adenocarcinoma and squamous cell carcinoma, respectively. There were 36 patients with tumors in the right lung and 25 patients with tumors present in the left lung, with 16 patients having stage I, 12 patients having stage II, 13 patients having stage III, and 20 patients had stage IV as per TNM staging. There were 31 patients suffering from tumors larger than 3 cm and 30 patients with tumors smaller than or equal to 3 cm. The two groups' general data were comparable ($P > 0.05$). The Hospital Ethics Committee provided their approval for this research.

2.2. Inclusion Criteria. (1) The diagnosis of NSCLC patients was made by clinicopathological examination [8]; (2) the Karnofsky Performance Status (KPS) score was >60; (3) life expectancy was >6 months; (4) all patients signed their informed consent and volunteered to take part in the study.

2.3. Exclusion Criteria. (1) Patients suffering from cardiopulmonary dysfunction; (2) patients having other malignant tumor diseases; (3) patients with severe hepatic and renal insufficiency; (4) patients with serious cardiovascular and cerebrovascular diseases; (5) patients with a history of pulmonary fibrosis or interstitial disease; (6) patients having a history of infusion reaction after antibody treatment; (7) patients with uncorrected thrombocytopenia or coagulopathy.

2.4. Methods. The control group received an anti-PD-1 monoclonal antibody and the observation group received microwave ablation in combination with an anti-PD-1 monoclonal antibody.

2.4.1. Microwave Ablation. The patient was fasted for 6 h before surgery. Half an hour before surgery, the patient was given 0.5 mg atropine sulfate, 10 mg diazepam intramuscular injection, and 30 mg codeine tablet oral treatment. Ten minutes before surgery, the patient was given a 10 mg bucinperazine intramuscular injection. The puncture point, direction, and depth of the needle were determined according to the tumor site revealed by the recent chest CT, and the puncture point was marked on the surface of the chest wall. At the puncture site, local anesthesia was administered using 5–15 mL of 1% lidocaine. The patient was told to hold his breath, and the microwave ablation antenna was inserted at the predetermined site and heated for 3-5 min at the power of 60-75 W. When the tumor diameter was smaller than or equal to 3 cm, one-point ablation was given; and when the maximum tumor diameter was greater than 3 cm, single-needle multipoint ablation or multineedle ablation was given according to the tumor shape. For tumor > 3 cm, the ablation range was 0.5-1.0 cm beyond the tumor edge, and it was appropriate when there was a ~0.5 cm wide ground glass reaction zone around the tumor on the lung window. During and 12 h after surgery, symptomatic treatments, including ECG monitoring, oxygen inhalation, blood oxygen saturation detection, intermittent listening to double-lung breath sounds, infection prevention, and hemostasis, were given to the patient. On day 1 postoperatively, a chest X-ray examination was performed to observe whether the patient had pneumothorax, liquid pneumothorax, and other complications.

2.4.2. Anti-PD-1 Monoclonal Antibody Therapy. The patient was treated by intravenous infusion of nivolumab injection (Bristol-Myers Squibb holdings Pharma, Ltd. Liability Company, USA, Registration Certificate No.: S20180014) at a dose of 3 mg/kg for 60 min. The treatment lasted for 6 cycles, with a drip every 14 days.

2.5. Observational Indices. (1) Clinical efficacy: the curative effects of the two groups were evaluated according to the response evaluation criteria in solid tumors RECISTI.1,

which included complete remission (CR), partial remission (PR), stable disease (SD), and progressed disease (PD). CR: the patient's lesion disappeared entirely, and the maintenance period lasted more than 4 weeks; PR: more than 30% of the lesion's diameter was shortened, and the maintenance period lasted 4 weeks; SD: the curative effect failed to meet PR and PD standards; PD: the tumor's total length and diameter grew by more than or equal to 20%, or new lesions developed. Response rate (RR) = (CR + PR)/total number of cases × 100%. Total effective rate = significant effective + effective. (2) Levels of T cell subsets: five milliliters of fasting venous blood was drawn from each patient in the two groups before and after treatment. The blood was subjected to centrifugation for 15 minutes at 3000 rpm to separate the serum. The levels of T cell subsets (CD3+, CD4+, and CD8+) were measured via flow cytometry according to the operation instructions. (3) Serum tumor markers: the levels of squamous cell carcinoma antigen (SCCA), cytokeratin Ig fragment (CYFRA21-1), and carcinoembryonic antigen (CEA) in serum were determined by electrochemiluminescence immunoassay. (4) Appropriate amount of cancer cells was extracted by percutaneous puncture, and RNA was extracted by extraction kit. Extraction and reverse transcription were performed with reverse transcription kits. The nuclear factor kappa B (NF-κB), protease C (PKC), and mitogen-activated protein kinases (MAPK) genes were amplified by PCR kit. The kits were obtained from SBS Genetech Co., Ltd. (Beijing, China). Prior to and following the treatment, a comparison was drawn between the two groups mRNA expression levels of NF-κB, PKC, and MAPK. (5) Long-term prognosis: telephone and outpatient services were employed for carrying out follow-up. In the first year, follow-ups were conducted once per month; in the second and third years, they were conducted once every three months and once every six months, respectively. The two groups' survival times were noted, and the survival of both groups was analyzed via the Kaplan-Meier method. (6) Occurrence of adverse reactions: the WHO criteria were used for evaluating the adverse reactions. Adverse reactions were classified into levels 0 to 4. The incidence of digestive tract reaction, liver and kidney function impairment, bone marrow transplantation, hematotoxicity, and peripheral neurotoxicity were compared between both groups

2.6. Statistical Analysis. All the data of this survey were entered into Excel without communication between two people and processed with the statistical software SPSS24.0. Mean ± SD ($\bar{x} \pm s$) represented the measurement data. When the measurement data conformed to the normal distribution and the variance was homogeneous, a t-test was adopted. The counting data were described by cases and %. Fisher's exact probability method and the χ^2 test were both utilized to compare the disordered classification data, and both tests were two-sided. $P < 0.05$ demonstrated statistical significance.

3. Results

3.1. Clinical Efficacy Comparison between the Two Groups. The observation group's RR was 80.33%, and the control group's RR was 62.30%, with statistically significant differences between the two groups ($P < 0.05$, Table 1).

3.2. Comparison of T Lymphocyte Subsets between the Two Groups. Prior to treatment, no considerable differences were observed between the two groups in regard to their CD3+, CD4+, or CD8+ levels (all $P > 0.05$). Upon treatment, the CD3+ and CD4+ levels increased and CD8+ levels reduced in both groups. The observation group's each index had an increased degree of improvement as compared to the control group, with statistically significant differences ($P < 0.05$, Table 2).

3.3. Comparative Analysis between the Two Groups' Serum Tumor Markers. Prior to treatment, no considerable differences were observed between the two groups in regard to their serum levels of CYFRA21-1, SCCA, or CEA (all $P > 0.05$). Following treatment, both groups' serum levels of SCCA, CYFRA21-1, and CEA decreased, and the observation group's indices were lesser as compared to the control group, with significant differences ($P < 0.05$, Table 3).

3.4. Comparison of Expression Levels of NF-κB, PKC, and MAPK mRNA between the Two Groups. There were no considerable differences between the two groups mRNA expression levels of NF-κB, PKC, and MAPK, prior to treatment (all $P > 0.05$). Following the treatment, the expression levels of NF-κB mRNA, PKC mRNA, and MAPK mRNA of both groups were reduced, and the observation group's indices were lesser than those of the control group, with significant differences (all $P < 0.05$, Table 4).

3.5. Comparison of the Two Groups' Survival Time. The observation groups' 1-, 2-, and 3-year survival rates (57.38%, 39.34%, and 29.51%) were greater than the control group (32.79%, 18.03%, and 8.20%), with statistically significant differences (all $P < 0.05$; Table 5 and Figures 1–3).

3.6. Comparison Analysis of Adverse Reactions between the Two Groups. No considerable differences were observed in the occurrence of gastrointestinal reaction, liver and kidney function impairment, bone marrow suppression, hematotoxicity, and peripheral neurotoxicity between both the groups (all $P > 0.05$, Table 6).

4. Discussion

Percutaneous microwave ablation is a relatively safe minimally invasive treatment. The only common contraindications are uncorrectable thrombocytopenia and coagulation disorders, and the surgery can even be carried out in the clinic. Patients with pulmonary dysfunction may experience a temporary exacerbation of respiratory symptoms prior to treatment and require oxygen therapy for a period of time [9]. Microwave ablation is a local treatment. For patients having peripheral lung cancer with tumor diameter < 3 cm, a single-needle ablation can completely inactivate the tumors. However, for tumors with a diameter > 5 cm, many residues remain after treatment, which may lead to tumor recurrence [10]. Multipoint, multidirectional, and multilevel

Table 1: Clinical efficacy comparison between the two groups (cases, %).

Group	CR	PR	SD	PD	RR
Observation group ($n = 61$)	29 (47.54)	20 (32.79)	8 (13.11)	4 (6.56)	49 (80.33)
Control group ($n = 61$)	20 (32.79)	18 (29.51)	14 (22.95)	9 (14.75)	38 (62.30)
χ^2					4.848
P					0.028

Note: CR: complete remission; PR: partial remission; SD: stable disease; PD: progressed disease; RR: response rate.

Table 2: Comparison of the two groups' T lymphocyte subsets ($\bar{x} \pm s$, %).

Group	CD3+		CD4+		CD8+	
	Before treatment	After treatment	Before treatment	After treatment	Before treatment	After treatment
Observation group ($n = 61$)	55.86 ± 5.70	67.41 ± 6.74[a]	36.73 ± 3.11	42.34 ± 3.45[a]	29.88 ± 2.49	20.74 ± 1.87[a]
Control group ($n = 61$)	55.18 ± 4.33	64.47 ± 6.08[a]	36.45 ± 3.07	40.16 ± 2.92[a]	29.44 ± 2.47	23.60 ± 2.16[a]
t	0.741	2.535	0.502	3.777	0.989	7.814
P	0.460	0.013	0.617	<0.001	0.325	<0.001

Note: compared to the same group's pretreatment data, [a]$P < 0.05$.

Table 3: Comparison of serum tumor markers between the two groups ($\bar{x} \pm s$).

Group	SCCA (ng/mL)		CYFRA21-1 (μg/L)		CEA (μg/L)	
	Before treatment	After treatment	Before treatment	After treatment	Before treatment	After treatment
Observation group ($n = 61$)	9.50 ± 0.94	3.57 ± 0.56[a]	26.55 ± 2.74	12.80 ± 2.37[a]	66.07 ± 5.46	42.50 ± 4.38[a]
Control group ($n = 61$)	9.66 ± 0.99	5.73 ± 0.64[a]	25.91 ± 2.47	16.33 ± 3.08[a]	67.98 ± 5.40	46.35 ± 4.52[a]
t	0.911	19.867	1.348	7.036	1.939	4.765
P	0.364	<0.001	0.180	<0.001	0.055	<0.001

Note: compared to the same group's pretreatment data, [a]$P < 0.05$.

Table 4: Comparison of expression levels of NF-κB, PKC, and MAPK mRNA between the two groups ($\bar{x} \pm s$).

Group	NF-κB mRNA		PKC mRNA		MAPK mRNA	
	Before treatment	After treatment	Before treatment	After treatment	Before treatment	After treatment
Observation group ($n = 61$)	0.91 ± 0.19	0.24 ± 0.12[a]	0.90 ± 0.14	0.24 ± 0.11[a]	0.93 ± 0.14	0.21 ± 0.11[a]
Control group ($n = 61$)	0.90 ± 0.11	0.53 ± 0.12[a]	0.91 ± 0.12	0.45 ± 0.15[a]	0.92 ± 0.14	0.48 ± 0.14[a]
t	0.446	13.325	0.337	8.469	0.322	11.795
P	0.656	<0.001	0.737	<0.001	0.748	<0.001

Note: compared to the same group's pretreatment data, [a]$P < 0.05$.

Table 5: Comparison of the two groups' survival time (cases, %).

Group	Follow-up for 1 year		Follow-up for 2 years		Follow-up for 3 years	
	Survival	Death	Survival	Death	Survival	Death
Observation group ($n = 61$)	35 (57.38)	26 (42.62)	24 (39.34)	37 (60.66)	18 (29.51)	43 (70.49)
Control group ($n = 61$)	20 (32.79)	41 (67.21)	11 (18.03)	50 (81.97)	5 (8.20)	56 (91.80)
Log-rank χ^2	7.980		9.039		11.210	
P	0.005		0.003		0.001	

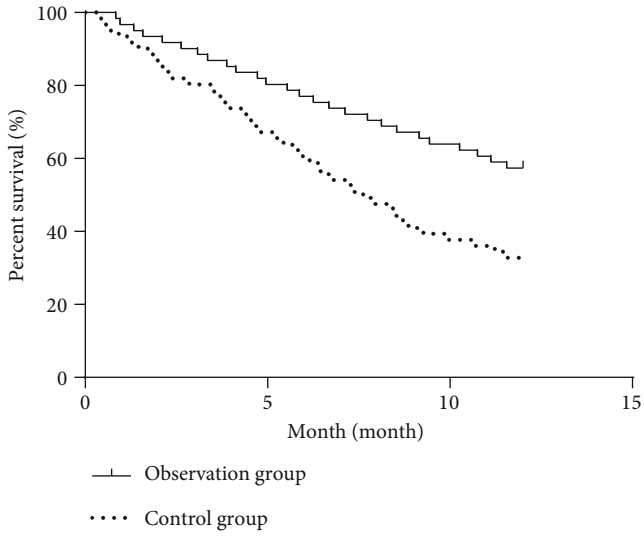

Figure 1: Survival curve of 1-year follow-up.

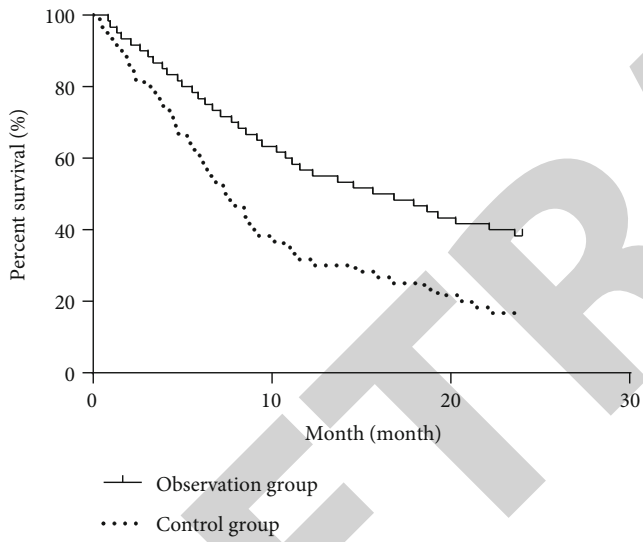

Figure 2: Survival curve of 2-year follow-up.

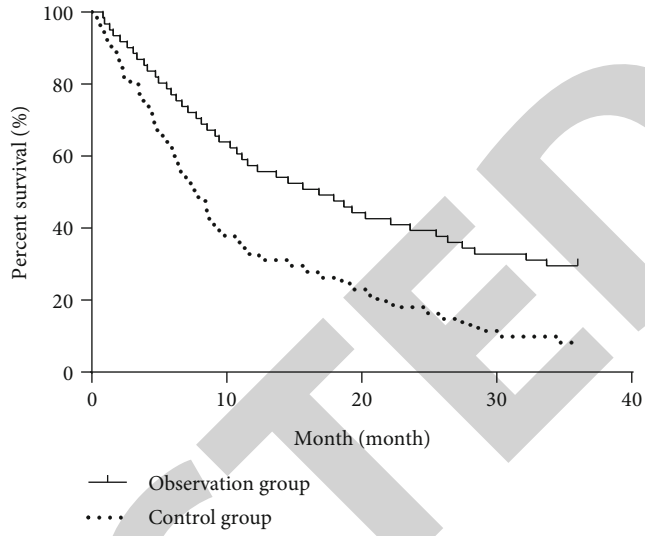

Figure 3: Survival curve of 3-year follow-up.

microwave ablation should be applied to tumors with a diameter ≥ 3 cm, and the inactivation range should be extended to 0.5-1.0 cm beyond the tumor edge as far as possible. However, distant metastasis or lymph node metastasis usually exists in advanced lung cancer, so microwave ablation alone is not suitable for the treatment of this kind of tumor. PD-1 is an important immune checkpoint and is a protective molecule of the body's immune system. By interacting with PD-L1, PD-1 can inhibit the inflammatory damage caused by T cell overactivation and effectively maintain the body's peripheral tolerance. Utilizing this characteristic, tumor cells overexpress immune checkpoint molecules to inhibit human immune system response, escape immune surveillance, and promote tumor cell growth [11, 12]. The immunosuppressive tumor microenvironment can activate the PD-1/PD-L1 signaling pathway, and blocking the PD-1/PD-L1 signaling pathway reverses the tumor immune microenvironment and increases the body's immune system's capability of killing the cancerous cells. The anti-PD-1 monoclonal antibody can effectively block the PD-1/PD-L1 signaling pathway. In the present study, the observation groups' patients received microwave ablation in combination with the anti-PD-1 monoclonal antibody, so that the efficacy of microwave ablation can be enhanced and the effect of immunotargeted therapy can be fully played to. In this study, RR (80.33%) in the observation group was substantially elevated than the RR of the control group (62.30%) following the treatment, and the improved levels of CD3+, CD4+, and CD8+ in the observation group were greater than the control group after treatment, implying that microwave ablation in combination with anti-PD-1 monoclonal antibody was superior to the lone use of anti-PD-1 monoclonal antibody for treating the NSCLC and can enhance the patients' cellular immunity in a more effective manner. CD3+ T lymphocytes can play an immune role in clearing tumor cells. CD4+ T lymphocytes, as auxiliary T cells, can not only play a direct killing role on tumor cells but also have immune memory function, playing a secondary immune role. CD8+ T lymphocytes are cytotoxic T lymphocytes, which can negatively regulate tumor immune response and can be used to evaluate the patient's autoimmune function [13, 14]. In the process of the development of NSCLC, apoptosis of tumor-specific T cells and PD-1-dependent and PD-1-independent mechanisms of mediation are closely related. PD-1-dependent mechanism can promote the immune escape of tumor cells in NSCLC patients. Peripheral blood T lymphocytes in NSCLC patients may show abnormal expression levels, including decreased CD3+ and CD4+ cells and increased CD8+ cells. Anti-PD-1 monoclonal antibody therapy can effectively improve the level of T lymphocytes in peripheral blood, relieve tumor load, and restore abnormal lymphocyte subsets [15]. Microwave ablation promoted tumor tissue necrosis and enhanced the effect of immunotherapy by improving the permeability of cell membrane and nuclear membrane. Therefore, the

Table 6: Comparison analysis of adverse reactions between the two groups (cases, %).

Group	Observation group ($n = 61$)			Control group ($n = 61$)			χ^2	P/Fisher's exact probability value
	I/II grade	III grade	Total incidence	I/II grade	III grade	Total incidence		
Gastrointestinal reaction	14 (22.95)	1 (1.64)	15 (24.59)	14 (22.95)	2 (3.28)	16 (26.23)	0.043	0.835
Liver and kidney function impairment	1 (1.64)	1 (1.64)	2 (3.28)	2 (3.28)	1 (1.64)	3 (4.92)	—	1.000
Bone marrow suppression	14 (22.95)	2 (3.28)	16 (26.23)	13 (21.31)	1 (1.64)	14 (22.95)	0.177	0.674
Hematotoxicity	7 (11.48)	1 (1.64)	8 (13.11)	4 (6.56)	0 (0.00)	4 (6.56)	1.479	0.224
Peripheral neurotoxicity	4 (6.56)	1 (1.64)	5 (8.20)	5 (8.20)	1 (1.64)	6 (9.84)	0.100	0.752

improvement effect of the T lymphocyte subgroup level in the observation group was better. Earlier research shows that microwave ablation can promote the patient's immune response to malignant tumors [16]. Our study's findings are in accordance with those of the earlier research.

Serum tumor markers refer to substances produced, secreted, or released by tumor cells into body fluid, blood, cells, or tissues that can reflect the presence and growth of the tumor. The expression level of serum tumor markers in normal or benign tissues is extremely low, and its level is highly associated with the incidence and progression of malignant tumors. Thus, it can reflect the case classification of tumor tissues and be used for disease analysis. As a soluble glycoprotein antigen, CEA is widely present in embryonic tumor and adenocarcinoma tissues, and its positive rate in lung adenocarcinoma is significantly higher than that in squamous cell carcinoma [17]. CYFRA21-1, the soluble fragment of cytokeratin Ig, is widely present in the cytoplasm of epithelial tumors such as esophageal cancer and lung cancer. It is a new tumor marker and can be used for the early diagnosis and prognosis of NSCLC [18]. Squamous cell carcinoma patients' serum contains significant amounts of SCCA [19]. The current research demonstrated that after treatment, serum levels of SCCA, CYFRA21-1, and CEA significantly decreased in the observation group in comparison to the control group, suggesting that anti-PD-1 monoclonal antibody and microwave ablation together could more effectively regulate the level of tumor markers. This may be because of the fact that the thermal effect of microwave ablation promotes irreversible necrosis of tumor tissue, destroys tumor cells in large quantities, and reduces the tumor load of the body. The combined therapy had an obvious tumor reduction effect, and the observation groups' level of serum tumor marker was more significantly reduced.

Previous research demonstrated that the PKC, MAPK, and NF-KB pathways are highly associated with the formation of VEGF. A series of cascade reactions among the three pathways can promote the synthesis and secretion of VEGF and promote tumor angiogenesis [20]. According to the current research, the NF-KB mRNA, PKC mRNA, and MAPK mRNA expression levels in the observation group were substantially enhanced as compared to the control group following the treatment, suggesting that microwave ablation in combination with anti-PD-1 monoclonal antibody may play a therapeutic effect by affecting PKC, MAPK, and NF-KB pathways, but there is no relevant clinical study at present. There, more research must be conducted to determine its precise mode of action. In this study, the observation group's 1-, 2-, and 3-year follow-up survival rates (32.79%, 18.03%, and 8.20%) were greater as compared to the control group (57.38%, 39.34%, and 29.51%), suggesting that combination therapy can more effectively enhance the patients' long-term prognosis.

In the current research, there were no considerable differences in the incidences of digestive tract reaction, liver and kidney function impairment, bone marrow suppression, hematotoxicity, and peripheral neurotoxicity between both groups. Although an additional treatment method was added to the observation group, adverse reactions were not aggravated, indicating that microwave ablation was safe.

In conclusion, percutaneous microwave ablation combined with an anti-PD-1 monoclonal antibody was effective in the treatment of NSCLC. This combined therapy could effectively improve the level of T lymphocyte subsets and long-term prognosis with good safety and clinical value.

Data Availability

The labeled dataset used to support the findings of this study is available from the corresponding author upon request.

Conflicts of Interest

The authors declare no competing interests.

References

[1] S. Jonna and D. S. Subramaniam, "Molecular diagnostics and targeted therapies in non-small cell lung cancer (NSCLC): an update," *Discovery Medicine*, vol. 27, no. 148, pp. 167–170, 2019.

[2] M. Alexander, S. Y. Kim, and H. Cheng, "Update 2020: management of non-small cell lung cancer," *Lung*, vol. 198, no. 6, pp. 897–907, 2020.

[3] F. Vari, D. Arpon, C. Keane et al., "Immune evasion via PD-1/PD-L1 on NK cells and monocyte/macrophages is more prominent in Hodgkin lymphoma than DLBCL," *Blood*, vol. 131, no. 16, pp. 1809–1819, 2018.

Hindawi
Computational and Mathematical Methods in Medicine
Volume 2023, Article ID 9793878, 1 page
https://doi.org/10.1155/2023/9793878

Retraction

Retracted: Electroacupuncture Treats Myocardial Infarction by Influencing the Regulation of Substance P in the Neurovascular to Modulate PGI2/TXA2 Metabolic Homeostasis via PI3K/AKT Pathway: A Bioinformatics-Based Multiomics and Experimental Study

Computational and Mathematical Methods in Medicine

Received 12 December 2023; Accepted 12 December 2023; Published 13 December 2023

This article has been retracted by Hindawi, as publisher, following an investigation undertaken by the publisher [1]. This investigation has uncovered evidence of systematic manipulation of the publication and peer-review process. We cannot, therefore, vouch for the reliability or integrity of this article.

Please note that this notice is intended solely to alert readers that the peer-review process of this article has been compromised.

Wiley and Hindawi regret that the usual quality checks did not identify these issues before publication and have since put additional measures in place to safeguard research integrity.

We wish to credit our Research Integrity and Research Publishing teams and anonymous and named external researchers and research integrity experts for contributing to this investigation.

The corresponding author, as the representative of all authors, has been given the opportunity to register their agreement or disagreement to this retraction. We have kept a record of any response received.

References

[1] P. Zhang, Y. Wang, X. Xing et al., "Electroacupuncture Treats Myocardial Infarction by Influencing the Regulation of Substance P in the Neurovascular to Modulate PGI2/TXA2 Metabolic Homeostasis via PI3K/AKT Pathway: A Bioinformatics-Based Multiomics and Experimental Study," *Computational and Mathematical Methods in Medicine*, vol. 2022, Article ID 5367753, 15 pages, 2022.

Hindawi
Computational and Mathematical Methods in Medicine
Volume 2022, Article ID 5367753, 15 pages
https://doi.org/10.1155/2022/5367753

Research Article

Electroacupuncture Treats Myocardial Infarction by Influencing the Regulation of Substance P in the Neurovascular to Modulate PGI2/TXA2 Metabolic Homeostasis via PI3K/AKT Pathway: A Bioinformatics-Based Multiomics and Experimental Study

Ping Zhang,[1] Yanyan Wang,[2] Xiaomin Xing,[1] Hu Li,[1] Xiaojing Wang,[1] Hanlin Zhang,[1] Xin Wang,[1] Xiubin Li,[3] Yanju Li,[1] and Qian Wang[4]

[1]*Department of Rehabilitation, The Second Affiliated Hospital of Shandong First Medical University, Taian, 271000, China*
[2]*Taian Traffic Hospital, Taian, 271000, China*
[3]*Department of Neurology, The Second Affiliated Hospital of Shandong First Medical University, Taian, 271000, China*
[4]*Postdoctoral Workstation, Department of Central Laboratory, The Affiliated Taian City Central Hospital of Qingdao University, Taian 271000, China*

Correspondence should be addressed to Yanju Li; liyanju@sdfmu.edu.cn and Qian Wang; qianqianwangxi@163.com

Received 26 July 2022; Revised 9 August 2022; Accepted 11 August 2022; Published 22 September 2022

Academic Editor: Min Tang

Acute myocardial infarction (AMI) is the most severe form of coronary heart disease caused by ischemia and hypoxia. The study is aimed at investigating the role of neuropeptides and the mechanism of electroacupuncture (EA) in acute myocardial infarction (AMI) treatment. Compared with the normal population, a significant increase in substance P (SP) was observed in the serum of patients with AMI. PGI2 expression was increased in the SP-treated AMI mouse model, and TXA2 expression was decreased. And PI3K pathway-related genes, including *Pik3ca*, *Akt*, and *Mtor*, were upregulated in myocardial tissue of SP-treated AMI patients. Human cardiomyocyte cell lines (HCM) treated with SP increased mRNA and protein expression of PI3K pathway-related genes (*Pik3ca*, *Pik3cb*, *Akt*, and *Mtor*). Compared to MI control and EA-treated MI rat models, *Myd88*, *MTOR*, *Akt1*, *Sp*, and *Irak1* were differentially expressed, consistent with in vivo and in vitro studies. EA treatment significantly enriched PI3K/AKT signaling pathway genes within MI-associated differentially expressed genes (DEGs) according to Kyoto Encyclopedia of Genes and Genomes (KEGG). Furthermore, it was confirmed by molecular docking analysis that PIK3CA, AKT1, and mTOR form stable dockings with neuropeptide SP. PI3K/AKT pathway activity may be affected directly or indirectly by EA via SP, which corrects the PGI2/TXA2 metabolic imbalance in AMI. MI treatment is now better understood as a result of this finding.

1. Introduction

Acute myocardial infarction (AMI) is the most severe manifestation of coronary heart disease. More and more young people are suffering from AMI, one of China's most critical public health problems [1]. It is primarily caused by ruptured coronary atherosclerotic plaques, which activates the body's platelets and coagulation process, eventually leading to thrombosis and coronary artery blockage [2].

AMI causes ischemia and hypoxia in the myocardium, which can cause pain, anxiety, and changes in cardiac function and promote sympathetic nerve activity. Neuropeptides are important prognostic markers of AMI [3–6]. The release of neuropeptide Y (NPY) from nerve fibers in the myocardium reduces blood flow to the vascular tissue in the infarct area [7]. Evidence suggests that substance P (SP) has a vasodilatory effect on cardiomyocytes and a cardioprotective effect during ischemic injury [8–11]. SP reduces the

likelihood of MI-induced arrhythmias, because it activates the PI3K/AKT signaling pathway and phosphorylates GSK-3, thus enhancing the expression of anti-apoptosis-related proteins and inhibiting the expression of proapoptosis proteins, thereby reducing inflammatory responses, thus protecting the heart [12]. PI3K/AKT signaling is a key regulatory pathway in the development of ischemic arrhythmias. Inhibition of this pathway causes mitochondrial damage leading to apoptosis in cardiomyocytes, and low AKT phosphorylation and high miRNA-1 levels inhibit membrane ion channel expression [12]. This changes the ion flow density, cardiac action potential duration, and cell conductivity, thereby inducing ischemic arrhythmias.

Electroacupuncture (EA) combines traditional manual acupuncture with modern electrotherapy and is now widely used to treat many conditions [13]. EA is commonly used to treat neurovascular disorders such as stroke, chronic neuropathic pain, and neurodegenerative diseases such as Alzheimer's disease [14–18]. EA exerts neuroprotective effects by enhancing anti-inflammatory response to inhibit abnormal glial cell activation and prevent neuronal loss [19]. Studies have also demonstrated that EA increases the expression of NPY in the hypothalamus and attenuates the stress response under chronic stress conditions [20, 21]. Further, EA also induces NPY expression in the paraventricular nucleus and inhibits antihypertensive and sympathetic activities [22]. EA exerts its protective effect by activating sympathetic alpha-adrenergic receptors in myocardial ischemic injury [23, 24]. EA reduces heart rate, ST segment, and infarct size, thereby alleviating myocardial injury in rats with AMI [25]. However, the mechanisms of EA in AMI treatment are largely unknown. Therefore, we speculate that EA may treat AMI by modulating neuropeptide expression.

The integration of computational techniques into traditional medicine is necessary for the integration of systems biology into traditional medicine based on a holistic approach [26–36]. In order to analyze the targets and key pathways associated with AMI treated with EA in rat models, data from the Gene Expression Omnibus (GEO) database were retrieved in this study. Moreover, neuropeptide docking with target proteins was examined. It provides new ideas for clinical treatment and drug development of AMI.

2. Materials and Methods

2.1. Patients. All patient samples were collected with informed consent in accordance with ethical standards. After blood samples were collected and centrifuged to extract serum, they were stored in ultracryogenic freezers and thawed at post-room temperatures. RNA was also extracted directly from blood cells.

2.2. AMI Animal Model. We purchased fifteen SPF Balb/c mice (6-week-old males) from Shanghai SLAC Laboratory Animal Co. Ltd. The mice were prebred for three days, then randomly divided into three groups; the first group was the surgical group, without ligation of the left anterior descending branch; the second group was the AMI group; and the third group was the AMI+SP group. Following shaving of the surgical scope, the surgical area was disinfected with 75% ethanol and anesthesia was administered by intraperitoneal injection with 3% sodium pentobarbital (80 mg/kg). Following anesthesia, tracheal intubation was performed to monitor the mouse's respiratory condition, and chest fluctuation was consistent with ventilator frequency (110 bpm), indicating successful intubation. With a 7-0 needle suture, mice were posed left lateral supine so their hearts were fully exposed, a little pericardium was torn, and the left anterior coronary artery descending was exposed. Afterwards, the chest was stitched layer by layer with muscles and skin. Observe the mice closely after the surgery to determine their basic health. The tracheal intubation was removed after the mice naturally awoke. Within 45 minutes after surgery, mice were injected with SP (5 nmol/kg), where the first and second groups received equal amounts of saline; about 1 week after cultivation, cardiac blood was collected, and the mice were sacrificed. Following the procedure above, mice were quickly removed, washed in ice saline to ensure no obvious blood stains, frozen at -20°C for 15 minutes, then cut into 1 mm thick slices, placed in 5 mL 1% TTC phosphate buffer (pH 7.4) and 37°C water bath for 15 minutes, and then weighed.

2.3. Cell Culture and RT-qPCR. DMEM high-glucose medium, supplemented with 20% FBS, 1% double antibody, and 37°C 5% CO_2, was used to culture human cardiomyocyte (HCM) cells. Inoculation is performed at constant temperatures and humidity.

RNA extraction was performed with Trizol for cell, blood samples, and tissues, where tissue suspension was required before tissue RNA extraction, and then, Trizol was added for RNA extraction. Extracted RNA was immediately reverse transcribed into cDNA (Takara Reverse Transcription Kit) and stored at-20°C for further detection. They were thawed at room temperature, and cDNA was performed according to the RT-PCR kit of cell organisms. Among them, $2^{-\Delta\Delta Ct}$ calculations were performed, with GAPDH as an internal reference.

2.4. ELISA. NPY and SP-1 concentrations were determined using the Invitrogen ELISA kit, and human serum was diluted 100-fold. Invitrogen ELISA kit was used to determine plasma levels after centrifuging rat blood to obtain 1000-fold diluted plasma.

2.5. Tissue and Cellular Protein Extraction. Infarct myocardial tissue was extracted using RIPA (blue); supplemented with protease inhibitors and phosphatase inhibitors by a homogenizer (Tanon), for 30 minutes on ice; and centrifuged at 4°C 12,000 rpm for 5 min; absorbed supernatants were incubated at 100°C for 10 min, and protein denaturation was performed in a refrigerator at -20°C. Proteins were denatured at 100°C for 10 minutes and stored at -20°C after being treated with SP1 (1 mol/L and 5 mol/L) for 24 h in RIPA supplemented with protease inhibitors and phosphatase inhibitors.

2.6. Western Blot. Proteins were treated at different concentrations of SDS-PAGE (Yarase) and then gel electrophoresis at 10% gel at 120 V constant pressure for 100 to 120 min and 300 mA for 90 minutes; PVDF membranes were closed with 5% BSA for 1 h, blocked overnight with TBST, and the following day were incubated with the secondary antibodies for 2 h.

2.7. Disease-Associated Genes. We downloaded two datasets (GSE54132, GSE61840) relevant to EA treatment of MI from the NCBI GEO database (https://www.ncbi.nlm.nih.gov/geo/), and the platform annotation files were Illumina HiSeq 2000 Rat Gene expression arrays (GPL14844). Two MI rats, three EA-treated MI rats, and three normal rats are included in GSE54132; two MI rats, two EA-treated MI rats, and two normal rats are included in GSE61840.

2.8. DEGs Associated with EA+MI. Combining the GSE54132 and GSE61840 datasets and preprocessing (background correction, normalisation, and log2 transformation) were done with R 4.0.2 (https://www.R-project.org). Multiple probes corresponding to a common gene were averaged to determine its expression level. To eliminate batch effects between the two datasets, the "sva" package was used. DEGs with $P < 0.05$ were screened with the "limma" package, using |log2 fold change (FC)| ≥1.00 as the cut-off point for selecting DEGs. R software was used to plot heat maps and volcano maps related to EA+MI.

2.9. GO and KEGG Pathway Enrichment Analysis of DEGs. DAVID online tool was used to annotate DEGs based on GO terms. There were three categories of biological processes (BP), cellular components (CC), and molecular functions (MF) included in the GO analysis. The Kyoto Encyclopedia of Genes and Genomes (KEGG) analysis was also completed. In order to understand the specific mechanisms of EA treatment of MI, we used the pathview-Bioconductor software (version 3.15) package to map signaling pathways.

2.10. Protein and Neuropeptide Docking. Peptide-core protein docking was performed between SP and the receptor protein to investigate their interaction. By homology modeling and exporting the 3D structure to PDB, we constructed SP's sdf structure from the PubChem database. We first downloaded the PDB format of the receptor core protein from the PDB website (http://www.rcsb.org/), dehydrated and dephosphorylated the protein using PyMOL software, and converted the SP and core protein structural domains to the PDBqt format using AutoDockTools 1.5.6 software. In order to calculate the molecular binding energy and show the results of molecular docking, the Vina script was run. The binding energy of a ligand and receptor can be less than zero, and spontaneous binding can take place. Vina binding energies ranging from -5.0 kcal/mol are used to evaluate the accuracy of bioinformatics predictions for ligand-receptor complexes.

2.11. Statistical Method. All experiments were performed three times. The data are presented as mean ± SD (standard deviation). Chi-square tests were used to analyze frequency differences between two groups, and *t*-tests were used to analyze differences between independent samples. $P < 0.05$ was considered statistically significant.

3. Results

3.1. SP Expression Was Increased in AMI Patients. Neuropeptides play roles in numerous diseases. Therefore, to investigate the role of SP in AMI, we collected blood from patients with AMI, and the expression of the neuropeptides was measured using RT-qPCR. Compared to the normal population, an increase in expression of SP, angiotensin II (Ang II), and NPY was observed in the serum of AMI patients. Among these, there was a significant increase in SP levels in AMI patients (Figure 1(a)). ELISA results revealed that as compared to the normal population, no significant difference ($P > 0.001$) in NPY levels was observed in the serum of AMI patients (Figure 1(b)). AMI patients' serum SP levels were significantly higher than those in the normal population, as shown in Figure 1(c) ($P < 0.001$). The results of this study indicate a significant increase in SP levels in AMI patients; however, its role in the disease is unclear.

3.2. Mice with AMI Can Benefit from SP. To investigate the effect of SP on acute MI, we established a mouse model of acute MI by ligation of the left anterior coronary artery descending and observed the effect of SP on AMI (Figure 2(a)). We used myocardial infarcted mice as control groups, and the SP-acting mice had both decreased infarct area weight and infarct tissue proportion (infarcted myocardial weight/total heart weight), indicating that SP was protective against AMI (Figures 2(b) and 2(c)).

3.3. SP Influences PGI2/TXA2 Axis Balance by Altering the PI3K/AKT Pathway. Our results show a protective effect of SP on AMI; however, SP's mechanism of action on AMI is unclear. In addition to the rupture of coronary artery plaque to form a clot that blocks the lumen of the artery, an increase in oxygen consumption by the myocardium and coronary artery spasm can also induce AMI [1, 2]. Coronary spasms are caused by various factors, like prostacyclin (PGI2) and thromboxane A2 (TXA2) [3, 4]. Therefore, ELISA was used to check the protein levels of PGI2 and TXA2 in the sera of the mice. As shown in Figures 3(a) and 3(b), as compared to normal mice, the levels of PGI2 and TXA2 were elevated in acute MI mice. Further, compared to the control group, the levels of PGI2 were higher in SP-treated MI mouse models. However, compared to the control group, a decrease in the levels of TXA2 was observed in SP-treated MI mouse models. Therefore, we hypothesized that SP affected MI by altering PGI2/TXA2 balance.

In the SP group, *Pik3ca*, *Akt*, and *Mtor* gene expression was increased, as shown in Figure 3(c). Therefore, we hypothesized that the PI3K/AKT pathway was involved in the mechanism of action of SP in AMI. We used western blotting to determine the expression of AKT, p-AKT, and mTOR proteins. The results reveal an increase in AKT, p-AKT, and mTOR expression in AMI mice treated with SP compared to the control (Figure 3(d)).

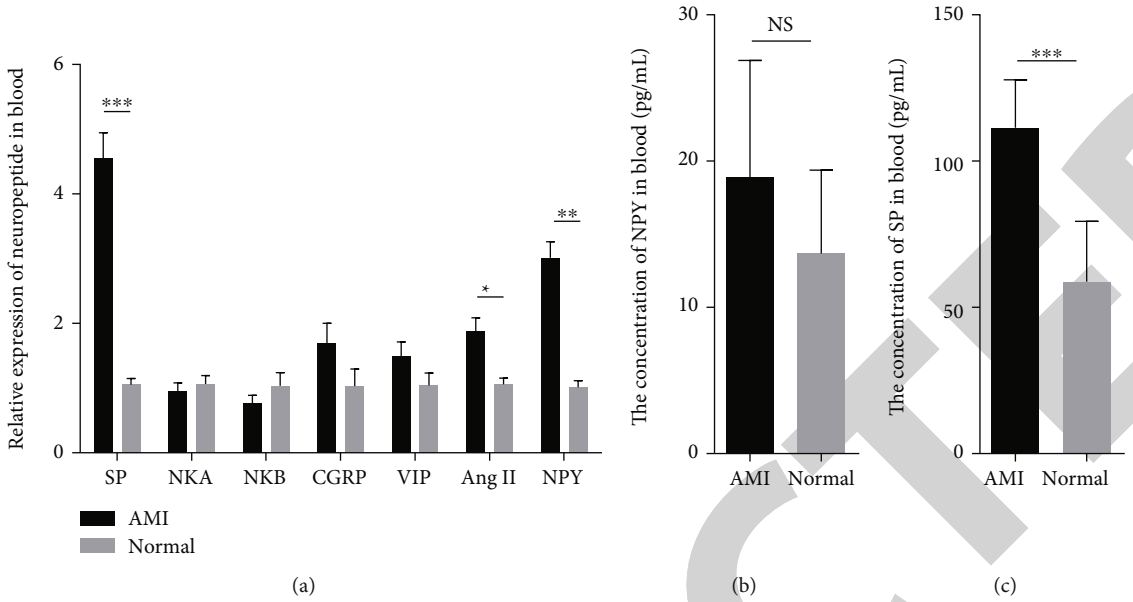

Figure 1: SP expression is increased in AMI patients. (a) RT-PCR showed that SP, Ang II, and NPY were increased in AMI patients. (b) ELISA results show NPY levels in the serum of AMI patients. (c) ELISA results reveal higher levels of SP in the serum of AMI patients. $^{*}P < 0.05$, $^{**}P < 0.01$, and $^{***}P < 0.001$.

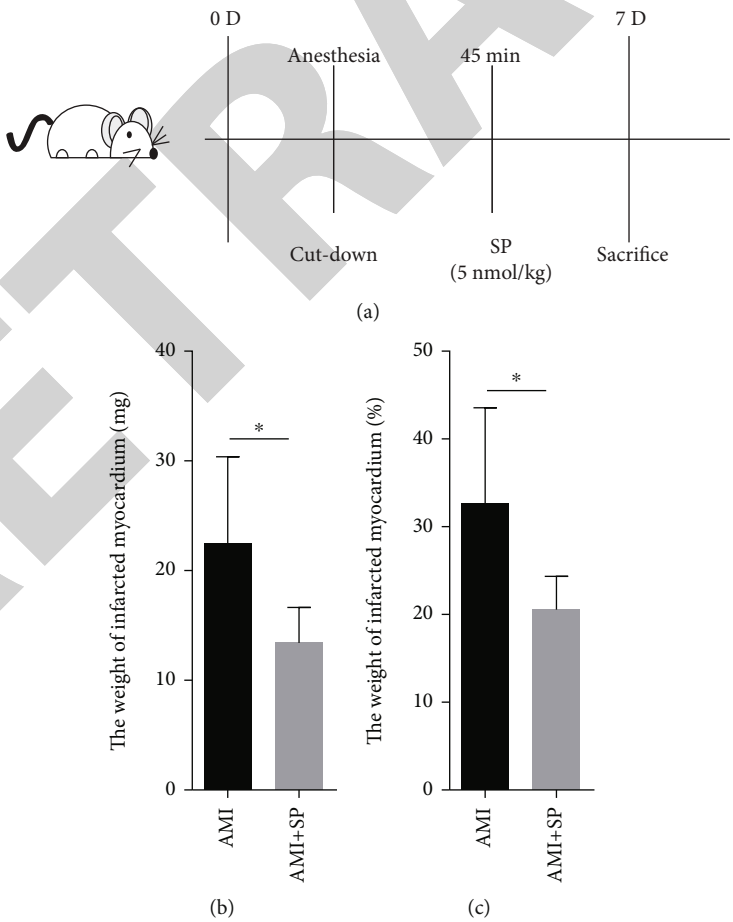

Figure 2: SP can improve the symptoms in the AMI mouse model: (a) schematic representation of the AMI mouse model; (b) the weight of infarcted myocardium (45 min); (c) the weight of infarcted myocardium (7 d); $^{*}P < 0.05$.

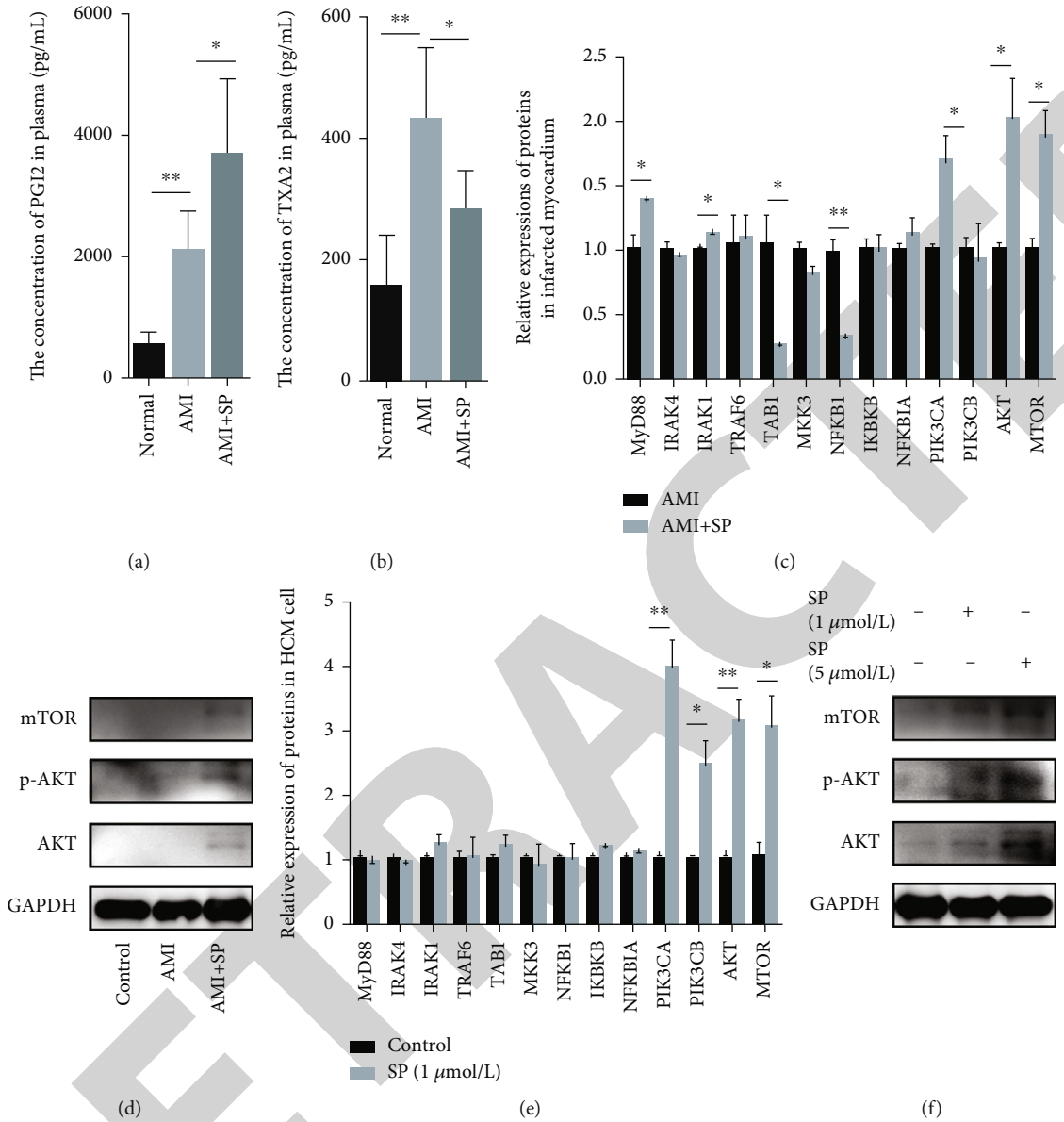

Figure 3: SP affects the PGI2/TXA2 balance by influencing the PI3K/AKT pathway. (a) Determination of PGI2 concentrations in mouse serum by ELISA; (b) determination of TXA2 concentrations in mouse serum by ELISA; (c) RT-PCR of *Myd88*, *Irak1*, *Tab1*, *Nf-κb1*, *Pik3c1*, *Akt*, and *Mtor* gene expression in infarcted myocardial tissues of mice; (d) expression of MTOR, p-AKT, AKT, and GAPDH genes in infarcted myocardial tissues of mice by western blot; (e) expression of *Myd88*, *Irak1*, *Tab1*, *Nf-κb1*, *Pik3c1*, *Akt*, and *Mtor* genes after SP treatment; (f) expression of MTOR, p-AKT, AKT, and MTOR after SP treatment by western blot.

To further analyze the mechanism of action of SP on cardiomyocytes, the human cardiomyocyte cell line HCM was treated with SP. RT-qPCR results revealed an increase in the expression of PI3K pathway-related genes (*Pik3ca*, *Pik3cb*, *Akt*, and *Mtor*) in HCM cells treated with SP (Figure 3(e)) compared to untreated HCM cells. The protein expression of these genes, as confirmed by western blotting, was consistent with RT-PCR results. Therefore, it is tempting to conclude that SP promotes AKT, p-AKT, and mTOR expression in cardiomyocytes (Figure 3(f)). Taken together, we show that SP influences the PGI2/TXA2 hemostasis by the PI3K/AKT pathway, thereby alleviating the symptoms of AMI.

3.4. Gene Expression Analysis of MI-Related Genes Treated with EA. GSE54132 and GSE61840 datasets were retrieved from the GEO database. The datasets used the same platform (GPL14844, Illumina HiSeq 2000 array) for the high-throughput mRNA sequencing of the EA-treated MI rat model. The gene expression was normalized after preprocessing and background correction. Differentially expressed genes (DEG) were screened using linear models for microarray data (limma) package. There were 551 DEGs between the MI rat model and control rats, of which 346 were expressed upregulated while 205 were expressed downregulated. However, in EA-treated MI rats, a total of 541 DEGs were observed, of which 197 were upregulated, and 344 were

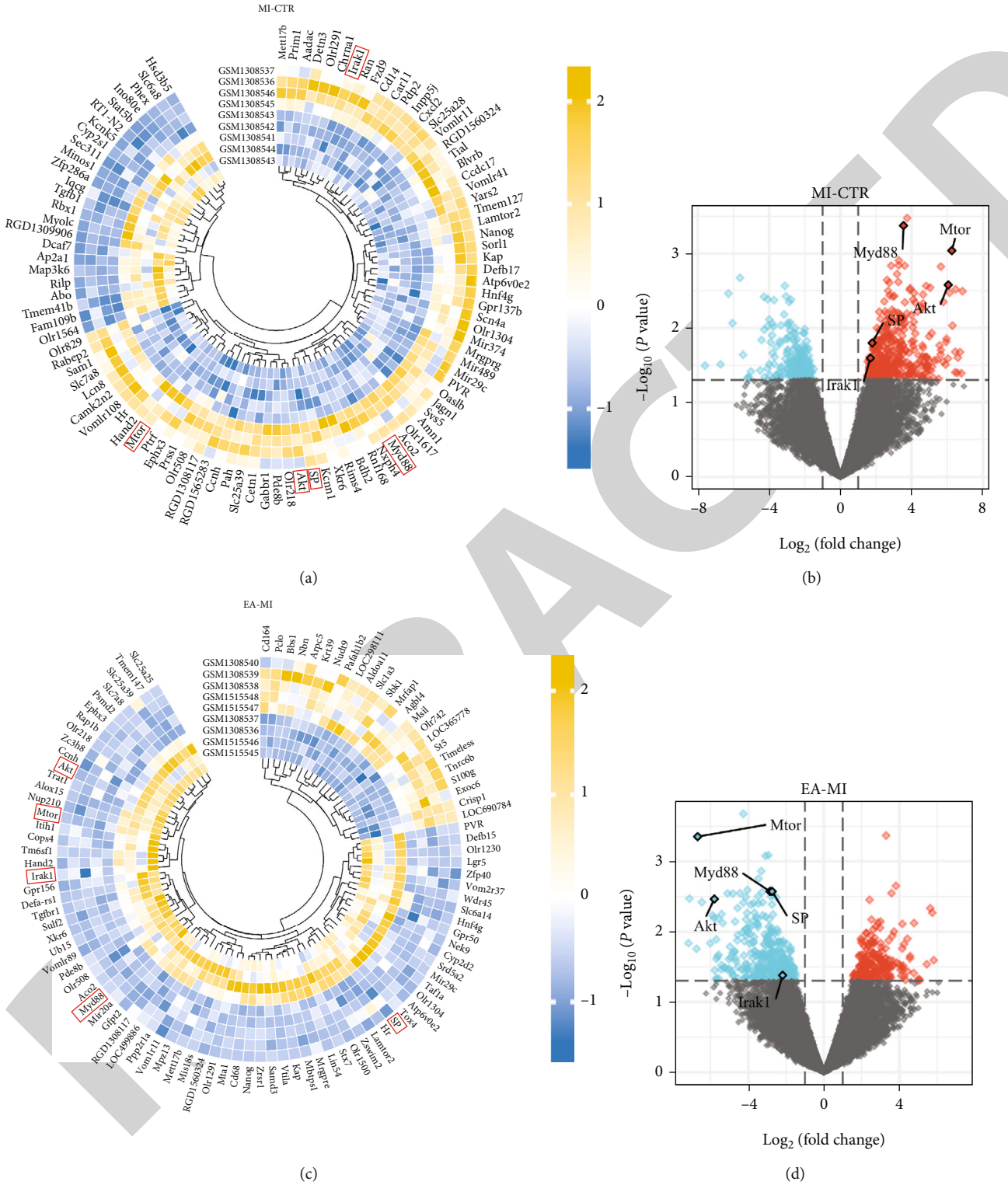

Figure 4: DEGs associated with EA+MI based on microarray data. (a) Heat map of MI-CTR differentially expressed genes; (b) heat map of MI-CTR differentially expressed volcanoes; (c) heat map of EA+MI differentially expressed genes; (d) heat map of EA+MI differentially expressed volcanoes. Blue represents ascending genes; red represents descending genes. Genes marked with an asterisk have been validated in the current experiment.

downregulated. The top 100 genes with the highest expression in MI-CTR (control) and EA-treated MI rats were screened for hierarchical cluster analysis, and the cluster heat map (Figures 4(a) and 4(c)) and volcano map (Figures 4(b) and 4(d)) were constructed. Differential expression of *Myd88*, *Mtor*, *Akt1*, *Sp*, and *Irak1* was observed between MI-CTR

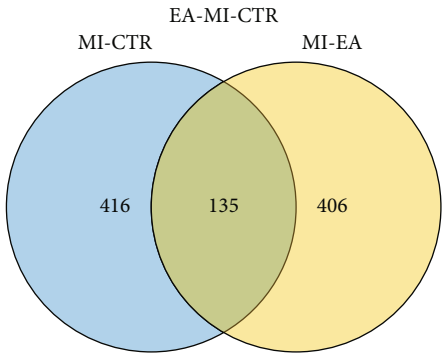

Figure 5: Venn diagram showing EA treatment targets for MI.

Table 1: Target expression in MI-CTR and EA+MI.

Gene symbol (Rattus norvegicus)	MI-CTR		EA+MI	
	log_2FC	P value	log_2FC	P value
Myd88	3.54	$P < 0.001$	-2.85	0.003
MTOR	6.26	$P < 0.001$	-6.68	$P < 0.001$
AKT1	6.06	0.003	-5.80	0.003
SP	1.79	0.016	-2.74	0.003
Irak1	1.69	0.025	-2.18	0.042

and EA-treated MI rats, consistent with the experimental results. There was no significant difference in the expression profile of other genes.

3.5. DEG Related to EA-Treated MI. The VennDiagram R package was used to reduplicate the intersection of DEG in MI-CTR and EA-treated MI [37]. The results reveal 135 DEGs, of which 119 were upregulated and 16 were downregulated in MI. In the EA-treated MI model, 16 genes were upregulated, and 119 were downregulated. There was an inverse correlation between DEG on the MI-CTR and EA-treated MI group. This indicates that EA treatment significantly reversed the expression of DEG in MI compared to the control group. Therefore, all 135 DEGs could be used as a potential target for EA treatment of MI (Figure 5). Table 1 shows the expression of the specific gene targets validated in the previous experiments in the MI-CTR and EA-treated MI groups.

3.6. GO and KEGG Pathway Enrichment Analysis of DEGs. The Database for Annotation, Visualization and Integrated Discovery (DAVID) was used for data processing and analysis, and $P < 0.05$ was used as a criterion selection of genes for enrichment analysis. Gene Ontology (GO) analysis revealed 135 DEGs and the biological processes, including positive regulation of tumor necrosis factor production, tumor necrosis factor superfamily cytokine production, cellular responses to oxidized low-density lipoprotein (LDL) particle stimulation, carboxylic acid transaminase, stimulation of LDL particles, carboxylic acid transmembrane transport, and organic acid transmembrane transport. Molecular functions include neutral amino acid transmembrane transporter activity, amino acid transmembrane transporter activity, alanine, carboxylic acid, and organic acid transmembrane transporter activity. The cellular components enriched were late endosomal membranes, lysosomal membranes, lysosomal vacuolar membranes, proton-transporting V-type ATPase complex AB, and the transcriptional regulator complex (Figures 6(a) and 6(b)). Pathway enrichment analysis was performed using the Kyoto Encyclopedia of Genes and Genomes (KEGG) database (Figure 6(c)). KEGG pathway analysis of 135 DEGs mainly enriched the NF-κB signaling pathway, collecting ductal acid secretion, steroid hormone biosynthesis, rheumatoid arthritis, PI3K/AKT signaling pathway, etc. The pathview-Bioconductor software (version 3.15) was used to show the potential signaling pathways associated with EA treatment of MI (Figure 6(d)).

3.7. SP-Core Protein Docking. Linear structure modeling was performed on the neuropeptide amino acid sequence and exported in PDB format. Three dimensional (3D) structures of the core proteins MYD88, IRAK1, NFKB1, PIK3CA, AKT1, and MTOR were downloaded from the PDB database and exported in PDB format, and SP as the core structural domain was converted using AutoDockTools 1.5.6 software. The results reveal that the binding energies of the core proteins PIK3CA, AKT1, and mTOR to SP were below -5.0 kcal/mol, and the Root Mean Square Deviation (RMSD) was <5.00 (Table 2). Combining the RMSD, chemical energy and docking model, the core protein AKT1 formed the most stable docking bond with SP. Finally, the results were exported using Vina and PyMOL, and the 3D molecular docking with protein ligands was demonstrated using Discovery Studio 2019 software (Figure 7) (Table 2).

4. Discussion

Substance P (SP) is a tachykinin located mainly in the sensory nerves and abundantly found in the cerebrum and intestinal region. It is widely distributed in the central nervous system and gastrointestinal system. It has nociceptive transmission, participates in the inflammatory response and immune regulation, and affects reproductive endocrine functions. In the heart, SP is usually located in the coronary artery [38–40]. To a lesser extent, the peripheral sensory nerves are located in coronary endothelial cells [41]. Thus, SP is a modulator of perception and released in response to changes in coronary blood flow or pressure, such as during myocardial ischemia [42]. SP is released within a minute of ischemic injury [41], and SP level remains elevated even during the reperfusion phase [10]. There is substantial evidence that SP has a cardioprotective effect in ischemic injury by mediating potent coronary dilatory effect on cardiomyocytes [8–11]. SP acts as an immunomodulator by binding to the neurokinin-1 receptor (NK-1R). NK-1R antagonism inhibits the beneficial effects of SP in restoring contractile function and coronary blood flow. In mouse isolated perfusion heart model, NK-1R blocking resulted in increased left ventricle (LV) diastolic blood pressure (DBP) and decreased systolic function. In contrast, adding exogenous SP decreased LV DBP and improved systolic function,

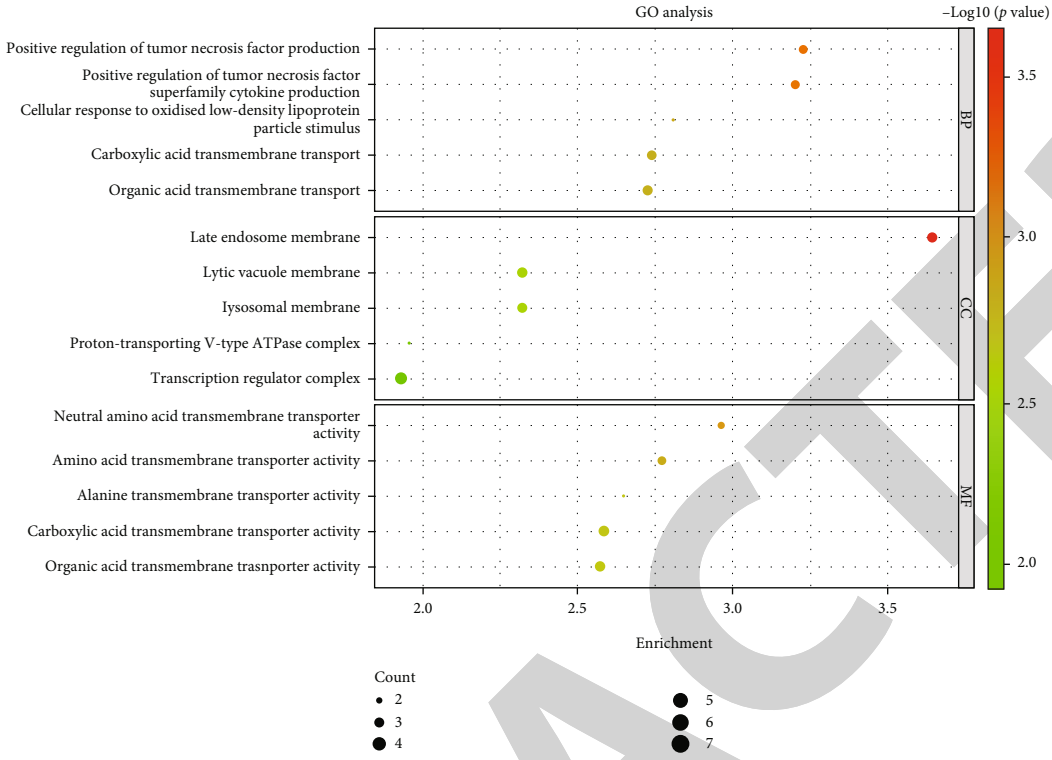

(a)

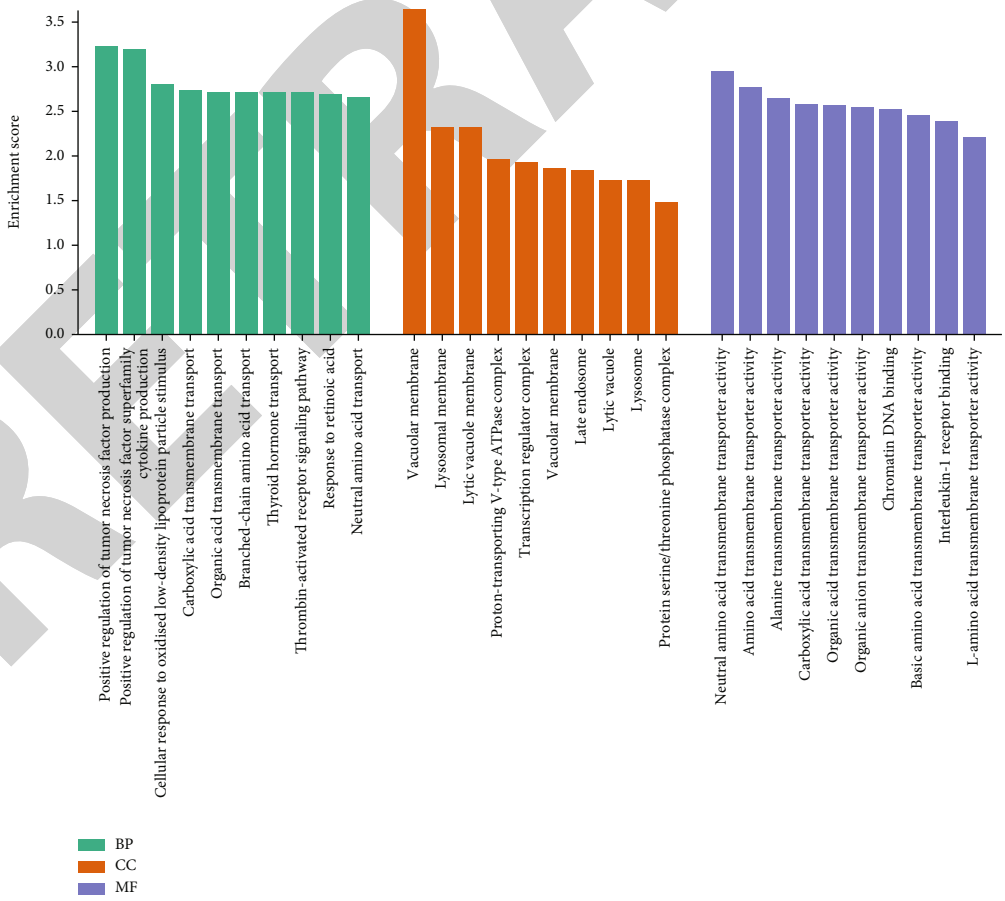

(b)

Figure 6: Continued.

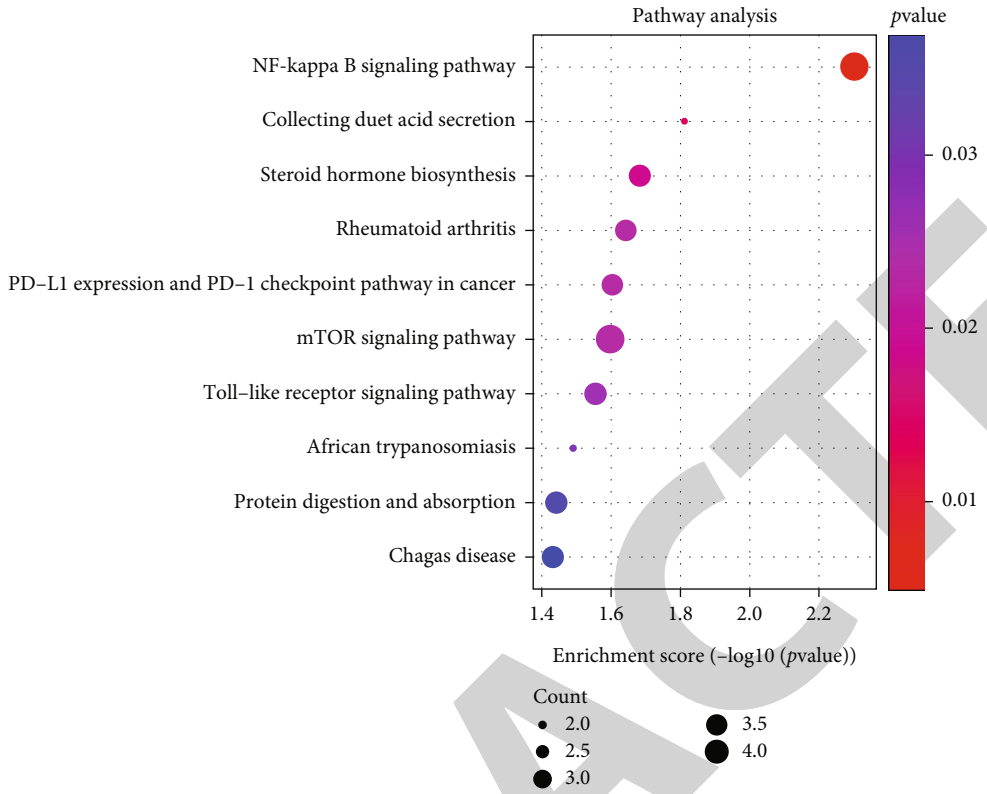

(c)

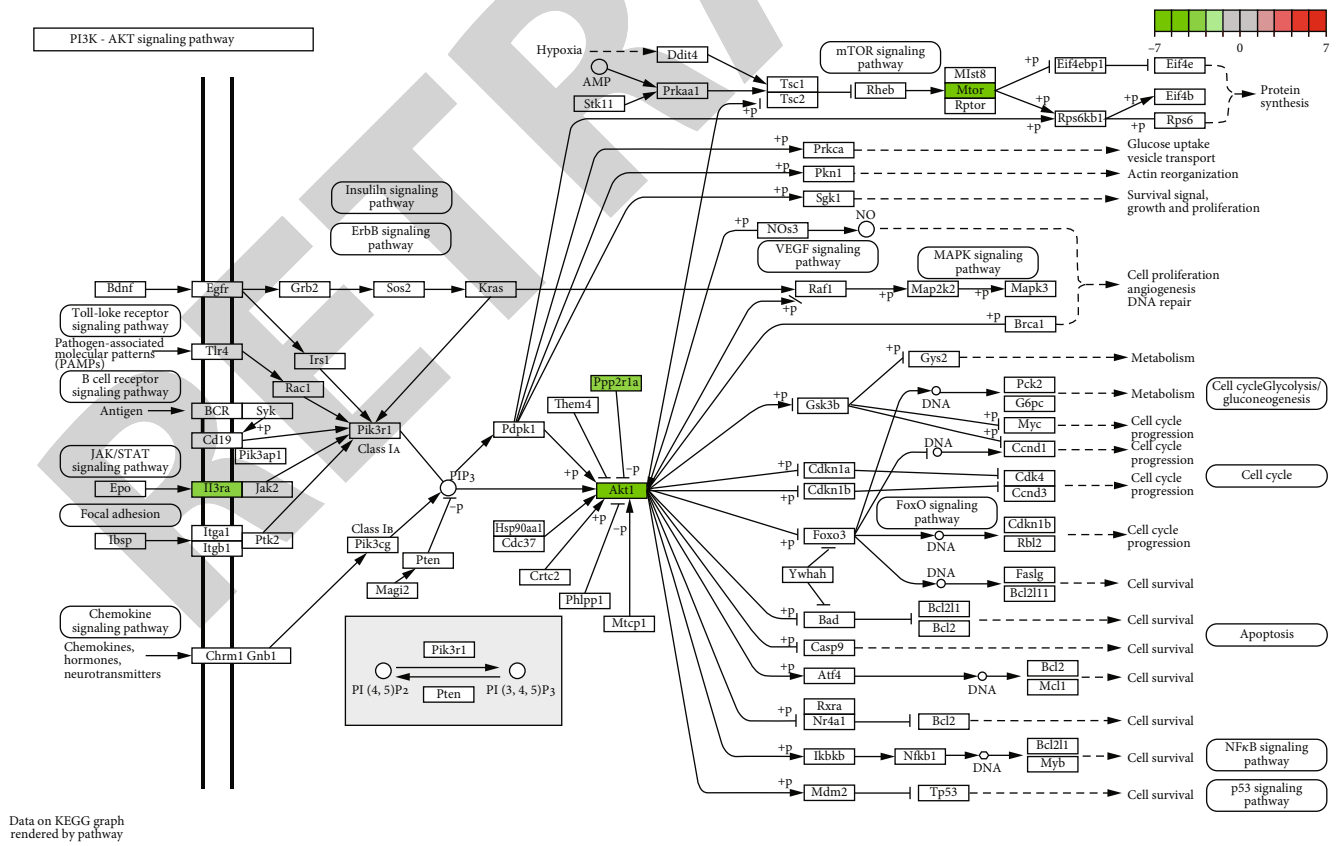

(d)

Figure 6: DEG enrichment analysis using GO and KEGG. (a) GO functional analysis bubble diagram; (b) GO functional analysis histogram; (c) KEGG functional analysis bubble diagram; (d) PI3K/AKT signaling pathway.

Table 2: Docking results for neuropeptide SP with core proteins using AutoDock Vina.

Protein	Compound	Structure	Vina (kcal·mol^{-1})	RMSD
Myd88 (5AIU)	Substance P	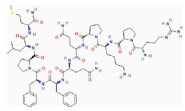	-1.5	0
Irak1 (6BFN)	Substance P	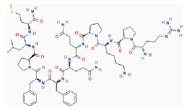	-4.4	2.372
Nfkb1 (5LW1)	Substance P	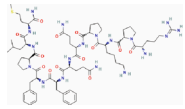	-4.5	0
Pik3ca (5SX8)	Substance P	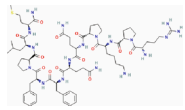	-8.4	2.029
AKT1 (4EJN)	Substance P	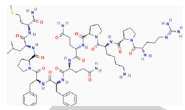	-8.5	1.315
Mtor (2L0X)	Substance P	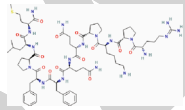	-5.4	3.0

suggesting that exogenous SP could also provide additional protective effects over endogenous SP [8, 10].

EA has a protective role in myocardial ischemic injury [23, 24]. EA reduces heart rate, ST segment, and MI area and alleviates myocardial injury in rats with AMI [25]. EA may also have a beneficial effect on ischemic heart disease such as MI by reducing lipid peroxidation; promoting energy metabolism, myocardial oxygen demand, and myocardial enzyme activity; and altering cellular ultrastructure. However, its mechanism of action is not yet clear [43–45].

Various studies have shown that the mechanism of EA treatment is closely related to SP. The SP-mediated pathway may be involved in the analgesic effect of EA in rats. Studies have shown that inhibiting the SP signaling can significantly enhance the analgesic effect of EA [46, 47]. EA may also improve gastrointestinal symptoms by reducing the SP expression in the colonic mucosa of patients with irritable bowel syndrome [48]. Additionally, in hypertension or colitis rat models, increased SP expression at acupoints leads to neurogenic inflammation, extravasation of plasma, and accumulation of subcutaneous water content. This results in high conductance and low impedance, triggering acupuncture signaling [49, 50]. Elevated SP levels also increase the therapeutic effect of EA [51, 52]. Consistent with previous studies, our results reveal that SP was differentially expressed in MI-CTR and EA-treated MI rat models, suggesting that SP may be involved in the effect of EA treatment on AMI.

Several studies have shown that EA mediates its effect via the PI3K/AKT pathway. EA significantly activates the PI3K/AKT signaling pathway in ischemic brain tissue, thereby exerting a neuroprotective effect in ischemic stroke, thus improving learning and memory function in a cerebral ischemia/reperfusion injury animal model [53, 54]. EA ameliorates denervation-induced skeletal muscle atrophy in rats via the PI3K/AKT signaling pathway [55]. In addition, EA reduces pulmonary vascular remodeling in the COPD model via the PI3K/AKT signaling pathway. In spontaneously hypertensive rats, EA reduces phenotypic transformation of vascular smooth muscle cells via the PI3K/AKT signaling pathway [56, 57]. Our results reveal that AKT and PIK3CA expression was upregulated in AMI myocardial tissues and that AKT1 was differentially expressed in MI-CTR and EA-treated MI rats. Therefore, EA may play a therapeutic role in AMI via the PI3K/AKT pathway.

PGI2/TXA2, a vasomodulator, was also involved in the EA's mechanism of action. Acute alcoholic liver injury animals showed higher levels of the vasoconstrictor TXA2 and decreased levels of the vasodilator PGI2; EA stimulation partially restored levels of PGI2/TXA2 in liver tissue [58]. EA also affects vascular function in various diseases, including vascular dementia, by reducing vascular hyporesponsiveness in a portal hypertension rat model [25, 59]. The dynamic homeostasis of PGI2/TXA2 is essential in maintaining normal vascular tone and patency, and an elevated ratio is associated with atherosclerosis [60]. Consistent with the previous studies, we report that both PGI2 and TXA2 levels were elevated in the AMI mouse model and the involvement of PGI2/TXA2 in the effect of EA treatment on AMI.

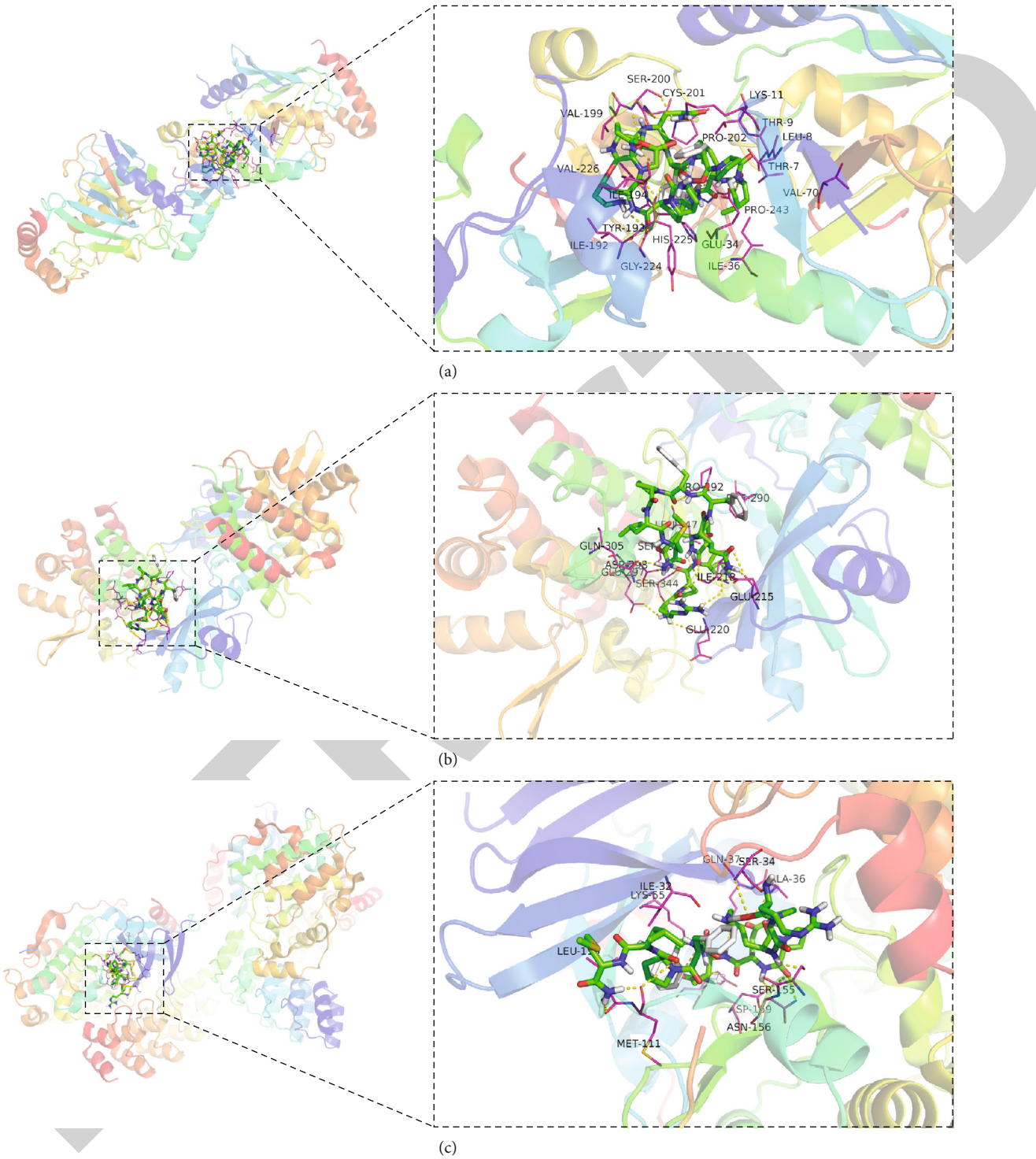

Figure 7: Continued.

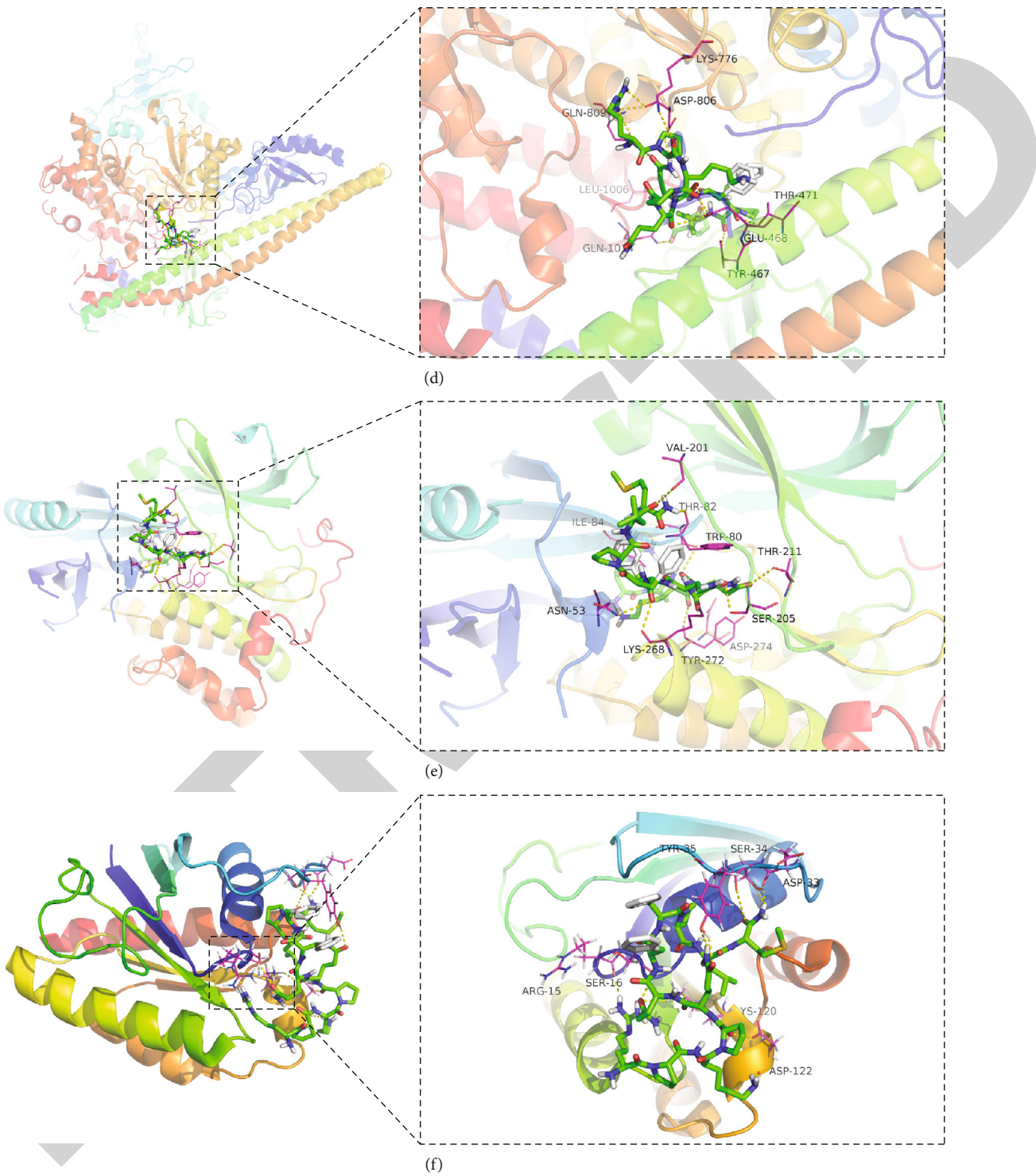

Figure 7: Molecular docking model of neuropeptide SP-core protein, Myd88-substance P-3D (a), Irak1-substance P (b), Nfkb1-substance P (c), Pik3ca-substance P-3D (d), AKT1-substance P (e), and MTOR-substance P (f).

Atherogenesis is caused by a buildup of PGI2 in the body, which inhibits TXA2, an arachidonic acid metabolite implicated in platelet aggregation [61]. TXA2 is released by cardiac muscle under hypoxia and early reoxygenation conditions [62, 63], and cardiac-derived TXA2 could be responsible for initiating the reperfusion injury in the heart [64]. Prostacyclin (PGI2) is an endogenous prostaglandin formed and released by endothelial cells with antiplatelet, vasodilatory, and cytoprotective properties [65]. PGI2 can also inhibit endothelial cell apoptosis and decomposition, which protects vascular integrity [66]. Due to vasodilatory properties, PGI2 is currently used in treating pulmonary hypertension and critical limb ischemia [67, 68]. It has been shown that patients after coronary stenting treated with low-dose prostacyclin have

improved endothelial function due to reduced levels of the soluble endothelial biomarker, sE-selectin. In this study, PGI2 and TXA2 were elevated in mice with AMI compared with normal mice. Further, in the SP-treated AMI mouse model, the levels of PGI2 were higher than in the control mice. Compared to the control group, a decrease in TXA2 levels was observed in the SP-treated AMI mouse model. Therefore, it is likely that SP may have a protective effect on AMI by altering the balance of PGI2/TXA2.

In this study, upregulation in the expression of PI3K pathway-related genes, including *Pik3ca*, *Akt*, and *Mtor*, was observed in infarcted myocardial tissue of mice by RT-PCR. Western blotting results reveal an increase in expression of AKT, p-AKT, and MTOR in AMI treated with SP. Further, human cardiomyocyte cells (HCM) treated with SP increased mRNA and protein expression of PI3K/AKT pathway-related genes (PIK3CA, PIK3CB, AKT, and MTOR). In addition, analysis of high-throughput sequencing data retrieved from the GEO database showed a differential expression of *Myd88*, *Mtor*, *Akt1*, *Sp*, and *Irak1* in MI-CTR and EA-treated MI rat models. These results were consistent with the in vivo and in vitro studies, while the remaining genes showed no significant differences. KEGG analysis of DEG in EA-treated MI tissues showed significant enrichment of the PI3K/AKT signaling pathway. Molecular docking analysis also confirmed that core proteins PIK3CA, AKT1, and MTOR formed stable docking bonds with SP with binding energies below -5.0 kcal/mol. The core protein AKT1 formed the most stable docking model with SP. Therefore, we postulate that SP promotes the expression of AKT, p-AKT, and MTOR in cardiomyocytes, thereby improving cardiomyocyte survival via NK-1R activation. Our study is based on previous reports and clinical data, validated by in vivo and in vitro studies. However, the number of clinical samples was limited and requires further in vivo validations.

5. Conclusion

EA regulates PGI2/TXA2 metabolism directly or indirectly through SP to reduce myocardial cell injury and alleviate the symptoms of AMI by affecting PI3K/AKT pathway activity. It provides an idea for clinical drug research and development.

Data Availability

This study's raw data can be downloaded from the database, and the experimental data can be obtained from the corresponding authors.

Conflicts of Interest

The authors declare no competing interests.

Authors' Contributions

PZ, YW, QW, XX, HL, XW, HZ, XW, YL, and XL proposed and designed the study. PZ, YW, QW, XX, HL, YL, and XL collected and analysed the data. PZ, YL, and XL provided the analysis tools and performed quality control. PZ, YW, QW, XX, HL, Xiaojing W, HZ, XW, YL, and XL wrote the manuscript. All authors contributed to the article and approved the submitted version.

Acknowledgments

Thanks are due to all those who worked on this study. The present study was funded by Shandong Medical and Health Technology Development Fund (202103070325), Shandong Province Traditional Chinese Medicine Science and Technology Project (M-2022216), and Nursery Project of the Affiliated Tai'an City Central Hospital of Qingdao University (2022MPM06).

References

[1] A. Ahmadi, J. Leipsic, R. Blankstein et al., "Do plaques rapidly progress prior to myocardial infarction?: the interplay between plaque vulnerability and progression," *Circulation Research*, vol. 117, no. 1, pp. 99–104, 2015.

[2] T. Su, S. Chang, P. Chen, and Y. Chan, "Temporal trends in treatment and outcomes of acute myocardial infarction in patients with chronic obstructive pulmonary disease: a nationwide population-based observational study," *JAHA*, vol. 6, no. 3, article e004525, 2017.

[3] A. Nobian, A. Mohamed, and I. Spyridopoulos, "The role of arginine vasopressin in myocardial infarction and reperfusion," *Kardiologia Polska*, vol. 77, no. 10, pp. 908–917, 2019.

[4] T. Rajtik, P. Galis, L. Bartosova, L. Paulis, E. Goncalvesova, and J. Klimas, "Alternative RAS in various hypoxic conditions: from myocardial infarction to COVID-19," *IJMS*, vol. 22, no. 23, article 12800, 2021.

[5] J. J. V. McMurray, M. A. Pfeffer, K. Swedberg, and V. J. Dzau, "Which inhibitor of the renin–angiotensin system should be used in chronic heart failure and acute myocardial infarction?," *Circulation*, vol. 110, no. 20, pp. 3281–3288, 2004.

[6] W. Feng, J. Yang, W. Song, and Y. Xue, "Crosstalk between heart failure and cognitive impairment via hsa-miR-933/RELB/CCL21 pathway," *BioMed Research International*, vol. 2021, Article ID 2291899, 16 pages, 2021.

[7] N. Herring, "Autonomic control of the heart: going beyond the classical neurotransmitters," *Experimental Physiology*, vol. 100, no. 4, pp. 354–358, 2015.

[8] J.-Y. Ren, J.-X. Song, M.-Y. Lu, and H. Chen, "Cardioprotection by ischemic postconditioning is lost in isolated perfused heart from diabetic rats: involvement of transient receptor potential vanilloid 1, calcitonin gene-related peptide and substance P," *Regulatory Peptides*, vol. 169, no. 1-3, pp. 49–57, 2011.

[9] E. E. Ustinova, D. Bergren, and H. D. Schultz, "Neuropeptide depletion impairs postischemic recovery of the isolated rat heart: role of substance P," *Cardiovascular Research*, vol. 30, no. 1, pp. 55–63, 1995.

[10] L. Wang and D. H. Wang, "TRPV1 gene knockout impairs postischemic recovery in isolated perfused heart in mice," *Circulation*, vol. 112, no. 23, pp. 3617–3623, 2005.

[11] B. Zhong and D. H. Wang, "TRPV1 gene knockout impairs preconditioning protection against myocardial injury in isolated perfused hearts in mice," *American Journal of Physiology-Heart and Circulatory Physiology*, vol. 293, no. 3, pp. H1791–H1798, 2007.

[12] M.-C. Xu, H.-M. Shi, X.-F. Gao, and H. Wang, "Salidroside attenuates myocardial ischemia–reperfusion injury via PI3K/Akt signaling pathway," *Journal of Asian Natural Products Research*, vol. 15, no. 3, pp. 244–252, 2013.

[13] B.-A. Jia, C. Y. Cheng, Y. W. Lin, T. C. Li, H. J. Liu, and C. L. Hsieh, "The 2 Hz and 15 Hz electroacupuncture induced reverse effect on autonomic function in healthy adult using a heart rate variability analysis," *Journal of Traditional and Complementary Medicine*, vol. 1, no. 1, pp. 51–56, 2011.

[14] A. W. N. Leung, L. C. W. Lam, A. K. L. Kwan et al., "Electroacupuncture for older adults with mild cognitive impairment: study protocol for a randomized controlled trial," *Trials*, vol. 16, no. 1, p. 232, 2015.

[15] Y. Jia, X. Zhang, J. Yu et al., "Acupuncture for patients with mild to moderate Alzheimer's disease: a randomized controlled trial," *BMC Complementary and Alternative Medicine*, vol. 17, no. 1, p. 556, 2017.

[16] D. Wang, L. Li, Q. Zhang et al., "Combination of electroacupuncture and constraint-induced movement therapy enhances functional recovery after ischemic stroke in rats," *Journal of Molecular Neuroscience*, vol. 71, no. 10, pp. 2116–2125, 2021.

[17] F. Zou, Y.-F. Lin, S.-G. Chen et al., "The impact of electroacupuncture at Hegu, Shousanli, and Quchi based on the theory "treating flaccid paralysis by Yangming alone" on stroke patients' EEG: a pilot study," *Evidence-based Complementary and Alternative Medicine*, vol. 2020, Article ID 8839491, 9 pages, 2020.

[18] J. Wang, X. Zheng, B. Liu et al., "Electroacupuncture alleviates mechanical allodynia of a rat model of CRPS-I and modulates gene expression profiles in dorsal root ganglia," *Frontiers in Neurology*, vol. 11, article 580997, 2020.

[19] J. Zhao, L. Wang, and Y. Li, "Electroacupuncture alleviates the inflammatory response via effects on M1 and M2 macrophages after spinal cord injury," *Acupuncture in Medicine*, vol. 35, no. 3, pp. 224–230, 2017.

[20] J. Sun, X. Wu, Y. Meng et al., "Electro-acupuncture decreases 5-HT, CGRP and increases NPY in the brain-gut axis in two rat models of diarrhea-predominant irritable bowel syndrome(D-IBS)," *BMC Complementary and Alternative Medicine*, vol. 15, no. 1, p. 340, 2015.

[21] Y. Yang, H. Yu, R. Babygirija et al., "Electro-acupuncture attenuates chronic stress responses via up-regulated central NPY and GABAA receptors in rats," *Frontiers in Neuroscience*, vol. 14, article 629003, 2021.

[22] Q. Zhang, Y. Tan, X. Wen, and F. Li, "Involvement of neuropeptide Y within paraventricular nucleus in electroacupuncture inhibiting sympathetic activities in hypertensive rats," *International Journal of Hypertension*, vol. 2022, Article ID 9990854, 11 pages, 2022.

[23] Z. Li, C. Wang, A. F. T. Mak, and D. H. K. Chow, "Effects of acupuncture on heart rate variability in normal subjects under fatigue and non-fatigue state," *European Journal of Applied Physiology*, vol. 94, no. 5-6, pp. 633–640, 2005.

[24] X. Hu, X. Yang, and H. Jiang, "Role of sympathetic nervous system in myocardial ischemia injury: beneficial or deleterious?," *International Journal of Cardiology*, vol. 157, no. 2, p. 269, 2012.

[25] C. Zhu, S. Wu, X. Wu et al., "Effect of electroacupuncture at Wushu acupoints of the cardiopulmonary meridian on the autophagy in rats with acute myocardial ischemia," *Evidence-based Complementary and Alternative Medicine*, vol. 2022, Article ID 2114517, 10 pages, 2022.

[26] S. Lee, "Systems biology - a pivotal research methodology for understanding the mechanisms of traditional medicine," *Journal of Pharmacopuncture*, vol. 18, no. 3, pp. 11–18, 2015.

[27] C. Jansen, J. D. Baker, E. Kodaira et al., "Medicine in motion: opportunities, challenges and data analytics-based solutions for traditional medicine integration into western medical practice," *Journal of Ethnopharmacology*, vol. 267, article 113477, 2021.

[28] R. Guo, X. Luo, J. Liu, L. Liu, X. Wang, and H. Lu, "Omics strategies decipher therapeutic discoveries of traditional Chinese medicine against different diseases at multiple layers molecular-level," *Pharmacological Research*, vol. 152, article 104627, 2020.

[29] A. Zhang, H. Sun, and X. Wang, "Potentiating therapeutic effects by enhancing synergism based on active constituents from traditional medicine," *Phytotherapy Research*, vol. 28, no. 4, pp. 526–533, 2014.

[30] R. Li, Q. Li, and Q. Ji, "Molecular targeted study in tumors: from western medicine to active ingredients of traditional Chinese medicine," *Biomedicine & Pharmacotherapy*, vol. 121, article 109624, 2020.

[31] X. Kang, Y. Sun, B. Yi et al., "Based on network pharmacology and molecular dynamics simulations, baicalein, an active ingredient of Yiqi Qingre Ziyin method, potentially protects patients with atrophic rhinitis from cognitive impairment," *Frontiers in Aging Neuroscience*, vol. 14, article 880794, 2022.

[32] L. Lu, X. Kang, B. Yi et al., "Exploring the mechanism of Yiqi Qingre Ziyin method in regulating neuropeptide expression for the treatment of atrophic rhinitis," *Disease Markers*, vol. 2022, Article ID 4416637, 12 pages, 2022.

[33] Q. Zhang, J. Yang, C. Yang, X. Yang, and Y. Chen, "Eucommia ulmoides Oliver-Tribulus terrestris L. drug pair regulates ferroptosis by mediating the neurovascular-related ligand-receptor interaction pathway- a potential drug pair for treatment hypertension and prevention ischemic stroke," *Frontiers in Neurology*, vol. 13, article 833922, 2022.

[34] Y. Zhang, J. Zhang, C. Sun, and F. Wu, "Identification of the occurrence and potential mechanisms of heterotopic ossification associated with 17-beta-estradiol targeting MKX by bioinformatics analysis and cellular experiments," *PeerJ*, vol. 9, article e12696, 2022.

[35] C. P. Ong, "Science in Chinese medicine," *Life Res*, vol. 4, 6 pages, 2021.

[36] K. Gao, X. Gao, and X. Xiao, "Study on the medication rule of herbs for uterine bleeding in ancient Chinese medicine," *Life Res*, vol. 4, no. 2, p. 17, 2021.

[37] H. Chen and P. C. Boutros, "VennDiagram: a package for the generation of highly-customizable Venn and Euler diagrams in R," *BMC Bioinformatics*, vol. 12, no. 1, p. 35, 2011.

[38] C.-J. Dalsgaard, A. Franco-Cereceda, A. Saria, J. M. Lundberg, E. Theodorsson-Norheim, and T. Hökfelt, "Distribution and origin of substance P and neuropeptide Y-immunoreactive nerves in the guinea-pig heart," *Cell and Tissue Research*, vol. 243, no. 3, pp. 477–485, 1986.

[39] M. Reinecke, E. Weihe, and W. G. Forssmann, "Substance P-immunoreactive nerve fibers in the heart," *Neuroscience Letters*, vol. 20, no. 3, pp. 265–269, 1980.

[40] J. Wharton, J. M. Polak, G. P. McGregor, A. E. Bishop, and S. R. Bloom, "The distribution of substance p-like immunoreactive nerves in the guinea-pig heart," *Neuroscience*, vol. 6, no. 11, pp. 2193–2204, 1981.

[41] P. Milner, V. Ralevic, A. M. Hopwood et al., "Ultrastructural localisation of substance P and choline acetyltransferase in

Hindawi
Computational and Mathematical Methods in Medicine
Volume 2023, Article ID 9834985, 1 page
https://doi.org/10.1155/2023/9834985

Retraction

Retracted: Expression of GMFB in High-Grade Cervical Intraepithelial Neoplasia and Its Role in Cervical Cancer

Computational and Mathematical Methods in Medicine

Received 12 December 2023; Accepted 12 December 2023; Published 13 December 2023

This article has been retracted by Hindawi, as publisher, following an investigation undertaken by the publisher [1]. This investigation has uncovered evidence of systematic manipulation of the publication and peer-review process. We cannot, therefore, vouch for the reliability or integrity of this article.

Please note that this notice is intended solely to alert readers that the peer-review process of this article has been compromised.

Wiley and Hindawi regret that the usual quality checks did not identify these issues before publication and have since put additional measures in place to safeguard research integrity.

We wish to credit our Research Integrity and Research Publishing teams and anonymous and named external researchers and research integrity experts for contributing to this investigation.

The corresponding author, as the representative of all authors, has been given the opportunity to register their agreement or disagreement to this retraction. We have kept a record of any response received.

References

[1] J. Tian, J. Wang, Y. Chi, Z. Han, D. Zhang, and H. Zhang, "Expression of GMFB in High-Grade Cervical Intraepithelial Neoplasia and Its Role in Cervical Cancer," *Computational and Mathematical Methods in Medicine*, vol. 2022, Article ID 7784921, 8 pages, 2022.

Hindawi
Computational and Mathematical Methods in Medicine
Volume 2022, Article ID 7784921, 8 pages
https://doi.org/10.1155/2022/7784921

Research Article

Expression of GMFB in High-Grade Cervical Intraepithelial Neoplasia and Its Role in Cervical Cancer

Jun Tian,[1] **Jianqing Wang**,[2] **Yinxiu Chi**,[1] **Zhongbao Han**,[1] **Dongliang Zhang**,[1] **and Hu Zhang**[1]

[1]*Jiangsu Vocational College of Medicine, Yancheng, Jiangsu 222005, China*
[2]*Department of Gynecology, Yancheng First People's Hospital, Yancheng, Jiangsu 222005, China*

Correspondence should be addressed to Jun Tian; yctj2008_edu@163.com

Received 8 August 2022; Revised 8 September 2022; Accepted 12 September 2022; Published 22 September 2022

Academic Editor: Min Tang

Cervical intraepithelial neoplasia (CIN) is a collective term for specific precancerous lesions associated with cervical cancer (CC). Although it has been affirmed with slow development of several levels of cellular changes, the existing poor prognosis calls for an urgent need to diagnose CIN at early stage and be aware of markers related to its pathogenesis and prognosis. We explored the expression level of a newly marker GMFB and its regulatory effect on CIN and CC. Patient samples and cell models were included. Bioinformatic studies were taken to predict its binding to miR-143-3p, miR-26b-5p, miR-191-5p, and miR-223-3p. Luciferase reporter and RNA pull-down assays were used to validate the prediction. Edu assay and flow cytometry were used to measure the regulation of GMFB on proliferation and apoptosis of CC cells. qRT-PCR was used for mRNA expression level detection. The results showed that GMFB was targeted by miR-143-3p, miR-26b-5p, miR-191-5p, and miR-223-3p. It had elevated expression in both CIN and CC samples. GMFB had highly prognostic value for CIN, and lymph node metastasis of CC was much associated with high GMFB expression level. Besides, silencing of GMFB inhibited CC cell proliferation and elevated cell apoptosis. In conclusion, we determined that GMFB has regulatory effect on high grade CIN and CC, which could lighten a novel way in exploring their pathogenesis and improving accuracy of prognosis.

1. Introduction

Cervical intraepithelial neoplasia (CIN) is a collective term for specific precancerous lesions associated with cervical invasive carcinoma [1]. CIN consists of cervical carcinoma in situ and cervical dysplasia and reflects the continuous progress of cervical cancer (CC). CC is a series of pathological changes, from cervical dysplasia (mild to medium severe) to carcinoma in situ, then early invasive carcinoma, and finally invasive carcinoma [2]. CIN is usually caused by certain types of human papillomavirus (HPV) and is subclassed into CIN 1, 2, and 3 as severity increases. It is diagnosed in view of the proportion of abnormal cells occupying the cervical epithelium [3]. CIN is classified as precancerous disease, even though only 9% of CIN 1 would develop into CIN 3 [4], and approximately 30% of CIN 3 would develop into CC [5].

CC is the most common gynecologic malignancy, with the highest incidence rate of carcinoma in situ among patients aged 30 to 35 years, and that of invasive carcinoma among patients aged 45 to 55 years. In recent years, its onset population is becoming younger [6]. Researchers have found that persistent HPV infection, approximately 10–25 years, would induce CIN to progress into CC [7, 8]. These slow cellular changes calls for an urgent need to diagnose CIN at early stage and be aware of markers related to its pathogenesis and prognosis.

In 2020, LCoR expression was found to be correlated with CIN II progression, and RIP140 expression increases significantly as CIN grade progresses, underlining their potential role in the development of precancerous lesions [9]. In 2021, it was found in CIN samples that WAPL activates estrogen receptor signaling in early tumorigenesis of CIN, serving as a direct role in its induction [10]. Glia

maturation factor-β (GMFB) is identified as the growth and differentiation factor of glia and neurons. It has been reported that GMFB induces ferroptosis in early diabetic retinopathy [11]. Besides, Sun et al. have pointed that GMFB is a novel biomarker and therapeutic target for hepatocellular carcinoma [12]. Nevertheless, there is few reports analyzing the role GMFB in high grade CIN or CC.

MicroRNAs (miRNAs) are small noncoding RNA molecules that combine with the 3′-untranslated region (UTR) of target mRNAs and modulate the expression of genes [13]. miRNAs affect the progression of several cancer types, including CC, by altering the biological activities of pro-or suppressor genes [14]. For example, miR-186-3p reduces tumorigenesis of CC by targeting IGF1 [15]. miR-411 hinders CC progression via binding to STAT3 [16]. In 2020, as miRNAs evolved into a versatile tool to distinguish genetical differences of cellular product [17, 18] and a diagnostic marker for various types of cancer, Wittenborn et al. discovered that a subpanel of six miRNAs (hsa-miR-26b-5p, hsa-miR-142-3p, hsa-miR-143-3p, hsa-miR-191-5p, hsa-miR-223-3p, and has-miR-338-3p) marked the CIN progress process and early stages of cervical squamous cell carcinoma [19]. Therefore, we set about investigation from the common target gene of these 6 miRNA markers and found that GMFB was targeted by miR-143-3p, miR-26b-5p, miR-191-5p, and miR-223-3p in common.

In summary, we proposed the hypothesis that GMFB has regulatory effect on high grade CIN and CC, which could lighten a novel way in exploring their pathogenesis and improving accuracy of prognosis.

2. Materials and Methods

2.1. Bioinformatic Studies. GMFB was found to be potentially targeted by miR-143-3p, miR-26b-5p, miR-191-5p, and miR-223-3p in common using the microRNA Target Prediction Database (miRDB, https://www.mirdb.org/), which is a dedicated database released in Dec 2018, included more than 8,500 experimental supporting articles on miRNA-target interactions. The overall survival curve with low/high GMFB TPM was referred from the Gene Expression Profiling Interactive Analysis (GEPIA, http://gepia.cancer-pku.cn/), which was developed by Professor Zhang Zemin Laboratory in 2017, Peking University. The platform includes RNA sequencing data of 8587 normal tissues and 9736 tumor tissues from The Cancer Genome Atlas (TCGA) and Genotype-Tissue Expression (GTEx) databases, mainly used for gene correlation analysis, dimensionality reduction analysis, gene expression analysis, survival analysis, similar gene prediction, etc.

2.2. Patient Samples. A total of 15 cervical mucosal samples were collected from CIN patients during cervical biopsies, with 15 control samples collected from normal volunteers. A total of 15 carcinoma samples were collected from CC patients during hysterectomies, with another 15 control samples collected from normal volunteers. All patients were enroll in Yancheng First People's Hospital from Jan. 2020 to Jan. 2021 and informed with consent, along with normal volunteers. Patients with recurrence of cervical malignancies, undergoing treatment, or vaccination against HPV were excluded. This study was approved by the Ethics Committee of Yancheng First People's Hospital.

2.3. Cell Culture. H8 (BFN607200572, BLUEFBIO, Shanghai, China) cells were cultured in DMEM high glucose medium (Gibco, USA) supplemented with 10% fetal bovine serum (FBS) and 1% penicillin/streptomycin (P/S). C33A (CL-0045, Procell, Wuhan, Hubei, China) cells were cultured in Minimum Essential Medium (Gibco, USA) supplemented with 10% FBS+1% P/S. HEK293T (CL-0005, Procell, Wuhan, Hubei, China) cells were cultured in DMEM high glucose medium (Gibco, USA) supplemented with 10% fetal bovine serum (FBS) and 1% penicillin/streptomycin (P/S). All cells were grown at 95% air and 5% CO_2 at 37°C and used 48 h later for subsequent experiments.

2.4. Cell Transfections. Short hairpin RNA (shRNA) against GMFB (sh-GMFB#1 and #2) and its negative control (sh-NC) were purchased from Fenghui Biotechnology (Changsha, Hunan, China). NC mimics, miR-143-3p mimics, miR-26b-5p mimics, miR-191-5p mimics, and miR-223-3p mimics were obtained from GenePharma Co., Ltd. (Shanghai, China). All plasmids were cotransfected into C33A cells using Lipofectamine™ 3000 transfection reagent (L3000015, Thermo Fisher, USA) according to the product's instructions. The cells were cultured at 37°C for 24 days and analyzed.

2.5. Quantitative Real-Time Polymerase Chain Reaction (qRT-PCR). Total RNA was extracted from C33A cells, cervical mucosal samples or carcinoma samples using TRIzol Reagent (15596-026, Ambion, USA). Hifair® II 1st Strand cDNA Synthesis Kit (11119ES60, Yeasen, Shanghai, China) was used for reverse transcription. SYBR Green FAST Mastermix was used for PCR process (Qiagen, Dusseldorf, Germany). The relative expression level was analyzed by the $2^{-\Delta\Delta CT}$ method. GAPDH was used to normalize the expression of corresponding gene. The primer sequences were listed below: GMFB: (F) 5′-GTCCTGTTGGATGTAAGCCT-3′, (R) 5′-TGGTTAGTTCAGCTGTCTGG-3′; GAPDH: (F) 5′-TCAAGATCATCAGCAATGCC-3′, (R) 5′-CGATACCAAAGTTGTCATGGA-3′.

2.6. RNA Pull-Down Assay. RNA pull-down assay was conducted using CIN tissues and Pierce™ Magnetic RNA-Protein Pull-Down Kit (20164, Thermo Fisher, USA). Biotin-labeled probes targeting GMFB (bio-GMFB) and the negative control-biotin (bio-NC) were mixed with streptavidin magnetic beads (80 μl), washed twice using TRIS buffer and incubated at room temperature for 25 min. The CIN tissues were lysed and mixed with pretreated magnetic beads labeled with probes overnight at 4°C. The magnetic beads were treated with 60 μl elution buffer for 45 min at 37°C to extract GMFB -associated miRNAs, followed by qRT-PCR analysis.

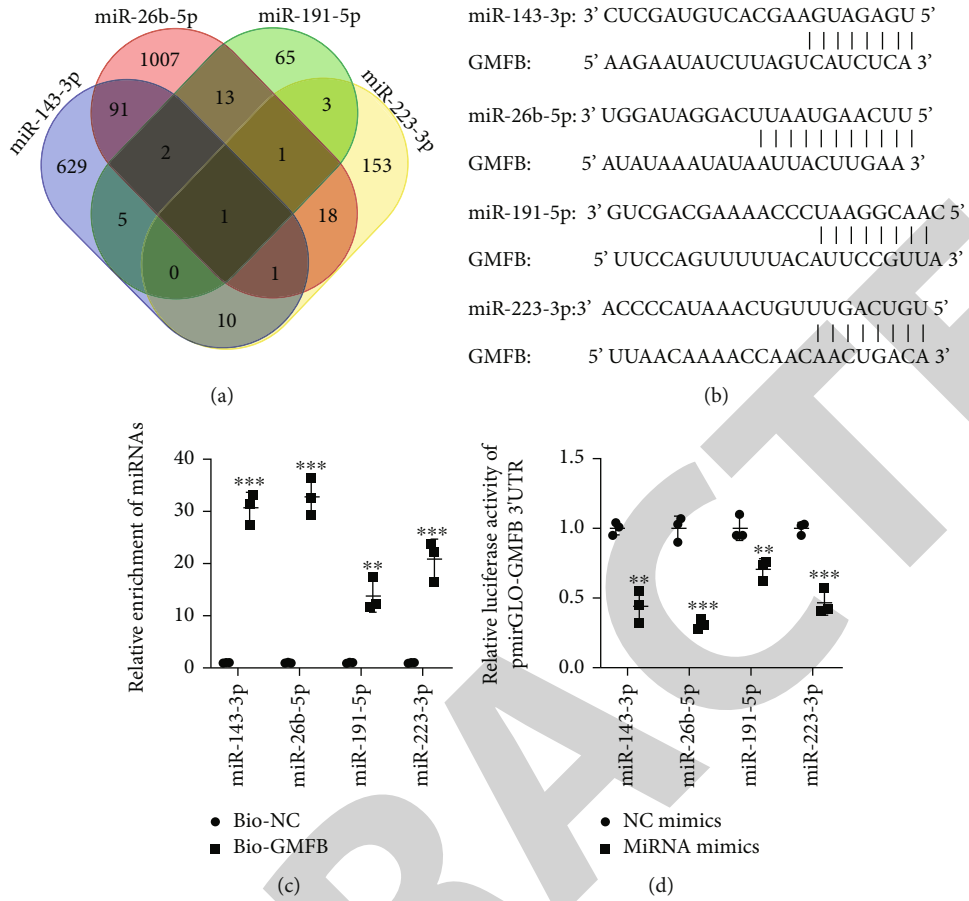

FIGURE 1: GMFB is targeted by miR-143-3p, miR-26b-5p, miR-191-5p, and miR-223-3p (a) miRNAs listed in previous paper [19] and their common target GMFB predicted by miRDB. (b) Binding sites between GMFB and corresponding miRNAs predicted by miRDB. (c) Relative enrichment of miRNAs in CIN tissue bind to bio-GMFB/NC, detected by RNA pull-down assay. (d) Relative luciferase activity of pmirGLO-GMFB 3′UTR in HEK293T cells transfected by corresponding miRNA mimics. $^{**}P < 0.01$, $^{***}P < 0.001$.

2.7. Luciferase Reporter Assay. GMFB 3′UTR was loaded in pmirGLO dual-luciferase vectors (Promega, Madison, WI, USA). HEK293T cells cotransfected with NC mimics, miR-143-3p mimics, miR-26b-5p mimics, miR-191-5p mimics, and miR-223-3p mimics together with luciferase reporter vectors were seeded in 24-well plates. Luciferase activities were determined and normalized using Dual-Luciferase Reporter Assay System (Promega).

2.8. Edu Assay. Edu assay was conducted using EdU Cell Proliferation Kit (E607204-0050, Sangon Biotech, Shanghai, China). The EdU solution was added to the cell complete medium at 1 : 500 ratio to make 2x EdU medium and added to the original cell medium to obtain 1x EdU solution (the final concentration of EdU was 10 μM). The 24-well plates were incubated with 300 μl of EdU medium per well for 2 h and the medium was discarded. The plates were washed twice using 1X PBS for 5 min each. The plates were treated with 150 μl of 4% paraformaldehyde per well at room temperature for 30 min, and then 100 μl of the configured detection mixture per well free of light at room temperature for 30 minutes. The plates were washed with 300 μl of 0.5% Triton X-100 cell permeabilization solution for 2 to 3 times for 10 min each and then added and treated with 300 μl 1x Hoechst of staining solution per well for 20 to 30 minutes at room temperature. Cells were washed twice with 300 μl PBS per well. A fluorescence microscope photograph was taken immediately after the staining.

2.9. Flow Cytometry. Cells were centrifuged at 300 g and 4°C for 5 min. Afterwards, they were washed twice with pre-cooled PBS, with a centrifugation at 300 g and 4°C for 5 min each time. Then, the cells were resuspended with 100 l 1 × binding buffer. Five μl annexin V-FITC and 10 μl PI Staining Solution were mixed with the cells. The reaction lasted for 10-15 min without light at room temperature. The mixture was treated with 400 L 1 × binding buffer and placed on ice, and the samples were detected by flow cytometry within 1 hour. The assay was conducted using annexin V-FITC/PI Apoptosis Detection Kit (A211-01, Vazyme, Nanjing, Jiangsu, China). FITC+ and PI− cells were defined as apoptotic cells.

2.10. Statistical Analysis. SPSS 20.0 statistical software was used for statistical analysis. All experiments were performed thrice independently. All the data were expressed as mean

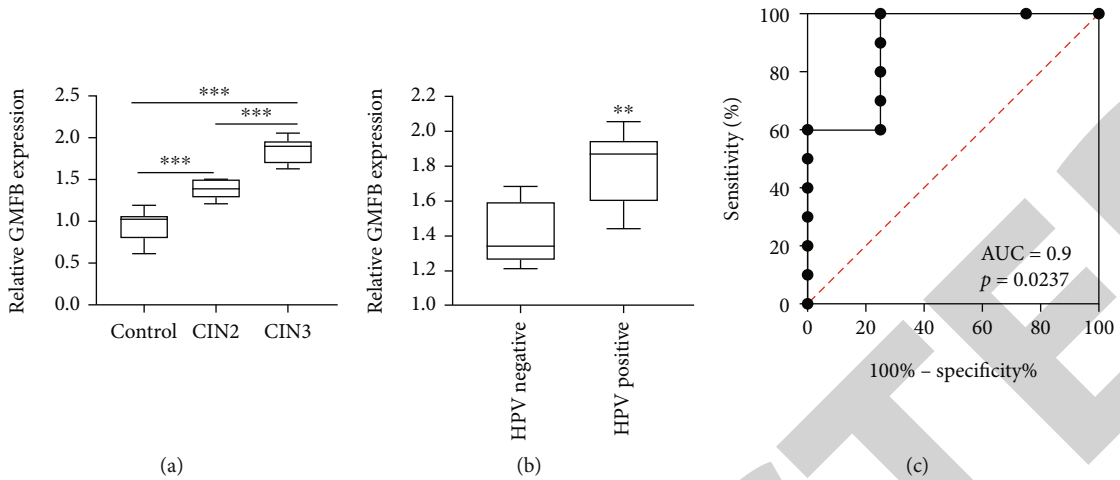

Figure 2: GMFB shows upregulation in high-grade CIN (a) Relative GMFB expression in control and high-grade CIN groups (CIN 2 and CIN 3), detected by qRT-PCR. (b) Relative GMFB expression in HPV negative and positive groups, sampled from high-grade CIN patients, detected by qRT-PCR. (c) ROC curve of GMFB expression in dead and survived patients. $^{**}P < 0.01$, $^{***}P < 0.001$.

± SD with $P < 0.05$ as a statistical significance. One-way analysis of variance (ANOVA) with Dunnett's test and student's *t*-test were used for comparison between groups. Sensitivity and specificity were calculated, with ROC curves built by mapping true-positive rate (sensitivity) against false-positive rate (1 – specificity).

3. Results

3.1. GMFB Is the Target of miR-143-3p, miR-26b-5p, miR-191-5p, and miR-223-3p. Previous paper [19] has discovered that miR-143-3p, miR-26b-5p, miR-191-5p, and miR-223-3p could serve as the biomarkers of CIN. miRDB was used to predict their common target, and it turned out that GMFB was targeted by these miRNAs in common (Figure 1(a)). Their binding sites were shown in Figure 1(b). Detected by RNA pull-down assay, bio-GMFB group had relatively higher enrichment of miR-143-3p, miR-26b-5p, miR-191-5p, and miR-223-3p in CIN tissue than bio-NC group (Figure 1(c)). Luciferase reporter assay results demonstrated that in HEK293T cells transfected with miRNA mimics, miR-143-3p, miR-26b-5p, miR-191-5p, and miR-223-3p groups, all showed relatively lower luciferase activity of pmirGLO-GMFB 3′UTR than cells transfected with NC mimics, suggesting that GMFB was directly targeted by miR-143-3p, miR-26b-5p, miR-191-5p, and miR-223-3p (Figure 1(d)). These results suggested that GMFB was the target of miR-143-3p, miR-26b-5p, miR-191-5p, and miR-223-3p.

3.2. GMFB Shows Upregulation in High-Grade CIN. Cervical mucosal samples were collected from normal volunteers and CIN patients to determine their GMFB expression levels. qRT-PCR results suggested that GMFB expression elevated significantly in CIN 2 and CIN 3 groups than in the control group, with evidently higher level in CIN 3 group than in the CIN 2 group (Figure 2(a)). Researches before have elucidated that the presence of HPV elevated the future risk of high grade CIN [20] and would even cause CC by a persistent infection [8]. Therefore, to further investigate GMFB expression in high-grade CIN, 15 patients with CIN 2-3 were divided into a positive group [10] and a negative group [5] according to HPV type, their information detailed in Table 1. Detected by qRT-PCR, HPV positive group showed significantly higher expression of GMFB than HPV negative group (Figure 2(b)). ROC curve analysis were performed using samples from 10 patients reported dead and 5 survived patients as negative control. The ROC curve was made according to the GMFB expression in corresponding samples, which showed that AUC was 0.9 ($P = 0.0237 < 0.05$), much close to 1, indicating GMFB had highly prognostic value for CIN (Figure 2(c)). These results showed that GMFB was upregulated in high-grade CIN samples, especially in HPV positive ones and could serve as the diagnostic marker for CIN prognosis.

Table 1: List of patients with CIN 2-3.

No.	CIN level	Age	HPV type
1	2	37	Negative
2	2	32	Positive
3	2	33	Positive
4	2	28	Negative
5	3	48	Negative
6	3	41	Positive
7	3	43	Positive
8	3	42	Positive
9	3	34	Positive
10	3	31	Negative
11	3	36	Negative
12	3	42	Positive
13	2	40	Positive
14	2	27	Positive
15	3	41	Positive

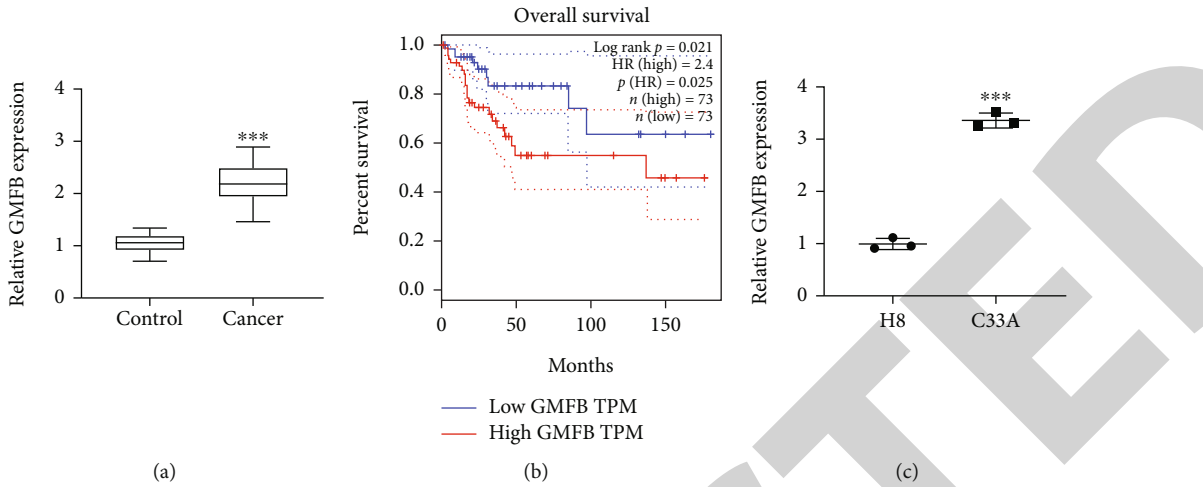

Figure 3: GMFB shows upregulation in high-grade CC (a) Relative GMFB expression in control and cervical cancer groups, detected by qRT-PCR. (b) Overall survival curves of patients with high/low GMFB expression, referred from GEPIA. (c) Relative GMFB expression in H8 and C33A cells, detected by qRT-PCR. $^{***}P < 0.001$.

3.3. GMFB Is Upregulated in CC. To measure the expression level of GMFB in CC, paracancerous tissues and CC tissues were sampled as the control group and the cancer group. qRT-PCR results suggested that GMFB was significantly upregulated in the cancer group compared to that in the control group (Figure 3(a)). Overall survival curves provided by GEPIA database revealed that CC patients with low survival rate had high expression of GMFB, indicating that GMFB was related to the poor prognosis of CC (Figure 3(b)). To further determine the association between GMFB expression and the clinicopathological features of CC patients, 15 CC patients were enrolled for analysis with their information detailed in Table 2, which turned out that lymph node metastasis was much associated with high GMFB expression level (Figure 3(c)). Lymph node metastasis has been reported to be the main metastatic pathway and the most critical factor in the prognosis and recurrence of CC [21], thus confirming and explaining the poor prognostic value of GMFB in CC diagnosis. Detected by qRT-PCR, C33A cells showed significantly higher expression level of GMFB than H8 cells, again validating our finding, and was chosen to be our experimental subject in in vitro assays. These results suggested that GMFB was upregulated in CC tissues and cells and was related to the poor prognosis of CC.

3.4. GMFB Is an Oncogene in CC. To investigate the regulatory effect of GMFB on CC, sh-GMFB was transfected into C33A cells, interference efficiency detected by qRT-PCR (Figure 4(a)). Assessed by Edu assay, C33A cells transfected with sh-GMFB showed significantly less Edu positive cells (Figure 4(b)), indicating that sh-GMFB attenuated the proliferation of C33A cells. Furthermore, flow cytometry results suggested the apoptosis rate of C33A cells transfected with sh-GMFB was significantly increased (Figure 4(c)) compared to those transfected with sh-NC, demonstrating that sh-GMFB suppressed the proliferation of C33A by promoting apoptosis. These results suggested that GMFB was an oncogene in CC that regulate cell proliferation by controlling apoptosis.

Table 2: Association of GMFB expression and the clinicopathological features of patients with cervical cancer.

Characteristics	Patient $n = 15$	GMFB expression Low $n = 7$	GMFB expression High $n = 8$	P
Age				
50	8	3	5	0.6193
≥50	7	4	3	
FIGO stage				
I	11	5	6	>0.9999
II	4	2	2	
Tumor diameter				
≤4 cm	12	6	6	>0.9999
4 cm	3	1	2	
Differentiation grade				
Middle + low	9	5	4	0.6084
High	6	2	4	
Lymph node metastasis				
Yes	7	0	7	0.0014**
No	8	7	1	
Vasoinvasion				
Yes	4	2	2	>0.9999
No	11	5	6	

**Significant P values ($P < 0.01$).

4. Discussion

CIN, serving as the precancerous lesions of CC, became the target direction for research related to CC in recent years. In 2013, Tornesello et al. mentioned that the detection of p16INK4a and Ki67 improves the identification of

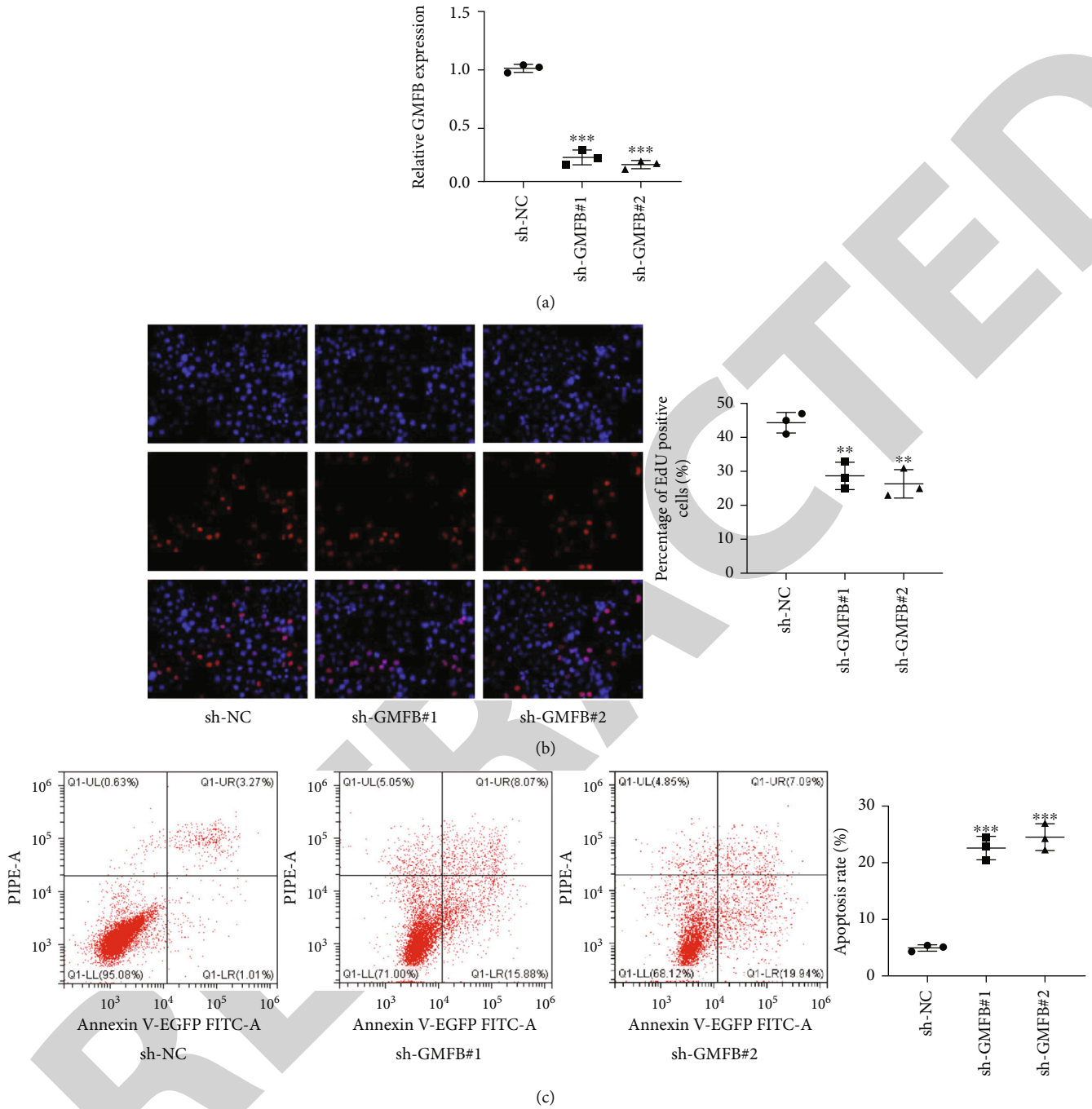

Figure 4: GMFB is an oncogene in CC. (a) Relative interference efficiency of C33A transfected with sh-GMFB. (b) Proliferation of C33A cells and percentage of Edu positive cells, assessed by Edu assay. (c) Apoptosis rate of C33A cells, assessed by flow cytometry. $^{**}P < 0.01$, $^{***}P < 0.001$.

premalignant lesions that have a high risk to evolve into invasive CC, such as CIN [22]. In 2019, Huang et al. put forward that 54.8% of the gene mutations detected in CIN specimens occurred in CC specimens as well [23]. It was measured in [24] 2017 that the immunoreactivity of both cytoplasmic and nuclear p16INK4A was absent in normal cervical tissue, while positive in CIN 1 (25%), CIN 2 (50%), CIN 3 (75%), squamous cell carcinoma (75%), and adenocarcinoma (100%) suggesting the prognostic value of p16INK4A in the management of CC. These results were consistent with our finding that there exists specific proteins which were upregulated in both CC and CIN specimens. The qRT-PCR results suggested that GMFB expression was elevated significantly in the CIN groups than in the control group, with evidently higher level in the high-grade CIN group. The HPV positive group showed significantly higher expression of GMFB than the HPV negative group. The ROC curve analysis

indicated that GMFB has highly prognostic value for CIN. CC specimen suggested that GMFB expression is elevated in CC tissues and cells and marked the poor prognosis of CC.

Glia maturation factor (GMF), first isolated from bovine brain in 1972, is a growth and differentiation factor [25], consisting of GMF-γ and GMFB. In 1989, GMFB was first purified from crude GMF [26]. Previous work has found that the expression of GMFB would elevate due to neuroinflammation and neurodegeneration, to modulate the expression of neurotrophin, granulocyte-macrophage colony-stimulating factor and superoxide dismutase [27]. In 2010, GMFB expression in serous ovarian carcinoma was found to be significantly enhanced than that in normal epithelium, benign serous adenoma, and borderline serous adenoma tissues and was associated with poor disease-free survival and overall survival [28]. In 2020, Sun et al. have proposed that GMFB expression was significantly upregulated in patients with hepatocellular carcinoma and positively coexpressed with tumor node metastases stage and histopathological grade of hepatocellular carcinoma [12]. However, the regulatory effect of GMFB in CIN and CC has few relevant reports.

It has been reported that silencing of GMFB hindered cell proliferation and migration in hepatocellular carcinoma [12]. Our results proved GMFB to share similar behavior in CIN/CC as in other carcinomas, which has not previously been reported. Especially, to investigate the regulatory effect of GMFB on CC, Edu assay and flow cytometry were performed. The results suggested that compared to the control group, the sh-GMFB group showed suppressed proliferation of C33A, suggesting that GMFB is an oncogene in CC that regulate cell proliferation by controlling apoptosis.

There are several limitations in our study. First, the in vivo experiments were not performed to verify the effect of GMFB on tumor growth and metastasis. Additionally, whether GMFB promoted CC cell proliferation via regulating signaling pathways was unclear. Therefore, further researches will be carried out to perfect our study.

In conclusion, the regulatory effect of GMFB on CIN and CC was detected in our research, with the inner mechanism explored on account of apoptosis and proliferation, which proved for the first time that GMFB could be considered as a prognostic predictor for CIN/CC patients.

Data Availability

The corresponding author is responsible to the data, and we will provide the original data if necessary.

Conflicts of Interest

The authors declare no conflicts of interest.

Acknowledgments

We appreciate all the participants in this work.

References

[1] Y. Chen, X. Qiu, W. Wang et al., "Human papillomavirus infection and cervical intraepithelial neoplasia progression are associated with increased vaginal microbiome diversity in a Chinese cohort," *BMC infectious diseases*, vol. 20, no. 1, p. 629, 2020.

[2] J. Zhang, K. Cheng, and Z. Wang, "Prevalence and distribution of human papillomavirus genotypes in cervical intraepithelial neoplasia in China: a meta-analysis," *Archives of Gynecology and Obstetrics*, vol. 302, no. 6, pp. 1329–1337, 2020.

[3] I. T. Øvestad, B. Engesæter, M. K. Halle et al., "High-grade cervical intraepithelial neoplasia (CIN) associates with increased proliferation and attenuated immune signaling," *International Journal of Molecular Sciences*, vol. 23, no. 1, p. 373, 2022.

[4] A. G. Ostör, "Natural history of cervical intraepithelial Neoplasia," *International Journal of Gynecological Pathology*, vol. 12, no. 2, pp. 186–192, 1993.

[5] M. R. McCredie, K. J. Sharples, C. Paul et al., "Natural history of cervical neoplasia and risk of invasive cancer in women with cervical intraepithelial neoplasia 3: a retrospective cohort study," *The Lancet Oncology*, vol. 9, no. 5, pp. 425–434, 2008.

[6] A. Buskwofie, G. David-West, and C. A. Clare, "A review of cervical cancer: incidence and disparities," *Journal of the National Medical Association*, vol. 112, no. 2, pp. 229–232, 2020.

[7] A. B. Moscicki, M. Schiffman, A. Burchell et al., "Updating the natural history of human papillomavirus and anogenital cancers," *Vaccine*, vol. 30, pp. F24–F33, 2012.

[8] M. Schiffman, P. E. Castle, J. Jeronimo, A. C. Rodriguez, and S. Wacholder, "Human papillomavirus and cervical cancer," *Lancet*, vol. 370, no. 9590, pp. 890–907, 2007.

[9] T. L. R. Vogelsang, E. Schmoeckel, C. Kuhn et al., "Regulation of LCoR and RIP140 expression in cervical intraepithelial neoplasia and correlation with CIN progression and dedifferentiation," *Journal of Cancer Research and Clinical Oncology*, vol. 146, no. 7, pp. 1847–1855, 2020.

[10] K. Kumagai, M. Takanashi, S. I. Ohno et al., "WAPL induces cervical intraepithelial neoplasia modulated with estrogen signaling without HPV E6/E7," *Oncogene*, vol. 40, no. 21, pp. 3695–3706, 2021.

[11] C. Liu, W. Sun, T. Zhu et al., "Glia maturation factor-β induces ferroptosis by impairing chaperone-mediated autophagic degradation of ACSL4 in early diabetic retinopathy," *Redox Biology*, vol. 52, p. 102292, 2022.

[12] W. Sun, C. Hu, T. Wang et al., "Glia maturation factor beta as a novel biomarker and therapeutic target for hepatocellular carcinoma," *Frontiers in Oncology*, vol. 11, 2021.

[13] T. X. Lu and M. E. Rothenberg, "MicroRNA," *Journal of allergy and clinical immunology*, vol. 141, no. 4, pp. 1202–1207, 2018.

[14] Y. Wang, A. Chen, C. Zheng, and L. Zhao, "miR-92a promotes cervical cancer cell proliferation, invasion, and migration by directly targeting PIK3R1," *Journal of clinical laboratory analysis*, vol. 35, no. 8, p. e23893, 2021.

[15] X. Lu, X. Song, X. Hao et al., "miR-186-3p attenuates tumorigenesis of cervical cancer by targeting IGF1," *World Journal of Surgical Oncology*, vol. 19, no. 1, p. 207, 2021.

[16] D. Shan, Y. Shang, and T. Hu, "MicroRNA-411 inhibits cervical cancer progression by directly targeting STAT3," *Oncology research*, vol. 27, no. 3, pp. 349–358, 2019.

Hindawi
Computational and Mathematical Methods in Medicine
Volume 2023, Article ID 9852615, 1 page
https://doi.org/10.1155/2023/9852615

Retraction

Retracted: Acupuncture Enhances Gastrointestinal Motility and Improves Autonomic Nervous Function in Patients with Septic Gastrointestinal Dysfunction

Computational and Mathematical Methods in Medicine

Received 5 December 2023; Accepted 5 December 2023; Published 6 December 2023

This article has been retracted by Hindawi, as publisher, following an investigation undertaken by the publisher [1]. This investigation has uncovered evidence of systematic manipulation of the publication and peer-review process. We cannot, therefore, vouch for the reliability or integrity of this article.

Please note that this notice is intended solely to alert readers that the peer-review process of this article has been compromised.

Wiley and Hindawi regret that the usual quality checks did not identify these issues before publication and have since put additional measures in place to safeguard research integrity.

We wish to credit our Research Integrity and Research Publishing teams and anonymous and named external researchers and research integrity experts for contributing to this investigation.

The corresponding author, as the representative of all authors, has been given the opportunity to register their agreement or disagreement to this retraction. We have kept a record of any response received.

References

[1] L. Ban, Y. Pu, H. Huang, B. You, W. Chen, and Y. Wang, "Acupuncture Enhances Gastrointestinal Motility and Improves Autonomic Nervous Function in Patients with Septic Gastrointestinal Dysfunction," *Computational and Mathematical Methods in Medicine*, vol. 2022, Article ID 1653290, 8 pages, 2022.

Hindawi
Computational and Mathematical Methods in Medicine
Volume 2022, Article ID 1653290, 8 pages
https://doi.org/10.1155/2022/1653290

Research Article

Acupuncture Enhances Gastrointestinal Motility and Improves Autonomic Nervous Function in Patients with Septic Gastrointestinal Dysfunction

Lihong Ban,[1] **Yongpeng Pu**,[1] **Huanyuan Huang**,[2] **Bin You**,[3] **Wei Chen**,[1] **and Yanzhen Wang**[1]

[1]*Department of Critical Medicine, The First People's Hospital of Lanzhou City, Lanzhou, Gansu 730050, China*
[2]*Department of Clinical Laboratory, The First People's Hospital of Lanzhou City, Lanzhou, Gansu 730050, China*
[3]*Department of Rehabilitation Medicine, The First People's Hospital of Lanzhou City, Lanzhou, Gansu 730050, China*

Correspondence should be addressed to Yanzhen Wang; wyshno1@163.com

Received 11 August 2022; Revised 26 August 2022; Accepted 29 August 2022; Published 21 September 2022

Academic Editor: Min Tang

Gastrointestinal dysfunction (GD) is a common complication after endotoxemia, which can further aggravate the progress of infection. Acupuncture uses metal needles of different shapes and techniques to stimulate specific points on the human body, which are effective in treating various diseases, including gastrointestinal diseases. We aimed at exploring the clinical effect of acupuncture on the recovery of visceral sensation, proximal gastric compliance, and autonomic nervous function in patients with septic GD. A total of 73 sepsis with GD patients were selected using modified single section ultrasonography combined with clinical symptoms in the First People's Hospital of Lanzhou City during 2019. The participants were randomly allocated to routine-treatment (control group) and study group receiving acupuncture. The indexes before and after treatment included gastric residue, gastric dilatation, pressure and volume, gastric compliance, autonomic nerve function, APACHE II score, and infection index were measured and compared. Before treatment, there was no significant difference in the basic information of the two groups, including gastric volume and pressure, gastric residue, gastric compliance, autonomic nerve function, and APACHE II score. After treatment, the maximum gastric volume and pressure, gastric residue, and APACHE II score of the two groups were significantly improved ($P < 0.05$). In addition, the maximum gastric volume and pressure of the study group were significantly higher, while gastric residual, autonomic nerve function, and APACHE II were significantly lower than those of the control group ($P < 0.05$). However, our results showed that acupuncture did not further reduce inflammatory markers, including white blood cells, C-reactive protein, and procalcitonin. To sum up, on the basis of basic treatment, the application of acupuncture can further improve the clinical symptoms of GD in patients with sepsis, enhance gastrointestinal motility, and improve autonomic nervous function, which is worthy of clinical application and promotion.

1. Introduction

Sepsis causes homeostasis imbalance and leads to multiple organ dysfunction, which determines its high risk and refractory [1, 2]. Gastrointestinal tract is the main target organ and "stress response center" of sepsis. Gastrointestinal dysfunction (GD) is the most common and important prognostic factor in multiple organ dysfunction syndrome (MODS) [3]. Similarly, GD is also the "starting organ", which can expand the inflammatory response and affect the prognosis of sepsis [4]. GD induced by sepsis is a clinical manifestation that involves impaired gastrointestinal function after the systemic inflammatory response caused by infection, and is one of the essential causes of exacerbation and death in critically ill patients [5]. In addition, gastrointestinal dysfunction in sepsis accounts for a large proportion of MODS, with a high morbidity and mortality rate, and an extremely poor prognosis [6]. Therefore, actively improving

the gastrointestinal function of patients is of great significance to improve the success rate of sepsis treatment.

For GD, the current western medicine treatment mode is mainly based on its etiology and clinical symptoms, such as antidiarrheal, analgesic, laxative, and promoting gastric motility [5]. However, there are still some patients with GD eventually leading to further deterioration of infection [7]. In recent years, traditional Chinese medicine treatment has been proved to have significant improvement effect in the study of gastrointestinal function in patients with sepsis [6, 8]. Therefore, to explore the characteristic therapy of traditional Chinese medicine and to use the advantages of traditional Chinese medicine to treat this disease has broad prospects and important significance.

Currently, a large number of studies have found that acupuncture plays an important role in gastrointestinal motility [7, 9]. Acupuncture, as the most commonly used technique in traditional Chinese medicine, mainly uses metal needles of different shapes and different techniques to stimulate certain acupoints on the human body. Through the channels and acupoints, adjust the human body viscera qi to achieve the purpose of treatment [10]. It has been reported that acupuncture can promote the recovery of gastrointestinal function in patients with GD after abdominal surgery on the basis of conventional western medicine treatment [11]. Also, acupuncture can reduce the systemic inflammatory response of patients with sepsis, promote the recovery of body functions, and improve clinical symptoms and prognosis. Acupuncture has a significant improvement effect on GD induced by sepsis, which mainly focuses on 2 aspects: inhibition of inflammation and immune promotion.

Based on previous studies, our aim is to confirm therapeutic effect of acupuncture in patients with septic GD. The indexes included gastric residue, gastric dilatation, pressure and volume, gastric compliance, autonomic nerve function, acute physiology, and chronic health evaluation II (APACHE II) score and infection index were detected before and after treatment. This study will provide further evidence as to whether acupuncture should be included in enhanced recovery for patients with septic GD.

2. Methods

2.1. Study Design. This study is a prospective, observational, and randomized control trial. It was conducted in 2019 and approved by the Ethics Committee of the First People's Hospital of Lanzhou City (approval number: G2019-7). All procedures were performed in accordance with the relevant guidelines and regulations. Informed consent forms have been obtained from all representatives of the patients.

2.2. Patients. A total of 73 patients with septic GD were selected from the First People's Hospital of Lanzhou City and randomly divided into control group ($n = 36$) and study group ($n = 37$) [12]. Inclusion criteria: (1) conform to the diagnosis criteria of sepsis as proposed in the Third International Consensus Definitions for Sepsis and Septic Shock (Sepsis-3) [13]]; (2) conform to the diagnostic criteria of GD grade II-III; (3) patients and their families received acupuncture treatment. Exclusion criteria: (1) did not meet the diagnostic criteria of sepsis and GD grade II-III; (2) mental disorders, pregnant women, or lactating women; (3) ICU stay < 3 days; (4) ≤18 years of age; (5) esophagus, stomach, or intestinal medical and surgical histories or primary injury to the gastrointestinal tract; (6) patients and their families were unwilling to receive acupuncture treatment. There were 18 males and 18 females in the control group, with an average age of 70.32 ± 8.58 years old. In the study group, there were 19 males and 18 females, with an average age of 70.22 ± 9.14 years old. There was no significant difference in gender or age between the two groups.

2.3. Determination of White Blood Cells (WBC), C-Reactive Protein (CRP), and Procalcitonin (PCT) Levels. After 8 h of fasting, 5 ml of fasting peripheral venous blood was collected from the patient, and the samples were immediately tested on the machine for CRP and PCT. The WBC count was performed using a Glitter GRT-6001 hematology analyzer. CRP level was evaluated using Myriad BC5390 fully automated hematology analyzer for latex-enhanced immunoturbidimetric assay. PCT assay was conducted using Radiometer AQT90 rapid immunoassay and time-resolved fluorescence immunoassay.

2.4. Ultrasonic. The modified single section method of gastric antrum was used for obtaining the contraction area of gastric antrum of patients before and after treatment of acupuncture. The superior mesenteric vein, the abdominal aorta, and the left lobe of the liver were used as sinusoidal landmarks, and the sinusoids were probed at the mid-upper abdominal body surface landmark points to determine the size of the sinusoidal area during fasting. The gastric cavity was filled with warm water orally in healthy subjects and via gastric tube in critically ill patients. The maximum diastolic area of the gastric sinus was measured immediately after filling, and then repeated every 5 minutes until the liquid dark area in the stomach disappeared, which was the gastric emptying time (GET).

2.5. Treatments. On the basis of anti-infection and organ function support treatment, the control group was treated with gastrointestinal motility drugs. Referring to the International Guidelines for the Treatment of Sepsis and Infectious Shock (2016), the treatment for the control group included: (1) organ support treatment by ventilator, hemofiltration, and vasoactive drugs to maintain basic vital signs; (2) symptomatic treatment such as fluid resuscitation and anti-infection; (3) protection of the gastrointestinal barrier mucosa when GD occurred; (4) regulation of microecology, improvement of intestinal microcirculation, and reduction of gastrointestinal mucosal permeability; and (5) symptomatic support treatment such as strengthening enteral nutrition and promoting gastrointestinal motility.

In contrast, on the basis of anti-infection and organ function support treatment, the study group was given an acupuncture treatment. Acupuncture will be performed by a licensed acupuncturist who holds a China Acupuncturist Certification, with at least 2 years of clinical experience in

acupuncture. Acupuncture points included Shangwan, Zhongwan, Xiawan, bilateral Tianshu, Guanyuan, Qihai, bilateral Zusanli, and bilateral Gongsun. Both groups were observed for 1 week. The needle used is 'Hua Tuo brand' disposable sterile needles, with diameter 0.30 mm and length 40 mm, the manufacturer is Suzhou Medical Supplies Factory Co. The site of insertions will be swabbed and disinfected with 75% alcohol before needle insertion.

Shangwan is located in the Ren channel. It is the meeting point with the foot yangming stomach meridian and the hand sun small intestine meridian and has the function of strengthening the spleen and stomach, and of clearing and distributing turbidity. Positioned on the anterior median line, 5 inches above the umbilicus; the operation is to pierce 1 inch directly and retain the needle for 30 minutes.

Zhongwan is located in the Ren channel, and is a point of the foot yangming stomach, and a point of the eight Hui points of the internal organs, with the effect of tonifying the middle and benefiting the qi, raising the clear, and lowering the turbid denial. Positioned on the front median line, 4 inches above the umbilicus, or at the midpoint of the joint line between the umbilicus and the thoracic sword; the operation is to pierce 1 inch directly and keep the needle for 30 minutes.

Xiawan is located in the Ren vessel, it is a meeting point with the foot taiyin spleen meridian and has the function of transporting and raising the clear. It is positioned on the front median. It is located on the anterior midline, 2 inches above the umbilicus; the operation is to pierce 1 inch directly and keep the needle for 30 minutes.

Bilateral tianshu isocated in the foot yangming stomach meridian, it is a point of the large intestine, with the effect of clearing turbidity from the internal organs. Positioned at 2 inches next to the middle of the umbilicus; the operation is to pierce 1 inch directly and retain the needle for 30 minutes.

Bilateral zusanli is a joint point of the foot yangming stomach meridian and is the lower joint point of the foot yangming stomach, which can be tonified if the spleen and stomach are deficient. It is positioned at the calvaria point (flexed knee, in the lateral recess of the patellar ligament. It is located 3 inches below the calvaria point (in the lateral recess of the patellar ligament), 1 finger outside the anterior tibial crest; the operation is to pierce 1 inch directly and retain the needle for 30 minutes.

Guan Yuan is on the midline of the abdomen, three inches below the umbilicus, and the midpoint from the Guanyuan to the navel is the Qihai; the operation is to pierce 1 inch directly and retain the needle for 30 minutes.

Bilateral Gongsun is located on the medial edge of the foot, just below the base of the first metatarsal; the operation is to pierce 1 inch directly and retain the needle for 30 minutes.

2.6. Adverse Events. If some adverse events including severe convulsions pain were caused by acupuncture intervention, aggravating symptoms, or other critical diseases occur during treatment and cannot be continued, the researchers found serious safety problems, as well as patients cannot stick to treatment for a variety of reasons, the patients will be dropped out of the study.

2.7. Observed Indexes

(1) The indexes, including the initial and maximal pressure and volume, symptom scores under different gastric dilatation volumes and gastric compliance were obtained with the Synectice Visceral Stimulator (SVS)/Barostat before and 1 week after the treatment. Bamstat can maintain the set pressure or volume level through electronic feedback mechanism, and measure the corresponding changes of gas volume or pressure in the airbag. SVS/Barostat was used for isovolumic mechanical gastric distention; 50 ml volume was increased every 2 minutes from 0. The symptom scores of abdominal distension, epigastric pain, nausea, and vomiting were recorded when the volume was 200 ml, 300 ml, and 400 ml, respectively. Each symptom was divided into 0-3 points (0 = no symptom, 1 = mild symptom, need attention to feel the symptom exists, 2 = moderate symptom, can feel the symptom exists, but can tolerate, 3 = severe symptom, unbearable). At the same time, the initial volume (the volume at which the subject began to feel discomfort or fullness in the upper abdomen when receiving the stimulation of gastric distention) and the maximal volume (the volume at which the subject began to feel pain or unbearable in the upper abdomen when receiving the stimulation of gastric distention) were recorded, as well as the corresponding initial pressure and maximal pressure. Besides, automatically generated gastric compliance was also recorded

(2) Autonomic nervous function was evaluated as followed. In brief, 15 minutes electrocardiograph (ECG) was recorded as baseline ECG. Then, isovolumic mechanical gastric dilatation was performed by barostat, and when the volume of gas injected into the balloon reached the maximum tolerated volume, 15 minutes ECG was recorded in the study group and the control group. After then, in the study group, acupuncture was performed for 20 minutes, and ECG was recorded 15 minutes after acupuncture. While in the control group, acupuncture was not performed, and the ECG was recorded for 15 minutes. Heart rate variability analysis indexes, including low frequency (LF: 0.04-0.15 Hz), high frequency (HF: 0.15-0.40 Hz), and very low frequency (VLF: below 0.03 Hz) were calculated at baseline in the maximal tolerance state and after acupuncture, respectively

(3) APACHE II score was calculated with the worst physiologic parameters during the first 24 hours before and after treatment to measure the clinical severity of each patient's objective physical condition upon presentation [14]

2.8. Statistical Methods. SPSS 22.0 was used for statistical analysis. The measurement data were expressed by (mean ± standard deviation) and compared with analysis of variance. $P < 0.05$ meant the difference was significant.

3. Results

3.1. Application of Ultrasonic Modified Single Section of Gastric Antrum in the Diagnosis of Patients with Septic GD. The modified single section method of gastric antrum can be used for the diagnosis of patients with septic GD by obtaining the contraction area of gastric antrum. As shown in Figure 1(a), before acupuncture, result of ultrasonography indicates the increased contraction area of the gastric antrum. After acupuncture for two days, the contraction area of the gastric antrum was decreased compared with that before acupuncture treatment (Figure 1(b)). After acupuncture for five days, the contraction area of the gastric antrum was further decreased and was basically restored to a normal condition (Figure 1(C)).

Before treatment (−1 and 0 days), both groups had significant delayed gastric emptying (defined as gastric residual volume (GRV)s ≥ 500 ml, lasting for ≥ 2 days). Compared with the results of GRVs on the day of treatment, GRVs of the two groups were significantly decreased after treatment ($P < 0.001$). In addition, compared with the control group, GRVs in the study group reduced more significantly after treatment ($P < 0.01$ and $P < 0.001$), as shown in Figure 2.

3.2. Comparison of the Initial and Maximal Pressure and Volume between the Two Groups. Before treatment, there was no significant difference in initial pressure and initial volume between the study group and the control group. After treatment, the initial pressure and initial volume of the two groups both increased, and the study group increased more ($P < 0.05$). Besides, before treatment, there was no significant difference in maximal pressure and maximal volume between the study group and the control group. After treatment, the maximal pressure and maximal volume of the two groups both increased, and the study group increased more ($P < 0.05$), as shown in Table 1.

3.3. Comparison of Symptom Scores under Different Gastric Dilatation Volumes between the Two Groups. Before treatment, when the expansion volume was 200 ml, 300 ml, and 400 ml, there was no significant difference in symptom scores (including epigastric pain, fullness, and nausea or vomiting) between the two groups. However, after treatment, when the expansion volume was 200 ml, 300 ml, and 400 ml, the symptom scores of the two groups all decreased, and the decrease of the study group was more obvious ($P < 0.05$), as shown in Table 2.

3.4. Comparison of Gastric Compliance between the Two Groups. Before treatment, there was no significant difference in gastric compliance between the study group and the control group ($P > 0.05$). After treatment, the gastric compliance of the two groups both improved, and the improvement of the study group was more obvious ($P = 0.0033$ and $P < 0.0001$), as shown in Table 3.

3.5. Effect of Acupuncture on Autonomic Nervous Function in Patients with Septic GD. Compared with baseline state, the HF in the maximal tolerance state showed a downward trend ($P < 0.05$), which indicated that expansion could reduce the HF, that was, the tension of vagus nerve; while the LF and VLF in the maximal tolerance state showed an upward trend ($P < 0.05$), which indicated that expansion could increase the LF and VLF, that was, the tension of sympathetic nerve. However, acupuncture could adjust the downward trend of HF and the upward trend of LF and VLF caused by gastric distention, that was, acupuncture could adjust the downward trend of vagus nerve tension and the upward trend of sympathetic nerve tension caused by gastric distention, so as to improve vagus nerve tension and reduce sympathetic nerve tension, as shown in Table 4.

3.6. Comparison of APACHE II Score, Abdominal Circumference and Intraperitoneal Pressure between the Two Groups. After treatment, APACHE II score and intraperitoneal pressure were lower in both groups than before treatment, and the improvements of the study group were more obvious than those of the control group ($P < 0.05$). However, there was no significant difference in abdominal circumference between the two groups before and after treatment, as shown in Table 5.

Comparison of infection indexes between the two groups. After treatment, WBC, CRP, and PCT in both groups were significantly decreased ($P < 0.05$), but acupuncture could not further reduce these inflammatory indexes, as shown in Table 6.

4. Discussion

GD is one of the main manifestations of multiple organ dysfunction syndrome (MODS) caused by sepsis [15, 16]. Its clinical manifestations are abdominal distension, vomiting, and diarrhea caused by more gastric residues, as well as intestinal dyskinesia, stress ulcer, and gastrointestinal bleeding [17]. When these symptoms appear at the same time, the mortality of patients can be significantly increased [3]. GD caused by sepsis is mainly mediated by inflammation, which can destroy the integrity of intestinal epithelium and the ability of immune response, leading to GD [18]. In addition, the inflammatory reaction can also increase the intestinal permeability, leading to bacteria passing through the intestinal wall, promoting the further development of sepsis, forming a vicious circle [19].

Weakness of spleen and stomach is the pathogenesis of GD in sepsis, often accompanied by fatigue, anorexia, pale complexion, palpitations, chest tightness, shortness of breath, excessive sweating, and other symptoms [20]. These phenomena of spleen and stomach weakness can be fundamentally improved by tonifying the spleen and stomach, supporting healthy qi, strengthening the main body, and fighting the enemy "syndrome differentiation and treatment, overall regulation" is an important principle of TCM treatment of diseases [21, 22]. In this study, we selected patients with GD in the late stage of sepsis, most of them were weak in spleen and stomach, sepsis patients were in a high metabolic state, and metabolic pathways were abnormal. If at this time the spleen and stomach function is damaged, the blood biochemical source is deficient, the patient's nutritional status is low, the healthy qi is deficient,

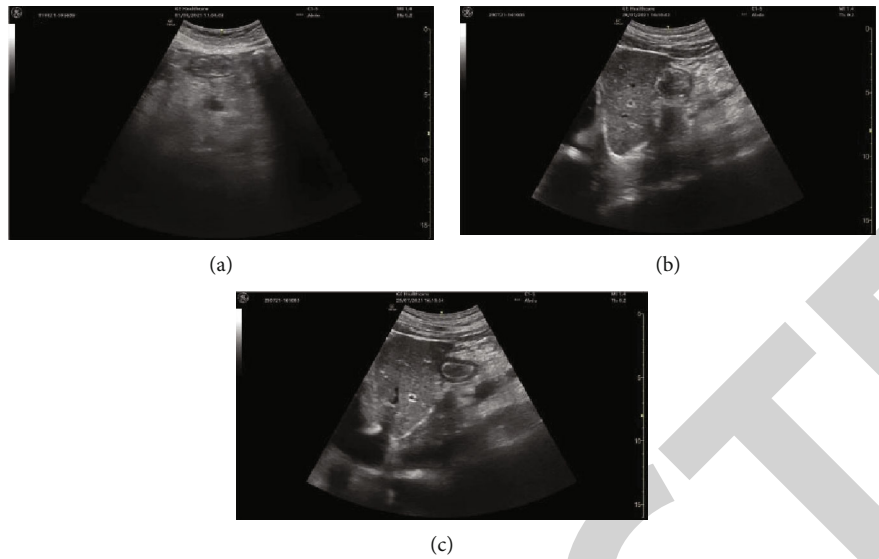

Figure 1: Ultrasonogram of GD at different time points. (a) Before acupuncture, result of ultrasonography indicates the increased contraction area of the gastric antrum. (b) After acupuncture for two days, result of ultrasonography indicates the decreased contraction area of the gastric antrum compared with that before acupuncture treatment. (c) After acupuncture for five days, result of ultrasonography indicates that the contraction area of the gastric antrum was decreased compared with that before acupuncture treatment and was basically restored to a normal condition.

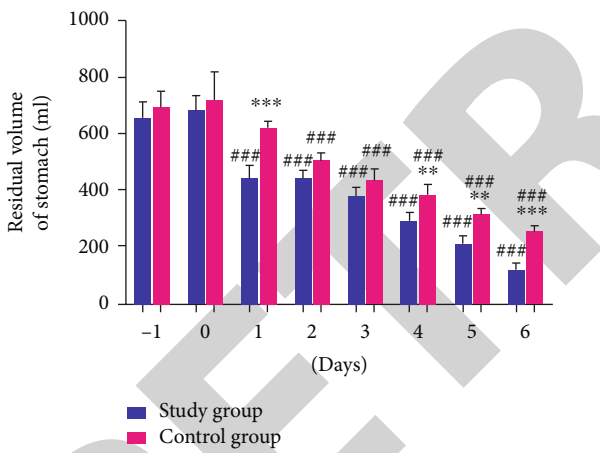

Figure 2: Delayed gastric emptying (gastric residual volume) from the day before treatment to the sixth day after treatment with gastrointestinal motility drugs (control group) and acupuncture (study group). Acupuncture caused a smaller gastric residual volume. $^{###}P < 0.001$, days 0-6 vs. day -1, $^{**}P < 0.01$, $^{***}P < 0.001$, control group vs. study group.

and the human body's ability to remove pathogenic factors is reduced, thus prolonging the course of sepsis.

The essence of acupuncture is to stimulate healthy qi by triggering and strengthening the body's homeostasis function and regulating the body's innate immunity, so as to assist the weakness and relieve the strong [23]. Acupuncture can play a two-way regulatory role in gastrointestinal tract, and has its special advantages in the treatment of acute and critical patients [24]. First, acupuncture therapy is simple, convenient, and low-cost, which can greatly reduce the medical burden of patients and society, with high clinical feasibility. Secondly, acupuncture therapy does not need to be absorbed through gastrointestinal tract, which reduces the burden of gastrointestinal tract. Our study applied ultrasonography to assess the effect of acupuncture on the contraction area of gastric antrum in patients, and found that before acupuncture, the contraction area of the gastric antrum was increased. After acupuncture for two days, the contraction area of the gastric antrum was decreased compared with that before acupuncture treatment. After acupuncture for five days, the contraction area of the gastric antrum was further decreased and was basically restored to a normal condition. Moreover, after treatment, the maximal pressure and maximal volume of the two groups both increased, and the study group increased more. As far as we know, HF, LF, and VLF are widely accepted as markers of the autonomic nervous functions [25]. Based on this, our study found acupuncture could adjust the downward trend of vagus nerve tension and the upward trend of sympathetic nerve tension caused by gastric distention, so as to improve vagus nerve tension and reduce sympathetic nerve tension. In addition, gastric residual, intra-abdominal pressure was decreased, and gastric compliance was improved in both groups after treatment. In addition, the recovery of gastric function in the study group was more significant than that in the control group [26]. The above data show that acupuncture can promote intestinal peristalsis, improve gastrointestinal rhythm, and restore gastric motility in patients with sepsis GD. Furthermore, the APACHE II score, WBC, CRP, and RCT of the two groups after treatment were lower than those before treatment, indicating that the treatment of the two groups had an improvement effect. However, there was no significant difference in WBC, CRP, and RCT between the two groups after treatment. Considering that the decrease of inflammation level between the two groups

Table 1: Comparison of the initial and maximal pressure and volume between the two groups.

Observed indexes	Control group ($n = 36$)		Study group ($n = 37$)	
	Before treatment	After treatment	Before treatment	After treatment
Initial pressure (mmHg)	4.62 ± 1.06	6.15 ± 1.61*	4.84 ± 1.24	8.44 ± 1.93*,#
Initial volume (ml)	302.20 ± 36.41	401.34 ± 56.85*	297.11 ± 33.37	492.32 ± 54.68*,#
Maximal pressure (mmHg)	9.19 ± 1.81	12.51 ± 1.86*	9.65 ± 1.79	13.69 ± 2.11*,#
Maximal pressure (ml)	425.08 ± 76.662	693.43 ± 80.86*	433.45 ± 49.76	820.71 ± 77.43*,#

Note: * meant $P < 0.05$ vs. before treatment; # meant $P < 0.05$ vs. after treatment in control group.

Table 2: Comparison of symptom scores under different gastric dilatation volumes between the two groups.

Observed indexes	Control group ($n = 36$)		Study group ($n = 37$)	
	Before treatment	After treatment	Before treatment	After treatment
Epigastric pain				
200 ml	0.94 ± 0.23	0.72 ± 0.45	0.95 ± 0.23	0.05 ± 0.23*,#
300 ml	1.86 ± 0.76	1.06 ± 0.47*	1.62 ± 0.72	0.62 ± 0.49*,#
400 ml	2.42 ± 0.65	1.47 ± 0.65*	2.27 ± 0.80	1.00 ± 0.08*,#
Fullness				
200 ml	1.08 ± 0.28	0.97 ± 0.17	1.14 ± 0.35	0.30 ± 0.46*,#
300 ml	1.97 ± 0.70	1.33 ± 0.79*	1.65 ± 0.86	0.862 ± 0.48*,#
400 ml	2.39 ± 0.69	1.89 ± 0.68*	2.49 ± 0.61	1.32 ± 0.67*,#
Nausea or vomiting				
200 ml	1.00 ± 0.24	0.67 ± 0.48	0.97 ± 0.29	0.11 ± 0.31*,#
300 ml	1.78 ± 0.68	1.14 ± 0.59*	1.92 ± 0.80	0.65 ± 0.54*,#
400 ml	2.19 ± 0.82	1.44 ± 0.69*	1.95 ± 0.81	0.97 ± 0.50*,#

Note: * meant $P < 0.05$ vs. before treatment; # meant $P < 0.05$ vs. after treatment in control group.

Table 3: Comparison of gastric compliance between the two groups.

	Before treatment	After treatment	t	P
Control group ($n = 36$)	45.55 ± 13.20	55.31 ± 13.99*	3.043	0.0033
Study group ($n = 37$)	45.78 ± 14.96	68.45 ± 17.11*,#	6.067	<0.0001
t	0.0695	3.587		
P	0.9448	0.0006		

Note: * meant $P < 0.05$ vs. before treatment; # meant $P < 0.05$ vs. after treatment in control group.

Table 4: Effect of acupuncture on autonomic nervous function in patients with septic GD.

Observed indexes	Control group ($n = 36$)			Study group ($n = 37$)		
	Baseline	Before treatment	After treatment	Baseline	Before acupuncture	After acupuncture
HF (ms^2)	615.1 ± 214.8	345.1 ± 132.1*	299.1 ± 108.9*	662.6 ± 209.9	357.7 ± 162.8*	608.9 ± 308.0#
LF (ms^2)	601.0 ± 221.8	798.4 ± 250.7*	788.7 ± 207.9*	546.8 ± 248.0	888.1 ± 320.5*	600.7 ± 168.7#
VLF (ms^2)	1497.1 ± 482.5	2038.4 ± 503.0*	1891.2 ± 369.4*	1401.3 ± 453.9	1893.4 ± 440.0*	1459.6 ± 438.3#

Note: * meant $P < 0.05$ vs. baseline; # meant $P < 0.05$ vs. before acupuncture.

is more likely related to comprehensive treatment such as anti-infection, fluid resuscitation, clearance of inflammatory mediators, mechanical ventilation, and organ function support. Finally, although the abdominal circumference of the two groups did not change much before and after treatment, it cannot be completely denied that the treatment did not

Table 5: Comparison of APACHE II score, abdominal circumference, and intraperitoneal pressure between the two groups.

Observed indexes	Control group ($n = 36$)		Study group ($n = 37$)	
	Before treatment	After treatment	Before treatment	After treatment
APACHE II score	21.08 ± 2.38	16.36 ± 2.69*	21.16 ± 2.21	14.62 ± 1.46*,#
Abdominal circumference (cm)	109.62 ± 8.37	106.12 ± 7.82	109.5 ± 7.99	105.08 ± 7.55
Intraperitoneal pressure (mmHg)	14.66 ± 1.24	12.48 ± 2.11 ∗	14.87 ± 1.33	10.63 ± 1.62 ∗,#

Note: ∗ meant $P < 0.05$ vs. before treatment; # meant $P < 0.05$ vs. after treatment in control group.

Table 6: Comparison of infection indexes between the two groups.

Observed indexes	Control group ($n = 36$)		Study group ($n = 37$)	
	Before treatment	After treatment	Before treatment	After treatment
WBC ($\times 10^9$/l)	14.03 ± 2.43	8.35 ± 0.76*	14.80 ± 2.30	8.43 ± 0.97*
CRP (mg/l)	127.92 ± 26.67	34.73 ± 10.44*	127.92 ± 29.14	37.05 ± 12.50*
PCT (ng/ml)	8.07 ± 1.59	2.02 ± 0.57*	8.10 ± 1.52	1.94 ± 0.57*

Note: * meant $P < 0.05$ vs. before treatment.

reduce the effect of abdominal circumference; it may also be related to the edema changes of patients before and after treatment.

However, there are limitations in the study. First, the sample size was relatively small in the study. More studies should be conducted in the future. Second, the trial lacked a sham acupuncture control group because most of the Chinese patients had been treated with acupuncture and it was difficult to blind the subjects.

5. Conclusion

The clinical application of acupuncture in the treatment of sepsis patients with GD can significantly reduce gastric residual, abdominal pressure, improve abdominal distension, promote gastrointestinal peristalsis and gastric motility, and restore gastrointestinal autonomic nerve function. In the early stage of sepsis, abdominal distension, vomiting, intestinal dyskinesia, and more gastric residue can be used as appropriate.

Data Availability

Data are available from the corresponding author under reasonable requests.

Conflicts of Interest

The authors declare that they have no conflicts of interest.

Acknowledgments

This work was supported by the Lanzhou Talent Innovation and Entrepreneurship Project (2019-RC-67).

References

[1] P. Bajracharya, S. Kalra, S. Dhingra, A. Sood, A. K. Yadav, and M. Kanitkar, "Acute kidney injury in the pediatric intensive care unit at a tertiary care hospital of the armed forces: a cross-sectional observational study," *Medical Journal, Armed Forces India*, vol. 76, no. 1, pp. 84–88, 2020.

[2] Q. Y. Yang, J. Ouyang, and J. D. Yang, "Sepsis as an important risk factor for gastrointestinal bleeding in acute coronary syndrome patients: two case reports," *Medicine (Baltimore)*, vol. 97, no. 36, article e12273, 2018.

[3] D. Govil and D. Pal, "Gastrointestinal motility disorders in critically ill," *Indian Journal of Critical Care Medicine*, vol. 24, Supplement 4, pp. S179–S182, 2020.

[4] Y. Zhang, Z. Zhao, E. Tang, Y. Hu, and J. Mao, "Additional traditional Chinese medicine on gastrointestinal dysfunction in patients with sepsis: a systematic review and meta-analysis," *Pakistan Journal of Pharmaceutical Sciences*, vol. 29, Supplement 2, pp. 663–669, 2016.

[5] H. F. Li, G. Q. Hu, and W. W. Liu, "Clinical trials of acupuncture of Jiaji (EX-B2) for treatment of gastrointestinal dysfunction in sepsis patients," *Zhen Ci Yan Jiu= Acupuncture Research*, vol. 44, no. 1, pp. 43–46, 2019.

[6] Q. Cao, Y. Liu, Y. Wu et al., "Profilin 2 promotes growth, metastasis, and angiogenesis of small cell lung cancer through cancer-derived exosomes," *Aging (Albany NY)*, vol. 12, no. 24, pp. 25981–25999, 2020.

[7] X. Mao, S. Guo, W. Ni et al., "Electroacupuncture for the treatment of functional dyspepsia: a systematic review and meta-analysis," *Medicine (Baltimore)*, vol. 99, no. 45, article e23014, 2020.

[8] W. J. Li, C. Gao, L. X. An, Y. W. Ji, F. S. Xue, and Y. Du, "Perioperative transcutaneous electrical acupoint stimulation for improving postoperative gastrointestinal function: a randomized controlled trial," *Journal of Integrative Medicine*, vol. 19, no. 3, pp. 211–218, 2021.

[9] S. Uchida, F. Kagitani, and I. Sato-Suzuki, "Somatoautonomic reflexes in acupuncture therapy: a review," *Autonomic Neuroscience*, vol. 203, pp. 1–8, 2017.

[10] W. W. Tao, H. Jiang, X. M. Tao, P. Jiang, L. Y. Sha, and X. C. Sun, "Effects of acupuncture, tuina, tai chi, qigong, and traditional Chinese medicine five-element music therapy on symptom management and quality of life for cancer patients: a

Hindawi
Computational and Mathematical Methods in Medicine
Volume 2023, Article ID 9780394, 1 page
https://doi.org/10.1155/2023/9780394

Retraction

Retracted: Hub Genes and Long Noncoding RNAs That Regulates It Associated with the Prognosis of Esophageal Squamous Cell Carcinoma Based on Bioinformatics Analysis

Computational and Mathematical Methods in Medicine

Received 12 December 2023; Accepted 12 December 2023; Published 13 December 2023

This article has been retracted by Hindawi, as publisher, following an investigation undertaken by the publisher [1]. This investigation has uncovered evidence of systematic manipulation of the publication and peer-review process. We cannot, therefore, vouch for the reliability or integrity of this article.

Please note that this notice is intended solely to alert readers that the peer-review process of this article has been compromised.

Wiley and Hindawi regret that the usual quality checks did not identify these issues before publication and have since put additional measures in place to safeguard research integrity.

We wish to credit our Research Integrity and Research Publishing teams and anonymous and named external researchers and research integrity experts for contributing to this investigation.

The corresponding author, as the representative of all authors, has been given the opportunity to register their agreement or disagreement to this retraction. We have kept a record of any response received.

References

[1] J. Lu, R. Li, M. Fang, and S. Ke, "Hub Genes and Long Noncoding RNAs That Regulates It Associated with the Prognosis of Esophageal Squamous Cell Carcinoma Based on Bioinformatics Analysis," *Computational and Mathematical Methods in Medicine*, vol. 2022, Article ID 6027058, 11 pages, 2022.

Hindawi
Computational and Mathematical Methods in Medicine
Volume 2022, Article ID 6027058, 11 pages
https://doi.org/10.1155/2022/6027058

Research Article

Hub Genes and Long Noncoding RNAs That Regulates It Associated with the Prognosis of Esophageal Squamous Cell Carcinoma Based on Bioinformatics Analysis

Jun Lu,[1] Ruichao Li,[2] Minghao Fang,[1] and Shun Ke[1]

[1]*Department of Emergency Medicine & Intensive Care Unit, Tongji Hospital, Tongji Medical College, Huazhong University of Science and Technology, Wuhan 430030, China*
[2]*Department of General Medicine, Tongji Hospital, Tongji Medical College, Huazhong University of Science and Technology, Wuhan 430030, China*

Correspondence should be addressed to Shun Ke; keshun@tjh.tjmu.edu.cn

Received 5 August 2022; Accepted 27 August 2022; Published 19 September 2022

Academic Editor: Min Tang

Objective. Through bioinformatics analysis methods, the public databases GEO and TCGA were used to research mRNA and squamous cell carcinoma of the esophagus, construct a lncRNA-mRNA network, and screen hub genes and lncRNAs related to prognosis. *Method*. Download esophageal squamous cell carcinoma-related mRNA and lncRNA datasets GEO and TCGA public datasets, as well as clinical data, use bioinformatic tools to perform gene differential expression analysis on the datasets to obtain differentially expressing mRNA (DEmRNA) and lncRNA (DElncRNA), and plot volcano plots and cluster heatmaps. The differential intersection of differentially expressed DEmRNA and DElncRNA was extracted by Venn diagram and imported into CytoScape software, a regulatory network visualization software, to construct a lncRNA-mRNA network and use cytoHubba and MCODE plug-ins to screen hub genes and key lncRNAs. The DEmRNA in the network was imported into the Gene and Protein Interaction Retrieval Database (STRING), gene-encoded protein–protein interactions (PPI) network maps were created, and the genes in the PPI network maps were submitted to GO functional annotation and pathway enrichment analysis using Kyoto Encyclopedia of Gene Genomes (KEGG) (KEGG). The link between hub gene and prognosis was studied using the clinical data collected by TCGA. *Result*. Retrieve the datasets GSE23400 and GSE38129 from the GEO database and the esophageal squamous cell carcinoma-related mRNAs from TCGA databases and then obtain intersection. Differentially regulated genes revealed a correlation of 326 (up) with 191 (down) in terms of the differential intersection; for this study, we need to collect the GSE130078 dataset from GEO, as well as the lncRNAs from TCGA databases that are connected to esophageal squamous cell cancer. There were 184 differentially up- and downregulated genes in the differential intersection. A differential intersection network of the differential intersection lncRNA-mRNA network allowed us to identify the hub genes, including COL5A2 (COL3A1), COL1A1 (COL1A1), CTD-2171N6.1 (CTD-2171N6.1), and RP11-863P13.3 (RP11-863P13.3). The extracellular matrix, which is important in protein digestion and absorption, was shown to be the primary site of functional enrichment, as shown by GO/KEGG analysis. Squamous cell carcinoma of the mouth and throat is associated with a poor prognosis because of a change in the extracellular matrix structure caused by specific long noncoding RNA (lncRNA) regulatory upregulation. *Conclusion*. For the purpose of predicting the prognosis of cancer of the esophagus, researchers studied the esophageal squamous cell carcinoma-related hub genes and important noncoding RNAs (ncRNAs).

1. Introduction

Eosophageal carcinoma (EC) is one of the most prevalent cancers in the world [1]. Cancer is the third most common and the fourth most deadly disease on China's mainland [2]. Esophageal squamous cell carcinoma (ESCC), which accounts for 90% of all esophageal cancer patients worldwide, is the most common pathological diagnosis [3]. Early ESCC patients had a five-year survival rate of up to 90%. According to the Centers for Disease Control and Prevention, 50 percent of

Table 1: DEmRNA result statistics table.

Statistical information		Threshold dissimilarity		Gene variants		Samples	
Data sources	Platform	FC	*P*_value	Up	Down	Tumor	Normal
GSE23400	GPL96	1.5	0.05	614	570	53	53
GSE38129	GPL571	1.5	0.05	1056	990	30	30
TCGA	HTSeq	1.5	0.05	1417	1630	161	12

Table 2: DElncRNA.

Data information		Difference threshold		Differential number of lncRNAs		Number of samples	
Data sources	Platform	FC	*P*_value	Up	Down	Tumor	Normal
GSE130078	HiSeq 2000	1.5	0.05	512	302	Twenty-three	Twenty-three
TCGA	HTSeq	1.5	0.05	1266	1000	161	12

ESCC patients in China have already had tumor metastases. Following surgical treatment, radiation therapy, and chemotherapy, survival rate after five years is under twenty percent [4, 5]. There is no doubt that the best chance of a cure lies on an early diagnosis and the presence of metastases in other parts of the body. Consequently, novel early screening markers and treatment targets are needed. It is thought that long noncoding RNA (lncRNA) plays an important role in tumor formation and growth because of its length of over 200 nucleotides [6]. Previous studies have shown that acute myeloid leukemia is characterized by a high degree of downregulation of the microRNA known as miR-192. It is able to influence tumor cell proliferation and cell cycle progression by interaction with cyclin CCNT2, which is responsible for regulating cell proliferation and cell cycle progression [7]. Esophageal squamous cell carcinoma has a decreased expression of long-chain noncoding NKILA that inhibits cell proliferation and migration by preventing the NF-B signaling pathway from activating [8]. The miR-7/HOXB13 axis can be activated by circular RNA CIRS-7 to increase the development and metabolism of esophageal squamous cell carcinoma [9]. Although noncoding RNAs (lncRNAs) have recently risen to the forefront of tumor formation and development studies, no studies have looked at lncRNAs as potential tumor indicators in esophageal squamous cell carcinoma.

As part of this study, we used the combined analysis of GEO and TCGA to screen out the differential expression profiles of long noncoding RNA (lncRNA) and short noncoding RNA (mRNA) in esophageal squamous cell carcinoma and constructed a network and selected hub genes using cytoscape. We then used clinical samples to verify the final prognosis of the hub gene and the feasibility as a prognostic marker for this type of cancer.

2. Materials and Methods

2.1. Data Collection. Esophageal squamous cell carcinoma-related mRNA and lncRNA datasets from the TCGA database can be downloaded from GSE23400, GSE38129, and GSE130078 gene probe matrices, respectively, from the Gene Expression Omnibus (GEO, http://www.ncbi.nlm.nih.gov/geo/), as well as GPL96, GPL571, and HiSeq 2000 annotation information file of the corresponding platform and then convert the probe IDs of the probe matrix in the dataset into the gene IDs and Ensembl gene IDs in the annotation information.

2.2. Differential Expression and Differential Intersection. Standard data were obtained by filtering and normalizing the data, and the log2 fold change (FC) absolute values of greater than 1.5 were used as a standard for differential gene screening. This allowed researchers to identify the mRNAs that were differentially expressed (DEmRNA) and lncRNAs that were differentially expressed (DElncRNA). DEmRNA and DElncRNA are the intersections of the datasets GSE23400 and GSE38129 and the mRNA- and lncRNA-related datasets in the TCGA database, respectively, taken from the intersection.

2.3. Construct lncRNA-mRNA Network and Protein-Protein Interaction Network Diagram. Introducing the intersection of DEmRNA and DElncRNA into cytoScape v3.7 [10] software, build lncRNA-mRNA network and use cytoHubba and MCODE plug-ins to obtain hub genes and key lncRNAs. Using the STRING [11] online tool, analyze the protein-protein interaction (PPI) through DEmRNA. Select Required Confidence (combined score) > 0.7 as the threshold for protein-protein interaction to construct a PPI network graph.

2.4. Enrichment Analysis and Survival Analysis. As a statistically significant function and signaling path, DEmRNA enrichment pathways are analyzed using GO functional annotation and Kyoto Encyclopedia of Genes and Genomes (KEGG) path analysis; a statistically significant result is one that has a *P* value that is less than 0.05. The survival curve between the hub gene and disease-free survival (DFS) was produced for prognostic analysis using esophageal squamous cell carcinoma survival data taken from the TCGA

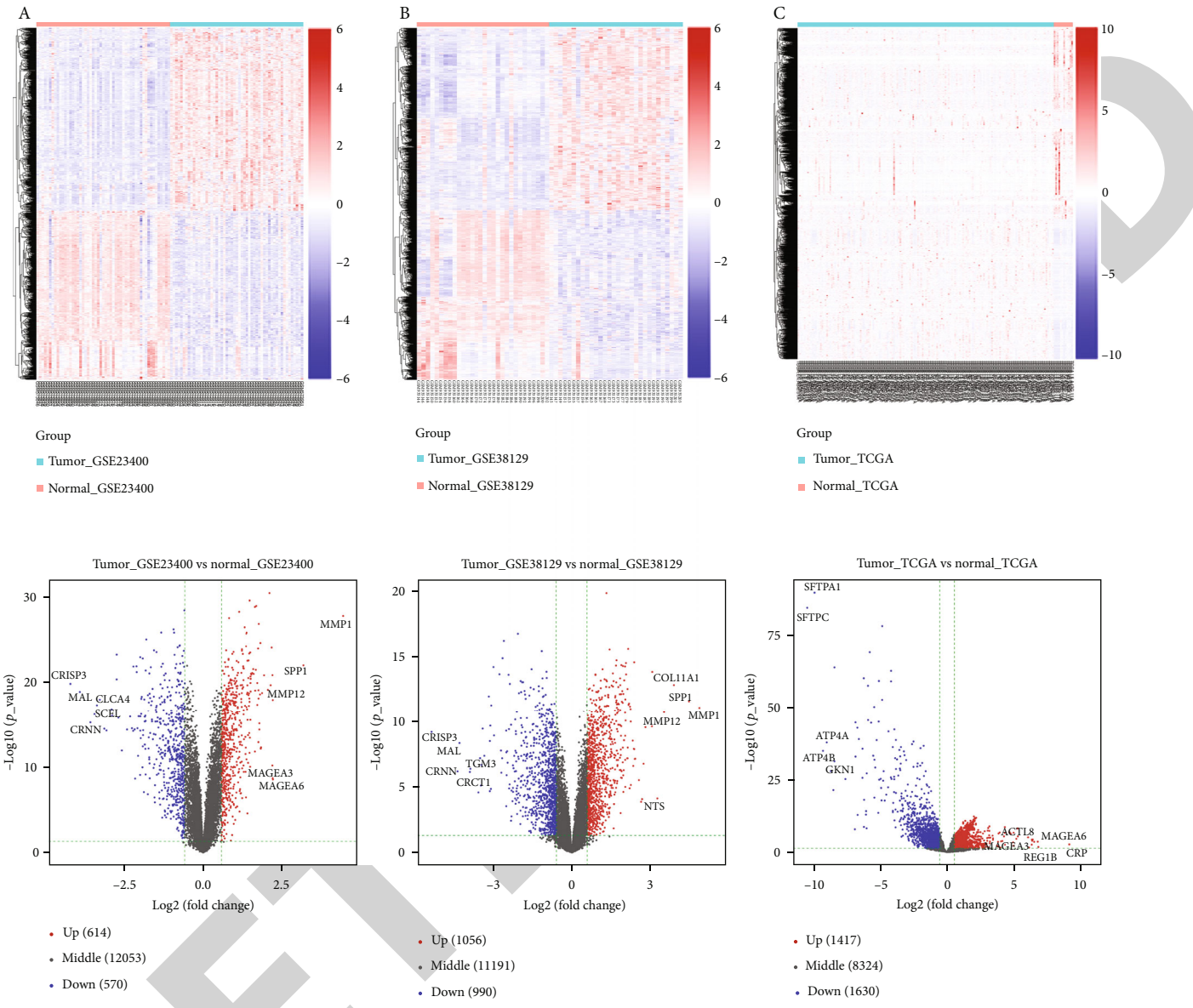

(a)

Figure 1: Continued.

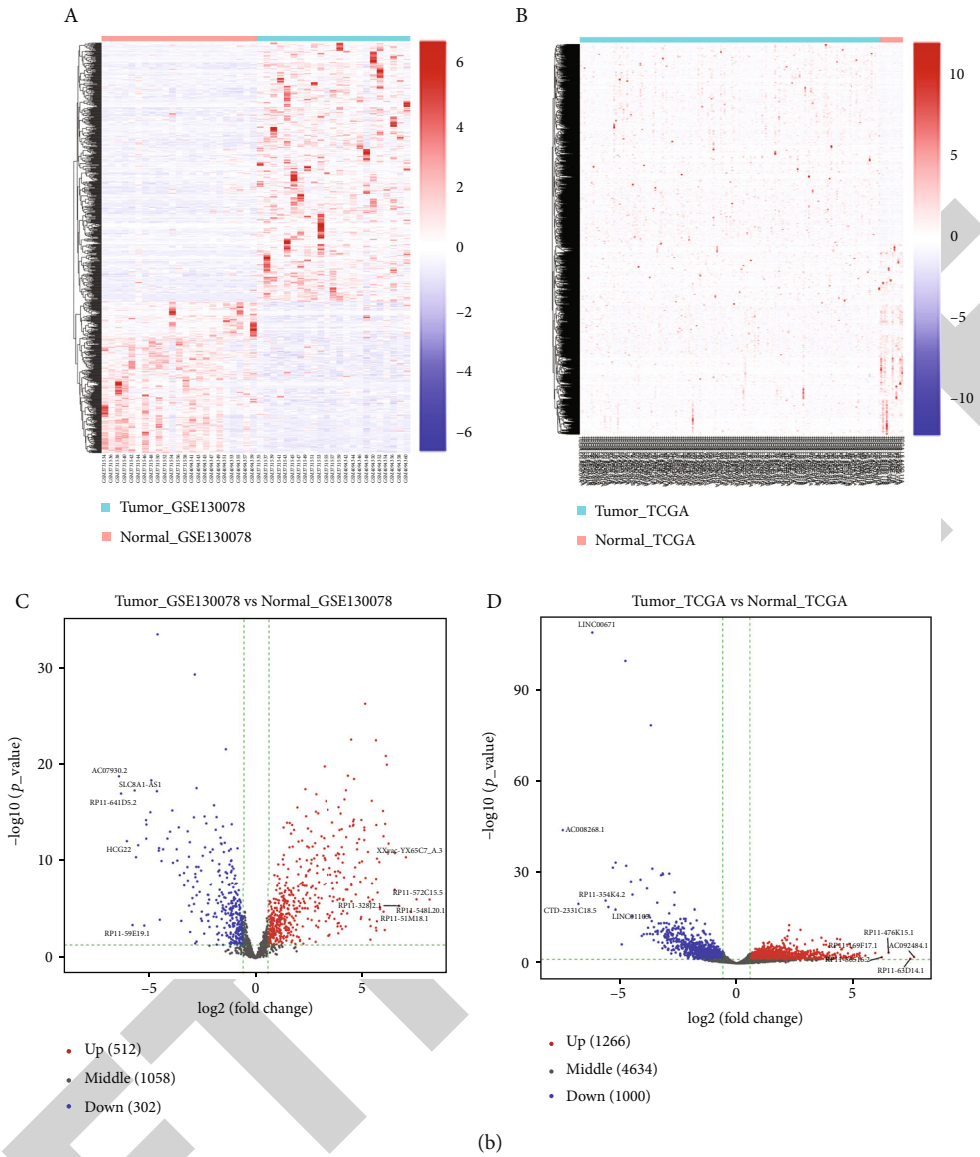

(b)

Figure 1: (a) DEmRNA thermal map and volcano diagram. (b) Heatmap and volcano map of DElncRNA.

database. This was done in order to determine the likelihood of a favorable outcome.

2.5. Statistical Methods. Use R language limma or edgeR package [12] to calculate differential expression, and draw Venn diagram to take differential intersection. Through CytoScape software, build lncRNA-mRNA network to screen hub genes and key lncRNAs. Stitch together a PPI network with the help of the STRING database, and then, do a survival study using the Kaplan-Meier curve.

3. Results

3.1. DEmRNA and DElncRNA Screening Findings. DEmRNAs screened from the three datasets of GSE23400, GSE38129, and TCGA are shown in Table 1, and the number of DElncRNAs screened from the two datasets of GSE130078 and TCGA is shown in Table 2. Cluster analysis was performed on the screened differential genes marking the differential genes with significant differences, and cluster heatmaps and volcano maps were drawn (Figures 1(a) and 1(b)).

3.2. Difference Intersection and Venn Diagram. The intersection analysis of DEmRNA and DElncRNA indicated 326 differentially upregulated genes and 191 differentially downregulated genes, respectively. There were 184 differentially upregulated lncRNAs and 57 differentially downregulated lncRNAs. Then, a Venn diagram was constructed (Figures 2(a) and 2(b)).

3.3. Analysis of lncRNA-mRNA and PPI Network and Enrichment Results. A lncRNA-mRNA regulatory network was constructed with the help of CytoScape (Figure 3). Analyzing the established lncRNA-mRNA regulatory network indicated that lncRNA-RP11-863P13.3, RP11-576I22.2, and CTD-2171N6.1 can govern the upregulation of MMP11,

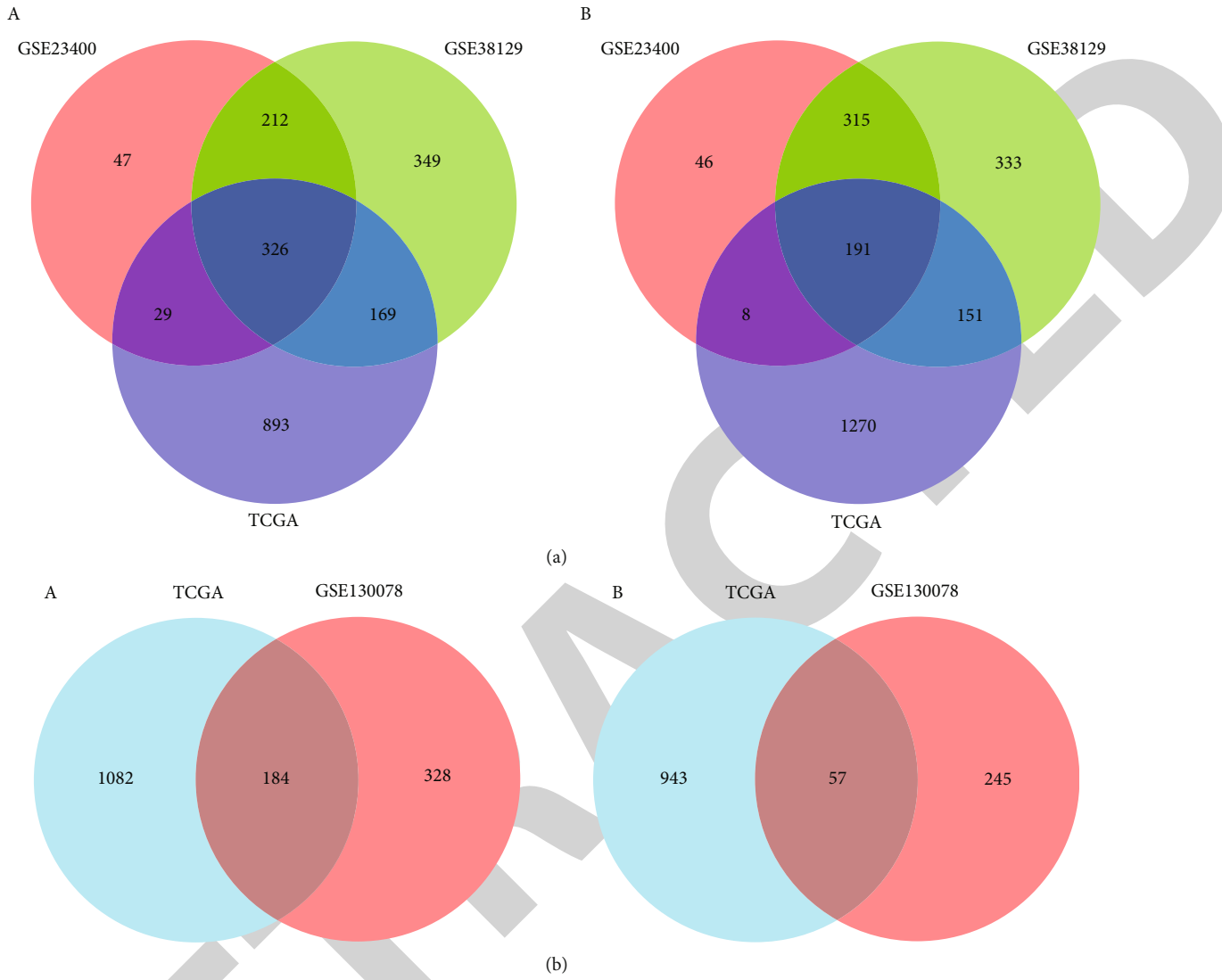

Figure 2: (a) Venn diagram of DEmRNA intersection. (b) Venn diagram of DElncRNA intersection.

THY1, and 16 more genes. MAMDC2-AS1 is the closest downregulated lncRNA related with gene regulation, interacting with 19 genes, including FHL1 and TGFBR3. Afterwards, using the online application STRING, a PPI network was constructed for the mRNAs that were the most directly influenced by lncRNAs. In addition, the hub genes were excluded from the analysis as a result of the connection degree of each gene (in this investigation, the top 10 genes with the highest connection degree were selected) (Figure 4(a)). It was shown that COL5A2, COL3A1, and COL1A1 as well as other hub genes had a greater influence on the lncRNA-mRNA regulatory network of esophageal squamous cell carcinoma than other hub genes. Biological process (BP), molecular function (MF), and cellular component (CC) are the three gene function categories identified by the GO and KEGG enrichment analyses of the genes in the aforementioned PPI network. The enrichment results revealed that the pathway with the highest enrichment score in BP was composed of extracellular matrix (Figure 4(b)), that the pathway with the highest enrichment score in CC was fibrillar collagen trimer (Figure 4(c)), and that the pathway with the highest enrichment score in MF is for the extracellular matrix structural components that confer tensile strength (Figure 4(d)). The protein digestion and absorption pathway received the greatest enrichment score according to KEGG (Figure 4(e)).

3.4. Survival Analysis. The selected hub genes of COL1A2, COL3A1, and COL5A2 were drawn using the Kaplan-Meier survival curve to analyze the clinical prognosis. These genes were chosen based on the clinical data provided by TCGA. It was discovered that all three of the hub genes, COL1A2, COL3A1, and COL5A2, had significant levels of expression. In addition, the disease-free survival duration of patients who had esophageal squamous cell carcinoma and had these hub genes in high expression was dramatically reduced (Figure 5). This suggests that it has certain clinical significance when determining the prognosis of patients who have esophageal squamous cell carcinoma.

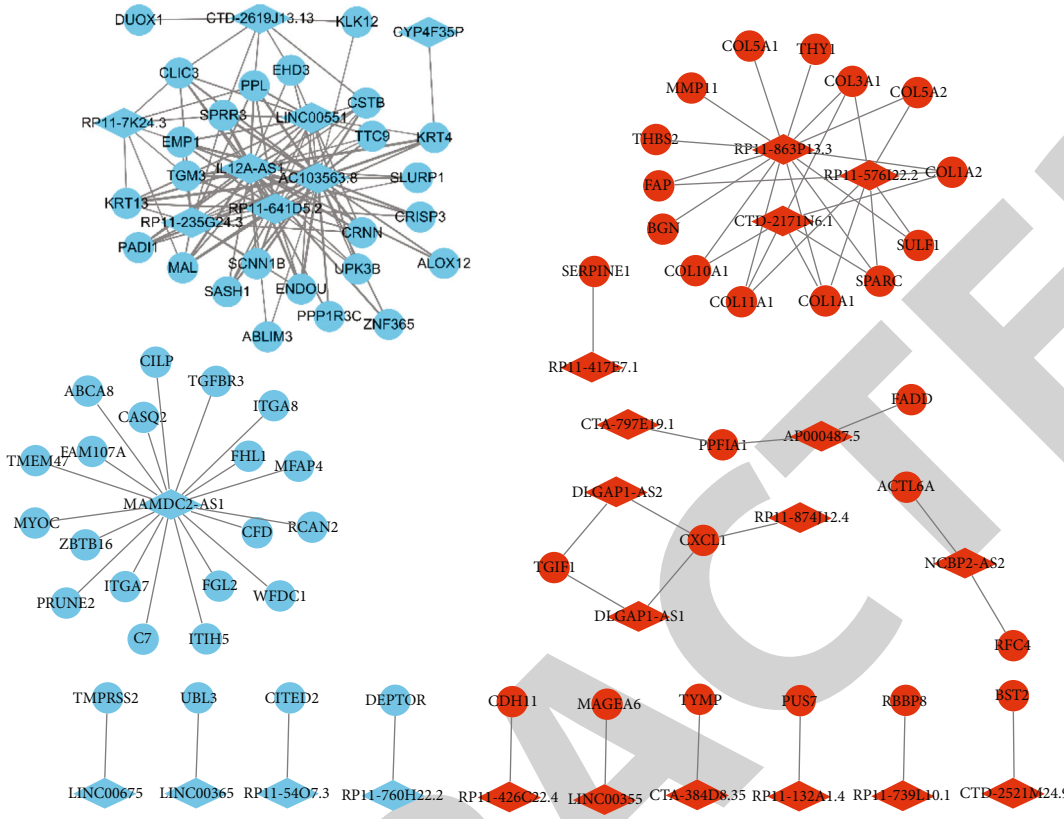

Figure 3: Schematic of the lncRNA-mRNA regulation network.

4. Discussion

As we all know, little is known about the lncRNA signatures of HCC patients. One piece of study established six lncRNA signatures with the intention of predicting recurrence-free survival in HCC. Wu et al. then investigated these signatures in a specific HCC cohort in which the tumor may be removed [13, 14]. This research utilized lncRNA signatures to construct a lncRNA-mRNA interaction network in patients with esophageal squamous cell carcinoma. The researchers then screened interacting hub genes to predict survival, which is more accurate and clinically relevant than simply screening lncRNA features from the perspective of cellular function correlation. In this work, we examined the differential lncRNAs and mRNAs in esophageal squamous cell carcinoma and paracancerous tissue using a combined TCGA-GEO analysis and then calculated expression correlation between the above differential intersection lncRNA and differential intersection mRNA in TCGA data. After the lncRNA-mRNA relationship pair with the correlation coefficient greater than 0.7 was selected, we constructed the lncRNA-mRNA regulatory network with CytoScape. Subsequently, the STRING database was used to predict the hub gene to construct a PPI network to enrich the GO and KEGG pathways. We examined the influence of hub gene expression related with lncRNA on disease-free survival in esophageal squamous cell carcinoma using TCGA clinical prognostic data.

I is a fibrillar collagen found abundantly in bone, cornea, dermis, and tendon [15–17]. This gene is linked to osteogenesis imperfecta types I through IV, Ehlers-Danlos syndrome VIIA, classic Ehlers-Danlos syndrome, Caffey disease, and idiopathic osteoporosis. A reciprocal translocation between chromosomes 17 and 22, where this gene and the platelet-derived growth factor gene are situated, is related with dermatofibrosarcoma protuberans, a particular kind of skin tumor caused by aberrant production of growth factors. For this gene, two transcripts with alternate polyadenylation signals have been discovered [18–21]. In this study, clinical prognostic analysis based on TCGA revealed that the high expression of four genes, majority, caused by mutations, mount faucet, the faucet, and signs of abating, may considerably reduce the disease-free survival of esophageal squamous cell carcinoma and worsen the prognosis. These genes are COL1A1, COL1A2, COL3A1, and COL5A2. Therefore, we hypothesize that the high expression of the COL collagen family is associated with a worse prognosis for esophageal squamous cell carcinoma.

Extracellular matrix (ECM) is a type of insoluble structural component that mostly consists of collagen, elastin, proteoglycans, and glycoproteins. ECM can influence biological processes such as cell differentiation, proliferation, adhesion, morphogenesis, and phenotypic expression, according to studies [22]. Malignant tumor formation, progression, invasion, and metastasis are frequently accompanied by alterations in the extracellular matrix and expression of cell surface

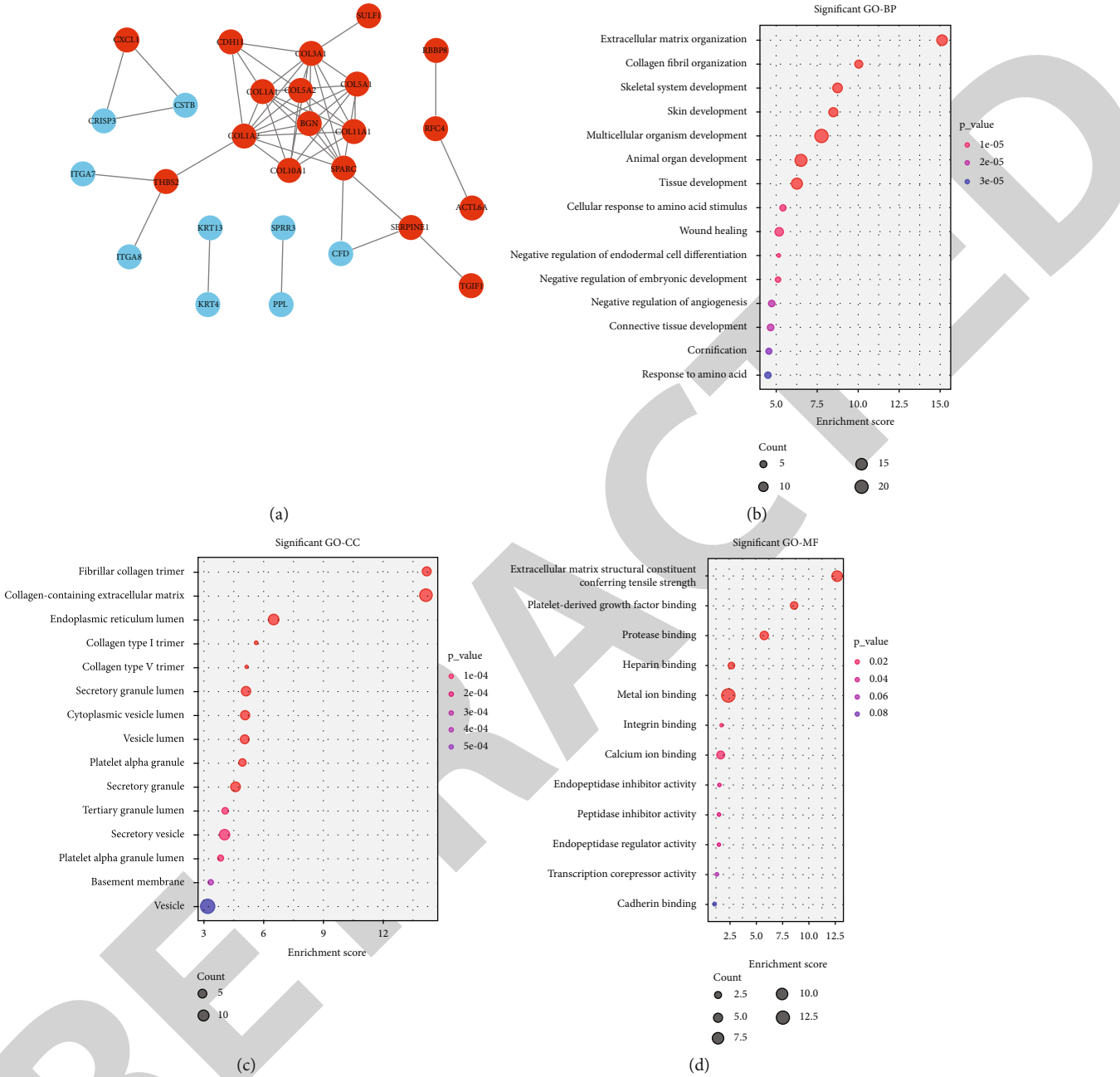

Figure 4: Continued.

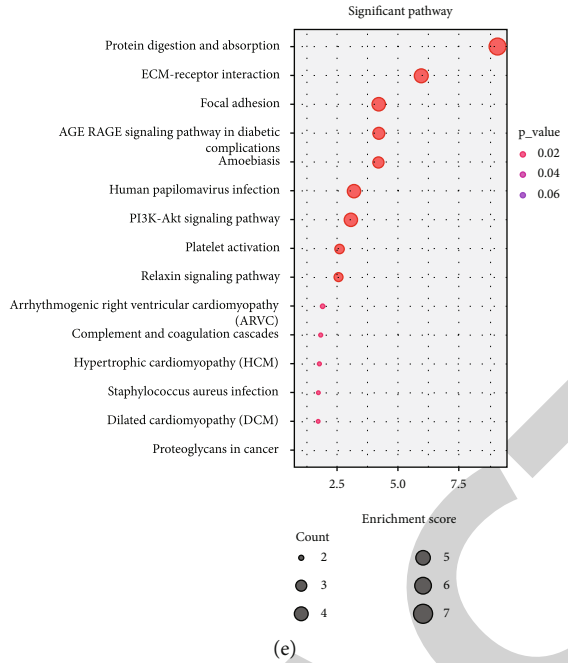

(e)

Figure 4: Analysis of PPI network and hub gene enrichment.

receptors [23]. Not only was the high level of LN and 61 significantly codistributed in human hepatocellular carcinoma (HCC) tissue but also the high level expression was negatively correlated with the prognosis of liver cancer patients, indicating that HCC cells may receive signals from LN via the 61 receptor, thereby causing the cancer to spread. Normal hepatocytes do not have a basement membrane and express the specific integrin family receptor 61 of laminin (LN). In the first stages of liver cancer's pathophysiology, portal vein invasion, intrahepatic metastasis, and extrahepatic metastases in the lungs and bones are common occurrences. The key aspects that decide a patient's prognosis with regard to liver cancer are the presence of invasion, metastasis, and postoperative recurrence of the disease. Matrix metalloproteinases, also known as MMPs, are responsible for the breakdown of extracellular matrix, also known as ECM. This is one of the most important links in the process of tumor cell invasion and metastasis. The presence of increased MMP levels and activity has been linked to a wide variety of cancerous tumors [24]. Among the GO annotation and KEGG pathway enrichment results, the related pathway of extracellular matrix property change has the highest enrichment score in extracellular matrix organization, fibrous collagen trimming, and extracellular matrix structure, indicating that COL collagen family represented by COL1A1 can result in a poor prognosis for patients by participating in the change of ECM properties to promote the generation and development of cancer cells. In this study, the pathway with the highest enrichment score in BP is extracellular matrix, the pathway with the highest enrichment score in CC is fibrillar collagen trimer, and the pathway with the highest enrichment score in MF is for the extracellular matrix structural components that confer tensile strength. The protein digestion and absorption pathway received the greatest enrichment score according to KEGG.

Epigenetics is a discipline of biology that investigates the heritable changes in gene expression and the stability of DNA sequence, which are necessary not only for the expansion and differentiation of cells but also for the occurrence and progression of cancers. DNA methylation, histone changes, and recently found noncoding RNAs are the key epigenetic processes [25]. Functional RNA molecules that cannot be translated into proteins are referred to as noncoding RNAs. Common regulatory noncoding RNAs include small interfering RNAs, microRNAs, piRNAs, and long noncoding RNAs [26]. Numerous studies have demonstrated that noncoding RNAs play an increasingly crucial role in epigenetic control. lncRNA participates in several biological processes, including the dose compensation effect, epigenetic control, cell cycle regulation, and cell differentiation regulation, among others, which play an important role, becoming a hot spot in genetics research. Tongji University used an integrated genomic data analysis method to research clinically relevant cancer lncRNAs and found two important prostate cancer lncRNA genes [27]. Studies have shown that lncRNA GLCC 1 binds to HSP 90 chaperones to form an RNA-protein complex, which stabilizes c-Myc in ubiquitination degradation in the cytoplasm to determine the transcription of its target gene LDHA and then to promote the genesis and glucose metabolism of colorectal cancer [28]. The interaction between HNF1A-AS1 and Egr1 promotes the ubiquitination and degradation of p21 that is mediated by CD34. This increases the expression of cyclin-dependent enzyme 2 (Kalindi kunj), kinases, and cyclin E1 and decreases the expression of p21, hence promoting the development of gastric cancer [6, 29]. These findings demonstrate that lncRNAs can influence gene expression via different pathways to mediate the evolution of tumor malignancy. This study revealed that the three noncoding RNA genes involved, engage

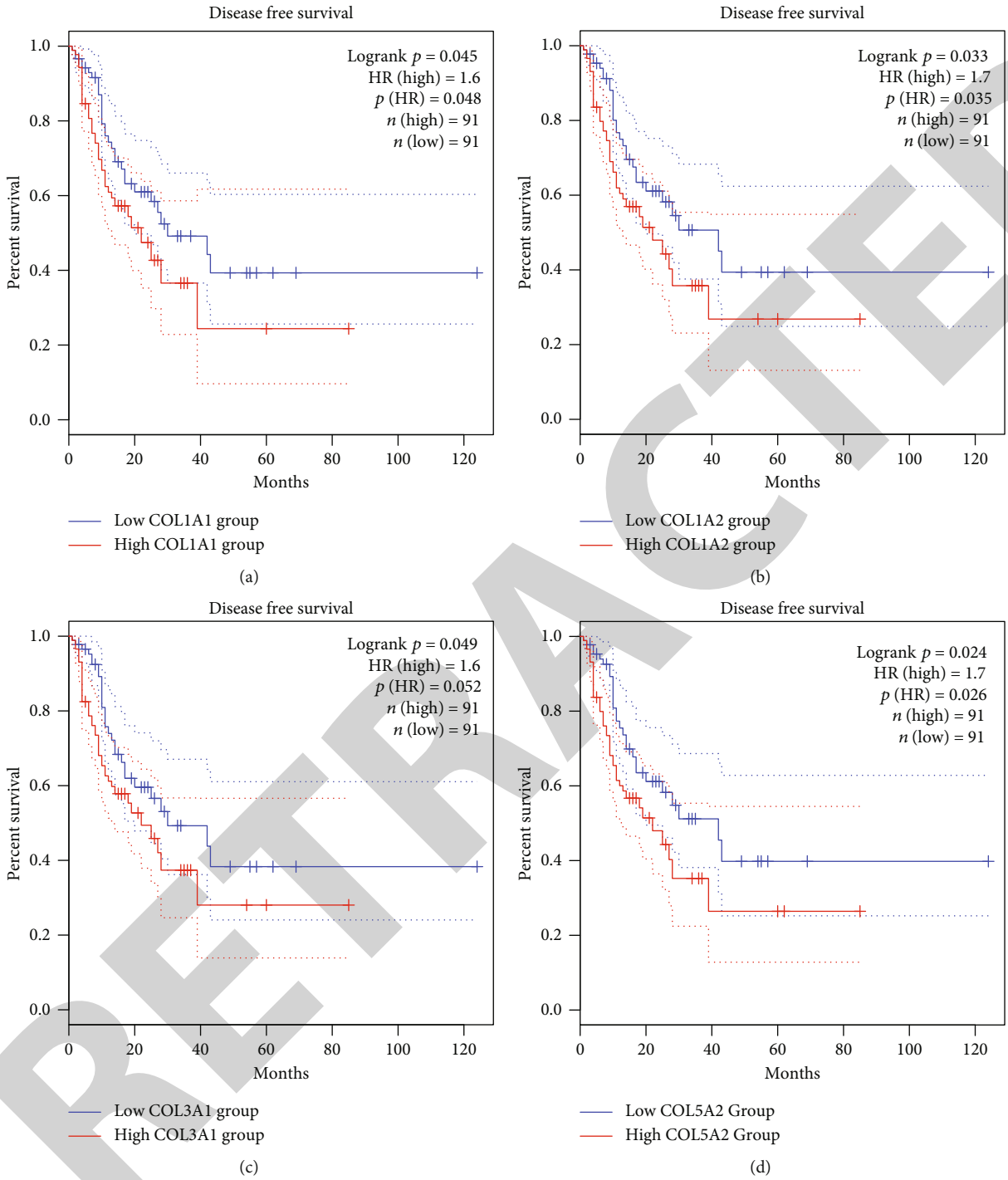

Figure 5: Hub gene and DFS prognosis analysis.

in self, and CTD-2171N6.1 may upregulate the expression of the COL collagen family member COL1A1 and are also interconnected. Significant portions of the dataset are expressed in esophageal squamous cell carcinoma-affected tissues. Therefore, we examined whether lncRNA-RP11-863P13.3, RP11-576I22.2, and CTD-2171N6.1 may contribute to a poor prognosis in patients with esophageal squamous cell carcinoma by promoting the change of ECM characteristics through the upregulation of Exon 1, Ccl5, COL3A1, and fabricating. The lncRNA-mRNA regulatory network of esophageal squamous cell carcinoma had the most pronounced effect on the hub genes COL5A2, COL3A1, COL1A1, and others.

Bioinformatics analysis was used in this work to identify the COL collagen family genes and three critical lncRNAs associated with the poor clinical prognosis of esophageal squamous cell carcinoma. But we did not conduct in vitro and in vivo functional experiments to further analyze the mechanism due to all kinds of objective reasons, which is

the biggest deficiency of this study. We will further study the expression regulation mechanism of related molecules in this study when the experimental conditions are met.

In conclusion, we have discovered three new lncRNAs as independent biological predictors of esophageal squamous cell carcinoma prognosis using bioinformatics, clinical data, and genetic profiles of thoroughly screened cohorts. To examine the progression process of ESCC and the particular mechanisms of action of these lncRNAs, however, it will be necessary to corroborate our findings in future research.

Data Availability

The labeled dataset used to support the findings of this study is available from the corresponding author upon request.

Conflicts of Interest

The authors declare that there are no conflicts of interest.

Acknowledgments

This work is supported by the National Natural Science Foundation of China (82002621) and Natural Science Foundation of Hubei Province (2021CFB380).

References

[1] R. L. Siegel, K. D. Miller, and A. Jemal, "Cancer statistics, 2020," *CA: a Cancer Journal for Clinicians*, vol. 70, no. 1, pp. 7–30, 2020.

[2] K. Sudo, K. Kato, J. Matsuzaki et al., "Development and validation of an esophageal squamous cell carcinoma detection model by large-scale microRNA profiling," *JAMA Network Open*, vol. 2, no. 5, p. e194573, 2019.

[3] F. Bray, J. Ferlay, I. Soerjomataram, R. L. Siegel, L. A. Torre, and A. Jemal, "Global cancer statistics 2018: GLOBOCAN estimates of incidence and mortality worldwide for 36 cancers in 185 countries," *CA: a Cancer Journal for Clinicians*, vol. 68, no. 6, pp. 394–424, 2018.

[4] J. Maret-Ouda, K. Wahlin, M. Artama et al., "Risk of esophageal adenocarcinoma after antireflux surgery in patients with gastroesophageal reflux disease in the Nordic countries," *JAMA Oncology*, vol. 4, no. 11, pp. 1576–1582, 2018.

[5] M. Suntharalingam, K. Winter, D. Ilson et al., "Effect of the addition of cetuximab to paclitaxel, cisplatin, and radiation therapy for patients with esophageal cancer: the NRG oncology RTOG 0436 phase 3 randomized clinical trial," *JAMA Oncology*, vol. 3, no. 11, pp. 1520–1528, 2017.

[6] H. T. Liu, S. Liu, L. Liu, R. R. Ma, and P. Gao, "EGR1-mediated transcription of lncRNA-HNF1A-AS1 promotes cell-cycle progression in gastric cancer," *Cancer Research*, vol. 78, no. 20, pp. 5877–5890, 2018.

[7] K. Shun, L. Rui-Chao, L. Jun, M. Fan-Kai, F. Yi-Kuan, and F. Ming-Hao, "MicroRNA-192 regulates cell proliferation and cell cycle transition in acute myeloid leukemia via interaction with CCNT2," *International Journal of Hematology*, vol. 106, no. 2, pp. 258–265, 2017.

[8] K. Shun, L. Rui-Chao, M. Fan-Kai, and F. Ming-Hao, "NKILA inhibits NF-κB signaling and suppresses tumor metastasis," *Aging (Albany NY)*, vol. 10, no. 1, pp. 56–71, 2018.

[9] L. Rui-Chao, K. Shun, M. Fan-Kai et al., "CiRS-7 promotes growth and metastasis of esophageal squamous cell carcinoma via regulation of miR-7/HOXB13," *Cell Death & Disease*, vol. 9, no. 8, p. 838, 2018.

[10] P. Shannon, A. Markiel, O. Ozier et al., "Cytoscape: a software environment for integrated models of biomolecular interaction networks," *Genome Research*, vol. 13, no. 11, pp. 2498–2504, 2003.

[11] C. von Mering, M. Huynen, D. Jaeggi, S. Schmidt, P. Bork, and B. Snel, "STRING: a database of predicted functional associations between proteins," *Nucleic Acids Research*, vol. 31, no. 1, pp. 258–261, 2003.

[12] M. D. Robinson, D. J. McCarthy, and G. K. Smyth, "EdgeR: a bioconductor package for differential expression analysis of digital gene expression data," *Bioinformatics (Oxford, England)*, vol. 26, no. 1, pp. 139-140, 2010.

[13] J. X. Gu, X. Zhang, R. C. Miao et al., "Six-long non-coding RNA signature predicts recurrence-free survival in hepatocellular carcinoma," *World Journal of Gastroenterology*, vol. 25, no. 2, pp. 220–232, 2019.

[14] Y. Wu, P. S. Wang, B. G. Wang, L. Xu, W. X. Fang, and X. F. Che, "Genomewide identification of a novel six-lncRNA signature to improve prognosis prediction in resectable hepatocellular carcinoma," *Cancer Medicine*, vol. 7, pp. 6219–6233, 2018.

[15] S. Yue, D. Zipeng, Z. Xun, Z. Xiaotian, W. Guoqing, and L. Fan, "Down-regulation of the let-7i facilitates gastric cancer invasion and metastasis by targeting COL1A1," *Protein & Cell*, vol. 10, no. 2, pp. 143–148, 2019.

[16] Z. Wenfeng, Y. Yan, Z. Fayun, Z. Chunling, and L. Wei, "Chrysin promotes osteogenic differentiation via ERK/MAPK activation," *Protein & Cell*, vol. 4, no. 7, pp. 539–547, 2013.

[17] M. Lars, A. Junya, T. Ryuji et al., "Inhibition of microRNA-29b reduces murine abdominal aortic aneurysm development," *The Journal of Clinical Investigation*, vol. 122, no. 2, pp. 497–506, 2012.

[18] J. Rui and W. Changli, "MiR-29b-3p reverses cisplatin resistance by targeting COL1A1 in non-small-cell lung cancer A549/DDP cells," *Cancer Management and Research*, vol. 12, pp. 2559–2566, 2020.

[19] M. Klaassens, E. Reinstein, Y. Hilhorst-Hofstee et al., "Ehlers–Danlos arthrochalasia type (VIIA–B) – expanding the phenotype: from prenatal life through adulthood," *Clinical Genetics*, vol. 82, no. 2, pp. 121–130, 2012.

[20] L. Zhytnik, K. Maasalu, T. Reimand, B. H. Duy, S. Kõks, and A. Märtson, "Inter- and intrafamilial phenotypic variability in individuals with collagen-related osteogenesis imperfecta," *Clinical and Translational Science*, vol. 13, no. 5, pp. 960–971, 2020.

[21] C. Teresa, S. J. Menashe, and B. H. Taragin, "Radiographic overlap of recurrent Caffey disease and chronic recurrent multifocal osteomyelitis (CRMO) with considerations of molecular origins," *Pediatric Radiology*, vol. 50, no. 5, pp. 618–627, 2020.

[22] H. Fujii, N. Kawada, and Japan Study Group of NAFLD, "The role of insulin resistance and diabetes in nonalcoholic fatty liver disease," *International Journal of Molecular Sciences*, vol. 21, no. 11, p. 3863, 2020.

Hindawi
Computational and Mathematical Methods in Medicine
Volume 2023, Article ID 9860406, 1 page
https://doi.org/10.1155/2023/9860406

Retraction

Retracted: The Significance of Implementing Bilevel Positive Airway Pressure under Cluster Nursing in Improving the Survival Possibility of Patients with Severe Pulmonary Infection Complicated by Respiratory Failure

Computational and Mathematical Methods in Medicine

Received 5 December 2023; Accepted 5 December 2023; Published 6 December 2023

This article has been retracted by Hindawi, as publisher, following an investigation undertaken by the publisher [1]. This investigation has uncovered evidence of systematic manipulation of the publication and peer-review process. We cannot, therefore, vouch for the reliability or integrity of this article.

Please note that this notice is intended solely to alert readers that the peer-review process of this article has been compromised.

Wiley and Hindawi regret that the usual quality checks did not identify these issues before publication and have since put additional measures in place to safeguard research integrity.

We wish to credit our Research Integrity and Research Publishing teams and anonymous and named external researchers and research integrity experts for contributing to this investigation.

The corresponding author, as the representative of all authors, has been given the opportunity to register their agreement or disagreement to this retraction. We have kept a record of any response received.

References

[1] X. Fang and H. Yang, "The Significance of Implementing Bilevel Positive Airway Pressure under Cluster Nursing in Improving the Survival Possibility of Patients with Severe Pulmonary Infection Complicated by Respiratory Failure," *Computational and Mathematical Methods in Medicine*, vol. 2022, Article ID 2324797, 8 pages, 2022.

Hindawi
Computational and Mathematical Methods in Medicine
Volume 2022, Article ID 2324797, 8 pages
https://doi.org/10.1155/2022/2324797

Research Article

The Significance of Implementing Bilevel Positive Airway Pressure under Cluster Nursing in Improving the Survival Possibility of Patients with Severe Pulmonary Infection Complicated by Respiratory Failure

Xiao Fang and Haiyan Yang

Department of Emergency Intensive Care Unit, Nanjing First Hospital, Nanjing Medical University, Nanjing, Jiangsu 210014, China

Correspondence should be addressed to Haiyan Yang; fanfanmama0271@sina.com

Received 28 July 2022; Revised 23 August 2022; Accepted 27 August 2022; Published 19 September 2022

Academic Editor: Min Tang

Objective. To explore the significance of bilevel positive airway pressure (BIPAP) under cluster nursing in improving the survival probability of patients with severe pulmonary infection (SPI) complicated by respiratory failure (RF). *Methods*. This research included 153 SPI patients complicated by RF (SPI + RF) admitted between January 2020 and March 2022, including 55 cases in group A who were treated with BIPAP under cluster care during hospitalization, 47 cases in group B receiving invasive continuous mechanical ventilation during hospitalization, and 51 cases in group C treated with BIPAP under routine care during hospitalization. The three cohorts were compared regarding pre- and posttreatment serum inflammatory factors (IFs), blood gas (BG) parameters, heart rate (HR), and respiratory rate (RR). Besides, the cumulative time of ventilator use, successful ventilator weaning rate, mortality, and incidence of adverse events were counted. Finally, patients were scored for their psychological state using the Hamilton Anxiety/Depression Scale (HAMA/HAMD). *Results*. The posttreatment TNF-α, IL-6, PCT, WBC, and $PaCO_2$ reduced statistically in all the three groups, with the lowest levels found in group A and the highest in group B ($P < 0.05$); while PaO_2 and SpO_2 increased, with the highest values found in group A and the lowest in group B ($P < 0.05$). Among the three groups, group A had the shortest duration of ventilator use, the highest successful weaning rate, and the lowest incidence of adverse events ($P < 0.05$). Besides, HAMA and HAMD scores were the lowest in group A among the three groups, while those in group B were higher compared with group C ($P < 0.05$). *Conclusion*. The implementation of BIPAP under cluster nursing can effectively reduce inflammatory responses of SPI + RF patients, improve their vital signs, and enhance their psychological state, which has extremely high clinical application value.

1. Introduction

Pulmonary infection (PI) refers to inflammation of the lung parenchyma due to infection, usually caused by virus or bacterial infection [1]. The incidence of PI keeps increasing, in parallel with the aging of population in China [2]. In addition, due to the continuous decline of physical function in the elderly population, once pulmonary infection occurs, most of the cases are severe and difficult to treat [3]. Moreover, PI can lead to hypoxia and metabolic dysfunction, which can easily cause respiratory failure (RF) and other complications, posing a serious threat to patients' life safety [4]. Therefore, timely and effective treatment is of great clinical significance to reduce the mortality of severe pulmonary infection (SPI) complicated with RF (SPI + RF) and improve patients' outcomes [5].

The traditional treatment of SPI + RF mainly adopts tracheal intubation and ventilators [6]. Although this can establish an effective artificial respiration channel and maintain the patient's normal breathing, it is very likely to cause severe invasive stress and inflammatory reactions after intubation, resulting in other complications [7]. At the same time, endotracheal intubation will also make the patient very uncomfortable and increase the pain of the patient [8]. Not

only that, but more and more studies have pointed out that the success rate of endotracheal intubation is getting lower and lower in recent years [9, 10]. In contrast, bilevel positive airway pressure (BIPAP), with the advantage lay in the noninvasive treatment that can lower the risk of traumatic infection and reduce complications and improve safety, has been well received in clinic [11]. In addition, effective nursing intervention during treatment for patients with SPI + RF has been shown to reduce complications and significantly improve the prognosis of patients after treatment [12].

The application of personalized nursing strategies in disease treatment has gradually become a clinical consensus. For example, continuous nursing based on the Omaha system can improve the fatigue and mental state of patients with lung cancer during chemotherapy [13], and nursing care given at home can improve the quality of life of patients with gastric cancer [14] and so on. This fully shows that the development of personalized nursing strategies has an important effect on improving the treatment effect of various diseases. Of them, cluster nursing, a comprehensive and continuous nursing plan integrating the practice of evidence-based hospitals and patients' conditions, has achieved excellent results in the treatment of pressure ulcers, gastroenteritis, and other diseases as well as in the intensive care unit (ICU) [15–17]. However, its employment in SPI + RF and bilevel positive airway pressure (BIPAP) remains rarely reported.

We speculate that cluster nursing can effectively improve the patient's treatment experience and safety during the BIPAP treatment of patients with SPI combined with RF, which is of great significance to the patient's rehabilitation. Consequently, this research is carried out to provide effective treatment measures for the future clinical treatment of SPI + RF and reduce its harm.

2. Materials and Methods

2.1. Study Area. The study was carried out at department of emergency intensive care unit, Nanjing First Hospital from January 2020 to April 2022.

2.2. General Information. This research enrolled 153 SPI + RF patients admitted between January 2020 and March 2022 and grouped them as follows based on the difference in the treatment and care during hospitalization: group A ($n = 55$; BIPAP under cluster care), group B ($n = 47$; invasive continuous mechanical ventilation), and group C ($n = 51$; BIPAP under routine care). This study was conducted in strict accordance with the Declaration of Helsinki, and all subjects in the study signed the informed consent form by the patients themselves (or their immediate family members).

2.3. Eligibility Criteria. The included participants were all diagnosed as SPI by X-ray examination, arterial blood analysis, and routine blood tests and met the diagnostic criteria for RF [18] and all indications for mechanical ventilation [19], with complete medical records and no serious medical diseases nor lung tumors. On the contrary, those with severe liver and kidney dysfunction, mental disorders, RF caused by other diseases, drug allergies, or immune diseases were excluded. Besides, referrals, as well as those who refused, contradicted medical investigators and were unable to take care of themselves were ruled out.

2.4. Treatment Schemes. After admission, all patients were given routine treatments such as anti-inflammatory, blood pressure maintenance, cough relief, expectorant, and water-electrolyte balance adjustment. BIPAP: a Philips Respironics bilevel ventilator was adopted, and the nasal mask was selected, which was adjusted to self-trigger time control mode. The initial value was set to 6-8 cm H2O, which was gradually increased to an appropriate level within 5-20 minutes; the positive expiratory pressure was 4-6 cm H2O and could be increased according to the patient's RF degree. In patients with spontaneous breathing, the inspiratory time was usually set as 0.8-1.2 s with the inspiratory ratio of 1 : 1.5-2.0. At the beginning of ventilation, the nursing staff paid close attention to the patient's flatulence and other adverse reactions to make timely adjustments. In addition, according to the specific situation of the patient, the ventilator was temporarily stopped to perform operations such as drinking water and expectorating sputum, and weaning was performed until the patient could complete spontaneous breathing. Invasive continuous mechanical ventilation: first, an artificial airway was established, and the auxiliary control ventilation mode was used. When the patient's spontaneous breathing frequency was lower than the preset frequency or the patient's inspiratory efforts cannot trigger the ventilator, BIPAP was performed with the preset tidal volume and ventilation frequency; and if the patient's inspiratory can trigger the ventilator, the ventilation was performed with a higher frequency than the preset frequency and then gradually transition to synchronous intermittent mandatory pressure support ventilation until weaning.

2.5. Nursing Measures. Routine nursing: nursing staff informed patients of the treatment principles, precautions, and other contents, so that patients can better cooperate to complete the treatment. Basic psychological counseling was also given to eliminate patients' adverse emotions. The ward was maintained quiet and clean to create a good environment. Besides, patients' vital signs were closely watched, the respiratory tract was kept unobstructed, and sputum aspiration was provided. Cluster nursing: nursing staff involved in cluster nursing all mastered certain professional knowledge. A working group was established to discuss and improve nursing contents and implement nursing intervention strictly according to the plan. In addition, nurses took the initiative to communicate with patients to share past successful cases, as well as disease-related knowledge, matters needing attention in daily life, so as to improve patients' confidence in treatment and degree of coordination. Family members were also instructed to understand and master the relevant dietary management, so that patients eat high protein and vitamin foods. Furthermore, the respiratory tract care of the patients was carried out by special personnel,

and sputum suction machines were used if necessary for those with cough difficulties. Moreover, oral care was given regularly, and medical instruments and ventilator pipes were disinfected regularly. After weaning, patients were assisted to complete simple rehabilitation training, the oxygen demand was ensured, and their vital signs were closely observed.

2.6. Endpoints. Serum inflammatory factors (IFs), including tumor necrosis factor α (TNF-α), interleukin 6 (IL-6), procalcitonin (PCT), and white blood cell (WBC), were detected by ELISA before and after treatment. A blood gas (BG) analyzer detected the following BG parameters before and after treatment: oxygen partial pressure (PaO_2), arterial partial pressure of carbon dioxide ($PaCO_2$), and blood oxygen saturation (SpO_2). Pre- and posttreatment heart rate (HR) and respiratory rate (RR) were also recorded. The cumulative time of ventilator use, successful weaning rate (-
number of people who successfully removed mechanical ventilation equipment/total number × 100%), mortality (patients who died during treatment/total number × 100%), and incidence of adverse reactions (the number of adverse reactions/total number × 100%) were counted. Hamilton Anxiety Scale (HAMA) and Depression Scale (HAMD) were utilized for psychological state evaluation of patients [20]: the HAMA score includes 14 items, and the HAMD score includes 17 items. The alternative answers are asymptomatic, mild, moderate, severe, and very severe, with scores ranging from 0 to 4, with higher scores representing anxiety (depression) the more serious the situation is.

2.7. Statistics and Methods. SPSS23.0 performed statistical analysis of the data. The Chi-square test identified the differences of count data denoted by (%); one-way ANOVA and LSD intragroup tests were used for comparison of measurement data expressed as ($\bar{\chi} \pm s$). Statistical significance was indicated by $P < 0.05$.

3. Results

3.1. Summary of Results. In this experiment, the posttreatment TNF-α, IL-6, PCT, WBC, and PaCO2 reduced statistically in all the three groups, with the lowest levels found in group A and the highest in group B ($P < 0.05$); while PaO2 and SpO2 increased, with the highest values found in group A and the lowest in group B ($P < 0.05$). Among the three groups, group A had the shortest duration of ventilator use, the highest successful weaning rate, and the lowest incidence of adverse events ($P < 0.05$). Besides, HAMA and HAMD scores were the lowest in group A among the three groups ($P < 0.05$).

3.2. Patient Data. Patients' clinical data like age, BMI, sex, living environment, disease type, ethnicity, and smoking history were collected and statistically analyzed (Table 1). The results showed that there were no significant differences in age, BMI, gender, living environment, disease type, ethnicity, and smoking history among the three groups ($P > 0.05$), confirming that the three groups were comparable.

3.3. Alterations of Pre- and Posttreatment IFs. First, we detected pre- and posttreatment alterations in IFs in the three groups. The results identified nonsignificant differences among the groups prior to treatment ($P > 0.05$) and notably reduced levels after treatment ($P < 0.05$). The posttreatment TNF-α levels in groups A, B, and C were (2.48 ± 0.21) mg/L, (3.14 ± 0.33) mg/L, and (2.93 ± 0.25) mg/L, respectively, with the lowest in group A and the highest in group B ($P < 0.05$, Figure 1(a)). The posttreatment IL-6 levels in groups A, B, and C were (8.44 ± 0.78) μg/L, (11.07 ± 1.10) μg/L, and (9.65 ± 0.66) μg/L, respectively, with the level in group C higher than group A and lower than group B ($P < 0.05$, Figure 1(b)). The comparison of posttreatment PCT levels among the three groups also revealed the lowest level in group A and the highest in group B ($P < 0.05$, Figure 1(c)). At last, the WBC of group A after treatment was $(10.46 \pm 2.87) \times 109$/L, which was lower compared with groups B and C; the WBC of group B after treatment was $(14.86 \pm 3.08) \times 109$/L, higher versus group C ($P < 0.05$, Figure 1(d)).

3.4. Alterations of Pre- and Posttreatment BG Function. Subsequently, we compared alterations in BG function among the three groups. The results also determined no difference in pretreatment PaO_2, $PaCO_2$, and SpO_2 among the three groups ($P > 0.05$). Increased PaO_2 was observed in all the three groups after treatment, with the highest and the lowest level found in group A (71.91 ± 6.60 mmHg) and group B (59.92 ± 6.47 mmHg), respectively ($P < 0.05$, Figure 2(a)). A decrease in $PaCO_2$ was found in all the three groups after treatment; the posttreatment $PaCO_2$ in group A was (37.28 ± 3.70) mmHg, which was lower versus groups B and C, while that in group B was (44.98 ± 4.61) mmHg, higher than group C ($P < 0.05$, Figure 2(b)). SpO_2 was also elevated in the three groups after treatment, and the increase in Group A was the most significant, followed by group C ($P < 0.05$, Figure 2(c)).

3.5. Changes in Pre- and Posttreatment Vital Signs. Similarly, HR and RR differed insignificantly among the three groups prior to treatment ($P > 0.05$). After treatment, the HR of group A was (80.47 ± 4.90) beats/min, which was lower versus groups B and C, while the HR of group B was (92.06 ± 5.15) beats/min, higher than that of group C ($P < 0.05$, Figure 3(a)). The posttreatment RR levels of groups A, B, and C were (20.8 ± 22.04) times/min, (25.02 ± 1.85) times/min, and (22.65 ± 0.06) times/min, respectively, with that in group A being the highest and that in group B higher than group C ($P < 0.05$, Figure 3(b)). The posttreatment HR and RR in both groups was decreased compared with their pretreatment levels ($P < 0.05$).

3.6. Comparison of Therapeutic Effects. All patients in groups A and C were treated successfully with no patient death, while one patient died in group B. The three groups presented no significant difference in mortality ($P > 0.05$). The duration of ventilator use in groups A, B, and C was (95.08 ± 16.31) h, (114.25 ± 25.66) h, and (101.62 ± 15.10) h, respectively, with that in group B being the longest and

Table 1: Patient data.

	Group A ($n = 55$)	Group B ($n = 47$)	Group C ($n = 51$)	F or χ^2	P
Age	64.6 ± 5.5	65.6 ± 4.1	64.9 ± 3.9	0.621	0.539
BMI (kg/m^2)	25.61 ± 4.27	26.50 ± 3.36	26.02 ± 3.54	0.707	0.495
Gender				0.020	0.990
Men	32 (58.18)	28 (59.57)	30 (58.82)		
Woman	23 (41.81)	19 (40.23)	21 (41.18)		
Type of disease				0.136	0.998
Infectious pneumonia	30 (54.55)	26 (55.32)	29 (56.86)		
Aspiration pneumonia	17 (30.91)	15 (31.91)	15 (29.41)		
Bronchiolitis	8 (14.51)	6 (12.77)	7 (13.73)		
Nationality				1.024	0.599
Han	50 (90.91)	45 (95.74)	48 (94.12)		
Minority	5 (9.09)	2 (4.26)	3 (5.88)		

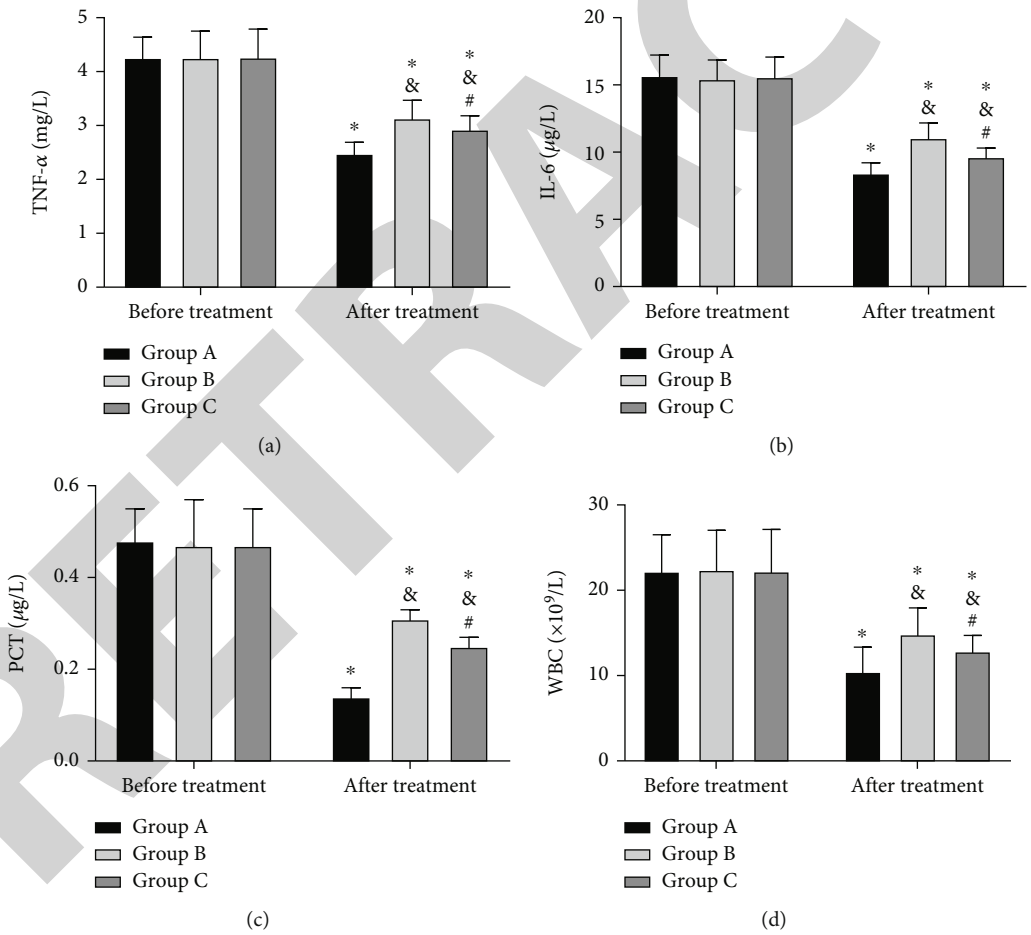

Figure 1: Alterations of pre- and posttreatment IFs. (a) Comparison of TNF-α among the three groups before and after treatment. (b) Comparison of IL-6 among the three groups before and after treatment. (c) Comparison of PCT among the three groups before and after treatment. (d) Comparison of WBC among the three groups before and after treatment. $^*P < 0.05$ compared to before treatment, $^\&P < 0.05$ compared to group A, $^\#P$ compared to group B.

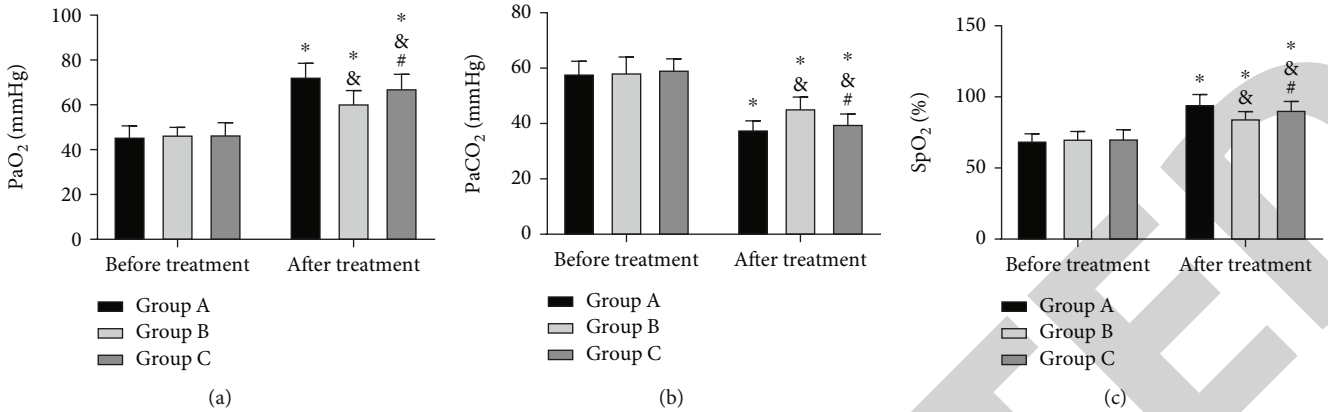

Figure 2: Alterations of pre- and posttreatment BG function. (a) Comparison of PaO2 among the three groups before and after treatment. (b) Comparison of PaCO2 among the three groups before and after treatment. (c) Comparison of SpO2 among the three groups before and after treatment. $^{*}P < 0.05$ compared to before treatment, $^{\&}P < 0.05$ compared to group A, $^{\#}P$ compared to group B.

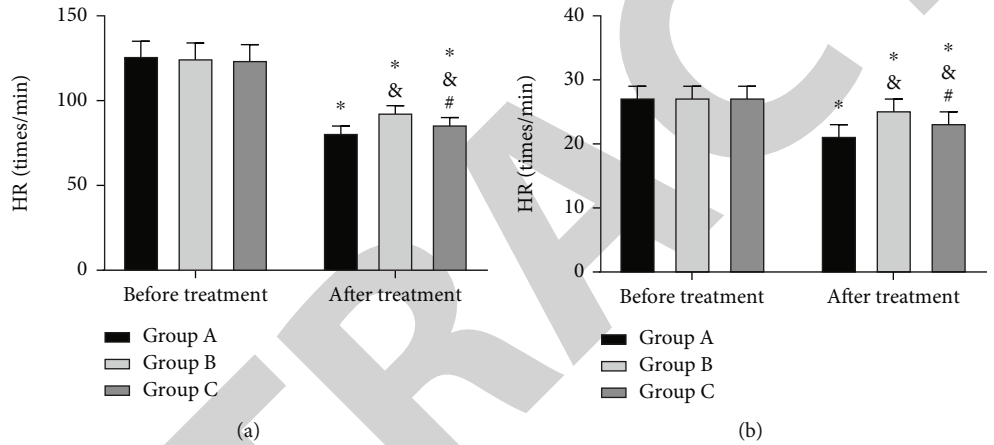

Figure 3: Changes in pre- and posttreatment vital signs. (a) Comparison of HR among the three groups before and after treatment. (b) Comparison of RR among the three groups before and after treatment. $^{*}P < 0.05$ compared to before treatment, $^{\&}P < 0.05$ compared to group A, $^{\#}P$ compared to group B.

that in group A being the shortest ($P < 0.05$). In addition, the successful weaning rate of group A was 100%, versus 98.04% in group C, with no marked difference between them ($P > 0.05$); while the successful weaning rate of group B was only 91.49%, lower than that of group A ($P < 0.05$, Table 2).

3.7. Comparison of Incidence of Adverse Reactions. Over the course of treatment, the incidence of adverse events observed in group A was 5.45%, the lowest of the three groups ($P < 0.05$); the incidence in group B was 29.79%, which was not significantly different from 13.73% in group C ($P < 0.05$), but higher than Group A ($P < 0.05$, Table 3).

3.8. Comparison of Psychological Scores. Finally, we evaluated and compared patients' psychological status among the three groups. HAMA and HAMD scores in group A were calculated to be (22.55 ± 1.92) and (24.78 ± 1.69), respectively, which were the lowest among the three groups. While HAMA and HAMD scores in group B were (34.30 ± 1.76) and (34.98 ± 2.07), respectively, which were higher versus group A. HAMA and HAMD scores in group C were higher compared with group A and lower versus group B ($P < 0.05$, Figures 4(a) and 4(b)).

4. Discussion

At present, the treatment of SPI patients mainly focuses on anti-infection, maintenance of patients' respiratory function, and improvement of acid-base metabolism balance [21, 22]. Among them, BIPAP has gradually become the first choice for SPI + RF, and how to further improve the therapeutic efficacy of patients is the hotspot of clinical research [23–25]. Therefore, this study may be of great implications for the application of BIPAP under cluster nursing and for further improving the therapeutic effect of SPI + RF in the future.

Endotoxin produced by pathogens can stimulate immune cells to release massive inflammatory factors, leading to endothelial cell adhesion and neutrophil proliferation, during which proteases are released in large quantities, causing damage to vascular endothelial cells and epithelial cells, and finally causing pulmonary fibrosis and microthrombosis [26, 27]. Therefore, the level of IFs in the body is of great

Table 2: Comparison of therapeutic effects.

	Group A ($n = 55$)	Group B ($n = 47$)	Group C ($n = 51$)	F or χ^2	P
Time of ventilator use (h)	95.08 ± 16.31	114.25 ± 25.66*	101.62 ± 15.10*#	12.700	<0.001
Successful weaning rate	55 (100.0)	43 (91.49%)*	50 (98.04)	6.220	0.045
Mortality	0 (0.0)	1 (2.13%)	0 (0.0)	2.270	0.321

Table 3: Comparison of incidence of adverse reactions.

	Group A ($n = 55$)	Group B ($n = 47$)	Group C ($n = 51$)	χ^2	P
Bloating	1 (1.82)	4 (8.51)	2 (3.92)		
Sore throat	1 (1.82)	5 (10.64)	2 (3.92)		
Malnutrition	0 (0.0)	2 (4.26)	1 (1.96)		
Chest tightness	1 (1.82)	3 (6.38)	2 (3.92)		
Incidence of adverse reactions (%)	5.45%	29.79%*	13.73%	11.570	0.003

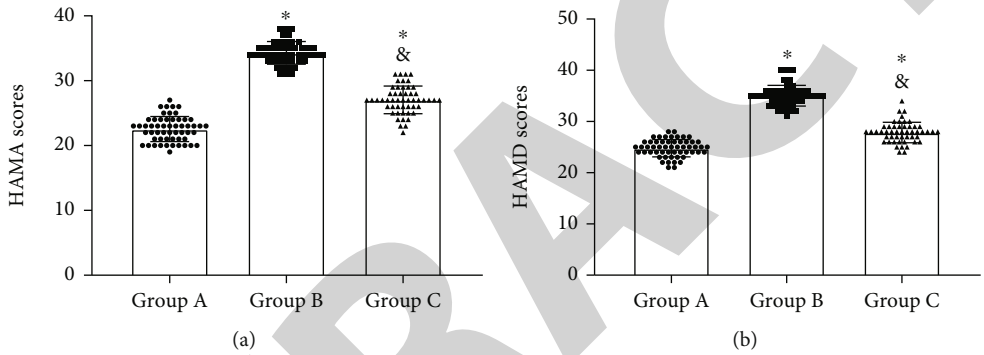

Figure 4: Comparison of psychological scores. (a) Comparison of HAMA scores. (b) Comparison of HAMD Scores. $^*P < 0.05$ compared to group A, $^\#P$ compared to group B.

significance in evaluating the development of SPI + RF. In this research, TNF-α, IL-6, PCT, and WBC were reduced statistically in all the three groups after treatment, with lower levels in groups A and C compared with group B, indicating that BIPAP was better than conventional mechanical ventilation in alleviating patients' inflammatory responses, which was consistent with past literature [28, 29]. Besides, we found better improved BG function and vital signs in groups A and C after treatment, further demonstrating the excellent application effect of BIPAP. Previous studies have suggested that BIPAP therapy can warm and humidify the inhaled gas through the upper respiratory tract, meet the needs of mask mechanical ventilation, shorten the hospitalization time of RF patients, and reduce the rate of tracheal intubation; in SPI, it can also effectively remove a large amount of inflammatory secretions in the airway, reduce airway obstruction, and improve lung ventilation and ventilation function [30, 31]. Therefore, under BIPAP, not only the high resistance in the airway can be overcome but also the workload of the respiratory muscles and the oxygen consumption can be reduced, so as to avoid the overwork of the respiratory muscles, improve the compliance of the lungs, and adjust the oxygen partial pressure, ultimately lowering the possibility of damage to the body and other organs. This study identified a lower incidence of adverse reactions in groups A and C compared with group B, which can also illustrate this point of view. Second, better survey results and lower HAMA and HAMD scores were determined in group A versus group C, which we think is due to the application effect of cluster nursing. Through cluster nursing, the professionalism and dynamics of nursing services can be guaranteed, reflecting the pertinence and integrity of nursing measures [32, 33]. Among them, the psychological attention to patients can enable them to fully understand the treatment methods and related operations, as well as self-regulation of bad emotions. Postural care can prevent reflux, aspiration, etc., to improve the comfort of treatment. Phlegm-expelling nursing is the focus of cluster nursing, which aims to ensure the unobstructed respiratory tract. Diet care can scientifically guide patients' diet and ensure balanced nutrition. And regular cleaning of oral secretions in oral care can ensure oral hygiene and avoid complications such as flatulence. All these measures of cluster nursing explain significantly accelerated physical rehabilitation and psychological improvement of patients compared with conventional nursing, indicating the important role of cluster nursing in future treatment of SPI + RF. In a previous study, we also found that cluster nursing can also reduce bilirubin levels, improve jaundice symptoms, and shorten the course of the disease in neonatal ABO solution treatment [34]; this also illustrates once again the citation value of cluster nursing in clinical practice. And for patients with gestational hypertension

combined with osteoarthritis, the use of cluster nursing can reduce patient negative emotions, increase satisfaction, and improve maternal and infant outcomes [35]. It can be seen that cluster nursing is suitable for patients with various diseases, different genders, and different ages and has important clinical research significance.

Of course, due to the small number of cases included in this experiment, there may be chance of statistical calculation results, so we need to include more patient data for verification in the follow-up. Second, since there is no unified guideline for cluster nursing in clinic at present, the specific protocols implemented in this study may still have room for improvement. In addition, we need to follow up all study subjects for a longer time to evaluate their long-term outcomes.

5. Conclusion

The implementation of BIPAP under cluster nursing can effectively reduce inflammatory responses of SPI + RF patients, improve their vital signs, and enhance their psychological state, which has extremely high clinical application value.

Data Availability

The datasets used and/or analyzed during the current study are available from the corresponding author on reasonable request.

Conflicts of Interest

The authors have no conflicts of interest to declare.

References

[1] H. L. Twigg, G. M. Weinstock, and K. S. Knox, "Lung microbiome in human immunodeficiency virus infection," *Translational Research*, vol. 179, pp. 97–107, 2017.

[2] D. K. Meyerholz and A. P. Beck, "Histopathologic evaluation and scoring of viral lung infection," *Methods in Molecular Biology*, vol. 2099, pp. 205–220, 2020.

[3] W. V. Lin, R. L. Kruse, K. Yang, and D. M. Musher, "Diagnosis and management of pulmonary infection due to _Rhodococcus equi_," *Clinical Microbiology and Infection*, vol. 25, no. 3, pp. 310–315, 2019.

[4] F. Touchon, Y. Trigui, E. Prud'homme et al., "Awake prone positioning for hypoxaemic respiratory failure: past, COVID-19 and perspectives," *European Respiratory Review*, vol. 30, no. 160, p. 210022, 2021.

[5] A. R. Falsey, P. A. Hennessey, M. A. Formica, C. Cox, and E. E. Walsh, "Respiratory syncytial virus infection in elderly and high-risk adults," *New England Journal of Medicine*, vol. 352, no. 17, pp. 1749–1759, 2005.

[6] R. Scala and L. Pisani, "Noninvasive ventilation in acute respiratory failure: which recipe for success?," *European Respiratory Review*, vol. 27, no. 149, 2018.

[7] G. D. Perkins, C. Ji, B. A. Connolly et al., "Effect of noninvasive respiratory strategies on intubation or mortality among patients with acute hypoxemic respiratory failure and COVID-19: the RECOVERY-RS randomized clinical trial," *JAMA*, vol. 327, no. 6, pp. 546–558, 2022.

[8] T. Yang, Y. Shen, J. G. Park et al., "Outcome after intubation for septic shock with respiratory distress and hemodynamic compromise: an observational study," *BMC Anesthesiology*, vol. 21, no. 1, p. 253, 2021.

[9] J. Zhang, X. He, J. Hu, and T. Li, "Failure of early extubation among cases of coronavirus disease-19 respiratory failure: case report and clinical experience," *Medicine (Baltimore)*, vol. 99, no. 27, article e20843, 2020.

[10] M. Antonelli, E. Azoulay, M. Bonten et al., "Year in review in intensive care medicine, 2008: II. Experimental, acute respiratory failure and ARDS, mechanical ventilation and endotracheal intubation," *Intensive Care Medicine*, vol. 35, no. 2, pp. 215–231, 2009.

[11] S. L. Raidal, C. S. M. Catanchin, L. Burgmeestre, and C. T. Quinn, "Bi-level positive airway pressure for non-invasive respiratory support of foals," *Frontiers in Veterinary Science*, vol. 8, article 741720, 2021.

[12] R. Pan, G. Y. Chen, J. Wang et al., "Bi-level nasal positive airway pressure (BiPAP) versus nasal continuous positive airway pressure (CPAP) for preterm infants with birth weight less than 1500 g and respiratory distress syndrome following INSURE treatment: a two-center randomized controlled trial," *Current Medical Science*, vol. 41, no. 3, pp. 542–547, 2021.

[13] L. Ning, C. Yuan, Y. Li et al., "Effect of continuous nursing based on the Omaha system on cancer-related fatigue in patients with lung cancer undergoing chemotherapy: a randomized controlled trial," *Annals of Palliative Medicine*, vol. 10, no. 1, pp. 323–332, 2021.

[14] S. Bilgin and S. Gozum, "Effect of nursing care given at home on the quality of life of patients with stomach cancer and their family caregivers' nursing care," *European Journal of Cancer Care*, vol. 27, no. 2, article e12567, 2018.

[15] S. Roberts, E. McInnes, T. Bucknall, M. Wallis, M. Banks, and W. Chaboyer, "Process evaluation of a cluster-randomised trial testing a pressure ulcer prevention care bundle: a mixed-methods study," *Implementation Science*, vol. 12, no. 1, p. 18, 2017.

[16] M. Saukkoriipi, A. M. Tuomikoski, P. Sivonen et al., "Clustering clinical learning environment and mentoring perceptions of nursing and midwifery students: a cross-sectional study," *Journal of Advanced Nursing*, vol. 76, no. 9, pp. 2336–2347, 2020.

[17] S. Martin-Iglesias, M. J. Santamaria-Martin, A. Alonso-Alvarez et al., "Effectiveness of an educational group intervention in primary healthcare for continued exclusive breast-feeding: PROLACT study," *BMC Pregnancy Childbirth*, vol. 18, no. 1, p. 59, 2018.

[18] L. J. Staub, R. R. Mazzali Biscaro, E. Kaszubowski, and R. Maurici, "Lung ultrasound for the emergency diagnosis of pneumonia, acute heart failure, and exacerbations of chronic obstructive pulmonary disease/asthma in adults: a systematic review and meta-analysis," *The Journal of Emergency Medicine*, vol. 56, no. 1, pp. 53–69, 2019.

[19] T. Pham, L. J. Brochard, and A. S. Slutsky, "Mechanical ventilation: state of the art," *Mayo Clinic Proceedings*, vol. 92, no. 9, pp. 1382–1400, 2017.

[20] Y. Duan, J. Wei, W. Geng et al., "Research on cognitive function in anxious depression patients in China," *Journal of Affective Disorders*, vol. 280, pp. 121–126, 2021.

Hindawi
Computational and Mathematical Methods in Medicine
Volume 2023, Article ID 9824960, 1 page
https://doi.org/10.1155/2023/9824960

Retraction

Retracted: Efficacy and Prediction Model Construction of Drug-Coated Balloon Combined with Cutting Balloon Angioplasty in the Treatment of Drug-Eluting Stent In-Stent Restenosis

Computational and Mathematical Methods in Medicine

Received 12 December 2023; Accepted 12 December 2023; Published 13 December 2023

This article has been retracted by Hindawi, as publisher, following an investigation undertaken by the publisher [1]. This investigation has uncovered evidence of systematic manipulation of the publication and peer-review process. We cannot, therefore, vouch for the reliability or integrity of this article.

Please note that this notice is intended solely to alert readers that the peer-review process of this article has been compromised.

Wiley and Hindawi regret that the usual quality checks did not identify these issues before publication and have since put additional measures in place to safeguard research integrity.

We wish to credit our Research Integrity and Research Publishing teams and anonymous and named external researchers and research integrity experts for contributing to this investigation.

The corresponding author, as the representative of all authors, has been given the opportunity to register their agreement or disagreement to this retraction. We have kept a record of any response received.

References

[1] H. Wu, T. Yu, T. Fan, and W. Liao, "Efficacy and Prediction Model Construction of Drug-Coated Balloon Combined with Cutting Balloon Angioplasty in the Treatment of Drug-Eluting Stent In-Stent Restenosis," *Computational and Mathematical Methods in Medicine*, vol. 2022, Article ID 9832622, 8 pages, 2022.

Hindawi
Computational and Mathematical Methods in Medicine
Volume 2022, Article ID 9832622, 8 pages
https://doi.org/10.1155/2022/9832622

Research Article

Efficacy and Prediction Model Construction of Drug-Coated Balloon Combined with Cutting Balloon Angioplasty in the Treatment of Drug-Eluting Stent In-Stent Restenosis

Haokun Wu, Tianhao Yu, Ting Fan, and Wenjun Liao

Guangdong Second Provincial General Hospital, Guangzhou, Guangdong 510317, China

Correspondence should be addressed to Haokun Wu; xnkwhk@163.com

Received 30 June 2022; Revised 9 August 2022; Accepted 24 August 2022; Published 19 September 2022

Academic Editor: Min Tang

Objective. To investigate the efficacy of drug-coated balloon (DCB) combined with cutting balloon angioplasty (CBA) in the treatment of drug-eluting stent in-stent restenosis (DES-ISR) and to construct a predictive model for the occurrence of DES-ISR. *Methods*.According to the criteria of diagnosis, inclusion, and exclusion, DES-ISR patients who were treated in the outpatient and inpatient departments of cardiovascular medicine of Second People's Hospital of Guangdong Province from July 2021 to December 2021 were included. A total of 72 cases were planned to be enrolled, including 36 cases in the control group and 36 cases in the experimental group. The control group was treated with DCB, and the experimental group was combined with CBA. The treatment success rate, coronary angiography results before and after surgery, and the incidence of major adverse cardiovascular events during the follow-up period were compared between the two groups. Seventy-two DES-ISR patients were divided into ISR group and 59 non-ISR patients were divided into non-ISR group. The clinical data of the two groups were compared to analyze the risk factors affecting the occurrence of DES-ISR, and the prediction model was established. *Results*. The surgical success rate of the experimental group was 94.44% (34/36), which was higher than the 77.78% (28/36) of the control group ($P < 0.05$). The minimum lumen diameter (MLD) of the experimental group 6 months after operation was greater than that of the control group, the late lumen loss (LL) and lumen stenosis rate were higher than those in the control group, and the incidence of major adverse cardiovascular events was lower than that in the control group ($P < 0.05$). In the ISR group, the proportion of patients with abnormal BMI, smoking, hypertension, diabetes, and family history of coronary heart disease and multivessel coronary artery disease was higher than that in the non-ISR group, the degree of stenosis target lesion was higher than that in the non-ISR group, the diameter of target lesion and stent diameter were smaller than those in the non-ISR group, and the length of target lesion and stent length were longer than those in the non-ISR group; the number of stents was more than that in the non-ISR group ($P < 0.05$). Combined hypertension, multiple coronary artery lesions, stenosis target lesion degree ≥85.05%, and target lesion length ≥36.88 mm were risk factors for DES-ISR, and target lesion diameter ≥3.15 mm and stent diameter ≥3.15 mm were protective factors ($P < 0.05$). The prediction model of DES-ISR was obtained by multiple logistic regression analysis, $P = 1[1 + e^{(2.281+3.321X_{\text{hypertension}}+3.427X_{\text{umber of arterial lesions}}+3.359X_{\text{stenosis target lesion degree}}-3.143X_{\text{target lesion diameter}}+0.650X_{\text{target lesion length}}-10.159X_{\text{stent diameter}})}]$. The Hosmer-Lemeshow test showed that Hosmer-Lemeshow $\chi^2 = 0.925$, $P = 0.413$; the ROC curve analysis showed that the AUC of the prediction model for the occurrence of DES-ISR was 0.924, the SE value was 0.022, and the 95% CI was 0.880-0.967. *Conclusion*. DCB combined with CBA has good clinical efficacy in the treatment of DES-ISR, which can reduce the rate of lumen stenosis and the incidence of adverse cardiovascular events. The prediction model established according to risk factors has high predictive value for the occurrence of DES-ISR.

1. Introduction

Coronary atherosclerotic heart disease is a heart disease caused by atherosclerotic lesions in the coronary vessels, resulting in stenosis or obstruction of the vascular lumen, resulting in myocardial ischemia, hypoxia, or necrosis [1]. At present, 7.3 million people die of ischemic heart disease every year in the world, ranking first among all diseases, accounting for 12.8% of all deaths from diseases [2]. Currently, percutaneous coronary drug-eluting stent (DES) has become the main means for the treatment of coronary heart disease, but the occurrence of in-stent restenosis (ISR) limits its long-term clinical benefits [3]. Although DES has been widely used and the design of stent structures has been continuously improved, the incidence of ISR in patients with DES is still as high as 10% [4]. ISR refers to restenosis of coronary artery in-stent lesions caused by coronary artery endothelial injury and gradual proliferation of intimal tissue caused by percutaneous coronary interventional therapy, and its mechanism includes biological, mechanical, and technical factors [5]. Relevant studies have pointed out that due to factors such as poor vascular endothelialization, local allergic reactions, and individual differences, there are still a considerable proportion of patients with adverse clinical and anatomical characteristics, and the analysis of risk factors affecting the occurrence of ISR in patients and effective intervention can reduce the risk of ISR [6, 7]. Balloon dilation is the main treatment for ISR. Domestic studies have shown that, compared with conventional high-pressure balloons, cutting balloon angioplasty (CBA) can squeeze and cut plaques to a certain extent, reduce complications such as vascular dissection and loss, and can increase immediate lumen acquisition rate and minimum lumen area after stent implantation [8]. Previous studies have pointed out that because of its ability to provide anti-restenosis drugs to the vascular endothelium and the avoidance of multilayer stent implantation, the drug-coated balloon (DCB) has received different clinical indications including the treatment of ISR in the past few years [9]. Therefore, this study combined the two in the clinical treatment of DES-ISR, aiming to explore its clinical efficacy on DES-ISR, and to construct a prediction model for the occurrence of DES-ISR, so as to provide reference for the clinical prevention and treatment of the disease.

2. Materials and Methods

2.1. Clinical Data. DES-ISR patients treated in the outpatient and inpatient departments of Department of Cardiovascular Medicine of the Second People's Hospital of Guangdong Province from July 2021 to December 2021 were included according to diagnosis, inclusion, and exclusion criteria. A total of 72 cases were planned to be enrolled, including 36 cases in the control group and 36 cases in the experimental group. There was no significant difference in general data between the two groups ($P > 0.05$), as shown in Table 1. This study has been approved by the hospital medical ethics committee.

2.1.1. Diagnostic Criteria. ISR is diagnosed according to relevant guidelines [10]: multi-projection coronary angiography or intracoronary imaging examinations indicated that the diameter of the stent lumen of the coronary target vessel has a stenosis of ≥50%, including coronary artery within 5 mm of both ends of the stent.

2.1.2. Inclusion Criteria. (1) Aged 18-80 years old, male or non-pregnant woman; (2) patients treated with DCB implantation and diagnosed with ISR 6-12 months after operation; (3) lesion length ≤40 mm; (4) subjects who understood the purpose of the experiment, voluntarily participated, and signed the written informed consent; (5) patients diagnosed with DES-ISR by coronary angiography after 6-9 months of PCI; (6) complete clinical data.

2.1.3. Exclusion Criteria. (1) Patients allergic to paclitaxel drugs; (2) patients with contraindications of antithrombotic drugs; (3) patients who were intolerant or allergic to more than one anti-platelet aggregation drug; (4) patients with myocardial infarction within one week; (5) patients with history of cerebrovascular accident or peptic ulcer or gastric bleeding within 6 months, or who were judged to be bleeding constitution by researchers; (6) restenosis in left main trunk stent; (7) lesion length >40 mm; (8) there was more than one layer of stent in the target vessel; (9) ISR lesions with residual stenosis >40% after conventional pretreatment; (10) glycated hemoglobin ≥9%; (11) patients with other types of heart disease; (12) subjects had poor compliance and could not complete the study as required.

2.1.4. Criteria for Dropout and Exclusion of Cases. (1) Those who did not meet the criteria and were mistakenly included; (2) patients who failed to follow the prescribed treatment regimen after inclusion; (3) patients whose treatment was discontinued or lost to follow-up for other reasons resulting in missing or no test records. For the included cases, those who meet one of the above criteria were excluded. All the excluded cases should be explained the reasons for exclusion, and their observation table should be kept for future reference

2.2. Methods

2.2.1. Control Group. The target blood vessel was examined by IVUS, and the high-pressure balloon was fully predilated. DCB of appropriate size was selected after coronary angiography showed no dissection, residual stenosis of less than 40%, and distal blood flow of TIMI grade 3 (Yinyi Biological Technology Co., LTD, Qingzhou® Coronary Drug Delivery System). The relevant longitudinal length of its expanded area should be larger than that of the pre-expanded balloon, and the diameter of DCB should be higher than that of the pre-expanded balloon, so as to ensure that DCB can cover the pre-expanded area by 2-3 mm on both sides and prevent the geographical loss of DCB. The operation should be carried out as soon as possible after the DCB contacted the blood, and the expansion time was 60-90s. IVUS examination was performed after treatment.

Table 1: Comparison of general data between the experimental group and the control group.

General data	Experimental group (n =36)	Control group (n =36)	χ^2 /t	P
Gender male (cases)	20	22	0.229	0.633
Age (years)	67.28 ± 5.04	66.06 ± 5.01	1.030	0.307
Abnormal BMI (cases)	20	23	0.520	0.471
Smoking (cases)	17	18	0.056	0.814
Hypertension (cases)	14	17	0.510	0.475
Diabetes (cases)	15	17	0.225	0.635
Hyperlipidemia (cases)	4	6	0.465	0.496
Family history of coronary heart disease (cases)	18	17	0.056	0.814

2.2.2. Treatment Method of Experimental Group. IVUS was used to examine the target vessels, and the high-pressure balloon was fully predilated, and then a cutting balloon was used to dilate the lesions (the model of the cutting balloon was selected according to the ratio of 1 : 1 to the actual stent diameter). During the dilation of the lesion, the cut balloon was slowly pressurized and predilated for 2 to 3 times. DCB was applied and other steps were the same as the control group after coronary angiography showed no dissection, residual stenosis of less than 40%, and distal blood flow of TIMI grade 3.

2.3. Clinical Data Collection. The patient's baseline data and clinical data were collected using the information system of hospital, mainly including demographic characteristics [age, gender, BMI (normally 18.5 ~ 23.9 kg/m^2), etc.], cardiovascular risk factors (such as smoking, hypertension, diabetes, hypercholesterolemia, hyperuricemia, and family history of coronary heart disease), angiographic information (such as multivessel disease, target lesion location, double vessel disease, degree of stenosis target lesion, and length of target lesion), surgical steps (such as stent length and stent diameter), and postoperative medication (such as statins, beta-blockers, ACEIs, ARBs, and calcium channel blockers).

2.4. Evaluation Criteria of Curative Effect [11]. Successful treatment: after treatment, the lumen of the target vessels was significantly enlarged, the residual stenosis of the main branch vessels was <20%, and the residual stenosis of the branch vessels was <30%. Angiography showed that blood flow of TIMI grade 3 was obtained, and there were no major clinical complications during hospitalization, and no recurrence occurred 6 months after surgery.

2.5. Coronary Angiography. All patients underwent coronary angiography before surgery, immediately after surgery, and 6 months after surgery. Coronary quantitative analysis software was used to analyze the imaging data of coronary angiography, mainly including minimal lumen diameter (MLD), reference vessel diameter (RVD), late lumen loss (LL), and lumen stenosis rate.

2.6. Statistical Processing. SPSS 22.0 software was used to process data, enumeration data were expressed as %, and differences between groups were compared by χ^2 test; measurement data were expressed as $\bar{x} \pm s$ after normality test, and differences between groups were compared by t test. Logistic regression was used to analyze the risk factors for DES-ISR. The Hosmer-Lemeshow test was used to analyze the degree of fitting between the prediction model and the standard curve. ROC curve was used to analyze the predictive value of the model for DES-ISR occurrence. $P < 0.05$ indicated that the difference was statistically significant.

3. Results

3.1. Comparison of Therapeutic Effects between the Two Groups. The surgical success rate of the experimental group was 94.44% (34/36), which was higher than 77.78% (28/36) of the control group ($\chi^2 = 0.041$, $P < 0.05$).

3.2. Comparison of Coronary Angiography Results between the Two Groups before and 6 Months after Surgery. There was no significant difference in preoperative RVD and MLD immediately after operation between the two groups ($P > 0.05$); the MLD of the experimental group was higher than that of the control group 6 months after surgery, and the LL and lumen stenosis rate were higher than those of the control group ($P < 0.05$), as shown in Table 2.

3.3. Comparison of the Incidence of Major Adverse Cardiovascular Events between the Two Groups. The incidence of major adverse cardiovascular events in the experimental group was lower than that in the control group ($P < 0.05$), as shown in Table 3.

3.4. Univariate Analysis of Factors Affecting the Occurrence of DES-ISR. In the ISR group, the proportion of patients with abnormal BMI, smoking, hypertension, diabetes, and family history of coronary heart disease and multivessel coronary artery disease was higher than that in the non-ISR group, the degree of stenosis target lesion was higher than that in the non-ISR group, the diameter of target lesion and stent diameter were smaller than that in the non-ISR group, the length of target lesion and stent was longer than that in the non-ISR group, and the number of stents was higher than that of the non-ISR group ($P < 0.05$), as shown in Table 4.

3.5. Multivariate Analysis of Factors Affecting the Occurrence of DES-ISR. Combined hypertension, multivessel coronary lesions, stenosis target lesion degree ≥85.05%, and target lesion length ≥36.88 mm were risk factors affecting the occurrence of DES-ISR, and target lesion diameter

Table 2: Comparison of coronary angiography results between the two groups before and 6 months after surgery.

Group	n	MLD (mm)		Lumen stenosis rate (%)		RVD (mm)	LL (mm)
		Immediately after surgery	Six months after surgery	Before surgery	Six months after surgery		
Experimental group	36	0.98 ± 0.17	1.79 ± 0.32	69.78 ± 5.31	24.19 ± 3.19	2.89 ± 0.47	0.51 ± 0.13
Control group	36	0.96 ± 0.19	1.51 ± 0.28	71.57 ± 5.05	30.07 ± 3.52	2.83 ± 0.51	0.67 ± 0.14
t		0.471	3.951	1.466	7.427	0.519	5.025
P		0.639	<0.001	0.147	<0.001	0.605	<0.001

Table 3: Comparison of the incidence of major adverse cardiovascular events between the two groups (cases, %).

Group	n	Target vessel revascularization	Target lesion revascularization	Nonfatal myocardial infarction	All-cause mortality	Incidence
Experimental group	36	1	0	2	1	11.11 (4)
Control group	36	2	1	5	2	30.56 (11)
χ^2						4.126
P						0.042

≥3.15 mm and stent diameter ≥3.15 mm were protective factors ($P < 0.05$), as shown in Table 5.

3.6. Establishment of the Prediction Model and Analysis of the Calibration Degree of the Model. The prediction model of the occurrence of DES-ISR was obtained by multivariate logistic regression analysis, $P = 1[1 + e^{(2.281+3.321X_{\text{hypertension}} + 3.427X_{\text{number of arterial lesions}}+3.359X_{\text{stenosis target}}}$ lesion degree $3.143X_{\text{target lesion diameter}}+0.650X$ $_{\text{target lesion length}}-10.159$ $X_{\text{stent diameter}})]$. The Hosmer-Lemeshow test showed that Hosmer-Lemeshow $\chi^2 = 0.925$, $P = 0.413$, as shown in Figure 1.

3.7. Prediction Efficiency Analysis of the Prediction Model. According to the ROC curve analysis, the AUC of the prediction model to predict the occurrence of DES-ISR was 0.924, the SE value was 0.022, and the 95% CI was 0.880-0.967, as shown in Figure 2.

4. Discussion

ISR is a major clinical problem after interventional therapy, which is mainly caused by coronary intimal hyperplasia, and oral administration alone to reduce the incidence of ISR is ineffective and has side effects [12]. Relevant studies have pointed out that DCB treatment for DES-ISR patients can improve the degree of in-stent stenosis [13, 14]. It has also been reported that CBA can reduce the incidence of repeated ISR and have less lumen loss than ordinary high-pressure balloon preconditioning [15, 16]. DCB is a commonly used treatment for coronary artery diseases, which can treat stenosis or occlusive vascular diseases by carrying chemotherapy drugs to the surface of the diseased vessels. The chemical drug paclitaxel on its surface makes full contact with the vascular wall of the lesion through balloon dilation and quickly penetrates into the arterial wall to inhibit intimal hyperplasia and prevent vascular restenosis [17, 18]. Studies have shown that although DCB can release anti-proliferative drugs to the coronary vascular wall through balloon dilation of local vessels to achieve the effect of inhibiting intima hyperplasia, some patients will still have adverse cardiovascular events in later stage, which affects the prognosis [19, 20]. Some scholars have found that the combination of CBA on the basis of DCB in the treatment of ISR can achieve a better therapeutic effect [21, 22]. This study found that the surgical success rate of the experimental group was higher than that of the control group, and after 6 months of surgery, the MLD, LL, and the lumen stenosis rate were higher than those of the control group, indicating that DCB combined with CBA has a good clinical effect on the treatment of DES-ISR and can reduce the lumen stenosis rate. The reason is that the drug balloon effectively reduces the inflammatory response of the intima of blood vessels and inhibits intima hyperplasia in the short term after surgery. In addition, precise expansion with CBA can prevent the balloon from sliding out of the stent, resulting in stent edge injury. Cutting treatment can cut the new intima tissue, which is theoretically helpful for the uptake of drugs delivered by DCB, thus improving the therapeutic effect [23]. In addition, the results show that combined treatment can reduce the incidence of adverse cardiovascular events, which is mainly related to the fact that CBA can squeeze and cut plaque to a certain extent, reduce complications such as vascular dissection and loss, and increase the immediate lumen acquisition rate, and retreatment reduces the circumferential force of the blood

Table 4: Univariate analysis of factors affecting the occurrence of DES-ISR.

Factors	ISR group (n =72)	Non-ISR group (n =59)	χ^2 /t value	P value
Age (years)	65.08 ± 5.38	64.34 ± 5.07	0.804	0.423
Gender (cases)				
Male	42	35	0.013	0.909
Female	30	24		
Abnormal BMI (cases)	43	20	8.663	0.003
Smoking (cases)	35	13	9.866	0.002
Hypertension (cases)	31	9	11.816	0.001
Diabetes (cases)	32	11	9.789	0.002
Hyperlipidemia (cases)	10	8	0.003	0.957
Family history of coronary heart disease (cases)	35	12	11.267	0.001
Platelets ($*10^{11}$)	1.07 ± 0.19	1.13 ± 0.24	1.597	0.113
LVEF (%)	60.32 ± 5.09	59.83 ± 5.11	0.547	0.585
Number of arterial lesions (cases)				
Multivessel lesions	61	29	19.081	<0.001
Single-vessel lesion	11	30		
Target lesion location (cases)				
Anterior descending branch	42	34	0.009	0.996
Circumflex branch	13	11		
Right coronary artery	17	14		
Stenosis target lesion degree (%)	88.34 ± 3.16	81.62 ± 3.86	10.958	<0.001
Target lesion diameter (mm)	2.85 ± 0.51	3.51 ± 0.59	6.866	<0.001
Target lesion length (mm)	41.69 ± 4.32	31.53 ± 5.04	12.422	<0.001
Stent implantation time (years)	4.07 ± 0.59	4.13 ± 0.67	0.545	0.587
Stent length (mm)	23.58 ± 2.73	21.09 ± 2.25	5.614	<0.001
Stent diameter (mm)	3.09 ± 0.18	3.26 ± 0.16	5.651	<0.001
Number of stents	1.95 ± 0.32	1.53 ± 0.21	8.665	<0.001
Postoperative medication (cases)				
Statins	71	56	0.862	0.930
Beta-blockers	59	48		
ACEI	37	34		
ARB	18	11		
Calcium channel blockers	30	25		

vessel wall and reduces the elastic recoil rate of the blood vessel wall [24].

Clinical data showed that the occurrence of DES-ISR was mainly related to local factors such as stent margins and the focal site, and it mostly occurred 6 months after surgery [25, 26]. It has been reported that the causes of ISR mainly include insufficient stent expansion, abnormal intimal hyperplasia, or new atherosclerosis, but the risk factors for the occurrence of DES-ISR are still inconclusive [27]. Therefore, this study analyzed the relevant factors affecting its occurrence. Related reports have shown that after coronary stenting, there is a significant correlation between diabetes and ISR, and diabetes is associated with clinical outcomes such as stent thrombosis and major adverse cardiac events after PCI [6]. ISR may occur in diabetic patients due to insulin resistance and complex underlying lesions. However, the results of this study showed that it was not related to the occurrence of ISR, which may be related to the small sample size of this study, so the sample size should be increased for further analysis in the later stage. Previous studies have found that the characteristics of coronary artery lesions, including the number of vessels, length, location, nature, and stenosis degree of coronary artery lesions, can affect the occurrence of ISR [28]. Studies have confirmed that the incidence of ISR in patients with multivessel lesions is higher than that in patients with single-vessel lesion. The diameter of diseased vessels and the length of total lesions are also predictors of restenosis, and the incidence of ISR increases significantly when the diameter of vessels is too small [29] .In this study, it was found that multivessel coronary artery lesions, stenosis target lesion degree ≥85.05%, and target lesion length ≥36.88 mm were risk factors affecting the occurrence of DES-ISR, and target lesion diameter ≥3.15 mm and stent diameter ≥3.15 mm were protective factors. It indicates that the increased length of implanted stents and the smaller diameter of stents significantly

Table 5: Multivariate analysis of factors affecting the occurrence of DES-ISR.

Index	β	*SE*	Wald's χ^2	*OR*	*95% CI*	*P* value
Abnormal BMI	2.281	1.282	3.166	9.786	0.793~120.750	0.076
Smoking	2.153	1.328	2.628	8.611	0.638~116.266	0.106
Hypertension	3.321	1.501	4.895	27.688	1.461~524.770	0.027
Diabetes	0.248	1.196	0.043	1.281	0.123~13.359	0.836
Family history of coronary heart disease	2.487	1.273	3.817	12.025	0.992~145.777	0.051
Number of arterial lesions	3.427	1.458	5.525	30.784	1.767~536.293	0.019
Stenosis target lesion degree	3.359	1.298	6.697	28.760	2.259~366.164	0.010
Target lesion diameter	-3.143	1.355	5.380	0.043	0.003~0.614	0.021
Target lesion length	0.650	0.211	9.490	1.916	1.267~2.897	0.002
Stent length	2.798	1.434	3.807	16.412	0.987~272.773	0.052
Stent diameter	-10.159	3.452	8.661	0.000	0.000~0.034	0.003
Number of stents	0.099	1.112	0.008	1.104	0.125~9.762	0.929
Constant	2.281	1.282	3.166	9.786	0.793~120.750	0.076

Assignment: abnormal BMI (yes was 1, no was 0); smoking (yes was 1, no was 0); hypertension (yes was 1, no was 0); diabetes (yes was 1, no was 0); family history of coronary heart disease (yes was 1, no was 0); number of coronary artery lesions (multiple vessels was 1, single vessel was 0); stenosis target lesion degree (≥85.05% was 1, <85.05% was 0); target lesion diameter (≥3.15 mm was 1, <3.15 mm was 0); stent diameter (≥3.15 mm was 1, <3.15 mm was 0); target lesion length (≥36.8 mm was 1, <36.88 mm was 0); stent length (≥22.07 mm was 1, <22.07 mm was 0); number of stents (≥2 was 1, <2 was 0).

increase the incidence of ISR. The matching of the stent diameter and the diameter of the blood vessel is very important to reduce the risk of restenosis, and longer stents are important risk factors for restenosis and ST. This study also found that hypertension is also a risk factor for the occurrence of ISR, which is mainly related to vascular endothelial dysfunction in patients with hypertension.

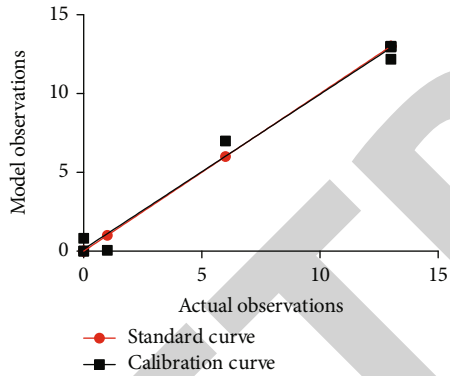

Figure 1: Calibration analysis of the prediction model.

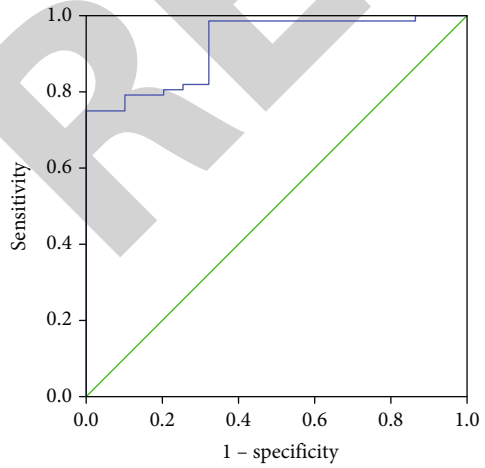

Figure 2: ROC curve analysis of the prediction model predicting the occurrence of DES-ISR.

At present, it is believed that identifying possible high-risk patients with ISR through the predictive model will help clinicians to carry out targeted doctor-patient communication and health education, so that patients can clearly realize the importance of postoperative rehabilitation. Adhering to the secondary prevention of coronary heart disease and developing individualized control programs for high-risk factors can theoretically further reduce the incidence of ISR after PCI, thus improving the expected prognosis of patients as much as possible. In this study, a prediction model was established according to various risk factors. The Hosmer-Lemeshow test and ROC curve analysis showed that the model has high predictive value for the occurrence of ISR, so it may be applied to the early prediction of ISR.

In conclusion, DCB combined with CBA has good clinical efficacy in the treatment of DES-ISR, which can reduce the rate of lumen stenosis and the incidence of adverse cardiovascular events. The prediction model established according to risk factors has high predictive value for the occurrence of DES-ISR in patients.

Data Availability

The labeled dataset used to support the findings of this study is available from the corresponding author upon request.

Conflicts of Interest

The authors declare no competing interests.

Acknowledgments

This research was supported by Medical Scientific Research Foundation of Guangdong Province, China (No. B2021227).

References

[1] S. C. Liang, J. Zhang, J. Li et al., "Systematic review and re-evaluation of the efficacy of drug interventions to prevent contrast-induced acute kidney injury after coronary intervention," *China Journal of Evidence-Based Medicine*, vol. 22, no. 5, p. 10, 2022.

[2] W. W. Chen, R. L. Gao, L. S. Liu et al., "Summary of China cardiovascular disease report 2013," *Chinese Journal of Circulation*, vol. 29, no. 7, p. 5, 2014.

[3] N. Kobayashi, M. Yamawaki, S. Mori et al., "Stentless strategy by drug-coated balloon angioplasty following directional coronary atherectomy for left main bifurcation lesion," *Journal of Interventional Cardiology*, vol. 2021, no. 3, pp. 1–7, 2021.

[4] Y. Sheng and J. B. Hou, "Research progress on the treatment strategies of coronaryin-stentrestenosis," *Journal of Cardiovascular Rehabilitation Medicine*, vol. 30, no. 2, pp. 4-5, 2021.

[5] M. S. Sabatine, B. A. Bergmark, S. A. Murphy et al., "Percutaneous coronary intervention with drug-eluting stents versus coronary artery bypass grafting in left main coronary artery disease: an individual patient data meta-analysis," *Lancet*, vol. 398, no. 10318, pp. 2247–2257, 2021.

[6] H. F. Lee, Y. W. Cheng, J. R. Peng et al., "Impact of chronic kidney disease on long-term outcomes for coronary in-stent restenosis after drug-coated balloon angioplasty," *Journal of Cardiology*, vol. 78, no. 6, pp. 564–570, 2021.

[7] L. Pan, W. Lu, Z. Han et al., "Clinical outcomes of drug-coated balloon in coronary lesions: a real-world, all-comers study," *Clinical Research in Cardiology*, vol. 6, no. 8058, pp. 1–19, 2021.

[8] L. Hou, L. L. Lu, H. S. Zeng et al., "Application of cutting balloon combined with drug-coated balloon in primary coronary lesions," *Heart Journal*, vol. 34, no. 1, p. 23, 2022.

[9] S. Cao, T. He, J. Xie et al., "Drug-coated balloon angioplasty versus balloon angioplasty for treating patients with in-stent restenosis in the femoropopliteal artery: a meta-analysis," *Medicine*, vol. 100, no. 16, article e25599, 2021.

[10] Interventional Cardiology Group of Cardiovascular Branch of Chinese Medical Association, Professional Committee of Thrombosis Prevention and Treatment of Cardiovascular Physicians Branch of Chinese Medical Association, and Editorial Board of Chinese Journal of Cardiovascular Disease, "Guidelines for percutaneous coronary intervention in China (2016)," *Chinese Journal of Cardiovascular Diseases*, vol. 44, no. 5, pp. 382–400, 2016.

[11] H. B. Yan, C. S. Ma, and Y. Huo, *Guidelines for Percutaneous Coronary Intervention in the United States*, China Environmental Science Press, Beijing, 2006.

[12] F. F. Zhang, Y. T. Xie, L. T. Liu et al., "Analysis of the influencing factors of restenosis after percutaneous coronary drug-eluting stent [J]," *Journal of Practical Medicine*, vol. 36, no. 14, pp. 1946–1951, 2020.

[13] X. Hao, D. Huang, Z. Wang, J. Zhang, H. Liu, and Y. Lu, "Study on the safety and effectiveness of drug-coated balloons in patients with acute myocardial infarction," *Journal of Cardiothoracic Surgery*, vol. 16, no. 1, pp. 178–182, 2021.

[14] W. Wang, B. Wang, Y. Chen, and S. Wei, "Late stent thrombosis after drug-coated balloon coronary angioplasty for in-stent restenosis," *International Heart Journal*, vol. 62, no. 1, pp. 171–174, 2021.

[15] I. P. van Wijck, S. Holewijn, L. A. van Walraven, and M. M. Reijnen, "Drug-coated balloon angioplasty for the treatment of edge stenosis after self-expanding covered stent placement for superficial femoral artery occlusive disease," *Vascular*, vol. 29, no. 1, pp. 108–115, 2021.

[16] K. Bhatia, I. N. Akhtar, Y. Akinci et al., "Drug-eluting balloon angioplasty for in-stent restenosis following carotid artery stent placement," *Journal of Neuroimaging*, vol. 30, no. 3, pp. 267–275, 2020.

[17] R. W. Yeh, W. Bachinsky, R. Stoler et al., "Rationale and design of a randomized study comparing the agent drug coated balloon to plain old balloon angioplasty in patients with in-stent restenosis," *American Heart Journal*, vol. 241, no. 13, pp. 101–107, 2021.

[18] D. Giacoppo, F. Alfonso, B. Xu et al., "Drug-coated balloon angioplasty versus drug-eluting stent implantation in patients with coronary stent restenosis," *Journal of the American College of Cardiology*, vol. 75, no. 21, pp. 2664–2678, 2020.

[19] H. Jin, C. T. Qiu, Y. C. Sun et al., "Comparison of cutting balloon and semi-compliant balloon for pre-dilation of coronary bifurcation lesions," *Chinese Tissue Engineering Research*, vol. 24, no. 22, pp. 3540–3546, 2020.

[20] Q. Y. Li, G. Li, and J. H. Tao, "Feasibility and safety of rotational atherectomy combined with cutting balloon in the treatment of severe coronary calcification lesions," *Chongqing Medicine*, vol. 48, no. 2, pp. 233–236, 2019.

[21] W. Liu, Y. Yao, Z. Jiang et al., "3-year outcomes in patients with heavily calcified lesions undergoing percutaneous coronary intervention using cutting balloons," *BMC Cardiovascular Disorders*, vol. 22, no. 1, pp. 187–195, 2022.

[22] M. Li, J. Hou, X. Gu, R. Weng, Z. Zhong, and S. Liu, "Incidence and risk factors of in-stent restenosis after percutaneous coronary intervention in patients from southern China," *European Journal of Medical Research*, vol. 27, no. 1, pp. 12–16, 2022.

[23] X. M. Zong, H. B. Sun, and B. Q. Li, "Application of drug-coated balloon combined with cutting balloon pre-dilation in bifurcation lesions," *Chinese Journal of Evidence-Based Cardiovascular Medicine*, vol. 10, no. 11, p. 4, 2018.

[24] M. Li and Y. H. Jia, "Study on the relationship between lipid metabolism and prognosis in patients with coronary heart disease complicated with diabetes mellitus," *Journal of Integrated Traditional Chinese and Western Medicine Cardiovascular and Cerebrovascular Diseases*, vol. 20, no. 4, p. 4, 2022.

[25] K. Zhang, T. X. Li, Z. L. Wang et al., "Factors affecting in-stent restenosis after angioplasty with the Enterprise stent for intracranial atherosclerotic diseases," *Scientific Reports*, vol. 11, no. 1, p. 10479, 2021.

[26] C. H. Pan, S. C. Chien, C. J. Chen et al., "Circulating level of microRNA-142-5p is a potential biomarker for predicting in-stent restenosis: a case–control study," *BMC Cardiovascular Disorders*, vol. 21, no. 1, p. 77, 2021.

[27] F. Levent, O. Senoz, S. V. Emren, Z. Y. Emren, and R. B. Gediz, "Is coronary artery tortuosity a predisposing factor for drug-eluting stent restenosis?," *Herz*, vol. 47, no. 1, pp. 73–78, 2022.

[28] M. Yi, S. Xu, Q. Liu, and X. Ke, "Analysis of risk factors for restenosis within 2 years of drug-eluting stents and

Hindawi
Computational and Mathematical Methods in Medicine
Volume 2023, Article ID 9868302, 1 page
https://doi.org/10.1155/2023/9868302

Retraction

Retracted: Efficacy and Risk Factors of Pyrrotinib in Second- and Third-Line Treatments for HER2-Positive Advanced Breast Cancer

Computational and Mathematical Methods in Medicine

Received 12 December 2023; Accepted 12 December 2023; Published 13 December 2023

This article has been retracted by Hindawi, as publisher, following an investigation undertaken by the publisher [1]. This investigation has uncovered evidence of systematic manipulation of the publication and peer-review process. We cannot, therefore, vouch for the reliability or integrity of this article.

Please note that this notice is intended solely to alert readers that the peer-review process of this article has been compromised.

Wiley and Hindawi regret that the usual quality checks did not identify these issues before publication and have since put additional measures in place to safeguard research integrity.

We wish to credit our Research Integrity and Research Publishing teams and anonymous and named external researchers and research integrity experts for contributing to this investigation.

The corresponding author, as the representative of all authors, has been given the opportunity to register their agreement or disagreement to this retraction. We have kept a record of any response received.

References

[1] X. Wang, Y. Huang, Z. Yang et al., "Efficacy and Risk Factors of Pyrrotinib in Second- and Third-Line Treatments for HER2-Positive Advanced Breast Cancer," *Computational and Mathematical Methods in Medicine*, vol. 2022, Article ID 7864114, 8 pages, 2022.

Hindawi
Computational and Mathematical Methods in Medicine
Volume 2022, Article ID 7864114, 8 pages
https://doi.org/10.1155/2022/7864114

Research Article

Efficacy and Risk Factors of Pyrrotinib in Second- and Third-Line Treatments for HER2-Positive Advanced Breast Cancer

Xiaolei Wang,[1] Yuxia Huang,[2] Zhen Yang,[1] Yang Yang,[1] Fenfen Wei,[1] Min Yan,[1] and Fanfan Li[1]

[1]*Department of Oncology, The Second Affiliated Hospital of Anhui Medical University, Hefei 230601, China*
[2]*Department of Medical Oncology, Chizhou Second People's Hospital, Chizhou, Anhui 247100, China*

Correspondence should be addressed to Fanfan Li; 15040140141@xs.hnit.edu.cn

Received 2 August 2022; Accepted 31 August 2022; Published 17 September 2022

Academic Editor: Min Tang

A study to examine the efficacy and risk factors associated with pyrrotinib in the second- and third-line treatment of advanced breast cancer with Human epidermal growth factor receptor 2- (HER2-) positive cells was conducted. Progression-free survival (PFS) was assessed as the primary endpoint, and the objective response rate (ORR), overall survival (OS), and safety were secondary endpoints. Across all the patients, the ORR was 48.57%, and the disease control rate (DCR) was 94.29%. In the follow-up period, the median PFS was 15 months, and second-line treatment had significantly longer PFS than third-line treatment ($P = 0.027$). The OS among all the patients was up to 28 months, but the median OS has not yet been reached. Diarrhea (69.57%) was the most important AE, mainly in grades 1 and 2. According to the COX regression analysis, brain metastasis was a risk factor for PFS, while second-line treatment and capecitabine chemotherapy were relevant to a longer PFS correlation among patients. In the second- and third-line treatment, pyrrotinib is still highly effective and safe. Pyrrotinib is a potential ideal salvage treatment plan for patients who failed in first-line treatments.

1. Introduction

Breast cancer, the leading cause of cancer death in women, is the most common malignant cancer in women [1, 2]. The latest data on the global cancer burden showed more than 2.26 million new cases of breast cancer and 2.2 million lung cancer in 2016, and breast cancer became the most prevalent cancer in the world [3, 4]. Breast cancer is a highly heterogeneous tumor with diverse histological morphology and genotypes. Human epidermal growth factor receptor 2- (HER2-) positive breast cancer refers to ERBB2/neu proto-oncogene amplification or HER2 transmembrane receptor protein overexpression, which accounts for about 15%–20% of all breast cancers in incidence [5, 6]. HER2-positive breast cancer is characterized by its proclivity for recurrence, highly aggressive metastasis, rapid progression, and poor prognoses [7, 8]. Based on the characteristics, anti-HER2-targeted drug therapy is considered effective in inhibiting tumor progression and prolonging the survival of patients.

With the continuous research into breast cancer's immune phenotype, more targeted drugs have been developed. Currently, the common clinical targeted therapy drugs for HER2-positive breast cancer mainly include tyrosine kinase inhibitors, monoclonal antibodies, and antibody-drug conjugates. However, the effect of targeted therapy in some patients has been unsatisfactory because of drug resistance. Therefore, it is necessary to develop more types of anti-HER2-targeted drugs. A new type of oral pan-ErbB receptor tyrosine kinase inhibitor, pyrrotinib, has been developed by China independently [9]. Its mechanism of action is as follows: it irreversibly binds to the ATP binding site of EGFR/HER1, HER2, and HER4 to prevent the formation of homo/heterodimers between the HER family, inhibit autophosphorylation, and block downstream signal transmission, thereby inhibiting tumor growth [9–11]. The actual effect of pyrrotinib in clinical application still needs more case support, even though it has achieved high evaluations in clinical trials I, II, and

III phases [12, 13]. The effectiveness in treating HER2-positive breast cancer in first-line treatment has been proved, while no reports have explored the efficacy in second-line and third-line treatment. What is important is that previous studies were limited to the analysis of treatment effects and ignored the observation of factors affecting treatment efficacy.

We review the efficacy of pyrrotinib in the second- and third-line breast cancers with HER2-positive and analyze the factors that affect treatment efficacy in this study. This is the first evidence-based study to analyze the factors affecting the efficacy of pyrrotinib in HER2-positive breast cancer.

2. Methods

2.1. Patient. Thirty-five patients with HER2-positive breast cancer treated with pyrrotinib between December 2018 and October 2021 were admitted to the study. Clinical data were complete in all patients. Inclusion criteria are as follows: (1) patients met the diagnostic criteria for HER2-positive breast cancer; that is, their primary or metastatic tissue specimens were immunohistochemically HER2 positive ("+++") or exhibited positive fluorescence in situ hybridization (FISH) ("+"); (2) patients were adult females; (3) patients had at least one measurable lesion, meeting the curative effect according to the response evaluation criteria in solid tumors (RECIST 1.1) evaluation conditions; (4) the patients received pyrrotinib treatment regimens; (5) their expected survival time was at least three months; and (6) the patients' physical functions tolerated pyrrotinib treatment, and there were no treatment contraindications. Exclusion criteria are as follows: (1) patients were undergoing other clinical trials; (2) they lacked follow-up data; and (3) psychiatric patients who cannot receive medication.

2.2. Ethical Statement. Based on meeting the Declaration of Helsinki, The Second Affiliated Hospital of Anhui Medical University (PY-YX2021-46) ethics committee approved this study. Studying retrospectively waived informed consent due to its retrospective nature.

2.3. Treatment Plan and Follow-Up. All patients received pyrrotinib for second-line or third-line treatment after the first-line. The patients took pyrrotinib maleate tablets orally (Jiangsu Hengrui Pharmaceutical Co., Ltd., National Medicine Zhunzi H20180013, 80 mg/tablet) at 4 tablets/320 mg, QD. After patients tolerated this regimen, the dose was increased to 5 tablets/400 mg, QD. Patients undergoing anti-HER2 second-line and third-line treatments were treated with combined chemotherapy regimens: capecitabine, tigeo, gemcitabine, taxanes, vinorelbine, and etoposide. Treatment efficacy was evaluated every two cycles (every six weeks). Treatment plans were adjusted when patients had grade 1 (mild reactions, no treatment required) or 2 (moderate response, requiring treatment) side effects. When side effects of grade 3 (severe reaction, life-threatening but recoverable) and above occurred, the dosages of the drugs were adjusted according to the types of side effects, or the number of combined chemotherapy drugs was reduced. All patients received long-term follow-ups, and the end of their follow-up period was defined as disease progression or the intolerance of treatment. All patients completed the study, and no patients dropped out of the study halfway through.

2.4. Treatment Efficacy and Adverse Events (AEs) Evaluation. Based on the RECIST (version 1.1), efficacy was evaluated [10] as complete response (CR), partial response (PR), stable disease (SD), and disease progression (PD). The objective response rate (ORR) is the sum of the proportions of CR and PR, and the disease control rate (DCR) is the proportions of CR, PR, and SD. In addition, all patients' survival times were recorded in detail.

AEs were classified into grades 1 through 5 based on National Cancer Institute Common Terminology Criteria for Adverse Events (NCI-CTC 4.0) [11].

2.5. Risk Factor Analysis Strategy. To analyze risk factors, ORR and PFS, AEs grade 3 or higher were used as dependent variables. Age, ECOG scores, WHO grades, ER, PR, P53/P63, pathological type, comorbidities, surgery, vascular tumor thrombus, the combined chemotherapy regimen, the number of pyrrotinib treatment lines, and the location of metastasis were used as dependent variables. The single-factor and multifactor logistic regression or the COX regression analysis models were used for correlation analysis.

2.6. Statistical Analysis. We performed statistical analysis by SPSS 26.0. We expressed enumeration data as cases (percentage) [n (%)], and performed the χ^2 test to test for significance. We analyzed correlations via the single-factor and multifactor logistic regression or the COX regression analysis models. The Kaplan-Meier survival curve was used to evaluate the survival time of patients. $P < 0.05$ means the difference was significant.

3. Results

3.1. Baseline. 35 breast cancer patients with HER2-positive were included, including 22 second-line cases and 13 third-line cases involving pyrrotinib. The patients aged 29 to 70 years (average of 49.4 ± 9.3 years). In addition, 71.43% of the patients had an ECOG score less than or equal to 1 at the start of treatment. Most patients (62.86%) had a WHO classification of grade 2, and only two patients had a family history of breast cancer. The main combination chemotherapy regimen was capecitabine (40.00%), followed by albumin paclitaxel (22.86%). Figure 1 shows the details of pyrrotinib use, and there were no statistical differences in baseline data between the groups ($P > 0.05$) (Table 1).

3.2. The Efficacy of Pyrrotinib. Table 2 shows the best response to pyrrotinib targeted therapy for all HER2-positive breast cancer patients which can be assessed. Only two patients achieved CR (1 in second-line and 1 in third-line treatment), and 15 patients achieved PR (12 in second-line and 3 in third-line treatment). A total of 15 cases reached SD, and 3 cases with PD. The ORR was 48.57%, and the DCR was 94.29%. There

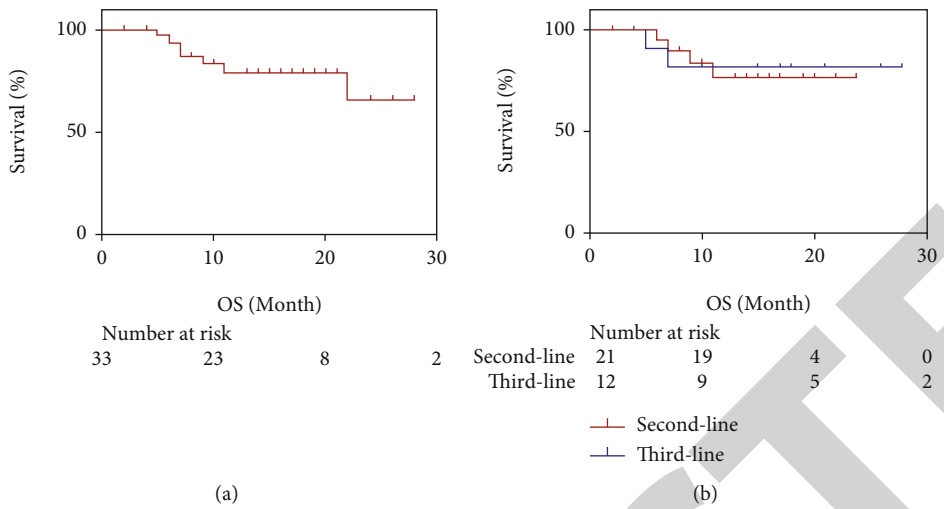

Figure 1: The overall survival of the patients. (a) The Kaplan-Meier curve of OS in patients undergoing second-line and third-line treatment, where the log-rank $P > 0.05$ between groups; (b) the Kaplan-Meier curve of OS in all patients.

Table 1: Baseline data of breast cancer patients with HER2-positive.

Items	Second-line ($n = 22$)	Third-line ($n = 13$)	Total ($n = 35$)
Age (years)	50.9 ± 9.5	46.5 ± 8.8	49.4 ± 9.3
ECOG score [n (%)]			
0~1	16 (72.73)	9 (69.23)	25 (71.43)
2	6 (27.27)	4 (30.77)	10 (28.57)
WHO grade [n (%)]			
II	15 (68.18)	7 (53.85)	22 (62.86)
III	7 (31.82)	6 (46.15)	13 (37.14)
ER [positive, n (%)]	11 (50.00)	6 (46.15)	17 (48.57)
PR [positive, n (%)]	13 (59.09)	7 (53.85)	20 (57.14)
P53/P63 [positive, n (%)]	9 (40.91)	4 (30.77)	13 (37.14)
Pathological type [n (%)]			
Invasive carcinoma	11 (50.00)	6 (46.15)	17 (48.57)
Invasive ductal carcinoma	6 (27.27)	3 (23.08)	9 (25.71)
Other	5 (22.73)	4 (30.77)	9 (25.71)
Family history [yes, n (%)]	1 (4.55)	1 (7.69)	2 (5.71)
Complications [yes, n (%)]	5 (22.73)	2 (15.38)	7 (20.00)
Surgery [yes, n (%)]	15 (68.18)	10 (76.92)	25 (71.43)
Vascular tumor thrombus [positive, n (%)]	8 (36.36)	2 (15.38)	10 (28.57)
Combination chemotherapy [n (%)]			
Capecitabine	10 (45.45)	4 (30.77)	14 (40.00)
Albumin paclitaxel	6 (27.27)	2 (15.38)	8 (22.86)
Gemcitabine	2 (9.09)	2 (15.38)	4 (11.43)
Other	4 (18.18)	5 (38.46)	9 (25.71)

was no significant difference in ORR and DCR between second-line and third-line treatment ($P > 0.05$) regimens. As the follow-up period ended, 26 patients (17 in the second-line and 9 in the third-line) survived, with a survival rate of 74.29%.

As of follow-ups to December 2021, 16 patients had progressed (8 in second-line and 8 in the third-line treatment). Their PFS was as high as 28 months, and the median PFS was 15 months (Figure 2(a)). PFS was significantly longer than in third-line treatment (HR = 0.27, 95% CI: 0.087–0.862, $P = 0.027$) (Figure 2(b)).

At the end of the follow-up period, 26 patients (74.29%) were alive; seven had passed away, and two were lost to follow-up. The overall OS was 2–28 months, but the median OS was not yet reached (Figure 1(a)). No

Table 2: The best response to pyrrotinib targeted therapy for all HER2-positive breast cancer patients.

Efficacy	Second-line ($n = 22$)	Third-line ($n = 13$)	Total
CR	1 (4.55)	1 (7.69)	2 (5.71)
PR	12 (54.55)	3 (23.08)	15 (42.86)
SD	8 (36.36)	7 (53.85)	15 (42.86)
PD	1 (4.55)	2 (15.38)	3 (8.57)
ORR	13 (59.09)	4 (30.77)	17 (48.57)
DCR	21 (95.45)	11 (84.62)	33 (94.29)
Survival rate [n (%)]	17 (77.27)	9 (69.23)	26 (74.29)

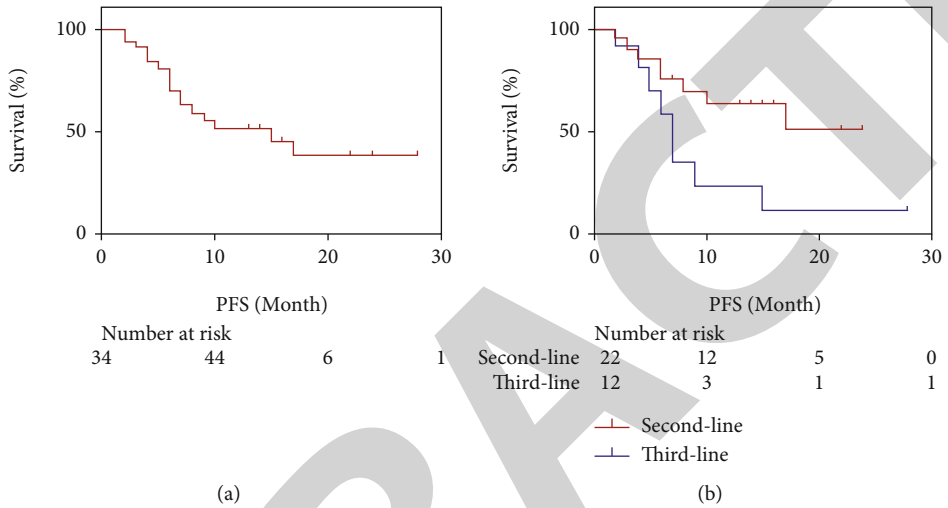

Figure 2: The progression-free survival of patients. (a) The Kaplan-Meier curve of PFS in patients undergoing second-line and third-line treatment, where the log-rank $P = 0.027$ between groups; (b) the Kaplan-Meier curve of PFS in all patients. PFS refers to progression-free survival.

significant difference was observed in OS between second-line and third-line treatment patients (HR = 1.16, 95% CI: 0218–06.158, $P = 0.864$) (Figure 1(b)).

3.3. Safety Analysis of Pyrrotinib. AE details are shown in Table 3. The most common side effect of the patients in the study was diarrhea, with an incidence of 69.57%, but grade 3 diarrhea was rare, with only three cases that have occurred. Diarrhea was relieved after reducing drug dosages until it was reduced to grade 1. Five patients had grade 2–3 neutropenia, and one case of grade 3 thrombocytopenia was documented. Other side effects were observable, including anemia, vomiting, skin rashes, hand-foot syndrome, elevated transaminase, hypertension, and peripheral neuritis. Their incidence was low, and there were no grade 3 AEs.

3.4. Risk Factors for the Efficacy of Pyrrotinib. We further incorporated the significant factors ($P < 0.01$) into a multivariate logistic regression model. The analysis results showed that after excluding confounding factors, comorbidities (OR = 1.380, 95% CI: 1.027–1.664) were independent factors influencing the ORR of pyrrotinib during the treatment. In addition, surgery (OR = 0.905, 95% CI: 0.695–0.980) was associated with a higher ORR (Table 4).

In the univariate analysis, variables related to PFS were obtained, including age, ECOG score, the number of treatment lines, pyridoxine chemotherapy drugs, pathological types, and brain metastases. After incorporating them into a multivariate model for further analysis, the results showed that after controlling for other potential confounding factors, brain metastasis (HR = 1.425, 95% CI: 1.138–2.502) was an independent risk factor for PFS, while second-line treatment (HR = 0.362) and capecitabine chemotherapy (HR = 0.880) were associated with a longer PFS ($P < 0.05$) (Table 5).

3.5. Risk Factors for the Safety of Pyrrotinib. Next, we analyzed the risk factors for the safety of pyrrotinib. Multivariate logistic regression analysis showed that patients 50 years old or older (OR = 1.263) and those with an ECOG score of 2 (OR = 1.185) were associated with more grade 3 AEs, whereas combined capecitabine chemotherapy (OR = 0.893) was associated with a reduced incidence of grade 3 AEs (Table 6).

4. Discussion

Pyrrotinib has been approved for HER2-positive advanced breast cancer treatment because of the significant outcomes in the recent phase II and phase III clinical studies in China [14, 15]. Previous studies, however, mainly analyzed the results of pyrrotinib applied to first-line treatment.

Table 3: The AEs of HER2-positive breast cancer patients [n (%)].

AEs	Grade			Total
	1	2	≥3	
Hematological AEs				
Anemia	3	2	0	5
Neutropenia	0	2	3	5
Thrombocytopenia	0	0	1	1
Non-hematological AEs				
Diarrhea	19	3	3	25
Vomiting	1	0	0	1
Skin rash	2	0	0	2
Hand-foot syndrome	2	0	0	2
Other AEs				
Elevated transaminase	1	0	0	1
Hypertension	3	0	0	3
Peripheral neuritis	2	1	0	3

Table 4: Multivariate logistic regression analysis of ORR.

Variables	OR	95% CI	P
Age (>50 years old vs. ≤50 years old)	1.063	0.859~1.303	0.296
Comorbidities (yes vs. no)	1.380	1.027~1.664	0.020
Surgery (yes vs. no)	0.905	0.695~0.980	0.032
Pathological type (invasive cancer vs. other)	1.125	0.730~1.308	0.296

Table 5: Multivariate logistic regression analysis of ORR.

Variables	HR	95% CI	P
Age (>50 years old *vs* ≤50 years old)	1.132	0.806~1.362	0.239
ECOG score (2 points vs. ≤1 point)	1.285	0.859~1.933	0.088
Number of treatment lines (second-line vs. third-line)	0.362	0.119~0.895	0.005
Chemotherapy drugs (capecitabine vs. others)	0.880	0.567~0.994	0.036
Hormone status (positive vs. negative)	0.925	0.445~1.369	0.167
Pathological type (invasive cancer vs. other)	1.125	0.859~1.492	0.265
Brain metastasis (yes vs. no)	1.425	1.138~2.502	0.007

Table 6: Multivariate logistic regression analysis of the safety of pyrrotinib for the treatment of HER2-positive breast cancer.

Variables	OR	95% CI	P
Age (>50 years old *vs.* ≤50 years old)	1.263	1.059~1.738	0.042
ECOG score (2 points vs. ≤1 point)	1.185	1.032~1.835	0.035
Comorbidities (yes vs. no)	1.180	0.927~1.625	0.094
Chemotherapy drugs (capecitabine vs. others)	0.893	0.627~0.964	0.014

Therefore, we focused on the efficacy and safety of pyrrotinib in second-line and third-line HER2-positive advanced breast cancer in this study, and by analyzing the treatment data of each patient, we sought to shed light on these issues.

This study showed that pyrrotinib is still significantly affected during the second-line and third-line treatment of HER2-positive advanced breast cancer. The overall ORR of the patients was as high as 48.57% (59.09% in the second-line treatment regimen and 30.77% in the third-line treatment regimen), and the DCR was as high as 94.29%. Although this ORR was not as ideal as the results of Phase II and III clinical studies [13, 16], considering the baseline characteristics of these local patients, the complexity of their combined chemotherapy regimens and the impact of the failure of patients' first-line treatments, these results were ideal. In addition, efficacy was improved compared with the currently recommended lapatinib [17, 18] combined chemotherapy regimen (48.57% vs. 34.4%).

In terms of survival, this cohort showed satisfactory PFS and OS. PFS was up to 28 months, the median PFS was 15 months, and OS was up to 28 months. The median OS has not yet been reached. The median is predicted based on the survival curve. OS will reach 35 months.

The NCCN guidelines list several treatment options for HER2-positive advanced breast cancer patients whose first-line treatment with trastuzumab failed [19–21]. These options include switching to a regimen containing lapatinib, continuous administration of trastuzumab while switching to other chemotherapeutic drugs, terminating chemotherapy, and trastuzumab plus lapatinib dual-targeted therapy and TDM1 administration. TDM1 is not yet available in China, and most patients are not suited for dual-targeted therapy. Also, patients often cannot afford the expensive anti-HER2 costs. As an anti-HER2-targeted drug independently developed by China, pyrrotinib has cost advantages, and more importantly, it seems to have a better effect in patients [22–24]. Most cases (27 cases) in this cohort were patients who failed first-line trastuzumab treatment. After pyrrotinib was combined with chemotherapy, 94.29% (33 cases) of the patients showed clinical improvement and had survived by the end of the follow-up period, with a rate as high as 74.29% (26 cases). Combined with the results of this study, we believe that for most Chinese patients with HER2-positive advanced breast cancer and who underwent failed first-line treatments with trastuzumab, pyrrotinib plus chemotherapy is most likely the new ideal choice.

The efficacy of pyrrotinib in the second-line and third-line treatment was observed. The ORR, DCR, and OS were not significantly different, while the median PFS of second-line treatment patients was higher than third-line. Treatment times were also significantly longer. This may have been due to the greater tolerance of targeted therapy and (or) chemotherapy drugs among third-line treatment patients after first-line and second-line treatment [25–27]. In addition, current studies rarely analyze the potential influencing factors of the efficacy of pyrrotinib. Therefore, we further analyzed the possible influencing factors of patients' ORR and PFS. The results showed that after excluding confounding factors, comorbidities (OR = 1.380, 95% CI: 1.027–1.664) were independent factors influencing the ORR of pyrrotinib during the treatment, and surgery was associated with a higher ORR. For PFS, brain metastasis (HR = 1.425), the number of medication lines (HR = 0.362), and capecitabine chemotherapy (HR = 0.880) are potential influencing factors identical to those of the previous trastuzumab treatment [28–31].

Regarding safety, diarrhea was still the most common side effect among patients, but diarrhea above grade 3 was rare, consistent with the previous study. One patient developed grade 3 neutropenia and thrombocytopenia at the same time. This patient changed chemotherapeutic drugs twice in succession; thus, these side effects were considered to be caused by chemotherapeutic drugs. The incidence of other AEs was relatively low, especially for vomiting and hand-foot syndrome. Compared with lapatinib, pyrrotinib is an irreversible tyrosine kinase inhibitor whose mechanism of action is different [23]. Similarly, multivariate logistic regression analysis showed that an age of 50 years old or older (OR = 1.263) and an ECOG score of 2 (OR = 1.185) were associated with a greater incidence of grade 3 AEs. In contrast, combined capecitabine chemotherapy (OR = 0.893) was associated with a lower incidence of grade 3 AEs, suggesting that capecitabine can be selected as a combination chemotherapy regimen to reduce the occurrence of adverse reactions.

There are 2 limitations to this study. First, the small sample size and the lack of a single center limited the applicability of the research results. In addition, this study was a retrospective study without prospective randomization. Therefore, there may have been significant biases in the sociological characteristics, physiological status, tumor characteristics, and other baseline characteristics of the patients. There was a difference in the number of combined chemotherapy drugs between the two groups. Despite these limitations, this was the first observational study to analyze the use of pyrrotinib for the second-line and third-line treatment of HER2-positive advanced breast cancer. It initially demonstrates the use of pyrrotinib in such second-line and third-line treatment and the huge potential of its full-line treatment. Also, combined with an analysis of efficacy and factors influencing safety, this study can be a useful reference for clinical practice.

5. Conclusion

Pyrrotinib combined with chemotherapy has good efficacy and high safety in the second- and third-line treatment of HER2-positive advanced breast cancer.

Data Availability

The datasets used and analyzed during the current study are available from the corresponding author upon reasonable request.

Conflicts of Interest

The authors declare that they have no conflicts of interest.

Acknowledgments

This work was supported by the Nature Science Foundation of Anhui Province (2019A0258).

References

[1] I. R. Macpherson, P. Spiliopoulou, S. Rafii et al., "A phase I/II study of epertinib plus trastuzumab with or without chemotherapy in patients with HER2-positive metastatic breast cancer," *Breast Cancer Research*, vol. 22, no. 1, p. 1, 2019.

[2] C. Saura, M. Oliveira, Y. H. Feng et al., "Neratinib plus capecitabine versus lapatinib plus capecitabine in HER2-positive metastatic breast cancer previously treated with ≥2 HER2-directed regimens: phase III NALA trial," *Journal of Clinical Oncology*, vol. 38, no. 27, pp. 3138–3149, 2020.

[3] H. Squires, M. Stevenson, E. Simpson, R. Harvey, and J. Stevens, "Trastuzumab emtansine for treating HER2-

positive, unresectable, locally advanced or metastatic breast cancer after treatment with trastuzumab and a taxane: an evidence review group perspective of a NICE single technology appraisal," *PharmacoEconomics*, vol. 34, no. 7, pp. 673–680, 2016.

[4] V. Diéras, D. Miles, S. Verma et al., "Trastuzumab emtansine versus capecitabine plus lapatinib in patients with previously treated HER2-positive advanced breast cancer (EMILIA): a descriptive analysis of final overall survival results from a randomised, open-label, phase 3 trial," *The Lancet Oncology*, vol. 18, no. 6, pp. 732–742, 2017.

[5] S. Dawood, K. Broglio, A. U. Buzdar, G. N. Hortobagyi, and S. H. Giordano, "Prognosis of women with metastatic breast cancer by HER2 status and trastuzumab treatment: an institutional-based review," *Journal of Clinical Oncology*, vol. 28, no. 1, pp. 92–98, 2010.

[6] L. Gianni, W. Eiermann, V. Semiglazov et al., "Neoadjuvant chemotherapy with trastuzumab followed by adjuvant trastuzumab versus neoadjuvant chemotherapy alone, in patients with HER2-positive locally advanced breast cancer (the NOAH trial): a randomised controlled superiority trial with a parallel HER2-negative cohort," *Lancet*, vol. 375, no. 9712, pp. 377–384, 2010.

[7] X. Lu, J. Ma, J. Chu et al., "MiR-129-5p sensitizes the response of her-2 positive breast cancer to trastuzumab by reducing Rps6," *Cellular Physiology and Biochemistry*, vol. 44, no. 6, pp. 2346–2356, 2018.

[8] Z. Rezaei, A. Sebzari, D. M. Kordi-Tamandani, and K. Dastjerdi, "Involvement of the dysregulation of miR-23b-3p, miR-195-5p, miR-656-5p, and miR-340-5p in trastuzumab resistance of HER2-positive breast cancer cells and system biology approach to predict their targets involved in resistance," *DNA and Cell Biology*, vol. 38, no. 2, pp. 184–192, 2019.

[9] H. A. Blair, "Pyrotinib: first global approval," *Drugs*, vol. 78, no. 16, pp. 1751–1755, 2018.

[10] X. Li, C. Yang, H. Wan et al., "Discovery and development of pyrotinib: a novel irreversible EGFR/HER2 dual tyrosine kinase inhibitor with favorable safety profiles for the treatment of breast cancer," *European Journal of Pharmaceutical Sciences*, vol. 110, pp. 51–61, 2017.

[11] J. Meng, X. Liu, S. Ma et al., "Metabolism and disposition of pyrotinib in healthy male volunteers: covalent binding with human plasma protein," *Acta Pharmacologica Sinica*, vol. 40, no. 7, pp. 980–988, 2019.

[12] C. Wang, Y. Lin, Y. Zhou et al., "Pyrotinib with trastuzumab and aromatase inhibitors as first-line treatment for HER2 positive and hormone receptor positive metastatic or locally advanced breast cancer: study protocol of a randomized controlled trial," *BMC Cancer*, vol. 20, no. 1, p. 653, 2020.

[13] Q. Li, X. Guan, S. Chen et al., "Safety, efficacy, and biomarker analysis of pyrotinib in combination with capecitabine in HER2-positive metastatic breast cancer patients: a phase I clinical trial," *Clinical Cancer Research*, vol. 25, no. 17, pp. 5212–5220, 2019.

[14] A. Wing, C. A. Fajardo, A. D. Posey Jr. et al., "Improving CART-cell therapy of solid tumors with oncolytic virus-driven production of a bispecific T-cell engager," *Cancer Immunology Research*, vol. 6, no. 5, pp. 605–616, 2018.

[15] A. E. Chung, K. Shoenbill, S. A. Mitchell et al., "Patient free text reporting of symptomatic adverse events in cancer clinical research using the National Cancer Institute's patient-reported outcomes version of the common terminology criteria for adverse events (PRO-CTCAE)," *Journal of the American Medical Informatics Association*, vol. 26, no. 4, pp. 276–285, 2019.

[16] F. Ma, Q. Ouyang, W. Li et al., "Pyrotinib or lapatinib combined with capecitabine in HER2-positive metastatic breast cancer with prior taxanes, anthracyclines, and/or Trastuzumab: a randomized, phase II study," *Journal of Clinical Oncology*, vol. 37, no. 29, pp. 2610–2619, 2019.

[17] H. Shawky and H. Tawfik, "All-oral combination of lapatinib and capecitabine in patients with brain metastases from HER2-positive breast cancer - A phase II study," *Journal of the Egyptian National Cancer Institute*, vol. 26, no. 4, pp. 187–194, 2014.

[18] G. Metro, J. Foglietta, M. Russillo et al., "Clinical outcome of patients with brain metastases from HER2-positive breast cancer treated with lapatinib and capecitabine," *Annals of Oncology*, vol. 22, no. 3, pp. 625–630, 2011.

[19] T. B. Bevers, B. O. Anderson, E. Bonaccio et al., "NCCN clinical practice guidelines in oncology: breast cancer screening and diagnosis," *Journal of the National Comprehensive Cancer Network*, vol. 7, no. 10, pp. 1060–1096, 2009.

[20] P. D. Beitsch, P. W. Whitworth, K. Hughes et al., "Underdiagnosis of hereditary breast cancer: are genetic testing guidelines a tool or an obstacle?," *Journal of Clinical Oncology*, vol. 37, no. 6, pp. 453–460, 2019.

[21] W. J. Gradishar, B. O. Anderson, J. Abraham et al., "Breast cancer, version 3.2020, NCCN clinical practice guidelines in oncology," *Journal of the National Comprehensive Cancer Network*, vol. 18, no. 4, pp. 452–478, 2020.

[22] J. J. Guo, X. D. Jiao, Y. Wu, B. D. Qin, K. Liu, and Y. S. Zang, "Response to pyrotinib in a Chinese patient with bone-metastatic scrotal Paget's disease harboring triple uncommon HER2 mutation: a case report," *Oncotargets and Therapy*, vol. - Volume 13, pp. 6289–6293, 2020.

[23] J. Dai, Y. Chen, C. Tang et al., "Pyrotinib in the treatment of human epidermal growth factor receptor 2-positive metastatic breast cancer: a case report," *Medicine (Baltimore)*, vol. 99, no. 25, article e20809, 2020.

[24] T. M. Nordmann, O. Messerli-Odermatt, L. Meier et al., "Sequential somatic mutations upon secondary anti-HER2 treatment resistance in metastatic ERBB2S310F mutated extramammary Paget's disease," *Oncotarget*, vol. 10, no. 62, pp. 6647–6650, 2019.

[25] M. R. Akbari, S. Sadrkhanlou, and A. Mirmohammadsadeghi, "Surgical outcome of single inferior oblique myectomy in small and large hypertropia of unilateral superior oblique palsy," *Journal of Pediatric Ophthalmology and Strabismus*, vol. 56, no. 1, pp. 23–27, 2019.

[26] A. Patel, N. Unni, and Y. Peng, "The changing paradigm for the treatment of HER2-positive breast cancer," *Cancers*, vol. 12, no. 8, p. 2081, 2020.

[27] E. Krasniqi, G. Barchiesi, L. Pizzuti et al., "Immunotherapy in HER2-positive breast cancer: state of the art and future perspectives," *Journal of Hematology & Oncology*, vol. 12, no. 1, p. 111, 2019.

[28] J. Sato, A. Shimomura, J. Kawauchi et al., "Brain metastasis-related microRNAs in patients with advanced breast cancer," *PLoS One*, vol. 14, no. 10, article e0221538, 2019.

[29] H. Y. Lee, J. Cha, S. K. Kim et al., "C-MYC drives breast cancer metastasis to the brain, but promotes synthetic lethality with TRAIL," *Molecular Cancer Research*, vol. 17, no. 2, pp. 544–554, 2019.

Hindawi
Computational and Mathematical Methods in Medicine
Volume 2023, Article ID 9757648, 1 page
https://doi.org/10.1155/2023/9757648

Retraction

Retracted: Comparison of Effectiveness as well as Advantages and Disadvantages of Different Dimensions of Hysterosalpingo-Contrast Sonography for Diagnosis of Lesions Associated with Female Infertility

Computational and Mathematical Methods in Medicine

Received 12 December 2023; Accepted 12 December 2023; Published 13 December 2023

This article has been retracted by Hindawi, as publisher, following an investigation undertaken by the publisher [1]. This investigation has uncovered evidence of systematic manipulation of the publication and peer-review process. We cannot, therefore, vouch for the reliability or integrity of this article.

Please note that this notice is intended solely to alert readers that the peer-review process of this article has been compromised.

Wiley and Hindawi regret that the usual quality checks did not identify these issues before publication and have since put additional measures in place to safeguard research integrity.

We wish to credit our Research Integrity and Research Publishing teams and anonymous and named external researchers and research integrity experts for contributing to this investigation.

The corresponding author, as the representative of all authors, has been given the opportunity to register their agreement or disagreement to this retraction. We have kept a record of any response received.

References

[1] R. Pei, "Comparison of Effectiveness as well as Advantages and Disadvantages of Different Dimensions of Hysterosalpingo-Contrast Sonography for Diagnosis of Lesions Associated with Female Infertility," *Computational and Mathematical Methods in Medicine*, vol. 2022, Article ID 7508880, 7 pages, 2022.

Hindawi
Computational and Mathematical Methods in Medicine
Volume 2022, Article ID 7508880, 7 pages
https://doi.org/10.1155/2022/7508880

Research Article

Comparison of Effectiveness as well as Advantages and Disadvantages of Different Dimensions of Hysterosalpingo-Contrast Sonography for Diagnosis of Lesions Associated with Female Infertility

Rudi Pei

Department of Ultrasound, Pukou Branch Hospital of Jiangsu People's Hospital, Nanjing Pukou Central Hospital, Nanjing, Jiangsu 211800, China

Correspondence should be addressed to Rudi Pei; peirudi4@163.com

Received 6 August 2022; Revised 23 August 2022; Accepted 27 August 2022; Published 16 September 2022

Academic Editor: Min Tang

Background and Objective. With social pressures and changes in lifestyle habits, the incidence of female infertility has increased in recent years. How to make timely and accurate assessment of the patency of the fallopian tubes in infertile women is of great importance in the clinical management of infertility. Therefore, this study aims to provide a reference for the future clinical application of hysterosalpingo-contrast sonography (HyCoSy) by comparing the advantages and disadvantages of different dimensions of HyCoSy for the diagnosis of female infertility. *Methods*. Forty subjects who underwent routine two-dimensional (2D) vaginal ultrasound, three-dimensional HyCoSy (3D-HyCoSy), and four-dimensional HyCoSy (4D-HyCoSy) examinations from January 2021 to July 2022 at the ultrasound department of Pukou Branch of Jiangsu Province Hospital were enrolled to this study. Fallopian tubal recanalization by hydrotubation (FTRH) was used as the gold standard to compare the efficacy of 2D vaginal ultrasound, 3D-HyCoSy, and 4D-HyCoSy in assessing the subjects for the presence of polyps, myomas, and other occupants in the uterine cavity or uterine adhesions. *Results*. A total of 18 cases of uterine cavity lesions, 11 of pelvic lesions, and 11 of ovarian lesions were identified by FTRH, while 80 fallopian tubes were found in 40 patients and 71 tubal obstructions were detected by FTRH. Vaginal ultrasound assessment of uterine cavity, pelvis, ovarian lesions, and tubal obstruction was moderately consistent with FTRH (Kappa = 0.616, 0.673, 0.654, and 0.640), 3D-HyCoSy was in good agreement with FTRH (Kappa = 0.812, 0.910, 0.906, and 0.894), and 4D-HyCoSy was in good agreement with FTRH (Kappa = 0.914, 0.903, 1.000, and 0.942), with 4D-HyCoSy being in good agreement with FTRH had the highest agreement. *Conclusion*. 4D-HyCoSy can be used as an effective tool for clinical diagnosis of female tubal obstruction infertility and provide a reference basis for the design of subsequent clinical treatment plans.

1. Introduction

With social pressures and changes in lifestyle habits, the incidence of female infertility has increased in recent years [1]. Surveys show that more than 300,000 new cases of infertility have been reported worldwide in 2020, an increase of 4-5 times compared to 2000 [2]. The occurrence of infertility not only increases a woman's mental stress, but also brings great economic pressure, which seriously affects the normal life of patients [3]. Currently, the clinical causes of infertility are extremely complex and can be caused by lesions of the uterus, fallopian tubes, and ovaries, among which tubal factors are the most common, accounting for about 25-50% of all patients [4]. Infertile women often have symptoms such as obesity, chronic lower abdominal pain, and obvious dysmenorrhea, and many infertile women do not have any clinical symptoms [5]. There is no way to diagnose the cause of infertility based on these clinical symptoms alone. A series of tests are needed to help diagnosis. Therefore, how to make timely and accurate assessment of the patency of the fallopian tubes in infertile women is of great importance in the clinical management of infertility [6]. Currently, there are various clinical methods

for the evaluation of tubal obstruction, such as hysterosalpingography under X-ray, uterine tubal fluid, FTRH, and hysterosalpingography under ultrasound [7]. Among them, fallopian tubal recanalization by hydrotubation (FTRH) is used as the most effective and accurate way to diagnose tubal patency and is the gold standard for infertility testing [8]. However, FTRH is extremely invasive and the test is expensive and carries a greater risk of use, which limits it from being the first choice for infertility testing [9]. Because of this, the search for an effective, safe, and accurate test is a hot topic in modern infertility diagnosis and treatment.

Hysterosalpingo-contrast sonography (HyCoSy) is a noninvasive, radiation-free test that did not gain clinical attention in the early stages of development because of unsatisfactory visualization and radiation exposure [10]. With the continuous development of contrast agents and ultrasonography technology, three-dimensional HyCoSy (3D-HyCoSy) and four-dimensional HyCoSy (4D-HyCoSy) have been developed, and the quality of their image quality has been improved dramatically on the basis of the original HyCoSy, which has been preliminarily confirmed for morphological assessment of the fallopian tubes. For example, Hong's research shows that 3D-HyCoSy can accurately assess the state of pelvic adhesions in women and can be used for the assessment of tubal obstruction in women with infertility [11]. Pan said that 4D-HyCoSy has a very comprehensive imaging effect on women's fallopian tubes, pelvis, and uterus. Endometrial thickness, fallopian tube wall, ovarian motility, etc. can be clearly observed, which has important research significance for evaluating female infertility [12]. Since HyCoSy is noninvasive, has no allergy and anesthesia risks, is radiation-free, and allows conception within a short period of time after the test, if its role in infertility evaluation can be confirmed, it will be an important enhancement for the future treatment of infertility.

Therefore, this study aims to provide a reference for the future clinical application of HyCoSy by comparing the advantages and disadvantages of different dimensions of HyCoSy for the diagnosis of female infertility.

2. Materials and Methods

2.1. Study Area. The study was carried out at the Department of Ultrasound, Pukou Branch Hospital of Jiangsu People's Hospital, from January 2021 to July 2022.

2.2. Research Subjects. Forty subjects who underwent routine two-dimensional (2D) vaginal ultrasound, 3D-HyCoSy, and 4D-HyCoSy examinations in the Ultrasound Department of Pukou Branch of Jiangsu Province Hospital from January 2021 to July 2022 were enrolled to retrospective analysis, and the basic patient data are shown in Table 1. The experiment was conducted in strict compliance with the Declaration of Helsinki, and all subjects signed an informed consent form.

2.3. Inclusion and Exclusion Criteria. Inclusion criteria are as follows: 3-7 d after the end of menstruation, with no sexual intercourse during this period; routine blood and white blood test results were normal; and age >22 years old.

Table 1: Basic data of the subjects.

Patient information	*n*
Age	28.18 ± 3.66
Weight (kg)	55.58 ± 10.32
Height (cm)	158.65 ± 6.76
Family history of illness	
Have	2 (5.00)
None	38 (95.00)
History of miscarriage	
Have	4 (10.00)
None	36 (90.00)
Smoking	
Yes	8 (20.00)
No	32 (80.00)
Drinking	
Yes	7 (17.50)
No	33 (82.50)
Sleep situation	
Normal	16 (40.00)
Irregular	24 (60.00)
Place of residence	
City	29 (72.50)
Rural	11 (27.50)

Exclusion criteria are as follows: infertility caused by endocrine abnormalities in the woman and semen abnormalities in the men; the presence of acute inflammation of the internal and external genitalia and subacute or acute attacks of chronic inflammation; and vaginal bleeding.

2.4. Main Instruments and Reagents. Color Doppler ultrasound diagnostic instrument (GE Voluson E10, USA), transvaginal 4-dimensional ultrasound probe (GE RIC5-9-D, center frequency 5.0-9.0 MHz, USA), and Sonovir contrast agent (Bracco Suisse SA, SFDA Approval No. J20130045).

2.5. Testing Methods. Altogether 5 mL of saline was filled into the glass bottle with powdered Sonovir, and 2 mL was collected and added into 18 mL of saline to make 20 mL of Sonovir dilution solution. A routine 2D vaginal ultrasound was performed to clarify patients' bilateral ovaries, pelvis, and uterus (Figure 1); after routine disinfection and laying towels, a disposable silicone rubber double shot hysterosalpingogram tube was inserted vaginally into the uterine cavity, and 1.2-2.5 mL of saline was injected into the balloon. Subsequently, 5 mL of saline was extracted and injected into the subject's uterine cavity through the contrast tube to observe intrauterine polyps, myomas, and other occupancies or uterine adhesions. In 3D-HyCoSy, start the 3D mode prescan, keep the probe position fixed under the transverse uterine section, select the 3D mode after starting the contrast condition, adjust the pelvis to be echo-free, and adjust the sampling frame larger to ensure the observation range. The contrast dilution was injected slowly and uniformly into the uterine cavity, and the collection of

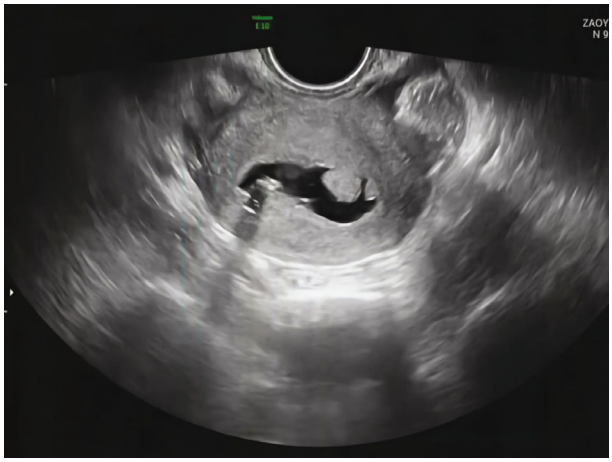

Figure 1: Saline hysterosalpingogram.

3D volume data was started when the two uterine horns became highly echogenic. After image acquisition, the pelvic and periovarian contrast distribution was observed via 2D contrast mode. The images are acquired 3 times continuously and stored for backup. When evaluation is needed, the images are pulled out, rotated, and cut, and the gain is adjusted for comprehensive analysis. For 4D-HyCoSy, in the center plane, start the contrast condition and 4D scan mode, turn down the gain, and turn up the sampling frame. During the process of contrast injection into the catheter, real-time dynamic observation of the high echo of contrast filling and flow in the uterine cavity and fallopian tubes is made to make a diagnosis, and the video can be played back frame by frame for analysis after being called up.

2.6. Results Assessment. All imaging results were reviewed by our two senior imaging physicians using a double-blind method, and subjects were analyzed for uterine, ovarian, and pelvic lesions and tubal patency based on 2D vaginal ultrasound, 3D-HyCoSy, and 4D-HyCoSy images. According to the Clinical Application Guideline of Ultrasonography in China, the subject's fallopian tubes were visualized throughout and traveled naturally, there was no resistance when pushing the contrast agent, the contrast agent was wrapped around the ovaries in a circular pattern, and the contrast agent was diffused evenly in the pelvis. Tubal development is discontinuous, local slender, nodular, or thickened, and there is resistance when injecting contrast medium, and after stopping injection of contrast medium, some contrast media recycle back to the inner orifice of the uterus (or even external orifice of the cervix). The contrast medium diffused slowly from the fallopian tube to the ovary and surrounded the ovary in an arc or semiring shape. The diffusion and sparse results of the contrast medium in the pelvic cavity were evaluated as tubal obstruction. The fallopian tube is not developed throughout the whole process (or only the proximal end of the fallopian tube), and the official cavity is slender, stiff, and curved. There was a great resistance when injecting the contrast medium. After stopping the contrast injection, almost all the contrast agent returned to the ectocervix and the external vaginal opening. It was evaluated as fallopian tube obstruction when there was no contrast agent around the ovaries and no contrast agent diffusion in the pelvis. When the results of the evaluation by two physicians were in dispute, the opinion of a third physician was sought.

2.7. Outcome Measures. The results of the FTRH examination [13] were employed as the gold standard to compare the effectiveness of different dimensions of the HyCoSy examination results in assessing the subjects for the presence of polyps, leiomyomas, and other occupancies in the uterine cavity or uterine adhesions. The calculation of diagnostic efficacy are as follows: both FTRH and this method were judged to be positive, regarded as true positive, and marked as a; both FTRH and this method were judged to be negative, regarded as true negative, and marked as b; FTRH is judged as positive, this method is judged as negative, it is regarded as false negative, and marked as c; FTRH is judged as negative, this method is judged as positive, it is regarded as false positive, and marked as d. Sensitivity $= a/(a + c) \times 100\%$; Specificity $= b/(b + d) \times 100\%$; Diagnostic accuracy $= (a + d)/(a + b + c + d) \times 100\%$.

2.8. Statistical Methods. Statistical analysis was performed using SPSS 22.0 software. The measurement data were recorded as $(\bar{\chi} \pm s)$, and the counting data were recorded as (%). Comparisons were made using the chi-square test, and differences were considered statistically remarkable at $P < 0.05$.

3. Results

3.1. Summary of Results. Vaginal ultrasound assessment of uterine cavity, pelvis, ovarian lesions, and tubal obstruction was moderately consistent with FTRH (Kappa = 0.616, 0.673, 0.654, and 0.640), 3D-HyCoSy was in good agreement with FTRH (Kappa = 0.812, 0.910, 0.906, and 0.894), and 4D-HyCoSy was in good agreement with FTRH (Kappa = 0.914, 0.903, 1.000, and 0.942), with 4D-HyCoSy being in good agreement with FTRH had the highest agreement.

3.2. Image Results. FTRH results manifested that uterine cavity lesions were detected in 18 patients, pelvic lesions in 11 cases, and ovarian lesions in 11 cases in 40 patients. A total of 80 fallopian tubes were found in 40 patients, and 71 tubal obstructions were examined by FTRH. Typical findings of vaginal ultrasound, 3D-HyCoSy, and 4D-HyCoSy are shown in Figures 2 and 3.

3.3. Comparison of Uterine Cavity Lesion Screening. Vaginal ultrasound detected 14 uterine cavity lesions with a diagnostic sensitivity of 50.00%, specificity of 77.27%, accuracy of 65.00%, and moderate concordance with FTRH (Kappa = 0.616, $P < 0.05$, Table 2). 3D-HyCoSy found 16 cases with a diagnostic sensitivity of 72.22%, specificity of 86.36%, accuracy of 80.00%, and good agreement with FTRH (Kappa = 0.812, $P < 0.05$, Table 3). 4D-HyCoSy discovered 17 cases with a diagnostic sensitivity of 94.44%, specificity of 100.0%, accuracy of 97.50%, and good agreement with FTRH (Kappa = 0.914, $P < 0.05$, Table 4).

3.4. Comparison of Pelvic Pathology Screening. 16 pelvic lesions were tested by vaginal ultrasound, 10 pelvic lesions were found by 3D-HyCoSy, and 13 pelvic lesions were examined by 4D-

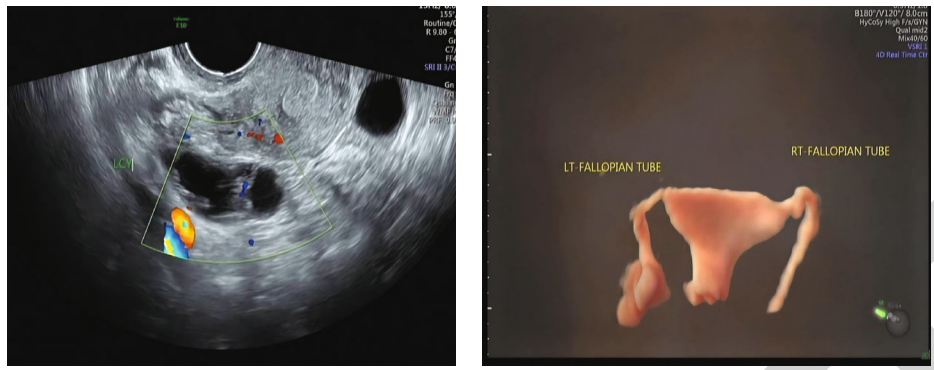

(a) (b)

Figure 2: Female, 29 years old: (a) vaginal ultrasound reveals hydrosalpinx on the left fallopian tube. (b) 4D-HyCoSy examination reveals a contrast collection at the end of the left tubal dilatation.

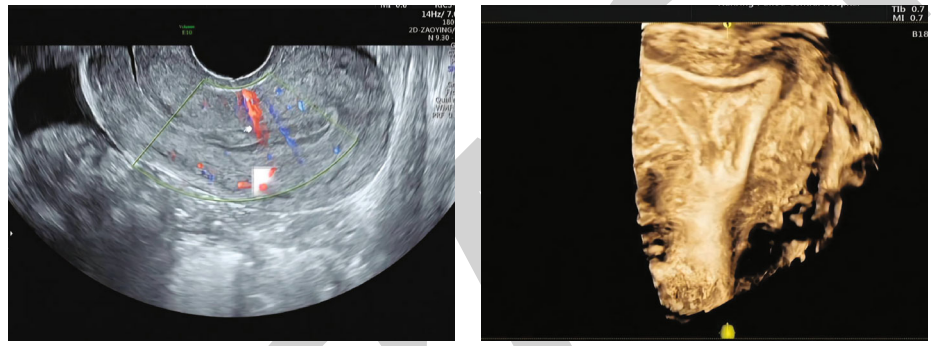

(a) (b)

Figure 3: Female, 32 years old: (a) endometrial polyp seen on vaginal ultrasound. (b) 3D-HyCoSy examination reveals endometrial polyps.

Table 2: Diagnostic effectiveness of vaginal ultrasound and FTRH for uterine cavity lesions.

		FTRH		Total	Kappa	*P*
		(+)	(-)			
Vaginal ultrasound	(+)	9	5	14	0.616	<0.05
	(-)	9	17	26		
Total		18	22			

Table 3: Diagnostic effectiveness of 3D-HyCoSy and FTRH for uterine cavity lesions.

		FTRH		Total	Kappa	*P*
		(+)	(-)			
3D-HyCoSy	(+)	13	3	16	0.812	<0.05
	(-)	5	19	24		
Total		18	22			

HyCoSy. The diagnostic sensitivity, specificity, and accuracy of vaginal ultrasound were 63.64%, 64.52%, and 67.50%, respectively, with moderate agreement with FTRH (Kappa = 0.673, $P < 0.05$, Table 5). The diagnostic sensitivity, specificity, and accuracy of 3D-HyCoSy were 81.82%, 96.55%, and 92.50%, respectively, which were in good agreement with FTRH (Kappa = 0.910, $P < 0.05$, Table 6). The diagnostic sensitivity, specificity, and accuracy of 4D-HyCoSy were 90.91%, 89.66%, and 90.00%, respectively, which were in good agreement with FTRH (Kappa = 0.903, $P < 0.05$, Table 7).

Table 4: Diagnostic effectiveness of 4D-HyCoSy and FTRH for uterine cavity lesions.

		FTRH		Total	Kappa	*P*
		(+)	(-)			
4D-HyCoSy	(+)	17	0	17	0.914	<0.05
	(-)	1	22	23		
Total		18	22			

3.5. Comparison of Ovarian Lesion Screening. 9 ovarian lesions were tested by vaginal ultrasound, the diagnostic sensitivity was 45.45%, the specificity was 86.21%, and the accuracy was 75.00% (Kappa = 0.654, $P < 0.05$, Table 8). 12 ovarian lesions were found by 3D-HyCoSy, the diagnostic sensitivity was 90.91%, the specificity was 93.10%, and the accuracy was 92.50% (Kappa = 0.906, $P < 0.05$, Table 9). And 11 ovarian lesions were examined by 4D-HyCoSy, and it is completely consistent with the inspection results of FTRH (Kappa = 1, Table 10).

Table 5: Diagnostic effectiveness of vaginal ultrasound versus FTRH for pelvic lesions.

		FTRH (+)	FTRH (-)	Total	Kappa	*P*
Vaginal ultrasound	(+)	7	9	16		
	(-)	4	20	24	0.673	<0.05
Total		11	29			

Table 6: Diagnostic effectiveness of 3D-HyCoSy versus FTRH for pelvic lesions.

		FTRH (+)	FTRH (-)	Total	Kappa	*P*
3D-HyCoSy	(+)	9	1	10		
	(-)	2	28	27	0.910	<0.05
Total		11	29			

Table 7: Diagnostic effectiveness of 4D-HyCoSy versus FTRH for pelvic lesions.

		FTRH (+)	FTRH (-)	Total	Kappa	*P*
4D-HyCoSy	(+)	10	3	13		
	(-)	1	26	27	0.903	<0.05
Total		11	29			

Table 8: Diagnostic effectiveness of vaginal ultrasound and FTRH on ovarian lesions.

		FTRH (+)	FTRH (-)	Total	Kappa	*P*
Vaginal ultrasound	(+)	5	4	9		
	(-)	6	25	31	0.654	<0.05
Total		11	29			

Table 9: Diagnostic effectiveness of 3D-HyCoSy and FTRH on ovarian lesions.

		FTRH (+)	FTRH (-)	Total	Kappa	*P*
3D-HyCoSy	(+)	10	2	12		
	(-)	1	27	28	0.906	<0.05
Total		11	29			

3.6. Comparison of Tubal Patency Test Results. Vaginal ultrasound detected 54 obstructions with a diagnostic sensitivity of 70.42%, specificity of 55.56%, accuracy of 68.75%, and moderate agreement with FTRH (Kappa = 0.640, $P < 0.05$, Table 11). 3D-HyCoSy found obstruction in 67 strips with a diagnostic sensitivity of 92.96%, specificity of 88.89%, accuracy of 92.50%, and good agreement with FTRH (Kappa = 0.894, $P < 0.05$, Table 12). 4D-HyCoSy identified obstruction in 68 entries with a diagnostic sensitivity of 95.77%, specificity of 100.0%, accuracy of 96.25%, and good agreement with FTRH (Kappa = 0.942, $P < 0.05$, Table 13).

Table 10: Diagnostic effectiveness of 4D-HyCoSy and FTRH on ovarian lesions.

		FTRH (+)	FTRH (-)	Total	Kappa	*P*
4D-HyCoSy	(+)	11	0	11		
	(-)	0	29	29	1.000	<0.05
Total		11	29			

4. Discussion

The fallopian tubes have the role of transporting sperm, picking up eggs, and being transported by fertilized eggs to the uterine cavity, and they occupy a dominant position among all the factors that cause infertility in women [14]. Thus, the correct and accurate assessment of tubal blockage is of great importance for the diagnosis and treatment of infertility. And for tubal obstruction assessment, both 3D-HyCoSy and 4D-HyCoSy also revealed superior results [15, 16]. However, few studies have been conducted to compare the effectiveness of 3D-HyCoSy with 4D-HyCoSy. Hence, this study is an essential reference for the further popularization of HyCoSy use. At the same time, for the increasing incidence of female infertility, finding the cause of infertility quickly and accurately is the key to complete clinical treatment and achieve normal pregnancy. By exploring the application of HyCoSy, it is also beneficial to better grasp the assessment of the causes of female infertility in the future, so as to provide patients with more reliable diagnosis and treatment advice.

In this study, we found that both 3D-HyCoSy and 4D-HyCoSy had better diagnostic results for infertility than 2D vaginal ultrasound, but the evaluation results of 4D-HyCoSy for uterine cavity, pelvis, ovarian lesions, and tubal patency were more consistent with laparoscopic tubal lavage, indicating that 4D-HyCoSy has a higher clinical application prospect. Previous studies have pointed out that although the clear images of 3D-HyCoSy provide a more visual and three-dimensional view of the course and morphology of the fallopian tubes, there are certain limitations, such as the fact that only one 3D image can be obtained per 3D-HyCoSy examination. And the start time and speed of the scan and the timing of the contrast agent need to be strictly controlled during the scan. At the same time, since the probe cannot be moved during 3D-HyCoSy, it is necessary to rely on the experience of the examiner to judge the depth, angle, and range of the scan, etc. Therefore, 3D-HyCoSy requires high professional skills of the operator, and only after proficiency can images of good quality be obtained [17–19]. The 4D-HyCoSy is a 3D volumetric database with high frame rate, which can display the whole process of contrast agent entering the uterine cavity from the catheter and developing the fallopian tubes in real time. The image is dynamic and clear, and it is convenient to observe the degree of patency

Table 11: Diagnostic effectiveness of vaginal ultrasound versus FTRH for tubal obstruction.

		FTRH		Total	Kappa	*P*
		(+)	(-)			
Vaginal ultrasound	(+)	50	4	54		
	(-)	21	5	26	0.640	<0.05
Total		71	9			

Table 12: Diagnostic effectiveness of 3D-HyCoSy versus FTRH for tubal obstruction.

		FTRH		Total	Kappa	*P*
		(+)	(-)			
3D-HyCoSy	(+)	66	1	67		
	(-)	5	8	13	0.894	<0.05
Total		71	9			

Table 13: Diagnostic effectiveness of 4D-HyCoSy versus FTRH for tubal obstruction.

		FTRH		Total	Kappa	*P*
		(+)	(-)			
4D-HyCoSy	(+)	68	0	68		
	(-)	3	9	12	0.942	<0.05
Total		71	9			

of the fallopian tubes, the morphology of the tubal and uterine cavities, and the diffusion of contrast agent in the pelvis. The scanning process can rotate the plane to select the best viewing and acquisition angles [20, 21]. We believe that the reason for some discrepancies in the results of the two examinations may lie in the shorter image scanning time of 3D-HyCoSy, when a transient blockage and spasm of the fallopian tubes may have been caused by the accumulation of air bubbles, leading to misdiagnosis. Besides, 3D-HyCoSy is a posterior-to-forward sweep, and the position of the fallopian tubes needs to be predicted in relation to the uterus and ovaries to determine the time to activate the 3D mode; otherwise, the contrast agent may diffuse into the pelvis and interfere with the image or "off-target" the distal fallopian tubes [22]. Moreover, 3D-HyCoSy is susceptible to the influence of contrast agents that diffuse into the pelvis, parametrial venous reflux, and myometrium, and there are more confounding factors in the evaluation of the final results [23], while 4D-HyCoSy acquires a video recording that dynamically records the entire process of contrast medium entering the uterine cavity and flowing into the fallopian tube to its ejection from the umbilical end. Its advantage is that it allows dynamic observation and frame-by-frame playback, which is more conducive to clinical observation of the details of the fallopian tube and confirmation of the presence of diffusion and backflow [24]. Finally, the 4D-HyCoSy examination also allows the probe to be moved during the examination to find the most ideal viewing angle, thus allowing a more effective evaluation of the difference in bilateral fallopian tube visualization time [25]. Nevertheless, there are still several issues that deserve attention. For example, due to the lack of clinical guidelines for 4D-HyCoSy, some of the diagnostic criteria are still not quantified; there may be some subjective differences in the judgment of the results, which need to be evaluated in conjunction with patients' specific situation and physicians' opinion. In some children with severe tubal occlusion, the injected contrast agent may diffuse or return to other surrounding organs, so it should be pushed as slowly as possible to prevent reflux. If the uterus is positioned too far forward or backward, the position of the uterus can be adjusted by filling the bladder to prevent leakage of the contrast medium.

Of course, since this study is a retrospective analysis and the number of subjects is small, we cannot exclude that there may be chance in the test results. Subsequently, we need to conduct randomized controlled trials to further confirm the advantages and disadvantages of 3D-HyCoSy versus 4D-HyCoSy as soon as possible. In the meantime, we need to conduct a trial on the effect of infertility treatment under 4D-HyCoSy guidance to provide a more comprehensive reference for the future use of HyCoSy. Of course, the most critical point is that because neither 3D-HyCoSy nor 4D-HyCoSy has been widely used in clinical practice, there is a lack of unified clinical manipulation and evaluation guidelines for the evaluation of female infertility by 3D-HyCoSy and 4D-HyCoSy. This is also a big problem to realize the clinical application of 3D-HyCoSy and 4D-HyCoSy. Therefore, we hope that more researchers can join in the research on the diagnosis of female infertility by 3D-HyCoSy and 4D-HyCoSy and realize the popularization and use of 3D-HyCoSy and 4D-HyCoSy as soon as possible.

5. Conclusion

4D-HyCoSy can be used as an effective tool for clinical diagnosis of female tubal obstruction infertility and provide a reference basis for the design of subsequent clinical treatment plans.

Data Availability

The datasets used and analyzed in the current study would be available from the corresponding author upon request.

Ethical Approval

This study was approved by the Human Research Ethical Committee of Pukou Branch Hospital of Jiangsu People's Hospital (Approval No.2022-SR-006).

Conflicts of Interest

The author declares that there are no competing interests.

Hindawi
Computational and Mathematical Methods in Medicine
Volume 2023, Article ID 9806902, 1 page
https://doi.org/10.1155/2023/9806902

Retraction

Retracted: Comparison of Efficacy and Psychology of Breast-Conserving Surgery and Modified Radical Mastectomy on Patients with Early Breast Cancer under Graded Nursing

Computational and Mathematical Methods in Medicine

Received 5 December 2023; Accepted 5 December 2023; Published 6 December 2023

This article has been retracted by Hindawi, as publisher, following an investigation undertaken by the publisher [1]. This investigation has uncovered evidence of systematic manipulation of the publication and peer-review process. We cannot, therefore, vouch for the reliability or integrity of this article.

Please note that this notice is intended solely to alert readers that the peer-review process of this article has been compromised.

Wiley and Hindawi regret that the usual quality checks did not identify these issues before publication and have since put additional measures in place to safeguard research integrity.

We wish to credit our Research Integrity and Research Publishing teams and anonymous and named external researchers and research integrity experts for contributing to this investigation.

The corresponding author, as the representative of all authors, has been given the opportunity to register their agreement or disagreement to this retraction. We have kept a record of any response received.

References

[1] T. Ren, J. Wu, L. Qian, J. Liu, and K. Ni, "Comparison of Efficacy and Psychology of Breast-Conserving Surgery and Modified Radical Mastectomy on Patients with Early Breast Cancer under Graded Nursing," *Computational and Mathematical Methods in Medicine*, vol. 2022, Article ID 4491573, 7 pages, 2022.

Hindawi
Computational and Mathematical Methods in Medicine
Volume 2022, Article ID 4491573, 7 pages
https://doi.org/10.1155/2022/4491573

Research Article

Comparison of Efficacy and Psychology of Breast-Conserving Surgery and Modified Radical Mastectomy on Patients with Early Breast Cancer under Graded Nursing

Tiantian Ren, Jianli Wu, Lu Qian, Jing Liu, and Kan Ni

Department of Thyroid and Breast Surgery, Affiliated Hospital of Nantong University, Nantong, Jiangsu 226000, China

Correspondence should be addressed to Kan Ni; ntnikan@163.com

Received 1 August 2022; Revised 26 August 2022; Accepted 30 August 2022; Published 16 September 2022

Academic Editor: Min Tang

Objective. To compare the efficacy and psychology of breast-conserving surgery and modified radical mastectomy in patients with early breast cancer (BC) under graded nursing. *Methods.* Forty-one early breast-conserving surgery BC patients admitted to our hospital from April 2020 to March 2022 were regarded as group A, and 52 with modified radical surgery were seen as group B. The operating time, intraoperative bleeding, postoperative drainage, and hospital stay were compared, and the postoperative adverse effects were counted. In addition, patients' psychology and quality of life were assessed using the HAMD, HAMA, and QLSBC rating scales. At the time of discharge, a treatment satisfaction survey was conducted. *Results.* The operative time, intraoperative bleeding, postoperative drainage, and hospital stay of patients in group A were lower than those in group B ($P < 0.05$). After treatment, the HAMD and HAMA scores were lower in group A than in group B, while the QLSBC scores and treatment satisfaction were higher ($P < 0.05$). *Conclusion.* Breast-conserving surgery under graded nursing is less damaging to early BC patients. It can effectively shorten the postoperative recovery process and improve the psychology and quality of life, so it has higher clinical applicability.

1. Introduction

Breast cancer (BC), an extremely common clinical malignancy, has a high incidence worldwide [1]. It mostly occurs in the mammary duct epithelium, and middle-aged and older women are the most prevalent group, and the incidence has shown a younger trend [2]. With the continuous development of modern medical technology, the rate of early BC diagnosis is increasing, and surgical treatment remains the best treatment option. Traditional radical mastectomy requires the entire breast and surrounding tissues to be removed due to the large excision range, which is rarely used in clinical practice [3]. The modified version of radical surgery has gradually developed into a common clinical procedure because of the surgical preservation of the pectoralis muscle and better postoperative appearance [4]. However, for young women, the lack of breasts after radical surgery will greatly impact the patient's self-esteem, affect future marital relationships, breastfeeding, etc., making patients prone to anxiety, depression, low self-esteem, and other negative emotions, affecting the treatment effect [5]. But breast-conserving surgery can effectively solve this problem without affecting the treatment effect, and improve the aesthetics of BC treatment [6].

In modern health care, the intervention of nursing tools is likewise one of the most vital aspects of improving patient outcome [7]. Several studies have shown the positive impact of applying individualized care strategies for various types of oncology patients [8], but there is still a lack of uniform clinical standard guidelines for BC. Through access to literature, we discovered that graded nursing is a type of service that is graded according to the severity of illness of patients and implemented in a targeted, detailed, and precise manner in relation to their actual condition [9]. It has been shown to exert excellent effects in the surgical treatment of diseases such as gastric cancer and lung cancer [10]. Recently, our hospital has been gradually promoting the use of graded nursing in all departments and expects to improve the

quality of medical services and patients' treatment experience in this way.

Thus, this research will provide a reliable reference and guidance for future clinical treatment of early BC patients by comparing the assessment of outcomes and the impact of psychology between breast-conserving surgery and modified radical surgery under graded nursing.

2. Materials and Methods

2.1. Study Area. The study was carried out at Department of Thyroid and Breast Surgery, Affiliated Hospital of Nantong University from April 2020 to April 2022.

2.2. General Data. Ninety-three patients with early BC admitted to our hospital from April 2020 to March 2022 were enrolled to this research. Among them, 41 patients received breast-conserving surgery were regarded as group A, and 52 with modified radical mastectomy were considered as group B. All the above subjects signed the informed consent form.

2.3. Inclusion and Exclusion Criteria. Inclusion criteria: all the selected patients were confirmed as early BC by pathological examination, and all of them chose to be treated in our hospital after diagnosis; patients have not received chemotherapy, radiotherapy, or endocrine therapy either preoperatively or prior to puncture; those with TNM stage I-II (The staging standard is based on the BC Staging Guidelines [11]) and those with complete medical records; patients or their immediate family members signed an informed consent form.

Exclusion criteria: those with other malignancies; those with multiple chronic diseases; those with cardiovascular and cerebrovascular diseases; those with organ dysfunction; those with drug allergies; those who suffer from mental illness or physical disability that prevents them from taking care of themselves; contraindication to surgery; transferred patients.

2.4. Hospitalization Management. Both groups of patients were admitted to the hospital using graded nursing [12]. The nursing team was led by the head nurse to establish a nursing plan, standardize the process and quality, and give patients a grade classification based on their own conditions, and implement targeted measures considering the classification. It is more helpful for patients with complex conditions to receive timely and active intervention and ensure the quality of nursing. Furthermore, nurses should help patients prepare for operation, including notification of surgical procedures, presentation of successful cases, and emotional counseling. After surgery, patients' vital signs are closely observed, healthy diet is instructed, upper limb function exercises are carried out in a timely manner, and professional guidance is provided to improve their discomfort and prognosis.

2.5. Operation Treatment. The surgeries of both groups were performed by the same surgical team in our hospital. Group A: with the lesion as the center, radial, transverse, or curved incision was chosen according to the location of the tumor, and the base of the tumor and normal breast tissue were excised at 1 cm from the tumor. The excised tissues were subjected to rapid cryopathological examination to mark the internal, external, upper, lower, and basal locations of the incision margin. When the diagnosis is positive at the incision margin, it is necessary to expand the excision again until the test is negative. Then, lymph node dissection is performed in the range of axillary vein, deep surface of pectoralis minor muscle and anterior border of latissimus dorsi muscle, and a drainage tube is disposed in the incision, sutured, and pressure bandaged. Group B: after intravenous compound inhalation anesthesia, the surgical incision was decided according to the size of the affected breast and the location of the tumor, etc. The surgical incision was made 2-5 cm from the outer edge of the tumor and a fusiform incision was made. After cutting the skin of patients' affected breast, the affected breast was excised from the surface of the pectoralis major muscle using an electric knife to free the flap superiorly to the clavicle, inferiorly to the superior edge of the rectus abdominis sheath, internally to the parasternal sternum, and externally to the anterior edge of the latissimus dorsi. Patients' axilla was disposed of by making an incision and lifting the pectoralis major and pectoralis minor muscles inward and upward with a thyroid pull hook to fully expose his axilla. The axillary lymph nodes on the affected side of patients and the lymph nodes between the pectoralis major and minor muscles were removed. Patients' surgical wound was irrigated and soaked using distilled water (45°C), followed by routine placement of a drainage tube and suturing of the incision.

2.6. Outcome Measures. The operative indexes of both groups were compared, including operation time, intraoperative blood loss, postoperative drainage, and hospital stay. The postoperative complications of the two groups of patients were counted, and the incidence of complications = the number of complications/total number × 100%. And the treatment satisfaction before discharge was calculated through the self-made satisfaction scale, the alternative answers are very satisfied, satisfied, dissatisfied, total satisfaction = (very satisfied + satisfied)/total × 100%. The psychological scores after treatment were evaluated by HAMD [13] and HAMA [14] scores, HAMD includes 17 survey items, HAMA includes 14 survey items, and the alternative answers are asymptomatic (0 points), mild (1 point), moderate (2 points), severe (3 points), and very severe (4 points), the higher the score, the more severe the depression and anxiety. The Quality-of-Life Scale for BC (QLSBC) [15] was used to assess the posttreatment quality of life in both groups, including four dimensions of physical functioning, social functioning, psychology, and faith factors, with higher scores indicating higher quality of life.

2.7. Statistical Methods. Data were analyzed statistically using SPSS24.0 software. Thereinto, the counting data were represented as (%) and compared through the chi-square test, while the measurement data were expressed in $(\bar{}\chi \pm s)$ and assessed through t-test and paired t-test. The difference was statistically marked ($P < 0.05$).

3. Results

3.1. Summary of Results. The operative time, intraoperative bleeding, postoperative drainage, and hospital stay of

patients in group A were lower than those in group B ($P < 0.05$). After treatment, the HAMD and HAMA scores were lower in group A than in group B, while the QLSBC scores and treatment satisfaction were higher ($P < 0.05$).

3.2. Baseline Data Comparison. The general data such as age and BMI of patients were counted (Table 1). Both groups revealed no statistical difference ($P > 0.05$), suggesting that there was comparability between groups and that subsequent experimental analysis could be performed.

3.3. Comparison of Operative Indexes between Groups. It can be seen that the operative time was shorter in group A than in group B (59.07 ± 9.79 min *vs.* 96.19 ± 12.85 min, $P < 0.05$, Figure 1(a)). The intraoperative bleeding in group A was (45.95 ± 8.27 mL), also lower than group B ($P < 0.05$, Figure 1(b)). The postoperative drainage was lower in group A than in group B ($P < 0.05$, Figure 1(c)). The length of stay in group A was (3.36 ± 0.88 d), which was dramatically shorter than that in group B ($P < 0.05$, Figure 1(d)).

3.4. Comparison of Postoperative Adverse Reactions. In group A, 2.44% (1 case) of patients had incision infection, 2.44% (1 case) had nausea and vomiting, 2.44% (1 case) had upper limb swelling, and 2.44% (1 case) had subcutaneous effusion. The total incidence of adverse reactions was 9.76%. While in group B, 1.92% (1 case) of patients had incision infection, 3.85% (2 cases) had nausea and vomiting, 3.85% (2 cases) had upper limb swelling, 1.92% (1 case) had flap necrosis, and 1.92% (1 case) had subcutaneous effusion. The total incidence was 13.46%. There was no marked difference in the incidence of postoperative adverse reactions between groups ($P > 0.05$, Table 2).

3.5. Comparison of Psychology before and after Treatment. Changes in patients' psychology are equally one of the important aspects that need to be brought to clinical attention in healthcare services nowadays. Thus, we compared the changes in psychological scores of patients before and after treatment. It turned out that the differences in HAMD and HAMA scores before treatment were not statistically obvious ($P > 0.05$). The HAMD score in group A was (8.78 ± 3.18) after treatment, which was lower than that in group B ($P < 0.05$, Figure 2(a)) The HAMA score was (8.34 ± 3.50), which was similarly lower than in group B ($P < 0.05$, Figure 2(b)). In addition, the HAMD and HAMA scores were remarkably lower in both groups after treatment than before treatment ($P < 0.05$).

3.6. Comparison of Quality of Life before and after Treatment. Likewise, quality of life, another aspect of modern clinical services that deserves attention, is a direct reflection of patient recovery and prognosis to a large extent. There was no difference in the scores of each dimension of QLSBC score between groups before treatment ($P > 0.05$), while the somatic function score in group A was (58.10 ± 5.64) after treatment, which was dramatically higher than that in group B ($P < 0.05$, Figure 3(a)). But the psychology score in group A was (76.93 ± 4.34), also dramatically higher than in group B ($P < 0.05$, Figure 3(b)). The social functioning domain scores of patients in group A were also higher than those in group B ($P < 0.05$, Figure 3(c)). And the faith factor score in group A was (44.46 ± 5.58), which was higher than that in group B (35.87 ± 7.21), ($P < 0.05$, Figure 3(d)).

Table 1: Baseline datasheet.

	Group A ($n = 41$)	Group B ($n = 52$)	t or χ^2	P
Age	64.07 ± 4.95	62.77 ± 9.27	0.811	0.420
BMI (kg/m2)	26.11 ± 3.03	25.32 ± 3.33	1.181	0.241
Living environment			0.862	0.353
In the city	26 (63.41)	28 (53.85)		
In the countryside	15 (36.59)	24 (46.15)		
Type of cancer			0.797	0.372
Ductal cancer	41 (100.0)	51 (98.08)		
Lobular cancer	0 (0.0)	1 (1.92)		
Drinking			0.001	0.982
Yes	4 (9.76)	5 (9.62)		
No	37 (90.24)	47 (90.38)		
Family history of illness			0.145	0.703
Have	1 (2.44)	2 (3.85)		
None	40 (97.56)	50 (96.15)		
Pathological stage			0.091	0.764
Stage I	21 (51.22)	25 (48.08)		
Stage II	20 (48.78)	27 (51.92)		

3.7. Treatment Satisfaction Comparison. The treatment satisfaction survey in both groups denoted that 58.54% of patients in group A were very satisfied and only 7.32% were dissatisfied, with an overall satisfaction rate of 92.68%. While only 36.54% of patients in group B rated very satisfied, and 26.92% rated unsatisfied, for a total rate of 73.08%. The total satisfaction was dramatically higher in group A than in group B ($P < 0.05$, Table 3).

4. Discussion

BC, one of the most common female tumors, has seriously affected the lives of more than 1.2 million female patients worldwide [16]. For early BC, timely surgical procedures can effectively mitigate the pathological development of BC and provide for patient safety [17]. However, because the tumor lesion invades normal breast tissue, most patients may require total removal of the entire breast tissue during surgery [18]. And that is why it is also necessary to pay closer attention to the changes in x patients to soothe the psychological burden caused by mastectomy and provide them with prognosis [18]. Graded nursing, one of the common nursing strategies clinically, has achieved extremely excellent results in the treatment of dementia and diabetes [19, 20], but its effectiveness in BC is indistinct.

Currently, personalized care strategies are also one of the extremely important key aspects in modern oncological

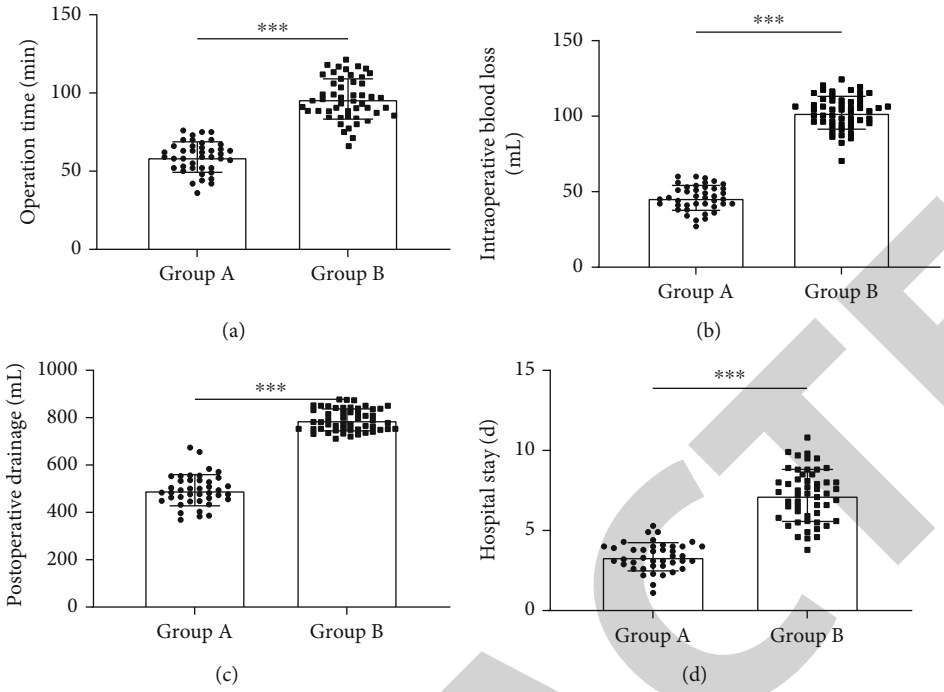

Figure 1: Comparison of surgical indicators between groups. (a) Comparison of operative time between groups. (b) Comparison of intraoperative bleeding between groups. (c) Comparison of postoperative drainage between groups. (d) Comparison of length of stay between groups. $^{***}P < 0.005$.

Table 2: Postoperative adverse reactions.

	Incision infection	Nausea and vomiting	Upper limb swelling	Flap necrosis	Subcutaneous effusion	Total incidence (%)
Group A ($n = 41$)	1 (2.44)	1 (2.44)	1 (2.44)	0 (0.00)	1 (2.44)	9.76
Group B ($n = 52$)	1 (1.92)	2 (3.85)	2 (3.85)	1 (1.92)	1 (1.92)	13.46%
χ^2						0.302
P						0.583

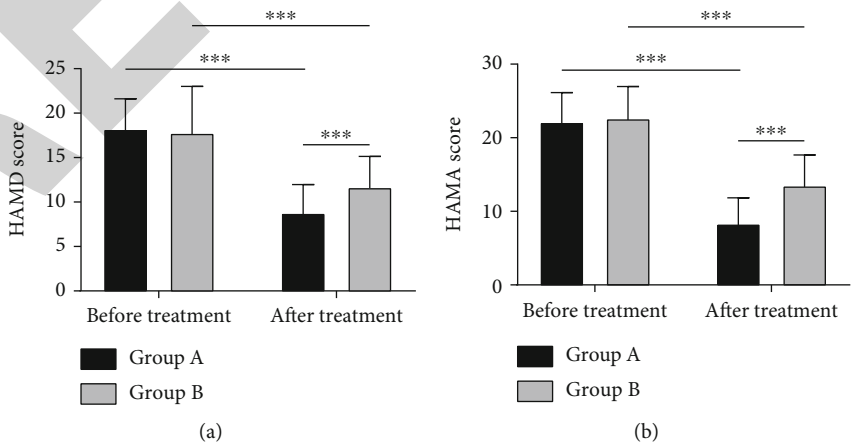

Figure 2: Comparison of psychology before and after treatment. (a) Comparison of HAMD scores of both groups before and after treatment. (b) Comparison of HAMA scores of both groups before and after treatment. $^{***}P < 0.005$.

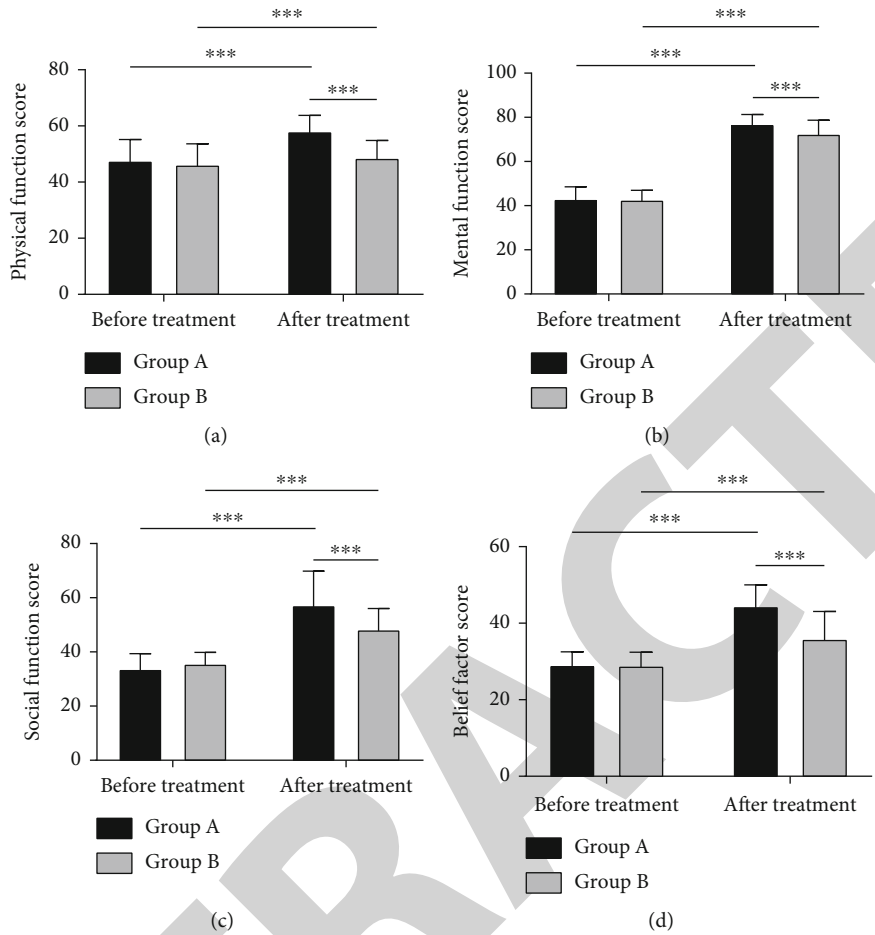

Figure 3: Comparison of quality of life before and after treatment. (a) Comparison of somatic function scores of both groups before and after treatment. (b) Comparison of psychology scores of both groups before and after treatment. (c) Comparison of functioning domain scores of both groups before and after treatment. (d) Comparison of faith factor scores of both groups before and after treatment. $^{***}P < 0.005$.

Table 3: Treatment satisfaction survey.

	Very satisfied	Satisfied	Dissatisfied	Total satisfaction (%)
Group A ($n = 41$)	24 (58.54)	14 (34.15)	3 (7.32)	92.68
Group B ($n = 52$)	19 (36.54)	19 (36.54)	14 (26.92)	73.08
χ^2				5.899
P				0.015

diseases. Among them, graded nursing, as an excellent nursing management model, has the core concept of patient-centeredness and different treatment measures for patients' conditions through environmental management, psychological guidance, health education, and adjustment of restraint measures under the guidance of nursing humanistic care principles and other methods. It cannot only improve their hospital comfort and eliminate negative emotions but also enhance their treatment effects and recovery to a certain extent [21, 22]. In the case of BC surgery patients, this research can lay the foundation for further promotion and application of subsequent graded nursing. In previous studies, graded nursing has achieved excellent results in the treatment of diabetes, meningioma, and other diseases, and it has been found to improve the nursing efficiency of cardiothoracic surgery patients and alleviate the negative emotions of patients [23–25]. At present, the idea that "individualized nursing strategies can improve the overall recovery of the disease" has been unanimously recognized by the clinic [26]. Therefore, for patients with BC surgery, the application of this study can provide a reliable reference for the follow-up treatment and nursing of BC, further protect the life safety of patients, and lay a foundation for the promotion and application of graded nursing.

First, we compared the surgical conditions of both groups, and the operative time, intraoperative bleeding, postoperative drainage, and hospital stay of patients in group A were shorter than those in group B, suggesting that our breast-conserving surgery is less damaging to those with early BC and can effectively shorten their postoperative recovery. In a previous study, we also found that the postoperative recovery process was shorter in patients undergoing breast-conserving surgery than those with conventional radical surgery [27], which could also verify the accuracy of this experiment. The feasibility of breast-conserving surgery was confirmed in the NSABP B-06 study in 1995 [28]; because breast-conserving surgery removes only a small area of tissue within the breast when removing the tumor, it can avoid the invasive operation of modified radical surgery with extensive removal of breast contents, skin flaps, and other tissues to a certain extent. So, it causes less damage to the tissues surrounding the lesion within the breast and shortens the postoperative recovery time of patients [29]. Besides, breast-conserving surgery cannot only preserve the breast to the maximum extent and ensure its shape and function to meet the cosmetic needs of patients as much as possible but also safeguard the psychology of patients and reduce the possibility of negative emotions [30]. In the follow-up investigation of the psychology scores of both groups, we also found that the postoperative HAMD and HAMA scores of patients in group A were lower than those of group B, indicating that the postoperative psychology of patients with breast-conserving surgery was more excellent. The lower psychological burden caused by breast-conserving surgery on patients has been mentioned several times in previous studies [31, 32]. In addition, in previous studies, we also found that graded care can also improve the psychological state of stroke and pancreatitis [33, 34], so the improvement of psychological state of patients in the two groups may also be affected by graded care. But this effect is positive for the patient's recovery. Nevertheless, we found no statistical difference in the incidence of adverse reactions between groups, which may be due to statistical contingency caused by small number of cases. It may also be because the subjects were all early BC patients, and therefore generally had a better postoperative recovery and a lower incidence of adverse effects. This will be verified as soon as possible in the follow-up experiments. Finally, we compared the quality of life between both groups, and the QLSBC score of patients in group A was higher, which indicated that the quality of life of those undergoing breast-conserving surgery was better after treatment. And this we presume is also because breast-conserving surgery causes less damage to patients. Meanwhile, the improvement of patients' negative emotions can more effectively enhance their postoperative recovery and quality of life. More than that, the treatment satisfaction rate was also higher in group A than in group B. It also once again indicates that breast-conserving surgery is more applicable in BC treatment and more recommended for clinical preference. Of course, the application of breast conserving surgery in the treatment of BC has been clinically verified many times [35, 36], and this study further highlights the future significance of breast conserving surgery in the treatment of BC through the comparison with modified radical mastectomy. This will undoubtedly be of great help to the choice of surgical treatment for BC patients.

5. Conclusion

Breast-conserving surgery under graded nursing is less damaging to early BC patients. It can effectively shorten the postoperative recovery process and improve the psychology and quality of life, so it has higher clinical applicability.

Data Availability

The datasets used and/or analyzed during the current study are available from the corresponding author on reasonable request.

Conflicts of Interest

The authors have no conflicts of interest to declare.

References

[1] S. H. Jafari, Z. Saadatpour, A. Salmaninejad et al., "Breast cancer diagnosis: imaging techniques and biochemical markers," *Journal of Cellular Physiology*, vol. 233, no. 7, pp. 5200–5213, 2018.

[2] U. M. Fahad, "Breast cancer: current perspectives on the disease status," *Advances in Experimental Medicine and Biology*, vol. 1152, pp. 51–64, 2019.

[3] J. Y. S. Tsang and G. M. Tse, "Molecular classification of breast cancer," *Advances in Anatomic Pathology*, vol. 27, no. 1, pp. 27–35, 2020.

[4] M. M. Al Awayshih, M. N. Nofal, and A. J. Yousef, "Modified radical mastectomy for male breast cancer," *The American journal of case reports*, vol. 20, pp. 1336–1339, 2019.

[5] H. Qiu, W. H. Xu, J. Kong, X. J. Ding, and D. F. Chen, "Effect of breast-conserving surgery and modified radical mastectomy on operation index, symptom checklist-90 score and prognosis in patients with early breast cancer," *Medicine (Baltimore)*, vol. 99, no. 11, article e19279, 2020.

[6] S. Sinnadurai, A. Kwong, M. Hartman et al., "Breast-conserving surgery versus mastectomy in young women with breast cancer in Asian settings," *BJS Open*, vol. 3, no. 1, pp. 48–55, 2019.

[7] P. Lumbiganon, R. Martis, M. Laopaiboon et al., "Antenatal breastfeeding education for increasing breastfeeding duration," *Cochrane Database of Systematic Reviews*, vol. 2016, no. 12, article CD006425, 2016.

[8] D. Arikpo, E. S. Edet, M. T. Chibuzor, F. Odey, D. M. Caldwell, and Cochrane Developmental, Psychosocial and Learning Problems Group, "Educational interventions for improving primary caregiver complementary feeding practices for children aged 24 months and under," *Cochrane Database of Systematic Reviews*, vol. 2018, no. 5, article CD011768, 2018.

[9] S. R. Komprood, "Nursing student attitudes toward oncology nursing: an evidence-based literature review," *Clinical Journal of Oncology Nursing*, vol. 17, no. 1, pp. E21–E28, 2013.

[10] L. M. Aitken, G. Williams, M. Harvey et al., "Nursing considerations to complement the surviving sepsis campaign

Hindawi
Computational and Mathematical Methods in Medicine
Volume 2023, Article ID 9789418, 1 page
https://doi.org/10.1155/2023/9789418

Retraction

Retracted: Effects of Thoracic Paravertebral Block on Postoperative Anxiety and Depression for Patients Undergoing Thoracoscopic Lung Cancer Radical Surgery

Computational and Mathematical Methods in Medicine

Received 12 December 2023; Accepted 12 December 2023; Published 13 December 2023

This article has been retracted by Hindawi, as publisher, following an investigation undertaken by the publisher [1]. This investigation has uncovered evidence of systematic manipulation of the publication and peer-review process. We cannot, therefore, vouch for the reliability or integrity of this article.

Please note that this notice is intended solely to alert readers that the peer-review process of this article has been compromised.

Wiley and Hindawi regret that the usual quality checks did not identify these issues before publication and have since put additional measures in place to safeguard research integrity.

We wish to credit our Research Integrity and Research Publishing teams and anonymous and named external researchers and research integrity experts for contributing to this investigation.

The corresponding author, as the representative of all authors, has been given the opportunity to register their agreement or disagreement to this retraction. We have kept a record of any response received.

References

[1] C. Geng, C. Tong, H. Li, S. Shi, J. Yu, and L. Huang, "Effects of Thoracic Paravertebral Block on Postoperative Anxiety and Depression for Patients Undergoing Thoracoscopic Lung Cancer Radical Surgery," *Computational and Mathematical Methods in Medicine*, vol. 2022, Article ID 7629012, 6 pages, 2022.

Hindawi
Computational and Mathematical Methods in Medicine
Volume 2022, Article ID 7629012, 6 pages
https://doi.org/10.1155/2022/7629012

Research Article

Effects of Thoracic Paravertebral Block on Postoperative Anxiety and Depression for Patients Undergoing Thoracoscopic Lung Cancer Radical Surgery

Congfu Geng,[1] Chunting Tong,[1] Houxiang Li,[1] Shaojiang Shi,[1] Jiancheng Yu,[1] and Lei Huang[2]

[1]*Department of Anesthesiology, Jinhu People's Hospital, Huai'an, 211600 Jiangsu, China*
[2]*Department of Anesthesiology, The First Affiliated Hospital of Soochow University, Suzhou, 215006 Jiangsu, China*

Correspondence should be addressed to Lei Huang; huanglei2014@suda.edu.cn

Received 12 August 2022; Revised 24 August 2022; Accepted 29 August 2022; Published 16 September 2022

Academic Editor: Min Tang

This study is aimed at investigating the effect of thoracic paravertebral block (TPVB) on the occurrence of chronic postoperative pain, postoperative anxiety, and depression in patients undergoing thoracoscopic radical lung cancer surgery. A total of 120 patients who underwent thoracoscopic radical lung cancer surgery in our hospital from June 2019 to March 2021 were included. There were 62 males and 58 females, with an age of 18-75 years old and a body mass index of 20-28 kg/m^2. Patients were divided into two groups using the random number table method, TPVB group ($n = 60$) and normal saline group (control group, $n = 60$). Two-point nerve block was performed at T5-6 and T6-7 levels. Patients in the TPVB group received nerve block with 15 mL of 0.375% ropivacaine hydrochloride, while those in the control group received 5 mL of 0.9% normal saline. The numeric rating scale (NRS) scores at rest and during movement at 24 and 48 hours after surgery and the number of times the button on the patient-controlled analgesia pressed at 24 h after surgery in two groups were recorded. All patients were followed up by outpatient visits or phone visits at 1 year after surgery and assessed using Leeds Assessment of Neuropathic Symptoms and Signs (LANSS) pain scale and Hospital Anxiety and Depression Scale (HADS). According to the inclusion, exclusion, and drop-out criteria, 108 patients were finally included, with 52 patients in the TPVB group and 56 patients in the control group. There was no statistically significant difference between the two groups in terms of age, sex, height, body weight, body mass index, ASA classification, and operation time ($P > 0.05$). NRS pain scores at 24 h ($P = 0.0108$) and 48 h ($P = 0.0000$) after surgery, the number of times pressing patient-controlled analgesia at 24 h after surgery ($P = 0.0000$), the LANSS scores ($P = 0.0000$), HADS anxiety score ($P = 0.0000$), and depression scores ($P = 0.0000$) at 1 year after surgery in the TPVB group were both significantly lower than those in the control group. To sum up, ultrasound-guided TPVB can effectively relieve pain at 48 hours after thoracoscopic lung cancer radical surgery and chronic postoperative pain at 6 months after V thoracoscopic lung cancer radical surgery.

1. Introduction

Pain is one of the most important causes of stress in patients undergoing surgery, which can lead to increased postsurgical stress response and various cardiovascular and cerebrovascular complications and affect the quality of life of patients following surgery [1]. For patients undergoing thoracic surgery, postoperative pain obviously impairs patients' ability to take deep breaths, to cough, and to clear sputum, thus leading to complications such as lung infection. If pain management is inadequate, postoperative pain can even develop into neuropathic pain [2], which seriously affects the quality of life of patients and even leads to severe anxiety and depression.

Lung cancer is one of the most common malignant tumors all over the world, with high mortality and morbidity and a tendency to metastasize, which threatens human health and life [3]. Thoracoscopic lung cancer radical

surgery is currently the mainstream treatment for lung cancer. One major advantage of video-assisted thoracoscopic lung cancer radical surgery is preservation of chest wall, thus reducing tissue and nerve damage at the surgical incision site, which can not only reduce surgical trauma but also obviously reduce postoperative pain, speed up the recovery of patients after surgery, and shorten the length of hospital stay [4].

The analgesic effect of thoracic paravertebral block (TPVB) is similar to that of epidural analgesia, which can obviously reduce the incidence of chronic postoperative pain in patients undergoing thoracoscopic radical resection of lung cancer [5]; there are few studies investigating the effect of TPVB and chronic pain on patients' quality of life after surgery. Therefore, in this study, we conducted a one-year follow-up of patients undergoing thoracoscopic lung cancer radical surgery; assessed chronic postoperative pain, anxiety, and depression by using Leeds Assessment of Neuropathic Symptoms and Signs (LANSS) and the Hospital Anxiety and Hospital Anxiety and Depression Scale (HADS); and explored the effect of TPVB on postoperative pain, anxiety, and depression in these patients.

This study investigated the effect of TPVB on the occurrence of chronic postoperative pain, postoperative anxiety, and depression in patients undergoing thoracoscopic radical lung cancer surgery, so as to provide a reference for clinical promotion of TPVB and enhancement of chronic postoperative pain management.

2. Subjects and Methods

2.1. Subjects. This was a double-blind randomized controlled study. This study was approved by the ethics committee of our hospital (clinical trial number: ChiCTR20190516003). Written informed consent was obtained from all patients included in the study. This study complied with the Declaration of Helsinki and adheres to CONSORT guidelines.

A total of 120 patients who thoracoscopic lung cancer radical surgery in our hospital from June 2019 to March 2021 were included. The inclusion criteria were as follows: patients who were aged 18-75 years with body mass index of 20-28 kg/m^2, American Society of Anesthesiologists (ASA) I or II, operative time of <4 hours, and no surgical history, as well as no history of psychiatric and neurological diseases. Exclusion criteria were as follows: aged ≥76 years, allergy to anesthetic drugs, puncture site infection, history of chest surgery or trauma, history of chronic pain, and history of psychiatric and neurological disorders, including depressive or anxious tendencies. Drop-out criteria were as follows: patients who were lost to follow-up patients who were unable to cooperate properly with assessment, and patients who received other surgical treatment during follow-up.

2.2. Methods. Patients were divided into two groups using a random number table: TPVB group and normal saline group (control group). All procedures were performed by a senior attending physician who had more than 5 years of experience in TPVB and completed more than 50 cases of TPVB alone. The physician was unaware of treatment assignments. The injectable drugs are prepared by a physician before the procedure. None of patients received preconditioning before entering the operating room. After patients entered the operating room, vital signs were monitored routinely, including heart rate, blood pressure, oxygen saturation (pulse oximetry), invasive arterial blood pressure, and bispectral index (BIS) [6]. All patients underwent combined intravenous-inhalational general anesthesia with conventional doses of anesthetic drugs including fentanyl (0.5 μg/kg), rocuronium (0.6 mg/kg), and sevoflurane (1–1.5%) calculated based on patients' body weight, and then, bronchial intubation was performed. After patients were turned to the lateral decubitus position, the position of the T5 spinous process was determined by manual palpation, the ultrasound probe was oriented vertically perpendicular to the midline and then moved upward to check the spinous process and confirm the structures, such as transverse process and pleura. After routine disinfection, two-point nerve block was performed at T5-6 and T6-7 levels, it is needed to confirm that the tip of the nerve block needle passed through the costotransverse ligament and entered in the paravertebral space, and there was no blood return after pulling back. For patients in the TPVB group, 15 mL of 0.375% ropivacaine hydrochloride was slowly injected at the two points. For patients in the control group, 15 mL of 0.9% normal saline was slowly injected [7].

After surgery, all patients were treated with intravenous patient-controlled analgesia (PCA, adding 1.2 mg fentanyl into normal saline to make a total volume of 100 mL) for postoperative analgesia. The PCA was set as a basal infusion rate of 2 mL/h, a bolus dose of 2 mL, with lockout time of 15 min. When pain control was not satisfactory, patients were encouraged to self-administer bolus doses of medication by pressing the PCA button. If postoperative pain is still not effectively relieved, additional nonsteroidal analgesic drugs can be administered; if the pain is still not relieved, consultation with an anesthesiologist may be necessary [8].

The numerical rating scale (NRS) pain scores at rest and during movement and the number of times the button on the PCA pressed at 24 h and 48 h after surgery were recorded. All patients were followed up by outpatient visits or phone visits at one year after surgery and analyzed using the LANSS scale and HADS. A LANSS score of ≥12 indicates the presence of neuropathic pain, and further treatment for chronic pain is recommended for such patients. A score of ≥11 on either HADS depression subscale (HADS-D) or anxiety subscale (HADS-A) indicates the presence of anxiety and depressive symptoms [9]. Throughout the study, patients, anesthesiologist, and surgeon were both unaware of treatment assignments; the physicians who assessed the outcomes during follow-up via outpatient visits or phone visits were also unaware of treatment assignments in order to prevent bias in assessment of subjective outcomes.

2.3. Statistical Analysis. Statistical analysis was carried out using SPSS software (version 24.0, IBM, New York, NY, USA). Continuous variables with normal distribution are expressed as the mean ± SD, and comparisons between

groups were conducted by using two independent sample t -test. Continuous variables with a skewed distribution are expressed as median (M) and interquartile ranges (IQR). Categorical data are expressed as number and percentages. Differences between groups were analyzed with the chi squared (χ^2) test or Fisher's exact test. $P < 0.05$ was considered to indicate a statistically significant difference.

3. Results

3.1. Baseline Characteristics of Patients. A total of 120 patients were initially enrolled in this study. According to the aforementioned inclusion, exclusion, and drop-out criteria, 108 patients were finally included, with 52 patients in the TPVB group and 56 patients in the control group. Analgesia was generally satisfactory in patients of the TPVB group within 48 hours after surgery, and no patients required consultation with an anesthesiologist due to inadequate analgesia within 48 h after surgery.

There was no statistically significant difference between the two groups in terms of age, sex, height, body weight, body mass index, ASA classification, and operation time ($P > 0.05$, Table 1).

3.2. NRS Scores at 24 h and 48 h after Surgery and the Number of Times Pressing PCA at 24 h after Surgery in Each Group. At 24 h and 48 h after surgery, NRS scores at rest and during movement were significantly lower in the TPVB group compared with the control group ($P = 0.0108$, $P = 0.0000$, $P = 0.0000$, and $P = 0.0002$, Table 2). At 24 h after surgery, the number of times pressing PCA was also significantly reduced in the TPVB group compared with the control group ($P = 0.0000$, Table 2).

3.3. The Number of Patients with LANSS of ≥12 Points at 1 Year after Surgery. The incidence of neuropathic pain (LANSS ≥ 12) in the TPVB group at 1 year after surgery was significantly lower than that in the control group ($P = 0.0000$, Table 3).

3.4. The Number of Patients with HADS-A/HADS-D Score of ≥11 at 1 Year Postoperatively between the Two Groups. The incidence of anxiety and depression (HADS-A/HADS – D score ≥ 11) was significantly lower in the TPVB than in the control group at 1 year after surgery ($P = 0.0000$, Tables 4 and 5).

4. Discussion

In this randomized, double-blind, controlled study, we compared patients' baseline characteristics and found that there was no statistically significant difference between the two groups in terms of age, sex, height, body weight, body mass index, ASA classification, and operation time ($P > 0.05$). It has been reported that TPVB can effectively relieve postoperative pain in patients undergoing thoracoscopic radical lung cancer surgery, which provides good analgesia [10]. Consistent with previous study, we compared the NRS pain scores at 24 h and 48 h after surgery and the number of times pressing PCA at 24 h after surgery between the two groups. The results showed that at 24 h and 48 h after surgery, NRS scores at rest and during movement were significantly lower in the TPVB group compared with the control group ($P = 0.0108$, $P = 0.0000$, $P = 0.0000$, and $P = 0.0002$). At 24 h after surgery, the number of times pressing PCA was also significantly reduced in the TPVB group compared with the control group ($P = 0.0000$).

During one-year postoperative follow-up by outpatient visits or phone visits, we also used the LANSS scale and the HADS to assess the occurrence of neuropathic pain, anxiety, and depression, respectively, in patients of the two groups. The LANSS scale is the most commonly used reliable scale for diagnosing the degree of neuropathic pain in different diseases, the specificity reached a high of 93%, and sensitivity reached a high of 83% [11]. In our study, we found that the incidence of neuropathic pain (LANSS ≥ 12) in the TPVB group at 1 year after surgery was significantly lower than that in the control group. Moreover, the HADS was originally developed by Zigmond and Snaith in 1983, which is the most used screening tool for assessing anxiety and depression among general hospital patients. The HADS consists of two subscales: HADS-A and HADS-D. According to the developers of HADS, a score of 0-7 is considered normal, 8–10 indicates possible, and 11–21 indicates definite. A previous study documented that using a cut-off of 9 for anxiety or depression can yield better sensitivity and specificity [12]. To screen out patients who need further treatment, a cut-off score of 11 was used in this study; patients with HADS-A/HADS-D score above 11 were recommended to undergo further specialist examination and treatment. Of note, the results showed that the incidence of anxiety and depression (HADS-A/HADS – D score ≥ 11) at 1 year after surgery in patients receiving TPVB was significantly lower compared with that in the control group ($P = 0.0000$).

Numerous studies have shown that TPVB can reduce postoperative pain in patients undergoing thoracoscopic radical resection of lung cancer, and the underlying mechanism has also been widely discussed. More studies choose to perform TPVB before induction of general anesthesia in patients, which can not only ensure safety during surgery and avoid serious complications but also allow determination of blocking range and exclude cases with poorer outcomes, making the conclusions more accurate [6]. In order to meet the requirements of randomized, double-blind controlled design, we chose to perform ultrasound-guided TPVB after induction of general anesthesia in patients; this can not only ensure the safety of the operation but also avoid the influence of knowledge about treatment assignments from subjects and/or surgeons on outcomes during follow-up. TPVB is performed by injecting local anesthetic adjacent to the thoracic vertebra close to where the spinal nerves emerge from the intervertebral foramina. This allows for continuous nerve blockage in multiple contiguous thoracic dermatomes above and below the injection site. And it is possible to visualize whether the drugs are injected into the target area by ultrasound, thus effectively reducing the occurrence of adverse events, such as accidental intravascular injection. The use of ultrasound can obviously improve block success rates when compared to the blind techniques [13].

Table 1: Comparison of baseline characteristics of patients between the two groups.

	TPVB group ($n = 52$)	Control group ($n = 56$)	T/χ^2	P value
Age (year)	57.1 ± 11.8	59.8 ± 11.0	1.2307	0.2212
Sex (male/female)	29/23	31/25	0.0019	0.9652
Height (cm)	165.2 ± 7.2	164.5 ± 8.0	0.4767	0.6346
Body weight (kg)	62.9 ± 8.9	61.7 ± 10.4	0.6419	0.5223
Body mass index (kg/m^2)	22.9 ± 2.4	22.7 ± 2.9	0.3888	0.6982
ASA I/II	15/37	16/40	0.0010	0.9748
Operative time (min)	146.5 ± 24.2	141.0 ± 22.3	1.2292	0.2217

TPVB: thoracic paravertebral block; ASA: American Society of Anesthesiologists.

Table 2: Comparison of NRS pain score and the number of times the button on the PCA was pressed at different time points after surgery between two groups.

	TPVB group ($n = 52$)	Control group ($n = 56$)	t value	P value
NRS pain score at rest at 24 h after surgery	2.6 ± 1.0	3.1 ± 1.0	2.5963	0.0108
NRS pain score at rest at 48 h after surgery	3.1 ± 1.0	4.0 ± 1.0	4.6733	0.0000
NRS pain score during movement at 24 h after surgery	1.5 ± 0.7	2.0 ± 0.3	4.8852	0.0000
NRS pain score during movement at 48 h after surgery	2.0 ± 1.0	2.7 ± 0.9	3.8284	0.0002
The number of times pressing PCA at 24 h after surgery	3.2 ± 1.4	6.2 ± 2.3	8.1118	0.0000

TPVB: thoracic paravertebral block; PCA: patient-controlled analgesia; NRS: numeric rating scale.

Table 3: Comparison of the incidence of postoperative chronic pain at 1 year after surgery between the two groups.

Groups	TPVB group	Control group	Total	χ^2	P value
LANSS ≥ 12	9 (17.3%)	33 (58.9%)	42 (38.9%)	19.6537	0.0000
LANSS < 12	43 (82.7%)	23 (41.1%)	66 (61.1%)		
Total	52	566	108		

TPVB: thoracic paravertebral block; LANSS: Leeds Assessment of Neuropathic Symptoms and Signs.

Table 4: Comparison of the incidence of anxiety in the two groups after surgery.

Anxiety	TPVB group	Control group	Total	χ^2	P value
HADS – A score ≥ 11	2 (3.8%)	22 (39.3%)	24 (22.2%)	19.5930	0.0000
HADS – A score < 11	50 (96.2%)	34 (60.7%)	84 (77.8%)		
Total	52	56	108		

Table 5: Comparison of the incidence of depression in the two groups after surgery.

Depression	TPVB group	Control group	Total	χ^2	P value
HADS – D score ≥ 11	0 (0%)	23 (41.1%)	23 (21.3%)	27.1361	0.0000
HADS – D score < 11	52 (100%)	33 (58.9%)	85 (78.7%)		
Total	52	56	108		

The possible mechanisms underlying neuropathic pain include the follows: damaged nerve fibers caused by demyelination generate spontaneous and continuous ectopic discharges, resulting in peripheral sensitization; abnormal neural electrical activity continues to be transmitted to the central nervous system, leading to central sensitization [14]. Local persistent inflammation caused by surgical trauma can also lead to increased excitability of nerve endings, thus aggravating peripheral and central sensitization. TPVB with local anesthetic drugs blocks the continuous ectopic discharge generated by damaged nerve fibers, thereby reducing the occurrence of central and peripheral sensitization. To a certain extent, TPVB plays a role in preventing or delaying the occurrence of pathological pain [15]. A previous study has shown

that injection of local anesthetics into the thoracic paravertebral space can lead to sensory blockade of 9-10 spinal nerve dermatomes, which produces analgesic effects similar to thoracic epidural nerve block [16], but TPVB is more simple and safe than thoracic epidural nerve block, so it has obvious advantages over intercostal nerve block and thoracic epidural nerve block in clinical application. In the present study, postoperative chronic pain was objectively evaluated by using the Chinese version of the LANSS scale; the results further confirmed the role of TPVB in reducing the incidence of postoperative chronic pain.

Chronic pain can affect patients not only physically but also mentally. In this study, the HADS was used to assess the occurrence of anxiety and depression in patients at 1 year after surgery. The results showed that the incidence of anxiety or depression was significantly higher in patients who did not receive TPVB compared with those who received TPVB. However, considering that many factors may contribute to the occurrence of anxiety and depression, evidence is inadequate to support the causal relationship between the incidence of anxiety, depression, and the incidence of neuropathic pain, as well as the use of TPVB during surgery; further investigations are needed to confirm this finding.

The study still has some limitations. First, the mechanisms of chronic postoperative pain and pathological pain are complex, which can be influenced by many factors [17]. TPVB cannot eliminate the occurrence of postoperative chronic pain completely. In addition, pain assessment for each patient was only performed at 48 hours and one year after surgery, the development and occurrence of chronic pain in patients during this period were not recorded, patients may often still need to receive further pain treatment during the follow-up period, and this may cause the incidence of postoperative chronic pain observed in this study to be higher than the actual situation. Second, this is a single-center study with a relatively small number of patients; although there was no significant difference in the general condition of the two groups, there may still be some bias. Third, many subjective scales were used in this study, and these scales are subjective; more objective indicators, such as assessment of mechanical pain thresholds in the skin using von Frey filaments, and diagnosis of anxiety and depression, involving the use of objective, quantifiable criteria, might provide more convincing evidence. Furthermore, in the present study, we only described the possible mechanism of TPVB to improve postoperative chronic pain and did not explore the specific mechanism of TPVB to improve postoperative anxiety and depression, which deserves further study.

5. Conclusions

Our findings showed that general anesthesia combined with TPVB could significantly reduce postoperative pain in patients undergoing thoracoscopic radical lung cancer surgery. Our findings also showed that TPVB could significantly reduce the incidence of neuropathic pain, as well as the incidence of anxiety and depression symptoms at 1 year after surgery. Our findings had implications for improving clinical application of TPVB and enhancing postoperative pain management.

Data Availability

Data generated or analyzed in this work were available from the corresponding author on reasonable request.

Conflicts of Interest

All authors confirm that there are no conflicts of interest existing in this study.

References

[1] E. M. O'Brien, R. M. Staud, A. D. Hassinger et al., "Patient-centered perspective on treatment outcomes in chronic pain," *Pain Medicine*, vol. 11, no. 1, pp. 6–15, 2010.

[2] J. Lovich-Sapola, C. E. Smith, and C. P. Brandt, "Postoperative pain control," *The Surgical Clinics of North America*, vol. 95, no. 2, pp. 301–318, 2015.

[3] A. G. Schwartz and M. L. Cote, "Epidemiology of lung cancer," *Advances in Experimental Medicine and Biology*, vol. 893, pp. 21–41, 2016.

[4] R. K. Elmallah, M. Chughtai, A. Khlopas et al., "Pain control in total knee arthroplasty," *The Journal of Knee Surgery*, vol. 31, no. 6, pp. 504–513, 2018.

[5] W. G. Andrews and S. Paul, "Techniques of video-assisted thoracoscopic surgery lobectomy and critical review of published data," *Future Oncology*, vol. 12, no. 23s, pp. 31–33, 2016.

[6] K. Kang, X. Meng, B. Li et al., "Effect of thoracic paravertebral nerve block on the early postoperative rehabilitation in patients undergoing thoracoscopic radical lung cancer surgery," *World Journal of Surgical Oncology*, vol. 18, no. 1, p. 298, 2020.

[7] L. Sun, Q. Li, Q. Wang, F. Ma, W. Han, and M. Wang, "Bilateral thoracic paravertebral block combined with general anesthesia vs. general anesthesia for patients undergoing off-pump coronary artery bypass grafting: a feasibility study," *BMC Anesthesiology*, vol. 19, no. 1, p. 101, 2019.

[8] J. Xu, M. Pu, X. Xu, J. Xiang, and X. Rong, "The postoperative analgesic effect of intercostal nerve block and intravenous patient-controlled analgesia on patients undergoing lung cancer surgery," *American Journal of Translational Research*, vol. 13, no. 8, pp. 9790–9795, 2021.

[9] C. Figueras, A. Matamalas, J. Pizones, L. Moreno-Manzanaro, J. Betegón, and J. Bagó, "The relationship of kinesiophobia with pain and quality of life in idiopathic scoliosis," *Spine (Phila Pa 1976)*, vol. 46, no. 21, pp. 1455–1460, 2021.

[10] Q. W. Huang, J. B. Li, Y. Huang, W. Q. Zhang, and Z. W. Lu, "A comparison of analgesia after a thoracoscopic lung cancer operation with a sustained epidural block and a sustained paravertebral block: a randomized controlled study," *Advances in Therapy*, vol. 37, no. 9, pp. 4000–4014, 2020.

[11] M. Bennett, "The LANSS Pain Scale: the Leeds assessment of neuropathic symptoms and signs," *Pain*, vol. 92, no. 1, pp. 147–157, 2001.

[12] W. Ye, S. K. Shi, J. M. Xu, and J. L. Ji, "An analysis of anxiety and depression of 957 inpatients in Chinese," *Chinese Journal of Behavioural Medicine and Brain Sciences*, vol. 4, no. 4, p. 198, 1995.

Hindawi
Computational and Mathematical Methods in Medicine
Volume 2023, Article ID 9803037, 1 page
https://doi.org/10.1155/2023/9803037

Retraction

Retracted: Mechanisms of Banxia Xiexin Decoction Underlying Chronic Atrophic Gastritis via Network Pharmacology, Molecular Docking, and Molecular Dynamics Simulations

Computational and Mathematical Methods in Medicine

Received 5 December 2023; Accepted 5 December 2023; Published 6 December 2023

This article has been retracted by Hindawi, as publisher, following an investigation undertaken by the publisher [1]. This investigation has uncovered evidence of systematic manipulation of the publication and peer-review process. We cannot, therefore, vouch for the reliability or integrity of this article.

Please note that this notice is intended solely to alert readers that the peer-review process of this article has been compromised.

Wiley and Hindawi regret that the usual quality checks did not identify these issues before publication and have since put additional measures in place to safeguard research integrity.

We wish to credit our Research Integrity and Research Publishing teams and anonymous and named external researchers and research integrity experts for contributing to this investigation.

The corresponding author, as the representative of all authors, has been given the opportunity to register their agreement or disagreement to this retraction. We have kept a record of any response received.

References

[1] C. Chang, W. Feng, M. Sun, X. Yu, and Z. Sun, "Mechanisms of Banxia Xiexin Decoction Underlying Chronic Atrophic Gastritis via Network Pharmacology, Molecular Docking, and Molecular Dynamics Simulations," *Computational and Mathematical Methods in Medicine*, vol. 2022, Article ID 4237040, 13 pages, 2022.

Hindawi
Computational and Mathematical Methods in Medicine
Volume 2022, Article ID 4237040, 13 pages
https://doi.org/10.1155/2022/4237040

Research Article

Mechanisms of Banxia Xiexin Decoction Underlying Chronic Atrophic Gastritis via Network Pharmacology, Molecular Docking, and Molecular Dynamics Simulations

Cheng Chang,[1,2] Weiqi Feng,[3] Min Sun,[4] Xiaowen Yu,[5] and Zhiguang Sun[1,2]

[1]*Nanjing University of Chinese Medicine, Nanjing 210023, China*
[2]*Jiangsu Provincial Second Chinese Medicine Hospital, The Second Affiliated Hospital of Nanjing University of Chinese Medicine, Nanjing 210017, China*
[3]*Department of Respiration, Zhenjiang Hospital of Chinese Traditional and Western Medicine, Zhenjiang 212000, China*
[4]*College of Special Education, Nanjing Normal University of Special Education, Nanjing 210038, China*
[5]*Zhenjiang Hospital Affiliated to Nanjing University of Chinese Medicine, Zhenjiang 212000, China*

Correspondence should be addressed to Xiaowen Yu; fsyy02221@njucm.edu.cn and Zhiguang Sun; zhiguangsun@njucm.edu.cn

Received 11 August 2022; Revised 23 August 2022; Accepted 26 August 2022; Published 15 September 2022

Academic Editor: Min Tang

Chronic atrophic gastritis (CAG) is a common chronically digestive disease which is notoriously characterized by atrophy of the epithelium and glands of the gastric mucosa, reduced number, thinning of the gastric mucosa, thickening of the mucosal base, or pyloric glandular hyperplasia and intestinal glandular hyperplasia, or with atypical hyperplasia. Banxia Xiexin decoction (BXD) has been applied for two thousand years and is considered an effective therapy for functional dyspepsia, gastroesophageal reflux disease and colon cancer. In this current study, to probe into the underlying mechanism of BXD on CAG, network pharmacology was conducted to collect druggable ingredients and predicted targets of BXD and the CAG-associated targets were harvested to take intersection with druggable ingredients from BXD predicted targets to obtain potential critical action targets. Subsequently, GO enrichment analysis and Kyoto Encyclopedia of Genes and Genomes pathway enrichment analysis were conducted to elucidate the underlying mechanisms and roles from the perspective of overall pathways and cellular functions. Eventually, molecular docking integrated with molecular dynamics simulations was conducted to further investigate the mechanism of action of BXD active ingredients on CAG from drug molecule-target interactions and to provide a theoretical basis for BXD drug development.

1. Introduction

Chronic atrophic gastritis (CAG) is a common chronically digestive disease which is notoriously characterized by atrophy of the epithelium and glands of the gastric mucosa, reduced number, thinning of the gastric mucosa, thickening of the mucosal base, or pyloric glandular hyperplasia and intestinal glandular hyperplasia, or with atypical hyperplasia [1, 2]. The representative clinical manifestation involved vague pain in the upper abdomen, fullness, belching, loss of appetite, wasting, anaemia, etc. [3]. It is a nonspecific and multicausal disease or precancerous lesion. Clinical and epidemiological evidence has suggested the repeated inflammation of gastric mucosa, Helicobacter pylori's infection, and gastric mucosal lesion induced by alcohol or an unhealthy diet are the dominating pathological factors of CAG [4, 5]. However, compared with the imperious command for the effective therapeutic approaches currently, there is still a lack of effective clinical therapy for CAG.

Traditional Chinese medicine (TCM) has been prevalently acknowledged as the treasure trove of natural compounds with pronounced clinical efficacy [6]. As reported before, many TCMs can improve CAG, such as berberine [7] and Jianpiyiqi formula [8]. Banxia Xiexin decoction (BXD), as a classic prescription Treatise on Febrile Diseases (Shanghan Lun), has been applied for two thousand years

and is considered an effective therapy for functional dyspepsia, gastroesophageal reflux disease, and colon cancer [9–11]. Moreover, BXD has been documented to affect drug sensitivity in gastric cancer cells [12]. The classic TCM prescription BXD is composed of seven medicinal herbs, including *Pinelliae Rhizoma* (Ban Xia), *Coptidis Rhizoma* (Huang Lian), *Scutellariae Radix* (Huang Qin), *Zingiberis Rhizoma* (Gan Jiang), *Ginseng Radix* (Ren Shen), *Jujubae Fructus* (Da Zao), and *Glycyrrhizae Radix* (Gan Cao). Drawing on previous studies, BXD has yielded various anti-inflammatory and antioxidative pharmacological effects, and the therapeutic effects on CAG and Ulcerative colitis (UC) are confirmed evidence [11, 13]. Pharmacological research demonstrated that the master ingredient of BXD which encompasses alkaloids and flavonoids could exert therapeutic effects on CAG by regulating inflammatory response and protecting from H. pylori infection and interfering with H. pylori growth and virulence [14]. Nevertheless, the detailed mechanism of BXD on CAG remains unveiled.

Network pharmacology is an emerging method to shed light on the process of disease development from the perspective of scientific biology and the equilibrium of biological network, to understand drug-organism interactions from a holistic viewpoint of promoting or restoring the equilibrium of biological network, and to guide the discovery of new drugs, which coincides with the theory of Traditional Chinese Medicine and is widely utilized for the exploration of mechanisms of Traditional Chinese Medicine [15, 16]. Currently, with the prevalence and development of computational chemistry methods and the proposed theoretical basis of the computer-aided drug designing (CADD) receptor-ligand interaction hypothesis and molecular simulations, structural biology combined with kinetic simulation methods promotes the processes of drug discovery and elucidation of target interactions [17].

In our current study, network pharmacology was initially conducted to screen out potential druggable ingredients of BXD and probe into the underlying biological mechanism by which BXD on the treatment of CAG from a systemic perspective and at the molecular level. Subsequently, the herb-biological function network of BXD was established to illustrate the regulatory effect of BXD for the treatment of CAG. Key targets were selected to perform the molecular docking procedure for predicting binding energy and screening potential therapeutic ingredients. Eventually, the target-compound complexes were conducted molecular dynamics simulation and performed binding free energy calculations via Gromacs 2020 software and MMPBSA procedure.

2. Materials and Methods

2.1. Network Pharmacology Analysis

2.1.1. Identification of the Active Compounds of BXD and Compound Data Collection. Bioinformatics was conducted to identify and comprehensively collect underlying therapeutic druggable compounds of BXD. The whole procedure was described as follows. Initially, the online database Traditional Chinese Medicine Systems Pharmacology Analysis Database and Analysis Platform (http://tcmspw.com/tcmsp.php) was conducted to screen potential active compounds from BXD by, respectively, importing *Pinelliae Rhizoma* (Ban Xia), *Coptidis Rhizoma* (Huang Lian), *Scutellariae Radix* (Huang Qin), *Zingiberis Rhizoma* (Gan Jiang), *Ginseng Radix* (Ren Shen), *Jujubae Fructus* (Da Zao), and *Glycyrrhizae Radix* (Gan Cao) as keywords [18]. Additionally, a literature search in PubMed Central of the NCBI database (https://www.ncbi.nlm.nih.gov/) was conducted as supplementary compounds of BXD. Eventually, all obtained compounds with the predicted drug properties were uploaded on ProTox-II (https://tox-new.charite.de/protox_II/index.php?site=home) which is an online database for predicting the toxicity of compounds [19]. Active compounds with low toxic doses and filtered with the criterion of oral bioavailability (OB $\geq$ 30%) and drug-likeness (DL $\geq$ 0.18) and the mol2 format files of selected active compounds were downloaded for further target prediction. Subsequently, macromolecular targets of active ingredients were predicted via SwissTargetPrediction (http://www.swisstargetprediction.ch/index.php) and PharmMapper Server (http://www.lilab-ecust.cn/pharmmapper/) which were prevalently utilized for potential target identification [20, 21]. Eventually, all prediction targets corresponding to components obtained from the above database search were imported into Venny 2.1 (https://bioinfogp.cnb.csic.es/tools/venny/index.html) to combine duplicate item.

2.2. CAG-Associated Target Collection. To comprehensively collect CAG-associated targets, six resources of disease online databases including CTD (http://ctdbase.org/), OMIM (http://omim.org/) DisGeNET (http://www.disgenet.org/), NCBI Gene (https://www.ncbi.nlm.nih.gov), and GENECARD (https://www.genecards.org/) were utilized by importing the keyword of chronic atrophic gastritis [22–24]. Considering that CAG is a type of chronic gastritis which exerts similar aetiology and pathology, we supplemented chronic gastritis-related targets and the overall aggregated targets were imported into Excel software for merging and removing repeated targets. The predicted potential targets for drugs of BXD and CAG-associated targets were derived from the intersection as potential targets of BXD on CAG.

2.3. Enrichment Analysis and Network Construction. Gene Ontology (GO) and Kyoto Encyclopedia of Genes and Genomes (KEGG) pathway enrichment analyses were conducted on the Metascape database (http://metascape.org) by importing key targets which refer to the intersection of CAG-related targets and BXD predicted targets [25]. GO-(Gene Ontology-) related biological processes (BP), cellular components (CC), molecular functions (MF) and KEGG pathways, GO enrichment, and KEGG pathway enrichment analyses were conducted to probe into the underlying mechanism of BXD in CAG at holistic systematic perspective, offering molecular mechanism demonstration for BXD treatment of CAG. To visualize the analysis results, RStudio

was utilized for presenting enrichment analysis results. Eventually, the network that encompasses the association between active ingredients and corresponded targets was constructed via Cytoscape 3.7.1 software (http://www.cytoscape.org/) [26].

2.4. Construction of the Protein-Protein Interaction (PPI) Network. To explore the protein and protein interactions among the key targets and illustrate the underlying mechanism, the PPI network was performed and visualized utilizing the Cytoscape software and Metascape online serve, which contains six PPI online serve sourceSTRING (https://string-db.org/) and Metascape online database servers were performed to obtain the associated analysis results of predicted protein interactions [27].

The method of central network evaluation is prevalently acknowledged as the most common and master measure for screening core proteins in PPI networks. Initially, the PPI networks of BXD targets and CAG-associated targets were integrated into an intersection as key targets. Subsequently, the Cytoscape plugin, STRING, and Metascape were conducted for assessing the intersection.

2.5. Validation of the Binding Capacity Between Active Ingredients and Key Targets by Molecular Docking. Computer-aided drug design, development, and target prediction have recently emerged as an important method for understanding biological regulatory mechanisms, which provides a theoretical basis for the design and discovery of new drug targets. AutoDock 1.5.6 (http://autodock.scripps.edu/) and instadock (https://hassanlab.org/instadock) are gratuitous and brilliant software for drug discovery with excellent docking accuracy and speed that combines predictive physics-based methods with machine learning techniques to accelerate drug discover [27–29]. The structures of active ingredients obtained from PubChem (https://pubchem.ncbi.nlm.nih.gov/) were prepared and optimized using ChemOffice and OpenBabel software for structure optimization, format conversion, charge correction, and energy minimization [30]. The PDB files of enzymes from tryptophan metabolism with the best structural resolution coupled with endogenous ligands were downloaded from the RCSB Protein Data Bank (https://www.rcsb.org/) and were predicted using the AlphaFold database, which is a state-of-the-art AI system developed by DeepMind that computationally predicts protein structures with unprecedented accuracy and speed (https://alphafold.ebi.ac.uk/) [31]. The flies with PDB formats of key targets were subsequently optimized by Discovery Studio 4.5 to perform hydrogenation and structural modification procedure. The parameters for the grid box and docking pocket were collected from the published report, and PyMOL 2.2.0 was used to obtain boxes from the selection plugin to obtain grid box parameters. After setting the grid parameters for the protein binding pocket, a genetic algorithm was implemented, and docking run options were set to the default parameters; eventually, the dpf file was exported. The docking results were visualized utilizing Discovery Studio Visualizer 4.5 for docking pattern visualization.

2.6. Molecular Dynamics (MD) Simulation. In the validation of the Binding Capacity Between Active Ingredients and Key Targets by Molecular Docking Simulation parameters, during the protein-ligand complex simulation, all proteins were utilized amber99sb-ildn force field to process protein, and small molecules were processed with acpype (http://bio2byte.be/acpype) to generate gro and itp files [32].

After the docking procedure for obtaining optimal conformation, the molecular dynamics (MD) simulations were conducted utilizing GROMACS 2020.6 software; TIP3P was selected as the force field of water molecules. The simulation box was set at 1.0 nm to ensure the distance between the atoms of the protein-ligand complex, and the edge of the box is appropriate for periodicity conditions. Fill the entire box with water using the solvate command, and add SOL items to the molecules section of the top file after running and add ions, default add NA and CL; -neutral command was performed to balance the simulation system to neutral. Then, the steepest descent method was performed to simulate and optimize the system for energy reduction; subsequently, the energy minimization and duration 10 ns constraint dynamics was conducted. Eventually, the index file was created, and md simulation was performed for 200 ns. All MD simulations were performed under an isothermal and isostatic ensemble with a temperature of 298.15 K and a pressure of 1 atmosphere. The temperature and pressure were controlled by the V-rescale and Parrinello-Rahman methods, respectively, and the temperature and pressure coupling constants were 0.1 and 0.5 ps, respectively. Except for the protein prodrug ligand simulation time of 50 ns, the MD simulation time of the other three systems was 200 ns.

It can be applied to each compound.

2.7. Binding Free Energy Calculations using the Born Surface Area (MM/GBSA) Method. Eventually, the MMPBSA process in GROMACS was utilized to calculate the binding energy, and the following equation was utilized: ΔGbind = Gcomplex – Gfree-protein – Gfree-ligand.

MM is van der Waals and electrostatic energy (ΔGvdw + ΔGele); PB is polar solvation (ΔGpolar); SA is nonpolar solvation (ΔGnonpolar).

In the MM/GBSA calculations, the protein-ligand binding free energy is calculated based on MD simulation trajectories and compared with experimental binding data to build and validate the new model. The free energy changes during ligand-protein binding to form complexes are described by the original MM/GBSA according to the equations as the sum of different interactions. The basic principle is to calculate the difference between the bound and unbound free energies of two solventized molecules or to compare the free energies of different solventized conformations of the same molecule.

3. Results

3.1. Target Prediction and Functional Analysis of the Regulatory Effects of BXD on CAG. To collect and screen potentially druggable compounds from BXD, TCMSP online

databases (https://tcmspw.com/index.php) were utilized for online searching. Based on the four predicted parameters of drugs including oral bioavailability (OB), drug-likeness (DL), toxicity prediction, and Caco-2 parameters obtained through ADME, ninety-two ingredients were selected as potential druggable active compounds of BXD, and the detailed information and structures were presented at (). Subsequently, the Venn diagram of ingredients was conducted. We found that there are a total of 182 potential active druggable ingredients in BXD, 15 ingredients in Banxia, 22 ingredients in Renshen, 5 ingredients in Shengjiang, 92 ingredients in Gancao, 14 ingredients in Huanglian and 36 ingredients in Huangqin which were identified out. The composition and content ratio of druggable potential in BXD were confirmed by a previous study which performed an LC-MS analysis to identify the principal characteristic peaks associated with a BXD fingerprint. Saponins, flavonoids and alkaloids were identified as the master abundant compounds that mainly exist in Renshen, Gamcao, Huangqin, and Huanglian, which is consistent with our results (Figures 1(a) and 1(b)) [33, 34].

3.2. Network Construction and Enrichment Analysis of Key Targets. After collecting the CAG-associated targets from six sources, the disease targets were taken at the intersection with BXD predicted targets to obtain key targets of BXD on CAG. There are a total of 134 key targets screened out, and the detailed target information is presented in Figure 2(a).

To explore the potential mechanism of clinical therapeutic effects of BXD on CAG, GO-related biological processes, cellular components, molecular functions, and KEGG pathways enriched analysis were performed on Metascape online serve by importing 134 key targets and, respectively, submitting enrichment analysis. To obtain better visualization of enrichment analysis, Rstudio was utilized to present Go and KEGG enrichment results (Shown in Figures 2(b)–2(d)). The enrichment analysis results indicated that the key targets were mainly enriched into 10 biological processes including cellular response to chemical stress, response to oxidative stress, and cellular response to oxidative stress biological process. The molecular function was mainly involved in protein serine/threonine kinase activity, phosphatase binding, and endopeptidase activity. The cellular component results suggested that these 134 key targets were dominating existing in membrane raft, membrane microdomain and membrane region. Moreover, the KEGG pathways (Figure 3) were enriched into TNF signaling pathway, cellular apoptosis, PI3K-Akt signaling pathway, C-type lectin receptor signaling pathway, and NF-kappa B signaling pathway, which were involved in Gastric mucosa inflammatory response, cellular apoptosis, and integrity of gastric mucosa cells, exerting a crucial role in CAG disease.

3.3. Analyses of the Key Target-Based Specific Protein Interaction Network. To explore the protein interaction of 134 key targets that BXD involved in the treatment of CAG, the gene list of targets was imported on Metascape and String online serve (Figure 4(a)). The protein and protein interaction (PPI) result demonstrated that the key targets were clustered as Figure 4(b) and the master protein clusters were involved in pathways in cancer, gastrin signaling pathway, and MAPK signaling pathway. These pieces of evidence revealed that BXD may exert a therapeutic role on CAG by regulating the protein interactions of the gastrin signaling pathway and MAPK signaling pathway.

3.4. Molecular Docking of Ingredients and Targets. To probe into the potential mechanism of BXD on CAG, the small molecules that filtered with the properties of drug properties were screened out for performing molecular docking procedures with key targets in CAG. All the pdb formats of targets were collected from RCSB Protein Data Bank (https://www.rcsb.org/), and the parameters of binding pocket of targets were obtained from the PyMOL 2.2.0 software. Eventually, the molecular docking procedure was performed by utilizing Vina software. The hot map (Figure 5) demonstrated that three targets encompassing NR3C1, NOS2, and IL-2 displayed impressive binding energy with the compounds from BXD, and it is worth noting that these compounds who represent considerable binding energy with the inflammatory targets were majorly originated from Huanglian, Huangqin, and Gancao, which was consistent with previous studies. Subsequently, we selected three target-ligand complexes to visualize the binding pattern, and the results were present. The visualization of three target-compound complexes was presented and analyzed by the Discovery studio 4.0 visualizer, and the binding pattern of NR3C1-coptisine indicated that there are three binding interactions encompassing van der vaals, Pi-Alkyl, and Pi-Pi T-shaped, which constituted the hydrophobic pocket contributing to the relatively low binding energy. In the dissection of the binding pattern of NOS2-palmidin A, three hydrogen bonds were observed interacting with TRP372, MET374, and SER242. These amino acid residues of NOS2 constitute a hydrophilic pocket that strongly interacts with the hydroxyl group of palmidin A. In the dissection of the binding pattern predicted in Discovery Studio presented in the 3D and 2D graphs, 2 hydrogen bonds between IL-2 and licocoumarone were observed. In the complex of IL-2 and licocoumarone, CYS31 (2.95 Å) and GLN74 (3.27 Å) interact with the hydroxide radical group of licocoumarone, forming 2 hydrogen bonds; moreover, PHE78 and LEU70 constitute the hydrophobic pocket that is beneficial to the stabilization of the complex (Figures 6(a)–6(f)). Based on the results described above, the conclusion could be drawn that coptisine, palmidin A, and licocoumarone could constitute stable complexes with NR3C1, NOS2, and IL-2 with low binding free energy and good binding pattern, which subsequently explored and unveiled the potential compound-target pharmacological interaction.

3.5. Molecular Dynamics Simulations and Analysis of Molecular Dynamics Trajectories. Subsequently, Gromacs-2019.5 was used to perform protein-ligand complex molecular dynamics simulation (MDS), which is beneficial for evaluating the stability of the ligand and protein complex. Based on the docking scores between 152 druggable compounds from BXD and selected key targets coupled

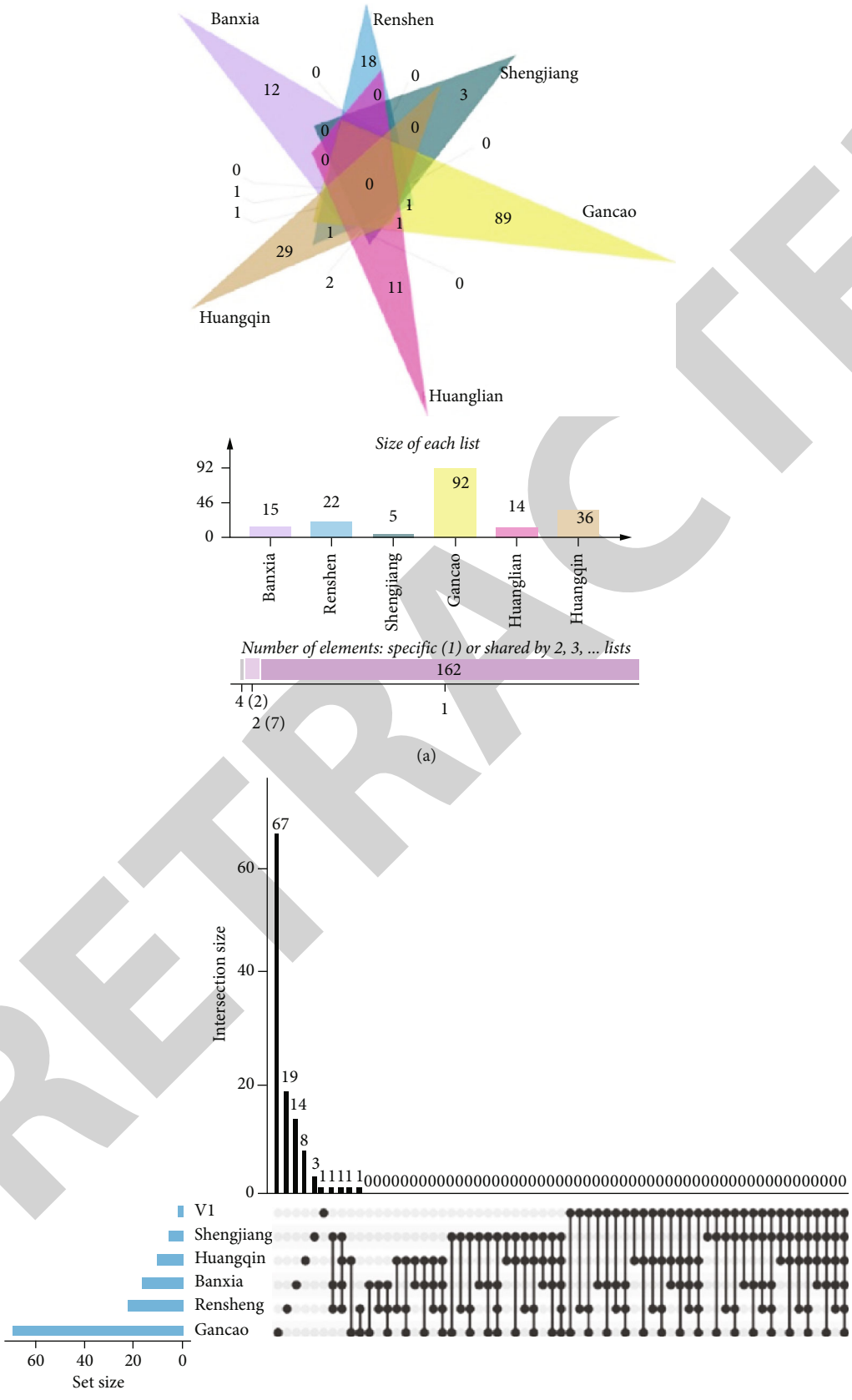

Figure 1: (a) The Venny plot of druggable ingredients from six herbs of BXD. (b) The UpSet graph coupled with elements of ingredients from six herbs of BXD.

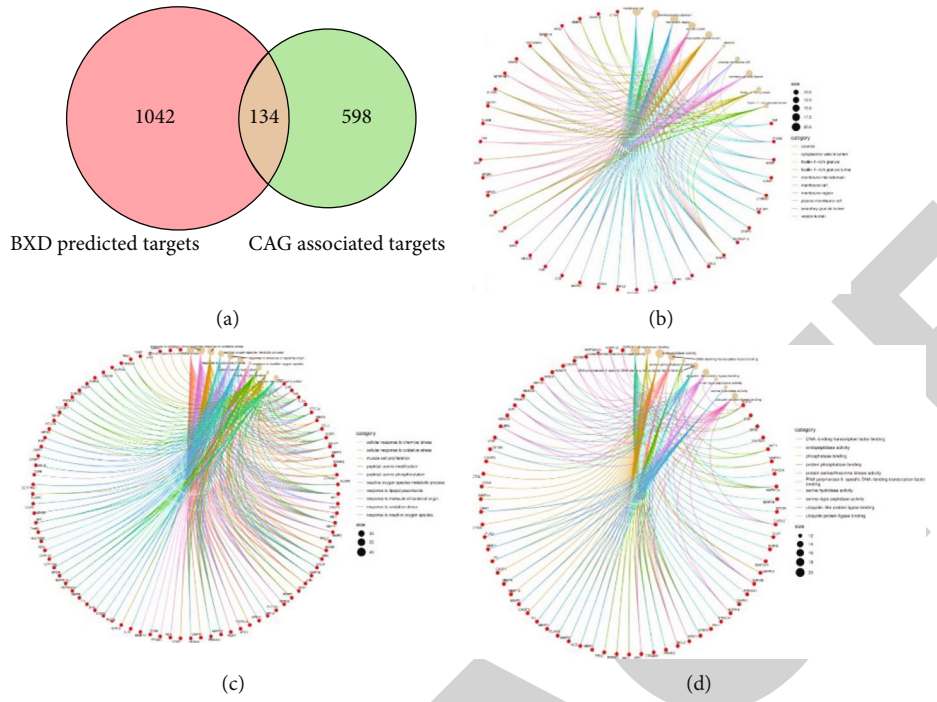

Figure 2: Go and KEGG pathways analysis. (a) Intersection diagram of BXD predicted targets and CAG-related targets. (b–d) GO-related biological processes, cellular components, and molecular functions enrichment analysis of key targets.

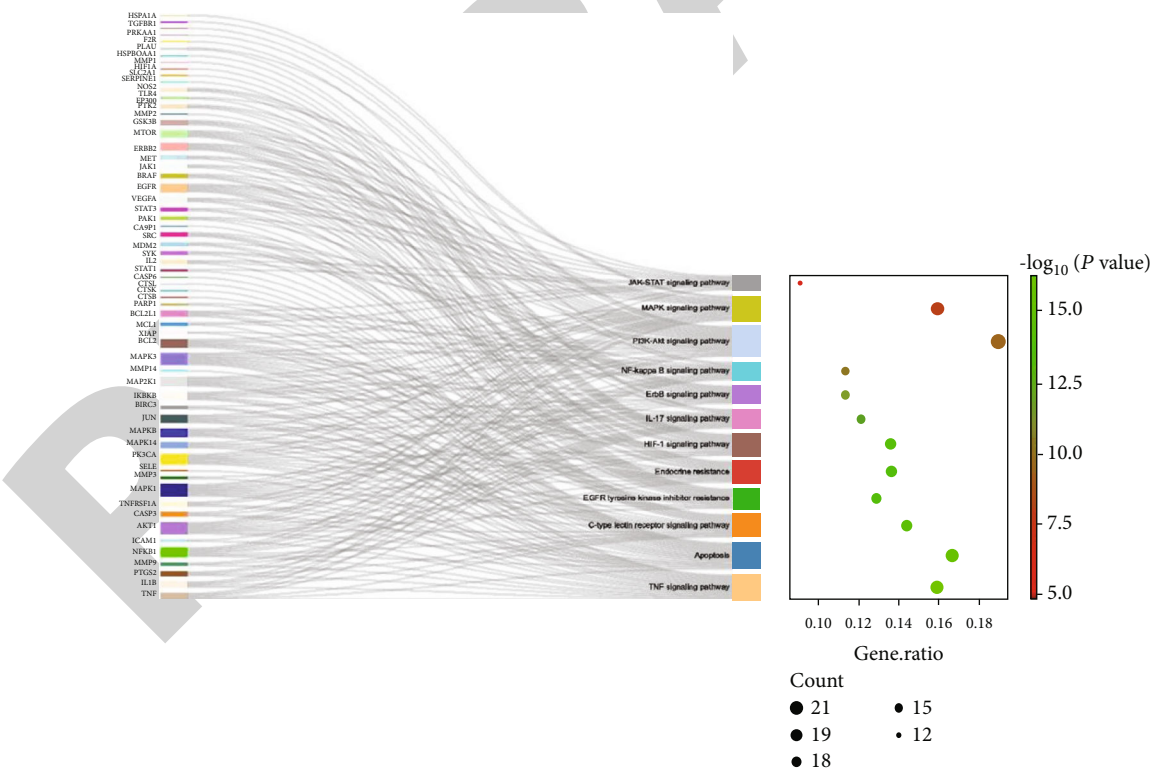

Figure 3: The KEGG pathway enrichment analysis of key targets. The squares represent target and pathway information, respectively, and the pathways are sequenced by gene ratio.

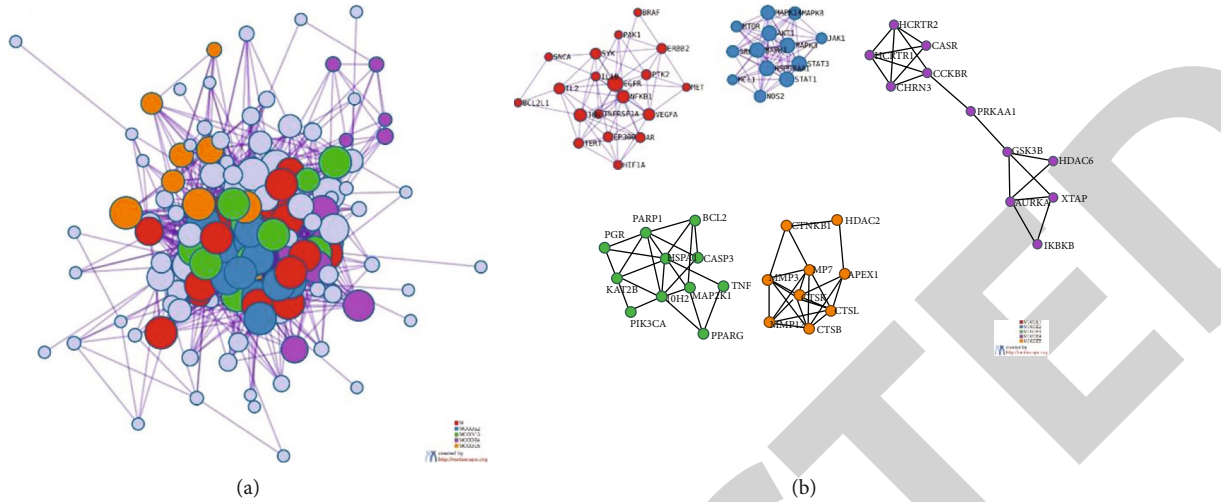

(a) (b)

Figure 4: Graph of protein-protein interactions. (a) General view of the interactions of proteins and clustered proteins. (b) Five protein clusters are associated with the Gastrin signaling pathway, MAPK signaling pathway, Apoptosis, G alpha (q) signalling events and collagen catabolic process. These circles represent the target protein, and the line represents the interaction of the target protein.

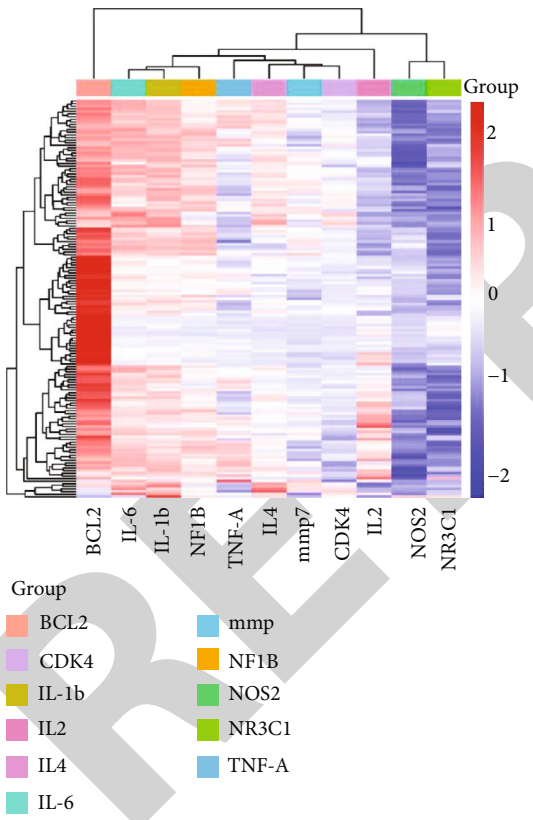

Figure 5: Heat map of docking energies.

with the visualization of binding pattern, three complexes including NR3C1-coptisine, NOS2-palmidin A, and IL-2-licocoumarone were selected, and their conformational behaviour was analyzed via molecular dynamics simulations and MMPBSA calculations (displayed in Figures 7(a)–7(i)). During the 100 ns molecular dynamics simulation, coptisine, palmidin A, and licocoumarone exhibited a wide range of interactions with various residues at the binding site, suggesting that three ligands form a stable complex with NR3C1, NOS2, and IL-2. Additionally, the root-mean-square deviation (RMSD) of the protein backbone and coptisine, palmidin A, and licocoumarone was of low magnitude, ranging in fluctuation, which is another strong indication of conformational stability that the protein had achieved with the ligand molecules. After analyzing hydrogen bond formation in the 100 ns of MDS, coptisine, palmidin A, and licocoumarone form 1, 2, and 2 hydrogen bonds with NR3C1, NOS2, and IL-2, respectively, as indicated by the docking pattern. Subsequently, we utilized molecular mechanics Poisson Boltzmann surface area calculations (MMPBSA) to obtain the van der Waals energy, electrostatic energy, polar solvation energy and SASA energy of coptisine, palmidin A, and licocoumarone complexed with NR3C1, NOS2, and IL-2, where positive values are unfavorable for interaction and negative values are favorable. In the MMPBSA calculations, the total binding free energy of -63.180, -52.778, and -43.012 kcal/mol, suggesting the strong interactions between protein ligands and high stability of the complexes formed.

3.6. Free Energy of Binding and Interacting Residue Results in Molecular Dynamics Simulation. Binding free energy is of great importance in the drug discovery process which could provide more accurate and detailed energy information [35]. A host of methods for calculating the binding free energy has been put forward in the last decades, for example, Thermodynamics Integration (TI), Free Energy Perturbation (FEP, MM/PB(GB)SA), and Linear Interaction Energy (LIE). The method of MM/PB(GB)SA is widely acknowledged as the most common and prevalent approach for calculating receptor-ligand binding free energy by researchers [36]. The main principle of program calculation of molecular Mechanics/Poisson Boltzmann (Generalized Born) Surface Area is to split the binding free energy into a molecular mechanics term and solvation energy. The

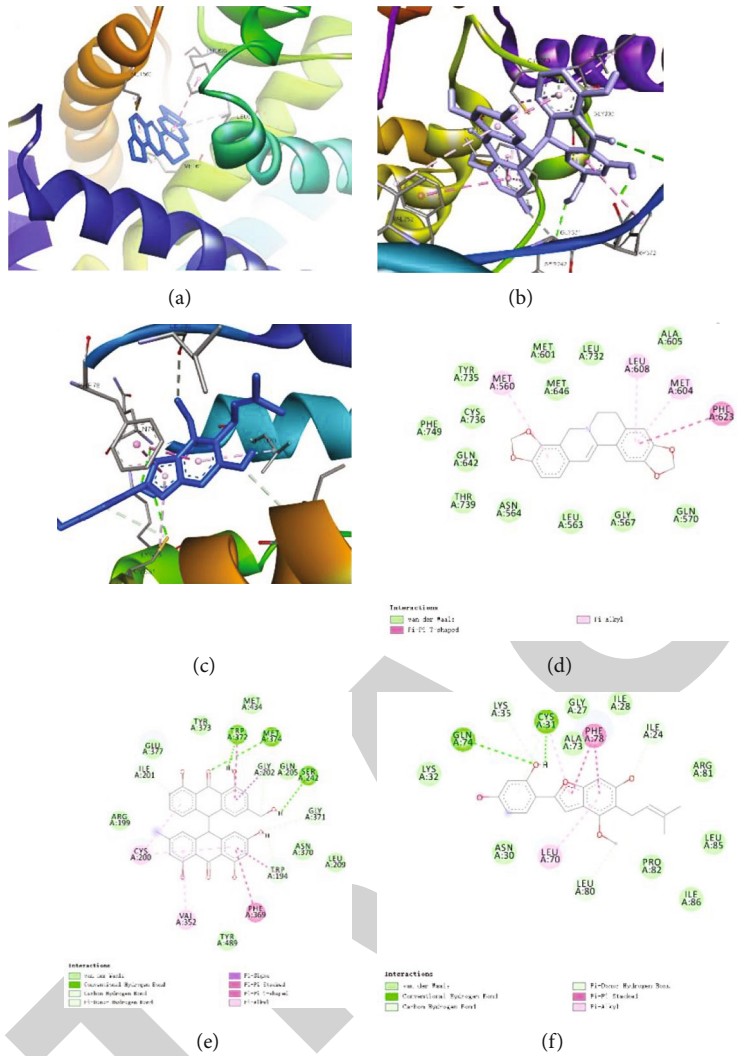

Figure 6: The interaction profile for three complexes. (a–c) Overall structure of NR3C1-coptisine, NOS2-palmidin A and IL-2-licocoumarone complex, (2d) binding modes of NR3C1-coptisine, NOS2-palmidin A, and IL-2-licocoumarone were presented as (d–f).

underlying mechanism is to evaluate the discrepancy between the binding free energy of two solventized molecules in bound and unbound states, as well as to calculate the free energy of the same molecule in different solvated confirmations. After conducting the molecular dynamics simulation procedure, the md trajectories were utilized for the free energy of binding calculation, and the results of the contribution of amino acid residues to the ligand-protein binding energy are shown in (Figures 8(a)–8(c)).

4. Discussion

TCM has unique therapeutic efficacy in clinical practice; many traditional Chinese prescriptions have been utilized to treat CAG, encompassing Zuojin Pill, Moluodan, and BXD [9, 37, 38]. Particularly, BXD has been widely utilized for treating various treatments of gastrointestinal diseases, including delayed diarrhea, ulcerative colitis, and ethanol-induced chronic gastritis, and exerted prominent therapeutic effects [11, 39]. Increasing emerging evidence has confirmed the anti-inflammatory and antitumor effects of the natural ingredients in BXD; additionally, the master compounds including baicalin and berberine have been identified and validated the treatments on CAG by various LC-MS analyses and pharmacological research. Nevertheless, in comparison with the precise clinical efficacy and the long history of the application of TCM, there is a relative lack of research on the mechanism of TCM. Accordingly, considering the multicomponent and multitarget characterization of TCM, the method of network pharmacology has been applied to study the potential mechanism of TCM and a series of progress was accomplished [40, 41]. In our current study, we initially explored the potential mechanism of BXD on CAG via the method of network pharmacology considering the definitive clinical efficacy of BXD.

TNF signaling pathway, PI3K-Akt signaling pathway, and NF-kappa B signaling pathway are common inflammatory associated pathways that CAG is involved in, and many traditional Chinese medicines have been reported to modulate these inflammatory pathways. For example, NF-kappa B and TNF signaling pathway have been reported to be associated with the helicobacter pylori

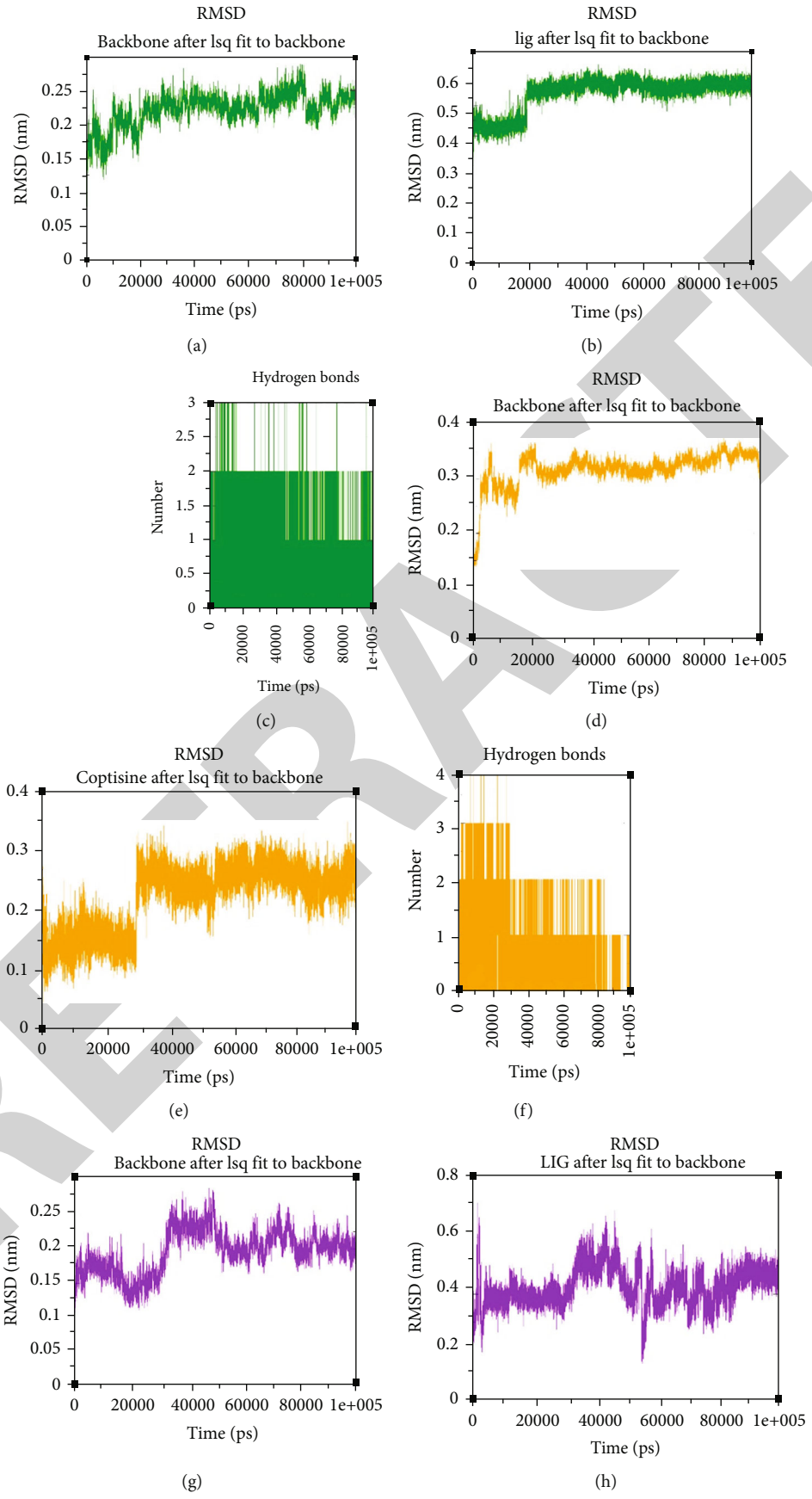

Figure 7: Continued.

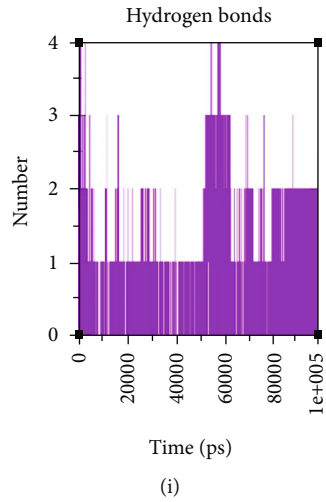

Figure 7: The RMSD results and Hbonds analysis of NOS2-palmidin A, NR3C1-coptisine, and IL-2-licocoumarone complex. (a–c) The RMSD of NOS2, RMSD of palmidin A relative to NOS2, and change in the number of hydrogen bonds during 100 ns simulation. (b–d) The RMSD of NR3C1, RMSD of coptisine relative to NR3C1, and change in the number of hydrogen bonds during 100 ns simulation. (d–e) The RMSD of IL-2, RMSD of licocoumarone relative to IL2, and change in the number of hydrogen bonds during 100 ns simulation.

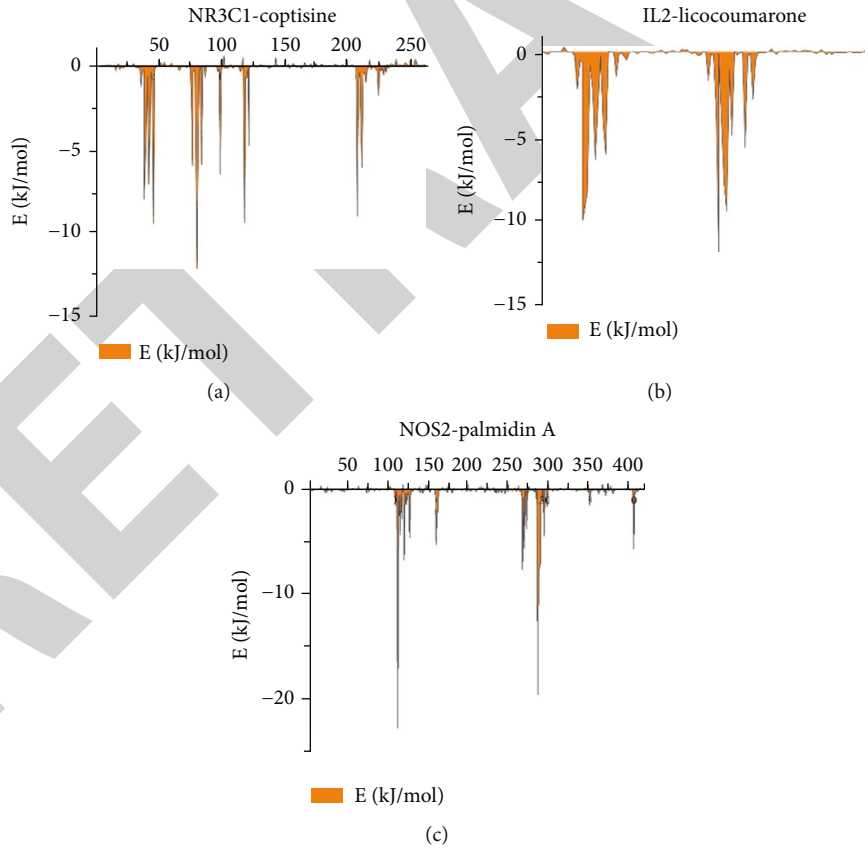

Figure 8: The graph of free energy contribution of amino acid residues to ligand-protein binding in three protein-ligand complexes.

gastrointestinal infection in CAG, and many traditional Chinese medicines have accomplished good results in the anti-inflammatory treatment of gastritis which encompassing Gancao, Huanglian and Huangqin [42–47]. Additionally, various herbal natural compounds have been reported for their anti-inflammatory pharmacological effects in the treatment of gastritis and have been developed as clinical agents, for example, 18β-glycyrrhetinic

acid (GRA) demonstrated in vivo pharmacological effects in the treatment of H. pylori gastritis infection. Berberine and baicalin also have been demonstrated in the treatment of CAG [48–50]. Consistently, the network pharmacology results from our study suggested that there are a total of 152 druggable ingredients in BXD and the target enrichment analysis demonstrated that the major pathways BXD involved in treating CAG were TNF signaling pathway, cellular apoptosis, PI3K-Akt signaling pathway, C-type lectin receptor signaling pathway, and NF-kappa B signaling pathways. These pathways are closely associated with the inflammatory response and the gastrointestinal environment.

The interactions of proteins are of crucial importance in normal biological processes. Cells receive signals from exogenous or endogenous sources and regulate their gene expression through their specific signaling pathways in order to maintain their normal biological properties. Proteins play an important role in this process, as they can internally regulate and mediate many biological activities of the cell. Although some proteins can function as monomers, most proteins act with chaperone molecules or form complexes with other proteins to perform their functions [51]. Accordingly, the protein interaction results also suggested the therapeutic role of CAG by regulating the protein interactions of the gastrin signaling pathway and MAPK signaling pathway. Considering that most small-molecule drugs exert their therapeutic effects mainly by acting on receptors to activate or inhibit. Remarkably, interactions between drugs and targets are the basis of biological effects. Many interaction modes exert a crucial role in the identification and binding of proteins and drugs [52]. However, they differ in stability and binding due to differences in binding energy and effective radius. In this study, three master interaction modes are introduced as described previously. Hydrogen bonding, with an average binding energy of 5 kJ/mol, is a weak electrostatic attraction between an electronegative hydrogen atom and an electronegative heteroatom and plays an important role in drug-target interactions. With the development of structural biology and computational chemistry, more and more natural compounds are being revealed for their pharmacological effects and developed as small molecule drugs, which accelerated drug development and mechanism discovery. Therefore, we attempted to explore the therapeutic effects of BXD on CAG from the perspective of drug-target interactions via the method of molecular docking and molecular dynamics simulation. After the docking procedure between 152 ingredients and selected key targets, the compounds with better results in docking with inflammatory targets were mostly from Gancao, Huanglian, and Huangqin herbs in BXD. Subsequently, molecular dynamics simulation was performed to validate the activity and stability of the active ingredient and the target protein during the binding process and calculate the contribution of amino acid residues to the binding free energy. The results demonstrated that palmidin A, licocoumarone, and coptisine could form stable complexes with NOS2, IL-2, and NR3C1, providing a theoretical basis for drug development and mechanism study of BXD for CAG.

There are some limitations in our study. First, we did not perform the relevant assays to determine the effect of BXD on CAG. Besides, the relation of BXD and signaling pathways and protein complexes was not verified by experiments. All these limitations will be perfected in the future study.

In conclusion, our study elucidated the potential mechanisms of BXD underlying CAG via network pharmacology, molecular docking, and molecular dynamics simulations, which might provide theoretical value for the treatment of CAG.

Data Availability

Data appear in the submitted article.

Conflicts of Interest

The authors reported that there is no conflict of interest.

Authors' Contributions

Cheng Chang and Weiqi Feng contributed equally to this work.

References

[1] Y. K. Wang, L. Shen, T. Yun, B. F. Yang, C. Y. Zhu, and S. N. Wang, "Histopathological classification and follow-up analysis of chronic atrophic gastritis," *World Journal of Clinical Cases*, vol. 9, no. 16, pp. 3838–3847, 2021.

[2] H. Yang, X. Y. Zhou, and B. Hu, "The 'reversibility' of chronic atrophic gastritis after the eradication ofHelicobacter pylori," *Postgraduate Medicine*, vol. 134, no. 5, pp. 474–479, 2022.

[3] S. C. Shah, M. B. Piazuelo, E. J. Kuipers, and D. Li, "AGA clinical practice update on the diagnosis and management of atrophic gastritis: expert review," *Gastroenterology*, vol. 161, no. 4, pp. 1325–1332.e7, 2021.

[4] H. Hsieh, H. B. Yang, B. S. Sheu, and Y. J. Yang, "Atrophic gastritis in Helicobacter pylori-infected children," *Helicobacter*, vol. 27, no. 3, article e12885, 2022.

[5] B. Annibale, G. Esposito, and E. Lahner, "A current clinical overview of atrophic gastritis," *Expert Review of Gastroenterology & Hepatology*, vol. 14, no. 2, pp. 93–102, 2020.

[6] C. C. Xue, A. L. Zhang, K. M. Greenwood, V. Lin, and D. F. Story, "Traditional chinese medicine: an update on clinical evidence," *Journal of Alternative and Complementary Medicine*, vol. 16, no. 3, pp. 301–312, 2010.

[7] Y. Tong, L. Liu, R. Wang et al., "Berberine attenuates chronic atrophic gastritis induced by MNNG and its potential mechanism," *Frontiers in Pharmacology*, vol. 12, article 644638, 2021.

[8] Z. Yan, T. Xu, Y. Xu, W. Chen, Z. An, and F. Zhu, "Jianpiyiqi formula ameliorates chronic atrophic gastritis in rats by modulating the Wnt/β-catenin signaling pathway," *Experimental and Therapeutic Medicine*, vol. 22, no. 2, p. 878, 2021.

[9] Q. Ji, Y. Yang, X. Song, X. Han, and W. Wang, "Banxia Xiexin decoction in the treatment of chronic atrophic gastritis: a protocol for systematic review and meta-analysis," *Medicine (Baltimore)*, vol. 99, no. 42, article e22110, 2020.

[10] B. Wang, K. W. Zeng, Z. F. Hong et al., "Banxia Xiexin decoction (& x534a;& x590f;& x6cfb;(sic)& x6c64;) treats diabetic

gastroparesis through PLC-IP3-Ca2+/NO-cGMP-PKG signal pathway," *Chinese Journal of Integrative Medicine*, vol. 26, no. 11, pp. 833–838, 2020.

[11] Y. Yu, G. Zhang, T. Han, and H. Huang, "Analysis of the pharmacological mechanism of Banxia Xiexin decoction in treating depression and ulcerative colitis based on a biological network module," *BMC Complement Med Ther*, vol. 20, no. 1, p. 199, 2020.

[12] X. Feng, F. Xue, G. He, Q. Ni, and S. Huang, "Banxia xiexin decoction affects drug sensitivity in gastric cancer cells by regulating MGMT expression via IL-6/JAK/STAT3-mediated PD-L1 activity," *International Journal of Molecular Medicine*, vol. 48, no. 2, 2021.

[13] B. Li, J. Rui, X. Ding, and X. Yang, "Exploring the multicomponent synergy mechanism of Banxia Xiexin decoction on irritable bowel syndrome by a systems pharmacology strategy," *Journal of Ethnopharmacology*, vol. 233, pp. 158–168, 2019.

[14] Q. Ji, Y. Yang, X. Song, X. Han, and W. Wang, "Banxia Xiexin decoction in the treatment of chronic atrophic gastritis," *Medicine*, vol. 99, no. 42, p. e22110, 2020.

[15] C. Nogales, Z. M. Mamdouh, M. List, C. Kiel, A. I. Casas, and H. H. H. W. Schmidt, "Network pharmacology: curing causal mechanisms instead of treating symptoms," *Trends in Pharmacological Sciences*, vol. 43, no. 2, pp. 136–150, 2022.

[16] C. Hao da and P. G. Xiao, "Network pharmacology: a Rosetta Stone for traditional Chinese medicine," *Drug Development Research*, vol. 75, no. 5, pp. 299–312, 2014.

[17] T. Usha, D. Shanmugarajan, A. K. Goyal, C. S. Kumar, and S. K. Middha, "Recent updates on computer-aided drug discovery: time for a paradigm shift," *Current Topics in Medicinal Chemistry*, vol. 17, no. 30, pp. 3296–3307, 2017.

[18] J. Ru, P. Li, J. Wang et al., "TCMSP: a database of systems pharmacology for drug discovery from herbal medicines," *Journal of Cheminformatics*, vol. 6, no. 1, p. 13, 2014.

[19] P. Banerjee, A. O. Eckert, A. K. Schrey, and R. Preissner, "ProTox-II: a webserver for the prediction of toxicity of chemicals," *Nucleic Acids Research*, vol. 46, no. W1, pp. W257–W263, 2018.

[20] A. Daina, O. Michielin, and V. Zoete, "SwissTargetPrediction: updated data and new features for efficient prediction of protein targets of small molecules," *Nucleic Acids Research*, vol. 47, no. W1, pp. W357–W364, 2019.

[21] X. Wang, Y. Shen, S. Wang et al., "PharmMapper 2017 update: a web server for potential drug target identification with a comprehensive target pharmacophore database," *Nucleic Acids Research*, vol. 45, no. W1, pp. W356–W360, 2017.

[22] J. Piñero, J. Saüch, F. Sanz, and L. I. Furlong, "The DisGeNET cytoscape app: exploring and visualizing disease genomics data," *Computational and Structural Biotechnology Journal*, vol. 19, pp. 2960–2967, 2021.

[23] A. P. Davis, C. J. Grondin, R. J. Johnson et al., "Comparative Toxicogenomics Database (CTD): update 2021," *Nucleic Acids Research*, vol. 49, no. D1, pp. D1138–D1143, 2021.

[24] N. Rappaport, M. Twik, I. Plaschkes et al., "MalaCards: an amalgamated human disease compendium with diverse clinical and genetic annotation and structured search," *Nucleic Acids Research*, vol. 45, no. D1, pp. D877–D887, 2017.

[25] Y. Dai, X. Chen, H. Yang et al., "Evidence construction of Huangkui capsule against chronic glomerulonephritis: a systematic review and network pharmacology," *Phytomedicine*, vol. 102, article 154189, 2022.

[26] P. Shannon, A. Markiel, O. Ozier et al., "Cytoscape: a software environment for integrated models of biomolecular interaction networks," *Genome Research*, vol. 13, no. 11, pp. 2498–2504, 2003.

[27] D. Szklarczyk, A. L. Gable, D. Lyon et al., "STRING v11: protein-protein association networks with increased coverage, supporting functional discovery in genome-wide experimental datasets," *Nucleic Acids Research*, vol. 47, no. D1, pp. D607–D613, 2019.

[28] S. Forli, R. Huey, M. E. Pique, M. F. Sanner, D. S. Goodsell, and A. J. Olson, "Computational protein-ligand docking and virtual drug screening with the AutoDock suite," *Nature Protocols*, vol. 11, no. 5, pp. 905–919, 2016.

[29] T. Mohammad, Y. Mathur, and M. I. Hassan, "InstaDock: A single-click graphical user interface for molecular docking-based virtual high-throughput screening," *Briefings in Bioinformatics*, vol. 22, no. 4, 2021.

[30] S. Kim, J. Chen, T. Cheng et al., "PubChem in 2021: new data content and improved web interfaces," *Nucleic Acids Research*, vol. 49, no. D1, pp. D1388–D1395, 2021.

[31] S. K. Burley, C. Bhikadiya, C. Bi et al., "RCSB Protein Data Bank: powerful new tools for exploring 3D structures of biological macromolecules for basic and applied research and education in fundamental biology, biomedicine, biotechnology, bioengineering and energy sciences," *Nucleic Acids Research*, vol. 49, no. D1, pp. D437–D451, 2021.

[32] A. W. Sousa da Silva and W. F. Vranken, "ACPYPE - AnteChamber PYthon Parser interfacE," *BMC Research Notes*, vol. 5, no. 1, p. 367, 2012.

[33] J. W. Shi, Z. Z. Li, J. S. Wu et al., "Identification of the bioactive components of Banxia Xiexin decoction that protect against CPT-11-induced intestinal toxicity via UPLC-based spectrum-effect relationship analyses," *Journal of Ethnopharmacology*, vol. 266, p. 113421, 2021.

[34] Y. Wang, R. Xu, J. Xiao et al., "Quantitative analysis of flavonoids, alkaloids and saponins of Banxia Xiexin decoction using ultra-high performance liquid chromatography coupled with electrospray ionization tandem mass spectrometry," *Journal of Pharmaceutical and Biomedical Analysis*, vol. 88, pp. 525–535, 2014.

[35] J. Setiadi and S. Kuyucak, "Free-energy simulations resolve the low-affinity Na^+-high-affinity Asp binding paradox in Glt_{Ph}," *Biophysical Journal*, vol. 117, no. 4, pp. 780–789, 2019.

[36] M. G. Nixon and E. Fadda, "Binding free energies of conformationally disordered peptides through extensive sampling and end-point methods," *Methods in Molecular Biology*, vol. 2039, pp. 229–242, 2019.

[37] W. Zhou, H. Zhang, X. Wang et al., "Network pharmacology to unveil the mechanism of Moluodan in the treatment of chronic atrophic gastritis," *Phytomedicine*, vol. 95, article 153837, 2022.

[38] J. Wen, S. Wu, X. Ma, and Y. Zhao, "Zuojin pill attenuates _Helicobacter pylori_ -induced chronic atrophic gastritis in rats and improves gastric epithelial cells function in GES-1 cells," *Journal of Ethnopharmacology*, vol. 285, article 114855, 2022.

[39] H. Y. Lu, J. Qin, N. Han, F. Xie, L. Gong, and C. Li, "Banxia Xiexin decoction is effective to prevent and control irinotecan-induced delayed diarrhea in recurrent small cell lung cancer," *Integrative Cancer Therapies*, vol. 17, no. 4, pp. 1109–1114, 2018.

Hindawi
Computational and Mathematical Methods in Medicine
Volume 2023, Article ID 9829453, 1 page
https://doi.org/10.1155/2023/9829453

Retraction

Retracted: Effects of Peripherally Inserted Central Catheter (PICC) Catheterization Nursing on Bloodstream Infection in Peripheral Central Venous Catheters in Lung Cancer: A Single-Center, Retrospective Study

Computational and Mathematical Methods in Medicine

Received 5 December 2023; Accepted 5 December 2023; Published 6 December 2023

This article has been retracted by Hindawi, as publisher, following an investigation undertaken by the publisher [1]. This investigation has uncovered evidence of systematic manipulation of the publication and peer-review process. We cannot, therefore, vouch for the reliability or integrity of this article.

Please note that this notice is intended solely to alert readers that the peer-review process of this article has been compromised.

Wiley and Hindawi regret that the usual quality checks did not identify these issues before publication and have since put additional measures in place to safeguard research integrity.

We wish to credit our Research Integrity and Research Publishing teams and anonymous and named external researchers and research integrity experts for contributing to this investigation.

The corresponding author, as the representative of all authors, has been given the opportunity to register their agreement or disagreement to this retraction. We have kept a record of any response received.

References

[1] Q. Hu, Y. Su, and L. Yan, "Effects of Peripherally Inserted Central Catheter (PICC) Catheterization Nursing on Bloodstream Infection in Peripheral Central Venous Catheters in Lung Cancer: A Single-Center, Retrospective Study," *Computational and Mathematical Methods in Medicine*, vol. 2022, Article ID 2791464, 7 pages, 2022.

Hindawi
Computational and Mathematical Methods in Medicine
Volume 2022, Article ID 2791464, 7 pages
https://doi.org/10.1155/2022/2791464

Research Article

Effects of Peripherally Inserted Central Catheter (PICC) Catheterization Nursing on Bloodstream Infection in Peripheral Central Venous Catheters in Lung Cancer: A Single-Center, Retrospective Study

Qiu Hu,[1] YanHong Su,[2] and Li Yan [3]

[1]*Department of Internal Medicine of Chest Oncology, Hubei Cancer Hospital, Tongji Medical College, Huazhong University of Science and Technology, No. 116, Zhuodaoquan South Road, Hongshan District, Wuhan 430079 Hubei Province, China*
[2]*Internal Department, Wuhan Third Hospital & Tongren Hospital of Wuhan University, No. 216, Guanshan Avenue, Hongshan District, Wuhan 430074, China*
[3]*Department of General Practice, Zhongnan Hospital of Wuhan University, 169 Donghu Road, Wuchang District, Wuhan, 430071 Hubei, China*

Correspondence should be addressed to Li Yan; kc@bbc.edu.cn

Received 24 June 2022; Revised 7 July 2022; Accepted 18 July 2022; Published 15 September 2022

Academic Editor: Min Tang

Background. Peripherally inserted central catheter (PICC), as one of the important intravenous routes for the rescue and treatment of critically ill patients, has been widely used in the fluid resuscitation of critically ill patients in intensive care. In particular, PICC can be widely used in the treatment of cancer patients. With the wide application of peripheral central venous catheterization, the clinical findings of bloodstream infection complications caused by PICC have gradually attracted the attention of doctors and patients. *Aims*. To investigate the effect of specialized placement and PICC placement care on patients with lung cancer who underwent PICC puncture. Patients were selected and divided into a comparison group and an observation group of 40 patients each according to the randomized residual grouping method. In the comparison group, routine PICC placement and catheter maintenance were performed, while the observation group was provided with specialized placement and PICC placement care. The differences in immune and tumor marker levels and nursing compliance between the two groups were observed and compared before and after nursing care. *Results*. There was no significant difference in the comparison of tumor marker levels between the two groups of patients before care, while the levels of CYFRA21-1, CA125, and VGEF in the observation group were significantly lower than those in the comparison group after care, and this difference was statistically significant ($P < 0.05$). There was no statistically significant difference in the comparison of immune levels between the two groups before care ($P > 0.05$), while the comparison of CD4+, CD3+, and CD4+/CD8+ after care was significantly different and higher in the observation group than in the comparison group, and the comparison was statistically significant ($P < 0.05$). The compliance rate of 93.8% in the observation group was significantly higher than that of 77.9% in the comparison group, and this difference was statistically significant for comparison ($P < 0.05$). *Conclusion*. PICC placement care is more effective in patients with lung cancer and performing PICC puncture, significantly improves patients' immune and tumor marker levels, improves patients' negative emotions, reduces disease uncertainty, and improves nursing compliance.

1. Introduction

Lung cancer is the malignancy that causes the most deaths worldwide, and most patients are already in the middle to late stages when they are diagnosed, making chemotherapy one of the main clinical treatment methods [1]. Transcatheter PICC provides a painless, safe, and sustainable intravenous chemotherapy access for clinical chemotherapy, but the catheter retention period is prone to complications due to factors such as nursing staff's operating technique and

individual patient's immune status [2]. Central venous catheter-associated bloodstream infection is one of the serious complications after PICC placement, and according to relevant data, the morbidity and mortality rate of patients with BIS is about 20% [3]. It is of positive significance to explore an ideal care plan to reduce the risk of BIS and improve the clinical chemotherapy outcome.

2. Material and Methods

2.1. Patient Eligibility Criteria. Eighty patients with lung cancer who underwent PICC puncture were selected as the subjects of the retrospective study and were divided into 40 cases each in the comparison group and the observation group according to the random remainder grouping method, and both groups were placed with single-lumen 4F or 5F catheters from BD, USA, under aseptic conditions: chills, except fever due to infection at other sites, positive culture of pathogenic bacteria in catheter blood, and significant decrease or return to normal temperature after perturbation; catheter blood and peripheral blood both cultured the same kind of bacteria or fungi. Patients with lung cancer chemotherapy all meet the indications for PICC tubes [4]: (i) lack of peripheral venous access, (ii) infusion of irritating drugs such as chemotherapy, and (iii) need for prolonged intravenous therapy. The drug flow rate is not affected by the patient's body position; the exterminate of chemotherapeutic drugs is effectively avoided; it can be retained for a long time, up to 1 year. It is not only beneficial to the treatment of patients but also more convenient for nursing work.

2.2. Exclusion Criteria. Inclusion criteria are as follows: (i) all patients in this study met the diagnostic criteria for lung cancer in the Chinese Medical Association Clinical Guidelines for Lung Cancer (2018 edition) [5] and were diagnosed with lung cancer by X-ray, magnetic resonance imaging, pathological examination, and clinical confirmation; (ii) Eastern Cooperative Oncology Group (ECOG) score [6]: 0-2, acquired drug resistance after care and expected survival time ≥3 months; and (iii) indications for PICC placement chemotherapy were met, clinical symptoms such as cough and blood in sputum were present, medical records were complete, and no previous chemotherapy or other related treatment had been received.

Exclusion criteria are as follows: (i) patients with severe infections, severe cognitive impairment, or previous history of psychiatric disease prior to inclusion; (ii) patients with combined speech and communication impairment, poor compliance, patients who did not agree to peripheral central venous line placement, or patients who were deemed unsuitable for inclusion for other reasons; and (iii) patients with underlying diseases such as severe diabetes, hypertension, or cardiac disease requiring hospitalization.

2.3. Methods. In the comparison group, routine PICC placement and catheter maintenance were performed; i.e., the peripheral central venous catheter was placed in strict accordance with the peripheral central venous catheter placement specification, and the correct position of the catheter tip could be confirmed by taking a film after placement, and sterile gauze should cover the puncture site after puncture, and then, bandage and hemostat should be performed. The patients were instructed to avoid strenuous movements of the punctured limb within 3 d of placement, were instructed how to properly maintain the peripheral central venous catheter, and were instructed to wear loose and comfortable clothing as much as possible during the placement process.

In the observation group, specialized catheter placement and PICC placement care were implemented; i.e., the dedicated PICC nurse correctly assessed the patient's vascular condition before placement and properly disinfected the patient's skin and operator's hand in the puncture area: maximum sterile barrier protection during placement, strict aseptic operation, gentle and steady tube delivery, and successful one-time puncture and tube delivery as far as possible; 24 h after placement, she was responsible for changing the dressing at the puncture site; after placement, the routine is as follows: catheter maintenance management, daily observation and assessment of the indwelling catheter, whether there are signs of infection such as redness, swelling, heat, and pain in the puncture area, and monitoring and following up the quality of PICC maintenance throughout the process. During the infusion period, the tube is flushed with 20 ml saline before and after infusion and sealed with sodium heparin saline after infusion; during the interinfusion deception period, the dressing and heparin cap are changed once every 7 d; if the dressing is loose, wet, and rolled edge, or there is blood in the heparin cap, the dressing and heparin cap are changed at any time. Nurses actively observe patients daily and immediately draw blood cultures according to the US CDC standards for monitoring catheter-associated bloodstream infections when patients show signs of infection such as cold collars, elevated body temperature ($T \geq 38^{\circ}C$) or decreased body temperature ($T \leq 36^{\circ}C$ in children), and decreased blood pressure for unknown reasons and when it is difficult to explain the infection in other parts of the state. If a set of peripheral venous blood is collected from a patient with a retained PICC and another set is collected from the catheter, the time of blood collection from both sources must be close (no more than Min); if 2 sets of peripheral blood cultures are collected aseptically from a patient who needs to have a PICC removed, the catheter is removed aseptically and the tip of the catheter is cut off for 5 cm for semiquantitative culture.

2.4. Observation Indicators. Eichmann Retroflex flow cytometer detects CD4+, CD3+, and CD4+/CD8+. Adherence: no nonadherent behavior was considered as complete adherence: the presence of 1~2 nonadherent behaviors was considered as partial adherence; the presence of 3 or more nonadherent behaviors was considered as nonadherence; complete adherence and partial adherence were counted as adherence rate.

2.5. Statistical Analysis. All statistical data in this study were entered into excel software by the first author and the corresponding author, respectively, and the statistical processing software was SPSS25.0 for calculation. Repeated measure analysis of variance between groups was used to measure

Table 1: Comparison of general information between the two groups [n, ($\bar{x} \pm s$)].

Group	Gender (male/female)	Average age (years)	Tumor diameter (cm)	Pathological type		
				Salmon carcinoma	Carcinoma ma	Squamous carcinoma
Comparison group (40)	28/12	36.63 ± 8.32	13.31 ± 1.67	10	22	8
Observation group (40)	29/11	36.62 ± 8.31	13.33 ± 1.25	11	23	6
χ^2/t	0.061	0.007	0.074	0.065	0.051	0.346
P	0.805	0.995	0.941	0.799	0.822	0.556

the measurement expressed as mean ± standard deviation ($X \pm S$). Count data expressed as a percentage (%) were tested by χ^2. Univariate and logistic multivariate regression analyses were used to compare the influencing factors, and the risk factors with significant differences were screened. Correlation test used logistic regression linear correlation analysis. Included data that did not conform to a normal distribution were described by M(QR), using the Mann-Whitney test. All statistical tests were two-sided probability tests. The statistical significance was $P < 0.05$.

3. Results

3.1. General Information Comparison. There was no statistically significant difference between the two groups by t-test and chi-square test when comparing the general data such as gender, mean age, tumor diameter, and pathological type ($P > 0.05$) (see Table 1).

3.2. Comparison of Tumor Marker Levels. Before care, there was no significant difference in the comparison of tumor marker levels between the two groups, and after care, the levels of CYFRA21-1, CA125, and VGEF in the observation group were significantly lower than those in the comparison group, and this difference was statistically significant ($P < 0.05$) (see Figure 1).

3.3. Comparison of Immune Levels. There was no statistically significant difference in the comparison of immune levels between the two groups before care ($P > 0.05$), while the comparison of $CD4^+$, $CD3^+$, and $CD4^+/CD8^+$ after care was significantly different and higher in the observation group than in the comparison group, and the comparison was statistically significant ($P < 0.05$) (see Figure 2).

3.4. Nursing Compliance. The compliance rate of 93.8% in the observation group was significantly higher than that of 77.9% in the comparison group, and this difference was statistically significant for comparison ($P < 0.05$) (see Figure 3).

4. Discussion

PICC, as one of the important intravenous routes for the resuscitation treatment of critically ill patients, has been widely used for fluid resuscitation, administration of radioactive drugs and antibiotics, parenthetical nutrition (PN), and hemodynamic monitoring in critically ill patients [7]. PICC is widely used mainly because of its easy maintenance, convenient operation, long retention time, and high safety [8]. PICC is especially performed. With the widespread use of peripheral central venous cannulae in the treatment of cancer patients, it has been found that complications from PICC-induced bloodstream infections are gradually gaining the attention of physicians and patients [9]. Once a bloodstream infection is formed, it will inevitably increase the physical and mental burden of the patient and at the same time reduce the initiative and motivation of the patient, which ultimately affects the prognosis to a great extent [10]. Relevant research data show that the mortality rate of bloodstream infections due to PICC is about 11.6% [11]. In order to improve clinical outcomes, the incidence of PICC bloodstream infections must be effectively controlled, and effective nursing measures must be taken [12]. In recent years, PICC has provided a painless, safe, and continuous intravenous chemotherapy access for oncology patients [13]. Oncology patients not only rely on PICC to complete chemotherapy but also need to rely on PICC for nutritional support [14]. Therefore, PICC plays an important role in the whole oncology treatment process, and whether PICC can be left for a long time depends on the catheter care quality emeritus, and once BSI occurs, it will affect the patient's prognosis and catheter retention time [15]. Doing specialized PICC placement care is an important measure to reduce PICC-associated bloodstream infection and prolong catheter retention time [16].

The levels of CYFRA21-1, CA125, and VGEF in the observation group after our study care were significantly lower than those in the comparison group, indicating that PICC placement care was more effective in patients with lung cancer and who underwent PICC puncture and significantly improved the level of tumor markers in patients. CYFRA21-1 is a soluble fragment of incineration, which is widely distributed in Bellamy or squamous epithelium, and CYFRA21-1 can be released into the blood when tumor cells are Elysee or necrotic, which has a high diagnostic and efficacy assessment application value for patients [17]. CA125 is a saccharine protein with low concentration in the serum of healthy individuals, which is released into the blood when tumor infiltration occurs in the organism, and its half-life is short and metabolism is fast, and its detection level can be used to reflect the recent efficacy of tumor treatment [18]. The results of our study showed that the levels of CYFRA21-1, CA125, and VGEF in the observation group were significantly lower than those in the prewar and comparison groups, indicating that specialized PICC placement care can effectively improve the patient's condition and indirectly inhibit tumor cell proliferation. Therefore, professional PICC placement process and

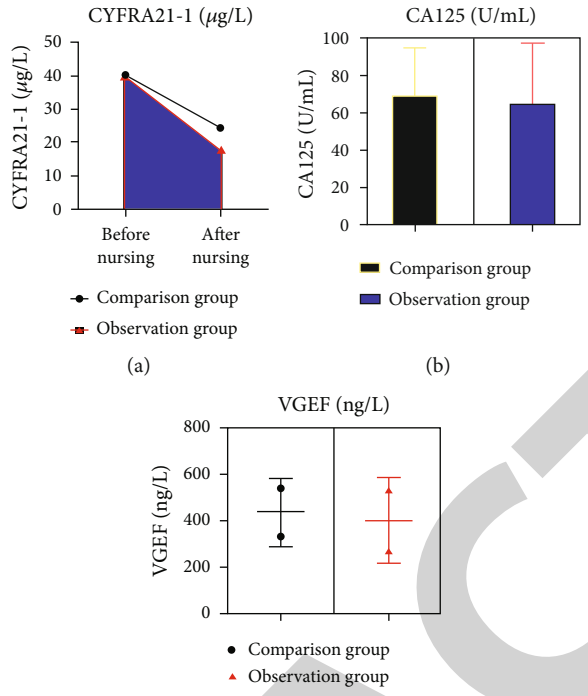

Figure 1: Comparison of tumor marker levels. All tumor marker level data in this study were entered into excel software by the first author and the corresponding author, respectively, and the statistical processing software was SPSS25.0 for calculation, expressed as mean ± standard deviation using independent sample t-test. It was found that the levels of CYFRA21-1, CA125, and VGEF in the observation group were significantly lower than those in the comparison group after care, and this difference was statistically significant ($P < 0.05$).

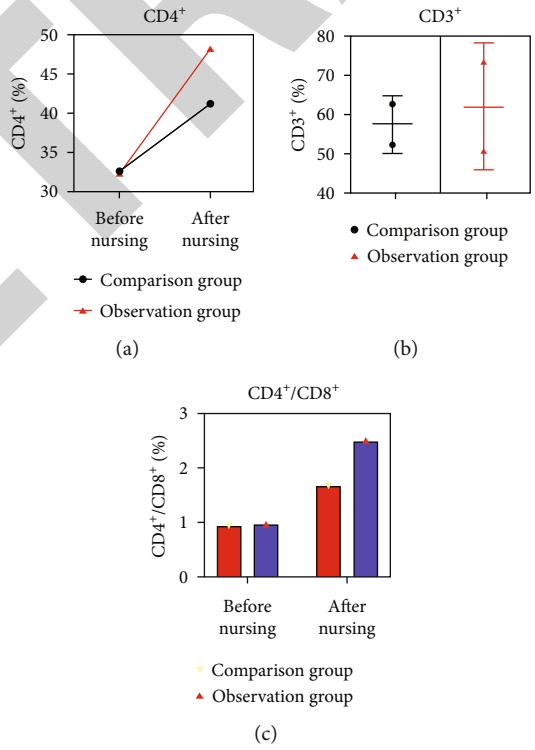

Figure 2: Comparison of tumor marker levels. All tumor marker level data in this study were entered into excel software by the first author and the corresponding author, respectively, and the statistical processing software was SPSS25.0 for calculation, and the independent samples t-test was used to express the mean ± standard deviation. The differences in CD4+ (a), CD3+ (b), and CD4+/CD8+a (c) in the observation group after nursing were significantly higher than those in the control group, and the comparison was statistically significant ($P < 0.05$).

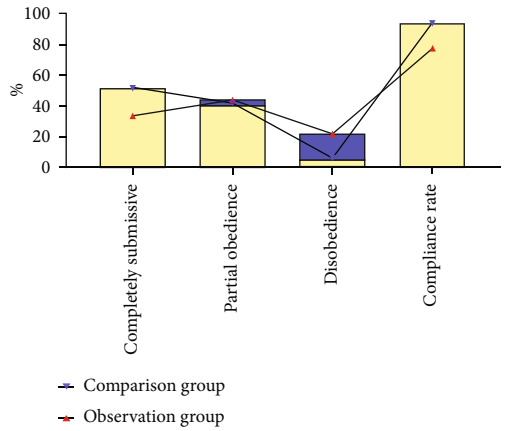

Figure 3: Nursing adherence. All nursing compliance data of our study were entered into Excel software by the first and corresponding authors, respectively, and the statistical processing software was SPSS25.0 for calculation expressed as a percentage (%) with χ^2 test, and it was found that the compliance rate of 93.8% in the observation group was significantly higher than that of 77.9% in the comparison group, and this difference was statistically significant ($P < 0.05$).

maintenance quality management are the key to prevent BSI [19]. Studies have shown that unskilled punctures, violation of aseptic principles, and irregular routine maintenance of catheters contribute to the occurrence of PICC-associated BSI [20]. Professionalized PICC placement care can both effectively prevent the occurrence of catheter-associated bloodstream infections and enhance nurses' professional skills and professional honor [21].

The difference in CD4+, CD3+, and CD4+/CD8+ after nursing care in our study was significant and higher in the observation group than in the comparison group, indicating that PICC placement nursing is more effective in patients with lung cancer and performing PICC puncture and significantly improves patient immunity. PICC placement catheter infections are mostly caused by bacteria from the skin at the insertion site migrating outside the catheter lumen via subcutaneous tunnels [22]. Bacteria cultured from fibrin adhesion at the catheter tip after perturbation were identical to those isolated from bacterial cultures on the surfaces of items in the surrounding environment such as bedside tables and infusion stands [23]. Bacterial cultures of tubercular secretions also contained the above-mentioned bacteria, suggesting that exogenous bacterial colonization is the main cause of venous catheter infection. The occurrence, development, and metastasis of tumors are closely related to the immune function of the body [24]. The immune function of the body is mostly suppressed in patients with malignant tumors, and the body's antitumor capacity and antitoxic side effects are diminished [25]. CD3+ cells can enhance the body's antitumor immune response, and CD4+/CD8+ mainly reflects the tumor cell killing activity [26]. Our study of catheter placement and catheter maintenance by a dedicated PICC nurse following a specialized standard procedure resulted in a lower infection rate of catheter-associated bloodstream infections than reported in the literature [27]. Therefore, good patient vascular assessment, skin disinfection and hand disinfection of the puncture before PICC placement, strict aseptic operation during placement, proper catheter maintenance after placement, and enhanced patient education are key aspects to prevent PICC-associated infections, improve patient immunity, and prolong catheter retention time [28]. PICC can not only serve as an intravenous nutrition supplementation channel for lung cancer patients but also as a PICC that is important in the treatment of lung cancer patients, as it can not only reduce the financial burden of patients but also reduce the waste of resources, improve the compliance of lung cancer patients, and ultimately improve the prognosis if the PICC time is long enough (until the end of chemotherapy) [29]. However, clinical research data show that as PICC is more and more widely used, the consequent incidence of PICC vascular infection is also increasing year by year, which subsequently affects the late treatment outcome of lung cancer patients to a great extent.

The compliance rate of 93.8% in the observation group of our study was significantly higher than that of 77.9% in the comparison group, indicating that PICC placement care is more effective and improves nursing compliance for patients with lung cancer, and PICC puncture is performed. Due to clinical treatment needs, lung cancer patients mostly need to go through six chemotherapy cycles, about half a year. The frequent peripheral puncture and stimulation by chemotherapeutic drugs not only cause complications such as phlebitis but also invariably increase the probability of drug leakage, resulting in local tissue necrosis and other conditions [30]. PICC overcomes the shortcomings of multiple acupuncture and effectively avoids the problem of repeated punctures by means of intravenous placement and establishment of a continuous drug delivery channel [31]. And the channel can be used not only as a chemotherapy drug delivery channel but also as a nutritional resupply channel for patients, thus reducing the pain of patients during treatment and recovery [32]. Therefore, PICC is important in the treatment of lung cancer patients [33].

In conclusion, PICC placement care is effective for patients with lung cancer who have undergone PICC puncture, and it significantly improves patients' immune and tumor marker levels, improves patients' negative emotions, reduces disease uncertainty, and increases nursing compliance.

Data Availability

No data were used to support this study.

Conflicts of Interest

There are no conflicts of interest.

Authors' Contributions

Qiu Hu and YanHong Su are co-first authors, and both authors contributed equally to this work.

References

[1] S. Jaber, C. Paugam, E. Futier et al., "Sodium bicarbonate therapy for patients with severe metabolic acidaemia in the intensive care unit (BICAR-ICU): a multicentre, open-label, randomised controlled, phase 3 trial," *The Lancet*, vol. 392, no. 10141, pp. 31–40, 2018.

[2] S. Duwadi, Q. Zhao, and B. S. Budal, "Peripherally inserted central catheters in critically ill patients - complications and its prevention: a review," *International Journal of Nursing Sciences*, vol. 6, pp. 99–105, 2019.

[3] M. Pan, A. Meng, R. Yin et al., "Nursing interventions to reduce peripherally inserted central catheter occlusion for cancer patients: a systematic review of literature," *Cancer Nursing*, vol. 42, no. 6, pp. E49–E58, 2019.

[4] S. Coppola, A. Caccioppola, S. Froio, and D. Chiumello, "Sodium bicarbonate in different critically ill conditions: from physiology to clinical practice," *Anesthesiology*, vol. 134, no. 5, pp. 774–783, 2021.

[5] Chinese Medical Association, Chinese Medical Association Oncology Branch, Chinese Medical Association Journal Press, "Chinese Medical Association Lung Cancer Clinical Diagnosis and Treatment Guidelines (2018 Edition)," *Chinese Journal of Oncology*, vol. 40, no. 12, pp. 935–964, 2018.

[6] E. Boran, G. Ramantani, N. Krayenbühl et al., "High-density ECoG improves the detection of high frequency oscillations that predict seizure outcome," *Clinical Neurophysiology*, vol. 130, pp. 1882–1888, 2019.

[7] X. Chen, L. Zhou, Y. Tan, and Z. Tao, "Selection of PICC catheter location in neonates via evidence-based ACE Star model," *Zhong Nan Da Xue Xue Bao Yi Xue Ban*, vol. 45, no. 9, pp. 1082–1088, 2020.

[8] H. Qian, J. Liu, C. Xu, W. Zhu, and L. Chen, "Predisposing factors and effect of bundle nursing in PICC-related upper extremity deep venous thrombosis in patients with non-Hodgkin's lymphoma undergoing chemotherapy," *American Journal of Translational Research*, vol. 13, no. 8, pp. 9679–9686, 2021.

[9] H. Xu, W. Yang, Y. Liu, X. Mu, Y. Liu, and H. Hu, "Analysis of nursing effect and impact of narrative nursing model on anxiety of tumor patients with PICC under chemotherapy," *Evidence-based Complementary and Alternative Medicine*, vol. 2021, Article ID 3698845, 7 pages, 2021.

[10] Y. Hu, Y. Ling, Y. Ye et al., "Analysis of risk factors of PICC-related bloodstream infection in newborns: implications for nursing care," *European Journal of Medical Research*, vol. 26, no. 1, p. 80, 2021.

[11] Q. Zhang, A. Qian, and W. Chen, "Analysis of PICC based on dysfunction module personalized nursing treatment in chemotherapy of advanced esophageal cancer," *Journal of Healthcare Engineering*, vol. 2021, Article ID 8997915, 10 pages, 2021.

[12] M. E. Lacostena-Pérez and A. M. Buesa-Escar, Eds.A. M. Gil-Alós, "Complications related to the insertion and maintenance of peripheral venous access central venous catheter," *Enfermería Intensiva (English ed.)*, M. E. Lacostena-Pérez and A. M. Buesa-Escar, Eds., vol. 30, no. 3, pp. 116–126, 2019.

[13] R. J. Chan, S. Northfield, E. Larsen et al., "Central venous access device securement and dressing effectiveness for peripherally inserted central catheters in adult acute hospital patients (CASCADE): a pilot randomised controlled trial," *Trials*, vol. 18, no. 1, p. 458, 2017.

[14] F. Qi, H. Cheng, X. Yuan, and L. Zhang, "Comparison of PICC and TIVAP in chemotherapy for patients with thyroid cancer," *Oncology Letters*, vol. 20, no. 2, pp. 1657–1662, 2020.

[15] Y. Wang and L. Zhao, "Diagnosis and management of secondary malposition of PICC into the azygos vein," *The Journal of Vascular Access*, vol. 23, pp. 450–454, 2022.

[16] B. Galen, S. Baron, S. Young, A. Hall, L. Berger-Spivack, and W. Southern, "Reducing peripherally inserted central catheters and midline catheters by training nurses in ultrasound-guided peripheral intravenous catheter placement," *BMJ Quality and Safety*, vol. 29, no. 3, pp. 245–249, 2020.

[17] J. Zhou and L. Wang, "Application of a nursing data-driven model for continuous improvement of PICC care quality," *Journal of Healthcare Engineering*, vol. 2022, Article ID 7982261, 8 pages, 2022.

[18] C. M. Rickard, N. M. Marsh, J. Webster et al., "Peripherally inserted central catheter dressing and securement in patients with cancer: the PISCES trial. Protocol for a 2x2 factorial, superiority randomised controlled trial," *BMJ Open*, vol. 7, no. 6, article e015291, 2017.

[19] L. Liu, J. Huang, Z. Wu, and Y. Ma, "Effectiveness and safety of catheter removal alone versus standard anticoagulation therapy after catheter removal for peripherally inserted central catheter (PICC)-related thrombosis," *Annals of Translational Medicine*, vol. 9, no. 24, p. 1778, 2021.

[20] Y. Gao, Y. Liu, H. Zhang, F. Fang, and L. Song, "The safety and accuracy of ECG-guided PICC tip position verification applied in patients with atrial fibrillation," *Therapeutics and Clinical Risk Management*, vol. 14, no. 14, pp. 1075–1081, 2018.

[21] J. T. Silva, A. Lagares-Velasco, M. Fernández-Ruiz, G. González-Monterrubio, M. D. Pérez-Cárdenas, and J. M. Aguado, Eds.F. López-Medrano, "Peripherally inserted central venous catheter placed and maintained by a dedicated nursing team for the administration of antimicrobial therapy vs. another type of catheter: a retrospective case-control study," *Enfermedades Infecciosas y Microbiología Clínica*, J. T. Silva, A. Lagares-Velasco, M. Fernández-Ruiz, G. González-Monterrubio, M. D. Pérez-Cárdenas, and J. M. Aguado, Eds., vol. 38, no. 9, pp. 425–430, 2020.

[22] T. Kleidon, A. J. Ullman, L. Zhang et al., "How does your PICC-COMPARE? A pilot randomized controlled trial comparing various PICC materials in pediatrics," *Journal of Hospital Medicine*, vol. 13, no. 8, pp. 517–525, 2018.

[23] G. Wang, Y. Li, C. Wu et al., "The clinical features and related factors of PICC-related upper extremity asymptomatic venous thrombosis in cancer patients: a prospective study," *Medicine*, vol. 99, no. 12, article e19409, 2020.

[24] R. Sharp, P. Carr, J. Childs et al., "Catheter to vein ratio and risk of peripherally inserted central catheter (PICC)-associated thrombosis according to diagnostic group: a retrospective cohort study," *BMJ Open*, vol. 11, no. 7, article e045895, 2021.

[25] C. Jie, P. Chunxue, X. Jiawei, L. Hongmei, and Q. Huohong, "Multidisciplinary cooperative mode led by infusion nurse specialists used to ensure the nursing quality of peripherally inserted central catheters in China: a 5-year retrospective study," *The Journal of Vascular Access*, vol. 21, 2021.

[26] R. Zhang, P. Chen, L. Yang, Y. Li, Y. Zong, and L. Deng, "Prevention of hematogenous infection in peripheral venous catheterization with integrated medical assistance in patients undergoing chemotherapy," *Annali Italiani di Chirurgia*, vol. 92, pp. 70–76, 2021, PMID: 33746117.

Hindawi
Computational and Mathematical Methods in Medicine
Volume 2023, Article ID 9856372, 1 page
https://doi.org/10.1155/2023/9856372

Retraction

Retracted: Correlation Analysis of Serum Pepsinogen, Interleukin, and TNF-α with Hp Infection in Patients with Gastric Cancer: A Randomized Parallel Controlled Clinical Study

Computational and Mathematical Methods in Medicine

Received 12 December 2023; Accepted 12 December 2023; Published 13 December 2023

This article has been retracted by Hindawi, as publisher, following an investigation undertaken by the publisher [1]. This investigation has uncovered evidence of systematic manipulation of the publication and peer-review process. We cannot, therefore, vouch for the reliability or integrity of this article.

Please note that this notice is intended solely to alert readers that the peer-review process of this article has been compromised.

Wiley and Hindawi regret that the usual quality checks did not identify these issues before publication and have since put additional measures in place to safeguard research integrity.

We wish to credit our Research Integrity and Research Publishing teams and anonymous and named external researchers and research integrity experts for contributing to this investigation.

The corresponding author, as the representative of all authors, has been given the opportunity to register their agreement or disagreement to this retraction. We have kept a record of any response received.

References

[1] S. Hao, M. Shou, J. Ma, Y. Shu, and Y. Yu, "Correlation Analysis of Serum Pepsinogen, Interleukin, and TNF-α with Hp Infection in Patients with Gastric Cancer: A Randomized Parallel Controlled Clinical Study," *Computational and Mathematical Methods in Medicine*, vol. 2022, Article ID 9277847, 7 pages, 2022.

Hindawi
Computational and Mathematical Methods in Medicine
Volume 2022, Article ID 9277847, 7 pages
https://doi.org/10.1155/2022/9277847

Research Article

Correlation Analysis of Serum Pepsinogen, Interleukin, and TNF-α with Hp Infection in Patients with Gastric Cancer: A Randomized Parallel Controlled Clinical Study

Shunxin Hao,[1] Minyue Shou,[2] Jing Ma,[3] Yongqian Shu,[2] and Yuanyuan Yu[4]

[1]*Department of General Surgery, Wuhan University of Science and Technology Hospital, China 430065*
[2]*The First Affiliated Hospital of Nanjing Medical University (Department of Oncology), China 210029*
[3]*Zhongshan Hospital Affiliated to Fudan University, China 200032*
[4]*Department of Geriatrics, Wuhan Hospital of Traditional Chinese Medicine, 49 Lihuangpi Road, Jiangan District, Wuhan City, Hubei Province, China*

Correspondence should be addressed to Yuanyuan Yu; wzy@bbc.edu.cn

Received 28 June 2022; Revised 30 July 2022; Accepted 2 August 2022; Published 14 September 2022

Academic Editor: Min Tang

Background. Gastric cancer pathological biopsy and visual examination have been the gold standard for gastric cancer diagnosis, but their operation is costly, demanding, and risky, so it is especially important to find an effective examination method in clinical practice. *Aims*. To investigate the correlation between serum pepsinogen I (PGI), pepsinogen II (PGII), pepsinogen I and II ratio (PGR), IL-6, and TNF-α and Helicobacter pylori (Hp) infection in patients with gastric cancer. *Materials and Methods*. Fifty patients with Hp-infected gastric cancer admitted to the Department of Gastroenterology of our hospital from January 2019 to December 2021 were selected for the study as the observation group, and another 50 patients without Hp-infected gastric cancer were selected as the comparison group to compare the correlation analysis of PGI, PGII, PGR, IL-6, and TNF-α with Hp infection between the two groups after admission and treatment. *Results*. After measurement, PGI and PGII in the observation group were significantly lower than those in the comparison group, and TNF-α, IL-18, and IL-6 in the observation group were significantly higher than those in the comparison group, and the comparative differences were all statistically significant ($P < 0.05$). The results of multivariate logistic regression model analysis of independent risk factors for gastric cancer showed that IL-18, hs-CRP, and tumor necrosis factor- (TNF-) α were risk factors for Hp infection in gastric cancer. *Conclusion*. The expression of IL-18, hs-CRP, and TNF-α factors in Hp-infected gastric cancer patients is correlated. IL-6, IL-18, and TNF-α are involved in the entire process from the onset to the development of Hp-positive gastric mucosal inflammation in patients, which is of great value in the diagnosis of gastric cancer and helps to assess the degree of progression and prognosis of gastric cancer.

1. Introduction

Epidemiological surveys in recent years have shown that the global morbidity and mortality of gastric cancer have been decreasing year by year, but it is still a common clinical malignant tumor [1]. The incidence of gastric cancer in my country ranks first among various malignant tumors, and it also accounts for 35% of the global incidence [2]. Epidemiological surveys have shown that with age, the incidence of H. pylori infection will continue to increase [3]. In recent years, studies have confirmed that H. pylori is closely related to the occurrence of gastric cancer, because H. pylori can cause damage to the gastrointestinal mucosa and promote the regeneration of gastrointestinal cells, thereby increasing the risk of injury [4]. H. pylori infection can increase the generation of oxygen free radicals, which leads to the peroxidation of gastric mucosal epithelium, which induces symptoms such as acid reflux, nausea, upper abdominal pain, and belching and is closely related to the incidence of gastric cancer [5]. Interleukin-18 (IL-18), high-sensitivity C-reactive protein

(hs-CRP), and tumor necrosis factor-α (TNF-α) are highly sensitive markers of inflammatory factors [6]. Studies have confirmed that these inflammatory factors can induce and aggravate inflammatory responses, and IL-18 is involved in the occurrence and development of various malignant tumors including gastric cancer through various mechanisms [7]. After the inflammatory reaction, due to the continuous increase of free radicals and the generation of superoxide, the cells undergo peroxidative damage, resulting in long-term cellular tumors and gastric cancer [8]. H. pylori is a Gram-negative bacterium with multiple genotypes and secretes a variety of exogenous toxins [9]. It can damage the gastric mucosal epithelium, and the damage mechanisms include cell DNA damage, mitochondrial base expression affecting gastric mucosal epithelial cells, and cell proliferation disorders .

Studies have shown that H. pylori is closely related to gastritis, peptic ulcer, and gastric cancer. H. pylori infection is an important factor in the incidence of gastric cancer and is listed as the first carcinogen by the World Health Organization [10]. The relationship between H. pylori infection and cell proliferation and apotheosis is a current research hotpot [11]. The stability of the gastric environment requires a balance between proliferation and apotheosis of gastric colossal cells. Although the rate of cell loss caused by apotheosis is comparable to the rate of new cell formation, H. pylori infection will affect this balance and lead to the occurrence of many gastric diseases [12]. It has been suggested that Hp infection affects PG changes, and Hp infection plays an important role in gastric carcinogenesis, but its exact mechanism of action is not clear. Hp is a trigger for a number of diseases, and Hp activates disease cells, causing them to accumulate in the gastric mucosal tissues, creating a mediated inflammatory response, and the levels of cytokines in chronic gastritis vary significantly. The higher the level of Hp in the patient, the more severe the degree of infection of the patient's gastric mucosa, and the degree of erosion of the Hp-positive gastric mucosa by disease cells has an important relationship with the density of Hp. Peptic ulcer is a common gastrointestinal disease with a complex etiology, and Hp infection is one of its important causes. We believe that Hp infection affects PG changes and Hp infection plays an important role in gastric carcinogenesis, but its specific mechanism of action is not clear. The reason why Hp affects PG changes and causes cancer may be related to chronic inflammatory stimulation of Hp leading to atrophic intestinalization of gastric tissues and damage to PG genes, and some scholars believe that it is related to the host's own immune disorder caused by Hp. In this study, 100 patients admitted to our hospital from January 2016 to January 10, 2020, were selected for exploration and analysis and the correlation analysis of serum pepsin, IL-6, and TNF-α with Hp infection in patients with gastric cancer. The report is as follows.

2. Material and Methods

2.1. Research Object. Fifty cases of Hp-infected gastric cancer patients admitted to the Department of Gastroenterology of our hospital were selected for the study as the observation group, and another 50 cases of patients without Hp infection were selected as the comparison group. Inclusion criteria [13]: (i) after gastroscopic biopsy histopathological examination, pathology and imaging consistent with the diagnosis of gastric cancer; (ii) age 18-65 years, no history of special medication (gastric mucosal protective agents, nonsteroidal anti-inflammatory drugs, acid suppressants, and antibacterial drugs) in the previous 2 months, all selected patients accepted and voluntarily joined the experiment; (iii) no history of relevant vaccinations, approved by the hospital ethics committee and those who signed the informed consent. Exclusion criteria: (i) with infectious diseases, (ii) with severe liver and kidney impairment, and (iii) with mental illness (interfering with our study or affecting the results of the trial).

2.2. Methods. Serum-related factor assay: 2 ml of fasting elbow venous blood was collected from both groups in the early morning, and the serum was separated after centralization at 3000 r/min for l0min, and the level of CRP was measured by enzyme-linked immunodeficient assay kit (Bioengineering Shanghai Co., Ltd.); IL-18 and TNF-α were measured by IMMU-NITE1000 luminescence analyzer (Thermo Fisher) (kit: Institute of Radiology and Immunology, PLA General Hospital). The 2000 luminescence instrument from Abbott and the accompanying PGI and PGII reagents were used to determine PGI and PGII levels and calculate the PGI/PGII (PGR) ratio, which was determined by the luminescence method; patients were kept in a fasting state before undergoing gastropod, 3 ml of venous blood was collected, serum was separated to obtain serum and tested, and the degree of gastric colossal inflammation was measured. The degree of inflammation of the gastric mucous was observed with a low-mounted microscope, and the values of IL-6, IL-18, and TNF-α were recorded and analyzed.

Hp assay: the anti-Hp antibody characterization kit (Shanghai Changchun Technology Co., Ltd., enzyme-linked immunodeficient assay) was used to detect the level of Hp-IgG antibody in the serum of the two groups of patients.

2.3. Statistical Analysis. All statistical data in this study were entered into Excel software by the first author and the corresponding author, respectively, and the statistical processing software was SPSS 25.0 for calculation. Repeated measures analysis of variance between groups was used to measure the measurement expressed as mean ± standard deviation ($X \pm S$). Count data expressed as a percentage (%) were tested by χ^2. Univariate and logistic multivariate regression analysis was used to compare the influencing factors, and the risk factors with significant differences were screened. Correlation test used logistic regression linear correlation analysis. Included data that did not conform to a normal distribution were described by M (QR), using the Mann–Whitney test. All statistical tests were two-sided probability tests. The statistical significance was $P < 0.05$.

Table 1: Comparison of baseline information between the two groups of patients.

Group	Average age (years)	Gender (male/female)	Lesion diameter (cm)	Body mass index (kg/m^2)	Tumor classification	
					Gastric body cancer	Gastric sinus cancer
Comparison group (50)	69.83 ± 5.13	23/27	4.50 ± 1.25	22.32 ± 1.16	22	28
Observation group (50)	68.72 ± 3.16	26/24	4.40 ± 1.01	22.11 ± 1.10	21	29
t	1.303	0.360	0.440	0.929	0.041	
P	0.196	0.548	0.661	0.355	0.840	

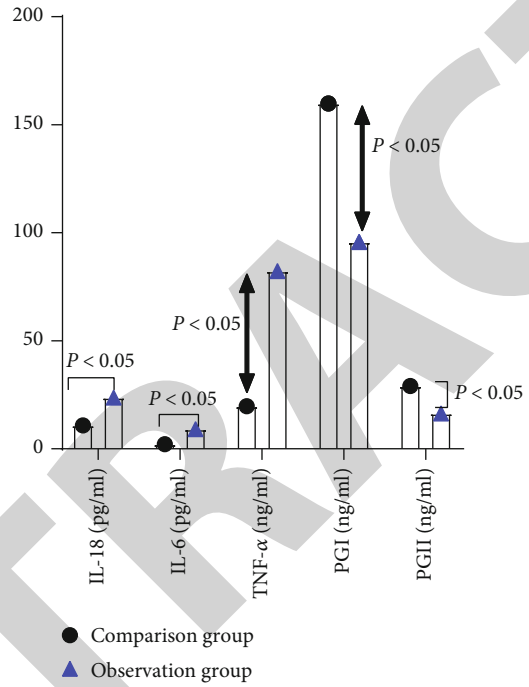

Figure 1: Comparison of serum indicators. In this study, the statistics of the pain VAS scores of the two groups of patients were entered into Excel software by the first and corresponding author, respectively, and the included data were tested using the Shapiro-Wilk method of mean ± standard deviation of the measured data conforming to a normal distribution. And independent sample or paired sample t-tests were implemented between or within groups. PGI and PGII in the observation group were significantly lower than those in the comparison group, and TNF-α, IL-18, and IL-6 in the observation group were significantly higher than those in the comparison group, and the comparative differences were all statistically significant ($P < 0.05$).

3. Results

3.1. Comparison of Baseline Data. The differences in mean age, gender, lesion diameter, tumor classification, and body mass index between the two groups were not statistically significant ($P > 0.05$). See Table 1.

3.2. Serum Index Comparison. After measuring, PGI (95.76 ± 3.14) and PGII (16.36 ± 4.90) in the observation group were significantly lower than those in the comparison group, and TNF-α (82.28 ± 4.24), IL-18 (19.76 ± 3.14), and IL-6 (9.13 ± 1.01) in the observation group were significantly higher than those in the comparison group, and the differences were statistically significant ($P < 0.05$). See Figure 1.

3.3. Comparison of Gastric Cancer Stage and Related Indicators. The higher clinical stage of gastric cancer led to higher serum gastrin-17, CEA, and CA199 levels and lower pepsinogen I levels, and the comparative differences were statistically significant ($P < 0.05$). However, the differences of pepsinogen I/pepsinogen II and H. pylori positivity rates in patients with different gastric cancer stages were not statistically significant ($P > 0.05$). See Figure 2.

3.4. Multiword Regression Analysis. The variables with significant differences were assigned, namely, IL-18, CA199, CEA, hs-CRP, and TNF-α (normal = 1, abnormal = 0). The results of multivariate logistic regression model analysis of independent risk factors for gastric cancer showed that IL-

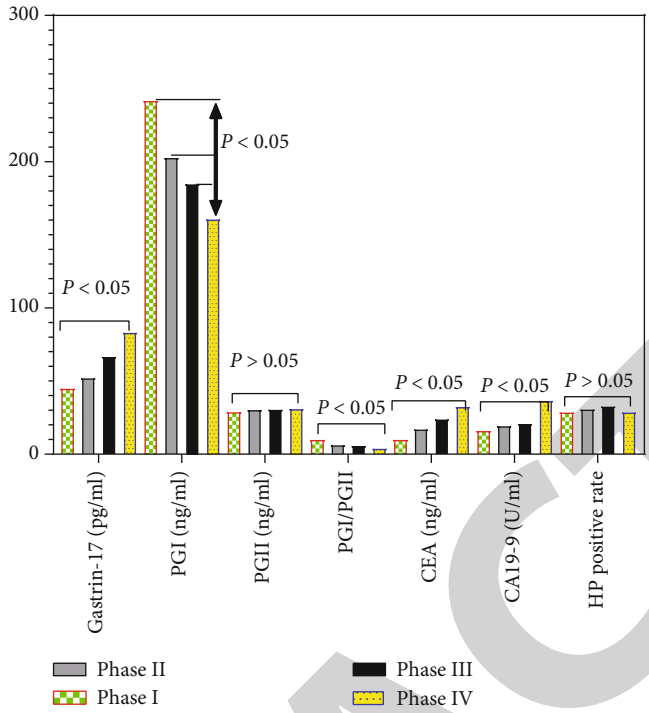

Figure 2: Comparison of gastric cancer staging and related indicators. In this study, statistics of pain VAS scores for both groups were entered into Excel software by the first and corresponding authors, respectively, and measures of gastrin-17, CEA, CA199, PGI, and PGI/PGII were tested for inclusion by the Shapiro-Wilk method of mean ± standard deviation. And independent sample or paired sample t -tests were implemented between or within groups, and HP-positive rate count data were expressed as whole numbers and found by chi-square test. Higher clinical stage of gastric cancer resulted in higher serum gastrin-17, CEA, and CA199 levels and lower PGI levels, all with statistically significant differences in comparison ($P < 0.05$). However, the differences in PGI/PGII and HP-positive rates were not statistically significant in patients with different gastric cancer stages ($P > 0.05$).

Table 2: Multiword logistic regression analysis.

	b	SE (b)	Wald	P	OR	OR 95% CI
IL-18	2.026	0.952	4.370	0.023	7.656	1.110-5.760
CA199	-0.203	0.708	0.053	0.742	0.761	0.150-3.780
CEA	0.502	0.710	0.376	0.527	1.633	0.330-7.970
hs-CRP	4.932	1.409	10.412	0.003	1.910	7.021-217.402
TNF-α	-1.915	0.908	4.309	0.023	0.110	0.020-0.840

18, hs-CRP, and TNF-α were risk factors for Hp infection in gastric cancer, and the comparative differences were all statistically significant ($P < 0.05$). See Table 2.

4. Discussion

Hp infection is an important trigger of chronic gastritis and peptic ulcer, and research data show that some immune mechanisms and inflammatory responses play an important role in the pathogenesis of gastric mucosa, and nowadays, diseases due to cytokine triggers are getting more and more attention [14]. Hp-positive chronic gastritis and peptic ulcer make some cells in patients to form an immune response, in which endocrine secretion of serum IL-6, IL-8, and TNF-α and other cytokines is endocrine raised [15]. Hp is the trigger of some diseases, Hp activates disease cells and causes them to accumulate in the gastric mucosal tissue, forming a mediated inflammatory response, and the levels of cytokines in chronic gastritis differ significantly [16]. The higher the level of Hp in the patient, the more severe the degree of infection of the patient's gastric mucosa, and the degree of erosion of the Hp-positive gastric mucosa by the disease cells has an important relationship with the density of Hp [17]. Peptic ulcer is a common gastrointestinal disease with a complex etiology, and Hp infection is one of its important causes [18].

We found that Hp can secrete a large number of pathogenic factors via regulation of relevant signaling pathways, and long-term persistent Hp infection induces immune and inflammatory responses and produces carcinogenic substances, thus playing a role in the progression of precancerous diseases [19]. In addition, persistent Hp infection leads to an increased rate of DNA damage, and inflammation can lead

to the production of large amounts of superoxide and free radicals, reducing the concentration of vitamin C in the gastric juice [20]. This makes the cells less tolerant to oxidative damage and prone to peroxidative damage [21]. The possible mechanisms linking Hp infection to the development of gastric cancer are considered to include the following: oxidative damage, type of Hp strain, genetic variants and differences in their expression, and abnormal kinetics related to gastric mucosal epithelial cells [22–25].

Our study showed showing that serum IL-6 and 1L-18 has an important factor in gastrointestinal diseases and also provides a diagnostic basis for patients with early gastric cancer [26]. Elevated serum IL-6 levels have been reported to be positively correlated with the development of bone tumors, and higher levels of IL-6 have been found in tumor cells and tumor-associated macrophages, and it has been found that tumor cells may produce higher levels of IL-6 during proliferation, invasion, or metastasis [27]. Elevated serum IL-6 levels were positively correlated with tumor load and disease progression, and IL-6 levels were significantly elevated in patients with gastric cancer with lymph node metastasis [28]. Serum pepsinogen, an endoproteinase with digestive function, is divided into two subgroups, PGI and PGII, according to immunology and biochemistry [29]. Among them, PGI is mainly expressed in cervical mucus cells and principal cells of the gastric fundus and is especially highly expressed in the gastric mucosa of embryos [30]. Among them, PGII is mainly expressed with all duodenal Brunner's gland and gastric glands and to a lesser extent in prostate and pancreas [31]. Most of the synthesized pepsinogen is secreted into the gastric lumen and activated into pepsin by the action of acidic gastric juice, and the pepsinogen that enters the circulation is very stable [32]. The measurement of serum pepsinogen changes can reflect the degree of gastric mucosal lesions and differentiation, which is beneficial for the early diagnosis of gastric cancer and is important for the prevention of gastric cancer, and it is also considered to be the best serological indicator for the histology of gastric mucosa [33]. Therefore, it is considered that serum pepsinogen can be used for the initial screening of gastric cancer and as an ideal tumor marker for the diagnosis of gastric cancer [34].

In our study, pepsinogen I and pepsinogen II in the observation group were significantly lower than those in the comparison group, and TNF-α and IL-6 in the observation group were significantly higher than those in the comparison group after measurement. The findings may suggest that elevated IL-6 levels may be an indicator of further deterioration of gastric cancer patients or suggest that the tumor may metastasize, suggesting appropriate therapeutic measures to control the development of the disease, and the experimental results have some clinical guidance [35]. TNF-α is one of the cytokines with the strongest antitumor effect, and both in vivo and ex vivo experiments have shown that TNF-α has very significant antitumor effect. Patients with higher tumor TNF-α values are more prone to metastasis and recurrence after treatment [36]. Therefore, TNF-α can be used as an important marker for tumor recurrence and metastasis, as well as an indicator for identifying pretumor lesions, and the experimental results are consistent with the literature [37]. The mean value of serum TNF-α in patients with lymph node metastasis from gastric cancer was nearly 6-fold higher than normal, and the mean value of serum TNF-α in patients with postoperative recurrence was nearly 3-fold higher than normal, which may be due to increased tumor load and excessive release of TNF-α from activated lymphocytes in vivo, resulting in increased serum TNF-α levels [38].

Our study also suggests that the determination of TNF-α activity in serum of gastric cancer patients, like the determination of IL-6, can be used as an adjunct to observe the progress of patients' disease and judge the deterioration or tumor metastasis, which has some reference value for clinicians [39]. Since the level of serum pepsinogen directly reflects the function of gastric mucosa, the significant decrease in serum pepsinogen I level in gastric cancer patients suggests that the secretion capacity of gastric mucosa of gastric cancer patients is reduced, and the significant decrease in serum pepsinogen I level in gastric cancer patients is related to atrophy, intestinalization, and reduced secretion of gastric mucosa in gastric cancer patients [41]. There was no statistically significant change in serum PC II levels in gastric cancer patients, which may be related to the wide distribution of 11 cells secreting pepsinogen [42]. A significant decrease in serum pepsinogen I is clinically important for the monitoring of early gastric cancer, and pepsinogen I and pepsinogen II are elevated in patients with gastric ulcer, whereas serum PGI and pepsinogen II are significantly lower in patients with cancer [43].

Multifactorial logistic regression analysis in our study showed that serum pepsinogen I, TNF-α, and IL-6 in gastric cancer were independent risk factors for Hp infection as a complication of gastric cancer. It indicates that serum pepsinogen and IL-6 tests can predict Hp infection in gastric cancer [44]. We believe that serum pepsinogen and IL-6 predicting Hp infection in gastric cancer also has some limitations to some extent, but the combination of separate tests can be used to improve the sensitivity of detection, early detection of Hp infection in gastric cancer, early intervention, and improve the survival rate of patients [45]. Existing clinical studies have shown that peripheral blood of gastric cancer patients showed a significant increase in serum pepsinogen, IL-6, which was correlated with tumor diameter and highly pelvic lymph node metastasis in gastric cancer patients, which is considered a factor associated with gastric cancer development and prognosis. IL-6 is a functional protein, mainly expressed by macrophages and epidermal cells, and is a common inflammatory factor with immunomodulatory and inflammation-mediated response. It has an important role in tissue injury and repair stages. Studies have shown phantom that the expression capacity of IL-6 is significantly lower in healthy humans than in patients with gastrointestinal diseases. IL-8 is mainly secreted by macrophages and epidermal cells and is also a common inflammatory factor with inflammation-mediating and endothelial cell proliferation effects, accelerating angiogenesis role. IL-8 has an important role at the beginning of the pathogenesis of diseases such as insulin, inflammation, and

xanthogranuloma. TNF-α is a class of cytokines with multiple activities, which can overactivate leukocytes. This increases the adhesion of leukocytes to endothelial cells and makes leukocytes more easily phagocytized. The current study showed that when patients were infected with Hp, the concentration of TNF-α in the organism was significantly increased.

In conclusion, the expression of IL-18, hs-CRP, and TNF-α factors in Hp-infected gastric cancer patients is correlated, and IL-6, IL-18, and TNF-α are involved in the entire process from the onset to the development of inflammation in the Hp-positive gastric mucosa of patients, which is of great value in the diagnosis of gastric cancer and helps to assess the degree of progression and prognosis.

Data Availability

No data were used to support this study.

Conflicts of Interest

There are no conflicts of interest.

Authors' Contributions

Shunxin Hao and Minyue Shou contributed equally to this work.

References

[1] I. Jacobs, R. Tibosch, P. Geomini, S. Coppus, M. Y. Bongers, and N. van Hanegem, "Atypical diametric polyps and the incidence of diametric cancer: a retrospective cohort study," *BJOG : An International Journal of Obstetrics and Gynaecology*, vol. 127, no. 8, pp. 994–999, 2020.

[2] L. Adomaitienė, R. Nadišauskienė, M. Nickkho-Amiry et al., "Proliferation in postmenopausal endometrial polyps-a potential for malignant transformation," *Medicina (Kaunas, Lithuania)*, vol. 55, no. 9, p. 543, 2019.

[3] B. Davis, "Endometrial stromal polyps in rodents: biology, etiology, and relevance to disease in women," *Toxicologic Pathology*, vol. 40, no. 3, pp. 419–424, 2012.

[4] M. Lee, J. Piao, and M. J. Jeon, "Risk factors associated with endometrial pathology in premenopausal breast cancer patients treated with tamoxifen," *Yonsei Medical Journal*, vol. 61, no. 4, pp. 317–322, 2020.

[5] S. R. de Rijk, M. E. Steenbergen, T. E. Nieboer, and S. F. Coppus, "Atypical endometrial polyps and concurrent endometrial cancer," *Obstetrics and Gynecology*, vol. 128, no. 3, pp. 519–525, 2016.

[6] M. G. Munro, "Uterine polyps, adenomyosis, leiomyomas, and endometrial receptivity," *Fertility and Sterility*, vol. 111, no. 4, pp. 629–640, 2019.

[7] C. T. Tien, P. C. Li, and D. C. Ding, "Outcome comparison between vaginoscopy and standard hysteroscopy: a retrospective cohort study," *Journal of the Chinese Medical Association*, vol. 84, no. 5, pp. 536–539, 2021.

[8] X. Enlan, *Hysteroscopy and Atlas*, Henan Science and Technology Press, Zhengzhou, 2009.

[9] Z. Wu, *Newly Edited Practical Obstetrical and Gynecological Ultrasonography*, Tianjin Science and Technology Translation and Publishing Company, Tianjin, 2007.

[10] S. Salim, H. Won, E. Nesbitt-Hawes, N. Campbell, and J. Abbott, "Diagnosis and management of endometrial polyps: a critical review of the literature," *Journal of Minimally Invasive Gynecology*, vol. 18, no. 5, pp. 569–581, 2011.

[11] T. J. Clark and H. Stevenson, "Endometrial polyps and abnormal uterine bleeding (AUB-P): what is the relationship, how are they diagnosed and how are they treated?," *Best Practice & Research. Clinical Obstetrics & Gynaecology*, vol. 40, pp. 89–104, 2017.

[12] L. M. Chen, H. W. Zhang, Q. Wang, Q. Li, and L. Sui, "Application of vaginoscopy in the diagnosis and treatment of occult vaginal high-grade squamous intraepithelial lesions," *Zhonghua Fu Chan Ke Za Zhi*, vol. 56, no. 8, pp. 569–575, 2021.

[13] P. M. De Silva, A. Carnegy, P. P. Smith, and T. J. Clark, "Vaginoscopy for office hysteroscopy: a systematic review & meta-analysis," *European Journal of Obstetrics, Gynecology, and Reproductive Biology*, vol. 252, pp. 278–285, 2020.

[14] W. Krois, L. Schmölz, M. Wagner et al., "Cysto-vaginoscopy of a 3D-printed cloaca model: a step toward personalized noninvasive preoperative assessment in patients with complex anorectal malformations," *European Journal of Pediatric Surgery*, vol. 32, no. 2, pp. 210–214, 2022.

[15] J. Johary, M. Xue, B. Xu, D. Xu, and A. Aili, "Use of hysteroscope for vaginoscopy or hysteroscopy in adolescents for the diagnosis and therapeutic management of gynecologic disorders: a systematic review," *Journal of Pediatric and Adolescent Gynecology*, vol. 28, no. 1, pp. 29–37, 2015.

[16] J. Dubuisson, C. Kaczmarek, and F. Constantin, "Management of mid-urethral slings erosions by vaginoscopy using the GelPOINT® system (with video)," *Gynécologie obstétrique fertilité & sénologie*, vol. 48, no. 10, pp. 772-773, 2020.

[17] N. Latchana, I. Esemuede, A. Harzman, M. Arnold, and S. Husain, "Colonoscope-mediated vaginoscopy for diagnostic evaluation of colovaginal fistulas," *Techniques in Coloproctology*, vol. 21, no. 5, pp. 397–399, 2017.

[18] H. O. Chapa and G. Venegas, "Vaginoscopy compared to traditional hysteroscopy for hysteroscopic sterilization. A randomized trial," *The Journal of Reproductive Medicine*, vol. 60, no. 1-2, pp. 43–47, 2015.

[19] R. S. Nakhal, D. Wood, and S. M. Creighton, "The role of examination under anesthesia (EUA) and vaginoscopy in pediatric and adolescent gynecology: a retrospective review," *Journal of Pediatric and Adolescent Gynecology*, vol. 25, no. 1, pp. 64–66, 2012.

[20] S. Yıldız, M. Ekin, H. Cengiz, H. Dağdeviren, and C. Kaya, "Vaginal foreign body: successful management with vaginoscopy," *Journal of the Turkish German Gynecological Association*, vol. 14, no. 1, pp. 46-47, 2013.

[21] C. Leutert, X. von Krueger, J. Plöntzke, and W. Heuwieser, "Evaluation of vaginoscopy for the diagnosis of clinical endometritis in dairy cows," *Journal of Dairy Science*, vol. 95, no. 1, pp. 206–212, 2012.

[22] V. Billone, C. Amorim-Costa, S. Campos et al., "Laparoscopy-like operative vaginoscopy: a new approach to manage mesh erosions," *Journal of Minimally Invasive Gynecology*, vol. 22, no. 1, p. 10, 2015.

[23] S. F. Ngu, V. Y. Cheung, and T. C. Pun, "Randomized study of vaginoscopy and H Pipelle vs traditional hysteroscopy and

Hindawi
Computational and Mathematical Methods in Medicine
Volume 2023, Article ID 9854393, 1 page
https://doi.org/10.1155/2023/9854393

Retraction

Retracted: MDH1 and MDH2 Promote Cell Viability of Primary AT2 Cells by Increasing Glucose Uptake

Computational and Mathematical Methods in Medicine

Received 5 December 2023; Accepted 5 December 2023; Published 6 December 2023

This article has been retracted by Hindawi, as publisher, following an investigation undertaken by the publisher [1]. This investigation has uncovered evidence of systematic manipulation of the publication and peer-review process. We cannot, therefore, vouch for the reliability or integrity of this article.

Please note that this notice is intended solely to alert readers that the peer-review process of this article has been compromised.

Wiley and Hindawi regret that the usual quality checks did not identify these issues before publication and have since put additional measures in place to safeguard research integrity.

We wish to credit our Research Integrity and Research Publishing teams and anonymous and named external researchers and research integrity experts for contributing to this investigation.

The corresponding author, as the representative of all authors, has been given the opportunity to register their agreement or disagreement to this retraction. We have kept a record of any response received.

References

[1] M. Hu, J. Yang, Y. Xu, and J. Liu, "MDH1 and MDH2 Promote Cell Viability of Primary AT2 Cells by Increasing Glucose Uptake," *Computational and Mathematical Methods in Medicine*, vol. 2022, Article ID 2023500, 15 pages, 2022.

Hindawi
Computational and Mathematical Methods in Medicine
Volume 2022, Article ID 2023500, 15 pages
https://doi.org/10.1155/2022/2023500

Review Article

MDH1 and MDH2 Promote Cell Viability of Primary AT2 Cells by Increasing Glucose Uptake

Mu Hu, JieLai Yang, Yang Xu, and Jiao Liu

Department of Orthopedics, Ruijin Hospital, Shanghai Jiao Tong University School of Medicine, No. 999 Hope Road, Jiading District, Shanghai 201801, China

Correspondence should be addressed to Jiao Liu; bosch0912@163.com

Received 23 June 2022; Revised 11 August 2022; Accepted 16 August 2022; Published 14 September 2022

Academic Editor: Min Tang

Background. Acute lung injury (ALI) is a clinical disease with high morbidity and mortality, with limited treatment means. For primary alveolar epithelial type II (AT2) cells, glycolysis is an essential bioenergetic process. However, the significance of AT2 cell glycolysis in sepsis ALI remains unknown. *Methods and Results*. In the current study, based on microarray analysis, real-time quantitative PCR, and Western blotting, we found that the hsa00020: citrate cycle pathway was inactivated, specifically its downstream gene: malate dehydrogenase 1 (MDH1) and MDH2 in ALI. In this context, lipopolysaccharides (LPS) were used to construct the septic-ALI mouse model and the biological function of MDH1 and MDH2 in primary alveolar epithelial type II (AT2) cells was explored. Through CCK-8, EdU, transwell, and apoptosis assays, we found that MDH1 and MDH2 promoted the cell vitality of AT2 cells, which relied on MDH1 and MDH2 to promote the glucose intake of AT2 cells. *Conclusion*. Overall, these findings suggest that targeting MDH1/MDH2-mediated AT2 cell glycolysis may be a potential strategy for ALI patients.

1. Introduction

Acute lung injury (ALI) is a frequent cause of respiratory failure that is characterized by the sudden onset of noncardiogenic pulmonary edema, inflammatory cell infiltration, and decreased gas exchange, culminating in severe hypoxemia and dyspnea that necessitates mechanical ventilation [1]. Sepsis is characterized by excessive inflammatory reactions that may cause severe cell and tissue damage as well as organ dysfunction such as ALI. Despite that numerous clinical trials and studies have been performed, there is no effective treatment strategy for treating ALI. The development of new therapeutic strategies is a hot issue to solve the clinical dilemma of ALI.

Alveolar epithelial type II (AT2) cell is one of the key cells to maintain the stability of the pulmonary environment and plays a role in secretion and regeneration in the alveoli [2]. The regeneration of alveolar epithelial cells is very important for the recovery of lung diseases, including ALI [3]. It was reported that AT2 cells are a kind of metabolically active lung cell that is essential for surfactant generation and alveolar balance [2]. However, the significance of AT2 cell metabolism in organ harm in sepsis, particularly ALI, is unknown.

Based on the microarray analysis previously [4], it was found that malate dehydrogenase 1 (MDH1) and MDH2 were substantially lower expressed in peripheral blood of septic-ALI patients compared with healthy donors. However, the biological functions of MDH1 and MDH2 in ALI remain unknown.

MDH1 silencing has been reported to induce cell death in lung cancer cell lines [5]. In addition, silencing MDH2 inhibited the proliferation, migration, and invasion while promoting cell apoptosis of endometrial cancer cells [6]. We speculated that MDH1 and MDH2 improved ALI by promoting the proliferation and inhibiting the apoptosis of AT2 cells.

MDH1 and MDH2 were the downstream genes of hsa00020: citrate cycle (TCA cycle) TCA cycle is the central pathway of almost all individual metabolic pathways, and the ultimate co-oxidation pathway of carbohydrates, fats, and amino acids [7]. In the role of oxidative catabolism of

carbohydrates (such as glucose), the TCA cycle provides a precursor for many biosynthetic pathways [7]. Therefore, the abnormal TCA cycle may have a certain influence on glucose uptake.

In this study, we speculate that MDH1 and MDH2 may promote the oxidative catabolism of glucose by activating the TCA cycle and then promote the uptake of glucose by cells. Glucose is vital to cell physiology as the primary energy source of cell [8]. Our results indicate that MDH1 and MDH2 may improve ALI injury by promoting glucose uptake in AT2 cells.

2. Material and Method Microarray Analysis

The microarray analysis data was obtained from the GSE32707 dataset [2], which included the peripheral blood raw mRNA data of 34 healthy donors and 30 septic-ALI patients. Differentially expressed genes (DEGs) were screened using the R language software package "limma." Screening criteria are as follows: fold change ≥ 2 and FDR < 0.05.

2.1. Septic-ALI Mouse Model. Twenty adult male C57BL/6 mice (six to eight weeks) were purchased from Saiye Biotechnology Co. Ltd. (Shanghai, China) and maintained under controlled temperature and humidity in specific pathogen-free conditions. The mice were divided in two groups randomly and equally: PBS (phosphate buffer saline, YS-10572R, Shanghai Yaji Biotechnology Co. Ltd., China) and LPS(lipopolysaccharide, SMB00610, Merck, USA) group. For the LPS group (ALI model), the mice were subjected to 25 mg/kg of 100 μl LPS via intratracheal instillation. For the PBS group (control model), the mice were subjected to 100 μl PBS via intratracheal instillation. Mice were sacrificed using the spinal dislocation method. Animal experiments were approved by the animal care and use committee of Ruijin Hospital, Shanghai Jiao Tong University.

2.1.1. Mouse Pulmonary Function Detection. The whole body scanning system (WBP-4MR, Shanghai Tawang Intelligent Technology Co. Ltd., China) was used to detect the airway resistance of mice and 50% exhalation flow rate of all mice.

2.1.2. Extraction of Primary AT2 Cells. Mice were sacrificed using the spinal dislocation method and were soaked in 75% alcohol for 2 min, and the lung tissues were collected. The lung tissue was cut into pieces and cleaned with PBS 3 times. The clipped tissue was digested with DNase I and trypsin for 20 min, and the supernatant was filtered by 70 μm and 40 μm mesh. Three culture dishes, A, B, and C, were taken, and cell suspension was planted into dish A. After standing at 37° for 20 min, the cell suspension of dish A was transferred to dish B for culture. After standing at 37° for 20 min, the cell suspension of dish B was transferred to dish C for culture. Dish C was AT2 cells, and the epithelial cell special culture medium (McM-314, Ningbo Mingzhou Biotechnology Co. Ltd., China) was changed every other day.

2.2. Real-Time Fluorescence Quantitative PCR (RT-PCR). Total RNA of primary AT2 cells was extracted by TRIzol Reagent (Shanghai Donghuan Biotechnology Co. Ltd., China). Total RNA was reversed into cDNA using the BioSci™ WitEnzy First-strand cDNA Synthesis Kit (8072031, Beijing Dake Biotechnology Co. Ltd., China). PCR was performed using the 2X SYBR Green qPCR Master Mix (Shanghai Donghuan Biotechnology Co. Ltd., China). GAPDH was used as internal reference. Relative gene expression was calculated using the $2^{-\Delta\Delta Ct}$ method. The primers used in this study were shown in Supplement Table 1.

2.3. Western Blot (WB). RIPA lysate (Shanghai Donghuan Biotechnology Co. Ltd., China) was used to lysate primary AT2 cells. Protein quantification was performed using the BCA kit (PC0020, Shanghai Jizhi Biochemical Technology Co. Ltd., China). 20 μl of protein was added to SDS-page gel and then transferred to the PVDF membrane. The PVDF membrane was sealed with 5% milk for 1 h. All primary antibodies in this experiment were as follows: MDH1 (AB175455, Abcam, USA), MDH2 (AB181873, Abcam, USA), and GAPDH (AB8245, Abcam, USA). The rabbit monoclonal [M87-3] anti-mouse IgG1, IgG2a, IgG2b H&L (ab125907, Abcam, USA) was used as second antibody. ECL kit solution A: solution B = 1 : 1 (Shanghai Donghuan Biotechnology Co. Ltd., China) was used for protein detection. The ECL system (Bio-Rad, Hercules, USA) was used to observe protein bands, and ImageJ software version 21.0 was used to calculate gray values.

2.4. Cell Culture and Transfection. Before transfection, 1 × 10^6 AT2 cells were inoculated into 6-well plates and epithelial cell special culture medium (McM-314, Ningbo Biotechnology Co. Ltd., China) was used to culture cells for 2 h. Small interfering RNA(SI)-MDH1, SI-MDH2, Si-negative control (NC), overexpressed- (OE-) MDH1 plasmid, OE-MDH2 plasmid, and OE-NC plasmid were purchased from GenePharma (Shanghai, China). siRNA and OE plasmids were transfected into AT2 cells using Lipofectamine 3000 Reagent (GenePharma, Shanghai, China). Follow-up experiments were performed after 48 h transfection.

2.5. Glucose Uptake Test. 2-NBDG (a fluorescent-labeled 2-deoxyglucose analogue, B6035, ApexBio, Shanghai, China) can be used as a tracer to assess cellular glycogen metabolism (phosphorylated by hexokinase and retained in cells). 4000/each well primary AT2 cells were inoculated in 24-well plates, and 2-NBDG of 200 μm/ml was added into each well and incubated for 2 h. Images were captured with a fluorescence microscope (CKX53, Olympus, Japan) and analyzed with Image-Pro Plus 6.0.

2.6. Enzyme-Linked Immunosorbent Assay (ELISA). The Mouse Interleukin 6 (IL-6) ELISA Kit (YX-E20012, Wuhan YIPu Biotechnology Co. Ltd., China) and Mouse IL-17A ELISA Kit (AB199081, Shenzhen Haisian Biotechnology Co. Ltd., China) were used to detect the concentration of IL-6 and IL-17A in cell or tissue lysis fluid.

2.7. Immunofluorescence. Primary AT2 cells were immobilized using 4% buffered paraformaldehyde, and then anti-IL-6 antibody [EPR16610-69] (AB179570, Abcam, USA)

and anti-IL-17A antibody were used to incubate overnight. The cells were washed with PBS and treated with goat anti-Mouse IgG H&L (Alexa Fluor® 488) (AB150113, Abcam, USA) at room temperature for 1 h. The nuclei were stained with DAPI (AB104139, Abcam, USA). Images were captured with a fluorescence microscope (CKX53, Olympus, Japan) and analyzed with Image-Pro Plus 6.0.

2.8. Hematoxylin and Eosin (HE) Staining and Masson's Trichrome Staining. The lung tissues of mice were fixed with 4% paraformaldehyde, embedded in paraffin, and cut into 5 μm thick sections. The HE staining kit (G1120-100, Beijing Solebo Technology Co. Ltd., China) and Masson trichromatic staining kit (G1340, Beijing Solebo Technology Co. Ltd., China) were used to observe lung cell morphology and collagen deposition under a fluorescence microscope (CKX53, Olympus, Japan).

2.9. Cell Counting Kit-8 (CCK-8). Two thousand of AT2 cells were inoculated in 96-well plates, and 10 μl CCK8 solution (Shanghai Donghuan Biotechnology Co. Ltd., China) and 90 μl high-glucose DMEM medium (12430062, Thermo Fisher Scientific, USA) or glucose-free DMEM medium (A90113, Shanghai Jizhi Biochemical Technology Co. Ltd., China) were added to each well. After incubation in the incubator for 2 hours, the absorbance at 450 nm was measured with a microplate reader (NanoDrop 2000c, Thermo Fisher Scientific, USA).

2.10. EdU Cell Proliferation. Two thousand of AT2 cells were inoculated in 96-well plates for 24 h. Then fixed cells with 4% paraoxide for 30 min and incubate with anti-Brdu antibody [IIB5] (AB8152, ABACam, USA) for 60 min. The absorbance at 450 nm was measured with a microplate reader (NanoDrop 2000c, Thermo Fisher Scientific, USA).

2.11. Transwell. AT2 cells (200 μl, 2000 cells per well) were collected and suspended in serum-free medium and then transferred to the hydrated matrix chamber (3421, Corning, USA). The subcompartment was cultured overnight in 600 μl epithelial cell special culture medium [9]. The cells on the upper surface of the cell were cultured, and the cells on the lower surface of the cell were fixed with anhydrous ethanol and stained with 0.1% crystal violet for half an hour. Cells were observed under an inverted microscope [10].

2.12. Apoptosis Detection. Tissue (digested with DNase I and trypsin) or cells were collected, and cells were gently resuspended with 1 ml PBS. 50 μl 1x binding buffer and 2.5 μl annexin v-FITC were added to each well and incubated at room temperature for 10–15 min away from light. Add 5 μl PI staining solution to each well, and incubate for 5–10 min on ice away from light. 100 μl 1x binding buffer was added, and cell apoptosis was detected by BD FACSCalibur flow cytometry (Becton, Dickinson and Company, USA). Annexin V-FITC was green fluorescence and PI was red fluorescence.

2.13. Data Analysis. All statistical analyses were performed using SPSS 22.0 software (SPSS Inc., Chicago, IL, USA), expressed as mean ± standard deviation ($X \pm S$). Wilcox tests were used to compare the two groups of independent samples. Kruskal-Wallis tests were used to compare multiple independent samples. $P < 0.05$ was considered statistically significant.

3. Results

3.1. The Construction of the Septic-ALI Mouse Model. Compared with PBS-treated mice ($N = 10$), the airway resistance (Figure 1(a)) and 50% exhalation flow rate (Figure 1(b)) of LPS-treated mice ($N = 10$) were substantially reduced. Masson's staining ($N = 5$, Figure 1(c)) and HE staining ($N = 5$, Figure 1(d)) showed that the lung tissues of mice in the LPS group were substantively damaged compared with those in the PBS group. In addition, RT-PCR ($N = 10$, Figure 1(e)) and ELISA ($N = 10$, Figure 1(f)) results showed that the expression of IL-6 and IL-17A was substantially increased in the lung tissues of mice in the LPS group compared with the PBS group. These results suggested that the LPS-induced septic-ALI mouse model was successfully established.

3.2. TCA Cycle Pathway Was Deactivated in the Septic-ALI Mouse Model. Based on the GSE32707 dataset, we screened the DEGs in the peripheral blood of healthy donors ($N = 34$) and septic-ALI patients ($N = 30$) and 3918 downregulated genes and 1372 upregulated genes were found in the peripheral blood of septic-ALI patients compared with healthy donors (Figure 2(a)). KEGG analysis showed that 393 DEGs were significantly enriched in the hsa01100: metabolic pathways, and 15 DEGs (ACLY, ACO1, CS, DLAT, DLST, FH, IDH1, IDH3A, MDH1, MDH2,PDHA1, PDHB, SDHA, SUCLA2, and SUCLG2) were significantly enriched in hsa00020: TCA cycle (Figure 2(b)). According to the GSE32707 dataset, it was found that except IDH1, all the other 14 genes had downregulated expression in the peripheral blood of septic-ALI patients (Figure 2(c)). In addition, RT-PCR results showed that CS, DLAT, MDH1, MDH2, and PDHA1 were substantially downregulated in lung tissues of septic-ALI mice ($N = 10$) compared with control mice ($N = 10$) (Figure 2(d)). Moreover, the downregulated expression of MDH1 and MDH2 in septic-ALI mice compared with control mice was confirmed via WB assay ($N = 5$, Figure 2(e)) and immunofluorescence ($N = 5$, Figure 2(f)). These data suggested that the TCA cycle pathway was inactivated in septic-ALI mice.

3.3. MDH1 And MDH2 Promoted the Cell Viability of Primary AT2 Cells by Enhancing Glucose Uptake. MDH1 and MDH2 were silenced or overexpressed in primary AT2 cells, and the knockdown or overexpression efficiency of MDH1 and MDH2 were detected by RT-PCR (Figures 3(a) and 3(b)) and WB (Figures 3(c) and 3(d)). Glucose uptake assay results showed that MDH1 or MDH2 silencing inhibited the glucose uptake, while MDH1 or MDH2 overexpression promoted the glucose uptake of primary AT2 cells (Figure 3(e)). The proliferation of primary AT2 was dependent on glucose

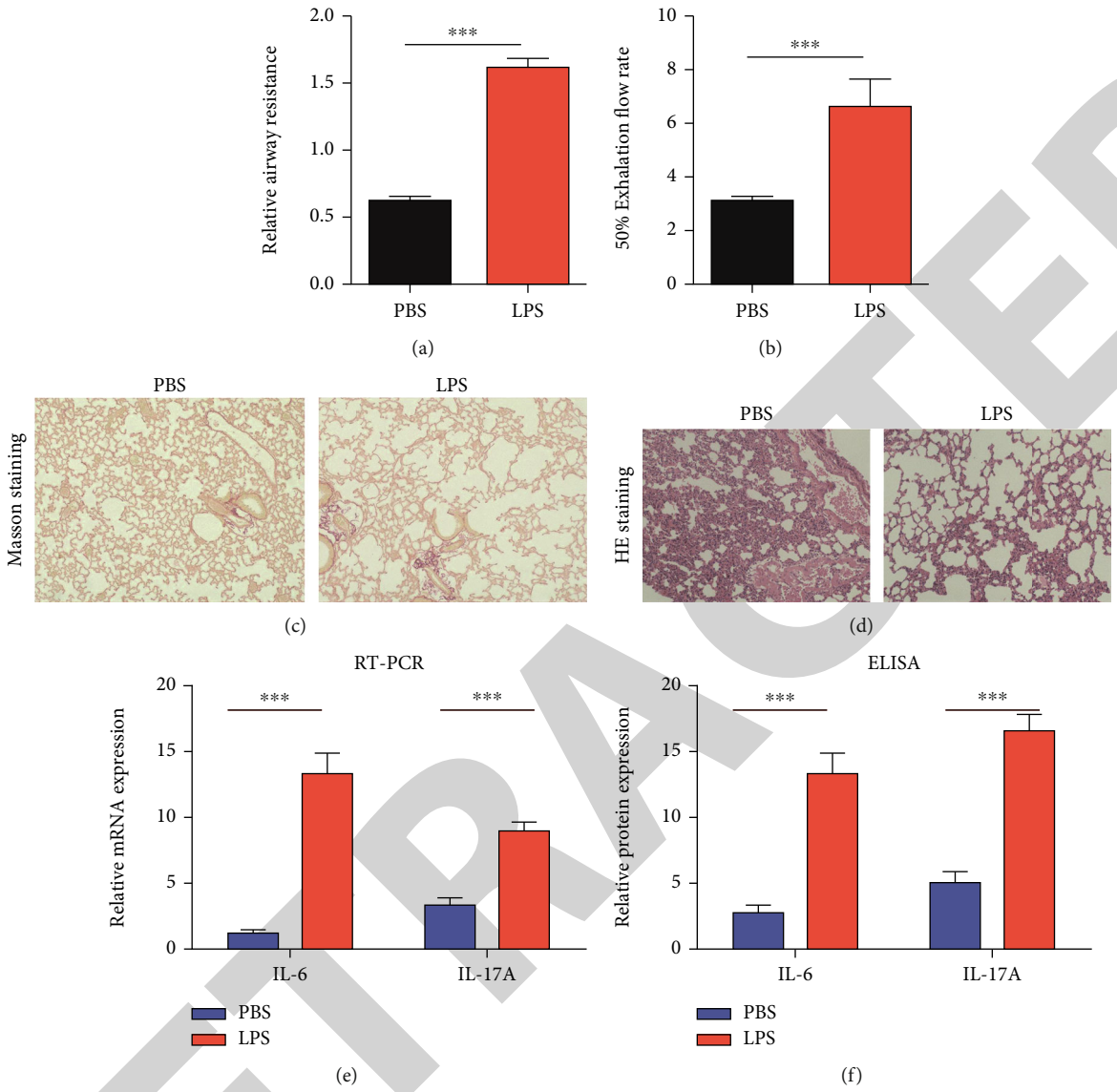

Figure 1: Construction of septic-ALI mouse model. (a) The airway resistance, (b) the 50% exhalation flow rate, (c) Masson's staining, and (d) HE staining of LPS-treated mice and PBS-treated mice. (e) RT-PCR and (f) ELISA were used to detect the expression of IL-6 and IL-17A. *** $P < 0.001$.

(Figure 3(f)). In 100% high-glucose medium, MDH1 or MDH2 silencing inhibited the proliferation of primary AT2 cells. Overexpression of MDH1 or MDH2 promoted the proliferation of primary AT2 cells (Figure 3(g)). However, in 100% glucose-free medium, MDH1 or MDH2 silencing or overexpression had no significant effect on the proliferation of primary AT2 cells (Figure 3(h)). Moreover, overexpression of MDH1 or MDH2 promoted the proliferation of primary AT2 cells in 100% high-glucose medium via EdU assays (Figure 3(i)). These results suggested that MDH1 or MDH2 promoted the proliferation of primary AT2 cells by enhancing glucose uptake. The invasion of primary AT2 cells was dependent on glucose (Figure 3(j)). In 100% high-glucose medium, MDH1 or MDH2 silencing inhibited while MDH1 or MDH2 overexpression promoted the proliferation of primary AT2 cells (Figure 3(k)). However, in 100% glucose-free medium, MDH1 or MDH2 silencing or MDH1 or MDH2 overexpression had no significant effect on the invasion of primary AT2 cells (Figure 3(l)). These results shown that by promoting glucose uptake, MDH1 or MDH2 promoted the invasion of primary AT2 cells.

3.4. MDH1 or MDH2 Inhibited the Apoptosis of Primary AT2 Cells by Promoting Glucose Uptake. Compared with PBS-treated mice, the apoptosis ratio of primary AT2 cells of LPS-treated mice was substantially enhanced (Figure 4(a)). Low-level glucose promoted the apoptosis ratio of primary AT2 cells (Figure 4(b)). In 100% high-glucose medium, MDH1 or MDH2 silencing promoted the apoptosis of primary AT2 cells. However, overexpression of MDH1 or MDH2 inhibited the apoptosis of primary AT2 cells

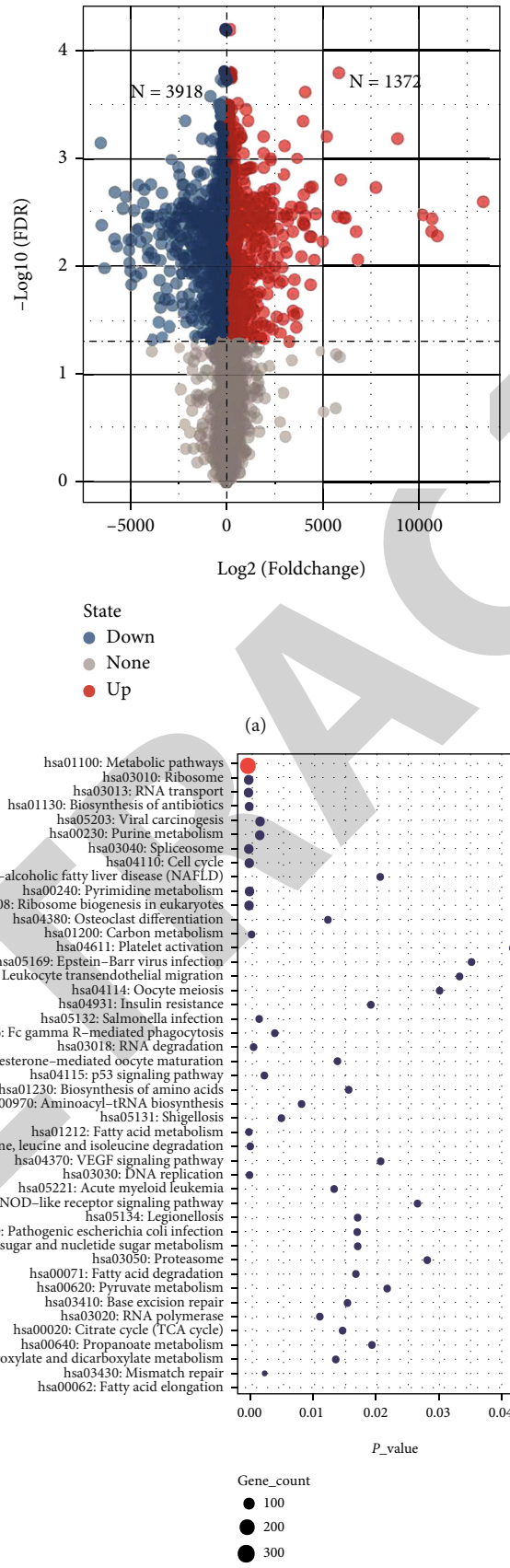

Figure 2: Continued.

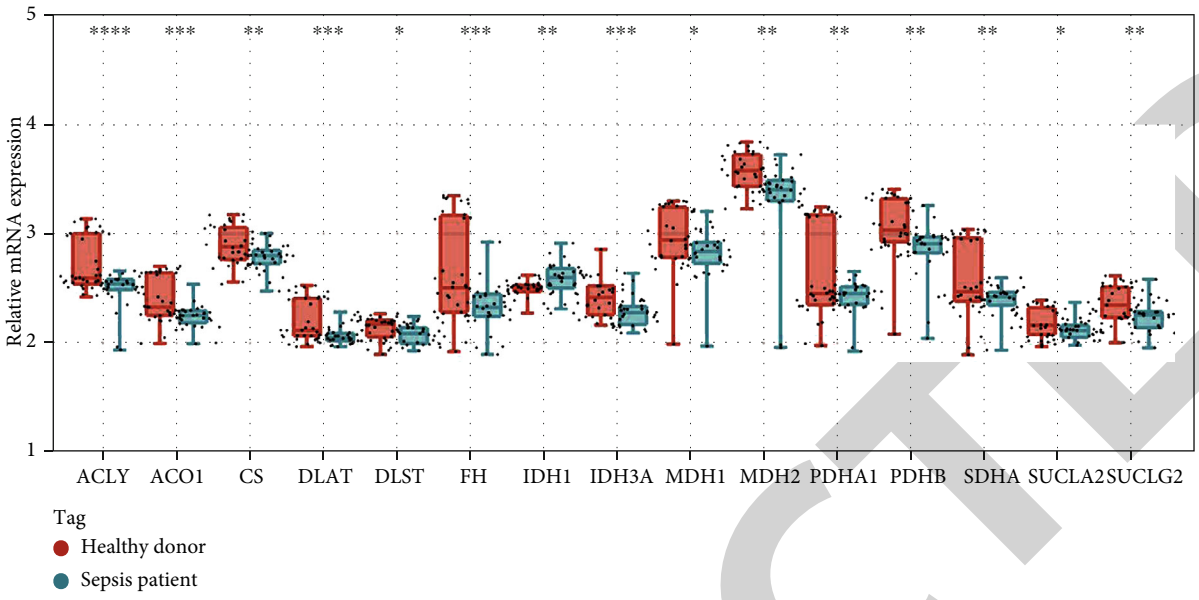

(c)

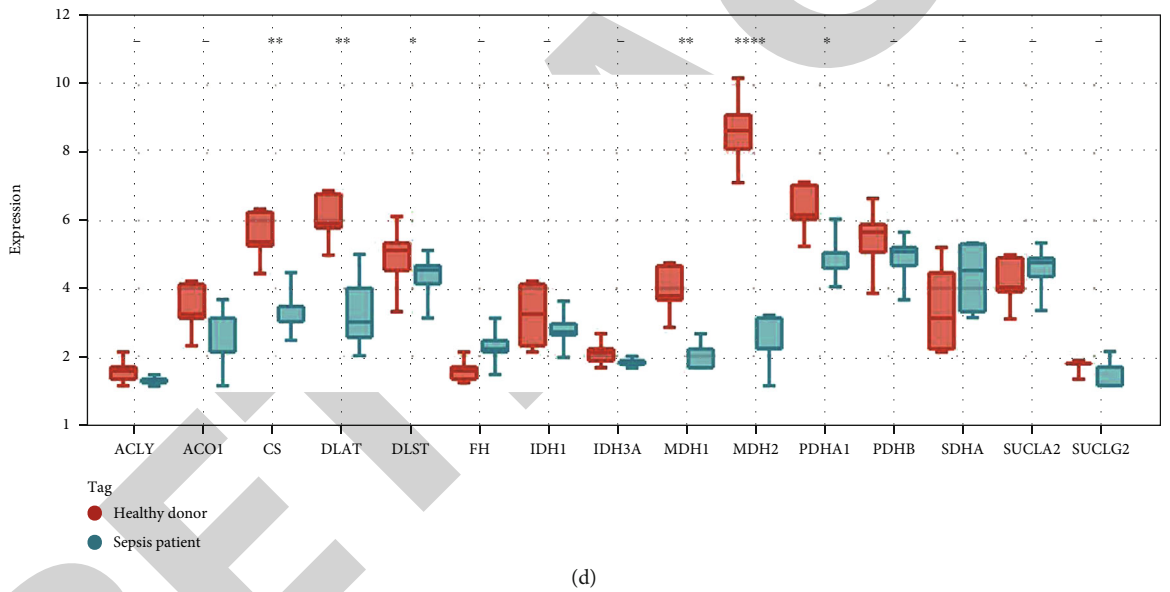

(d)

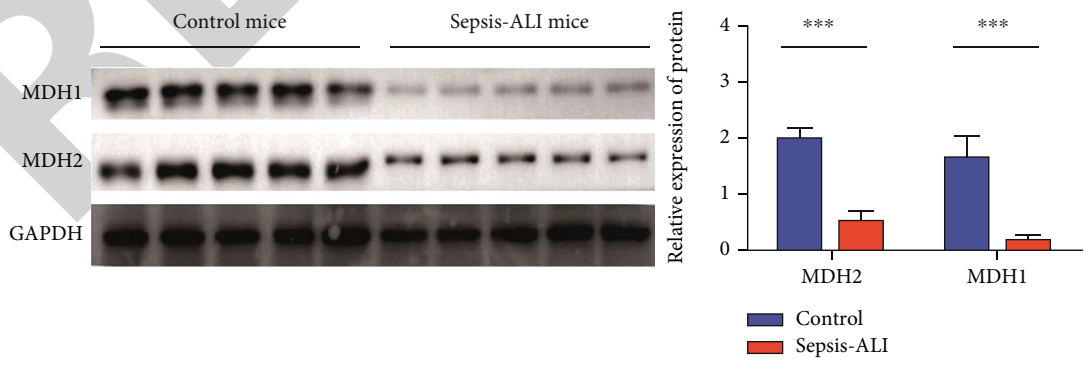

(e)

Figure 2: Continued.

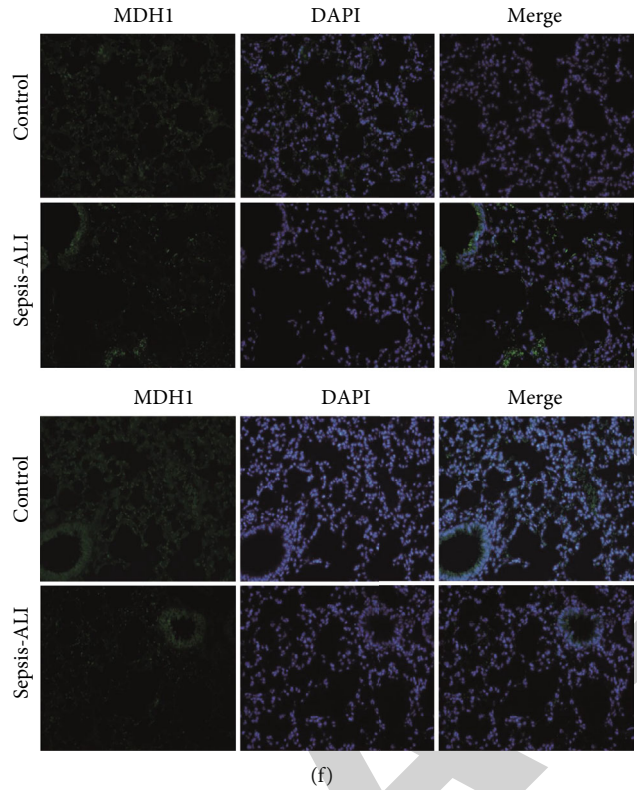

(f)

Figure 2: The TCA cycle pathway was inactivated in primary AT2 cells of septic-ALI mice. (a) Screening for differentially expressed genes in the peripheral blood of healthy donors ($N = 34$) and septic-ALI patients ($N = 30$). (b) KEGG analysis of 3918 downregulated genes and 1372 upregulated genes. (c, d) Expression of ACLY, ACO1, CS, DLAT, DLST, FH, IDH1, IDH3A, MDH1, MDH2, PDHA1,PDHB, SDHA, SUCLA2, and SUCLG2 was detected in the (c) GSE32707 dataset, or in septic-ALI mice ($N = 10$) and control mice ($N = 10$) via RT-PCR detection in (d) AT2 cells. (e, f) Expression of MDH1 and MDH2 was done via (e) WB assay ($N = 5$) and (f) immunofluorescence assay in AT2 cells ($N = 5$). $^{*}P < 0.05$, $^{**}P < 0.01$, $^{***}P < 0.001$.

(Figure 4(c)). These results indicated that MDH1 or MDH2 inhibited the apoptosis of primary AT2 cells by promoting glucose uptake.

4. Discussion

In this study, through microarray analysis, we initially found that the downstream genes of TCA cycle: ACLY, ACO1, CS, DLAT, DLST, FH, IDH1, IDH3A, MDH1,MDH2, PDHA1, PDHB, SDHA, SUCLA2, and SUCLG2, had substantially reduced expression in blood of septic-ALI patients compared to healthy donors. Metabolites associated with the TCA cycle have been reported to control transcription factors and chromatin modifications that alter cell function and fate [11]. It is suggested that the deactivation of the TCA cycle may affect the development of septic-ALI disease.

Based on the results of RT-PCR and WB, we found that MDH1 and MDH2 were substantially downregulated in lung tissues of septic-ALI mice compared with control mice. It has been reported that miRNA-126-5p exerted growth inhibition function by inhibiting MDH1 in non-small cell lung cancer cells [12]. MDH2 promoted the proliferation and inhibited apoptosis of endometrial cancer cells by inhibiting PTEN [13]. MDH1 and MDH2 may regulate the proliferation and apoptosis of lung cells. AT2 cell is one of the key cells that maintain the integrity of lung tissues [14]. In this study, we found that MDH1 or MDH2 silencing inhibited the proliferation and promoted the apoptosis of primary AT2 cells. In addition, we found that silencing MDH1 or MDH2 inhibited the invasion ability of primary AT2 cells. These results suggest that MDH1 and MDH2 promoted the activity of primary AT2 cells.

MDH1 and MDH2 play important roles in energy metabolism of the TCA cycle [15]. In this study, MDH1 and MDH2 promoted the proliferation and invasion, while inhibiting apoptosis in a glucose-dependent manner in primary AT2 cells, which was not reported before. The study reports that MDH1 was overexpressed in cancer and promoted glycolysis through NAD (nicotinamide adenine dinucleotide) production, which in turn promotes pancreatic cancer cell proliferation and metabolism [16]. However, the relationship between MDH2 and glycolysis remained unknown. Glycolysis is one of the classic pathways through which cells metabolize acetyl CoA, which was essential for maintaining TCA cycle activity [17]. Moreover, high levels of acetyl CoA promoted histone

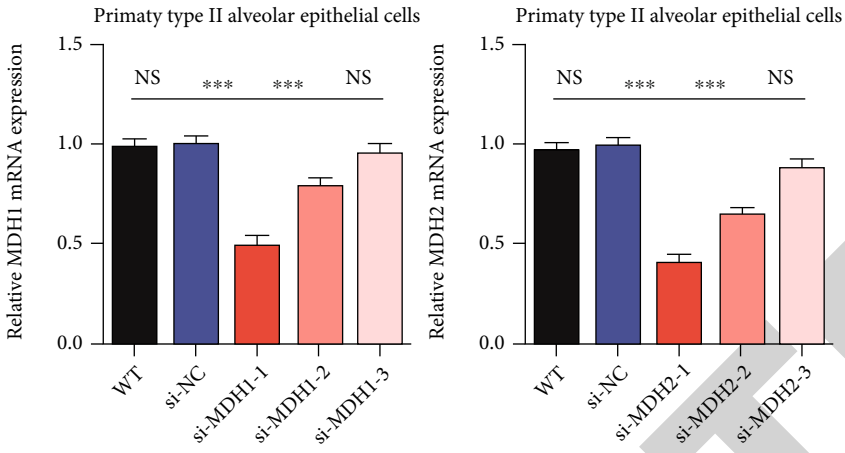

(a)

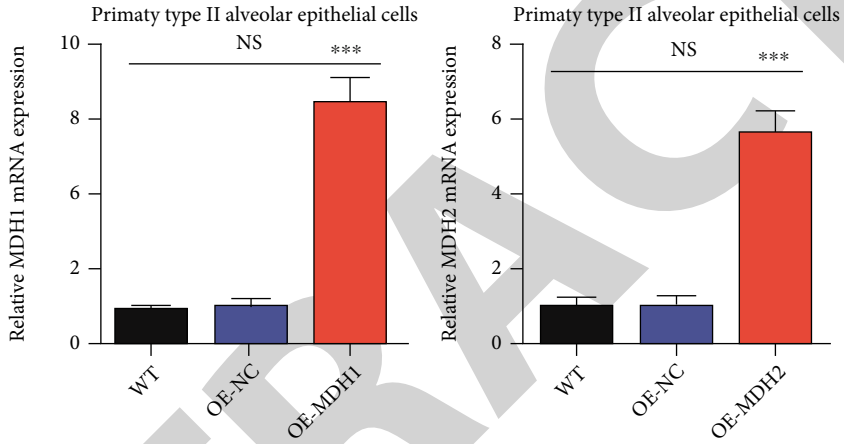

(b)

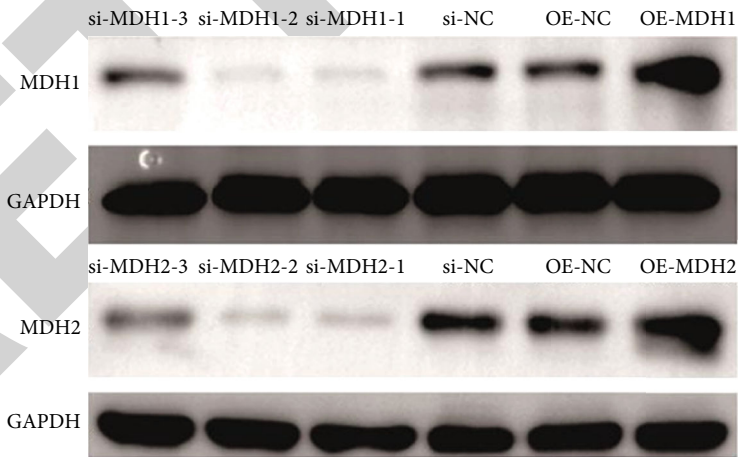

(c)

Figure 3: Continued.

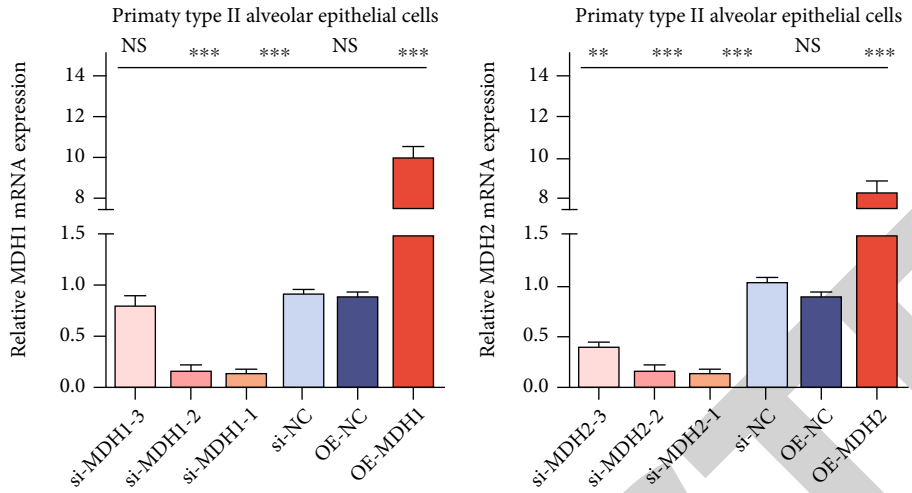

(d)

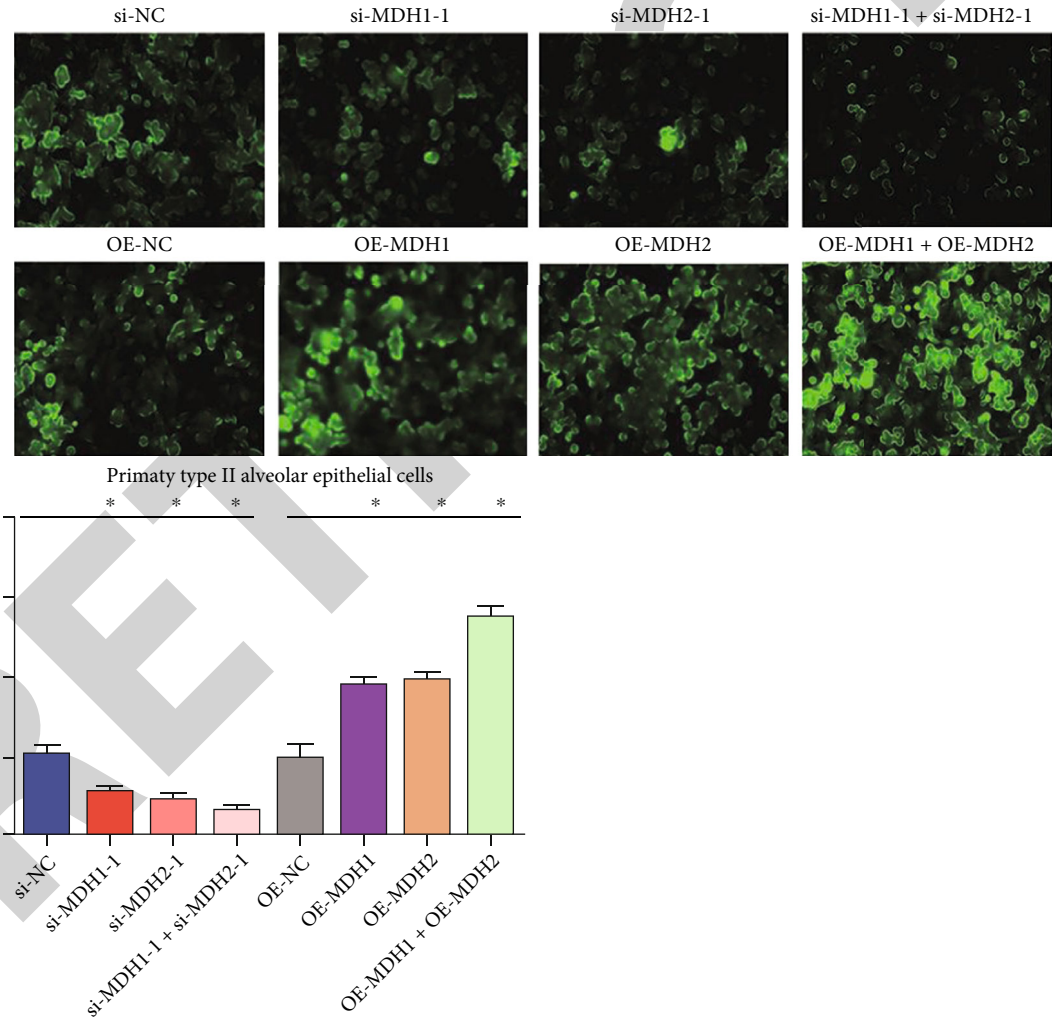

(e)

Figure 3: Continued.

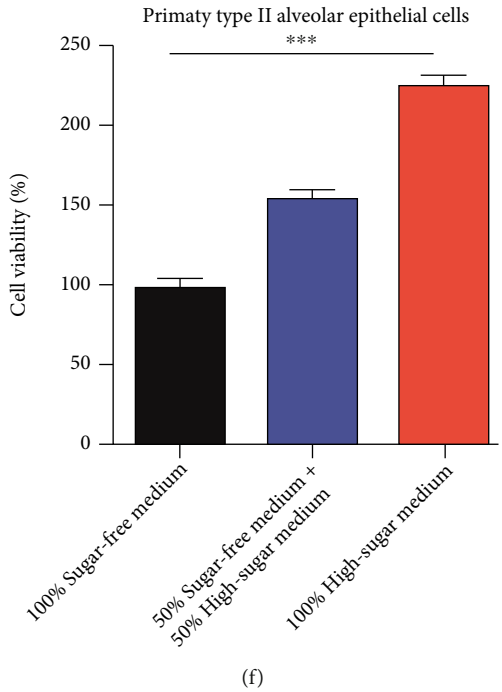

(f)

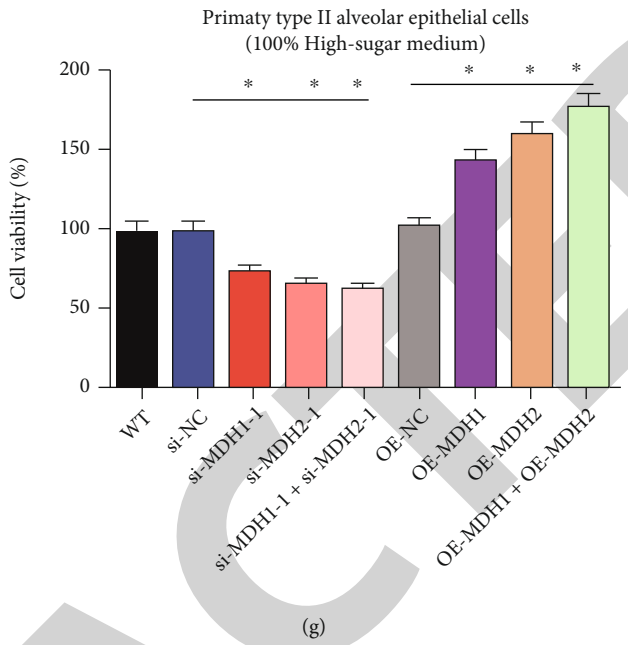

(g)

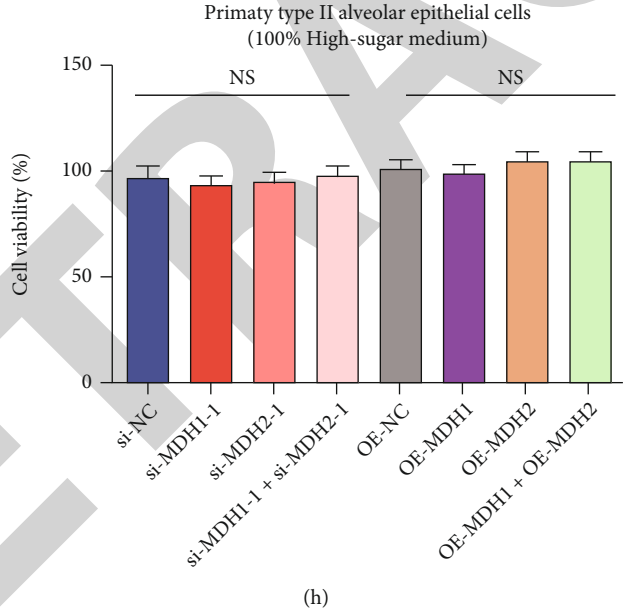

(h)

Figure 3: Continued.

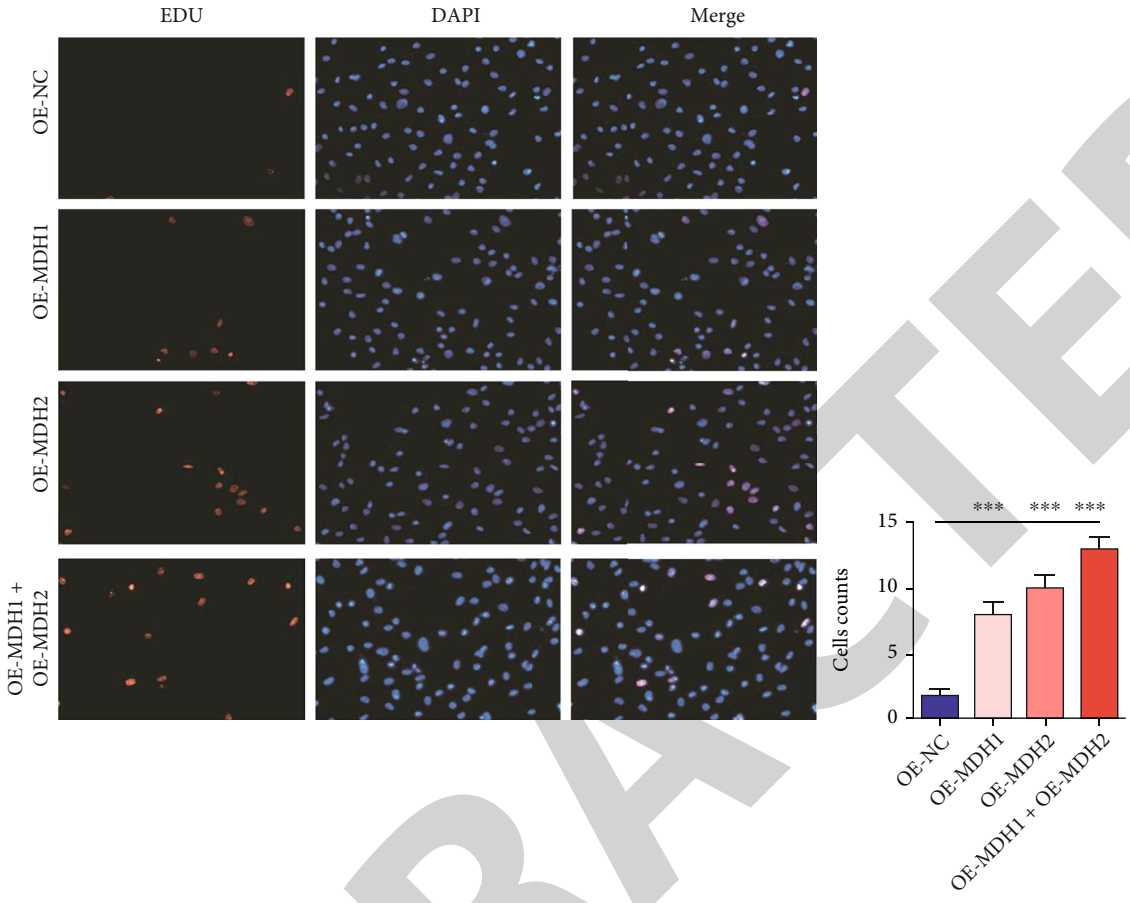

(i)

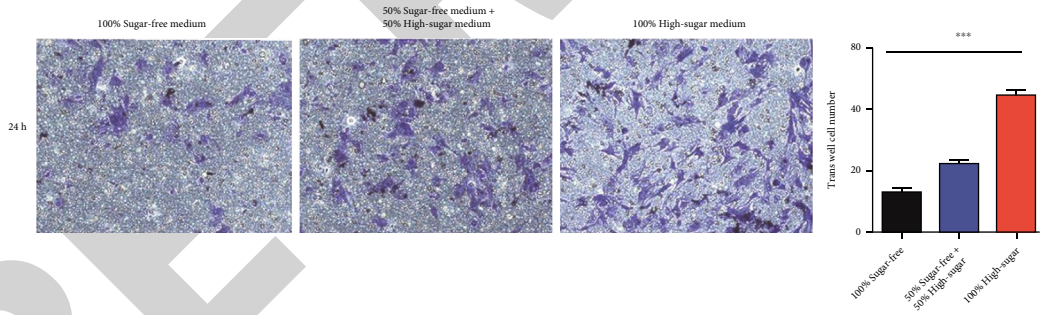

(j)

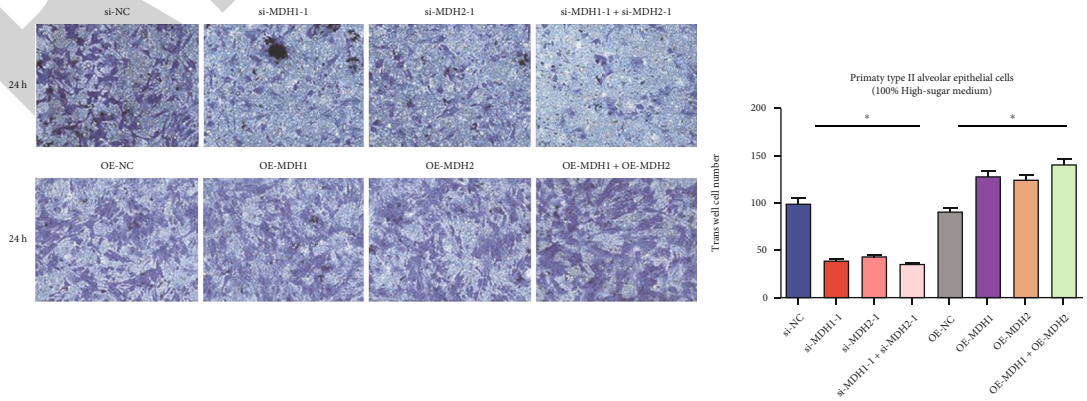

(k)

Figure 3: Continued.

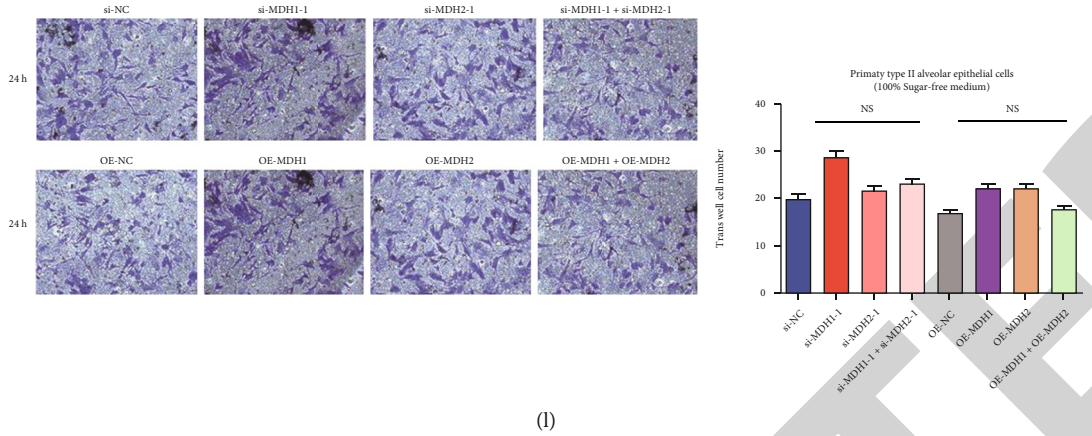

(l)

Figure 3: MDH1 or MDH2 promoted the proliferation and invasion of primary AT2 cells by promoting glucose uptake. (a, b) RT-PCR and (c, d) WB were used to detect the effect of siRNA and overexpressed plasmid on AT2 cells. (e) MDH1 or MDH2 promoted the glucose uptake of AT2 cells. (f) The proliferation of AT2 cells was dependent on glucose. (g, h) The effect of MDH1 or MDH2 on the proliferation of AT2 cells was measured in (g) 100% high-glucose medium or (h) 100% glucose-free medium via CCK-8. (i) The effect of MDH1 or MDH2 on the proliferation of AT2 cells was measured via EdU assays in 100% high-glucose medium. (j) The invasion of AT2 cells was dependent on glucose. (k, l) The effect of MDH1 or MDH2 on the invasion of AT2 cells was measured in 100% high-glucose medium (k) or 100% glucose-free medium (l) via transwell assay. $^{*}P < 0.05$, $^{**}P < 0.01$, $^{***}P < 0.001$; NS: no significance.

acetylation, putting cells into a proanabolic state, thereby promoting cell growth [18]. However, whether MDH1 and MDH2 increased the glucose uptake of primary AT2 cells by promoting glycolysis or other approaches remained to be further confirmed [18].

MDH is a typical multisubstrate enzyme, and its catalytic kinetic reaction mechanism is a strict sequential catalytic mechanism, that is, in the presence of the coenzyme NADH or NAD+, it must first bind to the coenzyme before it can be combined with the substrate (oxaloacetate or malate) [19] combined to catalyze the reaction, and then, oxaloacetate must be released from the active site of the enzyme first, and NAD+ or NADH is released, so it is called a typical NAD+-dependent dehydrogenase [20]. Acid dehydrogenase (ICDH, EC1.1.1.42) catalyzes the conversion of isocitrate into α-ketoglutarate to generate NADPH [21]. Therefore, the activities of MDH, G-6-PDH, and ICDH in vivo are directly related to the level of NADPH production, thereby controlling fat deposition in the body. Studies have shown that NADPH-producing enzyme activity has a more direct effect on the fat storage rate than the lean meat rate [22]. The activity of the NADPH-generating enzyme was positively correlated with the backfat thickness of live pigs [23]. The results of the study showed that the correlation coefficients between MDH and backfat thickness and lean meat percentage were 0.36 and −0.612, respectively [24]. The study found that using NADPH-producing enzyme activity as an early selection index to select lean pigs has more advantages than using backfat thickness as a selection index and control body fat deposition [25]. Studies have shown that NADPH-producing enzyme activity has a more direct effect on the fat storage rate than the lean meat rate [26]. The activity of the NADPH-generating enzyme was positively correlated with the backfat thickness of live pigs [27]. Malate dehydrogenase is an extremely important oxidoreductase in the aerobic decomposition of the TCA cycle in biological tissues. Malate can be oxidized to oxaloacetate in the mitochondrial matrix, and oxaloacetate can be reduced to malate in the cytoplasm [28]. MDH shuttles between the matrix and the cytoplasm, maintaining a dynamic balance of enzymatic reactions. The MDH gene can regulate the growth of muscle fibers. The expression level of the MDH gene has a very significant positive correlation with fatty acid synthesis in adipose tissue. The expression level of the MDH gene was positively correlated with fatty acid synthesis in adipose tissue.

The expression levels of adipose and subcutaneous adipose inner layers of the back are the highest, and the expression levels are the lowest in the longissimus dorsi muscle and the superficial adipose tissue of the heart; the order of MDH gene expression in male Rongchang pig tissues from high to low is as follows: abdomen subcutaneous fat, intermuscular fat, outer layer of dorsal subcutaneous fat, perirenal fat, lesser omentum, and inner layer of dorsal subcutaneous fat; this gene has the highest expression in the intermuscular adipose tissue of male Rongchang pigs and is expressed in the longissimus dorsi muscle, lowest expression. The analysis of the relative expression of the MDH2 gene in different tissues of the same breed and same sex showed that the data showed that the expression level was basically the highest in the psoas major muscle. Relatively speaking, the expression in each adipose tissue was lower than that in the muscle. However, the expression of lesser omentum, perirenal fat, and intermuscular fat in female Rongchang pigs was higher than that in psoas muscle. Its specific mechanism of action needs to be further studied. The trend of expression differences can be seen that the expression trends of MDH1 and MDH2 genes in various tissues are basically the same in male Landrace pigs, female Landrace pigs, male Rongchang pigs, and female Rongchang pigs. The expression changes

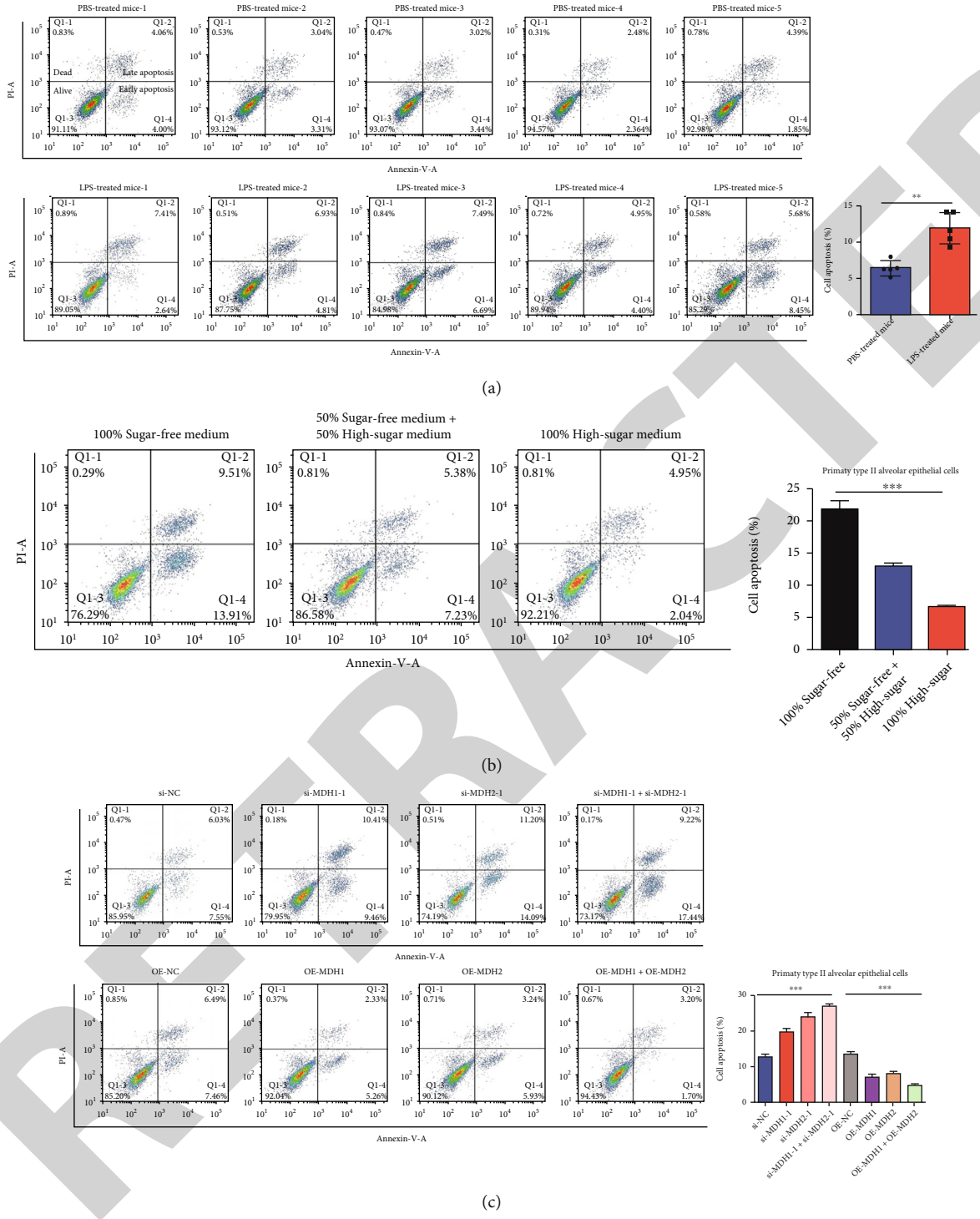

Figure 4: MDH1 or MDH2 inhibited the apoptosis of primary AT2 cells by promoting glucose uptake. (a) The apoptosis ratio of primary AT2 cells was detected in PBS- or LPS-treated mice. (b) The apoptosis of AT2 cells was dependent on glucose. (c) The effect of MDH1 or MDH2 on the apoptosis of AT2 cells was measured in 100% high-glucose medium via flow cytometry. $^{***}P < 0.001$.

in the outer layer, back subcutaneous fat, inner layer, and abdominal subcutaneous fat and in muscles (longissimus dorsi and psoas major) were basically the same, and the expression changes in visceral fat (perirenal fat, lesser omentum, cardiac surface fat, and large muscle) were basically the same. The omentum expression trends were significantly different.

In conclusion, MDH1 and MDH2 were substantially reduced expression in the lung tissues of septic-ALI. The upregulated MDH1 and MDH2 promoted the cell viability of primary AT2 cells by enhancing its glucose uptake. MDH1 and MDH2 are expected to be potential targets for treating septic-ALI patients.

Data Availability

No data were used to support this study.

Conflicts of Interest

All authors declare no conflict of interest.

Authors' Contributions

All authors designed the study, performed the experiments, and wrote the paper. LJ supervised the study and revised the paper.

Acknowledgments

This work was supported by the National Natural Science Foundation of China, no. 2019 81971869.

Supplementary Materials

Supplemental Table 1: primer sequences for quantitative real-time PCR. *(Supplementary Materials)*

References

[1] M. Akram, "Citric acid cycle and role of its intermediates in metabolism," *Cell Biochemistry and Biophysics*, vol. 68, no. 3, pp. 475–478, 2014.

[2] T. Dolinay, Y. S. Kim, J. Howrylak et al., "Inflammasome-regulated cytokines are critical mediators of acute lung injury," *American Journal of Respiratory and Critical Care Medicine*, vol. 185, no. 11, pp. 1225–1234, 2012.

[3] E. A. Hanse, C. Ruan, M. Kachman, D. Wang, X. H. Lowman, and A. Kelekar, "Cytosolic malate dehydrogenase activity helps support glycolysis in actively proliferating cells and cancer," *Oncogene*, vol. 36, no. 27, pp. 3915–3924, 2017.

[4] D. R. Janz and L. B. Ware, "Biomarkers of ALI/ARDS: pathogenesis, discovery, and relevance to clinical trials," *Seminars in Respiratory and Critical Care Medicine*, vol. 34, no. 4, pp. 537–548, 2013.

[5] A. Lima Queiroz, B. Zhang, D. E. Comstock et al., "miR-126-5p targets malate dehydrogenase 1 in non-small cell lung carcinomas," *Biochemical and Biophysical Research Communications*, vol. 499, no. 2, pp. 314–320, 2018.

[6] I. Martinez-Reyes and N. S. Chandel, "Mitochondrial TCA cycle metabolites control physiology and disease," *Nature Communications*, vol. 11, no. 1, p. 102, 2020.

[7] P. Mergenthaler, U. Lindauer, G. A. Dienel, and A. Meisel, "Sugar for the brain: the role of glucose in physiological and pathological brain function," *Trends in Neurosciences*, vol. 36, no. 10, pp. 587–597, 2013.

[8] G. Michal, "On representation of metabolic pathways," *Biosystems*, vol. 47, no. 1-2, pp. 1–7, 1998.

[9] Y. Nie, Z. Wang, G. Chai et al., "Dehydrocostus lactone suppresses LPS-induced acute lung injury and macrophage activation through NF-κB signaling pathway mediated by p38 MAPK and Akt," *Molecules*, vol. 24, no. 8, p. 1510, 2019.

[10] Z. Nova, H. Skovierova, and A. Calkovska, "Alveolar-capillary membrane-related pulmonary cells as a target in endotoxin-induced acute lung injury," *International Journal of Molecular Sciences*, vol. 20, no. 4, p. 831, 2019.

[11] T. Parimon, C. Yao, B. R. Stripp, P. W. Noble, and P. Chen, "Alveolar epithelial type II cells as drivers of lung fibrosis in idiopathic pulmonary fibrosis," *International Journal of Molecular Sciences*, vol. 21, no. 7, p. 2269, 2020.

[12] A. J. Paris, K. E. Hayer, J. H. Oved et al., "STAT3-BDNF-TrkB signalling promotes alveolar epithelial regeneration after lung injury," *Nature Cell Biology*, vol. 22, no. 10, pp. 1197–1210, 2020.

[13] Y. P. Wang, W. Zhou, J. Wang et al., "Arginine methylation of MDH1 by CARM1 inhibits glutamine metabolism and suppresses pancreatic cancer," *Molecular Cell*, vol. 64, no. 4, pp. 673–687, 2016.

[14] H. C. Yang, Wu, Yen et al., "The redox role of G6PD in cell growth, cell death, and cancer," *Cells*, vol. 8, no. 9, p. 1055, 2019.

[15] S. L. Zhou, M. Z. Li, Q. H. Li, J. Q. Guan, and X. W. Li, "Differential expression analysis of porcine MDH1, MDH2 and ME1 genes in adipose tissues," *Genetics and Molecular Research : GMR*, vol. 11, no. 2, pp. 1254–1259, 2012.

[16] Y. Zhuang, J. Xiang, W. Bao et al., "MDH2 stimulated by estrogen-GPR30 pathway down-regulated PTEN expression promoting the proliferation and invasion of cells in endometrial cancer," *Translational Oncology*, vol. 10, no. 2, pp. 203–210, 2017.

[17] J. Hao, L. Ren, L. Zhang, D. Kong, and L. Hao, "Aldosterone-induced inflammatory response of mesangial cells via angiotension II receptors," *Journal of the Renin-Angiotensin-Aldosterone System*, vol. 16, no. 4, pp. 739–748, 2015.

[18] J. Paquin-Veillette, F. Lizotte, S. Robillard et al., "Deletion of AT2 receptor prevents SHP-1-induced VEGF inhibition and improves blood flow reperfusion in diabetic ischemic hindlimb," *Arteriosclerosis, Thrombosis, and Vascular Biology*, vol. 37, no. 12, pp. 2291–2300, 2017.

[19] D. Zha, H. Cheng, W. Li et al., "High glucose instigates tubulointerstitial injury by stimulating hetero-dimerization of adiponectin and angiotensin II receptors," *Biochemical and Biophysical Research Communications*, vol. 493, no. 1, pp. 840–846, 2017.

[20] N. A. da Silva, F. T. Borges, E. Maquigussa, V. A. Varela, M. V. S. Dias, and M. A. Boim, "Influence of high glucose on mesangial cell-derived exosome composition, secretion and cell communication," *Scientific Reports*, vol. 9, no. 1, p. 6270, 2019.

[21] C. Li, L. Cao, and Q. Zeng, "Astragalus prevents diabetic rats from developing cardiomyopathy by downregulating angiotensin II type2 receptors' expression," *Journal of Huazhong University of Science and Technology. Medical Sciences*, vol. 24, no. 4, pp. 379–384, 2004, PMID: 15587404.

[22] K. Shahveisi, S. H. Mousavi, M. Hosseini et al., "The role of local renin-angiotensin system on high glucose-induced cell toxicity, apoptosis and reactive oxygen species production in PC12 cells," *Iranian Journal of Basic Medical Sciences*, vol. 17, no. 8, pp. 613–621, 2014.

[23] L. R. B. Santos, C. Muller, A. H. de Souza et al., "NNT reverse mode of operation mediates glucose control of mitochondrial NADPH and glutathione redox state in mouse pancreatic β-cells," *Molecular Metabolism*, vol. 6, no. 6, pp. 535–547, 2017.

[24] H. Kou, S. Gui, Y. Dai, Y. Guo, and H. Wang, "Epigenetic repression of AT2 receptor is involved in β cell dysfunction and glucose intolerance of adult female offspring rats exposed to dexamethasone prenatally," *Toxicology and Applied Pharmacology*, vol. 404, p. 115187, 2020, Epub 2020 Aug 11.

Hindawi
Computational and Mathematical Methods in Medicine
Volume 2023, Article ID 9878272, 1 page
https://doi.org/10.1155/2023/9878272

Retraction

Retracted: Clinical Application of Digital 3D Reconstruction and 3D Printing Technology in Endometrial Cancer (EC) Surgery

Computational and Mathematical Methods in Medicine

Received 12 December 2023; Accepted 12 December 2023; Published 13 December 2023

This article has been retracted by Hindawi, as publisher, following an investigation undertaken by the publisher [1]. This investigation has uncovered evidence of systematic manipulation of the publication and peer-review process. We cannot, therefore, vouch for the reliability or integrity of this article.

Please note that this notice is intended solely to alert readers that the peer-review process of this article has been compromised.

Wiley and Hindawi regret that the usual quality checks did not identify these issues before publication and have since put additional measures in place to safeguard research integrity.

We wish to credit our Research Integrity and Research Publishing teams and anonymous and named external researchers and research integrity experts for contributing to this investigation.

The corresponding author, as the representative of all authors, has been given the opportunity to register their agreement or disagreement to this retraction. We have kept a record of any response received.

References

[1] F. Luo and Q. Yang, "Clinical Application of Digital 3D Reconstruction and 3D Printing Technology in Endometrial Cancer (EC) Surgery," *Computational and Mathematical Methods in Medicine*, vol. 2022, Article ID 9180216, 8 pages, 2022.

Hindawi
Computational and Mathematical Methods in Medicine
Volume 2022, Article ID 9180216, 8 pages
https://doi.org/10.1155/2022/9180216

Research Article

Clinical Application of Digital 3D Reconstruction and 3D Printing Technology in Endometrial Cancer (EC) Surgery

Fang Luo and Qin Yang

Department of Gynecology, Wuhan Puren Hospital, 430081, China

Correspondence should be addressed to Qin Yang; dpp@bbc.edu.cn

Received 7 July 2022; Revised 3 August 2022; Accepted 27 August 2022; Published 14 September 2022

Academic Editor: Min Tang

Aims. We use CTA and magnetic resonance data to use digital three-dimensional reconstruction and 3D printing technology to reproduce the solid replication of the uterus and surrounding tissues in vitro, fully evaluate the adjacency of tumor tissues with surrounding important organs, blood vessels, and lymph nodes, and reduce the impact. The normal organ structure and function of the surgeon can shorten the operation time, reduce the bleeding during the operation, and reduce the perioperative complications of the patient to improve the prognosis of the patient. *Materials and Methods*. Select 40 EC patients and divide them into group A (3D reconstruction data is transmitted to 3D printing equipment according to the results of CTA and MRI examination, and a 3D model is printed out according to the ratio of 1 : 1 for evaluation and judgment before surgery) and group B (according to MRI imaging examination, there were 20 cases each). Different surgical conditions, quality of life, adverse reactions, and clinical efficacy were evaluated in each group. *Results*. The operation time, the time of the first anus exhaust, the hospitalization time after the operation, and the blood loss of the operation in group A were significantly lower than those in group B. Statistics showed that the difference was significant ($P < 0.05$). The quality of life scores of emotion, cognition, society, and overall health of group A were significantly higher than those of group B, while physical score, fatigue, nausea, vomiting, and pain were lower than those of group B, which were statistically significant ($P < 0.05$). Both groups of patients had complications after the operation, and they were asked to be followed up at the outpatient clinic 3 months after the operation. All patients recovered well. There were 19 and 18 patients in groups A and B, respectively, complaining of improvement in clinical symptoms, and the difference was not statistically significant ($P < 0.05$). *Conclusion*. With the support of digital three-dimensional reconstruction and 3D printing technology, complex operations can be accurately performed, improving the efficacy and safety of patients after EC surgery, improving patient outcomes and quality of life, improving EC positioning accuracy, and reducing tumor residue.

1. Introduction

Surgery is the main treatment method for endometrial cancer (EC). Surgery for early EC is called full staging surgery. This surgery involves the removal of lymph nodes near the pelvic cavity and abdominal aorta. Lymphatic vessels are the main metastasis route of gynecological tumors [1]. Lymphadenectomy is very important for the staging of EC, identifying high risk factors for recurrence, survival prognosis, and whether it can benefit from chemotherapy or radiotherapy. The key step of surgery is to identify blood vessels and their adjacent structures, especially for variant blood vessels [2]. Abdominal great vessel injury is not common but it is fatal. It can make decisions about abnormal conditions more effectively during the operation, thereby improving the accuracy and efficiency of abdominal para-aortic lymphadenectomy. Surgery for advanced EC is called cytoreductive surgery. The smaller the residual tumor during the operation, the better the postoperative prognosis. A number of studies have also indicated that cytoreductive surgery can achieve no residual to the naked eye, which can significantly improve the overall survival of patients. How to remove all primary and secondary tumors as much as possible is the goal of cytoreductive surgery, which is why it needs to be

Table 1: Comparison of general information between the two groups [$n(\bar{x} \pm s)$].

Group	Age (year)	Height (cm)	Weight (kg)	Tumor diameter (cm)	Histological grade		
					Well differentiated	Medium differentiation	Poor differentiation
Group A (20)	49.78 ± 3.32	161.78 ± 6.20	48.34 ± 2.65	4.51 ± 0.82	10	9	1
Group B (20)	50.62 ± 2.71	159.62 ± 5.21	47.26 ± 1.64	4.52 ± 0.81	11	7	3
χ^2/t	-0.877	1.193	1.550	-0.087	0.024	0.020	0.130
P	0.386	0.240	0.129	0.931	0.877	0.887	0.718

fully evaluated before surgery. Therefore, an accurate and sufficient assessment must be performed before EC surgery to determine whether neoadjuvant chemotherapy is required before surgery, to estimate the risk of surgery, and to do a good job in preoperative doctor-patient communication and perioperative treatment [3].

The specific application of digital 3D reconstruction technology and 3D printing technology in clinical obstetrics and gynecology is to perform abdominal and pelvic CTA and MRI scans under conventional or specific sequence conditions, collect all data and use biomedical software for 3D reconstruction to construct a 3D abdomen and pelvic cavity structure diagram, and then conduct detailed observations of all-round, various systems or parts to provide clinicians with more information for diagnosis, so consider the use of digital three-dimensional reconstruction and 3D printing to assist in EC surgery [4]. The digital 3D visualization model reconstructed by applying digital 3D reconstruction technology based on the CTA and MRI original data sets has the functions of visualization, three-dimensionalization, and rotation. The direction, mass, and the relationship between important blood vessels and surrounding important organs and blood vessels can be clearly understood. It is shown in front of us to facilitate the design of surgery and guide the implementation of surgery [5]. Digital three-dimensional reconstruction and 3D printing technology provide precise and detailed personalized anatomical data and guidance basis for the precise implementation of surgery, which can provide surgeons with more information during diagnosis and treatment, so as to predict intraoperative conditions in advance [6]. Use 3D printing models to explain to patients and their families before surgery so that they have the opportunity to understand their condition, surgery process, and prognosis [7–9]. At present, there are some precedents for the application of 3D printing technology in the field of obstetrics and gynecology, but there is no report of the application of this technology to EC surgery at home and abroad. This study intends to conduct a clinical application study of digital 3D reconstruction and 3D printing technology in EC surgery and explore the clinical application of 3D printing technology in surgery. The current research results are reported as follows.

2. Material and Methods

2.1. General Information. The clinical data of 40 EC patients who were treated in our hospital from January 2021 to July 2021 were selected as the subjects of this prospective study, and according to the random number table method, they were divided into group A and group B with 20 cases each. Before the start of the study, the patients and their families were informed of their informed consent in accordance with the principles of voluntariness, confidentiality, benefit, and harmlessness and approved by the medical ethics committee of our hospital. In all cases, an experienced physician with a senior professional title in obstetrics and gynecology performed vaginal speculum, bimanual and triadic examinations under the condition of emptying the bladder and relaxing abdomen to determine the size of the tumor and parauterine infiltration, strictly. According to the 2018 F1GO diagnostic criteria, each patient was accurately staged: surgical treatment: phase I: total hysterectomy plus bilateral appendage resection; stage II and stage III A: extensive total uterus plus bilateral adnexectomy, pelvic lymphadenectomy, and para-aortic lymph node sampling. General data such as gender and age of the two groups of patients had no effect on this test, as shown in Table 1. The records of all patients in this study are kept in the hospital as required. The identity of the patient is confidential. All patients gave informed consent before enrollment, the content and process of the experiment were introduced as well as related risks and possible adverse reactions, and an informed consent form was signed after obtaining the consent of the patients.

2.2. Inclusion and Exclusion Criteria. Inclusion criteria: (i) all patients in this study met the diagnostic criteria for uterine fibroids in the "Chinese Expert Consensus on the Diagnosis and Treatment of Uterine Fibroids" [10]. All selected patients were women of childbearing age, and ultrasound and MRI showed multiple uterine fibroids. (ii) There are indications for surgery: accompanied by symptoms such as abnormal menstruation, pelvic pain, or compression, uterine fibroids are the cause of infertility and miscarriage, fibroids grow too fast, etc. (iii) The patient has strong uterine retention willingness, agrees to surgery, has good communication skills, and cooperates with follow-up after discharge. Exclusion criteria: (i) those who refused to undergo surgery, combined with severe heart, lung, liver, and kidney diseases, or acute and chronic systemic and vaginal infections, combined with FG00, type 1, and type 8 fibroids; (ii) relevant auxiliary examinations indicated suspected pelvic malignancy, combined with adenomyosis/tumor, related imaging examination and gynecological examination showed severe pelvic-abdominal adhesions; (iii) the surgical method was changed during the operation, and there was a history of myomectomy, who could not cooperate with the follow-up.

2.3. Build a 3D Model. Acquisition of raw data (i) MRI scan: use United Imaging uMR780 3.0T superconducting MR scanner to perform horizontal, coronal, and sagittal multidirectional scans. The layer thickness is set to 4 mm, and the layer spacing is 0-1 mm. T2WI sagittal and transverse axis TR 3938 ms, TE 154.7 ms, read FOV 240; fat suppression T2WI coronal and transverse axis TR 4630 ms, TE 113.6 ms, read FOV 240. The horizontal axis of FSE-T1WI is TE 735 ms, TR 10.92 ms, and the readout FOV is 350. DWI (Diffusion Weighted Imaging) horizontal axis, *b* value is 50,800, read FOV 350. 3D sagittal DYN dynamic enhancement, TR 4.1 ms, TE 1.87, read FOV 300, a total of 12 scans in the same scan slice. (ii) CTA scan: a GE Optima660 64-slice spiral CT scanner is used. The patient was placed in a supine position, and the scan ranged from the upper edge of the twelfth thoracic vertebra to the upper femur. Tube voltage is 120 kV, automatic tube current. The layer thickness is 0.625 mm and the pitch is 1.375. Iohexol (containing 350 mg/ml of iodine) was used as the enhanced scanning contrast agent, and the injection flow rate was 3.5 ml/s. Scans were performed in the arterial phase, portal phase, and delayed phase. The arterial phase adopts the contrast medium tracking technology. When the CT value of the abdominal aorta is greater than/equal to 120 HU, the scan is triggered. The venous phase starts scanning at about 55-60 s after the drug is sprayed, and the delay period starts at about 240 s.

3D modeling and graphics processing: input the patient's CTA scan and magnetic resonance result data into the Mimics 20.0 computer software and then reconstruct according to the image scan result, transfer the data to the 3D printing device, and print out the model according to the ratio of 1 : 1. The material used is ABS engineering plastics (ABS) to reshape the three-dimensional model. The printer supporting software is Maker Ware™ Bundle 2.0.

2.4. Surgical Methods. The surgical method for the two groups of patients was total hysterectomy plus bilateral appendage resection for stage I patients, extensive hysterectomy plus bilateral appendage resection for stage II and III A patients, and pelvic lymphadenectomy and para-aortic lymph node sampling surgery. The chief surgeon used different anatomical information references for the two groups to guide the operation. During the operation of group A, the chief surgeon referred to the corresponding 3D printed model to guide the operation, and during the operation of group B, the chief surgeon referred to the corresponding B-ultrasound results, MRI film, and report. Guide the surgical operation. All patients underwent intravenous general anesthesia under tracheal intubation, took the position of bladder lithotripsy, head low buttock high, disinfection and spreading sterile towels followed conventional bladder lithotomy. The specific surgical process will not be described in detail and has no effect on this study.

2.5. Observation Indicators. During the operation, gauze strips were used to stop bleeding, and the difference in the weight of the gauze strips between wet and dry conditions was used to estimate the amount of bleeding. Quality of life score: the quality of life measurement scale (WHOQOL-100) is used as a postoperative quality of life questionnaire for patients. The patient will be followed up by telephone after 3 months of treatment to evaluate the quality of life: the core scale for cancer patients is used for evaluation. The core scale (EORTC QLQ2C30) is a system for measuring the quality of life of cancer patients developed systematically by the European Organization for Research and Treatment of Cancer (EORTC). There are 30 items in total. Article 29 and Article 30 are divided into 7 levels. The answer options range from 1 to 7 points; the other items are divided into 4 levels: from nothing to a little bit, to more than 4 points, 1 to 4 points directly, usually divided into several aspects. There are 15 domains, divided into 4 functional domains: physical, cognitive, emotional, and social functions, 3 symptom domains such as fatigue, pain, nausea, and vomiting, 1 overall health status/quality of life domain, and 6 individual domains (each as a domain), add the scores of the items contained in each domain, and divide by the number of items contained in the domain to get the score of the domain. Significance of the scoring rules: the more the score for function and overall health, the better the function and the quality of life, the higher the score for symptoms, the more the patient's symptoms of discomfort and the worse the quality of life. Cronbach's α values measured before use were all greater than 0.914. Patients or their accompanying family members should fill in the information independently before treatment and 3 months after treatment without being affected by any internal or external factors. The test will be completed within 57 minutes.

2.6. Statistical Analysis. All statistical data in this study were entered into Excel. Each parameter data is mentioned as mean ± SD and statistically analysed by employing one-way ANOVA followed Tukey's multiple comparisons post hoc test. Comparison was made within the group for before and after the drug treatment and between the groups for after drug treatment effect. $P < 0.05$ is considered as statistically significant.

3. Results

3.1. General Information Comparison. The age, height, weight, tumor diameter, histological grade, and other general data of the two groups of patients were not significantly different by *t*-test and chi-square test ($P > 0.05$). See Table 1.

3.2. Comparison of Surgical Conditions. During the perioperative period, the operation time and surgical blood loss of group A were significantly lower than those of group B ($P < 0.05$). After the operation, the hospitalization time after the operation and the time of the first anus exhaust of the patients in group A were significantly lower than those in group B. Statistics showed that the difference was significant ($P < 0.05$). See Figure 1.

3.3. Comparison of Quality of Life Scores. The two groups of patients were followed up after 3 months of treatment to evaluate the quality of life of the patients. The quality of life scores of the patients in group A, such as emotional score,

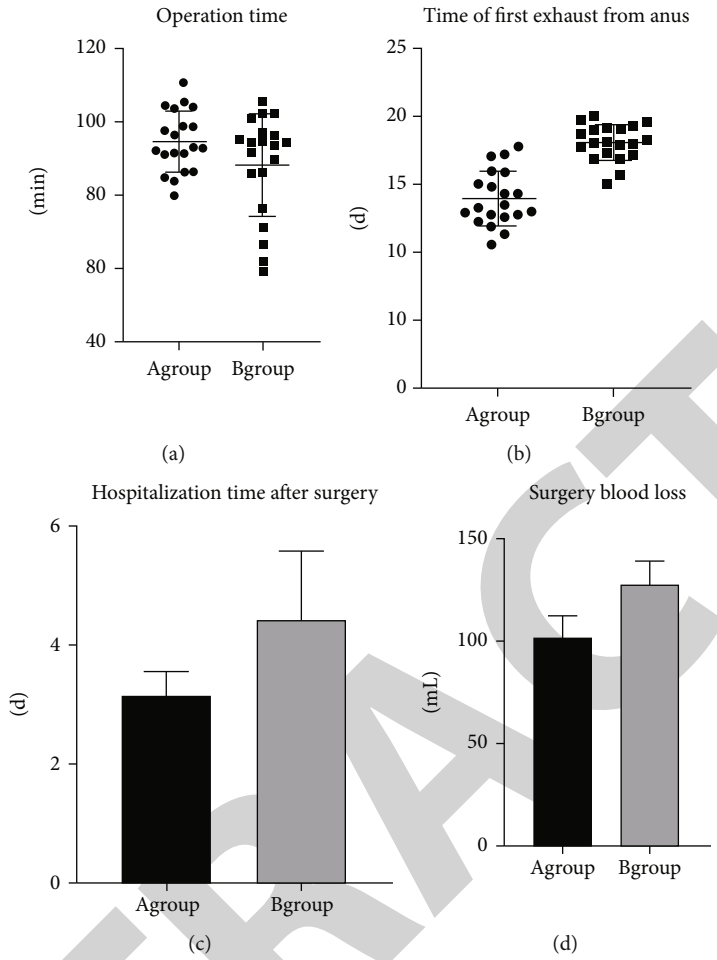

Figure 1: Comparison of surgical conditions.

cognitive score, social score, and overall health score, were significantly higher than those in group B. The scores of nausea and vomiting and pain scores were lower than those of group B, which were statistically significant ($P < 0.05$). See Figure 2.

3.4. Complications and Follow-Up Analysis. Both groups of patients had complications after the operation, and they were asked to be followed up at the outpatient clinic 3 months after the operation. All patients recovered well. There were 19 and 18 patients in groups A and B, respectively, complaining of improvement in clinical symptoms, and the difference was not statistically significant ($P < 0.05$).

3.5. Typical Cases. Wang Mou, 45 years old, was admitted to the hospital due to "irregular vaginal bleeding for more than half a month." Ultrasound revealed an enlarged uterus (about 11.2 cm × 5.9 cm × 9.4 cm) and a heterogeneous echo group in the uterine cavity, about 9.8 cm × 4.6 cm in size; the boundary is clear, the internal echo is chaotic, and irregular anechoic areas can be seen. The proposed diagnosis is "postmenopausal vaginal bleeding, the cause is yet to be investigated. EC has not been ruled out" and admitted to the hospital. Examination found fracture invasion and cervical cancer, parauterine tissue ligaments, appendages or lymph nodes significantly enlarged, triad examination showed palpable hard or enlarged cervical canal, main ligament or sliding belt thickened and decreased elasticity, appendage mass and swollen and fixed lymph nodes at the pelvic wall. This case is an EC patient. MRI findings: T1W image shows that the tumor and uterine muscle are isosignal. T2W is like a tumor with a medium-to-high signal intensity. The signal intensity is between the normal endometrium and the uterine muscle. After the enhanced scan, the blood supply of the tumor is lower than that of the normal uterine muscle. Signal, segmental interruption of the uterine junction is invaded by the muscle layer (Figure 3). The three-dimensional reconstruction results show that the cervix is enlarged and the blood supply is abundant. The blood is supplied by the descending branches of the bilateral uterine arteries, the left internal pudendal artery, and the right vaginal artery (Figure 4). In 3D printing, plastic model results clearly show the tumor's anatomical location and adjacent relationship with surrounding tissues. The model is based on three-dimensional reconstruction data, so the anatomical position of the tumor and the relationship with surrounding organs and blood vessels are the same as the three-dimensional reconstruction results. Through three-dimensional reconstruction combined with 3D printing, combined with dynamic images and static models, it assists in preoperative tumor positioning,

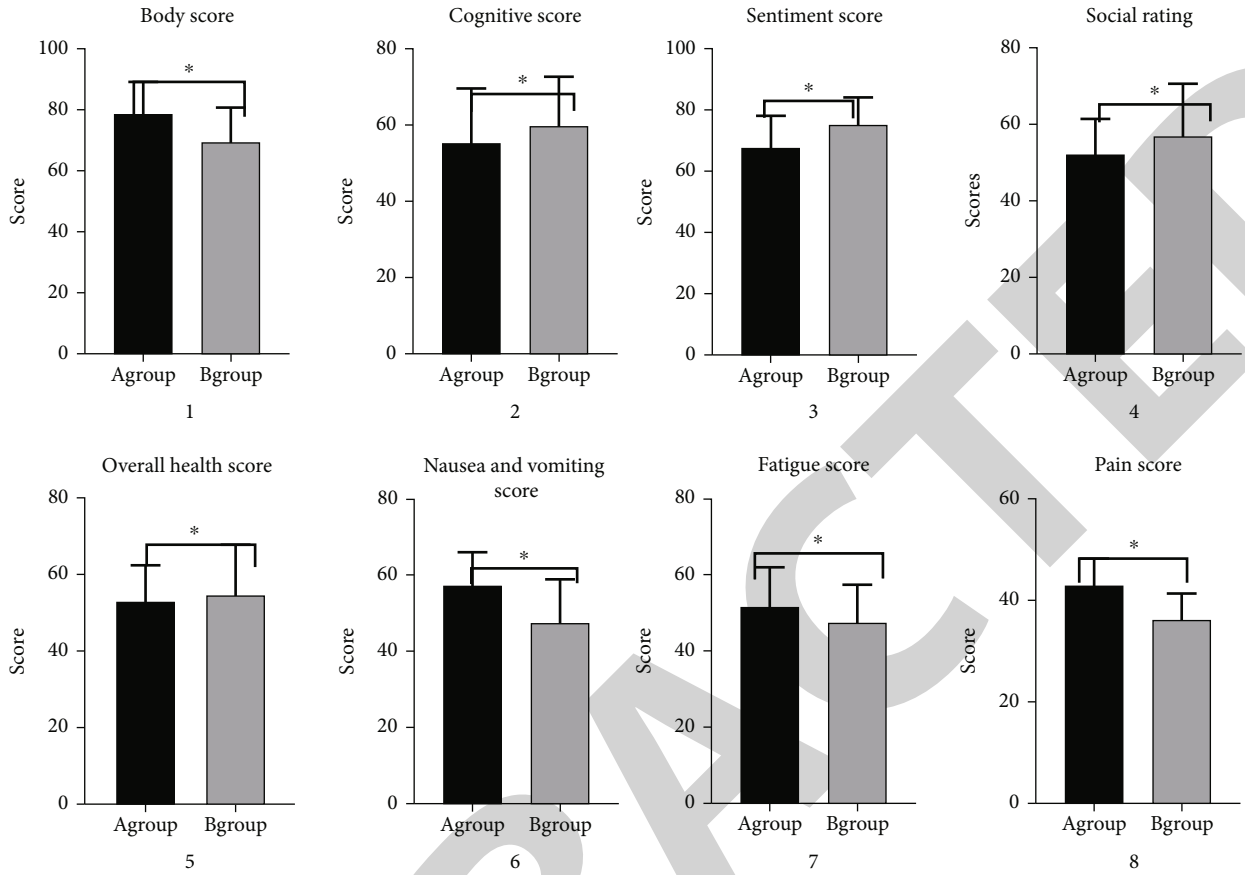

Figure 2: Comparison of quality of life scores between the two groups ($^*P < 0.05$).

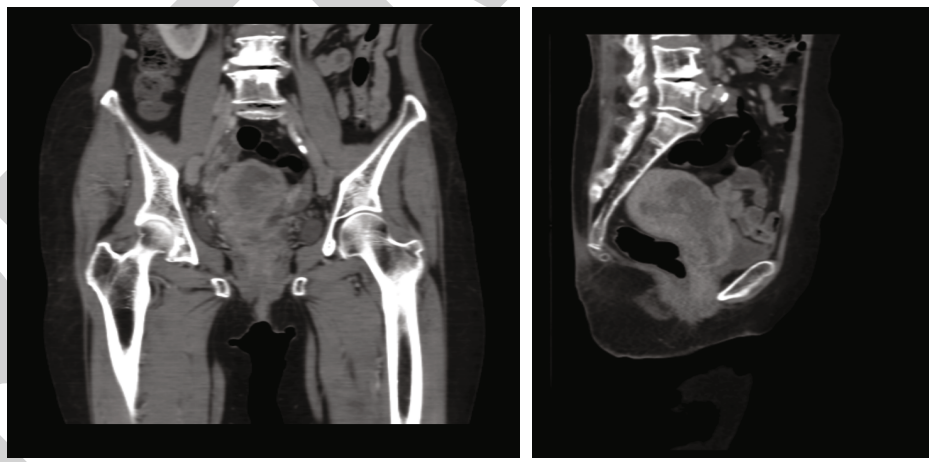

Figure 3: MRI image of the abdomen. There are soft tissue density tumors in the uterine cavity; the density of which is lower than that of the strengthened normal uterine muscle. The tumor is cauliflower-like or nodular, and the surrounding can be surrounded by lower-density intrauterine effusion. When the tumor invades the muscle layer, it strengthens. The normal uterine muscle has limited or diffuse low density, thinning of the muscle layer, and tumor invasion often manifests as blurred uterine edges or soft tissue strips or nodules.

judging the involvement of surrounding vital organs and large blood vessels, and formulating a preoperative plan (Figure 5).

4. Discussion

Myomectomy can not only preserve the fertility of the patient, but more importantly, it can maintain the physiological function of the uterus and the integrity of the anatomical structure of the pelvic floor, with the physical and mental health of the patients [11]. LM has the advantages of short hospital stay, less postoperative pain, less local adhesion, beautiful incision, and quick postoperative recovery, and its clinical application is becoming more and more extensive. 3D printing technology is a rapid prototyping

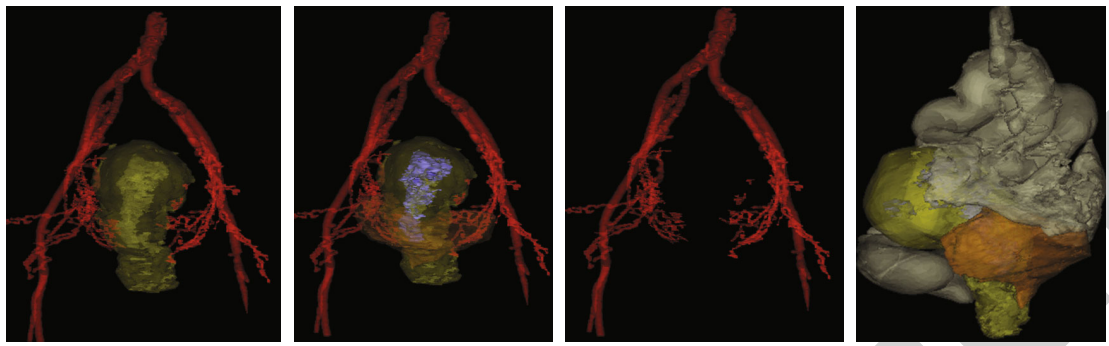

Figure 4: Three-dimensional reconstruction image of the uterus and main blood vessels. The pelvic mass is located on the right side and has a clear boundary with the uterus. The right ovarian artery is visible and thickened, but it bypasses the surface of the mass. The blood flow inside the mass is extremely sparse, and there is no obvious vascular network.

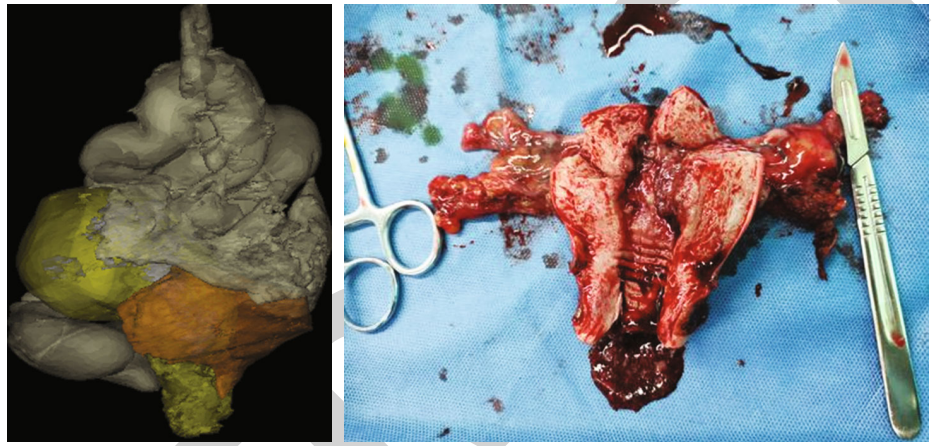

Figure 5: 3D printed EC model and pictures of surgically removed tumors.

manufacturing technology that can turn virtual 3D reconstruction models into reality. Its biggest advantage is that it is not limited by the shape of molds and objects. In theory, objects of any shape can be printed, and the supported printing consumables are extremely high. Abundant, suitable for the manufacture of individualized, small batch products [12], since its emergence in the 1990s, the application of 3D printing technology has been active in manufacturing and other fields. Over time, the advancement of technology and the development of materials have prompted this technology to break through the field of industrial mold manufacturing [13]. The current exploration of 3D printing technology has penetrated into all aspects of the medical field. From the most basic medical model making to the most cutting-edge 3D bioprinting, it has shown quite broad development prospects. This technology is often used clinically to print organ models of specific cases as samples for anatomical cognition and surgical assistance. Since the lesion parts of different cases are different and the structure of human organs itself is complex, 3D printing technology is used in medical application scenarios. Compared with traditional manufacturing technology, it has incomparable advantages in flexibility, economy, time saving, etc., and it fits perfectly with the concepts of precision medicine and individualized medicine [14].

In this study, the operation time, first anal exhaust time, postoperative hospital stay, average number of myomectomy, and surgical blood loss were significantly lower in group A than in group B, suggesting that when all or most of the myomas were removed, there is significant relief of the mass effect of fibroids, so that the uterus can return to normal shape and function, and improved related clinical symptoms. The comparison of the data of the two groups in this study can confirm that the 3D model does play an important role in adjuvant LM in the treatment of multiple fibroids. The improvement of fibroid localization accuracy reduces the possibility of residual and recurrence of fibroids [15]. The lack of palpation feel of LM was a common limitation of the two groups. The traditional MRI images used in group B were not intuitive, and the location of multiple fibroids was unclear, which easily led to the omission of tiny fibroids.

In this study, there was no significant difference in ovarian function-related indicators between the two groups of patients before treatment. After treatment, the recovery of estradiol, follicle-stimulating hormone, and luteinizing hormone in group A was better than that in group B, suggesting the ascending branch of the arteries. Ovarian function-related hormone levels were not significantly changed in patients with occlusion; that is, ascending artery occlusion

may not affect ovarian function in patients. Ascending artery occlusion did not significantly change the quality of sexual life of patients, which may be related to the fact that ascending artery occlusion did not change the level of hormones in the ovary of patients. This study is aimed at using 3D printing technology to reproduce the uterus and uterine fibroids in vitro, determine the scope of preoperative lesions, and complete preoperative doctor-patient communication, surgical plan planning, and preoperative rehearsal, so as to make the surgical operation process easier. It is carried out smoothly, minimizing the impact on the structure and function of the uterus of the recipient, reducing the probability of postoperative complications and the possibility of recurrence, and reducing the impact on the patient's pregnancy and normal uterine physiology. At present, 3D printing technology is widely used in many fields such as medicine, aviation, and education and gradually shows its advantages in the medical field. Now, with the advantages of customization of 3D printing technology, it is possible to design individual differentiated treatment plans [16]. 3D printing technology has been studied in the fields of lung cancer, gastrointestinal malignant tumor, bone tumor, kidney tumor, biliary tract tumor, and other fields, and the effect is remarkable, and the results have been unanimously affirmed [17]. There are relevant mature technologies in these two aspects, and we always pay attention to the most cutting-edge research progress in the world. At present, the previous operation has been carried out and achieved ideal results, which proves that the research plan is feasible. The application of 3D printing technology in laparoscopic myomectomy has reached the domestic advanced level; through the application of this technology, precision surgery is carried out, in order to reduce intraoperative bleeding and injury, shorten the operation time, reduce patient recurrence, reduce patient costs, etc. It can be popularized and applied at the grassroots level [18–21].

This study has some shortcomings due to the lack of resources in the selected hospital. First, the production cost of 3D printing models is still relatively high. Due to specific conditions such as funding, the number of samples included in this study is small, which may cause certain statistical problems, bias. Secondly, because the production process of color 3D printing is more complicated, the production cycle of the model is longer (about 5 days on average). If the research team can obtain the model earlier, it can gain more time for understanding the condition and improving the surgical plan; finally, because the density of the uterus, fibroids, and the adjacent soft tissue is close, the threshold range is not clear, the modeling is difficult, and this step depends on the participation of radiologists, due to the insufficient follow-up period in this study, so the postoperative pregnancy rate cannot be followed up for the time being. Although the application of 3D printing technology in making medical models and assisting surgical operations is relatively mature, its application in the field of obstetrics and gynecology is still rarely reported, and its effect still needs more relevant clinical research to confirm. In summary, 3D printing provides a uterus and its fibroid model with the characteristics of three-dimensional, vivid, and high reduction, which improves the positioning accuracy of multiple fibroids, reduces the probability of residual and recurrence of fibroids, and helps to improve the efficacy, efficiency, and safety of surgery.

5. Conclusion

In summary, the use of digital three-dimensional reconstruction and 3D printing technology can guide the precise operation of surgery, improve the efficacy and safety of patients after EC surgery, improve patient recovery and quality of life, improve the positioning accuracy of EC surgery, and guide surgery which has a certain effect.

Data Availability

No data were used to support this study.

Conflicts of Interest

There are no conflicts of interest.

Authors' Contributions

We confirm that the manuscript has been read and approved by all named authors and that there are no other persons who satisfied the criteria for authorship but are not listed. We further confirm that the order of authors listed in the manuscript has been approved by all of us.

Acknowledgments

The study was supported by Project No. WX21Z33, Fund Project: Clinical application of digital 3D reconstruction and 3D printing technology in endometrial cancer surgery.

References

[1] M. H. Vetter, B. Smith, J. Benedict et al., "Preoperative predictors of endometrial cancer at time of hysterectomy for endometrial intraepithelial neoplasia or complex atypical hyperplasia," *American Journal of Obstetrics and Gynecology*, vol. 222, no. 1, pp. 60.e1–60.e7, 2020.

[2] M. A. Clarke, B. J. Long, A. D. Morillo, M. Arbyn, J. N. Bakkum-Gamez, and N. Wentzensen, "Association of endometrial cancer risk with postmenopausal bleeding in women: a systematic review and meta-analysis," *JAMA Internal Medicine*, vol. 178, no. 9, pp. 1210–1222, 2018.

[3] R. Murali, D. F. Delair, S. M. Bean, N. R. Abu-Rustum, and R. A. Soslow, "Evolving roles of histologic evaluation and molecular/genomic profiling in the management of endometrial cancer," *Journal of the National Comprehensive Cancer Network*, vol. 16, no. 2, pp. 201–209, 2018.

[4] R. C. Arend, B. A. Jones, A. Martinez, and P. Goodfellow, "Endometrial cancer: molecular markers and management of advanced stage disease," *Gynecologic Oncology*, vol. 150, no. 3, pp. 569–580, 2018.

[5] N. Colombo, C. Creutzberg, F. Amant et al., "ESMO-ESGO-ESTRO consensus conference on endometrial cancer: diagnosis, treatment and follow-up," *International Journal of Gynecologic Cancer*, vol. 26, no. 1, pp. 2–30, 2016.

Hindawi
Computational and Mathematical Methods in Medicine
Volume 2023, Article ID 9864531, 1 page
https://doi.org/10.1155/2023/9864531

Retraction

Retracted: Continuous Renal Replacement Therapy for Hypertension Complicated by Refractory Heart Failure: An Analysis of Safety and Nursing Highlights

Computational and Mathematical Methods in Medicine

Received 12 December 2023; Accepted 12 December 2023; Published 13 December 2023

This article has been retracted by Hindawi, as publisher, following an investigation undertaken by the publisher [1]. This investigation has uncovered evidence of systematic manipulation of the publication and peer-review process. We cannot, therefore, vouch for the reliability or integrity of this article.

Please note that this notice is intended solely to alert readers that the peer-review process of this article has been compromised.

Wiley and Hindawi regret that the usual quality checks did not identify these issues before publication and have since put additional measures in place to safeguard research integrity.

We wish to credit our Research Integrity and Research Publishing teams and anonymous and named external researchers and research integrity experts for contributing to this investigation.

The corresponding author, as the representative of all authors, has been given the opportunity to register their agreement or disagreement to this retraction. We have kept a record of any response received.

References

[1] M. Zhang and J. Li, "Continuous Renal Replacement Therapy for Hypertension Complicated by Refractory Heart Failure: An Analysis of Safety and Nursing Highlights," *Computational and Mathematical Methods in Medicine*, vol. 2022, Article ID 7951744, 8 pages, 2022.

Hindawi
Computational and Mathematical Methods in Medicine
Volume 2022, Article ID 7951744, 8 pages
https://doi.org/10.1155/2022/7951744

Research Article

Continuous Renal Replacement Therapy for Hypertension Complicated by Refractory Heart Failure: An Analysis of Safety and Nursing Highlights

Miaoli Zhang and Jingfeng Li

Department of Fourth Cardiovascular Medicine, The Affiliated Chuzhou Hospital of Anhui Medical University, The First People's Hospital of Chuzhou, Chuzhou, Anhui 239000, China

Correspondence should be addressed to Jingfeng Li; a17201009@stu.ahu.edu.cn

Received 1 August 2022; Accepted 27 August 2022; Published 14 September 2022

Academic Editor: Min Tang

Objective. This research is aimed at analyzing the safety profile and nursing highlights of continuous renal replacement therapy (CRRT) for hypertension (HT) complicated by refractory heart failure (RHF). *Methods*. Sixty-six HT + RHF patients admitted between March 2018 and December 2021 were enrolled and assigned to two groups: a CRRT group with 33 cases treated with CRRT and a control group with 33 cases intervened by routine treatment. The therapeutic effect and alterations of cardiac function (CF) indexes were observed in both cohorts. Besides, statistics were made in terms of serum B-type natriuretic peptide (BNP), C-reactive protein (CRP) and mean arterial pressure (MAP) concentrations, time of asthma relief, heart rate recovery (HRR), edema resolution, and hospitalization, as well as incidence of adverse reactions (ARs). Finally, pre- and posttreatment psychological quality and pain of both cohorts of subjects were assessed using the self-rating anxiety and depression scale (SAS and SDS) and visual analogue scale (VAS), respectively. *Results*. CRRT group exhibited higher overall response rate and better CF than control group ($P < 0.05$), with lower BNP, CRP, and MAP levels, and shorter time of asthma relief, HRR, edema resolution, and hospitalization ($P < 0.05$); the incidence of ARs was similar ($P > 0.05$); for both groups, the scores of SAS, SDS, and VAS reduced statistically after treatment ($P < 0.05$). *Conclusion*. CRRT can effectively improve the therapeutic effect and CF of patients with HT complicated by RHF, to protect the health and safety of patients.

1. Introduction

Hypertension (HT) is an extremely prevalent chronic disease among the middle-aged and elderly; the clinical manifestations are paroxysmal or persistent dizziness, headache, insomnia, memory loss, and limb numbness, which have a serious impact on the quality of life and physical and mental health of patients [1]. Cardiocerebral disorders and renal dysfunction are common complications in hypertensive patients [2]. HT has been confirmed as the major risk factor for heart failure (HF), and due to the high age of hypertensive patients and the deterioration of physical functions, HF often develops into refractory critical diseases, and it is manifested as continuous aggravating palpitations, dyspnea, chest tightness, asthma, etc., which eventually lead to large-area myocardial infarction or myocardial fibrosis, posing a serious threat to patients' life safety [3]. Refractory heart failure (RHF) is in the severe stage of HF, when the renal blood flow is significantly reduced, accompanied by abnormal blood flow distribution, renal interstitial edema, and obviously decreased glomerular filtration rate, which can directly cause acute renal failure in severe cases [4]. This process can also lead to a substantial decline in cardiac output, most of which are accompanied by compensatory enhancement of neurohumoral factor activity and vasoconstriction, further increasing the cardiac load and aggravating the pathological development of RHF [5]. Therefore, correcting the renal blood flow in RHF is of great significance for disease treatment. Affected by RHF, the sensitivity of the patient's kidney to diuretics is greatly reduced that has been unable to meet

the treatment requirements [6]. Besides, due to the influence of neuroendocrine system activation, diuretic resistance, electrolyte disorder, and other factors, there is an urgent need to find a safer and more effective treatment in clinical practice [7].

At present, comprehensive treatment is mostly adopted for the clinical treatment of HT complicated by RHF clinically (HT + RHF); although it has certain therapeutic effect, the occurrence of adverse reactions (ARs) in the long-term treatment process worsens the final prognosis of patients [8, 9]. Therefore, the clinic is urgently looking for a more effective RHF treatment method, to protect the life safety of patients. With the continuous progress of medical technology, continuous renal replacement therapy (CRRT) has gradually become an important therapy for the treatment of critical diseases. Through extracorporeal circulation blood purification technology, water and solute are continuously and slowly removed to achieve the goal of stabilizing blood circulation and reducing the mortality of critically ill patients [10], such as CRRT reduces the mortality of patients with acute kidney injury and can effectively treat severe hyperkalemia [11, 12] and so on. CRRT has been increasingly applied to the treatment of HF, with many studies indicating its favorable efficacy in HF that is superior to conventional treatment; meanwhile, the application of nursing intervention has a positive effect on improving patient outcomes [13, 14]. However, little is known about the safety profile of this therapy in HT + RHF. Consequently, this paper evaluates the safety of CRRT in HT + RHF patients and analyzes the nursing highlights, to provide reliable evidence and methods for future clinical management of HT + RHF.

2. Materials and Methods

2.1. Study Area. The study was carried out of from March 2018 to February 2022.

2.2. Data Collection. With the approval of the Ethics Committee of our hospital, 66 HT + RHF patients admitted between March 2018 and December 2021 were enrolled and grouped as follows: a CRRT group with 33 cases treated with CRRT and a control group with 33 cases intervened by routine treatment. Additionally, all patients accepted individualized nursing strategies for blood purification tailored treatment formulated by our hospital. The eligible patients, all aged ≥50, met the diagnostic criteria of HT + RHF [15, 16] and agreed to receive CRRT treatment, with complete medical records, high compliance, and voluntary participation in this trial. In contrast, hospital referrals or those with communication barriers, physical impairment, other major diseases, infectious diseases, or short survival time were excluded.

2.3. Treatment Strategies. Control group: patients underwent a series of routine tests after admission. Their blood pressure (BP) and intracranial pressure were controlled to prevent complications. In addition to real-time monitoring of BP and blood oxygen, routine treatments such as cardiotonic, diuresis, vasodilator, and angiotensin-converting enzyme inhibitors were applied. Then, 25 mg sodium nitroprusside was added into 5% glucose solution for slow intravenous drip (6-12 drops/min), and the solution was changed every 6-8 hours. The treatment lasted for 14 days. CRRT group: based on the above treatment, patients in this group were given CRRT. The femoral vein double-lumen hemodialysis catheter was used to establish vascular access. All patients were treated with continuous veno-venous hemofiltration (CVVH), using AQU, Flex, ACH-10 pipelines, as well as MT-100, AEF-13, and HF1200 filters, with low molecular heparin anticoagulation as the main treatment. Each treatment lasted for 8 hours for a total of 14 days. Patients' vital signs, coagulation function, and electrolyte status were closely monitored, and corresponding adjustments were made according to patients' different reactions.

2.4. Nursing Strategies. Both groups received intensive care. After admission, the medical staff monitored the patients' BP, blood sugar, heart rate, and other vital signs three times a day and recorded them. In addition, health education was carried out for patients and their accompanying families to help them understand the disease, build up confidence, and improve treatment compliance. Furthermore, the medical staff paid attention to the presence of anxiety, nervousness, and other adverse emotions in patients and conducted timely communication and guidance to ease their mood and give them care and encouragement. Furthermore, the intravenous indwelling needle was selected when possible, the inspection of patients was strengthened, and the liquid medicine was replaced in time; oral care such as oxygen inhalation and sputum aspiration was provided for patients in need. Since infusion pump administration requires patients to stay in bed for a long time, HT + RHF patients have limited activities and are at high risk of pressure ulcers. Therefore, the nursing staff carried out a dynamic risk assessment of pressure ulcers and gave timely and reasonable interventions. What is more, the ward was ventilated regularly, and patients and their families were guided on standardized and reasonable diet, as well as infection prevention. Moreover, patients were encouraged to exercise moderately within their physical tolerance to prevent muscle atrophy. And according to the different needs of patients, corresponding intervention guidance was given in a timely manner until they were discharged from hospital.

2.5. Endpoints. The outcome measures were as follows [17]: (1) therapeutic effects (markedly effective: BP returned to normal, with alleviated HF symptoms and significantly improved cardiac function (CF); effective: the BP was significantly reduced, with certain improvement in HF symptoms and CF; ineffective: no obvious changes in BP, symptoms, etc., the total effective rate = (markedly effective + effective)/total × 100%); (2) alterations of CF indexes after treatment: left ventricular ejection fraction (LVEF), left atrial pressure (LAP), cardiac index (CI), stroke volume (SV); (3) serum levels of B-type natriuretic peptide (BNP), C-reactive protein (CRP), and mean arterial pressure (MAP) after treatment;

(4) clinical indices: asthma relief time, heart rate recovery (HRR) time, edema resolution time, and hospitalization time; (5) incidence of ARs (incidence of ARs = number of adverse reactions/total number × 100%); (6) psychological quality and pain: psychological quality and pain before and after the intervention were assessed using the self-rating anxiety and depression scale (SAS and SDS) [18] and visual analogue scale (VAS) [19], respectively. The higher the SAS and SDS scores, the more severe the patient's anxiety and depression; the higher the VAS score, the more obvious the patient's pain.

2.6. Statistical Processing. Data processing employed SPSS22.0. The intergroup difference of count data (denoted by percentage) used the chi-square test. The quantitative data were given (mean ± standard deviation), and the t test and paired t test were used to analyze the data that conformed to a normal distribution. For all analyses, differences were significant when P values < 0.05.

3. Results

3.1. Summary of Results. CRRT group exhibited higher overall response rate and better CF than control group ($P < 0.05$), with lower BNP, CRP, and MAP levels, and shorter time of asthma relief, HRR, edema resolution, and hospitalization ($P < 0.05$); the incidence of ARs was similar ($P > 0.05$); for both groups, the scores of SAS, SDS, and VAS reduced statistically after treatment ($P < 0.05$).

3.2. Patients' General Information. Patients' general data, including age, BMI, course of HT, sex, exercise habits, living environment, and ethnicity, were collected. After statistical analysis, we found no statistical difference in general data between groups ($P > 0.05$, Table 1), confirming the experimental comparability of the two groups.

3.3. Therapeutic Effects of Two Groups. After treatment, the number of cases of markedly effective, effective, and ineffective in CRRT group was 18 (54.55%), 13 (39.39%), and 2 (6.06%), respectively, with an overall response rate of 93.94%, versus 75.76% in control group. Apparently, the therapeutic effect was statistically higher in CRRT compared with control group ($P < 0.05$, Table 2).

3.4. Alterations of CF Indexes after Treatment. After treatment, the LVEF of CRRT group was (36.84 ± 7.06)%, higher than that of (33.26 ± 7.49)% in control group ($P < 0.05$, Figure 1(a)); the LAP of CRRT and control group groups was (12.87 ± 4.69) mmHg and (17.54 ± 5.96) L/min/m^2, respectively, indicating a significantly lower posttreatment LAP in CRRT group ($P < 0.05$, Figure 1(b)); the intergroup comparison of CI revealed a higher posttreatment CI in CRRT group compared with control group ($P < 0.05$, Figure 1(c)); finally, it can be seen that the SV value of CRRT group was (63.55 ± 9.70) mL, which was also higher when compared to control group ($P < 0.05$, Figure 1(d)).

3.5. Changes of Clinical Indices. The asthma relief time of CRRT and control groups was (3.7 ± 0.9) d and (5.9 ± 1.1) d, respectively, revealing notably faster asthma relief in patients treated with CRRT ($P < 0.05$, Figure 2(a)). The HRR time of CRRT group was (8.3 ± 1.2) d, shorter than that in control group ($P < 0.05$, Figure 2(b)). Comparing the edema resolution time, we also found that CRRT group took less time to resolve edema than control group ($P < 0.05$, Figure 2(c)). Shorter hospitalization time was also determined in CRRT group compared with control group (16.1 ± 2.4) d vs. (20.7 ± 1.8) d, with statistical significance ($P < 0.05$, Figure 2(d)).

3.6. Serum Indexes and MAP Levels in Both Groups after Treatment. The BNP levels in both cohorts were detected after treatment, and a notably higher BNP level was determined in CRRT group (529.00 ± 65.75) μg/L compared with control group ($P < 0.05$, Figure 3(a)). Similarly, the CRP of CRRT group was (12.40 ± 1.33) mg/L, lower than that of the control group ($P < 0.05$, Figure 3(b)). Finally, the MAP were counted and the results determined a markedly lower MAP in CRRT group versus control group ($P < 0.05$, Figure 3(c)).

3.7. Incidence of ARs in Two Groups. According to statistics, no serious ARs occurred in both cohorts of patients during the treatment. In CRRT group, nausea and vomiting, abdominal pain, hypotension, and gingival bleeding were found in 1 case each, with a total AR rate of 12.12%; while in control group, the above ARs were observed in 2, 2, 0, and 1 case, respectively, with an overall AR rate of 15.15%. The two groups showed no statistical difference in the AR rate ($P > 0.05$, Table 3).

3.8. Alterations of Psychological Quality and Pain in Both Groups before and after Treatment. Both groups showed adverse emotions such as depression and anxiety and strong pain before treatment, with no evident difference in SAS, SDS, and VAS scores ($P > 0.05$). Nor were there any notable differences in the above scores between them after treatment ($P > 0.05$), but compared with the baseline (before treatment), the scores of SAS, SDS, and VAS in both groups reduced statistically ($P < 0.05$, Figures 4(a)–4(c)).

4. Discussion

CRRT, as a blood purification technology widely used in clinical practice, has achieved remarkable results in the cardiovascular field [20]. CRRT has been found to reduce cardiac load, stabilize CF, restore the body's (especially kidney) sensitivity to diuretics, and improve oxygen supply and RHF status [21]. Therefore, an in-depth exploration of the application of CRRT in RHF may provide a more reliable safety guarantee for RHF patients in the future.

In this study, we observed better therapeutic effects in RHF patients treated with CRRT, with significantly improved CF after treatment and shorter time of asthma relief, HRR, and hospitalization, confirming the excellent application effect of CRRT on RHF, which is consistent with the results of previous studies [22, 23]. Compared with routine hemodialysis treatment, CRRT can more effectively remove fluid and stabilize hemodynamics while regulating fluid balance through continuous and slow blood

Table 1: General information.

	CRRT group ($n = 33$)	Control group ($n = 33$)	χ^2 or t/P
Age	69.5 ± 6.2	69.9 ± 6.0	0.266/0.791
BMI (KG/m^2)	27.0 ± 2.5	27.8 ± 1.7	1.520/0.133
Duration of hypertension (years)	5.2 ± 2.0	5.4 ± 1.4	0.668/0.507
Gender			0.062/0.804
Male	19 (57.58%)	18 (54.55%)	
Female	14 (42.42%)	15 (45.45%)	
Exercise habits			0.061/0.806
Yes	17 (51.52%)	16 (48.48%)	
No	16 (48.48%)	17 (51.52%)	
Living environment			0.262/0.609
In the city	20 (60.61%)	22 (66.67%)	
In rural areas	13 (39.39%)	11 (33.33%)	
Nationality			0.569/0.451
Han nationality	30 (90.91%)	28 (84.85%)	
Minority	3 (9.09%)	5 (15.15%)	

Table 2: Clinical curative effects.

Group	n	Markedly effective	Effective	Ineffective	Overall response rate
CRRT group	33	18 (54.55%)	13 (39.39%)	2 (6.06%)	31 (93.94%)
Control group	33	10 (30.30%)	15 (45.45%)	8 (24.24%)	25 (75.76%)
χ^2					4.243
P					0.039[a]

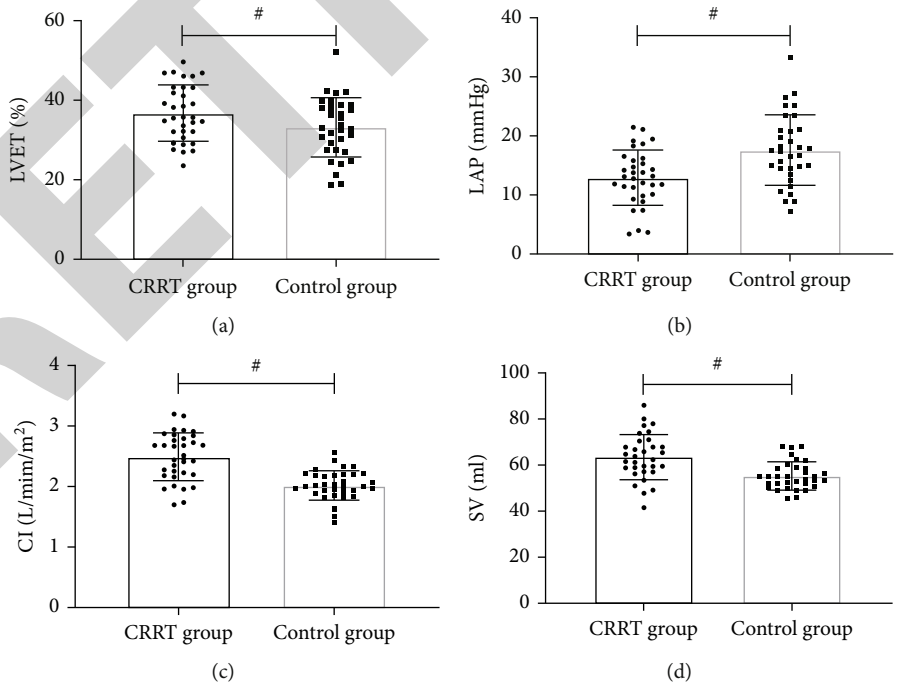

Figure 1: Alterations of CF indexes after treatment. (a) Comparison of LVEF between CRRT group and control group. (b) Comparison of LAP between CRRT group and control group. (c) Comparison of CI between CRRT group and control group. (d) Comparison of SV between CRRT group and control group. Note: # indicates that the difference between the two groups is statistically significant ($P < 0.05$).

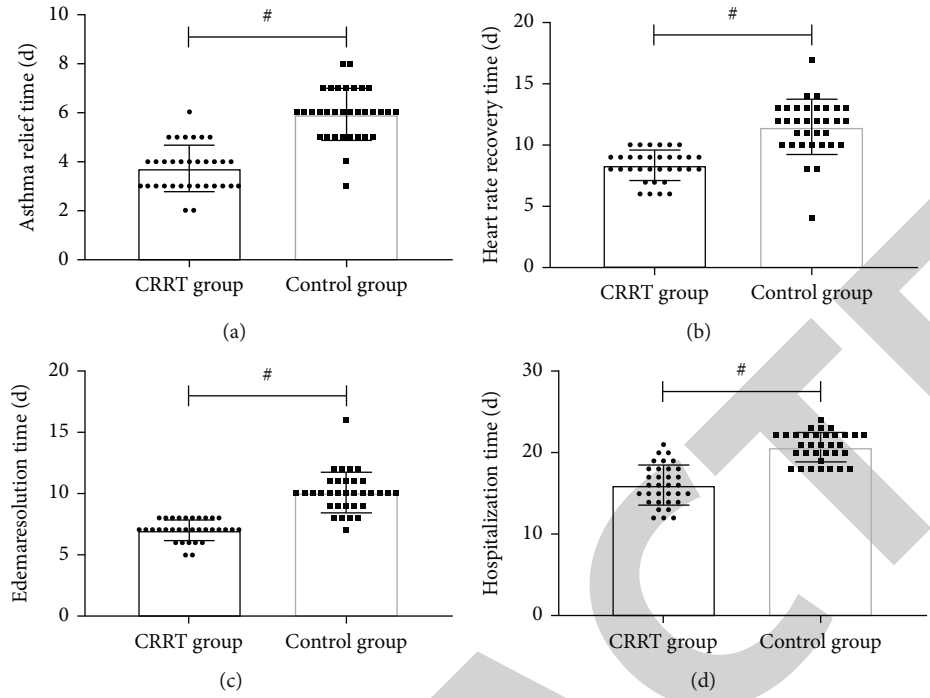

Figure 2: Changes of clinical indices. (a) Comparison of asthma relief time. (b) Comparison of heart rate recovery time. (c) Comparison of edema resolution time. (d) Comparison of hospitalization time. Note: # indicates that the difference between the two groups is statistically significant ($P < 0.05$).

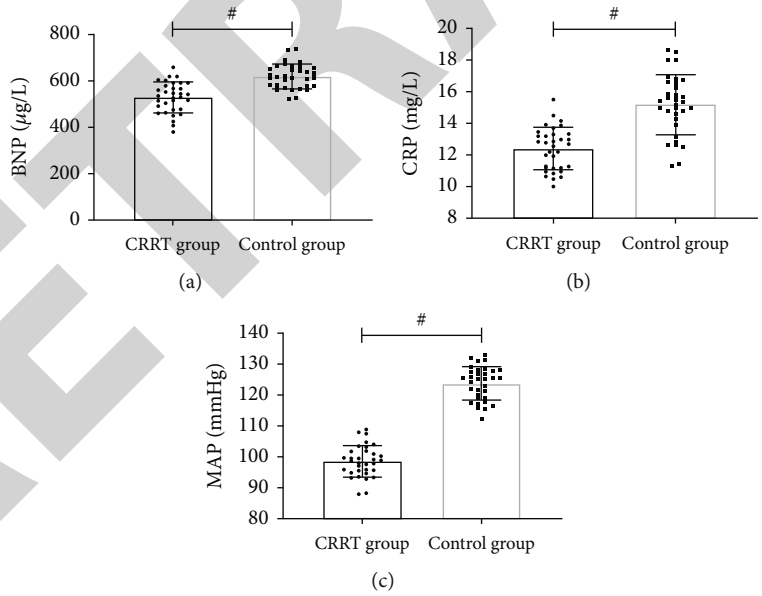

Figure 3: Serum indexes and MAP levels in both groups after treatment. (a) Comparison of BNP between CRRT group and control group. (b) Comparison of CRP between CRRT group and control group. (c) Comparison of MAP between CRRT group and control group. Note: # indicates that the difference between the two groups is statistically significant ($P < 0.05$).

purification, with no obvious impact on the cardiovascular system [24]. Moreover, the hemofilters used in CRRT have the advantages of good compatibility, strong adsorption capacity, and permeability, allowing them to adsorb or remove inflammatory factors as well as small and medium molecular toxins, thus inhibiting the high decomposition state and keeping the balance of water, electrolyte, and acid-base [25]. At the same time, CRRT has the characteristics of favorable safety, high tolerance in patients, and high success rate of treatment and is simple to operate and can

Table 3: Adverse reactions of two groups.

Group	n	Feel sick and vomit	Stomach ache	Low blood pressure	Bleeding gums	ARs
CRRT group	33	1 (3.03%)	1 (3.03%)	1 (3.03%)	1 (3.03%)	4 (12.12%)
Control group	33	2 (6.06%)	2 (6.06%)	0 (0.00%)	1 (3.03%)	5 (15.15%)
χ^2						0.129
P						0.720

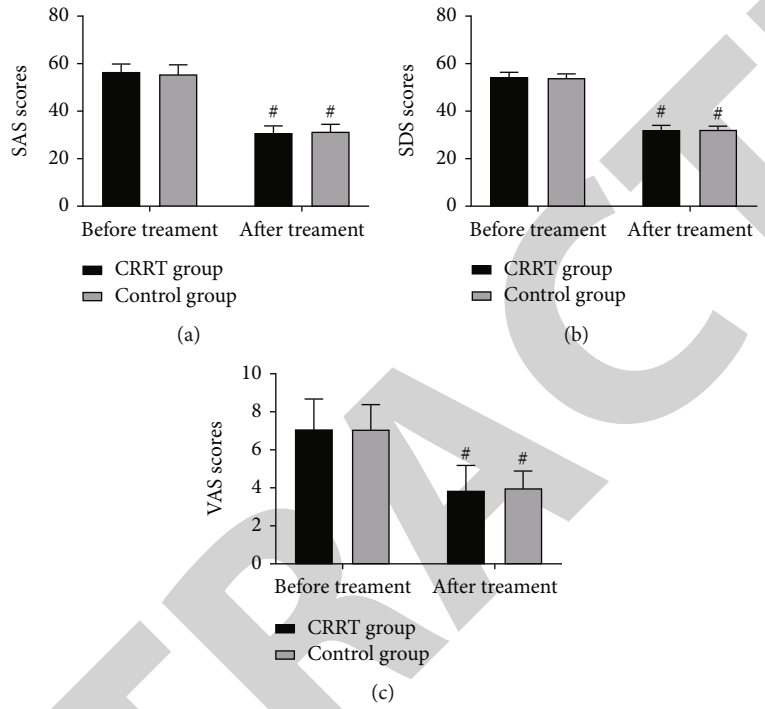

Figure 4: Alterations of psychological quality and pain in both groups before and after treatment. (a) Comparison of SAS scores before and after treatment. (b) Comparison of SDS scores before and after treatment. (c) Comparison of VAS scores before and after treatment. Note: # indicates that there is a statistically significant difference between the same group and the same group before treatment ($P < 0.05$).

be implemented at the bedside, especially for critically ill patients [26]. It is pointed out that the long duration of routine hemodialysis has a great influence on hemodynamics and even the therapeutic effect and may cause arrhythmia, hypotension, and even aggravation of HF and other ARs [27]. This is also consistent with our findings, indicating that CRRT is more suitable for the treatment of RHF. Moreover, CRRT is shown to remove inflammatory mediators released in large quantities due to HF-induced cardiomyocyte injury and necrosis, protect the functions of cardiomyocytes and vascular endothelial cells, and promote the recovery of CF [28], which may be one of the reasons for the better improvement of patients with CRRT. Compared with previous research results [29, 30], the excellent therapeutic effect of CRRT can just make up for the limitations of insufficient clinical treatment plans and poor therapeutic effect for RHF at this stage and provide more reliable treatment services for RHF patients, guaranteeing life safety of RHF patients.

In addition, lower posttreatment BNP, CRP, and MAP were observed in CRRT group versus control group, which can also testify the improvement effect of CRRT on RHF. We believe that CRRT plays the role of solute clearance by means of convection and dispersion and introduces arteriovenous blood into the semipermeable membrane filter with good permeability, in which the small molecular weight solute and water can clear the solute and water through the pressure gradient on both sides of the semipermeable membrane, thus reducing the burden on heart and kidney, keeping blood in a balanced state, restoring myocardial elasticity, improving CF, and reducing the synthesis and release of BNP and inflammatory factors [31–34]. However, its specific mechanism needs to be confirmed by further studies. There was no difference in ARs between the two groups, which indicates that CRRT has good safety. However, an expanded sample size is also needed for confirmation. Finally, since the application of CRRT in RHF is not common at present, targeted nursing strategies are also the focus of clinical attention. Combined with previous research and nursing experience, this study mainly focused on the psychological state, pain, and rehabilitation training of patients treated with CRRT. The experimental results showed decreased scores of SAS, SDS, and VAS in both cohorts after treatment,

which preliminarily indicated the successful implementation of the nursing program. Modern medical services are not only limited to the pathological treatment of patients' diseases but also need to pay attention to the physical and psychological rehabilitation of patients in an all-round way [35, 36]. Therefore, more meticulous, professional, and individualized nursing services play an extremely critical role in it [33, 37]. For RHF patients with more severe disease, difficult treatment and poor prognosis, it is more worthwhile to adopt a unique nursing strategy. The targeted care for CRRT in this study also successfully improved the patient's psychological state and reduced the patient's pain experience during treatment, which is of great significance to improving the current overall medical service. However, due to the lack of nursing guidelines for CRRT at present, there may still be room for improvement in this nursing program. Further research will be carried out on the nursing of RHF patients treated with CRRT.

In future studies, we also need to increase the number of cases and extend the study cycle to evaluate the impact of CRRT on patient outcomes and obtain more comprehensive results. At the same time, the improvement mechanism of CRRT on various functions of RHF patients is still worth further exploring, which will also be the focus of our follow-up research.

5. Conclusion

CRRT can effectively improve the therapeutic effect and CF of patients with HT complicated by RHF, with extremely high clinical application value.

Data Availability

The data presented in this study are available upon request from the corresponding author.

Conflicts of Interest

The authors declare that the research was conducted in the absence of any commercial or financial relationships that could be construed as a potential conflict of interest.

References

[1] G. Lamirault, M. Artifoni, M. Daniel, N. Barber-Chamoux, and Nantes University Hospital Working Group on Hypertension, "Resistant hypertension: novel insights," *Current Hypertension Reviews*, vol. 16, no. 1, pp. 61–72, 2020.

[2] K. E. Di Palo and N. J. Barone, "Hypertension and heart failure: prevention, targets, and treatment," *Heart Failure Clinics*, vol. 16, no. 1, pp. 99–106, 2020.

[3] J. Slivnick and B. C. Lampert, "Hypertension and heart failure," *Heart Failure Clinics*, vol. 15, no. 4, pp. 531–541, 2019.

[4] L. J. Rose-Jones, "Heart failure: advanced refractory heart failure," *FP Essentials*, vol. 506, pp. 31–42, 2021.

[5] M. Griffin, A. Soufer, E. Goljo et al., "Real world use of hypertonic saline in refractory acute decompensated heart failure: a U.S. center's experience," *JACC Heart Failure*, vol. 8, no. 3, pp. 199–208, 2020.

[6] L. Cappannoli, R. Scacciavillani, E. Rocco et al., "Cardiac contractility modulation for patient with refractory heart failure: an updated evidence-based review," *Heart Failure Reviews*, vol. 26, no. 2, pp. 227–235, 2021.

[7] D. Aslan Kutsal, O. Yildirimturk, A. Sungur, M. A. Sungur, M. Kayahan, and B. Gungor, "Peritoneal dialysis for refractory heart failure: a single-center experience," *Therapeutic Apheresis and Dialysis: Official Peer-reviewed Journal of the International Society for Apheresis, the Japanese Society for Apheresis, the Japanese Society for Dialysis Therapy*, 2021.

[8] L. Cappannoli, R. Scacciavillani, E. Rocco et al., "Cardiac contractility modulation: a treatment option for patients with refractory heart failure," *Giornale Italiano di Cardiologia*, vol. 22, no. 3, pp. 212–220, 2021.

[9] A. Pandey, K. V. Patel, M. Vaduganathan et al., "Physical activity, fitness, and obesity in heart failure with preserved ejection fraction," *JACC Heart Failure*, vol. 6, no. 12, pp. 975–982, 2018.

[10] S. Tandukar and P. M. Palevsky, "Continuous renal replacement therapy: who, when, why, and how," *Chest*, vol. 155, no. 3, pp. 626–638, 2019.

[11] K. R. P. Medina-Liabres and S. Kim, "Continuous renal replacement therapy in elderly with acute kidney injury," *The Korean Journal of Internal Medicine*, vol. 35, no. 2, pp. 284–294, 2020.

[12] P. Houzé, F. J. Baud, J. H. Raphalen et al., "Continuous renal replacement therapy in the treatment of severe hyperkalemia: an in vitro study," *The International Journal of Artificial Organs*, vol. 43, no. 2, pp. 87–93, 2020.

[13] D. S. Goumenos, E. Papachristou, and M. Papasotiriou, "Renal replacement therapy in patients with heart and kidney failure," *Prilozi*, vol. 37, no. 2-3, pp. 43–47, 2016.

[14] H. A. Schaubroeck, S. Gevaert, S. M. Bagshaw, J. A. Kellum, and E. A. Hoste, "Acute cardiorenal syndrome in acute heart failure: focus on renal replacement therapy," *European Heart Journal Acute Cardiovascular Care*, vol. 9, no. 7, pp. 802–811, 2020.

[15] I. E. Chazova, "Arterial hypertension in the light of current recommendations," *Terapevticheskiĭ Arkhiv*, vol. 90, no. 9, pp. 4–7, 2018.

[16] M. G. Crespo-Leiro and E. Barge-Caballero, "Advanced heart failure: definition, epidemiology, and clinical course," *Heart Failure Clinics*, vol. 17, no. 4, pp. 533–545, 2021.

[17] R. Antonione, S. Nodari, and M. Fieramosca, "Selection criteria to palliative care implementation in advanced heart failure," *Giornale Italiano di Cardiologia*, vol. 21, no. 4, pp. 272–277, 2020.

[18] T. Yue, Q. Li, R. Wang et al., "Comparison of hospital anxiety and depression scale (HADS) and Zung self-rating anxiety/depression scale (SAS/SDS) in evaluating anxiety and depression in patients with psoriatic arthritis," *Dermatology*, vol. 236, no. 2, pp. 170–178, 2020.

[19] V. Finsen, S. Hillesund, and I. Fromreide, "The reliability of remembered pretreatment visual analog scale scores among hand-surgery patients," *Journal of Hand and Microsurgery*, vol. 12, no. 1, pp. 8–12, 2020.

[20] A. Davenport and P. M. Honore, "Continuous renal replacement therapy under special conditions like sepsis, burn, cardiac failure, neurotrauma, and liver failure," *Seminars in Dialysis*, vol. 34, no. 6, pp. 457–471, 2021.

[21] A. Karkar, "Continuous renal replacement therapy: principles, modalities, and prescription," *Saudi Journal of Kidney Diseases and Transplantation*, vol. 30, no. 6, pp. 1201–1209, 2019.

Hindawi
Computational and Mathematical Methods in Medicine
Volume 2023, Article ID 9805943, 1 page
https://doi.org/10.1155/2023/9805943

Retraction

Retracted: Study on the Effect of Self-Made Lifei Dingchuan Decoction Combined with Western Medicine on Cough Variant Asthma

Computational and Mathematical Methods in Medicine

Received 1 August 2023; Accepted 1 August 2023; Published 2 August 2023

This article has been retracted by Hindawi following an investigation undertaken by the publisher [1]. This investigation has uncovered evidence of one or more of the following indicators of systematic manipulation of the publication process:

(1) Discrepancies in scope

(2) Discrepancies in the description of the research reported

(3) Discrepancies between the availability of data and the research described

(4) Inappropriate citations

(5) Incoherent, meaningless and/or irrelevant content included in the article

(6) Peer-review manipulation

The presence of these indicators undermines our confidence in the integrity of the article's content and we cannot, therefore, vouch for its reliability. Please note that this notice is intended solely to alert readers that the content of this article is unreliable. We have not investigated whether authors were aware of or involved in the systematic manipulation of the publication process.

Wiley and Hindawi regrets that the usual quality checks did not identify these issues before publication and have since put additional measures in place to safeguard research integrity.

We wish to credit our own Research Integrity and Research Publishing teams and anonymous and named external researchers and research integrity experts for contributing to this investigation.

The corresponding author, as the representative of all authors, has been given the opportunity to register their agreement or disagreement to this retraction. We have kept a record of any response received.

References

[1] J. Li, Z. Huang, K. Li, X. Jian, and B. Liang, "Study on the Effect of Self-Made Lifei Dingchuan Decoction Combined with Western Medicine on Cough Variant Asthma," *Computational and Mathematical Methods in Medicine*, vol. 2022, Article ID 9803552, 8 pages, 2022.

Hindawi
Computational and Mathematical Methods in Medicine
Volume 2022, Article ID 9803552, 8 pages
https://doi.org/10.1155/2022/9803552

Research Article

Study on the Effect of Self-Made Lifei Dingchuan Decoction Combined with Western Medicine on Cough Variant Asthma

Jiachun Li,[1] **Ziliang Huang**,[2,3] **Keying Li**,[4] **Xiaoyun Jian**,[1] **and Binghui Liang**[1,4]

[1]*Department of Respiratory Medicine, Foshan Hospital of Traditional Chinese Medicine, Guangzhou University of Traditional Chinese Medicine, Foshan, Guangdong 528000, China*
[2]*The Third School of Clinical Medicine, Guangzhou University of Chinese Medicine, Guangzhou, Guangdong 510145, China*
[3]*Department of Traditional Chinese Medicine, The Sixth Affiliated Hospital of Guangzhou Medical University, Qingyuan People's Hospital, Qingyuan, Guangdong 511518, China*
[4]*The Eighth School of Clinical Medicine, Guangzhou University of Chinese Medicine, Foshan, Guangdong 528000, China*

Correspondence should be addressed to Jiachun Li; lijiach25@163.com

Received 27 June 2022; Revised 1 August 2022; Accepted 23 August 2022; Published 12 September 2022

Academic Editor: Min Tang

Aims. To observe the clinical efficacy of self-made Lifei Dingchuan decoction combined with western medicine in the treatment of cough variant asthma (phlegm-heat accumulation in the lung syndrome). *Materials and Methods*. The clinical data of 90 patients with cough variant asthma who were hospitalized in the Department of Respiratory Medicine of our hospital from January 2020 to April 2022 were selected as the research objects, and they were equally divided into the observation group and the reference group according to different treatment methods, 45 cases in each group. The group was treated with traditional montelukast sodium chewable tablet and salmeterol fluticasone mixed powder inhalation, and the observation group was treated with self-made Lifei Dingchuan decoction on the basis of the control group, saturation, pH, partial pressure of oxygen in arterial blood, partial pressure of carbon dioxide, length of stay, and hospitalization costs. *Results*. After the patients underwent self-made Lifei Dingchuan decoction, there were significant differences between the observation group and the reference group in terms of heart rate, respiratory rate, blood oxygen saturation, pH value, arterial blood oxygen partial pressure, carbon dioxide partial pressure, and within the group. There was a statistical difference ($P < 0.05$). The adverse reactions in patients with cough variant asthma after treatment showed that the red throat, shortness of breath, chest tightness, and dry mouth in the observation group were significantly different from those in the control group ($P < 0.05$). After investigation, follow-up, and statistics, the hospitalization time, hospitalization cost, asthma exacerbation control time, effective rate, and recurrence rate were compared between the two groups, and the differences between the two groups were statistically significant ($P < 0.05$). *Conclusion*. The study on the clinical efficacy and low hospitalization cost of the self-prepared lung and asthma-restorative soup in patients with cough variant asthma significantly improved the patients' arterial oxygen saturation, acid-base value, arterial partial pressure of oxygen, and partial pressure of carbon dioxide and effectively controlled the heart rate and respiratory rate with high safety, which is worth further promotion.

1. Introduction

Cough variant asthma (CVA) is one of the most frequent respiratory diseases. Cough variant asthma is a specific type of asthma in which cough is the only or main clinical manifestation without obvious signs or symptoms such as wheezing and shortness of breath, but with airway hyperresponsiveness. The main manifestation is an irritating dry cough [1]. The cough is usually more intense, with nocturnal cough as its important feature, and severe cases are accompanied by chest tightness and shortness of breath [2]. The incidence of CVA has been increasing year by year in recent years, and 41.95% of all chronic cough patients in China in 2021 were further developed from CVA [3]. It is highly likely that nearly 30%

of patients with CVA without clinical diagnosis and treatment will eventually develop and evolve into typical asthma [4].

At present, it is believed that the pathogenesis of this disease is similar to that of typical asthma. The etiology includes genetic factors, allergic factors, infectious factors, and a series of physical and chemical factors. It has the physiological and pathological characteristics of chronic airway inflammation, airway remodeling, and airway hyperresponsiveness. It may be related to the sensitization of cough receptors and the increased wheezing threshold. Commonly used therapeutic drugs include inhaled corticosteroids (ICS), leukotriene receptor antagonists, bronchodilators, antihistamines, mast cell membrane stabilizers, macrolides, expectorants, and immunomodulators and have curative effect on CVA, but long-term use will produce side effects, and the recurrence rate is high once it is stopped. In addition, nondrug treatment methods such as specific immunotherapy will be used clinically. Although it is expected to cure the disease, the course of treatment is long, and the compliance of children is poor.

Cough variant asthma belongs to the category of cough, whooping cough, and pharyngogenic cough in Chinese medicine. In recent years, TCM has conducted some research on its mechanism and treatment, and certain progress has been made [5]. Traditional Chinese medicine has accumulated rich experience in the diagnosis and treatment of pulmonary cough and asthma and has formed a large number of effective prescriptions and medicines [6]. Modern TCM studies have shown significant efficacy in improving the clinical symptoms of CVA patients [7]. The results of Chinese medicine compound for the treatment of cough variant asthma suggest that it has a certain inhibitory effect on the pathological changes such as airway hyperreactivity, chronic allergic inflammation of airways, and bronchospasm in cough variant asthma [8].

2. Material and Methods

2.1. Research Object. This study included 90 patients with cough variant asthma who were hospitalized in the Department of Respiratory Medicine of our hospital from January 2018 to April 2022 as the research subjects, and were divided into an observation group and a reference group with 45 cases in each group. The age group is between 18 and 65 years old. Western medicine diagnostic criteria for cough variant asthma: referring to the 2016 Guidelines for the Diagnosis and Prevention of Bronchial Asthma by the Respiratory Group of the Chinese Medical Association, the diagnostic criteria for CVA were formulated: (1) cough persisted for >4 weeks, often during exercise and at night and (or) early morning onset or aggravation, mainly dry cough without wheezing; (2) no signs of clinical infection or ineffective after prolonged antibiotic treatment; (3) effective antiasthma drug diagnostic treatment; (4) to exclude chronic cough caused by other causes; (5) positive bronchial provocation test and (or) PEF day – to – day variability rate (continuous monitoring for 2 weeks) ≥ 13%; (6) personal or first- and second-degree relatives with a history of allergic diseases or allergen test positive. As there is no unified standard for TCM syndrome differentiation of cough variant asthma in China, the TCM diagnostic criteria are based on preliminary clinical observation and review of literature on cough variant asthma syndrome research in recent years. The national planning textbooks "Traditional Chinese Medicine" and "Traditional Chinese Medicine Clinical Diagnosis and Treatment Guidelines-Cough Variant Asthma" published in "Journal of Traditional Chinese Medicine" in 2016 [9] formulate the TCM diagnostic criteria for cough variant asthma: (1) recurrent cough, it was paroxysmal and aggravated at night, in the morning or after activities; (2) expectoration with thick yellowish sputum. (3) Throat red (swollen), shortness of breath, chest tightness, dry mouth, dry stool (or) constipation, yellow urine, red tongue, and yellow greasy coating.

2.2. Include Exclusion Criteria. Inclusion criteria [9]: (i) meeting the above diagnostic criteria for cough variant asthma in Western medicine, meeting the diagnostic criteria in TCM and the TCM evidence of phlegm-heat in the lung; (ii) no obvious signs of infection at the time of inclusion in the trial, informed consent of the legal guardian to be tested; (iii) voluntary cooperation with the study, hospitalization days > 1 d. Exclusion criteria: (i) combined with other primary diseases of the lung, combined with serious primary diseases of the heart, liver, kidney, and hematopoietic system, psychiatric patients diseases, and psychiatric patients; (ii) those with other pathologies that reduce the likelihood of enrollment or complicate enrollment according to the investigator's judgment, those who had already taken Chinese and Western medicine for cough within 12 hours before the visit; (iii) those who were participating in clinical trials of other drugs and those with poor compliance that could easily cause shedding.

2.3. Methods. The reference group was treated with nasal catheter oxygen and conventional montelukast sodium tablets and salmeterol fluticasone mixed powder inhaler and oral montelukast sodium (Merck Sharp & Dohme Limited National Quota J20130054). Dosage: 10 mg/dose, 1 time daily, nightly at bedtime. Salmeterol fluticasone mixed powder inhaler, one inhalation in the morning and one in the evening every day, after the cough improved to once daily inhalation, the course of treatment for 1 month. In the observation group, the treatment was based on the control group, i.e., 10 g of roasted ephedra, 10 g of dilaemon, 10 g of bitter almonds, 10 g of scape seeds, 10 g of perilla seeds, 10 g of semen, 10 g of Qianhu, 10 g of mulberry bark, 10 g of Scutellaria, and 10 g of Yujin. During the treatment period, all other Chinese and Western medicine drugs for CVA were stopped. Patients were advised to prevent colds, eat a light diet, relax their emotions, exercise appropriately, avoid eating fatty, sweet, greasy and sizzling products, avoid raw and cold food, and avoid contact with any allergens as much as possible.

2.4. Statistical Analysis. SPSS 27.0 statistical software was used for analysis. Count data were expressed as the number of cases, and differences between the three groups were compared using chi-square test. If the measurement data obeyed normal distribution and the variance between the groups

Table 1: Comparison of baseline data of two groups of patients.

Group	Average age (years)	Gender (men and women)	Common causes (n (%))				
			Exposure to allergens	Exposure to irritants	Allergic rhinitis	Respiratory infection	Premature withdrawal
Reference group (45)	47.91 ± 3.71	25/20	5 (11.11)	9 (20.00)	7 (15.56)	5 (11.11)	6 (13.33)
Observation group (45)	49.16 ± 5.62	22/23	8 (17.78)	6 (13.33)	4 (8.89)	6 (13.33)	9 (20.00)
t	-4.608	0.943			0.000		
P	0.115	0.445			1.000		

was the same, the data were expressed as mean ± standard deviation, and the differences between groups were compared using one-way ANOVA, and if the sample our data did not meet several conditions mentioned above, the data were expressed as median/interquartile spacing, and the comparison between the three groups was done using multiple independent sample our rank sum test (Kruskal-Wallis H test) with the test level $a = 0.05$.

3. Results

3.1. Baseline Data Comparison. The average age, gender, and common causes of patients in the observation group were not significantly different from those in the reference group, and the differences were not statistically significant ($P > 0.05$) (see Table 1).

3.2. Evaluation of Clinical Efficacy. There were statistically significant differences in heart rate, respiratory rate, oxygen saturation, acid-base value, arterial partial pressure of oxygen, and partial pressure of carbon dioxide between groups and within groups in the observation group and the reference group ($P < 0.05$). This result indicates a better clinical efficacy (see Figure 1).

3.3. Treatment Safety Evaluation. Drug toxicities after treatment in patients with cough variant asthma showed that symptoms such as red throat, shortness of breath, chest tightness, and dry mouth in the observation group were significantly different from those in the control group ($P < 0.05$). This result indicates a better treatment safety (see Figure 2).

3.4. Treatment Benefit Analysis. There were statistically significant differences between the two groups in terms of length of stay, hospital costs, time to control asthma exacerbation, efficiency, and recurrence rates ($P < 0.05$). This result indicates a better treatment benefit score for the treatment (see Figure 3).

4. Discussion

Most scholars believe that similar to typical asthma, on the one hand, the patient's own congenital constitution, "genetic quality," immune status, mental state, health status, and other subjective factors, in addition to allergens, bacterial and viral infections, changes in climate, excessive exercise, occupational environment, and food and drugs, may be factors that promote the occurrence, and the pathogenesis of CVA is complex and clinically unclear, and studies have found that CVA and typical asthma have similar pathological features [10], such as the presence of specific inflammatory patterns and airway remodeling [12]. CVA patients only cough without wheezing, and there are nowadays three explanations for this phenomenon: the degree of ASR is lower in CVA compared to asthma, the wheezing threshold of CVA causing wheezing, and the coughing receptor sensitivity is also increased [13]. The bronchoconstriction reflex and the cough reflex are two interrelated and independent types of reflexes, and most of their cough receptors are present in the patient's airways, which are physically stimulated by the deformation of the airways due to bronchoconstriction and chemically stimulated by inflammatory mediators [14]. This causes the clinical symptoms of cough in patients, and the absence of cough receptors in the small airways will only result in contracture of the airways during an asthma attack, which will result in wheezing symptoms and croup in the lungs [15].

CVA is a specific type of asthma with chronic cough as the main clinical symptom, and its physiopathology is characterized by airway hyperresponsiveness, chronic airway inflammation, and airway remodeling. The pathogenetic factors are not clear, but are currently thought to be closely related to genetic factors, infectious factors, allergic factors, and some physicochemical factors. Because its clinical symptoms sometimes manifest only as cough, parents are very likely to ignore it or treat it as a simple cough, resulting in failure to treat or mistreatment and further development of typical asthma. Western medical treatment is similar to that of bronchial asthma and is graded. Commonly used drugs include low doses of ICS, leukotriene receptor antagonists, B2 agonists, and H2 receptor antagonists. Long-term use of hormones can produce many adverse effects, such as affecting the people's growth and development, bone metabolism, and immune function. Inhaled glucocorticoids can also cause oral Candida infections. Many scholars now believe that leukotriene receptor antagonists have comparable efficacy with ICS and advocate the use of leukotriene receptor antagonists instead of inhaled glucocorticoids as the drug of choice during cough variant asthma exacerbations. However, montelukast sodium as a representative drug of leukotriene receptor antagonists also has some problems, such as being more expensive and producing side effects such as allergy, diarrhea, and headache. In contrast, Chinese herbal medicine has the advantages of being cheaper and having fewer adverse effects when taken for a long time to treat this disease.

We studied that phlegm-heat-contained lung disease is a common type of this disease, once sick, the disease evil is easy to turn heat from Yang, so having the most heat

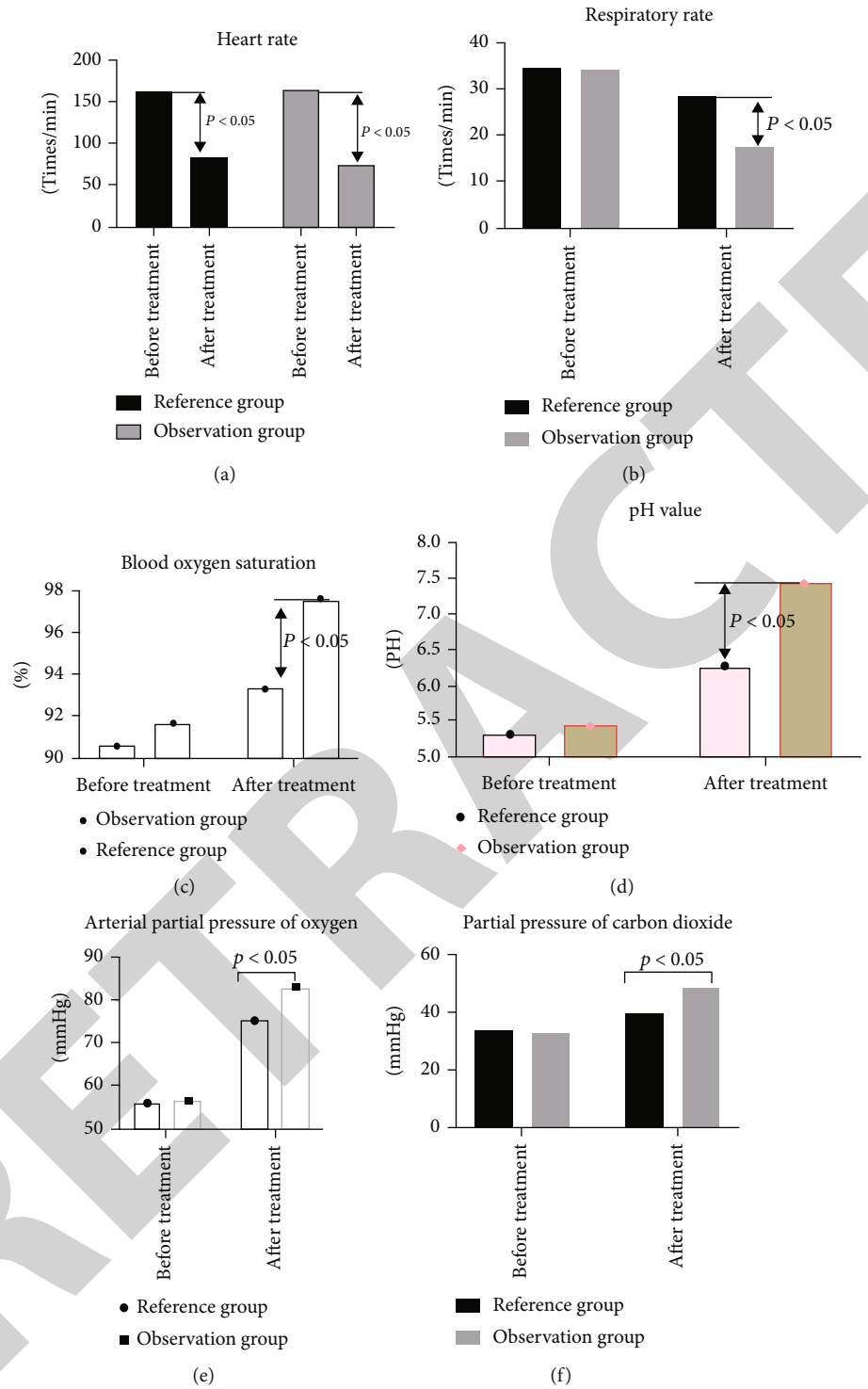

Figure 1: Evaluation of clinical efficacy; in our study, data on evaluation of clinical efficacy was statistically analyzed and calculated using SPSS 26.00 statistical software. The measured data were expressed as median, and the analysis of variance using repeated measures showed that patients underwent after Feidingchuan decoction; the heart rate, respiratory rate, blood arterial oxygen saturation, pH value, arterial blood oxygen partial pressure, and carbon dioxide partial pressure between the observation group and the reference group were significantly different between and within the group, with statistical differences ($P < 0.05$).

evidence, whenever the regulation is not proper, it is easy to feel the external evil, and the external evil inside turns fire into heat [16]. The lung is a delicate organ with a clear deficiency, and it is not resistant to phlegm and heat, so the lung loses its ability to declaim and descend, resulting in cough due to Qi rebellion [17]. With deficiencies in the lungs, spleen, and kidneys, prolonged illness leads to deficiency, irregular elevation of the lungs, failure of the spleen to

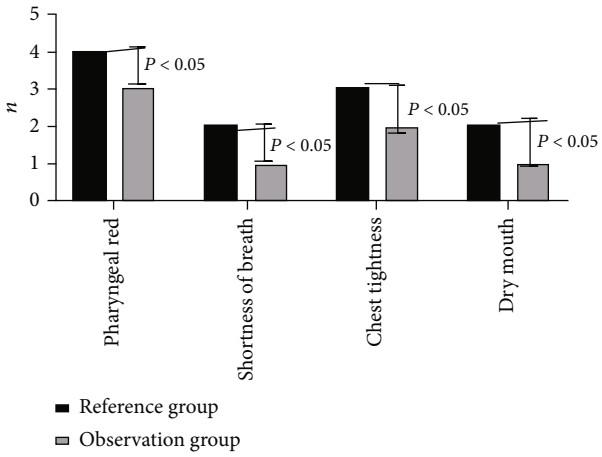

Figure 2: Treatment safety evaluation; in our study, data on treatment safety evaluation was statistically analyzed and calculated using SPSS 26.00 statistical software. The measured data were expressed as median, and the analysis of variance using repeated measures showed that with cough variant asthma, the drug toxicity and side effects of the patients after treatment showed that the red throat, shortness of breath, chest tightness, and dry mouth in the observation group were significantly different from those in the control group ($P < 0.05$).

exercise and transport, and inability of the kidneys to transpire, resulting in stagnation of fluids, phlegm, and phlegm-heat interconnection and phlegm-qi rebellion, leading to cough [18]. Therefore, those with CVA with phlegm-heat-infused lung type often have recurrent cough, especially at night, and are often accompanied by real hot symptoms such as thick sputum, red face and lips, thirst, yellow urine, and constipation [19]. Based on our years of clinical experience, we combined the etiology and pathogenesis of CVA and established the treatment rules, focusing on clearing the lung and resolving phlegm, lowering qi, relieving cough, and calming asthma, and applied the self-prepared Rational Lung and Asthma Determining Tang to treat the evidence of phlegm and heat in the lung of CVA [20]. Self-designed Ruling Lung and Asthma Tang is derived from the combination of Self-designed Ruling Lung and Asthma Tang and Self-designed Ruling Lung and Asthma Tang [21]. This formula is the most typical one in the treatise on typhoid fever, and it is used to treat sun diseases in which sweating does not work or is misdirected as the lower evil qi enters the lung and turns into heat, which is smothered in the lung [22]. Pu Fu-Chou, a famous Chinese medicine practitioner, said that the self-prepared Rational Lung and Asthma Determining Soup can be used both to manage cold qi and to bring down fire qi, or for anyone with uncontrollable sweating [23]. It has therapeutic effects such as clearing heat and promoting lung-heating to stop coughing and calm asthma and is mainly used for coughing and shortness of breath caused by external internal heat and can be used for coughing and heat caused by wind and cold foreign to the interior [24]. It can be used for coughing and shortness of breath caused by heat entering the lungs from the wind and cold [25].

As a traditional ancient formula in Fushou Jingmen-Phlegm Gate, it is clearly stated in the original text that "specializes in treating snooze and asthma, with very rapid results [26]." It has the effect of promoting the lung and lowering qi, clearing heat, and resolving phlegm and can be used to treat asthma with phlegm-heat stagnation in the lung and can be used for asthmatic cough with croupy sound in the larynx or with vicious chills and fever, which is a symptom of wind-cold external bundle and phlegm-heat internal accumulation [27]. All of the self-prepared Ruling the Lung and Fixing Asthma Tang can treat the imbalance of the declination and purification of the lung qi and can also be clinically applied to some respiratory diseases with heat congestion in the lung [28]. The main pathogenic factor of Self-Designed Luling and Asthma Determining Tang is the external wind-cold evil, and Self-Designed Luling and Asthma Determining Tang is the phlegm evil, and this formula is formed by combining the two after cutting them according to experience, which can be effective in clearing the lung and resolving phlegm, lowering qi, and relieving cough and asthma.

Our study found that after the patients had undergone self-preparation of Ruling Lungs and Asthma Treatment Tang, there were significant differences in heart rate, respiratory rate, blood arterial oxygen saturation, acid-base value, arterial partial pressure of oxygen, and partial pressure of carbon dioxide between the observation group and the reference group, and there were statistically significant differences in adverse reactions after treatment in patients with cough variant asthma, including red throat, shortness of breath, chest tightness, and dry mouth in the observation group compared with the reference group. This indicates the clinical efficacy and low hospitalization cost of the self-prepared lung and asthma treatment for patients with cough variant asthma, which significantly improved the patients' arterial oxygen saturation, acid-base value, arterial partial pressure of oxygen, and partial pressure of carbon dioxide and effectively controlled the heart rate and respiratory rate with high safety. The main efficacy and mechanism of action of the self-prepared lung stabilization soup we studied are as follows: to treat the lung, we need to resolve the depression of lung qi and restore the normal elevation function of lung qi [29]. In this formula, sizzling ephedra is pungent and dispersing to promote the lung and bitter to lower the qi, which is the key medicine to promote the lung, open the coup, open the hairy orifices, promote the lung health, make the lung qi smooth, and restore the normal function of the lung division of suction and descent. Di Long is cold and descending, penetrating the upper and lower, good at enlightening the upper and declaring and lowering lung qi, draining lung heat and relieving cough and asthma, draining the lower, opening the state capital, and removing dampness and drenching [31]. The combination of the two drugs, one cold and one warm, one ascending and one descending, and the reasonable use of Xuan Dao and Tongluo, can make the evil of dampness and heat go away from the bottom. Bitter almonds, scape seeds, perilla seeds, and half-xia all have the effect of lowering qi, resolving phlegm, and relieving cough and asthma. Bitter almonds are bitter to lower the qi, moisten the stool, and warm to cathartic, while ephedra is pungent and dispersing, favoring the surface, and bitter almonds are bitter and descending, favoring the lining,

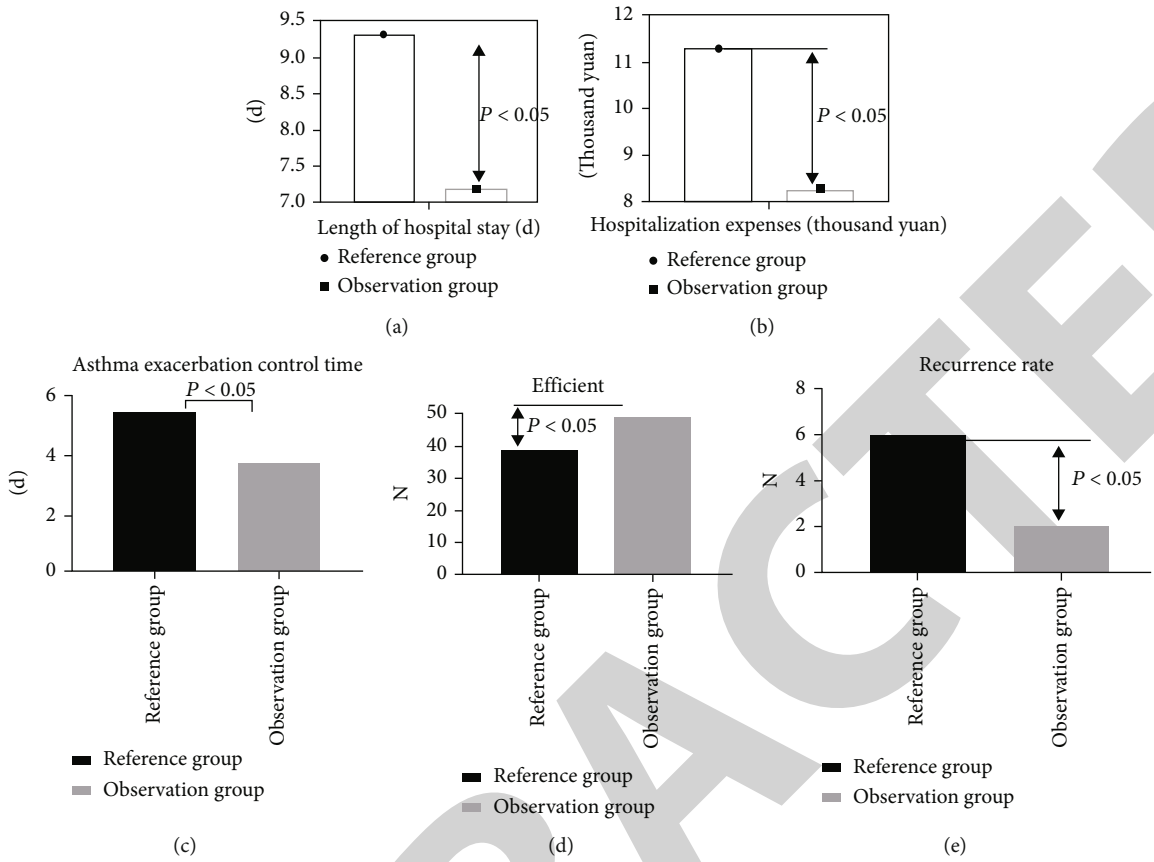

Figure 3: Analysis of treatment benefit; in our study, data on treatment benefit analysis was statistically analyzed and calculated using SPSS 26.00 statistical software. The measured data were expressed as median, and the analysis of variance using repeated measures showed that after survey follow-up and statistics, the hospitalization time, hospitalization cost, asthma exacerbation control time, effective rate, and recurrence rate of the patients in the two groups were significantly different between and within the group ($P < 0.05$).

which can restore the cathartic effect of lung qi and enhance the effect of ephedra in relieving cough and asthma. Daphne scabra is pungent and cold, smooth and downward, bitter and cold and subduing, and is specialized in dipping watery drinks and phlegm fire in the lung to calm cough and asthma. Perilla seeds are smooth and straight down and are mainly descending in nature, and are good at lowering lung qi and resolving phlegm and saliva; when qi is lowered and phlegm is eliminated, cough and asthma will be calmed. The combination of Radix Panax notoginseng, dampness, phlegm, and reversion can help Zizyphus to lower qi, resolve phlegm, and calm asthma, and the combination with almond can strengthen the function of suction. Scutellaria baicalensis, Morinda citrifolia, Qianhu, and Yujin are the adjuvants. Scutellaria baicalensis is bitter-cold in nature and enters the lung meridian to clear the heat in the upper jiao, so it is used with the pungent and warm Radix Panax notoginseng, which is used to clear heat and dispel phlegm [35]. The bitter cold of Scutellaria baicalensis and the warmth of Ephedra are mutually restrained, which enhances its effect on asthma without contributing to internal heat and does not cause the cold of Scutellaria baicalensis to deeply stagnate in the body and stagnate the qi, which can clear lung heat, dissolve phlegm and dampness, and relieve cough and asthma [36]. Mulberry bark, which is sweet in taste and cold in nature, can clear lung heat and relieve asthma as its main action. Mulberry bark, which can stabilize vital energy and compensate for deficiency by replenishing deficiencies, is usually used mainly to clear lung heat as well as relieve cough [37]. In combination with Scutellaria baicalensis, the heat-releasing power is even greater, and the sweet taste and cold nature of mulberry bark can counteract the bitter taste of Scutellaria baicalensis, clearing lung heat without harming Yin. Qian Hu descends Qi and dissolves phlegm, expels wind-heat, and is an important medicine for treating phlegm and Qi, and its use with ephedra's cold and heat can strengthen its power to expel lung heat [38]. It is pungent and can disperse, which can open the lung Jin's depression, release the depressed qi, and remove the fire evil then the cough will heal itself.

Our study is a retrospective randomized controlled study, and although it has some advantages in etiological inference, our study still has the following shortcomings. First, our study is a case-control study, not a randomized controlled trial, and is not blinded, so there is still some risk of bias; second, our study is a single-center clinical study, and the sample size included is small, and it still needs to be followed up by increasing the sample size and conducting multicenter. Finally, the clinical follow-up period of our study was relatively short, and long-term clinical follow-up is still needed.

In conclusion, the study of the clinical efficacy and low hospitalization cost of the self-prepared lung and asthma-restorative soup in patients with cough variant asthma significantly improved the patients' arterial oxygen saturation, acid-base value, arterial partial pressure of oxygen, and partial pressure of carbon dioxide and effectively controlled the heart rate and respiratory rate with high safety, which is worth further promotion.

Data Availability

No data were used to support this study.

Conflicts of Interest

The authors declare that they have no conflicts of interest.

Authors' Contributions

Jiachun Li and Ziliang Huang contributed to this work equally.

Acknowledgments

This work was supported by the Foshan Science and Technology Innovation Project (grant no. 2018AB001321) and Scientific Research Projects of Administration of Traditional Chinese Medicine of Guangdong Province (grant no. 20201341).

References

[1] Y. Luo, C. Z. Wang, J. Hesse-Fong, J. G. Lin, and C. S. Yuan, "Application of Chinese medicine in acute and critical medical conditions," *The American Journal of Chinese Medicine*, vol. 47, no. 6, pp. 1223–1235, 2019.

[2] L. M. Chavez, S. S. Huang, I. Mac Donald, J. G. Lin, Y. C. Lee, and Y. H. Chen, "Mechanisms of acupuncture therapy in ischemic stroke rehabilitation: a literature review of basic studies," *International Journal of Molecular Sciences*, vol. 18, no. 11, p. 2270, 2017.

[3] Y. Du, L. Zhang, W. Liu et al., "Effect of acupuncture treatment on post-stroke cognitive impairment: a randomized controlled trial," *Medicine (Baltimore)*, vol. 99, no. 51, article e23803, 2020.

[4] L. Lu, X. G. Zhang, L. L. Zhong et al., "Acupuncture for neurogenesis in experimental ischemic stroke: a systematic review and meta-analysis," *Scientific Reports*, vol. 6, no. 1, article 19521, 2016.

[5] Q. Cui, Y. L. Zhang, Y. H. Ma et al., "A network pharmacology approach to investigate the mechanism of Shuxuening injection in the treatment of ischemic stroke," *Journal of Ethnopharmacology*, vol. 257, article 112891, 2020.

[6] L. L. D. Zhong, W. Kun, N. Shi et al., "Evidence-based Chinese medicine clinical practice guideline for stroke in Hong Kong," *Chinese Medicine*, vol. 15, no. 1, p. 116, 2020.

[7] W. Yang, M. Q. Li, Y. Li et al., "Exploring Chinese medicine and Western medicine group modules in acute phase of ischemic stroke disease," *Zhongguo Zhong yao za zhi= Zhongguo Zhongyao Zazhi= China Journal of Chinese Materia Medica*, vol. 43, no. 3, pp. 618–626, 2018.

[8] Y. Zhou, J. Liao, Z. Mei, X. Liu, and J. Ge, "Insight into crosstalk between ferroptosis and necroptosis: novel therapeutics in ischemic stroke," *Oxidative Medicine and Cellular Longevity*, vol. 2021, Article ID 9991001, 19 pages, 2021.

[9] F. Xiaochun, D. Xiaozheng, S. Liping, L. Shuangzhu, W. Rui, and L. Jian, "Guidelines for clinical diagnosis and treatment of s in traditional Chinese medicine's cough variant asthma (development)," *Journal of Pediatrics of Traditional Chinese Medicine*, vol. 12, no. 5, pp. 1–4, 2016.

[10] J. Zhang, C. Lu, X. Wu, D. Nie, and H. Yu, "Neuroplasticity of acupuncture for stroke: an evidence-based review of MRI," *Neural Plasticity*, vol. 2021, Article ID 2662585, 14 pages, 2021.

[11] Y. Yu, G. Zhang, J. Liu, T. Han, and H. Huang, "Network meta-analysis of Chinese patent medicine adjuvant treatment of poststroke depression," *Medicine (Baltimore)*, vol. 99, no. 31, article e21375, 2020.

[12] S. C. Donnelly, "Traditional Chinese medicine treatment post-stroke and a significant reduction in presentation to healthcare providers," *QJM: An International Journal of Medicine*, vol. 112, no. 6, p. 397, 2019.

[13] Y. Yang, M. Zhang, J. Zhao, S. Song, F. Hong, and G. Zhang, "Effect of traditional Chinese medicine emotional therapy on post-stroke depression: a protocol for systematic review and meta-analysis," *Medicine (Baltimore)*, vol. 100, no. 14, article e25386, 2021.

[14] W. Cai, C. Mueller, Y. J. Li, W. D. Shen, and R. Stewart, "Post stroke depression and risk of stroke recurrence and mortality: a systematic review and meta-analysis," *Ageing Research Reviews*, vol. 50, pp. 102–109, 2019.

[15] J. Wang, J. Pei, D. Khiati et al., "Acupuncture treatment on the motor area of the scalp for motor dysfunction in patients with ischemic stroke: study protocol for a randomized controlled trial," *Trials*, vol. 18, no. 1, p. 287, 2017.

[16] J. Li, M. Yuan, Y. Liu, Y. Zhao, J. Wang, and W. Guo, "Incidence of constipation in stroke patients: a systematic review and meta-analysis," *Medicine (Baltimore)*, vol. 96, no. 25, article e7225, 2017.

[17] W. Peng, R. Lauche, C. Ferguson, J. Frawley, J. Adams, and D. Sibbritt, "Efficacy of Chinese herbal medicine for stroke modifiable risk factors: a systematic review," *Chinese Medicine*, vol. 12, no. 1, pp. 1–29, 2017.

[18] M. J. Zeng, L. J. Li, and Z. Q. Wu, "Chinese herbal medicine Buyang Huanwu decoction combined with acupuncture to treat sequela of apoplexy: a meta-analysis of randomized controlled trials," *Annals of Palliative Medicine*, vol. 10, no. 2, pp. 1685–1692, 2021.

[19] A. L. Yang, Q. H. Liang, H. J. Cui, H. J. Zhou, J. K. Luo, and T. Tang, "Angiogenesis opens a way for Chinese medicine to treat stroke," *Chinese Journal of Integrative Medicine*, vol. 19, no. 11, pp. 815–819, 2013.

[20] Y. X. Wang, L. T. Wang, Z. W. Huang, T. L. Li, and X. F. Ouyang, "Effectiveness of traditional Chinese medicine in treating gastrointestinal dysfunction in patients with acute stroke: a systematic review and meta-analysis of 16 randomized controlled trials," *Annals of Palliative Medicine*, vol. 10, no. 11, pp. 11808–11820, 2021.

[21] Z. Junhua, F. Menniti-Ippolito, G. Xiumei et al., "Complex traditional Chinese medicine for poststroke motor dysfunction: a systematic review," *Stroke*, vol. 40, no. 8, pp. 2797–2804, 2009.

Hindawi
Computational and Mathematical Methods in Medicine
Volume 2023, Article ID 9850396, 1 page
https://doi.org/10.1155/2023/9850396

Retraction

Retracted: The Relationship between Angiotensin–Neprilysin Treatment, Echocardiographic Parameters, and NT-proBNP Levels in HFpEF Patients with Acute Decompensated Heart Failure

Computational and Mathematical Methods in Medicine

Received 5 December 2023; Accepted 5 December 2023; Published 6 December 2023

This article has been retracted by Hindawi, as publisher, following an investigation undertaken by the publisher [1]. This investigation has uncovered evidence of systematic manipulation of the publication and peer-review process. We cannot, therefore, vouch for the reliability or integrity of this article.

Please note that this notice is intended solely to alert readers that the peer-review process of this article has been compromised.

Wiley and Hindawi regret that the usual quality checks did not identify these issues before publication and have since put additional measures in place to safeguard research integrity.

We wish to credit our Research Integrity and Research Publishing teams and anonymous and named external researchers and research integrity experts for contributing to this investigation.

The corresponding author, as the representative of all authors, has been given the opportunity to register their agreement or disagreement to this retraction. We have kept a record of any response received.

References

[1] X. Zhang, S. Yang, and Z. Xu, "The Relationship between Angiotensin–Neprilysin Treatment, Echocardiographic Parameters, and NT-proBNP Levels in HFpEF Patients with Acute Decompensated Heart Failure," *Computational and Mathematical Methods in Medicine*, vol. 2022, Article ID 4298644, 6 pages, 2022.

Hindawi
Computational and Mathematical Methods in Medicine
Volume 2022, Article ID 4298644, 6 pages
https://doi.org/10.1155/2022/4298644

Research Article

The Relationship between Angiotensin–Neprilysin Treatment, Echocardiographic Parameters, and NT-proBNP Levels in HFpEF Patients with Acute Decompensated Heart Failure

Xiaoliang Zhang, Song Yang, and Zhonglin Xu

Department of Cardiovascular, The Ninth People's Hospital of Chongqing, No. 69, Jialing Village, Beibei District, Chongqing 400700, China

Correspondence should be addressed to Xiaoliang Zhang; 466240716@qq.com

Received 24 July 2022; Revised 24 August 2022; Accepted 2 September 2022; Published 12 September 2022

Academic Editor: Min Tang

Background. The valsartan-sacubitril therapy improved the outcomes of patients with acute decompensated heart failure (ADHF) of a reduced ejection fraction (HFrEF). In ADHF patients with preserved ejection fraction (HFpEF), it is not yet clear whether the same treatment regimen may be safely used to treat ADHF. *Methods*. For this study, HFpEF patients hospitalized due to ADHF were enrolled. Following hemodynamic stabilization, patients were randomized into two groups that were treated with enalapril or sacubitril-valsartan. In this trial, the primary efficacy outcomes were changes in echocardiographic parameters and NT-proBNP levels from baseline to 8 weeks treatment. *Results*. ARNI treatment resulted in a significant decrease in NT-proBNP levels and an increase in LVEF in patients with HFpEF. However, HFpEF patients that underwent ARNI treatment achieved better outcomes than did patients that underwent ACEI treatment. *Conclusion*. Sacubitril-valsartan treatment, which lowered NT-proBNP levels and improved cardiac function, was more effective in HFpEF patients with acute decompensated heart failure than enalapril.

1. Introduction

The worldwide public health concern of heart failure (HF) affects around 2% of people in developed countries [1, 2], resulting in symptoms associated with insufficient cardiac output [2, 3]. The three subtypes of heart failure are HF with reduced left ventricular ejection fraction (HFrEF) EF <40% (amended to ≤ 35%), HF with preserved LVEF (HFpEF) in patients with an EF greater than 50%, LV diastolic dysfunction, and evidence of structural heart disease (HFmrEF) in patients with an LVEF of 40-49%, diastolic dysfunction, increased BNP concentrations, and evidence of structural heart disease [4, 5]. The etiology and pathophysiological characteristics of HFpEF are complex and heterogeneous [6, 7], and even individuals specializing in HF may have difficulty accurately diagnosing this disease.

Succinylcholinesterase inhibitor (SCIE) therapy, which includes sacubitril and/or valsartan, has been shown to reduce symptoms and lower the odds of hospitalization owing to HF and cardiovascular death in chronic HFrEF patients relative to outcomes associated with the angiotensin-converting enzyme inhibitor (ACEI) enalapril, while is the gold standard approach to treating these patients [8]. Sacubitril-valsartan therapy was connected to substantial improvements in the severity of clinical symptoms among HFrEF patients as defined by hospitalization, LVE, NYHA NT-proBNP, and cardiovascular mortality in phase III randomized PARADIGM-HF study [9–11]. More recent studies have expanded on the findings of this trial and examined the establishment of multidrug regimens incorporating both neprilysin inhibitors and renin-angiotensin-aldosterone system (RAS) blockers [12].

The safety and efficacy of sacubitril-valsartan treatment were further compared to those of enalapril following hemodynamic stabilization in patients hospitalized with ADHF in the PIONEER-HF trial [13]. In this study, sacubitril-

valsartan therapy was shown to be more effective than enalapril in reducing NT-proBNP concentrations in patients, whereas no differences in angioedema, hyperkalemia, worsening renal function, or symptomatic hypotension rates were evident among these groups [14, 15].

Up to now, sacubitril-valsartan does not have an indication in patients with HF with preserved ejection fraction (HFpEF) [16]. However, none of contemporary therapies was able to reduce HFpEF mortality. While sacubitril-valsartan was increasingly recognized as an efficacious treatment for HFrEF patients, whether it is similarly safe and effective in HFpEF patients undergoing hospitalization for acute decompensated HF remains to be established. The goal of this research was to compare the safety and efficacy of sacubitril-valsartan with enalapril in patients with heart failure, and treatment regimens in HFpEF patients hospitalized for ADHF. Our results suggest that sacubitril-valsartan treatment reduces NT-proBNP levels and improves cardiac function, and is more effective than enalapril in patients with HFpEF with acute decompensated heart failure. This provides new insights into the clinical treatment of HFpEF.

2. Material and Methods

2.1. Trial Design. The design for this trial has previously been published [14]. Study participants with ADHF were randomized, masked, and actively controlled to receive either enalapril or sacubitril-valsartan at the start of their stay in the hospital. The Chongqing Ninth People's Hospital's ethical committees have approved this study's protocol.

2.2. Patient Recruitment. The criteria for patient recruitment are as described previously [14]; in short, patients had to be at least 18 years old, have an LVEF of at least ≤ 50%, have BNP below ≤ 400 pg/mL, or N-terminal pro-B-type natriuretic peptide (NT-proBNP) values below ≤ 1600 pg/mL, and had been diagnosed with primary acute decompensated HF, which includes signs of fluid overload. Patients were enrolled while still hospitalized between 24 h and 10 days following initial hospital presentation. Patient randomization was only performed after hemodynamic stabilization, defined by an SBP ≥100 mmHg for at least 6 h without increases in i.v. diuretic doses and without the need for the administration of i.v. vasodilators over the past 6 h or i.v. inotropic agents over the past 24 h. Consent to treatment in the form of a written document was provided by every patient.

2.3. Trial Procedures. The criteria for patient recruitment were as described previously [14]; briefly, treatment with sacubitril-valsartan and enalapril (ACEI group) was randomized to patients. A fixed-dose combination of sacubitril-valsartan (either 24 mg of sacubitril with 26 mg of valsartan or 49 mg of sacubitril with 51 mg of valsartan as a fixed-dose combination) or enalapril (either 2.5 mg or 5 mg) was given twice daily to patients as an initial dosage. Blinding was achieved by providing all patients with a placebo resembling the other drugs. While patients in the enalapril group were administered enalapril and the placebo with their first dose, individuals treated with sacubitril-valsartan initially received two doses of placebos resembling both trial drugs such that a minimum washout period of 36 h prior to sacubitril-valsartan administration could be ensured, after which the appropriate trial drug and placebo were administered beginning with the third dose. A minimum of six hours of close observation followed the third dosage before patients were allowed to discharge. The sacubitril-valsartan dosage was tinkered with over the eight-week study period, with 97 and 103 mg twice-daily objectives for the two drugs. It was planned to have follow-up appointments in weeks one and two, and then every other week after that. On the morning of the eight-week follow-up appointment, the last medicine dosages were administered.

2.4. Trial Outcomes. This study's main finding was the time-averaged proportionate change in NT-proBNP levels between baseline and 4, 8, and 12 weeks after efficient treatment, as were echocardiographic parameters, including left ventricular end-diastolic dimension (LVEDD), left ventricular ejection fraction (LVEF), left ventricular end-systolic volume (LVESV), and left ventricular end-diastolic volume (LVEDV).

2.5. Statistical Analysis. All statistical analyses were performed using SPSS 21.0 (IL, USA). The Cox proportional-hazard models were used to compute hazard ratios and 95 percent confidence intervals (CIs), and log-rank test was used to compare the ACEI and ARNI treatment groups. It may not be feasible to replicate the conclusions reached from these intervals since the CIs for outcomes other than the main effectiveness outcome were not corrected for multiple comparisons. Treatment efficacy consistency was assessed in six pre-specified subgroups as well as six further exploratory subgroups. $p < 0.05$ was the significance threshold.

3. Results

3.1. The Impact of Sacubitril-Valsartan Treatment on Echocardiographic Parameters. Data from 127 patients who met the specified study inclusion criteria were gathered from the hospital information system registry of the Ninth People's Hospital of Chongqing between January 2018 and May 2019. Patient's characteristics at baseline are shown in Table 1. Patients in the ARNI and ACEI treatment groups exhibited a mean (±SD) age of 70.0 and 71.5 years, respectively (p =0.8563). The ARNI group consisted of 32 females (57.1%) and 24 males (42.9%) while the ACEI group consisted of 32 females (51.6%) and 30 males (48.4%). The mean SBP of patients in the ARNI and ACEI groups was 136.5 and 135.5 mmHg, respectively (p =0.7244), while corresponding DBP values were 76.5 and 77.0 mmHg (p = 0.6832). In total, 8 (13.8%) and 10 (16.1%) of patients in the ARNI and ACEI groups had a history of smoking. No significant difference in the history of hypertension prior to HF was evident in these groups [42 (72.4%) vs 43 (69.4%), respectively, p =0.7126]. The history of diabetes mellitus was comparable between these patient cohorts [21 (36.2%)

Table 1: General clinical data for patients in the ARNI and ACEI treatment groups.

Factors	ARNI $N=58$	ACEI $N=62$	p-value
Age	71.5 (66.0, 74.5)	70.0 (64.0, 72.0)	0.8563
Gender			
Male	24	30	0.5471
Female	32	32	
Smoking			
Yes	8	10	0.7203
No	50	52	
Hypertension			
Yes	42	43	0.7126
No	16	19	
Diabetes			
Yes	21	26	0.5206
No	37	36	
SBP (mmHg)	136.5 (128.5, 153)	135.5 (129.0, 155.0)	0.7244
DBP (mmHg)	76.5 (71.5, 92.0)	77.0 (72.5, 91.0)	0.6832
LVEF (%)	24.8 ± 5.7	26.3 ± 6.1	0.6274
LVEDD (mm)	61.3 ± 5.6	60.8 ± 6.7	0.6828
LVEDV (mL)	176.4 ± 14.6	182.4 ± 15.4	0.7144
LVESV (mL)	96.4 ± 11.7	98.7 ± 13.2	0.6632

vs 26 (41.9%), respectively, $p=0.5206$]. Analysis of confounding factors showed that there were no differences in the baseline BP, age, gender, or medical history of the ACEI and ARNI patient groups.

Patients in the ARNI group had pre- and post-treatment LVEF values of 24.8 ± 5.7 and 44.3 ± 5.1, respectively, as shown in Tables 1 and 2, while for patients in the ACEI group, these respective values were 26.3 ± 6.1 and 36.3 ± 3.8. While significant increases in LVEF were evident in both groups, these increases were greater for HFpEF patients in the ARNI group. Pre- and post-treatment LVEDD values in the ARNI group were 61.3 ± 5.6 and 50.2 ± 4.6, respectively, while those in the ACEI group were 60.8 ± 6.7 and 54.6 ± 5.3. Pre- and post-treatment LVEDV values in the ARNI group were 176.4 ± 14.6 and 118.4 ± 17.6, while those in the ACEI group were 182.4 ± 15.4 and 146.3 ± 12.4, respectively. The LVESV values were 96.4 ± 11.7 before and after treatment in the ARNI group vs. 42.6 ± 14.7 after treatment, while those in the ACEI group were 98.7 ± 13.2 and 67.3 ± 16.7, respectively. The differences of LVEF, LVEDD, LVEDV, and LVESV values before and after treatment in ARNI group were significantly higher than those in ACEI group, suggesting that HFpEF patients that underwent ARNI treatment achieved better outcomes than did patients that underwent ACEI treatment (Table 2).

3.2. Changes in NT-proBNP Concentrations. To confirm the influence of ARNI and ACEI treatment on NT-proBNP expression, we firstly analyzed the baseline of NT-proBNP concentration in ARNI and ACEI pre-treatment groups. ELISA results showed that the NT-proBNP concentrations of the two groups did not vary (3284.62 ± 317.64 pg/mL vs. 3184.75 ± 486.37 pg/mL, Figure 1). In the two groups, after ARNI or ACEI treatment, the concentration of NT-proBNP was significantly higher than pre-treatment (Figure 2), and the concentration of NT-proBNP was dramatically lower in ARNI treatment group compared with ACEI treatment group (Figure 2).

4. Discussion

Up to now, sacubitril-valsartan does not have an indication in patients with HF with preserved ejection fraction (HFpEF) [16]. However, none of contemporary therapies is able to reduce HFpEF mortality. While sacubitril-valsartan is increasingly recognized as an efficacious treatment for HFrEF patients, whether it is similarly safe and effective in HFpEF patients undergoing hospitalization for acute decompensated HF remains to be established. NT-proBNP levels and echocardiographic parameters in patients with acute decompensated HFpEF were the focus of this study, which aims to compare the effects of sacubitril-valsartan and ACEI therapy. When follow-up was performed 8 weeks post-treatment, sacubitril-valsartan was found to be associated with significantly greater echocardiographic improvement and reduced NT-proBNP levels relative to those in HFpEF patients that underwent ACEI treatment. While LVEF improved significantly in both treatment groups, these improvements were more pronounced for individuals that were subject to ARNI treatment as compared to ACEI treatment. Several prior studies have reported similar LVEF improvement in patients diagnosed with HFrEF [17–20]. The PARAGON-HF study determined that sacubitril-valsartan treatment was associated with more pronounced absolute and relative benefit as compared to valsartan in HFpEF patients when this therapeutic regimen was initiated during the high-risk window following hospitalization, in line with the present study [21]. ARNI patients also exhibited significantly greater reductions in LVEDD, LVEDV, and LVESV as compared to the ACEI group. Similar left ventricular volume improvements have also been reported in other studies [22–25].

While NT-proBNP levels fell for patients in both treatment groups, these decreases were more pronounced in the ARNI group relative to the ACEI group. Patients with HFrEF have shown a decrease in NT-proBNP levels after treatment with sacubitril-valsartan [26–28]. Patients with acutely decompensated HF were not included in the PARADIGM-HF study since it focused on ambulatory patients with chronic HFrEF [29]. After randomization, 48-26%of patients in the sacubitril-valsartan and enalapril therapy groups had NT-proBNP levels reduced by more than >30% from baseline to one month after randomization, respectively [30]. Predischarge beginning of sacubitril-valsartan medication led in a 28 percent decline in NT-proBNP levels at discharge, according to a transitional trial of hospitalized acute decompensated HF patients [31]. In addition to LVEF, several other factors such as BMI, age, and creatinine clearance can also impact NT-proBNP levels [32]. In contrast to prior studies, HFpEF patients included

Table 2: General clinical data for patients following ARNI and ACEI treatment.

Factors	ARNI treatment		ACEI treatment	
	Before	After	Before	After
LVEF (%)	24.8 ± 5.7	44.3 ± 5.1**,#	26.3 ± 6.1	36.3 ± 3.8*
LVEDD (mm)	61.3 ± 5.6	50.2 ± 4.6**,#	60.8 ± 6.7	54.6 ± 5.3*
LVEDV (mL)	176.4 ± 14.6	118.4 ± 17.6**,#	182.4 ± 15.4	146.3 ± 12.4*
LVESV (mL)	96.4 ± 11.7	42.6 ± 14.7**,#	98.7 ± 13.2	67.3 ± 16.7*

*$p < 0.05$ and **$p < 0.01$ compared with the before group; #$p < 0.05$ compared with ACEI treatment.

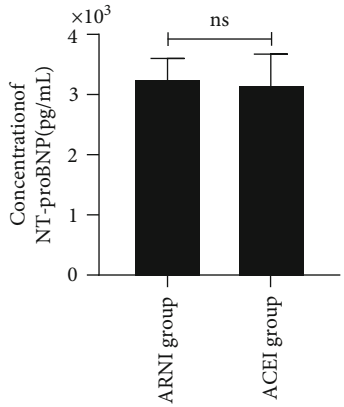

Figure 1: Pre-treatment NT-proBNP levels. Concentrations of NT-proBNP were compared at baseline between the ARNI and ACEI treatment groups. ns: no significance. ARNI group, $N = 58$; ACEI group, $N = 62$.

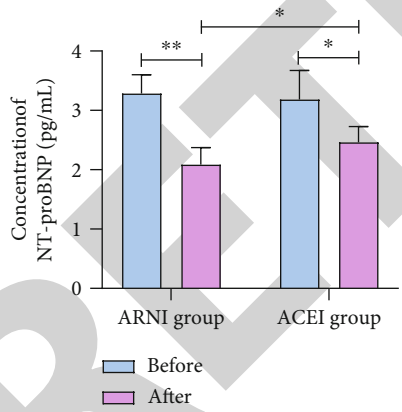

Figure 2: Pre- and post-treatment NT-proBNP levels. Concentrations of NT-proBNP were compared at baseline and at follow-up between the ACEI and ARNI treatment groups. *$p < 0.05$, **$p < 0.01$. ARNI group, $N = 58$; ACEI group, $N = 62$.

herein underwent in-hospital randomization to undergo ARNI or ACEI treatment, while NT-proBNP levels were measured several weeks post-treatment. The results of this study, together with data from the PIONEER-HF and PARADIGM-HF trials, support the ability of sacubitril-valsartan treatment to rapidly decrease NT-proBNP levels irrespective of HF patient subtyping.

PIONEER-HF trial results provided an extended evidence base with respect to the utilization of sacubitril-valsartan in patients for whom little or no other data were available, including individuals with new-onset HF, individuals hospitalized for acute decompensated HF, individuals not receiving traditional RAS inhibitor therapy, or patients not receiving high dosages of HF medicines prescribed in accordance with current guidelines [33–35].

These findings support the safety of starting sacubitril-valsartan treatment in individuals with acute decompensated HFpEF. It was shown that sacubitril-valsartan was well tolerated throughout the in-hospital beginning phase of the PIONEER-HF trial and in a follow-up, open-label extension research.

Data Availability

The data and study materials that support the findings of this study will be available to other researchers from the corresponding authors on reasonable request.

Ethical Approval

This study was carried out in accordance with guidelines outlined in the Declaration of Helsinki and approved by the Ethics Committee of The Ninth People's Hospital of Chongqing.

Consent

Informed consent was obtained from all individual participants included in the study.

Conflicts of Interest

The authors have no relevant financial or non-financial interests to disclose.

Authors' Contributions

Xiaoliang Zhang contributed to the conceptualization; Xiaoliang Zhang and Song Yang contributed to the data curation; Xiaoliang Zhang contributed to the funding acquisition; Xiaoliang Zhang and Zhonglin Xu contributed to the investigation; Xiaoliang Zhang contributed to the project administration; Xiaoliang Zhang and Song Yang contributed to the writing - original draft; all authors contributed to the writing - review and editing.

Acknowledgments

The research was supported by grants from Chongqing Science and Health Joint medical scientific research project (2019QNXM036).

References

[1] L. Sinnenberg and M. M. Givertz, "Acute heart failure," *Trends in Cardiovascular Medicine*, vol. 30, no. 2, pp. 104–112, 2020.

[2] E. Tanai and S. Frantz, "Pathophysiology of heart failure," *Comprehensive Physiology*, vol. 6, no. 1, pp. 187–214, 2015.

[3] M. Arrigo, F. Ruschitzka, and A. J. Flammer, "Acute heart failure," *Therapeutische Umschau*, vol. 75, no. 3, pp. 155–160, 2018.

[4] K. Swedberg, "Heart failure subtypes: pathophysiology and definitions," *Diabetes Research and Clinical Practice*, vol. 175, article 108815, 2021.

[5] L. W. Liang and Y. J. Shimada, "Endotyping in heart failure-identifying mechanistically meaningful subtypes of disease," *Circulation Journal*, vol. 85, no. 9, pp. 1407–1415, 2021.

[6] B. A. Borlaug, "The pathophysiology of heart failure with preserved ejection fraction," *Nature Reviews. Cardiology*, vol. 11, no. 9, pp. 507–515, 2014.

[7] J. J. Park, I. C. Hwang, S. H. Kang, J. B. Park, J. H. Park, and G. Y. Cho, "Myocardial strain for heart failure with preserved ejection fraction but without diastolic dysfunction," *ESC Heart Fail*, 2022.

[8] M. Packer, J. McMurray, A. S. Desai et al., "Angiotensin receptor neprilysin inhibition compared with enalapril on the risk of clinical progression in surviving patients with heart failure," *Circulation*, vol. 131, no. 1, pp. 54–61, 2015.

[9] L. Vicent, A. Ayesta, A. Esteban-Fernández et al., "Sex influence on the efficacy and safety of Sacubitril/valsartan," *Cardiology*, vol. 142, no. 2, pp. 73–78, 2019.

[10] B. Quiroga, A. de Santos, D. Sapiencia, Y. Saharaui, and V. Álvarez-chiva, "Experiencia clinica con sacubitrilo/valsartan en pacientes con insuficiencia renal: la vision del nefrologo," *Nefrologia (Engl Ed)*, vol. 39, no. 6, pp. 646–652, 2019.

[11] R. M. Burke, J. K. Lighthouse, D. M. Mickelsen, and E. M. Small, "Sacubitril/valsartan decreases cardiac fibrosis in left ventricle pressure overload by restoring PKG signaling in cardiac fibroblasts," *Circulation. Heart Failure*, vol. 12, no. 4, article e005565, 2019.

[12] K. F. Docherty, M. Vaduganathan, S. D. Solomon, and J. J. V. McMurray, "Sacubitril/valsartan: neprilysin inhibition 5 years after PARADIGM-HF," *JACC Heart Fail*, vol. 8, no. 10, pp. 800–810, 2020.

[13] E. J. Velazquez, D. A. Morrow, A. D. DeVore et al., "Rationale and design of the com _P_ ar _I_ son _O_ f sacubitril/valsarta _N_ versus _E_ nalapril on _E_ ffect on nt-p _R_ o-bnp in patients stabilized from an acute _H_ eart _F_ ailure episode (PIONEER-HF) trial," *American Heart Journal*, vol. 198, pp. 145–151, 2018.

[14] E. J. Velazquez, D. A. Morrow, A. DeVore et al., "Angiotensin-neprilysin inhibition in acute decompensated heart failure," *The New England Journal of Medicine*, vol. 380, no. 6, pp. 539–548, 2019.

[15] A. D. DeVore, E. Braunwald, D. A. Morrow et al., "Initiation of angiotensin-neprilysin inhibition after acute decompensated heart failure: secondary analysis of the open-label extension of the PIONEER-HF trial," *JAMA Cardiology*, vol. 5, no. 2, pp. 202–207, 2020.

[16] M. Gori, E. D'Elia, and M. Senni, "Sacubitril/valsartan therapeutic strategy in HFpEF: clinical insights and perspectives," *International Journal of Cardiology*, vol. 281, pp. 158–165, 2019.

[17] G. Vitale, G. Romano, A. di Franco et al., "Early effects of sacubitril/valsartan on exercise tolerance in patients with heart failure with reduced ejection fraction," *Journal of Clinical Medicine*, vol. 8, no. 2, p. 262, 2019.

[18] M. V. Polito, A. Silverio, A. Rispoli et al., "Clinical and echocardiographic benefit of Sacubitril/Valsartan in a real- world population with HF with reduced ejection fraction," *Scientific Reports*, vol. 10, no. 1, p. 6665, 2020.

[19] S. Straw, C. A. Cole, M. McGinlay et al., "Guideline-directed medical therapy is similarly effective in heart failure with mildly reduced ejection fraction," *Clinical Research in Cardiology*, 2022.

[20] C. da Luz Goulart, P. Agostoni, E. Salvioni et al., "Exercise oscillatory breathing in heart failure with reduced ejection fraction: clinical implication," *European Journal of Preventive Cardiology*, vol. 29, no. 12, pp. 1692–1698, 2022.

[21] M. Vaduganathan, B. L. Claggett, A. S. Desai et al., "Prior heart failure hospitalization, clinical outcomes, and response to sacubitril/valsartan compared with valsartan in HFpEF," *Journal of the American College of Cardiology*, vol. 75, no. 3, pp. 245–254, 2020.

[22] S. Gubelli and M. Caivano, "Case of a patient with heart failure, dilated cardiomyopathy and atrial fibrillation treated with sacubitril/valsartan," *Current Medical Research and Opinion*, vol. 35, sup3, pp. 19–22, 2019.

[23] A. A. House, C. Wanner, M. J. Sarnak et al., "Heart failure in chronic kidney disease: conclusions from a Kidney Disease: Improving Global Outcomes (KDIGO) Controversies Conference," *Kidney International*, vol. 95, no. 6, pp. 1304–1317, 2019.

[24] M. Abdelhamid, G. Rosano, M. Metra et al., "Prevention of sudden death in heart failure with reduced ejection fraction: do we still need an implantable cardioverter-defibrillator for primary prevention?," *European Journal of Heart Failure*, 2022.

[25] B. Chapman, A. S. Hellkamp, L. E. Thomas et al., "Angiotensin receptor neprilysin inhibition and associated outcomes by race and ethnicity in patients with heart failure with reduced ejection fraction: data from CHAMP-HF," *Journal of the American Heart Association*, vol. 11, no. 12, article e022889, 2022.

[26] D. L. Mann, S. J. Greene, M. M. Givertz et al., "Sacubitril/valsartan in advanced heart failure with reduced ejection fraction: rationale and design of the LIFE trial," *JACC Heart Fail*, vol. 8, no. 10, pp. 789–799, 2020.

[27] J. L. Januzzi Jr., M. F. Prescott, J. Butler et al., "Association of change in N-terminal pro-B-type natriuretic peptide following initiation of sacubitril-valsartan treatment with cardiac structure and function in patients with heart failure with reduced ejection fraction," *JAMA*, vol. 322, no. 11, pp. 1085–1095, 2019.

[28] D. Pascual-Figal, R. Wachter, M. Senni et al., "NT-proBNP response to sacubitril/valsartan in hospitalized heart failure patients with reduced ejection fraction: TRANSITION study," *JACC Heart Fail*, vol. 8, no. 10, pp. 822–833, 2020.

Hindawi
Computational and Mathematical Methods in Medicine
Volume 2023, Article ID 9790685, 1 page
https://doi.org/10.1155/2023/9790685

Retraction

Retracted: To Study the Effect of Individualized Nursing Model Based on MDT Concept on Limb Function Recovery and Quality of Life in Patients with Breast Cancer

Computational and Mathematical Methods in Medicine

Received 5 December 2023; Accepted 5 December 2023; Published 6 December 2023

This article has been retracted by Hindawi, as publisher, following an investigation undertaken by the publisher [1]. This investigation has uncovered evidence of systematic manipulation of the publication and peer-review process. We cannot, therefore, vouch for the reliability or integrity of this article.

Please note that this notice is intended solely to alert readers that the peer-review process of this article has been compromised.

Wiley and Hindawi regret that the usual quality checks did not identify these issues before publication and have since put additional measures in place to safeguard research integrity.

We wish to credit our Research Integrity and Research Publishing teams and anonymous and named external researchers and research integrity experts for contributing to this investigation.

The corresponding author, as the representative of all authors, has been given the opportunity to register their agreement or disagreement to this retraction. We have kept a record of any response received.

References

[1] Y. Chen, F. Luo, and G. Shi, "To Study the Effect of Individualized Nursing Model Based on MDT Concept on Limb Function Recovery and Quality of Life in Patients with Breast Cancer," *Computational and Mathematical Methods in Medicine*, vol. 2022, Article ID 1032503, 6 pages, 2022.

Hindawi
Computational and Mathematical Methods in Medicine
Volume 2022, Article ID 1032503, 6 pages
https://doi.org/10.1155/2022/1032503

Research Article

To Study the Effect of Individualized Nursing Model Based on MDT Concept on Limb Function Recovery and Quality of Life in Patients with Breast Cancer

Yue Chen, Feng Luo, and Guo Shi

Department of Breast and Thyroid Surgery, First Affiliated Hospital, Chongqing Medical University, Chongqing, China 400016

Correspondence should be addressed to Feng Luo; 202547@hospital.cqmu.edu.cn

Received 3 August 2022; Revised 11 August 2022; Accepted 27 August 2022; Published 9 September 2022

Academic Editor: Min Tang

Objective. To study the value of the individualized nursing model based on the concept of multidisciplinary team (MDT) on recovery of limb function and quality of life in patients with breast cancer. *Methods*. A total of 110 breast cancer patients admitted to our hospital from January 2021 to December 2021 were selected as the research objects. The 110 breast cancer patients were divided into the research group ($n = 55$) and the control group ($n = 55$) according to the random number table method. The control group received routine care. The research group implemented individualized nursing based on the MDT concept on the basis of routine nursing. The disabilities of the arm, shoulder, and hand (DASH) scores before nursing and 1 month after nursing were studied in the two groups, Hamilton anxiety scale (HAMA) score, Hamilton depression scale (HAMD) score, and Functional Assessment of Cancer Therapy-B (FACT-B) score. *Results*. After 1 month of nursing, the DASH score of the research group was lower than that of the control group, and the difference was statistically significant ($P < 0.05$), and after 1 month of nursing, the HAMA score of the research group was lower than that of the control group ($P < 0.05$). After 1 month of nursing, the HAMD scale score of the research group was lower than that of the control group, and the difference was statistically significant ($P < 0.05$). After 1 month of nursing, the FACT-B score of the research group was higher than that of the control group, and the difference was statistically significant ($P < 0.05$). *Conclusion*. The individualized nursing model based on the MDT concept has high application value for breast cancer patients. This nursing model can improve the function of limb movement, relieve the patient's anxiety and depression, and improve the patient's quality of life. This nursing model is worthy of clinical promotion.

1. Introduction

There are 5.7 million female breast cancer patients in the world by 2018. In China, breast cancer with 573000 confirmed number has become the most popular among women in 2018 [1]. In recent years, more and more breast cancer patients have been discovered and treated in a timelier manner because of the continuous improvement of diagnosis and treatment technology and people's health awareness with surgery as the center. The lack of breasts after surgery and various side effects of chemotherapy not only bring huge psychological pressure to patients but also seriously affect the quality of life of patients. The comprehensive treatment mode supplemented by chemotherapy, radiotherapy, and endocrine and targeted therapies has significantly improved the survival rate of breast cancer [2–5]. But shoulder joint dysfunction is still one of the most common complications of breast cancer patients [6–8].

Tumor treatment is becoming more and more complex, alone cannot meet the needs of diagnosis, treatment, and prevention of breast cancer and other tumor diseases [9–14]. The management of breast cancer patients requires the collaboration of experts in different fields. Multidisciplinary model (MDT) arises at the historic moment and gradually develops. As early as 1966, B. Fisher and E. Fisher and De Lena et al. published that breast cancer, as a systemic disease, should need comprehensive management and systemic systematic treatment in the early stage [15, 16].

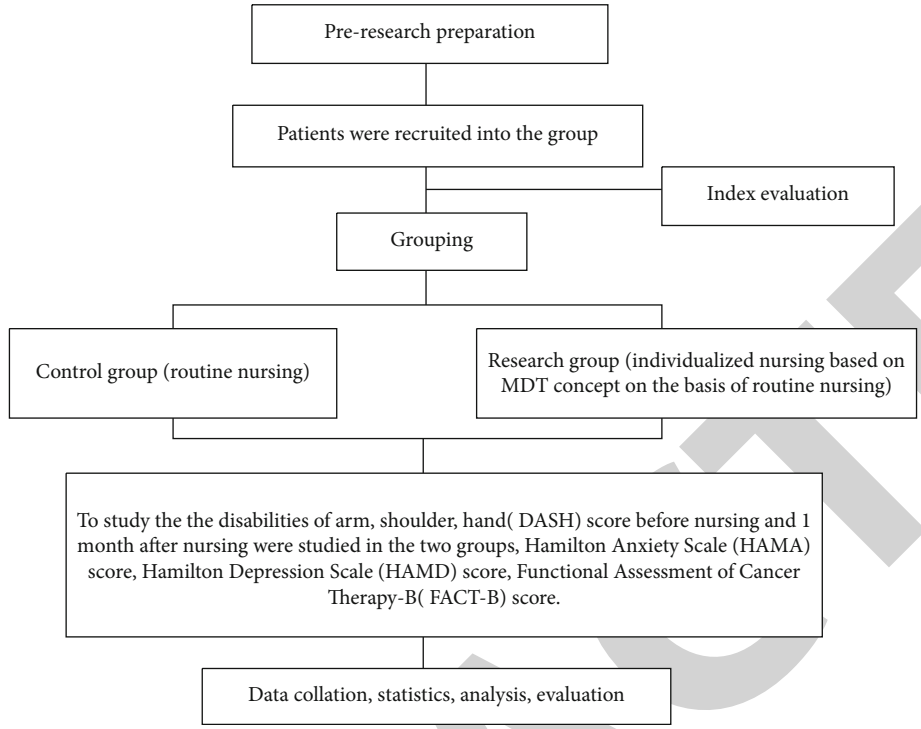

Figure 1: Technical route.

MDT can establish a multidisciplinary platform for correct and rapid diagnosis of diseases, strengthening interdisciplinary communication, collecting data fully and accurately, formulating treatment plans according to evidence-based medicine. Through joint discussion, multidisciplinary experts communicate with each other timely and fully, which helps to reduce the probability of negligence in diagnosis and treatment. It is of great benefit to the improvement of the prevention, diagnosis, and treatment of breast cancer [17, 18]. Therefore, this study selected 110 breast cancer patients as the research object to detect the influence of individualized nursing model based on MDT concept on limb function recovery and quality of life of breast cancer patients.

2. Materials and Methods

2.1. General Information. A total of 110 patients with breast cancer treated from Jan. 2021 to Dec. 2021 were selected. 110 cases with breast cancer were randomly divided into the research group ($n = 55$) and the control group ($n = 55$). All patients in the research group were female, who are aged 22 to 64 years old with an average of 49.45 ± 5.16 years. Pathological classification: 30 cases of noninvasive carcinoma and 25 cases of invasive carcinoma. In the control group, all were female patients, aged 21-65 years, with an average of 49.48 ± 5.23 years. Pathological classification: 29 cases of noninvasive carcinoma and 26 cases of invasive carcinoma. There was no significant difference in general data between the two groups ($P > 0.05$).

Inclusion criteria: (1) all patients met the diagnostic criteria for breast cancer and were pathologically diagnosed as breast cancer; (2) after the researcher stated the purpose of the study, volunteer to participate in the researcher; (3) patients who would undergo axillary lymph node dissection; (4) the patients could learn to use WeChat platform for intervention feedback; and (5) clear consciousness, normal language expression, strong reading ability and unhindered communication with researchers.

Exclusion criteria: (1) mental and cognitive disorders; (2) severe heart failure, renal failure, and liver disease; (3) edema symptoms such as nephrogenic, cardiogenic, and malnutrition; and (4) bilateral breast cancer, recurrence, and other organ metastasis.

Exclusion criteria: (1) patients who did not complete all intervention and data collection and (2) the patients dropped out of the study.

2.2. Methods

2.2.1. Technical Route. The technical route is shown in Figure 1.

2.2.2. Intervention Programme. The control group received routine nursing, including admission education, preoperative preparation, diet guidance, rehabilitation exercise guidance, and discharge guidance. Patients were instructed to raise the affected limb after operation and massage the affected limb with appropriate strength. The intervention lasted for 1 month.

Research group scheme: implement individualized care based on the MDT concept on the basis of routine care. (1) Individualize nursing based on the concept of MDT. Organize a case discussion meeting once a week to communicate among team members. The nurse in charge of the bed reports the mental and physical condition of the patient, the

specialist reports the operation of the patient, the rehabilitation physician, and the psychologist physicians and nutritionists are, respectively, responsible for solving the problems of patients' rehabilitation, psychology, diet, etc. (2) Establish an individualized care team based on the MDT concept. It consists of oncology specialists, tube nurses, specialist nurses, rehabilitation specialists, psychologists, nutritionists, imaging specialists, plastic surgeons, etc. The radiologists are responsible for evaluating the imaging results of patients, and specialist nurses formulate nursing plans based on the discussion content, as follows. ① Use nutritional risk screening and assessment for patients. Table (NRS-2002) is used for nutritional risk assessment. The measures for those who are sensitive to surgical fasting and fasting are that patients who are to be operated can take 1 bottle of perioperative clear drink 355 mL (surgical energy) before 12:00 after dinner before surgery. One more bottle can be taken before 6:00 in the morning for one operation. If there is no nausea and vomiting within 6 hours after the operation, a total of 1 bottle can be consumed in small amounts and multiple times. After 6 hours, normal food can be taken. ② Breast cancer patients are prone to complications such as lymphedema and skin flap necrosis after surgery. Demonstrate how to perform manual lymphatic drainage for patients and their families. The superficial lymph nodes of the back and groin should be massaged in sequence, and the scar tissue should be gently massaged along the breast surgery incision. It is advisable not to have redness after massage. After the surgical sutures were removed, the patients were required to perform manual lymphatic drainage 3 times a day, and the duration of a single session was 10 minutes. ③ Rehabilitation function training: 1-2 days after the operation, the wrist and elbow joints will be active. At the same time, the grip power ball will start to perform no more than 3 groups of 10 times a day, and the shoulder joint will be active on the third day. When the activity is above 90°, the grip strength training can be increased to 5 sets of 15-20 times per day. 7-10 days start to strengthen the shoulder joint lifting, back extension, abduction, and rotation exercises. After 14 days, you can start wall climbing exercise, ring exercise, etc. After 1 month, you can start mild resistance exercise, 2-3 times a week, with a 48-hour interval between every 2 training sessions. Under the guidance of a rehabilitation specialist, adjust the range of motion of the shoulder joint and grip strength exercises according to the patient's pain and increased drainage. Deep breathing exercises should be combined during exercise. ④After breast cancer surgery, it is easy to have low self-esteem, depression, anxiety, and other psychology disorders. Psychologists evaluate the patient's psychological state, actively talk with the patient, listen to the patient's confidence, and summarize the patient's psychological problems when listening to confidence. The causes are analyzed in depth, and then, patients are given comfort and enlightenment according to the causes. Positive suggestion, biofeedback, relaxation training, and other methods are used for psychological counseling, nurses in tube bed strengthen communication with patients, and family members and spouses are encouraged to give more support to patients.

2.3. Observation Indicators

(1) The quality of life measurement scale (Functional Assessment of Cancer Therapy-B (FACT-B)) scores of breast cancer patients before and after nursing in the two groups were studied. The FACT-B scale [19] includes a total of 36 items in 5 areas, including four areas: physiological status, social and family status, emotional status, and functional status. Entries require reverse scoring. The total score of the scale ranges from 0 to 144 points. The higher the score, the better the quality of life in the corresponding field

(2) To study the scores of Hamilton anxiety scale (HAMA), the score criteria of HAMA scale were applied to assess anxiety state [20]

(3) To study the scores of Hamilton depression scale (HAMD), the score standard of HAMD scale [21] <8 means the patient is normal and has no depression; the score 8~20 means the patient has the possibility of depression; the score 21~35 means the patient must have depression; the score > 35 means the patient's depression is serious

(4) The upper extremity dysfunction rating scale (disabilities of the arm, shoulder, and hand (DASH)) scores before and after nursing in the two groups were studied. The DASH scale [22] has a total of 30 questions, and each question is scored from 1 to 5. The higher the score, the more serious the dysfunction. Calculate the score according to $[(\text{total score}/\text{number of answers}) - 1] \times 25$

2.4. Statistical Analysis. IBM SPSS 24.0 software was applied for statistical analysis. The measurement data were expressed by mean ± standard deviation. The counting data were expressed by frequency or rate. The t-test was used when measurement data obey normal distribution, and rank sum test was used when it did not obey normal distribution. The χ^2 test was used to compare the classified counting data. Repeated measurement data were analyzed by repeated measurement analysis of variance. Main effect test results were used when there was no interaction, and simple effect analysis was carried out when there was interaction. $P < 0.05$ indicated that the difference between groups is statistically significant.

3. Results

3.1. The Scores of DASH Scale before Nursing and 1 Month after Nursing in Two Groups. Following one-month nursing, the score of DASH scale in the study cohort was higher than that in the control cohort, and the difference was statistically significant ($P < 0.05$). This result indicated that the DASH score of the research group was better than that of the control group. All results are shown in Table 1.

3.2. The Scores of HAMA Scale before Nursing and 1 Month after Nursing in Two Groups. One month after nursing, the score of HAMA scale in the research group was lower than that in the control group, and the difference was statistically

Table 1: The DASH score of two groups before nursing and 1 month after nursing.

Grouping	Before nursing	After one month of nursing
Control group	75.54 ± 2.19	41.82 ± 1.11*
Research group	75.55 ± 2.12	25.69 ± 1.03*
t value	0.024	78.998
P value	0.981	0.000

Note: * represents that after one month of nursing in this group, compared with that before nursing, $P < 0.05$.

significant ($P < 0.05$). This result indicated that the HAMA scores of the research group were better than those of the control group. All results are shown in Table 2.

3.3. The Scores of HAMD Scale in Two Groups Were Studied. Following one-month nursing, the score of HAMD scale in the research group was lower than that in the control group, and the difference was statistically significant ($P < 0.05$). This result indicated that the HAMD scale of the research group was better than that of the control group. All results are shown in Table 3.

3.4. The FACT-B Scores of the Two Groups Were Observed. Following one-month nursing, the FACT-B score of the research group was higher than that of the control group, and the difference was statistically significant ($P < 0.05$). This result indicated that the FACT-B scores of the research group were better than those of the control group. All results are shown in Table 4.

4. Discussion

The evidence has reported that for patients, MDT can effectively improve the survival rate of patients [23–31], increase patients' satisfaction [32], pay attention to patients' mental health [33], and improve the timeliness and accuracy of diagnosis [34]. For medical staff, MDT can enhance interdisciplinary communication and interaction, improve consistency in the implementation of guidelines, and provide a platform for specialist education to increase access to clinical trials. This study selected 110 breast cancer patients as the research object to detect the influence of individualized nursing model based on MDT concept on limb function recovery and quality of life of breast cancer patients.

The results of this study showed that after individualized nursing based on MDT concept, the score of DASH scale was lower than that of routine nursing, the score of HAMA and HAMD scale was lower than that of routine nursing, and the score of FACT-B was higher than that of routine nursing. It is proved that the application value of individualized nursing based on MDT concept in breast cancer patients is more significant, and it is more helpful to improve limb motor function, relieve anxiety and depression, and improve the quality of life. This is mainly because, on the one hand, breast cancer treatment will no longer belong to nurses but to the entire breast cancer treatment team.

Table 2: The HAMA scores of the two groups before nursing and 1 month after nursing.

Grouping	Before nursing	After one month of nursing
Control group	8.45 ± 1.33	6.59 ± 1.17*
Research group	8.51 ± 1.29	4.08 ± 0.15*
t value	0.240	15.781
P value	0.811	0.000

Note: * represents that after one month of nursing in this group, compared with that before nursing, $P < 0.05$.

Table 3: The score of HAMD scale before nursing and 1 month after nursing in two groups.

Grouping	Before nursing	After one month of nursing
Control group	10.89 ± 2.12	7.32 ± 1.22*
Research group	10.92 ± 2.09	6.11 ± 0.13*
t value	0.075	7.314
P value	0.941	0.000

Note: * represents that after one month of nursing in this group, compared with that before nursing, $P < 0.05$.

Table 4: The FACT-B scores of the two groups prenursing and after 1-month nursing.

Grouping	Before nursing	After one month of nursing
Control group	60.39 ± 2.84	77.09 ± 4.33*
Research group	60.44 ± 2.77	85.17 ± 3.04*
t value	0.093	11.326
P value	0.926	0.000

Note: * represents that after one month of nursing in this group, compared with that before nursing, $P < 0.05$.

Breast cancer MDT team experts include breast surgery, oncology, pathology, imaging (ultrasound, mammography, magnetic resonance, and nuclear medicine), radiotherapy, and breast specialist nurses. The UK Department of Health defines MDT as "experts from different medical fields discuss patients' treatment decisions together at a specific time and place (or by remote/video or teleconference) and each expert can make diagnosis and treatment decisions about patients independently." According to the specific situation, it can include drug therapists, geneticists, physiotherapists, psychologists, plastic surgeons, dietitians, and social workers [35, 36]. This study introduces the concept of multidisciplinary teamwork, in which breast cancer specialist nurses play a leading role, and imaging technologists, oncologists, and pharmacists assume different responsibilities in the team. When specialist nurses encounter problems that cannot be dealt with alone, they contact team members for multidisciplinary consultation and discussion. Members of different disciplines perform their own functions, complement each other, and formulate standardized and targeted diagnosis and treatment plans so that various disciplines integrate and promote each other and reach a consensus on treatment

methods and ideas. It has improved the medical risk prevention ability of specialist nurses and improved the nursing quality of breast cancer patients.

Secondly, the members of the individualized nursing group based on the concept of MDT cooperate with each other and give patients professional, standardized, and systematic nursing intervention, which can improve the nursing quality and improve the prognosis of patients. Its purpose is to transform the traditional empirical therapy into modern teamwork therapy and individualized therapy [37, 38]. First of all, on the premise of accurate diagnosis, the diagnosis process of patients usually includes the first clinical consultation of patients, the improvement of imaging examination, the final pathological diagnosis of tumor puncture, and the formulation of individual treatment plan according to the specific condition of the patient. Specifically, breast cancer patients after routine examination, by imaging doctors, to judge the specific condition of upper limb dysfunction, upper limb edema and other symptoms, by the MDT team to formulate a nursing plan, under the guidance of the MDT team for treatment and nursing, until the upper limb edema symptoms are eliminated, so as to correct the condition of upper limb dysfunction and improve the quality of life [39, 40].

Third, MDT explores disease treatment strategies by establishing a multidisciplinary platform, taking people as the fundamental principle, and relying on team members of various disciplines, rather than the traditional form of "disease-centered." Specifically, in the intervention, rehabilitation physicians instruct patients to exercise upper limb function, which can effectively improve limb function. Psychologists evaluate the psychological state of patients in time, devote themselves to solving the actual psychological problems of patients, use positive suggestion, biofeedback, relaxation training, and other methods for psychological counseling, and strengthen communication between nurses and patients. Encouraging family members and spouses to give more support to patients can effectively alleviate patients' anxiety and depression, make patients have more confidence in treatment, and improve patients' compliance. This study still has some shortcomings. Firstly, the quality of this study is limited due to the small sample size we included in the study. Secondly, this research is a single-center study and our findings are subject to some degree of bias. Therefore, our results may differ from those of large-scale multicenter studies from other academic institutes. This research is still clinically significant and further in-depth investigations will be carried out in the future.

To sum up, the individualized nursing model based on the MDT concept has high application value for breast cancer patients. This nursing model can improve the function of limb movement, relieve the patient's anxiety and depression, and improve the patient's quality of life. This nursing model is worthy of clinical promotion.

Data Availability

The datasets used and analyzed during the current study are available from the corresponding author upon reasonable request.

Conflicts of Interest

The authors declare that they have no competing interests.

References

[1] W. Qiaozhen, "Effect of comprehensive nursing intervention on quality of life of breast cancer patients during postoperative chemotherapy," *China Journal of Coal Industry Medicine*, vol. 20, no. 1, pp. 77–80, 2017.

[2] C. Wanqing, "Analysis of incidence and mortality of breast cancer in 2014 Chinese women," *Chinese Journal of Oncology*, vol. 40, no. 1, pp. 5–13, 2018.

[3] L. Fan, K. Strasser-Weippl, J. J. Li et al., "Breast cancer in China," *The Lancet Oncology*, vol. 15, no. 7, pp. e279–e289, 2014.

[4] A. Pei, "Inner experience of fertility preservation decision-making in young women with early breast cancer," *Nursing management in China*, vol. 22, no. 3, pp. 354–358, 2022.

[5] Q. Hui, L. June, and H. Jing, "A qualitative study on the experience of upper limb lymphedema in postoperative patients with breast cancer," *Chinese Journal of Modern Nursing*, vol. 25, no. 13, pp. 1641–1645, 2019.

[6] L. Yuhuan and L. Liu, "Clinical application of improved individualized nursing combined with quality control circle in improving functional exercise compliance of affected limbs in postoperative patients with breast cancer," *Contemporary nurses (first ten-day issue)*, vol. 25, no. 5, pp. 183–185, 2018.

[7] K. Hayes, M. Callanan, J. Walton, A. Paxinos, and G. A. Murrell, "Shoulder instability: management and rehabilitation," *Journal of Orthopaedic & Sports Physical Therapy*, vol. 32, no. 10, pp. 497–509, 2002.

[8] X. Qian and F. Luo, "Advances in evaluation and treatment of axillary reticulum syndrome in patients with breast cancer," *Journal of Nursing*, vol. Magazine 36, no. 3, pp. 111-112, 2021.

[9] M. G. Wiggans, S. A. Jackson, B. M. Fox et al., "The preoperative assessment of hepatic tumours: evaluation of UK regional multidisciplinary team performance," *HPB Surgery*, vol. 2013, Article ID 861681, 7 pages, 2013.

[10] H. Weili, L. Zhao, and Z. Heling, "Effect of neoadjuvant chemotherapy in patients with breast cancer," *Chinese Journal of Gerontology*, vol. 42, no. 7, pp. 1598–1601, 2022.

[11] J. Prades, E. Remue, E. van Hoof, and J. M. Borras, "Is it worth reorganising cancer services on the basis of multidisciplinary teams (MDTs)? A systematic review of the objectives and organisation of MDTs and their impact on patient outcomes," *Health Policy*, vol. 119, no. 4, pp. 464–474, 2015.

[12] B. Kane and S. Luz, ""Do no harm": fortifying MDT collaboration in changing technological times," *International Journal of Medical Informatics*, vol. 82, no. 7, pp. 613–625, 2013.

[13] R. G. Gish, R. Lencioni, A. M. Di Bisceglie, J. L. Raoul, and V. Mazzaferro, "Role of the multidisciplinary team in the diagnosis and treatment of hepatocellular carcinoma," *Expert Review of Gastroenterology & Hepatology*, vol. 6, no. 2, pp. 173–185, 2012.

[14] W. Lina, Z. Pei, and G. Huanzhi, "Application of MDT nursing intervention in prevention of postoperative lymphedema in patients with breast cancer," *Inner Mongolia Medical Journal*, vol. 53, no. 10, pp. 1262-1263, 2021.

Hindawi
Computational and Mathematical Methods in Medicine
Volume 2023, Article ID 9786485, 1 page
https://doi.org/10.1155/2023/9786485

Retraction

Retracted: Diagnostic Values of Advanced Glycation End Products and Homocysteine in Patients with Alzheimer's Disease and Sarcopenia

Computational and Mathematical Methods in Medicine

Received 12 December 2023; Accepted 12 December 2023; Published 13 December 2023

This article has been retracted by Hindawi, as publisher, following an investigation undertaken by the publisher [1]. This investigation has uncovered evidence of systematic manipulation of the publication and peer-review process. We cannot, therefore, vouch for the reliability or integrity of this article.

Please note that this notice is intended solely to alert readers that the peer-review process of this article has been compromised.

Wiley and Hindawi regret that the usual quality checks did not identify these issues before publication and have since put additional measures in place to safeguard research integrity.

We wish to credit our Research Integrity and Research Publishing teams and anonymous and named external researchers and research integrity experts for contributing to this investigation.

The corresponding author, as the representative of all authors, has been given the opportunity to register their agreement or disagreement to this retraction. We have kept a record of any response received.

References

[1] X. Zhang, Y. Meng, W. Zhang et al., "Diagnostic Values of Advanced Glycation End Products and Homocysteine in Patients with Alzheimer's Disease and Sarcopenia," *Computational and Mathematical Methods in Medicine*, vol. 2022, Article ID 8949048, 8 pages, 2022.

Hindawi
Computational and Mathematical Methods in Medicine
Volume 2022, Article ID 8949048, 8 pages
https://doi.org/10.1155/2022/8949048

Research Article

Diagnostic Values of Advanced Glycation End Products and Homocysteine in Patients with Alzheimer's Disease and Sarcopenia

Xuelian Zhang, Yunxia Meng, Weiwei Zhang, Luhang Shi, Xia Liu, Lijuan Zhang, and Qiaoling Liu

Geriatrics Department, The First People's Hospital of Lianyungang, Xuzhou Medical University Affiliated Hospital of Lianyungang, The First Affiliated Hospital of Kangda College of Nangjing Medical University, Jiangsu 222002, Jiangsu, China

Correspondence should be addressed to Qiaoling Liu; liuqiaoling_edu@outlook.com

Received 2 August 2022; Revised 14 August 2022; Accepted 23 August 2022; Published 9 September 2022

Academic Editor: Min Tang

This study is aimed at exploring the diagnostic value of advanced glycation end products (AGEs) and homocysteine (Hcy) in Alzheimer's disease (AD) complicated with sarcopenia (SP) and to analyze the risk factors related to AD complicated with SP. A total of 168 patients admitted to our hospital from November 2019 to December 2021 were enrolled. Patients were divided into the NC (no SP and AD) group with 29 cases, the AD group with 39 cases, the AD+SP group with 35 cases, and the SP group with 65 cases. The general information, Mini-Mental State Examination (MMSE) scores, and serum levels of AGEs and Hcy among the four groups were compared. Unordered logistic regression was used to analyze the influencing factors of SP patients complicated with dementia. The AGE level was higher in the AD or AD+SP group than the NC or SP group ($P < 0.05$). There was no significant difference between the SP group and the NC group or between the AD group and the AD+SP group ($P > 0.05$). The Hcy level was higher in the SP or AD group than the NC group ($P < 0.05$). There were no significant differences between the AD group and NC group or between the SP group and AD+SP group ($P > 0.05$). The ROC curve of serum AGEs and Hcy for the diagnosis of AD showed that the area under curve (AUC) was 0.887, $P < 0.05$ (95% CI: 0.821-0.954, sensitivity: 80.95%, specificity: 73.81%) and 0.7423, $P < 0.05$ (95% CI: 0.6382-0.8465, sensitivity: 60.42%, specificity: 57.59%), respectively. The ROC curve of serum AGEs and Hcy for the diagnosis of SP showed that the AUC was 0.5533, $P > 0.05$ (95% CI: 0.4294-0.6771) and 0.8744, $P < 0.05$ (95% CI: 0.8006-0.9483). Age ($P < 0.001$), depression ($P = 0.001$), malnutrition ($P = 0.002$), and BMI ($P < 0.001$) were independent influencing factors of SP complicated with AD in elderly inpatients. In conclusion, combined serum AGEs and Hcy had a good diagnostic value for AD combined with SP, which may be helpful for early detection of patient condition.

1. Introduction

Alzheimer's disease (AD), a common clinical degenerative disease of the central nervous system, is mainly characterized by destabilization of the neuronal network and neuronal death. Its two major pathological features are the formation of extracellular insoluble senile plaques and the tangles of intracellular neuronal fibers [1, 2]. The etiology and pathogenesis of senile dementia are still unclear, and it is mostly considered to be a complex brain disease involving multiple factors and multiple pathological pathways. Sarcopenia (SP) is a new type of geriatric syndrome that has become popular in recent years, which refers to an age-related decrease in muscle mass, accompanied by the decrease in muscle strength and/or physical function [3]. In China, SP is still in the stage of low awareness rate and lack of awareness of prevention and treatment. The main clinical manifestations of SP are the decrease in mobility and body balance and difficulty in completing daily activities such as walking and sitting, and adverse events, such as falls, fragility fractures, and osteoporosis, are prone to occur [4]. Age, exercise, diabetes, inflammatory cytokines, vitamin D,

hormone levels, etc., are all high-risk factors for SP, but their correlations need further study.

Increasing studies have shown that AD and SP have many overlapping phenomena in the pathogenesis and pathological changes [5, 6]. Studies have reported that at least 40% of patients diagnosed with SP have pathological changes in AD [7]. Studies have shown that early intervention for SP makes the disease reversible to a certain extent [8], but the current treatment for AD only controls symptoms and delays the progression of the disease. Therefore, it is crucial to study the possible common pathogenesis of AD and SP and their relationship and thus to explore their common biomarkers, so as to implement early diagnosis and intervention for AD and SP patients.

In recent years, the relationship between advanced glycation end products (AGEs) and AD has attracted more and more attention. AGEs are stable end products generated by nonenzymatic reaction between free amino groups, such as groups of proteins, lipids, nucleic acids, and other macromolecules and carbonyl groups of glucose or other reducing sugars. Under normal conditions, AGEs-modified proteins act as a signal to participate in the removal of aging tissues and structural reconstruction in the body. Under pathological conditions, AGEs can cause the abnormity of cellular structure and function of tissues, resulting in a series of pathological changes [9]. Current research shows that AGEs accelerate human aging and are related to the occurrence of a variety of chronic degenerative diseases [10], and it is believed that AGEs may also be one of the causes of AD. However, there are few studies related to SP and AGEs, which needs further exploration.

Homocysteine (Hcy) belongs to a noncoded amino acid and a transitional product of methionine cycle. As a neurotoxin, Hcy maintains normal physiological level by remethylation to methionine, among which vitamin B6, folic acid, and B12 are common nutrients in the diet [11]. Recent studies have also demonstrated that Hcy is a risk factor for cardiovascular and cerebrovascular diseases [12]. Geisel et al. have shown that Hcy can activate N-methyl-D-aspartate receptor (NMDAR), leading to neuronal death in the hippocampus [13]. Hcy also has an excitotoxic effect on hippocampal neurons, inducing dementia [13]. Importantly, Hcy was considered a main risk coefficient for AD as high plasma concentrations were related to the progression of this disease [14]. High Hcy serum concentration was also associated with behavioral and psychological evidence of AD [15]. However, its relation to SP and whether it could be used as a biomarker for early diagnosis of SP remains unexplored.

Therefore, this study is aimed at explore the diagnostic values of AGEs and Hcy underlying the pathogenesis of AD and SP and possible relationship between them and search possible laboratory markers with diagnostic value, which provides clinical possibilities for early detection, diagnosis, and prevention of the disease.

2. Materials and Methods

2.1. General Data. A total of 168 patients admitted to the Department of Neurology in our hospital from November 2019 to December 2021 were collected, including 102 males and 66 females, with an age distribution of 64-88 years, and an average age of 71.40 ± 6.18 years. This study was approved by the Ethics Committee of our hospital, and the informed consent was signed before treatment. Inclusion criteria are as follows: (1) age ≥ 60 years old; (2) well informed and agreed to participate in this study; (3) able to read, write, and speak Chinese normally and able to complete the questionnaire; and (4) able to move freely and able to complete pace, grip strength, and balance tests. Exclusion criteria are as follows: (1) a history of intracranial infection and other serious autoimmune diseases; (2) serious diseases (malignant tumors, severe liver, and kidney damage), etc.; and (3) MRI or CT confirmed cerebral infarction or cerebral hemorrhage and hemiplegia patients. According to whether the patients had SP and dementia, they were divided into the no SP and AD (NC) group ($n = 29$), the AD group ($n = 39$), the AD and SP group ($n = 35$), and the SP group ($n = 65$).

2.2. Data Collection. Within 4 h after admission, nervous system physical examination of all the inclusive research objects was performed by professional neurologists with information and medical history recorded. The anticoagulation tubes were used to store the fasting elbow venous blood drawn early in the morning. After 1 h, the serum was separated by centrifugation of 3000 r/min for 10 min. The separated serum was dispensed with the frozen pipe to freeze up at -80°C refrigerator for detection of indicators such as blood biochemistry, serum AGES, and Hcy. Within 48 h of admission, the head CT or skull MR, cerebrovascular and carotid duplex ultrasound, electrocardiogram, chest X-ray, and other inspections were performed. Basic information, such as name, gender, age, height, and weight, were collected. Smoking, drinking, hypertension, diabetes history, and stroke history were collected. MMSE and HIS scale were evaluated. Body mass index = body weight/height^2 (kg/m^2). All experiments on humans were conducted in accordance with the Declaration of Helsinki (1964) and were approved by the ethical committee of the First People's Hospital of Lianyungang.

2.3. Detection of Serum AGEs and Hcy. Serum AGE and Hcy kits were purchased from Wuhan Canvest Biotechnology Co., Ltd. The frozen specimens (50 μL of serum) were placed in a 37°C water bath for instant dissolution once obtained and then measured by double-sandwich enzyme-linked immunosorbent assay (ELISA). In the process, a full-wavelength GeminiXPS fluorescent microplate reader was used for analysis, and the experimental steps were shown in the instructions of the kit.

2.4. Analysis of Risk Factors. Diagnostic criteria for risk factors are as follows: (1) hypertension: had a history of hypertension or were taking antihypertensive drugs; systolic blood pressure ≥ 140 mmHg and/or diastolic blood pressure ≥ 90 mmHg measured in resting state for 2 consecutive times without taking antihypertensive drugs; (2) diabetes: had a history of diabetes or were taking hypoglycemic drugs/

insulin to control blood glucose; fasting blood glucose (FBG) ≥ 7.00 mmol/L, 2 h postprandial glucose (2hPG) ≥ 11.10 mmol/L, with or without diabetes symptoms; (3) smoking: average smoking ≥ 10 cigarettes/day and duration >1 year; (4) drinking: drinking any beer, liquor, or wine, average ethanol intake ≥ 30 g/day and duration > 1 year.

2.5. Mini-Mental State Examination (MMSE). The MMSE scale was currently the most commonly used and influential scale in the world. The scale included orientation, memory, calculation and attention, recall ability, and language ability. Language ability included naming ability, repetition ability, three-step commands, reading ability, writing ability, and structural ability, with a total score of 30 points, and it took about 5-10 minutes [16]. 27-30 points were normal, and <27 points were AD. Dementia criteria are as follows: illiteracy ≤ 17 points, primary school education (education years ≤ 6 years) ≤ 20 points, middle school (including technical secondary school) ≤ 22 points, and college and above (including junior college) ≤ 23 points. Dementia degree evaluation: 21-24 points were mild; 10-20 points were moderate; ≤9 points were severe.

2.6. Montreal Cognitive Assessment (MoCA). Montreal Cognitive Assessment (MoCA) included visuospatial and executive function (0-5 points), attention (0-6 points), delayed recall memory (0-5 points), naming (0-3 points), language (0-3 points), abstraction (0-2 points), and orientation (0-6 points), with a total score of 30 points [17]. When the score was less than or equal to 18 points, the patient was identified as dementia. Dementia degree evaluation: 18-15 points were mild; 15-10 points were moderate; ≤9 points were severe.

2.7. Diagnosis of SP. This study used the diagnostic criteria of the Asian Working Group for Sarcopenia (AWGS) (2019) [3] to diagnose SP. (1) Appendicular skeletal muscle mass index (ASMI) measurement: it was measured by bioelectrical impedance analysis (Inbody S10), where ASMI < 7.0 kg/m^2 for males and <5.7 kg/m^2 for females were defined as the decline of skeletal muscle mass. (2) Grip strength measurement: it was measured by the grip strength tester (Xiangshan EH101). The research subjects were required to hold the grip strength meter with all their strength when standing, and the left and right hands were measured 3 times, respectively, and the maximum value was taken. Men < 28 kg and women < 18 kg were the decline of grip strength. (3) Physical activity ability: it was measured by the 6 m pace measurement method. The pace of ≤1.0 m/s was regarded as the decline of physical function. SP was diagnosed when a subject had a decrease in skeletal muscle mass accompanied by a decrease in grip strength or physical function.

2.8. Assessment of Mental State. The Geriatric Depression Scale (GDS-5) was used to evaluate the depressive symptoms of the research subjects. It contained 5 items totally, and the subjects answered "yes" or "no." The answer "yes" was scored 1 point, "no" was scored 0 points, and the total score over 2 points indicated that there may be depressive symptoms [8].

2.9. Assessment of Nutritional Status. The nutritional status was assessed using the mini nutritional assessment-short form (MNA-SF), with 14 points as total scores, 12-14 points as normal nutritional status, 8-11 points as the risk of malnutrition, and 0 ~ 7 points to malnutrition [18].

2.10. Statistical Analysis. SPSS 20.0 software was used for statistical analysis of data. Measurement data were expressed as mean ± standard deviation, and ANOVA was used for comparison between groups; enumeration data was expressed as the number of cases (%), and chi-square test was used for comparison between groups; unordered logistic regression was used to analyze the influencing factors of SP patients complicated with AD. The area under the curve of AGEs and Hcy in the diagnosis of AD and SP; the corresponding sensitivity, specificity, and 95% confidence interval were calculated. The test standard was $\alpha = 0.05$, and $P < 0.05$ was considered statistically significant.

3. Results

3.1. Comparison of Basic Data among Four Groups. Among the included patients, 65 (38.69%) were in the SP group, and 39 (23.21%) were in the AD group; 35 (20.83%) were in the AD+SP group, and 29 (17.27%) were in the NC group. Statistical analysis showed that there were significant differences in age, BMI, hypertension, DM, cerebrovascular disease, osteoporosis, education level, depression, and nutritional status among the patients in each group ($P < 0.05$ or $P < 0.001$). At the same time, there were no significant differences in gender, cardiovascular disease, currently smoking, falls in the last 12 months and daily medication > 4 kinds among the patients in each group ($P > 0.05$), as shown in Table 1.

3.2. Comparison of Serum AGE Level among Four Groups. There was a statistically significant difference in serum AGEs among four groups ($P < 0.05$.) Pairwise comparison showed that the level of AGEs in the AD group was higher than that in the SP group, and the difference was statistically significant ($P < 0.05$); the level of AGEs in the AD group was higher than that in the NC group, and the difference was statistically significant ($P < 0.05$); the level of AGEs in the AD +SP group was higher than that in the SP group, and the difference was statistically significant ($P < 0.05$); the level of AGEs in the AD+SP group was higher than that in the NC group, and the difference was statistically significant ($P < 0.05$); there was no significant difference between the SP group and the NC group or between the AD group and the AD+SP group ($P > 0.05$) (Figure 1).

3.3. Comparison of Serum Hcy Level among Four Groups. There was a statistically significant difference in Hcy among four groups. Pairwise comparison showed that the level of Hcy in the SP group was higher than that in the NC group, and the difference was statistically significant ($P < 0.05$); the level of Hcy in the AD group was higher than that in the NC group, and the difference was statistically significant ($P < 0.05$); the level of Hcy in the AD+SP group was higher than that in the NC group, and the difference was statistically significant ($P < 0.05$); there was no significant

Table 1: Basic data in four groups.

Item	NC	SP	AD	AD+SP	P
Age (year)	80.59 ± 7.36	84.22 ± 7.13	87.88 ± 6.72	90.48 ± 5.21	<0.001
Gender					
Male	19 (65.52)	40 (61.52)	23 (58.97)	20 (57.14)	0.763
Female	10 (34.48)	25 (38.45)	16 (41.03)	15 (42.86)	
BMI ($x \pm s$)	24.33 ± 2.58	21.62 ± 2.36	26.08 ± 3.11	21.64 ± 3.18	<0.001
Comorbidity					
Hypertension	21 (72.41)	36 (55.37)	34 (69.23)	27 (77.14)	0.008
DM	15 (51.72)	24 (36.91)	35 (89.74)	14 (40.00)	0.012
Cardiovascular disease	9 (31.03)	21 (32. 30)	16 (41.03)	15 (42.86)	0.071
Cerebrovascular disease	19 (65.52)	38 (58.44)	24 (61.54)	29 (82.85)	0.032
Osteoporosis	7 (24.08)	31 (47.68)	9 (23.08)	11 (31.43)	<0.001
Education level					
≤6 years	1 (3.44)	4 (6.15)	6 (15.38)	2 (5.71)	<0.001
>6 years and <12 years	14 (48.16)	28 (43.06)	20 (51.28)	26 (74.29)	
≥12 years	13 (44.72)	33 (50.75)	12 (30.77)	8 (22.86)	
Currently smoking	3 (10.32)	3 (4.61)	3 (7.69)	2 (5.71)	0.407
Falls in the last 12 months	8 (27.52)	2 (33.83)	12 (30.77)	9 (25.71)	0.476
Daily medication > 4 kinds	17 (58.48)	34 (52.29)	26 (66.66)	22 (62.85)	0.243
Depression	1 (3.44)	9 (13.84)	7 (17.95)	7 (20.00)	<0.001
Malnutrition	2 (6.88)	18 (27.68)	8 (20.51)	21 (60.00)	<0.001

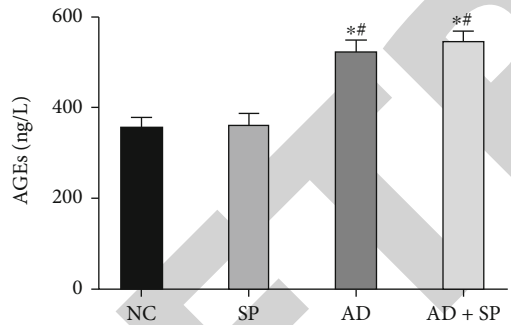

Figure 1: Serum AGEs level in four groups. Note: $^{*}P < 0.05$, vs. the NC group; $^{\#}P < 0.05$, vs. the SP group.

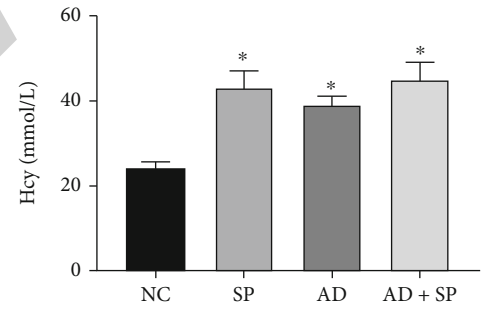

Figure 2: Serum Hcy level in four groups. Note: $^{*}P < 0.05$, vs. the NC group.

difference between the AD group and SP group or between the SP group and AD+SP group or between the AD group and AD+SP group ($P > 0.05$) (Figure 2).

3.4. Diagnostic Characteristic Curves of Subjects. The ROC curve of serum AGEs for the diagnosis of AD showed that the area under curve (AUC) was 0.887, $P < 0.05$ and 95% CI was 0.821-0.954, indicating that serum AGEs have a high diagnostic value for AD, and the critical value of serum AGEs for the diagnosis of AD was 518.5 ng/L, with a diagnostic sensitivity of 80.95% and a specificity of 73.81%. The ROC curve of serum AGEs for the diagnosis of SP showed that the AUC was 0.5533, $P > 0.05$ and 95% CI was 0.4294-0.6771, indicating that serum AGEs have no diagnostic value for SP (Figure 3).

The ROC curve of serum Hcy for the diagnosis of AD showed that the AUC was 0.7423, $P < 0.05$ and 95% CI was 0.6382-0.8465, $P < 0.05$, indicating that serum Hcy has a diagnostic value for AD, with a diagnostic sensitivity of 60.42% and a specificity of 57.59%. The ROC curve of serum Hcy for the diagnosis of SP showed that the AUC was 0.8744, $P < 0.05$ and 95% CI was 0.8006-0.9483, indicating that serum Hcy has a good diagnostic value for SP, and the critical value of serum Hcy for the diagnosis of SP was 34.5, with a diagnostic sensitivity of 88.10% and a specificity of 72.16% (Figure 4).

The ROC curve of combined AGEs and Hcy for the diagnosis of AD and SP showed that the AUC was 0.9311, $P < 0.05$; 95% CI was 0.8845-0.9818, $P < 0.05$; the sensitivity was 88.10%, and the specificity was 78.57%, indicating that combined serum AGEs and Hcy have a good diagnostic value for AD and SP (Figure 5).

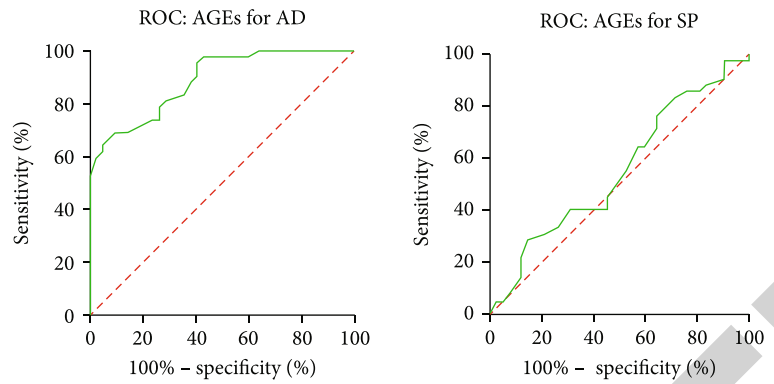

Figure 3: ROC curve of AGEs for the diagnosis of AD and SP.

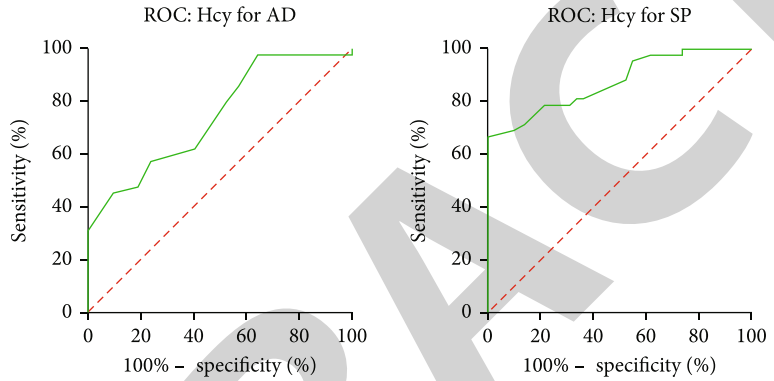

Figure 4: ROC curve of serum Hcy for the diagnosis of AD and SP.

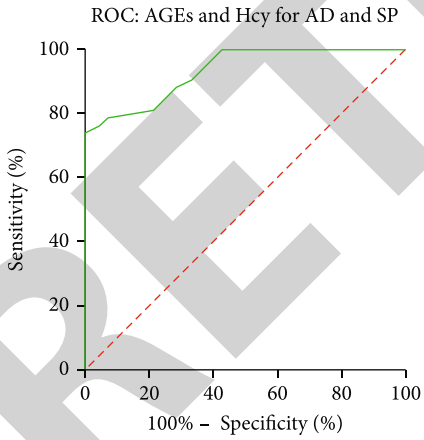

Figure 5: ROC curve of combined AGEs and Hcy for the diagnosis of AD and SP.

3.5. Logistic Regression Analysis of the Influencing Factors of SP Complicated with AD in Elderly Inpatients. Taking the NC group as the reference group, the abovementioned statistically significant factors were incorporated into the disordered logistic regression model. The results showed that age ($P < 0.001$), depression ($P = 0.001$), malnutrition ($P = 0.002$), and BMI ($P < 0.001$) were all independent influencing factors in the SP+AD group, as shown in Table 2.

4. Discussion

AD, a neurological disease with a high incidence rate among middle-aged and elderly people, seriously affects the quality of life and physical and mental health of the elderly and also brings a heavy burden to the family and society. SP, an age-related decline in skeletal muscle mass, muscle strength, and/or physical activity, is associated with adverse outcomes in older adults, such as decreased functional status, falls, poor quality of life, and increased mortality [6]. SP is considered an important public health problem due to its important clinical, economic, and social consequences and has now been formally recognized as a muscle disease. More and more studies have shown that AD and SP have a common pathogenesis. Researches on the possible risk factors of AD and SP, early intervention, and early diagnosis are essential to improve the treatments of patients and reduce the burden on families and society.

There are many studies on the relationship between AGEs and AD, and the main mechanisms leading to the pathogenesis may be as follows: AGEs can lead to the occurrence and development of AD through a variety of ways, such as modifying Aβ and Tau proteins, triggering inflammatory responses, causing mitochondrial dysfunction, producing oxidative stress damage and affecting cell metabolism, the cycle of neurons, autophagy, and the permeability of the blood-brain barrier, etc. [19]. There are few studies on AGEs and SP, most of which show that AGEs

Table 2: The influencing factors of SP and/or AD in each group.

Groups	Variables	P	SE	Wald X^2	P	OR (95% CI)
SP	Intercept	3.784	1.856	4.387	0.035	—
	Age	0.046	0.023	8.201	0.004	1.028 (1.017-1.093)
	BMI	-0.392	0.059	44.384	<0.001	0.703 (0.619-0.770)
	Depression	2.108	0.676	9.703	0.002	7.764 (2.140-28.525)
	Osteoporosis	1.092	0.311	12.632	<0.001	2.897 (1.633-5.437)
AD	Intercept	-9.337	2.876	11.517	0.001	—
	Age	0.112	0.034	12.341	<0.001	1.112 (1.045-1.170)
	Education level ≥ 6 years	2.273	0.663	12.444	<0.001	10.144 (2.802-36.662)
	Malnutrition	1.056	0.532	4.521	0.032	2.954 (1.088-8.091)
	Depression	1.907	0.709	7.317	0.006	6.546 (1.675-25.524)
AD+SP	Intercept	-12.976	4.573	8.309	0.003	—
	Age	0.223	0.046	19.972	< 0.001	1.227 (1.138-1.392)
	BMI	-0.415	0.081	25.535	< 0.001	0.633 (0.549-0.768)
	Malnutrition	1.626	0.572	8.556	0.002	4.907 (1.685-14.108)
	Depression	2.419	0.810	9.338	0.001	10.873 (2.345-49.885)

The first P represented the regression coefficient. The second P is a parameter used to determine the result of a hypothesis test, with $P < 0.05$ indicates significance.

play an important role in the regulation of calcium and phosphorus, increasing serum calcium ion concentration and improving neuromuscular activity, and can also bind to vitamin D receptors, increasing the production of osteocalcin and osteopontin [20]. A study has revealed that the reduced vitamin D level can affect the homeostasis of insulin resistance in the elderly, thereby promoting the occurrence of SP [21]. In this study, AGEs in the AD group and the AD+SP group were significantly higher than those in the NC group and the SP group, and the difference was statistically significant, which was consistent with literature reports, suggesting that AGEs may promote the occurrence and development of AD through the abovementioned various mechanisms. The sensitivity and specificity of AGEs for the diagnosis of AD were calculated by drawing the ROC curve. The ROC curve of serum AGEs for the diagnosis of AD showed that the AUC was 0.887, $P < 0.05$ and 95% CI was 0.821-0.954, indicating that serum AGEs had a high diagnostic value for AD, and the critical value of serum AGEs for the diagnosis of AD was 518.5 ng/L, with a diagnostic sensitivity of 80.95% and a specificity of 73.81%. The ROC curve of serum AGEs for the diagnosis of SP showed that the AUC was 0.5533, $P > 0.05$, and 95% CI was 0.4294-0.6771, indicating that serum AGEs had no diagnostic value for SP.

Hcy, a sulfur-containing amino acid, is involved in the methionine cycle and is the product of methionine demethylation [22]. Some cross-sectional studies and prospective longitudinal epidemiological studies have shown that high Hcy level may increase the risk of AD [23]. However, a recent study has demonstrated that the elevated Hcy level is not associated with the occurrence, severity and progression of AD [24]. Studies have shown that high Hcy level may have an independent role in the pathogenesis of SP, and some cross-sectional studies have also shown that Hcy level is upregulated in SP patients [25]. The KIM study has revealed that high Hcy level is associated with brain atrophy, but whether reducing Hcy level can delay the progression of dementia or prevent the progression of neurodegenerative disease requires further research [26]. The ROC curve of serum Hcy for the diagnosis of AD showed that the AUC was 0.7423, $P < 0.05$, and 95% CI was 0.6382-0.8465, $P < 0.05$, indicating that serum Hcy had a significant diagnostic value for AD, with a diagnostic sensitivity of 60.42% and a specificity of 57.59%. The ROC curve of serum Hcy for the diagnosis of SP showed that the AUC was 0.8744, $P < 0.05$, and 95% CI was 0.8006-0.9483, indicating that serum Hcy had a good diagnostic value for SP, and the critical value of serum Hcy for the diagnosis of SP was 34.5, corresponding to a diagnostic sensitivity of 88.10% and a specificity of 72.16%. The ROC curve of combined AGEs and Hcy for the diagnosis of AD and SP showed that the AUC was 0.9311, $P < 0.05$; 95% CI was 0.8845-0.9818, $P < 0.05$; the sensitivity was 88.10%, and the specificity was 78.57%, indicating that combined serum AGEs and Hcy had a good diagnostic value for AD and SP.

The results of this study showed that the risk of SP complicated with AD increased by 1.221 times per year as the elderly patients aged. Under normal circumstances, the muscle mass and muscle strength of the human body will change with age. For most people over 50 years old, the muscle mass of the legs will decrease at a rate of 1% to 2% per year, and the muscle strength will also decrease by 1.5% to 5.0% per year [27]. At present, the biggest known risk factor for AD is increasing age, as is proved in its prevalence. Therefore, in clinical work, attention should be paid to screening for SP and AD in elderly patients.

This study also showed that elderly inpatients with or at risk of malnutrition are more likely to develop SP complicated with AD compared with elderly inpatients with normal nutrition (OR = 4.907, 95% CI: 1.685-14.108, $P = 0.002$). This may be due to the fact that malnutrition can lead to lower serum

albumin level in patients. Protein is a component of muscle, and low protein intake can lead to low muscle mass, which leads to SP. Studies have found that AD patients have a higher risk of malnutrition compared with people with normal cognitive function [28]. It can be seen that attention should be paid to the nutritional status of elderly inpatients clinically. For patients at risk of malnutrition, further screening for SP and AD should be performed, and interventions such as nutritional supplementation and exercise training should be taken as soon as possible.

It is worth noting that the risk of SP complicated with AD in the elderly patients with depression in this study was 10.873 times that of the elderly patients without depression. There may be common pathophysiological mechanisms between SP and mental disorders (depression, AD). Skeletal muscle can release neurotrophic factors that nourish neuron growth and differentiation during contraction, which can have a positive effect in mood changes [29]. In addition, depression can reduce appetite, and result in insufficient protein intake, thereby causing the decreased muscle mass. A meta-analysis by Taiwanese scholars also has shown that with exclusion of confounding factors such as age, gender, cognitive function, and physical activity; SP is positively correlated with depression (OR = 1.821, 95% CI: 1.160-2.859) [30]. There is also a significant correlation between depression and AD in the elderly. Neurodegenerative changes [26], vascular damage, and neuroinflammatory changes [31], etc., are the common pathophysiological mechanisms between depression and AD. Another meta-analysis has shown that the prevalence rate of depression in mild AD patients was 32% (95% CI: 27%-37%), that is, 1 out of every 3 mild AD patients has a simultaneous suffer from depression [32]. In conclusion, screening for depressive symptoms in the elderly is critical for identifying SP and AD.

5. Conclusion

The combined serum AGEs and Hcy have a good diagnostic value for AD complicated with SP, which can help to detect the patient's condition early. In addition, age, depression, malnutrition and BMI are independent influencing factors of SP complicated with AD in elderly inpatients. These patients should be given sufficient attention in treatment and daily life.

Data Availability

The datasets used and/or analyzed during the current study are available from the corresponding author upon request.

Conflicts of Interest

The authors declared no potential conflicts of interest with respect to the research, authorship, and/or publication of this article.

Acknowledgments

This study was supported by the Jiangsu Provincial Health and Family Planning Commission scientific research project (LR2021048).

References

[1] J. Y. Nau, "100 years later, what to know about Maillard reaction and French fries toxicity?," *Revue Médicale Suisse*, vol. 10, no. 424, pp. 772-773, 2014.

[2] Z. S. Khachaturian, "Revised criteria for diagnosis of Alzheimer's disease: National Institute on Aging-Alzheimer's Association diagnostic guidelines for Alzheimer's disease," *Alzheimers Dement*, vol. 7, no. 3, pp. 253–256, 2011.

[3] L. K. Chen, J. Woo, P. Assantachai et al., "Asian working group for sarcopenia: 2019 consensus update on sarcopenia diagnosis and treatment," *Journal of the American Medical Directors Association*, vol. 21, no. 3, pp. 300–307.e2, 2020.

[4] C. Beaudart, M. Zaaria, F. Pasleau, J. Y. Reginster, and O. Bruyère, "Health outcomes of sarcopenia: a systematic review and meta-analysis," *PLoS One*, vol. 12, no. 1, article e0169548, 2017.

[5] V. Jakus, K. Bauerová, and N. Rietbrock, "Effect of aminoguanidine and copper (II) ions on the formation of advanced glycosylation end products. In vitro study on human serum albumin," *Arzneimittel-Forschung*, vol. 51, no. 4, pp. 280–283, 2001.

[6] A. Kuhla, S. C. Ludwig, B. Kuhla, G. Münch, and B. Vollmar, "Advanced glycation end products are mitogenic signals and trigger cell cycle reentry of neurons in Alzheimer's disease brain," *Neurobiology of Aging*, vol. 36, no. 2, pp. 753–761, 2015.

[7] E. Zengarini, R. Giacconi, L. Mancinelli et al., "Prognosis and interplay of cognitive impairment and sarcopenia in older adults discharged from acute care hospitals," *Journal of Clinical Medicine*, vol. 8, no. 10, p. 1693, 2019.

[8] S. K. Weeks, P. E. McGann, T. K. Michaels, and B. W. J. H. Penninx, "Comparing various short-form Geriatric Depression Scales leads to the GDS-5/15," *Journal of Nursing Scholarship*, vol. 35, no. 2, pp. 133–137, 2003.

[9] P. Salahuddin, G. Rabbani, and R. H. Khan, "The role of advanced glycation end products in various types of neurodegenerative disease: a therapeutic approach," *Cellular & Molecular Biology Letters*, vol. 19, no. 3, pp. 407–437, 2014.

[10] S. Y. Ko, H. A. Ko, K. H. Chu et al., "The possible mechanism of advanced glycation end products (AGEs) for Alzheimer's disease," *PLoS One*, vol. 10, no. 11, article e0143345, 2015.

[11] G. N. Welch and J. Loscalzo, "Homocysteine and atherothrombosis," *The New England Journal of Medicine*, vol. 338, no. 15, pp. 1042–1050, 1998.

[12] M. Krautwald and G. Münch, "Advanced glycation end products as biomarkers and gerontotoxins - a basis to explore methylglyoxal-lowering agents for Alzheimer's disease?," *Experimental Gerontology*, vol. 45, no. 10, pp. 744–751, 2010.

[13] J. Geisel, U. Hübner, M. Bodis et al., "The role of genetic factors in the development of hyperhomocysteinemia," *Clinical Chemistry and Laboratory Medicine*, vol. 41, no. 11, pp. 1427–1434, 2003.

[14] M. S. Morris, "Homocysteine and Alzheimer's disease," *Lancet Neurology*, vol. 2, no. 7, pp. 425–428, 2003.

Hindawi
Computational and Mathematical Methods in Medicine
Volume 2023, Article ID 9847256, 1 page
https://doi.org/10.1155/2023/9847256

Retraction

Retracted: Cognitive Function and Vitamin D Status in the Chinese Hemodialysis Patients

Computational and Mathematical Methods in Medicine

Received 5 December 2023; Accepted 5 December 2023; Published 6 December 2023

This article has been retracted by Hindawi, as publisher, following an investigation undertaken by the publisher [1]. This investigation has uncovered evidence of systematic manipulation of the publication and peer-review process. We cannot, therefore, vouch for the reliability or integrity of this article.

Please note that this notice is intended solely to alert readers that the peer-review process of this article has been compromised.

Wiley and Hindawi regret that the usual quality checks did not identify these issues before publication and have since put additional measures in place to safeguard research integrity.

We wish to credit our Research Integrity and Research Publishing teams and anonymous and named external researchers and research integrity experts for contributing to this investigation.

The corresponding author, as the representative of all authors, has been given the opportunity to register their agreement or disagreement to this retraction. We have kept a record of any response received.

References

[1] J. Zhang, J. Hu, R. Zhou, and Y. Xu, "Cognitive Function and Vitamin D Status in the Chinese Hemodialysis Patients," *Computational and Mathematical Methods in Medicine*, vol. 2022, Article ID 2175020, 6 pages, 2022.

Hindawi
Computational and Mathematical Methods in Medicine
Volume 2022, Article ID 2175020, 6 pages
https://doi.org/10.1155/2022/2175020

Research Article

Cognitive Function and Vitamin D Status in the Chinese Hemodialysis Patients

Jing Zhang,[1] **Jun Hu**,[2] **Ru Zhou**,[1] **and Yuzhen Xu**[3]

[1]*Department of Nephrology, Wannan Medical College Affiliated Yijishan Hospital, Wuhu, Anhui Province 241001, China*
[2]*Hemodialysis Center, Wannan Medical College Affiliated Yijishan Hospital, Wuhu, Anhui Province 241001, China*
[3]*Department of Rehabilitation, The Second Affiliated Hospital of Shandong First Medical University, Taian, Shandong Province 271000, China*

Correspondence should be addressed to Jing Zhang; jingzhang721@163.com, Jun Hu; yjsyyhujun@163.com, and Yuzhen Xu; tianyayizhe@126.com

Received 19 June 2022; Accepted 23 August 2022; Published 9 September 2022

Academic Editor: Min Tang

Objective. Vitamin D insufficiency and the cognitive function decline are both common in patients receiving hemodialysis (HD). The present study evaluated the relation between cognitive function and circulating vitamin D levels in HD patients in Wannan Medical College Affiliated Yijishan Hospital, China. *Methods*. This study was conducted in 80 patients receiving HD in Wannan Medical College Affiliated Yijishan Hospital. To measure cognitive function, Montreal Cognitive Assessment-Basic (MoCA-B) Chinese Version was used. The 25-hydroxyvitamin D [25(OH)D], which is applied to assess vitamin D status, was tested. One-way ANOVA, Tukey post hoc test, and the correlation and regression analysis were used in this study. *Results*. Based on the MoCA-B, cognitive function decline (the scores below 26) was present in 28 HD patients, accounting for 35% (28/80). The mean age of these patients is 50.5 ± 10.9 years old. The mean level of 25(OH)D was 16.1 ± 7.3 ng/ml in 80 HD patients. In univariate analysis, there was a significant relationship between MoCA-B score and serum 25(OH)D level ($p < 0.05$). The level of 25(OH)D was positively correlated with MoCA-B score ($r = 0.312$, $p = 0.023$), and the association was independent of demographic and clinical features. *Conclusions*. Vitamin D insufficiency may contribute to cognitive function decline in HD patients. Serum level of 25(OH)D is an independent protective factor of cognitive function in the HD patients.

1. Introduction

Chronic kidney disease (CKD) has become a major public health problem worldwide. According to the 2012 national epidemiological survey, the overall prevalence of CKD was 10.8% [1] in China, that is, there are about 130 million patients with CKD in China. CKD are independent risk factors for cognitive dysfunction [2]. Cognitive function decline is common in dialysis patients, with the prevalence of mild to moderate cognitive dysfunction up to 70% in hemodialysis (HD) population [3]. What is more, cognitive dysfunction is an independent predictive factor for all-cause mortality in the patients undergoing HD. Therefore, cognitive function decline will become a more and more serious problem in this population [4].

Vitamin D is a kind of fat-soluble seco-steroid necessity for calcium uptake and bone metabolism [5], which is mainly synthesized in the skin after sun exposure. Vitamin D insufficiency has been reported to be common among patients with CKD [6] because of declined renal function and vitamin D metabolism disorder [7]. Vitamin D insufficiency has also been related to many statuses, such as obesity, cardiovascular, and neurodegenerative diseases [8, 9]. Some literatures have demonstrated that vitamin D is closely related to cognitive function decline [10, 11]. Therefore, vitamin D insufficiency is considered as a potentially reversible hazard factor of declined cognitive function. However, little is known about the relationship between the level of vitamin D and the cognitive function in HD patients of China.

25-Hydroxyvitamin D [25(OH)D] (with a half-life of 2-3 weeks [12]) is a metabolite of vitamin D and is also considered as the main circulating form of vitamin D. It is widely applied to assess vitamin D status. Thus, in this study, our

purpose is to assess the association between 25(OH)D level and cognitive function in HD patients at a single hemodialysis center.

2. Patients and Methods

2.1. Study Population. All the HD participants (from Wannan Medical College Affiliated Yijishan Hospital) were patients aged 30–82 years who were receiving HD more than 6 months. The study was approved by the Ethics Committee of Yijishan Hospital Affiliated to Wannan Medical College. The written approval consents from participants and/or their guardians were obtained prior to enrollment in the study. Exclusion criteria were: age < 18years or >90years; HD vintage < 6 months; suffered from dementia, cerebrovascular disease, infection, or other serious illnesses such as malignancy during the 6 months before the study; unable or unwilling to answer the questionnaire. None of the patients had taken vitamin D during the study.

2.2. Hemodialysis. All the patients were receiving conventional HD (thrice weekly, 4 h each time) through autologous arteriovenous fistula and used "Gambro" HD machine, "Gambro" Polyflux L capillary dialyzers, and bicarbonate dialysate. The blood flow ranged from 220 to 260 ml/min with a dialysate flow of 500 ml/min. All the patients were injected intravenously with low molecular heparin before HD for anticoagulation, according to body weight (60-80 IU/kg). All of them were treated with recombinant human erythropoietin (rhEPO) according to their anemia status and L-Carnitine after each session of HD.

2.3. Laboratory Measurements. The clinical, laboratory tests in HD patients were performed at the beginning of the study. Blood for assessment of biochemical characteristics were collected from the HD patients, after fasting for more than 8 hours. The isolated serum samples were measured for the biochemical parameters, such as albumin, blood glucose, renal function (including blood urea nitrogen and serum creatinine), lipids profiles (including total cholesterol, triglycerides, high-density lipoprotein cholesterol, and low-density lipoprotein cholesterol), calcium and phosphorus and intact parathyroid hormone (iPTH), and vitamin D status [25(OH)D].

2.4. Cognitive Assessment Examination. The Chinese translation version of MoCA-B test was administered in all participants. The full score of MoCA-B test is 30, and a score below 26 is indicative of cognitive function decline. The testing personnels have been trained by the neurologist.

2.5. Statistical Analyses. All the data were analyzed by SPSS 22.0 statistical software. The continuous variables were expressed as means (standard deviation), and categorical variables were summarized as numbers and percentages. One-way ANOVA and subsequent Tukey post hoc test were used to analyze the data between the groups. Further, the correlation and regression analyses between demographic, clinical laboratory features, and MoCA-B scores were performed. $p < 0.05$ was regarded as a significant difference.

Table 1: Demographic information and laboratory data and MoCA-B scores of HD patients ($N = 80$).

Characteristics	Outcomes
Age, yr (range)	52.3 ± 11.1 (30-82)
Males, *N* (%)	43 (53.75)
Females, *N* (%)	37 (46.25)
Education, yr N (%)	
0-3	13 (16.25)
3-6	35 (43.75)
6-12	30 (37.5)
>12	2 (2.50)
Antecedents, N (%)	
Diabetes	38 (47.5)
Hypertension	8 (10.0)
Glomerulonephritis	32 (40.0)
Others	2 (2.5)
Duration of HD (months)	53.6 ± 26.4
Smokers, *N* (%)	3(3.75)
Predialysis SBP, mmHg	140.2 ± 20.3
Predialysis DBP, mmHg	73.3 ± 9.5
MAP, mmHg	95.6 ± 11.4
MoCA-B score	26.1 ± 2.0 (22-30)
MoCA − B score < 26	
N (%)	28 (35)
Age, yr	50.5 ± 10.9
Clinical laboratory characteristics	
25(OH)D, ng/ml	16.1 ± 7.3
Hb, g/l	112.6 ± 16.8
Alb, g/l	40 ± 4.4
BUN, mmol/l	24.4 ± 8.4
Scr, μmol/l	877.1 ± 231.3
Ca, mmol/l	2.4 ± 0.2
P, mmol/l	1.7 ± 0.5
BG, mmol/l	5.3 ± 2.0
TC, mmol/l	4.0 ± 1.0
TG, mmol/l	1.7 ± 0.8
HDL-C, mmol/l	1.3 ± 0.3
LDL-C, mmol/l	2.2 ± 0.7
iPTH, pg/ml	317.5 ± 317.4

Continuous variables are expressed as means ± SD, and categorical variables were summarized as numbers (percentages). SBP: systolic blood pressure; DBP: diastolic blood pressure; MAP: mean arterial pressure; 25(OH)D: 25 hydroxyvitamin D; Hb: hemoglobin; Alb: albumin; BUN: blood urea nitrogen; Scr: serum creatinine; Ca: calcium; P: phosphorus; BG: blood glucose; TC: total cholesterol; TG: triglyceride; HDL-C: high-density lipoprotein cholesterol; LDL-C: low-density lipoprotein cholesterol; iPTH: intact parathyroid hormone; mM: mmol/l.

Table 2: Demographic, laboratory features, and MoCA-B scores of three groups.

Variable	Tertile 1	Tertile 2	Tertile 3	p
25(OH)D(ng/ml)	≤10.77	10.77-19.24	>19.24	—
Age (yr)	53 ± 12.5	49.6 ± 10.6	54.2 ± 9.9	0.206
Male (n)	15	12	16	0.624
Female (n)	11	15	11	0.569
Education (yr)	6.7 ± 2.4	6.6 ± 2.4	7.0 ± 2.4	0.074
Smokers (n)	1	1	1	—
SBP, mmHg	144.2 ± 19.2	145.0 ± 18.0	131.5 ± 21.3	0.097
DBP, mmHg	74.8 ± 11.2	74.9 ± 8.9	70.1 ± 8.2	0.324
Duration of dialysis (months)	48.8 ± 31.5	53.7 ± 24.1	48.4 ± 23.2	0.247
Hb, g/l	113.1 ± 22.2	110.6 ± 15.1	113.9 ± 12.2	0.812
Alb, g/l	39.5 ± 5.4	38.9 ± 4.2	41.7 ± 2.7	0.746
BUN, mmol/l	20.5 ± 5.5	22.1 ± 7.3	20.8 ± 5.6	0.692
Scr, μmol/l	837.0 ± 241.8	853.7 ± 242.1	939.3 ± 203.6	0.186
Ca, mmol/l	2.4 ± 0.2	2.3 ± 0.2	2.4 ± 0.2	0.717
P, mmol/l	1.7 ± 0.4	1.7 ± 0.5	1.7 ± 0.5	0.826
BG, mmol/l	5.3 ± 2.7	5.3 ± 1.9	5.3 ± 1.0	0.844
TC, mmol/l	4.0 ± 1.0	4.0 ± 1.0	3.9 ± 1.0	0.656
TG, mmol/l	1.7 ± 0.7	1.8 ± 1.0	1.6 ± 0.7	0.532
HDL-C, mmol/l	1.3 ± 0.3	1.3 ± 0.3	1.3 ± 0.3	0.781
LDL-C, mmol/l	2.2 ± 0.8	2.2 ± 0.6	2.1 ± 0.7	0.889
iPTH, pg/ml	292.5 ± 253.5	332.1 ± 305.3	326.5 ± 266.9	0.068
MoCA-B score	24.8 ± 1.7	26.0 ± 1.8	27.5 ± 1.7	0.042

25(OH)D: 25-hydroxyvitamin D; SBP: systolic blood pressure; DBP: diastolic blood pressure; MAP: mean arterial pressure; Hb: hemoglobin; Alb: albumin; BUN: blood urea nitrogen; Scr: serum creatinine; Ca: calcium; P: phosphorus; BG: blood glucose; TC: total cholesterol; TG: triglyceride; HDL-C: high-density lipoprotein cholesterol; LDL-C: low-density lipoprotein cholesterol; iPTH: intact parathyroid hormone.

3. Results

The demographic information and clinical laboratory data and MoCA-B scores of patients receiving HD are presented in Table 1. In total, 80 subjects comprising 43 (53.75%) males and 37 (46.25%) females were enrolled to this study, and fortunately, no one dropped out of this research. The average age of the subjects was 52.3 ± 11.1 years old (from 30 to 82 years old). The primary causes contributed to HD are chronic glomerulonephritis, hypertension, and diabetes, accounting for 40%, 10%, and 47.5%, respectively.

In our study, the mean MoCA-B score of all the participants was 26.0 ± 2.0 (ranged between 22 and 30). 28 patients showed cognitive function decline (MoCA − B score < 26), accounting for about 35%. The mean age of those patients with MoCA − B score < 26 is 50.5 ± 10.9 years old. The demographic, laboratory features, and MoCA-B scores of the participants were displayed in Table 2. There was no significant difference in demographic and laboratory features except MoCA-B scores. From Table 2, we can see that the lower the 25(OH)D level, the worse the cognitive function may be.

The Spearman rank correlation test (Table 3) shows MoCA-B score was positively correlated with 25(OH)D ($r = 0.312$, $p = 0.023$). However, MoCA-B score showed no correlation with demographic parameters (such as age, sex, and years of education) and other clinical parameters (such as concentrations of hemoglobin and other biochemical parameters).

Table 4 presented the association of serum 25(OH) D tertiles with MoCA-B scores in the HD patients. After adjusting age, sex, education, smoking, HD duration, and the clinical and laboratory parameters (such as SBP, DBP, Hb, Alb, BUN, Scr, Ca, P, BG, iPTH, TC, TG, HDL-C, and LDL-C), compared with the subjects in tertiles 1 [25(OH)D ≤ 10.77 ng/ml], there was significant protection for cognitive function with the subjects in tertiles 3 [25(OH)D > 19.24 ng/ml] (OR = 2.113; 95% CI 0.971-4.397; $p = 0.037$). The average MoCA-B score (26.0 ± 1.8) of subjects in tertiles 2 [25(OH)D: 10.77–19.24 ng/ml] increased, compared with that in tertiles 1(OR = 2.203; 95% CI 1.732-2.488,p =0.261), but there was no significant statistical difference between two groups (tertiles 1 versus tertiles 2).

4. Discussion

In our current study, HD patients had a relative high prevalence of cognitive function decline, and the level of serum 25(OH)D is positively related to the MoCA-B score in the

Table 3: Correlation analysis between MoCA-B and various parameters.

	r	p
Age (yr)	0.347	0.231
Male (n)	0.376	0.356
Education (yr)	0.221	0.279
Smokers (n)	0.768	0.697
SBP, mmHg	0.531	0.133
DBP, mmHg	0.651	0.098
Duration of dialysis(months)	0.257	0.146
Hb, g/l	0.374	0.333
Alb, g/l	0.419	0.103
BUN, mmol/l	0.544	0.265
Scr, μmol/l	0.731	0.247
Ca, mmol/l	0.424	0.421
P, mmol/l	0.537	0.258
BG, mmol/l	0.471	0.394
TC, mmol/l	0.604	0.136
TG, mmol/l	0.495	0.289
HDL-C, mmol/l	0.537	0.686
LDL-C, mmol/l	0.289	0.691
iPTH, pg/ml	0.114	0.218
25(OH)D, ng/ml	0.312	0.023

SBP: systolic blood pressure; DBP: diastolic blood pressure; MAP: mean arterial pressure; 25(OH)D: 25 hydroxyvitamin D; Hb: hemoglobin; Alb: albumin; BUN: blood urea nitrogen; Scr: serum creatinine; Ca: calcium; P: phosphorus; BG: blood glucose; TC: total cholesterol; TG: triglyceride; HDL-C: high-density lipoprotein cholesterol; LDL-C: low-density lipoprotein cholesterol; iPTH: intact parathyroid hormone.

HD population. This relationship was independent of demographic and clinical laboratory features. Our results also demonstrated that the high level of 25 (OH)D in serum was an independent protective factor for predicting good cognitive function in Chinese HD patients.

Cognitive function decline can occur at all stages of CKD, including early stage [13] and end stage [14]. In addition to cardiovascular complications, the neurologic complications are also very prevalent in CKD patients, especially in dialysis patients. One of the neurological complications is cognitive function decline [15], which is remarkably associated with CKD, but not with age and other potential confounders [16]. The cognitive function of HD patients of all ages is worse than individuals of the general population of the same age [3]. In our current study, 35% HD patients appeared cognitive function decline, which is different from our previous study [17] that reported that only 15% HD patients appeared cognitive function decline. The main reason may be lie in the different assessment method and the different primary disease causing end stage renal disease (ESRD). In this study, diabetes was the primary disease in almost half of the HD patients (accounting for 47.5%), whereas this proportion accounted for only 32% in our previous study [17]. In the Miskulin's Cohort Study [18], diabetes is the primary cause in 47% of patients with ESRD, which is similar to this study. Diabetes and ESRD are both independent risk factors for cognitive function decline because advanced glycosylation end-product accumulation may trigger vascular endothelial dysfunction [19] and impaired cerebral blood flow in ESRD, which finally contributed to cognitive function decline. However, there are few studies about the combined impact of diabetes and ESRD on cognitive function. In the future, we will focus on the cognitive function of the patients with diabetic ESRD.

The poor cognitive function is high prevalent in elderly population [13]. The older the age, the greater the decline of cognitive function every year, regardless of sex, race, education, stroke history, or cause of renal failure [20]. However, the result of our study presented differently. The average age of HD patients with cognitive function decline in our study is only 50.5 ± 10.9 years old, which is similar to a seven-year study [21]. In that study, not only elderly but also younger aged dialysis patients (mean age: 51.81 ± 14.05 years old) presented significant cognitive function decline. Therefore, HD patients may have a high risk of cognitive function decline even at younger ages.

The causes of poor cognitive function are not fully understood in the adult population receiving HD, and several factors might be involved in the high prevalence of cognitive function decline and rapid deterioration in HD patients. The uremic toxins has been reported to potentially lead to poor cognitive function, because cognitive function was improved with the restoration of renal function after kidney transplantation [22]. In addition, there are other risk factors between cognitive function decline and ESRD.

Vitamin D is gradually recognized and attached importance because of its effect on cognitive function. Vitamin D levels are decreased in population suffered from mild cognitive impairment [23], and vitamin D insufficiency is a potential risk factor for cognitive function decline in the general population [10]. A part of the reason is that higher circulating levels of 25(OH)D exerts vasculoprotective and neuroprotective properties to improve cognitive function. The mechanism involved in inhibiting proinflammatory factors, antioxidation, immunoregulation, and enhanced nerve conduction [24]. 25(OH)D insufficiency is also associated with endothelial dysfunction [25], which is related to cognitive impairment [26]. An animal experimental study [27] also found that increasing the level of 25(OH)D could prevent the age-related cognitive function decline in aged rats. The reason was that vitamin D was thought to strengthen hippocampal synaptic function in aged rats.

Despite of different subjects, the mean level of serum 25(OH)D is 16.1 ± 7.3 ng/ml in this study, which is similar to the previous report (the mean level of serum $25(\mathrm{OH})\mathrm{D} \pm \mathrm{SD}$ was 17.26 ± 7.4 ng/ml) [28]. We also found an association between serum low levels of vitamin D [assessed by 25(OH)D] and cognitive function decline in Chinese HD patient, which is also consistent with Kamran's study of HD patients in the United States [28]. In this study, patients with higher 25(OH)D tertile had significantly higher MoCA-B scores. The spearman correlation test shows that the serum 25(OH)D level is positively related to MoCA-B scores ($r = 0.312$; $p < 0.05$). However, not all literatures report such association. A study by Jovanovich et al. [29] of 605 veterans with advanced CKD and chronic dialysis reported that the

Table 4: Association of serum 25(OH) D tertiles with MoCA-B scores.

	ORs (95% CI), p value		
	Tertile 1	Tertile 2	Tertile 3
N	26	27	27
	1 (reference)	2.203 (1.732-2.488), $p = 0.261$	2.113 (0.971-4.397), $p = 0.037$

Adjusted for age, sex, education, smoking, duration of HD, SBP, DBP, Hb, Alb, BUN, Scr, Ca, P, BG, iPTH, TC, TG, HDL-C, and LDL-C; SBP: systolic blood pressure; DBP: diastolic blood pressure; Hb: hemoglobin; Alb: albumin; BUN: blood urea nitrogen; Scr: serum creatinine; Ca: calcium; P: phosphorus; BG: blood glucose; iPTH: intact parathyroid hormone; TC: total cholesterol; TG: triglyceride; HDL-C: high-density lipoprotein cholesterol; LDL-C: low-density lipoprotein cholesterol.

levels of plasma 25(OH)D could not independently predict TICSm score, a method for measuring cognitive function in advanced CKD and ESRD. This discrepancy may lie in: (1) different investigation methods (face to face questionnaire and telephone survey); (2) different method for measuring cognitive function (MoCA-B and TICSm); (3) different research objects (men and women are almost equally divided and nearly entirely men); (4) racial differences.

Except for the correlation between serum 25(OH)D and MoCA-B scores, previous studies have confirmed the associations between higher SBP and DBP and cognitive impairment in the general population [30]. However, other studies suggested that there was no relationship between changes in SBP or intradialytic change in blood pressure with cognitive function decline [31]. Our study also found there is no relationship between SBP and cognitive function. The main cause may be that the subjects are different. The elevated iPTH levels were associated with impaired cognitive function in the patients suffered from secondary hyperparathyroidism due to calcium deficit rather than renal function impairment [32], whereas nocturnal daily HD improved cognitive function, which may be partly due to reduced iPTH levels [33]. However, we did not find an independent relationship between iPTH levels and cognitive function in HD patients.

In conclusion, serum 25(OH)D affects cognitive function in HD patients. The level of serum 25(OH)D may play independent roles in cognitive function decline. The potential mechanism needs to be further explored.

5. Limitations of the Study

There were several limitations in this study. In the first place, the sample of the patient population is relatively small (only 80 patients), which may produce selection bias and made this study underpowered. Thus, it is recommended to expand the sample sizes, and we are convinced that expanding the sample size would more reveal that whether reduced 25(OH)D raises the incidence of cognitive function decline in the HD patients. Second of all, the average age of HD patients is only 52.3 years in this study, which is slightly younger than the present age in many developed populations [34]. Therefore, the results of this study could not represent HD patients in other dialysis centers.

Data Availability

The data used to support the findings of this study are available from the corresponding author upon reasonable request.

Conflicts of Interest

The authors have declared no conflict of interest.

Authors' Contributions

Jing Zhang and Jun Hu contributed equally to this work.

Acknowledgments

This study was funded by grants from the Youth Research Fund of Wannan Medical College (WK2019F15) and University Natural Science Research Project of Anhui Province (KJ2019A0409).

References

[1] L. Zhang, F. Wang, L. Wang et al., "Prevalence of chronic kidney disease in China: a cross-sectional survey," *Lancet*, vol. 379, no. 9818, pp. 815–822, 2012.

[2] J. M. Bugnicourt, O. Godefroy, J. M. Chillon, G. Choukroun, and Z. A. Massy, "Cognitive disorders and dementia in CKD: the neglected kidney-brain axis," *Journal of the American Society of Nephrology: JASN*, vol. 24, no. 3, pp. 353–363, 2013.

[3] E. O'Lone, M. Connors, P. Masson et al., "Cognition in people with end-stage kidney disease treated with hemodialysis: a systematic review and meta-analysis," *American Journal of Kidney Diseases*, vol. 67, no. 6, pp. 925–935, 2016.

[4] A. A. Pereira, D. E. Weiner, T. Scott, and M. J. Sarnak, "Cognitive function in dialysis patients," *American Journal of Kidney Diseases*, vol. 45, no. 3, pp. 448–462, 2005.

[5] A. G. Turner, M. A. Hanrath, H. A. Morris, G. J. Atkins, and P. H. Anderson, "The local production of $1,25(OH)_2D_3$ promotes osteoblast and osteocyte maturation," *The Journal of Steroid Biochemistry and Molecular Biology*, vol. 144, no. Part A, pp. 114–118, 2014.

[6] A. Levin, G. L. Bakris, M. Molitch et al., "Prevalence of abnormal serum vitamin D, PTH, calcium, and phosphorus in patients with chronic kidney disease: results of the study to evaluate early kidney disease," *Kidney International*, vol. 71, no. 1, pp. 31–38, 2007.

[7] Y. C. Li, "Vitamin D: roles in renal and cardiovascular protection," *Current Opinion in Nephrology and Hypertension*, vol. 21, no. 1, pp. 72–79, 2012.

[8] M. Cekic, S. M. Cutler, J. W. Van Landingham, and D. G. Stein, "Vitamin D deficiency reduces the benefits of progesterone treatment after brain injury in aged rats," *Neurobiology of Aging*, vol. 32, no. 5, pp. 864–874, 2011.

[9] K. Rajakumar, J. D. Fernstrom, M. F. Holick, J. E. Janosky, and S. L. Greenspan, "Vitamin D status and response to vitamin D

Hindawi
Computational and Mathematical Methods in Medicine
Volume 2023, Article ID 9758487, 1 page
https://doi.org/10.1155/2023/9758487

Retraction

Retracted: Identification of Molecular Targets and Underlying Mechanisms of Xiaoji Recipe against Pancreatic Cancer Based on Network Pharmacology

Computational and Mathematical Methods in Medicine

Received 5 December 2023; Accepted 5 December 2023; Published 6 December 2023

This article has been retracted by Hindawi, as publisher, following an investigation undertaken by the publisher [1]. This investigation has uncovered evidence of systematic manipulation of the publication and peer-review process. We cannot, therefore, vouch for the reliability or integrity of this article.

Please note that this notice is intended solely to alert readers that the peer-review process of this article has been compromised.

Wiley and Hindawi regret that the usual quality checks did not identify these issues before publication and have since put additional measures in place to safeguard research integrity.

We wish to credit our Research Integrity and Research Publishing teams and anonymous and named external researchers and research integrity experts for contributing to this investigation.

The corresponding author, as the representative of all authors, has been given the opportunity to register their agreement or disagreement to this retraction. We have kept a record of any response received.

References

[1] C. Xia, D. Chen, G. Wang et al., "Identification of Molecular Targets and Underlying Mechanisms of Xiaoji Recipe against Pancreatic Cancer Based on Network Pharmacology," *Computational and Mathematical Methods in Medicine*, vol. 2022, Article ID 4640849, 17 pages, 2022.

Hindawi
Computational and Mathematical Methods in Medicine
Volume 2022, Article ID 4640849, 17 pages
https://doi.org/10.1155/2022/4640849

Research Article

Identification of Molecular Targets and Underlying Mechanisms of Xiaoji Recipe against Pancreatic Cancer Based on Network Pharmacology

Cunbing Xia,[1,2] Dexuan Chen,[1,2] Gaoyuan Wang,[1,2] Haijian Sun,[1,2] Jingran Lin,[1,2] Chen Chen,[1,2] Tong Shen,[1,2] Hui Cheng,[1,2] Chao Pan,[1,2] Dong Xu,[3] Hongbao Yang,[4] Yongkang Zhu ,[1,2] and Hong Zhu [1,2]

[1]*Department of General Surgery, Affiliated Hospital of Nanjing University of Chinese Medicine, Jiangsu Province Hospital of Chinese Medicine, Nanjing, Jiangsu 210029, China*
[2]*The Inheriting Studio of National Famous Old Chinese Medicine Experts-Zhu Yongkang (National Traditional Chinese Medicine Science and Education 2022 No. 75), Nanjing, Jiangsu 210029, China*
[3]*Pancreas Center, The First Affiliated Hospital of Nanjing Medical University, Nanjing, Jiangsu 210029, China*
[4]*Center for New Drug Safety Evaluation and Research, Institute of Pharmaceutical Science, China Pharmaceutical University, Nanjing, Jiangsu 211198, China*

Correspondence should be addressed to Yongkang Zhu; zhuyk8888@126.com and Hong Zhu; njtcm1998@163.com

Received 12 August 2022; Accepted 24 August 2022; Published 8 September 2022

Academic Editor: Min Tang

Traditional Chinese medicine (TCM) is applied in the anticancer adjuvant therapy of various malignancies and pancreatic cancer included. Xiaoji recipe consists several TCM materials with anticancer activities. In our work, we intended to analyze the molecular targets as well as the underlying mechanisms of Xiaoji recipe against pancreatic cancer. A total of 32 active components and 522 potential targets of Xiaoji recipe were selected using the TCMSP and SwissTargetPrediction databases. The potential target gene prediction in pancreatic cancer was performed using OMIM, Disgenet, and Genecards databases, and totally, 998 target genes were obtained. The component-disease network was constructed using the Cytoscape software, and 116 shared targets of pancreatic cancer and Xiaoji recipe were screened out. As shown in the protein–protein interaction (PPI) network, the top 20 hub genes such as TP53, HRAS, AKT1, VEGFA, STAT3, EGFR, and SRC were further selected by degree. GO and KEGG functional enrichment analysis revealed that Xiaoji recipe may affect pancreatic cancer progression by targeting the PI3K/AKT and MAPK signaling pathways. Moreover, we performed *in vitro* assays to explore the effect of Xiaoji recipe on pancreatic cancer cells. The results revealed that Xiaoji recipe suppressed the viability and migration and promoted the apoptosis of pancreatic cancer cells via the inactivation of PI3K/AKT, MAPK, and STAT3 pathways. The findings of our study suggested the potential of Xiaoji recipe in the targeting therapy of pancreatic cancer.

1. Introduction

Pancreatic cancer is a fatal malignancy and ranks the seventh leading cause of cancer-related death in both sexes, with approximately 5 million new cases and 466000 death cases in 2020 [1]. Many risk factors may contribute to the development of pancreatic cancer, including genetic background, obesity, type II diabetes, and tobacco smoking [2]. The chemotherapy with gemcitabine is regarded as the first-line treatment for pancreatic cancer, with 23.8% clinical response and a 5-year survival rate of 2% [3, 4]. However, the prognosis of pancreatic cancer patients is still unsatisfactory due to the late diagnosis, early metastasis, and limited chemotherapy effects [5]. Therefore, it is imperative to investigate potent treatment options to improve the clinical outcome of anticancer therapy in pancreatic cancer.

Traditional Chinese medicine (TCM), especially Chinese herbal medicines and acupuncture, is used to treat advanced

cancers with low-toxic effects and is reported to increase physical function, reduce symptoms, and improve the life quality of patients [6, 7]. Increasing studies have demonstrated the antitumor effects of TCM on the proliferation, metastasis, and tumorigeneis in cancer development [8]. In pancreatic cancer, it has been reported that scoparone inhibits tumor progression via PI3K/Akt signaling pathway [9]. Besides, a proteoglycan extracted from *Ganoderma lucidum* can induce cancer cell apoptosis [10]. The prescription of Xiaoji recipe is mainly composed of *Curcuma zedoaria* (10 g, E Zhu), *Polygonum cuspidatum* (10 g, Huzhang), *clematis root* (10 g, Weilingxian), *Rhizoma Paridis* (10 g, Zhonglou), and *Eupolyphaga Steleophaga* (10 g, Tubiechong). The main functions of Xiaoji recipe is to eliminate the heat and dampness and promote the blood circulation and can be used in the antitumor therapy for various cancers. *Curcuma zedoaria* (Zingiberaceae) is reported to inhibit the development of gastric carcinoma, breast cancer as well as liver cancer [11–14]. *Polygonum cuspidatum* is used for the therapy of multiple diseases including hypertension, diabetes, and atherosclerosis [15–17], and its extracts have been reported with anticancer effects in lung cancer, osteosarcoma, and breast cancer [18–20]. The extracts of *Rhizoma Paridis* is revealed to suppress the cancer development in non-small-cell lung carcinoma, colon cancer, and hepatocarcinoma [21–23]. *Eupolyphaga Steleophaga* is reported to be used in the treatment of fractures, falls, uterine fibroids, or menstrual problems [24], while its effects in cancer are not fully understood.

Network-based pharmacology is widely used in drug discovery by predicting potential mechanisms via exploring the targets of drugs, diseases, and their biomolecular networks [25, 26]. In TCM, a holistic perspective has long been at the heart of the herbal treatment of various diseases. TCM prescriptions have holistic theory and rich experience in multicomponent therapy, which provides a bright prospect for systematic treatment of complex diseases. Therefore, linking emerging network science with ancient TCM will provide new methods and opportunities to discover bioactive components and biomarkers, reveal mechanisms of action, and explore the scientific basis of TCM formulations based on complex biological systems [27]. Moreover, network-based pharmacology is becoming a frontier research field in current cancer drug research. For example, Huang et al. have explored the potential effect of Tao Hong Si Wu decoction for treating breast cancer according to network pharmacology and experimental [28].

Signaling pathways such as the phosphoinositide 3 kinase/AKT (PI3K/AKT) signaling pathway, signal transducer and activator of transcription 3 (STAT3) signaling pathway, and mitogen-activated protein kinases (MAPK) signaling pathway are important in the pathological process of pancreatic cancer and are frequently activated in pancreatic cancer. They are associated with poor prognosis of pancreatic cancer. Aberrant activation of these pathways are involved in cell survival, cell cycle progression, and cell apoptosis [29, 30]. Targeting these signaling pathways may be an approach to cancer treatment.

In our study, we intended to explore the potential core targets and pathways of Xiaoji recipe against pancreatic cancer based on the TCM network pharmacology approach. The findings of our study may provide clues for the targeting therapy of Xiaoji recipe in pancreatic cancer.

2. Materials and Methods

2.1. Cell Culture and Treatment. Pancreatic cell lines (CFPAC (cat. no. CRL-1918; PANC1, cat. no. CRL-1469)) were provided by the ATCC (American Type Culture Collection, USA), CFPAC cell line was cultured in Iscove's modified Dulbecco's medium. PANC1 cell line was cultured in Dulbecco's modified Eagle's medium (DMEM, Cytiva, Shanghai, China). Both culture mediums were maintained in an incubator supplemented with g 10% FBS (Beyotime, Shanghai, China) at 37°C and 5% CO_2. To evaluate the effects of Xiaoji recipe on cell malignant behaviors *in vitro*, the CFPAC and PANC1 cells were treated with 150 μg/ml or 300 μg/ml Xiaoji recipe.

2.2. Cell Viability. The viability of pancreatic cancer cells was measured using a Cell Counting Kit-8 (CCK-8; MCE, Inc., Shanghai, China). The treated CFPAC and PANC1 cells were grown into 96-well plates at 2000 cells/well and incubated for 24, 48, and 72 h, followed with addition of 10 μl CCK-8 solution, followed with incubation for another 2 h at 37°C. A microplate reader (HBS-1096A, DeTie Laboratory Equipment Co., Ltd., Nanjing, China) was used to determine the absorbance at 450 nm.

2.3. Wound Healing Assay. The treated CFPAC and PANC1 cells were plated into 6-well plates supplemented with medium and 1.5% fetal bovine serum and cultured to reach 90% confluence. Then, the plates were scratched using a 10 μl pipette tip. A microscope (Olympus, Shanghai, China) was used to photograph the wound healing distance at 0 and 48 h.

2.4. Flow Cytometry Analysis. The apoptosis of CFPAC and PANC1 cells after indicated treatments was assessed by flow cytometry analysis. CFPAC and PANC1 cells were harvested, washed with PBS, and resuspended in a 500 μl mixture with 5 μl Annexin and 10 μl propidium iodide (7-AAD; Multi-Sciences Biotech, Co., Ltd., Hangzhou, China). Finally, cell apoptosis rate was detected using a flow cytometer and analyzed with the FlowJo software. The apoptosis rate in each group was calculated by Q2 (late apoptosis) + Q3 (early apoptosis).

2.5. Western Blot. RIPA lysis buffer (Beyotime, Shanghai, China) was used to collect the protein in treated CFPAC and PANC1 cells. The concentration of collected proteins was evaluated using a BCA Protein Assay kit (Beyotime, Shanghai, China). Then, the proteins were separated with 10% SDS-PAGE gels and electrotransferred on the PVDF membranes. The Protein-Free Rapid Blocking Buffer (Epizyme, Shanghai, China) was used to block the membranes for 1 h, which were then cultured with the primary antibodies against AKT1 (1 : 1000, Abcam, USA), STAT3 (1 : 1000, Abcam, USA), EGFR (1 : 1000, Abcam, USA), MAPK3 (1 : 1000, Abcam, USA) at 4°C overnight, and

Table 1: Relation between potential targets and active components in Xiaoji recipe.

Component name	Degree	Betweenness centrality	Closeness centrality	Eccentricity
Bisdemethoxycurcumin	36	0.049102808	0.422096317	4
Luteolin	31	0.024267623	0.408219178	4
Quercetin	30	0.021502194	0.403794038	4
Flavone	30	0.029632826	0.412742382	4
Beta-ecdysone	27	0.02982601	0.40599455	4
Physovenine	22	0.016298752	0.38501292	4
(4aS,6aR,6aS,6bR,8aR,10R,12aR,14bS)-10-hydroxy-2,2,6a,6b,9,9,12a-heptamethyl-1,3,4,5,6,6a,7,8,8a,10,11,12,13,14b-tetradecahydropicene-4a-carboxylic acid	18	0.011697317	0.37913486	4
Pennogenin	18	0.008901981	0.375314861	5
ClematosideA′_qt	17	0.010539948	0.37721519	4
Picralinal	16	0.007242384	0.373433584	4
Rhein	16	0.009358031	0.371571072	4
Pennogenin VI	16	0.006015765	0.371571072	5
Pennogenin VII	16	0.006015765	0.371571072	5
6,8-Dihydroxy-7-methoxyxanthone	14	0.005718922	0.362530414	4
Physciondiglucoside	11	0.005127525	0.362530414	4
Diosgenin	10	0.002912114	0.357314149	5
Beta-sitosterol	9	0.011919371	0.355608592	4
Polysaccharide	9	0.003448702	0.347319347	5
Hederagenin	8	0.004162798	0.357314149	4
Stigmasterol	6	0.00185844	0.347319347	4
Wenjine	5	0.001187609	0.326039387	5
Cholesterol	5	0.005333285	0.344110855	4
Embinin	4	0.001738369	0.337868481	5
Dioscin I	4	3.06*E*-04	0.333333333	5
Dioscin II	4	3.06*E*-04	0.333333333	5
Torachrysone-8-O-beta-D-(6′-oxayl)-glucoside	3	2.64*E*-04	0.334831461	5
Heptyl phthalate	3	7.37*E*-04	0.336343115	4
Pariphyllin	3	1.43*E*-04	0.328918322	5

GAPDH (1 : 1000, Abcam, USA) served as an internal reference. Next, the membranes were washed with TBST and cultured with corresponding secondary antibodies (1 : 2000, Abcam, USA) for 2 h at room temperature. Finally, the protein signal was detected using a Biosharp ECL detection kit (Biosharp, Beijing, China) and analyzed with ImageJ software.

2.6. Exploration of Active Components and Potential Targets of Xiaoji Recipe. Xiaoji recipe is a traditional Chinese prescription composed of *Curcuma zedoaria* (E Zhu), *Polygonum cuspidatum* (Huzhang), *clematis root* (Weilingxian), *Rhizoma Paridis* (Zhonglou), and *Eupolyphaga Steleophaga* (Tubiechong). The active components of these TCM materials were searched on the Traditional Chinese Medicine Systems Pharmacology Database and Analysis Platform (TCMSP, http://lsp.nwu.edu.cn/tcmsp.php) [31] under the condition of oral bioavailability (OB) ≥ 30% and drug–likeness (DL) ≥ 0.18 and TCMID database (http://119.3.41.228:8000/tcmid/) [32]. The component structures obtained from the PubChem (https://pubchem.ncbi.nlm.nih.gov/) [33] and TCMSP databases were input into the SwissTargetPrediction database (http://www.swisstargetprediction.ch/) [34] for the prediction of the underlying target genes of main components in Xiaoji recipe.

2.7. Exploration of Potential Targets of Pancreatic Cancer. The potential target genes of pancreatic cancer were searched in the Disgenet (https://www.disgenet.org/) [35], OMIM (https://omim.org/) [36], and Genecards (https://www.genecards.org/) [37] databases using the "pancreatic ductal adenocarcinoma" as the keyword.

2.8. The Screening of Component-Disease Targets and Network Construction. The 522 targets of Xiaoji recipe and 998 targets of pancreatic cancer were imported into the Venny2.1 software, and the obtained Venn diagram showed 116 shared targets of the pancreatic cancer and the components of Xiaoji recipe. The drug-component-target-disease network was constructed using the Cytoscape 3.8.2 software and analyzed with the Network Analyzer function. The hub genes were analyzed and selected based on the topological

Table 2: Active ingredients of Xiaoji recipe.

Mol ID	Molecule name	OB (%)	DL	Chinese medicinal materials
MOL000296	Hederagenin	36.91	0.75	*Curcuma zedoaria*
MOL000906	Wenjine	47.93	0.27	*Curcuma zedoaria*
MOL000940	Bisdemethoxycurcumin	77.38	0.26	*Curcuma zedoaria*
MOL013281	6,8-Dihydroxy-7-methoxyxanthone	35.83	0.21	*Polygonum cuspidatum*
MOL013287	Physovenine	106.21	0.19	*Polygonum cuspidatum*
MOL013288	Picralinal	58.01	0.75	*Polygonum cuspidatum*
MOL002259	Physciondiglucoside	41.65	0.63	*Polygonum cuspidatum*
MOL002268	Rhein	47.07	0.28	*Polygonum cuspidatum*
MOL002280	Torachrysone-8-O-beta-D-(6′-oxayl)-glucoside	43.02	0.74	*Polygonum cuspidatum*
MOL000358	Beta-sitosterol	36.91	0.75	*Polygonum cuspidatum*, *clematis root*, *Eupolyphaga Steleophaga*
MOL000492	(+)-catechin	54.83	0.24	*Polygonum cuspidatum*
MOL000006	Luteolin	36.16	0.25	*Polygonum cuspidatum*
MOL000098	Quercetin	46.43	0.28	*Polygonum cuspidatum*
MOL001663	(4aS,6aR,6aS,6bR,8aR,10R,12aR,14bS)-10-hydroxy-2,2,6a,6b,9,9,12a-heptamethyl-1,3,4,5,6,6a,7,8,8a,10,11,12,13,14b-tetradecahydropicene-4a-carboxylic acid	32.03	0.76	*Clematis root*
MOL002372	(6Z,10E,14E,18E)-2,6,10,15,19,23-hexamethyltetracosa-2,6,10,14,18,22-hexaene	33.55	0.42	*Clematis root*
MOL000449	Stigmasterol	43.83	0.76	*Clematis root*
MOL005594	ClematosideA′_qt	37.51	0.76	*Clematis root*
MOL005598	Embinin	33.91	0.73	*Clematis root*
MOL005603	Heptyl phthalate	42.26	0.31	*Clematis root*
	Dioscin I			*Rhizoma Paridis*
	Dioscin II			*Rhizoma Paridis*
	Diosgenin			*Rhizoma Paridis*
	Flavone			*Rhizoma Paridis*
	Pariphyllin			*Rhizoma Paridis*
	Pennogenin			*Rhizoma Paridis*
	Pennogenin VI			*Rhizoma Paridis*
	Pennogenin VII			*Rhizoma Paridis*
	Polysaccharide			*Rhizoma Paridis*
	Beta-ecdysone			*Rhizoma Paridis*
	Cholesterol			*Eupolyphaga Steleophaga*
	Flavacin			*Eupolyphaga Steleophaga*
	Hypoxanthine			*Eupolyphaga Steleophaga*

analysis, and the degree value indicates the relation between the components and targets (Table 1).

2.9. Protein–Protein Interaction (PPI) Network Construction. The interaction of the 116 component-disease targets was explored on the STRING platform (https://cn.string-db.org/) [38] under "*Homo sapiens*." The protein was presented as nodes, and the association between proteins was shown as edges in the PPI network, and the size and shade of color represented the value of degree. Furthermore, based on the topological analysis, the results from the STRING database were analyzed with the Cytoscape 3.8.2 software using the Network Analyzer function, and the core targets

Table 3: Active ingredients and their potential targets in Xiaoji recipe.

Name	Ingredients (*n*)	Predicted targets (*n*)
Curcuma zedoaria (Ezhu)	3	159
Polygonum cuspidatum (Huzhang)	10	313
Clematis root (Weilingxian)	7	107
Rhizoma Paridis (Zhonglou)	10	271
Eupolyphaga Steleophaga (Tubiechong)	4	44

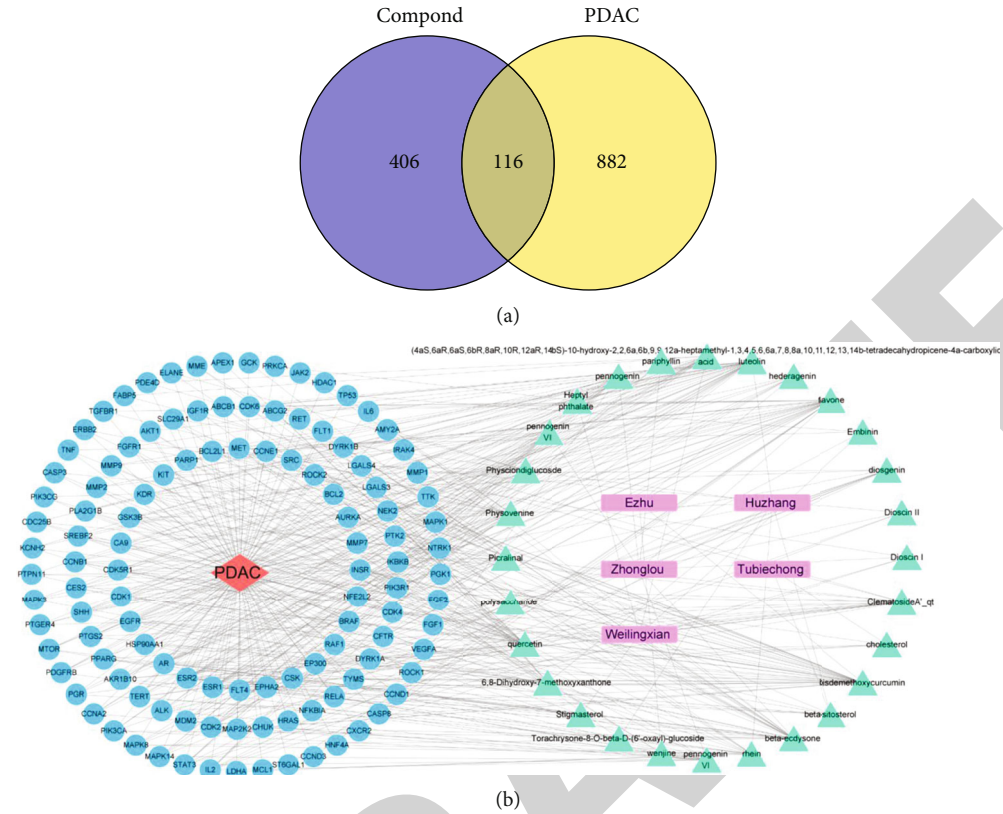

Figure 1: Construction of the target gene network of pancreatic cancer and Xiaoji recipe. (a) The Venn diagram of potential targets of main active components in Xiaoji recipe and pancreatic cancer. (b) The component-disease target network.

were selected under the condition of degree value over the average. The top 30 targets were selected and exported the bar graph using the R 4.0.5 software. Based on the clustering analysis, the results from the STRING database were imported into the Cytoscape 3.8.2 software and analyzed using the Molecular Complex Detection (MCODE) plugin. Three gene clusters were obtained, and 2 core genes (HSP90AA1, CDK6) were selected.

2.10. GO and KEGG Functional Enrichment Analysis. Gene Ontology (GO) analysis including the biological process (BP), molecular function (MF), and cellular components (CC) and the biological pathway (KEGG) enrichment analysis of 116 disease-component targets were performed using the R software with Bioconductor package under p value < 0.05. The results were exported with the bar graphs and pathway maps.

2.11. Statistical Analysis. All experiments were completed three times independently. The results were analyzed using GraphPad 8 software and presented as the mean ± SD. Student's t-test was used to compare the difference between two groups, and one-way ANOVA was used for multiple group comparisons. $p < 0.05$ indicates statistical significance.

3. Results

3.1. Active Ingredients and Their Potential Targets in Xiaoji Recipe. We found 32 potential active ingredients of Xiaoji recipe *Curcuma zedoaria* (E Zhu), *Polygonum cuspidatum* (Huzhang), *clematis root* (Weilingxian), *Rhizoma Paridis* (Zhonglou) and *Eupolyphaga Steleophaga* (Tubiechong) based on the TCMSP database, under OB ≥ 30% and DL ≥ 0.18 and TCMID database (Table 2). There were 3 ingredients from *Curcuma zedoaria*, 10 ingredients from *Polygonum cuspidatum*, 7 ingredients from *clematis root*, 10 ingredients from *Rhizoma Paridis*, and 4 ingredients from *Eupolyphaga Steleophaga* (Table 3). *Curcuma zedoaria*, *Polygonum cuspidatum*, and *clematis root* share the same ingredient beta-sitosterol. Based on the SwissTargetPrediction platform, we performed the prediction of the potential targets of active components in *Curcuma zedoaria* (E Zhu), *Polygonum cuspidatum* (Huzhang), *clematis root* (Weilingxian), *Rhizoma Paridis* (Zhonglou), and *Eupolyphaga Steleophaga*. Totally, 522 target genes of these active ingredients of Xiaoji recipe were screened out, and there were 159 targets for *Curcuma zedoaria*, 313 targets for *Polygonum cuspidatum*, 107 targets for *clematis root*, 271 targets for *Rhizoma Paridis*, and 44 targets for *Eupolyphaga Steleophaga* (Table 3).

3.2. Construction of the Target Gene Network of Pancreatic Cancer and Xiaoji Recipe. We searched the potential targets in the OMIM, Disgenet, and Genecards using the keywords "pancreatic ductal adenocarcinoma," and totally, 998 potential targets of PDAC were obtained. Venny 2.1 software was used to select the shared targets for PDAC and Xiaoji recipe, and the results showed that there were 116 shared targets in the intersection area (Figure 1(a)). Then, the 32 active

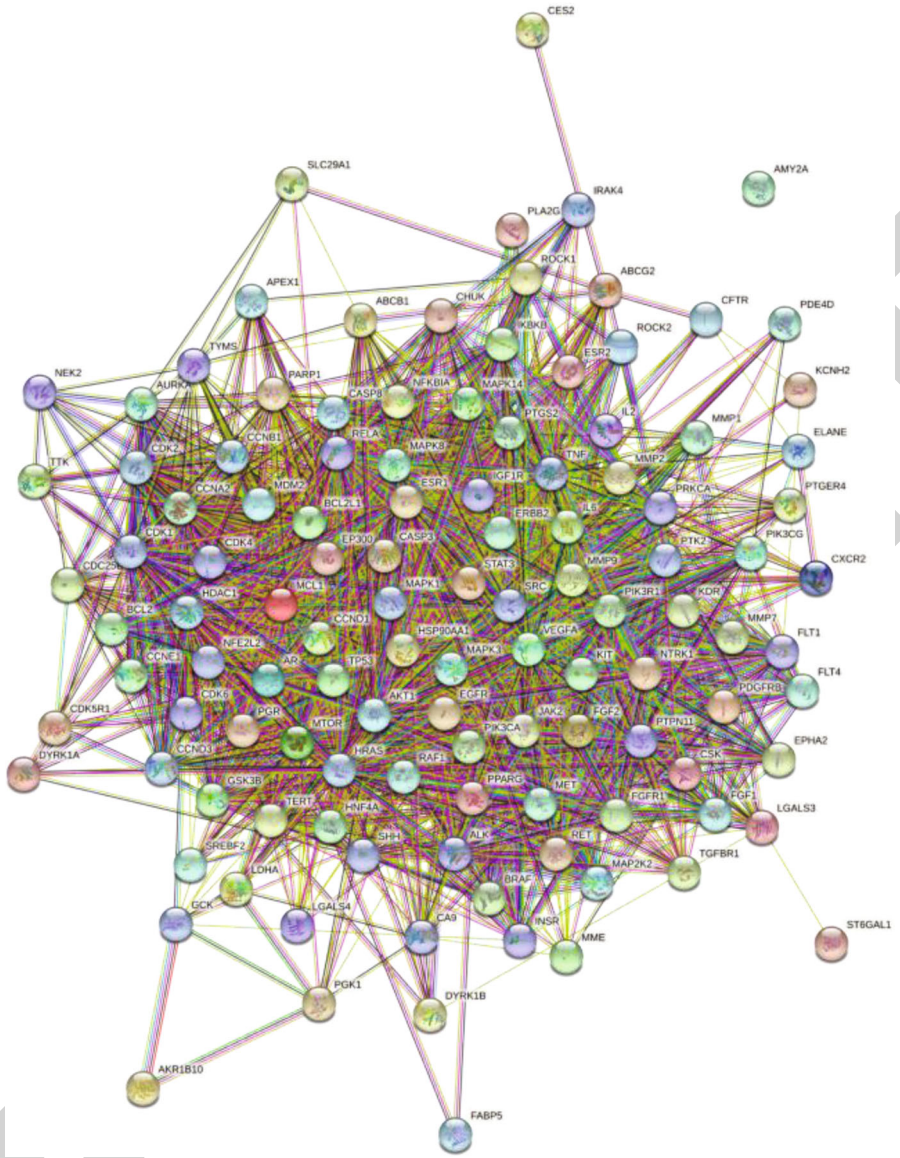

(a)

Figure 2: Continued.

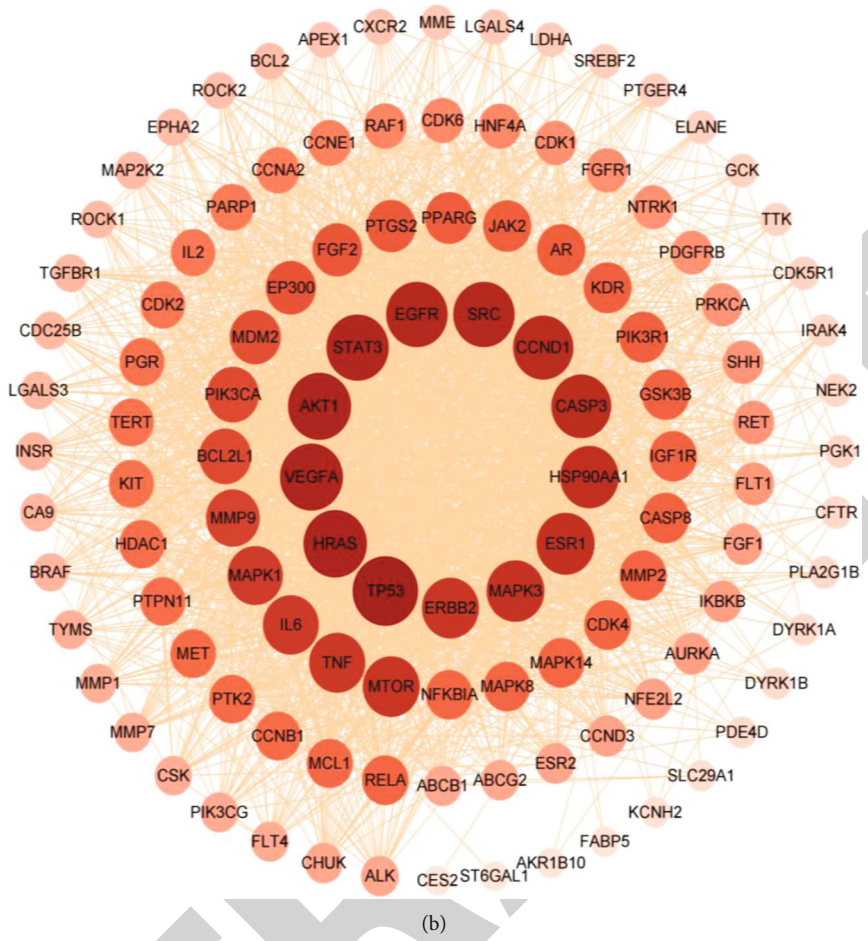

(b)

Figure 2: Construction of the PPI network and analysis of targets of Xiaoji recipe in pancreatic cancer. (a) The PPI network of 116 compound-disease target genes. (b) The topological analysis of the 116 compound-disease target genes.

ingredients in Xiaoji recipe and 116 compound-disease targets were input into the Cytoscape 3.8.2 software, and we deleted 4 isolated components that were not intersected with the targets. The remaining 28 active components were marked in red in Table 2. The main active biomolecules were analyzed using the Network Analyzer function. As shown in Figure 1(b), the red button represented the disease, the blue bubbles represented the 116 compound-disease targets, the purple rectangle represented the Chinese medical materials, and the green triangles represented the 28 active ingredients in Xiaoji recipe. The top five core ingredients were bisdemethoxycurcumin, luteolin, quercetin, flavone, and beta-ecdysone, as shown in Table 1.

3.3. Construction of the PPI Network and Analysis of Targets. The PPI network was constructed based on the STRING database and Cytoscape software to investigate the underlying interaction among the 116 targets. Based on the topology analysis, the 116 compound-disease targets were input in the STRING platform for the protein-protein interaction network construction. There were 116 nodes and 2210 edges (Figure 2(a)). Further, the interaction data from the STRING database were imported into the Cytoscape software for the interaction network. The degree was determined by the size and color shade of the nodes (Figure 2(b)). TP53, HRAS, VEGFA, AKT1, STAT3, EGFR, and SRC were the core target genes.

The hub genes in the network were identified by the top 30 targets ranked by degree on the PPI network, which was performed using the R 4.0.5 software as shown in Figure 3(a). Moreover, based on the clustering analysis and analysis using Cytoscape software, three gene clusters were obtained with two core target genes, HSP90AA1 and CDK6, which were potentially involved in the development of PDAC (Figure 3(b)).

3.4. GO and KEGG Pathway Enrichment Analysis. Based on the GO enrichment analysis, the biological process, cellular component, and molecular function of the 116 component-disease targets were analyzed using R software. The results revealed that the target genes were enriched in 2144 BP, 50 CC expression process, and 132 MF-related process. The biological functions of targets mainly included the peptidyl-serine modification and phosphorylation, positive modulation of protein serine/threonine kinase activity and MAP kinase activity, and gland development (Figure 4). The molecular functions mainly included the protein tyrosine kinase activity, phosphatase binding, insulin receptor substrate binding, and

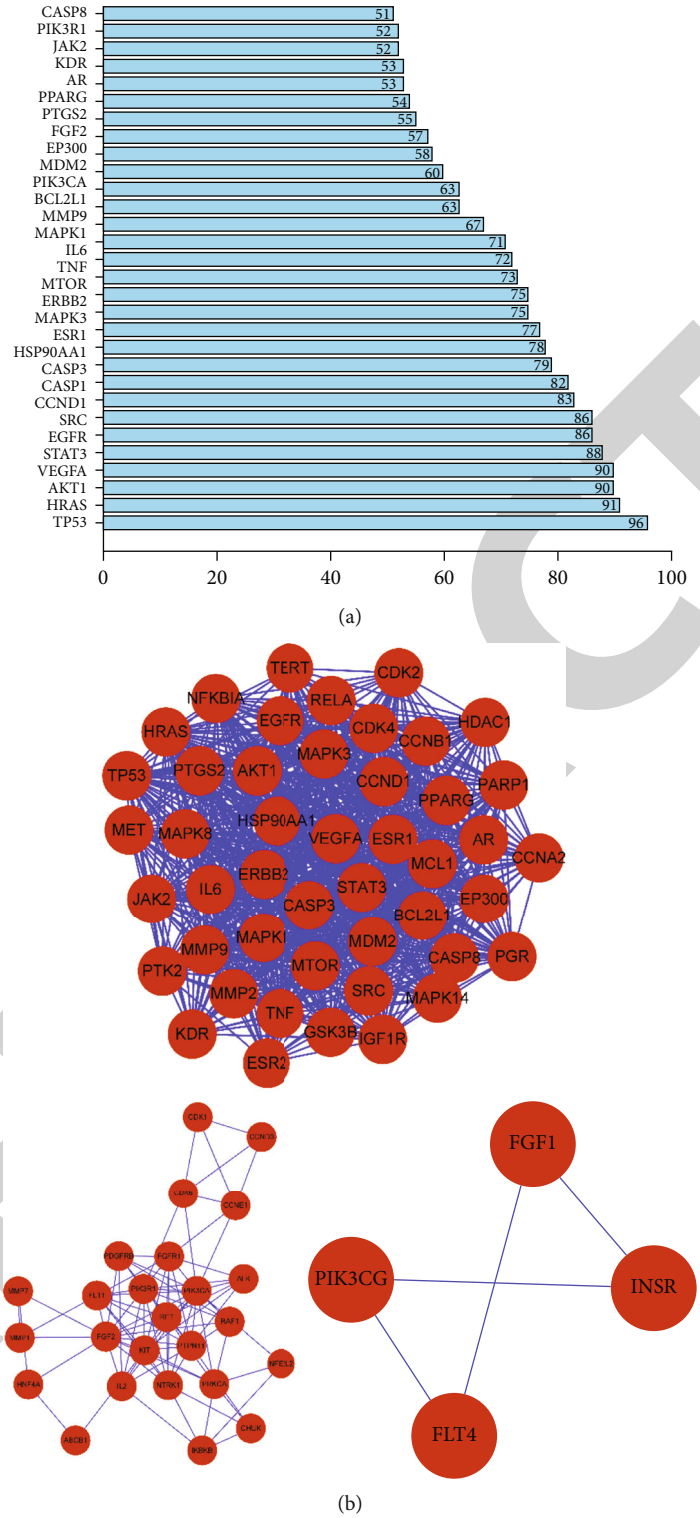

Figure 3: The analysis of compound-disease hub genes. (a) The top 30 genes from the PPI network based on the topological analysis. (b) The clustering analysis of the PPI network.

growth factor binding (Figure 5). The cellular component mainly included the transferase complex, protein kinase complex, serine/threonine protein kinase complex, membrane raft, and transcription regulator complex (Figure 6).

A total of 159 KEGG signaling pathways of the 116 shared target genes were obtained using the R software. The top 20 significant signaling pathways were shown in histograms. The results revealed that these targets were closely

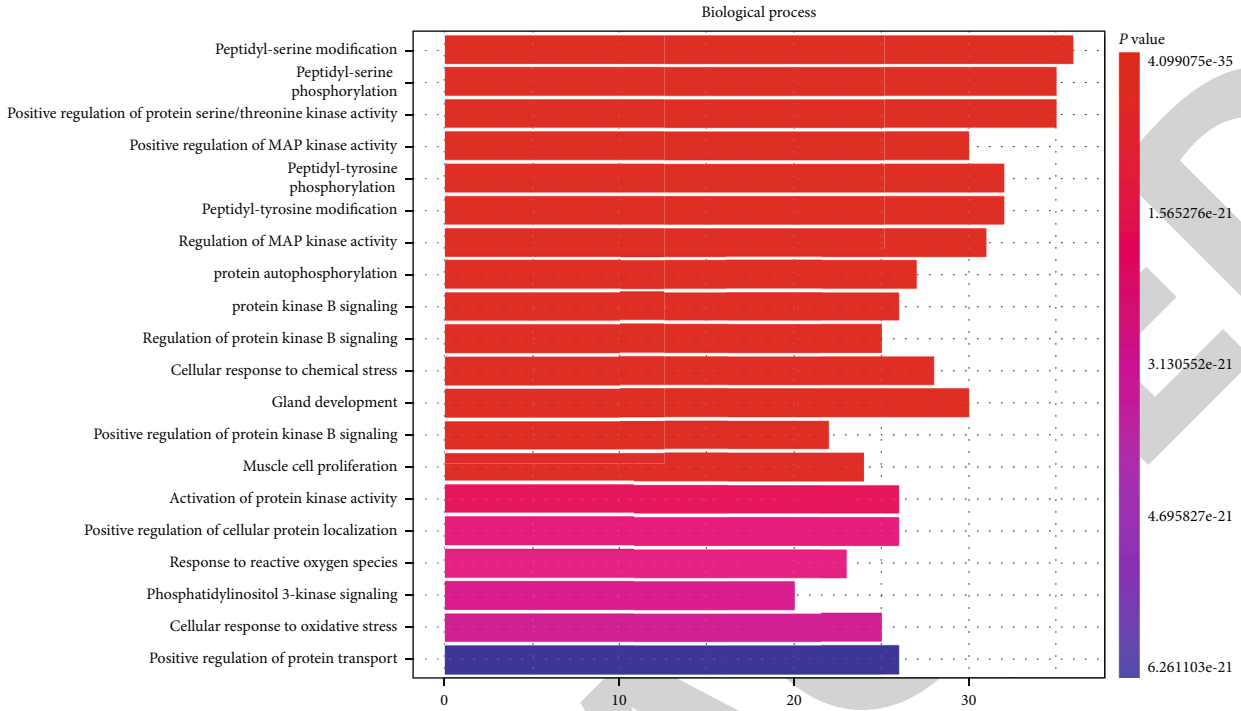

Figure 4: GO analysis for biological process of component-disease targets.

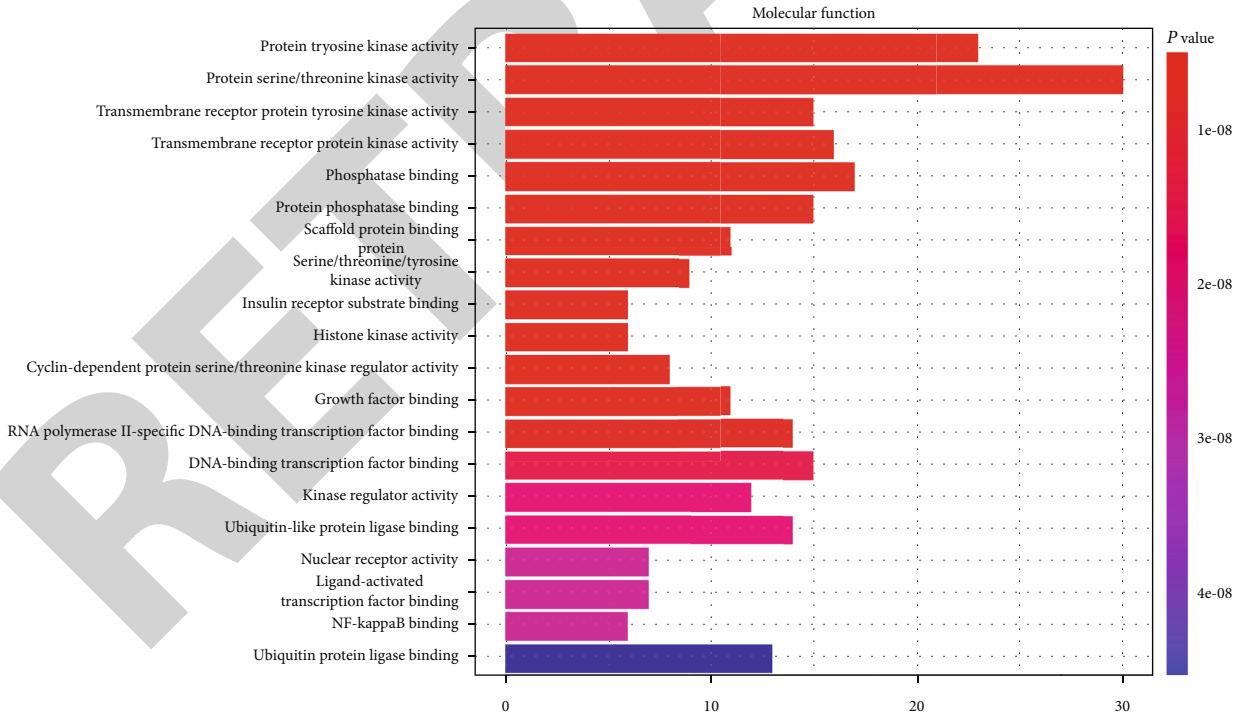

Figure 5: GO analysis for molecular function of component-disease targets.

associated with the PI3K-AKT pathway, EGFR tyrosine kinase inhibitor resistance, endocrine resistance and MAPK signaling, and pancreatic cancer, which may improve the understanding of the molecular mechanism associated with pancreatic cancer progression (Figure 7). Moreover, the target genes involved in the PI3K-AKT and MAPK signalings in pancreatic cancer were shown in Figures 8(a) and 8(b).

3.5. Xiaoji Recipe Inhibited the Proliferation and Migration of Pancreatic Cancer Cells. Furthermore, we explored the

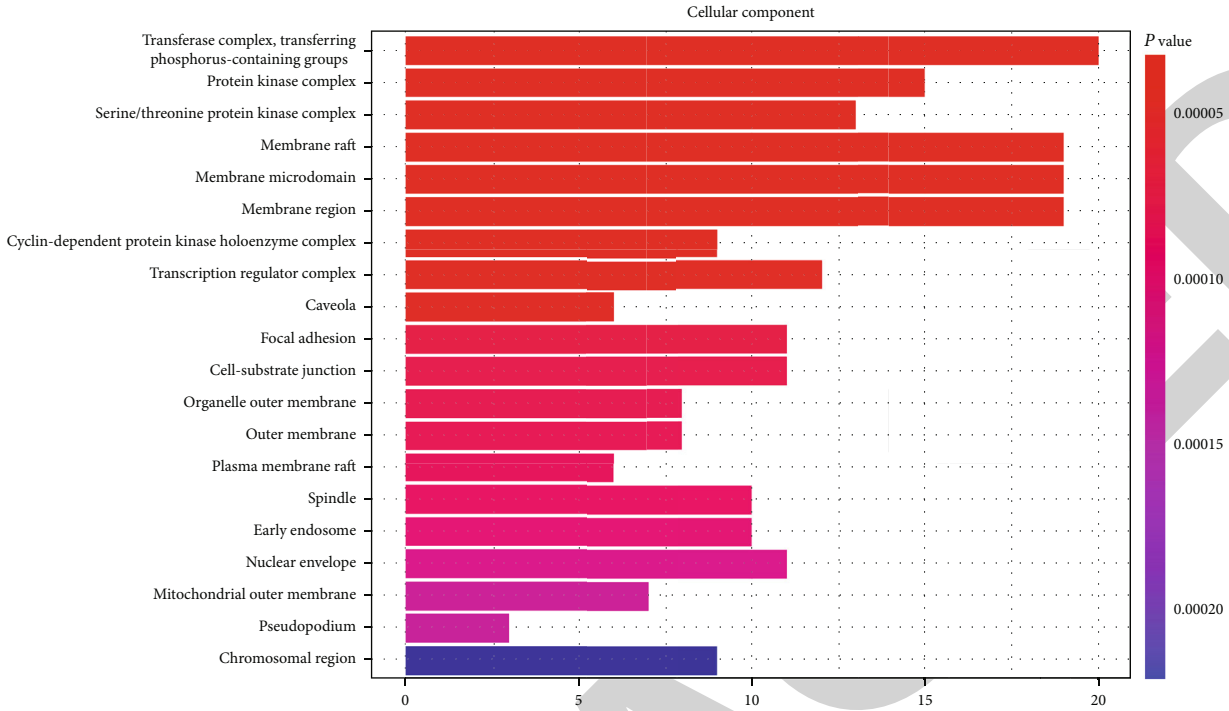

Figure 6: GO analysis for cellular component of component-disease targets.

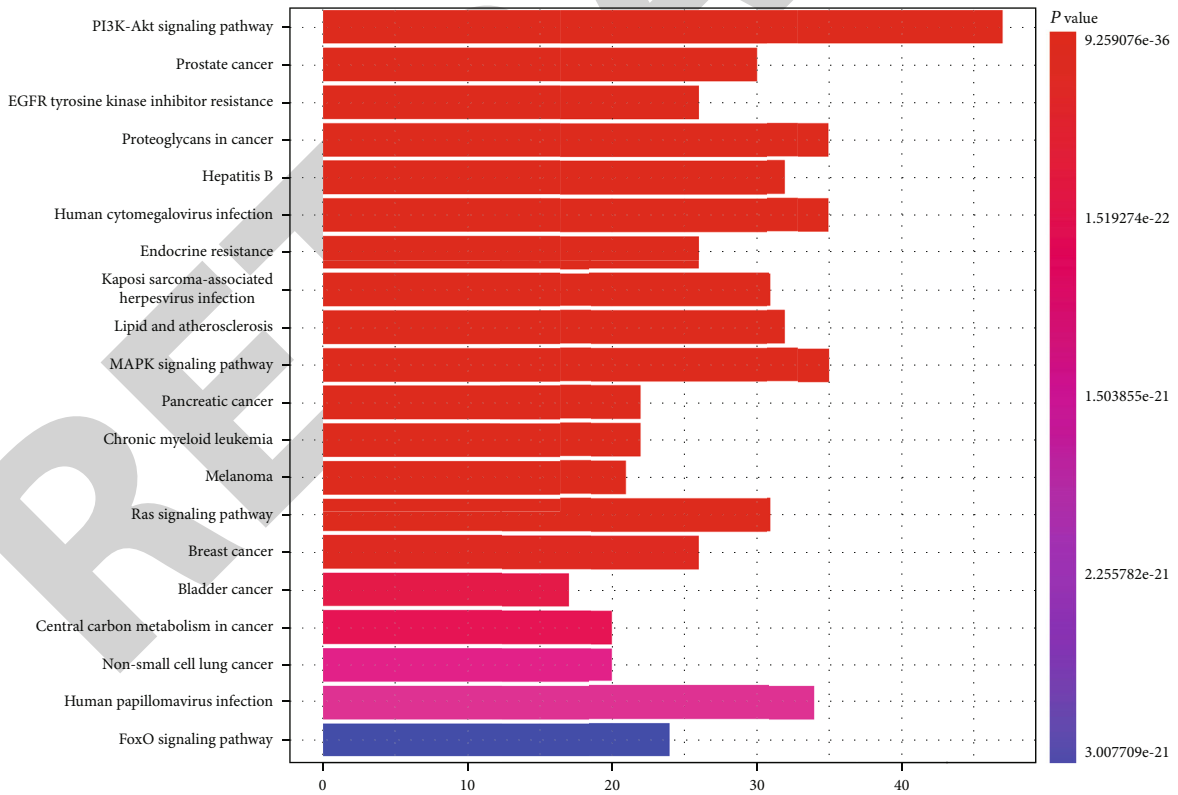

Figure 7: KEGG enrichment analysis of the Xiaoji recipe potential targets in pancreatic cancer.

effects of Xiaoji recipe on the malignant behaviors of pancreatic cancer cells. As revealed by the CCK-8 assay, the viability of CFPAC and PANC1 cells exhibited significant reduction with Xiaoji recipe treatment in a concentration-dependent way (Figures 9(a) and 9(b)). Furthermore, we conducted wound healing assays to explore the impact of Xiaoji recipe on pancreatic cancer cell migration. The results demonstrated that the migration ability of CFPAC and

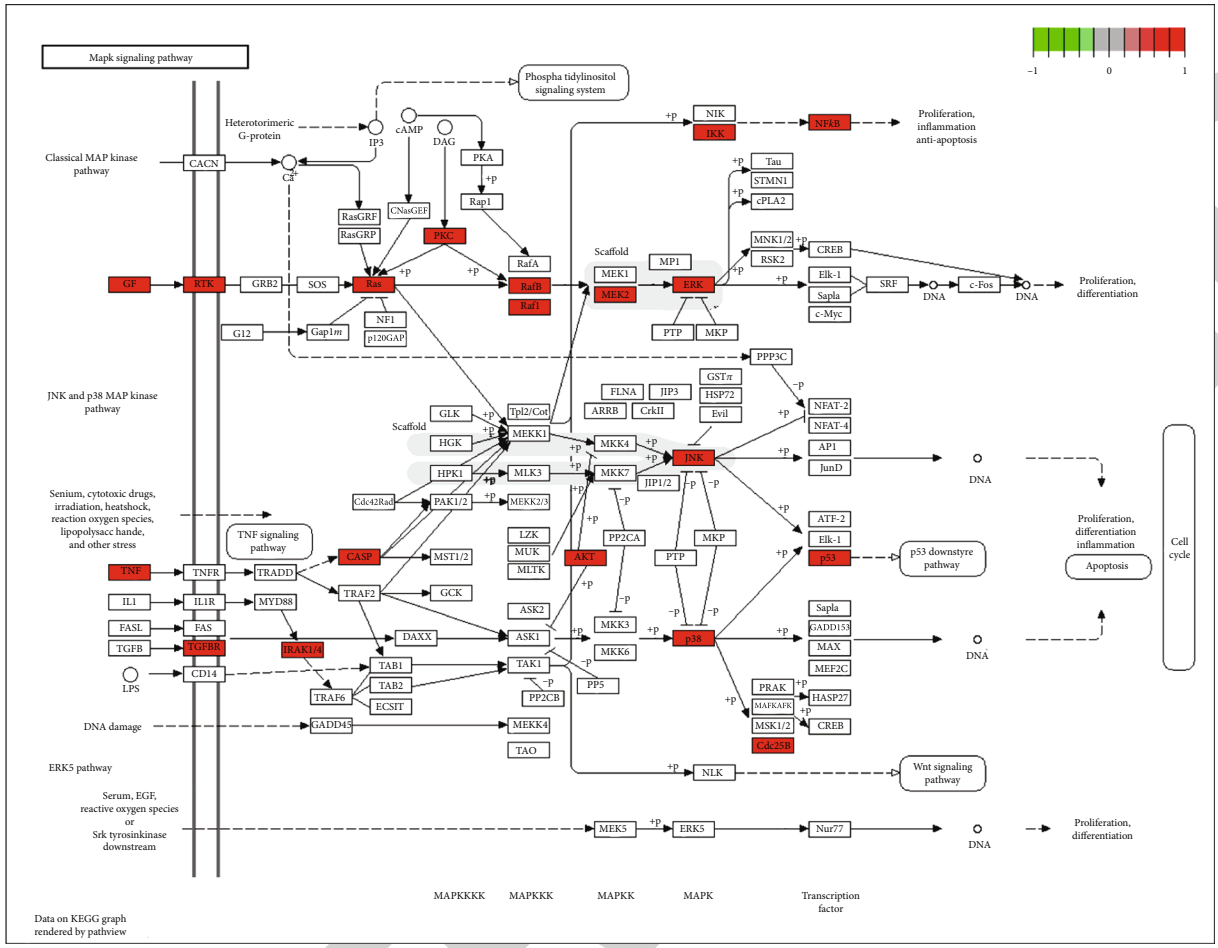

(a)

Figure 8: Continued.

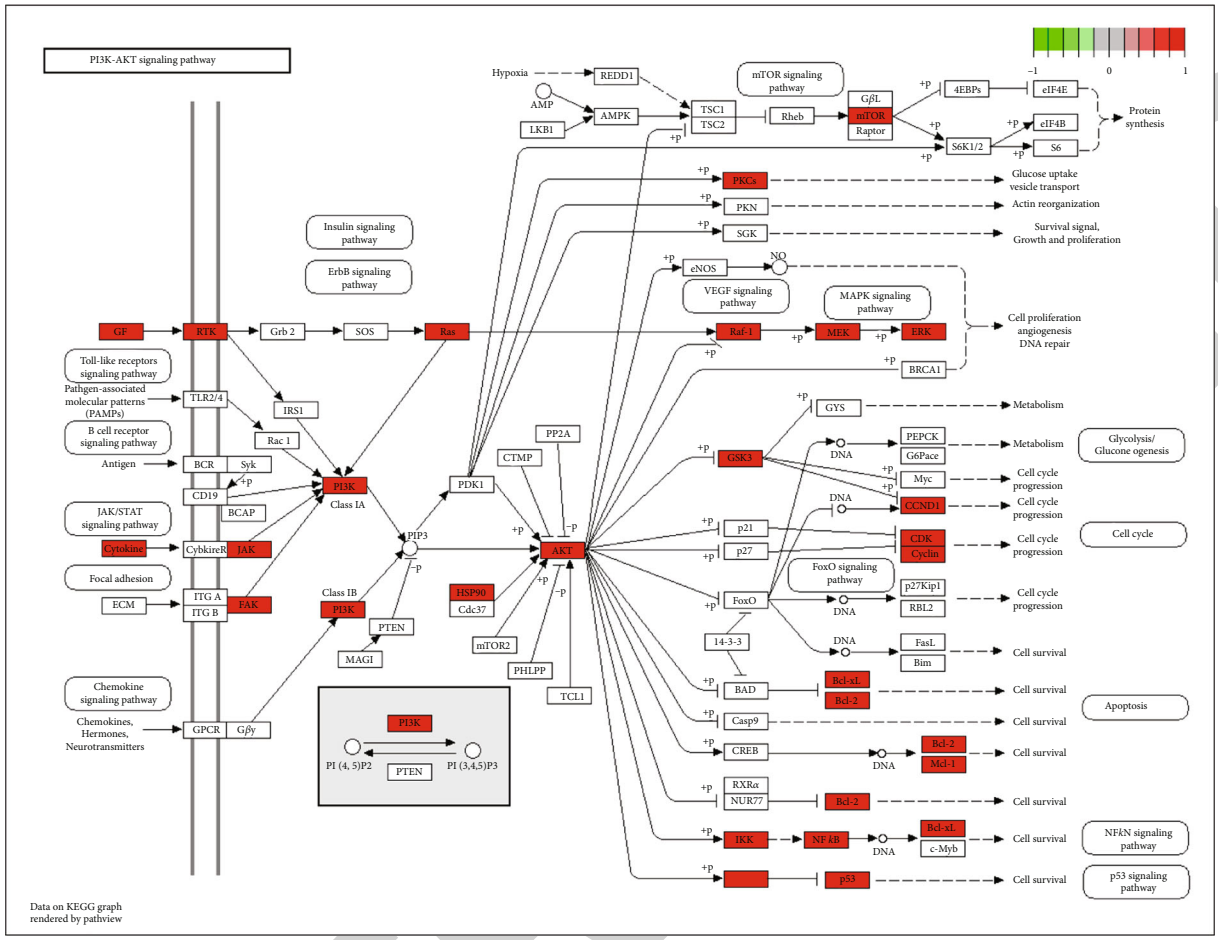

(b)

Figure 8: The related signaling pathways of component-disease targets. (a) The potential targets in MAPK signaling pathway. (b) The potential targets in PI3K/AKT signaling pathway.

PANC1 was significantly suppressed by the treatment of Xiaoji recipe, and the higher the concentration, the more significant the suppression (Figures 9(c) and 9(d)).

3.6. Xiaoji Recipe Promoted the Apoptosis of Pancreatic Cancer Cells In Vitro. The effects of Xiaoji recipe on the apoptosis of pancreatic cancer cells were explored using flow cytometry analysis. As shown in Figures 10(a) and 10(b), the apoptosis rate of CFPAC and PANC1 cells were continuously elevated as the concentration of Xiaoji recipe increased, which indicated that Xiaoji recipe facilitated pancreatic cancer cell apoptosis in a dose-dependent way.

3.7. Xiaoji Recipe Exerted Inhibitory Effects on the Activation of AKT, MAPK, and STAT3 Signaling Pathways. Whether Xiaoji recipe affected the activation of AKT, MAPK, and STAT3 signaling pathways was further explored. The protein expression of AKT1, STAT3, EGFR, and MAPK3 in pancreatic cancer cells was detected using Western blot. We found that the AKT1, STAT3, EGFR, and MAPK3 protein expression showed significant decrease in CFPAC and PANC1 cells after Xiaoji recipe treatment in a dose-dependent manner (Figures 11(a) and 11(b)).

4. Discussion

Pancreatic cancer, as one of the most fatal malignancies, is reported with increasing incidence in recent years. The prognosis of pancreatic cancer patients is still unsatisfying due to the atypical early symptoms and distal metastasis [39]. Thus, it is imperative to explore the underlying mechanism of pancreatic cancer pathogenesis. In our work, the primary active components of Xiaoji recipe and the potential targets and mechanisms in the treatment of pancreatic cancer were investigated based on network pharmacology. The exploration of underlying mechanism of Xiaoji recipe may provide evidence for the TCM therapy in pancreatic cancer.

Chinese herbal medicine (CHM) is indicated as a promising treatment option for multiple malignant diseases with unique clinical effects [40, 41]. As reported previously, Xiaoji recipe has been to inhibit cell migration and growth of lung adenocarcinoma and gastric cancer [42, 43]. Consistently, our study found that Xiaoji recipe repressed cell proliferation and migration while promoted cell apoptosis in pancreatic cancer. More importantly, the main active components of Xiaoji recipe were explored in our study. Bisdemethoxycurcumin, luteolin, quercetin, flavone, and beta-ecdysone

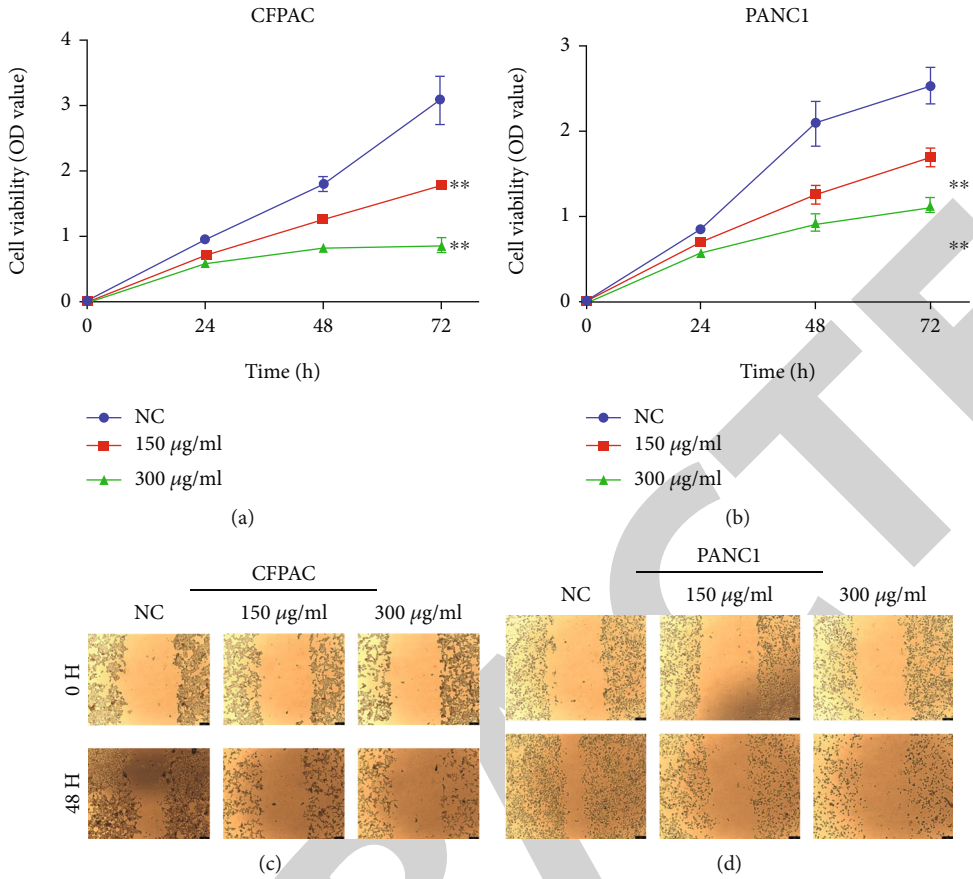

Figure 9: The effect of Xiaoji recipe on cell viability and migration in pancreatic cancer. (a) CCK-8 assays were used to evaluate the viability of CFPAC and PANC1 cells after the treatment of different concentrations of Xiaoji recipe. (b) The migration of CFPAC and PANC1 cells after indicated treatments was subject to wound healing assays. $^{**}p < 0.01$.

were the top five active ingredients ranked by degree according to the component-target-disease network, which were potentially the main active ingredients in the treatment of pancreatic cancer. Bisdemethoxycurcumin is reported with antifibrosis, antiapoptosis, antioxidant, and anti-inflammatory characteristic in various diseases [44–46]. Bisdemethoxycurcumin is also reported with antitumor effects in hepatocellular carcinoma, breast cancer, and non-small-cell lung cancer [47–49]. Luteolin is a flavonoid with anti-inflammation, antiallergy, and anticancer properties and suppresses cell transformation, metastasis, invasion, and angiogenesis in carcinogenesis [50–52]. It has also been reported to inhibit the invasion and epithelial-mesenchymal transition of pancreatic cancer cells by inactivating the STAT3 pathway [53]. Quercetin is reported with cytotoxic and antitumor effects and suppresses pancreatic cancer progression by inhibiting the STAT3 pathway activation [54]. The active ingredients possess different degrees of therapeutic effects on pancreatic cancer and are involved in various signaling pathways.

The component-disease network showed the target genes regulated by these active components in pancreatic cancer. The genes include EGFR, CDK1, MMP7, BCL2, and PARP1. Moreover, the PPI networks revealed that TP53, HRAS, VEGFA, AKT1, STAT3, EGFR, and SRC were the core target genes in the PPI network. The target genes were not mutually independent but were interacted with each other. The Xiaoji recipe may inhibit the progression of pancreatic cancer by regulating the multiple proteins. In line with our finding, all mentioned core target genes have been reported as major driver genes for pancreatic cancer [55–60].

GO and KEGG enrichment analysis revealed the biological process, molecular functions, cellular component as well as the related signaling pathways in the occurrence and progression of pancreatic cancer. There were 2144 BP, 50 CC expression process, and 132 MF-related process of these 116 component-disease targets. We also found that the enrichment of the 116 component-disease targets in the PI3K/AKT and MAPK pathways according to the KEGG analysis. PI3K/AKT pathway is critically involved in the regulation of malignant behaviors in pancreatic cancer, indicating that PI3K/AKT is a valuable target for pancreatic cancer therapy [30, 61]. The MAPK pathways are reported to regulate the tumor cell proliferation, differentiation, apoptosis, and resistance to drug therapy, and PI3K/AKT and Ras/MEK/MAPK pathways were the two main signaling in the downstream of EGFR [62]. In our study, we found that EFGR is one of the component-disease targets, and Xiaoji recipe may inhibit the activation of MAPK signaling by targeting EFGR in pancreatic cancer. In addition, we performed in vitro assays to demonstrate that Xiaoji recipe exerted inhibitory effects on the activation of PI3K/AKT, MAPK,

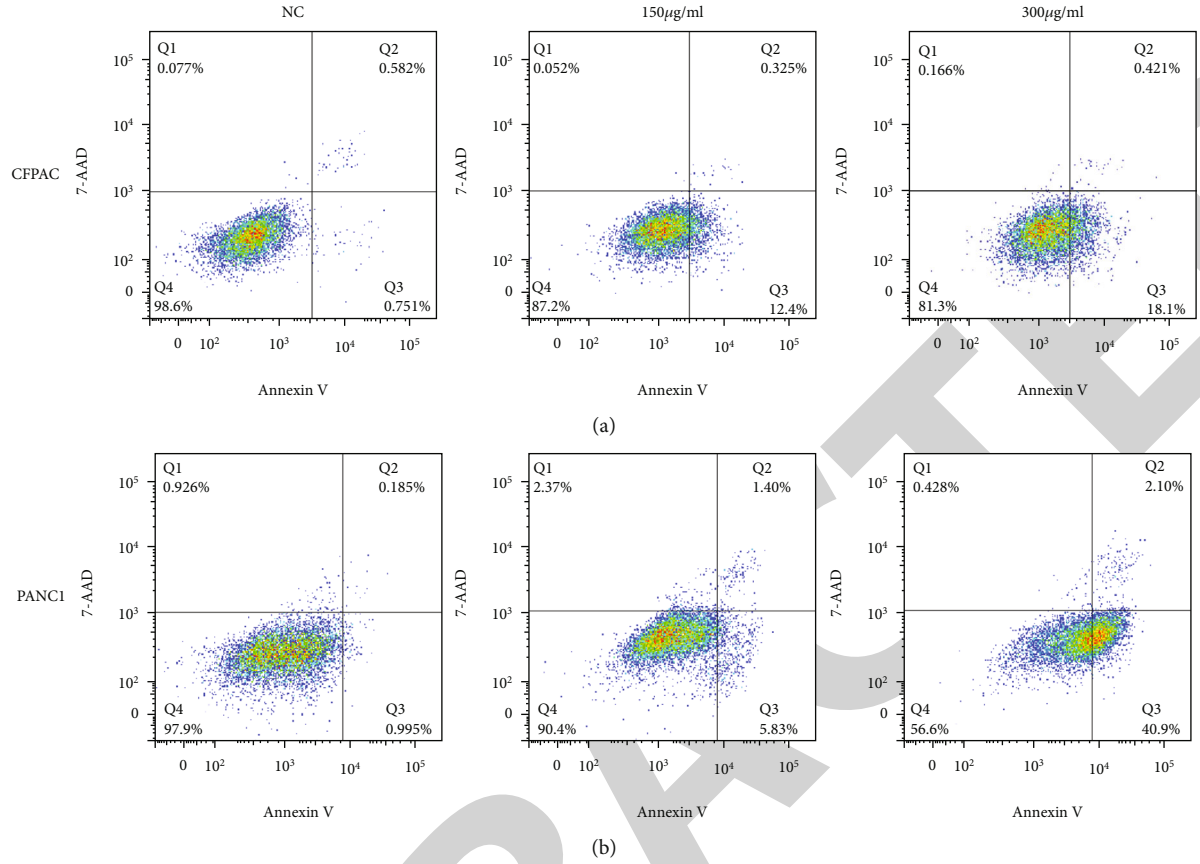

Figure 10: The effect of Xiaoji recipe on pancreatic cancer cell apoptosis. (a) The apoptosis rate of CFPAC and PANC1 cells after indicated treatments was subject to flow cytometry analysis.

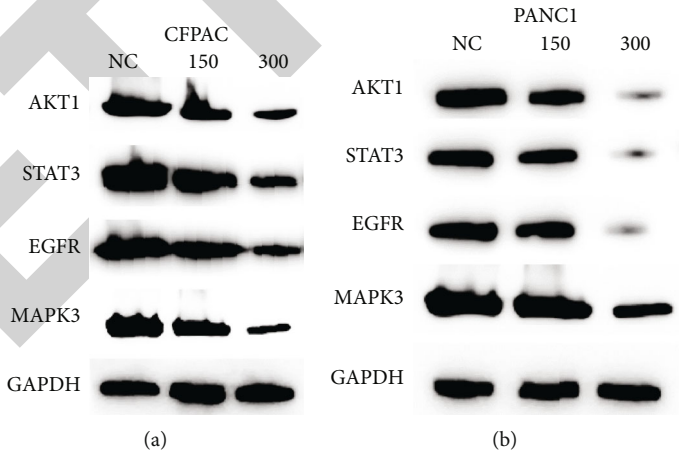

Figure 11: The effect of Xiaoji recipe on MAPK and PI3K/AKT signaling pathways. (a, b) The protein expression of AKT, STAT3, EGFR, and MAPK3 in CFPAC and PANC1 cells after indicated treatments.

and STAT3 signaling pathways. For all we know, these three signaling pathways are widely reported in the involvement of pancreatic cancer. Moreover, many literatures have supported that TCMs inhibit tumor progression via these signaling pathways [63–65].

In this study, the active ingredients and related targets of Xiaoji recipe in pancreatic cancer were explored, and the biological process, molecular function, cellular process, and related signaling pathways were under investigation based on the network pharmacology approach. Moreover, we also verified the effect of Xiaoji recipe on pancreatic cancer cell proliferation, migration, apoptosis, and relevant signaling pathways using in vitro assays. Xiaoji recipe significantly inhibited the proliferation, migration, AKT, MAPK, and

STAT3 signaling pathways and induced the apoptosis of pancreatic cancer cells, which indicated its potential in clinical therapy of pancreatic cancer patients.

However, our study also exists some limitations. First, the in vivo experiments of Xiaoji recipe on tumor growth were lack. Second, the specific mechanism of Xiaoji recipe on regulating the PI3K/AKT, MAPK, and STAT3 signaling pathways were not explored. More, the potential mechanism of Xiaoji recipe on regulating the core target genes of TP53, HRAS, VEGFA, AKT1, STAT3, EGFR, and SRC in pancreatic cancer were not shown. All these limitations will be perfected in the near future.

Data Availability

Data generated in this study are available from the corresponding author under reasonable requests.

Conflicts of Interest

There is no any conflict of interest.

Authors' Contributions

Cunbing Xia and Dexuan Chen contributed equally to this work.

References

[1] H. Sung, J. Ferlay, R. L. Siegel et al., "Global cancer statistics 2020: GLOBOCAN estimates of incidence and mortality worldwide for 36 cancers in 185 countries," *CA: a Cancer Journal for Clinicians*, vol. 71, no. 3, pp. 209–249, 2021.

[2] J. D. Mizrahi, R. Surana, J. W. Valle, and R. T. Shroff, "Pancreatic cancer," *Lancet*, vol. 395, no. 10242, pp. 2008–2020, 2020.

[3] M. Amrutkar and I. P. Gladhaug, "Pancreatic cancer chemoresistance to gemcitabine," *Cancers*, vol. 9, no. 11, article 157, 2017.

[4] D. D. Von Hoff, T. Ervin, F. P. Arena et al., "Increased survival in pancreatic cancer with nab-paclitaxel plus gemcitabine," *The New England Journal of Medicine*, vol. 369, no. 18, pp. 1691–1703, 2013.

[5] S. Zeng, M. Pöttler, B. Lan, R. Grützmann, C. Pilarsky, and H. Yang, "Chemoresistance in pancreatic cancer," *International Journal of Molecular Sciences*, vol. 20, no. 18, article 4504, 2019.

[6] Y. Zhang, Z. Wu, H. Yu et al., "Chinese herbal medicine Wenxia Changfu formula reverses cell adhesion-mediated drug resistance via the integrin β1-PI3K-AKT pathway in lung cancer," *Journal of Cancer*, vol. 10, no. 2, pp. 293–304, 2019.

[7] S. Wang, S. Long, Z. Deng, and W. Wu, "Positive role of Chinese herbal medicine in cancer immune regulation," *The American Journal of Chinese Medicine*, vol. 48, no. 7, pp. 1577–1592, 2020.

[8] Y. Wang, Q. Zhang, Y. Chen et al., "Antitumor effects of immunity-enhancing traditional Chinese medicine," *Biomedicine & Pharmacotherapy*, vol. 121, article 109570, 2020.

[9] N. Li, F. Yang, D. Y. Liu, J. T. Guo, N. Ge, and S. Y. Sun, "Scoparone inhibits pancreatic cancer through PI3K/Akt signaling pathway," *World Journal of Gastrointestinal Oncology*, vol. 13, no. 9, pp. 1164–1183, 2021.

[10] X. Wu, L. Jiang, Z. Zhang et al., "Pancreatic cancer cell apoptosis is induced by a proteoglycan extracted from Ganoderma lucidum," *Oncology Letters*, vol. 21, no. 1, p. 34, 2021.

[11] S. Lakshmi, G. Padmaja, and P. Remani, "Antitumour effects of isocurcumenol isolated from Curcuma zedoaria rhizomes on human and murine cancer cells," *International Journal of Medicinal Chemistry*, vol. 2011, Article ID 253962, 13 pages, 2011.

[12] T. K. Lee, D. Lee, S. R. Lee et al., "Sesquiterpenes from _Curcuma zedoaria_ rhizomes and their cytotoxicity against human gastric cancer AGS cells," *Bioorganic Chemistry*, vol. 87, pp. 117–122, 2019.

[13] X. F. Gao, Q. L. Li, H. L. Li et al., "Extracts from Curcuma zedoaria inhibit proliferation of human breast cancer cell MDA-MB-231 in vitro," *Evidence-Based Complementary and Alternative Medicine*, vol. 2014, Article ID 730678, 9 pages, 2014.

[14] H. Han, L. Wang, Y. Liu et al., "Combination of curcuma zedoary and kelp inhibits growth and metastasis of liver cancer in vivo and in vitro via reducing endogenous H2S levels," *Food & Function*, vol. 10, no. 1, pp. 224–234, 2019.

[15] M. Wu, X. Li, S. Wang et al., "Polydatin for treating atherosclerotic diseases: a functional and mechanistic overview," *Biomedicine & Pharmacotherapy*, vol. 128, article 110308, 2020.

[16] T. Yi, H. Zhang, and Z. Cai, "Analysis of rhizoma polygoni cuspidati by HPLC and HPLC-ESI/MS," *Phytochemical Analysis*, vol. 18, no. 5, pp. 387–392, 2007.

[17] Z. Sheng, B. Ai, L. Zheng, X. Zheng, Y. Yang, and Y. Shen, "Capability of polygonum cuspidatum extract in inhibiting AGEs and preventing diabetes," *Food Science & Nutrition*, vol. 7, no. 6, pp. 2006–2016, 2019.

[18] J. Zhao, B. Pan, X. Zhou et al., "Polygonum cuspidatum inhibits the growth of osteosarcoma cells via impeding Akt/ERK/EGFR signaling pathways," *Bioengineered*, vol. 13, no. 2, pp. 2992–3006, 2022.

[19] Y. W. Lin, F. J. Yang, C. L. Chen, W. T. Lee, and R. S. Chen, "Free radical scavenging activity and antiproliferative potential of Polygonum cuspidatum root extracts," *Journal of Natural Medicines*, vol. 64, no. 2, pp. 146–152, 2010.

[20] S. Chen, J. Tao, F. Zhong et al., "Polydatin down-regulates the phosphorylation level of Creb and induces apoptosis in human breast cancer cell," *PLoS One*, vol. 12, no. 5, article e0176501, 2017.

[21] J. Zhang, Y. Yang, L. Lei, and M. Tian, "Rhizoma Paridis saponins induces cell cycle arrest and apoptosis in non-small cell lung carcinoma A549 cells," *Medical Science Monitor : International Medical Journal of Experimental And Clinical Research*, vol. 21, pp. 2535–2541, 2015.

[22] X. Qian, L. Zhu, J. Hu et al., "_Rhizoma Paridis_ ethanol extract selectively inhibits the proliferation of HUVECs comparing to Lovo cells and shows anti-angiogenesis effects in a mouse model," *Journal of Ethnopharmacology*, vol. 143, no. 1, pp. 256–261, 2012.

[23] S. Man, H. Chai, P. Qiu et al., "Turmeric enhancing anti-tumor effect of _Rhizoma paridis_ saponins by influencing their metabolic profiling in tumors of H22 hepatocarcinoma mice," *Pathology, Research and Practice*, vol. 211, no. 12, pp. 948–954, 2015.

[24] D. T. Zhao, Y. J. Gao, W. J. Zhang et al., "Development a multi-immunoaffinity column LC-MS-MS method for comprehensive

investigation of mycotoxins contamination and co-occurrence in traditional Chinese medicinal materials," *Journal of Chromatography B*, vol. 1178, article 122730, 2021.

[25] Y. Jiang, M. Zhong, F. Long, R. Yang, Y. Zhang, and T. Liu, "Network pharmacology-based prediction of active ingredients and mechanisms of Lamiophlomis rotata (Benth) Kudo against rheumatoid arthritis," *Frontiers in Pharmacology*, vol. 10, article 1435, 2019.

[26] J. Sun, T. Han, T. Yang, Y. Chen, and J. Huang, "Interpreting the molecular mechanisms of Yinchenhao decoction on hepatocellular carcinoma through absorbed components based on network pharmacology," *BioMed Research International*, vol. 2021, Article ID 6616908, 22 pages, 2021.

[27] X. Wang, Z. Y. Wang, J. H. Zheng, and S. Li, "TCM network pharmacology: a new trend towards combining computational, experimental and clinical approaches," *Chinese Journal of Natural Medicines*, vol. 19, no. 1, pp. 1–11, 2021.

[28] S. Huang, Y. Chen, L. Pan et al., "Exploration of the potential mechanism of Tao Hong Si Wu decoction for the treatment of breast cancer based on network pharmacology and in vitro experimental verification," *Frontiers in Oncology*, vol. 11, p. 731522, 2021.

[29] M. Ligorio, S. Sil, J. Malagon-Lopez et al., "Stromal microenvironment shapes the intratumoral architecture of pancreatic cancer," *Cell*, vol. 178, no. 1, pp. 160–175, 2019.

[30] X. Xu, Y. Yu, K. Zong, P. Lv, and Y. Gu, "Up-regulation of IGF2BP2 by multiple mechanisms in pancreatic cancer promotes cancer proliferation by activating the PI3K/Akt signaling pathway," *Journal of Experimental & Clinical Cancer Research*, vol. 38, no. 1, p. 497, 2019.

[31] J. Ru, P. Li, J. Wang et al., "TCMSP: a database of systems pharmacology for drug discovery from herbal medicines," *Journal of Cheminformatics*, vol. 6, no. 1, pp. 1–6, 2014.

[32] X. Chen, H. Zhou, Y. B. Liu et al., "Database of traditional Chinese medicine and its application to studies of mechanism and to prescription validation," *British Journal of Pharmacology*, vol. 149, no. 8, pp. 1092–1103, 2006.

[33] S. Kim, J. Chen, T. Cheng et al., "PubChem in 2021: new data content and improved web interfaces," *Nucleic Acids Research*, vol. 49, no. D1, pp. D1388–D1395, 2021.

[34] A. Daina, O. Michielin, and V. Zoete, "SwissTargetPrediction: updated data and new features for efficient prediction of protein targets of small molecules," *Nucleic Acids Research*, vol. 47, no. W1, pp. W357–W364, 2019.

[35] J. Piñero, N. Queralt-Rosinach, A. Bravo et al., "DisGeNET: a discovery platform for the dynamical exploration of human diseases and their genes," *Database*, vol. 2015, article bav028, 2015.

[36] J. S. Amberger, C. A. Bocchini, F. Schiettecatte, A. F. Scott, and A. Hamosh, "OMIM.org: Online Mendelian Inheritance in Man (OMIM®), an online catalog of human genes and genetic disorders," *Nucleic Acids Research*, vol. 43, no. D1, pp. D789–D798, 2015.

[37] S. Fishilevich, R. Nudel, N. Rappaport et al., "GeneHancer: genome-wide integration of enhancers and target genes in GeneCards," *Database*, vol. 2017, 2017.

[38] D. Szklarczyk, A. L. Gable, K. C. Nastou et al., "The STRING database in 2021: customizable protein-protein networks, and functional characterization of user-uploaded gene/measurement sets," *Nucleic Acids Research*, vol. 49, no. D1, pp. D605–D612, 2021.

[39] Y. Wang, G. Yang, L. You et al., "Role of the microbiome in occurrence, development and treatment of pancreatic cancer," *Molecular Cancer*, vol. 18, no. 1, p. 173, 2019.

[40] J. L. Tang, B. Y. Liu, and K. W. Ma, "Traditional Chinese medicine," *Lancet*, vol. 372, no. 9654, pp. 1938–1940, 2008.

[41] R. Wang, H. Liu, Y. Shao et al., "Sophoridine inhibits human colorectal cancer progression via targeting MAPKAPK2," *Molecular Cancer Research*, vol. 17, no. 12, pp. 2469–2479, 2019.

[42] P. F. Chen, L. Pan, and Y. Q. Jin, "Effects of qingre xiaoji recipe on the migration, chemotaxis, and tube formation capability of human lung adenocarcinoma cell induced human umbilical vein endothelial cells," *Zhongguo Zhong Xi Yi Jie He Za Zhi*, vol. 33, no. 4, pp. 497–501, 2013.

[43] F. Zhou and X. H. Shen, "Effects of serum containing Yiqi Xiaoji recipe on cell line NKN-28 of gastric cancer," *Zhong Xi Yi Jie He Xue Bao*, vol. 5, no. 4, pp. 442–444, 2007.

[44] F. Jin, Y. Jin, J. Du et al., "Bisdemethoxycurcumin protects against renal fibrosis via activation of fibroblast apoptosis," *European Journal of Pharmacology*, vol. 847, pp. 26–31, 2019.

[45] J. Zhang, Y. Yang, H. Han, L. Zhang, and T. Wang, "Bisdemethoxycurcumin protects small intestine from lipopolysaccharide-induced mitochondrial dysfunction via activating mitochondrial antioxidant systems and mitochondrial biogenesis in broiler chickens," *Oxidative Medicine and Cellular Longevity*, vol. 2021, Article ID 9927864, 18 pages, 2021.

[46] F. Jin, X. Chen, H. Yan et al., "Bisdemethoxycurcumin attenuates cisplatin-induced renal injury through anti-apoptosis, anti-oxidant and anti-inflammatory," *European Journal of Pharmacology*, vol. 874, article 173026, 2020.

[47] C. Qiu, K. Liu, S. Zhang et al., "Bisdemethoxycurcumin inhibits hepatocellular carcinoma proliferation through Akt inactivation via CYLD-mediated deubiquitination," *Drug Design, Development and Therapy*, vol. 14, pp. 993–1001, 2020.

[48] C. H. Chou, H. K. Wang, Y. C. Lin et al., "Bisdemethoxycurcumin promotes apoptosis and inhibits the epithelial-mesenchymal transition through the inhibition of the G-protein-coupled receptor 161/mammalian target of rapamycin signaling pathway in triple negative breast cancer cells," *Journal of Agricultural and Food Chemistry*, vol. 69, no. 48, pp. 14557–14567, 2021.

[49] M. Xiang, H. G. Jiang, Y. Shu et al., "Bisdemethoxycurcumin enhances the sensitivity of non-small cell lung cancer cells to icotinib via dual induction of autophagy and apoptosis," *International Journal of Biological Sciences*, vol. 16, no. 9, pp. 1536–1550, 2020.

[50] M. Imran, A. Rauf, T. Abu-Izneid et al., "Luteolin, a flavonoid, as an anticancer agent: a review," *Biomedicine & Pharmacotherapy*, vol. 112, article 108612, 2019.

[51] Y. Lin, R. Shi, X. Wang, and H. M. Shen, "Luteolin, a flavonoid with potential for cancer prevention and therapy," *Current Cancer Drug Targets*, vol. 8, no. 7, pp. 634–646, 2008.

[52] J. Zhao, L. Li, Z. Wang et al., "Luteolin attenuates cancer cell stemness in PTX-resistant oesophageal cancer cells through mediating SOX2 protein stability," *Pharmacological Research*, vol. 174, p. 105939, 2021.

[53] X. Huang, S. Dai, J. Dai et al., "Luteolin decreases invasiveness, deactivates STAT3 signaling, and reverses interleukin-6 induced epithelial-mesenchymal transition and matrix metalloproteinase secretion of pancreatic cancer cells," *OncoTargets and Therapy*, vol. 8, pp. 2989–3001, 2015.

Hindawi
Computational and Mathematical Methods in Medicine
Volume 2023, Article ID 9891078, 1 page
https://doi.org/10.1155/2023/9891078

Retraction

Retracted: Effectiveness of Cognitive Behavior Therapy Combined with Eye Movement Desensitization and Reprocessing on Psychological Problems and Life Quality in Patients' Postfacial Trauma

Computational and Mathematical Methods in Medicine

Received 12 December 2023; Accepted 12 December 2023; Published 13 December 2023

This article has been retracted by Hindawi, as publisher, following an investigation undertaken by the publisher [1]. This investigation has uncovered evidence of systematic manipulation of the publication and peer-review process. We cannot, therefore, vouch for the reliability or integrity of this article.

Please note that this notice is intended solely to alert readers that the peer-review process of this article has been compromised.

Wiley and Hindawi regret that the usual quality checks did not identify these issues before publication and have since put additional measures in place to safeguard research integrity.

We wish to credit our Research Integrity and Research Publishing teams and anonymous and named external researchers and research integrity experts for contributing to this investigation.

The corresponding author, as the representative of all authors, has been given the opportunity to register their agreement or disagreement to this retraction. We have kept a record of any response received.

References

[1] Y. Lin, W. Lv, J. Xu, Y. Jiang, and Z. Chen, "Effectiveness of Cognitive Behavior Therapy Combined with Eye Movement Desensitization and Reprocessing on Psychological Problems and Life Quality in Patients' Postfacial Trauma," *Computational and Mathematical Methods in Medicine*, vol. 2022, Article ID 7822847, 7 pages, 2022.

Hindawi
Computational and Mathematical Methods in Medicine
Volume 2022, Article ID 7822847, 7 pages
https://doi.org/10.1155/2022/7822847

Research Article

Effectiveness of Cognitive Behavior Therapy Combined with Eye Movement Desensitization and Reprocessing on Psychological Problems and Life Quality in Patients' Postfacial Trauma

Yue Lin,[1] Wang Lv,[1] Jun Xu,[2] Yingying Jiang,[1] and Zheyan Chen[3]

[1]*Department of Emergency, Wenzhou People's Hospital, Wenzhou, Zhejiang 325000, China*
[2]*Department of Endoscopy Center, Wenzhou People's Hospital, Wenzhou, Zhejiang 325000, China*
[3]*Department of Plastic Surgery, Wenzhou People's Hospital, Wenzhou, Zhejiang 325000, China*

Correspondence should be addressed to Wang Lv; lvwangwz@outlook.com

Received 7 August 2022; Revised 22 August 2022; Accepted 26 August 2022; Published 7 September 2022

Academic Editor: Min Tang

Objective. To investigate the effectiveness of cognitive behavior therapy (CBT) combined with eye movement desensitization and reprocessing (EMDR) on the esteem, anxiety, depression, posttrauma stress disorder (PTSD), and posttraumatic growth in patients with facial trauma. *Methods*. A total of 92 facial trauma patients in Wenzhou People's Hospital from January 2017 to December 2019 were enrolled in this study. The patients were randomly divided into control group ($n = 46$) and intervention group ($n = 46$). Both of the control group and the intervention group received routine treatment, while the intervention group further received CBT combined with EMDR. Questionnaires were used to explore and record the general patient information. The Self-Esteem Scale (SES), Self-Anxiety Scale (SAS), Self-Depression Scale (SDS), Posttraumatic Stress Disorder Checklist Civilian Version (PCL-C), Posttraumatic Growth Inventory (PTGI), and World Health Organization Quality of Life-brief (WHOQOL-BREF) scores between the two groups were compared. *Results*. After CBT combined with EMDR intervention, the SDS and SAS scores in the intervention group were significantly decreased compared with the scores before intervention with statistically significance ($P < 0.001$). Furthermore, the PCL-C score in the intervention group showed significant decrease in comparison with the control group ($P < 0.001$), while the PTGI score in the intervention group was significantly higher than the control group ($P < 0.001$). The WHOQOL-BREF scores were increased after treatment in the two groups compared with the scores before treatment, and the scores in the intervention group were higher than those in the control group after treatment ($P < 0.01$). *Conclusion*. Psychological intervention therapy can effectively alleviate the anxiety, depression, and PTSD and improve the life quality and the recovery of facial trauma patients.

1. Introduction

Facial trauma as sign of injuries is a major challenge in public health in relation to the self-perception and self-esteem of patients [1]. Increasing evidence from psychology, anthropology, and socioeconomics has demonstrated that people with attractive facial appearance have an advantage in their social life [2–4]. Patients postfacial trauma usually receive negative social response during social interactions, leading to detrimental effects on their mental state such as depression, anxiety, and posttraumatic stress disorder (PTSD) [5, 6]. However, patients can also positively change their perspectives and undergo personal growth after a major life crisis or traumatic event [7], and this process is called posttraumatic growth (PTG). The psychological factors in the treatment of facial trauma should be paid more attention.

The PTSD treatment includes the psychological and pharmacological methods. For psychological treatment, there are trauma-focused psychological interventions such as exposure therapy and cognitive therapy and non-

trauma-focused psychological interventions such as relaxation, stress inoculation training, and interpersonal therapy [8]. Eye movement desensitization and reprocessing (EMDR) and cognitive behavioral therapy (CBT) are known as the trauma-focused psychological therapies. EMDR heals people from the emotional distress [9, 10] and is prevalently applied in the treatment of PTSD patients. It mainly consists of eight phases, including recalling an image, thought, emotion, and a bodily sensation related to the traumatic event, receiving bilateral stimulation such as taps, tones, or eye movements [11]. It has been reported that EMDR is effective treatment for psychopathology and psychological problems in patients with facial trauma, which helps them to desensitize discomfort caused by traumatic experiences and reprocess them in the individual's autobiographical memory, thus achieving the goal of relieving symptoms [12]. CBT is a trauma-focused psychotherapy whose effect has been demonstrated in multiple randomized controlled trials [13–15]. Currently, CBT is also regarded as a well-established intervention to treat posttraumatic stress and related symptoms [8, 16]. The World Health Organization has recommended CBT as a treatment option for posttraumatic stress with a focus on trauma [17].

In China, the psychological intervention of posttrauma patients is not widely available. Our study is aimed at exploring the effectiveness of CBT combined with EMDR for the psychological intervention of patients with facial trauma. The findings of our study may provide evidence for the clinical effect of CBT combined with EMDR.

2. Materials and Methods

2.1. Study Participants. By convenient sampling, 92 facial trauma patients in Wenzhou People's Hospital from January 2017 to December 2019 were selected for this study. Inclusion criteria are as follows: (1) participants were educated and could read and comprehend the content of questionnaires, (2) aged between 18 and 60, (3) patients are hospitalized with facial trauma without organic brain injury and did not require craniocerebral surgery, (4) no other life-threatening or disabling injuries, (5) clear in language expression and stable in disease condition, and (6) never received CBT or EMDR interventions. Exclusion criteria are as follows: (1) patients with history of depression, anxiety disorder, or schizophrenia; (2) patients experienced death of relatives or friends or great property loss in the trauma; (3) patients complicated with other physical diseases during the treatment; and (4) patients out of contact in the follow-up or refused to accept psychological intervention or scale evaluation. Body mass index (BMI) was measured using the formula: body mass (kg)/height squared (m^2). Significant difference between the two groups was found in the drinking history ($P < 0.05$), average length of hospital stay ($P < 0.001$), and hospitalization expenses ($P < 0.05$). There was no statistical difference in other baseline characteristics such as age, BMI, gender, and education level ($P > 0.05$). Our study was under the approval of the Ethics Committee of the Wenzhou People's Hospital, and all participants have signed the informed consent.

2.2. Methods. 92 patients with 49 males and 43 females were randomly divided into the control group and intervention group with 46 participants in each group. Patients in the control group received routine treatment, including the posttrauma treatment, condition monitoring, health education, diet guidance, medication guidance, regular ward rounds, rehabilitation nursing, and prevention of infection and other complications. Patients in the intervention group received CBT combined with EMDR based on the routine treatment procedures. The intervention duration was once every two days from hospitalization, 60-90 minutes each time. After discharge from hospital, patients were transferred to the psychological department for further treatment or home visit. The end of treatment was determined by the condition of patients and the joint agreement of therapists and patients. The explicit procedures were as follows: (1) psychological intervention team was established, including 2 physicians, 2 nurses in charge, and 3 follow-up therapists. All the staff had years of experience in diagnosis and treatment or nursing and received professional psychological training. There were 3 national second-level psychological consultants with years of experience in clinical CBT and EMDR operation; (2) CBT operation procedures [18], in trauma-focused CBT, besides the psychological education and anxiety management (such as muscle relaxation or breathing training), exposure (body and imagined), and cognitive reconstruction (check and challenge the idea of dysfunction) are the most critical factor. Complete treatment process included 12 times of interventions. The first intervention was the narrative memories of traumatic events, and patients described the event for multiple times (≥2 times). The second intervention included the interpretation of the treatment plan, the relaxation exercise and the trauma-focused psychological education, and the introduction of the following exposure practice. The third intervention included the practice of recalling the traumatic event, exposure, and homework, The fourth to ninth intervention included homework, the relaxation exercise, psychological education, strategy management, thought intrusion, thought prevention, etc. The tenth to twelfth interventions included systematic desensitization, evaluation of stress situation grade, and scale score; (3) EMDR operation [19], first, the consultant determined the most disturbing memories about the trauma event from patients, the related negative thoughts, disturbing emotions, and positions of the patients. Then, the patients were asked to focus on the traumatic event and simultaneously followed the bilateral finger movements of counselor for about 30 seconds. After exercises, patients were asked to share any emotions/flashbacks/perceptions they noticed in the process of visual stimulation. When the patient exhibited no more emotional outbursts or any other feelings associated with the target memory, the counselor evaluated the ability of patients of detailed description until the patients could think of the trauma without disturbing emotion or physical responses. Then, we chose other targets and repeated the same procedure (trauma identification, visual stimulation, and assessment). EMDR treatment ended when the patient was able to face the reformulated goals in the imagined future scenario

without emotional discomfort. The hospital stay length and treatment expense of the two groups were recorded.

2.3. Measures. The observation indicators were collected using questionnaires: (1) Self-Esteem Scale (SES), compiled by Rosenberg in 1965 with a total score of 40 [20]. The higher the score, the higher the self-esteem; (2) Self-Rating Anxiety Scale (SAS) and Self-Rating Depression Scale (SDS), compiled by W.K. Zung in 1965 and 1971 with a total score of 100. In the SAS, a higher score indicates a higher degree of anxiety: a score of 50-70 out of 100 suggests mild anxiety, 71-90 suggests moderate anxiety, and higher than 90 suggests severe anxiety. In the SDS, a higher score reflects a higher degree of depression: a score from 50 to 70 out of 100 represents mild depression, from 71 to 90 represents moderate depression, and higher than 90 represents severe depression; (3) PTSD Checklist-Civilian version (PCL-C) is used to evaluate the severity of PTSD symptoms. The intensity and frequency of PTSD symptoms were divided into five grades, and the higher the scores, the severer the PTSD symptoms. A total score of 38 to 49 was defined as a degree of PTSD, and those of 50 to 85 were diagnosed as PTSD. (4) Posttraumatic Growth Inventory (PTGI), compiled by Tedeschi et al., was used to assess the perceived degree of positive life change after traumatic events. It includes 21 items and explores 6 dimensions. The Likert 6-level scoring method is adopted with a total score of 105, and the higher the score, the more the posttraumatic growth. (5) World Health Organization Quality of Life-brief (WHOQOL-BREF) [21] includes a generic facet (overall quality of life and general health) and 4 domains such as physical health, psychological health, social relationships, and environment. The higher the scores, the better the quality of life. After the two groups of patients were admitted to the hospital and in stable condition, these scales were filled out under the guidance of the nurse in charge. Patients with writing ability filled out the scales by themselves, and those without writing ability were guided by the nurse. The questionnaires would be collected and checked once the patients finished. The SES, SAS, SDS, PCL-C, PTGI, and WHOQOL-BREF scales were also filled out by patients in the intervention group after the intervention period and patients in the control group in the follow-up after 15-30 days discharged of hospital.

2.4. Statistical Analysis. SPSS 21.0 was used to perform statistical analysis. The data were expressed as the number, percent, and mean ± SD. Paired t-test was used for univariate analysis before and after intervention, and Student's t-test was used for comparison between two groups. Chi-square (χ^2) test was used to assess the relationship between two categorical variables. The multivariate analysis was conducted with logistic regression analysis. $P < 0.05$ was considered statistically significant.

3. Results

3.1. Clinical Characteristics of Patients. A total of 92 cases with facial trauma were enrolled in this study. There were no statistical difference between the age, BMI, gender, place of residence, smoking history, marital history, record of children, career, education level, family monthly income, the forms of injury, treatment, complicated injury, and predicted prognosis between the intervention group and control group ($P > 0.05$). We also found the statistical difference in the drinking history ($P < 0.05$), length of hospital stay ($P < 0.001$), and treatment expenses between the two groups ($P < 0.05$), as shown in Table 1.

3.2. The Effect of Psychological Intervention on the Self-Esteem, Depression, and Anxiety of Patients. The effects of psychological intervention on the SES, SDS, and SAS scores before and after intervention are presented in Table 2. There was no significant difference in the SES score between the two groups before and after intervention ($P > 0.05$), but there were significant differences in SDS and SAS scores between the two groups before and after intervention ($P < 0.001$). A total of 43 patients (46.94%) in the two groups showed low self-esteem (SES < 20), 72 patients (78.26%) showed mild or more depression symptoms (SDS > 53), and 86 patients (93.48%) showed mild or more anxiety (SAS > 50).

During the follow-up period, there were 23 cases (25.00%) showed low self-esteem, 36 cases (39.13%) showed depression, and 44 cases (47.83%) showed anxiety in the control group. In the intervention group, there were 20 cases (21.74%) of low self-esteem, 9 cases (9.78%) of depression, and 19 cases (20.65%) of anxiety, respectively. The incidence of depression and anxiety was significantly different between the two groups ($P < 0.05$). The scores of depression and anxiety reduced significantly after intervention ($P < 0.05$), while the SES scores were not significantly affected. According to multivariate analysis, the SAS and SDS scores in the intervention group were significantly reduced compared with the control group ($P < 0.05$).

3.3. The Influence of Psychological Intervention on the PTSD and PTG of Patients. The effects of psychological intervention on PCL-C and PTGI scores are exhibited in Table 2. During the follow-up period after discharge from the hospital, 42 patients (91.30%) in the control group developed a certain degree of PTSD (PCL-C > 38), and 22 cases (47.83%) of them were diagnosed of PTSD (PCL-C > 50). For the intervention group, there were 15 patients (32.61%) developed a certain degree of PTSD (PCL-C > 38), among whom 6 cases (13.04%) were diagnosed of PTSD. Both univariate and multivariate analyses demonstrated lower total PCL-C scores and higher PTGI scores in the intervention group in comparison with the control group after intervention, with statistical differences ($P < 0.001$).

3.4. Comparison of the Treatment Outcome between the Two Groups on the Quality of Life. The WHOQOL-BREF scores of the two groups were also compared. The results indicated that the WHOQOL-BREF scores were both increased in two groups before and after the treatment. Moreover, after the treatment, the patients in the intervention group showed higher WHOQOL-BREF scores than those in the control

Table 1: Demographic and baseline characteristics of the two groups.

Factors	Control group ($n = 46$)	Intervention group ($n = 46$)	T/χ^2	P
Age (years)	28.70 ± 4.62	30.43 ± 5.47	1.64	0.10
BMI (kg/m^2)	20.79 ± 2.88	20.11 ± 2.66	1.17	0.24
Gender				
Male	25 (54.35)	24 (52.17)	0.04	0.83
Female	21 (45.65)	22 (47.83)		
Residence place				
Urban	43 (93.48)	43 (93.48)	0	1
Rural	3 (6.52)	3 (6.52)		
Smoking history				
No	36 (78.26)	34 (73.91)	0.24	0.63
Yes	10 (21.74)	12 (26.09)		
Drinking history				
No	28 (60.87)	41 (89.13)	9.8	<0.05
Yes	18 (39.13)	5 (10.87)		
Marital status				
Unmarried	11 (23.91)	21 (45.65)	5.27	0.07
Married	32 (69.57)	24 (52.17)		
Divorced	3 (6.52)	1 (2.17)		
Child				
No	24 (52.17)	25 (54.35)	0.04	0.83
Yes	22 (47.83)	21 (45.65)		
Career				
Farmer/migrant worker	10 (21.74)	7 (15.22)	1.99	0.57
Enterprises and public institutions	18 (39.13)	20 (43.48)		
Others	10 (21.74)	14 (30.43)		
Jobless	8 (17.39)	5 (10.87)		
Education level				
Junior-senior high school and below	15 (32.61)	10 (21.74)	2.55	0.28
College degree/bachelor and above	30 (65.22)	36 (78.26)		
Others	1 (2.17)	0 (0)		
Family monthly income				
<5000	6 (13.04)	10 (21.74)	1.21	0.27
≥5000	40 (86.96)	36 (78.26)		
Forms of injury				
Violence	8 (17.39)	7 (15.22)	1.13	0.77
Road accident	13 (28.26)	10 (21.74)		
Fall down	19 (41.3)	24 (52.17)		
Others	6 (13.04)	5 (10.87)		
Treatment				
Conservative treatment	32 (69.57)	36 (78.26)	0.9	0.34
Surgery	14 (30.43)	10 (21.74)		
Complicated injury				
No	29 (63.04)	28 (60.87)	0.05	0.83
Yes	17 (36.96)	18 (39.13)		
Predicted prognosis				
Favorable	34 (73.91)	37 (80.43)	0.56	0.46
Poor	12 (26.09)	9 (19.57)		
Hospital stay (days)	4.94 ± 1.73	3.07 ± 0.68	6.82	<0.001

Table 1: Continued.

Factors	Control group ($n = 46$)	Intervention group ($n = 46$)	T/χ^2	P
Expenses (thousand yuan)	6.37 ± 3.08	5.11 ± 2.61	2.12	<0.05

Table 2: Comparison of treatment outcomes between the two groups.

Indicators	Evaluation period	Control group ($n = 46$)	Intervention group ($n = 46$)	T	P	B	$^*P$
SES score	Before intervention	19.39 ± 4.71	19.54 ± 5.21	0.15	0.88	-0.65	0.49
	After intervention	20.76 ± 3.55	19.54 ± 5.21	0.22	0.83		
SDS score	Before intervention	63.39 ± 11.71	62.24 ± 7.90	0.55	0.58	-12.97	<0.001
	After intervention	59.98 ± 9.43	46.07 ± 7.10	8.00	<0.001		
SAS score	Before intervention	64.41 ± 10.13	65.43 ± 9.73	0.49	0.62	-14.99	<0.001
	After intervention	61.5 ± 6.40	46.09 ± 11.95	7.71	<0.001		
PCL-C score	After intervention	50.00 ± 7.87	22.85 ± 13.77	7.33	<0.001	-16.05	<0.001
PTGI score	After intervention	42.24 ± 6.18	52.17 ± 10.30	5.61	<0.001	10.40	<0.001

$^*P$ indicates the logistic regression P value.

Table 3: Comparison of the WHOQOL-BREF indicator between the two groups.

Indicator	Control group ($n = 46$)		Intervention group ($n = 46$)		F
	Before treatment	After treatment	Before treatment	After treatment	
Physical health	20.6 ± 4.0	22.2 ± 3.8	20.5 ± 3.6	23.8 ± 4.2	1.94
Psychological health	17.8 ± 3.8	19.3 ± 4.1	18.2 ± 3.6	20.7 ± 3.8	2.05**
Social relationships	8.7 ± 2.5	9.4 ± 3.2	8.9 ± 2.3	9.7 ± 2.6	6.37**
Environment	25.9 ± 4.2	27.2 ± 4.5	26.7 ± 4.6	29.4 ± 4.1	7.53

$^{**}P < 0.01$.

group, especially in the psychological health and social relationship fields ($P < 0.01$), which indicated the effect of CBT combined with EMDR on the improvement of life quality of patients with facial trauma, as shown in Table 3.

4. Discussion

The human face, characterized by the uniqueness, is a dynamic tool carrying information in social communication [22]. It is closely related to the sense of self, self-esteem, and identity [23, 24]. Patients with facial trauma due to violence, road accidents, burn injury, sports injuries, etc., often experience a variety of symptoms of emotional stress, including depression, anxiety, social phobia, low self-esteem, and frustration, resulting in susceptibility to psychological problems and poor life quality [25–27]. According to clinical researches, about 20%-30% patients with facial trauma show the symptoms and signs of anxiety [28, 29]. Moreover, patients with facial trauma showed increased PTSD incidence compared with the general population [30, 31]. In our study, we found that patients with facial trauma exhibited evident short-term symptoms of depression and anxiety. There were 78.26% of the patients with different degrees of depression and 93.48% of the patients of anxiety symptoms. In the follow-up periods, part of the control group patients could calm down by themselves, while there were still 39.13% of patients of depression and 47.83% of patients of anxiety to different degrees. The incidence of depression and anxiety was significantly different between the two groups ($P < 0.05$). The scores of depression and anxiety reduced significantly after intervention ($P < 0.05$), while the SES scores were not significantly affected. According to multivariate analysis, the SAS and SDS scores in the intervention group were significantly reduced compared with the control group ($P < 0.05$). Additionally, 47.83% of the patients presented the symptoms of PTSD. Therefore, patients with facial trauma are prone to adverse psychological emotions, and more attention should be paid to improving their mental health.

The management of psychological intervention of patients with facial trauma is still challenging. The EMDR and CBT are evidence-based treatment options for patients with PTSD [32]. Previous studies have compared the effect of EMDR and CBT for different mental disorders such as PTSD, obsessive-compulsive disorder, and panic disorder [33–35]. Both the two methods showed significant effect to alleviate the depression, anxiety, and behavior problems [36]. In our study, we provided CBT and EMDR interventions to patients from admission to hospital in stable condition to the follow-up home visit. After treatment, patients in the intervention group presented lower SDS, SAS, and PCL-C scores compared with the control group in the follow-up

periods ($P < 0.001$). There were 9.78% patients presented depression, 20.65% presented anxiety, and 13.04% presented PTSD in the intervention group. After treatment, the PTGI score of the intervention group was significantly higher than those of the control group ($P < 0.001$). The hospital stay ($P < 0.001$) and hospital expenses ($P < 0.05$) in the intervention group were significantly lower than the control group. Moreover, compared with the control group, patients in the intervention group showed improved physical health, psychological health, social relationship, and environment ($P < 0.01$). CBT combined with EMDR intervention was effective to improve the life quality of patients with facial trauma. Therefore, based on the trusted doctor-patient relationship, doctors should actively listen to the feelings of patients and adopt the CBT combined with EMDR to affect the negative thought of patients, promoting the establishment of right cognition and recovery from trauma.

In conclusion, based on the CBT combined with EMDR psychological intervention to the patients with facial trauma, we found that psychological intervention is effective to attenuate the depression, anxiety, and PTSD and improve the posttrauma growth self-esteem as well as life quality of patients with facial trauma. The finding of our study indicates the potential of CBT combined with EMDR in the psychological intervention of facial trauma patients in clinical practice.

Data Availability

Data generated in this study are available from the corresponding author under reasonable requests.

Conflicts of Interest

There is no any conflict of interest.

Acknowledgments

This work was supported by the Wenzhou Fundamental Research Projects (No. Y20190457).

References

[1] L. The, "Facial injuries," *Lancet (London, England)*, vol. 391, no. 10118, p. 282, 2018.

[2] M. Benzeval, M. J. Green, and S. Macintyre, "Does perceived physical attractiveness in adolescence predict better socioeconomic position in adulthood? Evidence from 20 years of follow up in a population cohort study," *PLoS One*, vol. 8, no. 5, article e63975, 2013.

[3] J. Cai, Y. Zheng, P. Li, B. Ye, H. Liu, and L. Ge, "The effect of romantic relationships on the evaluation of the attractiveness of one's own face," *i-Perception*, vol. 9, no. 2, p. 204166951876554, 2018.

[4] J. C. Nellis, M. Ishii, P. J. Byrne, K. D. O. Boahene, J. K. Dey, and L. E. Ishii, "Association among facial paralysis, depression, and quality of life in facial plastic surgery patients," *JAMA facial plastic surgery*, vol. 19, no. 3, pp. 190–196, 2017.

[5] V. Sahni, "Psychological impact of facial trauma," *Craniomaxillofacial trauma & reconstruction*, vol. 11, no. 1, pp. 015–020, 2018.

[6] V. Wright, "What it feels like to have a facial disfigurement," *BMJ (Clinical research ed)*, vol. 358, article j4068, 2017.

[7] R. G. Tedeschi and L. G. Calhoun, "The posttraumatic growth inventory: measuring the positive legacy of trauma," *Journal of traumatic stress*, vol. 9, no. 3, pp. 455–471, 1996.

[8] K. Cusack, D. E. Jonas, C. A. Forneris et al., "Psychological treatments for adults with posttraumatic stress disorder: a systematic review and meta-analysis," *Clinical psychology review*, vol. 43, pp. 128–141, 2016.

[9] E. Susanty, M. Sijbrandij, W. Srisayekti, Y. Suparman, and A. C. Huizink, "The effectiveness of eye movement desensitization for post-traumatic stress disorder in Indonesia: a randomized controlled trial," *Frontiers in Psychology*, vol. 13, article 845520, 2022.

[10] J. I. Bisson, N. P. Roberts, M. Andrew, R. Cooper, C. Lewis, and Cochrane Common Mental Disorders Group, "Psychological therapies for chronic post-traumatic stress disorder (PTSD) in adults," *The Cochrane database of systematic reviews*, vol. 12, p. CD003388, 2013.

[11] J. Sin, D. Spain, M. Furuta, T. Murrells, I. Norman, and Cochrane Schizophrenia Group, "Psychological interventions for post-traumatic stress disorder (PTSD) in people with severe mental illness," *The Cochrane database of systematic reviews*, vol. 2017, no. 1, article CD011464, 2017.

[12] N. E. Van Loey and M. J. Van Son, "Psychopathology and psychological problems in patients with burn scars," *American Journal of Clinical Dermatology*, vol. 4, no. 4, pp. 245–272, 2003.

[13] T. K. Jensen, T. Holt, S. M. Ormhaug et al., "A randomized effectiveness study comparing trauma-focused cognitive behavioral therapy with therapy as usual for youth," *Journal of Clinical Child & Adolescent Psychology*, vol. 43, no. 3, pp. 356–369, 2014.

[14] L. K. Murray, S. Skavenski, J. C. Kane et al., "Effectiveness of trauma-focused cognitive behavioral therapy among trauma-affected children in Lusaka, Zambia: a randomized clinical trial," *JAMA pediatrics*, vol. 169, no. 8, pp. 761–769, 2015.

[15] P. O'Callaghan, J. McMullen, C. Shannon, H. Rafferty, and A. Black, "A randomized controlled trial of trauma-focused cognitive behavioral therapy for sexually exploited, war-affected Congolese girls," *Journal of the American Academy of Child and Adolescent Psychiatry*, vol. 52, no. 4, pp. 359–369, 2013.

[16] R. A. Bryant, L. Kenny, N. Rawson et al., "Efficacy of exposure-based cognitive behaviour therapy for post-traumatic stress disorder in emergency service personnel: a randomised clinical trial," *Psychological Medicine*, vol. 49, no. 9, pp. 1565–1573, 2019.

[17] W. A. Tol, C. Barbui, and M. van Ommeren, "Management of acute stress, PTSD, and bereavement: WHO recommendations," *Journal of the American Medical Association*, vol. 310, no. 5, pp. 477-478, 2013.

[18] E. Santarnecchi, L. Bossini, G. Vatti et al., "Psychological and brain connectivity changes following trauma-focused CBT and EMDR treatment in single-episode PTSD patients," *Frontiers in Psychology*, vol. 10, p. 129, 2019.

[19] F. Shapiro, "The role of eye movement desensitization and reprocessing (EMDR) therapy in medicine: addressing the

Hindawi
Computational and Mathematical Methods in Medicine
Volume 2023, Article ID 9879301, 1 page
https://doi.org/10.1155/2023/9879301

Retraction

Retracted: The Impact of Standardized Health Education in Patients with Ischemic Stroke on Patient Management Satisfaction and Quality of Clinical Management Services

Computational and Mathematical Methods in Medicine

Received 12 December 2023; Accepted 12 December 2023; Published 13 December 2023

This article has been retracted by Hindawi, as publisher, following an investigation undertaken by the publisher [1]. This investigation has uncovered evidence of systematic manipulation of the publication and peer-review process. We cannot, therefore, vouch for the reliability or integrity of this article.

Please note that this notice is intended solely to alert readers that the peer-review process of this article has been compromised.

Wiley and Hindawi regret that the usual quality checks did not identify these issues before publication and have since put additional measures in place to safeguard research integrity.

We wish to credit our Research Integrity and Research Publishing teams and anonymous and named external researchers and research integrity experts for contributing to this investigation.

The corresponding author, as the representative of all authors, has been given the opportunity to register their agreement or disagreement to this retraction. We have kept a record of any response received.

References

[1] J. Chen and L. Xiang, "The Impact of Standardized Health Education in Patients with Ischemic Stroke on Patient Management Satisfaction and Quality of Clinical Management Services," *Computational and Mathematical Methods in Medicine*, vol. 2022, Article ID 5698400, 6 pages, 2022.

Hindawi
Computational and Mathematical Methods in Medicine
Volume 2022, Article ID 5698400, 6 pages
https://doi.org/10.1155/2022/5698400

Research Article

The Impact of Standardized Health Education in Patients with Ischemic Stroke on Patient Management Satisfaction and Quality of Clinical Management Services

Jing Chen[1] **and Lin Xiang**[2]

[1]*Department of Radiology, The Third People's Hospital of Hubei Province, Wuhan 430030, China*
[2]*Department of Neurology, Hubei No. 3 People's Hospital of Jianghan University, Wuhan 430030, China*

Correspondence should be addressed to Lin Xiang; b20160502114@stu.ccsu.edu.cn

Received 25 July 2022; Revised 5 August 2022; Accepted 16 August 2022; Published 7 September 2022

Academic Editor: Min Tang

Aim. Ischemic stroke is a common brain disease, which seriously affects the quality of life of patients. The purpose of this study was to evaluate the impact of the application of standardized health education in ischemic stroke patients on patient management satisfaction and clinical management service quality. *Methods*. 220 patients with ischemic stroke were chosen for study target. The research objects were randomly divided into control group ($n = 110$) and education group ($n = 110$) by odd even number draw lots. The control group conducted conventional treatment; on the basis of the control group, the education group received standardized health education. The impact of the application of standardized health education in patients with ischemic stroke on patient management satisfaction and clinical management service quality was analyzed. *Results*. The number of health error items in the two groups decreased significantly after 2 months and 3 months of treatment, contrast to before admission, and the number of health error items in the education group was lower than that in the control group, and the difference was statistically significant. After 3 months of treatment, the daily activity score increased and the neurological function score decreased in the two groups, and the daily activity score in the education group was higher than that in the control group, and the neurological function score was lower than that in the control group; the difference was statistically significant. The satisfaction scores of patients in the education group in different aspects such as staff working attitude, health management, diet management, and environmental management were higher than those in the control group, and the disparity was obvious. *Conclusion*. The application of standardized health education in patients with ischemic stroke has certain clinical value.

1. Introduction

Ischemic stroke is a common vascular brain illness with a complex pathogenesis that is significantly associated with environmental, genetic, and acquired genetic factors [1, 2]. Ischemic stroke is a condition in which patient's cerebral arteries are blocked, resulting in a dysfunctional blood supply to the brain, leading to partial brain tissue necrosis, which severely affects the patient's neurological function [3, 4]. The disease usually occurs suddenly. With the continuous evolution of ischemic stroke, patients' nerves are very vulnerable to damage, and its disability rate is high, which will lead to the obstruction of their limb motor ability, the impairment of their visual and auditory abilities, and the decline of their autonomous activity ability and motor ability, which will seriously influence the level of life of living sufferers [5, 6]. At present, intravenous thrombolysis is used to treat patients in clinic, which has good curative effect, but standardized management has not been formed in disease health education [7, 8]. Therefore, we should find a scientific and standardized health education method to carry out health management and education for their diseases, which can take a vital part in the healthy life, ability, and neurological function recovery of patients [9–11]. In this study, obtained in to our hospital, from September 2019 to December 2021, 220 patients with ischemic stroke were selected as

the research objects, and the health management education and training program was formulated to explore its application effect. Now it is reported as follows.

2. Materials and Methods

2.1. Study Subjects. 220 patients with ischemic stroke who came to the emergency department of our hospital from September 2019 to December 2021 were randomly divided into education group ($n = 110$) and control group ($n = 110$) by odd even number draw lots. During the study period, no suspension or shedding occurred in both groups. There were 52 males and 58 females in the education group. Aged from 24 to 72, the average age was 45.18 ± 5.46 years old. In the control group, there were 50 males and 60 females. Aged from 28 to 74, the average age was 45.74 ± 5.38 years old. There was no difference in general data such as gender and age of patients ($P > 0.05$), which was comparable. According to the diagnostic criteria for acute ischemic stroke in the "Chinese guidelines for the diagnosis and treatment of ischemic stroke 2014" [9] written by Peng et al. [12], the patient has severe coma and no active consciousness.

2.2. Inclusion and Exclusion Criteria. This study was approved by the ethics committee of our hospital. Inclusion criteria are as follows: (1) meet the above diagnostic criteria of ischemic stroke, (2) the surgical characteristics are relatively clear, (3) less than 79 years old, (4) surgery can be arranged within 72 hours after admission, and (5) the patient or his family members sign the medical documents and voluntarily participate. Exclusion criteria are as follows: (1) patients with severe autoimmune diseases, (2) those who had cerebral hemorrhage in the past, (3) patients with severe blood system diseases or coagulation dysfunction, (4) patients with malignant tumors, (5) people with mental disorders, and (6) the patient is in a coma.

2.3. Treatment Regimens. The control group: the patients were dealt with routine treatment, psychological repair activities, appropriate psychological counseling, and relieving the patients' mood, so as to recover quickly. It was suggested that patients should mainly eat light food.

The education group: implement standardized expert education methods for patients, and the contents were as follows:

(1) Establish a nursing expert group, the members of which were mainly composed of experienced clinicians and nurses. The members of the group cooperated closely to discuss nursing intervention measures. Make nursing and recuperation plans in time

(2) *Condition Monitoring, Dynamic Monitoring of Patients' Recovery Process, and Monitoring of Patients' Indicators*. Timely give feedback about the recovery of the disease, through reexamination and other ways to understand the patient's condition contrasted, and provide patients with a reasonable dietary plan

(3) Create a good ward environment. Ventilate the ward regularly, adjust the temperature to 27-32°C, the air humidity should be 60%-70%, and set warning signs in the ward to create a good environment for patients

(4) *Admission Nursing*. The admission nursing of patients required the consent of patients and their families. Under the guidance of doctors, the nursing staff carried out admission nursing in strict accordance with the nursing plan

(5) *Psychological Repair*. From the perspective of the patient's treatment process, it was inevitable to have negative emotions about the condition. Nursing staff need to appease patients' emotions, timely give feedback about the effect of patients in the treatment stage, and encourage patients to maintain a stable mood

(6) Establish a good doctor-patient relationship. When communicating with patients with ischemic stroke, medical staff should reasonably guide patients to communicate with them in combination with patients' emotions, so as to improve patients' enthusiasm for treatment cooperation

(7) *Strengthen Self-Management*. Send disease knowledge manuals and precautions to patients with ischemic stroke, so that patients can understand the disease precautions. The goal should be to improve patient management objectives and medical compliance behavior, so as to achieve patient self-management. Each time you visited patients, you should closely communicate with patients about disease precautions, understand patients' medication, explain the relationship between exercise, diet, and glucose metabolism, and strengthen patients' medical compliance behavior

(8) Establish the patient's disease management information, including the basic information of the patient's hospitalization, as well as the living ability and the disease management mode. Carry out neurological rehabilitation training and drug treatment for patients, as well as the key points of first aid after stroke

(9) *Discharge Education*. A series of common problems for patients discharged from hospital also need patients to carry out education, such as how to carry out disease self-management, self-care program, and scientific diet plan after discharge. Nurses recorded the above knowledge points into videos for patients to read and learn and finally continued to deepen their cognition and understanding of knowledge points, so as to achieve effective health education (Figure 1).

2.4. Follow-Up. (1) Standardize health education knowledge. Observe and record the health knowledge evaluation form of the two groups of patients, including stroke and treatment and rehabilitation knowledge, and count the relevant scores. (2) Service quality. The recovery status of patients was assessed by daily activity scale (Barthel Index scale) and neurological function rating scale (NIHSS), and their service and

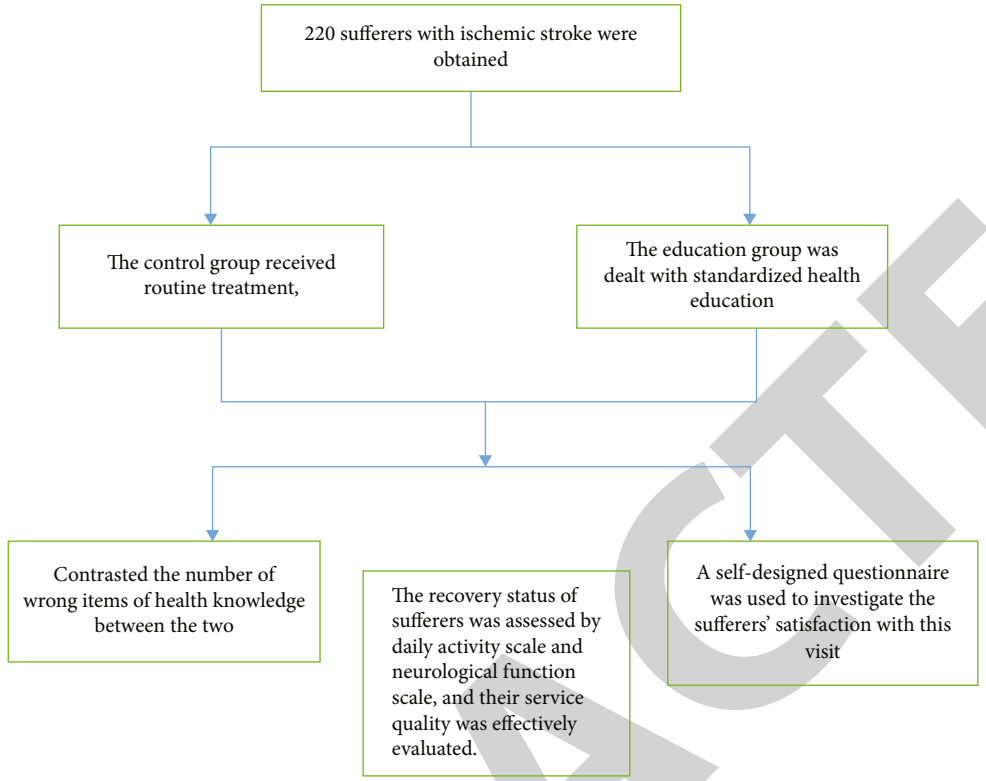

Figure 1: The application of standardized health education in patients with ischemic stroke can improve the ability of daily activities, enhance the repair of neural function, and increase the nursing satisfaction of patients.

Table 1: Comparison of the number of wrong items of health knowledge between the two groups (pieces, $\bar{x}\pm s$).

Category	Instances	On admission	Treatment for 2 months	Treatment for 3 months
Education group	110	31.35 ± 3.38	7.37 ± 1.79▲	6.34 ± 1.59▲
Control group	110	30.34 ± 6.57	12.31 ± 3.57▲	11.34 ± 3.98▲
t value		1.306	12.973	12.236
P value		0.194	0.000	0.000

Note: Compared with the same group at admission, ▲$P < 0.05$.

treatment were effectively evaluated. Barthel Index scores range from 0 to 100 points. The higher the score, the stronger the ability of daily activities; NIHSS score was 0-42 points. The higher the score, the more serious the nerve defect. (3) Management satisfaction. A self-made questionnaire was used to evaluate the patients' satisfaction with this visit, including the staff's working attitude, health management, food management, and environmental management. The total score of each part was 25 points, and the full score was set to 100 points

2.5. Data Analysis. SPSS 22.0 was utilized to evaluate quantitative data, and the assessment sample was normally distributed with equal variance and written as ($\bar{x}\pm s$). The t -test of paired samples was utilized for intracategory comparisons, while the t-test of independent samples was used for comparison between two categories. And the difference was taken clinically significant at $P < 0.05$.

3. Results

3.1. Comparison of Two Groups of Health Knowledge Analysis. On admission, there was no significant difference in health knowledge error item score between the two groups ($P > 0.05$). The number of health knowledge error item in the two groups decreased significantly after 2 months and 3 months of treatment compared with that before admission ($P < 0.05$), and the number of health knowledge error item in the education group was lower than that in the control group; the difference was statistically significant ($P < 0.05$), as shown in Table 1.

3.2. Comparison of Daily Activity and Neurological Function between the Two Groups. At admission, there was no significant difference in the scores of daily activity and neurological function between the two groups ($P > 0.05$). After 3 months of treatment, the scores of daily activity and neurological function of the two groups increased, and the scores

Table 2: Comparison of daily activity and neurological function between the two groups (points, $\bar{x}\pm s$).

Category	Instances	Daily activity ability		Neurological function score	
		On admission	Treatment for 3 months	On admission	Treatment for 3 months
Education group	110	56.58 ± 9.97	71.82 ± 7.43▲	22.13 ± 3.24	12.21 ± 2.19▲
Control group	110	55.04 ± 6.70	64.42 ± 6.06▲	22.56 ± 3.97	14.43 ± 3.92▲
t value		1.345	8.095	0.880	5.185
P value		0.180	0.000	0.380	0.000

Note: Compared with the same group at admission, ▲$P < 0.05$.

Table 3: Satisfaction of patients in the two groups (points, $\bar{x}\pm s$).

Category	Instances	Staff working attitude	Health management	Diet management	Environmental management
Education group	110	22.08 ± 1.64	23.31 ± 1.05	22.16 ± 1.09	22.82 ± 1.64
Control group	110	20.25 ± 2.38	21.14 ± 1.89	21.01 ± 1.27	20.28 ± 2.36
t value		6.640	10.526	7.207	9.270
P value		0.000	0.000	0.000	0.000

of daily activity and neurological function of the education group were higher than those of the control group and lower than those of the control group. The differences were statistically significant ($P < 0.05$), as shown in Table 2.

3.3. Analysis of Patients' Satisfaction in the Two Groups. The satisfaction scores of the patients in the education group in different aspects such as staff working attitude, health management, diet management, and environmental management were higher than those in the control group, and the difference was statistically significant ($P < 0.05$), as shown in Table 3.

4. Discussion

Ischemic stroke is a common brain disease, whose pathogenesis is closely related to external environment, psychological factors, and self-immunity. Clinically, the symptoms of ischemic stroke are coma, blurred consciousness, language function, and sensory nerve disorders, which may cause severe loss of activity [13–15]. Patients with ischemic stroke are very prone to ischemia, resulting in hypoxic necrosis of neurons in brain tissue, damage to neurons, and irreversible cell death, which will have a huge impact on the patient's neurological function, and the disease develops rapidly. Soon after, the patient has blurred consciousness, which seriously threatens the patient's life and health [16–18]. At present, hyperbaric oxygen therapy is used in clinic, which can effectively delay the patient's condition and effectively control the blood supply to the brain. However, 25% of patients have serious sequelae, patients' neurological function is damaged, and some patients' neurological function recovery is poor, which can effectively improve patients' activity and cognitive function [19]. Standard education is helpful to evaluate the degree of neurological impairment of ischemic stroke and lay a theoretical basis for the diagnosis of early patients.

With the continuous improvement of people's living standards and the improvement of people's dietary structure and lifestyle, the proportion of patients with ischemic stroke will continue to increase. Ischemic stroke is a common brain disease, which seriously affects people's quality of life. Therefore, patients need to take drugs for a long time to inhibit vascular blockage, but the patients' cognitive level of the disease is low and lack of systematic understanding, which affects the patients' life treatment [20, 21]. Especially in the elderly, the cognitive level of patients with ischemic stroke is low, and they do not listen to the advice of medical staff, which is not conducive to disease control. The difficulties in the management of patients with ischemic stroke are the long disease cycle, many complications, patients' emotional instability, and poor drug control effect.

The main advantages of the application of standardized health education: dynamically understand the situation of patients and timely monitor various indicators of patients, and medical staff should provide psychological guidance to patients, so as to grasp the basic situation of patients in time, so that patients can actively cooperate with treatment. This study found that the score of daily activity ability of patients in the education group was significantly higher than that in the control group, and the score of neurological function of patients in the education group was significantly lower than that in the control group. It shows that health standardization education can strengthen rehabilitation training for patients through careful, accurate, and standardized operation, so as to reduce patients' neurological function and improve patients' daily activity ability. Meglio et al. [22] have shown that humanistic care for patients with ischemic stroke can effectively improve their quality of life. When carrying out nursing intervention for patients with ischemic stroke, it is necessary to carry out psychological counseling, establish an optimistic attitude, and handle treatment correctly, which will make patients actively cooperate with treatment, build confidence, and make patients actively seek help. Pay a return visit to patients, monitor their condition in real time, and communicate with patients at any time, which is convenient for correcting patients' behavior in time and strengthening exercise and other aspects and will improve patients' health status in time. This study found that the satisfaction scores

of patients in the education group were higher than those in the control group in different aspects such as staff work attitude, health management, diet management, and environmental management. Narayan et al. [23] have conducted comprehensive nursing intervention on patients with ischemic stroke and found that the comprehensive nursing intervention group is significantly higher than the control group, and the cognition of the disease is relatively high. This is mainly because patients are optimistic after treatment with standardized education, and actively cooperate with doctors to significantly improve the curative effect and effectively improve the treatment effect of patients [24–26]. Therefore, health standardized education should be carried out in the treatment of patients with ischemic stroke, and psychological counseling and rehabilitation training should be included in the treatment of patients with ischemic stroke. It is beneficial to the recovery of patients. However, there are some shortcomings in this study, such as single center and small sample size, which lead to the limitations of the research results. It is necessary to design a multicenter and large sample study to further verify the test results.

5. Conclusion

To sum up, in the treatment of ischemic stroke patients with standardized health education, integrating psychological counseling and rehabilitation training into the treatment of ischemic stroke patients will help patients improve their psychology, establish a positive and optimistic attitude, and teach patients to master medical nursing knowledge and self-care methods. Through the scientific guidance of patients' psychology, diet, and environment, the symptoms of patients can be significantly alleviated, which is worthy of clinical promotion.

Data Availability

The data used to support the findings of this study are available from the corresponding author upon request.

Conflicts of Interest

The authors declare that they have no conflict of interest.

References

[1] C. D. Maida, R. L. Norrito, M. Daidone, A. Tuttolomondo, and A. Pinto, "Neuroinflammatory mechanisms in ischemic stroke: focus on cardioembolic stroke, background, and therapeutic approaches," *International Journal of Molecular Sciences*, vol. 21, no. 18, p. 6454, 2020.

[2] A. Acharya, P. Yogi, P. Singh, and T. R. Bhattarai, "Herlyn Werner Wunderlich syndrome presenting with ischemic stroke due to suspected paroxysmal nocturnal hemoglobinuria: a case report," *JNMA; Journal of the Nepal Medical Association*, vol. 59, no. 234, 2021.

[3] Y. Pan, X. Cai, J. Jing et al., "Stress hyperglycemia and prognosis of minor ischemic stroke and transient ischemic attack," *Stroke*, vol. 48, no. 11, pp. 3006–3011, 2017.

[4] M. Vucic, Z. Stanojkovic, A. Antic, J. Vucic, and V. Pavlovic, "Eval-uation of platelet activation in leukocyte -depletedplatelet concentrates during storage," *Bosnian Journal of Basic Medical Sciences*, vol. 292, no. 28, pp. 11631–11637, 2018.

[5] J. E. Siegler and S. Galetta, "Editors' note: safety and efficacy of dual antiplatelet pretreatment in patients with ischemic stroke dealt with IV thrombolysis: a systematic review and meta-analysis," *Neurology*, vol. 96, no. 3, pp. 134.1–13134, 2021.

[6] M. V. Diaz Rojas, T. C. Wu, L. Zhu et al., "Abstract P189: using telemedicine eliminates the weekend/after-hours effect in acute ischemic stroke patients receiving thrombolysis during a deadly pandemic," *Stroke*, vol. 52, Suppl_1, 2021.

[7] J. Jiang, C. Tan, W. Zhou et al., "Plasma C-reactive protein level and outcome of acute ischemic stroke patients treated by intravenous thrombolysis: a systematic review and meta-analysis," *European Neurology*, vol. 84, no. 3, pp. 145–150, 2021.

[8] R. Su, S. A. Cornelissen, M. Van Der Sluijs et al., "autoTICI: automatic brain tissue reperfusion scoring on 2D DSA images of acute ischemic stroke patients," *IEEE Transactions on Medical Imaging*, vol. 40, no. 9, pp. 2380–2391, 2021.

[9] T. Yamasaki, K. Hayashi, Y. Shibata et al., "Takotsubo cardiomyopathy following mechanical thrombectomy for acute ischemic stroke: illustrative case," *Journal of Neurosurgery: Case Lessons*, vol. 2, no. 9, 2021.

[10] J. Strause, K. B. Atsina, D. Bialo, J. Orwitz, R. L. Wolf, and B. Cucchiara, "Ischemic stroke associated with aneurysmal lenticulostriate vasculopathy and symmetric reversible basal ganglia lesions in COVID-19," *Journal of the Neurological Sciences*, vol. 426, article 117484, 2021.

[11] S. C. Kapur, K. Jeevesh, and V. K. Sharma, "Radiation exposure during computerized tomography-based neuroimaging for acute ischemic stroke: a case-control study," *Journal of Integrative Neuroscience*, vol. 20, no. 3, pp. 605–611, 2021.

[12] B. Peng, J. Ni, C. S. Anderson et al., "Implementation of a structured guideline-based program for the secondary prevention of ischemic stroke in China," *Stroke*, vol. 45, no. 2, pp. 515–519, 2014.

[13] R. Abdolahipour, A. Nowrouzi, M. B. Khalili, A. Meysamie, and S. Ardalani, "Aqueous Cichorium intybus L. seed extract may protect against acute palmitate-induced impairment in cultured human umbilical vein endothelial cells by adjusting the Akt/eNOS pathway, ROS: NO ratio and ET-1 concentration," *Journal of Diabetes and Metabolic Disorders*, vol. 19, no. 2, pp. 1045–1059, 2020.

[14] S. Nazik, V. Avci, and Z. Küskü Kiraz, "Ischemia-modified albumin and other inflammatory markers in thediagnosis of appendicitis in children," *Turkish Journal of Trauma and Emergency Surgery*, vol. 23, no. 4, pp. 317–321, 2016.

[15] W. Q. Chen, C. Li, W. M. Liang et al., "The roles of optogenetics and technology in neurobiology: a review," *Frontiers in Aging Neuroscience*, vol. 14, article 867863, 2022.

[16] P. Kiluk, A. Baran, M. Świderska, M. Maciaszek, and I. Flisiak, "Lp-PLA2 as a promising predictor of comorbidities in patients with severe psoriasis," *The Journal of Dermatological Treatment*, vol. 31, no. 5, pp. 524–530, 2020.

[17] L. Jackisch, W. Kumsaiyai, J. D. Moore et al., "Differential expression of Lp-PLA2 in obesity and type 2 diabetes and the influence of lipids," *Diabetologia*, vol. 61, no. 5, pp. 1155–1166, 2018.

[18] J. Cao, R. Hou, J. Lu et al., "The predictive value of β2-MG and TGF-β for elderly hypertensive nephropathy," *Experimental and Therapeutic Medicine*, vol. 17, no. 4, pp. 3065–3070, 2019.

Hindawi
Computational and Mathematical Methods in Medicine
Volume 2023, Article ID 9831659, 1 page
https://doi.org/10.1155/2023/9831659

Retraction

Retracted: Adverse Influences of Nonstrabismic Amblyopia on Quality of Life of Teenagers in China

Computational and Mathematical Methods in Medicine

Received 5 December 2023; Accepted 5 December 2023; Published 6 December 2023

This article has been retracted by Hindawi, as publisher, following an investigation undertaken by the publisher [1]. This investigation has uncovered evidence of systematic manipulation of the publication and peer-review process. We cannot, therefore, vouch for the reliability or integrity of this article.

Please note that this notice is intended solely to alert readers that the peer-review process of this article has been compromised.

Wiley and Hindawi regret that the usual quality checks did not identify these issues before publication and have since put additional measures in place to safeguard research integrity.

We wish to credit our Research Integrity and Research Publishing teams and anonymous and named external researchers and research integrity experts for contributing to this investigation.

The corresponding author, as the representative of all authors, has been given the opportunity to register their agreement or disagreement to this retraction. We have kept a record of any response received.

References

[1] Y. Wang and H. Wang, "Adverse Influences of Nonstrabismic Amblyopia on Quality of Life of Teenagers in China," *Computational and Mathematical Methods in Medicine*, vol. 2022, Article ID 2621991, 6 pages, 2022.

Hindawi
Computational and Mathematical Methods in Medicine
Volume 2022, Article ID 2621991, 6 pages
https://doi.org/10.1155/2022/2621991

Research Article

Adverse Influences of Nonstrabismic Amblyopia on Quality of Life of Teenagers in China

Yakun Wang and Hong Wang

Department of Ophthalmology, Clinical Medical College, Yangzhou University, Yangzhou 225000, China

Correspondence should be addressed to Yakun Wang; wjscui06@163.com

Received 9 August 2022; Revised 19 August 2022; Accepted 22 August 2022; Published 7 September 2022

Academic Editor: Min Tang

The aim of this study was to explore the influences of nonstrabismic amblyopia on quality of life in adolescents. Health-related quality of life (HRQoL) scale, a multidimensional construct that indicates a fundamental health outcome, was used to measure physical and psychosocial functioning of the adolescents. Forty teenagers with nonstrabismic amblyopia and 40 control teenagers without nonstrabismic amblyopia were recruited between April 2019 and July 2021. The anthropometric measures, body image, physical activity outcome, and HRQoL scores including physical health, emotional functioning, social functioning, and school functioning were compared between the two groups. The results revealed that teenagers with nonstrabismic amblyopia had less weekly sedentary time ($P < 0.001$), weekly total steps ($P < 0.001$), and worse school functioning ($P = 0.0211$) than control teenagers. No significant difference was found in anthropometric measures and body image between the two groups ($P > 0.05$). This study implied the needs for teenagers with nonstrabismic amblyopia to enhance physical activities. Teachers and parents are encouraged to pay more attention to teenagers with nonstrabismic amblyopia to improve their school functioning.

1. Introduction

Amblyopia is a neurodevelopmental disorder, affecting up to 5% of the general population [1]. For patients with amblyopia, monocular vision or binocular vision is decreased because of poor visual stimulation in childhood [2]. After uncorrected refractive errors, amblyopia is the second most common cause of poor vision in children and young adults [2, 3]. The most common amblyogenic factors include strabismus and anisometropia. Strabismus is noticeable, while other types of amblyopia were not easily to be recognized by parents. Children may go undetected until they are beyond the critical period of treatment efficacy. Anisometropic amblyopia shows high prevalence in school-age children [4, 5]. Despite it, investigations on nonstrabismic amblyopia in quality of life were very limited. This may be due to that nonstrabismic amblyopia is deemed less serious than strabismus-associated amblyopia, which has obvious emotional and psychosocial consequences [6, 7]. Moreover, many amblyopia-related studies focus on the effects of amblyopia treatment [8, 9] but not the condition itself, and recurrence of amblyopia occurs in 25% to 50% of children after successful treatment, and binocular vision rarely returns to normal after repair [10].

To assess the physical and social functioning, well-being, and mental health of children and adolescents, health-related quality of life (HRQoL) has aroused much interest [11]. Certain key aspects of health are not assessed by clinical or traditional physiological measurements but can be detected by HRQoL measures. Quality of life was defined as "the individual" perception of their position in life in the context of the culture and value systems in which they live and in relation to their goals, expectations, standards, and concerns by World Health Organization [12]. HRQoL is multidimensional and includes various subdimensions of subjective experience, such as social interaction, psychological well-being, physical activity, and school performance, reflecting individual self-assessment, perception of enjoyment and well-being, and satisfaction with functioning, life, and general health [13, 14]. In recent years, the evidence of the effects of amblyopia on HRQoL has been measured

[15]. Literatures point out that amblyopia indeed influences the individual together with family members [16], but the way in which amblyopia treatment has changed and some studies demonstrating that HRQoL implications of amblyopia are dated. Therefore, it is essential to reevaluate whether the influence of amblyopia on HRQoL has altered by changes in clinical practice. A previous study demonstrated that nonstrabismic amblyopia influences the quality of life of adults [17]. Currently, few studies have evaluated perspective quality of life in adolescents with nonstrabismic amblyopia.

Considering the importance of studying HRQoL, we performed a study to reveal the effects of nonstrabismic amblyopia on HRQoL in adolescents.

2. Methods

2.1. Participants. The study was conducted following the Declaration of Helsinki and was approved by the ethnical committee of Northern Jiangsu People's Hospital. Participants were recruited by department of ophthalmology in Northern Jiangsu People's Hospital. Written informed consent was gained from a parent or legal guardian before testing their child and after explanation of the nature and possible consequences of the study. Persons who visited the hospital underwent a complete eye examination including ocular motility test, slit lamp examination, refraction, cover-uncover test, and dilated retinal evaluation. The inclusion criteria were set as follows: (1) aged between 12 and 18 and (2) diagnosed with amblyopia [18]. The exclusion criteria were set as follows: (1) with strabismus [19], (2) with severe diseases that influence the daily life, and (3) unwilling to join in the study (for both teenager participants and their parents). Finally, 40 teenagers (male = 28 and female = 12) with nonstrabismic amblyopia were included, and 40 healthy teenagers (male = 23 and female = 17) without nonstrabismic amblyopia were recruited between April 2019 and July 2021.

2.2. HRQoL. The Pediatric Quality of Life Inventory (PedsQL) [20], recommended by Khairy et al. as a simple, easy, and reliable model for assessing HRQoL [21], was used in our study. The PedsQL questionnaire had 23 items in total and was divided into 4 domains regarding physical functioning (8 items) and psychosocial health (15 items). The latter one was further divided into social functioning (5 items), emotional functioning (5 items), and school functioning (5 items). Each item was reversely scored and linearly transformed, and higher scores indicate better HRQoL [20]. The transformation was set as follows: 0 = 100, 1 = 75, 2 = 50, 3 = 25, and 4 = 0. Children completed the PedsQL questionnaire by themselves after instructions from our research team. Children's self-reported HRQoL and their parents perceived children's HRQoL total scores were recorded.

2.3. Body Image Perception. Parents were invited to identify the most similar image with body of their children among various silhouettes to evaluate the parent's body image perception about their children [22]. There are two different silhouettes, actual figure and ideal figure, selected by the parents. Actual figure is the image that is believed to be the most similar with their children. Ideal figure is the image that is desired for their children. Overestimation of the body image means that actual figure is larger than ideal figure and vice versa. The profile series were divided based on the BMI categories determined by Cole's cut-off values: 1: underweight status, 2: normal weight status, 3: overweight status, and 4: obese status. Profiles 1 and 2 correspond to underweight; profiles 3, 4, and 5 correspond to normal weight; profiles 6 and 7 correspond to overweight; profiles 8 and 9 correspond to obesity.

2.4. Anthropometric Measuring. BMI was calculated as weight/height^2, which was used to assess the weight status of each participant according to Cole cut-off values by sex and age [23]. The units for weight and height were kilogram and meter. The waist/height ratio (WHTR) was calculated to reveal the cardiovascular risk with the cut-off value set as 0.5 [24, 25].

2.5. Physical Activity Variables. Sedentary time was monitored using ActiGraph accelerometry monitors (Actigraph, USA) and was analyzed using the ActiLife 6.13.3 software (ActiGraph) [26]. Accelerometers were fixed with an elastic belt around the waist in the right side. Teenagers worn the accelerometers for a week and removed the accelerometers when bathing, swimming, and showering. The Evenson cut points were used to calculate the minutes spent in physical activity per day [27]. Adolescents aged 5–17 were recommended by World Health Organization to perform at least one hour of moderate-to-vigorous PA (MVPA) per day [28], which was measured in this study, and at least 3 valid days were needed for inclusion in analyses.

2.6. Statistical Analysis. Data are expressed as N (%) or mean ± SD. All analyses were carried out using SPSS, version 22 (SPSS Inc. Chicago, IL, USA). Chi-square test and unpaired t test were applied. The significance threshold was set as $P \leq 0.05$.

3. Results

3.1. Comparison of the General Information between the Two Groups. General information including age, gender, and parents' education of teenagers in the healthy control and nonstrabismic amblyopia groups was collected. As revealed in Table 1, there is no significant difference among general information between the two groups ($P > 0.05$).

3.2. Comparison of the Anthropometric Measures between the Two Groups. Teenagers in the healthy control and nonstrabismic amblyopia groups had no significant differences in BMI and WHTR ($P > 0.05$, Table 2).

3.3. Comparison of the Body Image between the Two Groups. Teenagers in the healthy control and nonstrabismic amblyopia groups had no significant differences in body image ($P > 0.05$, Table 3).

Table 1: General information of the participants.

Parameters	Healthy control	Nonstrabismic amblyopia	P value
Age	15.89 ± 1.57	15.64 ± 1.13	0.5242
Gender			0.3524
Male	$n = 23$ (57.5%)	$n = 28$ (70%)	
Female	$n = 17$ (42.5%)	$n = 12$ (30%)	
Mother's education			0.8565
Low	$n = 7$ (17.5%)	$n = 11$ (27.5%)	
Medium	$n = 17$ (42.5%)	$n = 20$ (50%)	
High	$n = 6$ (40%)	$n = 9$ (22.5%)	
Father's education			0.4669
Low	$n = 3$ (7.5%)	$n = 5$ (12.5%)	
Medium	$n = 21$ (52.5%)	$n = 22$ (55%)	
High	$n = 6$ (40%)	$n = 3$ (7.5%)	

Data are expressed as N (%) or mean ± SD. Unpaired t test or chi-square test was conducted.

Table 2: Anthropometric measures of the participants.

Parameters	Healthy control	Nonstrabismic amblyopia	P value
BMI	19.21 ± 2.15	20.55 ± 2.36	0.1107
Normal weight	$n = 37$ (92.50%)	$n = 35$ (87.50%)	0.7449
Overweight	$n = 1$ (2.50%)	$n = 2$ (5.00%)	
Underweight	$n = 2$ (5.00%)	$n = 3$ (7.50%)	
Obese	$n = 0$ (0.00%)	$n = 0$ (0.00%)	
WHTR	0.47 ± 0.03	0.48 ± 0.03	0.1626
Non at risk	$n = 39$ (97.50%)	$n = 38$ (95.00%)	0.5562
At risk	$n = 1$ (2.50%)	$n = 2$ (5.00%)	

Data are expressed as N (%) or mean ± SD. Unpaired t test or chi-square test was conducted.

Table 3: Body image of the participants.

	Healthy control	Nonstrabismic amblyopia	P value
Under	$n = 6$ (15.00%)	$n = 4$ (10.00%)	0.7563
Correct	$n = 31$ (77.50%)	$n = 32$ (80.00%)	
Overestimation	$n = 3$ (7.50%)	$n = 4$ (10.00%)	

Data are expressed as N (%). Chi-square test was conducted.

3.4. Comparison of the Physical Activity Outcomes between the Two Groups. Teenagers in the healthy control and nonstrabismic amblyopia groups had no significant differences in daily MVPA ($P > 0.05$). However, the nonstrabismic amblyopia group showed longer weekly sedentary time and less weekly total steps than the control group ($P < 0.001$, Table 4).

3.5. Comparison of HRQoL of the Teenagers between the Two Groups. Teenagers in the healthy control and nonstrabismic amblyopia groups had no significant differences in scores of physical health, emotional functioning, and social functioning ($P > 0.05$). However, the nonstrabismic amblyopia group showed less school functioning scores than the control group ($P = 0.0211$, Table 5).

3.6. Comparison of HRQoL of the Parent Proxy-Reports between the Two Groups. As revealed in Table 6, there are no significant differences in physical health, emotional functioning, and social functioning of the parent proxy-reports between the two groups ($P > 0.05$). However, the nonstrabismic amblyopia group showed less school functioning scores than the control group ($P = 0.0017$).

4. Discussion

The subtypes of amblyopia (strabismic and nonstrabismic amblyopia) are not only disturbance of the development of the visual system at different points but also primarily different pathologic processes [29]. Some previous studies revealed the negative influence of strabismic amblyopia (or its treatment) on life of quality [30–32] while that of nonstrabismic amblyopia remains unknown. The study was designed to investigate the anthropometric measures, body image perception, physical activity outcomes, teenager-self reported, and parent-reported HRQoL from 40 teenagers with nonstrabismic amblyopia and 40 control teenagers. There were no significant differences between the general information including age, gender, and family education level of the teenagers in the two groups ($P > 0.05$). In addition, body image is a multifaceted mental representation of our bodies and their emotional experiences that is constantly updated. During adolescence, due to the constant physical and cognitive changes occurring, body image concerns occur frequently, thus increasing the evaluation and attention to the body and appearance. Sociocultural influences and social comparisons internalize the ideal of beauty, which leads to negative body image and dissatisfaction with appearance [33]. Therefore, adolescence is a time of significant physical and social change that can lead to negative body image. Perception of body image is associated with BMI and WHTR. However, reports about amblyopia and perception of body image are rare. Here, we found that the two groups also exhibited no significant differences in anthropometric measures including BMI and WHTR and perception of their parents on the body image ($P > 0.05$).

Amblyopia is associated with academic scores in mathematics, reading, social science, and science [34]. Consistent with previous literature, we found that adolescents with nonstrabismic amblyopia have worse school functioning than control peers ($P = 0.0211$), which might be associated with the vision loss in leaning period. Besides

Table 4: Physical activity outcome of the participants.

	Healthy control	Nonstrabismic amblyopia	P value
Daily MVPA			0.0979
Meet	$n = 17$ (38.3%)	$n = 10$ (38.3%)	
Not meet	$n = 23$ (61.7%)	$n = 30$ (61.7%)	
Weekly sedentary time	6322.44 ± 424.03	6885.43 ± 522.14	<0.001
Weekly total steps	54,178.23 ± 9627.18	52094.66 ± 9232.84	<0.001

Data are expressed as N (%) or mean ± SD. Unpaired t test or chi-square test was conducted.

Table 5: HRQoL of the participants.

	Healthy control	Nonstrabismic amblyopia	P value
Physical health	73.16 ± 13.64	72.89 ± 14.27	0.3066
Emotional functioning	72.21 ± 13.89	71.69 ± 13.21	0.0724
Social functioning	74.37 ± 12.12	72.33 ± 10.89	0.6123
School functioning	76.88 ± 14.03	73.14 ± 12.73	0.0211

Data are expressed as mean ± SD. Unpaired t test was conducted.

Table 6: HRQoL of the parent proxy-reports.

	Healthy control	Nonstrabismic amblyopia	P value
Physical health	82.52 ± 15.31	79.46 ± 10.95	0.9788
Emotional functioning	75.47 ± 12.48	73.85 ± 12.76	0.0901
Social functioning	76.58 ± 14.75	75.73 ± 12.64	0.1514
School functioning	84.12 ± 13.96	78.44 ± 12.93	0.0017

Data are expressed as mean ± SD. Unpaired t test was conducted.

school functioning, physical health, emotional functioning, social functioning are also important for adolescents. It was reported that the nonamblyopia group had significantly better motor competence on the physical activity than either the corrected amblyopia group or the noncorrected amblyopia group [35]. Moreover, quite a number of amblyopia patients believe that amblyopia affects their study and work to a certain extent and generally affects their lifestyle [36]. Previous study also showed that children with strabismus had lower physical health scores, worse emotional functioning, and school functioning than those without strabismus, while no difference was found in these parameters between child with our without amblyopia [37]. However, the present study revealed the no significant difference in physical health scores and emotional functioning between adolescents with or without nonstrabismic amblyopia ($P > 0.05$).

Moderate physical activity has positive association with high HRQoL (measured by the total PedsQL score) in children [38, 39]. According to meta-analyses by Wafa et al., children with higher physical activity levels had a better HRQoL [40]. The positive association of physical activity and HRQoL was consistent regardless of age, gender, weight, and socioeconomic characteristics [41]. In our study, adolescents with nonstrabismic amblyopia have longer weekly sedentary time and less weekly total steps than control peers ($P < 0.001$). Considering that adolescents with nonstrabismic amblyopia also had lower school functioning in HRQoL ($P = 0.0211$), the positive association of physical activity and HRQoL in nonstrabismic amblyopia was identified.

Moreover, HRQoL perceptions between children or adolescents and their parents are likely to be different with increasing age because the child may have a more complicated and distinct understanding of the world instead of simply accepting opinions from parents. Thus, Tsiros et al. made suggestions to attach importance to the parent's perceived HRQoL [42]. Williams et al. found that, compared with children below 12 years old, there is less agreement between child-reported and parent's perceived HRQoL for children at the age of 12 years [43]. In our research, the comparison results of the perceived HRQoL for their children in the two groups were no different from the teenager-reported HRQoL ($P > 0.05$), which is similar to a previous study [39]. Our study revealed that both teenager-reported HRQoL and parent's perceived HRQoL revealed the worse school functioning in nonstrabismic amblyopia ($P = 0.0017$), while there are no differences in physical health, emotional functioning, and social functioning ($P > 0.05$).

There are also some limitations in our study. First, participants were recruited from a small geographical area. Further studies are needed to determine whether the identified HRQoL is present nationwide. Moreover, many of the effects of amblyopia and/or its treatment on HRQoL are experienced by the children; however, parents' opinions and perspectives on treatment may directly or indirectly influence children's beliefs.

5. Conclusion

After controlling for gender, age, and education of parents, there is a significant difference in physical activities and social functioning between adolescents with or without nonstrabismic amblyopia, which highlights the needs for teenagers with nonstrabismic amblyopia to increase physical activities for improving physical health. Teachers and parents should pay more attention to teenagers with nonstrabismic amblyopia to enhance their school functioning.

Data Availability

Data used or generated in this study are available from the corresponding author under reasonable request.

Conflicts of Interest

All authors declare that no conflicts of interest in this study.

References

[1] J. Carlton, J. Karnon, C. Czoski-Murray, K. J. Smith, and J. Marr, "The clinical effectiveness and cost-effectiveness of screening programmes for amblyopia and strabismus in children up to the age of 4-5 years: a systematic review and economic evaluation," *Health Technology Assessment*, vol. 12, no. 25, pp. iii, xi–iii,194, 2008.

[2] E. Kanonidou, "Amblyopia: a mini review of the literature," *International Ophthalmology*, vol. 31, no. 3, pp. 249–256, 2011.

[3] A. L. Webber, "The functional impact of amblyopia," *Clinical & Experimental Optometry*, vol. 101, no. 4, pp. 443–450, 2018.

[4] M. Gupta, S. K. Rana, S. K. Mittal, and R. N. Sinha, "Profile of amblyopia in school going (5-15 years) children at state level referral hospital in Uttarakhand," *Journal of Clinical and Diagnostic Research*, vol. 10, no. 11, 2016.

[5] S. Ganekal, V. Jhanji, Y. Liang, and S. Dorairaj, "Prevalence and etiology of amblyopia in southern India: results from screening of school children aged 5-15 years," *Ophthalmic Epidemiology*, vol. 20, no. 4, pp. 228–231, 2013.

[6] S. R. Hatt, D. A. Leske, W. E. Adams, P. A. Kirgis, E. A. Bradley, and J. M. Holmes, "Quality of life in intermittent exotropia: child and parent concerns," *Archives of Ophthalmology*, vol. 126, no. 11, pp. 1525–1529, 2008.

[7] S. R. Hatt, D. A. Leske, P. A. Kirgis, E. A. Bradley, and J. M. Holmes, "The effects of strabismus on quality of life in adults," *American Journal of Ophthalmology*, vol. 144, no. 5, pp. 643–647, 2007.

[8] J. Carlton, "Identifying potential themes for the child amblyopia treatment questionnaire," *Optometry and Vision Science*, vol. 90, no. 8, pp. 867–873, 2013.

[9] K. Koklanis, L. A. Abel, and R. Aroni, "Psychosocial impact of amblyopia and its treatment: a multidisciplinary study," *Clinical & Experimental Ophthalmology*, vol. 34, no. 8, pp. 743–750, 2006.

[10] E. E. Birch, "Amblyopia and binocular vision," *Progress in Retinal and Eye Research*, vol. 33, pp. 67–84, 2013.

[11] M. Solans, S. Pane, M. D. Estrada et al., "Health-related quality of life measurement in children and adolescents: a systematic review of generic and disease-specific instruments," *Value in Health*, vol. 11, no. 4, pp. 742–764, 2008.

[12] Group, WH, "Development of the WHOQOL: rationale and current status," *International Journal of Mental Health*, vol. 23, no. 3, pp. 24–56, 1994.

[13] E. Petracci and G. Cavrini, "The effect of weight status, lifestyle, and body image perception on health-related quality of life in children: a quantile approach," *Quality of Life Research*, vol. 22, no. 9, pp. 2607–2615, 2013.

[14] L. Zhang, P. J. Fos, W. D. Johnson et al., "Body mass index and health related quality of life in elementary school children: a pilot study," *Health and Quality of Life Outcomes*, vol. 6, no. 1, p. 77, 2008.

[15] J. Carlton and E. Kaltenthaler, "Amblyopia and quality of life: a systematic review," *Eye (London, England)*, vol. 25, no. 4, pp. 403–413, 2011.

[16] V. Tailor, M. Bossi, J. A. Greenwood, and A. Dahlmann-Noor, "Childhood amblyopia: current management and new trends," *British Medical Bulletin*, vol. 119, no. 1, pp. 75–86, 2016.

[17] S. E. Kumaran, A. Rakshit, J. R. Hussaindeen, J. Khadka, and K. Pesudovs, "Does non-strabismic amblyopia affect the quality of life of adults? Findings from a qualitative study," *Ophthalmic & Physiological Optics*, vol. 41, no. 5, pp. 996–1006, 2021.

[18] M. M. Kates and C. J. Beal, "Amblyopia," *Jama*, vol. 325, no. 4, p. 408, 2021.

[19] K. B. Gunton, B. N. Wasserman, and C. DeBenedictis, "Strabismus," *Primary care*, vol. 42, no. 3, pp. 393–407, 2015.

[20] J. W. Varni, M. Seid, and C. A. Rode, "The PedsQL: measurement model for the pediatric quality of life inventory," *Medical Care*, vol. 37, no. 2, pp. 126–139, 1999.

[21] S. A. Khairy, S. R. Eid, L. M. el Hadidy, O. H. Gebril, and A. S. Megawer, "The health-related quality of life in normal and obese children," *Egyptian Pediatric Association Gazette*, vol. 64, no. 2, pp. 53–60, 2016.

[22] M. E. Collins, "Body figure perceptions and preferences among preadolescent children," *International Journal of Eating Disorders*, vol. 10, no. 2, pp. 199–208, 1991.

[23] T. J. Cole, K. M. Flegal, D. Nicholls, and A. A. Jackson, "Body mass index cut offs to define thinness in children and adolescents: international survey," *BMJ*, vol. 335, no. 7612, p. 194, 2007.

[24] M. Ashwell and S. D. Hsieh, "Six reasons why the waist-to-height ratio is a rapid and effective global indicator for health risks of obesity and how its use could simplify the international public health message on obesity," *International Journal of Food Sciences and Nutrition*, vol. 56, no. 5, pp. 303–307, 2005.

[25] H. D. McCarthy and M. Ashwell, "A study of central fatness using waist-to-height ratios in UK children and adolescents over two decades supports the simple message – 'keep your waist circumference to less than half your height'," *International Journal of Obesity*, vol. 30, no. 6, pp. 988–992, 2006.

[26] J. H. Migueles, C. Cadenas-Sanchez, U. Ekelund et al., "Accelerometer data collection and processing criteria to assess physical activity and other outcomes: a systematic review and practical considerations," *Sports Medicine*, vol. 47, no. 9, pp. 1821–1845, 2017.

[27] K. R. Evenson, D. J. Catellier, K. Gill, K. S. Ondrak, and R. G. McMurray, "Calibration of two objective measures of physical activity for children," *Journal of Sports Sciences*, vol. 26, no. 14, pp. 1557–1565, 2008.

[28] F. C. Bull, S. S. al-Ansari, S. Biddle et al., "World Health Organization 2020 guidelines on physical activity and sedentary behaviour," *British Journal of Sports Medicine*, vol. 54, no. 24, pp. 1451–1462, 2020.

[29] L. M. Tong, "Unifying concepts in mechanism of amblyopia," *Medical Hypotheses*, vol. 48, no. 2, pp. 97–102, 1997.

[30] A. N. Buffenn, "The impact of strabismus on psychosocial heath and quality of life: a systematic review," *Survey of Ophthalmology*, vol. 66, no. 6, pp. 1051–1064, 2021.

[31] K. B. Gunton, "Impact of strabismus surgery on health-related quality of life in adults," *Current Opinion in Ophthalmology*, vol. 25, no. 5, pp. 406–410, 2014.

Hindawi
Computational and Mathematical Methods in Medicine
Volume 2023, Article ID 9831697, 1 page
https://doi.org/10.1155/2023/9831697

Retraction

Retracted: MicroRNA-1306-5p Regulates the METTL14-Guided m6A Methylation to Repress Acute Myeloid Leukemia

Computational and Mathematical Methods in Medicine

Received 12 December 2023; Accepted 12 December 2023; Published 13 December 2023

This article has been retracted by Hindawi, as publisher, following an investigation undertaken by the publisher [1]. This investigation has uncovered evidence of systematic manipulation of the publication and peer-review process. We cannot, therefore, vouch for the reliability or integrity of this article.

Please note that this notice is intended solely to alert readers that the peer-review process of this article has been compromised.

Wiley and Hindawi regret that the usual quality checks did not identify these issues before publication and have since put additional measures in place to safeguard research integrity.

We wish to credit our Research Integrity and Research Publishing teams and anonymous and named external researchers and research integrity experts for contributing to this investigation.

The corresponding author, as the representative of all authors, has been given the opportunity to register their agreement or disagreement to this retraction. We have kept a record of any response received.

References

[1] J. Li, Y. Wu, M. Wang et al., "MicroRNA-1306-5p Regulates the METTL14-Guided m6A Methylation to Repress Acute Myeloid Leukemia," *Computational and Mathematical Methods in Medicine*, vol. 2022, Article ID 5787808, 12 pages, 2022.

Hindawi
Computational and Mathematical Methods in Medicine
Volume 2022, Article ID 5787808, 12 pages
https://doi.org/10.1155/2022/5787808

Research Article

MicroRNA-1306-5p Regulates the METTL14-Guided m6A Methylation to Repress Acute Myeloid Leukemia

Jiajia Li,[1] **Yanping Wu**,[1] **Meng Wang**,[1] **Xiaofeng Chen**,[1] **Zhongyu Li**,[1] **Xue Bai**,[1] **and Haotian Wu**[2]

[1]*Department of Hematology, The First Affiliated Hospital of Bengbu Medical College, Bengbu, Anhui, China*
[2]*Bengbu Medical College, Bengbu, Anhui, China*

Correspondence should be addressed to Jiajia Li; 13955207283@163.com

Received 10 August 2022; Revised 19 August 2022; Accepted 22 August 2022; Published 7 September 2022

Academic Editor: Min Tang

miRNA and m6A methylation are two key regulators in cancers. However, in acute myeloid leukemia (AML), the relationship of miRNA and m6A methylation remains unclear. The present work is aimed at determining the effect of m6A methylation induced by miRNAs on AML and its underlying mechanism. The expression of METTL14 was detected by qRT-PCR and western blot. The growth of HL-60 cells was analyzed by CCK-8, Transwell assay, and flow cytometry. Tumor-bearing mice were established, and Ki-67 staining assay was used to detect the proliferation *in vivo*. Dual luciferase reporter system detected the effect of miR-1306-5p on METTL14 luciferase activity. Dot blot analysis detected m6A methylation. We found that METTL14 was upregulated in AML patients and overexpressed METTL14 promoted AML development. Further analysis indicated that METTL14 was directly targeted by miR-1306-5p and overexpressed miR-1306-5p alleviated AML progression. In addition, m6A methylation level regulated by METTL14 could be affected by miR-1306-5p. In conclusion, we found that suppressed miR-1306-5p enhanced AML progression by elevating m6A methylation level via upregulating METTL14. These findings provided basis for the development of new strategies for treating AML.

1. Introduction

Acute myeloid leukemia (AML) is the most common malignant tumor of the hematopoietic system [1]. It is characterized by the malignant clonal proliferation of highly heterogeneous hematopoietic stem cells and precursor cells. It accounts for about 70% of adult acute leukemia [2]. Although with the continuous improvement of clinical and laboratory diagnosis and treatment methods, the prognosis of AML has been significantly improved, but there are still about 70% of patients who cannot survive more than 5 years after diagnosis [3, 4]. Therefore, searching for biomarkers associated to the occurrence, recurrence, and prognosis of AML is of great significance to the treatment for AML patients.

The AML pathogenesis is a multistep process, with disorders in genes and cell growth, resulting in progenitor cells and hematopoietic stem transforming into malignant ones [5]. As the most commonly used modification method in eukaryotic mRNA, N6-methyladenosine (m6A) methylation regulates the protein expressions after transcription with the same base sequence. The biological potentials of m6A modification is regulated by a methyltransferase complex, which consists of RNA methyltransferases ("writers"), demethylases ("erasers"), and m6A-binding proteins ("readers") [6]. m6A methylation is implemented by RBM15, ZC3H13, METTL3, METTL14, and WTAP, along with KIAA1429, while demethylation is carried out by demethylases FTO and ALKBH5. In addition, a specific group of RNA-binding proteins, including YTHDF1/2/3, YTHDC1/2, HNRNPA2B1, and LRPPRC, together with FMR1, can recognize m6A patterns and thus influence m6A function. There are already studies proving that m6A methylation has a huge effect on AML [7]. Feng et al. indicated that YBX1 was essential for the survival of AML cells by regulating BCL2 stability [8]. Pan et al. demonstrated that METTL3 mediated the adipogenesis to promote chemoresistance in AML [9]. In addition, the relationship

between METTL14 and AML is also reported in recent years. Li et al. pointed that METTL14 could promote the progression of AML via combining with long noncoding RNA UCA1 [10]. However, there is few studies focusing on the regulatory mechanism of this effect.

MicroRNA (miRNA) is a new short noncoding RNA molecule. Mainly through the complementary binding of miRNA and its target mRNA to hinder the translation of mRNA or cause the degradation of mRNA. Therefore, miRNAs are considered to be natural regulators of gene expression [11]. Several miRNAs are also found to play crucial roles in AML by regulating various kinds of biological processes, such as miRNA-485-5p, miR-126, and miR-204 [12–14]. In addition, as reported previously, miR-1306-5p is involved in the progression of many diseases, such as amelogenesis imperfecta, cerebral ischemia/reperfusion injury, and sepsis [15–17]. However, the role of miR-1306-5p in AML is obscure. Intriguingly, there are also studies proving that miRNA regulates m6A. Vittori et al. have stated that miR-3189-3p could negatively affect m6A-mediated cap-independent translation [18]. It is also found that METTL3-mediated m6A modification facilitated to upregulate miR-221-3p [19]. Nevertheless, the association of miR-1306-5p and m6A modification remains unclear.

In this research, we aimed to determine the effect of METTL14 on AML and its interactions with miR-1306-5p. We determined that METTL14 serves as the target of miR-1306-5p, suggesting that METTL14 regulated AML by miR-1306-5p.

2. Materials and Methods

2.1. Samples Information. Ten patients diagnosed with AML and 10 healthy volunteers treated from 2019 to 2021 by the First Affiliated Hospital of Bengbu Medical College (Department of Hematology) were selected as study subjects. The samples of peripheral venous blood were taken in postabsorptive state in the morning. The research protocol was signed approval by the Ethics Committee of The First Affiliated Hospital of Bengbu Medical College, and all participants were informed with consents. All subjects were informed with consent and agreed to this study.

2.2. Cell Culture and Transfection. The HL-60 cell line is a promyelocytic cell line derived from human leukemia. The cells are premyelocytes but can be induced *in vitro* to differentiate into different lineages of mature myeloid cells with different reagents [20]. It was selected as a study subject and purchased from Hasenbio (Wuxi, China). The cells were cultured in Dulbecco's modified Eagle's medium (Invitrogen) with fetal bovine serum (10%), penicillin (100 units/ml), and streptomycin (100 μg/ml) at preseted atmosphere (37°C, 5% CO_2). Over-METTL14 plasmid, siRNA of METTL14, miR-1306-5p mimics, and miR-1306-5p inhibitors (2 μg/ml) were designed and synthesized by GenePharma (Shanghai, China) and were transfected into HL-60 cells by using Lipofectamine 2000 according to the instructions (Invitrogen, 11668-027) when at 60-70% confluency. Cells were used for assays afterwards 48 h after transfection. METTL14 siRNA, sense, 5′-GGAUGAGUUAA UAGCUAAAUC-3′; antisense, 5′-UUUAGCUAUUAACU CAUCCUU-; miR-1306-5p mimics sense: 5′-CCACCUCCC CUGCAAACGUCCA-3′; miR-1306-5p mimics antisense: 5′ -UGGACGUUUGCAGGGGAGGUGG-3′; miR-1306-5p inhibitor: 5′-UGGACGUUUGCAGGGGAGGUGG-3′.

2.3. Quantitative Real-Time PCR (qRT-PCR) Assay. qRT-PCR was used to detect the RNA expression of METTL14 and miR-1306-5p. All the RNA was collected from blood, cell, or tissue samples using the miRNeasy extraction kit (QIAGEN). For quantitative analysis, the cDNA was reversed by miRNA Reverse Transcription Kit (MR101-01/02, Vazyme) and detected by all-in-one miRNA RT-qPCR Detection Kit (Q711-02, Vazyme) with U6 as the internal control. As for METTL14 mRNA detection, TRIzol (BS259A, Biosharp) was used for RNA isolation and PrimeScript RT Reagent kit (R223-01, Vazyme) was used to reverse RNA into cDNA. SYBR Green Real-Time PCR Master Mix (Q711-02, Vazyme) was used for RT-PCR assay with β-actin as the control. The primers for miR-1306-5p, U6, METTL14, and β-actin were listed as below: METTL14, sense, 5′- GAGTGTGTTTACGAAAATGGGGT-3′; antisense, 5′- CCGTCTGTGCTACGCTTCA-3′; β-actin: sense, 5′-AGCGAGCATCCCCCAAAGTT-3′, antisense: 5′-GGGCACGAAGGCTCATCATT-3′; U6: sense, 5′-CTCG CTTCGGCAGCACA-3′, antisense: 5′-AACGCTTCACG AATTTGCGT-3′; miR-1306-5p reverse primer: 5′-CTCA ACTGGTGTCGTGGAGTCGGCAATTCAGTTGAGTGG ACGTT-3′; miR-1306-5p sense: 5′-AATACCACCTCCCC TGCA-3′. $2^{-\Delta\Delta Ct}$ method was used for analysis of relative expression.

2.4. Western Blot. The western blot was used to detect protein expression of METTL14. In western blot analysis, RIPA lysis buffer (BL504A, Biosharp) was for protein extractions from cells and tissues. BCA assay (BL521A, Biosharp) was used for detection of protein concentrations. 30 μg protein loaded on SDS-PAGE was transferred to PVDF. Skim milk (5%) was used for blocking. Primary antibodies were added to the membranes for an overnight incubation at 4°C. Secondary antibodies (1/10000, BL003A, Biosharp) were added for 1 h incubation at 37°C. The ECL kit (WBKLS0100, Millipore) was used for detection of immunoreactive bands. The primary antibodies: METTL14 (1/1000, ab252562, Abcam, Cambridge, UK) and β-actin (1/1000, ab8227, Abcam, Cambridge, UK). ImageJ was used to quantify gray scale value of protein bands.

2.5. CCK-8 Assay. The CCK-8 assay was used to detect the proliferation of HL-60 cells affected by METTL14 and miR-1306-5p. Cell Counting Kit-8 (Dojindo, USA) was used in accordance with the instructions. HL-60 cells (2×10^3 cells/well) were seeded in 96-well plates. RPMI1640 Medium (containing 10% FBS) was used for incubation. 10 μl CCK-8 was added into each well 48 h after transfection followed and incubated for 3 h at 37°C. The absorbance was measured using a

Microplate Reader (Molecular Devices SpectraMax i3) at 450 nm.

2.6. Flow Cytometry. Flow cytometry was used to detect the apoptosis of HL-60 cells affected by METTL14 and miR-1306-5p. FACSVerse flow cytometry (BD Biosciences) was used for examination. Briefly, Annexin V-fluorescein isothiocyanate (FITC) Apoptosis Detection kit (HS-SJ069, Hasenbio) was used to detect the apoptosis at 48 h after transfection. Transfected HL-60 cells resuspended in binding buffer (500 μl) were stained with PI (5 μl, 50 μg/ml) and Annexin V-FITC (10 μl). The stain process was in the dark and lasted for 15 min at room temperature. FACSVerse flow cytometry (BD Biosciences) was used for examination.

2.7. Cell Migration and Invasion Assays. Transwell assays was used to detect the migration and invasion of HL-60 cells affected by METTL14 and miR-1306-5p. The images of Transwell assays were captured using a microscope. In migration assay, the upper chamber of Transwell (Corning) was loaded with 2×10^5 HL-60 cells in serum-free medium. The medium with 20% FBS were added to the lower well. The 4% formaldehyde was used for fixing, and crystal violet was added for 10 min staining. The incubation lasted for 24 h. In invasion assay, 40 μg Matrigel was used to coat the Boyden chambers (8 μm inserts) in 24-well plate, and all the procedures after were the same as migration assay.

2.8. Dual-Luciferase Reporter Assay. Dual-Luciferase Reporter Assay was used to detect the regulatory of miR-1306-5p to METTL14. The target miRNA of METTL14 was based on the online software TargetScan (http://www.targetscan.org/vert_72/). It suggested a binding site between METTL14 and miR-1306-5p. The sequence of 3′ UTR of METTL14 containing wild-type and mutant binding sites were subcloned into pmirGLO vector. Lipofectamine 3000 was used to transfect the vectors into HL-60 cells, including miR-1306-5p mimics and miR-NC. Relative luciferase activities were analyzed using Dual-Luciferase Reporter detection System (Promega) at 48 h after transfection.

2.9. Dot Blot Analysis. Dot blot analysis was used to detect the m6A methylation levels affected by METTL14 and miR-1306-5p. Nitrocellulose membranes were collected from denatured and spotted RNA samples under vacuum. After UV cross-linking, the 5% nonfat dry milk was used for 1 h blocking in 0.1% PBST (HS-SJ021, Hasenbio). Rabbit anti-m6A antibody (1 : 500, ab284130, Abcam, Cambridge, UK) was added to the membranes at 4°C overnight. After being washed, the blot was mixed with goat anti-rabbit IgG (H+L) (1 : 500, ab7090, Abcam, Cambridge, UK for 1 h incubation at 25°C. The imaging system (Roche LightCycler® 480II) was used for scanning.

2.10. Tumor Xenograft in Nude Mice. Tumor xenograft in nude mice was established for *in vivo* assays. Nude BALB/c Mice (4–6 weeks) was purchased from Comparative Medicine Center of Yangzhou University. The animal laboratory (pathogen-free) was presented for transfer stay. The mice were divided into 4 group ($N = 5$) at random. HL-60 cells were injected into the mice (neck and back) at 0.1 ml suspension (1×10^6): Tumor volume $(\text{mm}^3) = \text{length} \times \text{width}^{2/}2$ [21]. After 2 weeks, the mice were sacrificed by an overdose of pentobarbital sodium (100 mg/kg). The whole experimental process complied with the Guide for the Care and Use of Laboratory Animals published by the US National Institutes of Health. All procedures about animal treatment have approval by the Ethics Committee of Laboratory Animal Use of The First Affiliated Hospital of Bengbu Medical College.

2.11. Ki-67 Staining Assay. Ki-67 staining assay was used to detect the proliferation affected by miR-1306-5p *in vivo*. It was performed on tumor tissue as a measurement of in situ proliferation. The 4% paraformaldehyde was used for fixing. The 0.1% sodium citrate and 0.1% Triton X were used for permeabilization. The tissues were then sliced into 4 μm sections. The 3% bovine serum albumin/5% goat serum was used for preincubation in PBS for 1 h. Primary antibodies anti-Ki67 (1 : 100, ab15580, Abcam, Cambridge, UK) were added for 1 h. Peroxidase-labelled polymer-conjugated secondary antibodies (1 : 1000, ab214880, Abcam, Cambridge, UK) were added for a 45 min incubation. DAKO Liquid DAB Substrate-Chromogen System was used for 5 min incubation with 3, 3′-diaminobenzidine DAB (DAKO, France). Hematoxylin was used for counterstaining. Then, the sections were dehydrated and coverslipped. The slices were incubated for 1 min by adding 150 μl hematoxylin at a dark room. And then, the slices were washed back to blue and dehydrated and sealed with neutral resin. Images were taken using immunofluorescence microscope (Leica, IX71).

2.12. Statistical Analysis. All experiments in this study should be performed three times. GraphPad Prism 5.0 was used for analysis with data expressed as mean ± standard deviation (SD). The statistical significance between two or more groups were analyzed using student's t-test or one-way analysis of variance (ANOVA) followed by Tukey's test. $P < 0.05$ was considered statistically significant.

3. Results

3.1. METTL14 Was Upregulated in Patients with AML. It was suggested that METTL14 expression was remarkably upregulated in AML patients compared with the NC group (Figures 1(a) and 1(b)), indicating that METTL14 may be involved in AML progression.

3.2. Overexpression METTL14 Promoted AML Development. In order to confirm the effect of METTL14 on AML, the loss and gain function assays of METTL14 on AML were performed *in vitro* and *in vivo*. *In vitro*, we found that overexpressed METTL14 could promote HL-60 cell proliferation, invasion, and migration and inhibit the apoptosis compared with NC group. Meanwhile, suppressed METTL14 showed opposite results in HL-60 cells (Figures 2(a)–2(d)). *In vivo*

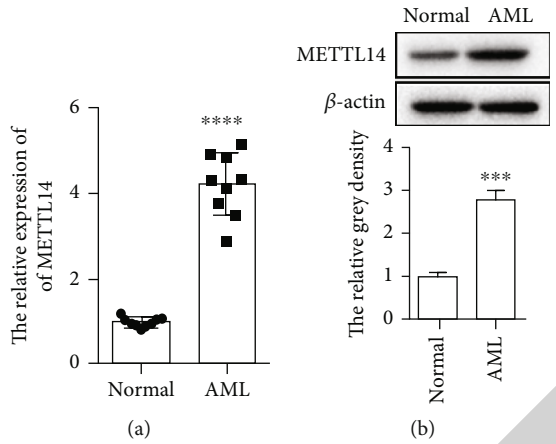

Figure 1: METTL14 was upregulated in patients with AML. (a) qRT-PCR was used to detect the expression of METTL14 in the patients of AML. (b) Western blot analysis was used to detect the expression of METTL14 in the patients of AML at protein level with β-actin as the control. Data are presented as mean ± SD. $^{***}P < 0.005$, $^{****}P < 0.001$.

analysis indicated that the tumor volume and weight were significantly increased with overexpressed METTL14 and greatly decreased with suppressed METTL14, compared with NC group after 28 days of tumor-bearing (Figures 2(e) and 2(f)). Ki-67 staining analysis showed overexpressed METTL14 significantly promoted proliferation while suppressed METTL14 showed the opposite effect (Figure 2(g)). These results demonstrated that the overexpression of METTL14 promoted AML development.

3.3. miR-1306-5p Directly Targeted METTL14. Increasing numbers of genes have been proved to participate in various miRNA-regulated processes. In the present study, TargetScan (https://www.targetscan.org/vert_80/) was used to predict the miRNAs which could bind with METTL14. The result showed that there was a binding site of miR-1306-5p and 3′ UTR of METTL14 (Figure 3(a)). Dual luciferase report system assay indicated that the relative luciferase activity was significantly decreased in the METTL14 WT group with miR-1306-5p overexpression compared with the NC group. However, the luciferase activity was not changed in the METTL14 Mut group after miR-1306-5p overexpression compared with the NC group. (Figure 3(b)). The results showed that compared with the NC group, the expression of miR-1306-5p was reduced in AML patients (Figure 3(c)). The expression of METTL3 was decreased by miR-1306-5p mimics and increased by miR-1306-5p inhibitors (Figures 3(d) and 3(e)). These results were also confirmed by qRT-PCR *in vivo* (Figure 3(f)). These results suggested that METTL14 was directly targeted by miR-1306-5p.

3.4. Overexpression miR-1306-5p Alleviated AML Development. The function of miR-1306-5p in AML development was also detected *in vitro* and *in vivo*. The results showed that miR-1306-5p mimics could inhibit HL-60 cell proliferation, invasion, and migration while promoting the apoptosis of HL-60 compared with the NC group *in vitro*. Meanwhile, miR-1306-5p inhibitors showed the opposite results (Figures 4(a)–4(d)). Further analysis *in vivo* indicated that the tumor volume and weight were significantly decreased with miR-1306-5p mimics and increased with miR-1306-5p inhibitors when compared with the NC group at 28 days after tumor-bearing (Figures 4(e) and 4(f)). Ki-67 staining analysis showed miR-1306-5p increase significantly suppressed proliferation while miR-1306-5p inhibition showed the opposite effect (Figure 4(g)). These results demonstrated that miR-1306-5p alleviated AML development.

3.5. m6A Methylation Level Was Affected by miR-1306-5p. In order to know whether the effect of miR-1306-5p on AML development was related to m6A methylation changes, detection of m6A methylation levels was performed with METTL14 and miR-1306-5p separately controlled as single variable. As shown in Figure 5(a), the m6A methylation level was significantly elevated with overexpressed METTL14 and decreased with suppressed METTL14 both *in vitro* and *in vivo*. While with miR-1306-5p as single variable, further analysis showed the opposite changes in m6A methylation level (Figure 5(b)). In addition, rescue experiment revealed that the elevated (decreased) m6A methylation level caused by overexpressed (suppressed) METTL14 could be partially reversed by miR-1306-5p mimics (inhibitors) (Figure 5(c)). These results demonstrated that the METTL14-regulated m6A methylation level could be affected by miR-1306-5p.

4. Discussion

AML is an aberrant clonal malignancy of immature myeloid hematopoietic cells in the bone marrow [22, 23]. The etiology and pathogenesis of AML have not been fully elucidated, leaving much to be explored in clinical treatment, drug selection and prognostic judgment. In the present study, we demonstrated that suppression of miR-1306-5p promoted AML by regulating METTL14-guided m6A methylation.

N6-Methyladenosine (m6A) methylation modification is the most commonly used modification method in eukaryotic mRNA. It regulates mRNA, lncRNA, and miRNA under the reversible coregulation of related enzymes [24, 25] and

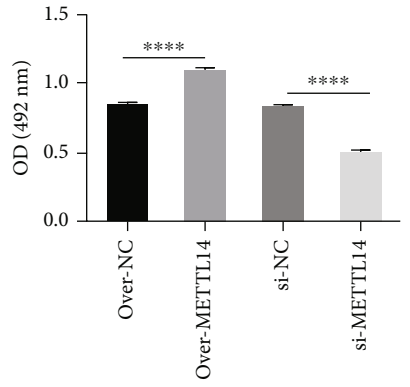

(a)

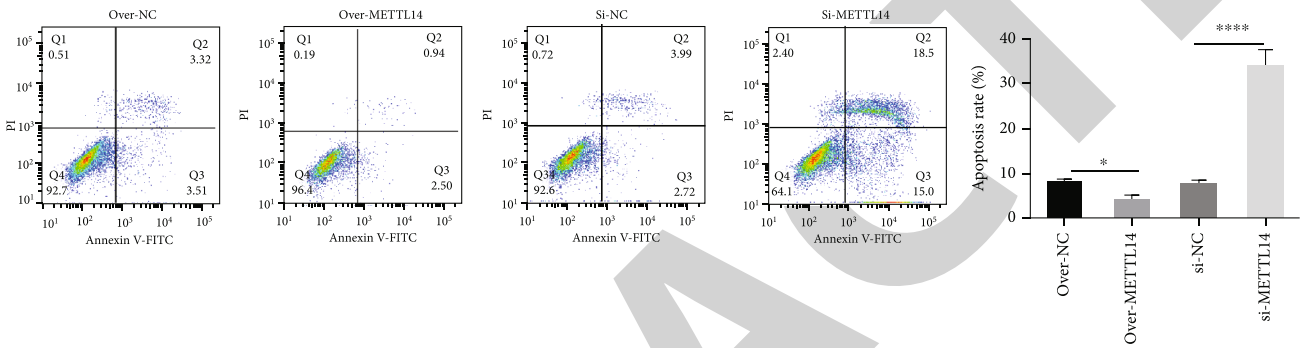

(b)

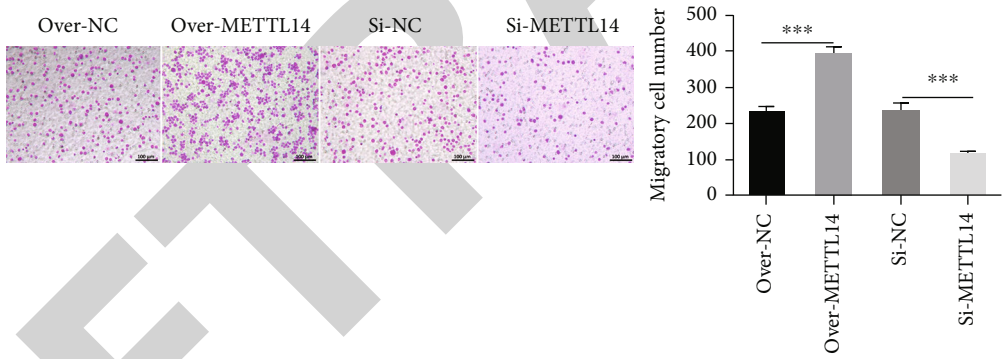

(c)

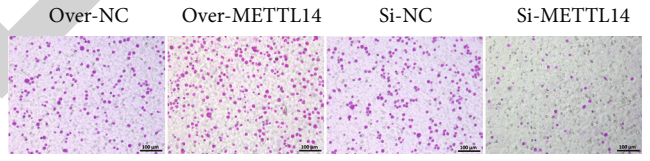

(d)

Figure 2: Continued.

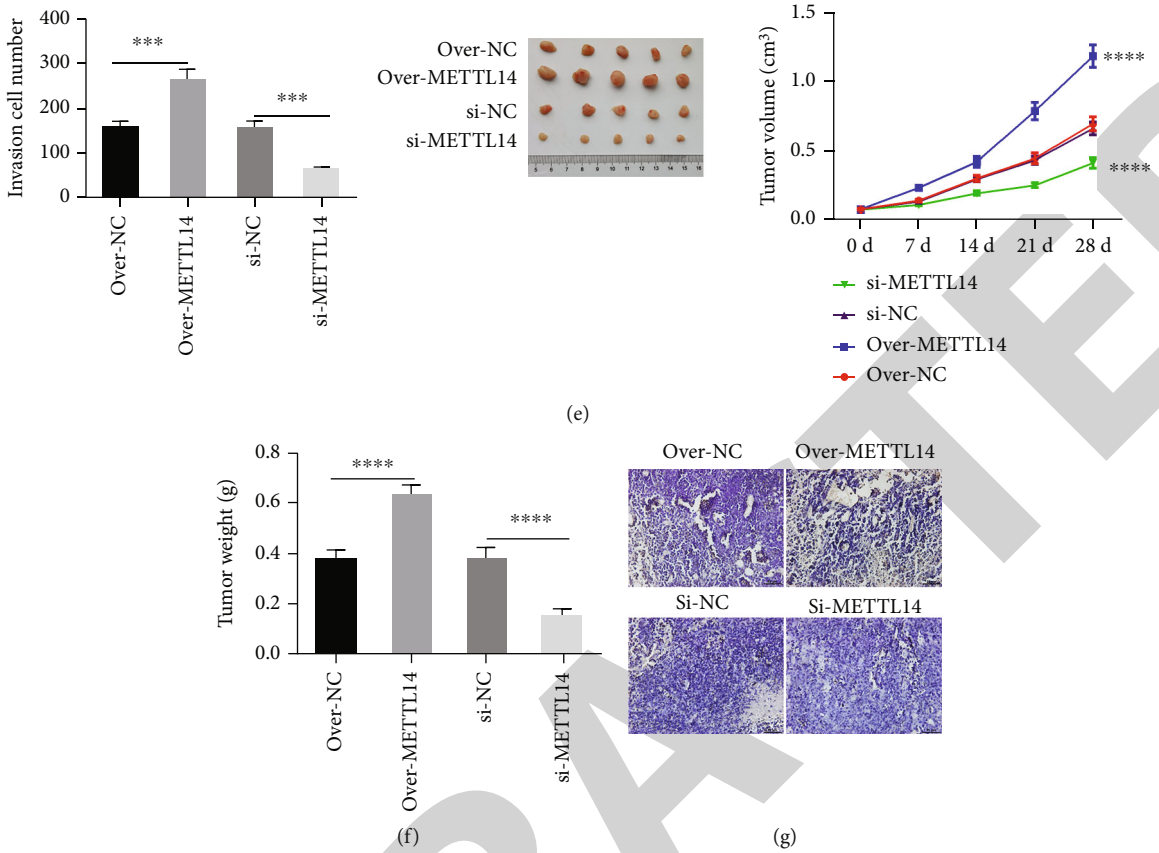

Figure 2: Overexpression METTL14 promote AML development. (a) CCK-8 was used to detect the proliferation of HL-60 cells affected by METTL14. (b) Flow cytometry was used to detect the apoptosis of HL-60 cells affected by METTL14. (c, d) Transwell assay was used to detect the migration and invasion of HL-60 cells affected by METTL14, bar = 100 μm. (e, f) Tumor volume and weight was detected in the tumor-bearing mice at 0, 7, 14, 21, and 28 days after tumor-bearing with HL-60 cells. (g) Proliferation was detected in vivo by Ki-67 staining assay affected by METTL14, *bar* = 25 μm. Data are presented as mean ± SD. $^{*}P < 0.05$, $^{***}P < 0.005$, and $^{****}P < 0.001$.

accounts for the metabolic process of abundant mRNAs, including methyltransferase-like protein 3 (METTL3), methyltransferase-like protein 14 (METTL14), and wilms tumor 1-associated protein (WTAP) [26]. Increasing numbers of evidence also demonstrated that m6A methylation has important value in the development and prognosis of AML [27]. Weng et al. revealed that METTL14 promotes leukemogenesis and inhibited hematopoietic stem/progenitor differentiation through mRNA m6A modification [28]. There was also reports stating that METTL14 gene polymorphisms influence the risk of leukemia in southern Chinese children and might be potential biomarkers for pediatric leukemia chemotherapeutics [29]. However, there are few reports specially analyzing the specific regulatory effect of METTL14 on m6A methylation. *In vivo* assay was also neglected in the previous works. Consistent with previous report, we found that METTL14 was upregulated in patients with AML and overexpressed METTL14 could promote HL-60 cell proliferation, invasion and migration and inhibit the apoptosis in vitro. At the same time, overexpressed METTL14 promoted cell growth in vivo. We found that m6A methylation level was increased with overexpressed METTL14 and decreased with suppressed METTL14 both *in vitro* and *in vivo*. These results indicated that overexpressed METTL14 promote AML development by elevating m6A methylation level.

miRNA is a series of small noncoding RNAs that regulate gene expression at the posttranscriptional or translational level [30, 31]. It plays an important role in various biological processes such as cell differentiation, proliferation, and apoptosis. More and more evidence show that miRNAs serve as key regulators of AML [11, 31]. miR-1306-5p was found to decrease cerebral ischemia/reperfusion injury *in vitro* by targeting BIK [16]. It was also confirmed to regulate ameloblast differentiation by regulating genes related to amelogenesis imperfecta [15] and inhibit the malignant behavior of osteosarcoma cells [32]. However, the specific biological roles of miR-1306-5p and its indirect interactions and regulation of m6A in AML remain poorly understood. As is well known, miRNA is capable of regulating physiological and pathological processes via binding to the 3′ UTR of target mRNA translation to inhibit mRNA expression. Accordantly, a previous report demonstrated that miR-1306-5p exerted functions in the development of melanoma via targeting PCGF2 [33]. Similarly, in our work, we found that METTL14 was directly targeted by miR-1306-5p from

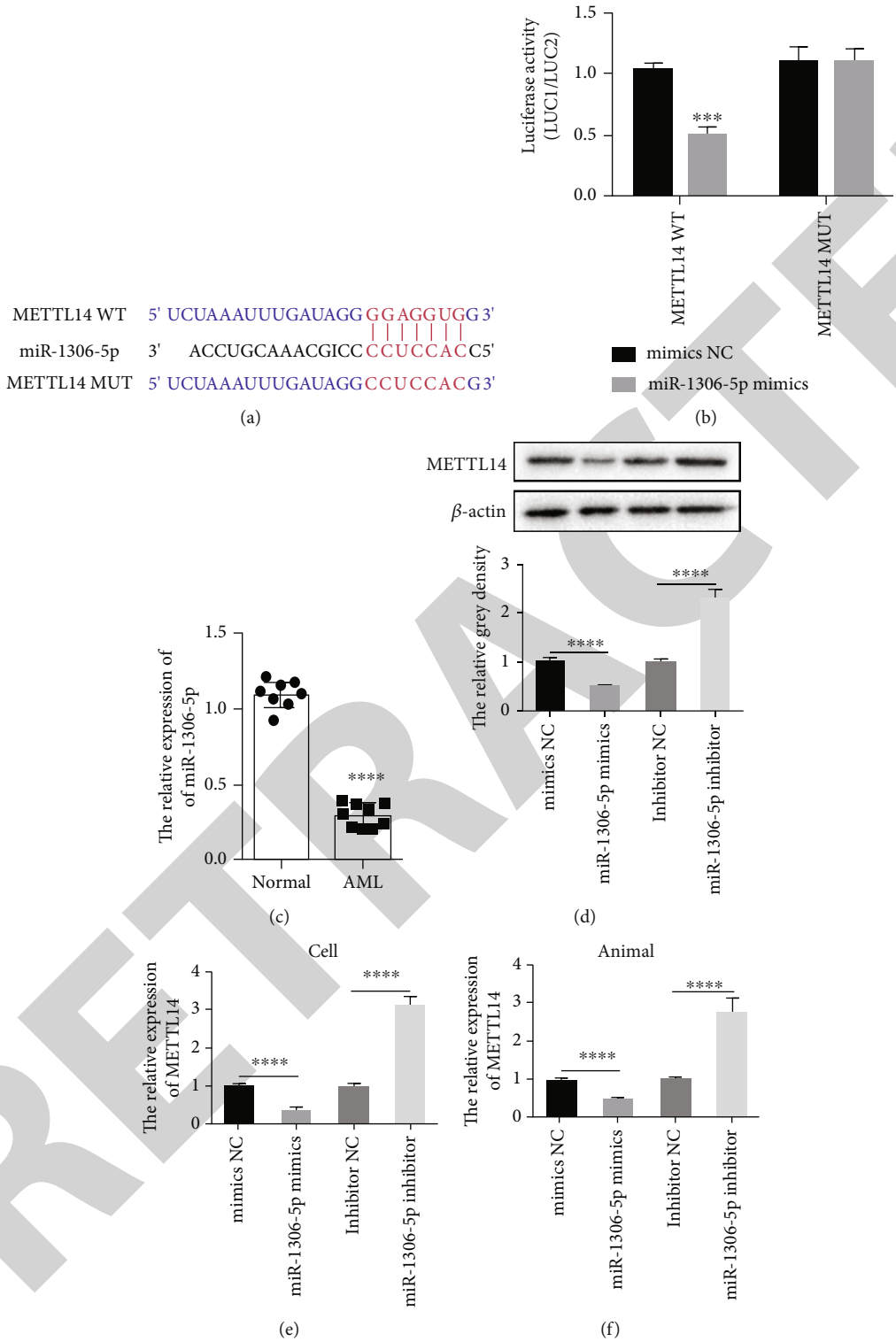

FIGURE 3: METTL14 is a direct target of miR-1306-5p. (a) The binding site of miR-1306-5p to METTL14 was predicted by TargetScan. (b) Dual luciferase report system assay was used to detect the regulatory of miR-1306-5p to METTL14. (c) The expression of miR-1306-5p in the AML patients was detected by qRT-PCR, U6 acts as an internal control. (d, e) qRT-PCR and western blot analysis were used to detect the expression of METTL3 affected by miR-1306-5p in vitro. (f) qRT-PCR analysis was used to detect the expression of METTL3 affected by miR-1306-5p *in vivo* with β-actin as the control. Data are presented as mean ± SD. $^{***}P < 0.005$, $^{****}P < 0.001$.

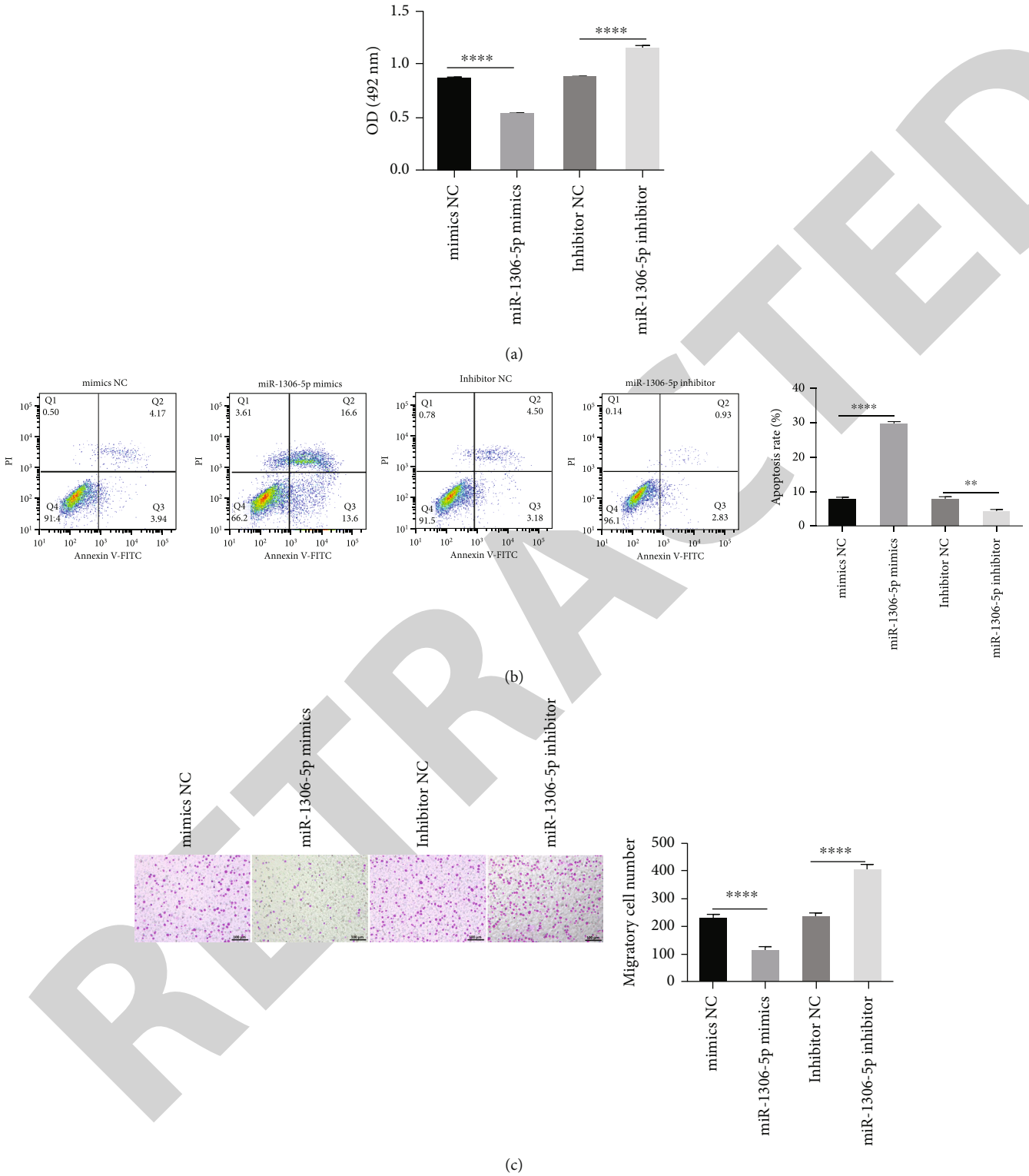

Figure 4: Continued.

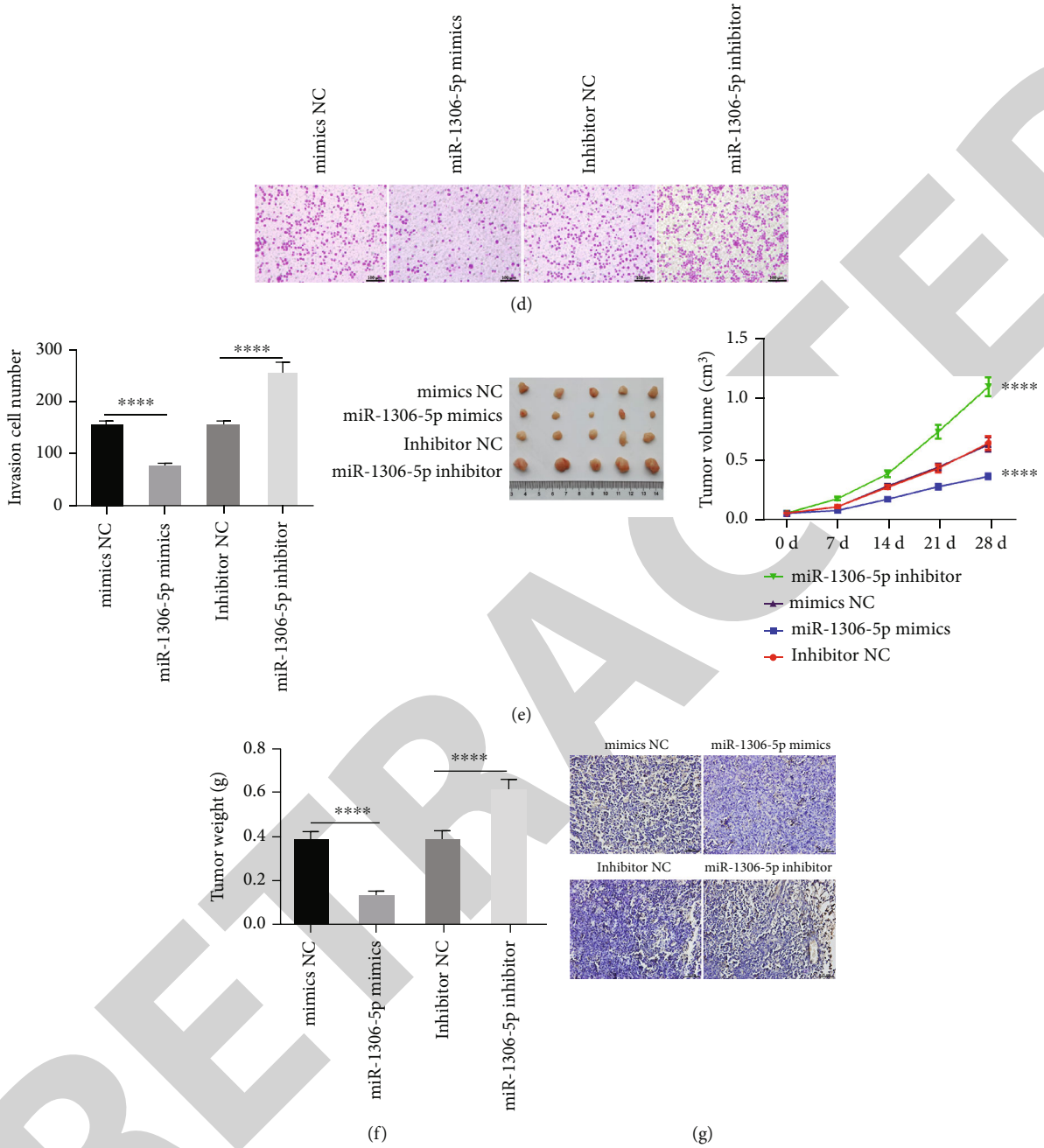

Figure 4: Overexpression miR-1306-5p alleviated AML development. (a) CCK-8 was used to detect the proliferation of HL-60 cells affected by miR-1306-5p. (b) Flow cytometry was used to detect the apoptosis of HL-60 cells affected by miR-1306-5p. (c, d) Transwell assay was used to detect the migration and invasion of HL-60 cells affected by miR-1306-5p, bar = 100 μm. (e, f) Tumor volume and weight was detected in the tumor-bearing mice at 0, 7, 14, 21, and 28 days after tumor-bearing with HL-60 cells, respectively. (f) Proliferation affected by miR-1306-5p *in vivo* was detected by Ki-67 staining assay, bar = 25 μm. Data are presented as mean ± SD. $^{*}P < 0.05$, $^{***}P < 0.005$, and $^{****}P < 0.001$.

bioinformatics prediction and luciferase reporter assays. Further analysis indicated that miR-1306-5p was lowly expressed in AML patients, and overexpression miR-1306-5p alleviated AML development via inhibiting HL-60 cell proliferation, invasion, and migration and promoting the apoptosis in vitro. At the same time, overexpressed miR-1306-5p suppressed cell growth in vivo. Consistent with our finding, miR-1306-5p also plays a protective role against Alzheimer's disease [34]. In addition, a former literature displayed that a certain miRNA regulated METTL14 to hinder osteoblastic bone formation via m6A methylation [35]. In line with the above literature, it was also found that the elevated (decreased) m6A methylation level caused by overexpressed (suppressed) METTL14 could be partially reversed by miR-

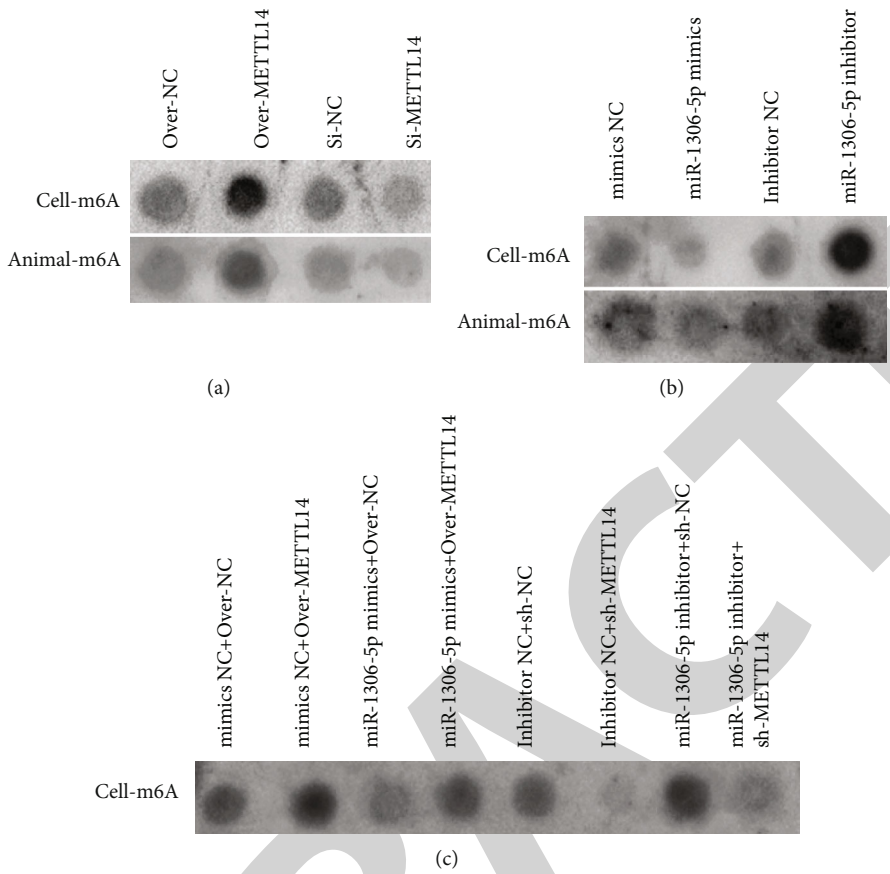

Figure 5: m6A methylation level was affected by miR-1306-5p. (a) Dot blot analysis was used to detect the m6A methylation levels affected by METTL14. (b) Dot blot analysis was used to detect the m6A methylation levels affected by miR-1306-5p. (c) Rescue experiment was used to detect m6A methylation level changes caused by miR-1306-5p-regulated METTL14.

1306-5p mimics (inhibitors). These results demonstrated that m6A methylation level regulated by METTL14 could be affected by miR-1306-5p. Taken together, we demonstrated that downregulation of miR-1306-5p promoted AML development via elevating METTL14-mediated m6A methylation level.

Nevertheless, more investigation on clinical level and more intensive molecular mechanisms are also needed to strengthen these findings. How METTL14 affect m6A molecularly in AML cell lines and whether there are more miRNAs or lncRNAs involved in the regulatory process remain unknown. Meanwhile, the number of samples drawn from patients needs to be enlarged to confirm these findings.

In summary, we found that METTL14 was upregulated in AML patients and overexpressed METTL14 promoted AML development. Further analysis indicated that downregulation of miR-1306-5p promoted AML development by elevating m6A methylation level via upregulating METTL14.

Data Availability

Data are available from the corresponding author under reasonable requirements.

Ethical Approval

All procedures performed in studies involving human participants were in accordance with the ethical standards of the First Affiliated Hospital of Bengbu Medical College and with the 1964 Helsinki declaration and its later amendments or comparable ethical standards. All animal experiments were approved by the First Affiliated Hospital of Bengbu Medical College.

Consent

Informed consent was obtained from all individual participants included in the study.

Conflicts of Interest

The authors declare that they have no conflicts of interest.

Acknowledgments

The study was supported by the 512 Talent Cultivation Program of Bengbu Medical College (by51202308), Bengbu Medical College Translational Medicine Key Project

(BYTM2019034), Anhui Natural Science Foundation Youth Project (2108085QH324), Outstanding young backbone talents in colleges and universities abroad visiting study and training project (gxgwfx2021030), Bengbu Medical College Graduate Research and Innovation Project (Byycxz21068), and National University Student Innovation and Entrepreneurship Project (202110367066).

References

[1] A. Kirtonia, G. Pandya, G. Sethi, A. K. Pandey, B. C. das, and M. Garg, "A comprehensive review of genetic alterations and molecular targeted therapies for the implementation of personalized medicine in acute myeloid leukemia," *Journal of Molecular Medicine (Berlin, Germany)*, vol. 98, no. 8, pp. 1069–1091, 2020.

[2] M. S. Infante, M. A. Piris, and J. A. Hernandez-Rivas, "Molecular alterations in acute myeloid leukemia and their clinical and therapeutical implications," *Medicina Clínica (Barcelona)*, vol. 151, no. 9, pp. 362–367, 2018.

[3] E. H. Estey, "Acute myeloid leukemia: 2019 update on risk-stratification and management," *American Journal of Hematology*, vol. 93, no. 10, pp. 1267–1291, 2018.

[4] M. Medinger, D. Heim, J. P. Halter, C. Lengerke, and J. R. Passweg, "Diagnosis and therapy of acute myeloid leukemia," *Therapeutische Umschau. Revue Therapeutique*, vol. 76, no. 9, pp. 481–486, 2019.

[5] S. Kayser and M. J. Levis, "Clinical implications of molecular markers in acute myeloid leukemia," *European Journal of Haematology*, vol. 102, no. 1, pp. 20–35, 2019.

[6] Q. Lan, P. Y. Liu, J. Haase, J. L. Bell, S. Hüttelmaier, and T. Liu, "The critical role of RNA m6A methylation in cancer," *Cancer Research*, vol. 79, no. 7, pp. 1285–1292, 2019.

[7] E. Yankova, D. Aspris, and K. Tzelepis, "The N6-methyladenosine RNA modification in acute myeloid leukemia," *Current Opinion in Hematology*, vol. 28, no. 2, pp. 80–85, 2021.

[8] M. Feng, X. Xie, G. Han et al., "YBX1 is required for maintaining myeloid leukemia cell survival by regulating BCL2 stability in an m6A-dependent manner," *Blood*, vol. 138, no. 1, pp. 71–85, 2021.

[9] Z. P. Pan, B. Wang, D. Y. Hou et al., "METTL3 mediates bone marrow mesenchymal stem cell adipogenesis to promote chemoresistance in acute myeloid leukaemia," *FEBS Open Bio*, vol. 11, no. 6, pp. 1659–1672, 2021.

[10] J. Li, Z. Li, X. Bai et al., "LncRNA UCA1 promotes the progression of AML by upregulating the expression of CXCR4 and CYP1B1 by affecting the stability of METTL14," *Journal of Oncology*, vol. 2022, Article ID 2756986, 13 pages, 2022.

[11] J. A. Wallace and R. M. O'Connell, "MicroRNAs and acute myeloid leukemia: therapeutic implications and emerging concepts," *Blood*, vol. 130, no. 11, pp. 1290–1301, 2017.

[12] W. Wang, H. R. Wang, W. G. Ji, S. L. Guo, and H. X. Li, "MiRNA-485-5p suppresses the proliferation of acute myeloid leukemia via targeting SALL4," *European Review for Medical and Pharmacological Sciences*, vol. 23, no. 11, pp. 4842–4849, 2019.

[13] E. R. Lechman, B. Gentner, S. W. K. Ng et al., "miR-126 regulates distinct self-renewal outcomes in normal and malignant hematopoietic stem cells," *Cancer Cell*, vol. 29, no. 4, pp. 602–606, 2016.

[14] A. S. Abdelhafiz, G. M. Elsayed, M. M. Saber, A. Gameel, and N. Hamdy, "Low expression of miR-204 is associated with expression of CD34 and poor performance status in denovo AML," *International Journal of Laboratory Hematology*, vol. 42, no. 3, pp. 263–269, 2020.

[15] H. Yoshioka, Y. Y. Wang, A. Suzuki et al., "Overexpression of miR-1306-5p, miR-3195, and miR-3914 inhibits ameloblast differentiation through suppression of genes associated with human amelogenesis imperfecta," *International Journal of Molecular Sciences*, vol. 22, no. 4, p. 2202, 2021.

[16] X. Chen, C. Li, J. Li, L. Sheng, and X. Liu, "Upregulation of miR-1306-5p decreases cerebral ischemia/reperfusion injury in vitro by targeting BIK," *Bioscience, Biotechnology, and Biochemistry*, vol. 83, no. 12, pp. 2230–2237, 2019.

[17] Z. Wang, C. Zhong, Y. Cao et al., "LncRNA DANCR improves the dysfunction of the intestinal barrier and alleviates epithelial injury by targeting the miR-1306-5p/PLK1 axis in sepsis," *Cell Biology International*, vol. 45, no. 9, pp. 1935–1944, 2021.

[18] C. Vittori, D. Jeansonne, H. Yousefi et al., "Mechanisms of miR-3189-3p-mediated inhibition of c-MYC translation in triple negative breast cancer," *Cancer Cell International*, vol. 22, no. 1, p. 204, 2022.

[19] J. Niu, B. Wang, T. Wang, and T. Zhou, "Mechanism of METTL3-mediated m6A modification in depression-induced cognitive deficits," *American Journal of Medical Genetics. Part B, Neuropsychiatric Genetics*, vol. 189, no. 3-4, pp. 86–99, 2022.

[20] J. Sai, M. Rogers, K. Hockemeyer, J. P. Wikswo, and A. Richmond, "Chapter two - study of chemotaxis and cell–cell interactions in cancer with microfluidic devices," in *Methods in Enzymology,*, T. M. Handel, Ed., pp. 19–45, Academic Press, 2016.

[21] M. Huang, Y. Huang, J. Guo et al., "Pyrido[2, 3-d]pyrimidin-7(8H)-ones as new selective orally bioavailable threonine tyrosine kinase (TTK) inhibitors," *European Journal of Medicinal Chemistry*, vol. 211, article 113023, 2021.

[22] M. Chopra and S. K. Bohlander, "The cell of origin and the leukemia stem cell in acute myeloid leukemia," *Genes, Chromosomes & Cancer*, vol. 58, no. 12, pp. 850–858, 2019.

[23] S. A. Sami, N. H. E. Darwish, A. N. M. Barile, and S. A. Mousa, "Current and future molecular targets for acute myeloid leukemia therapy," *Current Treatment Options in Oncology*, vol. 21, no. 1, p. 3, 2020.

[24] T. Wang, S. Kong, M. Tao, and S. Ju, "The potential role of RNA N6-methyladenosine in cancer progression," *Molecular Cancer*, vol. 19, no. 1, p. 88, 2020.

[25] S. Ma, C. Chen, X. Ji et al., "The interplay between m6A RNA methylation and noncoding RNA in cancer," *Journal of Hematology & Oncology*, vol. 12, no. 1, p. 121, 2019.

[26] S. Zaccara, R. J. Ries, and S. R. Jaffrey, "Reading, writing and erasing mRNA methylation," *Nature Reviews. Molecular Cell Biology*, vol. 20, no. 10, pp. 608–624, 2019.

[27] Z. Ianniello, A. Paiardini, and A. Fatica, "N6-Methyladenosine (m6A): a promising new molecular target in acute myeloid leukemia," *Frontiers in Oncology*, vol. 9, p. 251, 2019.

[28] H. Weng, H. Huang, H. Wu et al., "METTL14 inhibits hematopoietic stem/progenitor differentiation and promotes leukemogenesis via mRNA m^6A modification," *Cell Stem Cell*, vol. 22, no. 2, pp. 191–205.e9, 2018.

[29] A. Luo, L. Yang, M. Li et al., "Genetic variants in METTL14 are associated with the risk of acute lymphoblastic leukemia in southern Chinese children: a five-center case-control study,"

Hindawi
Computational and Mathematical Methods in Medicine
Volume 2023, Article ID 9850243, 1 page
https://doi.org/10.1155/2023/9850243

Retraction

Retracted: Efficacy of TACE+Radiofrequency Ablation +Sorafenib in the Treatment of Patients with Recurrent Liver Cancer and Construction of Prediction Model

Computational and Mathematical Methods in Medicine

Received 12 December 2023; Accepted 12 December 2023; Published 13 December 2023

This article has been retracted by Hindawi, as publisher, following an investigation undertaken by the publisher [1]. This investigation has uncovered evidence of systematic manipulation of the publication and peer-review process. We cannot, therefore, vouch for the reliability or integrity of this article.

Please note that this notice is intended solely to alert readers that the peer-review process of this article has been compromised.

Wiley and Hindawi regret that the usual quality checks did not identify these issues before publication and have since put additional measures in place to safeguard research integrity.

We wish to credit our Research Integrity and Research Publishing teams and anonymous and named external researchers and research integrity experts for contributing to this investigation.

The corresponding author, as the representative of all authors, has been given the opportunity to register their agreement or disagreement to this retraction. We have kept a record of any response received.

References

[1] A. Sun, S. Chen, M. Lin et al., "Efficacy of TACE+Radiofrequency Ablation+Sorafenib in the Treatment of Patients with Recurrent Liver Cancer and Construction of Prediction Model," *Computational and Mathematical Methods in Medicine*, vol. 2022, Article ID 6879035, 7 pages, 2022.

Hindawi
Computational and Mathematical Methods in Medicine
Volume 2022, Article ID 6879035, 7 pages
https://doi.org/10.1155/2022/6879035

Research Article

Efficacy of TACE+Radiofrequency Ablation+Sorafenib in the Treatment of Patients with Recurrent Liver Cancer and Construction of Prediction Model

Aimin Sun,[1] Shumei Chen,[2] Minggang Lin,[1] Dapeng Zhou,[3] Hongyan Zhang,[1] Cheng Sun,[1] and Pan Wang[4]

[1]*Department of Oncology, Qingdao Chengyang District People's Hospital, Qingdao, Shandong 226001, China*
[2]*Department of Outpatient, Qingdao Chengyang District People's Hospital, Qingdao, Shandong 226001, China*
[3]*Department of Interventional Medicine, Qingdao University, Qingdao, Shandong 226001, China*
[4]*Department of 3D Medical Printing Center, Qingdao Chengyang District People's Hospital, Qingdao Shandong 226001, China*

Correspondence should be addressed to Minggang Lin; lmg202206@126.com

Received 13 July 2022; Revised 8 August 2022; Accepted 20 August 2022; Published 7 September 2022

Academic Editor: Min Tang

Objective. This study is aimed at exploring the efficacy of transarterial chemotherapy embolization (TACE)+radiofrequency ablation+sorafenib in the treatment of patients with recurrent liver cancer and at constructing its prediction model. *Methods*. A total of 60 patients with recurrent liver cancer treated in our hospital from March 2020 to March 2022 were enrolled and divided into two groups according to treatment methods, with 30 patients in each group. Group A adopted TACE+radiofrequency ablation+sorafenib therapy while group B adopted TACE+radiofrequency ablation therapy. Clinical efficacy, complications, and adverse reactions of the two groups were observed. A total of 30 patients with nonrecurrent liver cancer in the same period were enrolled. 60 patients with recurrent liver cancer and 30 patients with nonrecurrent liver cancer were taken as the recurrence group and the nonrecurrence group, respectively. The baseline data and clinical data of the patients were queried by the Hospital Information System. The data included age, gender, Child-Pugh grade, HBV/HCV infection, portal vein tumor thrombus, degree of differentiation, vascular invasion, serum alpha fetal protein (AFP) level, number of tumors, maximum diameter of tumors, and number of nodules. The logistic regression analysis was used to analyze the independent risk factors for liver cancer recurrence. The Hosmer-Lemeshow test was used to analyze the degree of fitting between the prediction model and the standard curve. The ROC curve was used to analyze the predictive value of the model for liver cancer recurrence. *Results*. The objective effective rate and disease control rate in group A (33.33% and 70.00%) were higher than those in group B (10.00% and 43.33%), and the differences were statistically significant (both $P < 0.05$). There were no significant differences in the incidence of complications such as embolism syndrome, hand and foot skin reaction, gastrointestinal reaction, hypertension, diaphragmatic injury and bleeding, and biliary leakage and fever between the two groups (all $P > 0.05$). The proportions of patients in the recurrence group with portal vein tumor thrombus (PVTT), medium and high degree of differentiation, combined with vascular invasion, serum AFP level ≥ 400 ng/dL, multiple tumors, maximum tumor diameter ≥ 5 cm, combined with cirrhosis, and polynodules were all higher than those in the nonrecurrence group; the differences were statistically significant (all $P < 0.05$). Complication of PVTT, the degree of medium and high differentiation, and the maximum tumor diameter ≥ 5 cm were independent risk factors for recurrence of liver cancer (all $P < 0.05$). The prediction model of liver cancer recurrence was obtained by multiple regression analysis, $P = 1/[1 + e^{-(-5.441+6.154*\text{PVTT}+3.475*\text{differentiateddegree}+3.001*\text{maximumdiameteroftumor})}]$. The Hosmer-Lemeshow test showed that $\chi^2 = 1.558$ ($P = 0.992$). According to the ROC curve analysis, the AUC, SE, and 95% CI value of the prediction model for liver cancer recurrence were 0.977, 0.012, and 0.953-1.000, respectively. *Conclusion*. TACE+radiofrequency ablation+sorafenib is effective in the treatment of recurrent liver cancer, and the prediction model established based on the risk factor has high predictive value for patients with recurrent liver cancer.

1. Introduction

Primary liver cancer (PLC) is a common malignant tumor disease in clinical practice. Its mortality and morbidity of liver cancer rank the second and third, respectively, among all malignant tumor diseases, and its morbidity is relatively high in Asia [1, 2]. PLC includes intrahepatic bile duct carcinoma, hepatocellular carcinoma (HCC), and bile duct carcinoma. At present, radical therapies for PLC mainly include complete tumor resection and liver transplantation. Due to the serious shortage of liver transplantation donors, hepatectomy is still the first-line treatment for most PLC patients with good liver function reserve. However, the recurrence rate of PLC is still as high as 50%-70% within 5 years after surgery. Recurrence and metastasis after surgical resection can seriously affect the long-term survival and quality of life of PLC patients. Although a variety of adjuvant therapies are also used clinically to reduce postoperative recurrence, the effect is not satisfactory and needs to be further explored [3, 4]. At present, the main clinical treatment methods for patients with recurrent liver cancer include resectomy, transarterial chemotherapy embolization (TACE), targeted therapy, local ablation, radiofrequency ablation, and salvage liver transplantation. Hepatectomy is the gold standard for the treatment of recurrent liver cancer. However, hepatectomy is faced with problems such as acute liver failure and insufficient liver function reserve due to the small size of the liver after resection, and only 6%~31% of patients can be resected again. Radiofrequency ablation and repeated resection have similar survival rates. TACE and radiofrequency ablation are both effective methods for the treatment of recurrent liver cancer. Sorafenib is an oral multikinase inhibitor that prolongates survival of patients with advanced liver cancer. Sorafenib is a targeted therapy. The purpose of this study was to explore the effect of TACE+radiofrequency ablation+sorafenib in the treatment of patients with recurrent liver cancer and to provide reference for the prevention and treatment of recurrent liver cancer by constructing a prediction model for liver cancer recurrence. The report is as follows.

2. Data and Methods

2.1. General Data. A total of 60 patients with recurrent liver cancer treated in our hospital from March 2020 to March 2022 were enrolled and divided into group A and group B according to treatment methods, with 30 patients in each group. In group A, there were 19 males and 11 females. The age ranged from 39 to 64 years, with the average age of 54.30 ± 6.28 years. Complications included hypertension in 8 cases, diabetes in 3 cases, and others in 19 cases. In group B, there were 17 males and 13 females. The age range was 39-77 years, with an average of 55.43 ± 10.79 years. Complications included hypertension in 12 cases, diabetes in 5 cases, and others in 13 cases. During the same period, a total of 30 patients with nonrecurrent liver cancer were enrolled as the nonrecurrence group. There were 18 males and 12 females. The age range was 38-72 years, with an average of 55.36 ± 7.52 years. Complications included hypertension in 10 cases, diabetes in 4 cases, and others in 16 cases. The general data of the three groups were comparable (all $P > 0.05$). This study was approved by the Hospital Ethics Committee.

2.2. Inclusion Criteria. The inclusion criteria of this study are as follows: (1) age > 18, (2) all patients were diagnosed with recurrent liver cancer by clinicopathological diagnosis, (3) the maximum diameter of the tumor was 1-7 cm, (4) the life expectancy > 3 months, and (5) all patients participated in this study voluntarily.

2.3. Exclusion Criteria. The exclusion criteria of this study are as follows: (1) patients with other malignant tumor diseases, (2) patients with Child-Pugh grade C for liver function, (3) patients with severe organ dysfunction such as heart, lung, and kidney, (4) patients who cannot tolerate TACE and radiofrequency ablation or were allergic to sorafenib, and (5) patients with severe coagulation dysfunction that were uncorrectable.

2.4. Methods. Group A was treated with TACE+radiofrequency ablation+sorafenib, and group B was treated with TACE+radiofrequency ablation.

2.4.1. TACE. The femoral artery was punctured with Seldinger technique routinely, and the 5F catheter was placed. The catheter was placed at the opening of the celiac trunk artery for angiography to determine the tumor target vessel. Superselective intubation was performed into the tumor supplying artery. The tumor target vessel was embolized with fluorouracil 1000 mg, cisplatin 50 mg, pirarubicin 50 nmg+super liquefied lipiodol 5~10 mL. After the operation, hepatoprotective hydration treatment was performed.

2.4.2. Radiofrequency Ablation. After the TACE treatment for 2-4 weeks, radiofrequency ablation was performed. First, CT scanning was performed to determine the puncture point, and then, lidocaine was used for local anesthesia. Percutaneous puncture of intrahepatic lesions was performed under the guidance of the CT, and tumor ablation was performed according to the protocol. After that, CT scanning was performed to see whether the scope covered the target tumor. If it was not completely covered, radiofrequency ablation could be performed immediately. During radiofrequency ablation, all lesions should be ablated in one ablation process, including single nodule and polynodule patients.

2.4.3. Sorafenib Treatment. Seven days after intervention, sorafenib was given orally, 400 mg/time, twice a day for 4 weeks.

2.5. Observation Indicators. (1) The clinical efficacy of group A and group B was evaluated according to the efficacy evaluation criteria. (2) There is a comparison of complication rate between group A and group B. (3) A total of 30 patients with nonrecurrent liver cancer in the same period were selected, and 60 patients with recurrent liver cancer and 30 patients without recurrent liver cancer were divided into the recurrence group and the nonrecurrence group. The baseline data and clinical data of patients were queried by

Table 1: Comparison of clinical efficacy between the two groups [n (%)].

Group	CR	PR	SD	PD	ORR	DCR
Group A ($n = 30$)	1 (3.33)	9 (30.00)	11 (36.67)	9 (30.00)	10 (33.33)	21 (70.00)
Group B ($n = 30$)	0 (0.00)	3 (10.00)	10 (33.33)	17 (56.67)	3 (10.00)	13 (43.33)
χ^2-value					4.812	4.344
P value					0.028	0.037

CR: complete remission; PR: partial remission; SD: stable disease; PD progressive disease; ORR: objective response rate; DCR: (disease control rate).

Table 2: Comparison of complications and adverse reactions between the two groups [n (%)].

Group	Embolism syndrome	Hand-foot skin reaction	Gastrointestinal reaction	Hypertension	Diaphragm injury and bleeding	Biliary leakage and fever
Group A ($n = 30$)	28 (93.33)	23 (76.67)	27 (90.00)	9 (30.00)	12 (40.00)	10 (33.33)
Group B ($n = 30$)	27 (90.00)	21 (70.00)	23 (76.67)	12 (40.00)	10 (33.33)	7 (23.33)
χ^2-value		0.341	1.920	0.659	0.287	0.739
P value		0.559	0.166	0.417	0.592	0.390
Fisher's exact probability value	1.000					

hospital information system. Age, gender, Child-Pugh grade, HBV/HCV infection, portal vein tumor thrombus, differentiation degree, vascular invasion, serum AFP level, tumor number, tumor maximum diameter, number of nodules, and other data were included. Baseline data and clinical data were compared between the recurrence group and the nonrecurrence group. (4) Logistic multivariate regression analysis was used to analyze the independent risk factors of HCC recurrence. The baseline and clinical data of the recurrence group and the nonrecurrence group were statistically different. (5) Logistic regression was used to analyze the risk factors of HCC recurrence and establish a regression model. (6) The receiver operating characteristic (ROC) curve was used to calculate the discrimination of the prediction model.

2.6. Efficacy Evaluation Criteria. The treatment effects of the two groups were assessed according to the Response Evaluation Criteria in Solid Tumors (RECIST) [5] proposed by the American Cancer Institute. The treatment effects were divided into complete remission (CR), partial remission (PR), stable disease (SD), progressive disease (PD), objective response rate (ORR) = CR + PR, and disease control rate (DCR) = CR + PR + SD.

2.7. Statistical Method. All the data in this study were entered into Excel form without communication between two persons and analyzed and processed with statistical software SPSS 24.0. The measurement data were expressed in mean ± SD (±s). When the measurement data conform to the normal distribution and the variance was homogeneous, a t-test was adopted. The counting data were described by N and %. The disordered classification data were compared by the χ^2 test or Fisher's exact probability method. The logistic regression analysis was used to analyze the risk factors of liver cancer recurrence. The Hosmer-Lemeshow test was used to analyze the fitting degree between the prediction model and the standard curve. The ROC curve was used to analyze the predictive value of the model for recurrence of liver cancer. All tests were two-sided, and the difference was statistically significant when $P < 0.05$.

3. Results

3.1. Comparison of Clinical Efficacy between the Two Groups. The ORR and DCR in group A (33.33% and 70.00%) were higher than those in group B (10.00% and 43.33%). The differences were statistically significant (both $P < 0.05$, Table 1).

3.2. Comparison of Complications and Adverse Reactions between the Two Groups. There were no significant differences in the incidence of complications such as embolism syndrome, hand and foot skin reaction, gastrointestinal reaction, hypertension, diaphragmatic injury and bleeding, and biliary leakage and fever between the two groups (all $P > 0.05$) as shown in Table 2.

3.3. Univariate Analysis of Recurrence in Two Groups. The proportion of patients in the recurrence group with PVTT, medium and high degree of differentiation, combined with vascular invasion, serum AFP level ≥ 400 ng/dL, multiple tumors, maximum diameter ≥ 5 cm, combined with cirrhosis, and polynodules was higher than that in the nonrecurrence group; the differences were statistically significant (all $P < 0.05$), as shown in Table 3.

3.4. Logistic Multivariate Analysis of Recurrence in Two Groups. Complication of PVTT, the degree of medium and high differentiation and the maximum tumor diameter ≥ 5 cm were independent risk factors for recurrence of liver cancer (all $P < 0.05$), as shown in Table 4.

Table 3: Univariate analysis of recurrence in two groups [$\bar{x} \pm s$, n (%)].

Item	Recurrence group ($n = 60$)	Nonrecurrence group ($n = 30$)	χ^2 value	P value
Age (years)				
<60 years	37 (61.67)	18 (60.00)	0.023	0.878
≥60 years	23 (38.33)	12 (40.00)		
Gender				
Male	36 (60.00)	20 (66.67)	0.378	0.539
Female	24 (40.00)	10 (33.33)		
Child-Pugh grade				
Grade A	44 (73.33)	17 (56.67)	2.544	0.111
Grade B	16 (26.67)	13 (43.33)		
HBV/HCV infection				
No	39 (65.00)	14 (46.67)	2.777	0.096
Yes	21 (35.00)	16 (53.33)		
PVTT				
Yes	52 (86.67)	2 (6.67)	53.33	<0.001
No	8 (13.33)	28 (93.33)		
Degree of differentiation				
High differentiation	17 (28.33)	4 (13.33)	8.921	0.012
Medium differentiation	28 (46.67)	9 (30.00)		
Low differentiation	15 (25.55)	17 (56.67)		
Vascular invasion				
Yes	28 (46.67)	3 (10.00)	11.908	0.001
No	32 (53.33)	27 (90.00)		
Serum AFP level (ng/dl)				
<400	22 (36.67)	18 (60.00)	4.410	0.036
≥400	38 (63.33)	12 (40.00)		
Number of tumors				
Single	27 (54.00)	23 (76.67)	8.122	0.004
Multiple	33 (82.50)	7 (23.33)		
Maximum diameter of tumor (cm)				
<5	29 (48.33)	22 (73.33)	5.090	0.024
≥5	31 (51.67)	8 (26.67)		
Cirrhosis				
Yes	24 (40.00)	19 (63.33)	4.364	0.037
No	36 (60.00)	11 (36.67)		
Number of nodules				
Single nodule	25 (41.67)	20 (66.67)	5.000	0.025
Polynodule	35 (58.33)	10 (33.33)		

3.5. Establishment of Prediction Model and Analysis of Model Calibration Degree. The predictive model of liver cancer recurrence was obtained by multiple regression analysis, $P = 1/[1 + e^{-(-5.441+6.154*\text{PVTT}+3.475*\text{Degreeofdifferentiation}+3.001*\text{Maximumdiameteroftumor})}]$. The Hosmer-Lemeshow test showed that $\chi^2 = 1.558$ and $P = 0.992$ (Figure 1).

3.6. Prediction Efficiency Analysis of Prediction Model. According to ROC curve analysis, the AUC value, SE value, and 95% CI of the prediction model for HCC recurrence were 0.977, 0.012, and 0.953-1.000, respectively (Figure 2).

4. Discussions

Most recurrent liver cancer cannot tolerate secondary surgery because of specific tumor location, multiple recurrent foci, and complicated with severe cirrhosis. TACE is the preferred treatment for nonsurgical treatment of recurrent liver cancer [6–8]. TACE technology combines embolization and chemotherapy. Chemotherapy drugs can be injected through the hepatic artery to increase drug concentration in tumor tissue and reduce side effects of systemic chemotherapy. The use of iodized oil to suspend chemotherapy drugs can

Table 4: Logistic multivariate analysis of recurrence in two groups.

Item	β	SE	Wald χ^2	OR	95% CI	P value
PVTT	6.154	1.710	12.947	470.733	16.477~13448.349	< 0.001
Degree of differentiation	3.475	1.475	5.548	32.295	1.792~581.983	0.019
Vascular invasion	1.636	1.212	1.822	5.134	0.477~55.220	0.177
Serum AFP level (ng/dL)	1.705	1.151	2.196	5.502	0.577~52.479	0.138
Number of tumors	0.940	1.196	0.617	2.560	0.245~26.695	0.432
Maximum diameter of tumor	3.001	1.520	3.898	20.109	1.022~395.55	0.048
Cirrhosis	-2.997	1.587	3.566	0.050	0.002~1.120	0.059
Number of nodules	0.928	1.138	0.665	2.531	0.272~23.557	0.415
Constant	-5.441	1.857	8.581	0.004		0.003

PVTT: yes = 1 and no = 0; degree of differentiation: medium and high differentiation = 1 and low differentiation = 0; vascular invasion: yes = 1 and no = 0; serum AFP level (ng/dL): ≥400 = 1 and <400 = 0; number of tumors: multiple = 1 and single = 0; maximum diameter of tumor (cm): ≥5 = 1 and <5 = 0; cirrhosis: yes = 1 and no = 0; nodule number: polynodule = 1 and single nodule = 0.

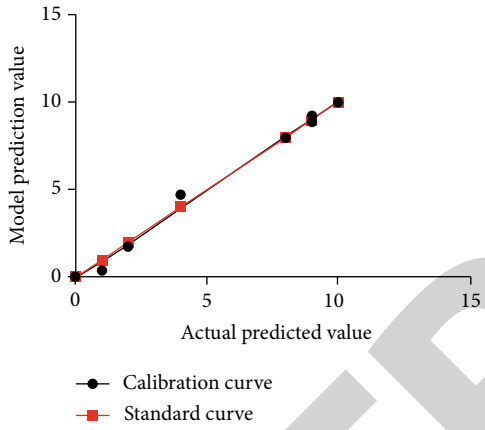

Figure 1: Analysis of model calibration degree.

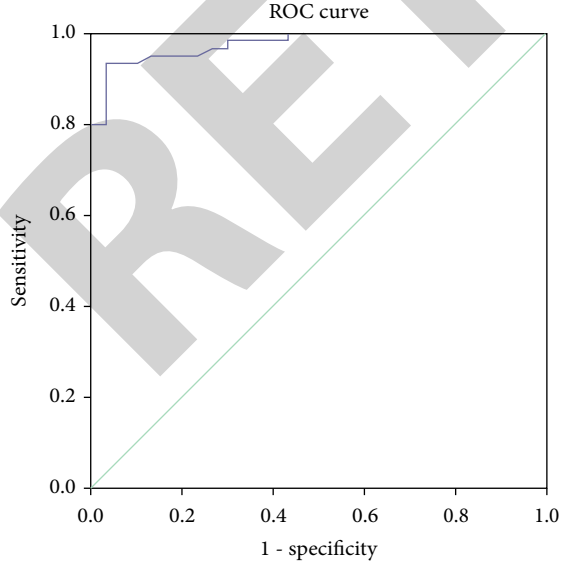

Figure 2: ROC curve analysis of prediction model for predicting liver cancer recurrence.

concentrate the drug in tumor tissue. Transcatheter therapy for liver cancer allows direct delivery of embolic agents to the liver tumor, preserving normal liver tissue, and promoting the absorption of drugs into cancer cells [9–11]. Radiofrequency ablation is considered to be a radical treatment strategy for PLC comparable to liver resection and liver transplantation, with the advantages of repeatable operation, less trauma and fewer complications. In addition to PLC, radiofrequency ablation can be applied to single or relatively limited intrahepatic recurrence to improve the long-term outcomes of patients [12, 13]. *Guidelines for the Diagnosis and Treatment of Primary Liver Cancer (2022)* [14] indicates that radiofrequency ablation is suitable for liver cancer patients with single tumor with diameter ≤ 5 cm, multiple tumors with maximum tumor with diameter ≤ 3 cm, tumor nodules with diameter ≤ 3 cm, no vascular invasion, and distant metastasis. For patients with single or multiple tumors that cannot be treated surgically, TACE combined with radiofrequency ablation can be used. Sorafenib is a molecular targeted drug, a multikinase inhibitor, which can effectively prolong the survival time of liver cancer patients. In addition, according to relevant studies, sorafenib can expand the range of radiofrequency ablation and improve the therapeutic effect of liver cancer treatment [15]. Treating liver cancer with TACE alone also has some limitations. TACE treatment of liver cancer can cause anoxic environment, induced VEGF expression, and neovascularization, while TACE combined with sorafenib to treat liver cancer can effectively inhibit regenerating blood vessels, reduce tumor recurrence and metastasis, and improve the therapeutic effect. In this study, the ORR and DCR of group A (33.33% and 70.00%) after treatment were higher than that of group B (10.00% and 43.33%) (both $P < 0.05$). Group A was given TACE+radiofrequency ablation+sorafenib, and group B was given TACE+radiofrequency ablation. These results indicated that the combination of TACE+radiofrequency ablation+sorafenib was more effective in the treatment of recurrent liver cancer, which may be related to the synergistic therapeutic effect of sorafenib with TACE and radiofrequency ablation. There were no significant differences in the incidence of complications such as embolism syndrome, hand and foot skin reaction, gastrointestinal

reaction, hypertension, diaphragmatic injury and bleeding, and biliary leakage and fever between the two groups (all $P > 0.05$). Although sorafenib was added in group A, there was no increase in the incidence of serious adverse reactions and complications indicating that sorafenib are safe for treatment.

Comparison of baseline and clinical data between the two groups showed that the proportion of patients in the recurrence group with PVTT, medium and high degree of differentiation, combined with vascular invasion, serum AFP level ≥ 400 ng/dL, multiple tumors, maximum diameter ≥ 5 cm, combined with cirrhosis, and polynodules was significantly higher than that in the nonrecurrence group (all $P < 0.05$). The results showed that the complication of PVTT, medium and high degree of differentiation, vascular invasion, serum AFP level ≥ 400 ng/dL, multiple tumors, maximum tumor diameter ≥ 5 cm, cirrhosis, and polynodules were related to the recurrence of liver cancer. The recurrence of liver cancer is generally caused by multicentric canceration, and the high recurrence rate after surgery also seriously affects the therapeutic effect. Early recurrence was mainly related to tumor size, vascular invasiveness, and higher AFP level in muscle serum of the primary tumor, while late recurrence was mainly related to etiology and cirrhosis background. Vascular invasion can lead to worse tumor stage and tumor progression in patients, and PVTT is a common complication in patients with liver cancer, indicating poor prognosis [16]. Tumor grade can significantly affect the independent influencing factors of long-term survival, and the histological grade of tumor can represent the biological aggressiveness of liver cancer. Multiple previous studies have shown that tumor grade is a negative prognostic indicator [17, 18], which is consistent with the results of our study. Serum AFP indicators play an important role in early detection, and serum AFP level can be used as an independent predictor of overall survival before salvage treatment, and a higher AFP level indicates a higher degree of malignancy of liver cancer [19]. The number and maximum diameter of tumors are related to the early recurrence of liver cancer. Large liver cancer with a diameter of >5 cm is highly invasive and has a high risk of recurrence, which may be related to large tumor size, compression or invasion of large blood vessels. Previous studies have also shown that cirrhosis and polynodules are risk factors for liver cancer recurrence [20–22]. The logistic multivariate analysis showed that PVTT, medium and high differentiation degree, and maximum tumor diameter ≥ 5 cm were independent risk factors for liver cancer recurrence (all $P < 0.05$). PVTT, serum AFP level ≥ 400 ng/dL, multiple tumors, cirrhosis, and polynodular were not the independent risk factors for liver cancer recurrence. This result may be related to the small number of cases in this study.

The identification of patients with recurrent liver cancer by predictive model is conducive to the timely intervention by clinicians and the development of individualized control programs for high risk factors, which is conducive to further reducing the recurrence rate of liver cancer and improving the prognosis of liver cancer patients. In this study, a prediction model was established based on various risk factors. The Hosmer-Lemeshow test and ROC curve analysis showed that the model had high predictive value for liver cancer recurrence and could be used in the early prediction of liver cancer recurrence.

In conclusion, TACE+radiofrequency ablation+sorafenib has a good clinical effect in the treatment of recurrent liver cancer, and the prediction model established based on risk factors has a high predictive value for the recurrence of liver cancer.

Data Availability

The labeled dataset used to support the findings of this study is available from the corresponding author upon request.

Conflicts of Interest

The authors declare no competing interests.

References

[1] X. Li, P. Ramadori, D. Pfister, M. Seehawer, L. Zender, and M. Heikenwalder, "The immunological and metabolic landscape in primary and metastatic liver cancer," *Nature Reviews. Cancer*, vol. 21, no. 9, pp. 541–557, 2021.

[2] Z. Liu, Y. Jiang, H. Yuan et al., "The trends in incidence of primary liver cancer caused by specific etiologies: results from the global burden of disease study 2016 and implications for liver cancer prevention," *Journal of Hepatology*, vol. 70, no. 4, pp. 674–683, 2019.

[3] Y. Sun, L. Wu, Y. Zhong et al., "Single-cell landscape of the ecosystem in early-relapse hepatocellular carcinoma," *Cell*, vol. 184, no. 2, pp. 404–421.e16, 2021.

[4] M. Yoshioka, N. Taniai, Y. Kawano et al., "Effectiveness of laparoscopic repeat hepatectomy for recurrent liver cancer," *Journal of Nippon Medical School*, vol. 86, no. 4, pp. 222–229, 2019.

[5] S. Litière, S. Collette, E. G. de Vries, L. Seymour, and J. Bogaerts, "RECIST - learning from the past to build the future," *Nature Reviews. Clinical Oncology*, vol. 14, no. 3, pp. 187–192, 2017.

[6] Y. Sun, S. Ji, H. Ji, L. Liu, and C. Li, "Clinical efficacy analysis of transcatheter arterial chemoembolization (TACE) combined with radiofrequency ablation (RFA) in primary liver cancer and recurrent liver cancer," *Journal of BUON*, vol. 24, no. 4, pp. 1402–1407, 2019.

[7] Y. Midorikawa, T. Takayama, M. Moriguchi et al., "Liver resection versus embolization for recurrent hepatocellular carcinoma," *World Journal of Surgery*, vol. 44, no. 1, pp. 232–240, 2020.

[8] B. Sarici, B. Isik, and S. Yilmaz, "Management of recurrent HCC after liver transplantation," *Journal of Gastrointestinal Cancer*, vol. 51, no. 4, pp. 1197–1199, 2020.

[9] X. Zhang, J. Zhou, D. D. Zhu et al., "CalliSpheres® drug-eluting beads (DEB) transarterial chemoembolization (TACE) is equally efficient and safe in liver cancer patients with different times of previous conventional TACE treatments: a result from CTILC study," *Clinical & Translational Oncology*, vol. 21, no. 2, pp. 167–177, 2019.

[10] J. Ji, J. Gu, J. Z. Wu et al., "The "six-and-twelve" score for recurrent HCC patients receiving TACE: does it still work?," *Cardiovascular and Interventional Radiology*, vol. 44, no. 5, pp. 720–727, 2021.

Hindawi
Computational and Mathematical Methods in Medicine
Volume 2023, Article ID 9892159, 1 page
https://doi.org/10.1155/2023/9892159

Retraction

Retracted: Efficacy Analysis of Comprehensive Nursing in the Care of Ovarian Carcinoma Treated with Paclitaxel Combined with Nedaplatin

Computational and Mathematical Methods in Medicine

Received 12 December 2023; Accepted 12 December 2023; Published 13 December 2023

This article has been retracted by Hindawi, as publisher, following an investigation undertaken by the publisher [1]. This investigation has uncovered evidence of systematic manipulation of the publication and peer-review process. We cannot, therefore, vouch for the reliability or integrity of this article.

Please note that this notice is intended solely to alert readers that the peer-review process of this article has been compromised.

Wiley and Hindawi regret that the usual quality checks did not identify these issues before publication and have since put additional measures in place to safeguard research integrity.

We wish to credit our Research Integrity and Research Publishing teams and anonymous and named external researchers and research integrity experts for contributing to this investigation.

The corresponding author, as the representative of all authors, has been given the opportunity to register their agreement or disagreement to this retraction. We have kept a record of any response received.

References

[1] Y. Li, J. Wu, and G. Zhu, "Efficacy Analysis of Comprehensive Nursing in the Care of Ovarian Carcinoma Treated with Paclitaxel Combined with Nedaplatin," *Computational and Mathematical Methods in Medicine*, vol. 2022, Article ID 9398823, 6 pages, 2022.

Hindawi
Computational and Mathematical Methods in Medicine
Volume 2022, Article ID 9398823, 6 pages
https://doi.org/10.1155/2022/9398823

Research Article

Efficacy Analysis of Comprehensive Nursing in the Care of Ovarian Carcinoma Treated with Paclitaxel Combined with Nedaplatin

Yahui Li,[1] **Jing Wu**,[2] **and Gehong Zhu**[1]

[1]*Department of Gynecology and Oncology, Shaanxi Cancer Hospital, Xi'an, 710061 Shaanxi, China*
[2]*Department of General Surgery, Shaanxi Cancer Hospital, Xi'an, 710061 Shaanxi, China*

Correspondence should be addressed to Gehong Zhu; zhugehong1688@163.com

Received 22 June 2022; Revised 5 August 2022; Accepted 17 August 2022; Published 6 September 2022

Academic Editor: Min Tang

Objective. To determine the effectiveness of comprehensive nursing in the care of ovarian carcinoma (OC) patients treated with paclitaxel (PTX) plus nedaplatin (NDP). *Methods.* The research population comprised 180 advanced OC patients who received treatment in the Shaanxi Cancer Hospital between November 2018 and November 2021. The enrolled cases were assigned to two groups based on different nursing plans: an observation group (OG) with 100 cases treated with comprehensive nursing and a control group (CG) with 80 cases intervened by conventional nursing. Intergroup comparisons were performed to identify statistical significance in terms of the following parameters: serum NGF, TK1, and CA15-3 levels; VAS, SAS, and SDS scores; nursing compliance; incidence of adverse reactions; and nursing satisfaction. *Results.* Compared with CG, OG showed the following: (1) lower posttreatment NGF, TK1, and CA15-3 levels; (2) lower scores of SAS and SDS; (3) higher nursing compliance; and (4) lower incidence of adverse reactions and higher nursing satisfaction after nursing. *Conclusions.* Comprehensive nursing far outperformed conventional nursing in the care of advanced OC patients treated with PTX plus NDP, which is worth popularizing.

1. Introduction

Ovarian carcinoma (OC) is one of the most deadly gynecological malignancies, ranking as the fifth leading cause of cancer deaths among women in many developed countries [1, 2]. It is a collection of heterogeneous tumors with different clinicopathological and molecular characteristics [3], with approximately 70-80% of cases being diagnosed at a late stage due to unconspicuous or nonspecific clinical presentations [4, 5]. Advances have been made in both traditional and new treatments for the disease over the past few decades [6]. Among various treatments, nedaplatin (NDP) plus paclitaxel (PTX) maintenance chemotherapy is a common approach, with evidence indicating that weekly dose-dense PTX combined with platinum can improve patient survival [7]. However, 60-70% of patients still face the risk of recurrence even after relevant treatment, which has a great impact on their 5-year survival [8]. This shows that after treatment, other means are needed to maintain the effect of treatment [9]. Nursing is a necessary means to maintain the therapeutic effect. Therefore, this research, which focuses on OC nursing, is of great significance to maintain a more effective therapeutic effect for patients with the disease, thereby reducing disease recurrence.

After a variety of treatment means, a good nursing model is conducive to patient recovery and maintains therapeutic effects [10, 11]. Comprehensive nursing is such a good and flexible nursing method that can be tailored according to the changes of patients' conditions. Its strong comprehensiveness can considerably ease surgery-induced negative psychological state of patients while helping them to develop a healthy lifestyle from the aspect eating habits, which is of great significance to patients' rehabilitation [12, 13]. However, there is scanty research on the employment of comprehensive nursing care in OC patients after chemotherapy. Consequently, this study assesses the effectiveness of

Table 1: Patient's general information.

Classification	Observation group ($n = 100$)	Control group ($n = 80$)	t/χ^2	P
Mean age (years)	48.11 ± 6.92	48.84 ± 6.46	0.72	0.470
BMI	27.34 ± 1.62	27.29 ± 1.39	0.22	0.827
Drinking			0.09	0.769
Yes	72 (72.00)	56 (70.00)		
No	28 (28.00)	24 (30.00)		
Smoking			0.01	0.919
Yes	88 (88.00)	70 (87.50)		
No	12 (12.00)	10 (12.50)		
Working state			1.42	0.233
Employed	78 (78.00)	68 (85.00)		
Unemployed	22 (22.00)	12 (15.00)		
Family type			2.51	0.113
Nuclear family	64 (64.00)	60 (75.00)		
Others	36 (36.00)	20 (25.00)		
Place of residence			0.01	0.945
Rural	37 (37.00)	30 (37.50)		
Urban	63 (63.00)	50 (62.50)		

comprehensive nursing on OC patients from various blood test indexes after treatment, as well as anxiety, depression, and various complications.

2. Methods

2.1. Study Population. The study population comprised 180 advanced OC patients who received treatment in the Shaanxi Cancer Hospital between November 2018 and November 2021. Based on different nursing plans, 100 cases receiving comprehensive nursing after treatment were included in the observation group (OG), and the other 80 cases receiving conventional nursing were included in the control group (CG). Inclusion criteria are as follows: all cases were diagnosed as OC by cytology or histopathological biopsy and received treatment treated in our hospital; age ≥ 18; active participation and cooperation of patients and their family members; and complete case data. Exclusion criteria are as follows: other malignant tumors; intolerance or contraindications to chemotherapy; primary diseases of blood system, or dysfunction of heart, liver, kidney and other organs; allergic constitution; and pregnant or lactating women. This study was conducted after obtaining approval from the Medical Ethics Committee of Shaanxi Cancer Hospital, and patients and their families signed informed consent.

2.2. Methods. The two cohorts of patients received the same treatment (PTX plus NDP) but different posttreatment nursing methods. The patients in CG were given conventional nursing, that is, monitoring the changes of vital signs, giving routine dietary guidance, helping patients with mobility difficulties to recover from exercise, daily cleaning of the ward to keep the environment clean, and instructing patients to review regularly upon their discharge from hospital, while the patients in OG received comprehensive care. All examinations were completed within 24 hours of admission. Upon patient admission, the medical staff carried out a detailed investigation and understanding of a series of personal-related conditions of the patient, as well as the patient's awareness of the complications related to the combination therapy of OC. Based on the investigation, a nursing plan suitable for each patient was developed. During the health education for patients, the medical staff not only distributed the relevant health manuals to them but also explained the relevant knowledge of OC in detail, including the occurrence, treatment, drug use, treatment of posttreatment complications (if any), and home care methods. Family members were also involved in learning to play a part in the care. In addition, health education was conducted once a week (2 h/time), and the frequency was adjusted according to the degree of knowledge acquired by patients and their families. Furthermore, the patients were cared for psychologically and emotionally. They were informed that negative emotions can easily worsen their illness. Psychological nursing was carried out in an environment in which interpersonal atmosphere and treatment are more harmonious, and appropriate encouragement was given to patients in time, so as to establish their confidence to recover from surgical treatment. The medical staff also reminded the patients of some precautions during treatment. For example, during health education, the patients were instilled with the need to strictly abide to the instructions of the medical staff during the operation and strictly follow the doctor's advice to use drugs and cannot stop taking drugs against the medical advice. After surgical treatment, medical staff deliberately set aside a period of time (about 10-15 min) every day to help patients with impaired mobility to do rehabilitation exercise. Moreover,

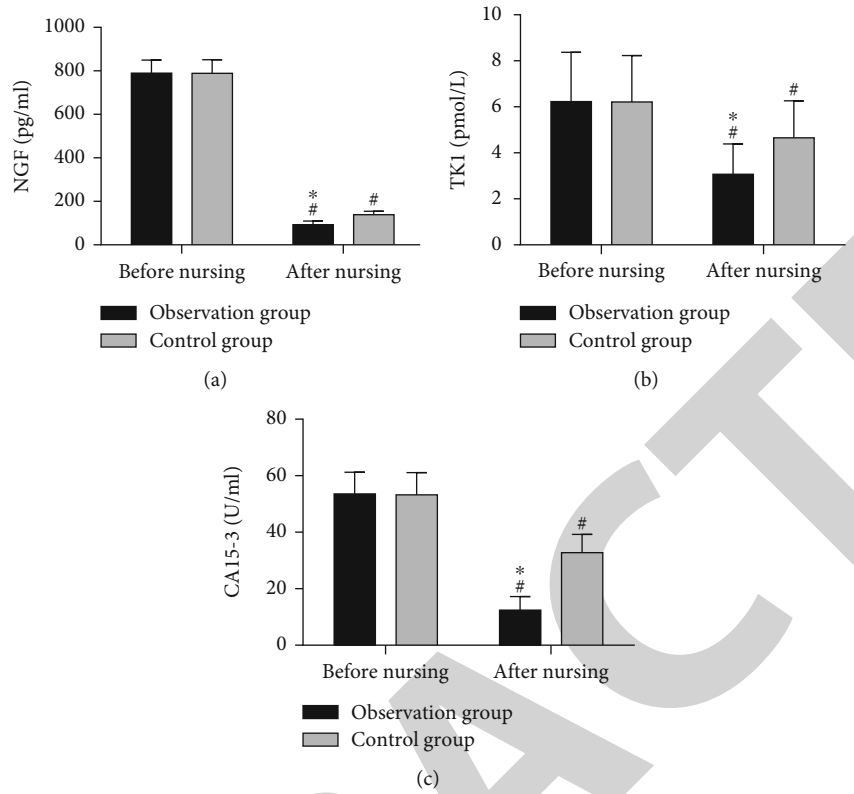

Figure 1: Serum levels of NGF, TK1, and CA15-3 in the two groups: (a) serum NGF levels before and after nursing in the two groups. (b) Serum TK1 levels in the two groups before and after nursing. (c) Serum CA15-3 levels before and after nursing in the two groups. Note: $^{\#}P < 0.05$ vs. before treatment; $^{*}P < 0.05$ vs. control group.

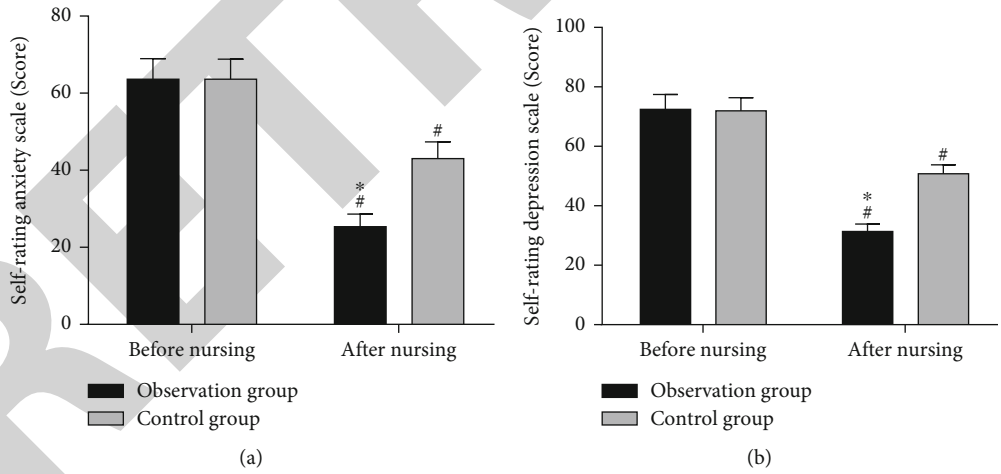

Figure 2: Mental health of patients in the two groups: (a) SAS scores before and after nursing in the two groups. (b) SDS scores of the two groups before and after nursing. Note: $^{\#}P < 0.05$ vs. before treatment; $^{*}P < 0.05$ vs. control group.

during and after treatment, patients were given dietary guidance, highlighting light diet, balanced nutrition, and more intake of food with high nutritional value and avoiding alcohol, tobacco, and greasy and spicy food. On the day before discharge, patients and their families were given postdischarge nursing guidance, covering medication, diet, exercise, and reexamination. They were also instructed to master the basic essentials of home nursing, disinfection, and isolation. Follow-up was conducted periodically. After that, they were followed up regularly.

2.3. Endpoints

2.3.1. Serum Nerve Growth Factor (NGF), Thymidine Kinase 1 (TK1), and Carbohydrate Antigen 15-3 (CA15-3). At admission and 30 days after nursing, 5 mL of fasting cubital

Table 2: Compliance of patients in the two groups.

Classification	Observation group ($n = 100$)	Control group ($n = 80$)	χ^2	P
Complete compliance	73 (73.00)	36 (45.00)	—	—
Partial compliance	24 (24.00)	24 (30.00)	—	—
Noncompliance	3 (3.00)	20 (25.00)	—	—
Total compliance (%)	97 (97.00)	60 (75.00)	19.30	<0.001

Table 3: Incidence of adverse reactions in the two groups.

Classification	Observation group ($n = 100$)	Control group ($n = 80$)	χ^2	P
Myelosuppression	0 (0.00)	2 (2.50)	—	—
Hair loss	2 (2.00)	4 (5.00)	—	—
Gastrointestinal discomfort	2 (2.00)	4 (5.00)		
Anemia	0 (0.00)	2 (2.50)	—	—
Total incidence (%)	4 (4.00)	12 (15.00)	6.64	0.01

Table 4: Nursing satisfaction of patients in the two groups.

Classification	Observation group ($n = 100$)	Control group ($n = 80$)	χ^2	P
Satisfied	70 (70.00)	34 (42.50)	—	—
Basically satisfied	28 (28.00)	30 (37.50)	—	—
Dissatisfied	2 (2.00)	16 (20.00)	—	—
Satisfaction (%)	98 (98.00)	64 (80.00)	16.00	<0.001

venous blood was collected into test tubes without anticoagulant and naturally agglutinated at indoor temperature for 20-30 min. After 10 min of centrifugation ($1500 \times g$ at 4°C), the serum was separated and stored at -20°C for subsequent detection of NGF, TK1, and CA15-3 via ELISA [14].

2.3.2. Mental Health (MH). The MH level of both groups was evaluated and compared at admission and 30 days after receiving nursing care, with the self-rating anxiety/depression scale (SAS/SDS) [15, 16] as evaluation criteria. The worse the MH level of patients, the higher the score.

2.3.3. Nursing Compliance. Patients' compliance during nursing care was also observed and compared. Complete compliance: the patient actively cooperates with medical staff in the nursing process. Partial compliance: the patient occasionally has irregular behaviors in the nursing process but continues to cooperate after being reminded by medical staff. Noncompliance: the patient is completely uncooperative with the medical staff.

2.3.4. Adverse Reactions (ARs). ARs, including myelosuppression, alopecia, gastrointestinal discomfort, and anemia, were compared.

2.3.5. Nursing Satisfaction. The nursing satisfaction assessed by the satisfaction questionnaire made by our hospital was also compared. The score ranged from 0 to 100, with a score of ≥85 and 84-60 indicating satisfied and basically satisfied, respectively. Higher scores suggest better nursing quality.

2.4. Statistical Methods. The software applied for statistical analysis and image rendering was SPSS 21.0 (Bizinsight Information Technology Co., Ltd.) and GraphPad Prism 6 (GraphPad Software, San Diego, USA), respectively. The statistical methods for the comparison of measurement data (mean age, body mass index (BMI), etc.) expressed as ($\bar{\chi} \pm s$) and counting data (drinking, smoking, etc.) were t -test and χ^2 test, respectively, and statistical significance was present when $P < 0.05$.

3. Results

3.1. General Data. The two groups exhibited no statistical differences in general information such as mean age, BMI, drinking/smoking (yes/no), working status, family type, and residence ($P > 0.05$) (see Table 1 for details).

3.2. Serum NGF, TK1, and CA15-3 Contents. Intergroup comparisons of serum NGF, TK1, and CA15-3 contents revealed statistically lower levels of these parameters in OG ($P < 0.05$). Figure 1.

3.3. Psychological Status. The intergroup comparison of MH revealed statistically lower SAS and SDS scores in OG versus CG after nursing intervention ($P < 0.05$). Figure 2.

3.4. Nursing Compliance. After statistical comparison, it was found that the total compliance was higher in OG than in CG ($P < 0.05$) Table 2.

3.5. Adverse Reactions. Comparing ARs between the two groups, we found an obviously lower incidence of ARs in OG compared with CG ($P < 0.05$) Table 3.

3.6. Nursing Satisfaction. The statistical comparison of patient satisfaction towards nursing revealed a statistically higher satisfaction degree in OG compared with CG ($P < 0.05$) Table 4.

4. Discussion

As one of the gynecological malignancies, OC is highly migratory and easily metastasized to abdominal organs, and in many cases, it has already metastasized once detected [17–19]. PTX plus NDP is a common method to treat OC; however, it is easy for cancer cells to develop drug resistance, leading to disease relapse [20]. Therefore, after treatment, a series of nursing measures are required to maintain the therapeutic effect and enable patients to recover effectively.

First, we found more significant deductions in cancer-related serum factors (NGF, TK1, and CA15-3) in OG compared with CG after nursing. TK1 plays a vital part in DNA synthesis and cell proliferation, with elevated expression in various cancers, which is a common prognostic factor of cancer [21]. NGF generally affects the nervous system; NGF and its precursor, proNGF, stimulate the survival or growth of cancer cells, respectively, which can enhance the invasiveness of cells [22]. CA15-3 is a common serological marker in various cancers, with elevated expression indicating further progression of cancer, but its sensitivity is poor [23]. The results of this study showed that comprehensive nursing had a better effect on reducing cancer-related factors than conventional nursing, which is consistent with the suggestion of Lu et al. [24] in the study on the care for OC. This is because compared with conventional nursing, comprehensive nursing is more integrated and targeted, and its clinical nursing methods, application of nursing management system, and nursing procedures are more standardized, with stricter management requirements for medical teams [25–27]. This study also found that after nursing, the scores of anxiety (SAS) and depression (SDS) were reduced in both cohorts, especially in OG. As we all know, negative emotions tend to aggravate patient's conditions and form a vicious circle. In order to get a good recovery, patients need to maintain psychologically healthy [22]. Therefore, great efforts should be made during the care to avoid such emotions in patients. In terms of nursing methods, comprehensive nursing has better and more detailed health education than conventional nursing, which enables patients and their families to fully understand the treatment process of chemotherapy and medication and to better deal with adverse reactions and complications caused by the drugs. Therefore, patients in OG with health education carried out from multiple dimensions were more confident. In addition, medical staff provided special psychological counseling to help patients build confidence during the comprehensive nursing process, so that the depression and anxiety patients in OG were validly eliminated. It is precisely because of that the therapeutic effect of OG is better, with more significant improvements in various factors.

This study also has shortcomings. Due to the influence of equipment and some other objective conditions, we were unable to detect more indicators. Besides, we have not yet developed a valid indicator to determine whether patients relapsed after treatment to help verify the maintenance of efficacy during care. In future research, we will continue to address these defects.

5. Conclusion

Collectively, comprehensive nursing has advantages over conventional nursing in the care of advanced OC patients treated with PTX plus NDP, which is worth popularizing.

Data Availability

The labeled dataset used to support the findings of this study are available from the corresponding author upon request.

Conflicts of Interest

The authors declare no competing interests.

References

[1] K. D. Miller, L. Nogueira, A. B. Mariotto et al., "Cancer treatment and survivorship statistics, 2019," *CA: a Cancer Journal for Clinicians*, vol. 69, no. 5, pp. 363–385, 2019.

[2] N. Howlader, K. A. Cronin, A. W. Kurian, and R. Andridge, "Differences in breast cancer survival by molecular subtypes in the United States," *Cancer Epidemiology, Biomarkers & Prevention*, vol. 27, no. 6, pp. 619–626, 2018.

[3] A. Markowska, S. Sajdak, A. Huczynski, S. Rehlis, and J. Markowska, "Ovarian cancer stem cells: a target for oncological therapy," *Advances in Clinical and Experimental Medicine*, vol. 27, no. 7, pp. 1017–1020, 2018.

[4] R. L. Siegel, K. D. Miller, S. A. Fedewa et al., "Colorectal cancer statistics, 2017," *CA: a Cancer Journal for Clinicians*, vol. 67, no. 3, pp. 177–193, 2017.

[5] M. E. Bregenzer, E. N. Horst, P. Mehta, C. M. Novak, T. Repetto, and G. Mehta, "The role of cancer stem cells and mechanical forces in ovarian cancer metastasis," *Cancers (Basel)*, vol. 11, no. 7, p. 1008, 2019.

[6] H. D. Liu, B. R. Xia, M. Z. Jin, and G. Lou, "Organoid of ovarian cancer: genomic analysis and drug screening," *Clinical & Translational Oncology*, vol. 22, no. 8, pp. 1240–1251, 2020.

[7] A. J. Cortez, P. Tudrej, K. A. Kujawa, and K. M. Lisowska, "Advances in ovarian cancer therapy," *Cancer Chemotherapy and Pharmacology*, vol. 81, no. 1, pp. 17–38, 2018.

[8] V. Gogineni, S. Morand, H. Staats et al., "Current ovarian cancer maintenance strategies and promising new developments," *Journal of Cancer*, vol. 12, no. 1, pp. 38–53, 2021.

[9] S. Morand, M. Devanaboyina, H. Staats, L. Stanbery, and J. Nemunaitis, "Ovarian cancer immunotherapy and personalized medicine," *International Journal of Molecular Sciences*, vol. 22, no. 12, p. 6532, 2021.

[10] T. T. Quinn, G. S. Miller, M. Rostek, M. S. Cabalag, W. M. Rozen, and D. J. Hunter-Smith, "Prosthetic breast

Hindawi
Computational and Mathematical Methods in Medicine
Volume 2023, Article ID 9838096, 1 page
https://doi.org/10.1155/2023/9838096

Retraction

Retracted: Identification of Prognostic Signature of Necroptosis-Related lncRNAs and Molecular Subtypes in Glioma

Computational and Mathematical Methods in Medicine

Received 5 December 2023; Accepted 5 December 2023; Published 6 December 2023

This article has been retracted by Hindawi, as publisher, following an investigation undertaken by the publisher [1]. This investigation has uncovered evidence of systematic manipulation of the publication and peer-review process. We cannot, therefore, vouch for the reliability or integrity of this article.

Please note that this notice is intended solely to alert readers that the peer-review process of this article has been compromised.

Wiley and Hindawi regret that the usual quality checks did not identify these issues before publication and have since put additional measures in place to safeguard research integrity.

We wish to credit our Research Integrity and Research Publishing teams and anonymous and named external researchers and research integrity experts for contributing to this investigation.

The corresponding author, as the representative of all authors, has been given the opportunity to register their agreement or disagreement to this retraction. We have kept a record of any response received.

References

[1] G. Zhang, R. Chen, L. Zhu et al., "Identification of Prognostic Signature of Necroptosis-Related lncRNAs and Molecular Subtypes in Glioma," *Computational and Mathematical Methods in Medicine*, vol. 2022, Article ID 3440586, 21 pages, 2022.

Hindawi
Computational and Mathematical Methods in Medicine
Volume 2022, Article ID 3440586, 21 pages
https://doi.org/10.1155/2022/3440586

Research Article

Identification of Prognostic Signature of Necroptosis-Related lncRNAs and Molecular Subtypes in Glioma

Guanghao Zhang, Rundong Chen, Luojiang Zhu, Hongyu Ma, Haishuang Tang, Chenghao Shang, Jing Wang, Deyu Zhang, Qiang Li, and Jianmin Liu

Neurovascular Center, Changhai Hospital, Naval Medical University, Shanghai 200003, China

Correspondence should be addressed to Qiang Li; lqeimm@126.com and Jianmin Liu; cnc@smmu.edu.cn

Received 5 July 2022; Revised 28 July 2022; Accepted 4 August 2022; Published 5 September 2022

Academic Editor: Min Tang

Background. In tumor progression and epigenetic regulation, long non-coding RNA (lncRNA) and necroptosis are crucial regulators. However, in glioma microenvironment, the role of necroptosis-related lncRNAs (NRLs) remains unknown. *Method*. In this study, the RNA-seq and clinical annotation of glioma patients were analyzed using the Cancer Genome Atlas (TCGA) and Chinese Glioma Genome Atlas (CGGA) databases. To investigate prognosis and tumor microenvironment of NRLs in gliomas, we conducted a prediction model based on the training cohort. The accuracy of the model was verified in the verification cohort. *Results*. A signature composed of 13 NRLs was identified, and all glioma patients were divided into two groups. We found that each group has unique survival outcomes, biological behaviors, and immune infiltrating status. The necroptosis-related lncRNA signature (NRLS) model was found to be an independent risk factor in multivariate Cox analysis. Immunosuppressive microenvironment was positively correlated with the high-risk group. Due to significantly different IC50 between risk groups, NRLS could be used as a guide for chemotherapeutic treatment. Further, the entire cohort was divided into two clusters depending on NRLs. Consensus clustering method and the risk scoring system were basically similar. Survival probability was higher in Cluster 2, while Cluster 1 has stronger immunologic infiltration. *Conclusion*. The predictive signature could be a prognostic factor independently and serve to detect the role of NRLs in glioma immunotherapy response.

1. Introduction

Glioma is the most frequently diagnosed malignant tumor in the central nervous system (CNS), accounting for about 30% of primary brain tumors and 80% of malignant brain tumors [1]. The latest 2021 WHO Classification of Tumors of the Central Nervous System integrated histological features and molecular phenotypes of tumors and further proposed the new tumor classification criteria, which focus on advancing the application of molecular diagnosis in the classification of CNS tumors [2]. In recent decades, molecular markers, including the isocratic dehydrogenase (IDH) mutation, the codeletion of chromosome arms 1p and 19q (1P/19q codeletion), and the H3 G34 mutant, have been demonstrated that play a significant role in the classification, grading, prognosis and treatment of gliomas [3–5]. However, these markers have limited sensitivity and accuracy [6]. On the other hand, multimodal treatment, including maximum surgical resection assisted by radiotherapy and simultaneous chemotherapy with temozolomide, has made great progress [7, 8]. However, some glioma patients are still resistant to current treatment strategies due to the presence of an immunosuppressive tumor microenvironment (TME) and tumor heterogeneity. The clinical outcomes of these patients are still unsatisfactory. Especially for glioblastoma, the median survival time was only 16 months [9]. As a result, it is critical to develop novel prognostic biomarkers and individualized molecular targets.

Necroptosis, a type of programmed cell death, was initially identified as a viable alternative to apoptosis due to the presence of death domain receptors [10]. Necroptosis differs from apoptosis and other forms of programmed cell necrosis in that it is not dependent on caspase activity. Instead, it requires RIPK3-dependent phosphorylation of MLKL [11]. This phosphorylation event causes MLKL to

produce large pores on the plasma membrane, which leads to damage-associated molecular patterns (DAMP) secretion, cell swelling, and membrane rupture. During necroptosis, different stages of cell disassembly can be observed, including organelle swelling, membrane rupture, and disassembly of the cytoplasm [12]. The expression of several key molecules associated with necroptosis, including CYLD, RIPK3, and MLKL, has been reported to be downregulated in some tumors [13], suggesting that cancer cells tend to escape from the necroptotic pathway. However, it has also been demonstrated that induction of necroptosis in tumor cells is not necessarily beneficial, cell rupture resulting from necroptosis and release of cell contents may act as a pro-inflammatory agent, in turn promoting tumor cell growth, angiogenesis, invasion, and metastasis [14].

In a word, the overall effect of necroptosis or its interaction with the surrounding environment on tumor progression remains to be investigated in different tumor microenvironments.

lncRNAs are a subclass of non-coding RNA with a length of up to 200 nucleotides that is abundant in organisms. Increasing evidence reports that lncRNAs are associated with malignant progression of glioma [15]. For instance, by binding to miR-302a, lncRNA HOXA-AS2 promotes KDM2A/JAG1 expression, thereby facilitating Treg cell proliferation and immune tolerance in glioma [16]; lncRNA.

NEAT1 activates NF-κB and PD-L1 to promote immune evasion by interacting with PTRF in glioblastoma [17](p1). On the other hand, numerous studies indicated that lncRNAs could also regulate necroptosis by acting as competitive endogenous RNA and influencing target gene expression. For example, LncCRLA overexpression inhibited necroptosis in lung adenocarcinoma cells via binding to the RIPK1 intermediate domain and then disrupting the RIPK1–RIPK3 interaction [18]. Besides lncRNAs associated with necroptosis, several lncRNAs associated with aging, pyroptosis, and 5-methylcytosine have been extensively reported in recent years [19–21]. Given NRLs are highly heterogeneous in terms of tumor phenotype and function, their function in glioma microenvironment is worth being fully investigated.

This study focused on the NRLs in glioma. We analyzed the RNA-seq data in TCGA and CGGA cohorts and identified 13 NRLs highly related to the prognosis of glioma patients. Based on this result, we construct a signature of NRLs and tried to regroup patients based on NRLS. Importantly, we found that each group has unique survival outcomes, biological behaviors, immune infiltrating status, and chemosensitivity. Moreover, we conducted a prediction model for predicting prognosis and verified that this model has excellent capability to predict the clinical outcomes of patients. We hope that this NRLS may serve as unique reference for the precision treatment and prognosis evaluation development of glioma.

2. Materials and Methods

2.1. Data Collection. The RNA sequencing counts matrix, including 663 samples (LGG+GBM) with paired clinical annotation as the training data, was obtained through Xena platform (http://xena.ucsc.edu/) [22]. Analogously, the RNA transcriptome count matrix of normal samples from the Genotype-Tissue Expression (GTEx) was retrieved. RNA-sequencing of TCGA-Glioma and GTEx-Brain were merged using the function "removeBatchEffect()" in "limma R" package to perform further analysis. The validation cohorts were obtained from the Chinese Glioma Genome Atlas (CGGA), which included mRNA count matrix and clinical annotation for 1018 samples (mRNAseq 693 +mRNA seq325) [23]. Patients who did not receive follow-up or whose overall survival (OS) was less than 30 days were removed.

2.2. Identification of Necroptosis-Related Gene and lncRNA. From recent publications, a list of 67 necroptosis-related genes from previous literature was obtained (Table S1). The "Deseq2" package was performed to obtain differentially expressed gene (DEGs) between merged TCGA-Glioma and GTEx-Brain, the |Log2FC| >2, and the adjusted P-value (adj. P) <0.05 as the screening condition. Then, we obtained 20 genes that overlapped between DEGs and necroptosis-related genes for further analysis. lncRNAs annotation according to the genome references consortium human build 38 was downloaded from the GENCODE website (http://www.gencodegenes.org/). Finally, 14086 lncRNAs from TCGA and 14086 lncRNAs from CGGA were identified. Pearson's correlation analysis among necroptosis-related genes and lncRNAs was utilized to get the necroptosis-related lncRNAs in both cohorts (TCGA and CGGA) with a threshold coefficient $|r| > 0.5$ and $P < 0.001$. Next, the repeated genes were applied to univariate Cox regression in two cohorts with a threshold of $P < 0.001$. For further analyses, we intersected the lncRNAs screened from the TCGA and CGGA cohorts. Subsequently, a total of 43 reliably expressed lncRNAs were detected.

2.3. Development and Validation of Necroptosis-Related lncRNAs Prognostic Signature. To determine the optimal coefficients for each prognostic signature, the LASSO Cox regression model was applied in TCGA training cohort [24]. LASSO coefficients were determined at one standard error (lamda 1SE) of the minimum mean cross-validation errors. The formula was given as follows:

$$\text{risk score} = \sum_{n=1}^{n} \beta_n \times x_n. \quad (1)$$

β_n means the LASSO regression coefficient for each lncRNA, and x_n denotes the expression profile of the selected lncRNA. With the assistance of "survminer" package, after the optimum cut-off value for the risk score was determined, patients were classified as high-risk or low-risk groups. Similarly, using the optimum cut-off value of the training cohort, we separated CGGA patients into high-risk and low-risk groups based on NRLS model to evaluate the accuracy of the prognostic signature. Then, we evaluated the survival difference between the two groups through the

Kaplan–Meier (KM) survival analysis and the log-rank test in the training and validation cohorts.

2.4. Independent Prognostic Analysis of Risk Scores Based on the TCGA and CGGA Datasets. We developed univariate Cox and multivariate Cox regression analyses to evaluate whether the risk score and clinicopathologic data (age, gender, grade, IDH status, and p/19q status) were independent variable factors in TCGA and CGGA cohorts. "forestplot" package was used to visualize the results of multiple multivariate Cox regression. We established a predictive model and nomogram to predict patient prognosis. To assess the predictive accuracy of this model at different time point, time-dependent receiver operating characteristic (ROC) curves were applied via "survivalROC" R package, and the area under the curve (AUC) values demonstrated distinction of this model.

2.5. Gene Set Enrichment Assessment. The cut-off values (|log2FC|≥2 and adj.*P*.Val<0.01) were used to distinguish the differential genes between high- and low-risk groups in TCGA cohort. Then, the DEGs were sorted according to the difference multiple. GSEA was conducted to examine discrepancies, related pathways, and biological processes between both risk groups. The enrichment degree and significance of DEGs in KEGG, GO, and Hallmark gene sets were calculated via the configuration of the "clusterProfiler" R package. The above three gene sets were downloaded from the Molecular Signatures Database (http://www.gsea-msigdb.org).

2.6. Tumor Immune Microenvironment (TIME) Analysis in Glioma. TIME reflects several terms, including immune cell infiltration, immune checkpoint expression profile, and levels of the anti-cancer immunity cycle [25]. Immune infiltration abundance of each sample from TCGA was quantified from 7 algorithms including CIBERSORT, XCELL, QUANTISEQ, TIMER, EPIC, and MCPcounter. Correlation of risk score with immune cell subpopulations was conducted by the Spearman correlation test. We use a bubble chart to visualize the result. To figure out stromal cells and immune cell abundance, "ESTIMATES" package was used to calculate the Stromalscore, Immunescore, and EstestimateScore. According to previous research, evaluation of anticancer immunity cycle includes 7 steps [26], and these steps can be quantified for single-sample Gene Set Enrichment Analysis (ssGSEA) based on the expression level of related genes in each sample. Every step was set to a value that indicated the degree of antitumor immunity upregulation. A boxplot depicts the expression level of immune checkpoints in low- and high-risk groups. In addition, to investigate the immunotherapeutic response, Tumor Immune Dysfunction and Exclusion (TIDE) web tool (http://tide.dfci.harvard.edu/) was employed to determine related scores of TIDE for every sample.

2.7. Sensitivity of Chemotherapeutic Agents Assessment. The Genomics of Drug Sensitivity in Cancer (GDSC; https://www.cancerrxgene.org/) website was applied to predict the sensitivity of each sample to chemotherapeutic agents. The half maximal inhibitory concentration (IC50) was determined using ridge regression and R package "pRRophetic."

2.8. Consensus Clustering. To decode the heterogeneity of patients based on 13 necroptosis-related lncRNAs. TCGA and CGGA cohorts were divided into two clusters via "ConsensusClusterPlus" R package with the parameters of 500 iterations and resample rate of 0.9. Then, the Kaplan–Meier survival was performed to evaluate the discrimination of consensus clustering and survival difference. Finally, a heat map was conducted to visualize the degree of immune infiltration between the two clusters.

2.9. Validations of Selected lncRNAs Using Quantitative Real-Time (qRT-PCR) in Tissue Samples. Five lncRNAs were chosen to verify the expression difference between non-tumor brain tissue and glioma. All glioma specimens and non-tumor brain tissues were obtained from the Department of Neurosurgery of Changhai Hospital between August 2021 and January 2022, including five non-tumor brain tissues, three WHO grade 2, three WHO grade 2, and four GBM. Non-tumor brain tissues were from patients who underwent temporal lobectomy for intractable epilepsy. All activities conducted with patient specimens collected were authorized by the Medical Ethics Committee of our hospital. Total RNA extraction was conducted via Trizol reagent. cDNA was synthesized according to the instruction of PrimeScriptTMRT Master Mix Kit. Next, qRT-PCR was conducted using LightCycler 480 real-time PCR system. GAPDH served as an internal control, while $2^{-\Delta\Delta Ct}$ method was used to standardize the results. The sequences of the primers were reported in Table S5.

3. Results

3.1. Screen of Prognostic NRLs in Glioma Patients. Figure 1(a) depicts the study's workflow. We first analyze the differences between glioma and normal samples to determine abnormally expressed necroptosis-related genes in glioma (Table S2). 20 genes were figured out, and 95.0% of these genes (19/20) were upregulated in glioma samples (Figures 1(b) and 1(c)). Next, Pearson's correlation analysis with Pearson's coefficient $|r| > 0.5$ and $P < 0.001$ retained a small number of intersected lncRNAs in TCGA and CGGA cohorts (Figure 1(d)). In the meantime, we performed univariate Cox analysis in each cohort and identified 43 intersecting lncRNAs related to prognosis (Figure 1(e) and Table S3).

3.2. Development and Verification of NRLs. To eliminate collinearity, 43 NRLs were included in LASSO Cox regression. According to lamda 1SE, 13 lncRNA with poor prognosis in glioma were selected to determine the risk score (Figures 2(a) and 2(b), Figure S1). The corresponding coefficient value was exhibited in Figure 2(c). To stratify samples into different risk groups, the optimal cut-off value derived from risk score in training cohort was determined using "survminer" R package (Figure S2). Based on the cut-off value, we divided the glioma patients into high-risk and low-risk groups. As visualized in KM survival analysis

FIGURE 1: Identifying prognostic genes for developing a risk model. (a) A workflow of study. (b) Volcano plot of differentially expressed genes analysis in glioma (TCGA cohort) compared with normal brain (GTEx). (c) Gene expression heat map. (d) Heat map showed the correlation of 20 necroptosis related with 43 lncRNAs. (e) Forest plot of the prognostic lncRNAs extracted by univariate Cox regression analysis.

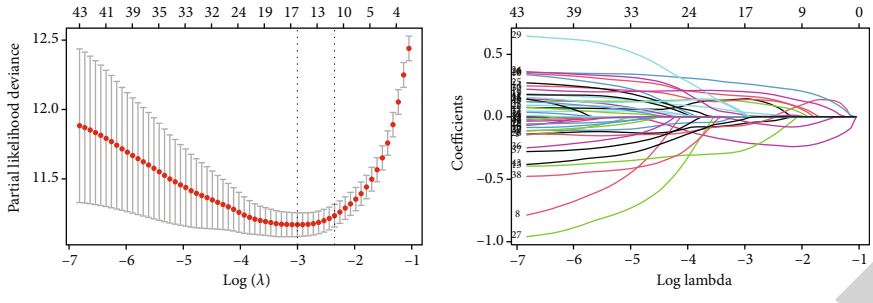

(a) (b)

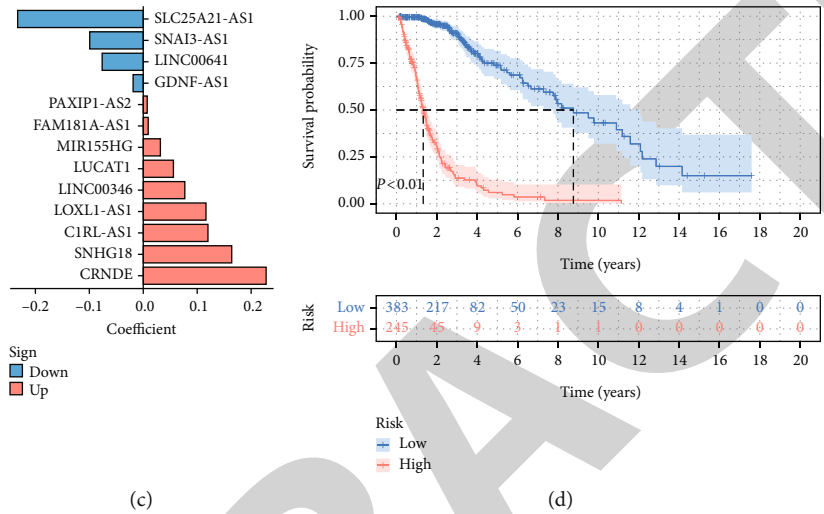

(c) (d)

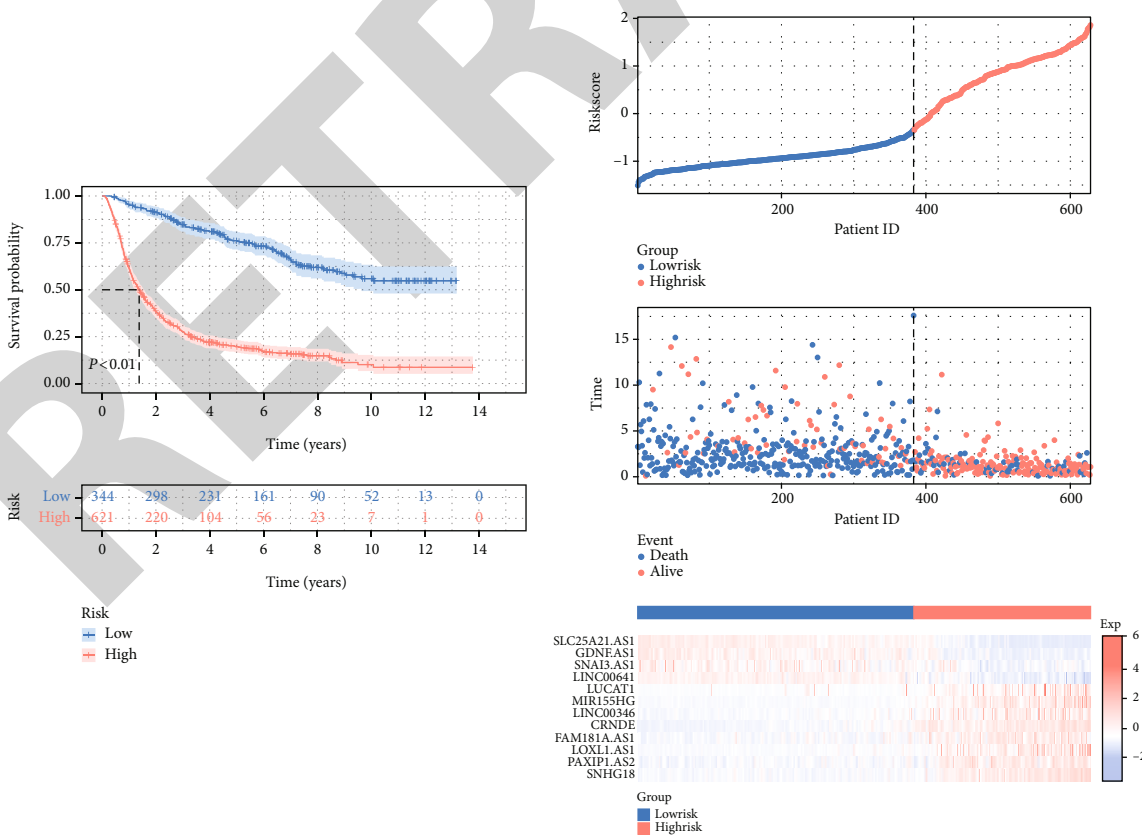

(e) (f)

Figure 2: Continued.

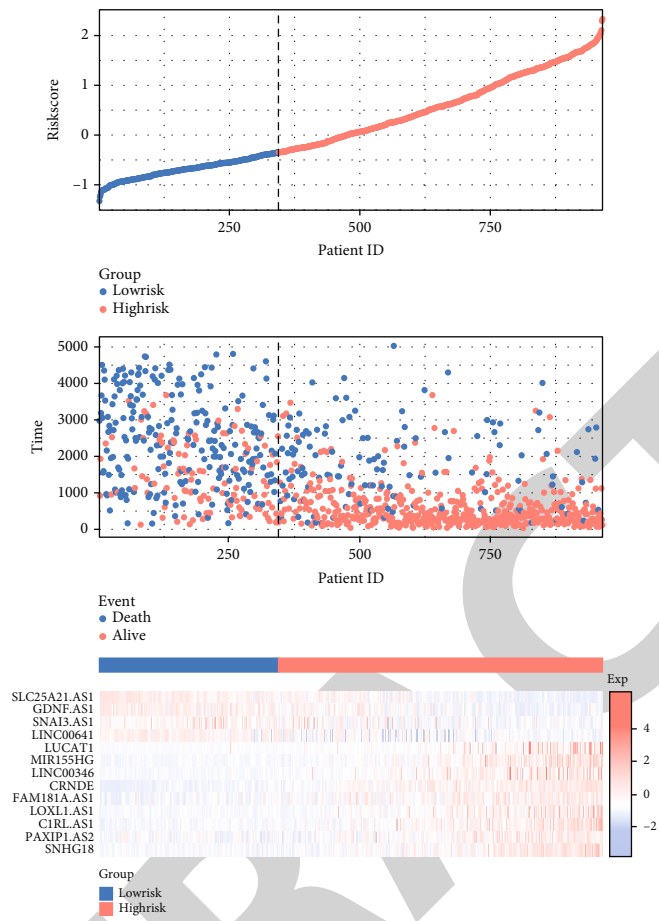

(g)

Figure 2: Development and validation of NRLs. (a) LASSO cox regression of 13 NRLs. (b) Cross-validation for tuning the parameter selection in the LASSO regression. (c) Coefficient of model regression. (d) Kaplan-Meier curves of high-risk group and low-risk group in TCGA. (e) Kaplan-Meier curves of high-risk group and low-risk group in CGGA. (f) Distribution of risk score and patients based on the risk score and heat map of 13 NRL expressions in TCGA. (g) Distribution of risk score and patients based on the risk score and heat map of 13 NRL expressions in CGGA.

for training and validation cohort, low-risk group had better survival outcomes than high-risk group (Figures 2(d) and 2(e)). Moreover, distributions of risk gene expression, risk score, and gene expression profile were plotted in TCGA and CGGA cohorts (Figures 2(f) and 2(g)). All these results indicated that risk score depending on NRLS could be an acceptable indicator in predicting the clinical outcome of glioma patients. Besides, whether the risk score can be used in different subgroups of glioma samples was exhibited in (Figures 3(a)–3(p)). We observed that the risk scoring system performed well in predicting the survival outcome of patients with different clinical situations. From the above results, the prediction potential of the risk scoring system based on NRLS was revealed.

3.3. Independent Predictive Ability of the NRLS in TCGA and CGGA. Univariate and multivariate Cox regression analyses were performed to verify whether the prediction signature is independent within both training and validation cohorts. Univariate Cox regression shows risk score, grade, age, and histology subtype in each cohort were significantly related to prognosis (Figure S3). Meanwhile, according to multivariate Cox regression, risk score could be a prognostic factor for both training and validation cohorts (Figures 4(a) and 4(b)). Thus, a prediction model and a nomogram were established. The sum of clinical parameters and risk scores could be used to predict 1-, 3-, and 5-year survival probabilities (Figure 4(c)). The area under the curve (AUC) for predicting 1-, 3-, and 5-year survival in TCGA were 0.88, 0.92, and 0.86, and in CGGA were 0.77, 0.83, and 0.84, respectively, which illustrated the precision of the prediction model is relatively high. Calibration curves at 1, 3, 5 years were plotted and attest proper consistency between actual survival and predicted survival from nomogram in both cohorts (Figures 4(f)–4(k)).

3.4. Analysis of Gene Set Enrichment. In order to have insights into the functional annotation of DEGs between different expression profiles, difference analysis was performed in high-risk and low-risk groups (Table S4). Then, GSEA is applied using gene ontology (GO), Kyoto Encyclopedia of Genes and Genomes (KEGG), and Hallmark gene sets. We selected terms

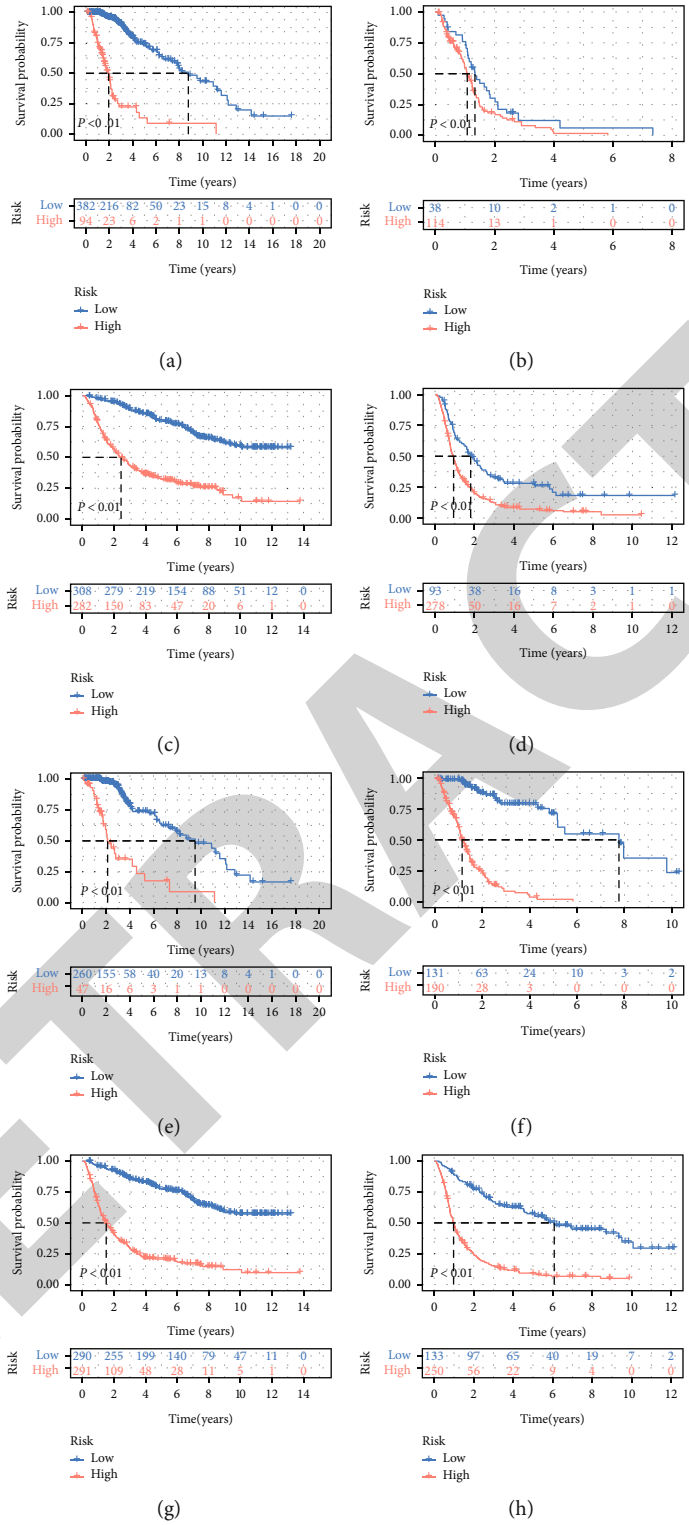

Figure 3: Continued.

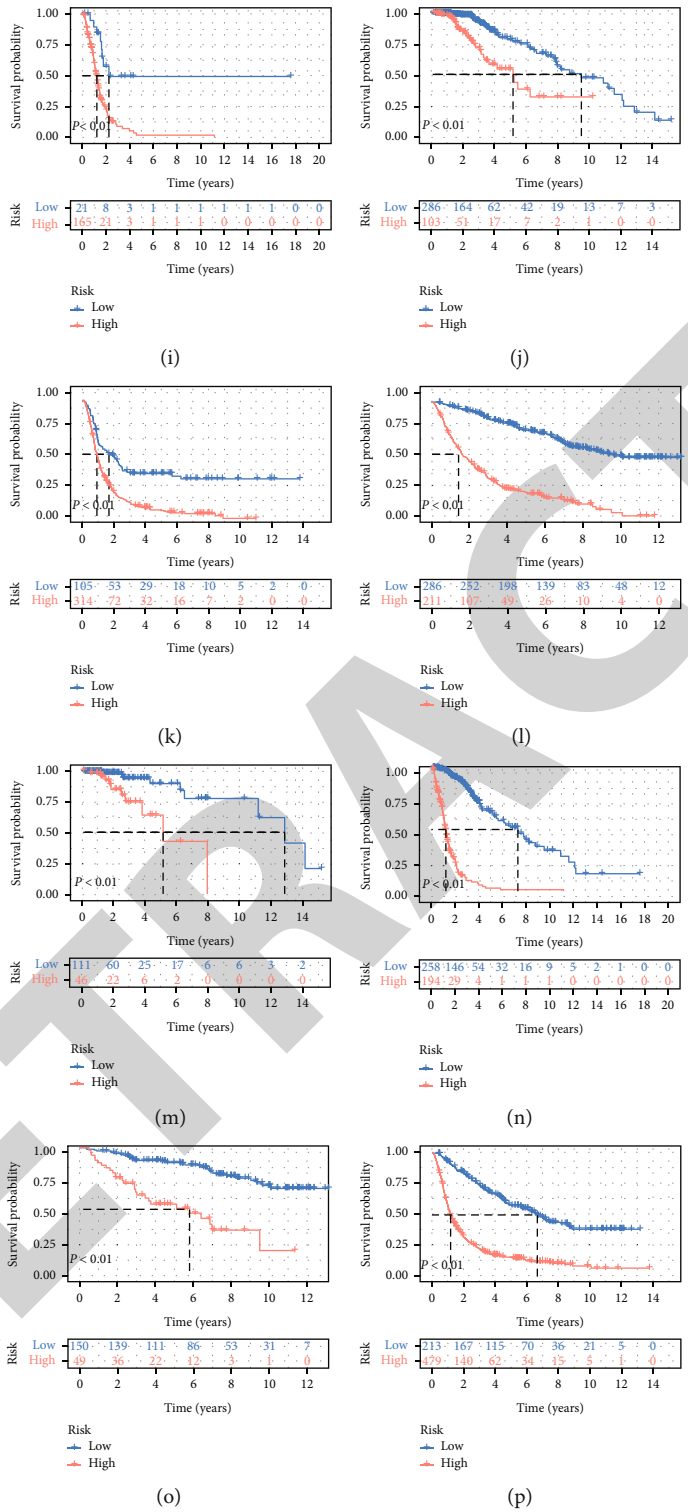

Figure 3: Subgroup analysis of high- and low-risk groups. (a) LGG in TCGA. (b) GBM in TCGA. (c) LGG in CGGA. (d) GBM in CGGA. (e) Young (age<45) in TCGA. (f) Old (age ≥45) in TCGA. (g) Young (age<45) in CGGA. (h) Old (age ≥45) in TCGA. (i) IDH wildtype in TCGA. (j) IDH mutant in TCGA. (k) IDH wildtype in CGGA. (l) IDH mutant in CGGA. (m) 1p9ql codeletion in TCGA. (n) 1p19ql non-codeletion in TCGA. (o) 1p9ql codeletion in CGGA. (p) 1p19ql non-codeletion in CGGA.

with adjusted P value > 0.01 and |NES|>1.5 for further analysis. We observed that high-risk group enriched multiple immune-related terms including IL2-STAT5 signaling, IL6-JAK-TAT3 signaling, and inflammatory response in Hallmark set (Figure 5(a)). Similarly, the results of KEGG and GO were also enriched in immune-related and oncogenic processes (Figures 5(b) and 5(c)). These results indicated distinct immune statuses in high-risk and low-risk groups.

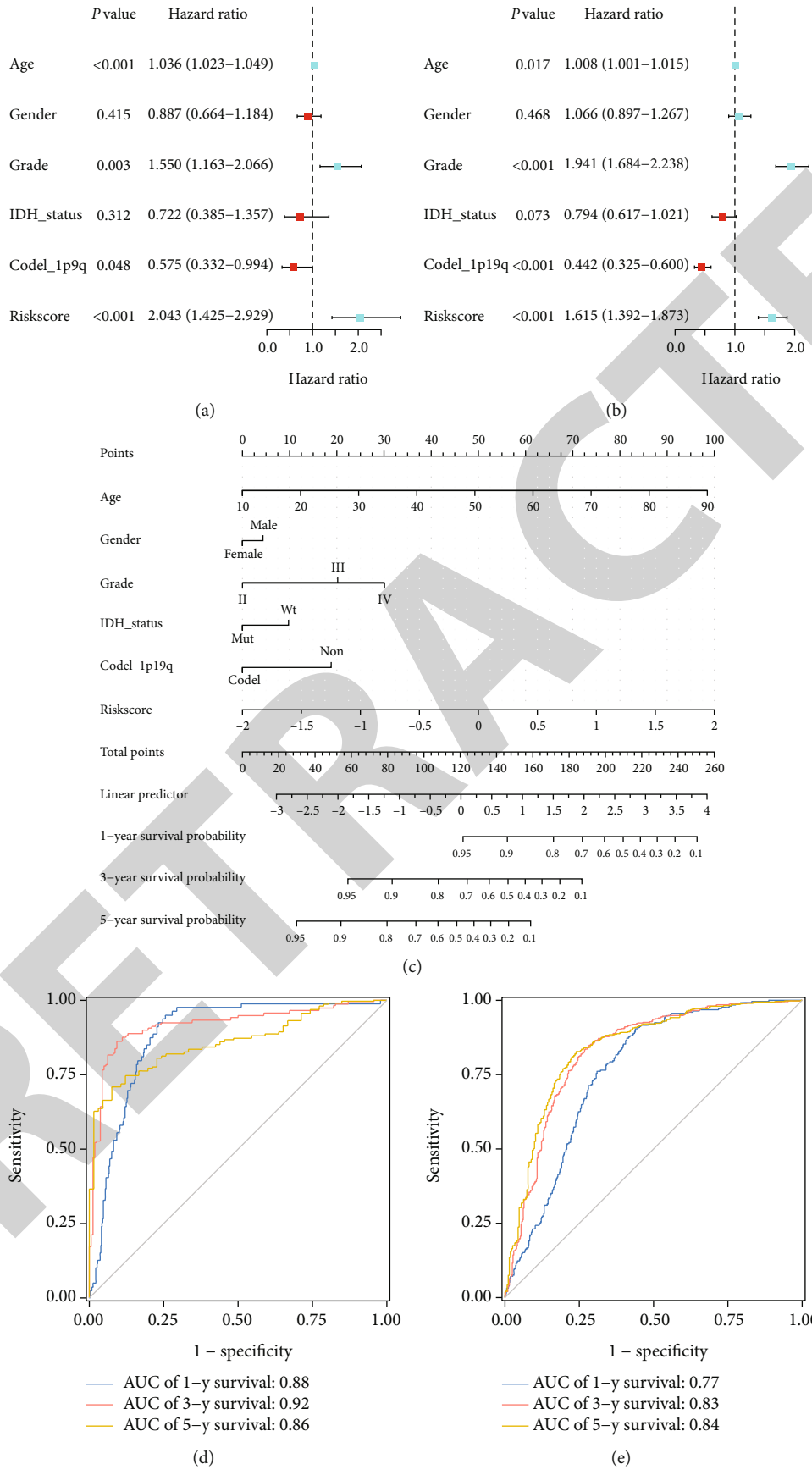

Figure 4: Continued.

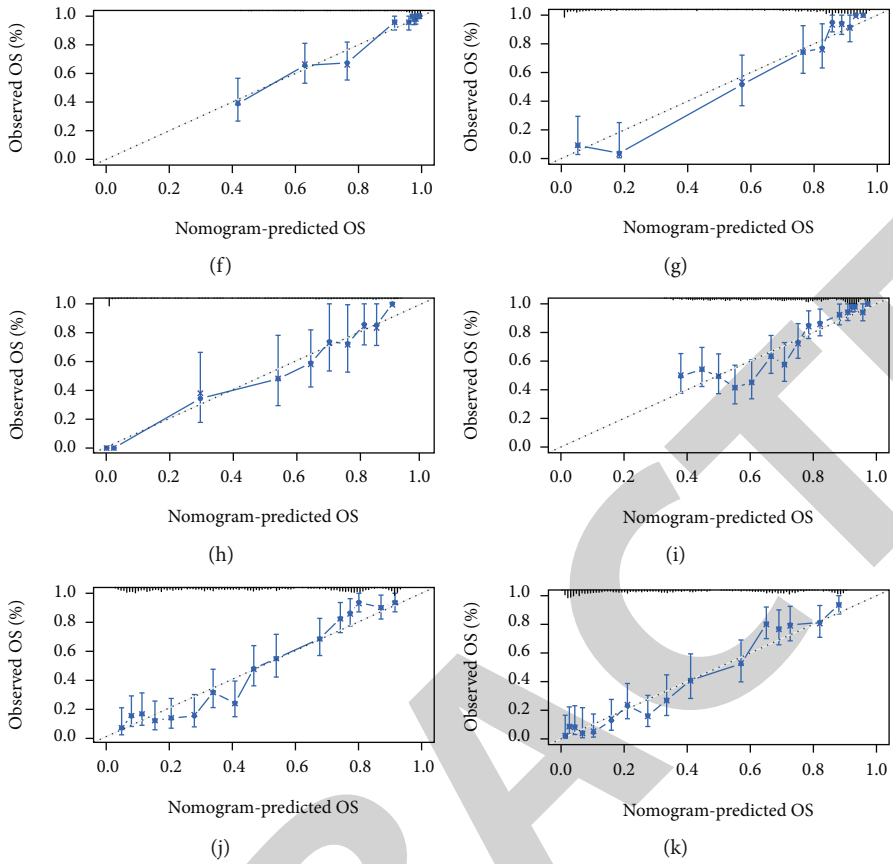

Figure 4: Independent prognosis analysis of risk score. (a, b) Multivariate COX Forest plot of risk score in TCGA and CGGA. (c) Nomograph plot of predicted 1-, 3-, and 5-year overall survival probability based on prognosis lncRNAs. (d) ROC curves of prognostic signature based on risk score in TCGA. (e) ROC curves of prognostic signature based on risk score in CGGA. (f–h) Calibration plots of the nomogram for predicting the probability of OS at 1, 3, and 5 years in TCGA. (i–k) Calibration plots of the nomogram for predicting the probability of OS at 1, 3, and 5 years in CGGA.

3.5. The Investigation of Immunity Factors in Risk Groups. Previous research indicated that necroptosis plays an important role in tumor immunotherapy [27]. To evaluate the heterogeneous immune condition between both risk groups, immune cell distribution of patients in TCGA cohort was analyzed using the CIBERSORT protocol; the result shows that, in the high-risk group, immune cells such as Tregs, resting NK cells, and M2 macrophages are significatively high (Figure 5(d)). Through applying correlation analysis, a positive correlation was revealed between the abundance of M2 macrophage cells and the abundance of CD8+ T cells ($r^2 = 0.59$). Moreover, Tregs were positively correlated with resting NK cells ($r^2 = 0.60$), and resting T cell CD4+ memory was negatively correlated with B cell plasma ($r^2 = -0.41$) (Figure 5(e)). Furthermore, we used various algorithms to investigate the relationship between risk score and the quantitative value of immune infiltration, we selected P value<0.001 to study further, the results obtained from the preliminary analysis are shown in Figure 5(f), more immune-suppressive cells such as cancer-associated fibroblast, M2 macrophage, Treg cell, T follicular helper cells, and T cell CD4+ Th2 are positively related to the risk score on different platforms, whereas NK cell activated cell, Monocyte, and CD4+ Th1 cells are neglective related to the risk score. Meanwhile, Spearman's correlation analysis showed that there were significant positive correlations between immune, stromal, and ESTIMATE scores as defined by "Estimate" package and risk score (Figures 5(g)–5(i)). Potential differences in immune microenvironment components between high-risk and low-risk groups were revealed based on this result.

3.6. Cancer Immunity Cycle and Immunotherapy Response Analysis in Risk Groups. The term "cancer immunity cycle" refers to the series of events that lead to an effective anticancer immune response [26]. Immunotherapy is based on the establishment or reestablishment of the cancer immunity cycle. We calculated the activity related to tumor circulation. The result is somewhat counterintuitive, although high-risk group demonstrated significantly stronger activity than low-risk group in several steps, including release of cancer cell antigens (step 1), CD8 T cell recruitment (step 4.3), and recognition of cancer cells by T cells (step 6); the high-risk group demonstrated significantly less activity in killing cancer cells (step 7) (Figure 6(a)). This phenomenon may be explained by the positive correlation between immune checkpoints and risk score, such as PD-L1

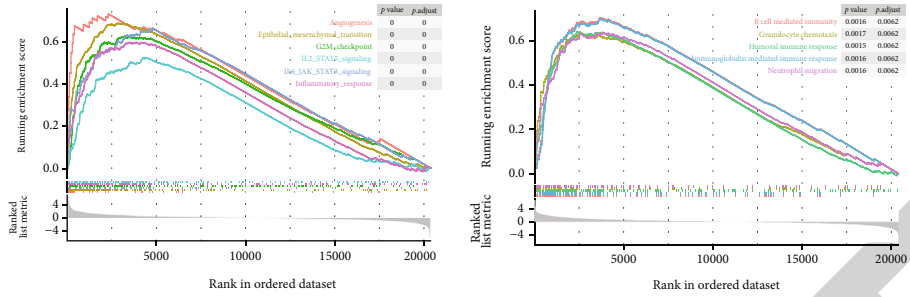

(a) (b)

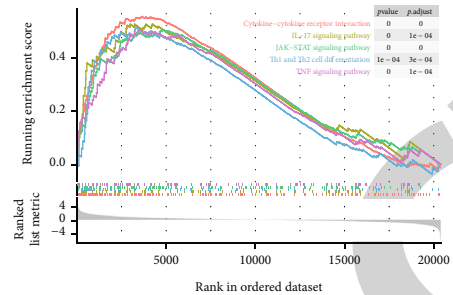

(c)

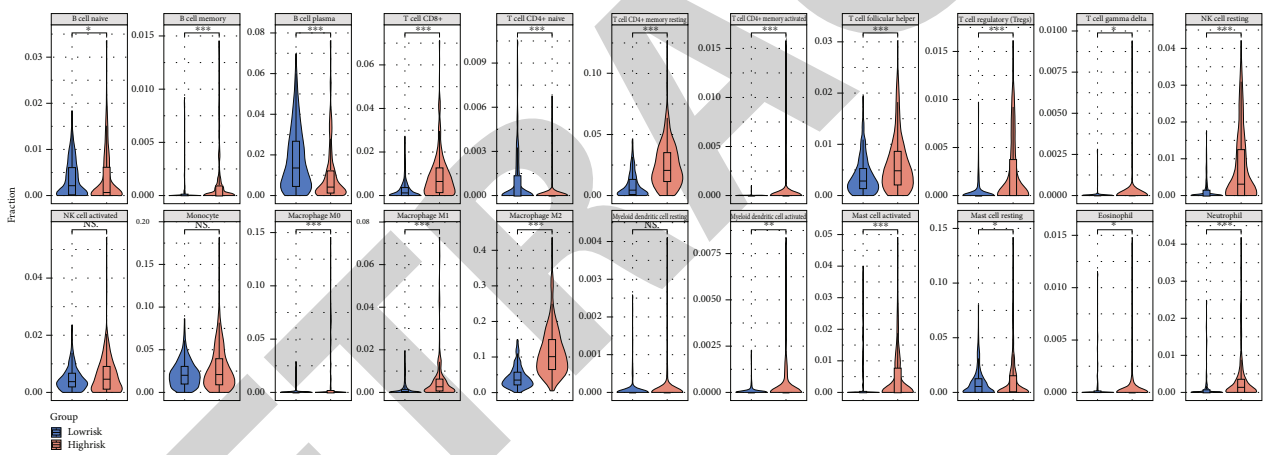

(d)

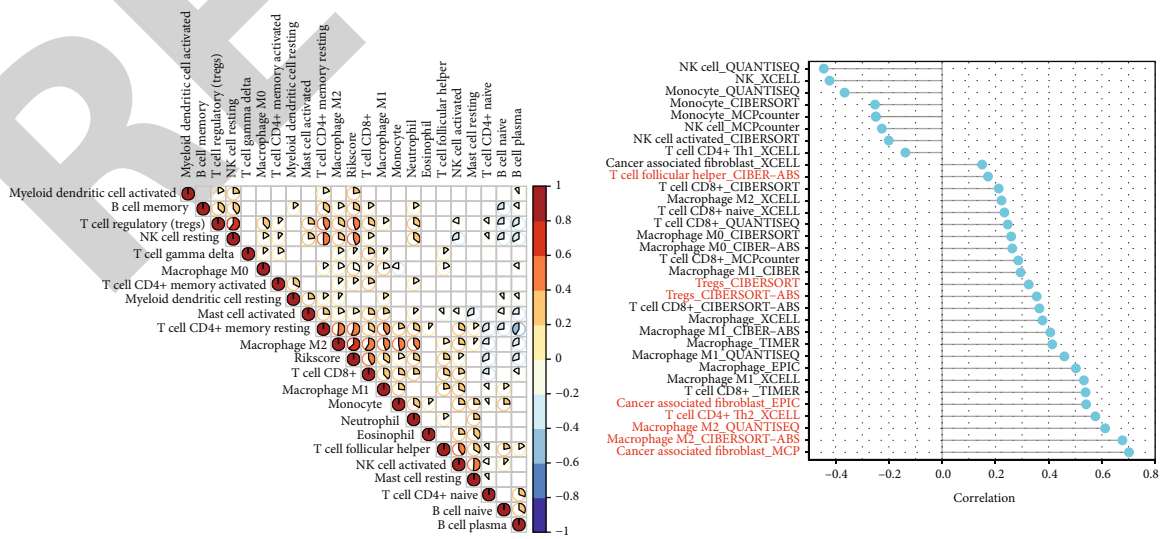

(e) (f)

Figure 5: Continued.

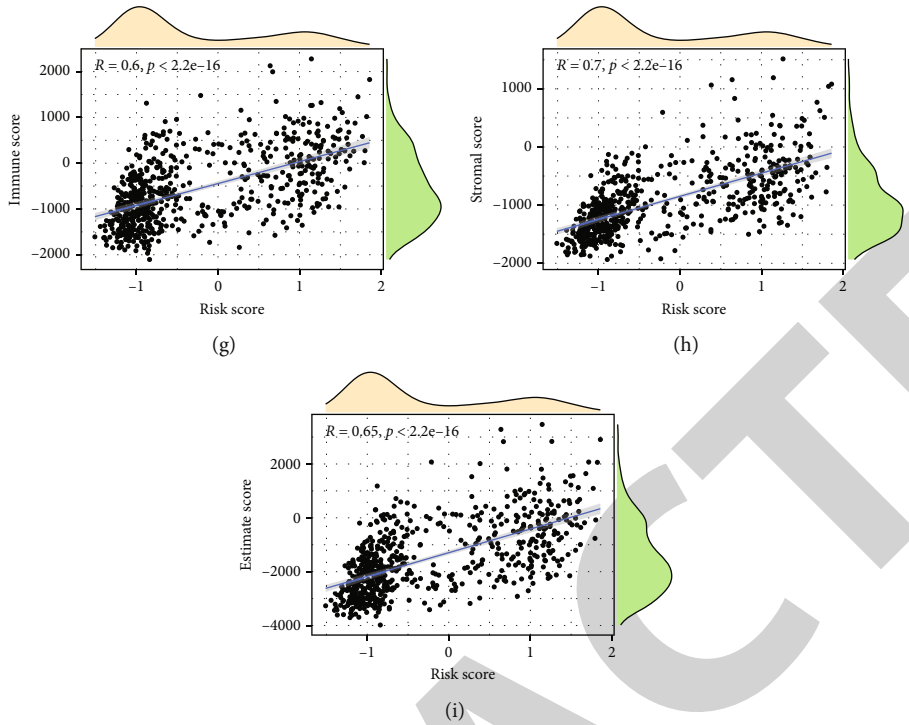

Figure 5: Functional and enrichment pathways and immune microenvironment analysis. (a–c) HALLMARK, GO (BP), KEGG pathway enrichment analyses in high-risk group. (d) The relationship between risk score and immune cell infiltration score. (e) Correlation of 22 types of immune cell subsets in the TCGA cohort. (f) The immune cell bubble of risk groups. (g–i) Correlation between risk score with immune score, stromal score, and ESTIMATE score.

(CD274), PD1 (PDCD1), and CTLA4 (Figures 6(b) and 6(c)). These findings indicated that high-risk group exerted a strong immune-suppressive microenvironment. Thus, we used "TIDE" web tool to predict the immune therapy response. We found that the high-risk group had significantly more immune dysfunction than low-risk group, and there was no significant difference in immune exclusion between the two groups (Figures 6(e) and 6(f)). In addition, TIDE score of high-risk group was significantly higher than that of the low-risk group (Figure 6(g)). These results suggested that the low-risk group is more susceptible to immunotherapy.

3.7. Necroptosis-Related lncRNA Signature in Prediction of Chemotherapeutics Response. Furthermore, we predicted the response of patients to 6 chemotherapeutic drugs including A-443654 (Akt inhibitor), Gefitinib (EGFR inhibitors), Temsirolimus (mTOR inhibitor), Trametinib (MEK inhibitor), Bortezomib (proteasome inhibitor), and Pazopanib (VEGF inhibitor). As illustrated in Figures 7(a)–7(f), the estimated IC50 values for selected agents were lower in patients with high-risk than low-risk group. These results may provide basis for the precise medication of glioma patients.

3.8. Molecular Classification Based on NRLs. Consensus clustering was used to regroup TCGA and CGGA cohorts for the expression profile of NRLs. According to the clustering heat maps and CDF curve, the optimal clustering number was determined to be $k=2$ (Figure 8(a)). Meanwhile, principal component analysis (PCA) and t-Distributed Stochastic Neighbor Embedding (t-SNE) method plotted patients in two-dimensional coordinate systems to demonstrate that the two clusters in the training and verification cohorts could be obviously distinguished (Figure 8(b), Fig S4). Cluster 1 demonstrated worse overall OS compared to Cluster 2 ($P < 0.01$) (Figure 8(c)). The alluvial diagram depicted the distribution of TCGA cohort across clusters and risk groups (Figure 8(d)). Moreover, the risk score for Cluster 1 was significantly higher than Cluster 2 (Fig S5). These results suggested potential differences in biological behavior and tumor microenvironment components between Cluster 1 and Cluster 2. Figure 8(e) shows a heat map of immune infiltrated cells generated utilizing various algorithms. We observed that Cluster 1 has stronger immune infiltration than Cluster 2. It might result in different immunotherapeutic responses. Therefore, we could consider Cluster 1 was more susceptible to immunotherapy.

3.9. Validation of the Expression of Selected NRL. We selected five NRLs to observe the difference in relative expression between glioma and non-tumor brain tissues, including LOXL1-AS1, CRNDE, FAM181A-AS1, SNAI3-AS1, and LINC00641. The result is shown in Figure 9; LOXL1-AS1, CRNDE, and FAM181A-AS1 were upregulated with the increase of glioma malignancy, while SNAI3-AS1 and LINC00641 were downregulated. This result is consistent with what we found in our bioinformatics analysis, suggesting that the signature based on NRLs could be used to predict the clinical outcome in glioma patients.

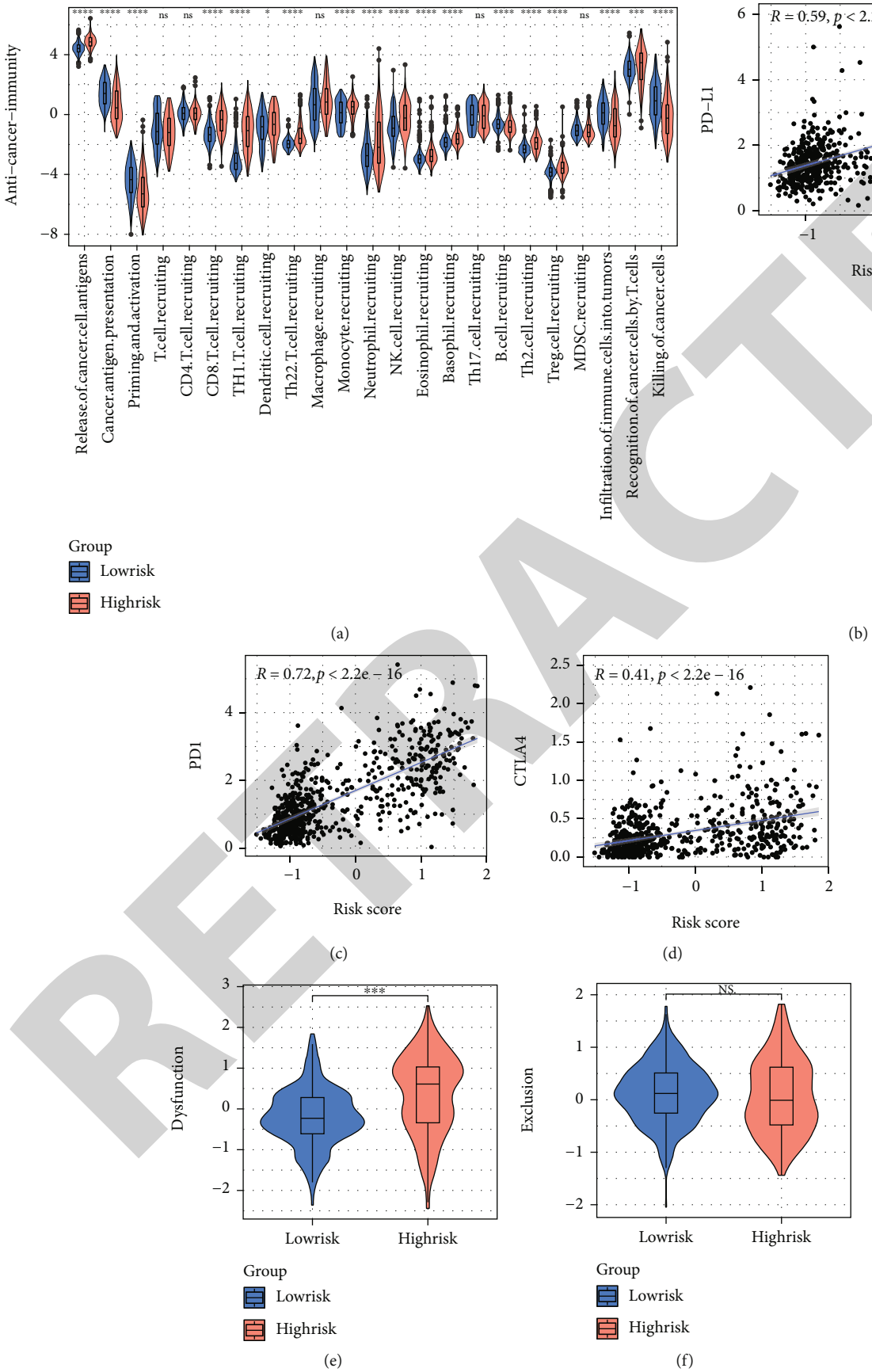

Figure 6: Continued.

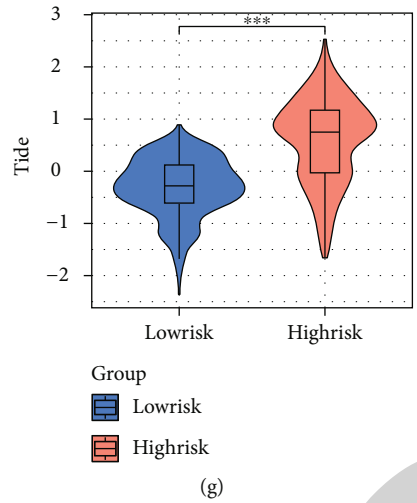

Figure 6: Cancer immunity cycle and Immunotherapy response analysis. (a) Correlation between the risk score and cancer immunity cycles. (b–d) Correlation between the risk score and PD-L1, PD1, and CTLA4 expressions. (e–g) Comparisons of TIDE scores between the two groups.

4. Discussion

In the current study, 43 NRLs were identified as having prognostic significance in TCGA and CGGA cohorts, and 13 of them were used to establish a NRLS for predicting the survival outcome of glioma patients using LASSO Cox method. Patients were divided into low- and high-risk groups according to the risk score's optimal cut-off value. After adjustment for clinicopathological factors by multivariate Cox analysis, NRLS can be applied as an independent predictive factor. Then, the development of nomograms assists clinicians in making clinical decisions. ROC curve and calibration plots verified the robust performance of prediction model. Further investigation was conducted into GESA, immune infiltration, immunotherapy, chemotherapy responses, and molecular subtype based on NRLS. Our findings shed new light on the role of NRLs in diagnosis and treatment of glioma.

The 5th edition of the WHO classification of central nervous system tumors, published in 2021, integrates histological and molecular phenotypes of glioma, established new tumor classification standards, and emphasizes the importance of molecular diagnosis in tumor classification. This update shows that intratumor molecular heterogeneity has become a major consideration in formulating treatment strategies [2]. For gliomas with the same grade and classification diagnosis, patients still have different clinical outcomes after standard treatment [28]. Necroptosis, as a subtype of programmed inflammatory cell death, can be detected in the necrotic area of the tumor [29]. Necroptosis has been reported to have both protumorigenic and antitumorigenic effects at different stages of tumorigenesis, invasion, and metastasis [30]. RIPK3 plays a crucial role in necroptosis under a variety of circumstances [31]. Previous studies have demonstrated that overexpression of RIPK3 is related to the poor prognosis of glioma patients [32, 33]. Necroptosis is required for tumorigenesis in highly malignant tumors [34, 35]. Several prediction models focused on the aging gene, ferroptosis gene, and pyroptosis gene have been developed in glioma. However, there is no report that has been published to decipher the correlation between NRLs and glioma. Here, the NRLS was constructed in this study by identifying 13 NRLs that were significantly associated with the survival outcomes of glioma patients. In addition, the establishment of nomogram helps physicians make clinical decisions.

In glioma, several of these NRLs had their biological functions confirmed. CRNDE was found to be linked to tumor progression and may serve as an independent prognostic factor for patients with glioma [36, 37]. Further research shows that CRNDE inhibition strengthens temozolomide chemosensitivity in glioblastoma by modulating PI3K/Akt/mTOR pathway [38]. FAM181A-AS1 was demonstrated that enhanced proliferation and survivability of glioma cells [39][(p2)]. LINC00346 was confirmed to regulate glioma angiogenesis, migration, invasion, and proliferation [40, 41]. The expression of LINC00461 was significantly increased in stem cell-like/anti-therapeutic GBM cells [42]. LOXL1-AS1 was also verified to increase the malignancy of gliomas via regulation of the miR-374b-5p/MMP14 axis [43]. Additionally, in our study, several genes previously unreported in glioma have significant prognostic value, necessitating more research.

Given the fundamental role in tumorigenesis, the glioma immune microenvironment has gained substantial attention [44, 45]. Recent reports have suggested that both CD4+ and CD8+ T cell activities are inhibited when the necroptotic is activated, resulting in antitumor immunity being blocked [43]. Upregulation of RIPK1 in tumor-associated macrophages (TAMs) also contributes to immune tolerance and resistance or immunotherapeutic [46]. Several IncRNAs have been investigated to modulate necroptosis by acting as competitive RNAs that interact with miRNA to influence the expression of target genes

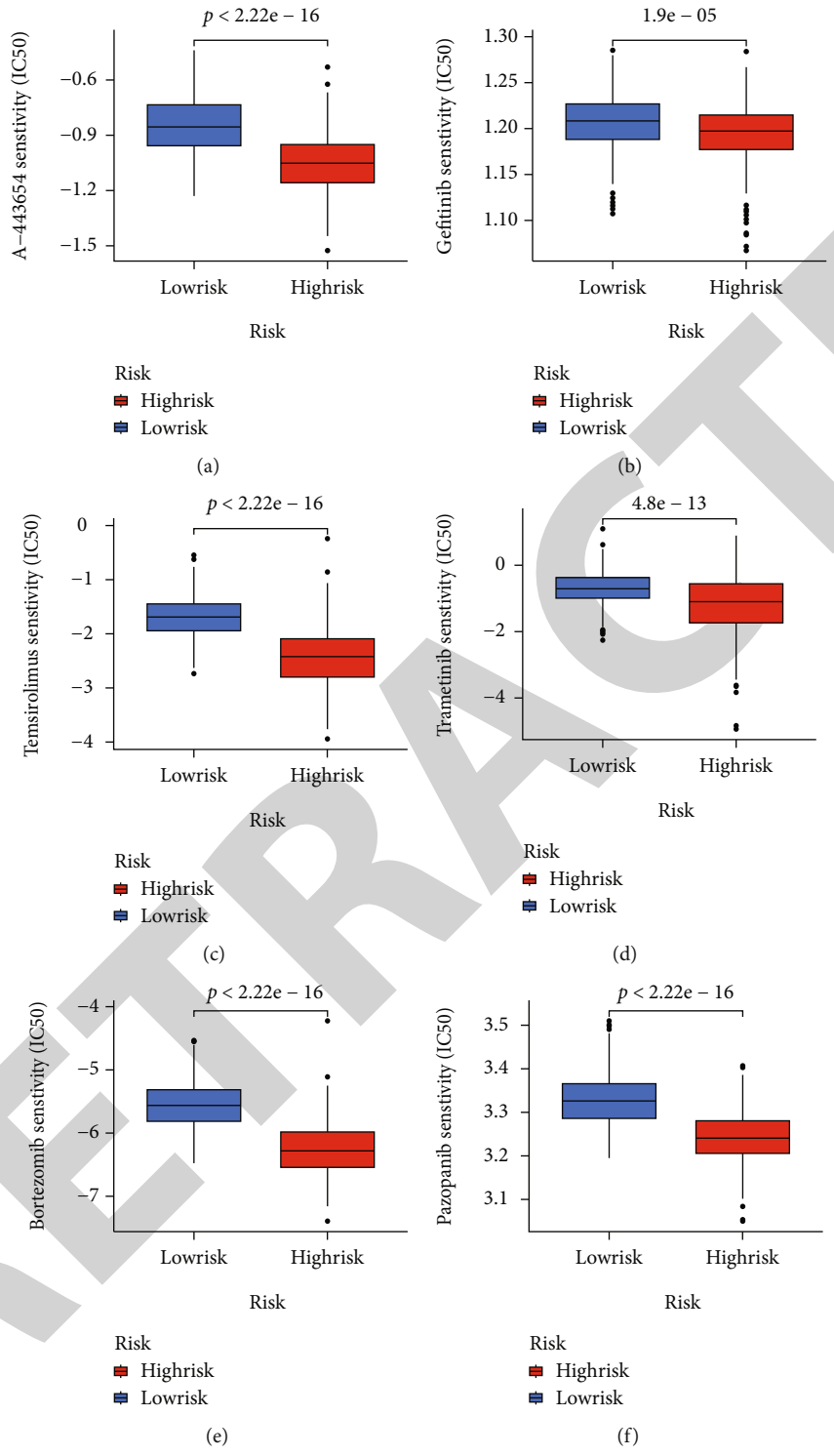

Figure 7: Predicted response of patients in TCGA cohort to chemotherapeutic agents in different risk groups.

[47, 48]. In our study, GO, KEGG, and Hallmark analyses via GSEA were performed between the high- and low-risk score groups. The majority of the results were immune-related signaling pathways. These findings indicated that immune status is different between high- and low-risk groups, particularly in the inflammatory response. Moreover, ImmuneScore was positively and significantly associated with risk score. As a result, a high-risk score implies a high level of immune infiltration. Necroptosis contributes to the infiltration of immunosuppressive cells such as transformation of tumor-associated macrophages to M2 phenotype in a STAT1-dependent manner, leading

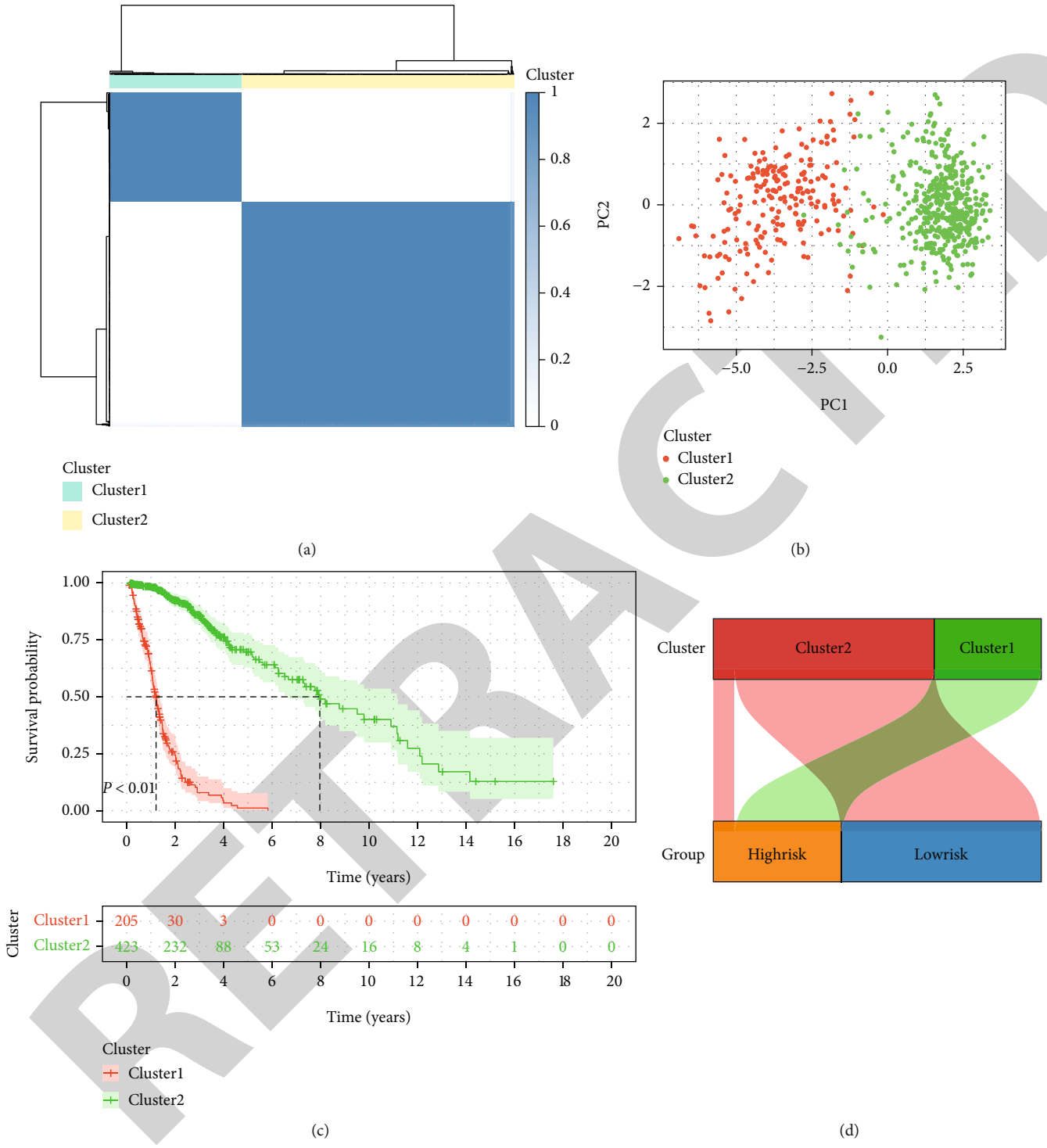

Figure 8: Continued.

(e)

Figure 8: Molecular classification based on NRLs and immune landscape analysis. (a) Patients are divided into two clusters by ConsensusClusterPlus. (b) PCA indicated that two clusters were obtained. (c) Overall survival of two clusters in TCGA. (d) Alluvial diagram of clusters and risk groups. (e) The heat map of immune cells in clusters via different platforms.

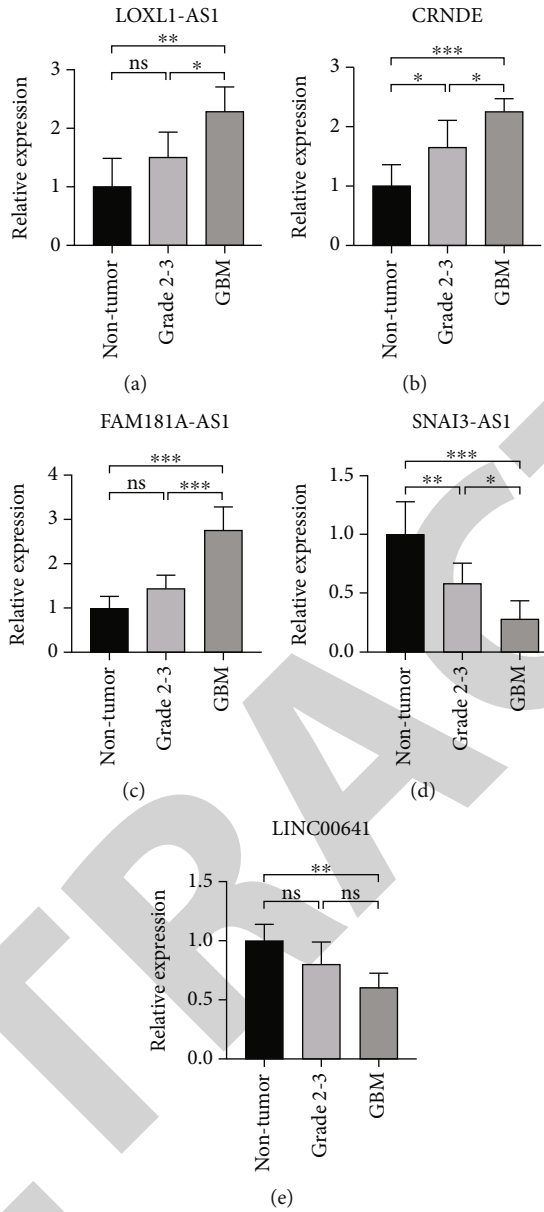

Figure 9: Validation of the expression levels of selected NRLs in 5 non-tumor brain tissues and 11 glioma tissues. (a) LOXL1-AS1. (b) CRNDE. (c) FAM18A-AS1. (d) SNAI3-AS1. (e) LINC00641.

to tumor immune escape and immunotherapy resistance [46]. Our findings indicated that high-risk patients exhibited an immunosuppressive phenotype, with more infiltrating M2 macrophages and Treg cells, as well as overexpression of immune checkpoint gene, which is consistent with previous studies [46]. Moreover, in our research, we observed that patients in high-risk group have worse response to immune checkpoint blockade (ICB) immune therapy.

Then, pRRophetic algorithm was employed to predict chemotherapeutics response of several drugs including A-443654 (AKT inhibitor), Gefitinib (EGFR inhibitors), Temsirolimus (mTOR inhibitor), Trametinib (MEK inhibitor), and Bortezomib (proteasome inhibitor). According to the findings, the cases in the high-risk group were more sensitive to the drugs.

Furthermore, using the consensus clustering algorithm, we identified two molecular patterns (Cluster 1 and Cluster 2) based on NRLS in both TCGA and CGGA cohorts. We observed that all the patients in Cluster 2 were in the low-risk group and that the risk scores for Cluster 1 were significantly higher than Cluster 2, indicating that the consensus clustering method and the risk scoring system were basically similar.

Despite the fact that we had used a variety of methods to asset our model, there were still some flaws and deficiencies. To begin, our current results are derived entirely from public databases, and further experimental validation of our bioinformatics analysis is required. Additionally, the molecular mechanism by which NRLs contribute to the development and progression of glioma cells is unknown, necessitating

further investigation. Finally, all the non-tumor brain tissues were obtained from temporal lobe, and more specimens from different locations are needed to improve the reliability of the results. In the future, we will collect additional samples to investigate the relationship between protein-level gene expression and glioma prognosis.

5. Conclusion

On this basis, our current research develops a theoretical foundation for NRLS prediction in glioma prognosis and immunotherapeutic response. This novel score may also reflect the state of NRLs and shed light on the close association between NRLs and the immunosuppressive phenotype in glioma. The robust NRLS-based risk score established in this study may have predictive value in glioma diagnosis and treatment from a clinical standpoint.

Data Availability

The data used to support the results are available at the TCGA (https://tcga-data.nci.nih.gov/tcga/), GTEx (https://www.gtexportal.org/), GSEA (http://www.gsea-msigdb.org/gsea/index.jsp), and CGGA (https://www.cgga.org.cn).

Conflicts of Interest

The authors declare that the research was conducted in the absence of any commercial or financial relationships that could be construed as a potential conflict of interest.

Authors' Contributions

J.L. and Q.L. designed the overall research strategy. G.Z. and R.C. collected the clinical information and atherosclerotic plaque samples. H.M. and L.Z. performed the experiments. G.Z. performed the bioinformatics analysis. G.Z., D.Z., and R.C. wrote the manuscript. H.T., C.S., and J.W. participated in data discussion. All authors contributed to the article and approved the submitted version. Guanghao Zhang and Rundong Chen contributed equally to this work and share first authorship.

Acknowledgments

We thank Dr. Jianming Zeng (University of Macau) and all the members of his bioinformatics team, biotrainee, for generously sharing their experience and codes. This study was supported by National Natural Science Foundation of China (Grant No. 81771266) and Shanghai Shenkang Three-year Action Plan Major Clinical Research Project (SHDC2020CR4037).

Supplementary Materials

Supplementary 1. Supplementary Figure 1 Kaplan-Meier curves of 13 identified NRLs in TCGA. (A–M) LUCAT1, MIR155HG, LINC00346, CRNDE, SLC25A21−AS1, GDNF−AS1, FAM181A−AS1, LOXL1−AS1, SNAI3−AS1, C1RL−AS1, PAXIP1−AS2, SNHG18, and LINC00641. Supplementary Figure 2 Optimal cut-off values for the risk scores. Supplementary Figure 3 (A) Univariate COX Forest plot of risk score and clinical subgroup in TCGA. (B) Univariate COX Forest plot of risk score and clinical subgroup in CGGA. Supplementary Figure 4 (A) PCA analysis showed the distribution of two clusters in TCGA cohort. (B) t-SNE analysis supported the stratification into two clusters in TCGA cohort. (C) PCA analysis showed the distribution of two clusters in the CGGA cohort. (D) t-SNE analysis supported the stratification into two clusters in CGGA cohort. Supplementary Figure 5 (A) Boxplot showed the comparisons of risk score in different clusters.

Supplementary 2. Supplementary Table (1) 67 necroptosis-related genes from previous literature.

Supplementary 3. Supplementary Table (2) Differentially expressed genes (DEGs) in normal samples and glioma.

Supplementary 4. Supplementary Table (3) Univariate Cox analysis in TCGA and CGGA cohorts.

Supplementary 5. Supplementary Table (4) Differentially expressed genes (DEGs) in high-risk and low-risk groups.

Supplementary 6. Supplementary Table (5) The primers sequences for five lncRNA.

References

[1] A. Omuro, "Glioblastoma and other malignant gliomas," *Journal of the American Medical Association*, vol. 310, no. 17, p. 1842, 2013.

[2] D. N. Louis, A. Perry, P. Wesseling et al., "The 2021 WHO classification of tumors of the central nervous system: a summary," *Neuro-Oncology*, vol. 23, no. 8, pp. 1231–1251, 2021.

[3] J. B. Iorgulescu, C. Sun, C. Neff et al., "Molecular biomarker-defined brain tumors: epidemiology, validity, and completeness in the United States," *Neuro-Oncology*, 2022.

[4] D. N. Louis, A. Perry, G. Reifenberger et al., "The 2016 World Health Organization classification of tumors of the central nervous system: a summary," *Acta Neuropathologica*, vol. 131, no. 6, pp. 803–820, 2016.

[5] H. G. Vuong, H. T. Le, and I. F. Dunn, "The prognostic significance of further genotyping H3G34 diffuse hemispheric gliomas," *Cancer*, vol. 128, no. 10, pp. 1907–1912, 2022.

[6] Y. F. Gao, X. Y. Mao, T. Zhu et al., "COL3A1 and SNAP91: novel glioblastoma markers with diagnostic and prognostic value," *Oncotarget*, vol. 7, no. 43, pp. 70494–70503, 2016.

[7] G. Lombardi, V. Barresi, A. Castellano et al., "Clinical management of diffuse low-grade gliomas," *Cancers*, vol. 12, no. 10, p. 3008, 2020.

[8] R. Stupp, M. Brada, M. J. Van Den Bent, J. C. Tonn, and G. E. S. M. O. Pentheroudakis, "High-grade glioma: ESMO Clinical Practice Guidelines for diagnosis, treatment and follow-up†," *Annals of Oncology*, vol. 25, Supplement 3, pp. iii93–iii101, 2014.

[9] M. R. Gilbert, J. J. Dignam, T. S. Armstrong et al., "A randomized trial of bevacizumab for newly diagnosed glioblastoma," *The New England Journal of Medicine*, vol. 370, no. 8, pp. 699–708, 2014.

[10] A. Degterev, Z. Huang, M. Boyce et al., "Chemical inhibitor of nonapoptotic cell death with therapeutic potential for ischemic brain injury," *Nature Chemical Biology*, vol. 1, no. 2, pp. 112–119, 2005.

[11] J. Zhao, S. Jitkaew, Z. Cai et al., "Mixed lineage kinase domain-like is a key receptor interacting protein 3 downstream component of TNF-induced necrosis," *Proc Natl Acad Sci USA.*, vol. 109, no. 14, pp. 5322–5327, 2012.

[12] Z. Su, Z. Yang, L. Xie, J. P. DeWitt, and Y. Chen, "Cancer therapy in the necroptosis era," *Cell Death and Differentiation*, vol. 23, no. 5, pp. 748–756, 2016.

[13] M. Ghandi, F. W. Huang, J. Jané-Valbuena et al., "Next-generation characterization of the cancer cell line encyclopedia," *Nature*, vol. 569, no. 7757, pp. 503–508, 2019.

[14] R. Weinlich, A. Oberst, H. M. Beere, and D. R. Green, "Necroptosis in development, inflammation and disease," *Nature Reviews. Molecular Cell Biology*, vol. 18, no. 2, pp. 127–136, 2017.

[15] Y. Jiang, L. Zhao, Y. Wu et al., "The role of NcRNAs to regulate immune checkpoints in cancer," *Frontiers in Immunology*, vol. 13, article 853480, 2022.

[16] C. Zhong, B. Tao, X. Li et al., "HOXA-AS2 contributes to regulatory T cell proliferation and immune tolerance in glioma through the miR-302a/KDM2A/JAG1 axis," *Cell Death & Disease*, vol. 13, no. 2, p. 160, 2022.

[17] K. Yi, X. Cui, X. Liu et al., "PTRF/Cavin-1 as a novel RNA-binding protein expedites the NF-κB/PD-L1 axis by stabilizing lncRNA NEAT1, contributing to tumorigenesis and immune evasion in glioblastoma," *Frontiers in Immunology*, vol. 12, article 802795, 2021.

[18] W. Min, L. Sun, B. Li, X. Gao, S. Zhang, and Y. Zhao, "lncCRLA enhanced chemoresistance in lung adenocarcinoma that underwent epithelial mesenchymal transition," *Oncology Research*, vol. 28, no. 9, pp. 857–872, 2021.

[19] G. Tanzhu, N. Li, Z. Li, R. Zhou, and L. Shen, "Molecular subtypes and prognostic signature of pyroptosis-related lncRNAs in glioma patients," *Frontiers in Oncology*, vol. 12, article 779168, 2022.

[20] H. Zhou, M. Meng, Z. Wang et al., "The role of m5C-related lncRNAs in predicting overall prognosis and regulating the lower grade glioma microenvironment," *Frontiers in Oncology*, vol. 12, article 814742, 2022.

[21] Z. Zhou, J. Wei, and W. Jiang, "Characterization of aging tumor microenvironment with drawing implications in predicting the prognosis and immunotherapy response in low-grade gliomas," *Scientific Reports*, vol. 12, no. 1, p. 5457, 2022.

[22] M. J. Goldman, B. Craft, M. Hastie et al., "Visualizing and interpreting cancer genomics data via the Xena platform," *Nature Biotechnology*, vol. 38, no. 6, pp. 675–678, 2020.

[23] Z. Zhao, K. N. Zhang, Q. Wang et al., "Chinese Glioma Genome Atlas (CGGA): a comprehensive resource with functional genomic data from Chinese glioma patients," *Genomics, Proteomics & Bioinformatics*, vol. 19, no. 1, pp. 1–12, 2021.

[24] S. H. Yu, J. H. Cai, D. L. Chen et al., "LASSO and bioinformatics analysis in the identification of key genes for prognostic genes of gynecologic cancer," *Journal of personalized medicine*, vol. 11, no. 11, p. 1177, 2021.

[25] D. C. Hinshaw and L. A. Shevde, "The tumor microenvironment innately modulates cancer progression," *Cancer Research*, vol. 79, no. 18, pp. 4557–4566, 2019.

[26] D. S. Chen and I. Mellman, "Oncology meets immunology: the cancer-immunity cycle," *Immunity*, vol. 39, no. 1, pp. 1–10, 2013.

[27] J. Sprooten, P. De Wijngaert, I. Vanmeerbeek et al., "Necroptosis in immuno-oncology and cancer immunotherapy," *Cell*, vol. 9, no. 8, p. E1823, 2020.

[28] Z. Hou, K. Zhang, X. Liu et al., "Molecular subtype impacts surgical resection in low-grade gliomas: a Chinese Glioma Genome Atlas database analysis," *Cancer Letters*, vol. 522, pp. 14–21, 2021.

[29] D. Jiao, Z. Cai, S. Choksi et al., "Necroptosis of tumor cells leads to tumor necrosis and promotes tumor metastasis," *Cell Research*, vol. 28, no. 8, pp. 868–870, 2018.

[30] J. Yan, P. Wan, S. Choksi, and Z. G. Liu, "Necroptosis and tumor progression," *Trends in Cancer*, vol. 8, no. 1, pp. 21–27, 2022.

[31] J. Lin, S. Kumari, C. Kim et al., "RIPK1 counteracts ZBP1-mediated necroptosis to inhibit inflammation," *Nature*, vol. 540, no. 7631, pp. 124–128, 2016.

[32] G. A. Vergara, G. C. Eugenio, S. M. F. Malheiros, E. D. S. Victor, and R. Weinlich, "RIPK3 is a novel prognostic marker for lower grade glioma and further enriches IDH mutational status subgrouping," *Journal of Neuro-Oncology*, vol. 147, no. 3, pp. 587–594, 2020.

[33] Y. Dong, Y. Sun, Y. Huang, B. Dwarakanath, L. Kong, and J. J. Lu, "Upregulated necroptosis-pathway-associated genes are unfavorable prognostic markers in low-grade glioma and glioblastoma multiforme," *Translational Cancer Research*, vol. 8, no. 3, pp. 821–827, 2019.

[34] L. Seifert, G. Werba, S. Tiwari et al., "The necrosome promotes pancreatic oncogenesis via CXCL1 and Mincle-induced immune suppression," *Nature*, vol. 532, no. 7598, pp. 245–249, 2016.

[35] M. Seehawer, F. Heinzmann, L. D'Artista et al., "Necroptosis microenvironment directs lineage commitment in liver cancer," *Nature*, vol. 562, no. 7725, pp. 69–75, 2018.

[36] S. Jing, Y. Y. Lu, J. K. Yang, W. Y. Deng, Q. Zhou, and B. H. Jiao, "Expression of long non-coding RNA CRNDE in glioma and its correlation with tumor progression and patient survival," *European Review for Medical and Pharmacological Sciences*, vol. 20, no. 19, pp. 3992–3996, 2016.

[37] M. Sorokin, M. Raevskiy, A. Zottel et al., "Large-scale transcriptomics-driven approach revealed overexpression of CRNDE as a poor survival prognosis biomarker in glioblastoma," *Cancers*, vol. 13, no. 14, p. 3419, 2021.

[38] Z. Zhao, M. Liu, W. Long et al., "Knockdown lncRNA CRNDE enhances temozolomide chemosensitivity by regulating autophagy in glioblastoma," *Cancer Cell International*, vol. 21, no. 1, p. 456, 2021.

[39] X. Jiang and D. Chen, "LncRNA FAM181A-AS1 promotes gliomagenesis by sponging miR-129-5p and upregulating ZRANB2," *Aging*, vol. 12, no. 20, pp. 20069–20084, 2020.

[40] X. Chen, D. Li, L. Chen et al., "Long noncoding RNA *LINC00346* promotes glioma cell migration, invasion and proliferation by up-regulating ROCK1," *Journal of Cellular and Molecular Medicine*, vol. 24, no. 22, pp. 13010–13019, 2020.

[41] C. Yang, J. Zheng, X. Liu et al., "Role of ANKHD1/LINC00346/ZNF655 feedback loop in regulating the glioma angiogenesis via staufen1-mediated mRNA decay," *Molecular Therapy-Nucleic Acids*, vol. 20, pp. 866–878, 2020.

[42] A. C. Wu, W. B. Yang, K. Y. Chang et al., "HDAC6 involves in regulating the lncRNA-microRNA-mRNA network to promote the proliferation of glioblastoma cells," *Journal of Experimental & Clinical Cancer Research: CR*, vol. 41, no. 1, p. 47, 2022.

[43] B. Yi, H. Li, H. Cai, X. Lou, M. Yu, and Z. Li, "*LOXL1-AS1* communicating with TIAR modulates vasculogenic mimicry in glioma via regulation of the *miR-374b-5p*/MMP14 axis,"

Hindawi
Computational and Mathematical Methods in Medicine
Volume 2023, Article ID 9863871, 1 page
https://doi.org/10.1155/2023/9863871

Retraction

Retracted: Influences of Antithrombotic Elastic Socks Combined with Air Pressure in Reducing Lower Extremity Deep Venous Thrombosis for Patients Undergoing Cardiothoracic Surgery

Computational and Mathematical Methods in Medicine

Received 5 December 2023; Accepted 5 December 2023; Published 6 December 2023

This article has been retracted by Hindawi, as publisher, following an investigation undertaken by the publisher [1]. This investigation has uncovered evidence of systematic manipulation of the publication and peer-review process. We cannot, therefore, vouch for the reliability or integrity of this article.

Please note that this notice is intended solely to alert readers that the peer-review process of this article has been compromised.

Wiley and Hindawi regret that the usual quality checks did not identify these issues before publication and have since put additional measures in place to safeguard research integrity.

We wish to credit our Research Integrity and Research Publishing teams and anonymous and named external researchers and research integrity experts for contributing to this investigation.

The corresponding author, as the representative of all authors, has been given the opportunity to register their agreement or disagreement to this retraction. We have kept a record of any response received.

References

[1] W. Fu, Q. Zhang, X. Sun, and Y. Gu, "Influences of Antithrombotic Elastic Socks Combined with Air Pressure in Reducing Lower Extremity Deep Venous Thrombosis for Patients Undergoing Cardiothoracic Surgery," *Computational and Mathematical Methods in Medicine*, vol. 2022, Article ID 1338214, 6 pages, 2022.

Hindawi
Computational and Mathematical Methods in Medicine
Volume 2022, Article ID 1338214, 6 pages
https://doi.org/10.1155/2022/1338214

Research Article

Influences of Antithrombotic Elastic Socks Combined with Air Pressure in Reducing Lower Extremity Deep Venous Thrombosis for Patients Undergoing Cardiothoracic Surgery

Weihong Fu,[1] Qun Zhang,[2] Xuemei Sun,[1] and Yan Gu[3]

[1]*Department of Thoracic Surgery, Affiliated Hospital of Nantong University, Nantong, 226001 Jiangsu, China*
[2]*Department of Cardiovascular Surgery, Affiliated Hospital of Nantong University, Nantong, 226001 Jiangsu, China*
[3]*Department of Surgery, Affiliated Hospital of Nantong University, Nantong, 226001 Jiangsu, China*

Correspondence should be addressed to Yan Gu; 1602409019@stu.suda.edu.cn

Received 10 August 2022; Revised 17 August 2022; Accepted 22 August 2022; Published 5 September 2022

Academic Editor: Min Tang

This study was designed to investigate the application and therapeutic effect of antithrombotic elastic socks combined with air pressure in the prevention of lower extremity deep venous thrombosis in patients undergoing cardiothoracic surgery. Sixty patients in cardiothoracic surgery of our hospital from January 2019 to December 2020 were randomly divided into a study group and control group. The control group was treated with routine treatment intervention. Based on routine treatment intervention, the study group was treated with antithrombotic elastic socks combined with pneumatic treatment intervention. The activated partial thromboplastin time (APTT), thrombin time (TT), femoral venous blood flow velocity of both lower limbs, and the incidence of lower extremity deep venous thrombosis (LEDVT), postoperative lower extremity swelling, inflammatory factors, and satisfaction were measured. After intervention, APTT (31.74 ± 1.15 s) and TT (14.58 ± 0.24 s) in the study group were higher than those in the control group APTT (25.13 ± 1.14 s) and TT (12.14 ± 0.23 s) ($P < 0.05$). The left lower limb femoral vein blood flow velocity and the right lower limb femoral vein blood flow velocity in the study group were better than those in the control group ($P < 0.05$). The incidence of postoperative lower limb swelling and deep vein in the study group was lower than that in the control group ($P < 0.05$). Serum tumor necrosis factor alpha and interleukin-6 concentrations in the study group were lower than those in the control group ($P < 0.05$). The satisfaction rate of patients in the study group (93.33%) was significantly higher than that in the control group (70.00%) ($P < 0.05$). In conclusion, after cardiothoracic surgery, antithrombotic elastic socks combined with air pressure can significantly reduce the incidence of LEDVT by improving patients' coagulation function, reducing inflammatory reaction. It is worthy of popularization and application in relevant surgery.

1. Introduction

Venous thrombosis is often caused by trauma and surgery, and abnormally coagulated blood can lead to partial or even complete obstruction of vascular lumen. Lower extremity deep venous thrombosis (LEDVT) is one of the most common surgical complications in clinic [1]. Surgical treatment is one of the main treatment methods for lesions in the esophagus, lungs, mediastinum, and other parts [2]. Cardiothoracic surgery is a clinical department mainly for major surgical treatment, mostly for elderly patients, and the surgical site involves important organs of the human body. The operation is complicated and traumatic, and the postoperative recovery is slow, which requires long-term bed rest and more complications. Cardiothoracic surgery, the patient needs to stay in bed for a long time after operation, resulting in slow and blocked blood reflux, which is very easy to be complicated with deep venous thrombosis of lower limbs [3]. LEDVT can lead to lower limb swelling, pain and other symptoms, and even fatal pulmonary embolism, threatening the life and health of patients. At present, the methods to prevent deep venous thrombosis mostly take drugs or

Table 1: Comparison of general data between the two groups.

Groups	n	Age (years)	Gender (n)		Height (cm)	Body weight (kg)	Operation time (min)
			Male	Female			
Control group	30	64.63 ± 5.44	18	12	162.86 ± 7.62	66.77 ± 11.53	194.52 ± 44.63
Study group	30	64.93 ± 5.68	15	15	462.66 ± 9.12	69.63 ± 10.40	176.71 ± 43.52
P		>0.05	>0.05		>0.05	>0.05	>0.05

physical methods to reduce the viscosity of blood and promote the blood circulation of lower limbs. However, it is difficult to control the dosage of drug prevention, which is easy to cause postoperative bleeding [4, 5]. Various physical prevention methods, including postoperative massage and electrical stimulation of calf muscles, are sometimes difficult to achieve the expected effect due to difficult control and large individual differences. Similarly, muscle electrical stimulation is difficult for most patients to accept because it increases the discomfort of postoperative patients.

The antithrombotic elastic socks are designed according to the characteristics of human physiological function, and the pressure decreases gradually from the distal ankle to the proximal end. The venous blood of the distal leg can be pumped back to the heart to improve the blood circulation of both lower limbs. The antithrombotic elastic socks cover the foot to the knee, and the feet expose the toes, which is the intervention to shrink calf muscles and prevent venous filling. Meanwhile, the antithrombotic elastic socks are convenient to observe the blood circulation and allow blood to flow back to the heart through progressive pressure [6, 7]. Pneumatic therapy is a kind of "physiological pump" simulating artificial massage, which compresses the muscles of both lower limbs by rapidly inflating and deflating the air bag in a short time, so as to accelerate the blood reflux in the venous cavity, accelerate the venous blood circulation, and rapidly increase the blood perfusion and oxygenation speed [8, 9]. Pneumatic therapy can increase the rate of venous return to enhance the blood circulation of the lower limbs and reduce the incidence of LEDVT [10].

The purpose of this study was to explore the application and therapeutic effect of antithrombotic elastic socks combined with pneumatic therapy in the prevention of lower extremity deep venous thrombosis in patients undergoing cardiothoracic surgery.

2. Data and Methods

2.1. General Information. A total of 60 patients admitted to cardiothoracic surgery from January 2019 to December 2020 were randomly divided into a study group ($n = 30$) and control group ($n = 30$). This study was approved by the medical ethics committee of the hospital and obtained the consent of the selected patients and their families, and all patients signed the informed consent form. Inclusion criteria were as follows: all patients need thoracic surgery, no surgical contraindications, and good compliance. Exclusion criteria were as follows: patients with coagulation dysfunction, heart and liver dysfunction, or cognitive impairment.

There was no significant difference in gender, age, height, weight, operation time, and other general data between the two groups ($P > 0.05$), as shown in Table 1.

2.2. Intervention Methods. Control group: routine nursing prevention was adopted. Before operation, nurses explained the principle and risk of lower extremity deep venous thrombosis to patients and their families and made a comprehensive evaluation, explain the methods and significance of prevention of postoperative deep venous thrombosis of lower limbs, and inform the patients of perioperative diet precautions and the significance of getting out of bed as soon as possible after operation. After operation, patients are encouraged to get out of bed early and step by step. The whole process must be completed under the supervision and guidance of nurses or accompanied by family members. If the patient is not fit to get out of bed, the nurse shall assist the patient in passive exercise after the condition is stable. Specific methods are as follows: start from the distal small joints of both lower limbs; perform flexion, extension, and lifting in the order from toe to hip joint, three times a day, 20 minutes each time; and teach the family members.

Study group: on the basis of the control group, medical elastic socks and pneumatic therapeutic instrument were used for prevention. (1) Before operation, measure the thinnest and coarsest circumference of the patient's lower leg, and select medical elastic socks of appropriate specification and length. The nurse shall help to wear medical elastic socks to ensure that the toes are exposed. Pay close attention to the tightness of medical elastic socks, the skin temperature on the back of the foot, and the pulsation of the artery on the back of the foot. During the period, pay attention to personal hygiene and replace and clean them frequently. (2) Use of pneumatic therapeutic instrument: the patient takes a flat lying position, puts his lower limbs into the sleeve of pneumatic therapeutic instrument, and the sole of the foot reaches the bottom of the sleeve with appropriate tightness. The pressure is set to 25-180 mmHg (1 mmHg = 0.133 kPa). According to the manufacturer's instructions, set the ankle 45 mmHg, lower leg 40 mmHg, and thigh 30 mmHg to ensure the blood flow to the proximal heart. When inflating, start from the air bag at the distal end of the lower limb and gradually inflate to the proximal end until the air bag at the root of the thigh is inflated and all the air bags in the sleeve are automatically and slowly vented [11]. The above methods were performed twice a day for 30 minutes each

Table 2: Comparison of coagulation function indexes between the two groups before and after intervention (s, $x \pm s$).

Groups	n	APTT		TT	
		Before intervention	After intervention	Before intervention	After intervention
Control group	30	20.83 ± 1.44	25.13 ± 1.14	11.08 ± 0.31	12.14 ± 0.23
Study group	30	20.80 ± 1.45	31.74 ± 1.15	11.12 ± 0.27	14.58 ± 0.24
t		0.085	20.105	0.441	32.062
P		>0.05	<0.05	>0.05	<0.05

Table 3: Comparison of blood flow velocity of the femoral vein of both lower limbs between the two groups before and after intervention (cm/s, $x \pm s$).

Groups	n	Left lower limb (cm/s, $x \pm s$)		Right lower limb (cm/s, $x \pm s$)	
		Before intervention	After intervention	Before intervention	After intervention
Control group	30	14.08 ± 3.31	16.19 ± 4.02	14.06 ± 3.20	16.13 ± 4.21
Study group	30	14.11 ± 3.21	19.50 ± 5.03	14.01 ± 3.01	19.20 ± 4.18
t		0.039	3.402	0.066	2.722
P		>0.05	<0.05	>0.05	<0.05

Table 4: Comparison of postoperative lower limb swelling and deep venous thrombosis between the two groups (cases (%)).

Groups	n	Postoperative lower limb swelling	Deep venous thrombosis
Control group	30	8 (26.67)	6 (20.00)
Study group	30	1 (3.33)	0 (0.00)
χ^2		6.40	6.67
P		<0.05	<0.05

time until the fifth day after operation. In addition to bathing or taking off and replacing in time in case of pollution, it is necessary to keep wearing medical elastic socks until the fifth day after operation, including functional exercise in bed and out of bed activities. In the course of treatment, closely observe the patient's reaction, and stop treatment immediately in case of complexion change, chest tightness, palpitation, etc.

2.3. Observation Indicators

(1) Coagulation function index: 3 mL of peripheral venous blood sample was collected from each patient before and after intervention. QLabs Electrometer (Micropoint Biotechnologies, Guangdong, China) was used to test the samples for activated partial thromboplastin time (APTT) and thrombin time (TT)

(2) Femoral vein blood flow velocity of both lower limbs: the femoral vein blood flow velocity of both lower limbs of the two groups was measured before and after the intervention

(3) The incidence of LEDVT in the two groups was recorded

(4) Lower extremity deep venous thrombosis: the peripheral diameters of lower leg and thigh were measured 1 day before operation and 1-3 days after operation, and the postoperative lower limb swelling of the two groups was comprehensively evaluated. Deep veins of lower limbs: the same doctor with ultrasonic diagnosis qualification shall detect the deep veins of both lower limbs of the two groups by ultrasonic detection on the first day before operation and the first to third days after operation, so as to determine whether there is lower limb venous thrombosis

(5) Tumor necrosis factor-α (TNF-α) and interleukin-6 (IL-6) were detected by ELISA as previously reported [12]. The kit was produced by Shanghai Kanglang Biotechnology Co., Ltd.

(6) Patients' satisfaction was evaluated by self-made questionnaire at discharge, including nursing staff's professional level, comfort, and working attitude. The full score is 100 points. A score of 90-99, 75-89, and less than 75 points meant that the patients are very satisfied, satisfied, and dissatisfied, respectively.

2.4. Statistical Analysis. The SPSS v20.0 software (IBM, USA) was used for data analysis. The comparison between the two groups of data adopts t-test, and all measurement data are expressed by mean ± standard deviation (mean ± SD). $P < 0.05$ is considered as the difference which is statistically significant.

Table 5: Comparison of serum inflammatory factors between the two groups ($x \pm s$).

Groups	TNF-α (ng/mL)		IL-6 (pg/mL)	
	Before intervention	After intervention	Before intervention	After intervention
Control group	2.86 ± 0.30	1.59 ± 0.21	24.65 ± 2.13	15.29 ± 0.95
Study group	2.81 ± 0.24	1.04 ± 0.32	26.65 ± 2.21	9.34 ± 0.88
t	0.668	5.241	0.012	6.214
P	>0.05	<0.05	>0.05	<0.05

Table 6: Comparison of patient satisfaction between the two groups (n (%)).

Groups	n	Very satisfied	Satisfied	Dissatisfied	Satisfaction rate
Control group	30	8 (26.67)	11 (36.67)	11 (36.67)	21 (70.00)
Study group	30	16 (53.33)	12 (40.00)	2 (6.67)	28 (93.33)
χ^2					5.269
P					<0.05

3. Results

3.1. Comparison of Coagulation Function Indexes between the Two Groups before and after Intervention. Before the intervention, there was no significant difference between APTT and TT in the two groups ($P > 0.05$). After the intervention of different modes, APTT and TT in the study group were significantly better than those in the control group ($P < 0.05$), as shown in Table 2.

3.2. Comparison of Blood Flow Velocity of the Femoral Vein of Both Lower Limbs between the Two Groups before and after Intervention. Before the intervention, there was no significant difference in the blood flow velocity of the lower limb femoral vein between the two groups ($P > 0.05$). After the intervention of different modes, the blood flow velocity of the lower limb femoral vein in the study group was significantly higher than that in the control group ($P < 0.05$), as shown in Table 3.

3.3. Comparison of Postoperative LEDVT Incidence between the Two Groups. There were 8 cases of postoperative lower limb swelling and 6 cases of deep venous thrombosis in the control group, with the incidence of about 26.67% and 20%. There was 1 case of postoperative lower limb swelling and 0 case of deep venous thrombosis in the study group, with the incidence of about 3.33% and 0.00%, which was significantly lower than that in the control group ($P < 0.05$), as revealed in Table 4.

3.4. Comparison of Serum Inflammatory Factor Expression between the Two Groups. Before the intervention, there was no significant difference between the serum inflammatory factor indexes TNF-α and IL-6 in the two groups ($P > 0.05$). After the intervention of different modes, the TNF-α and IL-6 in the study group were significantly lower than those in the control group ($P < 0.05$), as shown in Table 5.

3.5. Comparison of Patients' Satisfaction with Treatment between the Two Groups. The overall satisfaction rate of the study group was 93.33%, significantly higher than 70.00% of the control group ($P < 0.05$), as shown in Table 6.

4. Discussion

Deep venous thrombosis (DVT) is one of the most common perioperative complications, which can lead to pulmonary embolism and can even be life-threatening. In patients with pulmonary embolism, 90% of the thrombus is caused by the falling off of the deep venous thrombosis of the lower limbs and entering the pulmonary artery through the blood circulation [13]. With the continuous improvement of diagnostic technology, the incidence of the disease shows an increasing trend, however. The occult onset and delayed diagnosis of deep venous thrombosis may delay the best time of treatment. Therefore, it is of great significance to take active measures to prevent deep venous thrombosis [14].

The surgical trauma of cardiothoracic surgery is generally large and the postoperative stay in bed is long, suggesting that the prevention of postoperative deep venous thrombosis is particularly important. In this study, the average ages of the two groups were 64.63 ± 5.44 years and 64.93 ± 5.68 years. Most of the patients are elderly patients, with decreased cardiac output, slow blood flow, and even stasis. In addition, the patient fasted for a long time before operation, the body volume was relatively insufficient, and the blood viscosity increased, which increased the risk of postoperative deep venous thrombosis. Meanwhile, elderly patients with reduced postoperative activity and long resting time can cause slow blood flow; intraoperative operation and deep vein catheterization can cause vascular injury.

The principle of antithrombotic elastic socks is to accelerate the speed of venous blood circulation, reduce venous blood stasis, and then promote the blood circulation of the lower limb veins, which can continuously and effectively prevent lower limb deep venous thrombosis in patients undergoing cardiothoracic surgery. Barotherapeutic instrument, as a noninterventional therapeutic instrument, has the same principle of action as manual massage. The

mechanical pump is used to quickly inflate and exhaust the air bag on the sleeve in a very short time to squeeze the limbs, which can accelerate the blood circulation in the veins of the limbs and improve the blood perfusion and oxygenation of the limbs [15, 16]. Compared with manual massage, pneumatic therapeutic instrument has the advantages of simple operation, small individual difference, and no influence of body position. The research shows that the design of different pressure gradient can increase the blood flow rate and shorten the recovery time of skin temperature, which is of positive significance to prevent the occurrence of deep venous thrombosis after shell surgery. In addition, this operation can also reduce the workload of its nurses, so as to devote more energy to observing the changes of the disease and perioperative nursing, and significantly improve the satisfaction of patients with nursing work. By comparing the postoperative lower limb swelling, the incidence of postoperative deep venous thrombosis, hospitalization time, and hospitalization expenses between the two groups, we found that medical elastic socks combined with pneumatic therapeutic instrument can significantly improve the postoperative recovery, shorten the hospitalization time, save medical expenses, and improve the postoperative quality of life.

The results showed that before the intervention, there was no significant difference between APTT and TT, as well the blood flow velocity of the lower limb femoral vein in the two groups ($P > 0.05$). However, after the intervention of different modes, APTT and TT in the study group were significantly better than those in the control group ($P < 0.05$). Meanwhile, the blood flow velocity of the femoral veins in both lower limbs in the study group was significantly faster than that in the control group ($P < 0.05$). The reasons may be as follows: (1) the gradient pressure effect of antithrombotic elastic socks; (2) the compression frequency and inflation time were adjusted in time, and the air pressure gradually intervened in both lower limbs from the distal end to proximal end, so as to improve the hemodynamic indexes. Studies have shown that barotherapy can improve the biological activity of plasmin, promote fibrinolysis, inhibit the activation of procoagulant substances, and prevent coagulation factors from adhering to the intima of blood vessels. Our study showed that the incidence of postoperative lower limb swelling and deep vein in the study group was lower than that in the control group ($P < 0.05$). IL-6 and TNF-α are important inflammatory factors that mediate the process of platelet aggregation [17]. Some scholars believe that inflammatory factors may play key roles in the occurrence and development of LEDVT [18]. Consistently, our study found that before the intervention, there was no significant difference between the serum inflammatory factor indexes TNF-α and IL-6 in the two groups ($P > 0.05$). After the intervention of different modes, the TNF-α and IL-6 in the study group were significantly lower than those in the control group ($P < 0.05$). The decrease of the IL-6 and TNF-α expression indirectly suggested that the risk of LEDVT also decreases. In addition, our research demonstrated that the overall satisfaction rate of the study group was 93.33%, significantly higher than 70.00% of the control group ($P < 0.05$). All the above findings indicated that the use of antithrombotic elastic socks combined with pneumatic treatment may play a good effect in the prevention of LEDVT after cardiothoracic surgery.

5. Conclusion

The application of antithrombotic elastic socks combined with pneumatic therapy in perioperative patients of cardiothoracic surgery can effectively reduce the incidence of lower extremity deep venous thrombosis, improve patients' coagulation function, and improve satisfaction, which is worthy of clinical application.

Data Availability

Data generated during the study can be obtained from the corresponding author under reasonable request.

Conflicts of Interest

The authors declare that no conflicts of interest exist in this study.

Authors' Contributions

Weihong Fu and Qun Zhang contributed equally to this work.

References

[1] W. Zhang, J. Shen, and J. L. Sun, "Risk scores, prevention, and treatment of maternal venous thromboembolism," *World Journal of Clinical Cases*, vol. 8, no. 11, pp. 2210–2218, 2020.

[2] H. E. Garrett Jr. and C. L. Roper, "Surgical intervention in histoplasmosis," *The Annals of Thoracic Surgery*, vol. 42, no. 6, pp. 711–722, 1986.

[3] C. F. Evans, A. T. Iacono, P. G. Sanchez et al., "Venous thromboembolic complications of lung transplantation: a contemporary single-institution review," *The Annals of Thoracic Surgery*, vol. 100, no. 6, pp. 2033–2040, 2015, discussion 2039-40.

[4] X. Wang, G. Cao, W. Mao, W. Lao, and C. He, "Robot-assisted versus laparoscopic surgery for rectal cancer: a systematic review and meta-analysis," *Journal of Cancer Research and Therapeutics*, vol. 16, no. 5, pp. 979–989, 2020.

[5] M. A. Zayed, G. de Silva, R. Ramaswamy, and L. Sanchez, "Management of cavoatrial deep venous thrombosis: incorporating new strategies," *Seminars in Interventional Radiology*, vol. 34, no. 1, pp. 25–34, 2017.

[6] J. Zhang and J. L. Sun, "Severe venous thromboembolism in the puerperal period caused by thrombosis: a case report," *World Journal of Clinical Cases*, vol. 8, no. 7, pp. 1311–1318, 2020.

[7] D. H. Zhao, R. Xue, and X. R. Sun, "Quality improvement of nursing on patients with complex cerebral arteriovenous malformation undergoing hybrid surgery: a prospective single-center study," *Chinese Neurosurgical Journal*, vol. 7, no. 1, p. 23, 2021.

[8] M. Zuin, G. Rigatelli, C. Picariello, M. Carraro, P. Zonzin, and L. Roncon, "Prognostic role of a new risk index for the prediction of 30-day cardiovascular mortality in patients with acute

Hindawi
Computational and Mathematical Methods in Medicine
Volume 2023, Article ID 9769373, 1 page
https://doi.org/10.1155/2023/9769373

Retraction

Retracted: Clinical Value of Contrast-Enhanced Ultrasound in Breast Cancer Diagnosis

Computational and Mathematical Methods in Medicine

Received 5 December 2023; Accepted 5 December 2023; Published 6 December 2023

This article has been retracted by Hindawi, as publisher, following an investigation undertaken by the publisher [1]. This investigation has uncovered evidence of systematic manipulation of the publication and peer-review process. We cannot, therefore, vouch for the reliability or integrity of this article.

Please note that this notice is intended solely to alert readers that the peer-review process of this article has been compromised.

Wiley and Hindawi regret that the usual quality checks did not identify these issues before publication and have since put additional measures in place to safeguard research integrity.

We wish to credit our Research Integrity and Research Publishing teams and anonymous and named external researchers and research integrity experts for contributing to this investigation.

The corresponding author, as the representative of all authors, has been given the opportunity to register their agreement or disagreement to this retraction. We have kept a record of any response received.

References

[1] Y. Yuan, M. Xu, Y. Ren, L. He, J. Chen, and L. Sun, "Clinical Value of Contrast-Enhanced Ultrasound in Breast Cancer Diagnosis," *Computational and Mathematical Methods in Medicine*, vol. 2022, Article ID 2017026, 6 pages, 2022.

Hindawi
Computational and Mathematical Methods in Medicine
Volume 2022, Article ID 2017026, 6 pages
https://doi.org/10.1155/2022/2017026

Research Article

Clinical Value of Contrast-Enhanced Ultrasound in Breast Cancer Diagnosis

Yingying Yuan,[1] Ming Xu,[1] Yi Ren,[2] Lili He,[1] Jiejie Chen,[1] and Li Sun[1]

[1]*Department of Ultrasound, The Affiliated Huai'an No. 1 People's Hospital of Nanjing Medical University, Huai'an, Jiangsu 223300, China*
[2]*Department of Surgery of Thyroid Gland and Breast, The Affiliated Huai'an No. 1 People's Hospital of Nanjing Medical University, Huai'an, Jiangsu 223300, China*

Correspondence should be addressed to Ming Xu; mingxu1286@outlook.com

Received 13 August 2022; Revised 22 August 2022; Accepted 25 August 2022; Published 5 September 2022

Academic Editor: Min Tang

Breast cancer (BC) ranks first in morbidity and mortality among female malignant tumors worldwide. This study is aimed at clarifying clinical value of contrast-enhanced ultrasound (CEUS) in the diagnosis and differentiation of BC. A total of 108 BC patients admitted to our hospital from January 2019 to December 2021 were enrolled. All patients underwent conventional color Doppler ultrasound and CEUS imaging examination. All ultrasound images were analyzed by a senior (5+ years) sonographer. The lesion location, echo, size, and color Doppler flow imaging (CDFI) blood flow distribution of benign and malignant BC were assessed. The transverse and longitudinal diameters of malignant BC presented significant elevation compared with the control group ($P < 0.05$). CEUS is more reliable than conventional ultrasound in the differentiation of benign and malignant breast lesions, and CEUS has the best reliability. The comparison of CEUS observation indicators between benign and malignant groups demonstrated that CEUS enhancement patterns (time and intensity) and morphological features (lesion boundary, shape, range, homogeneity, and filling defect) presented statistical significance ($P < 0.01$). Irregular shape and range expansion were high-specificity indicators (all >90.00%); fast-forward, high enhancement, clear boundary, and range expansion were high-sensitivity (all >90.00%); and fast-forward, high enhancement, and clear boundary were low-specificity indicators (all <50.00%); moderate sensitivity is as follows: homogeneous enhancement and range expansion (all >80.00%). The area under curve of CEUS (0.735 ± 0.053) presented elevation relative to conventional ultrasound (0.901 ± 0.024), with statistical significance ($Z1 = 2.462$, $P < 0.05$). Relative to conventional ultrasound, the specificity and positive predictive value of CEUS presented elevation ($P < 0.05$). In conclusion, in the differentiation of benign and malignant breast lesions, CEUS has better diagnostic accuracy and reliability than conventional ultrasound. The diagnostic advantages of CEUS are to elevate the diagnostic specificity and positive predictive value and reduce the misdiagnosis rate.

1. Introduction

Breast cancer (BC) ranks first in morbidity and mortality among female malignant tumors worldwide. The incidence and mortality of BC in China are expected to continue to rise for a long time in the future. BC can be detected, diagnosed, and treated early through population screening, and the 5-year survival of BC patients diagnosed at an early stage can reach more than 90% [1]. Traditional breast imaging methods include magnetic resonance imaging (MRI), mammography (MG), and conventional ultrasound. MRI has high resolution for soft tissue and has obvious advantages in diagnosing multiple and small breast lesions. However, because of its insensitivity to microcalcification, it has little diagnostic value for early BC. Additionally, its examination technique is complex and time-consuming, has many contraindications, and is expensive, which is mainly used as a supplementary examination for difficult cases of MG and conventional ultrasound diagnosis [2–4]. Conventional ultrasound and MG are the most commonly used methods

for breast tumor screening, but the imaging features of conventional two-dimensional ultrasound and MG in some early stage and BI-RADS grade III and IV BCs are not obvious; thus, diagnosis is difficult. Zhang et al. compared the diagnostic performance of conventional gray-scale ultrasound, MG, and MRI for benign and malignant breast lesions and found that MRI accuracy and sensitivity in diagnosing breast diseases were 86.9% and 95.5%, respectively, whose diagnostic performance is better than conventional gray-scale ultrasound and MG [5]. However, MRI cannot dynamically observe the imaging features of lesions in real time, and there are many contraindications, such as severe contrast medium allergy, toxic effects on kidneys, claustrophobia, and contraindications to metal implant examinations.

Pathological examination has been the gold standard for diagnosis in cancer, and its role has also included the elucidation of etiology, pathogenesis, clinicopathological correlation, and prognostication. With the development of sophisticated techniques of examination, pathologists have continued to seek biological information regarding the different types of breast cancer that are linked to clinical data such as overall survival, disease-free survival, or quality of life, and they have continued to develop methods for the earlier detection of tumors and metastases [6].

Contrast-enhanced ultrasound (CEUS) is the use of contrast agents to strengthen contrast between blood vessels and surrounding tissues. It can display tiny ($<10\,\mu$m), low-velocity (< 1 mm/s) blood flow in real time that cannot be detected by conventional ultrasound and provide information on microcirculation perfusion in the lesion and the features such as number, thickness, shape, and spatial distribution of new blood vessels, which has great advantages in the differentiation of benign and malignant diseases and has been widely used to qualitatively diagnose tumors of the liver and other abdominal organs [7, 8].

In this study, we aimed to clarify the clinical value of contrast-enhanced ultrasonography in the diagnosis and differential diagnosis of BC.

2. Materials and Methods

2.1. General Data. A total of 108 BC patients admitted to our hospital from January 2019 to December 2021 were enrolled. This study was approved by the ethical approval and obtained informed consent of all patients. 108 BC patients were divided into 2 groups: malignant group ($n = 68$) and benign group ($n = 40$). All patients underwent conventional color Doppler ultrasound and CEUS imaging examinations, all of which were single lesions. The average age of patients was (53.37 ± 5.15) years old; the lesion diameter ranged 0.53-2.5 cm, average: (1.29 ± 0.41) cm. Inclusion criteria were as follows: (1) those with BC confirmed by surgery and pathology, (2) those who knew about this research, and themselves and their families had no objection to participating in the research and signed the relevant agreement in advance. Exclusion criteria were as follows: (1) those complicated with severe dysfunction of the heart, kidneys, or other important organs; (2) those with mental disorders; and (3) those with poor cooperation in clinical examination due to physiological or psychological factors.

2.2. Methods. The PHILIPS EPIQ7 color diasonograph (PHILIPS, USA) was used, with linear array probe frequency of 5-12 MHz. Microbubble ultrasound contrast agent SonoVue lyophilized powder (BRACCO, Italy) was used as contrast agent, 0.9% sodium chloride solution was added before use, and the suspension was shaken and left to stand for use [9]. Specific methods were as follows: the patients were instructed to take off the jacket and take the supine position, and after the upper arm was abducted, the high-frequency ultrasonography took the nipple as the center and was scanned from transverse, oblique, and longitudinal planes. The transverse and anterior-posterior long diameters of the largest section of the lesion, as well as the location, shape, boundary, and size of the lesion, were measured. The Doppler flow imaging mode was chosen to evaluate the blood flow of the lesions. The CEUS mode was chosen, the probe was lightly placed on the skin surface and fixed, and the focus was adjusted and kept at the same depth as the lesion. The patients were instructed to maintain regular breathing, bolus 2.4 mL of contrast medium through the cubital vein, and then the tube was flushed. The observation time was set of more than 180 s, and the images were stored in the ultrasound apparatus [10].

2.3. Ultrasound Observation Indicators. All ultrasound images were analyzed by a senior (5+ years) sonographer. Conventional ultrasound observed the location, echo, size of breast lesions, and color Doppler flow imaging (CDFI) of blood flow distribution, etc., in the lesions. The section with the most abundant blood flow in the lesion was chosen, and CEUS mode was switched to. After the contrast agent was bolus injected through the median cubital vein, the breast lesion enhancement time and the filling direction of the contrast agent, whether there were perforating vessels around the lesion, the peak time, peak enhancement degree, lesion enhancement range after CEUS, enhancement mode, lesion hyperenhancement duration, etc., were observed and recorded.

2.4. Statistical Analysis. SPSS 21.0 software was used for data processing. Measurement data were expressed as mean ± standard deviation, and four-table count data were expressed as frequency. (1) Taking the pathological diagnosis as the "gold standard," the sensitivity, specificity, positive and negative predictive values, misdiagnosis rate, and missed diagnosis rate of conventional ultrasound and CEUS were, respectively, calculated, and the McNemar exact test based on binomial distribution was used for comparison. (2) Receiver operating characteristic curve (ROC) of the two diagnostic methods was constructed, and Z test was performed to compare the area under curve (AUC) differences between the two. (3) Kappa consistency analysis with the "gold standard" was used to compare the reliability of the two diagnostic methods (kappa value < 0.40 meant poor consistency; 0.40-0.75 meant moderate consistency; > 0.75 meant high consistency). (4) Pearson X or continuous

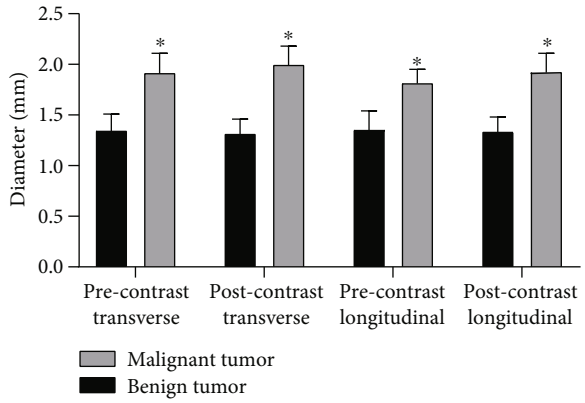

Figure 1: CEUS parameters of benign and malignant breast lesions. Note: $^*P < 0.05$, compared with benign tumor.

Table 1: Reliability comparison of two diagnostic methods.

Diagnostic methods	Pathological examination results		Kappa value	P
	Malignant ($n = 68$)	Benign ($n = 40$)		
Conventional ultrasound			0.571	
Malignant	40	18		
Benign	28	22		
CEUS			0.875	<0.01
Malignant	56	12		
Benign	12	28		
Total	68	40		

correction X test was used to compare CEUS observation indicators between groups. $P < 0.05$ was considered to be statistically significant.

3. Results

3.1. Clinical and Pathological Findings. All patients underwent needle biopsy or surgical treatment. Of the 108 breast lesions, 68 were confirmed to be breast malignant tumors by final pathological examination, including 53 invasive ductal carcinomas and ductal carcinoma in situ (DCIS), 4 encapsulated papillary carcinoma, and 2 mucinous carcinoma, while 40 were benign breast lesions, including 29 mastopathy and fibroadenoma, 8 intraductal papilloma, and 3 inflammatory lesions.

3.2. Comparison of CEUS Parameters between Benign and Malignant Breast Lesions. The changes of transverse and longitudinal diameters of malignant BC both presented elevation relative to benign one before and after CEUS ($P < 0.05$, Figure 1).

3.3. Reliability Comparison of Two Diagnostic Methods. With pathological diagnosis as the "gold standard," the kappa analysis of the two diagnostic methods and the "gold standard" demonstrated the moderate consistency of conventional ultrasound with "gold standard" (kappa value = 0.571) and the high consistency of CEUS with "gold standard" (kappa value = 0.875, $P < 0.01$), suggesting that CEUS may be more reliable than conventional ultrasound in the differentiation of benign and malignant breast lesions, and CEUS had the best reliability, as shown in Table 1.

3.4. Comparative Analysis of CEUS Observation Indicators and Pathological Diagnosis. The comparison of CEUS observation indicators between benign and malignant groups demonstrated that, except for the enhancement order ($P = 0.154$), CEUS enhancement patterns (time and intensity) and morphological features (lesion boundary, shape, range, homogeneity, and filling defect) presented statistical significance ($P < 0.01$).

Among them, irregular shape and range expansion were high-specificity indicators (all >90.00%); fast-forward, high enhancement, clear boundary, and range expansion were high-sensitivity indicators (all >90.00%); fast-forward, high enhancement, and clear boundary were low-specificity indicators (all <50.00%); moderate sensitivity was as follows: homogeneous enhancement and range expansion (all >80.00%).

It could be seen that CEUS image features may be used as an effective diagnostic indicator for benign and malignant breast lesions. However, the sensitivity and specificity within a single indicator and among multiple indicators vary greatly, and the improvement of accuracy depends on the combination of multiple indicators, as shown in Table 2.

3.5. AUC Comparison of Two Diagnostic Methods. Taking the sensitivity of conventional ultrasound and CEUS for the diagnosis of 68 lesions as the ordinate, and the 1-specificity as the abscissa, two ROC curves were constructed, and the AUCs were 0.735 ± 0.053 and 0.901 ± 0.024, respectively. CEUS curve was closer to the upper left of the coordinate, and CEUS and AUC presented elevation relative to conventional ultrasound, with statistical significance ($Z1 = 2.462$, $P < 0.05$), indicating that CEUS may be more valuable than conventional ultrasound in identifying benign and malignant breast lesions (Figure 2).

3.6. Accuracy Comparison of Two Diagnostic Methods. The McNemar exact test demonstrated that relative to conventional ultrasound, the specificity and positive predictive value of CEUS presented elevation ($P < 0.05$), whereas sensitivity and negative predictive value presented no difference ($P > 0.05$). It could be seen that elevating specificity and positive predictive value and reducing misdiagnosis rate were the diagnostic advantages of CEUS (Table 3).

4. Discussion

CEUS is a pure blood pool imaging technique. The size of the contrast agent used (about 2-6 μm in diameter) is comparable to that of red blood cells, and it cannot penetrate the vascular endothelial cell space to enter the surrounding tissue. It can display the microcirculation perfusion of lesions and surrounding tissues in real time and anatomical morphological characteristics such as the number, shape,

Table 2: The independent diagnostic efficacy of each CEUS observation indicator.

CEUS evaluation indicator	Pathological diagnosis (N) Malignant	Benign	Sensitivity	Specificity	P
Enhancement time					< 0.01
Fast-forward	64	14	96.77	34.29	
Same or slow-forward	4	26			
Enhancement intensity					
High enhancement	62	21	94.24	41.03	
Low or no enhancement	6	19			
Enhancement order					0.154
Centripetal	48	18			
Noncentripetal	20	22			
Lesion boundary					< 0.01
Clear	68	24	100.00	17.95	
Difficult to distinguish	0	16			
Lesion shape					< 0.01
Irregular	58	11	67.74	90.63	
Regular	10	29			
Enhancement homogeneity					< 0.01
Inhomogeneous	62	17	83.87	56.41	
Homogeneous	6	23			
Range expansion					< 0.01
Yes	61	11	90.65	90.63	
No	7	29			
Filling defect					< 0.01
Yes	20	5	72.26	89.74	
No	48	35			

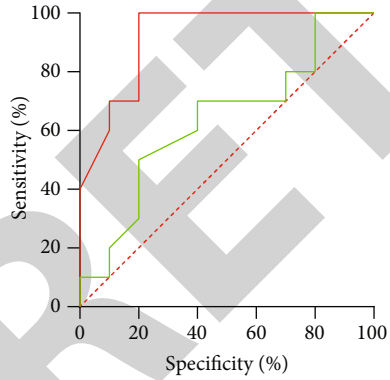

Figure 2: AUC of two diagnostic methods.

and spatial distribution of new blood vessels and indirectly reflect the hemodynamic characteristics through the enhancement mode, which has unique advantages in the differentiation of benign and malignant lesions [11]. In our study, the changes of transverse and longitudinal diameters of malignant BC both presented elevation relative to benign one before and after CEUS ($P < 0.05$).

In recent years, relevant studies have revealed that CEUS diagnostic performance in benign and malignant breast lesions is similar to or even slightly better than enhanced MRI [12, 13]. CEUS examination is more and more widely used clinically because of its simplicity, real-time dynamic observation, the ability to repeat multiple examinations, etc. The second-generation "pure blood pool" CEUS contrast agent represented by SonoVue can enter the breast tissue and capillary network of lesions and clearly and accurately display the microcirculation blood perfusion of lesions and surrounding glands in real time, which is helpful for diagnosis and differentiation of BC [14, 15]. Consistently, our study found that the kappa analysis of the two diagnostic methods and the "gold standard" demonstrated the moderate consistency of conventional ultrasound with "gold standard" (kappa value = 0.571) and the high consistency of CEUS with "gold standard" (kappa value = 0.875), suggesting that CEUS may be more reliable than conventional ultrasound in the differentiation of benign and malignant breast lesions, and CEUS had the best reliability.

Table 3: Accuracy of two diagnostic methods.

Diagnostic methods	Sensitivity	Specificity	Negative predictive value	Positive predictive value
Conventional ultrasound	80.65	61.55	80.00	62.50
CEUS	83.87	89.74	87.50	86.67

Although many domestic and foreign scholars have studied the CEUS sonographic features of breast malignancies, there is still a lack of unified diagnostic criteria, which limits the wide application of CEUS in breast diseases. CEUS is helpful for the diagnosis and differentiation of benign and malignant breast diseases [16, 17]. Herein, the BC enhancement range on CEUS was larger than that of conventional ultrasound. Breast malignancies are affected by vascular endothelial growth factor receptors, and there are many new microvessels around the tumor, which continuously infiltrate and grow into surrounding tissues. Thus, breast malignancy lesions are larger in CEUS than conventional gray-scale ultrasound, while benign breast lesions on CEUS presented no marked change in range relative to conventional gray-scale ultrasound [18].

Z test for AUC of two diagnostic methods demonstrated that CEUS had a higher diagnostic value (AUC: 0.901 ± 0.024), while conventional ultrasound had the lowest diagnostic value (AUC: 0.735 ± 0.053), with statistical significance. It is concluded that CEUS is superior to conventional ultrasound in terms of diagnostic accuracy, which is consistent with findings of Della and Arcovito [19]. There is a CEUS evaluation of irregular shape and inhomogeneous enhancement as malignant signs. The pairwise comparison of accuracy of three diagnostic methods by McNemar's exact test demonstrated that CEUS remarkably elevated diagnostic specificity and positive predictive value and reduced misdiagnosis rate, further validating the view of Chou et al. [20]. Though CEUS did not have obvious advantages in diagnostic sensitivity, negative predictive value, and missed diagnosis rate, CEUS correctly diagnosed many cases of BC classified as benign tumor by conventional ultrasound, avoiding delay in treatment due to missed diagnosis.

There are also some limitations in this study. First, some other factors may lead to these results, such as small sample size of this study and personal reasons of sonographers. Second, the CEUS real-time dynamic picture was not provided to show the pathological condition of BC patients. Thus, these interference factors will be avoided as possible as we can in the future study.

In conclusion, CEUS was superior to conventional ultrasound in diagnostic accuracy and reliability of benign and malignant breast lesions. The diagnostic advantage of CEUS was to elevate diagnostic specificity and positive predictive value and reduce misdiagnosis rate.

Data Availability

Data appears in the submitted manuscript.

Conflicts of Interest

The authors declare that there were no competing conflicts of interest.

Acknowledgments

This work was supported by the 2019 Medical Scientific Research Project of Provincial Health Commission (H2019048) and 2019 Six "One" Project for High-level Health Talents (LGY2019049).

References

[1] G. L. Menezes, F. M. Knuttel, B. L. Stehouwer, R. M. Pijnappel, and M. van den Bosch, "Magnetic resonance imaging in breast cancer: a literature review and future perspectives," *World Journal of Clinical Oncology*, vol. 5, no. 2, pp. 61–70, 2014.

[2] A. Chaiwerawattana, S. Thanasitthichai, S. Boonlikit et al., "Clinical outcome of breast cancer BI-RADS 4 lesions during 2003-2008 in the National Cancer Institute Thailand," *Asian Pacific Journal of Cancer Prevention*, vol. 13, no. 8, pp. 4063–4066, 2012.

[3] D. E. Kuczek, A. M. H. Larsen, M. L. Thorseth et al., "Collagen density regulates the activity of tumor-infiltrating T cells," *Journal for Immunotherapy of Cancer*, vol. 7, no. 1, p. 68, 2019.

[4] L. Tao, G. Huang, H. Song, Y. Chen, and L. Chen, "Cancer associated fibroblasts: an essential role in the tumor microenvironment," *Oncology Letters*, vol. 14, no. 3, pp. 2611–2620, 2017.

[5] J. Zhang, X. J. Lai, Q. L. Zhu et al., "Interobserver agreement for sonograms of breast lesions obtained by an automated breast volume scanner," *European Journal of Radiology*, vol. 81, no. 9, pp. 2179–2183, 2012.

[6] S. Masuda, "Pathological examination of breast cancer biomarkers: current status in Japan," *Breast Cancer*, vol. 23, no. 4, pp. 546–551, 2016.

[7] X. W. Bian, X. F. Jiang, J. H. Chen et al., "Increased angiogenic capabilities of endothelial cells from microvessels of malignant human gliomas," *International Immunopharmacology*, vol. 6, no. 1, pp. 90–99, 2006.

[8] T. R. Cox and J. T. Erler, "Molecular pathways: connecting fibrosis and solid tumor metastasis," *Clinical Cancer Research*, vol. 20, no. 14, pp. 3637–3643, 2014.

[9] I. Acerbi, L. Cassereau, I. Dean et al., "Human breast cancer invasion and aggression correlates with ECM stiffening and immune cell infiltration," *Integrative Biology*, vol. 7, no. 10, pp. 1120–1134, 2015.

[10] M. Golatta, D. Franz, A. Harcos et al., "Interobserver reliability of automated breast volume scanner (ABVS) interpretation and agreement of ABVS findings with hand held breast ultrasound (HHUS), mammography and pathology results," *European Journal of Radiology*, vol. 82, no. 8, pp. e332–e336, 2013.

[11] Y. Liu, J. Kim, F. Qu et al., "CT features associated with epidermal growth factor receptor mutation status in patients with lung adenocarcinoma," *Radiology*, vol. 280, no. 1, pp. 271–280, 2016.

[12] R. M. S. Sigrist, J. Liau, A. E. Kaffas, M. C. Chammas, and J. K. Willmann, "Ultrasound elastography: review of techniques and clinical applications," *Theranostics*, vol. 7, no. 5, pp. 1303–1329, 2017.

[13] R. Menezes, S. Sardessai, R. Furtado, and M. Sardessai, "Correlation of strain elastography with conventional sonography and FNAC/biopsy," *Journal of Clinical and Diagnostic Research*, vol. 10, no. 7, pp. TC05–TC10, 2016.

[14] J. H. Moon, S. H. Koh, S. Y. Park, J. Y. Hwang, and J. Y. Woo, "Comparison of the SRmax, SRave, and color map of strain-elastography in differentiating malignant from benign breast lesions," *Acta Radiologica*, vol. 60, no. 1, pp. 28–34, 2019.

Hindawi
Computational and Mathematical Methods in Medicine
Volume 2023, Article ID 9843413, 1 page
https://doi.org/10.1155/2023/9843413

Retraction

Retracted: Microarray and Bioinformatics Analysis of Differential Gene and lncRNA Expression during Erythropoietin Treatment of Acute Spinal Cord Injury in Rats

Computational and Mathematical Methods in Medicine

Received 5 December 2023; Accepted 5 December 2023; Published 6 December 2023

This article has been retracted by Hindawi, as publisher, following an investigation undertaken by the publisher [1]. This investigation has uncovered evidence of systematic manipulation of the publication and peer-review process. We cannot, therefore, vouch for the reliability or integrity of this article.

Please note that this notice is intended solely to alert readers that the peer-review process of this article has been compromised.

Wiley and Hindawi regret that the usual quality checks did not identify these issues before publication and have since put additional measures in place to safeguard research integrity.

We wish to credit our Research Integrity and Research Publishing teams and anonymous and named external researchers and research integrity experts for contributing to this investigation.

The corresponding author, as the representative of all authors, has been given the opportunity to register their agreement or disagreement to this retraction. We have kept a record of any response received.

References

[1] H. He, H. Huang, P. Hu, and Z. Chen, "Microarray and Bioinformatics Analysis of Differential Gene and lncRNA Expression during Erythropoietin Treatment of Acute Spinal Cord Injury in Rats," *Computational and Mathematical Methods in Medicine*, vol. 2022, Article ID 4121910, 13 pages, 2022.

Hindawi
Computational and Mathematical Methods in Medicine
Volume 2022, Article ID 4121910, 13 pages
https://doi.org/10.1155/2022/4121910

Review Article

Microarray and Bioinformatics Analysis of Differential Gene and lncRNA Expression during Erythropoietin Treatment of Acute Spinal Cord Injury in Rats

Haibo He,[1] **Hanwen Huang**,[2] **Panyong Hu**,[3] **and Zhong Chen**[2]

[1]*Department of Spinal Surgery, University of South China Affiliated Nanhua Hospital No. 336, Dongfeng South Road, Zhuhui District, Hengyang, Hunan, China*
[2]*Department of Spinal Surgery, Zhujiang Hospital of Southern Medical University, 253# Industry Road, 510280 Guangzhou, Guangdong, China*
[3]*Department of Spinal Surgery, Affiliated Hospital of Guilin Medical University, No. 15, Lequn Road, Guilin, Guangxi Zhuang Autonomous Region, China*

Correspondence should be addressed to Zhong Chen; chenzhong@smu.edu.cn

Received 5 July 2022; Revised 10 August 2022; Accepted 20 August 2022; Published 2 September 2022

Academic Editor: Min Tang

Purpose. We performed a genome-wide analysis of long noncoding RNA (lncRNA) expression to identify novel targets for the further study of recombinant human erythropoietin (rhEPO) treatment of acute spinal cord injury (SCI) in rats. *Methods*. Nine rats were randomly divided into 3 groups. No operation was performed in group 1. In groups 2 and 3, a laminectomy was performed at the 10th thoracic vertebra, and a contusion injury was induced by extradural application of an aneurysm clip. Group 1 rats did not receive any treatment, group 2 rats received a single intraperitoneal injection of normal saline, and group 3 rats received rhEPO. Three days after injury, spinal cord tissues were collected for RNA-Seq, microarray, differentially expressed genes (DEGs), Gene Ontology (GO) function enrichment, Kyoto Encyclopedia of Genes and Genomes (KEGG) pathway enrichment, and protein-protein interaction (PPI) analyses. *Results*. Compared with group 1, 4,446 genes were found to be differentially expressed in group 2. Furthermore, 99 lncRNAs were found to be changed in the injury group. The data indicate that 2,471 mRNAs were upregulated, and 1,975 mRNAs were downregulated in group 2 as compared with group 1. In addition, 45 of the lncRNAs were upregulated, and the other 44 lncRNAs were downregulated. The top 5 upregulated and top 5 downregulated lncRNAs that were different between group 2 and group 1 are shown. The top 5 downregulated and the top 5 upregulated lncRNAs that were different between group 3 and group 2 are shown. *Conclusion*. RhEPO treatment alters the expression profiles of the differentially expressed lncRNAs and genes beneficial to the development of new treatments.

1. Introduction

Spinal cord injury (SCI) is a global health problem, and each year, there are 15 to 40 acute SCIs per million persons commonly caused by high falls, community violence, recreational activities, and traffic accidents [1]. SCI can lead to serious damage to the nervous system, including quadriplegia and paraplegia, which seriously affect quality of life [2]. The pathophysiological mechanisms of SCI are complex and involve ischemia-reperfusion leading to endothelial dysfunction and vascular permeability changes, which induce a cascade of inflammation and subsequent neuronal death and loss of neurological function [3].

Although much research has been devoted to elucidate the complex pathophysiological processes that follow SCI, no definitive treatments have been developed. Early decompression surgery can have a positive impact on outcomes. The only pharmacological treatment that is known to ameliorate neurologic dysfunction after SCI is methylprednisolone (MP). Therefore, new therapeutic strategies to promote functional recovery in SCI patients are necessary, and a better understanding of the cellular and molecular

mechanisms of SCI may help in the development of new treatments [4].

Erythropoietin (EPO), also known as red blood cell (RBC) stimulating factor, is a human endogenous glycoprotein hormone that stimulates RBC production. The production of EPO is stimulated in a hypoxic environment, and EPO is used clinically for the treatment of anemia associated with renal insufficiency [5]. In a prior study, we reported that recombinant human erythropoietin (rhEPO) reduced apoptosis and inflammation and promoted myelin repair and functional recovery following compressive SCI in rats and that delayed treatment is equally effective [6]. To our knowledge no specific cellular and molecular studies have been undertaken to understand the mechanism by which rhEPO helps repair SCI.

Long noncoding RNAs (lncRNAs) [7] are RNA transcripts longer than 200 nucleotides that lack protein coding ability. Compared to well-studied protein-coding genes, the function of most lncRNAs has not been elucidated, even though a large number of genes have been identified [8, 9]. However, recent studies indicated that lncRNAs are important regulatory molecules in the human genome, which exert their biological control in various ways [10, 11]. lncRNAs have been associated with cell proliferation, survival, and differentiation, genomic stability, and chromatin remodeling [12–14]. With the development of high-throughput sequencing technology, more and more lncRNAs have been identified, and a recent study showed that lncRNA deregulation is an important factor in various nervous system pathologies and that it may play a crucial role in SCI [15].

Thus far, no studies have focused on the differential expression of lncRNAs and mRNAs in SCI treated with EPO. Thus, the purpose of this study was to examine differentially expressed lncRNAs and mRNAs by transcriptome sequencing (RNA-seq) in SCI tissues in a rat model treated with rhEPO. Data from this study may help the development of novel treatments for SCI.

2. Materials and Methods

2.1. Animals. The study protocols conformed to the Guide for the Care and Use of Laboratory Animals from the National Institutes of Health and were approved by the Animal Care and Use Committee of Southern Medical University. Nine adult male Sprague–Dawley rats (220–260 g) were purchased from the Animal Center of Southern Medical University. All rats were housed 3 per cage under temperature-controlled conditions, with a 12 h light/dark cycle, and had free access to tap water and food.

2.2. Experimental Design. The 9 rats were randomly divided into 3 groups: group 1, blank control group; group 2, SCI group; group 3, rhEPO treatment group. All rats were continuously observed and fed for 3 days prior to the experiments.

No procedures were performed on the rats in group 1. They were fed and had free access to water. In group 2, a laminectomy was performed at the 10^{th} thoracic vertebra, and contusion injury was induced by extradural application of an aneurysm clip. The spinal cord was clamped for 30 seconds. Penicillin (1,200,000 U/kg, intramuscular) was given immediately after injury for preventing infection of the surgical incision. An intraperitoneal injection of normal saline (5 ml/kg) was given within 2 hours of the injury and repeated for the next 3 days. Group 3 rats received the same injury as group 2 rats. In group 3, a rhEPO intraperitoneal infusion (3000 U/kg) was given within 2 hours of the injury, and the same rhEPO infusion was given for the next 3 days. As in group 2, penicillin was given immediately after the injury.

Three days after SCI, spinal cord tissue was collected from each rat for the experiments described below.

2.3. Surgical Procedures. Rats were deeply anesthetized with an intraperitoneal pentobarbital injection (40 mg/kg) and were fixed in the prone position. Back hair on the surgical area was removed with electric shaver, and the area was disinfected with 3% iodophor. After locating the T10 spinous process, a 2 cm midline incision was made on the midline of the back from the T8 to T12 vertebrae. The overlying musculature was separated laterally, and the spinal cord was exposed by a complete T10 level laminectomy. Subsequently, the spinal cord was subjected to extradural compression with a temporary aneurysm clip (70g force; 65821T; Rebstock, Dürbheim, Germany) for 30 seconds to induce a crush injury. The surgical site was closed using nondegradable sutures after removing the aneurysm clip, and then, the closed skin incision was disinfected again with 3% iodophor. During the procedure, body temperature was maintained with a heat lamp.

After surgery, all rats received 2 ml of 10% glucose solution, tramadol hydrochloride (50 mg/kg) for postoperative analgesia, and penicillin (800,000 U/kg) by intramuscular injection to prevent infection of the surgical incision. The rats were returned to their cages after they completely recovered from anesthesia.

The rats were fed normally with food and water for 3 days, and manual bladder evacuation was performed 3 times a day. On the third postoperative day, the wound was recut and 1 cm of spinal cord tissue was taken from the exposed spinal cord and rapidly frozen in liquid nitrogen. After the sample was completely frozen, it was stored in an airtight container at -80°C until RNA extraction.

2.4. RNA Extraction. RNA was extracted from spinal cord tissue using the TRIzol method, according to the manufacturer's instructions.

2.5. Microarray Analysis. The mRNA in spinal cord tissue samples was enriched with magnetic beads with the probe named oligo (dT). Subsequently, fragmentation buffer was added to break the mRNA into short fragments, and the mRNA was used as a template to synthesize cDNA using random hexamers. Double-stranded cDNA was then synthesized by the addition of buffer, dNTPs, and DNA polymerase I and RNase H. The double-stranded cDNA was then purified using AMPure XP beads.

Purified double-stranded cDNA was repaired, A-tailed, and ligated to the sequencing linker, and fragment size was selected using AMPure XP beads. Finally, PCR amplification was carried out, and the PCR product was purified with AMPure XP beads to obtain a final library.

After the library was constructed, preliminary quantification was performed using a Qubit 2.0 fluorometer (USA, Invitrogen), and the insert size of the library was subsequently detected using an Agilent 2100 bioanalyzer (USA, Agilent). After the insert was determined to be consistent with expectations, q-PCR was used to accurately quantify the effective concentration of the library to ensure library quality. After the quality of the library was confirmed, the high-throughput sequencing was conducted.

The raw reads, the data by sequencing, need to be filtered to eliminate low-quality reads in order to ensure the quality of the information analysis. The subsequent data obtained is recorded as total data. By removing the known ribosomal RNAs from the total data (28S rRNA, 18S rRNA, 12S rRNA, 5.8S rRNA, and 5S rRNA), high-quality, clean data was obtained. The ribosomal RNA that was removed was identified using the database of the National Center for Biotechnology Information (NCBI, https://www.ncbi.nlm.nih.gov). Subsequent microarray profiling was performed by the Boyue Biotechnology Company (Wuhan, China).

2.6. qRT-PCR Validation of Microarrays. To confirm the repeatability of the microarray assays, 6 additional rats were divided into 2 groups and treated the same as the rats in group 2 (SCI group) and group 3 (SCI+rhEPO group), respectively. After total RNA was extracted from the spinal cord of the 6 rats, qRT-PCR assays were performed. Briefly, the qRT-PCR assays consisted of 2 steps, RNA reverse transcription (RT) and qPCR detection. First, the PrimeScript™ RT reagent Kit with gDNA Eraser (TAKARA) was used to synthesize cDNA according to the manufacturer's instructions after removing the genomic DNA. RT-PCR was then performed using SYBR® Premix Ex Taq™ II (TAKARA). The reaction system consists of 10 μl SYBR® Premix Ex Taq™ II, 0.4 μl PCR Forward Primer (10 μM), 0.4 μl PCR Reverse Primer (10 μM), 2 μl cDNA, and 7.2 μl ddH_2O. The primer sequences were designed and synthesized in the laboratory by the Guangzhou cm biotechnology and are listed in Table 1. The reaction conditions were: 95°C for 10 minutes; a total of 40 cycles at 95°C for 15 seconds and 60°C for 20 seconds. Each sample tested in triplicate. Gene expression levels were normalized to glyceraldehyde 3-phosphate dehydrogenase (GAPDH) using the $\Delta\Delta$CT method. Finally, Student's t-test was used to examine differences between the 2 groups, and values of $p < 0.05$ were considered statistically significant.

2.7. Differentially Expressed Gene (DEG) Analysis and Gene Ontology (GO) Enrichment Analysis. DEG analysis refers to the identification of genes with significant differences in expression levels between different sample groups. The clean data was analyzed using the DESeq2 package (http://www.bioconductor.org/packages/release/bioc/html/DESeq2.html) in the R programming language (version 3.60) because our sample had only 3 per group [16]. When the biological repeat reaches 5 to 10, a better choice is to use a nonparametric method.

Table 1: The list of primers for qRT-PCR.

Primer	Sequence (5′to 3′)
Actin b-F	GTGATGGACTCCGGAGACG
Actin b-R	GTGGTGAAGCTGTAGCCACG
Ccl5-F	GAAGATCTCCACAGCTGCATC
Ccl5-R	GTGACAAAGACGACTGCAAGG
Ppbp-F	CTTCAGACTCAGACCTACATC
Ppbp-R	CCACATTGTCACAGTGCGC
Ahsp-F	CTCATGCCTGAAGAAGACATG
Ahsp-R	CAGAATGATCCTGTATTTGGC
Plk5-F	GCACCACCGCAACATCGTG
Plk5-R	GGTCACCTATCTTAACTTCCATG
Mmp7-F	GGACTGCAGACATCATAATTGG
Mmp7-R	GTGGCCAAGTTCATGAGTGG
Esrp2-F	GGGATGACAAACCACTAGCTG
Esrp2-R	CTTGCCCTCTGGTATTCACTG

DESeq2 is the most popular statistical method to analyze DEGs, and it can estimate variance-mean dependence in clean data, and test for differential expression based on a model using a negative binomial distribution. The log2-fold change (log2FC) and p values of the genes were calculated [17]. A gene was considered to be a DEG when the log2FC was >1 and the p value was <0.05. The lncRNA information was then extracted from DEG analysis result based on the lncRNA annotation information provided in the reference genome annotation file.

GO enrichment analysis is used to annotate genes and gene products and to provide gene function classification labels and background knowledge of gene function and has become a common approach for sequencing data processing [17–19]. GO enrichment analysis can be divided into 3 parts: molecular function (MF), biological process (BP), and cell composition (CC). GO annotation information of genes can be found by searching the GO database by species and genetic information. Based on the GO annotation of a gene, all of the genes of the species can be selected as background genes, and p values can be calculated using statistical methods. As such, distribution information and the significance of the gene collection of the GO category can be obtained.

To gain further insights into the changes of biological pathways in the cells of SCI rats, Kyoto Encyclopedia of Genes and Genomes (KEGG analysis) was performed. KEEG is a database of biochemical reactions, signaling pathways, metabolic pathways, and biological processes and can be used to identify the significant pathways associated with DEGs.

The clusterprofiler package (https://bioconductor.org/packages/release/bioc/html/ clusterProfiler.html) in the R programming language (version 3.60) allows 2 methods of analysis. In the analyses in this study, a value of $p < 0.05$ was considered to indicate statistical significance.

Table 2: The differential expression profile of the known mRNAs and lncRNAs.

Group	mRNA		lncRNA	
	Upregulation	Downregulation	Upregulation	Downregulation
G2 vs. G1	2471	1975	45	54
G3 vs. G2	151	76	9	5

The number of this table represented the quantity of differential expression of lncRNAs and mRNAs.

2.8. Protein-Protein Interaction (PPI) Network Construction. The Search Tool for the Retrieval of Interacting Genes (STRING, http://string-db.org/) is a database that aims to provide a critical assessment and integration of PPI, including direct (physical) and indirect (functional) associations [20]. In the PPI network built using the STRING online tool, each node signifies a gene, and the edges indicate interactions between nodes. The degree is defined as the number of edges linked to a given node.

Cytoscape is software that provides data integration and network visualization [21], especially in respect to the processing of databases of protein-protein interactions [22]. In the current study, the cytoHubba plug-in of Cytoscape (version 3.61) was used to screen the hub genes from the PPI network, and a node degree of ≥10 was screen as the hub genes from the PPI.

3. Results

3.1. Screening and Identification of DEGs. DEGs between samples were selected by differential multiples (log 2FC > 1) and a significance level of $p < 0.05$. Compared with group 1, 4,446 genes were found to be differentially expressed in group 2. Furthermore, 99 lncRNAs were found to be changed in the injury group. The data indicate that 2,471 mRNAs were upregulated, and 1,975 mRNAs were downregulated in group 2 as compared with group 1. In addition, 45 of the lncRNAs were upregulated, and the other 44 lncRNAs were downregulated (Table 2). A volcano plot was created that visually showed how the expressions of the lncRNAs and mRNAs changed dramatically (Figure 1).

A comparison of group 3 with group 2 identified 228 DEGs. Furthermore, 14 lncRNAs were found to be changed in group 3 as compared with group 2 (Table 2).

Cluster analysis of DEGs was used to determine the clustering pattern of DEGs in the different groups. The top 50 genes with the largest variance in expression between the different groups, including the known lncRNAs and mRNAs, were used for cluster analysis (Figure 2).

3.2. qRT-PCR. To further confirm the accuracy of the microarray assays, 6 differentially expressed mRNAs, including 3 upregulated mRNAs (Ccl5, Ppbp, and Ahsp) and 3 downregulated mRNAs (Plk5, Mmp7, and Esrp2), were randomly selected for qRT-PCR analysis to compare between group 3 (SCI + rhEPO group) and group 2 (SCI group).

As shown in Figure 3, the expression patterns of the selected mRNAs were consistent with the mRNA-seq results ($p < 0.05$ for each mRNA, Student's t test). These results indicated that the microarray were highly reliable.

3.3. Top Differentially Expressed lncRNAs between the Groups. The top 5 upregulated and top 5 downregulated lncRNAs that were different between group 2 and group 1 are shown in Table 3. The top 5 downregulated and the top 5 upregulated lncRNAs that were different between group 3 and group 2 are shown in Table 4.

3.4. GO and KEGG Pathway Enrichment Analyses. The gene function enrichment analysis was divided into 2 steps: gene function annotation and enrichment analysis. The 3 GO domains used to describe the gene product attributes were MF, BP, and CC (molecular function, biological process, and cell composition, respectively). GO analysis was performed for the DEGs between group 2 and group 1, and the top 15 are shown in Figure 4(a). As shown in the figure, the biological processes of the DEGs were primarily associated with positive regulation of the immune response, regulation of vesicle-mediated transport, regulation of leukocyte activation, wound healing, regulation of transmembrane transport, and other significant biological processes in SCI. In addition, the main 15 KEGG enrichment pathways were related to Epstein-Barr virus infection, focal adhesions, the calcium signaling pathway, retrograde endocannabinoid signaling, osteoclast differentiation, platelet activation, and systemic lupus erythematosus (SLE) and were highly significantly correlated with SCI (Figure 5(a)).

Furthermore, GO and KEGG enrichment analyses were performed between group 3 and group 2 to gain further insights into the changes of biological pathways associated with rhEPO treatment of SCI. GO enrichment analysis reveals 15 significant metabolic networks, including leukocyte chemotaxis, myeloid leukocyte migration, granulocyte migration, granulocyte chemotaxis, neutrophil migration, and other biological processes that were significantly enriched in group 3 (Figure 4(b)). KEGG enrichment analysis indicated that the enriched DEGs were associated with cytokine-cytokine receptor interaction, the chemokine signaling pathway, human cytomegalovirus infection, IL-17 signaling path, malaria, and herpes simplex infection (Figure 5(b)).

3.5. PPI Network Construction. Based on data from the STRING database with medium confidence (data chosen had a minimum required interaction score of >0.4), a PPI network with 809 nodes and 5,081 edges was constructed between group 2 and group 1 and was visualized using Cytoscape (Figure 6).

In the PPI network, 10 nodes were selected as hub genes using the Maximal Clique Centrality (MCC) method, which is available in the cytoHubba plug-in of Cytoscape. The hub genes were fibronectin 1 (FN1), protein tyrosine

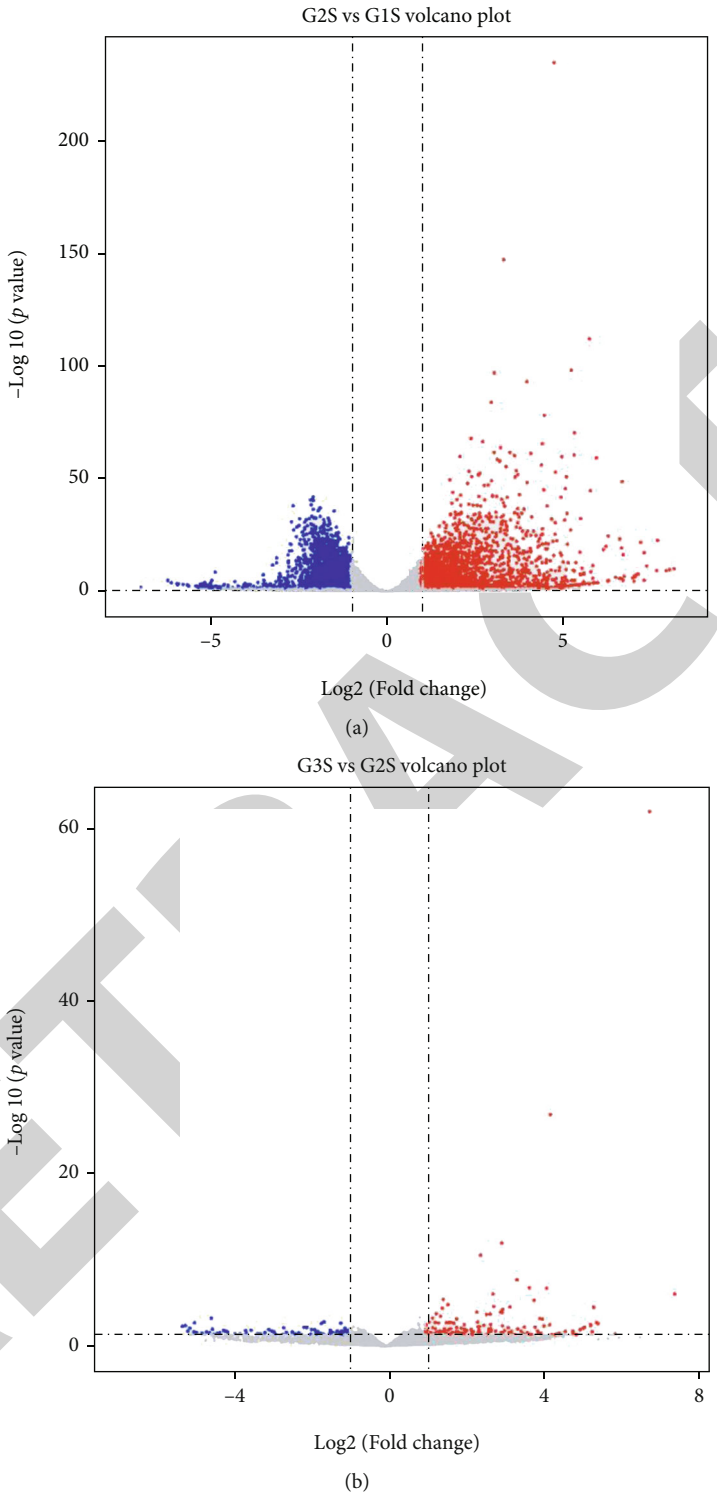

Figure 1: In the volcano diagram, each point represents a gene, and the X-axis represents the logarithm of the multiple of the difference in expression of a certain gene in the two samples; the Y-axis represents the statistically significant negative logarithm of the gene expression change. The larger the absolute value of the X-axis, the greater the fold change in expression between the two samples; the larger value of Y-axis, the more significant the differential expression, and the more reliable the DEGs obtained by screening. The blue dots (fold change < -1) in the figure represent downregulated DEGs, the red dots (fold change > 1) represent upregulated DEGs, and the grey dots represent non-DEGs.

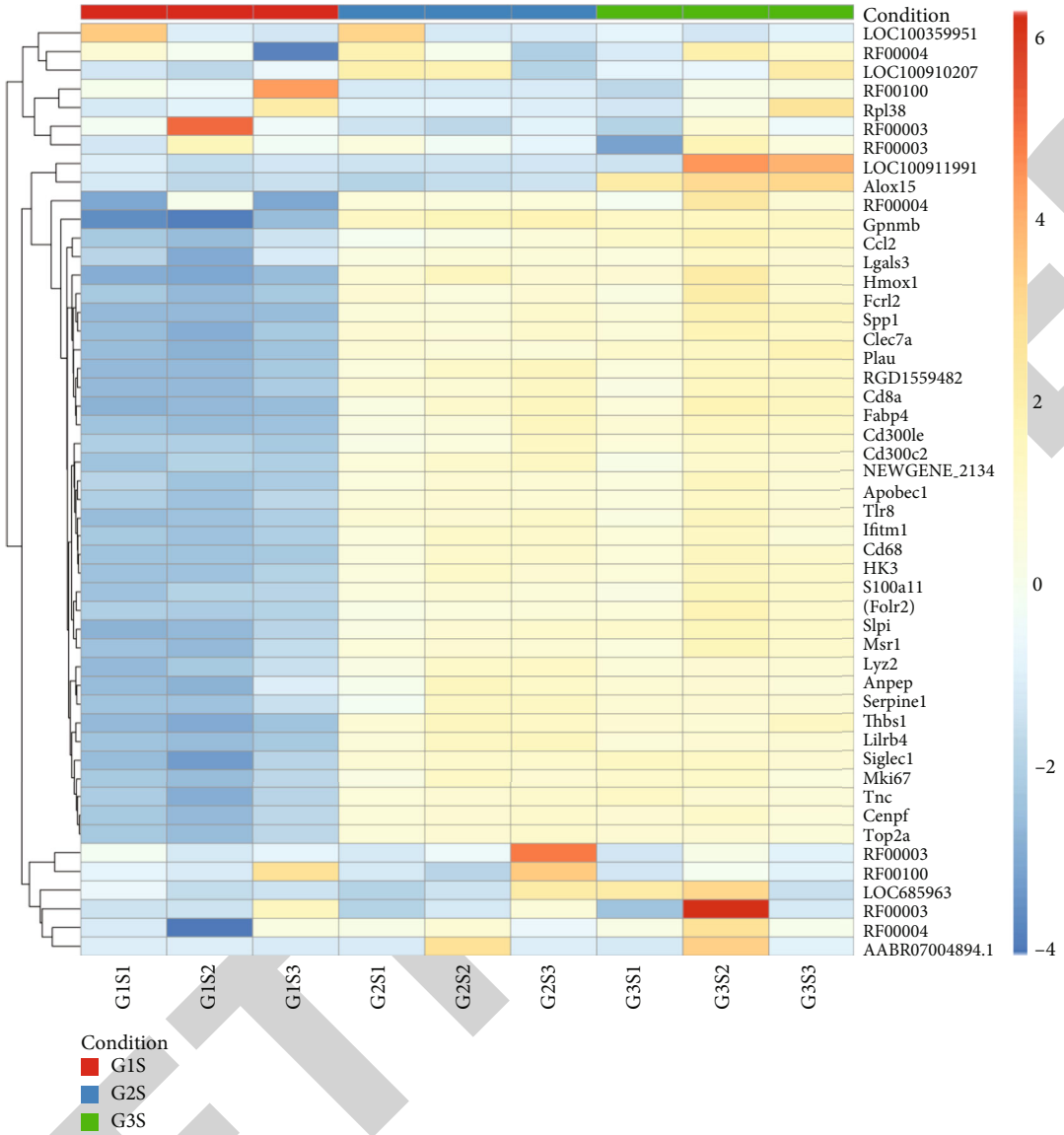

Figure 2: In the heatmap, the red color represents upregulated mRNAs or lncRNAs, and the blue color represents downregulated mRNAs or lncRNAs.

phosphatase receptor type C (PTPRC), cluster of differentiation 4 (CD44), cell division cycle 20 (CDC20), TYRO protein tyrosine kinase-binding protein (TYROBP), aurora kinase B (AURKB), toll-like receptor 2 (TlR2), angiotensinogen (AGT), Rac family small GTPase 2 (RAC2), and matrix metallopeptidase 9 (MMP9). Of the 10 hub genes, FN1 had the highest score of 108 (Table 5).

Similarly, a comparative study of group 3 and group 2 was conducted using the same methods. The constructed PPI network had 70 nodes and 129 edges (Figure 7). The top 10 key genes are shown in Table 6.

4. Discussion

In most cases, SCI is a disabling and irreversible disease that is associated with great social and economic cost to families and society [23]. SCI is a complex biological process that includes both primary and secondary damage and involves the nervous, immune, and vascular systems [24]. The initial mechanical trauma can lead to neuron necrosis and apoptosis, and the secondary damage often worsens the injury [25, 26]. Active research of SCI has made slow but consistent progress with respect to developing new treatments. With respect to mRNA and lncRNA, a recent study by Jin et al. [27] identified significant DEGs at 3 days, 2 weeks, and 1 month following SCI. Based on the results of Jin's study, we choose 3 days post-SCI as the time point of our study.

Our results demonstrated that the expressions of certain mRNAs and lncRNAs were dramatically changed 3 days after SCI. Furthermore, we identified 10 key genes in the injury group (group 2) and the rhEPO treatment group (group 3) that may play an important role in early acute phase of SCI. These genes may assist in further research of SCI and the development of new treatments.

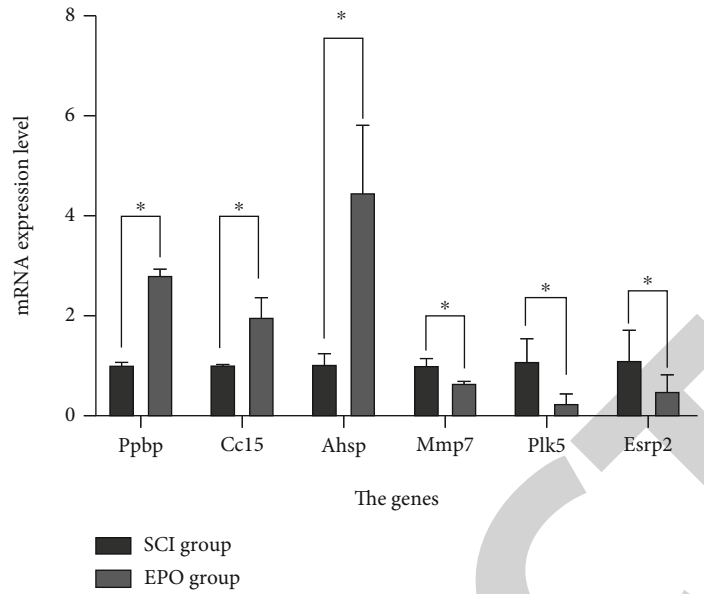

Figure 3: The qRT-PCR result was consistent with that of the microarray between group 3 and group 2, in that the first 3 mRNAs had a rising trend, while the last 3 mRNAs showed a downward trend. All 6 mRNA transcripts reached statistical significance ($p < .05$ for each mRNA, Student's T test), as seen in Figure 1. Verification expression levels of DEGs in qRT-PCR during EPO treatment of SCI in rats. DEGs: differentially expressed genes; SCI: spinal cord injury; EPO: erythropoietin.

Table 3: The top 5 upregulated and downregulated lncRNAs between the group 2 and group 1.

Upregulated lncRNAs			Downregulated lncRNAs		
ID	log2FC	p value	ID	log2FC	p value
AABR07030791.1	8.19	8.50E-11	AABR07028797.1	-6.05	0.000167407
AABR07049503.1	6.02	0.000129838	AC105485.2	-5.86	0.000437654
AABR07027569.3	6.01	0.000152459	AABR07028793.1	-5.61	0.00116144
AABR07038983.1	5.84	2.00E-09	AABR07048040.1	-5.55	0.004700986
AABR07021998.1	5.77	0.000287606	AABR07007879.1	-5.33	0.005198832

Table 4: The top 5 downregulated and upregulated lncRNAs between the group 3 and group 2.

Upregulated lncRNAs			Downregulated lncRNAs		
ID	log2FC	p value	ID	log2FC	p value
LOC100910750	5.34	0.023054	AABR07069008.3	-5.09	0.019272
AC096330.1	4.02	0.033215	AABR07044454.1	-5.04	0.008021
AABR07002674.1	3.86	0.007318	AABR07062344.2	-4.32	0.031877
AABR07007055.1	2.42	0.015358	AABR07051515.2	-4.12	0.021149
AABR07019254.2	2.40	0.027412	AABR07053771.1	-2.42	0.025481

The genes in the injury group (group 2) with significant changes in expression profiles were associated with the positive regulation of the immune response, regulation of vesicle-mediated transport, regulation of leukocyte activation, wound healing, regulation of transmembrane transport, and other significant biological processes. Previous studies have indicated that the primary cellular responses to SCI are inflammation and an immune response, which is consistent with our GO analysis results. SCI induces the activation of immune cells and inflammatory mediators, but the benefit of targeting the immune response to treat SCI is not clear [28].

Stimulation of the proliferation of leukocytes is also a key process of SCI that occurs from the immediate phase to the chronic repair phase. Our KEGG enrichment analysis demonstrated that the genes with changes of expression were involved in Epstein-Barr virus infection, focal adhesions, the calcium signaling pathway, retrograde endocannabinoid signaling, osteoclast differentiation, platelet activation, and SLE. In a prior study, KEGG enrichment

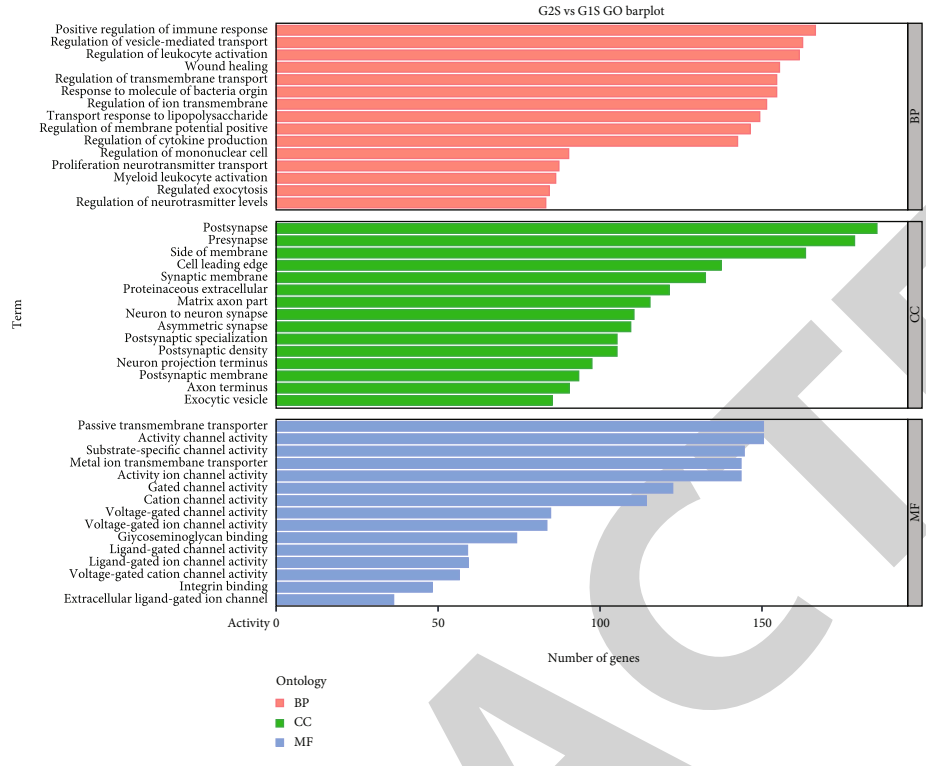

(a)

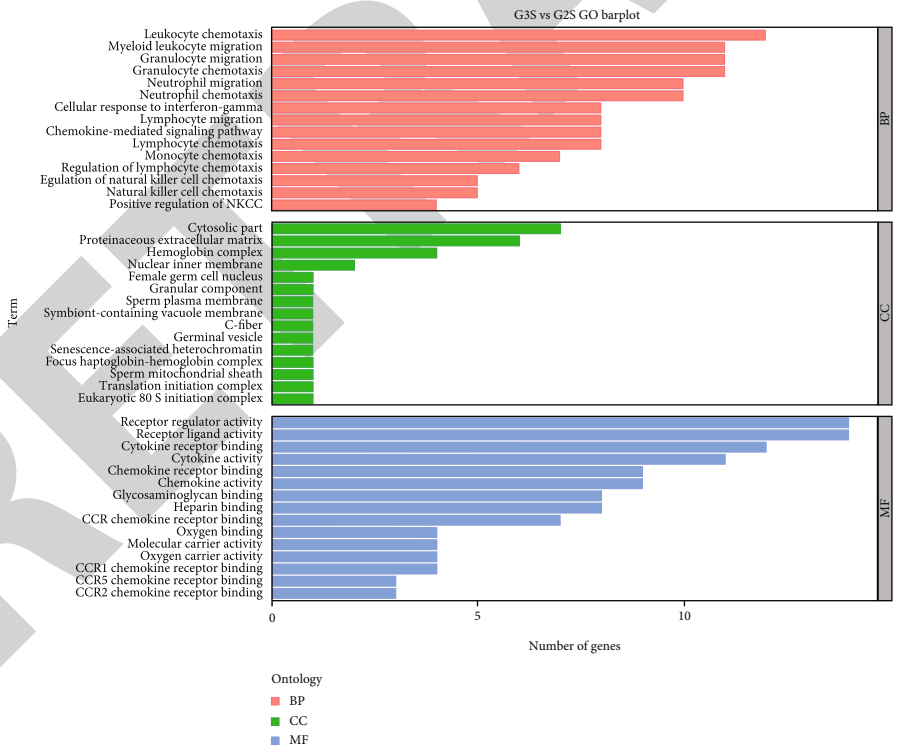

(b)

Figure 4: GO term enrichment analysis of mRNAs in the early acute phase of SCI. (a) GO annotations of DEGs with top 15 enrichment scores between group 1 and group 2. (b) GO annotations of DEGs with top 15 enrichment scores between group 3 and group 1. The red represents BC; the green represents CC; the blue represents MF. BC: biological process; CC: cell component; MF: molecular function.

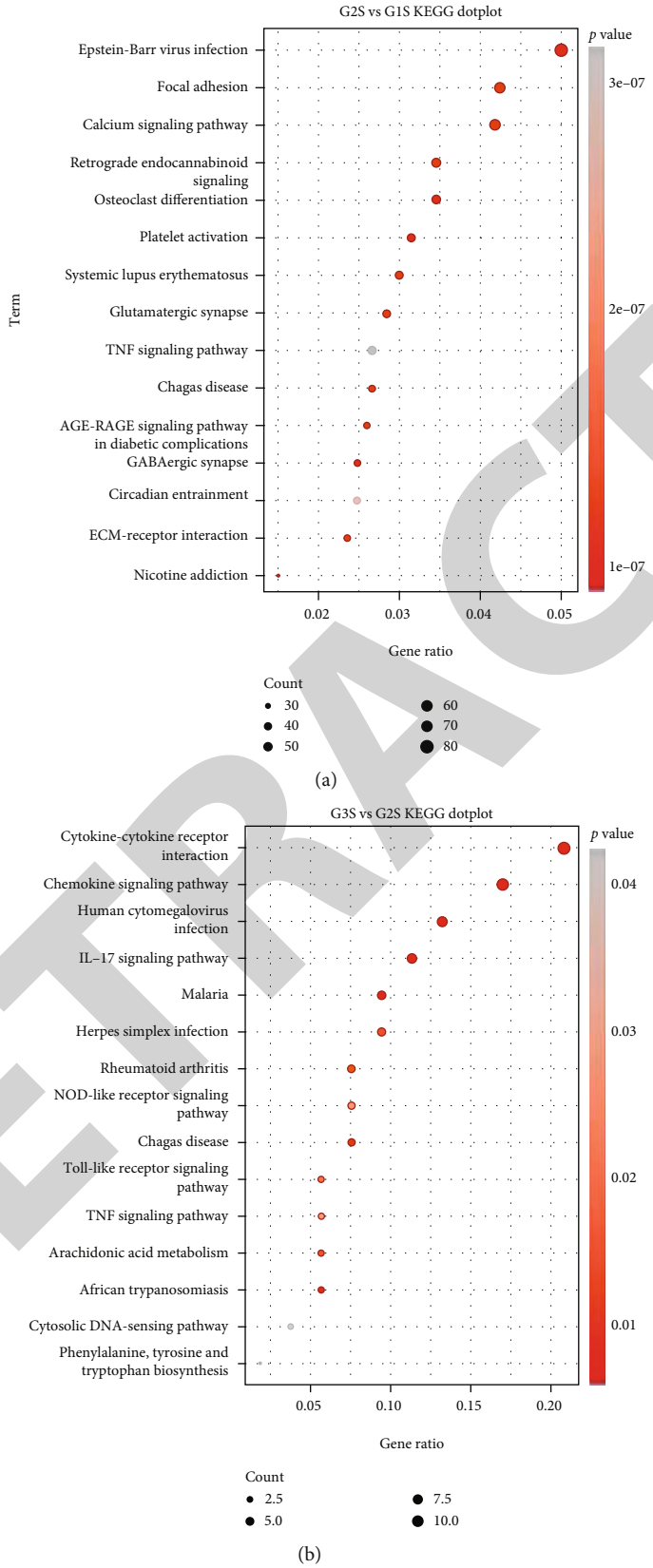

Figure 5: KEGG pathway analysis of DEGs in spinal cord samples in the subacute phase following SCI. (a) The top 15 KEGG analysis enrichment between group 2 and group 1. (b) The top 15 KEGG analysis enrichment between group 3 and group 2. The *X*-axis shows gene ratio, and the *Y*-axis shows the KEGG annotations. The larger the circle area, the more DEGs the pathway contains. KEGG: Kyoto Encyclopedia of Genes and Genomes.

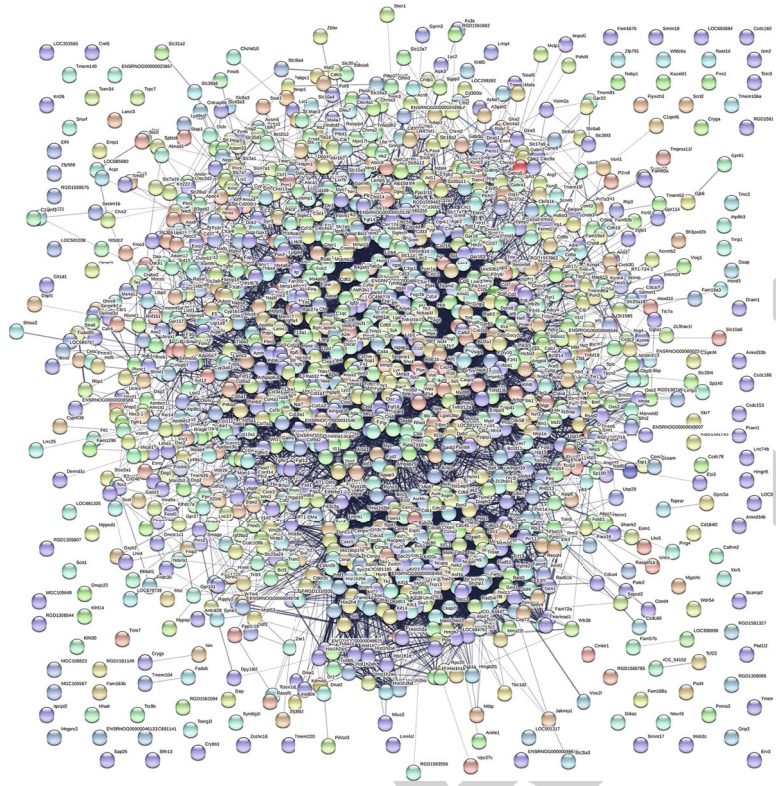

Figure 6: Interaction of protein-protein network analysis of DEGs between group 2 and group 1. Nodes represent DEGs. Lines indicate interactions between DEGs.

Table 5: The top 10 hub gene in the network between group 2 and group 1.

Rank	Name	Score	Rank	Name	Score
1	Fn1	108	6	Aurkb	61
2	Ptprc	85	7	Tlr2	60
3	Cd44	70	8	Agt	59
4	Cdc20	68	9	Rac2	58
5	Tyrobp	66	10	Mmp9	57

analysis revealed that the toll-like receptor signaling pathway, p53 signaling pathway, MAPK signaling pathway, and Jak–STAT signaling pathway were related to SCI [29]. Obviously, our findings are not completely consistent with that of the prior study. We postulate that the different results may be because specimens were collected at different time points. Our PPI network analysis, however, identified FN1, PTPRC, CD44, CDC20, TYROBP, AURKB, TlR2, angiotensinogen, AGT, RAC2, and MMP9 as the top 10 high-degree hub nodes, suggesting these genes may play an indispensable role in the pathophysiological processes of SCI.

Our previous studies showed that EPO reduces apoptosis and inflammation and promotes myelin repair and functional recovery following compressive SCI in rats from the perspective of bioinformatics. Our prior results were the basis for performing the current study to identify genes differentially expressed after SCI, and after treatment with rhEPO. In the rhEPO treatment group (group 3), the DEGs were significantly associated with leukocyte chemotaxis, myeloid leukocyte migration, granulocyte migration, granulocyte chemotaxis, and neutrophil migration. These findings confirm that the inflammatory response and inflammatory cell activation play an indispensable role in the repair of SCI. A prior study showed that blocking inflammation via the administration of anti-inflammatory drugs can reduce inflammation and partially restore locomotor activity following SCI [30].

Our KEGG pathway analysis indicated that the most significant pathways associated with SCI and repair were cytokine-cytokine receptor interaction, chemokine signaling, and IL-17 signaling pathways. Previous studies have reported that cytokines play an important role in central nervous system (CNS) immune system interactions, and SCI can initiate immune responses characterized by the synthesis and release of chemokines and cytokines [31, 32]. In addition, an increase of IL-17 concentration can result in the increase in the size of a lesion after SCI. Study has shown that reducing the expression of IL-17 and IL-17-related inflammatory factors can protect neurons and promote recovery after SCI [33]. In the PPI network developed in this study, the top 10 high-degree hub nodes (Ccl4, Ppbp, Cxcl13, Ahsp, Ccl5, Alas2, Npy, Gng13, Ccl2, and Hba2.) were all chemokines, which are a superfamily of secreted proteins involved in immune-regulatory and inflammatory processes. Study has shown that CXCL13/CXCR5 signaling

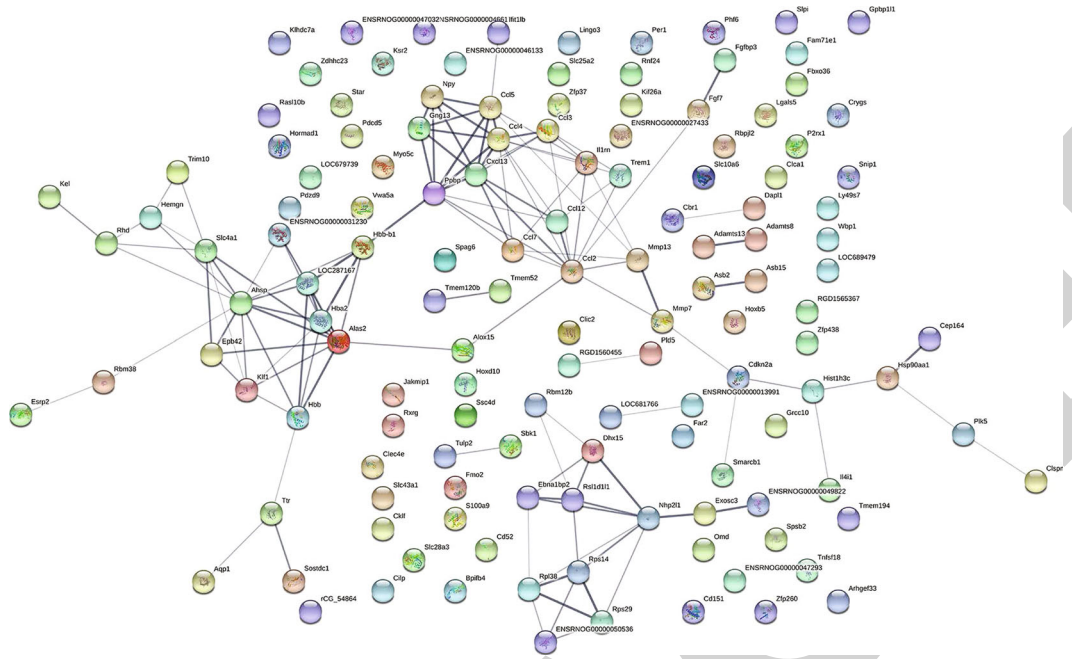

Figure 7: Interaction of protein-protein network analysis of DEGs between group 3 and group 2. Nodes represent DEGs. Lines indicate interactions between DEGs.

Table 6: The top 10 hub gene in the network between group 3 and group 2.

Rank	Name	Score	Rank	Name	Score
1	Ccl4	218	6	Alas2	121
2	Ppbp	193	7	Npy	120
3	Cxcl13	192	7	Gng13	120
4	Ahsp	127	9	Ccl2	106
5	Ccl5	125	10	Hba2	96

can promote diabetes-induced tactile allodynia through the production of proinflammatory cytokines in the spinal cord of male mice [34]. Additionally, Ppbp is a platelet-derived growth factor that belongs to the CXC chemokine family. Chio et al. [35] demonstrated that a traumatic brain injury can upregulate the expression of Ppbp in peripheral blood. Alas2 encodes a protein called heme that catalyzes the first step in the heme biosynthetic pathway and appears to promote a concurrent increase of neutrophilic metamyelocytes and mature CD71 erythroid cells [36]. Furthermore, endogenous neuropeptide Y (NPY) and the activation of its associated receptors can exert long-lasting spinal inhibitory control of neuropathic pain [37]. We speculate that EPO may influence the expression of NPY to achieve behavioral NPY-induced antinociception. Taken together, the aforementioned studies and our results lead us to hypothesize that EPO plays an important role in the acute phase of SCI by regulating the inflammatory response and affecting the synthesis and release of inflammatory factors and/or chemokines.

To our knowledge, this is the first study that has used bioinformatics methods to investigate EPO and the treatment of SCI. While we identified DEGs and lncRNAs associated with SCI, and EPO treatment, there are some shortcomings of this study. First, the small numbers of specimens may affect the reliability of the results. However, we reduced individual differences by mixing different samples from the same group. While we identified DEGs, we did not explore their functions, nor did we explore the specific mechanisms of the lncRNAs identified. In the acute phase of SCI, primary injury can lead to neuron death, demyelination in the spinal cord, and eventually, axonal dieback. In this study, we only examined tissue specimens at 1 time point. Future studies should examine and compare specimens at multiple time points after SCI.

5. Conclusion

In conclusion, we identified differential expression profiles of mRNAs and lncRNAs in spinal cord samples in the subacute phase following SCI. We also identified DEGs between normal spinal cord and injured spinal cord and between injured spinal cord and SCI treated with rhEPO. Critical pathways affected by rhEPO treatment of SCI were also identified. These results may offer new insights into the cellular and pathophysiological processes involved in SCI and insights for the development of new treatment methods.

Data Availability

No data were used to support this study.

Ethical Approval

The present study was approved by the ethics committee of the Zhujiang Hospital of Southern Medical University

(Guangzhou, China). All applicable international, national, and/or institutional guidelines for the care and use of animals were followed.

Conflicts of Interest

The authors declare that they have no conflict of interests.

References

[1] L. H. S. Sekhon and M. G. Fehlings, "Epidemiology, demographics, and pathophysiology of acute spinal cord injury," *Spine*, vol. 26, pp. S2–S12, 2001.

[2] C. S. Ahuja, S. Nori, L. Tetreault et al., "Traumatic spinal cord injury-repair and regeneration," *Neurosurgery*, vol. 80, no. 3S, pp. S9–S22, 2017.

[3] T. M. O'Shea, J. E. Burda, and M. V. Sofroniew, "Cell biology of spinal cord injury and repair," *The Journal of Clinical Investigation*, vol. 127, no. 9, pp. 3259–3270, 2017.

[4] Z. Li, I. H. T. Ho, X. Li et al., "Long non-coding RNAs in the spinal cord injury: novel spotlight," *Journal of Cellular and Molecular Medicine*, vol. 23, no. 8, pp. 4883–4890, 2019.

[5] R. H. Wenger and A. Kurtz, "Erythropoietin," *Comprehensive Physiology*, vol. 1, pp. 1759–1794, 2011.

[6] L. Yang, X. Yan, Z. Xu, W. Tan, Z. Chen, and B. Wu, "Delayed administration of recombinant human erythropoietin reduces apoptosis and inflammation and promotes myelin repair and functional recovery following spinal cord compressive injury in rats," *Restorative Neurology and Neuroscience*, vol. 34, pp. 647–663, 2015.

[7] L. G. St, C. Wahlestedt, and P. Kapranov, "The landscape of long noncoding RNA classification," *Trends in Genetics*, vol. 31, no. 5, pp. 239–251, 2015.

[8] T. Wu and Y. Du, "LncRNAs: From Basic Research to Medical Application," *International Journal of Biological Sciences*, vol. 13, no. 3, pp. 295–307, 2017.

[9] M. K. Iyer, Y. S. Niknafs, R. Malik et al., "The landscape of long noncoding RNAs in the human transcriptome," *Nature Genetics*, vol. 47, no. 3, pp. 199–208, 2015.

[10] T. R. Mercer, M. E. Dinger, and J. S. Mattick, "Long noncoding RNAs: insights into functions," *Nature Reviews Genetics*, vol. 10, no. 3, pp. 155–159, 2009.

[11] J. J. Quinn and H. Y. Chang, "Unique features of long noncoding RNA biogenesis and function," *Nature Reviews Genetics*, vol. 17, p. 47, 2016.

[12] A. Fatica and I. Bozzoni, "Long non-coding RNAs: new players in cell differentiation and development," *Nature Reviews Genetics*, vol. 15, no. 1, pp. 7–21, 2014.

[13] R. L. Siegel, K. D. Miller, and A. Jemal, "Cancer statistics, 2015," *CA: A Cancer Journal for Clinicians*, vol. 65, no. 1, pp. 5–29, 2015.

[14] B. Yu, S. Zhou, S. Yi, and X. Gu, "The regulatory roles of noncoding RNAs in nerve injury and regeneration," *Progress in Neurobiology*, vol. 134, pp. 122–139, 2015.

[15] I. A. Qureshi, J. S. Mattick, and M. F. Mehler, "Long noncoding RNAs in nervous system function and disease," *Brain Research*, vol. 1338, pp. 20–35, 2010.

[16] M. I. Love, W. Huber, and S. Anders, "Moderated estimation of fold change and dispersion for RNA-seq data with DESeq2," *Genome Biology*, vol. 15, no. 12, p. 550, 2014.

[17] J. Feng, C. A. Meyer, Q. Wang, J. S. Liu, X. Shirley Liu, and Y. Zhang, "GFOLD: a generalized fold change for ranking differentially expressed genes from RNA-seq data," *Bioinformatics*, vol. 28, no. 21, pp. 2782–2788, 2012.

[18] M. Ashburner, C. A. Ball, J. A. Blake et al., "Gene Ontology: tool for the unification of biology," *Nature Genetics*, vol. 25, no. 1, pp. 25–29, 2000.

[19] O. C. Gene, "The Gene Ontology (GO) project in 2006," *Nucleic Acids Research*, vol. 34, no. 90001, pp. D322–D326, 2006.

[20] D. Szklarczyk, A. Franceschini, S. Wyder et al., "STRING v10: protein–protein interaction networks, integrated over the tree of life," *Nucleic Acids Research*, vol. 43, no. D1, pp. D447–D452, 2015.

[21] M. E. Smoot, K. Ono, J. Ruscheinski, P. L. Wang, and T. Ideker, "Cytoscape 2.8: new features for data integration and network visualization," *Bioinformatics*, vol. 27, no. 3, pp. 431-432, 2011.

[22] P. Shannon, A. Markiel, O. Ozier et al., "Cytoscape: a software environment for integrated models of biomolecular interaction networks," *Genome Research*, vol. 13, no. 11, pp. 2498–2504, 2003.

[23] A. F. Cristante, F. T. Barros, R. M. Marcon, O. B. Letaif, and I. D. Rocha, "Therapeutic approaches for spinal cord injury," *Clinics*, vol. 67, no. 10, pp. 1219–1224, 2012.

[24] Y. Ding, Z. Song, and J. Liu, "Aberrant lncRNA expression profile in a contusion spinal cord injury mouse model," *BioMed Research International*, vol. 2016, Article ID 9249401, 10 pages, 2016.

[25] B. K. Kwon, W. Tetzlaff, J. N. Grauer, J. Beiner, and A. R. Vaccaro, "Pathophysiology and pharmacologic treatment of acute spinal cord injury," *The Spine Journal*, vol. 4, no. 4, pp. 451–464, 2004.

[26] J. W. McDonald and C. Sadowsky, "Spinal-cord injury," *The Lancet*, vol. 359, no. 9304, pp. 417–425, 2002.

[27] L. Jin, Z. Wu, W. Xu et al., "Identifying gene expression profile of spinal cord injury in rat by bioinformatics strategy," *Molecular Biology Reports*, vol. 41, no. 5, pp. 3169–3177, 2014.

[28] I. Pineau and S. Lacroix, "Proinflammatory cytokine synthesis in the injured mouse spinal cord: multiphasic expression pattern and identification of the cell types involved," *The Journal of Comparative Neurology*, vol. 500, no. 2, pp. 267–285, 2007.

[29] H. Zhou, Z. Shi, Y. Kang et al., "Investigation of candidate long noncoding RNAs and messenger RNAs in the immediate phase of spinal cord injury based on gene expression profiles," *Gene*, vol. 661, pp. 119–125, 2018.

[30] J. E. A. Wells, R. J. Hurlbert, M. G. Fehlings, and V. W. Yong, "Neuroprotection by minocycline facilitates significant recovery from spinal cord injury in mice," *Brain*, vol. 126, no. 7, pp. 1628–1637, 2003.

[31] L. Acarin, B. González, and B. Castellano, "Neuronal, astroglial and microglial cytokine expression after an excitotoxic lesion in the immature rat brain," *The European Journal of Neuroscience*, vol. 12, no. 10, pp. 3505–3520, 2000.

[32] A. Baek, S. Cho, and S. H. Kim, "Elucidation of gene expression patterns in the brain after spinal cord injury," *Cell Transplantation*, vol. 26, no. 7, pp. 1286–1300, 2017.

[33] G. Sun, S. Zeng, X. Liu et al., "Synthesis and characterization of a silica-based drug delivery system for spinal cord injury therapy," *Nano-Micro Letters*, vol. 11, no. 1, 2019.

[34] S. Liu, X. Liu, H. Xiong et al., "CXCL13/CXCR5 signaling contributes to diabetes-induced tactile allodynia via activating

Hindawi
Computational and Mathematical Methods in Medicine
Volume 2023, Article ID 9806791, 1 page
https://doi.org/10.1155/2023/9806791

Retraction

Retracted: GINS2 Is Downregulated in Peripheral Blood of Patients with Intervertebral Disk Degeneration and Promotes Proliferation and Migration of Nucleus Pulposus Cells

Computational and Mathematical Methods in Medicine

Received 5 December 2023; Accepted 5 December 2023; Published 6 December 2023

This article has been retracted by Hindawi, as publisher, following an investigation undertaken by the publisher [1]. This investigation has uncovered evidence of systematic manipulation of the publication and peer-review process. We cannot, therefore, vouch for the reliability or integrity of this article.

Please note that this notice is intended solely to alert readers that the peer-review process of this article has been compromised.

Wiley and Hindawi regret that the usual quality checks did not identify these issues before publication and have since put additional measures in place to safeguard research integrity.

We wish to credit our Research Integrity and Research Publishing teams and anonymous and named external researchers and research integrity experts for contributing to this investigation.

The corresponding author, as the representative of all authors, has been given the opportunity to register their agreement or disagreement to this retraction. We have kept a record of any response received.

References

[1] H. Jiang, H. Sun, J. Dai, C. Zhang, and X. Tang, "GINS2 Is Downregulated in Peripheral Blood of Patients with Intervertebral Disk Degeneration and Promotes Proliferation and Migration of Nucleus Pulposus Cells," *Computational and Mathematical Methods in Medicine*, vol. 2022, Article ID 1986348, 13 pages, 2022.

Hindawi
Computational and Mathematical Methods in Medicine
Volume 2022, Article ID 1986348, 13 pages
https://doi.org/10.1155/2022/1986348

Research Article

GINS2 Is Downregulated in Peripheral Blood of Patients with Intervertebral Disk Degeneration and Promotes Proliferation and Migration of Nucleus Pulposus Cells

Haitao Jiang, Hailang Sun, Jian Dai, Cheng Zhang, and Xiaoming Tang

Department of Orthopedics, The Affiliated Huaian No.1 People's Hospital of Nanjing Medical University, Huai'an, 223300 Jiangsu, China

Correspondence should be addressed to Xiaoming Tang; dr_tangxiaoming@outlook.com

Received 8 August 2022; Revised 15 August 2022; Accepted 18 August 2022; Published 2 September 2022

Academic Editor: Min Tang

GINS complex subunit 2 (GINS2) regulates the migration, invasion, and growth of cells in many malignant and chronic diseases. In the present study, we aimed to investigate the expression of GINS2 in the peripheral blood and nucleus pulposus (NP) cells of patients with intervertebral disk degeneration (IDD). GINS2 expression was detected using bioinformatics tools from the GEO public repository and validated using peripheral blood samples from IDD patients and healthy participants. GINS2 clinical significance was explored by the receiver operating curve (ROC) utilizing area under the curve (AUC). Moreover, the influences of GINS2 on cell viability, migration, and invasion were explored by MTT, wound healing, and transwell assays, whereas cell apoptosis was determined by flow cytometry. Expression levels of GINS2 in the peripheral blood were significantly lower in IDD patients than in healthy participants. Moreover, ROC obtained a significantly higher AUC of GINS2 in IDD patients. Further, overexpressed GINS2 increased the proliferation, migration, and invasion of NP cells while overexpressed GINS2 decreased the apoptotic property of cells compared to the NC plasmid and control groups. In conclusion, GINS2 might be a potential therapeutic target of IDD.

1. Introduction

Intervertebral disk degeneration (IDD) is a leading factor of discogenic lower back pain (LBP) [1–3]. IDD has been relegated to the disc tissue-based age-related process due to the continuously decreasing concentration of proteoglycan, which leads to decreased intervertebral height, the production of osteophytes, and endplate sclerosis [4, 5]. A normal human intervertebral disc is a fibrocartilaginous structure made of three main components, such as (1) cartilage endplates [6, 7]; (2) the annulus fibrosus (AF), composed of type I collagen and fibroblast-like cells [8]; and (3) nucleus pulposus (NP) originated of chondrocyte-like cells [9, 10]. Previous studies have found that the inherited factors were directly linked to the pathogenic factors (almost 70%) that were associated with IDD [11–13]. Thus, assessing the IDD mechanism from a genetic standpoint is crucial to address the present clinical concerns about chronic LBP.

GINS complex subunit 2 (GINS2), a member of the GINS family that also includes GINS2, GINS3, and GINS4 [14], plays an essential role in the DNA duplication [15]. Downregulation of GINS2 suppressed the growth of breast cancer cells by triggering endogenous DNA damage [16, 17]. Further, a study reported that unregulated expression of GINS2 initiated free survival of distant metastasis and therapeutic resistance of endocrine in patients with breast cancer [18]. Meanwhile, upregulated GINS2 urged the proliferation of HL60 cells in acute promyelocytic leukemia [19]. Moreover, overexpressed GINS2 promoted cell migration and proliferation and repressed apoptosis in lung cancer cell lines [20]. Nonetheless, the role of GINS2 in the peripheral blood and NP cells of patients with intervertebral disk degeneration (IDD) remains unknown.

In this study, we found that GINS2 was downregulated in the peripheral blood and NP cells of IDD patients and had a significant diagnostic value for IDD. Moreover, we

confirmed the promotive effects of GINS2 overexpression on the proliferation, migration, and invasion and the inhibitory effect on the apoptosis of NP cells. Our study might provide a novel target for IDD therapy.

2. Materials and Methods

2.1. Study Design. The present study is aimed at evaluating the GINS2 protein-coding gene expression using a GEO-based repository and further validates it retrospectively in the peripheral blood samples of IDD patients and healthy participants. Subsequently, the expression of GINS2 was achieved in IDD patients. Finally, GINS2 expression and its biological functions were analyzed in vitro using NP cells.

2.2. Enrollment of Patients. 60 participants with IDD ($n = 30$) and healthy control ($n = 30$) were retrospectively collected, along with the peripheral blood samples. The subjects were enrolled from June 2020 to June 2021.

2.3. Cell Culture and Cell Transfection. Human NP cells (CP-H170, Procell, Hubei, China) were used in the present study. Herein, cells were cultured in Roswell Park Memorial Institute (RPMI-1640) medium (Thermo Fisher Scientific, MA, USA) comprising 10% fetal bovine serum (FBS, Gibco, NY, USA) and penicillin in a 37°C and 5% CO_2 incubator. Furthermore, the cells were seeded onto a 12-well plate. GINS2-overexpression (GINS2-OE) plasmid, negative control (NC) plasmid, and blank control were transfected into NP cells by Lipofectamine 300 (Invitrogen, CA, USA) for 48 h. They were bought from GenePharma Biotechnology Co. Ltd., (Shanghai, China). Then, all the cells were obtained and utilized for subsequent experiments.

2.4. RNA Extraction. Total RNA was isolated from the whole blood cells of the peripheral blood samples utilizing phenol-chloroform solutions after handling the homogenization by guanidine isothiocyanate (kit for preparing TRIzol RNA, Thermo Fisher Scientific, Waltham, MA, USA). RNA concentrations were analyzed by a spectrophotometer (ND1000, NanoDrop Technologies, DE, USA).

2.5. RT-qPCR. Total RNA was isolated from the peripheral blood specimens by following TRIzol reagent protocols after transfection. Then, using the reverse transcript kit, the total RNA was reverse-transcribed to cDNA (Sangon Biological Engineering Co., Shanghai). Reaction steps of qPCR were carried out using SYBR Green PCR Master Mix (Applied Biosystems, USA) as follows: (1) for 10 min at 95°C (predenaturation); (2) for 15 s at 95°C (denaturation), for 15 s at 60°C (annealing), and for 20 s at 72°C (elongation); and (3) for 15 min at 72°C. At 4°C, reactions were discontinued. For each specimen, these three steps were followed, and a quantitative analysis of the data was performed based on a $2^{-\triangle\triangle CT}$ value. The RT primers utilized were as follows: GINS2, forward: 5′-AGGCGCCAGAGGCACCATGGAC-3′ and reverse: 5′-CATCCTGTGCGTTGGCTGCC-3′; β-actin, forward: 5′-GAGCGCGGCTACAGCTT-3′ and reverse: 5′-TCCTTAATGTCACGCACGATTT-3′.

2.6. Microculture Tetrazolium (MTT) Assay. MTT assay was carried out to evaluate the proliferation activity of the cell by following the manufacturer's protocols (Beyotime Biotech., Shanghai, China) [21]. NP cell lines were cultivated in 96-well plate at 5×10^3 cells/well density and then treated with overexpression of the GINS2 plasmid. 10 μL MTT reagent (Beyotime Biotech., Shanghai, China) was imparted into the well and further incubated for 4 h at 37°C. Each well's optical density (OD) value was evaluated by a microplate reader (Promega Corporation, Madison, WI, USA) at 490 nm. Results of the cell viability from three independent experiments were normalized to the control group and expressed as mean ± SD.

2.7. Transwell Assay. Matrigel was equally spread on the transwell chamber's bottom surface (Corning, Shanghai, China). After 10% FBS, 500 μL medium was put into the lower chamber, and 2×10^4 cells were added to the upper chamber. Then, cells on the upper surface were gently scraped, whereas the invasive cells on the lower surface were fixed and colored with crystal violet, followed by observation using a microscope (Olympus Corporation, Tokyo, Japan).

2.8. Wound Healing Assay. After the transfection of NP cells, the cells were treated with trypsin, planted into the 6-well plate, and cultivated till they reached 80% confluence of the medium. Then, the sterile pipette (200 μL) tip was used to scratch each well and washed with PBS solution numerous times to abolish cell debris. In the following 48 h, cells were incubated in medium (serum-free), and migrated cells to the surface of the wound were counted as fabricating an in vitro healing process. The display images of the wound healing assay were obtained by a light microscope (Olympus Corporation, Tokyo, Japan; magnification ×100), and the closure rate was evaluated. The relative ability of migratory cells was assessed by ImageJ software using the width at 0 h time point ((width of wound (0 − 24 h)/0 h width of wound) × 100%).

2.9. Apoptosis Assay. The cells were put into a 12-well plate after transfection, and NP cells were obtained from trypsin digestion without EDTA (Thermo fisher, Waltham, MA, USA). The rate of apoptotic cells was evaluated by Annexin V-PE/7-AAD (Sungene Biotech., Tianjin, China) following the manufacturer's protocols and instructions. Herein, cells were stained using 5 μL Annexin V-phycoerythrin (PE) and 5 μL 7-amino-actinomycin D at 37°C for 10 min. The cells were determined by flow cytometry (BD Aria III, New Jersey, USA).

2.10. Western Blotting. After 48 h posttransfection, the cells were kept in a 6-well plate and managed under suitable conditions. After the cells were put into the RIPA assay buffer (Beyotime Biotech., Shanghai, China), protein in equal amounts was parted by SDS-PAGE and transferred onto PVDF membranes (Bio-Rad, CA, USA). Then, the membranes were blocked with skim milk (5%), cleansed with Tris-buffered saline, and incubated with primary antibodies, GINS2 (1 : 200, ab197123, Abcam, MA, USA) and GAPDH (1 : 1000, 5174T, Cell Signaling Technology, MA, USA),

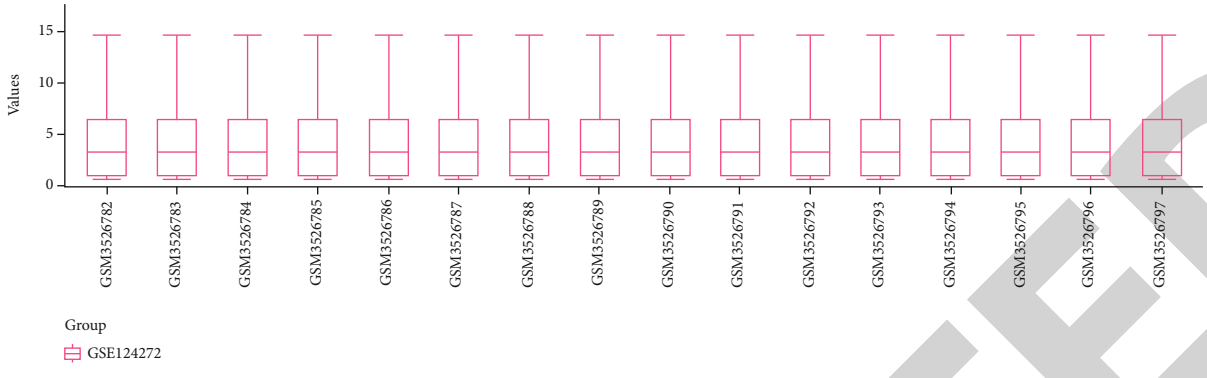

(a)

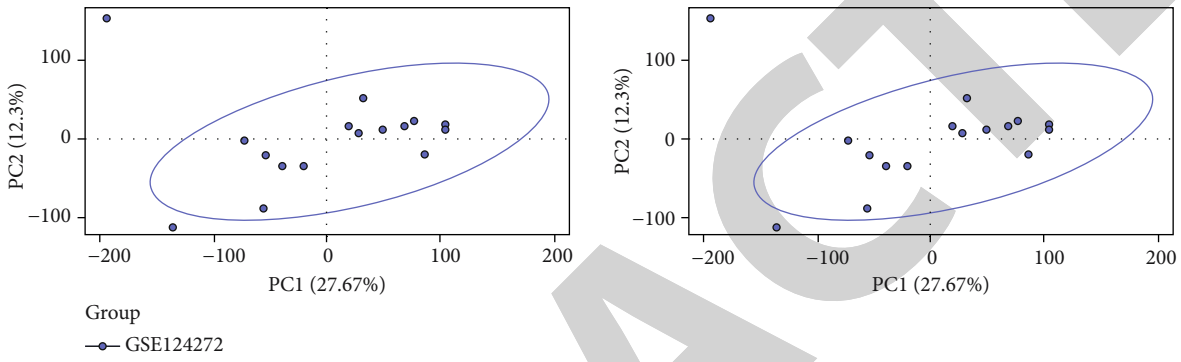

(b)

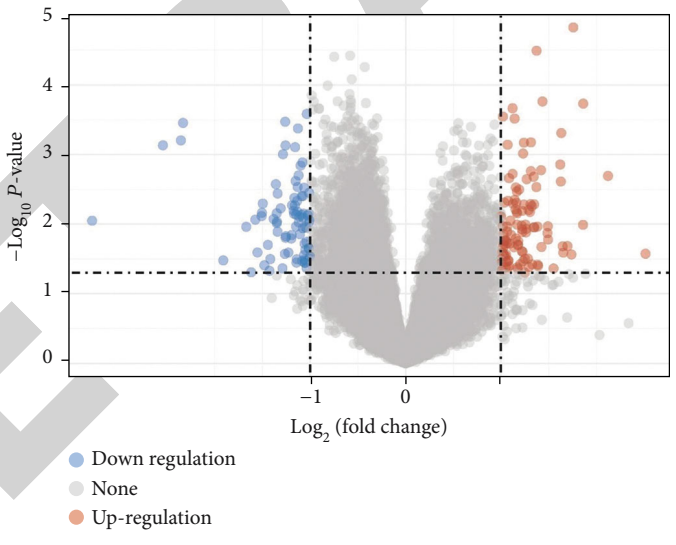

(c)

Figure 1: Continued.

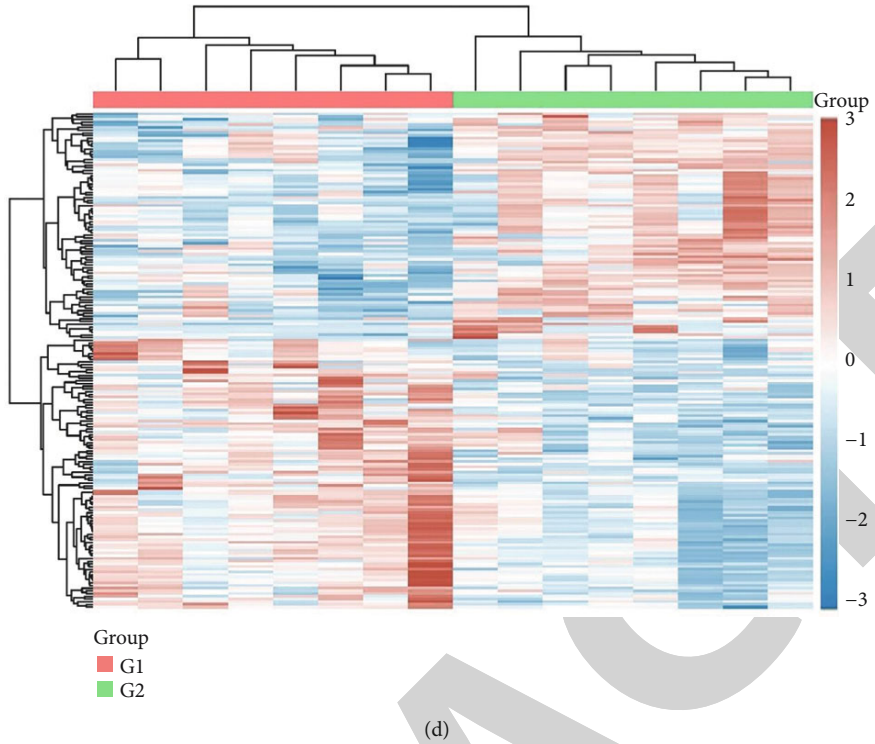

(d)

Figure 1: Screening of the genes between IDD patients and healthy control group. (a) The expression value of multiple genes shown in IDD patients versus healthy control by each of the eight microarray datasets of the GEO database (GSE124272) in the box plot. (b) PCA biplots of eight microarray datasets represented quality control measures. (c) Volcano plot is representing the dysregulated expression of genes. (d) Heatmap is showing the up- and downregulated expressed genes between two groups.

overnight at 4°C. After that, the membranes were incubated with secondary antibody HRP-conjugated goat antirabbit IgG heavy and light (1 : 2000, ab6721, Abcam) for 1 h. Furthermore, the membranes were analyzed by an ECL reagent (Thermo Scientific Pierce, IL, USA). The protein band was visualized with the internal reference of β-actin.

2.11. Bioinformatics and Statistical Analysis. Bioinformatics tools were used to create box plots, PCA biplots, volcano maps, and heatmaps. By utilizing the GEO database (GSE124272), the enriched signaling pathways were evaluated through the Kyoto Encyclopedia of Genes and Genomes (KEGG) and Gene Ontology (GO) databases. GraphPad (version 8, CA, USA) and SPSS software (version 20.0, IL, USA) were used for statistical analysis throughout the study, and all the data were represented as mean ± standard deviation. *T*-test and one-way and two-way ANOVA analyses were utilized to compare two or more groups. GINS2 clinical significance was explored using the receiver operating curve- (ROC-) based area under the curve (AUC) in the peripheral blood samples. $P < 0.05$ was contemplated as the threshold for providing statistical significance.

3. Results and Discussion

3.1. Discovery of GINS2 Expression in IDD. Eight microarray datasets of IDD patients compared to healthy controls were obtained from the GEO database (GSE124272) and used to screen for the GINS2 protein-coding gene utilizing bioinformatics tools, resulting in dysregulated gene expressions as determined by box plot, PCA biplot, volcano map, and heatmap analyses (see Figures 1(a)–1(d)). These eight datasets have demonstrated GINS2 expressions individually (see Figure 2(a)). PCA biplots were shown as the quantitative measure of eight microarray datasets (see Figure 2(b)). Based on these biplots of PCA, the present study involved all eight datasets for subsequent analysis. In the box plot, GINS2 expressions were significantly lower in IDD patients contrasted to a healthy group (see Figure 2(c), $P < 0.05$).

Moreover, the top 20 significant KEGG pathway enrichments in IDD patients and healthy groups based on the up- and downregulated genes were obtained utilizing the KEGG database (see Figure 3(a), $P < 0.05$). Likewise, significant top 20 GO enriched pathways related to the up- and downregulated genes were achieved using the GO database (see Figure 3(b), $P < 0.05$).

3.2. Validation and Clinical Significance of GINS2 in IDD Patients. To validate GINS2 expression levels in the peripheral blood from 30 IDD patients and 30 healthy participants, a scatter plot analysis was used. Herein, GINS2 expression was markedly decreased in the peripheral blood samples of IDD patients compared to the healthy group (see Figure 4(a), $P < 0.001$). Meanwhile, the demographical parameters of IDD patients and healthy participants are represented in Table 1, which showed no significant differences ($P > 0.05$). The ROC curve of GINS2 yielded a significantly high AUC of 0.8261 (95% confidence interval (CI) = 0.7051 ~ 0.9472,

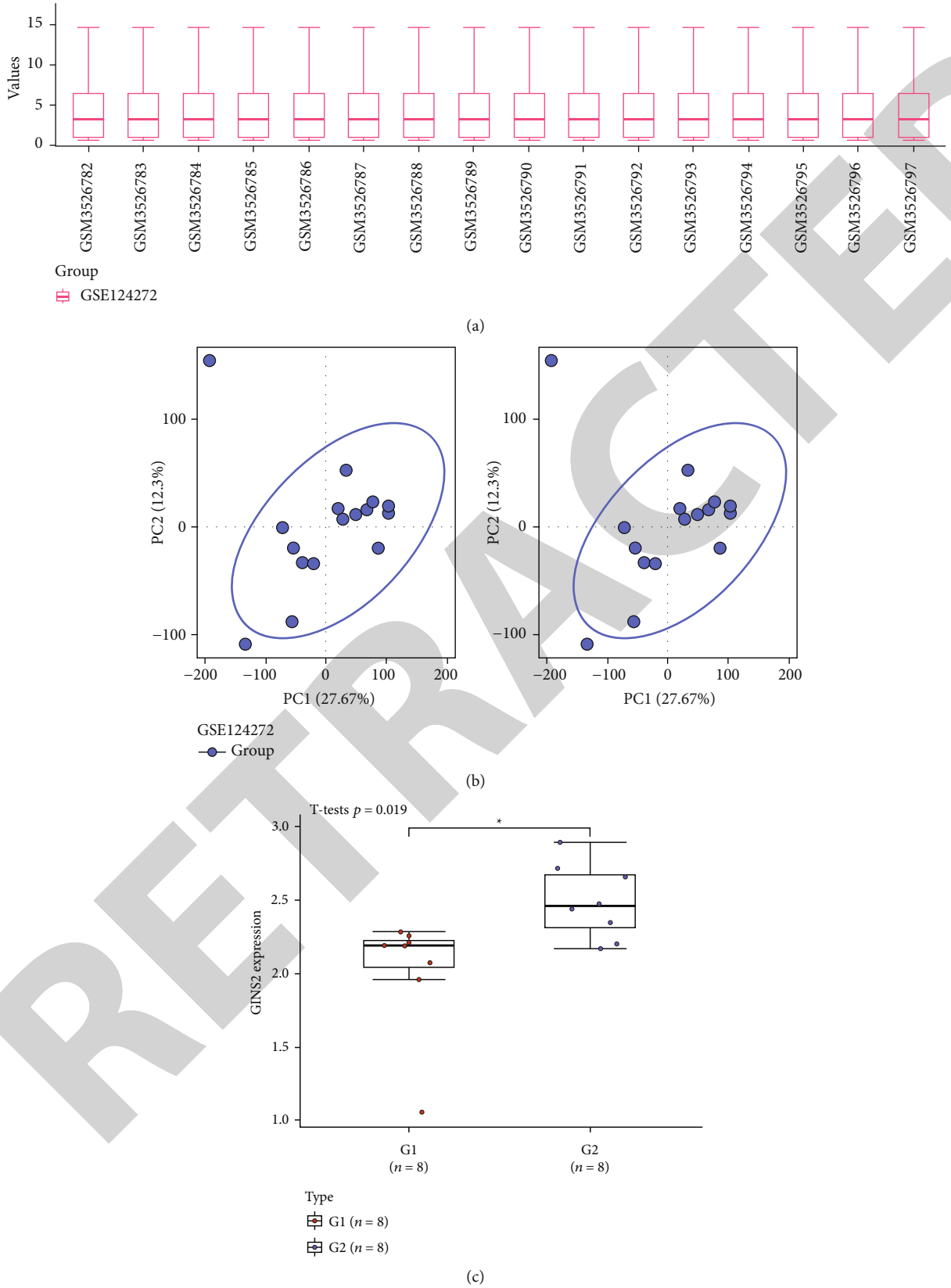

Figure 2: Discovery of the GINS2 between IDD patients and healthy control group. (a) The expression value of multiple genes observed in IDD patients versus healthy control by each of the eight microarray datasets of the GEO database (GSE124272) in the box plot. (b) PCA biplots of eight microarray datasets showed quality control measures. (c) GINS2 expression was measured in the peripheral blood from two groups of participants by box plots. G1: healthy group; G2: IDD group.

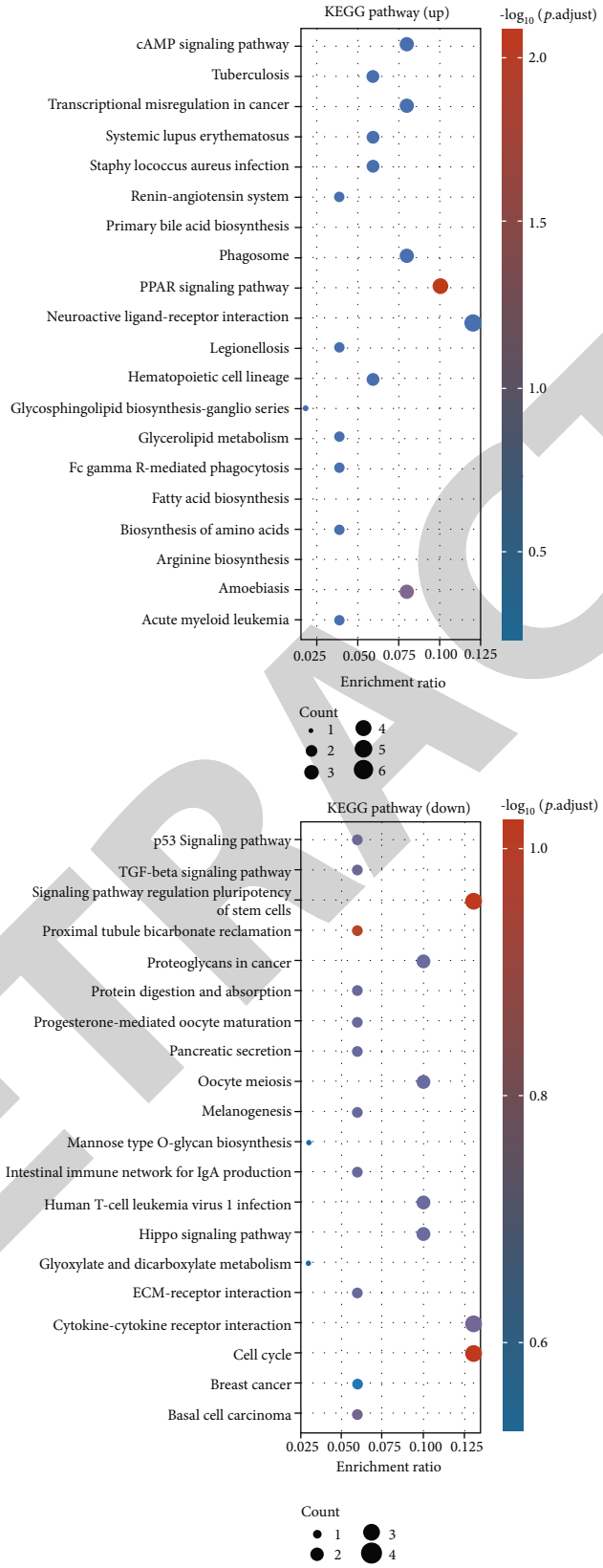

(a)

Figure 3: Continued.

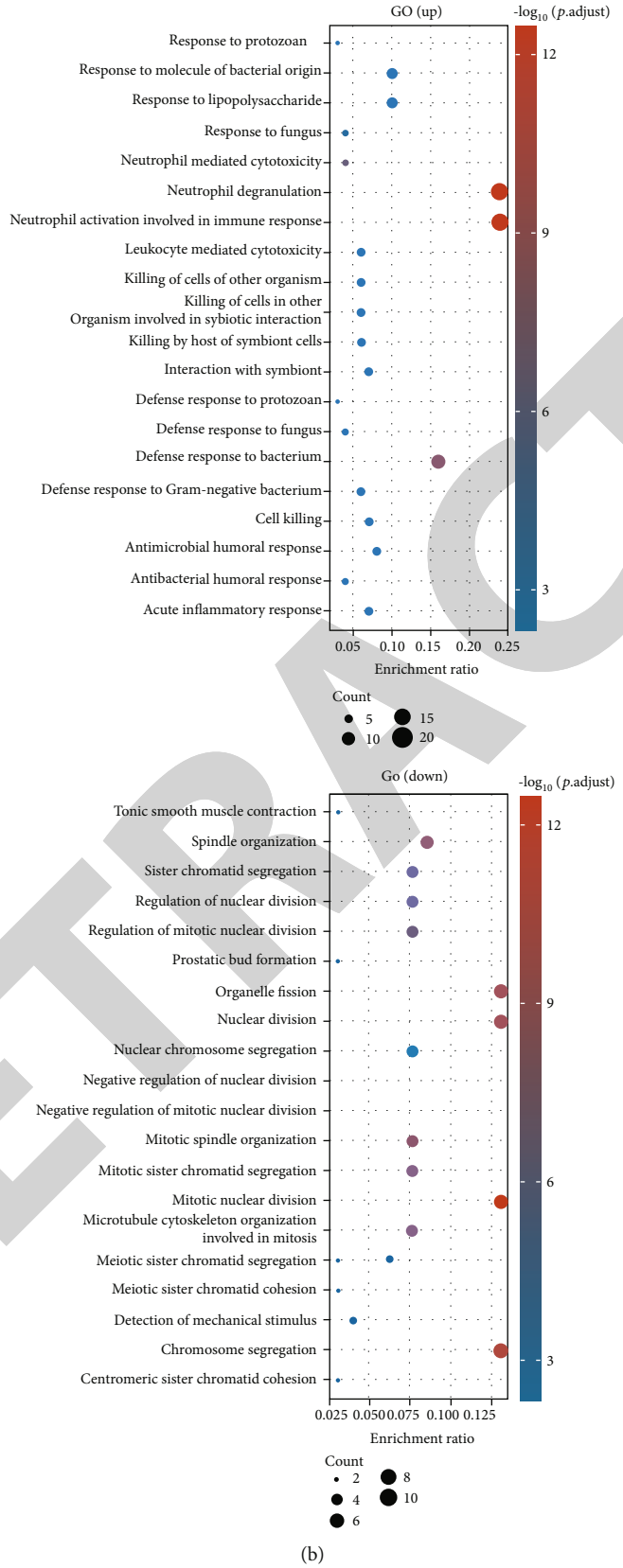

(b)

Figure 3: GO and KEGG pathway enrichment analysis. (a) The top significant KEGG-enriched pathways of the targeted genes in IDD are demonstrated individually in up- and downregulated manner. (b) The topmost GO enrichment pathways of the targeted genes in IDD are shown in a similar manner.

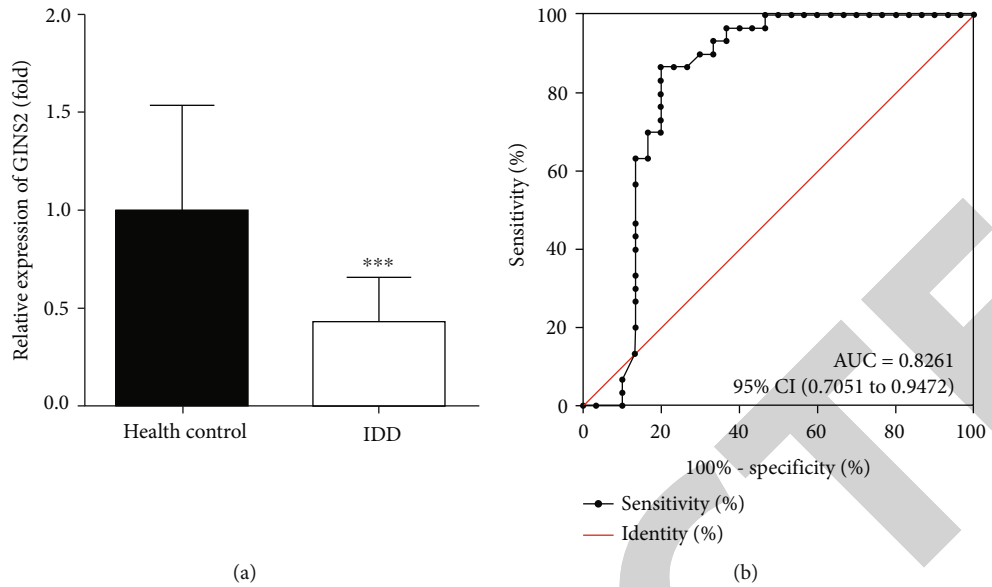

Figure 4: The validation of GINS2 expression in the peripheral blood samples between IDD patients and healthy control. (a) The histogram represented the overall validation of GINS2 in IDD patients and healthy control. (b) The clinical significance of GINS2 was measured by ROC curve for IDD patients.

Table 1: Clinical information of the patients and healthy controls.

	Control ($n = 30$)	IDD ($n = 30$)	P value
Age (years)	35.14 ± 4.21	36.22 ± 4.95	0.1166
BMI	24.31 ± 2.35	25.06 ± 2.78	0.0522
Gender (male/female)	18/12	11/19	0.8586

$P < 0.05$) in IDD patients (see Figure 4(b)). Thus, the diagnostic values of GINS2 may be used to precisely distinguish between IDD patients and healthy groups and further provide potential significance in diagnosing IDD.

3.3. Cell Proliferation, Migration, and Invasion Effects of GINS2 in NP Cells. The present study evaluated the biological functions of GINS2 by transfecting NP cells with the GINS2-OE and NC plasmids. WB analysis was utilized to determine the expression of GINS2 mRNA in NP cells transfected with NC plasmid, blank group, and GINS2-OE plasmid (see Figures 5(a) and 5(b), $P < 0.001$). GINS2 mRNA expression was significantly over/upregulated in NP cells following transfection with the GINS2-OE group compared to other groups ($P < 0.001$). Similarly, the CCK-8 assay demonstrated that the overexpression of GINS2 markedly increased cell viability (see Figure 5(c), $P < 0.001$), indicating that GINS2 upregulation may promote the proliferation of NP cells.

The migration and invasion abilities of cells are key indicators of tumor metastasis. The current study utilized wound healing and transwell assays to detect the metastatic capability of the tumor. Wound healing assay showed that the GINS2-OE significantly increased and promoted the migratory potential of NP cells when compared to the NC plasmid and blank groups (see Figures 5(d) and 5(e), $P < 0.001$). Subsequently, a transwell assay was utilized to determine the invasive ability of NP cells, which showed that GINS2-OE significantly promoted the invasion capability of NP cells when compared to other groups (see Figures 6(a) and 6(b), $P < 0.001$). Hence, the overexpression of GINS2 could promote NP cell migration and invasion.

3.4. Cell Apoptosis Effects of GINS2 in NP Cells. To determine the apoptosis effects of GINS2 in NP cells, Annexin V-PE/7-AAD staining was utilized. The apoptosis assay demonstrated that GINS2-OE significantly decreased the apoptosis rate in NP cells when compared to the NC plasmid and blank groups (see Figures 7(a)–7(d), $P < 0.001$). Thus, overexpression of GINS2 inhibited NP cell apoptosis.

4. Discussion

IDD is widely recognized as a major cause of LBP, a globally prevalent condition that imposes a vast social-economic burden and degrades the quality of life [22–24]. Disk degeneration is also associated with disk prolapse or herniation and sciatica, though it can be asymptomatic in some cases [25, 26]. In IDD cases, the intervertebral disk height and spinal column-based biomechanics are altered, which can have a significant effect on the behavior of other spinal structures, involving the ligaments and muscles [7]. In the long run, this

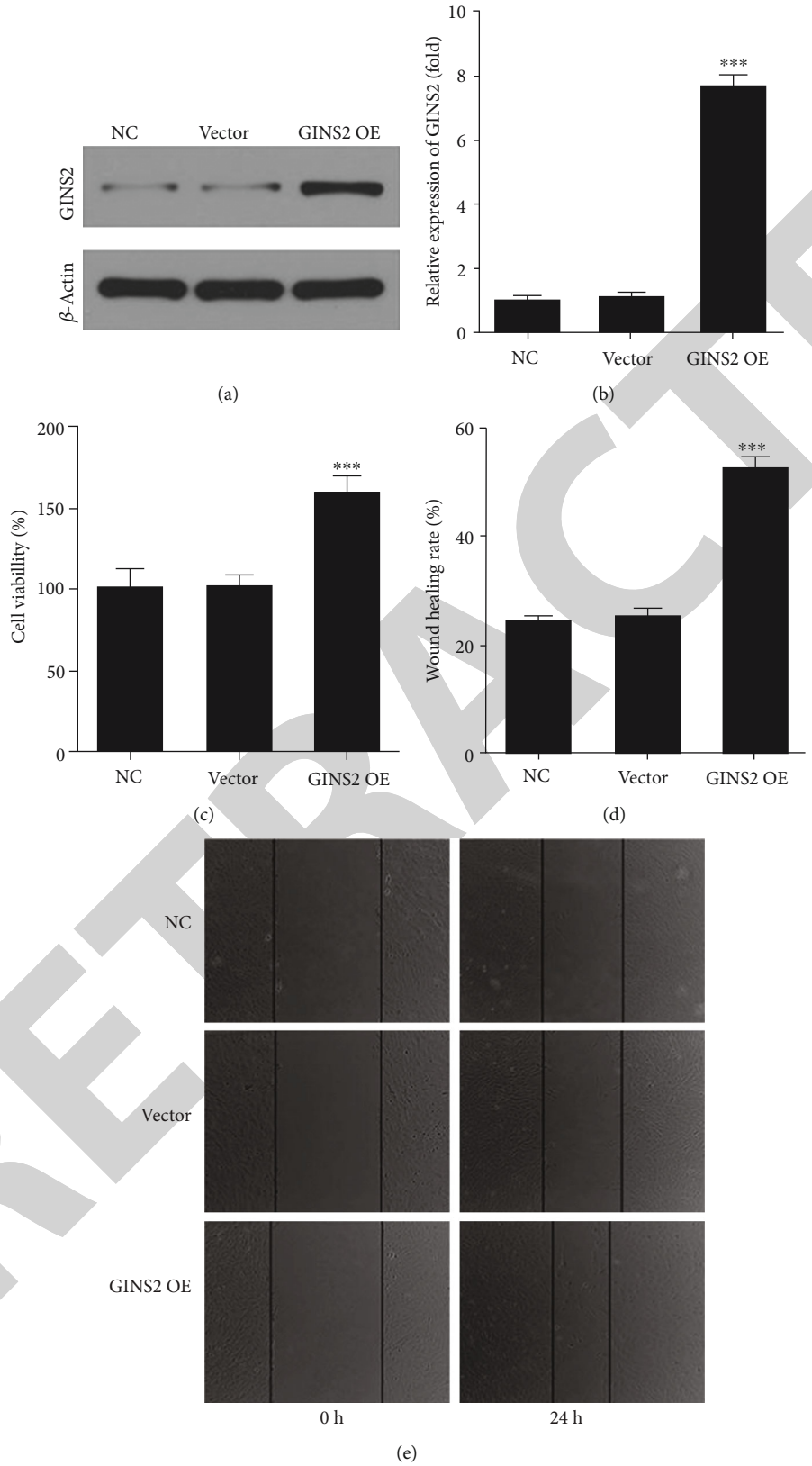

Figure 5: The biological mechanism of GINS2 in NP cells. (a, b) Western blot analysis represented the GINS2 mRNA expression in three groups of GINS2-OE, NC plasmid, and blank group. (c) MTT assay showed the cell proliferation or growth rate of three groups in transfected NP cells. (d) The wound healing rate was observed between the three groups. (e) Wound healing assay was performed to evaluate the migratory ability of transfected NP cells. NC plasmid, blank group, and GINS2-OE.

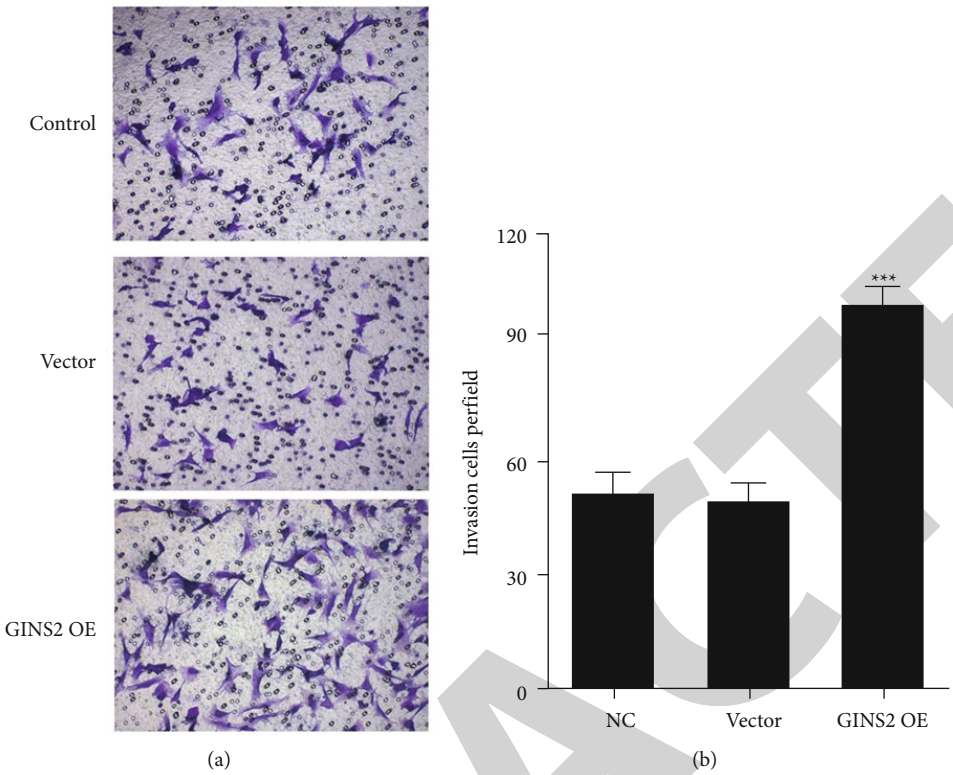

Figure 6: Effects of GINS2 on migration and invasion of NP cells. (a, b) Transwell assay was performed on NP cells and showed the invasive capacity of cells. NC plasmid, blank group, and GINS2-OE.

condition can progress to spinal stenosis [27], which is the main reason for pain and disability in the aged population [25]. Overall, IDD is a tangled process whose mechanism is not fully apprehended. Extracellular matrix degeneration, mechanical loading, extreme senescence, incremental secretions of inflammatory factors, and NP cell aberrant apoptosis have all been implicated in the development of IDD [28–32]. Thus, current research into NP cell apoptosis and targeted interventions may not only anticipate significant therapeutic strategies but also increase the underlying pathogenetic mechanisms of IDD.

GINS2 takes a crucial part in the replication activity and chromatin binding due to the complex structure as a heterotetramer [33]. In malignant cancers, such as cervical cancer, GINS2 was significantly upregulated in cancer cells and tumor tissues with an inverse correlation to overall survival in cervical cancer patients [34], whereas in thyroid cancer, GINS2 overexpression initiated the cancer cell proliferation and suppressed the apoptosis via LOXL2 and CITED2 mediation [35, 36]. Our study determined and confirmed the dysregulation of GINS2 expression in the peripheral blood samples from IDD patients and healthy participants. Our pathway enrichment analysis results indicated that GINS2 was involved in KEGG-enriched pathways, including p53 signaling pathways, cell cycles, extracellular matrix, and cytokine receptor interactions in IDD-based samples. Hence, on one hand, GINS2 was demonstrating downregulated expression in the peripheral blood samples from IDD, and on the other hand, GINS2 may take part in IDD pathogenesis via certain enriched pathways. Moreover, our study indicated that GINS2 protein-coding gene significantly differentiated IDD patients from the healthy group by representing an AUC of 0.8261. Thus, GINS2 protein-coding gene not only played a role in IDD pathogenesis but may also serve as a novel diagnostic biomarker for IDD by distinguishing IDD patients from healthy controls.

GINS2 was previously shown to influence the proliferation, migration, and invasion of non-small-cell lung cancer cells via PI3K/Akt and MEK/ERK signaling pathways [37]. Similarly, interfering with GINS2 inhibited cell viability, initiated cell cycle arrest, and facilitated apoptosis in pancreatic cancer cell lines using the MAPK/ERK pathway [38]. Our study evaluated the biological functions of GINS2 in NP cells by GINS2-OE and NC plasmids. Herein, consistent with the above-mentioned studies, our in vitro analysis revealed that the overexpression of GINS2 promoted cell proliferation, migration, and invasion of NP cells; meanwhile, it suppressed the apoptotic activity and vice versa. Thus, GINS2 may act as a potential therapeutic target for IDD.

Nonetheless, the current study has a few limitations. At first, the determination of GINS2 was screened using an online database of GEO, which could contain biased microarray results or samples. Second, GINS2 validation was carried out with a smaller size-based cohort; therefore, future studies are needed to carry out validation using a larger size-based cohort. Third, the present study was unable to include more clinical characteristics and risk factors for patients with IDD. Fourth, the GINS2 was evaluated and

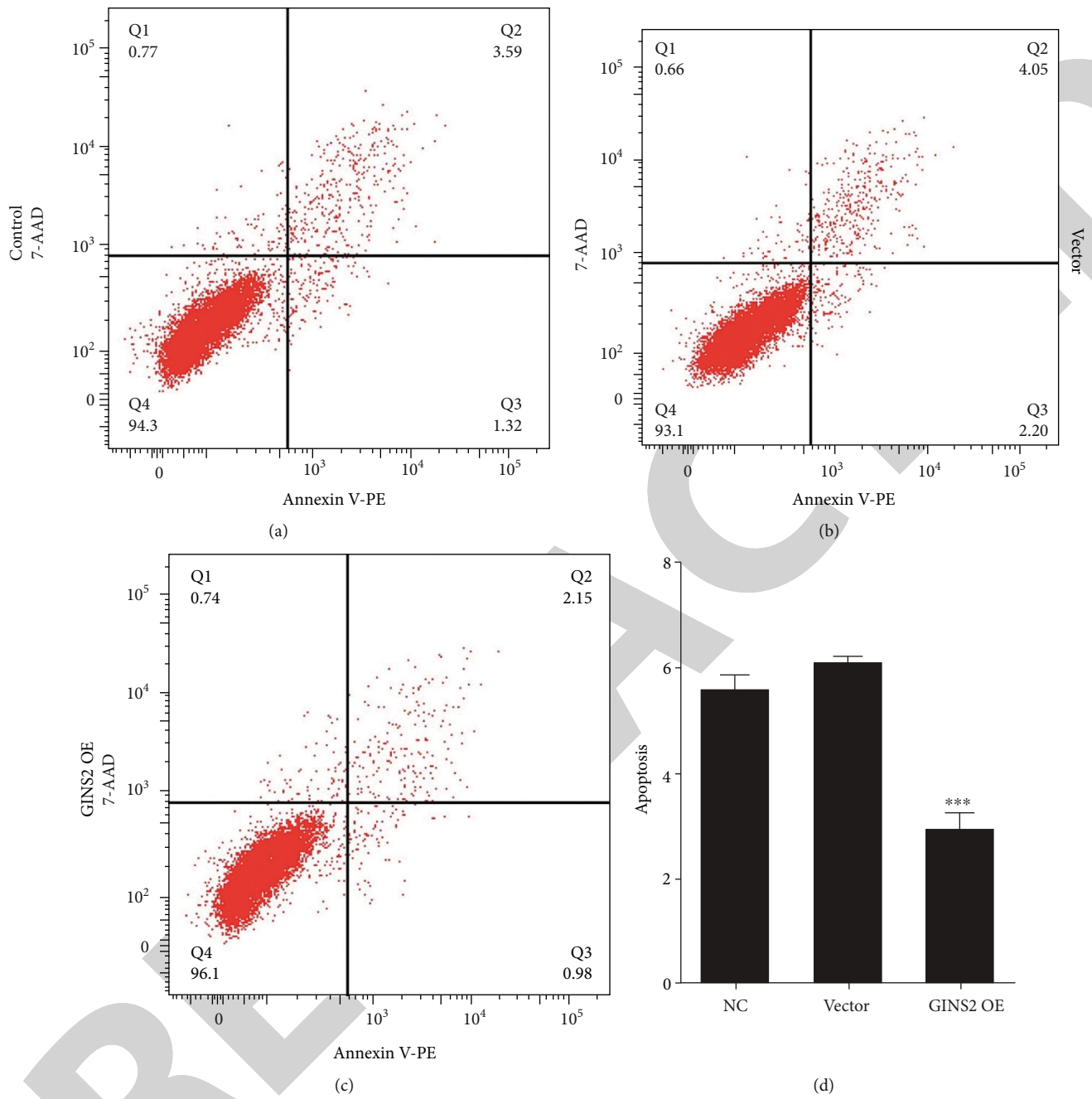

Figure 7: The apoptosis assay of NP cells. (a–d) NP cells transfected with GINS2-OE, NC plasmid, and blank group showed the apoptotic activity of cells.

compared using only the peripheral blood samples and NP cell lines without further validation of downregulating signaling pathways. Thus, future research is required to thoroughly determine and assess GINS2 in conjunction with other GINS family members, which might be taking part in the occurrence, development, and progression of IDD.

5. Conclusion

In conclusion, downregulation of GINS2 was observed in the peripheral blood and NP cells of IDD patients, which had a significant diagnostic value for IDD. Moreover, our study proved GINS2 overexpression promoted the proliferation, migration, and invasion and inhibited the apoptosis of NP cells, implying the biological role of GINS2 in IDD. GINS2 might be a novel target for IDD therapy.

Data Availability

The datasets used during the current study are available from the corresponding author on request.

Ethical Approval

All procedures performed in the studies involving human participants were in accordance with the ethical standards of the Affiliated Huaian No.1 People's Hospital of Nanjing Medical University committee and with the 1964 Helsinki declaration and its later amendments or comparable ethical standards.

Consent

Informed consent was obtained from all individual participants included in the study.

Conflicts of Interest

The authors declare that there is no conflict of interest regarding the publication of this paper.

Authors' Contributions

Haitao Jiang and Hailang Sun contributed equally to this work.

References

[1] M. G. Wiet, A. Piscioneri, S. N. Khan, M. N. Ballinger, J. A. Hoyland, and D. Purmessur, "Mast cell-intervertebral disc cell interactions regulate inflammation, catabolism and angiogenesis in discogenic back pain," *Scientific Reports*, vol. 7, no. 1, p. 12492, 2017.

[2] V. K. Podichetty, "The aging spine: the role of inflammatory mediators in intervertebral disc degeneration," *Cellular and Molecular Biology (Noisy-le-Grand, France)*, vol. 53, no. 5, pp. 4–18, 2007.

[3] M. Millecamps and L. S. Stone, "Delayed onset of persistent discogenic axial and radiating pain after a single-level lumbar intervertebral disc injury in mice," *Pain*, vol. 159, no. 9, pp. 1843–1855, 2018.

[4] A. G. Hadjipavlou, M. N. Tzermiadianos, N. Bogduk, and M. R. Zindrick, "The pathophysiology of disc degeneration: a critical review," *Journal of Bone and Joint Surgery. British Volume (London)*, vol. 90, no. 10, pp. 1261–1270, 2008.

[5] P. P. Raj, "Intervertebral disc: anatomy-physiology-pathophysiology-treatment," *Pain Practice*, vol. 8, no. 1, pp. 18–44, 2008.

[6] H. Liu, H. Kang, C. Song et al., "Urolithin A inhibits the catabolic effect of TNFα on nucleus pulposus cell and alleviates intervertebral disc degeneration in vivo," *Frontiers in Pharmacology*, vol. 9, p. 1043, 2018.

[7] L. Pimenta, L. Marchi, L. Oliveira, J. Nogueira-Neto, E. Coutinho, and R. Amaral, "Elastomeric lumbar total disc replacement: clinical and radiological results with minimum 84 months follow-up," *Int J Spine Surg*, vol. 12, no. 1, pp. 49–57, 2018.

[8] S. Yang, F. Zhang, J. Ma, and W. Ding, "Intervertebral disc ageing and degeneration: the antiapoptotic effect of oestrogen," *Ageing Research Reviews*, vol. 57, article 100978, 2020.

[9] F. C. Bach, S. A. de Vries, A. Krouwels et al., "The species-specific regenerative effects of notochordal cell-conditioned medium on chondrocyte-like cells derived from degenerated human intervertebral discs," *European Cells & Materials*, vol. 30, pp. 132–147, 2015.

[10] R. Rodrigues-Pinto, A. Berry, K. Piper-Hanley, N. Hanley, S. M. Richardson, and J. A. Hoyland, "Spatiotemporal analysis of putative notochordal cell markers reveals CD24 and keratins 8, 18, and 19 as notochord-specific markers during early human intervertebral disc development," *Journal of Orthopaedic Research*, vol. 34, no. 8, pp. 1327–1340, 2016.

[11] C. Bijkerk, J. J. Houwing-Duistermaat, H. A. Valkenburg et al., "Heritabilities of radiologic osteoarthritis in peripheral joints and of disc degeneration of the spine," *Arthritis and Rheumatism*, vol. 42, no. 8, pp. 1729–1735, 1999.

[12] P. N. Sambrook, A. J. MacGregor, and T. D. Spector, "Genetic influences on cervical and lumbar disc degeneration: a magnetic resonance imaging study in twins," *Arthritis and Rheumatism*, vol. 42, no. 2, pp. 366–372, 1999.

[13] M. C. Battie, T. Videman, L. E. Gibbons, L. D. Fisher, H. Manninen, and K. Gill, "1995 Volvo Award in clinical sciences. Determinants of lumbar disc degeneration. A study relating lifetime exposures and magnetic resonance imaging findings in identical twins," *A study relating lifetime exposures and magnetic resonance imaging findings in identical twins. Spine (Phila Pa 1976)*, vol. 20, no. 24, pp. 2601–2612.

[14] A. Gambus, R. C. Jones, A. Sanchez-Diaz et al., "GINS maintains association of Cdc45 with MCM in replisome progression complexes at eukaryotic DNA replication forks," *Nature Cell Biology*, vol. 8, no. 4, pp. 358–366, 2006.

[15] Y. Kubota, Y. Takase, Y. Komori et al., "A novel ring-like complex of Xenopus proteins essential for the initiation of DNA replication," *Genes & Development*, vol. 17, no. 9, pp. 1141–1152, 2003.

[16] J. K. Rantala, H. Edgren, L. Lehtinen et al., "Integrative functional genomics analysis of sustained polyploidy phenotypes in breast cancer cells identifies an oncogenic profile for GINS2," *Neoplasia*, vol. 12, no. 11, pp. 877–IN14, 2010.

[17] M. Thomassen, K. M. Jochumsen, O. Mogensen, Q. Tan, and T. A. Kruse, "Gene expression meta-analysis identifies chromosomal regions involved in ovarian cancer survival," *Genes, Chromosomes & Cancer*, vol. 48, no. 8, pp. 711–724, 2009.

[18] M. Zheng, Y. Zhou, X. Yang et al., "High GINS2 transcript level predicts poor prognosis and correlates with high histological grade and endocrine therapy resistance through mammary cancer stem cells in breast cancer patients," *Breast Cancer Research and Treatment*, vol. 148, no. 2, pp. 423–436, 2014.

[19] X. Zhang, L. Zhong, B. Z. Liu, Y. J. Gao, Y. M. Gao, and X. X. Hu, "Effect of GINS2 on proliferation and apoptosis in leukemic cell line," *International Journal of Medical Sciences*, vol. 10, no. 12, pp. 1795–1804, 2013.

[20] W. Tian, X. Yang, H. Yang, and B. Zhou, "GINS2 functions as a key gene in lung adenocarcinoma by WGCNA co-expression network analysis," *Oncotargets and Therapy*, vol. Volume 13, pp. 6735–6746, 2020.

[21] J. Zhu, C. Jiang, H. Hui et al., "Overexpressed lncRNA LINC00893 suppresses progression of colon cancer by binding with miR-146b-3p to upregulate PRSS8," *Journal of Oncology*, vol. 2022, Article ID 8002318, 2022.

[22] M. J. Prince, F. Wu, Y. Guo et al., "The burden of disease in older people and implications for health policy and practice," *Lancet*, vol. 385, no. 9967, pp. 549–562, 2015.

[23] H. B. Bressler, W. J. Keyes, P. A. Rochon, and E. Badley, "The prevalence of low back pain in the elderly," *A systematic review*

Hindawi
Computational and Mathematical Methods in Medicine
Volume 2023, Article ID 9796430, 1 page
https://doi.org/10.1155/2023/9796430

Retraction

Retracted: Multislice Computed Tomography Angiography Imaging Diagnosis of Lower Extremity Arteriosclerosis in Patients with Hypertension and Its Correlation with the Level of High-Sensitivity C-Reactive Protein

Computational and Mathematical Methods in Medicine

Received 5 December 2023; Accepted 5 December 2023; Published 6 December 2023

This article has been retracted by Hindawi, as publisher, following an investigation undertaken by the publisher [1]. This investigation has uncovered evidence of systematic manipulation of the publication and peer-review process. We cannot, therefore, vouch for the reliability or integrity of this article.

Please note that this notice is intended solely to alert readers that the peer-review process of this article has been compromised.

Wiley and Hindawi regret that the usual quality checks did not identify these issues before publication and have since put additional measures in place to safeguard research integrity.

We wish to credit our Research Integrity and Research Publishing teams and anonymous and named external researchers and research integrity experts for contributing to this investigation.

The corresponding author, as the representative of all authors, has been given the opportunity to register their agreement or disagreement to this retraction. We have kept a record of any response received.

References

[1] J. Huo, Z. Wu, H. Jiang, and H. Zhang, "Multislice Computed Tomography Angiography Imaging Diagnosis of Lower Extremity Arteriosclerosis in Patients with Hypertension and Its Correlation with the Level of High-Sensitivity C-Reactive Protein," *Computational and Mathematical Methods in Medicine*, vol. 2022, Article ID 1768208, 8 pages, 2022.

Hindawi
Computational and Mathematical Methods in Medicine
Volume 2022, Article ID 1768208, 8 pages
https://doi.org/10.1155/2022/1768208

Research Article

Multislice Computed Tomography Angiography Imaging Diagnosis of Lower Extremity Arteriosclerosis in Patients with Hypertension and Its Correlation with the Level of High-Sensitivity C-Reactive Protein

Jing Huo,[1] Zhongyin Wu,[2] Haijun Jiang,[2] and Hong Zhang[2]

[1]*Department of General Medicine, Affiliated Hospital of Chengde Medical College, Chengde, 067000 Hebei, China*
[2]*Department of Vascular Surgery, Affiliated Hospital of Chengde Medical College, Chengde, 067000 Hebei, China*

Correspondence should be addressed to Hong Zhang; 201311704@stu.lzjtu.edu.cn

Received 27 June 2022; Revised 30 July 2022; Accepted 5 August 2022; Published 31 August 2022

Academic Editor: Min Tang

The aim of this study was to investigate the relationship between multislice computed tomography (CT) angiography (MSCTA) imaging and high-sensitivity C-reactive protein (hs-CRP) in patients with hypertension and lower extremity arteriosclerosis. 68 hypertensive patients with lower extremity arteriosclerosis were selected as the observation group, and 68 healthy volunteers were selected as the control group to compare the differences in hs-CRP. According to the degree of stenosis, the patients were further divided into five grades: no obvious stenosis, mild stenosis, moderate stenosis, severe stenosis, and occlusion. The correlation between the degree of stenosis and the content of hs-CRP was compared. The changes of hs-CRP content before and after treatment were compared, and the difference of images before and after surgical treatment and the difference of hs-CRP expression in patients with occlusion were compared. Compared with the control group, the content of hs-CRP in the observation group was significantly higher ($P < 0.05$), and the degree of stenosis was positively correlated with the content of hs-CRP. After two weeks of treatment, the hs-CRP levels of patients with severe stenosis and occlusion were significantly lower than those before treatment ($P < 0.01$). The level of hs-CRP in patients with occlusion after arterial stent intervention was significantly lower than before, and the images also showed that the blood vessels were significantly expanded. The degree of stenosis in patients with lower extremity arteriosclerosis diagnosed by MSCTA imaging was closely related to the expression of hs-CRP in the patient, and a sustained high concentration of hs-CRP corresponded to a more severe degree of vascular occlusion. In conclusion, the hs-CRP can be used as one of the factors to predict and evaluate the occurrence of cardiovascular and cerebrovascular diseases.

1. Introduction

Worldwide, approximately 200 million people suffer from occlusion arteriosclerosis, which can be life-threatening in some cases [1]. Lower extremity arteriosclerosis is the manifestation of occlusion arteriosclerosis in the lower extremities. Occlusion arteriosclerosis is more common in the medium and large arteries at the lower end of the abdominal aorta. Due to atherosclerotic plaque and its internal hemorrhage or plaque rupture, secondary thrombosis leads to gradual lumen stenosis or occlusion, resulting in limb ischemia and other clinical manifestations [2, 3]. With the improvement of social living standards and the aging of the population, the incidence of lower extremity arteriosclerosis occlusion is increasing year by year. The main risk factors of lower extremity arteriosclerosis occlusion disease are hypertension, diabetes, hyperlipidemia, smoking, advanced age, etc. [4]. Studies have found that smoking and diabetes are the most harmful and can increase the incidence of arterial disease by 3 ~ 4 times [5]. The clinical manifestations are intermittent claudication and pain at rest, which can lead to dry gangrene or ulceration in severe cases [6]. Hypertension is one of the risk factors for arteriosclerotic occlusion disease. Although the risk is not as good as diabetes and

hyperlipidemia, the number of people suffering from hypertension is large, and it is also a cause that cannot be ignored [7]. Generally speaking, hypertension will cause a relatively large impact on the inner wall of the blood vessel, which will damage the inner wall of the blood vessel after a long time. After the function of the endothelium is damaged, the lipids in the blood are more likely to be deposited on the blood vessel wall, which promotes the occurrence and development of atherosclerosis [8]. On the contrary, the normal diastolic function of the blood vessels with atherosclerosis is weakened, the stiffness of the blood vessel wall increases, and the blood pressure rises again [9].

Multislice spiral computed tomography (CT) angiography (MSCTA) technology is the application of multislice spiral CT technology in angiography. It can quickly scan a large area without loss of spatial resolution, so that the carotid artery can be better displayed, and the aorta, iliac artery, and femoral artery can also be observed in one scan, effectively using intravascular contrast medium [10]. Because multilayer C can choose thinner layer thickness, the vascular tree of each part can be displayed with higher contrast, which is incomparable with single-layer spiral CT. MSCTA postimage processing techniques include multiplanar reconstruction (MPR), maximum density projection (MIP), volume reconstruction (AR), surface occlusion display (SSD), and simulated inner diameter display (VE) [10, 11]. MSCTA has gradually become an important method for the diagnosis of lower extremity vascular lesions because of its advantages of faster speed, thinner layers, and wider scanning.

High-sensitivity C-reactive protein (hs-CRP) is a nonspecific marker of acute phase systemic inflammation synthesized by the liver. It also specifically refers to C-reactive protein in plasma, which can clinically guide cardiovascular disease, neonatal bacterial infection, and kidney transplantation [12, 13]. Persistent low-level inflammation plays a major role in atherosclerosis, which produces aseptic inflammation due to accumulation of cholesterol and other lipids, resulting in elevated hs-CRP [14]. A large number of studies have shown that high-sensitivity C-reactive protein is mainly located in atherosclerotic plaques and can regulate monocyte aggregation. hs-CRP is a complement activator that coexists with membrane attack complexes in early atherosclerotic lesions, stimulates tissue factor production, and aggregated hs-CRP activates complement. Due to the activation of complement by chronic trace inflammatory factors, lipids are deposited on the vascular wall, and through infiltration and aggregation, vascular damage and atherosclerosis are caused [15]. Studies have found that hs-CRP can chemotactic monocytes at the site of vascular sclerosis, induce monocytes to produce tissue factor, activate complement, induce endothelial cells to produce adhesion factors, impair endothelial function, and accelerate the progression of arteriosclerosis. hs-CRP can also bind to lipoproteins, activate the complement system by the classical pathway, and then generate a large number of terminal complexes, causing vascular endothelial damage [16].

Table 1: Criteria for stenosis grading.

Grade	Degree of stenosis
Grade 1	No obvious stenosis
Grade 2	Mild stenosis (<50%)
Grade 3	Moderate stenosis (50%-70%)
Grade 4	Severe stenosis (71-99%)
Grade 5	Occlusion

Table 2: Comparison of clinical data.

Group	Cases	Gender		Age (years old)
		Males	Females	
Control group	68	37	31	56.23 ± 4.78
Observation group	68	40	28	52.13 ± 5.13

2. Methods

2.1. Data and Grouping. A total of 68 hypertension patients with lower extremity arteriosclerosis who underwent MSCTA examination in the hospital from January 2020 to January 2021 were selected as the observation group. Clinical manifestations included intermittent claudication, rest pain and/or night pain, pale skin, coolness or numbness, weakness, swelling or muscle atrophy of the affected limb, decreased skin temperature, ischemic cyanosis, gangrene, ulcer, thromboocclusion vasculitis (Buerger) syndrome (+), the pulse of the affected limb femoral artery, popliteal artery, posterior tibial artery, and dorsal foot artery. During the same period, 68 healthy volunteers were selected as the control group for the determination of the content of hs-CRP. This experiment was approved by the ethics committee of the hospital, and all experimental cases obtained the consent of the patients or their families and signed the informed consent.

Inclusive criteria are as follows: (i) hypertensive patients diagnosed as arteriosclerosis of lower limbs by MSCTA examination, (ii) at least 18 years old, and (iii) no history of contrast agent allergy.

Exclusion criteria are as follows: (i) patients whose lower extremity arteriosclerosis was caused by hyperlipidemia, diabetes, etc.; (ii) patients suffering from arteriosclerosis in other parts of the body and patients suffering from other cardiovascular diseases; (iii) patients suffering from serious body infections; (iv) patients who received kidney transplantation within the past month; and (v) patients who underwent intervention and surgical treatment.

2.2. Examination and Treatment. For the treatment of hypertension, oral nifedipine sustained-release tablets II was used twice a day in the morning and evening with a 12-hour interval. For patients with severe claudication, it should take some arterial dilation drugs (cilostazol), antiplatelet drugs (aspirin), or anticoagulant drugs (rivaroxaban) as prescribed by a doctor and prescribe some pain relievers if necessary. Patients with gangrene of limb ulcers required endovascular therapy and surgery. Conventional treatment

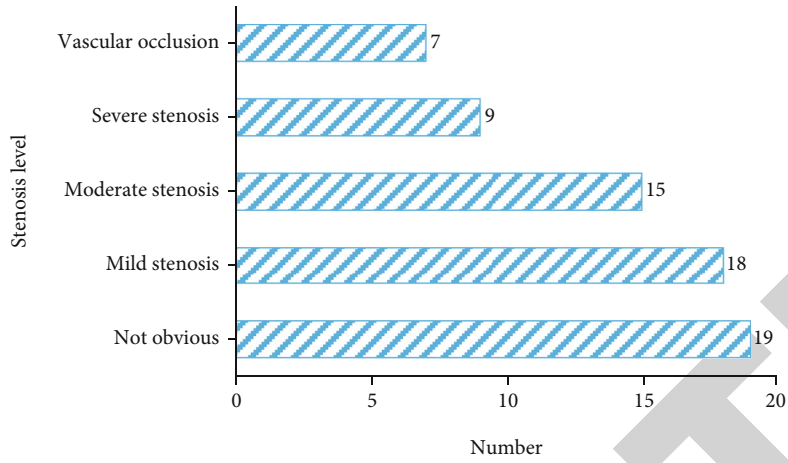

Figure 1: Distribution of the number of patients by degree of stenosis.

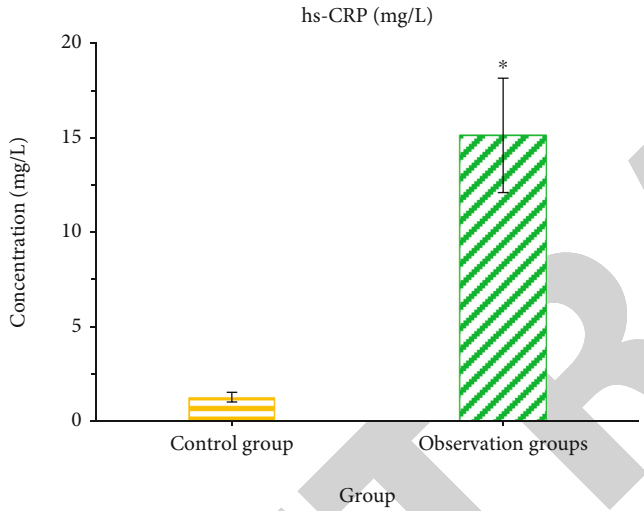

Figure 2: Comparison of the concentration of hs-CRP in the plasma of the control group and the observation group. *Compared with the control group, $P < 0.01$.

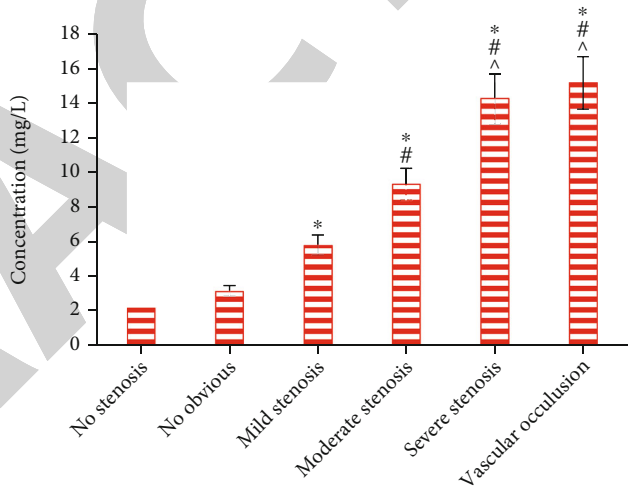

Figure 3: Comparison of concentrations of hs-CRP in each stenosis group. *Compared withthe insignificant stenosis group, $P < 0.05$; #compared with the mild stenosis group, $P < 0.05$; ^compared with the moderate stenosis group, $P < 0.05$.

included ① quitting smoking, which can significantly delay the further aggravation of the disease; ② reasonable arrangement of meals; ③ appropriate exercise to improve ischemia; and ④ attention to foot care to avoid limb injury. All patients were treated with antihypertensive and conventional treatment. No other treatment was performed if there was no obvious stenosis. Arterial dilation, antiplatelet, and anticoagulant drug treatment were performed for mild, moderate, and severe stenosis. Interventional therapy was performed for patients with occlusion, and reexamination should be performed six months after the end of treatment. For patients undergoing interventional therapy, MSCTA was detected, and the images were processed and analyzed using maximum density projection, volume reconstruction, and surface reconstruction techniques and were compared with the lower extremity arterial images of healthy volunteers.

3 mL of fasting venous blood was collected from patients in the observation group in the next morning after admission. The specific protein analyzer was used for inspection, and the content of high-sensitivity C-reactive protein in blood was obtained after analysis. The detection of hs-CRP in healthy volunteers was the same as above.

According to the patient's condition of lower extremity arteriosclerosis, the treatment should be carried out reasonably, and blood collection should be performed to detect the content of hs-CRP in the first and second weeks of drug treatment, conventional treatment, and interventional treatment. After treatment, the content of hs-CRP in patients with each stenosis grade was counted.

2.3. Stenosis Grading Method. The imaging data of MSCTA of 68 patients in the observation group were evaluated by two senior radiologists in a double-blind evaluation of the blood vessels of the lower extremities. The degree of stenosis of blood vessels in CTA-MIP and CTA-VR of the same patient was evaluated, respectively, and CTA-MPR technical analysis could be done if necessary. The lower extremity

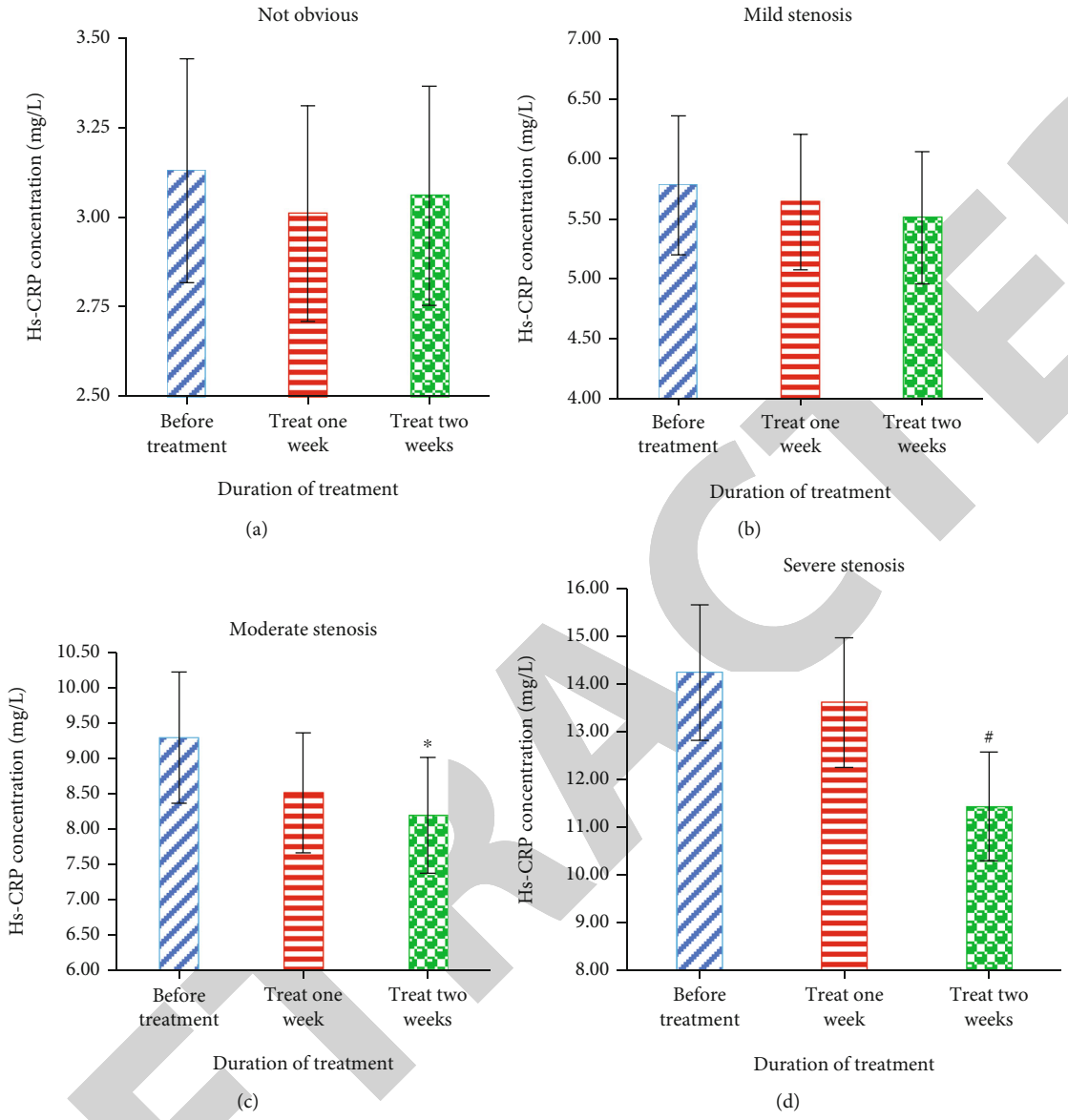

Figure 4: Continued.

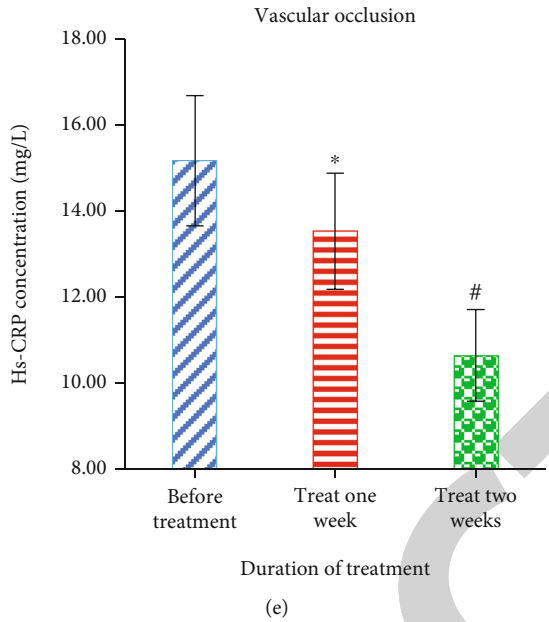

Figure 4: Expression of hs-CRP in each stenosis group after comprehensive treatment. (a–e) The expression levels of hs-CRP before treatment and after one week and two weeks of treatment in each group with no obvious stenosis, mild stenosis, moderate stenosis, severe stenosis, and occlusion, respectively. *Compared with that before treatment, $P < 0.05$; #compared with that before treatment, $P < 0.01$.

arteries were divided into 10 segments: lower abdominal aorta, common iliac artery, internal iliac artery, external iliac artery, femoral artery, popliteal artery, tibiofibular trunk, anterior tibial artery, posterior tibial artery, and peroneal artery. Each segment of blood vessels was graded into 5 grades according to the degree of stenosis. The calculation equation of the degree of stenosis was given as follows: degree of stenosis = [(diameter of the normal blood vessel at the proximal end of the stenosis − diameter of the blood vessel at the stenosis)/diameter of the normal blood vessel at the proximal end of the stenosis] × 100%.

Patients with multiple stenosis were classified according to the highest stenosis grade. The patients were grouped according to the grade of stenosis. The specific grades were shown in Table 1.

2.4. Data Processing Method. SPSS 23.0 software was used for statistical analysis of the data in this study. All data were expressed as mean ± standard deviation, the counting data are expressed as frequency, the data between observation groups were compared by t-test, and the data between multiple groups was compared by one-way analysis of variance. $P < 0.05$ indicated statistical significance.

3. Results

3.1. Data Statistics and Comparison. As shown in Table 2, the average age of healthy volunteers was 56.23 ± 4.78 years old, and the patients with lower extremity arterial stenosis were 40 males and 28 females, with an average age of 52.13 ± 5.13. There was no significant difference between the patients with lower extremity arteriosclerosis and the healthy persons in the clinical basic data ($P > 0.05$). In addition, according to the judgment of the doctor and the evaluation of the stenosis grade, the statistics of the number of volunteers with each stenosis grade were shown in Figure 1. 19 patients had no significant stenosis, 18 had mild stenosis, 15 had moderate stenosis, 9 had severe stenosis, and 7 had occlusion (Figure 1).

3.2. Comparison of the Content of hs-CRP. As shown in Figure 2, the content of hs-CRP in the plasma of patients with lower extremity arteriosclerosis was 1.26 ± 0.21 mg/L and that of healthy volunteers was 15.13 ± 4.42 mg/L. After comparison, it was found that there was a significant difference in the content of hs-CRP between the two groups ($P < 0.01$). This also showed that the plasma hs-CRP of patients with lower extremity arteriosclerosis was significantly higher than that of healthy volunteers.

3.3. Analysis of hs-CRP Content in Each Stenosis Group. The patients with lower extremity arterial stenosis in the observation group were regrouped according to the degree of stenosis, and the average levels of hs-CRP in each group were counted, as shown in Figure 3. Starting from the moderate stenosis group to severe stenosis group, each group had a significant difference compared with the previous group ($P < 0.05$). There was no significant difference in complete vascular occlusion compared to the severe stenosis group. This also showed that with the increase in the degree of stenosis, the patient's plasma hs-CRP also increased.

3.4. Comparison of hs-CRP Content after Treatment. As shown in Figure 4, patients with no obvious stenosis and mild stenosis had no significant change after comprehensive treatment compared with before treatment, and there was no

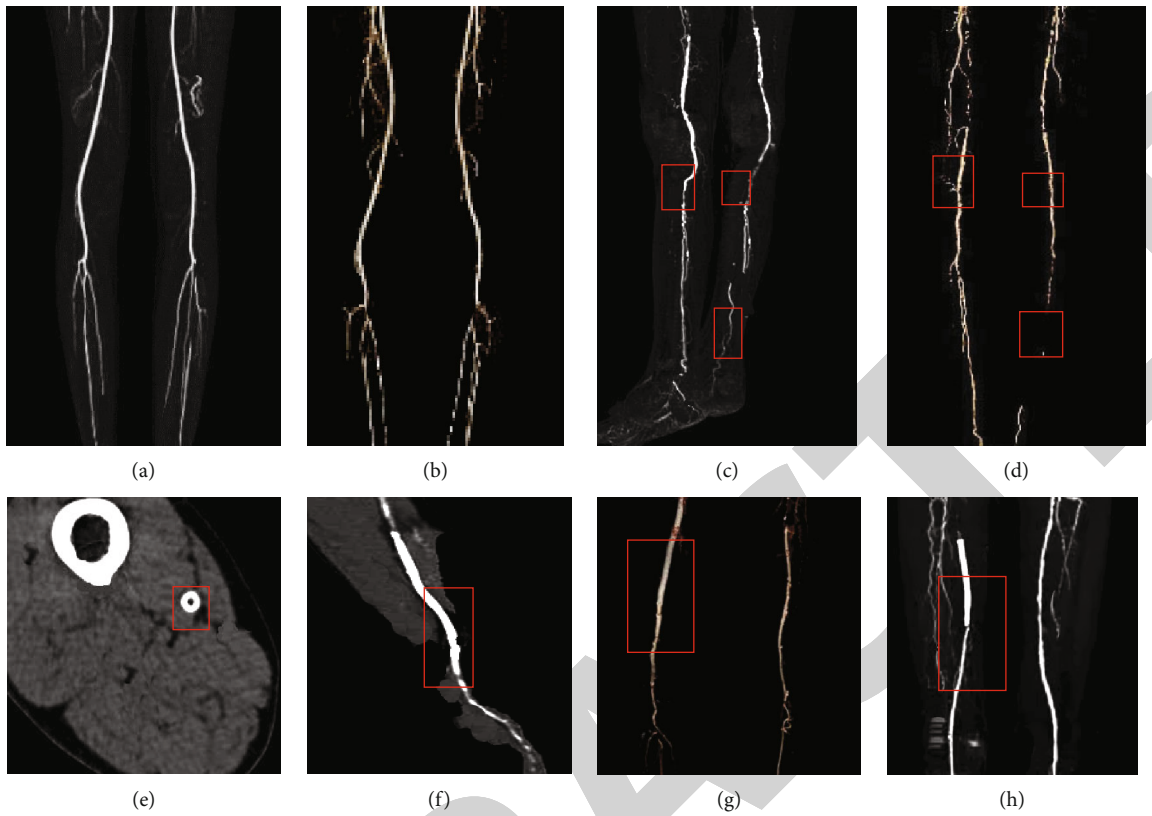

Figure 5: Comparison of MSCTA imaging processing before and after stent implantation in patients with lower extremity arterial occlusion. The marked part in red indicated the narrow part of the lower limb artery. (a, b) The imaging results of blood vessels of healthy volunteers. (c, d) The imaging results of the blood vessels of patients. (e) The CT plain scan results. (f) The CTA surface reconstructed image. (g) The image after boneless volume reconstruction. (h) The image constructed by the maximum density projection.

significant difference after comparison ($P < 0.05$). Compared with before treatment, the content of hs-CRP in patients with moderate stenosis was significantly lower after two weeks of treatment, and the difference was statistically significant ($P < 0.05$).

3.5. MSCTA Imaging and hs-CRP Analysis before and after Interventional Therapy. A patient with right femoral artery occlusion was diagnosed with MSCTA on admission and analyzed using maximum density projection and boneless volume reconstruction techniques. Afterwards, under the doctor's suggestion, he underwent femoral artery stent implantation, and he came to the hospital for reexamination and diagnosis. The patient's hs-CRP concentration at the first examination was 15.17 mg/L, as shown in the images after MSCTA imaging (Figures 5(c) and 5(d)). Compared with the blood vessels of healthy volunteers (Figures 5(a) and 5(b)), the patient's right femoral artery was significantly occlusion, with collateral circulation, the left femoral artery was narrowed and severely calcified, and the left tibial anterior and posterior tibial arteries were tiny. Six months after the right side received femoral artery stent implantation, the hs-crp concentration was 9.51 mg/L, which was significantly lower than that before treatment. After the consultation, it was found that the recovery state was good, and further reexamination, CT plain scan (Figure 5(e)) found that the stent was unobstructed, and no stenosis and thrombosis were found. The implanted vascular stent can be clearly seen in the CTA surface reconstruction (Figure 5(f)), the boneless volume reconstruction (Figure 5(g)), and the maximum density projection (Figure 5(h)).

4. Discussion

hs-CRP is an effective and sensitive marker of inflammation in vivo, which marks the acute phase of inflammation and can predict the occurrence of cardiovascular and cerebrovascular events. The process of atherosclerotic lesions is closely related to the inflammatory response caused by continuous and repeated damage of blood vessels. hs-CRP can activate phagocytes, activate complement, make vascular endothelial cells dysfunctional, promote foam cell formation, inhibit the survival and differentiation of endothelial progenitor cells, activate the intima of atherosclerosis, and further lead to the occurrence of atherosclerosis [17]. The results of this work found that patients with higher arterial stenosis had higher plasma hs-CRP, which to some extent indicated that patients with lower extremity arteriosclerosis caused by hypertension already had a certain inflammatory response. Therefore, in addition to MSCTA, hs-CRP can also be used as a reference index for the degree of disease. In a study on the association between hs-CRP and clinical outcomes in

patients with intermittent claudication in the past decade, it was found that elevated hs-CRP levels were significantly associated with cardiovascular-related and cancer-related deaths in patients with intermittent claudication [18]. In the study of psoriasis and cardiovascular disease risk, it was found that patients with psoriasis had a higher risk of subclinical atherosclerosis. hs-CRP is a useful marker of cardiovascular disease risk, and anti-inflammatory drugs not only play a key role in the treatment of psoriasis but also reduce cardiovascular risk by reducing levels of inflammatory markers including hs-CRP risk of disease [19]. In the study of the relationship between ultrasound and hs-CRP and carotid stenosis, it was found that high hs-CRP and the degree of carotid stenosis were closely related [20].

Digital subtraction angiography (DSA) has always been the gold standard for diagnosing lower extremity arteriosclerosis occlusion, but its disadvantage is trauma examination [21]. However, with the development and improvement of MSCTA, it has become the mainstream way of examining arterial blood vessels. In addition to its advantages of convenience, noninvasiveness, and high patient acceptance, MSCTA can more intuitively display the length of arterial vessels, the degree of stenosis, collateral circulation, and perivascular tissue. MSCTA has many image processing methods, and different processing techniques can be selected according to needs, which can provide a variety of rich image data for clinical practice [22]. In this work, the stenosis of lower extremity arteries can be clearly observed and classified according to the degree of stenosis by selecting maximum density projection, solvent reconstruction, and multiplanar reconstruction technology after MSCTA scanning. A study using MSCTA and DSA techniques to differentiate the internal iliac artery branch angiography in patients with pelvic tumors found that MSCTA has a great advantage over DSA in the evaluation of the branch vessels at the end of the internal iliac artery [23].

Since MSCTA can well analyze the degree of stenosis of blood vessels in patients through various imaging systems and hs-CRP is an important marker of vascular stenosis, there must be a certain correlation between the two. This experiment also found that the higher the stenosis degree, the higher the hs-CRP level of the patients, and the hs-CRP level of the patients with a high degree of stenosis was significantly different from that of the patients with a lower degree of stenosis ($P < 0.05$). In addition, this work also studied the hs-CRP level of patients after corresponding treatment of arteriosclerosis. The results showed that after treatment, the level of hs-CRP in patients with severe stenosis and occlusion was significantly reduced after two weeks of treatment ($P < 0.01$). A six-month follow-up visit to a patient with vascular occlusion treated with interventional stents also found that the occlusion blood vessels of the lower extremities were completely unblocked, and the level of hs-CRP in the body was significantly lower than before treatment. All the above experiments showed that the degree of vascular stenosis determined by MSCTA was closely related to the level of hs-CRP.

5. Conclusion

MSCTA imaging can clearly observe the degree of stenosis of lower extremity arteries, and it is also found that the level of hs-CRP in patients with hypertension is closely related to the degree of stenosis of lower extremity arteriosclerosis. Patients with severe vascular stenosis tend to have higher levels of hs-CRP in plasma. After treatment, patients' lower extremity vascular stenosis is reduced, and hs-CRP levels are also reduced. The disadvantage of this experiment is that there are too few experimental samples, which cannot more accurately reflect the relationship between MSCTA imaging and hs-CRP. In addition, considering that the treatment method is different for each patient, there was no significant difference in the hs-CRP level between mild and moderate patients before and after treatment. In follow-up studies, more experimental samples should be sought, especially to include more patients with severe stenosis and occlusion, and to develop better treatment modalities for classification.

Data Availability

The data used to support the findings of this study are available from the corresponding author upon request.

Conflicts of Interest

The authors declare no conflicts of interest.

Authors' Contributions

Jing Huo and Zhongyin Wu contributed equally to this work.

References

[1] I. Rencüzoğulları, T. Çınar, and Y. Karabağ, "Endothelin-1 and C reactive protein as potential biomarkers for restenosis in patients with arteriosclerosis obliterans," *Journal of Investigative Surgery*, vol. 34, no. 7, pp. 771-772, 2021.

[2] W. Lian, H. Nie, Y. Yuan, K. Wang, W. Chen, and L. Ding, "Clinical significance of endothelin-1 and C reaction protein in restenosis after the intervention of lower extremity arteriosclerosis obliterans," *Journal of Investigative Surgery*, vol. 34, no. 7, pp. 765–770, 2021.

[3] W. Yao, L. Wang, Q. Chen, F. Wang, and N. Feng, "Effects of valsartan on restenosis in patients with arteriosclerosis obliterans of the lower extremities undergoing interventional therapy: a prospective, randomized, single-blind trial," *Medical Science Monitor*, vol. 26, article e919977, 2020.

[4] M. Bossi, M. Tozzi, M. Franchin et al., "Cryopreserved human allografts for the reconstruction of aortic and peripheral prosthetic graft infection," *Annals of Vascular Diseases*, vol. 10, no. 4, pp. 391–397, 2017.

[5] Y. Watanabe, T. Miyata, K. Shigematsu et al., "Current trends in epidemiology and clinical features of thromboangiitis obliterans in Japan - a nationwide survey using the medical support system database," *Circulation Journal*, vol. 84, no. 10, pp. 1786–1796, 2020.

Hindawi
Computational and Mathematical Methods in Medicine
Volume 2023, Article ID 9804692, 1 page
https://doi.org/10.1155/2023/9804692

Retraction

Retracted: Influences of Airway Obstruction Caused by Adenoid Hypertrophy on Growth and Development of Craniomaxillofacial Structure and Respiratory Function in Children

Computational and Mathematical Methods in Medicine

Received 5 December 2023; Accepted 5 December 2023; Published 6 December 2023

This article has been retracted by Hindawi, as publisher, following an investigation undertaken by the publisher [1]. This investigation has uncovered evidence of systematic manipulation of the publication and peer-review process. We cannot, therefore, vouch for the reliability or integrity of this article.

Please note that this notice is intended solely to alert readers that the peer-review process of this article has been compromised.

Wiley and Hindawi regret that the usual quality checks did not identify these issues before publication and have since put additional measures in place to safeguard research integrity.

We wish to credit our Research Integrity and Research Publishing teams and anonymous and named external researchers and research integrity experts for contributing to this investigation.

The corresponding author, as the representative of all authors, has been given the opportunity to register their agreement or disagreement to this retraction. We have kept a record of any response received.

References

[1] H. Li, H. Wang, H. Hao, H. An, and H. Geng, "Influences of Airway Obstruction Caused by Adenoid Hypertrophy on Growth and Development of Craniomaxillofacial Structure and Respiratory Function in Children," *Computational and Mathematical Methods in Medicine*, vol. 2022, Article ID 5096406, 7 pages, 2022.

Hindawi
Computational and Mathematical Methods in Medicine
Volume 2022, Article ID 5096406, 7 pages
https://doi.org/10.1155/2022/5096406

Research Article

Influences of Airway Obstruction Caused by Adenoid Hypertrophy on Growth and Development of Craniomaxillofacial Structure and Respiratory Function in Children

Huina Li,[1] **Hongwei Wang**,[2] **Hengrui Hao**,[1] **Hong An**,[1] **and Hongya Geng**[3]

[1]*Department of Pediatrics, Xingtai People's Hospital, Xingtai, 054001 Hebei, China*
[2]*Department of Orthodontic, Hebei Eye Hospital, Xingtai, 054001 Hebei, China*
[3]*Department of Otolaryngology, Hebei Eye Hospital, Xingtai, 054001 Hebei, China*

Correspondence should be addressed to Huina Li; lihuinanurse@163.com

Received 22 June 2022; Revised 20 July 2022; Accepted 29 July 2022; Published 30 August 2022

Academic Editor: Min Tang

Adenoid hypertrophy (AH) is a common disease in otorhinolaryngology. Children with chronic snoring and hypoxia are susceptible to long-term nasal obstruction, while long-term open-mouth breathing may cause craniofacial bone development disorders and dull facial expressions, the so-called adenoid face. The purpose of this work is to analyze the influence of AH-induced airway obstruction (AO) on the growth and development of craniomaxillofacial structure and respiratory function (RF) in children. The clinical data of 56 AH children (observation group) and 42 healthy children with physical examination (control group) who visited the Hebei Eye Hospital during the same period were retrospectively analyzed. All children received acoustic rhinometry and X-ray cephalometric measurements. The upper airway structure, sleep disorder score, and *A*/*N* value of nasopharyngeal lateral X-ray images were compared between cases and controls. For AH children, sleep tests were also performed to assess their RF. X-ray cephalometric measurements of facial morphology showed obvious vertical growth, mandibular retrognathia, and enlarged mandibular angle in AH children. AH mainly affects the size of the nasopharyngeal and oropharyngeal airway. AH children presented with higher nasal airway resistance ($5.11 \pm 1.95\,cmH_2O/L\,min$) and lower nasopharyngeal volume (NPV) ($16.86 \pm 3.93\,cm^3$) than controls. Of the AH children, 45 had abnormal RF, including 4 with obstructive sleep apnea syndrome. The *A*/*N* value of nasopharyngeal lateral X-ray images was significantly higher in AH children than in controls. Besides, worse sleep quality was found in AH children. The above differences were all of statistical significance. The above indicates that AH can affect the size of the nasopharyngeal and oropharyngeal airway, change children's respiratory mode and RF, increase nasal resistance, and decrease NPV, resulting in upper respiratory tract stenosis, as well as craniomaxillofacial and oral malformations, which affects children's normal growth and development.

1. Introduction

Adenoid hypertrophy (AH), the most common cause of upper airway obstruction (AO) in children and adolescents, is a natural response to the increase of immune activity in childhood [1, 2]. The normal breathing pattern of human beings is nasal respiration, which means that air travels through the nasal, nasopharyngeal, oropharyngeal, and laryngopharyngeal cavity into the lower airway [3]. If the airflow is obstructed through the respiratory tract, that is, the passage is partially or completely blocked, the human body will adaptively change the nasal breathing mode into the oral breathing mode, so as to obtain sufficient ventilation to maintain normal physiological functions [4]. Open-mouth breathing (OMB), nasal diseases, asthma, speech disorders, and obstructive sleep apnea syndrome (OSAS) are common health issues that can be induced to some extent by inflammation and/or obstruction of the upper respiratory tract [5, 6]. The adenoid is a local immune organ [7] and an important part of the pharyngeal lymphatic ring, which, together with the palatine tonsil, lingual tonsil, eustachian tube tonsil, lateral pharyngeal bands, and posterior pharyngeal

lymphoid follicles, forms an endolymphatic ring, surrounding the airway and esophageal entrance [8, 9]. It is the site of the earliest exposure to inhaled and ingested antigens. When the adenoids or the peripheral lymphoid tissues are exposed to antigen stimulation and immune response occurs, adenoid tissue proliferates and increases in volume, resulting in AH [10].

AH can cause a wide spectrum of diseases, including secretory otitis media [11], sinusitis [12], obstructive sleep apnea-hypopnea syndrome (OSAHS) [13], lower respiratory tract inflammation [14], long-term hypoxia-induced abnormal growth and development, and mental and psychological disorders. AH is an important factor for children to breathe with their mouths open. Long-term OMB in childhood will inevitably lead to abnormal development of maxillofacial bone structure. For example, narrow dental arch, high-arched palate, anterior protrusion of upper incisors, crowded and uneven dentition leading to malocclusion, and uneven development of facial bones can cause abnormal development of nasal septum, resulting in deviation of nasal septum and turbinate hypertrophy [15, 16]. Children with OMB can suffer from sleep deprivation at night, long-term lack of oxygen, lethargy, and dull facial expression, resulting in the classic adenoid face [17]. As for the time of craniofacial development, the increase of upper airway resistance in any period may change the normal breathing mode and thus affect craniofacial development, while the age group with high incidence of AH is in the critical period of craniofacial development. At this stage, the detection and diagnosis of AH are still relatively complex, requiring nasal endoscopy, nasopharyngeal palpation, and X-ray examinations to make a definite diagnosis [18]. So far, the research on AH mainly focuses on its resultant nasal obstruction, while its effect on upper airway bone structure is rarely reported [19, 20].

Consequently, it is crucial to master diagnostic methods and timely judge the degree of illness. The novelty and motivation of the presented study is to use X-ray cephalometry as the breakthrough point to measure the maxillofacial structure of AH children in lateral cephalometric radiographs, so as to study the changes of facial morphology in AH children, and to analyze the impact of AH on children's respiratory function (RF).

2. Data and Methods

2.1. General Data. This research retrospectively analyzed the clinical data of 56 AH children (observation group) and 42 healthy children (control group) who visited the Hebei Eye Hospital between May 2020 and June 2021. Inclusion criteria for AH children are as follows: (1) age: 4-12 with a medical history ≥ 2 years; (2) presence of typical clinical symptoms such as nasal obstruction, sleep snoring, and OMB; and b(3) diagnosis of AH, with the A/N ratio of $X-$ ray lateral cephalogram ≥ 0.71, and adenoid blockage of posterior nostril $> 51\%$ by nasopharyngeal-fiberoscope. Exclusion criteria are as follows: (1) history of chronic rhinitis, turbinate hypertrophy, temporomandibular joint, or craniofacial trauma; (2) history of otolaryngology surgery or previous cranial-maxillofacial orthodontic treatment; and (3) congenital developmental disorders. The two cohorts of children were not statistically different in terms of gender, age, and other general data, indicating comparability (Table 1). This study was approved by the Ethics Committee of Xingtai People's Hospital, and the subjects' guardians all signed the informed consent.

2.2. Research Methods and Outcome Measures

(1) X-ray examination: all children underwent an X-ray skull examination. The lateral radiographs were fixed and measured when the child was in the standing position, with the midline of the skull vertical to the ground, the plane of the eyes and ears parallel to the ground, the mouth naturally closed, the facial muscles relaxed, and even breathing maintained. The outcome measures included the following: ANS-Me (distance from the anterior nasal spine to the submental point), N-ANS (distance from the nasion to the anterior nasal spine), FH ratio (ratio of anterior superior height to anterior inferior height), Ar-ANS (maxillary length: distance from the articulare to the anterior nasal spine), Go-Gn (mandibular body length: distance from the mandibular angle to the submental apex), Go-Ar (mandibular ramus height), SNA (anteroposterior position of maxillary basal bone and anterior skull base plane), SNB (anteroposterior position of mandibular basal bone and anterior skull base plane), ANB (anteroposterior position of upper and lower jaws), Go angel (vertical relationship of mandibular body relative to mandibular ramus), and MP-SN (angle between mandibular plane and anterior skull base plane)

(2) Upper airway measurement analysis by X-ray: A (the most protruding point across the lower margin of the adenoid is the vertical line of the external cranial tangent of the occipital slope. The distance between the most protruding point and the vertical foot is the thickness of the adenoid); N (the root of the pterygium meets the cranial surface of the ramp, and the length between the junction point and the point of the posterior nasal spine is the width of the bony nasopharyngeal cavity); PNS-R (the distance between the posterior nasal spinous point and the pharyngeal apex); PNS-UPW (the distance from the posterior nasal spinous point to the superior pharyngeal wall); SPP-SPPW (the distance from the back of the soft palate to the wall of the pharynx); U-MPW (the distance between the apical uvula and the middle pharyngeal wall); TB-TPPW (Pharyngeal airway space); and V-LPW (the distance between epiglottis valley and hypopharyngeal wall)

(3) Nasal airway volumetric measurement using acoustic rhinometry (AR): half an hour before the examination, the investigator entered the air-conditioned examination room that was maintained at 21°C with a humidity of 50%-60%. Nasopharyngeal volume

Table 1: General data.

	Gender (male/female)	Age	Delivery mode		Symptom			Type of hypertrophy	
			Natural childbirth	Cesarean delivery	Snoring	Mouth breathing	Both	Simple adenoid hypertrophy	Combined with tonsil hypertrophy
Observation group ($n = 56$)	34/22	6.36 ± 1.41	32 (57.1)	24 (42.9)	21 (37.5)	24 (42.9)	11 (19.6)	41 (73.2)	15 (26.8)
Control group ($n = 42$)	23/19	6.76 ± 1.54	25 (59.5)	17 (40.5)	—	—	—	—	—
χ^2/t	0.3495	1.3358	0.0559						
P	0.5544	0.1848	0.8131						

Table 2: Sagittal diameter of upper airway on cephalic radiographs.

Parameters	Observation group ($n = 56$)	Control group ($n = 42$)	t	P
A (mm)	16.13 ± 1.40	8.61 ± 1.88	22.7064	**<0.0001**
N (mm)	20.34 ± 1.55	19.85 ± 1.69	1.4898	0.1396
PNS-R (mm)	18.21 ± 1.41	19.80 ± 1.83	4.8596	**<0.0001**
PNS-UPW (mm)	9.16 ± 1.81	15.35 ± 1.97	16.1302	**<0.0001**
SPP-SPPW (mm)	10.83 ± 2.07	11.25 ± 1.84	1.0418	0.3001
U-MPW (mm)	9.70 ± 2.02	9.87 ± 1.49	0.4594	0.6469
TB-TPPW (mm)	8.93 ± 2.49	9.31 ± 2.33	0.7683	0.4442
V-LPW (mm)	18.87 ± 1.37	19.20 ± 1.82	1.0245	0.3082

Notes: Bold text means statistical significance.

Table 3: Comparison of craniofacial morphological parameters between the two groups of children.

Parameters	Observation group ($n = 56$)	Control group ($n = 42$)	t	P
ANS-Me (mm)	67.14 ± 5.73	63.40 ± 5.41	3.2744	**0.0015**
N-ANS (mm)	46.30 ± 3.72	49.53 ± 5.22	1.8453	0.0681
FH ratio	0.71 ± 0.10	0.79 ± 0.09	4.0886	**<0.0001**
Ar-ANS (mm)	78.89 ± 7.06	80.13 ± 7.49	0.8383	0.4040
Go-Gn (mm)	60.74 ± 5.48	61.95 ± 7.84	0.8992	0.3708
Ar-Gn (mm)	94.71 ± 7.08	94.29 ± 9.75	0.2471	0.8053
Go-Ar (mm)	45.82 ± 6.88	45.15 ± 8.07	0.4428	0.6589
SNA (°)	88.93 ± 4.53	89.26 ± 5.25	0.3333	0.7396
SNB (°)	76.69 ± 4.60	80.93 ± 5.22	4.2613	**<0.0001**
ANB (°)	8.61 ± 2.05	8.59 ± 2.03	0.0480	0.9618
MP-SN (°)	40.05 ± 5.76	34.32 ± 5.03	5.1411	**<0.0001**
Go angle (°)	134.23 ± 5.25	132.38 ± 5.33	1.7151	0.0896

(NPV) and nasal airway resistance (NAR) were measured by the acoustic reflection nasal measurement system (ECCOVISION, USA). Children were asked to sit quietly for a moment to prepare for examination, and the influences of temperature, humidity, movement, and noise on nasal mucosa were eliminated. When measuring, an appropriate nasal probe was used to prevent the nasal cavity from being deformed by extrusion. Breathing and swallowing were stopped during the test, and the left and right nasal cavities were tested separately

(4) RF determination: AH children were monitored for sleeping with a portable PSG device, with the detection time not less than 7 hours per night. Polysomnography was interpreted by two technicians and a pediatrician trained in sleep medicine, all blinded to clinical outcomes. Sleep stages were classified based on the American Academy of Sleep Medicine guidelines [21], and subjects with an obstructive apnea-hypopnea index (OAHI) score ≥ 1 were defined as OSAS [22]

(5) The sleep quality, efficiency, and time of both cohorts of children were assessed using the Pittsburgh Sleep Quality Index (PSQI) [23]. The scale consists of self-assessment items and other items, including seven modules: sleep quality, sleep latency, sleep duration, sleep efficiency, sleep disturbance, sleep medication, and daytime sleep dysfunction. On a scale of 0-21, higher scores are associated with more severe sleep disorders

2.3. Statistical Processing. Data analysis was performed by SPSS 22.0 (IBM SPSS 22.0, Chicago, IL), and statistical significance was considered when $P < 0.05$. A Chi-square test was used for counting data described in the form of n (%). The measurement data of normal distribution were represented by mean ± SD, and the difference was determined by an independent sample t-test.

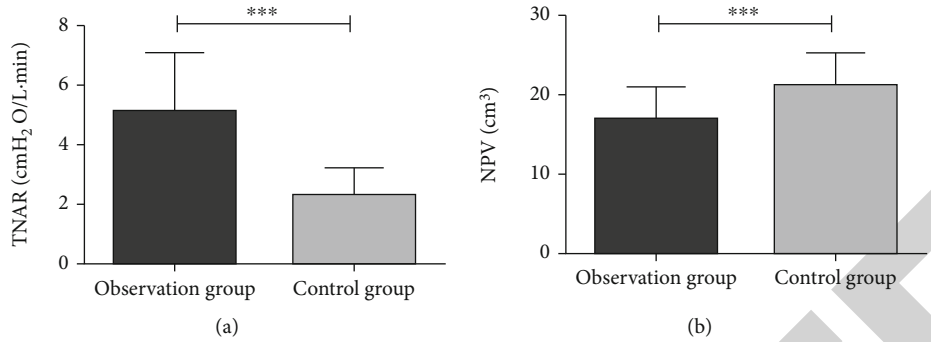

Figure 1: Comparison of acoustic rhinometry measurement parameters between two groups of children. (a) Comparison of total nasal airway resistance (TNAR). (b) Comparison of nasopharyngeal volume (NPV). $^{***}P < 0.001$.

3. Results

3.1. Sagittal Diameter of Upper Airway in Children. As shown in Table 2, the A value, PNS-R value, and PNS-UPW value showed statistically differences between the control group and the observation group, indicating that AH mainly affected the size of nasopharyngeal and oropharyngeal airway. While no significant difference was observed in the N value, indicating no difference in bony structure of nasopharyngeal cavity between the two groups, nor was there any statistical difference in other indicators, suggesting no difference in the middle and lower segments of the upper airway.

3.2. Cephalometric Parameters of Children. Among the craniofacial measurement parameters, SNB angle, MP-SN angle, and FH ratio showed statistical significance between groups. Meanwhile, a significant difference was observed in ANS-Me ($P < 0.05$). The other indexes were not statistically significant ($P > 0.05$) Table 3.

3.3. Nasal Airway Resistance Results in Two Groups. The results identified a lower total NAR (2.35 ± 0.83 cmH_2O/L min) in controls than in AH children (5.11 ± 1.95 cmH_2O/L·min) and a higher NPV in controls compared with cases (20.78 ± 4.44 cm^3 vs. 16.86 ± 3.93 cm^3), with statistical significance ($P < 0.05$) Figure 1.

3.4. Respiratory Function of Adenoidal Hypertrophy Children. The RF test results (Table 4) identified 11 children with an OAHI score of 0, 41 children with 0 < OAHI score < 1, and 4 with an OAHI score ≥ 1. The results indicate that 45 children developed respiratory dysfunction, including 4 with OASA.

3.5. Children's Sleep Quality and A/N Value of Nasopharyngeal X-Ray Lateral Films in Two Groups. After evaluating the sleep quality, we found that compared with controls, the sleep latency (23.09 ± 3.93 min) and PSQI score (14.46 ± 3.43 points) were significantly higher in AH children. A higher *A*/*N* value (0.89 ± 0.09) of nasopharyngeal X-ray lateral films was also determined in AH children (Figure 2).

Table 4: Results of respiratory function indexes in children with adenoid hypertrophy.

Measured value	Number	Percentage
OAHI = 0	11	19.6
0 < OAHI < 1	41	73.2
OAHI ≥ 1	4	7.2

4. Discussion

Adenoids are lymphatic organs located in the nasopharynx and the top of the posterior pharyngeal wall [8]. According to previous views, adenoids existed at birth, increased with age under physiological conditions, and reached their maximum size at the age of 6-7. They began to atrophy after the age of 10 and completely shrank by puberty, merging with the mucous membrane of the nasopharyngeal wall. AH is rare in adulthood [24, 25]. However, some other studies have shown that among adults with pharyngeal diseases, the proportion of adenoids remains high and hypertrophy is common [26]. The location and function determine that adenoids, once stimulated, will evoke immune responses, increase in volume, and occupy the space of the nasopharyngeal cavity, which may block the ventilation and drainage of posterior nostril and nasopharynx, resulting in pathological AH [10]. OMB is a reflex activity of the body to enlarge the upper airway. If the upper airway is blocked for a long time, children will still keep OMB even when the obstruction is removed, as the bad habit has already been developed. Craniofacial growth and development are influenced by both genetic factors and functional stimuli. According to Moss's functional matrix theory, the change of breathing pattern is bound to break the original balance of teeth, jaw, tongue, and muscles around the face, resulting in the growth and reconstruction of teeth and jaw to a new equilibrium, which will ultimately affect the position of teeth and the shape of jaw and give rise to craniomaxillofacial deformities [27].

In this study, the nasal RF and craniofacial morphology of AH children were objectively evaluated by AR and X-ray cephalometry. The results showed higher NAR and statistically lower NPV in AH children compared with controls. It shows that the nasal cavity and nasopharyngeal cavity became smaller after mechanical obstruction of

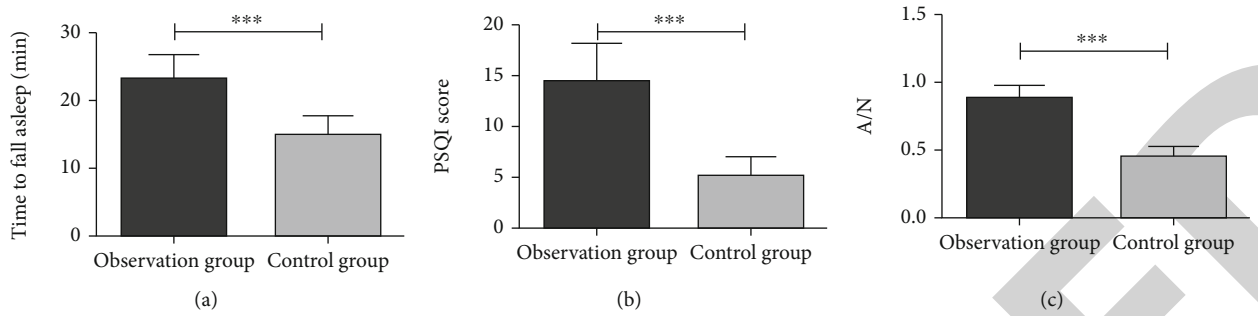

Figure 2: Comparison of sleep quality and A/N value of nasopharyngeal X-ray lateral films between the two groups. (a) Comparison of average sleep latency. (b) Comparison of PSQI score. (c) Comparison of A/N. $^{***}P < 0.05$.

adenoid tissue in children, resulting in nasal obstruction and nasal blood circulation disorders. Most of the previous studies on pediatric AH and craniofacial dysplasia did not objectively measure children's nasal RF but confirmed nasal AO only by OMB. Although some studies have also used the combination of signs and symptom scores to subjectively quantify the nasal opening degree, the reliability of subjective sensation of nasal obstruction is not high, because some children with AH are too young to accurately describe and express their feelings. The AR used in this study has obvious advantages because it does not rely on airflow in the nasal cavity, which is suitable for patients with complete nasal obstruction and kids aged under 3. The basic principle of AR is to describe the two-dimensional information of the cavity to be measured by using the acoustic reflection signals and to sketch the cross-sectional shape of nasal airway by measuring the amplitude of the reflected wave and the reflected time, which directly reflects the patency of the airway [28, 29]. Then, we observed the craniofacial morphology of two groups of children and found statistical differences in SNB angle, MP-SN angle, FH ratio, and ANS-Me. Nasal obstruction caused by AH will affect children's craniofacial development. First, it has a great impact on the position and morphology of mandible. The narrowing of the upper respiratory tract changes children's RF and breathing pattern, which triggers a certain degree of changes in oral muscles, as well as damage to the balance between oral muscles and the jaw, eventually leading to abnormal growth of the jaw and teeth, which is mainly manifested as mandibular retraction and smaller SNB angle on the sagittal plane, similar to previous studies [30, 31]. In addition, long-term OMB promoted the progressive extension of the head and neck, leading to an increase in craniocervical angle anteversion [32]. Wang et al. explored the influence of AH on both the morphological development characteristics of the upper airway and the craniofacial features in children. The results showed that AH altered a child's breathing mode and function by inducing upper airway stenosis, as well as craniomaxillofacial and oral deformities [16].

Finally, we observed the sleep quality and RF of children. Significantly worse sleep quality was observed in AH cases compared with healthy children; in addition, 45 AH children developed respiratory dysfunction, including 4 with OSAS. AH is considered the most important risk factor for the development of OSAS in children [33, 34]. Sleep monitoring is an important means to identify sleep-related respiratory disorders in children. The clinical manifestations of sleep-disordered breathing in children are different from those in adults, mainly characterized by obstructive hypopnea accompanied by varying number of apnea episodes and periodic hypoxemia. There is no obvious sleep structure disorder, and respiratory disorder is generally not accompanied by microawakening. In addition, children with similar severity of OSAS and similar adenoid or tonsil sizes have different clinical presentations [35]. All these suggest that the OSAS phenotype is highly variable. Hence, we should pay attention not only to apnea-hypopnea index but also to clinical manifestations, sleep structure characteristics, and respiratory regulation. It is important to note that if left untreated, OSAS can lead to neurobehavioral and cardiovascular complications and growth disorders [36]. Therefore, close attention should be paid to the sleep status of children with AH. However, this research still shows some limitations. As only 56 AH children were included in this study, the results may not be representative. Besides, people in plateau areas have respiratory compensation due to different growing environments, so differences in different growing environments need to be further analyzed.

5. Conclusion

To sum up, AH will significantly affect the growth of craniomaxillofacial structure of children and their RF, resulting in reduced sleep quality of such children. Oral respiration mainly affects mandibular development, which can cause back rotation or extension of mandible, decrease of mandibular body length, and lip tilt of upper and lower front teeth. However, it has little influence on maxillary development.

Data Availability

The labeled dataset used to support the findings of this study are available from the corresponding author upon request.

Conflicts of Interest

The authors declare no competing interests.

Acknowledgments

This project is supported by the Key Research and Development Projects in Xingtai, China (2020ZC348).

References

[1] X. Feng, G. Li, Z. Qu, L. Liu, K. Näsström, and X.-Q. Shi, "Comparative analysis of upper airway volume with lateral cephalograms and cone-beam computed tomography," *American Journal of Orthodontics and Dentofacial Orthopedics*, vol. 147, no. 2, pp. 197–204, 2015.

[2] L. V. Gankovskaya, V. P. Bykova, L. S. Namasova-Baranova et al., "Innate immunity gene expression by epithelial cells of upper respiratory tract in children with adenoid hypertrophy," *Auris Nasus Larynx*, vol. 45, no. 4, pp. 753–759, 2018.

[3] C. Popa, A. M. Bratu, and M. Petrus, "A comparative photoacoustic study of multi gases from human respiration: mouth breathing vs. nasal breathing," *Microchemical Journal*, vol. 139, pp. 196–202, 2018.

[4] C. Recinto, T. Efthemeou, P. T. Boffelli, and J. W. Navalta, "Effects of nasal or oral breathing on anaerobic power output and metabolic responses," *International Journal of Exercise Science*, vol. 10, no. 4, pp. 506–514, 2017.

[5] I. Brambilla, A. Pusateri, F. Pagella et al., "Adenoids in children: advances in immunology, diagnosis, and surgery," *Clinical Anatomy*, vol. 27, no. 3, pp. 346–352, 2014.

[6] G. Marseglia, P. Merli, D. Caimmi et al., "Nasal disease and asthma," *International Journal of Immunopathology and Pharmacology*, vol. 24, 4_suppl, pp. 7–12, 2011.

[7] G. Marseglia, D. Caimmi, F. Pagella et al., "Adenoids during childhood: the facts," *International Journal of Immunopathology and Pharmacology*, vol. 24, 4_suppl, pp. 1–5, 2011.

[8] L. Stanisce, E. Sims, C. Hou et al., "Differential cellular composition of human palatine and pharyngeal tonsils," *Archives of Oral Biology*, vol. 96, pp. 80–86, 2018.

[9] A. Arambula, J. R. Brown, and L. Neff, "Anatomy and physiology of the palatine tonsils, adenoids, and lingual tonsils," *World Journal of Otorhinolaryngology-Head and Neck Surgery*, vol. 7, no. 3, pp. 155–160, 2021.

[10] E. Kershaw and A. Poulios, "Adenoidal hypertrophy," in *Rhinology and Anterior Skull Base Surgery*, Springer, 2021.

[11] V. Bhat, I. P. Mani, R. Aroor, M. Saldanha, M. Goutham, and D. Pratap, "Association of asymptomatic otitis media with effusion in patients with adenoid hypertrophy," *Journal of Otology*, vol. 14, no. 3, pp. 106–110, 2019.

[12] A. M. Bulfamante, A. M. Saibene, G. Felisati, C. Rosso, and C. Pipolo, "Adenoidal disease and chronic rhinosinusitis in children—is there a link?," *Journal of Clinical Medicine*, vol. 8, no. 10, p. 1528, 2019.

[13] L. Shen, Z. Lin, X. Lin, and Z. Yang, "Risk factors associated with obstructive sleep apnea-hypopnea syndrome in Chinese children: a single center retrospective case-control study," *PLoS One*, vol. 13, no. 9, article e0203695, 2018.

[14] A. B. Goldsobel, "Risk of adenoid hypertrophy in children with allergic rhinitis," *Pediatrics*, vol. 110, Supplement_2, pp. 441-442, 2002.

[15] C. F. Koca, T. Erdem, and T. Bayındır, "The effect of adenoid hypertrophy on maxillofacial development: an objective photographic analysis," *Journal of Otolaryngology-Head & Neck Surgery*, vol. 45, no. 1, pp. 1–8, 2016.

[16] H. Wang, X. Qiao, S. Qi, X. Zhang, and S. Li, "Effect of adenoid hypertrophy on the upper airway and craniomaxillofacial region," *Translational Pediatrics*, vol. 10, no. 10, pp. 2563–2572, 2021.

[17] A. J. Sheeba and S. S. Bakshi, "Adenoid facies," *Anesthesiology*, vol. 129, no. 2, pp. 334–334, 2018.

[18] M. Sikorska-Żuk and M. Bochnia, "Halitosis in children with adenoid hypertrophy," *Journal of Breath Research*, vol. 12, no. 2, article 026011, 2018.

[19] C. M. Baldassari and S. Choi, "Assessing adenoid hypertrophy in children: X-ray or nasal endoscopy?," *The Laryngoscope*, vol. 124, no. 7, pp. 1509-1510, 2014.

[20] W. Chen, W. Cao, J. Shen, Z. Zhou, C. Chen, and Y. Fu, "The efficacy of om85-bv in the treatment of recurrent upper respiratory tract infection with adenoid hypertrophy and the preliminary exploration of potential therapeutic mechanism," *Lin Chuang er bi yan hou tou Jing wai ke za zhi= Journal of Clinical Otorhinolaryngology, Head, and Neck Surgery*, vol. 34, pp. 499–504, 2020.

[21] R. B. Berry, R. Budhiraja, D. J. Gottlieb et al., "Rules for scoring respiratory events in sleep: Update of the 2007 AASM manual for the scoring of sleep and associated events: deliberations of the sleep apnea definitions task force of the American Academy of Sleep Medicine," *Journal of Clinical Sleep Medicine*, vol. 8, no. 2012, pp. 597–619, 2012.

[22] M. J. Sateia, "International classification of sleep disorders-third edition," *Chest*, vol. 146, no. 5, pp. 1387–1394, 2014.

[23] A. Setyowati and M. H. Chung, "Validity and reliability of the Indonesian version of the Pittsburgh Sleep Quality Index in adolescents," *International Journal of Nursing Practice*, vol. 27, no. 5, article e12856, 2021.

[24] C. S. Handelman and G. Osborne, "Growth of the nasopharynx and adenoid development from one to eighteeen years," *The Angle Orthodontist*, vol. 46, no. 3, pp. 243–259, 1976.

[25] T. Ishida, A. Manabe, S.-S. Yang, H. S. Yoon, E. Kanda, and T. Ono, "Patterns of adenoid and tonsil growth in Japanese children and adolescents: a longitudinal study," *Scientific Reports*, vol. 8, no. 1, pp. 1–7, 2018.

[26] N. Yildirim, M. Şahan, and Y. Karslioğlu, "Adenoid hypertrophy in adults: clinical and morphological characteristics," *Journal of International Medical Research*, vol. 36, no. 1, pp. 157–162, 2008.

[27] S. Kyrkanides, T. Moore, J.-N. H. Miller, and R. H. Tallents, "Melvin Moss' function matrix theory–revisited," *Orthodontic Waves*, vol. 70, no. 1, pp. 1–7, 2011.

[28] H.-Y. Li, H. Engleman, C.-Y. Hsu et al., "Acoustic reflection for nasal airway measurement in patients with obstructive sleep apnea-hypopnea syndrome," *Sleep*, vol. 28, no. 12, pp. 1554–1559, 2005.

[29] E. Spataro and S. P. Most, "Measuring nasal obstruction outcomes," *Otolaryngologic Clinics of North America*, vol. 51, no. 5, pp. 883–895, 2018.

[30] D. Mahony, A. Karsten, and S. Linder-Aronson, "Effects of adenoidectomy and changed mode of breathing on incisor and molar dentoalveolar heights and anterior face heights," *Australian Orthodontic Journal*, vol. 20, no. 2, pp. 93–98, 2004.

[31] H. Özdemir, R. Altin, A. Söğüt et al., "Craniofacial differences according to AHI scores of children with obstructive sleep apnoea syndrome: cephalometric study in 39 patients," *Pediatric Radiology*, vol. 34, no. 5, pp. 393–399, 2004.

Hindawi
Computational and Mathematical Methods in Medicine
Volume 2023, Article ID 9819813, 1 page
https://doi.org/10.1155/2023/9819813

Retraction

Retracted: Systematic Evaluation of the Efficacy of Acupuncture Associated with Physical and Mental Intervention when Treating Idiopathic Tinnitus and the Improvement of Tinnitus Symptoms

Computational and Mathematical Methods in Medicine

Received 12 December 2023; Accepted 12 December 2023; Published 13 December 2023

This article has been retracted by Hindawi, as publisher, following an investigation undertaken by the publisher [1]. This investigation has uncovered evidence of systematic manipulation of the publication and peer-review process. We cannot, therefore, vouch for the reliability or integrity of this article.

Please note that this notice is intended solely to alert readers that the peer-review process of this article has been compromised.

Wiley and Hindawi regret that the usual quality checks did not identify these issues before publication and have since put additional measures in place to safeguard research integrity.

We wish to credit our Research Integrity and Research Publishing teams and anonymous and named external researchers and research integrity experts for contributing to this investigation.

The corresponding author, as the representative of all authors, has been given the opportunity to register their agreement or disagreement to this retraction. We have kept a record of any response received.

References

[1] Y. Li, D. Sang, Z. Wu, and X. Cao, "Systematic Evaluation of the Efficacy of Acupuncture Associated with Physical and Mental Intervention when Treating Idiopathic Tinnitus and the Improvement of Tinnitus Symptoms," *Computational and Mathematical Methods in Medicine*, vol. 2022, Article ID 6764909, 10 pages, 2022.

Hindawi
Computational and Mathematical Methods in Medicine
Volume 2022, Article ID 6764909, 10 pages
https://doi.org/10.1155/2022/6764909

Research Article

Systematic Evaluation of the Efficacy of Acupuncture Associated with Physical and Mental Intervention when Treating Idiopathic Tinnitus and the Improvement of Tinnitus Symptoms

Yan Li, Di Sang, Zeting Wu, and Xuemei Cao

Acupuncture & Moxibustion Dept., The Fourth Clinical Medical College of Guangzhou University of Traditional Chinese Medicine, Shenzhen 518000 Guangdong, China

Correspondence should be addressed to Xuemei Cao; 20201121065@stu.gzucm.edu.cn

Received 8 July 2022; Revised 4 August 2022; Accepted 16 August 2022; Published 30 August 2022

Academic Editor: Min Tang

Objective. To systematically evaluate the efficacy of acupuncture associated with physical and mental intervention when treating idiopathic tinnitus and the improvement of tinnitus symptoms, so as to supply evidence-based medicine for its popularization and adoption. *Methods*. PubMed, EMBASE, ScienceDirect, Cochrane Library, China knowledge Network Database (CNKI), China VIP Database, Wanfang Database, and China Biomedical Literature Database (CBM) online database were searched for the controlled trial of acupuncture associated with physical and mental intervention when treating idiopathic tinnitus. The retrieval time limit is from January 2010 to March 2022. Separately, two researchers extracted the data, and according to the Cochrane Handbook 5.3, the bias risk of each piece of literature was assessed. The collected data were measured using RevMan5.3 statistical software. *Results*. Finally, 5 CT articles were included in this study, with a total sample size of 282. Meta-analysis showed that the effective rate of the study group was significantly higher than that of the control group ($P < 0.05$). The scores of tinnitus disorder scale (THI) after treatment were analyzed by Meta. The THI scores of the study group after treatment were significantly lower than those before treatment. Meta-analysis of the severity of tinnitus after treatment showed that the severity of tinnitus in the observation group after treatment was significantly lower than that before treatment. There is a certain publication deviation in the literature, which may be related to the heterogeneity of the research and the small number of literatures. *Conclusion*. On the basis of acupuncture treatment, associated with physical and mental intervention is helpful to the recovery of patients with idiopathic tinnitus, can effectively improve their clinical symptoms, and is suitable for clinical application. A popularization of this concept in clinical practice is worth considering, but further research and follow-up with a higher methodological quality and longer intervention time are needed to confirm its efficacy.

1. Introduction

Idiopathic tinnitus refers to a kind of subjective tinnitus of unknown cause in clinic, that is, no distinct abnormality is found through the current examination, or there is a lack of clear causal relationship between abnormal examination results and tinnitus [1, 2]. It not only refers to the symptoms of tinnitus but also can be used as an independent disease. The onset of idiopathic tinnitus is acute or chronic, with or without hearing and psychological disorders, which is usually associated with hearing loss, noise exposure, aging, and stress. The auditory sensitivity in tinnitus population is 40-86% [3, 4]. Most research reports show that the prevalence of adult tinnitus is about 10-19%, and in recent years, the prevalence of adult tinnitus is increasing at an annual rate of 3%, and the incidence rate increases with age. It accounts for 31.4%, and about 1/3 of the elderly suffer from tinnitus for many years. People who are male, obese, or have long-term blood pressure, blood lipids, blood sugar, psychoemotional disorders, and other related diseases, or people with a history of occupational and recreational noise exposure have a higher incidence of tinnitus [5].

Currently, the specific pathogenesis of tinnitus is not completely clear. With the development of neuroimaging,

neurophysiology, neuropsychology, and so on, it is believed that tinnitus is driven by the following two mechanisms: one is the bottom-up mechanism related to hearing loss, and the other is the top-down mechanism related to insufficient noise elimination [5]. The course of tinnitus is often long, which will cause great harm to the physical and mental health of patients, and the related social and economic costs caused by its treatment are very high. Take the United States as an example, by the fiscal year 2012, the number of veterans who had received government disability pension for tinnitus alone had exceeded 970000 [6]. Since there is no standardized treatment plan at present, nonstandard and ineffective treatment can increase the cost of national health care [7]. According to relevant statistics in the United States, the annual government pension for tinnitus is more than $2.75 billion [8]. In China, there is no specific investigation in this regard, but the economic burden brought by tinnitus treatment cannot be ignored. In addition, tinnitus has a large impact on the life quality of patients, and the functional impairment caused by it mainly includes four aspects: thinking and emotion, sleep, hearing, and concentration [9, 10].

According to traditional Chinese medicine (TCM), tinnitus can be caused by exogenous and internal injuries. The pathogenesis of tinnitus can be divided into deficiency and excess, including wind-heat invasion, qi depression, inflammation of liver fire, hyperactivity of liver yang, stagnation of phlegm fire, and blood stasis. Deficiency syndrome includes deficiency of heart blood, deficiency of lung qi, weakness of spleen and stomach, deficiency of kidney essence, and loss of kidney yang [11, 12]. According to the bottom-up tinnitus mechanism, the damage of the peripheral auditory system leads to a decrease in the input signal from the cochlea to the brain, and the central auditory structure compensates the lost signal in the form of neuroplasticity. Of note, the weak cochlear signal is gradually amplified along the auditory pathway, increasing spontaneous and synchronous neural activity, which may lead to tinnitus in varying degrees. At present, with regard to the lack of specific treatment for idiopathic tinnitus, it has been found that TCM therapy such as TCM, acupuncture, moxibustion, acupoint injection, and five elements music can reduce the loudness of tinnitus and relieve the concomitant symptoms of tinnitus [13]. Acupuncture as a traditional means of TCM, based on the theory of viscera and meridians, according to the characteristics of patients' condition, acupuncture and manipulation were selected according to syndrome differentiation, which had a good effect when treating tinnitus [14]. Numerous literature studies have shown [15, 16] that acupuncture associated with nondrug interventions has better curative effect when treating idiopathic tinnitus, the therapeutic effect is better than that of rehabilitation therapy or acupuncture alone, and it has the advantages of fewer clinical adverse reactions. However, the effectiveness of TCM when treating idiopathic tinnitus has not been internationally recognized and needs to be supported by high-quality research evidence. In addition, there are large differences between different research designs, and there are many evaluation indicators. Common clinical manifestations include insomnia, anxiety, and depression, decreased concentration, and decreased speech comprehension, or other family life and work problems, and the higher the degree of tinnitus distress, the greater the likelihood of accompanying psychological, psychosomatic, and/or psychiatric comorbidities. Therefore, timely medical treatment should be recommended for such patients, and active and effective intervention should be given. Only the effectiveness of a certain literature or the improvement of a certain evaluation index is used to illustrate the clinical efficacy of TCM acupuncture associated with mind-body intervention when treating idiopathic tinnitus. The results are unconvincing and inconsistent across numerous studies. Under this background, it is very necessary to carry out further research on the efficacy of acupuncture associated with physical and mental intervention when treating idiopathic tinnitus. Therefore, this study systematically, quantitatively, and comprehensively analyzed the results of multiple independent studies of the same kind through. The purpose of this study was to evaluate the clinical efficacy of acupuncture combined with physical and mental intervention in the treatment of patients with idiopathic tinnitus through meta-analysis and to provide an objective basis for clinical application.

2. Research Contents and Methods

2.1. The Sources and Retrieval Methods of Documents. Search PubMed, EMBASE, ScienceDirect, Cochrane Library, China Journal full-text Database (CNKI), VIP full-text Database (VIP), Wanfang Database, and Chinese Biomedical Literature data (CBM); search relevant Chinese journals, conference papers, degree papers, etc.; and collect relevant data about acupuncture associated with physical and mental intervention when treating idiopathic tinnitus. Literature retrieval was carried out in the way of free words and subject words, with the key words of TCM acupuncture, physical and mental intervention, idiopathic tinnitus, tinnitus symptoms, improvement effect, meta-analysis, TCM acupuncture; idiopathic tinnitus; symptoms of tinnitus, etc., from January 2010 to March 2022.

2.2. Literature Inclusion and Exclusion Criteria

2.2.1. Literature Inclusion Criteria. (1) Research type: all the controlled trials (CT) of acupuncture associated with physical and mental intervention when treating idiopathic tinnitus, the search languages are Chinese and English; (2) object of study: patients with idiopathic tinnitus were clearly diagnosed; diagnostic criteria of western medicine: refer to the consensus of 2012 tinnitus experts and diagnostic criteria of idiopathic tinnitus in interpretation [17]; TCM syndrome differentiation criteria: refer to the TCM diagnostic criteria of tinnitus in the Clinical Research guidelines to treat tinnitus with new drugs of TCM [18]; (3) intervention measures: the study group received physical and mental intervention measures such as acclimatization therapy/five elements music therapy/cognitive behavioral therapy/TCM horn music, while the control group only received acupuncture or simple physical and mental intervention

2.2.2. Literature Exclusion Standard. (1) It is not a control study; (2) the data report is incomplete and the data cannot be used; (3) repeat the research content and take the latest research; (4) the evaluation of the curative effect of the study was not noticeable

2.3. Quality Evaluation and Data Extraction

(1) *Bias Risk Assessment Contained in the Study*. Evaluation was performed using the bias risk assessment tool recommended in Cochrane System Review Manual 5.3

(2) Data extraction and literature screening are done independently by two researchers, who collect literature, extract data, evaluate quality, and cross-check the results. When there are differences in opinion, discuss and resolve them or ask the third researcher for help. Note that Express document management software and Excel office software were used to manage and extract research data. If the data contained in the literature is incomplete, contact the author of this article to supplement it. The contents of data extraction contained (1) basic information: author, publication time, number of cases; (2) intervention measures: scheme, course of treatment; and (3) outcome indicators: total clinical effective rate, tinnitus disability assessment scale (THI) score and tinnitus evaluation questionnaire (TEQ).

2.4. Statistical Processing. RevMan5.3 software was adopted for meta-analysis. Counting data was indexed by relative risk (OR), and measurement data was indexed by mean difference (MD). The point estimate and 95% confidence interval (CI) of each effect are given. χ^2 test was adopted for heterogeneity test, and I^2 was adopted to judge the heterogeneity. Fixed effect models are used if there is no heterogeneity; if there is heterogeneity, subgroup analysis, sensitivity analysis, or descriptive analysis are used; and the random effect model is used if there is heterogeneity. The difference exhibited statistically noticeable ($P < 0.05$). Furthermore, the inverted funnel chart is drawn to measure the publication bias of the literature, and the Eggers's test is used to test the asymmetry of the funnel chart. Whenever the P value of this test is less than 0.1, the trim and fill method can be used to correct the funnel chart and adjust the effect of the potential release deviation.

3. Results and Analysis

3.1. The Results of Literature Retrieval and the Basic Situation of Literature Inclusion. We used a computer database to retrieve 1542 articles, 413 articles were eliminated after removing repeated studies, and 128 were retrieved by reading the titles and abstracts, after excluding irrelevant studies, reviews, case reports, and noncontrol literature, 74 articles were obtained, of which 69 had incomplete data and failed to highlight main outcomes, and finally contained 5 CT [13–20]. There were 282 samples analyzed by meta. The screening diagram of the literature is shown in Figure 1, and the basic characteristics of the contained literature are shown in Table 1.

3.2. Evaluation of the Quality of the Methodology Contained in the Literature. The five CT articles contained in this meta-analysis reported the baseline health status of the patients. All CT mentioned "random allocation," but did not specify the random method, and gave detailed intervention measures and treatment course. The reasons and number of blind method and lost follow-up or withdrawal were not described in detail in 5 CT articles. According to the Jadad scale, we can see that the CT of 5 articles is less than 2 points. The risk bias analysis is shown in Figures 2 and 3.

3.3. Meta-Analysis Result

3.3.1. Treatment Effective Rate. There were 5 CT studies contained in this study, with 282 samples. A meta-analysis was carried out on the treatment effectiveness. The results of the heterogeneity test indicated that $\text{Chi}^2 = 1.94$, $\text{df} = 3$, $P = 0.58$, and $I^2 = 0\%$, showing that the research data contained in the study show distinct heterogeneity, and the fixed effect model was adopted to analyze (Figure 4). It is suggested that acupuncture associated with physical and mental intervention has a noticeable effect on idiopathic tinnitus.

3.3.2. THI Scoring. There were 5 CT studies contained in this study, with 282 samples. The meta-analysis of THI scores after treatment was performed. The results of the heterogeneity test indicated that $\text{Chi}^2 = 22.26$, $\text{df} = 3$, $P < 0.0001$, and $I^2 = 87\%$, showing that the research data contained in the study show distinct heterogeneity. The random effect model was adopted to analyze (Figure 5). The THI score of the study group after treatment was noticeably lower ($P < 0.05$), suggesting that acupuncture associated with physical and mental intervention is helpful for the recovery of patients with idiopathic tinnitus.

3.3.3. TEQ Score. There were 5 CT studies contained in this study, with 282 samples. Meta-analysis was performed on the severity classification of tinnitus after treatment. The results of the heterogeneity test indicated that $\text{Chi}^2 = 16.81$, $\text{df} = 8$, $P = 0.03$, and $I^2 = 52\%$, showing that the research data contained in the study show distinct heterogeneity, and the random effect model (Figure 6) analysis shows that the severity of tinnitus in the study group after treatment was noticeably lower ($P < 0.05$).

3.3.4. Publication Bias Analysis. The inverted funnel chart was used to analyze the publication bias of the study with the treatment efficiency as the outcome index (Figure 7). The results indicated that most of the funnel charts were symmetrical and a few were asymmetrical, suggesting that there was a certain publication bias in the contained literature. This may be relevant to the heterogeneity of the study and the small number of contained literatures.

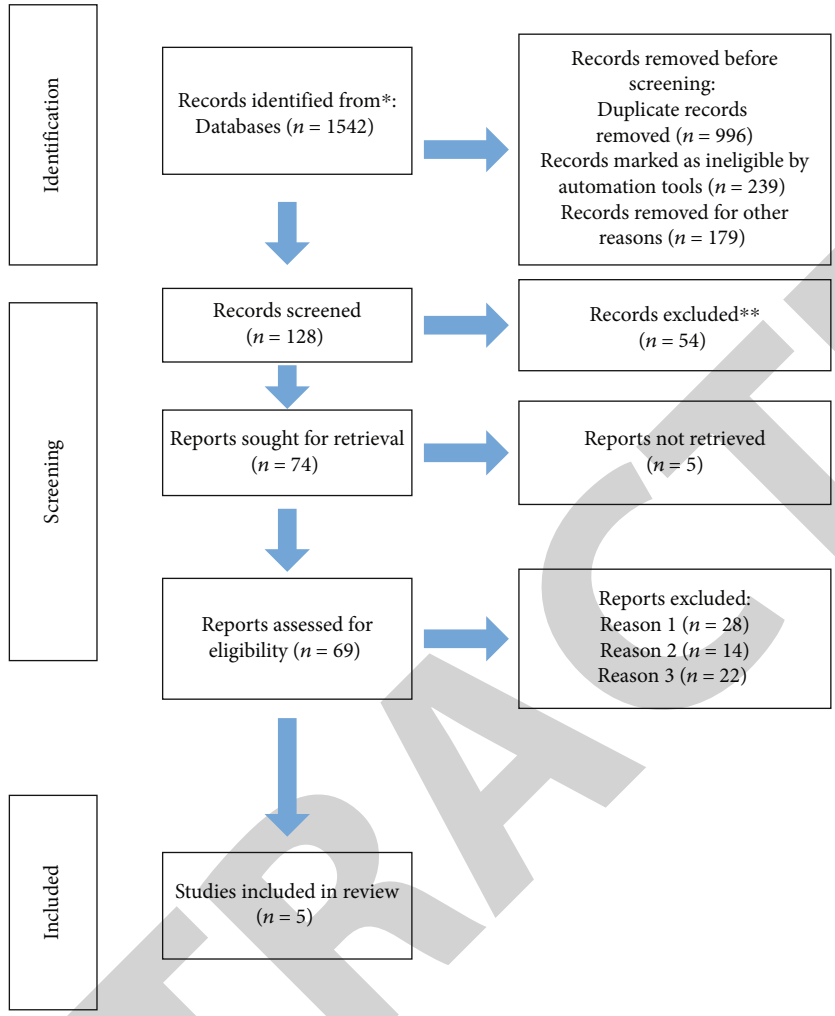

Figure 1: The screening diagram of the literature.

4. Analysis and Discussion

This study systematically, quantitatively, and comprehensively analyzed the results of multiple independent studies of the same kind through. Meta-analysis was performed to assess the clinical efficacy of acupuncture in the treatment of patients with idiopathic tinnitus in relation to physical and psychiatric interventions and to provide an objective basis for clinical application. With the aggravation of the aging population and the increase of environmental noise, the incidence of tinnitus is increasing year by year. According to epidemiological investigation, it is conservatively estimated that about 39 million elderly people in China suffer from tinnitus; 26 million tinnitus patients are seriously affected by tinnitus, and their life quality is seriously declining; 6.5 million patients are unable to live, work, and study normally because of tinnitus [24]. Tinnitus is still poorly understood as far as its mechanism is concerned. Some researchers such as Lee et al. [25] believe that the abnormal electrical activity of nerve fibers in the auditory conduction pathway is the basis of tinnitus, and the limbic system and autonomic nervous system are involved in the formation of tinnitus. Some researcher Qiu and Liu [26] also realized that nonauditory problems such as mental psychology, sleep, anxiety, and depression can also cause tinnitus and pointed out that after psychological and sleep problems were improved, tinnitus-related symptoms were also improved. In fact, in addition to ear surgery, diseases caused by tinnitus through surgical treatment can play a better effect, most other tinnitus can only be symptomatic treatment. Western medicine through the intervention of the primary disease, moderate improvement of inner ear microcirculation, and nutritional nerve drug treatment can improve tinnitus symptoms to a certain extent, but the cost of long-term use of western medicine is high, which will restrict patients with limited economic conditions.

The theory of TCM considers that the liver and the ear are closely related to the physiological functions, and the long-term emotional discomfort can lead to stagnation of liver qi, loss of relaxation, stagnation of qi mechanism, imbalance of ascending and descending, stagnation of fire for a long time, and stagnation of fire circulation. After disturbing the orifice, the disease will cause tinnitus. Therefore, liver-qi stagnation syndrome is a common syndrome of tinnitus. The "Nei Jing" clearly records tinnitus and expounds the pathogenesis of tinnitus from the perspective of TCM,

Table 1: Basic characteristics of literature.

Include the literature	Year of publication	N (C/T)	Intervention method		Outcome index	Course of treatment	Stochastic method	Blind or not
			C	T				
Liu and Feng [19]	2017	24/24	Vinpocetine + acupuncture	Vinpocetine + acupuncture therapy + acclimatization therapy	①②	1 month	Not mentioned	No
Wang and Wang [20]	2016	27/27	Dialectical acupuncture	Dialectical acupuncture + five elements music therapy	①②	4 weeks	Not mentioned	No
Zhang et al. [21]	2021	40/40	Cognitive behavioral therapy	Acupuncture therapy + cognitive behavioral therapy	②	4 weeks	Not mentioned	No
Guan [22]	2019	20/20	Acupuncture	Acupuncture therapy + horn music of TCM	①③	84 d	Not mentioned	No
Guan and Han [23]	2021	30/30	Acupuncture	Acupuncture therapy + psychological intervention + sound therapy	①②③	28 d	Not mentioned	No

Note: C: control group; T: research group. ① Treatment effective rate; ② THI score; ③ TEQ score.

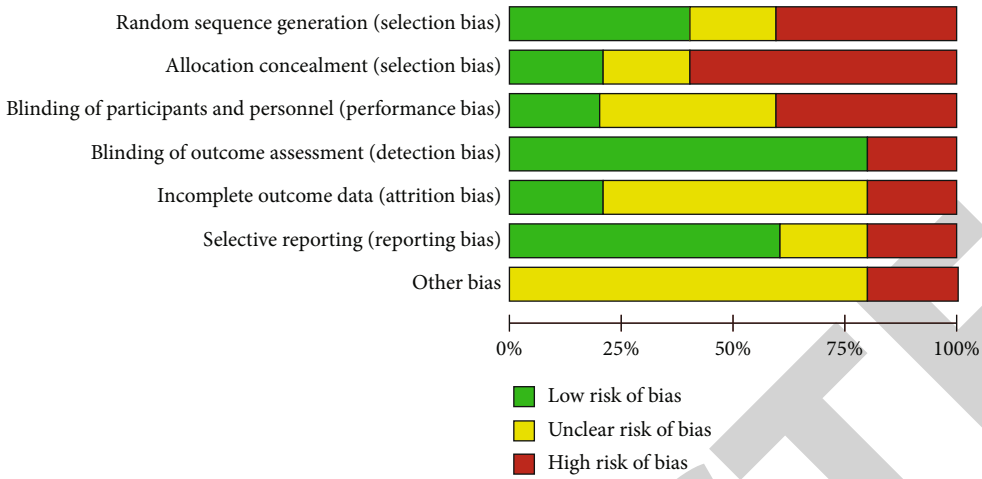

Figure 2: Risk of bias.

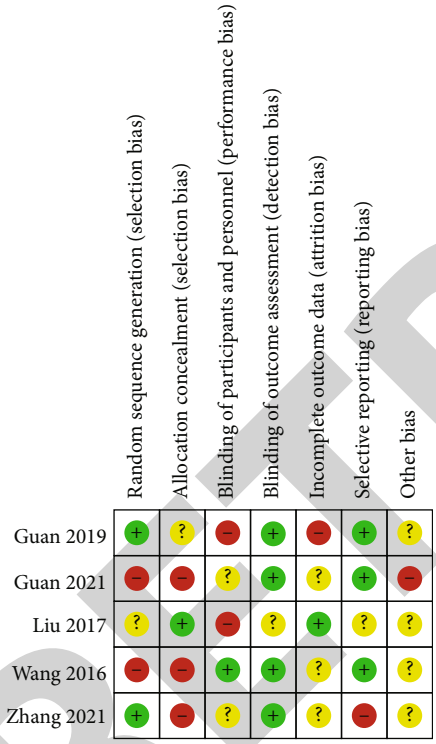

Figure 3: Risk of bias summary.

which believes that the occurrence of tinnitus is relevant to the internal organs and is closely relevant to the liver, spleen, and kidney. Yao et al. [13] believe that most of the patients with modern tinnitus are "liver depression," and the treatment of tinnitus from "liver depression" has received a good clinical effect. Acupuncture therapy in the external therapy of TCM shows a certain potential when treating tinnitus because of its low cost and outstanding effect. Acupuncture can improve the microcirculation of the inner ear, correct the hypoxia-ischemic state of cochlear cells, and regulate the release of neurotransmitters so as to repair inner ear cells and improve hearing. Researcher Gong et al. [27] evaluated the current situation of acupuncture treatment of tinnitus in China through meta-analysis and concluded that acupuncture therapy is distinctly better than drug therapy. This further provides a theoretical basis for acupuncture treatment of tinnitus. At present, there are many methods to treat tinnitus in western medicine, including masking therapy and acclimatization therapy, but the curative effect is unstable, so it is necessary to seek a more effective treatment of tinnitus.

The expert consensus in China pointed out that idiopathic tinnitus should be treated with tinnitus combined management (TCM), that is, tinnitus counseling, behavioral cognitive therapy, drug therapy, and sound therapy; and psychological counseling is the key (1). The American guidelines for Clinical Application of Tinnitus focus on persistent annoying tinnitus (the course of disease > 6 months). The guidelines believe that tinnitus can be improved spontaneously and lack of high-quality evidence to treat new tinnitus. It is considered to be related to the medical model of family doctors in the United States. In the United States, acute tinnitus is mainly treated by family doctors, and it is often beyond the acute stage when transferred to an ear, nose, and throat specialist for treatment. Often lose the opportunity to treat new tinnitus. This guide recommends cognitive behavioral therapy, sound therapy, hearing aid evaluation, etc. The European guidelines for multidisciplinary tinnitus: diagnosis, evaluation, and treatment strongly recommend cognitive behavioral therapy and cochlear implants for tinnitus patients with hearing loss, because the existing evidence shows that treatment measures may do more harm than good. They are opposed to repeated transcranial stimulation and drug therapy and do not comment on acclimatization therapy, sound therapy, and acupuncture therapy because of the low level of existing evidence [28, 29]. The clinical practice guide for the diagnosis and treatment of chronic tinnitus in Japan [30] discusses the treatment of chronic tinnitus (the course of disease is more than 3 months). In recent years, the therapeutic effects of tinnitus are quite different, and even the conclusions are contradictory. The German "Tinnitus Diagnosis and Treatment

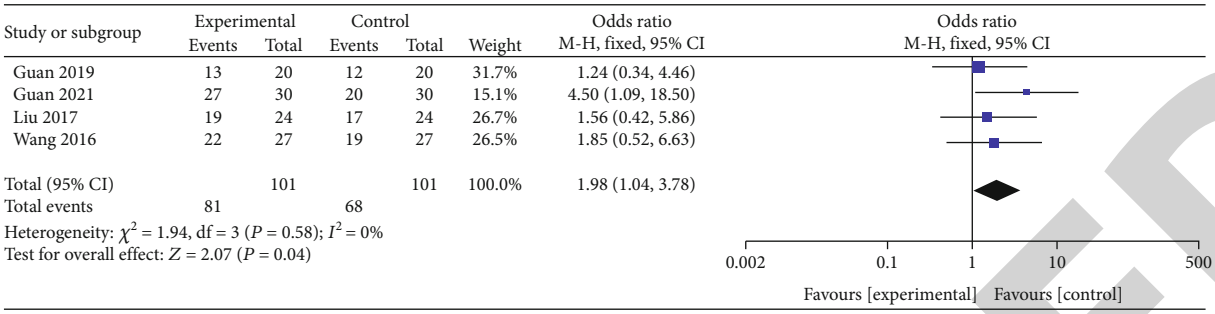

Figure 4: Forest plot of meta-analysis of effective rate of treatment.

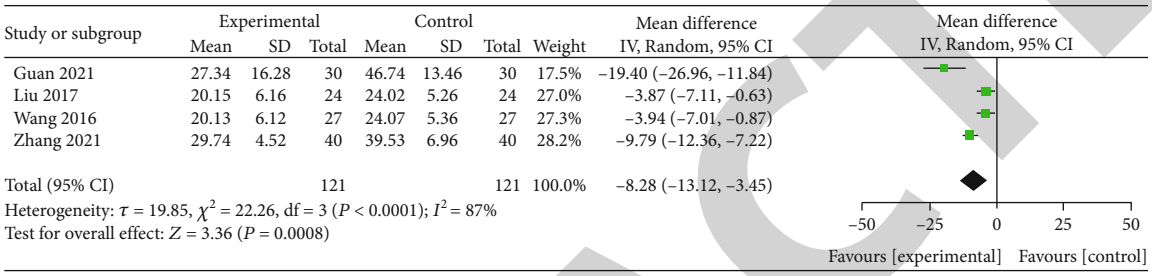

Figure 5: Forest plot of meta-analysis of THI score.

Outline" mainly refers to the treatment plan for sudden deafness when treating idiopathic tinnitus, but the efficacy lacks high-quality clinical evidence support.

Associated with the results of this study, there were 5 CTs contained, with 282 samples. Meta-analysis was conducted on the treatment effective rates. The results of the heterogeneity test indicated that $\text{Chi}^2 = 1.94$, df = 3, $P = 0.58$, and $I^2 = 0\%$, showing that the research data contained in the study show distinct heterogeneity. The fixed effect model analysis indicated that the treatment effective rate of the study group was noticeably better ($P < 0.05$). This shows that acupuncture associated with physical and mental intervention is effective when treating idiopathic tinnitus. From the literature contained in this study, a large number of studies on acupuncture associated with physical and mental intervention when treating idiopathic tinnitus have been carried out in China, including random control group, double-blind, and multicenter high-level research. It shows that TCM acupuncture associated with physical and mental intervention has high clinical value for patients with idiopathic tinnitus. The reason why this treatment scheme has a good curative effect is that acupuncture therapy can cure both the symptoms and root causes, starting with the source of the disease and selecting acupoints. It can not only noticeably improve the inner ear microcirculation and cochlear cell ischemia and hypoxia but also repair inner ear cells, noticeably improve the hearing level of patients, and generally not easy to relapse after treatment. Physical and mental intervention can systematically improve the physical and mental state and life quality of patients and further enhance the clinical efficacy. Meta-analysis was performed on the THI score and tinnitus severity classification after treatment. The results of the heterogeneity test indicated that THI score: $\text{Chi}^2 = 22.26$, df = 3, $P < 0.0001$, and $I^2 = 87\%$; severity of tinnitus: $\text{Chi}^2 = 16.81$, df = 8, $P = 0.03$, and $I^2 = 52\%$; the results indicated that the research data contained in the study show distinct heterogeneity. According to the random effect model analysis, the THI score and TEQ score of the study group were noticeably lower ($P < 0.05$). It is suggested that acupuncture associated with physical and mental intervention is helpful to the recovery of patients with idiopathic tinnitus. The decrease of THI score and TEQ score also fully confirmed the science and effectiveness of this treatment scheme. Acupuncture and physical and mental intervention treatment can noticeably improve the clinical symptoms of patients and accelerate the recovery of their condition. It also shows that this treatment scheme has a broad prospect of clinical application. The same idea can be found in the study put forward by Chen et al. [31]. They have applied new methods in the study, and the conclusions drawn can also give some support to this study. This paper still have some limitations: (1) the inclusion and exclusion criteria are stricter, and the final number of contained literature is less; (2) the follow-up time of all studies is short, so there are some limitations; (3) the evaluation of quality methodology contained in the literature is not high, and there is diversity in the use of acupuncture methods, the type of control group, the selection of outcome indicators, and physical and mental intervention measures, which increases the heterogeneity among studies. More large samples and high-quality randomized controlled trials are needed to provide evidence support for the efficacy of acupuncture when treating idiopathic tinnitus; (4) this paper failed to find the source of heterogeneity through subgroup analysis, which needs to be

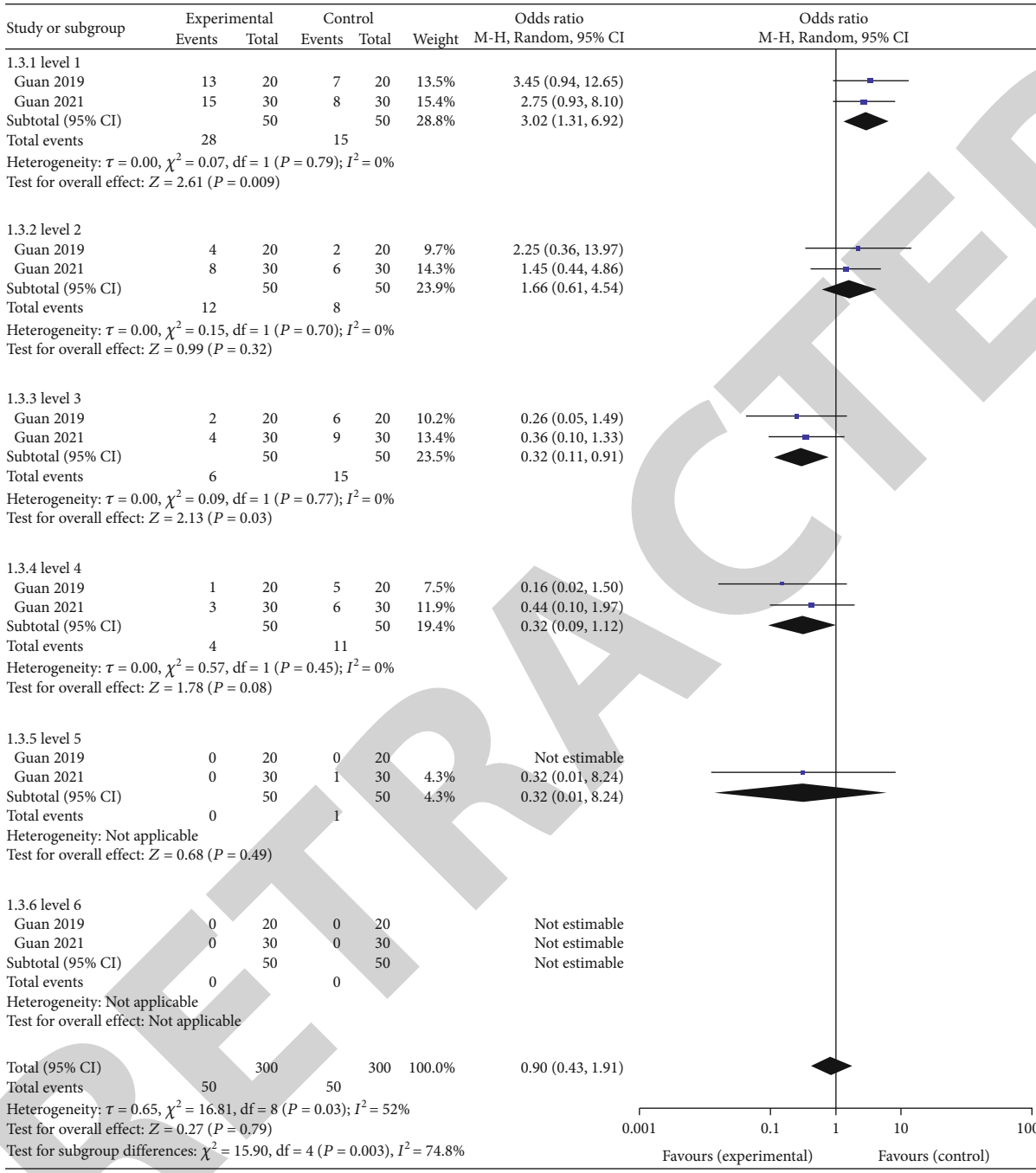

Figure 6: Forest plot of meta-analysis of TEQ score.

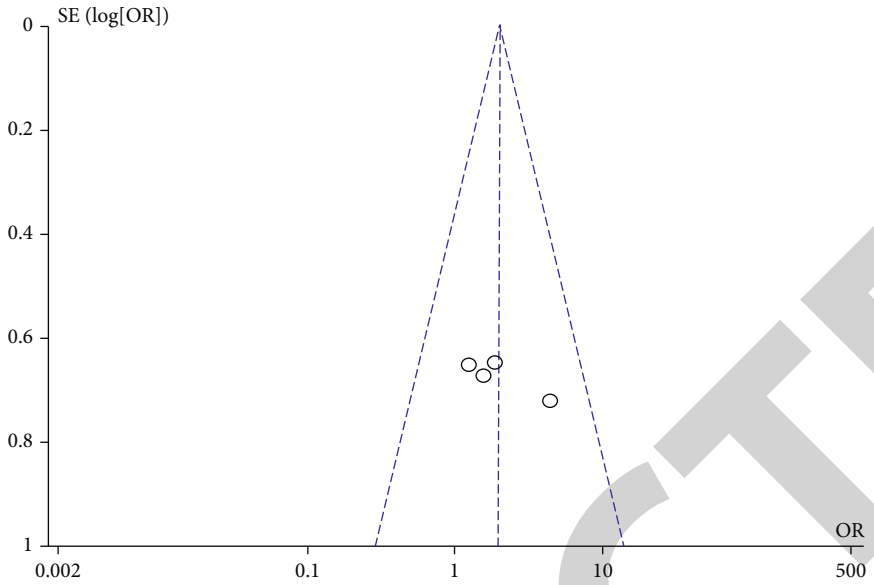

Figure 7: Funnel chart with effective treatment.

followed up by scholars to provide more support for acupuncture associated with physical and mental intervention when treating idiopathic tinnitus, and more high-quality controlled trials need to be performed to verify it.

5. Conclusion

To sum up, acupuncture associated with physical and mental intervention is effective when treating idiopathic tinnitus, which can noticeably reduce the severity of tinnitus, reduce the discomfort caused by tinnitus, enhance their hearing level, and improve their life quality. This conclusion is consistent with the original literature.

Data Availability

The datasets used and analyzed during the current study are available from the corresponding author upon reasonable request.

Conflicts of Interest

The authors declare that they have no conflicts of interest.

Acknowledgments

This study was supported by Three Projects' Chief Researcher Liu Baoyan of Chinese Academy of Traditional Chinese Medicine Clinical Evaluation Method Innovation Team (no.: SZSM201612001).

References

[1] S. Y. Yang, H. Liu, B. Wang, W. Zhang, and B. Zhao, "Research progress of idiopathic tinnitus," *Lin Chuang Er Bi Yan Hou Tou Jing Wai Ke Za Zhi*, vol. 33, no. 8, pp. 785–789, 2019.

[2] T. Diao, X. Ma, J. Li et al., "Long-term prognosis of tinnitus associated with idiopathic sudden sensorineural hearing loss," *Audiology & Neuro-Otology*, vol. 26, no. 6, pp. 461–469, 2021.

[3] T. Shim, Y. Chillakuru, P. Moncada et al., "Sensorineural hearing loss and tinnitus characteristics in patients with idiopathic intracranial hypertension," *Otology & Neurotology*, vol. 42, no. 9, pp. 1323–1328, 2021.

[4] P. Zhao, C. Jiang, H. Lv, T. Zhao, S. Gong, and Z. Wang, "Why does unilateral pulsatile tinnitus occur in patients with idiopathic intracranial hypertension?," *Neuroradiology*, vol. 63, no. 2, pp. 209–216, 2021.

[5] Y. Shiyu, L. Hui, W. Bing, Z. Wen, and Z. Bo, "Research progress of idiopathic tinnitus," *Journal of Clinical Otorhinolaryngology, Head and Neck Surgery*, vol. 33, no. 8, pp. 785–789, 2019.

[6] Y. Shirui, L. Fengying, L. Ying, and Z. Ying, "Research status of traditional Chinese and Western medicine on tinnitus," *Chinese Journal of Otorhinolaryngology with Integrated traditional Chinese and Western Medicine*, vol. 28, no. 5, pp. 386–390, 2020.

[7] D. J. Hoare, P. E. Gander, L. Collins, S. Smith, and D. A. Hall, "Management of tinnitus in English NHS audiology departments: an evaluation of current practice," *Journal of Evaluation in Clinical Practice*, vol. 18, no. 2, pp. 326–334, 2012.

[8] J. P. Funnell, C. L. Craven, S. D. Thompson et al., "Pulsatile versus non-pulsatile tinnitus in idiopathic intracranial hypertension," *Acta Neurochirurgica*, vol. 160, no. 10, pp. 2025–2029, 2018.

[9] J. A. Lansley, W. Tucker, M. R. Eriksen, P. Riordan-Eva, and S. E. J. Connor, "Sigmoid sinus diverticulum, dehiscence, and venous sinus stenosis: potential causes of pulsatile tinnitus in patients with idiopathic intracranial hypertension?," *AJNR. American Journal of Neuroradiology*, vol. 38, no. 9, pp. 1783–1788, 2017.

[10] J. Thielker, A. Heuschkel, D. Boeger et al., "Patients with non-idiopathic sudden sensorineural hearing loss show hearing improvement more often than patients with idiopathic sudden

Hindawi
Computational and Mathematical Methods in Medicine
Volume 2023, Article ID 9783405, 1 page
https://doi.org/10.1155/2023/9783405

Retraction

Retracted: Influence of Optimal Management of Hyperglycemia and Intensive Nursing on Blood Glucose Control Level and Complications in Patients with Postoperative Cerebral Hemorrhage

Computational and Mathematical Methods in Medicine

Received 12 December 2023; Accepted 12 December 2023; Published 13 December 2023

This article has been retracted by Hindawi, as publisher, following an investigation undertaken by the publisher [1]. This investigation has uncovered evidence of systematic manipulation of the publication and peer-review process. We cannot, therefore, vouch for the reliability or integrity of this article.

Please note that this notice is intended solely to alert readers that the peer-review process of this article has been compromised.

Wiley and Hindawi regret that the usual quality checks did not identify these issues before publication and have since put additional measures in place to safeguard research integrity.

We wish to credit our Research Integrity and Research Publishing teams and anonymous and named external researchers and research integrity experts for contributing to this investigation.

The corresponding author, as the representative of all authors, has been given the opportunity to register their agreement or disagreement to this retraction. We have kept a record of any response received.

References

[1] D. Sun, L. Sun, and F. Su, "Influence of Optimal Management of Hyperglycemia and Intensive Nursing on Blood Glucose Control Level and Complications in Patients with Postoperative Cerebral Hemorrhage," *Computational and Mathematical Methods in Medicine*, vol. 2022, Article ID 8553539, 7 pages, 2022.

Hindawi
Computational and Mathematical Methods in Medicine
Volume 2022, Article ID 8553539, 7 pages
https://doi.org/10.1155/2022/8553539

Research Article

Influence of Optimal Management of Hyperglycemia and Intensive Nursing on Blood Glucose Control Level and Complications in Patients with Postoperative Cerebral Hemorrhage

Dandan Sun, Liang Sun, and Fang Su

Neurosurgery, The First Affiliated Hospital of Soochow University, Suzhou 215006, China

Correspondence should be addressed to Fang Su; sufang1919@163.com

Received 10 July 2022; Revised 26 July 2022; Accepted 4 August 2022; Published 29 August 2022

Academic Editor: Min Tang

Background. Cerebral hemorrhage, also known as hemorrhagic stroke, is a common clinical cerebrovascular disease, accounting for about 10%-30% of stroke, with high morbidity and mortality. *Objective*. To observe the effect of optimal management of hyperglycemia and intensive nursing on blood glucose control level and complications in patients with postoperative cerebral hemorrhage. *Methods*. One hundred and eight patients with postoperative cerebral hemorrhage comorbid with stress hyperglycemia admitted to our neurosurgery department from February 2019 to February 2022 were selected and divided into a general group of 54 cases and an optimized group of 54 cases by simple random method. The general group was managed with conventional care, while the optimized group developed optimized management of hyperglycemia for intensive care. The indexes related to blood glucose control, electrolytes, National Institutes of Health Stroke Scale (NIHSS) scores, Barthel Index (BI) scores, and time to achieve blood glucose standard, insulin pumping time, patient satisfaction, and prognosis were compared between the two groups. *Results*. Before intervention, there was no statistical significance in the comparison of blood glucose control-related indicators and electrolytes between the two groups ($P > 0.05$). After 7 d and 14 d of intervention, the fasting blood glucose and 2 h postprandial blood glucose in the two groups were lower than before, while K+ and Na+ were higher than before ($P < 0.05$). The blood glucose indexes at the same time point in the optimized group were found to be lower than those in the general group by statistical analysis, but electrolytes were not statistically significant when compared with the general group ($P > 0.05$). In the optimized group, the time to achieve blood glucose standard (6.59 ± 1.94) d and insulin pumping time (7.14 ± 1.89) d were shorter than those in the general group [(7.48 ± 2.12) d and (8.58 ± 2.14) d], insulin dosage (748.85 ± 63.61) U was less than that in the general group (923.54 ± 84.14) U, and the incidence of hypoglycemia (3.70%) was lower than that in the general group (16.67%), and the satisfaction rate (92.59%) was higher than that of the general group (77.78%), which was statistically significant ($P < 0.05$). Before intervention, there was no significant difference in NIHSS score and BI score between the two groups ($P > 0.05$). After 7 d and 14 d of intervention, the NIHSS scores of the two groups were lower than before, while the BI scores were higher than before, and the NIHSS scores of the optimized group at the same time point were all lower than those of the general group, and the BI scores were higher than those of the general group ($P < 0.05$). The incidence of pulmonary infection (11.11%) and rebleeding (7.41%) in the optimized group were lower than those in the general group (25.93% and 22.22%), while deep vein thrombosis, multiple organ dysfunction syndrome (MODS), and death within 28 d was not statistically significant when compared with the general group ($P > 0.05$). *Conclusion*. Optimal management of hyperglycemia and intensive nursing can effectively control the blood sugar level of patients after cerebral hemorrhage, reducing insulin dosage, and the occurrence of hypoglycemia, pulmonary infection, and rebleeding.

1. Introduction

The formation of hematoma causes local brain tissue compression and ischemia, requiring surgical removal of the hematoma [1, 2]. Cerebral hemorrhage and surgery can cause stress response, with stress hyperglycemia as one of the main manifestations of stress hyperglycemia, but its mechanism is still unclear. Previous studies have shown that the disorder of neuroendocrine-humoral regulation system, abnormal secretion of various antiregulatory hormones, and disorder of blood glucose regulation-related hormones are one of the important mechanisms of stress hyperglycemia [3, 4].

It has been found that the incidence of stress hyperglycemia after cerebral hemorrhage is more than 50%, which is not only related to the severity of cerebral hemorrhage but also one of the independent risk factors affecting the neurological deficit and prognosis of patients with cerebral hemorrhage [5, 6]. At present, insulin is often used in clinical treatment of stress hyperglycemia, but there are still some patients with poor blood glucose control and many complications [7, 8]. Hyperglycemia optimal management intensive care is a care model focusing on glycemic control. This study observed the effect of hyperglycemia optimal management intensive care on the level of glycemic control and complications in postoperative patients with cerebral hemorrhage, which is reported below.

Core tips: stress hyperglycemia after cerebral hemorrhage is harmful, and effective control of blood glucose is the focus of postoperative treatment. In this study, patients with cerebral hemorrhage were treated with high blood glucose optimization management intensive nursing intervention. It was found that it can effectively control the blood glucose level of patients after cerebral hemorrhage, reduce the amount of insulin, and reduce the incidence of hypoglycemia, pulmonary infection, and rebleeding.

1.1. Data and Methods

1.1.1. Case Selection. Inclusion criteria: (1) the cerebral hemorrhage met the criteria of the Chinese Guidelines for the Diagnosis and Treatment of Cerebral Hemorrhage [9], and the location of the hemorrhage was confirmed by brain CT; (2) the age was 18-75 years old, regardless of gender; (3) all patients were treated with minimally invasive surgery; (4) two consecutive random blood glucose values > 11.1 mmol/L and normal glycosylated hemoglobin (HbA1c); (5) the blood glucose was controlled by insulin pump; (6) no previous history of diabetes mellitus, and preoperative blood glucose levels were normal; (7) consent signed by the patient or his family.

Exclusion criteria: (1) history of drug use affecting blood glucose; (2) hyperglycemia due to diabetes and other diseases; (3) previous history of long-term glucocorticoid use; (4) presence of gastrointestinal damage, chronic constipation, and abnormal liver and kidney function; (5) poor overall condition of the patient with an expected survival of less than 6 months; (6) concomitant malignancy.

1.1.2. Case Collection. One hundred and eight patients with postoperative cerebral hemorrhage comorbid with stress hyperglycemia admitted to our neurosurgery department from February 2019 to February 2022 were selected, of whom 58 were male and 50 were female; age ranged from 41 to 75 years, mean (61.89 ± 10.77) years, onset to admission time ranged from 3 h to 24 h, mean (7.89 ± 2.71) h. The simple randomization method was used to divide the patients into general group 54 cases and 54 cases in the optimized group, and the two groups of patients were comparable ($P > 0.05$).

1.2. Method. In the general group, conventional nursing management was adopted, and patients were instructed to eat low-salt, low-fat diet, quit smoking and alcohol, and were given comprehensive intervention such as reducing intracranial pressure, controlling blood pressure, blood lipids, antiplatelet, anticoagulation, nutritional nerve, and maintaining water and electrolyte balance. When the random blood glucose was >11.1 mmol/L, the continuous intravenous infusion of insulin was given. The blood glucose control objectives were fasting blood glucose < 6.1 mmol/L and postprandial 2 h blood glucose < 7.8 mmol/L.

The optimization group formulated hyperglycemia optimization management for intensive care. The intensive nursing intervention group was established to receive training on knowledge related to hyperglycemia optimization management, including the harm of stress hyperglycemia to the nervous system, the relationship between enteral nutrition and intravenous corresponding insulin dose, and hyperglycemia optimization management plan. The nursing staff performed all nursing operations according to the optimal hyperglycemia management plan, closely observed the condition, regularly monitored the blood glucose, and adjusted the nutrient intake and insulin dose according to the blood glucose monitoring results. If there is any abnormal blood glucose situation, it will be reported to the endocrinologist and neurosurgeon in time to give timely treatment. Insulin is administered by intravenous pump, and each insulin is administered for no more than 8 h. The nurse manager is responsible for monitoring the implementation of the program, including blood glucose monitoring, insulin dose adjustment, and data recording. Attention should be paid to identifying symptoms of hypoglycemia, especially in patients with disturbance of consciousness, such as sweating, rapid breathing, aggravation of disturbance of consciousness or blood glucose < 3.9 mmol/L immediately according to the hypoglycemic process, suspending insulin pumping, and quickly injecting 50% glucose injection.

1.3. Observation Indicators and Detection Methods. Blood glucose control-related indicators, electrolytes, National Institutes of Health Stroke Scale (NIHSS) score, Barthel index (BI) score, blood glucose compliance time, insulin pump time, patient satisfaction, and prognosis were compared between the two groups.

A total of 3 mL of venous blood specimens from the upper limbs of both groups were drawn before, 7 d and 14 d after the intervention, and fasting blood glucose and electrolyte indicators K+ and Na+ were measured by a fully automatic biochemical analyzer (Hitachi, model 7600, Japan). Blood was collected again 2 h after eating to test the postprandial 2 h blood glucose.

1.4. Score Standard. The satisfaction was measured by the hospital-made scale, including the environment, working ability of medical staff, and blood glucose control. The score was 0–100 points, and the score was proportional to the satisfaction. The score 90 or above was considered very satisfied, 70-90 was considered satisfied, and below 70 was considered dissatisfied. NIHSS score, with the range of 0-42 points, high or low score represented the size of nerve defect. BI score, with the range of 0-100 points, score level indicated the level of daily living ability.

1.5. Statistical Method. The data were processed by SPSS19.0. The K-S method was used to test the normality of measurement data such as age. The measurement data conforming to the normal distribution were described by $(\bar{\chi} \pm s)$. The t test was used for comparison. The enumeration data such as gender were described by the number of cases (%). The χ^2 test of four-grid table or row × list was used for comparison. $P < 0.05$ was statistically significant.

2. Results

2.1. Comparison of Baseline Data between Two Groups. There was no significant difference in the initial fasting blood glucose, body mass index, hematoma volume, admission GCS score, gender, age, smoking history, PT, Fib and PLT between the two groups ($P > 0.05$) (see Table 1).

2.2. Comparison of Blood Glucose Control between Two Groups. Before intervention, there was no significant difference in blood glucose control-related indicators between the two groups ($P > 0.05$). After 7 d and 14 d of intervention, the fasting blood glucose and 2 h postprandial blood glucose in the two groups were lower than those before intervention, and the blood glucose indexes at the same time point in the optimized group were statistically lower than those in the general group ($P < 0.05$) (see Table 2).

2.3. Comparison of Insulin Dosage and Blood Glucose Compliance Time between the Two Groups. The blood glucose compliance time and insulin pump time in the optimized group were shorter than those in the general group, the insulin dosage was less than that in the general group, and the incidence of hypoglycemia was lower than that in the general group, with statistical significance ($P < 0.05$) (see Table 3).

2.4. Comparison of Electrolyte between Two Groups. Before intervention, there was no significant difference in electrolyte between the two groups ($P > 0.05$). After 7 d and 14 d of intervention, K+ and Na+ in the two groups were higher than those before, but the electrolyte in the two groups at the same time was not statistically significant ($P > 0.05$) (see Table 4).

2.5. Comparison of Satisfaction between the Two Groups. The satisfaction of the optimized group was 92.59% (50/54), which was higher than 77.78% (42/54) of the general group, with statistical significance ($P < 0.05$) (see Table 5).

2.6. Comparison of NIHSS Score and BI Score between the Two Groups. Before intervention, there was no significant difference in NIHSS score and BI score between the two groups ($P > 0.05$). After 7 d and 14 d of intervention, the NIHSS score of the two groups decreased, while the BI score increased. The NIHSS score of the optimized group was lower than that of the general group at the same time point, and the BI score was higher than that of the general group ($P < 0.05$) (see Table 6).

2.7. Comparison of Prognosis between Two Groups. The incidence of pulmonary infection and rebleeding in the optimized group was lower than that in the general group, while the incidence of deep vein thrombosis, MODS, and death within 28 days in the optimized group was not statistically significant compared with that in the general group ($P > 0.05$) (see Table 7).

3. Discussion

Stress hyperglycemia is one of the common complications in neurocritical patients, and stress conditions can cause neuroendocrine disorders; as a result, stress hormones such as cortisol hormone, glucagon, and adrenal hormone are secreted in large amounts, promoting gluconeogenesis and causing massive hepatic glycogen synthesis. Neuroendocrine disorders can also lead to insulin resistance in the body [10–12]. Hematoma compression can lead to hypothalamus-pituitary-adrenal axis injury and reduce the biological uptake and utilization of glucose in peripheral tissues [13, 14]. In contrast, hyperglycemic state can affect brain tissue energy metabolism, leading to acidosis due to lactic acid accumulation and can induce oxidative stress, which aggravates neuronal cell damage and is detrimental to the prognosis of patients with cerebral hemorrhage [15, 16]. Therefore, clinical attention has been paid to the treatment of stress hyperglycemia in neurosurgical patients.

For patients with cerebral hemorrhage, dehydration to reduce intracranial pressure treatment can lead to blood viscosity, and the body is in a state of high catabolism after operation, which requires nutritional support treatment, and it is also easy to induce hyperglycemia [17, 18]. At present, the overall control effect of clinical stress hyperglycemia is not ideal. The reason for the poor therapeutic effect of insulin is not the problem of hyperglycemia, but the damage caused by large-scale blood glucose fluctuations and hypoglycemia [19, 20]. In this study, it was found that the fasting blood glucose and postprandial 2 h blood glucose of patients receiving intensive nursing intervention with optimized management of hyperglycemia after 7 d and 14 d were lower than those of patients receiving ordinary nursing intervention. The time of blood glucose reaching the standard and the time of insulin pump were shorter than those who received ordinary care intervention, the insulin dosage was less than those who received ordinary care intervention, and the incidence of hypoglycemia was lower than those who received ordinary care intervention. The above results suggest that intensive care for optimal management of hyperglycemia can effectively control the blood glucose level,

Table 1: Comparison of baseline data between the two groups.

Normal information	General group ($n = 54$)	Optimized group ($n = 54$)	χ^2/t	P
Gender [n (%)]				
Male	30 (55.56)	28 (51.85)	0.149	0.700
Female	24 (44.44)	26 (48.15)		
Age [($\bar{\chi} \pm s$), age]	61.74 ± 11.05	60.49 ± 11.41	0.578	0.564
Body mass index [($\bar{\chi} \pm s$), kg/m^2]	7.45 ± 2.86	7.91 ± 2.94	0.824	0.412
Initial fasting blood glucose [($\bar{\chi} \pm s$), mmol/L]	9.57 ± 1.45	9.74 ± 1.29	0.644	0.521
Admission GCS score [n (%)]				
9-12 minutes	35 (64.81)	32 (59.26)	0.354	0.552
>12 minutes	19 (35.19)	22 (40.74)		
Hematoma volume [($\bar{\chi} \pm s$), mL]	102.56 ± 35.89	99.74 ± 38.12	0.396	0.693
Smoking history [n (%)]				
Have	18 (33.33)	15 (27.78)	0.393	0.531
None	36 (66.67)	39 (72.22)		
PT [($\bar{\chi} \pm s$), s]	18.52 ± 4.56	18.39 ± 4.74	0.145	0.885
Fib [($\bar{\chi} \pm s$), g/L]	2.76 ± 1.02	2.71 ± 0.98	0.260	0.796
PLT [($\bar{\chi} \pm s$), ×109/L]	231.56 ± 74.88	227.96 ± 81.04	0.240	0.811

Table 2: Comparison of blood sugar control between the two groups [($\bar{\chi} \pm s$), mmol/L].

Group	n	Fasting blood sugar			2 h postprandial blood glucose		
		Before intervention	Intervention 7 d	Intervention 14 d	Before intervention	Intervention 7 d	Intervention 14 d
General group	54	9.57 ± 1.45	7.25 ± 1.23*	5.75 ± 0.84*	13.58 ± 3.85	10.05 ± 2.15*	8.15 ± 1.36*
Optimized group	54	9.74 ± 1.29	6.54 ± 1.04*	5.23 ± 0.67*	13.49 ± 3.79	8.56 ± 1.73*	5.57 ± 1.04*
t		0.644	3.239	3.556	0.122	3.968	11.074
P		0.521	0.002	0.001	0.903	0.000	0.000

Compared with before intervention, *$P < 0.05$.

Table 3: Comparison of insulin dosage and blood glucose reaching time between two groups.

Group	n	Blood sugar target time [($\bar{\chi} \pm s$)x, d]	Insulin pump time [($\bar{\chi} \pm s$), d]	Insulin dosage [($\bar{\chi} \pm s$), U]	Hypoglycemia [n (%)]
General group	54	7.48 ± 2.12	8.58 ± 2.14	923.54 ± 84.14	9(16.67)
Optimized group	54	6.59 ± 1.94	7.14 ± 1.89	748.85 ± 63.61	2(3.70)
χ^2/t		2.276	3.706	12.170	4.960
P		0.025	0.000	0.000	0.026

Table 4: Comparison of electrolytes between the two groups [($\bar{\chi} \pm s$), mmol/L].

Group	n	K^+			Na^+		
		Before intervention	Intervention 7 d	Intervention 14 d	Before intervention	Intervention 7 d	Intervention 14 d
General group	54	3.81 ± 0.15	4.15 ± 0.19*	4.23 ± 0.23*	134.25 ± 4.15	142.15 ± 6.98*	148.85 ± 6.11*
Optimized group	54	3.79 ± 0.18	4.18 ± 0.17*	4.25 ± 0.28*	132.98 ± 5.84	143.02 ± 5.84*	146.78 ± 8.54*
t		0.627	0.865	0.406	1.303	0.702	1.449
P		0.532	0.389	0.686	0.196	0.484	0.150

Compared with before intervention, *$P < 0.05$.

Table 5: Comparison of compliance between the two groups [n (%)].

Group	n	Very satisfied	Satisfy	Dissatisfied	Satisfaction
General group	54	19 (35.19)	23 (42.59)	12 (22.22)	42 (77.78)
Optimized group	54	28 (51.85)	22 (40.74)	4 (7.41)	50 (92.59)
χ^2					4.696
P					0.030

Table 6: Comparison of NIHSS scores and BI scores between the two groups [($\bar{\chi} \pm s$), minute].

Group	n	NIHSS score			BI score		
		Before intervention	Intervention 7 d	Intervention 14 d	Before intervention	Intervention 7 d	Intervention 14 d
General group	54	19.02 ± 4.74	16.52 ± 3.15*	12.23 ± 2.56*	48.52 ± 8.56	56.96 ± 7.45*	67.14 ± 6.22*
Optimized group	54	18.89 ± 4.58	14.49 ± 2.87*	10.04 ± 2.18*	47.63 ± 9.11	63.22 ± 6.57*	76.86 ± 6.35*
t		0.145	3.501	4.786	0.523	4.631	8.036
P		0.885	0.001	0.000	0.602	0.000	0.000

Compared with before intervention, *$P < 0.05$.

Table 7: Comparison of prognosis between the two groups [n (%)].

Group	n	Deep vein thrombosis	MODS	Lung infection	Rebleeding	Die within 28 days
General group	54	3 (5.56)	5 (9.26)	14 (25.93)	12 (22.22)	3 (5.56)
Optimized group	54	1 (1.85)	1 (1.85)	6 (11.11)	4 (7.41)	1 (1.85)
χ^2		1.039	2.824	3.927	4.696	1.039
P		0.308	0.093	0.048	0.030	0.308

reduce insulin dosage, and decrease hypoglycemia in patients after cerebral hemorrhage. This is due to high blood sugar optimization management intensive nursing intervention through regular monitoring of blood sugar, timely upload data to neurology and nutrition doctors, and jointly develop reasonable blood sugar control objectives, intervention of individualized insulin therapy, and nutritional intervention [21–23]. When insulin was injected intravenously, physiological insulin secretion mode was simulated as much as possible, and timely adjustment of enteral nutrition was helpful to control blood glucose fluctuation, effectively reduce blood glucose variability, and maintain blood glucose stability [24–26]. In this study, the electrolyte level was also detected. After intervention, K^+ and Na^+ in the two groups increased, but there was no significant difference between the two groups. Because both groups attach importance to maintaining water-electrolyte balance during treatment.

In this study, it was found that the NIHSS score of patients receiving intensive nursing intervention with optimized management of hyperglycemia after 7 d and 14 d was lower than that of patients receiving ordinary nursing intervention, while the BI score was higher than that of patients receiving ordinary nursing intervention. The results suggest that the intensive nursing of hyperglycemia optimization management can effectively improve the degree of nerve defect and the ability of daily living in patients with cerebral hemorrhage after operation. This is due to the optimal management of hyperglycemia intensive nursing intervention mode of patients with better blood glucose control can avoid hyperglycemia damage to neurons [27–29]. Hyperglycemia can increase the anaerobic metabolism of brain tissue, destroy mitochondria, produce a large number of free radicals, and increase the Ca2 + influx of nerve cells [30–32]. Hyperglycemia can also cause excessive release and accumulation of excitatory amino acids such as glutamate, causing neuronal damage [33, 34].

This study also found that the incidence of pulmonary infection and rebleeding in patients receiving intensive nursing intervention with optimized management of hyperglycemia was lower than that in patients receiving ordinary nursing intervention, while there was no significant difference in the incidence of deep vein thrombosis, MODS, and death within 28 days between the two groups. Those who received intensive nursing intervention for optimal management of hyperglycemia were more satisfied than those who received ordinary nursing intervention. The above results suggest that intensive nursing of high blood glucose optimization management can reduce the risk of pulmonary infection and rebleeding. This is related to the improvement of immune function after stable blood glucose control, and stable blood glucose also helps to protect vascular endothelial cells and blood-brain barrier and prevent secondary brain injury and rebleeding [35].

In conclusion, intensive care for optimal management of hyperglycemia can effectively control the blood glucose level of patients after cerebral hemorrhage, reducing

insulin dosage, and decreasing the occurrence of hypoglycemia, pulmonary infection, and rebleeding.

Data Availability

The labeled dataset used to support the findings of this study are available from the corresponding author upon request.

Conflicts of Interest

The authors declare no competing interests.

Acknowledgments

This study is sponsored by The First Affiliated Hospital of Soochow University.

References

[1] Z. Troiani, L. C. Ascanio, K. A. Yaeger, M. Ali, and C. P. Kellner, "Minimally invasive surgiscopic evacuation of intracerebral hemorrhage," *Journal of Neurointerventional surgery*, vol. 13, no. 4, p. 400, 2021.

[2] Y. Wei, X. J. Fan, M. H. Zhang et al., "The mechanisms of peiyuan-tong-nao capsule as a therapeutic agent against cerebrovascular disease," *World Journal of Traditional Chinese Medicine*, vol. 6, no. 3, pp. 331–340, 2020.

[3] G. Roberts, J. Sires, A. Chen et al., "A comparison of the stress hyperglycemia ratio, glycemic gap, and glucose to assess the impact of stress-induced hyperglycemia on ischemic stroke outcome," *Journal of Diabetes*, vol. 13, no. 12, pp. 1034–1042, 2021.

[4] G. Merlino, C. Smeralda, G. L. Gigli et al., "Stress hyperglycemia is predictive of worse outcome in patients with acute ischemic stroke undergoing intravenous thrombolysis," *Journal of Thrombosis and Thrombolysis*, vol. 51, no. 3, pp. 789–797, 2021.

[5] Z. Ament, M. B. Bevers, Z. Wolcott, W. T. Kimberly, and A. Acharjee, "Uric acid and gluconic acid as predictors of hyperglycemia and cytotoxic injury after stroke," *Translational Stroke Research*, vol. 12, no. 2, pp. 293–302, 2021.

[6] N. R. Klug, O. V. Chechneva, B. Y. Hung, and M. E. O'Donnell, "High glucose-induced effects on Na+-K+-2Cl−cotransport and Na+/H+ exchange of blood-brain barrier endothelial cells: involvement of SGK1, PKCβII, and SPAK/OSR1," *American Journal of Physiology*, vol. 320, no. 4, pp. C619–C634, 2021.

[7] R. A. Babel and M. P. Dandekar, "A review on cellular and molecular mechanisms linked to the development of diabetes complications," *Current Diabetes Reviews*, vol. 17, no. 4, pp. 457–473, 2021.

[8] Z. Heidary, H. Khalili, M. Mohammadi, M. T. Beigmohammadi, and A. Abdollahi, "Effect of magnesium loading dose on insulin resistance in patients with stress-induced hyperglycemia: a randomized clinical trial," *Journal of Intensive Care Medicine*, vol. 35, no. 7, pp. 687–693, 2020.

[9] Neurology Branch of Chinese Medical Association, Cerebrovascular Diseases Branch of Chinese Medical Association, "Guidelines for the diagnosis and treatment of cerebral hemorrhage in China (2019)," *Chinese Journal of Neurology*, vol. 52, no. 12, pp. 994–1005, 2019.

[10] B. P. Kilari, P. Mudgil, S. Azimullah, N. Bansal, S. Ojha, and S. Maqsood, "Effect of camel milk protein hydrolysates against hyperglycemia, hyperlipidemia, and associated oxidative stress in streptozotocin (STZ)-induced diabetic rats," *Journal of Dairy Science*, vol. 104, no. 2, pp. 1304–1317, 2021.

[11] S. R. Bampi, A. M. Casaril, M. Domingues et al., "Depression-like behavior, hyperglycemia, oxidative stress, and neuroinflammation presented in diabetic mice are reversed by the administration of 1-methyl-3-(phenylselanyl)-1 _H_ -indole," *Journal of Psychiatric Research*, vol. 120, no. 20, pp. 91–102, 2020.

[12] S. Rajendran and S. Vasudevan, "Activation of prophenoloxidase and hyperglycemia as indicators of microbial stress in the blue swimmer crab _Portunus pelagicus_," *Marine Pollution Bulletin*, vol. 160, no. 2, pp. 111711–1117114, 2020.

[13] D. F. Wu, Y. L. Wang, Y. Y. Wu, and S. Ding, "The protective effect of genipin on oxidative stress under hypoxia and hyperglycemia in retinal pigment epithelial cells," *Journal of Biomaterials and Tissue Engineering*, vol. 11, no. 11, pp. 2239–2245, 2021.

[14] T. S. Meshref, R. F. Abd El-Aal, M. A. Ashry, H. M. Imam, and A. B. Elden, "Impact of stress hyperglycemia on myocardial salvage in patients with ST-elevation myocardial infarction: cardiac magnetic resonance study," *Indian Heart Journal*, vol. 72, no. 5, pp. 462–465, 2020.

[15] L. G. Vicas, T. Jurca, I. Baldea et al., "Physalis alkekengi L. extract reduces the oxidative stress, inflammation and apoptosis in endothelial vascular cells exposed to hyperglycemia," *Molecules*, vol. 25, no. 16, p. 3747, 2020.

[16] F. A. Al-Salmi, "Efficacy of vanadyl sulfate and selenium tetrachloride as anti-diabetic agents against hyperglycemia and oxidative stress induced by diabetes mellitus in male rats," *Molecular Biology*, vol. 44, no. 1, pp. 94–104, 2022.

[17] A. Ahangarpour, A. A. Oroojan, L. Khorsandi, M. Kouchak, and M. Badavi, "Hyperglycemia-induced oxidative stress in isolated proximal tubules of mouse: the in vitro effects of myricitrin and its solid lipid nanoparticle," *Archives of Physiology and Biochemistry*, vol. 127, no. 5, pp. 422–428, 2021.

[18] M. Saeed, A. Sharif, S. U. Hassan, B. Akhtar, F. Muhammad, and M. Malik, "Cyperus iria aqueous-ethanol extract ameliorated hyperglycemia, oxidative stress, and regulated inflammatory cytokines in streptozotocin-induced diabetic rats," *Environmental Science and Pollution Research*, vol. 29, no. 3, pp. 4769–4784, 2022.

[19] R. A. Ajala-Lawal, N. O. Aliyu, and T. O. Ajiboye, "Betulinic acid improves insulin sensitivity, hyperglycemia, inflammation and oxidative stress in metabolic syndrome rats via PI3K/Akt pathways," *Archives of Physiology and Biochemistry*, vol. 126, no. 2, pp. 107–115, 2020.

[20] R. Shovit and K. S. Praveen, "Study of stress, anxiety and depression in type 2 diabetic model of zebrafish (Danio rerio)," *Bulletin of Pure and Applied Sciences, Zoology*, vol. 39, no. 1, pp. 25–35, 2020.

[21] R. J. Qin, D. Lin, U. N. Zhang, F. Xiao, and L. Guo, "Mst1 deletion reduces hyperglycemia-mediated vascular dysfunction via attenuating mitochondrial fission and modulating the JNK signaling pathway," *Journal of Cellular Physiology*, vol. 235, no. 1, pp. 294–303, 2020.

[22] T. F. Lee, S. M. Drake, G. W. Roberts et al., "Relative hyperglycemia is an independent determinant of in-hospital mortality in patients with critical illness," *Critical Care Medicine*, vol. 48, no. 2, pp. E115–E122, 2020.

[23] H. Miyauchi, K. Fujioka, S. Okubo et al., "Insulin therapy for hyperglycemia in neonatal sepsis using a preterm mouse

Hindawi
Computational and Mathematical Methods in Medicine
Volume 2023, Article ID 9861751, 1 page
https://doi.org/10.1155/2023/9861751

Retraction

Retracted: Analysis of the Relationship between Gut Flora Levels in Childhood Obese Population and Normal Healthy Population Based on Machine Learning

Computational and Mathematical Methods in Medicine

Received 12 December 2023; Accepted 12 December 2023; Published 13 December 2023

This article has been retracted by Hindawi, as publisher, following an investigation undertaken by the publisher [1]. This investigation has uncovered evidence of systematic manipulation of the publication and peer-review process. We cannot, therefore, vouch for the reliability or integrity of this article.

Please note that this notice is intended solely to alert readers that the peer-review process of this article has been compromised.

Wiley and Hindawi regret that the usual quality checks did not identify these issues before publication and have since put additional measures in place to safeguard research integrity.

We wish to credit our Research Integrity and Research Publishing teams and anonymous and named external researchers and research integrity experts for contributing to this investigation.

The corresponding author, as the representative of all authors, has been given the opportunity to register their agreement or disagreement to this retraction. We have kept a record of any response received.

References

[1] Y. Feng, X. Si, R. Zhu et al., "Analysis of the Relationship between Gut Flora Levels in Childhood Obese Population and Normal Healthy Population Based on Machine Learning," *Computational and Mathematical Methods in Medicine*, vol. 2022, Article ID 6860940, 9 pages, 2022.

Hindawi
Computational and Mathematical Methods in Medicine
Volume 2022, Article ID 6860940, 9 pages
https://doi.org/10.1155/2022/6860940

Research Article

Analysis of the Relationship between Gut Flora Levels in Childhood Obese Population and Normal Healthy Population Based on Machine Learning

Yaoqing Feng, Xia Si, Ruifang Zhu, Junxiang Chen, Wenting Zhao, Qian Wang, and Shifan Han

School of Nursing, Shanxi Medical University, 56 Xinjian South Road, Taiyuan, Shanxi Province 030001, China

Correspondence should be addressed to Shifan Han; shifan.han@sxmu.edu.cn

Received 16 June 2022; Revised 1 August 2022; Accepted 6 August 2022; Published 28 August 2022

Academic Editor: Min Tang

Aims. To explore the study of the relationship between the level of gut flora in childhood obese people and normal healthy people based on the analysis of machine learning. *Materials and Methods*. The stools of 54 normal weight, 53 overweight, and 59 obese children from May 2021 to May 2022 were selected. And DNA was extracted, and primers specific for the four bacteria were designed according to the specificity of the four bacteria to the 16 S rDNA gene sequences of the bacteria to be tested, and real-time fluorescence quantitative PCR reactions were performed to compare whether there was any difference in the number of the four bacteria between the three groups. *Results*. The results of agarose gel electrophoresis showed that the PCR amplification products of all four target bacteria showed clear bands at the corresponding positions, and no nonspecific bands appeared. When compared with the marker, the size matched with the target fragment, indicating good primer specificity. The comparison between normal body recombinant, super recombinant, and obese groups was statistically significant ($P < 0.05$) for rectal eubacteria, polymorphic anaplasma, bifidobacteria spp., and lactobacilli. The median number of bifidobacteria in the three groups was significantly higher than the median number of rectal eubacteria, polymorphomycetes, and lactobacilli. The difference in comparison was statistically significant ($P < 0.05$). Stratified analysis of children's age revealed that normal body composition of Lactobacillus decreased with increasing age, and the difference was statistically significant ($P < 0.05$). *Conclusion*. An increase in rectal eubacteria and a decrease in polymorphomycetes, bifidobacteria spp., and lactobacilli may be associated with the development of obesity. The numbers of rectal eubacteria, polymorphic methanobacteria, bifidobacteria spp., and lactobacilli in the intestine of normal weight and obese children were less affected by sex and age.

1. Introduction

With the development of the economy and the improvement of people's living standards, in the past three decades, the three indicators of body mass index, prevalence of obesity, and prevalence of overweight individuals have increased significantly worldwide. Health risks have received extensive attention from researchers around the world [1]. Prevention and treatment of obesity and related complications have been shown to be lengthy and complex, and successful strategies for treating obesity remain limited. Epidemiological studies have revealed potential environmental factors that affect obesity, including diet, energy expenditure, lack of sleep, endocrine disorders, chronic inflammation, and microbiome status, which may lead to an increased risk of obesity [2].

Under normal circumstances, the intestinal flora maintains a dynamic balance with the internal and external environment of the human body. Once this balance is broken, intestinal microbial structural imbalance will occur, which will lead to the occurrence and development of obesity and related metabolic diseases. Studies have shown that Firmicutes are closely related to obesity because they can better assist the body to absorb energy from the external environment [3]. In recent years, the relationship between intestinal flora and diseases has attracted extensive attention from

scholars at home and abroad, and many new research ideas have been proposed, some of which have also made breakthroughs [4]. However, there are still few studies on the relationship between gut microbiota and children of different weights, especially the relationship between overweight and obese children and some specific microbiota [5]. In order to reasonably integrate and correlate massive data with relevant biological information, so as to better serve practical applications, researchers have introduced machine learning methods into the analysis of gut microbiota data as early as six years ago [6]. Compared with classical statistical methods, machine learning is more suitable for dealing with large-scale learning problems and shows excellent performance when dealing with high-dimensional structured data obtained by metagenomic sequencing [7]. Machine learning methods can deeply mine the interaction information contained in the flora data by extracting features, which can deal with a variety of biological information problems, identify relevant biomarker variables based on sparse data, and prevent overfitting [8]. For multitask problems, the performance is improved by using information from various related tasks, for clustering feature analysis of unlabeled data [9]. We studied the characteristics of intestinal flora changes in obese children and explored the relationship between intestinal flora and obesity, in order to provide a theoretical basis for the prevention and treatment of obesity by regulating intestinal flora.

2. Material and Methods

2.1. Research Object. Stools of 54 normal weight, 53 overweight, and 59 obese children were selected from May 2021 to May 2022. Normal weight children and overweight and obese children were screened strictly according to the predefined inclusion and exclusion criteria, and fresh stools were collected using disposable stool collection tubes and stored at -80°C.

2.2. Inclusion and Exclusion Criteria. Inclusion criteria are as follows: (i) aged between 6 and 11 years old; (ii) meeting the criteria for determining normal weight, overweight, and obesity in children; comparison of BMI (kg/m^2) cut-off points [10] (see Table 1); and (iii) willing to participate in the study and obtain the consent of the guardian, voluntarily serve as the subject, and sign the informed consent. Exclusion criteria are as follows: (i) antibiotic use in the past 4 weeks; (ii) gastrointestinal disorders, past history of gastrointestinal disease or diarrhea, bloating, abdominal pain or constipation within the past 4 weeks, trauma, serious infection, and infectious disease; and (iii) hereditary obesity, drug-induced obesity, endocrine disorders, and metabolic diseases.

2.3. Methods

2.3.1. Fecal Genomic DNA Extraction. Weigh 200 mg of feces into a 2 ml centrifuge tube and place the tube on ice. Add 1.4 ml GSL to the centrifuge tube and shake intermittently for 1 min until the sample is well mixed. Incubate at 70°C for 5 min. Vortex for 15 seconds and centrifuge at 12000 pm for 1 minute. Pipette 1.2 ml of supernatant into a new 2 ml centrifuge tube. Take an inhibitor adsorbent tablet and add it to the supernatant, and shake it sufficiently to completely disperse and suspend the adsorbent tablet. Place at room temperature for 1 minute to promote the full effect of the adsorption sheet. Centrifuge at 12000 rpm for 3 minutes. Transfer the supernatant to a new 1.5 ml centrifuge tube and centrifuge again for 3 min. Transfer 200 μl of the supernatant to a new 1.5 ml centrifuge tube, then add 15 μl proteinase K and 200 μl GB, and vortex for 15 seconds. Incubate at 70°C for 10 minutes. After a brief centrifugation, add 200 absolute ethanol. Vortex to mix and briefly centrifuge again. The solution was transferred to an adsorption column and centrifuged at 12000 pm for 30 seconds, and the waste liquid was discarded. Add 500 μl GD, centrifuge for 30 seconds, and discard the waste liquid. Add 600 lPW, centrifuge for 30 seconds, then discard the waste liquid, and repeat the operation step 14. Centrifuge at 12000 pm for 2 minutes and discard the waste liquid. Place at room temperature for about 10 minutes to allow the residual liquid in the adsorbent material to dry. Put the adsorption column into a new 1.5 ml centrifuge tube, then add 50 μl TB dropwise to the middle of the adsorption membrane, place it at room temperature for 5 minutes, and then centrifuge for 2 minutes. The solution in the centrifuge tube is the extracted DNA.

Table 1: Comparison of different BMI cut-off points for children and adolescents aged 6-11 years in China.

Age (years)	Overweight	Obesity	Overweight	Obesity
6	16.8	18.4	16.7	18.4
7	17.2	19.2	16.9	18.8
8	17.8	20.1	17.3	19.5
9	18.5	21.1	17.9	20.4
10	19.3	22.2	18.7	21.5
11	20.1	23.2	19.6	22.7

2.3.2. Agarose Gel Electrophoresis of PCR Products. Add 20 ml of TBE (50×) to 980 ml of double-distilled water, and dilute to TBE (1×) for later use; weigh 1 g of agarose powder, add 100 l of TBE (1×), and shake gently. Heat in a microwave oven until the agarose is completely melted, cool to about 60°C, add 10 μl of GelRed dye, mix well, and pour it into the plastic plate with the comb inserted. After the gel has solidified, take out the comb, put the gel block into the electrophoresis tank, and add TBE (1×) buffer until the gel plate is covered. The DNA sample and loading buffer (6×) were mixed at a ratio of 5 : 1 and added to the sample well, and finally, the same volume of DNA marker was added. Turn on the power for electrophoresis, 120 V, 30 min. After the electrophoresis is completed, take pictures with a gel imaging analyzer. Under UV light, the band containing the target DNA was excised into a clean 1.5 ml centrifuge tube and weighed. According to the weight of the gel, the sol solution PN was added to the centrifuge tube in proportion (100 μl of PN solution was added to 0.1 g of the gel) and heated in a 50°C water bath until the gel block was completely dissolved. Put the adsorption column into the

collection tube, transfer the solution to the adsorption column, leave it at room temperature for 2 minutes, centrifuge at 12000 pm for 60 seconds, drain the waste liquid in the collection tube, then put the adsorption column back into the collection tube, add 6001 of rinse solution Centrifuge at PW.12000 pm for 1 minute, discard the waste liquid, and put the adsorption column back into the collection tube. Centrifuge again for 3 minutes. After centrifugation, the adsorption column was left at room temperature for 10 minutes. Put the adsorption column into a new 1.51 centrifuge tube, then add 50 μl of elution buffer TB dropwise to the middle of the adsorption membrane, leave it at room temperature for about 5 minutes, and centrifuge for 2 minutes. The solution in the centrifuge tube is the recovered gel. UV spectrophotometer detects the concentration: the DNA recovered from the above-mentioned cutting gel is used as the standard, and the concentration is detected by the UV spectrophotometer and converted into the corresponding copy number according to the formula: copy number = concentration (nggL) × 109 × 6.02 × 1031 (660 × the number of bases of the target gene). Preparation of standard curve: serially dilute each standard 10 times to form 10-10 copies/μl, and carry out real-time fluorescence quantitative PCR reaction. To avoid systematic and manual errors, three replicate wells were made for each concentration of standard template. Real-time fluorescent quantitative PCR reaction system 20 μ: DNA template 1 μl, upstream and downstream primers each 1 μl, 2×RealStar Green Fast Mixture (with Rox) 10 μl, and ddH_2O 7 μl. The amplification conditions of real-time quantitative PCR reaction were as follows: 95°C predenaturation for 2 minutes; 95°C denaturation for 15 s, Tm annealing for 30 s, 72°C extension for 30 s, 40 cycles; melting curve: 60°C to 95°C for each 0.3°C temperature increase to collect fluorescence. After the reaction, the StepOne software automatically draws a standard curve.

2.4. Statistical Analysis. The SPSS 27.0 statistical software was used for analysis. Count data were expressed as the number of cases, and differences between the three groups were compared using chi-square test. If the measurement data obeyed normal distribution and the variance between the groups was the same, the data were expressed as mean ± standard deviation, and the differences between groups were compared using one-way ANOVA, and if the sample data did not meet several conditions mentioned above, the data were expressed as median/interquartile spacing, and the comparison between the three groups was done using multiple independent sample our rank sum test (Alaska-Wallis H test) with the test level $a = 0.05$.

3. Results

3.1. Electrophoresis of PCR Products. The results of agarose gel electroplate showed that the PC amplification products of the four target bacteria all showed clear bands at the corresponding positions, and no nonspecific bands appeared. When compared with the marker, the size matched with the target fragment, indicating good primer specificity (see Figure 1).

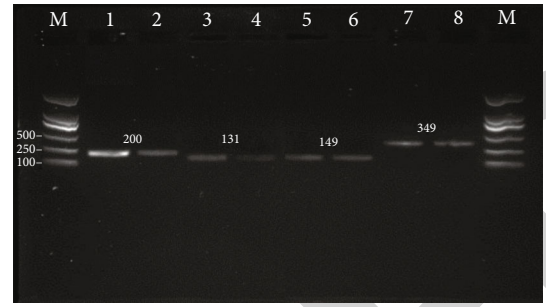

Figure 1: PCR product electroplate results (M: marker; 1, 2: rectal antibacterial; 3, 4: polymorphomycetes; 5, 6: Bifidobacterium spp.; 7, 8: Lactobacillus).

3.2. Differences in the Amount of Bacteria between Groups. The comparison of antibacterial rectum, Bacteroides polymorpha, Bifidobacterium, and Lactobacillus among the normal weight, overweight, and obese groups was statistically significant ($P < 0.05$). The median of Bifidobacterium in the three groups was significantly higher than that of antibacterial rectum, Bacteroides polymorpha, and Lactobacillus. The difference was statistically significant ($P < 0.05$) (see Figure 2).

3.3. Distribution Characteristics of Gut Microbiota in Different Genders. The gender stratified analysis of children showed that there was no significant difference in the distribution of intestinal flora among normal weight children, overweight children, and obese children ($P > 0.05$) (see Figure 3).

3.4. Distribution Characteristics of Gut Microbiota at Different Ages. The stratified analysis of children's age showed that the normal body weight Lactobacillus decreased with the increase of age, and the difference was statistically significant ($P < 0.05$), and the other differences were not statistically significant ($P > 0.05$) (see Figure 4).

4. Discussion

The intestinal flora is closely related to human health. With the deepening of the research on the intestinal flora, people have realized that the intestinal flora plays an important role in the process of energy intake, transformation, and storage [11]. More and more studies have found that the intestinal flora has a certain relationship with the occurrence and development of obesity. Therefore, an in-depth study of the relationship between the changes in the intestinal flora and obesity, especially the relationship between specific bacteria and obesity, can be used for obesity prevention and development. Treatment offers new directions [12]. Studies on the relationship between gut microbiota and obesity have mainly focused on the phylum level. Studies in both animals and humans have found that compared with the control group, the obese individuals have an increase in Firmicutes and a decrease in Bacteroidetes or Firmicutes/Pseudobacterium The proportion of Bacillus phyla increased [13]. Based on this, our study is aimed at exploring the relationship

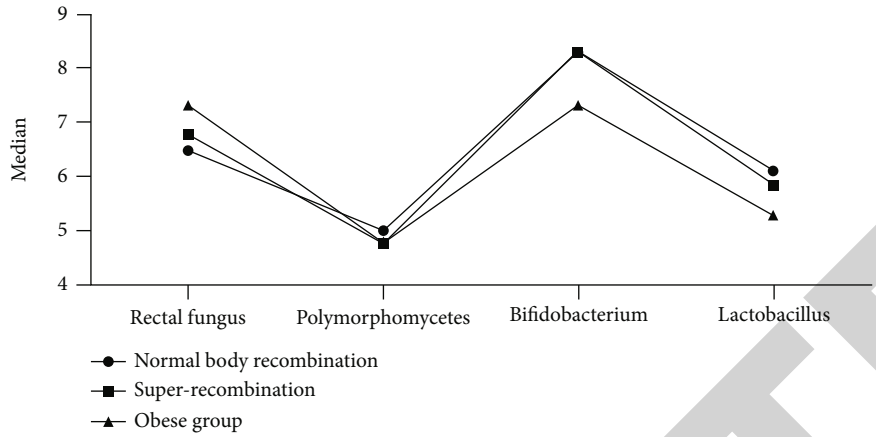

Figure 2: Differences in genus amounts between groups. In our study, data on differences in genus amounts between groups were statistically analyzed and calculated using the SPSS 27.0 statistical software. The measured data were expressed as median, and analysis of variance using repeated measures showed that rectal bacteria, polymorphic mimics, bactericidal spp., and bacilli were statistically significant ($P < 0.05$) when compared between the normal body recombination, super recombination, and obesity groups. The median number of bactericidal in the three groups was significantly higher than the median number of rectal bacteria, polymorphomycetes, and bacilli. The difference in comparison was statistically significant ($P < 0.05$).

between specific bacteria and obesity through quantitative research on specific bacteria [14]. Eubacterium rectum is a representative bacteria in the Firmicutes phylum, with the role of fermenting glucose or protein [15]. Eubacterium rectum contains genes related to resistant starch-degrading enzymes, which can reduce glycan-degrading enzymes, thereby increasing the expression process of selective amino acid and sugar transport, reducing the level of nicotinamide adenine dinucleotide (NADH), and promoting sugar fermentation [16]. Therefore, we have reason to think that Eubacterium rectum may be related to the host's energy metabolism. Bacteroides polymorpha is one of the most studied bacteria in the phylum Bacteroidetes. Because it contains 64 enzymes related to the degradation of polysaccharides, it has a strong ability to digest polysaccharides [17]. At the same time, it can hydrolyze and ferment exogenous fibrous substances and endogenous mucin to provide energy for the host [18]. Bacteroides polymorpha can also regulate and maintain the intestinal microecological balance by synthesizing vitamins, preventing the colonization of foreign bacteria, and enhancing the body's immunity [19]. Based on the characteristics of Eubacterium rectum and Bacteroides polymorpha, it can be speculated that changes in their numbers are closely related to obesity [20]. Probiotics refer to microorganisms that can benefit health after consumption, and the probiotics that exist in the human gut can also exert their beneficial effects by improving the intestinal microecological balance of the body. Bifidobacterium and Lactobacillus are the two most common probiotics [21]. On the one hand, the probiotic effect of bifidobacteria is to enhance the adsorption of intestinal mucosa by producing extracellular polysaccharides and colonize the surface of intestinal epithelial cells, thereby preventing the colonization of pathogens or opportunistic pathogens [22]. On the other hand, lactic acid and acetic acid are produced by decomposing carbohydrates, which makes the intestinal tract an acidic environment, thereby inhibiting the growth of spoilage bacteria and maintaining the microecological balance in the intestinal tract [23]. Lactobacillus is named because it can ferment sugars to produce lactic acid, so it can regulate intestinal microecology like Bifidobacterium [24]. Lactobacillus also has a role in regulating immune function, but there are relatively few studies on weight control [25].

Our study found that the number of Eubacterium rectum in the overweight and obese children was significantly higher than that in the normal weight group, and the number of Eubacterium rectum in the obese group was significantly higher than that in the overweight group. It is speculated that it may lead to obesity by increasing energy absorption [26]. Some scholars have found that compared with normal mice, germ-free mice can absorb dietary glucose and metabolize starch but lack the complex fiber for digestion, so they cannot obtain energy from indigestible polysaccharides [27]. This indicates that certain gut microbiota can lead to obesity by increasing energy acquisition from polysaccharide diet [28]. Eubacterium rectum may be one of these bacteria [29]. Bacteroides polymorpha belongs to the phylum Bacteroidetes, is a Gram-negative bacterium, and is one of the most important bacteria in the human body [30]. Some scholars have found that ordinary people contain about 30% of Bacteroides in the intestine, while only 3% of Bacteroides in obese people increased to 15% [31]. The same is true for studies in mice, where obese mice had less Bacteroides than wild-type mice when fed the same low-fat diet but increased Bacteroides when they lost weight [32]. However, some scholars have found that the number of Bacteroides in the intestine of obese people is significantly higher than that of the lean group, but considering that the method of in vitro culture combined with microscopy is used and the number of people in the study is small, it is impossible to make a firm conclusion on the results [33]. Some scholars found that the real-time fluorescence quantitative PC technology was used to quantify B. polymorpha in patients with type 2 diabetes and normal control groups and found that

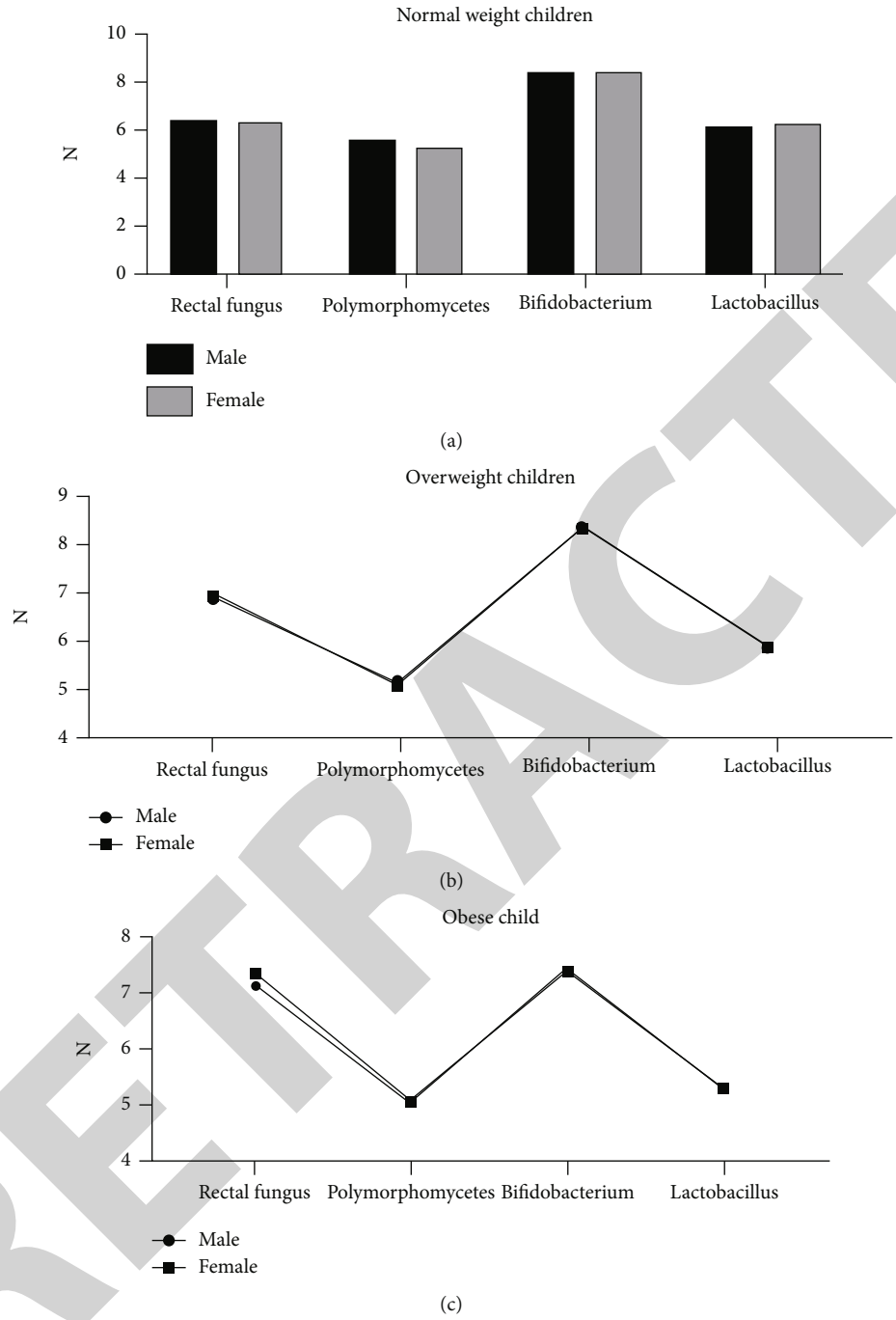

Figure 3: Characteristics of intestinal flora distribution among different genders of children. In our study, data on the characteristics of intestinal flora distribution among different genders of children were statistically analyzed and calculated using the SPSS 26.00 statistical software. The measured data were expressed as median, and the analysis of variance using repeated measures showed that the differences were not statistically significant ($P > 0.05$) when comparing the intestinal flora distribution characteristics of normal weight children, overweight children, and obese children, stratified by gender.

the number of B. polymorpha in the type 2 diabetes group was lower than that in the normal control group [34]. In the study of hypertension, the hypertensive group was significantly lower than the normal control group, and some scholars found that the use of Bacteroides polymorpha gavage in mice found that it has a weight loss effect [35]. A further study in obese patients found that the number of B. polymorpha in the gut could be restored to normal weight levels by bariatric surgery [36]. Both animal and human studies have demonstrated that the reduction of B. polymorpha is associated with obesity.

Our study found that the number of B. polymorpha in children with overweight and obesity was significantly higher than that in children with normal weight, but the

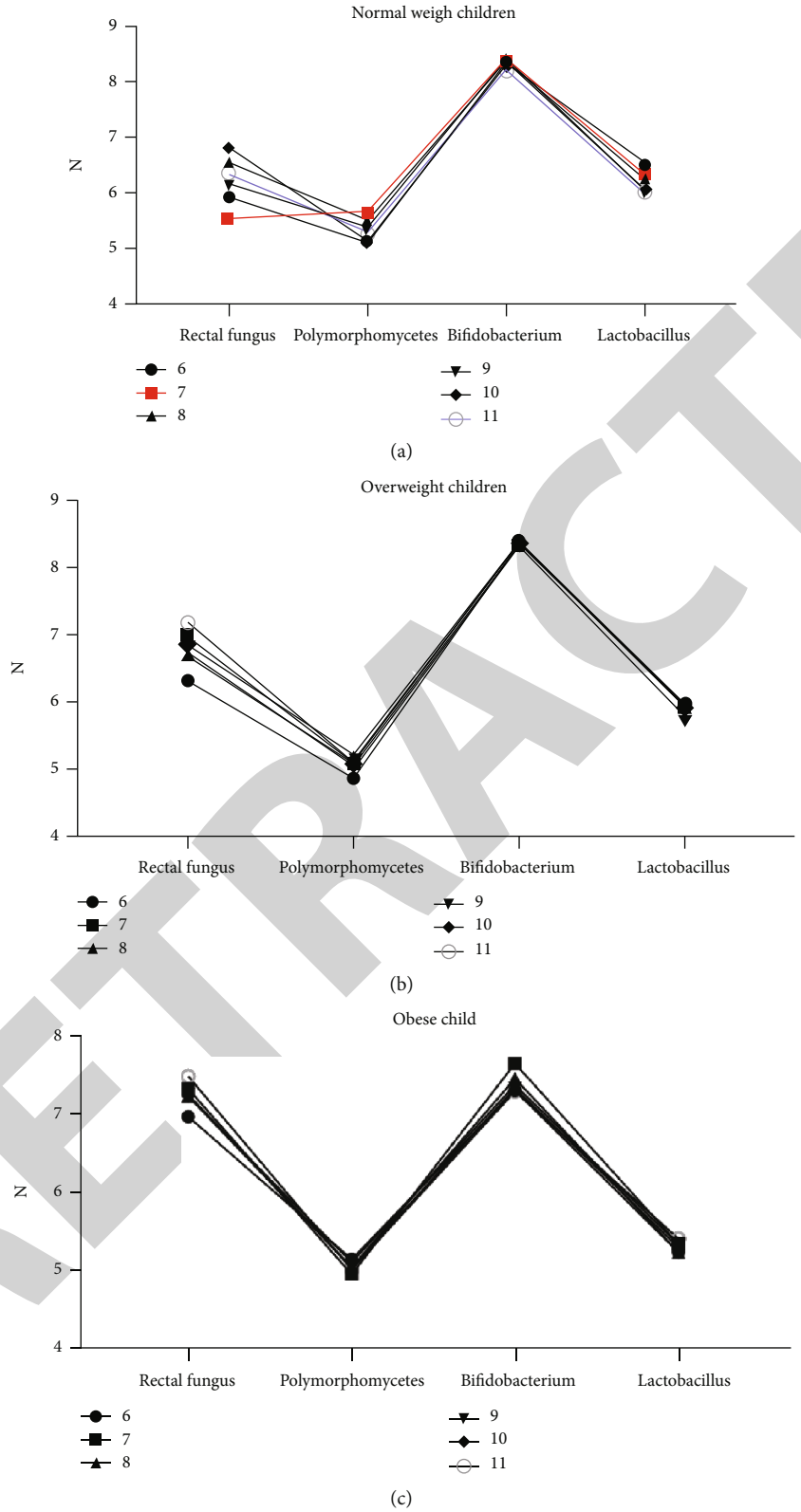

Figure 4: Comparison of intestinal flora distribution characteristics at different ages. In this study, statistical analysis of data on intestinal flora distribution characteristics at different ages was calculated using the SPSS26.00 statistical software. The measured data were expressed as mean ± standard deviation, and repeated measures ANOVA showed that stratified analysis of children's age revealed that normal body composition of Lactobacillus decreased with increasing age and the difference was statistically significant ($P < 0.05$); the rest of the differences were not statistically significant ($P > 0.05$).

difference between overweight and obesity groups was not statistically significant, indicating that the reduction of B. polymorpha may lead to the occurrence of overweight and obesity, but the specific mechanism is still unclear, and further research is needed. In our study, the four types of intestinal bacteria were stratified by gender and age among the three groups and found that the normal weight Lactobacillus decreased with the increase of age, and the difference was statistically significant. It indicated that the number of Lactobacillus in the normal body group was related to age, and the number of four bacteria in the other groups had nothing to do with age and gender. This is similar to the conclusion found in studies elsewhere in China that the distribution of gut microbiota in school-age children is less affected by children's gender and age. Lactobacillus is also a probiotic, which can ferment carbohydrates to produce a large amount of lactic acid, and is one of the important physiological flora of human [37]. In addition to improving immunity, anti-inflammatory, anticancer, etc., it also plays an important role in regulating intestinal flora [38]. A study found that the body weight and adipose tissue weight of mice fed with Lactobacillus were significantly lower than those in the control group, suggesting that Lactobacillus may control the growth of fat cells [39]. Studies have also found that Lactobacillus can significantly reduce abdominal fat and weight loss in obese mice, presumably by reducing fat absorption and affecting energy metabolism [40]. A number of epidemiological studies have found that cesarean section is a risk factor for childhood obesity. At the same time, some studies have pointed out that the intestinal tract of newborns born by cesarean section is mainly Lactobacillus, while the newborns born by cesarean section are mainly Staphylococcus and Acinetobacter [41]. Bifidobacterium belongs to Actinobacteria and is an important probiotic with the functions of improving immunity, antitumor, and antiaging and regulating intestinal flora [42]. It mainly regulates the intestinal flora through two aspects: on the one hand, by producing extrabacterial polysaccharides to enhance the adsorption to the intestinal mucosa and colonize the surface of intestinal epithelial cells, thereby preventing the colonization of pathogens or opportunistic pathogens [43]. On the other hand, by decomposing carbohydrates to produce lactic acid and acetic acid, the intestinal environment is acidic, thereby inhibiting the growth of spoilage bacteria [44]. Our study found that the number of Bifidobacterium in the obese group was significantly lower than that in the normal weight and overweight group, but the difference between the normal group and the overweight group was not statistically significant, indicating that the reduction of Bifidobacterium may be related to the occurrence of obesity [45]. The possible mechanism is that the reduction of bifidobacteria promotes the increase of harmful bacteria and destroys the stability of the intestinal mucosa, thereby unbalanced the absorption and metabolism of nutrients, leading to the occurrence of host obesity [46].

We have a small amount of research samples, and there are certain limitations. All the data in our experiments are relatively concentrated and underrepresented. The detection of only four intestinal species that may be related to obesity cannot represent the entire intestinal microbes. It is hoped that more bacteria will be screened in the future to provide more support for obesity research. Our study is a preliminary exploration of the relationship between gut microbiota and overweight and obesity, and other technical means are needed to conduct mechanism research to comprehensively describe the relationship between gut microbiota and overweight and obesity. In conclusion, the increase of Eubacterium rectum and the decrease of Bacteroides polymorpha, Bifidobacterium, and Lactobacillus may be related to the occurrence and development of obesity. Quantities of Eubacterium rectum, Bacteroides polymorpha, Bifidobacterium, and Lactobacillus in the gut of normal weight and obese children were less affected by sex and age.

Data Availability

No data were used to support this study.

Conflicts of Interest

The authors declare that they have no conflicts of interest.

Acknowledgments

This study was funded by the Shanxi Science and Technology Association.

References

[1] A. C. Gomes, C. Hoffmann, and J. F. Mota, "The human gut microbiota: metabolism and perspective in obesity," *Gut Microbes*, vol. 9, no. 4, pp. 308–325, 2018.

[2] A. Gupta, V. Osadchiy, and E. A. Mayer, "Brain-gut-microbiome interactions in obesity and food addiction," *Nature Reviews Gastroenterology & Hepatology*, vol. 17, no. 11, pp. 655–672, 2020.

[3] M. J. Saad, A. Santos, and P. O. Prada, "Linking gut microbiota and inflammation to obesity and insulin resistance," *Physiology (Bethesda, Md.)*, vol. 31, no. 4, pp. 283–293, 2016.

[4] A. Gasmi, P. K. Mujawdiya, L. Pivina et al., "Relationship between gut microbiota, gut hyperpermeability and obesity," *Current Medicinal Chemistry*, vol. 28, no. 4, pp. 827–839, 2021.

[5] S. J. Leigh and M. J. Morris, "Diet, inflammation and the gut microbiome: mechanisms for obesity-associated cognitive impairment," *Biochimica et Biophysica Acta - Molecular Basis of Disease*, vol. 2020, article 165767, p. 6, 2020.

[6] D. Pitocco, M. Di Leo, L. Tartaglione et al., "The role of gut microbiota in mediating obesity and diabetes mellitus," *European Review for Medical and Pharmacological Sciences*, vol. 24, no. 3, pp. 1548–1562, 2020.

[7] Q. Zeng, D. Li, Y. He et al., "Discrepant gut microbiota markers for the classification of obesity-related metabolic abnormalities," *Scientific Reports*, vol. 9, no. 1, p. 13424, 2019.

[8] Y. Kang and Y. Cai, "Gut microbiota and obesity: implications for fecal microbiota transplantation therapy," *Hormones (Athens, Greece)*, vol. 13, no. 3, pp. 223–234, 2017.

[9] K. E. Bouter, D. H. van Raalte, A. K. Groen, and M. Nieuwdorp, "Role of the gut microbiome in the pathogenesis of obesity and obesity-related metabolic dysfunction," *Gastroenterology*, vol. 152, no. 7, pp. 1671–1678, 2017.

[10] L. Hui, Z. Xinnan, J. Chengye, and J. Mi, "Study on the cut-off point of body mass index for overweight and obesity screening in Chinese children and adolescents aged 2-18 years," *Chinese Journal of Epidemiology*, vol. 31, no. 6, pp. 616–620, 2010.

[11] H. Zouhal, R. Bagheri, R. Triki et al., "Effects of Ramadan intermittent fasting on gut hormones and body composition in males with obesity," *International Journal of Environmental Research and Public Health*, vol. 17, no. 15, p. 5600, 2020.

[12] P. Wang, D. Li, W. Ke, D. Liang, X. Hu, and F. Chen, "Resveratrol-induced gut microbiota reduces obesity in high-fat diet-fed mice," *International Journal of Obesity*, vol. 44, no. 1, pp. 213–225, 2020.

[13] M. Uemura, F. Hayashi, K. Ishioka et al., "Obesity and mental health improvement following nutritional education focusing on gut microbiota composition in Japanese women: a randomised controlled trial," *European Journal of Nutrition*, vol. 58, no. 8, pp. 3291–3302, 2019.

[14] N. Vallianou, T. Stratigou, G. S. Christodoulatos, and M. Dalamaga, "Understanding the role of the gut microbiome and microbial metabolites in obesity and obesity-associated metabolic disorders: current evidence and perspectives," *Current Obesity Reports*, vol. 8, no. 3, pp. 317–332, 2019.

[15] Y. Xu, N. Wang, H. Y. Tan et al., "Panax notoginseng saponins modulate the gut microbiota to promote thermogenesis and beige adipocyte reconstruction via leptin-mediated AMPKα/STAT3 signaling in diet-induced obesity," *Theranostics*, vol. 10, no. 24, pp. 11302–11323, 2020.

[16] M. Green, K. Arora, and S. Prakash, "Microbial medicine: prebiotic and probiotic functional foods to target obesity and metabolic syndrome," *International Journal of Molecular Sciences*, vol. 21, no. 8, p. 2890, 2020.

[17] E. Denou, K. Marcinko, M. G. Surette, G. R. Steinberg, and J. D. Schertzer, "High-intensity exercise training increases the diversity and metabolic capacity of the mouse distal gut microbiota during diet-induced obesity," *American Journal of Physiology-Endocrinology and Metabolism*, vol. 310, no. 11, pp. E982–E993, 2016.

[18] J. Aron-Wisnewsky, M. V. Warmbrunn, M. Nieuwdorp, and K. Clément, "Metabolism and metabolic disorders and the microbiome: the intestinal microbiota associated with obesity, lipid metabolism, and metabolic health-pathophysiology and therapeutic strategies," *Gastroenterology*, vol. 160, no. 2, pp. 573–599, 2021.

[19] F. Hossain, S. Majumder, J. David, B. A. Bunnell, and L. Miele, "Obesity modulates the gut microbiome in triple-negative breast cancer," *Nutrients*, vol. 13, no. 10, p. 3656, 2021.

[20] S. Parida and D. Sharma, "The microbiome-estrogen connection and breast cancer risk," *Cell*, vol. 8, no. 12, p. 1642, 2019.

[21] J. B. Lone, W. Y. Koh, H. A. Parray et al., "Gut microbiome: microflora association with obesity and obesity-related comorbidities," *Microbial Pathogenesis*, vol. 124, pp. 266–271, 2018.

[22] S. V. Kumbhare, D. V. V. Patangia, R. H. Patil, Y. S. Shouche, and N. P. Patil, "Factors influencing the gut microbiome in children: from infancy to childhood," *Journal of Biosciences*, vol. 44, no. 2, p. 49, 2019.

[23] E. Barengolts, "Gut microbiota, prebiotics, probiotics, and synbiotics in management of obesity and prediabetes: review of randomized controlled trials," *Endocrine Practice*, vol. 22, no. 10, pp. 1224–1234, 2016.

[24] R. Scholz and T. Langmann, "Gut flora connects obesity with pathological angiogenesis in the eye," *EMBO Molecular Medicine*, vol. 8, no. 12, pp. 1361–1363, 2016.

[25] F. M. Gribble and F. Reimann, "Function and mechanisms of enteroendocrine cells and gut hormones in metabolism," *Nature Reviews Endocrinology*, vol. 15, no. 4, pp. 226–237, 2019.

[26] M. Romaní-Pérez, C. Bullich-Vilarrubias, I. López-Almela, R. Liébana-García, M. Olivares, and Y. Sanz, "The microbiota and the gut-brain axis in controlling food intake and energy homeostasis," *International Journal of Molecular Sciences*, vol. 22, no. 11, p. 5830, 2021.

[27] S. Coppola, C. Avagliano, A. Calignano, and C. R. Berni, "The protective role of butyrate against obesity and obesity-related diseases," *Molecules*, vol. 26, no. 3, p. 682, 2021.

[28] S. Reitmeier, S. Kiessling, T. Clavel et al., "Arrhythmic gut microbiome signatures predict risk of type 2 diabetes," *Cell Host & Microbe*, vol. 28, no. 2, pp. 258–272.e6, 2020.

[29] M. C. Dao and K. Clément, "Gut microbiota and obesity: concepts relevant to clinical care," *European Journal of Internal Medicine*, vol. 48, pp. 18–24, 2018.

[30] A. N. Hutchinson, L. Tingö, and R. J. Brummer, "The potential effects of probiotics and ω-3 fatty acids on chronic low-grade inflammation," *Nutrients*, vol. 12, no. 8, p. 2402, 2020.

[31] R. W. Stephens, L. Arhire, and M. Covasa, "Gut microbiota: from microorganisms to metabolic organ influencing obesity," *Obesity (Silver Spring)*, vol. 26, no. 5, pp. 801–809, 2018.

[32] G. V. Moreira, F. F. Azevedo, L. M. Ribeiro et al., "Liraglutide modulates gut microbiota and reduces NAFLD in obese mice," *The Journal of Nutritional Biochemistry*, vol. 62, pp. 143–154, 2018.

[33] H. Shi, Y. Yu, D. Lin et al., "β-glucan attenuates cognitive impairment via the gut-brain axis in diet-induced obese mice," *Microbiome*, vol. 8, no. 1, p. 143, 2020.

[34] J. R. Allegretti, Z. Kassam, B. H. Mullish et al., "Effects of fecal microbiota transplantation with oral capsules in obese patients," *Clinical Gastroenterology and Hepatology*, vol. 18, no. 4, pp. 855–863.e2, 2020.

[35] E. Lau, D. Carvalho, C. Pina-Vaz, J. A. Barbosa, and P. Freitas, "Beyond gut microbiota: understanding obesity and type 2 diabetes," *Hormones (Athens, Greece)*, vol. 14, no. 3, pp. 358–369, 2015.

[36] Y. Naito, T. Takagi, and R. Inoue, "Obesity and gut microbiome:their association to lower gastrointestinal disorders," *Nihon Shokakibyo Gakkai Zasshi*, vol. 118, no. 6, pp. 525–531, 2021.

[37] Y. Y. Lim, Y. S. Lee, and D. S. Q. Ooi, "Engineering the gut microbiome for treatment of obesity: a review of current understanding and progress," *Biotechnology Journal*, vol. 15, no. 10, article e2000013, 2020.

[38] A. F. Cătoi, D. C. Vodnar, A. Corina et al., "Gut microbiota, obesity and bariatric surgery: current knowledge and future perspectives," *Current Pharmaceutical Design*, vol. 25, no. 18, pp. 2038–2050, 2019.

[39] S. Moran-Ramos, B. E. López-Contreras, and S. Canizales-Quinteros, "Gut microbiota in obesity and metabolic abnormalities: a matter of composition or functionality?," *Archives of Medical Research*, vol. 48, no. 8, pp. 735–753, 2017.

[40] G. Lee, H. J. You, J. S. Bajaj et al., "Distinct signatures of gut microbiome and metabolites associated with significant fibrosis in non-obese NAFLD," *Nature Communications*, vol. 11, no. 1, p. 4982, 2020.

Hindawi
Computational and Mathematical Methods in Medicine
Volume 2023, Article ID 9847091, 1 page
https://doi.org/10.1155/2023/9847091

Retraction

Retracted: Long Noncoding RNA LINC00473 Ameliorates Depression-Like Behaviors in Female Mice by Acting as a Molecular Sponge to Regulate miR-497-5p/BDNF Axis

Computational and Mathematical Methods in Medicine

Received 5 December 2023; Accepted 5 December 2023; Published 6 December 2023

This article has been retracted by Hindawi, as publisher, following an investigation undertaken by the publisher [1]. This investigation has uncovered evidence of systematic manipulation of the publication and peer-review process. We cannot, therefore, vouch for the reliability or integrity of this article.

Please note that this notice is intended solely to alert readers that the peer-review process of this article has been compromised.

Wiley and Hindawi regret that the usual quality checks did not identify these issues before publication and have since put additional measures in place to safeguard research integrity.

We wish to credit our Research Integrity and Research Publishing teams and anonymous and named external researchers and research integrity experts for contributing to this investigation.

The corresponding author, as the representative of all authors, has been given the opportunity to register their agreement or disagreement to this retraction. We have kept a record of any response received.

References

[1] B. Li, H. Zhao, and J. Sun, "Long Noncoding RNA LINC00473 Ameliorates Depression-Like Behaviors in Female Mice by Acting as a Molecular Sponge to Regulate miR-497-5p/BDNF Axis," *Computational and Mathematical Methods in Medicine*, vol. 2022, Article ID 4244425, 12 pages, 2022.

Hindawi
Computational and Mathematical Methods in Medicine
Volume 2022, Article ID 4244425, 12 pages
https://doi.org/10.1155/2022/4244425

Research Article

Long Noncoding RNA LINC00473 Ameliorates Depression-Like Behaviors in Female Mice by Acting as a Molecular Sponge to Regulate miR-497-5p/BDNF Axis

Bo Li, Hongxia Zhao, and Junxia Sun

Department of Psychialogics, Binzhou Municipal Youfu Hospital, Binzhou, Shandong 256600, China

Correspondence should be addressed to Bo Li; bobonana1982@163.com

Received 6 July 2022; Revised 28 July 2022; Accepted 8 August 2022; Published 28 August 2022

Academic Editor: Min Tang

Background. Depression was a common life-threatening psychiatric disorder and occurs more frequently in women than in men. Long noncoding RNAs (lncRNAs), such as LINC00473, had been reported to be involved in the progression of depression. *Methods*. Chronic unpredictable moderate stress in mice (CUMS) was applied to construct a depression model. Subsequently, RT-qPCR was applied to check the level of LINC00473 and microRNA-497-5p (miR-497-5p) in the hippocampal region of the mice induced by CUMS. CUMS mice were injected with lentiviral vectors of LINC00473 (LV-LINC00473), miR-497-5p inhibitor, short hairpin- (sh-) brain-derived neurotrophic factor (sh-BDNF), or miR-497-5p mimic to evaluate depressive behaviors, including sucrose preference test, forced swim test, elevated plus maze, and tail suspension test. Moreover, the production of hypothalamic neurotransmitters was assessed with the usage of ELISA kits. Dual-luciferase reporter assay, RNA pull-down, and RIP analysis were performed to measure the relationship between miR-497-5p and LINC00473 or BDNF. Further, western blot was employed to determine the protein level of BDNF. *Results*. We discovered that LINC00473 level was downregulated in the female mice with depression, but not in male mice. Besides, the depressive behaviors induced by CUMS in mice, including the decrease of sucrose preference and time in open arm, as well as the increase of immobility time and swimming resting time were all ameliorated by LINC00473 overexpression. Moreover, the concentration of neurotransmitters was decreased in CUMS-induced mouse hypothalamus, which was blocked by LV-LINC00473 lentiviral vector administration. Mechanistically, LINC00473 directly targeted miR-497-5p. Absence of miR-497-5p revealed the antidepression effects on CUMS-induced mice, and miR-497-5p upregulation could counter the antidepressive impacts of LINC00473 upregulation on CUMS-induced mice. Furthermore, LINC00473 could target miR-497-5p to modulate BDNF level. Knockdown of BDNF could abrogate the improving influences of miR-497-5p suppression on CUMS-induced depression. *Conclusions*. LINC00473 ameliorated CUMS-caused depression by encouraging BDNF expression via binding to miR-497-5p, which might provide a potential therapeutic target for depression in females.

1. Introduction

Depression is currently one of the psychiatric disorders with the highest incidence, with a lifetime prevalence of up to 11%, and its main clinical feature is a long-lasting and significant depression, often accompanied by symptoms such as anhedonia, cognitive impairment, and metabolic disturbances [1]. Depression seriously reduces the quality of life of patients and even leads to suicidal tendencies, resulting in a heavy economic and medical burden for families and society [2]. The use of antidepressant medications is the main therapy method for many depression patients in recent years, while almost 40% of depression patients fail to show complete remission after an antidepressant trial, and about 20% patients showed no response to any intervention, partially due to the lack of notable biomarkers and reliable biological tests to diagnose depression [3]. The available results suggested that depression was a chronic multifactorial psychiatric disorder whose pathology is the result of biological, genetic, and environmental factors. Risk factors of depression included sex, age, stressful life events and social environment, among other factors [4]. Moreover, it was reported that

stress-related disorders often show gender differences, and women tended to have more severe symptoms of depression [5]. Numerous studies had shown that women remain at a high risk of developing depression for several years from adolescence to menopause, with women of reproductive age having 2-3 times the incidence of depressive disorders as men, and with declining estrogen levels after entering perimenopause, the risk of developing clinically significant depressive symptoms increases 2-4 times compared with before. However, the molecular mechanisms under gender differences of depression remained blurry.

Recent studies on lncRNAs had progressed rapidly, and a series of findings established that lncRNAs played important roles in various cellular processes, such as genomic imprinting, chromatin modification, transcriptional interference, and intranuclear trafficking, but a large number of lncRNA functions are still unknown and urgently studied. At present, many lncRNAs had been detected to exhibit significant alteration in expression levels during the process of studying the pathological mechanisms of depression. Therefore, the regulatory role of lncRNAs in depression has great potential for the study of their pathological mechanisms [6]. For example, a study showed that lncRNA MIR155HG overexpression exhibited the improvement action on depression in chronic unpredictable moderate stress- (CUMS-) treated mice [7]. Ni et al. found that by regulating Wnt/β-catenin pathway, lncRNA TCONS_00019174 exhibited antidepressant-like action on the mice induced by CUMS [8]. Further analysis targeting the gender difference demonstrated that the differential lncRNA expression was more significant in female patients than that in males. A research reported that the expression of LINC00473 was downregulated in depressed patients [9]. More interestingly, another study revealed that LINC00473 was decreased in depressed females only [10]. However, the functional role of LINC00473 in depression has not been clarified.

Recently, microRNAs (miRNAs), the small noncoding RNAs, were found to be functioned as important regulators in the higher functioning of brain [11]. Dysregulation of miRNAs was associated with various human neurological disorders, including neurodevelopmental disorders, neurodegenerative diseases, and affective psychiatric disorders. For instance, the expression of miR-146a was negatively correlated with the degree of depression [12]. Moreover, miR-124-3p expression was increased in the brain of the depressed patients, and similar results were obtained in the serum of depressed patients [13]. Additionally, miR-497 level was overexpressed in CUMS-induced rats [14]. However, the potential mechanism of miR-497-5p implicated in depression was largely unexplored.

In the present study, we established an animal depression model to explore the role of LINC00473 and the downstream mechanism mediated by LINC00473 and aimed to find a novel therapeutic target for depression treatment in females.

2. Materials and Methods

2.1. Experimental Animal. 86 C57BL/6 male mice (32 ± 2.6 g, 7 weeks) and 10 C57BL/6 female mice (30 ± 2.3 g, 7 weeks) were obtained from Shandong Animal Experiment Center. All mice were provided with free access to eat and drink water and fed with pellet feed. After adaptive feeding for one week, the experiments were performed. All experiments performed in the recent study were ratified by the Institute for Experimental Animals of Binzhou Municipal Youfu Hospital.

2.2. Chronic Unpredictable Moderate Stress (CUMS) Modeling. In brief, the mice in CUMS group were suffered from various stressors swimming in ice water for 24 h (6°C), fasting for 24 h, water prohibition for 24 h, overnight lighting for 12 h, day night reversal, interrupted noise stimulus for 24 h, and flash stimuli of certain frequency. The CUMS mice were given 6 weeks of continuous stress stimulation. Mice in the control group were housed in a separate room with no stressors.

2.3. Intraventricular Viral Vector Injection. This study used LINC00473 lentiviral vector (LV-LINC00473; RiboBio Co., Ltd., Guangzhou, China) construction, miR-497-5p mimic (RiboBio Co., Ltd.), sh-BDNF (RiboBio Co., Ltd.), and miR-497-5p inhibitor (RiboBio Co., Ltd.). A skin cut on the skull was made, and then, two small holes (bilateral hippocampi) were made by using a micro drill in the skull below the surface of dura: ML = ±1.4 mm, AP = −2.2 mm, and DV = −1.9 mm. Lentiviral injection was carried out at 1 week before model construction as previously described [14].

2.4. Cell Culture. HEK-293T cells (Shanghai Huiying Biotech Co., Ltd., Shanghai, China) were maintained in DMEM medium. The 10% fetal bovine serum, 100 U/mL penicillin, and 100 μg/mL streptomycin were put into the medium before culture.

2.5. RT-qPCR. After extraction of total RNA using TRIzol (Thermo Fisher, Shanghai, China), cDNA was gained with the usage of a reverse transcription kit. RNA concentration was determined by spectrophotometer ($1.9 < A260/A280 < 2.0$). Then, RT-qPCR was performed on the step one plus real-time PCR system (Thermo Fisher, USA). The relative levels of LINC00473 and miR-497-5p were calculated by using $2^{-\Delta\Delta Ct}$ method. The efficiency of the PCR should be between 90 and 110% ($3.6 > \text{slope} > 3.1$). The primers were listed as follows: LINC00473, F 5′-TGTGCACGCTTTCACAATGG-3′, R 5′-CTCTGGCATGGATTGGTGGT-3′; miR-497-5p, F 5′-CGCCAGCAGCACACTGTGG-3′, R 5′-GTGCAGGGTCCGAGGT-3′; GAPDH, F 5′-TGCAGTGGCAAAGTGGAGATT-3′, R 5′-TCGCTCCTGGAAGATGGTGAT-3′; and U6, F 5′-GCTTCGGCAGCACATATACTAAAAT-3′, R 5′-CGCTTCACGAATTTGCGTGTCAT-3′. U6 and GAPDH acted as the internal reference.

2.6. Bioinformatics Methods. The miRNA and lncRNA targets were predicted using a computer-aided algorithm from starbase (https://starbase.sysu.edu.cn/).

2.7. Sucrose Preference Test (SPT). As previously described [15], the mice were trained using a sucrose solution (1%,

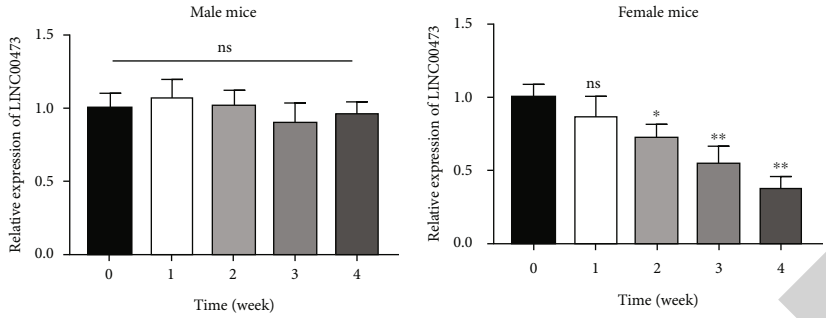

Figure 1: CUMS-induced LINC00473 downregulation in the hippocampal region of the female mice. (a and b) RT-qPCR for LINC00473 expression detection at 0, 1, 2, 3, and 4 weeks of stimulation in male and female mice. $N = 3$; $^{*}P < 0.05$ and $^{**}P < 0.01$.

w/*v*) for 24 h prior to the test. After that, the mice were maintained under fasting and anhydrous environment for 24 h and subsequently fed with 1% sucrose solution, followed by replacement of tap water. Finally, the mice were fed with tap water (200 mL) and 1% sucrose solution (200 mL) at the test day. The sucrose solution was changed once after 12 h.

2.8. Elevated Plus Maze (EPM). Mice were put into the cross maze at the same position with the head facing the direction of the open arm, initiating monitoring of the activity of the recorded animals over a 5 min period [16]. The collected indexes included the number of times that the mice entered the open and closed arms, as well as the dwell time in each arm. Finally, the behavioral changes of mice in each group were analyzed.

2.9. Forced Swimming Test (FST). FST was carried out according to the previously described [17]. The test animals were individually put into a Plexiglas cylinder (24 cm in height, 12 cm in diameter) with a water depth of 20 cm ($25 \pm 2^{\circ}$C). The animals that stopped struggling up to 2 s were regarded immobile. The immobility time was recorded. 1 h acclimatization of the mice was prerequisite before test.

2.10. Tail Suspension Test (TST). TST was performed as previously described [18]. Mice were suspended in a position 30 cm high with adhesive cloth at approximately 1 cm from the tail tip. The absence of any limb or body movements was defined as immobility, except those caused by respiration. TST was conducted for 6 min, and the immobility time was recorded. 1 h acclimatization of animals was prerequisite prior to test.

2.11. ELISA. Mouse hypothalamic tissues were collected and disrupted into a suspension, and then, the contents of norepinephrine (NE), dopamine (DA), and serotonin (5-HT) in the supernatant were measured using mouse enzyme-linked immunosorbent assay (ELISA) kits (Thermo Fisher, USA). Optical density (OD) values were measured at 450 nm using a Multiskan Mk3 microplate reader (Thermo Fisher, USA). All experiments were performed in triplicate.

2.12. Dual-Luciferase Reporter Assay. Wild-type (WT) LINC00473 and BDNF 3′UTR sequences with the binding site of miR-497-5p were cloned into pGL3 vector (Promega, Madison, WI, USA) to form LINC00473-WT and BDNF-WT. The mutant (MUT) LINC00473 and BDNF 3′UTR sequences with mutations in the potential binding sites of miR-497-5p were also synthesized to generate LINC00473-MUT and BDNF-MUT. Lipofectamine 3000 (Invitrogen, Carlsbad, CA, USA) was employed for cell transfection.

2.13. RNA Pull-Down Assay. The bio-probe-NC, bio-miR-497-5p-WT, and bio-miR-497-5p-MUT were synthesized and labeled by Biotin RNA Labeling Mix (Roche). HEK-293T cells were lysed by cell lysis buffer (Sigma). Then, cell lysates were incubated with biotin-labelled RNAs and streptavidin-agarose beads (Invitrogen). The enrichment of LINC00473 was measured using RT-qPCR analysis.

2.14. RIP Assay. Briefly, cell lysates was gained with the usage of a RIP kit (Geneseed, Guangzhou, China). Then, the magnetic beads conjugated with anti-Ago2 or anti-IgG were cultured in cell lysates. Finally, whether LINC00473 is bound to miR-497-5p was disclosed via determining the abundance of miR-497-5p and LINC00473 using RT-qPCR.

2.15. Western Blot. Total cell protein was extracted with RIPA lysate, and the protein concentration was determined using a BCA protein assay kit (Thermo Fisher, USA) in a microplate reader. After denaturation for 10 min with the addition of loading buffer, 50 μg of protein samples was subjected to SDS-PAGE and transferred onto PVDF membranes. The membrane was blocked with blocking solution (5% nonfat dry milk) for 2 h and subsequently washed three times using TBST. Specific primary and secondary antibodies were next added separately, followed by incubation on a shaker. ImageJ software was applied to detect and analyze the gray values of protein bands on the membrane. The primary antibodies included β-actin (1 : 1000 dilution, Abcam, ab8227, Cambridge, UK) and BDNF (1 : 1000 dilution, ab108319, Abcam).

2.16. Statistical Analysis. Data from the repeated three times were analyzed and compared using Student's *t*-test or analysis of variance, with statistically significant difference of $P < 0.05$.

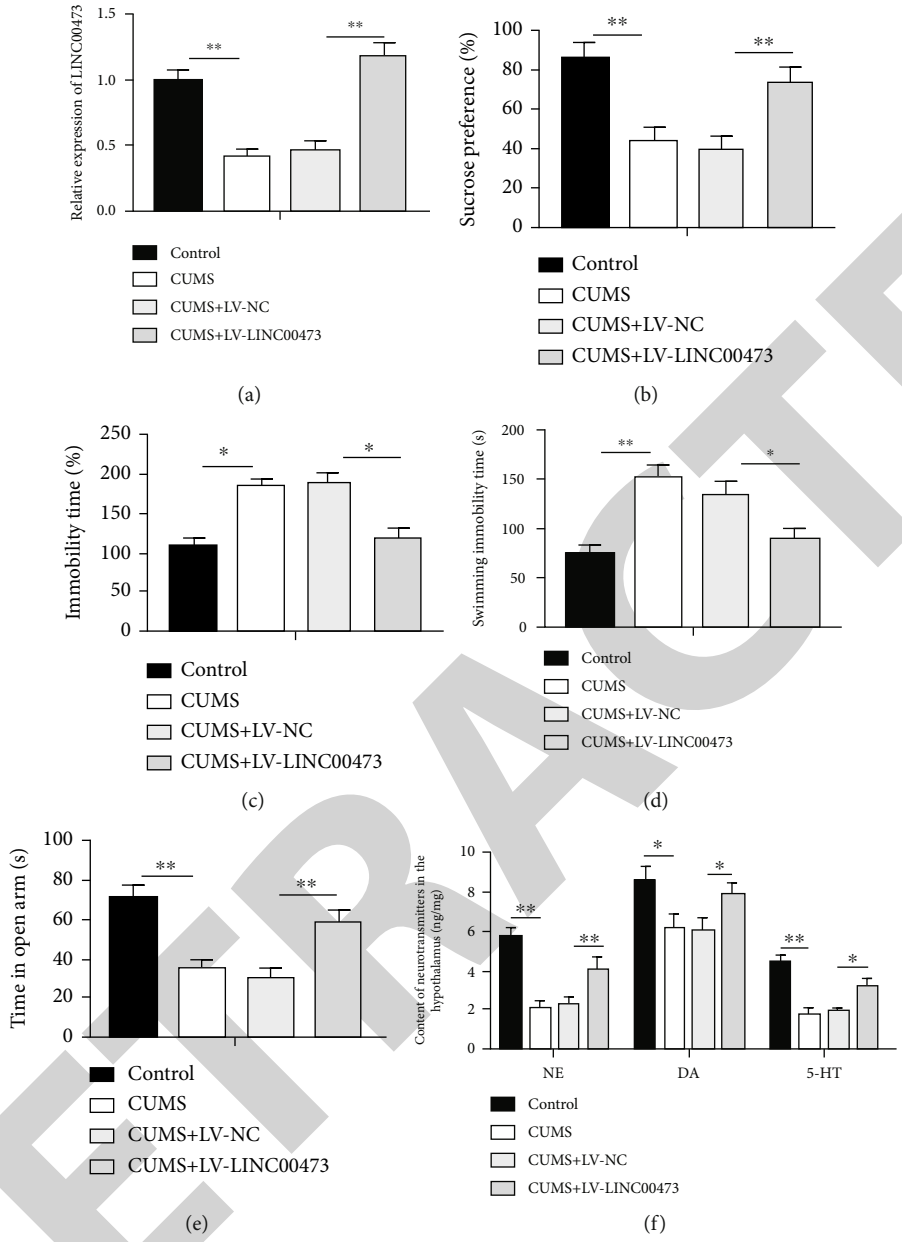

Figure 2: LINC00473 upregulation could improve CUMS-induced depression-like behaviors. LV-LINC00473 was injected into the hippocampal region of the CUMS-induced female mice. (a) The level of LINC00473 was tested by RT-qPCR. (b) Sucrose preference was measured by SPT test. (c) Immobility time was determined by TST. (d) Cold water immobility time in mice was determined by FST. (e) The time in open arm was calculated by EPM. (f) The concentration of hypothalamic neurotransmitters was measured by ELISA. $N = 3$; $^{*}P < 0.05$ and $^{**}P < 0.01$.

3. Results

3.1. CUMS-Induced LINC00473 Downregulation in the Hippocampal Region of the Female Mice. To study on the potential action of LINC00473 on the mice with depression, the expression of LINC00473 was detected in the mice induced by CUMS. The data showed that LINC00473 expression was gradually decreased in a time-dependent manner in CUMS female mice (Figure 1(b)), while there was no significant change in CUMS male mice (Figure 1(a)). Overall, LINC00473 was decreased in depressed female mice.

3.2. LINC00473 Upregulation Could Improve CUMS-Induced Depression-Like Behaviors. To further investigate the effect of LINC00473 overexpression on the depression-like behaviors of CUMS female mice, LV-LINC00473 lentiviral vector and its negative control were injected into the mouse hippocampal region for 48 h, respectively. RT-qPCR analysis indicated that LINC00473 was markedly retarded in CUMS-caused depressed mice, which was upregulated by LV-LINC00473 injection (Figure 2(a)). In addition, the results of behavioral test revealed that sucrose preference (Figure 2(b)) and time in open arm (Figure 2(e)) were dramatically increased, and

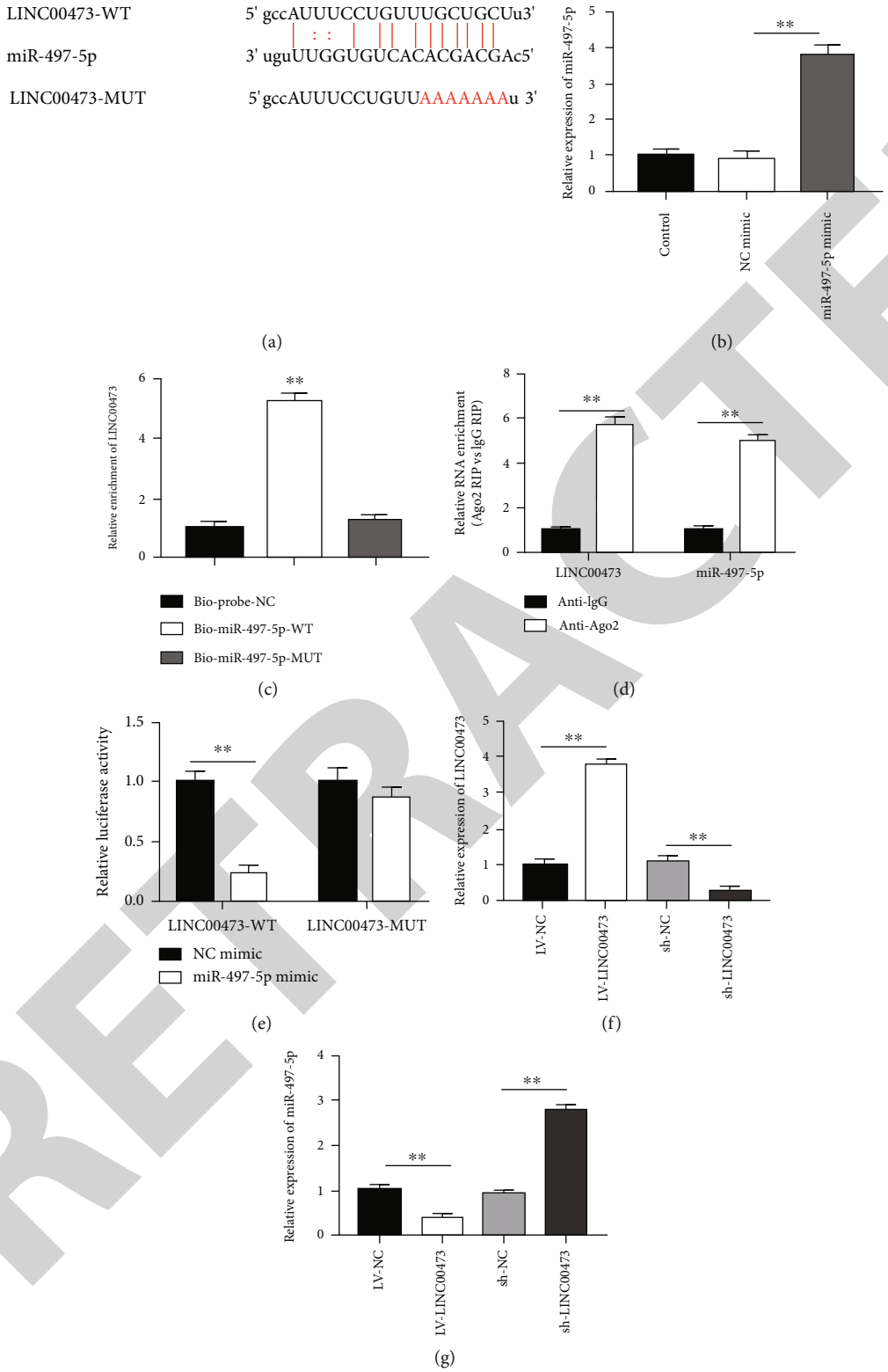

Figure 3: LINC00473 directly bound to miR-497-5p. (a) The predicted binding sites of miR-497-5p and LINC00473. (b) The overexpression efficiency of miR-497-5p mimic was verified. (c–e) RNA pull-down, dual-luciferase reporter, and RIP assays were used to examine relationship between miR-497-5p and LINC00473. (f) LINC00473 level examination in HEK-293T cells after transfection with LV-LINC00473 and sh-LINC00473. (g) miR-497-5p level determination in HEK-293T cells after transfection with LV-LINC00473 and sh-LINC00473. $N = 3$; $^{**}P < 0.01$.

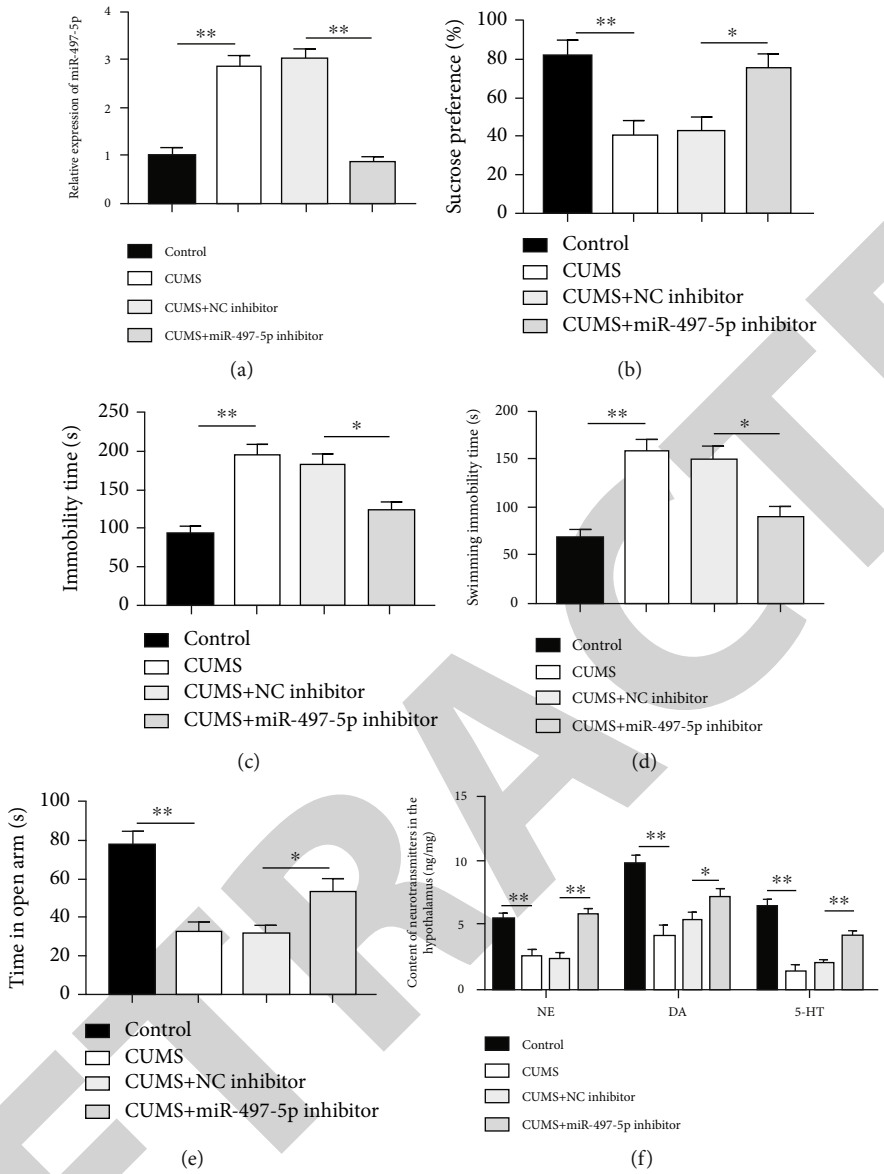

Figure 4: Downregulation of miR-497-5p alleviated depression-like behaviors induced by CUMS in female mice. The viral vectors containing miR-497-5p inhibitor were injected into the hippocampal region of the CUMS-induced female mice. (a) The miR-497-5p level was tested by RT-qPCR. (b) Sucrose preference tested in SPT. (c) Immobility time tested in TST. (d) Water immobility time tested in FST. (e) The time in open arm was tested by EPM. (f) The hypothalamic neurotransmitter concentration measurement. $N = 3$; $^{*}P < 0.05$ and $^{**}P < 0.01$.

immobility time of TST (Figure 2(c)) and the resting time in FST (Figure 2(d)) were markedly decreased compared with the CUMS-induced female mice. Moreover, the contents of neurotransmitters were obviously decreased in the hypothalamus of CUMS mice, which were rescued after LINC00473 overexpression (Figure 2(f)).

3.3. LINC00473 Directly Bound to miR-497-5p. Online bioinformatics databases (https://starbase.sysu.edu.cn/) showed that miR-497-5p was a putative target of LINC00473 (Figure 3(a)). As shown in Figure 3(b), we observed the successful overexpression efficiency of miR-497-5p mimic in HEK-293T cells. Our data revealed that LINC00473 was significantly pulled down by bio-miR-497-5p-WT (Figure 3(c)). Moreover, we found that the levels of LINC00473 and miR-497-5p were markedly increased in Ago2 precipitates compared with IgG (Figure 3(d)). The results from dual-luciferase reporter assay indicated that the luciferase activity was significantly suppressed in the LINC00473-WT group, but not in LINC00473-MUT group (Figure 3(e)). In addition, the data elaborated that LINC00473 was boosted by transfection with LV-LINC00473 and downregulated by transfection with sh-LINC00473 (Figure 3(f)). In addition, the results displayed that LINC00473 upregulation significantly suppressed miR-497-5p expression, while LINC00473 inhibition memorably elevated miR-497-5p expression (Figure 3(g)).

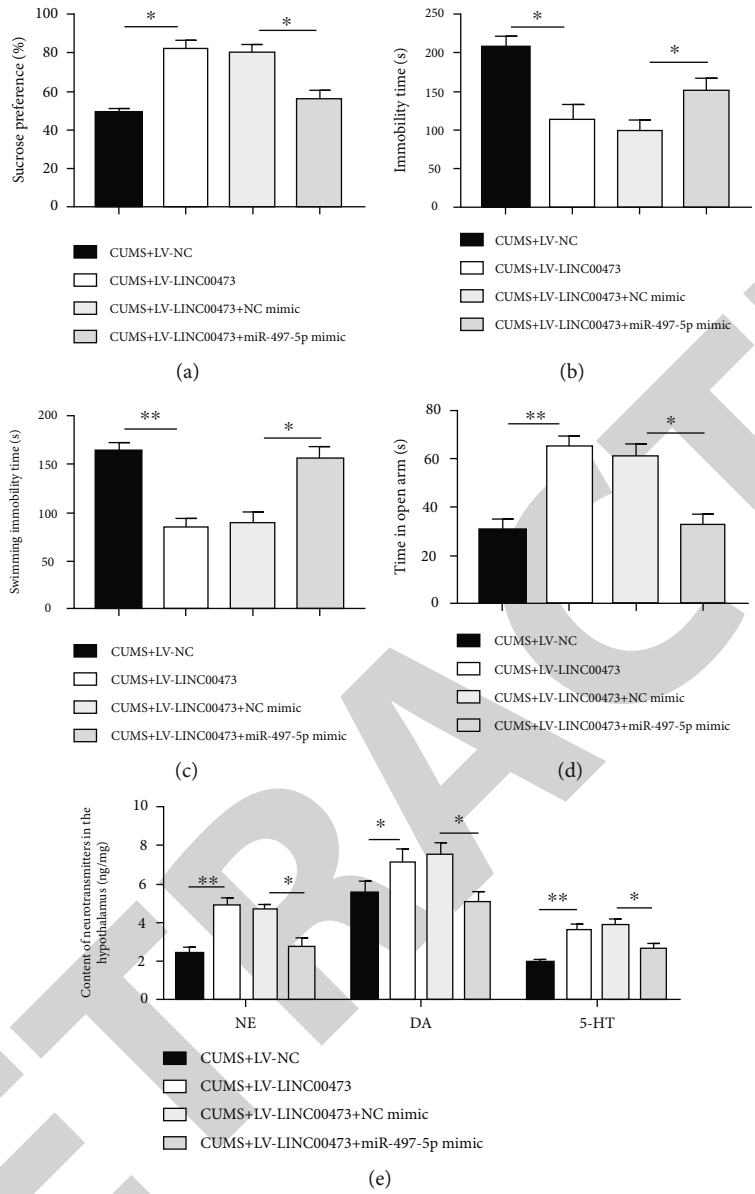

Figure 5: miR-497-5p upregulation could harbor the improving effects of LINC00473 overexpression on depression. LV-LINC00473 was coinjected with miR-497-5 mimic lentiviral vector into the hippocampal region of the CUMS-induced female mice. (a) Sucrose preference in SPT. (b) Immobility time of mice in TST. (c) Cold water immobility time of mice in FST. (d) Open arm time in EPM. (e) ELISA was used to detect the concentration of the hypothalamic neurotransmitters. $N = 3$; $^{*}P < 0.05$ and $^{**}P < 0.01$.

3.4. Inhibition of miR-497-5p Alleviated Depression-Like Behaviors Induced by CUMS in Female Mice. Although a research has shown that knockdown of miR-497 could improve rat depression [19], the detailed action of miR-497-5p in depression remains to be elucidated. Subsequently, viral vectors containing miR-497-5p inhibitor were injected into the hippocampal region of CUMS-induced mice. We found that miR-497-5p was prominently reduced after viral vector injection of miR-497-5p downregulation (Figure 4(a)). Moreover, miR-497-5p inhibitor alleviated depression-like behaviors induced by CUMS, including sucrose preference (Figure 4(b)), immobility time (Figure 4(c)), swimming immobility time (Figure 4(d)), and time in open arm (Figure 4(e)). Furthermore, the contents of NE, DA, and 5-HT reduced by CUMS treatment in female mice were upregulated by downregulation of miR-497-5p (Figure 4(f)).

3.5. miR-497-5p Upregulation Could Reverse the Improving Effects of LINC00473 Overexpression on Depression. To explore whether LINC00473 exerts its function by regulating miR-497-5p, rescue experiments were performed via coinjecting with LV-LINC00473 and miR-497-5 mimic into the hippocampal region of CUMS-induced female mice. We found that increase of miR-497-5p prominently reversed the boosting influences of LINC00473 overexpression on sucrose preference (Figure 5(a)), open arm time (Figure 5(d)), and hypothalamic neurotransmitter concentration (Figure 5(f)), as well as the inhibitory effects on resting time (Figure 5(b))

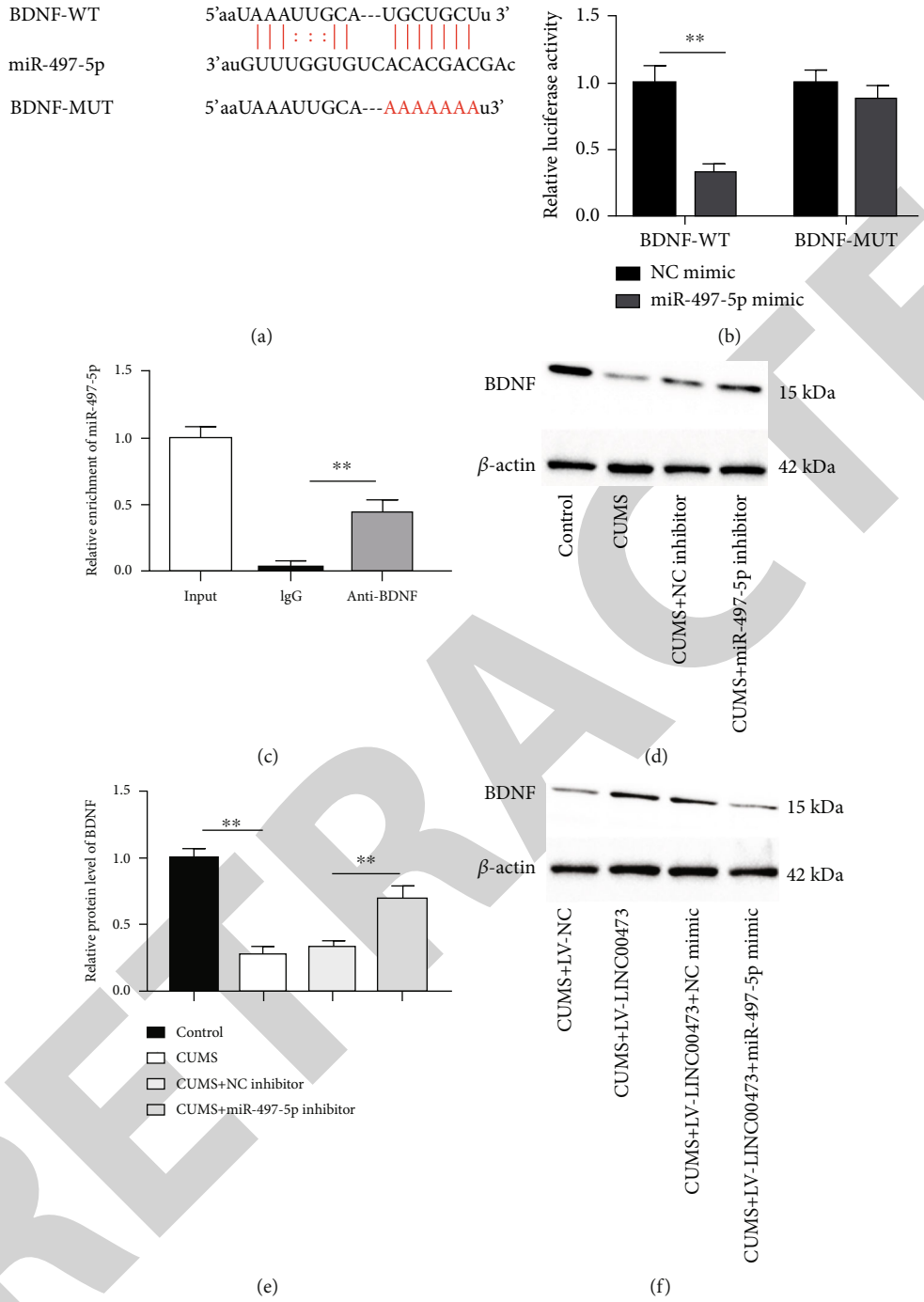

Figure 6: Continued.

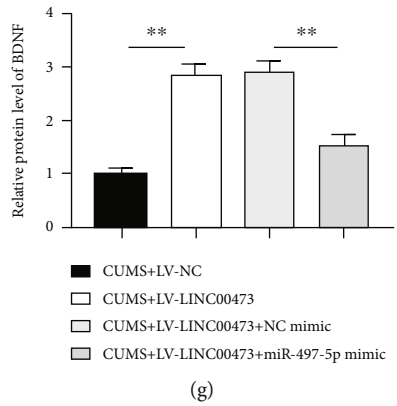

Figure 6: miR-497-5p negatively regulated BDNF expression. (a) The binding sites between BDNF and miR-497-5p were shown. (b and c) Dual-luciferase reporter and RIP assays were used to evaluate the correlation between BDNF and miR-497-5p. (d and e) BDNF protein expression examination in the hippocampus region of mice after miR-497-5p inhibitor injection. (f and g) BDNF protein expression detection in the hippocampus region of mice after coinjection of miR-497-5p mimic and LV-LINC00473. $N = 3$; $^{**}P < 0.01$.

and the cold water time (Figure 5(c)) in CUMS-induced female mice. Taken together, the above findings revealed that miR-497-5p upregulation could block the ameliorative effects of LINC00473 overexpression on depression.

3.6. miR-497-5p Negatively Regulated BDNF Expression. Then, we found that miR-497-5p could bind to BDNF 3′ UTR (Figure 6(a)). The results displayed that miR-497-5p mimic suppressed the luciferase activity in BDNF-WT group, while the luciferase activity showed no obvious change in BDNF-MUT group compared the NC mimic group (Figure 6(b)). RIP results further disclosed that the enrichment of miR-497-5p on BDNF antibody was substantially increased compared with IgG (Figure 6(c)). Moreover, we demonstrated that the protein expression of BDNF was downregulated after CUMS-induced depression in mice, which was partially reversed by miR-497-5p inhibitor (Figures 6(d) and 6(e)). Additionally, miR-497-5p mimic could partially abolish the promotion effect of LINC00473 overexpression on BDNF protein expression in depressed mice (Figures 6(f) and 6(g)).

3.7. BDNF Knockdown Abolished the Impacts of miR-497-5p Inhibitor on Depression. In depth, we investigated the functional role of BDNF in depression. CUMS-induced female mice were injected with miR-497-5p alone or coinjected with miR-497-5p inhibitor and sh-BDNF together. The efficiency of sh-BDNF was detected by western blot, and the data demonstrated that the protein expression of BDNF promoted by miR-497-5p inhibition was suppressed by BDNF knockdown in CUMS-induced mice (Figures 7(a) and 7(b)). Besides, we found that the promotion impacts of miR-497-5p inhibitor on sucrose preference (Figure 7(c)), open arm time (Figure 7(f)), and hypothalamic neurotransmitter concentration (Figure 7(g)) were harbored by BDNF downregulation in CUMS-induced female mice. Moreover, our results also suggested that the inhibition effects of miR-497-5p downregulation on resting time (Figure 7(d)) and the cold water resting time (Figure 7(e)) were partially blocked by BDNF knockdown in depressed mice.

4. Discussion

Depression is a commonly affective disorder with more than 60% of patients suffering from some degree of undertreatment and deterioration. Studies have proposed that biomarkers were the first choice for screening subtypes of psychiatric disorders [20]. Accumulating evidence indicated that in-depth exploration of the underlying molecular mechanisms of depression development contributed to search for new therapeutic biomarkers to inhibit this psychiatric disorder. Recently, the functional roles and actions of lncRNAs in depression have attracted the attention of researchers. For example, lncRNAGAS5 level was facilitated in depression-like behavioral mice, and GAS5 downregulation suppressed the contents of the inflammatory factors in depression mice [21]. In addition, highly expressed lncRNA MIR155HG was observed in CUMS-induced mice, which might exert protective effects on depression-like behaviors [7]. In the reported studies, LINC00473 downregulation facilitated trophoblast cell migration and invasion in preeclampsia [22]. Besides, LINC00473 could promote proliferation, migration, invasion, and inhibition of apoptosis of non-small-cell lung cancer cells by acting as a sponge of miR-497-5p [23].A study found that LINC00473 was dramatically repressed in the brain of depressed female patients [24]. Consistently, we discovered that LINC00473 was markedly reduced in the hippocampal region of CUMS-induced female mice, but not in male mice. Interestingly, overexpression of LINC00473 ameliorated depression in depressed female mice via upregulating proportion of sucrose consumed, time in open arm, and the contents of neurotransmitter including NE, DA, and 5-HT in the mouse hypothalamus, as well as upregulating immobility time and cold water immobility time.

Multiple miRNAs have been reported to be enriched in the central nervous system or aberrantly expressed in the brain. The specificity of certain neuronal miRNAs is due to their localization in the synaptic interstitial compartment, which was related to their ability to regulate the translation of their target mRNAs [25]. Increasing researches disclosed that many candidate miRNAs were found to potentially

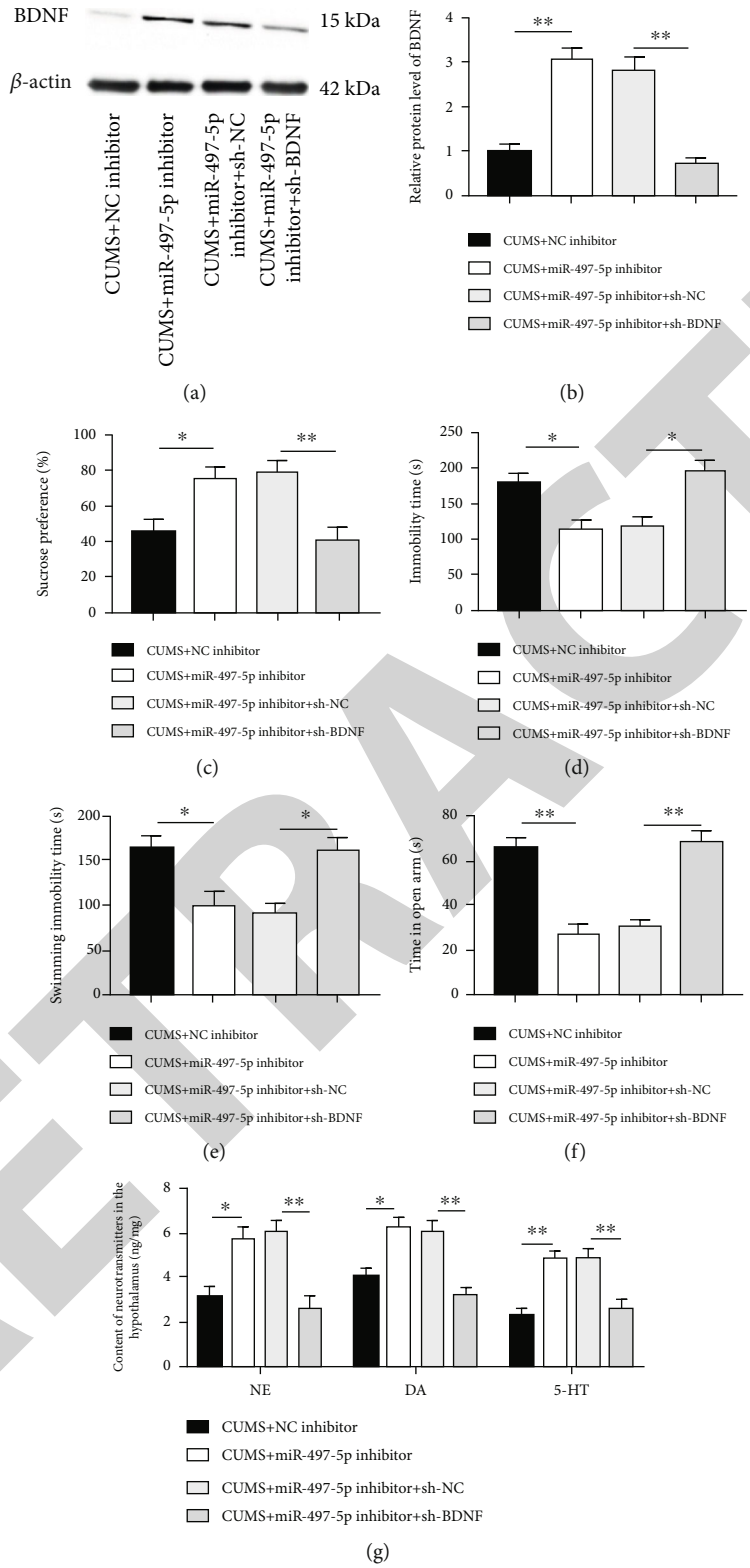

Figure 7: BDNF knockdown abolished the impacts of miR-497-5p inhibitor on depression. The hippocampal region of CUMS-induced depressed female mice was injected with miR-497-5p inhibitor alone or coinjected with miR-497-5p inhibitor and sh-BDNF lentiviral vector together. (a and b) The protein expression of BDNF in the hippocampus was tested by western blot. (c–f) Behavioral testing was carried out via evaluating sucrose preference in SPT, immobility time in TST, cold water immobility time in FST, and time in open arm in EPM. (g) The hypothalamic neurotransmitter concentration determination. $N = 3$; $^{*}P < 0.05$ and $^{**}P < 0.01$.

participate in the progression of depression. For example, the research reported that miR-124 was evidently higher in major depressive disorder patients than in healthy controls [25, 26]. The percentage and specificity of distinguishing patients suffering from major depressive disorder and healthy controls were 66.67%. Moreover, a study obtained the elevated miR-124 in depressed mice caused by CUMS, and suppression of miR-124 exhibited ameliorating impacts against depression via regulating SIRT1 [27]. Furthermore, miR-134 could interfere with dendritic spine growth by targeting LIMK-1, and miR-134 was downregulated when neurons were exposed to BDNF [28]. In our study, bioinformatics online tools predicted that LINC00473 might bind to miR-497-5p. Previous studies reported that miR-497-5p was a crucial regulator in inhibiting tumorigenesis, and the aberrant expression of miR-497-5p took part in tumor initiation, cancer cell growth, apoptosis, and invasion [29–32]. More importantly, miR-497 was verified to be increased in the mouse brain after cerebral ischemia, and inhibition of miR-497 could attenuate ischemic cerebral infarction [33]. Moreover, a study results revealed that miR-497 aggravated CUMS-induced depressed rats by modulating FGF2 [33]. More interestingly, LINC00473 was reported to enhance cell proliferation and invasion and inhibit apoptosis of non-small-cell lung cancer cells by sponging miR-497 [23]. However, whether LINC00473 was involved in depression progression in female mice by modulating miR-497-5p level remained uninvestigated. In our present study, we discovered that miR-497-5p could promote the development of depression, and miR-497-5p overexpression abolished the improving effects of LINC00473 upregulation on depression in female mice triggered by CUMS.

BDNF, a growth factor, was confirmed to be implicated in the development and progression of depression. Stress and depression could reduce the expression and function of BDNF in the areas related to depression, such as the PFC and hippocampus, and BDNF was also dramatically augmented in the blood of depressed patients [34]. Polymorphisms of BDNF interacted with estrogen and estrous cycle to influence the role of memory-related signaling systems [35]. The risk of individuals with BDNF mutations suffering from depression was higher than healthy people after exposure to early life stress or trauma. In addition, it has been found that normal BDNF levels contributed to the maintenance of antidepressant effects [36]. Moreover, excessive miR-134 levels inhibited the expression of CREB that could impair memory and plasticity, and the decrease of CREB in transcription factor in turn depressed BDNF expression, suggesting the antagonism effect between miR-134 and BDNF [26].Via bioinformatics analysis, we discovered that miR-497-5p could bind to BDNF and negatively modulated the expression of BDNF. Furthermore, BDNF interference could hinder the ameliorative effect of miR-497-5p inhibition on depression in depressed female mice. Additionally, overexpression of LINC00473 elevated the expression of BDNF via targeting miR-497-5p in female mice induced by CUMS.

In conclusion, we found that LINC00473 was downregulated in the CUMS-induced female mice, and its upregulation could alleviate depressive behaviors in female mice. Besides, LINC00473 showed the protective action on depressive-like behaviors via targeting miR-497-5p to modulate BDNF expression in depressed female mice. These results provided a new underlying mechanism of lncRNAs in the development of depression in females.

Data Availability

All data obtained or analyzed during this research are included in the manuscript.

Ethical Approval

This research was approved by the Binzhou Municipal Youfu Hospital.

Consent

Consent for publication was obtained from each author. All patients had read and signed the informed consent.

Conflicts of Interest

The authors declare that they have no competing interests.

Authors' Contributions

Bo Li designed this study. Hongxia Zhao performed the experimental work and wrote the manuscript. Junxia Sun performed statistical analysis as well as provided the figures. All authors read and approved the final manuscript.

References

[1] N. A. Nuñez, B. Joseph, M. Pahwa et al., "Augmentation strategies for treatment resistant major depression: a systematic review and network meta-analysis," *Journal of Affective Disorders*, vol. 302, pp. 385–400, 2022.

[2] R. C. Kessler, P. Berglund, O. Demler, R. Jin, K. R. Merikangas, and E. E. Walters, "Lifetime prevalence and age-of-onset distributions of DSM-IV disorders in the national comorbidity survey replication," *Archives of General Psychiatry*, vol. 62, no. 6, pp. 593–602, 2005.

[3] D. Warden, A. J. Rush, M. H. Trivedi, M. Fava, and S. R. Wisniewski, "The STAR∗D project results: a comprehensive review of findings," *Current Psychiatry Reports*, vol. 9, no. 6, pp. 449–459, 2007.

[4] S. L. Dubovsky, B. M. Ghosh, J. C. Serotte, and V. Cranwell, "Psychotic depression: diagnosis, differential diagnosis, and treatment," *Psychotherapy and Psychosomatics*, vol. 90, no. 3, pp. 160–177, 2021.

[5] P. Gdańska, E. Drozdowicz-Jastrzębska, B. Grzechocińska, M. Radziwon-Zaleska, P. Węgrzyn, and M. Wielgoś, "Anxiety and depression in women undergoing infertility treatment," *Ginekologia Polska*, vol. 88, no. 2, pp. 109–112, 2017.

[6] B. Labonté, O. Engmann, I. Purushothaman et al., "Sex-specific transcriptional signatures in human depression," *Nature Medicine*, vol. 23, no. 9, pp. 1102–1111, 2017.

[7] Z. Huan, Z. Mei, H. Na et al., "lncRNA MIR155HG alleviates depression-like behaviors in mice by regulating the miR-155/

Hindawi
Computational and Mathematical Methods in Medicine
Volume 2023, Article ID 9790315, 1 page
https://doi.org/10.1155/2023/9790315

Retraction

Retracted: Effects of Transcranial Magnetic Stimulation Combined with Computer-Aided Cognitive Training on Cognitive Function of Children with Cerebral Palsy and Dysgnosia

Computational and Mathematical Methods in Medicine

Received 12 December 2023; Accepted 12 December 2023; Published 13 December 2023

This article has been retracted by Hindawi, as publisher, following an investigation undertaken by the publisher [1]. This investigation has uncovered evidence of systematic manipulation of the publication and peer-review process. We cannot, therefore, vouch for the reliability or integrity of this article.

Please note that this notice is intended solely to alert readers that the peer-review process of this article has been compromised.

Wiley and Hindawi regret that the usual quality checks did not identify these issues before publication and have since put additional measures in place to safeguard research integrity.

We wish to credit our Research Integrity and Research Publishing teams and anonymous and named external researchers and research integrity experts for contributing to this investigation.

The corresponding author, as the representative of all authors, has been given the opportunity to register their agreement or disagreement to this retraction. We have kept a record of any response received.

References

[1] J. Chen, X. Yu, and G. Luo, "Effects of Transcranial Magnetic Stimulation Combined with Computer-Aided Cognitive Training on Cognitive Function of Children with Cerebral Palsy and Dysgnosia," *Computational and Mathematical Methods in Medicine*, vol. 2022, Article ID 5316992, 7 pages, 2022.

Hindawi
Computational and Mathematical Methods in Medicine
Volume 2022, Article ID 5316992, 7 pages
https://doi.org/10.1155/2022/5316992

Research Article

Effects of Transcranial Magnetic Stimulation Combined with Computer-Aided Cognitive Training on Cognitive Function of Children with Cerebral Palsy and Dysgnosia

Jun Chen, Xiaoming Yu, and Guangjin Luo

Department of Rehabilitation, Qingdao Women and Children's Hospital, Qingdao, Shandong 266034, China

Correspondence should be addressed to Jun Chen; jean_ch@sohu.com

Received 28 June 2022; Revised 29 July 2022; Accepted 8 August 2022; Published 26 August 2022

Academic Editor: Min Tang

Objective. This study is aimed at researching transcranial magnetic stimulation (TMS) effects combined with computer-aided cognitive training (CACT) on cognitive function of children suffering from cerebral palsy and dysgnosia. *Methods*. From December 2019 to October 2021, 86 children with cerebral palsy and dysgnosia who were treated at our hospital were recruited and assigned into observation and control groups ($n = 43$, each) using the random number table technique. The observation group received TMS combined with CACT (TMS+CACT), whereas the control group received only TMS. Chinese Wechsler Young Children Scale of Intelligence (C-WYCSI) and Chinese-Wechsler Intelligence Scale for Children (C-WISC) were used to evaluate the intelligence level of the two groups; Gross Motor Function Measure-88 (GMFM-88) of Fudan Chinese version was employed for evaluating the gross motor function of the two groups; a comparison was drawn among the two groups for the cerebral hemodynamic parameters before and after the treatment. *Results*. For young children, the verbal intelligence quotient (VIQ) scores at 6 and 12 weeks of treatment in the observation group were increased when compared to those in the control group (48.91 ± 3.70 vs. 47.32 ± 3.33, 54.25 ± 4.46 vs. 49.48 ± 3.36), and the observation group's performance intelligence quotient (PIQ) score at 12 weeks of treatment was higher as to that of the control group (65.38 ± 4.23 vs. 62.81 ± 4.74, all $P < 0.05$). For older age children, the observation group's VIQ and PIQ scores were greater than the control group's at 6 and 12 weeks of treatment, with statistical significance (63.80 ± 3.76 vs. 59.50 ± 5.32, 74.64 ± 12.04 vs. 65.08 ± 6.30; 63.91 ± 5.96 vs. 58.42 ± 3.70, 72.73 ± 5.06 vs. 66.42 ± 5.93; all $P < 0.05$). The GMFM-88 scale scores in both groups were increased after 6 and 12 weeks of treatment. After treatment for 12 weeks, the observation group's A-E scores were greater than those of the control group (all $P < 0.05$). The peak systolic velocity (V_s), end-diastolic velocity (V_d), and mean velocity (V_m) at the anterior cerebral artery (ACA), middle cerebral artery (MCA), and posterior cerebral artery (PCA) in the observation group were dramatically increased than those in the control group (all $P < 0.05$) after 12 weeks of treatment. *Conclusion*. TMS+CACT can effectively improve the intelligence level, cognitive ability, gross motor function, and cerebral blood flow of children suffering from cerebral palsy and intellectual disability.

1. Introduction

Cerebral palsy is a common pediatric nervous system disorder that can lead to disability and deformity. Dysgnosia is a common complication of cerebral palsy. According to relevant research, the incidence of cerebral palsy complicated with dysgnosia is as high as 55%~65%. The more serious the condition of children is, the more likely they are to be complicated with dysgnosia. Children with cerebral palsy and dysgnosia often show motor dysfunction, intellectual developmental disorder, and cognitive dysfunction, which can seriously affect their physical health and quality of life [1, 2]. Currently, no effective method for treating cerebral palsy exists. The key to the treatment of cerebral palsy with dysgnosia is to improve the level of children's intelligence, motor, and cognitive function. Routine rehabilitation intervention is often adopted in the clinical treatment of cerebral palsy with dysgnosia, but the treatment effect is not evident. Repetitive transcranial magnetic stimulation (rTMS) is a novel type of neuroelectrophysiological technology, which

is painless, noninvasive, easy to operate, and very safe. It can generate a certain intensity of time-varying magnetic field in a specific part outside the skull, induce an electric field in the brain, cause induced current, stimulate the nearby nerve tissue, and further affect the brain metabolism and the physiological hormone of neuroelectric activity. Currently, this technology has been widely used in the fields of psychological diseases and nervous system diseases [3, 4]. Cognitive training is a method that specialized doctors are responsible for or using computer platform to complete training items, including attention training, memory training, processing speed training, and flexibility training. It is easy to operate and has good compliance. Computer-aided cognitive training (CACT) is more convenient for children to train at home [5, 6]. The objective of this research was to explore the effects of TMS+CACT on cognitive function of children suffering from cerebral palsy and dysgnosia. The following is the report.

2. Materials and Methods

2.1. General Data. From December 2019 to October 2021, 86 children with cerebral palsy complicated by dysgnosia were treated in our hospital as outpatients or inpatients and were registered and randomized into observation and control groups utilizing the random number table method, having 43 cases in every group. The observation group had 25 males and 18 females; their ages ranged from 3 years and 11 months to 7 years, with an average of 67.07 ± 7.89 months; dysgnosia grade: mild in 17 cases, moderate in 20 cases, and severe in 6 cases; clinic classification of cerebral palsy: 33 cases of spastic type, 7 cases of mixed type, 2 cases of dyskinetic type, and 1 case of ataxic type. There were 22 males and 21 females in the control group; with an average of 68.30 ± 12.76 months, their ages were from 3 years and 11 months to 8 years; dysgnosia grade: mild in 18 cases, moderate in 18 cases, and severe in 7 cases; clinic classification of cerebral palsy: 30 cases of spastic type, 9 cases of mixed type, 3 cases of dyskinetic type, and 1 case of ataxic type. The general data of the two groups were comparable (all $P > 0.05$). The Hospital Ethics Committee gave its approval to this study. Diagnostic criteria: the diagnostic criteria and clinic classification of cerebral palsy were in line with the standards formulated by the Compilation Committee of *Guidelines for Rehabilitation and Treatment of Cerebral Palsy in China* [7] and conform to the classification guidelines for cerebral palsy in the *World Health Organization International Classification of Functioning, Disability, and Health* [8]. The diagnosis of dysgnosia conformed to the diagnostic criteria of intellectual developmental disorder in the *International Classification of Diseases 11th Revision (ICD-11)* [9]. Inclusion criteria: (1) all met the Western and Chinese diagnostic criteria; (2) age ≥ 3 years and 11 months; (3) the child was conscious and his/her vital signs were stable; (4) the study was voluntarily undertaken by all of the enrolled children and their families. Exclusion criteria: (1) children with central brain injury caused by progressive diseases such as cerebral edema and viral encephalitis; (2) children with water and electrolyte disorders; (3) children with epilepsy; (4) children with severe lung infection; (5) children with systemic immune system diseases; and (6) children suffering from extreme organ diseases such as heart, liver, and kidney dysfunctions.

2.2. Therapies. Both groups received routine rehabilitation training. The TMS+CACT was administered to the observation group, and the control group got administered by TMS only. TMS: the children were treated with TMS instrument with positioning treatment cap. The stimulation frequency was adjusted to 5-10 Hz, the stimulation intensity was 80%-100% resting state motion threshold (RMT), and the stimulation sites were F3 and F4 of EEG 10-20 system. The treatment was given once daily for 20 minutes, 5 times a week, and 20 times as a course. The treatment lasted for 3 courses. CACT: computer interactive table rehabilitation cognitive training software and MindWave Mobile Core attention training software were used to train the children's memory, executive, attention, and spatial vision abilities. The training content included (1) attention training: selecting the picture that was consistent with the reference picture from the screen pictures and selecting the picture from simple to complex; (2) memory training: including graphic memory and detail memory, memorizing screen pictures or texts, and answering relevant questions; (3) time and place orientation training: children are trained according to instructions or scene graphics; and (4) visual space and executive function training: in different content and different number of picture groups, selecting rotated reference pictures as visual space function training, and stick figure drawing as executive function training. In accordance with the type and severity of cognitive impairment, different combinations were used to conduct cognitive function training for patients; the training was provided once daily for 30 minutes, 5 times a week, while the training lasted for 12 weeks.

2.3. Observational Indexes. (1) Intelligence level: before and after treatment, the intelligence level of the younger children (3 years and 11 months to 6 years old) was evaluated by the Chinese Wechsler Young Children Scale of Intelligence (C-WYCSI) [10], while that of older children (6 to 16 years old) was assessed by Chinese-Wechsler Intelligence Scale for Children (C-WISC) [11]. Both sets of intelligence assessment tools had high reliability and validity. Each set of intelligence scale included two parts: speech and operation, and consists of 11 subitems, such as picture vocabulary, arithmetic, picture generalization, comprehension, animal laying eggs, picture filling, maze, visual analysis, wood block pattern, and geometric figure. The results of intelligence assessment include verbal intelligence quotient (VIQ) and performance intelligence quotient (PIQ), which are completed by professional testers in the Neurorehabilitation Department of the hospital. (2) Gross motor ability: before and after treatment, the gross motor function was evaluated by GMFM-88 Scale of Fudan Chinese version [12]. The scale had 88 items, which were distributed in 5 functional areas: (A) lying motion and turning over (17 items); (B) sitting motion (20 items); (C) crawling and kneeling motion (14

items); (D) standing (13 items); and (E) walking, running, and jumping (24 items). The score of each item was 0~3 points according to the degree of completion, and score for each functional area was obtained. The greater the child's gross motor performance, the higher the score. In order to reduce the error, the same doctor conducted blind evaluation before and after the treatment. (3) Comparison of the two groups' cerebral hemodynamic parameters before and after the treatment: color Doppler ultrasound was employed to evaluate peak systolic velocity (V_s), end-diastolic velocity (V_d), and mean velocity (V_m) at the anterior cerebral artery (ACA), middle cerebral artery (MCA), and posterior cerebral artery (PCA) before and after treatment in both groups.

2.4. Statistical Methods. The data were analyzed and processed using SPSS 20.0 statistical software. $\bar{x} \pm s$ was used to represent the measurement data. The intergroup comparison was executed with an independent sample t-test, while the intragroup comparison was done with a paired t-test before and after treatment. The χ^2 test was performed on the counting data, which was expressed as frequency and constituent ratio. A statistically significant difference was represented by $P < 0.05$.

3. Results

3.1. Comparison of C-WYCSI Scores of Young Children between Two Groups before and after Treatment. The VIQ and PIQ scores did not vary significantly among the two groups before treatment (both $P > 0.05$); however, VIQ and PIQ scores were higher in both groups after being treated for 3, 6, and 12 weeks. At 6 and 12 weeks of treatment, the observation group's VIQ score was greater than that of the control group, and the observation group's PIQ score was higher compared to the control group's at 12 weeks of treatment, both with statistical significance (all $P < 0.05$, Table 1).

3.2. Comparison of C-WISC Scores of the Older Children between Two Groups before and after Treatment. The VIQ and PIQ scores did not change significantly among the two groups prior to treatment (both $P > 0.05$). However, at 3, 6, and 12 weeks of treatment, the scores for VIQ and PIQ in the observation group and PIQ in the control group increased. After receiving treatment for 6 and 12 weeks, the control group's VIQ score improved. At 6 and 12 weeks after treatment, the observation group's VIQ and PIQ scores were greater than those of the control group, with statistical significances (all $P < 0.05$, Table 2).

3.3. Comparison of GMFM-88 Scale Scores between Two Groups before and after Treatment. The exercise ability scores among the two groups prior to treatment did not differ significantly ($P > 0.05$). Exercise ability scores, however, in both groups improved after receiving treatment for 6 and 12 weeks. The observation group's A~E scores were substantially greater than those of the control group following treatment for 12 weeks (all $P < 0.05$, Table 3).

3.4. Comparison of Cerebral Hemodynamic Parameters between Two Groups before and after Treatment. Prior to the treatment, no major differences could be observed among the two groups in the V_s, V_d, and V_m parameters of the ACA, MCA, and PCA (all $P > 0.05$). V_s, V_d, and V_m of ACA, MCA, and PCA in both the groups, however, improved after treatment for 6 and 12 weeks. V_s, V_d, and V_m of ACA, MCA, and PCA in the observation group were considerably greater compared to those in the control group after receiving treatment for 12 weeks (all $P < 0.05$, Table 4).

4. Discussion

Cerebral palsy is a refractory disease with a long course. Children with cerebral palsy often have perceptual, behavioral, sensory, cognitive, and other disorders, as well as varying degrees of mental retardation. If not treated in time, it may lead to lifelong disability and bring heavy burden to the family and society. The clinical treatment of cerebral palsy mostly adopts comprehensive treatment methods including physical therapy and cognitive function training. The working principle of TMS is to send pulse electric current into the coil and then generate pulse magnetic field around the coil. The induced current in the head is generated by the pulse magnetic field, which then activates the associated brain nerve units [13, 14]. The effects of different TMS frequencies on cortical metabolism and cerebral blood flow may vary. High-frequency stimulation can improve cerebral perfusion and local cerebral blood flow and metabolism, while low-frequency stimulation can reduce cerebral blood flow and metabolism. Compared with conventional electrical stimulation, TMS has the following characteristics: (1) easy to achieve deep brain stimulation. Surface electrode stimulation can make the electric field diffused rapidly and could not reach the deep brain. Implanting electrical stimulation cannot be extensively employed in clinical practice because it is traumatic, and the loss of magnetism in bone and muscle is small, due to which TMS can reach deep into the brain. (2) Less discomfort: electrical stimulation has strong stimulation to scalp and skull and can make the person produces strong discomfort. TMS does not act directly on nerves but can stimulate them by producing induced electrical current. The size of the induced current is inversely proportional to the resistance. There is no discomfort when induced current is applied to bone and scalp with large resistance. (3) Not direct contact with human body: magnetic stimulation equipment does not make direct contact with the human body, which can reduce the risk of injury to the human body. CACT began to appear in the 1990s and has been extensively utilized for treating cerebral infarction, brain injury, and other neurological diseases currently. Compared with traditional manual training, CACT has the following advantages. (1) By combining cognitive training with fun animations, it makes the treatment process more interesting through visual, auditory, tactile, and other multimedia technologies, which can better attract the attention and improve the cognitive function of children. (2) Through the standardized intervention method of the programmed training task module, it has strong repeatability and is easy to compare and promote the efficacy. (3) Individualized treatment plans can be developed according to the specific

Table 1: Comparison of C-WYCSI scores of young children between two groups before and after treatment ($\bar{x} \pm s$, points).

Group	VIQ score				PIQ score			
	Before treatment	Treatment for 3 weeks	Treatment for 6 weeks	Treatment for 12 weeks	Before treatment	Treatment for 3 weeks	Treatment for 6 weeks	Treatment for 12 weeks
Observation group ($n = 32$)	42.69 ± 3.65	46.09 ± 3.28[a]	48.91 ± 3.70[a]	54.25 ± 4.46[a]	52.84 ± 4.64	57.16 ± 4.86[a]	60.78 ± 4.18[a]	65.38 ± 4.23[a]
Control group ($n = 31$)	41.71 ± 3.51	44.81 ± 3.35[a]	47.32 ± 3.33[a]	49.48 ± 3.36[a]	52.13 ± 4.11	57.16 ± 3.48[a]	59.52 ± 3.33[a]	62.81 ± 4.74[a]
t value	1.083	1.542	1.783	4.778	0.646	0.005	1.327	2.269
P value	0.283	0.128	0.080	<0.001	0.521	0.996	0.190	0.027

Note: compared with before treatment, [a]$P < 0.05$.

Table 2: Comparison of C-WISC scores of the older children between two groups before and after treatment ($\bar{x} \pm s$, points).

Group	VIQ score				PIQ score			
	Before treatment	Treatment for 3 weeks	Treatment for 6 weeks	Treatment for 12 weeks	Before treatment	Treatment for 3 weeks	Treatment for 6 weeks	Treatment for 12 weeks
Observation group ($n = 11$)	51.55 ± 2.66	57.55 ± 4.08[a]	63.82 ± 3.76[a]	74.64 ± 12.04[a]	53.82 ± 4.53	60.55 ± 4.78[a]	63.91 ± 5.96[a]	72.73 ± 5.06[a]
Control group ($n = 12$)	50.92 ± 6.76	55.33 ± 5.87	59.50 ± 5.32[a]	65.08 ± 6.30[a]	53.25 ± 2.86	56.58 ± 3.34[a]	58.42 ± 3.70[a]	66.42 ± 5.93[a]
t value	0.298	1.040	2.228	2.414	0.363	2.320	2.681	2.732
P value	0.770	0.310	0.037	0.025	0.721	0.031	0.014	0.012

Note: compared with before treatment, [a]$P < 0.05$.

conditions of children. Real-time data analysis feedback can also be carried out in the training process, which can effectively stimulate the training enthusiasm of children and is conducive to follow-up rehabilitation.

TMS combined with CACT was utilized for treating the observation group in the present study. The observation group's VIQ score was greater than the control group's at 6 and 12 weeks, and the observation group's PIQ score was higher than that of the control group at 12 weeks, according to the results. At 6 and 12 weeks following treatment, the older children in the observation group had superior VIQ and PIQ scores than the control group. The observation group's scores of the A~E item on the GMFM-88 scale were greater than the control group's after 12 weeks of treatment, showing that TMS+CACT can successfully enhance the intelligence level and motor function of children suffering from cerebral palsy complicated by dysgnosia. Intracranial blood flow in children with brain injury is characterized by low speed and high resistance, showing sustained hypoperfusion and low circulation, which can affect the continued brain development of infants and young children. TMS can effectively improve the brain tissue perfusion in children with brain injury and promote their neuropsychological development [15]. According to relevant studies, TMS can effectively improve the motor function of children suffering from cerebral palsy. In other studies, TMS was applied to children with dysgnosia and showed significant effects [16]. Cognitive training can enhance synaptic efficiency and promote neural function reorganization, and children can improve their cognitive ability through repetitive exercises [17]. In the present study, the combined application of TMS and CACT further improved the children's intelligence, motor ability, and cognitive ability. TMS+CACT can effectively expand the cerebral vascular microcirculation, stimulate the activity of neurons and cells in the brain, and improve the intelligence and motor ability of children. TMS+CACT can effectively regulate the levels of serum markers related to cerebral nerve function in children. The stimulation coil of TMS instrument can generate the corresponding magnetic field, and the magnetic field through the skull will generate the corresponding induction current and finally play the role of regulating local neurons, which further promotes the recovery of brain nerve.

Dysgnosia in children with cerebral palsy is mostly caused by brain injury. Abnormal cerebral blood flow parameters can reflect the severity of brain injury and affect intellectual development [18, 19]. According to relevant studies, children with cerebral palsy with cerebral microcirculation disorders have slow cerebral artery blood flow and increased vascular resistance, which further influences dysgnosia [20]. Cerebral blood flow velocity is closely related to changes in local cerebral blood flow. Peak flow velocity and average flow velocity can be regarded as relative indicators of cerebral blood flow, and average flow velocity can reflect the degree of cerebrovascular filling. At 6 and 12 weeks of treatment, V_s, V_d, and V_m of ACA, MCA, and PCA improved in both groups. V_s, V_d, and V_m of ACA, MCA, and PCA in the observation group were considerably greater compared to those in the control group after treatment for 12 weeks (all $P < 0.05$). This indicates that repeated TMS combined with CACT can effectively improve cerebral blood flow, cerebral blood flow microcirculation disorder,

Table 3: GMFM-88 scores before and after treatment ($\bar{x} \pm s$, points).

Group	A				B				C				D				E			
	Before treatment	Treatment for 3 weeks	Treatment for 6 weeks	Treatment for 12 weeks	Before treatment	Treatment for 3 weeks	Treatment for 6 weeks	Treatment for 12 weeks	Before treatment	Treatment for 3 weeks	Treatment for 6 weeks	Treatment for 12 weeks	Before treatment	Treatment for 3 weeks	Treatment for 6 weeks	Treatment for 12 weeks	Before treatment	Treatment for 3 weeks	Treatment for 6 weeks	Treatment for 12 weeks
Observation group ($n = 34$)	32.84 ± 3.29	36.37 ± 2.84^a	41.55 ± 2.65^a	50.12 ± 4.60^a	16.84 ± 1.09	22.47 ± 2.51^a	28.49 ± 2.55^a	35.30 ± 3.20^a	6.53 ± 2.26	9.49 ± 2.11^a	13.51 ± 2.32^a	17.21 ± 1.58^a	5.00 ± 1.29	8.28 ± 2.25^a	11.44 ± 2.46^a	16.65 ± 3.65^a	2.74 ± 0.95	4.63 ± 1.23^a	6.51 ± 1.47^a	9.23 ± 2.38^a
Control group ($n = 43$)	32.56 ± 2.93	37.21 ± 2.53^a	40.81 ± 2.75^a	44.23 ± 2.83^a	16.51 ± 1.20	19.98 ± 2.27^a	25.00 ± 2.80^a	30.74 ± 4.21^a	6.30 ± 1.39	6.88 ± 1.33	9.37 ± 1.80^a	13.28 ± 4.28^a	5.21 ± 1.30	6.95 ± 1.09^a	8.14 ± 1.34^a	10.95 ± 2.48^a	2.65 ± 0.92	3.65 ± 0.92^a	4.53 ± 1.16^a	6.60 ± 1.76^a
t value	0.415	1.444	1.277	7.141	1.316	4.818	6.038	5.650	0.575	6.849	9.236	5.644	0.749	3.477	7.728	8.468	0.460	4.155	6.918	5.822
P value	0.679	0.152	0.205	<0.001	0.192	<0.001	<0.001	<0.001	0.567	<0.001	<0.001	<0.001	0.456	0.001	<0.001	<0.001	0.647	<0.001	<0.001	<0.001

Note: compared with before treatment, $^aP < 0.05$. A: lying motion and turning over; B: sitting motion; C: crawling and kneeling motion; D: standing; E: walking, running, and jumping.

Table 4: Comparison of cerebral hemodynamic parameters between two groups before and after treatment ($\bar{x} \pm s$).

Group	ACA				MCA				PCA			
	Before treatment	Treatment for 3 weeks	Treatment for 6 weeks	Treatment for 12 weeks	Before treatment	Treatment for 3 weeks	Treatment for 6 weeks	Treatment for 12 weeks	Before treatment	Treatment for 3 weeks	Treatment for 6 weeks	Treatment for 12 weeks
V_s												
Observation group ($n = 34$)	60.20 ± 8.34	67.33 ± 5.23[a]	74.59 ± 5.40[a]	82.90 ± 7.93[a]	69.23 ± 6.98	76.55 ± 5.28[a]	82.38 ± 4.90[a]	89.75 ± 7.20[a]	52.31 ± 4.39	56.87 ± 4.43[a]	60.47 ± 4.43[a]	66.63 ± 4.79[a]
Control group ($n = 43$)	58.39 ± 5.81	64.60 ± 5.18[a]	69.69 ± 5.18[a]	76.65 ± 7.55[a]	68.14 ± 4.74	74.06 ± 4.69[a]	79.44 ± 4.42[a]	84.29 ± 5.23[a]	51.23 ± 4.02	55.56 ± 3.11[a]	59.54 ± 3.16[a]	64.59 ± 3.94[a]
t value	1.168	2.437	4.295	3.741	0.852	2.319	2.924	4.026	1.189	1.584	1.117	2.156
P value	0.247	0.017	<0.001	<0.001	0.397	0.023	0.004	<0.001	0.238	0.117	0.267	0.034
V_d												
Observation group ($n = 34$)	21.43 ± 5.46	28.10 ± 3.96[a]	32.05 ± 3.88[a]	38.32 ± 5.30[a]	24.36 ± 5.40	30.57 ± 2.55[a]	33.57 ± 2.83[a]	38.09 ± 3.36[a]	15.21 ± 4.70	19.61 ± 4.40[a]	23.61 ± 4.26[a]	30.39 ± 6.83[a]
Control group ($n = 43$)	22.41 ± 3.41	26.69 ± 2.30***a***	29.58 ± 3.03[a]	33.62 ± 4.42[a]	23.67 ± 3.83	25.46 ± 3.90[a]	30.30 ± 3.77[a]	34.63 ± 4.88[a]	14.11 ± 2.82	17.46 ± 2.75[a]	20.80 ± 2.54[a]	24.23 ± 3.42[a]
t value	1.003	2.017	3.300	4.475	0.688	7.191	4.553	3.824	1.315	2.717	3.719	5.287
P value	0.319	0.048	0.001	<0.001	0.493	<0.001	<0.001	<0.001	0.193	0.008	<0.001	<0.001
V_m												
Observation group ($n = 34$)	35.36 ± 3.41	39.81 ± 2.30[a]	43.52 ± 3.72[a]	49.27 ± 3.75[a]	41.88 ± 4.51	47.84 ± 3.03[a]	51.76 ± 3.49[a]	57.17 ± 4.67[a]	26.78 ± 1.79	28.76 ± 1.75[a]	33.20 ± 5.01[a]	36.51 ± 5.78[a]
Control group ($n = 43$)	36.01 ± 4.42	40.27 ± 2.80[a]	43.08 ± 2.19[a]	46.42 ± 3.32[a]	41.02 ± 3.29	41.87 ± 3.19	46.77 ± 2.76[a]	49.79 ± 2.89[a]	26.11 ± 1.94	28.34 ± 1.19[a]	29.99 ± 1.74[a]	32.37 ± 2.30[a]
t value	0.770	0.837	0.673	3.721	1.008	8.914	7.353	8.811	1.672	1.282	3.971	4.364
P value	0.443	0.405	0.503	<0.001	0.316	<0.001	<0.001	<0.001	0.098	0.203	<0.001	<0.001

Note: compared with before treatment, [a]$P < 0.05$.

Hindawi
Computational and Mathematical Methods in Medicine
Volume 2023, Article ID 9891370, 1 page
https://doi.org/10.1155/2023/9891370

Retraction

Retracted: Meta-Analysis of the Effect of Nursing Intervention on Children with Type 2 Diabetes

Computational and Mathematical Methods in Medicine

Received 12 December 2023; Accepted 12 December 2023; Published 13 December 2023

This article has been retracted by Hindawi, as publisher, following an investigation undertaken by the publisher [1]. This investigation has uncovered evidence of systematic manipulation of the publication and peer-review process. We cannot, therefore, vouch for the reliability or integrity of this article.

Please note that this notice is intended solely to alert readers that the peer-review process of this article has been compromised.

Wiley and Hindawi regret that the usual quality checks did not identify these issues before publication and have since put additional measures in place to safeguard research integrity.

We wish to credit our Research Integrity and Research Publishing teams and anonymous and named external researchers and research integrity experts for contributing to this investigation.

The corresponding author, as the representative of all authors, has been given the opportunity to register their agreement or disagreement to this retraction. We have kept a record of any response received.

References

[1] L. Tang, Z. Xu, P. Yao, and H. Zhu, "Meta-Analysis of the Effect of Nursing Intervention on Children with Type 2 Diabetes," *Computational and Mathematical Methods in Medicine*, vol. 2022, Article ID 6185739, 10 pages, 2022.

Hindawi
Computational and Mathematical Methods in Medicine
Volume 2022, Article ID 6185739, 10 pages
https://doi.org/10.1155/2022/6185739

Research Article

Meta-Analysis of the Effect of Nursing Intervention on Children with Type 2 Diabetes

Liying Tang, Zhen Xu, Ping Yao, and Huiqin Zhu

Huzhou Central Hospital, Affiliated Central Hospital Huzhou University, Huzhou, Zhejiang 313000, China

Correspondence should be addressed to Huiqin Zhu; zhq1684@163.com

Received 12 July 2022; Revised 2 August 2022; Accepted 9 August 2022; Published 25 August 2022

Academic Editor: Min Tang

Objective. To systematically evaluate the effect of nursing intervention on children with type 2 diabetes. *Methods*. The randomized controlled trials (RCTs) on nursing intervention in children with type 2 diabetes in CNKI, VIP, WanFang, Chinese Biomedical Database (CBM), PubMed, The Cochrane Library, Embase, and Science were searched by the computer until July 2022. Two evaluators reviewed the articles, selected the information, and assessed their quality according to the inclusion criteria and exclusion criteria and then carried out meta-analysis with RevMan 5.3. *Results*. A total of 5 RCT studies were kept, including 319 patients with type 2 diabetes (≤21 years old), where 162 patients were in the nursing group and 157 patients were in the control group. Meta-analysis revealed that, compared with routine nursing, nursing intervention could effectively control children's fasting blood glucose (FBG) (MD = −1.68, 95% CI (-2.19, -1.17), $P < 0.00001$), 2 h postprandial blood glucose (2hPG) (MD = −4.01, 95% CI (-4.70, -3.33), $P < 0.00001$), fasting insulin (FINS) (MD = −7.42, 95% CI (-10.63, -4.20), $P < 0.00001$), 2 h postprandial insulin (2hINS) (MD = −58.18, 95% CI (-103.24, -13.11), $P = 0.01$), triglycerides (TG) (MD = −0.41, 95% CI (-0.56, -0.25), $P < 0.00001$), and systolic blood pressure (SBP) (MD = −8.85, 95% CI (-14.67, -3.03), $P = 0.003$) and effectively maintain patients' blood glucose at a normal level (MD = −8.85, 95% CI (-14.67, -3.03), $P = 0.003$), where all the differences were statistically significant. *Conclusion*. The existing evidence showed that nursing intervention has a significant effect in controlling normal blood glucose and improving insulin utilization in children with type 2 diabetes, which can effectively improve the therapeutic effect on children.

1. Introduction

Diabetes is a metabolic disease caused by impaired islet function and carbohydrate metabolism disorder. With the characteristics of long course and many complications, it has developed into one of the nine major diseases damaging human health [1, 2]. In 2015, it was reported that 415 million people aged 20-79 have diabetes, which is expected to reach 642 million by 2040 [3, 4]. Globally, the number of diabetes patients has quadrupled in the past few years, and 90% of diabetes patients are type 2 diabetes [5], which is mainly caused by insulin resistance due to various reasons [6]. Due to the change of dietary structure and the reduction of physical activity, obese children are gradually increasing, and the number of children and adolescents with type 2 diabetes is raising year after year [7], although type 1 diabetes is mostly in children. If effective methods are not used for timely treatment, acute complications such as impaired glucose tolerance and other chronic diseases are very likely to occur [8, 9]. Children and adolescent patients with type 2 diabetes need special medical treatment and care, since they are different from adults in many aspects, such as changes in insulin sensitivity, growth and development, self-management ability, and susceptibility to hypoglycemia related to sexual maturity [10–12]. In addition, long-term self-management education, reasonable diet, appropriate physical exercise, psychotherapy, etc. are also needed to prevent and reduce the occurrence of adverse reactions and complications [13, 14].

Some studies have pointed out that nursing intervention can effectively control the blood glucose of children with type 2 diabetes and improve their compliance with treatment, so as to delay the progress of the disease and improve patients' life experience [15–17], but there is still a lack of

relevant medical evidence. Therefore, we systematically evaluated the effect of nursing intervention in children with type 2 diabetes by retrieving relevant literature and applying meta-analysis method, so as to provide medical evidence for the clinical promotion and application of nursing intervention.

2. Data and Methods

2.1. Inclusion and Exclusion Criteria

2.1.1. Inclusion Criteria. The inclusion criteria are the following: (1) research type: randomized controlled trails (RCT); (2) patient information: children with type 2 diabetes, age ≤ 21 years old; (3) intervention measures: the nursing group was given other nursing interventions based on the routine nursing, and the control group was given routine nursing; (4) outcome indexes: literature with one of the following indicators can be included: fasting blood glucose (FBG, mmol/L), 2 h postprandial blood glucose (2hPG, mmol/L), fasting insulin (FINS, U/L), 2 h postprandial insulin (2hINS, U/L), triglycerides (TG, mmol/L), systolic blood pressure (SBP, mmHg), and total effectiveness of blood glucose control (cases).

2.1.2. Exclusion Criteria. The exclusion criteria are the following: (1) repeatedly published literature and (2) studies with incomplete information and unable to extract effective data.

2.2. Literature Retrieval Strategy. The RCTs on nursing intervention in children with type 2 diabetes in CNKI, VIP, WanFang, CBM, PubMed, The Cochrane Library, Embase, and Science were searched by the computer until July 2022. It was supplemented by manual secondary retrieval, so as to ensure the comprehensiveness of literature retrieval. The Chinese search takes "Nursing," "Child," and "diabetes mellitus, type 2" as the subject words for combined hybrid search. Taking WanFang database as an example, the search formula is as follows: (nursing OR intervention) AND (child OR teenagers OR children) and diabetes mellitus, type 2. English retrieval takes "nursing", "child", "diabetes mellitus, type 2," "randomized controlled trial" as the subject word for combinatorial hybrid retrieval. Taking PubMed as an example, the formula is as follows: (((((((((“Nursing”[Mesh])) OR (Nurse[Title/Abstract])) OR (Care[Title/Abstract])) OR (Caring[Title/Abstract])) OR (Intervention[Title/Abstract])) OR (Intervene[Title/Abstract])) AND (((((((“Child”[Mesh])) OR (Children[Title/Abstract])) OR (preschool[Title/Abstract])) OR (young[Title/Abstract])) OR (youngsters[Title/Abstract])) OR (teenagers[Title/Abstract]))) AND ((((((((((((((((((((“Diabetes Mellitus, Type 2”[Mesh]) OR (Diabetes Mellitus, Noninsulin-Dependent[Title/Abstract])) OR (Diabetes Mellitus, Ketosis-Resistant[Title/Abstract])) OR (Diabetes Mellitus, Ketosis Resistant[Title/Abstract])) OR (Ketosis-Resistant Diabetes Mellitus[Title/Abstract])) OR (Diabetes Mellitus, Non Insulin Dependent[Title/Abstract])) OR (Diabetes Mellitus, Non-Insulin-Dependent[Title/Abstract])) OR (Non-Insulin-Dependent Diabetes Mellitus[Title/Abstract])) OR (Diabetes Mellitus, Stable[Title/Abstract])) OR (Stable Diabetes Mellitus[Title/Abstract])) OR (Diabetes Mellitus, Type II[Title/Abstract])) OR (NIDDM[Title/Abstract])) OR (Diabetes Mellitus, Noninsulin Dependent[Title/Abstract])) OR (Diabetes Mellitus, Maturity-Onset[Title/Abstract])) OR (Maturity Onset Diabetes Mellitus[Title/Abstract])) OR (MODY[Title/Abstract])) OR (Diabetes Mellitus, Slow Onset[Title/Abstract])) OR (Type 2 Diabetes Mellitus[Title/Abstract])) OR (Noninsulin Dependent Diabetes Mellitus[Title/Abstract])) OR (Maturity Onset Diabetes[Title/Abstract])) OR (Type 2 Diabetes[Title/Abstract])) OR (Diabetes, Type 2[Title/Abstract]))) AND (“Randomized Controlled Trial” [Publication Type]).

2.3. Data and Relevant Information Extraction. Using an independent double-blind method, two researchers read the topics and abstracts for preliminary screening and then read the full text for rescreening. Extract data from the final included literature, cross-check it, and deliver the divergence to the third researcher to decide whether to include it after verification. The extracted information includes (1) the first author and the year of publication; (2) study design, patients number, age, and gender; (3) intervention measures, intervention time, and intervention cycle; and (4) outcome measures: FBG, 2hPG, FINS, 2hINS, TG, SBP, and total effectiveness of blood glucose control.

2.4. Study Quality Evaluation. The quality of the analyses is influenced by the bias risk of the included studies. In this study, two researchers evaluated the quality of articles using the bias risk assessment tool in RevMan 5.3. Negotiate and discuss the disagreement, and if necessary, invite a third researcher to determine the results. The risk of bias included in the literature was evaluated from six aspects: selection bias, performance bias, detection bias, attrition bias, reporting bias, and other bias. Each item is evaluated with "low risk," "high risk," and "unclear risk." If all of them meet the requirements of "low risk," they will be rated as class A; if some of them meet the requirements of "low risk," they will be rated as class B; and if none of them meet the requirements of "low risk," they will be rated as class C.

2.5. Data Analysis. RevMan 5.3 is applied to analyze these clinical data. If the outcome index is a continuous variable and the measurement units are the same, the weighted mean difference (MD) is used for data statistics and the 95% confidence interval is calculated. If the outcome is a binary variable, the odds ratio (OR) is used. This study detects the heterogeneity between studies by calculating the I^2 value. When $I^2 = 0$, there is no heterogeneity. When $0 < I^2 < 50\%$, the heterogeneity is small, and the fixed effect model is performed. When $I^2 \geq 50\%$, the heterogeneity is large, and the random effect model is adopted.

3. Results

3.1. Article Retrieval and Basic Characteristics of Included Literature. 1439 relevant literatures were initially detected, and 984 literatures were obtained after eliminating duplicate literatures. After excluding repeated publications, reviews,

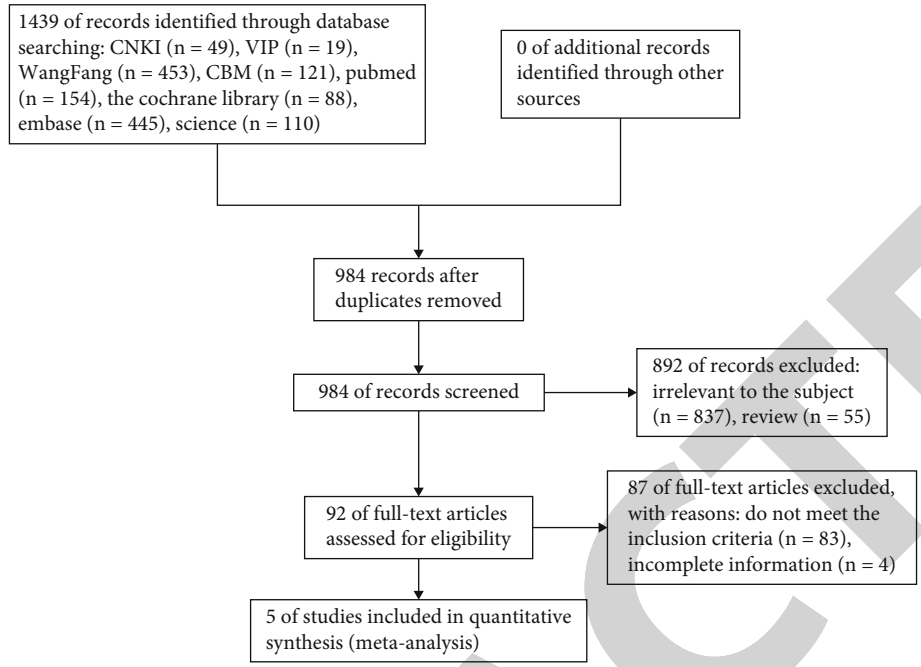

Figure 1: Article screening flow chart.

Table 1: Basic characteristics of the included study.

	Cases (*n*)		Gender (male/female, *n*)		Age (years)		
	Nursing group	Control group	Nursing group	Control group	Nursing group	Control group	Primary outcome
Ba et al. (2017) [18]	45	45	25/20	23/22	8.6 ± 1.2	9.8 ± 1.3	(7)
Chen et al. (2006) [19]	23	20	16/7	12/8	12.96 ± 1.52	12.15 ± 0.75	(1), (2), (3) (4), (5), (6), (7)
Li et al. (2011) [20]	24	24	14/10	13/11	12.9 ± 1.5	12.2 ± 0.8	(1), (2), (5), (6), (7)
Liang (2005) [21]	20	18	12/8	11/7	12.96 ± 1.52	12.5 ± 0.75	(1), (2), (3), (4), (5), (6), (7)
Yu (2016) [22]	50	50	28/22	27/23	10.5 ± 0.9	10.6 ± 1.1	(1), (2), (3), (4), (5), (6)

Primary outcome: (1): fasting blood glucose (FBG, mmol/L); (2) 2 h postprandial blood glucose (2hPG, mmol/L); (3): fasting insulin (FINS, U/L); (4): 2 h postprandial insulin (2hINS, U/L); (5): triglycerides (TG, mmol/L); (6): systolic blood pressure (SBP, mmHg); and (7): total effectiveness of blood glucose control (cases).

and noncompliance with the inclusion criteria through primary screening, 87 literatures were left. Finally, 5 RCTs were kept after excluding noncompliance with the inclusion criteria through secondary screening, with a total of 319 patients, where 162 was in the nursing group and 157 was in the control group. The article screening details and the basic information of these studies are shown in Figure 1 and Table 1, respectively.

3.2. Literature Quality Evaluation. In the 5 literatures, the clinical baselines of the nursing group and the control group including the gender, age, and prenursing indicators are comparable. RevMan 5.3 software was utilized to evaluate the bias risk of literature. Specifically, the patients in the five articles were randomly grouped, only one mentioned the use of random number table method, and the other four did not mention it. Besides, all the articles did not describe the detection bias and the quality of literature was all class B, see Table 2 and Figure 2 for more information.

3.3. Analyses and Results

3.3.1. Effect of Nursing Intervention on FBG. Four studies compared the FBG levels of the two groups, where the literature by Yu (2016) was eliminated to reduce the heterogeneity. Finally, 129 patients were included, where the number of patients in the nursing group and control group was 67 and 62, respectively. The results of meta-analysis showed that there was still a certain heterogeneity ($P = 0.08$, $I^2 = 60\%$), so the random effect (RE) model was adopted for analysis (MD = −1.68, 95% CI (-2.19, -1.17), $P < 0.00001$]) It can be considered that nursing intervention can effectively reduce the FBG level of children with type 2 diabetes, as shown in (Figure 3).

Table 2: The scale for assessing the report quality of clinical trials.

Literature year	Random sequence generation	Allocation concealment	Performance bias	Detection bias	Attrition bias	Reporting bias	Other bias	Quality
Ba et al. (2017) [18]	Unclear risk	Low risk	High risk	Unclear risk	Low risk	Unclear risk	Low risk	B
Chen et al. (2006) [19]	Unclear risk	Low risk	Unclear risk	Unclear risk	Low risk	Low risk	Low risk	B
Li et al. (2011) [20]	Unclear risk	Low risk	Unclear risk	Unclear risk	Low risk	Low risk	Low risk	B
Liang (2005) [21]	Unclear risk	Low risk	Unclear risk	Unclear risk	Low risk	Low risk	Low risk	B
Yu (2016) [22]	Low risk	Low risk	Unclear risk	Unclear risk	Low risk	Low risk	Low risk	B

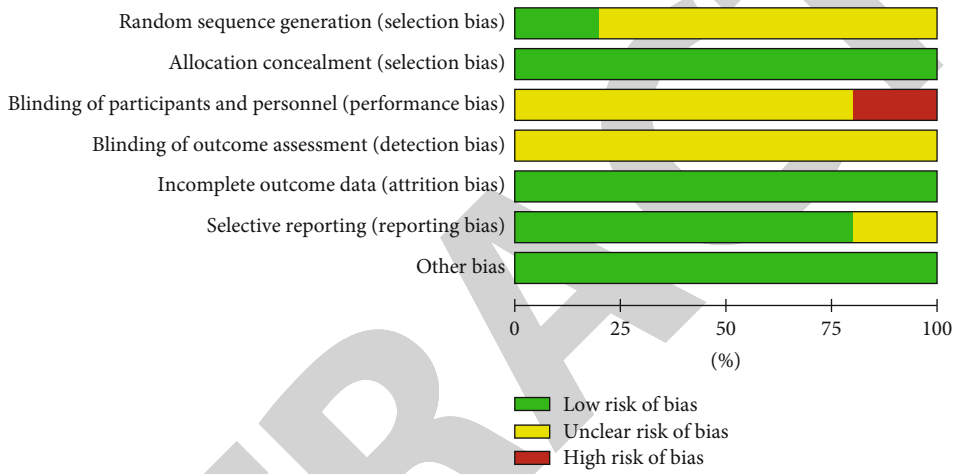

Figure 2: Included study bias risk assessment chart.

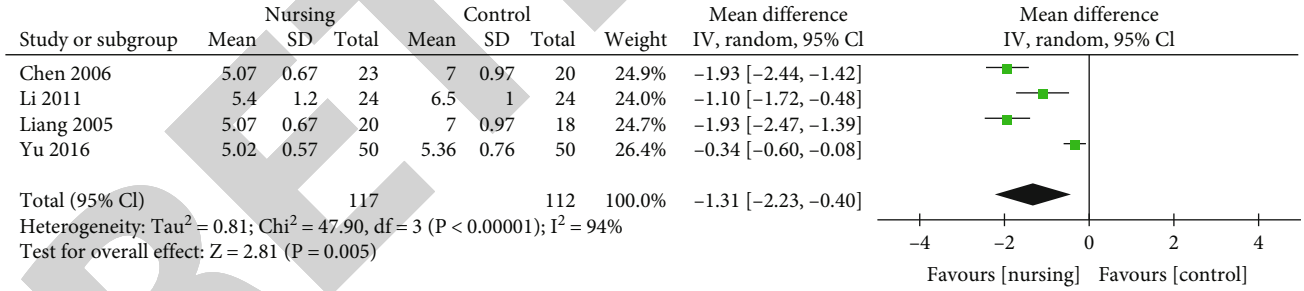

Figure 3: Effect of nursing intervention and routine nursing on fasting blood glucose (FBG).

3.3.2. Effect of Nursing Intervention on 2hPG. Four studies compared the levels of 2hPG in the two groups, where the literature by Yu (2016) was eliminated to reduce the heterogeneity. The results showed that the heterogeneity decreased significantly after removing sensitive articles ($P = 0.70$, $I^2 = 0$ %). Further, the FE model was used (MD = −4.01, 95% CI (-4.70, -3.33), $P < 0.00001$), indicating that nursing intervention can effectively reduce the level of 2hPG in children, as shown in Figure 4.

3.3.3. Effect of Nursing Intervention on FINS. Three studies compared the levels of FINS between the two groups, including 181 patients, where 93 in the nursing group and 88 in the control group. Since the heterogeneity of these studies was small ($P = 0.81$, $I^2 = 0\%$), the fixed effect (FE) model was performed for analysis (MD = −7.42, 95% CI (-10.63, -4.20), $P < 0.00001$), indicating that nursing intervention was better than routine nursing in reducing FINS in children with type 2 diabetes. More information is shown in Figure 5.

3.3.4. Effect of Nursing Intervention on 2hINS. As shown in Figure 6, three studies compared the levels of 2hINS. A total of 181 patients were collected, where 93 patients were divided into the nursing group and 88 patients were assigned

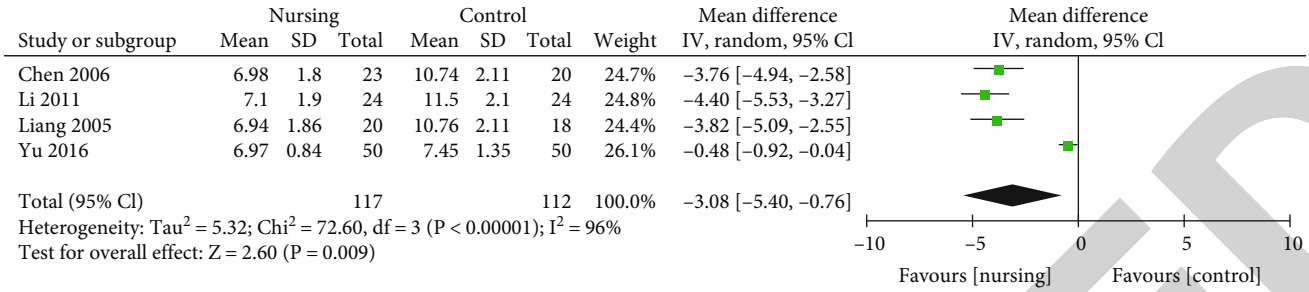

Figure 4: Effect of nursing intervention and routine nursing on 2 h postprandial blood glucose (2hPG).

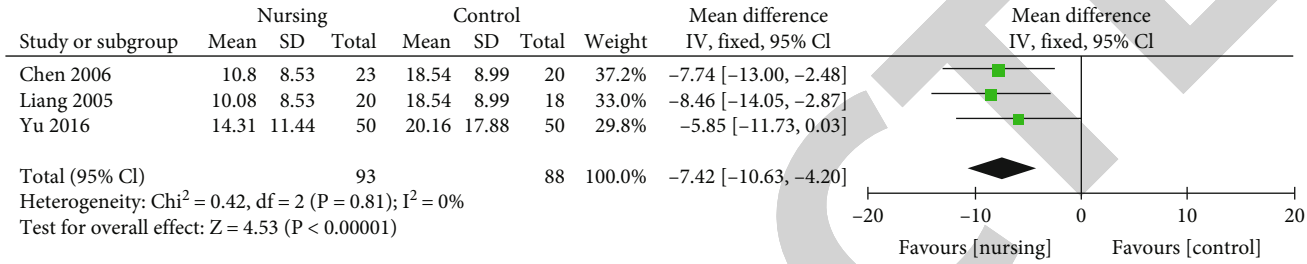

Figure 5: Effect of nursing intervention and routine nursing on fasting insulin (FINS).

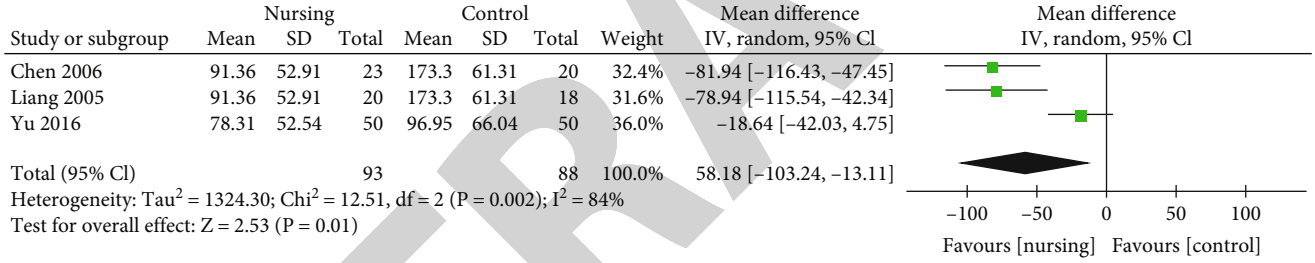

Figure 6: Effect of nursing intervention and routine nursing on 2 h postprandial insulin (2hINS).

to the control group. Some heterogeneity existed in the included studies ($P < 0.002$, $I^2 = 84\%$), and the RE model was used for analysis (MD = −58.18, 95% CI (-103.24, -13.11), $P = 0.01$). It can be considered that nursing intervention is better than routine nursing in reducing 2hINS in children with type 2 diabetes.

3.3.5. Effect of Nursing Intervention on TG. Four studies compared the TG levels of the two groups, a total of 117 (the nursing group) + 112 (the control group) patients. Due to the low heterogeneity between these studies ($P = 0.81$, $I^2 = 0\%$), the FE model was used for analysis (MD = −0.41, 95% CI (-0.56, -0.25), $P < 0.00001$). Meta-analysis results show that nursing intervention has a better control effect on TG level of patients (Figure 7).

3.3.6. Effect of Nursing Intervention on SBP. As shown in Figure 8, four studies compared the SBP levels, which have the same number patients as above. Because of the high heterogeneity between these studies ($P = 0.08$, $I^2 = 55\%$), the RE model was adopted (MD = −8.85, 95% CI (-14.67, -3.03), $P = 0.003$). It showed that nursing intervention has a better effect on the control of SBP in patients.

3.3.7. Effect of Nursing Intervention on the Total Effectiveness of Blood Glucose Control. As shown in Figure 9, four studies compared the total effectiveness of blood glucose control (112 patients in the nursing group and 107 patients in the control group). Due to the low heterogeneity of the included studies ($P = 0.58$, $I^2 = 0\%$), the fixed effect model was used for analysis (MD = 4.71, 95% CI (2.5, 8.88), $P < 0.00001$). It can be considered that nursing intervention can effectively control the blood glucose of children and maintain it at a normal level.

3.3.8. Funnel Chart of Publication Bias in Each Dimension. As shown in Figure 10, the funnel chart was used to detect publication bias of the literatures included in the study. The result showed that the dots are asymmetrically distributed on both sides of the vertical line, suggesting that there is a certain publication bias in the literature.

4. Discussion

Type 2 diabetes is rare in children with diabetes, accounting for about 5% of the incidence rate of diabetes in children [23]. The disease is a chronic disease with serious clinical

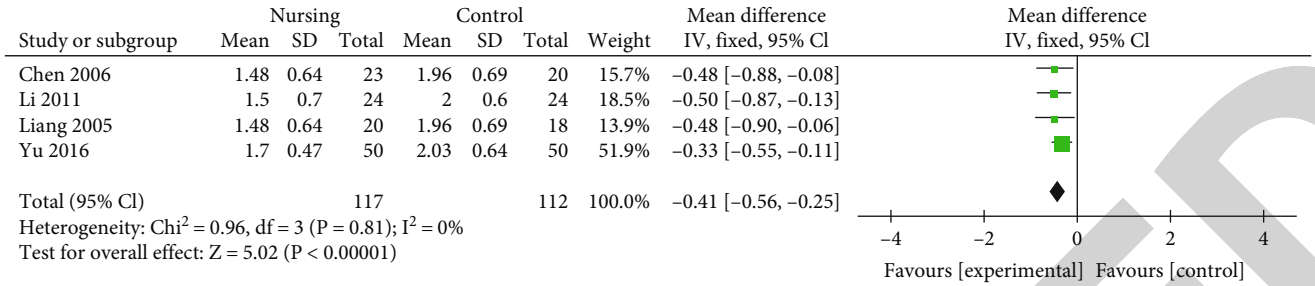

Figure 7: Effect of nursing intervention and routine nursing on triglycerides (TG).

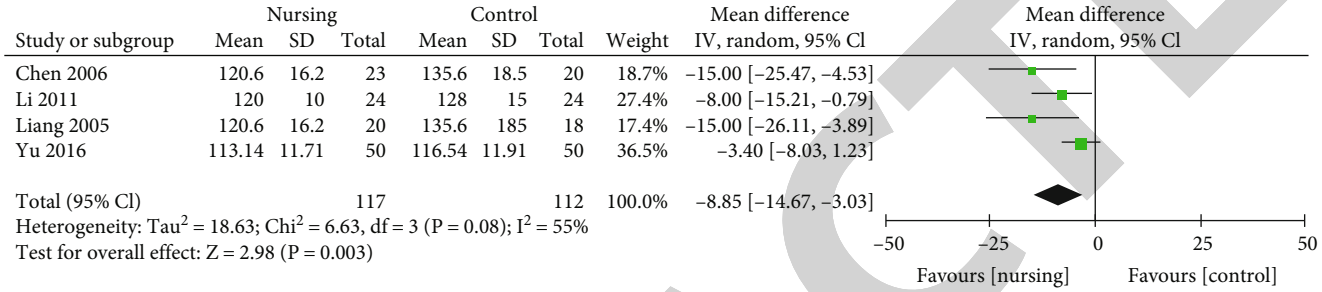

Figure 8: Effect of nursing intervention and routine nursing on systolic blood pressure (SBP).

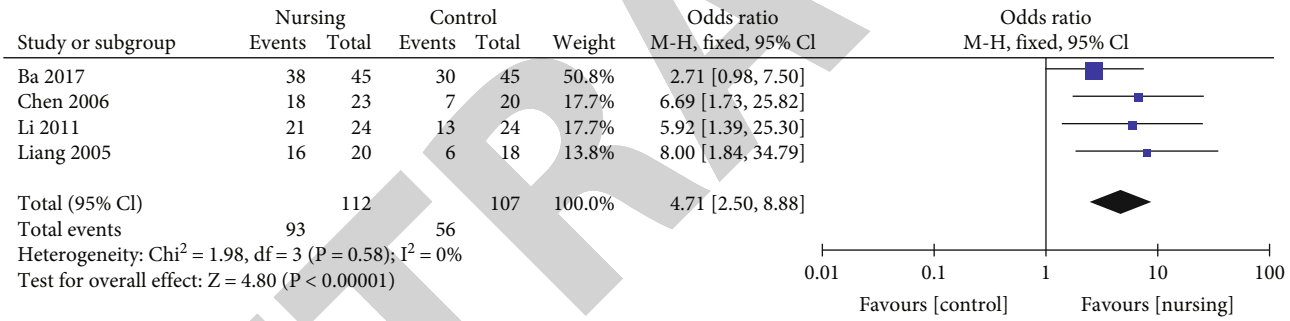

Figure 9: Effect of nursing intervention and routine nursing on total effectiveness of blood glucose control.

harm, which seriously endangers children's daily life [24, 25]. Since there is no complete cure at present, it is very important to take appropriate treatment measures to control blood glucose in the body [26]. The results of this study show that nursing intervention can significantly reduce the fasting blood glucose of children (MD = −1.68, 95% CI (-2.19, -1.17), $P < 0.00001$) and 2 h postprandial blood glucose (MD = −4.01, 95% CI (-4.70, -3.33), $P < 0.00001$) and strengthen the hypoglycemic effect. Compared with routine nursing, nursing intervention is more targeted, providing patients with diabetes education and life, emotional, and behavioral support, strengthening patients' understanding of the disease and enhancing the understanding to the important role of blood glucose in disease progression [27]. On the other hand, combined diet control, exercise therapy, bad behavior correction, blood glucose real-time monitoring, and other measures, nursing intervention plays a positive role in blood glucose control [28].

Insulin resistance and pancreatic β cell function defects are two pathological features of type 2 diabetes [29]. Due to the lack of effective use of insulin, the level of insulin secreted by the body is excessive, which makes the pancreatic β cell function gradually decreases [30]. Therefore, more attention should be paid to insulin resistance in the prevention and treatment of type 2 diabetes. The results of this study showed that, compared with routine nursing, nursing intervention can significantly reduce fasting insulin in children (MD = −7.42, 95% CI (-10.63, -4.20), $P < 0.00001$) and 2 h postprandial insulin (MD = −58.18, 95% CI (-103.24, -13.11), $P = 0.01$) and effectively promote the utilization of insulin in patients. The reason is that the nursing intervention mode strengthens the relevant behaviors and knowledge of patients and enables patients to better understand the problems existing in the process of disease management and actively correct them, which is conducive to the formation of patients' health awareness and improves their self-management ability by analyzing the problems existing in the process of insulin secretion, utilization, and conversion with patients and guiding patients to write disease diaries. Patients pay close attention to insulin and other indicators during treatment and communicate with doctors at any time, which is conducive to the doctors' timely

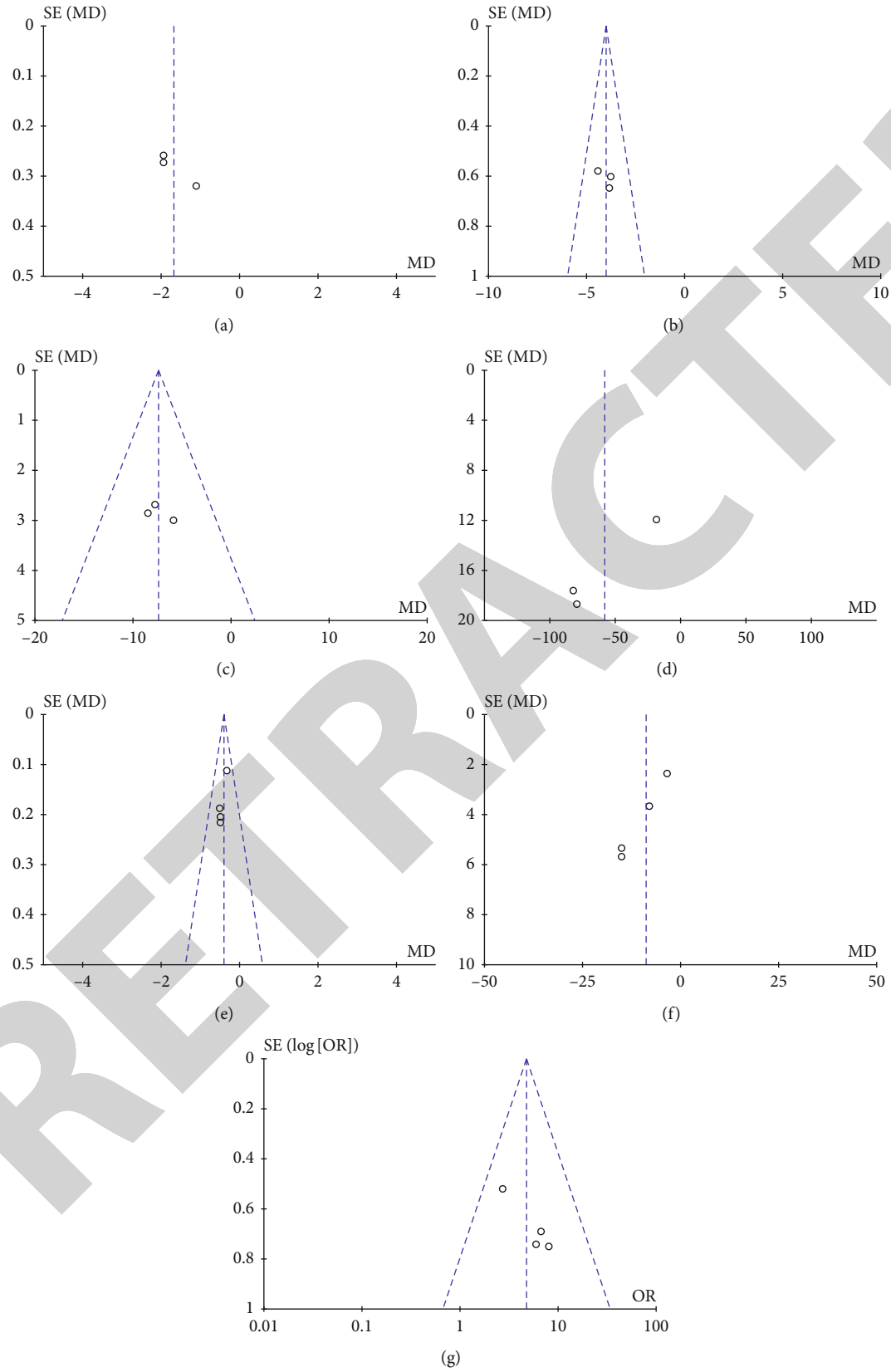

Figure 10: Funnel chart of publication bias in each dimension: (a) FBG, (b) 2hPG, (c) FINS, (d) 2hINS, (e) TG, (f) SBP, and (g) total effectiveness of blood glucose control.

feedback. Thus, it can promote the good use of insulin in patients and make the treatment effect more effective.

Studies have shown that history of hypertension, history of staying up late, and high triglycerides are possible influencing factors of type 2 diabetes [31–33]. Therefore, we will combine these basic clinical indicators to judge the patient's condition control. This study systematically discussed the effects of nursing intervention on triglycerides and systolic blood pressure by collecting data from some literatures. The results revealed that nursing intervention could effectively decrease the triglyceride level of children with type 2 diabetes (MD = −0.41, 95% CI (-0.56, -0.25), $P < 0.00001$) and maintain the systolic blood pressure of children in a normal state (MD = −8.85, 95% CI (-14.67, -3.03), $P = 0.003$). The reason is that triglycerides and systolic blood pressure are closely related to dietary obesity and lack of exercise [34, 35]. Therefore, in the process of nursing intervention, doctors and nurses will work with children and parents to formulate weight loss goals and take a step-by-step approach to gradually reduce weight. Dietitians should reasonably adjust their dietary structure. Special personnel were assigned to give specific exercise guidance, and the amount of therapeutic exercise was determined according to the height, weight, and obesity of each child. Through weight loss, diet, and exercise to guide children's daily life, their triglyceride and systolic blood pressure levels were improved.

The effectiveness of blood glucose control in children with type 2 diabetes is an important indicator for the systematic evaluation of this treatment measure [36]. This meta-analysis showed that nursing intervention applied to the treatment of children with type 2 diabetes could significantly improve the total effectiveness of blood glucose control (MD = 4.71, 95% CI (2.5, 8.88), $P < 0.00001$), and the difference was statistically significant. Compared with routine nursing, nursing intervention can effectively control patients' fasting blood glucose and 2 h postprandial blood glucose, improve patients' self-management ability, and guide patients to implement correct nursing behavior, so as to improve the total efficiency of blood glucose control [37].

This study has some limitations. (1) Due to the small number of children with type 2 diabetes, there are few articles on the effect of nursing intervention on the treatment of type 2 diabetes in children. In this meta-analysis, a total of 5 RCT studies of medium quality were collected, which still need to be supported by evidence-based articles of higher quality. (2) We only searched the literature in Chinese and English languages. After the search and screening, there are 4 Chinese articles and 1 English article, which may have problems such as publication bias and incomplete document collection. (3) In this analysis, we analyzed the seven outcome indicators of FBG, 2hPG, FINS, 2hINS, TG, SBP, and blood glucose control, but glycosylated hemoglobin (HbA1c,%) is also an important indicator to evaluate the treatment effect of children [38]. Since only two literatures in this study reported HbAc1 data, which is of little statistical value, it was not included in this analysis. (4) From the analysis results of seven outcome indicators, the results of FBG, 2hPG, 2hINS, and SBP have great heterogeneity. Analyzing the reasons that the research objects in Li (2011) and Yu (2016) included not only children with type 2 diabetes but also children with obesity and abnormal glucose metabolism. Although obesity and abnormal glucose metabolism are high-risk factors for type 2 diabetes, they can also affect the results. On the other hand, it may be related to nursing intervention measures and nursing time. Among the 5 articles, 4 introduced their nursing method as comprehensive nursing, and 1 did not introduce it; three articles introduced their nursing intervention about 18 months and the other two did not. Because the number of included literatures is too small to conduct subgroup analysis, this result needs more high-quality research support.

5. Conclusion

Nursing intervention has a significant effect in controlling blood glucose, promoting insulin utilization, improving triglyceride levels, and improving the total effective rate of blood glucose control in children with type 2 diabetes. Although the implementation of comprehensive nursing requires nurses to pay more time and energy, it provides a full range of services for children, has good clinical application value, and is worth promoting.

Data Availability

The labeled dataset used to support the findings of this study is available from the corresponding author upon request.

Conflicts of Interest

The authors declare no competing interests.

Acknowledgments

This work was supported by the Huzhou Central Hospital, Affiliated Central Hospital Huzhou University.

References

[1] S. Mashayekh-Amiri, S. Mohammad-Alizadeh-Charandabi, S. Abdolalipour, and M. Mirghafourvand, "Myo-inositol supplementation for prevention of gestational diabetes mellitus in overweight and obese pregnant women: a systematic review and meta-analysis," *Diabetology and Metabolic Syndrome*, vol. 14, no. 1, p. 93, 2022.

[2] V. Guerreiro, I. Maia, J. S. Neves et al., "Oral glucose tolerance testing at 1 h and 2 h: relationship with glucose and cardiometabolic parameters and agreement for pre-diabetes diagnosis in patients with morbid obesity," *Diabetology and Metabolic Syndrome*, vol. 14, no. 1, p. 91, 2022.

[3] L. C. Silva, B. M. Rocha, G. M. Escott et al., "Accuracy evaluation of 2021 chronic kidney disease epidemiology collaboration, full age spectrum and European kidney function consortium equations for estimating glomerular filtration rate in type 2 diabetes mellitus and healthy adults," *Clinica Chimica Acta*, vol. 534, pp. 14–21, 2022.

[4] R. D. Barmanray, N. Cheuk, S. Fourlanos, P. B. Greenberg, P. G. Colman, and L. J. Worth, "In-hospital hyperglycemia but not diabetes mellitus alone is associated with increased in-hospital mortality in community-acquired pneumonia

(CAP): a systematic review and meta-analysis of observational studies prior to COVID-19," *BMJ Open Diabetes Research & Care*, vol. 10, no. 4, article e002880, 2022.

[5] J. B. McGill, H. Haller, P. Roy-Chaudhury et al., "Making an impact on kidney disease in people with type 2 diabetes: the importance of screening for albuminuria," *BMJ Open Diabetes Research & Care*, vol. 10, no. 4, article e002806, 2022.

[6] H. Gemalmaz, C. Unal, and Y. Gültekin, "Evaluation of early postoperative period results of patients with type 2 diabetes taking oral anti-diabetics or insulin medications, with microalbuminuria and normal creatinine levels after coronary artery bypass," *The Heart Surgery Forum*, vol. 25, no. 3, pp. E407–E412, 2022.

[7] K. T. Kao, M. A. Sabin, G. M. Escott et al., "Type 2 diabetes mellitus in children and adolescents," *Australian Family Physician*, vol. 45, no. 6, pp. 401–406, 2016.

[8] S. J. Choo, H. G. Lee, C. J. Kim, and E. M. Yang, "Severe hypernatremia in soft drink ketoacidosis and hyperglycemic hyperosmolar state at the onset of type 2 diabetes mellitus: a case series of three adolescents," *Clinical Pediatric Endocrinology*, vol. 31, no. 2, pp. 81–86, 2022.

[9] B. Hu, L. Zhang, Z. S. Zhao, Y. C. Qi, W. Zhou, and Y. L. Ma, "The predictive value of thromboelastography (TEG) parameters in vascular complications in patients with type 2 diabetes mellitus," *Journal of Diabetes and Its Complications*, vol. 36, no. 8, article 108236, 2022.

[10] G. Beauchamp, M. M. Barr, A. Vergara, A. Ashraf, and F. Bril, "Treatment of hyperglycemia not associated with NAFLD improvement in children with type 2 diabetes mellitus," *International Journal of Pediatrics and Adolescent Medicine*, vol. 9, no. 2, pp. 83–88, 2022.

[11] H. Yokomichi, M. Mochizuki, R. Shinohara et al., "Gestational age, birth weight, and perinatal complications in mothers with diabetes and impaired glucose tolerance: Japan environment and children's study cohort," *PLoS One*, vol. 17, no. 6, article e0269610, 2022.

[12] V. A. Essuman, N. N. Tagoe, A. Essuman et al., "A cross-sectional study of ocular changes in children and adolescents with diabetes mellitus in selected health facilities in Ghana," *International Journal of Environmental Research and Public Health*, vol. 19, no. 9, p. 5295, 2022.

[13] Z. Li, X. Lei, B. Xu, S. Wang, T. Gao, and H. Lv, "Analysis of risk factors of diabetes peripheral neuropathy in type 2 diabetes mellitus and nursing intervention," *Experimental and Therapeutic Medicine*, vol. 20, no. 6, p. 1, 2020.

[14] Y. Zheng, B. Anton, J. Rodakowski et al., "Associations between implementation of the Caregiver Advise Record Enable (CARE) act and health service utilization for older adults with diabetes: retrospective observational study," *JMIR Aging*, vol. 5, no. 2, article e32790, 2022.

[15] E. Vlachou, A. Ntikoudi, D. A. Owens, M. Nikolakopoulou, T. Chalimourdas, and O. Cauli, "Effectiveness of cognitive behavioral therapy-based interventions on psychological symptoms in adults with type 2 diabetes mellitus: an update review of randomized controlled trials," *Journal of Diabetes and Its Complications*, vol. 36, no. 5, article 108185, 2022.

[16] R. Forde, O. Abiola, J. Anderson et al., "An integrated primary care-based programme of PRE-Pregnancy cARE to improve pregnancy outcomes in women with type 2 Diabetes (the PREPARED study): protocol for a multi-method study of implementation, system adaptation and performance," *BMC Primary Care*, vol. 23, no. 1, p. 76, 2022.

[17] P. Seferović, D. Farmakis, A. Bayes-Genis et al., "Biomarkers for the prediction of heart failure and cardiovascular events in patients with type 2 diabetes: a position statement from the Heart Failure Association of the European Society of Cardiology," *European Journal of Heart Failure*, vol. 24, no. 7, pp. 1162–1170, 2022.

[18] H. Ba, X. Yu, S. Han et al., "The clinical outcomes of nursing intervention for children with type 2 diabetes mellitus on the treatment adherence," *Biomedical Research (0970-938X)*, vol. 28, no. 15, 2017.

[19] X. Chen, J. Zhang, and Z. Zhang, "Observation on the effect of nursing intervention on the prevention and treatment of diabetes in children and adolescents," *Qilu Journal of Nursing*, vol. 12, p. 2, 2006.

[20] W. Li, J. Gu, H. Wei, and Y. Chen, "Discussion on the effect of nursing intervention in children with obesity and abnormal glucose metabolism," *Medical Theory and Practice*, vol. 24, no. 22, p. 3, 2011.

[21] R. Liang, "Observation on the prevention and treatment of type 2 diabetes in children and adolescents and the effect of nursing intervention," *Chinese Journal of Practical Nursing*, vol. 6, pp. 21–23, 2005.

[22] C. Yu, "Study on comprehensive intervention to prevent and treat type II diabetes and metabolic syndrome in obese children," *Diabetes New World*, vol. 2, p. 3, 2016.

[23] S. D. Brown, M. M. Hedderson, Y. Zhu et al., "Uptake of guideline-recommended postpartum diabetes screening among diverse women with gestational diabetes: associations with patient factors in an integrated health system in the USA," *BMJ Open Diabetes Research & Care*, vol. 10, no. 3, article e002726, 2022.

[24] M. Kumar, L. T. Ang, C. Ho et al., "Machine learning-derived prenatal predictive risk model to guide intervention and prevent the progression of gestational diabetes mellitus to type 2 diabetes: prediction model development study," *JMIR Diabetes*, vol. 7, no. 3, article e32366, 2022.

[25] E. K. Esdaile, J. Gillespie, L. A. Baur, L. M. Wen, and C. Rissel, "Australian state and territory eclectic approaches to obesity prevention in the early years: policy mapping and perspectives of senior health officials," *Frontiers in Public Health*, vol. 10, article 781801, 2022.

[26] S. M. Janssen, D. M. Connelly, C. Shields, and M. Landry, "Assessing physical function after completing a supervised education and exercise program in adults with type 2 diabetes and exploring exercise motivation at one-year follow up: a case series study," *Physiotherapy Theory and Practice*, vol. 7, pp. 1–14, 2022.

[27] Y. Chen, Q. Zhong, J. Luo et al., "The 6-month efficacy of an intensive lifestyle modification program on type 2 diabetes risk among rural women with prior gestational diabetes mellitus: a cluster randomized controlled trial," *Prevention Science*, vol. 13, pp. 1–13, 2022.

[28] C. E. Lloyd, A. Nouwen, N. Sartorius et al., "Prevalence and correlates of depressive disorders in people with type 2 diabetes: results from the International Prevalence and Treatment of Diabetes and Depression (INTERPRET-DD) study, a collaborative study carried out in 14 countries," *Diabetic Medicine*, vol. 35, no. 6, pp. 760–769, 2018.

[29] Y. Kim, J. H. Huh, M. Lee, E. S. Kang, B. S. Cha, and B. W. Lee, "Tolerability and effectiveness of switching to dulaglutide in patients with type 2 diabetes inadequately controlled with

Hindawi
Computational and Mathematical Methods in Medicine
Volume 2023, Article ID 9804870, 1 page
https://doi.org/10.1155/2023/9804870

Retraction

Retracted: A Preliminary Study on the Value of Intestinal Flora in Predicting Major Adverse Cardiovascular and Cerebrovascular Events in Patients with Refractory Hypertension

Computational and Mathematical Methods in Medicine

Received 12 December 2023; Accepted 12 December 2023; Published 13 December 2023

This article has been retracted by Hindawi, as publisher, following an investigation undertaken by the publisher [1]. This investigation has uncovered evidence of systematic manipulation of the publication and peer-review process. We cannot, therefore, vouch for the reliability or integrity of this article.

Please note that this notice is intended solely to alert readers that the peer-review process of this article has been compromised.

Wiley and Hindawi regret that the usual quality checks did not identify these issues before publication and have since put additional measures in place to safeguard research integrity.

We wish to credit our Research Integrity and Research Publishing teams and anonymous and named external researchers and research integrity experts for contributing to this investigation.

The corresponding author, as the representative of all authors, has been given the opportunity to register their agreement or disagreement to this retraction. We have kept a record of any response received.

References

[1] J. Jiao, Y. Zhang, P. Han, and S. Zhai, "A Preliminary Study on the Value of Intestinal Flora in Predicting Major Adverse Cardiovascular and Cerebrovascular Events in Patients with Refractory Hypertension," *Computational and Mathematical Methods in Medicine*, vol. 2022, Article ID 7723105, 7 pages, 2022.

Hindawi
Computational and Mathematical Methods in Medicine
Volume 2022, Article ID 7723105, 7 pages
https://doi.org/10.1155/2022/7723105

Research Article

A Preliminary Study on the Value of Intestinal Flora in Predicting Major Adverse Cardiovascular and Cerebrovascular Events in Patients with Refractory Hypertension

Jie Jiao,[1] **Yeping Zhang**,[2] **Pengda Han**,[3] **and Shuya Zhai**[4]

[1]*Heart Center and Beijing Key Laboratory of Hypertension, Beijing Chaoyang Hospital, Capital Medical University, Beijing, China*
[2]*Heart Center, Beijing Chaoyang Hospital, Capital Medical University, Beijing, China*
[3]*Beijing Emergency Medical Center, China*
[4]*Beijing Fengtai You'anmen Hospital, China*

Correspondence should be addressed to Jie Jiao; luckyguo111@sina.com

Received 6 July 2022; Revised 18 July 2022; Accepted 27 July 2022; Published 24 August 2022

Academic Editor: Min Tang

Objective. To investigate the value of intestinal flora in predicting major adverse cardiovascular and cerebrovascular events (MACCE) in patients with refractory hypertension (RH). *Methods*. 359 patients with RH hospitalized in our hospital from April 2020 to March 2021 were followed up for 1 year and selected for the study. These patients were divided into a MACCE group and no-MACCE group. Results were analyzed by comparing general information, the abundance of intestinal flora at the phylum level, and the abundance of intestinal flora at the species level between the two groups. The influence factors related to MACCE were evaluated using multifactor logistic regression analysis, and the value of intestinal flora in predicting MACCE was determined using receiver operating characteristic (ROC) and the area under ROC (AUC). *Results*. Systolic blood pressure was higher in the MACCE group than in the no-MACCE group ($P < 0.05$). The abundances of Actinomycetes and Verrucomicrobia were higher in the MACCE group than in the no-MACCE group, while unnamed viruses were the opposite ($P < 0.05$). The abundances of Eubacterium eligens, Akkermansia muciniphila, Prevotella stercorea, and Eubacterium rectale were lower in the MACCE group than in the no-MACCE group, while Escherichia coli, Clostridium hathewayi, and Ruminococcus gnavus were opposite ($P < 0.05$). Systolic blood pressure, Actinomycetes, unnamed viruses, Verrucomicrobia, Eubacterium eligens, Akkermansia muciniphila, Prevotella stercorea, Eubacterium rectale, Escherichia coli, Clostridium hathewayi, and Ruminococcus gnavus were closely associated with MACCE in RH patients ($P < 0.05$). In addition, Akkermansia muciniphila had the highest AUC among the single indicator but was still lower than the AUC of the combined detection. *Conclusion*. The increases of Actinomycetes, Verrucomicrobia, Escherichia coli, Clostridium hathewayi, and Ruminococcus gnavus and the decreases of unnamed viruses, Eubacterium eligens, Akkermansia muciniphila, Prevotella stercorea, and Eubacterium rectale were associated with MACCE in RH patients, and the combined detection may provide a method and idea for predicting and preventing MACCE.

1. Introduction

In China, the morbidity of hypertension is 18.8% in people aged ≥18, while the blood pressure control rate is only 6.1%, which is not only related to medication compliance and treatment timeliness but also related to the number of patients with refractory hypertension (RH) [1]. RH patients are more difficult to control their blood pressure. Poor blood pressure control has been proven to cause damage to target organs such as the heart, brain, and kidney and increase the risk of major adverse cardiovascular and cerebrovascular events (MACCE), threatening the life of patients. Thus, early predicting the risk of RH patients complicated with MACCE is of great significance for the prevention and treatment of MACCE and its adverse prognosis [2]. Intestinal flora contains a large number of diverse microorganisms and continuously exchanges information with the host, participating in multiple physiological processes such as digestion, intestinal

barrier, nervous system regulation, and metabolism [3, 4]. Compared with healthy people, hypertensive patients are significantly abnormal in the intestinal flora, which is closely associated with blood pressure level, indicating that the intestinal flora is related to the incidence and progression of hypertension. However, there is no data on whether intestinal flora is involved in the occurrence and prediction of MACCE in RH patients [5]. Based on the above background, this study attempted to explore the predictive value of intestinal flora in MACCE in RH patients, with the hope of providing evidence-based references for the mechanism of MACCE in RH patients. Details are as follows.

2. Materials and Methods

2.1. RH Patients. The study recruited 359 patients with RH hospitalized in our hospital from April 2020 to March 2021. During the 1-year follow-up, 4 patients were lost to follow-up and 355 patients were visited, including 179 females and 176 males, aged from 38 to 86 years, with an average of 56.64 ± 13.90 years. All patients signed the written informed consent. The study was permitted by the Ethics Committee of our hospital. All patients were divided into 2 groups, including a MACCE group and no-MACCE group.

Inclusion criteria are listed as follows: (i) patients meeting the diagnostic criteria of RH [1], (ii) patients who promised to cooperate with follow-up, (iii) patients whose age was more than 18, (iv) patients with over 1 year of survival rate, (v) patients without terminal diseases, and (vi) patients voluntarily signing informed consent. Exclusion criteria are as follows: (i) patients with acute gastroenteritis, (ii) patients with chronic intestinal disease, (iii) patients with malignant cancers, (iv) patients who had been treated with beneficial bacteria and antibacterial drugs within 1 month before enrollment, (v) patients lost to follow up, (vi) patients who could not communicate properly, and (vii) patients who had MACCE induced by vascular malformation, aneurysm, and hematologic diseases.

2.2. Method

2.2.1. Information Collection of RH Patients. General information questionnaire was performed to collect RH patient information, including age, gender, body mass index, diastolic blood pressure, systolic blood pressure, duration of disease, diabetes, hyperlipidemia, smoking, drinking, chronic renal insufficiency, and medication history.

2.2.2. Detection of Intestinal Flora. Reagents used in this study included Stool DNA Kit (Beijing Dingguo Changsheng Biotech, China) and $2 \times$ Taq PCR MasterMix (Solarbio, Beijing, China). Primer synthesis was performed by Sangon Biotech (Shanghai, China). Experiment instruments included an ultraviolet spectrophotometer (U-3900; Hitachi, Tokyo, Japan), polymerase chain reaction (PCR) thermocycler (9600; PerkinElmer, Boston, MA, USA), automatic PCR analysis system (LightCycler 480, Roche, Basel, Switzerland), and ultraviolet transmission and reflection analyzer (FS-312; Shanghai Fusheng Biotech, China).

2 g of midstream stools was collected from RH patients using a special stool collector, and DNA was extracted using a stool DNA Kit. DNA purification and concentration were analyzed by an ultraviolet spectrophotometer, and DNA integrity was determined by agarose gel electrophoresis. The OD260/OD280 of purified DNA with high purity is between 1.6 and 1.8. Then, V3-V4 variable regions of microbial 16 SrDNA were amplified by PCR with primers (forward, 5′-GTGT GYCAGCMGCCGCGGTAA-3′ and reverse, 5′-CCGGAC TACNVGGGTWTCTAAT-3′) with the reaction at 94°C for 3 min, 27 cycles at 94°C for 30 s, 72°C for 30 s, and 72°C for 10 min and then identified by high-throughput sequencing using an Illumina HiSeq sequencer, followed by bioinformatics analysis. The DNA was quantified by quantitative real-time PCR with a PCR thermocycler. Double barcode was introduced into the primer area for PCR amplification to prevent amplification bias and the occurrence of chimeric sequences to ensure the satisfactory concentration of amplification products in the minimum cycle number of samples.

When investigating microbial diversity, operational taxa are introduced to facilitate analysis and improve efficiency. Representative sequences of the operational taxonomic unit were selected and compared with ribosomal RNA data of Greengenes Database 13-8 version based on 99% sequence similarity clustering to obtain the annotation information of species. Single sequences and chimeric sequences without duplication were taken out, and the confidence threshold was set to 70% to obtain the composition of the tested samples at phylum and species classification levels. The species abundance spectrum was evaluated according to the proportion of phylum and species in the total number of sequences.

2.3. Observation Indexes. The observation indexer were as follows: (1) general information was compared between the two groups. (2) The abundance of intestinal flora at the phylum level was compared between the two groups. (3) The abundance of intestinal flora at the species level was compared between the two groups. (4) The influence factors of RH complicated with MACCE were analyzed between the two groups. (5) The predictive value of intestinal microbiota-related indexes for MACCE was assessed between the two groups.

2.4. Statistical Analysis. All data were analyzed using SPSS24.0. Attribute data were compared using the χ^2 test and expressed as n (%), while variables data were compared with Student's t-tests and expressed as means ± standard deviations (SD). The factors related to MACCE were evaluated using multifactor logistic regression analysis, and the value of intestinal flora in predicting MACCE was determined using receiver operating characteristic (ROC) and the area under ROC (AUC). $P < 0.05$ indicated statistical significance.

3. Results

3.1. Comparison of General Informal. During the 1-year follow-up, 4 cases were lost to follow-up and 355 cases were visited. As a result, MACCE occurred in 169 cases (47.61%), including 55 cases with cerebral hemorrhage, 62 cases with

cerebral infarction, 44 cases with acute myocardial infarction, and 8 cases with cardiovascular and cerebrovascular event-related death. 186 cases (52.39%) did not occur with MACCE. The results showed that there was no significant difference in age, gender, body mass index, diastolic blood pressure, duration of disease, diabetes, hyperlipidemia, smoking, drinking, chronic renal insufficiency, and medication history when comparing the two groups (Table 1). But, systolic pressure is higher in the MACCE group than in the no-MACCE group ($P < 0.05$) (Table 1).

3.2. Comparison for the Abundance of Intestinal Flora at the Phylum Level. The results showed that the abundances of Actinomycetes and Verrucomicrobia were higher in the MACCE group than in the no-MACCE group, while the abundance of unnamed virus had the opposite results ($P < 0.05$) (Table 2).

3.3. Comparison for the Abundance of Intestinal Flora at the Species Level. The results showed that the abundances of Eubacterium eligens, Akkermansia muciniphila, Prevotella stercorea, and Eubacterium rectale were lower in the MACCE group than in the no-MACCE group, while the abundances of Escherichia coli, Clostridium hathewayi, and Ruminococcus gnavus were opposite ($P < 0.05$) (Table 3).

3.4. Multiple-Factor Analysis of RH Complicated with MACCE. MACCE occurrence was taken as the dependent variable, and the comparison index between the two groups ($P < 0.05$) was taken as the independent variable. As shown in Table 4, systolic pressure, Actinomycetes, unnamed virus, Verrucomicrobia, Eubacterium eligens, Akkermansia muciniphila, Prevotella stercorea, Escherichia coli, Eubacterium rectale, Clostridium hathewayi, and Ruminococcus gnavus were all associated with MACCE in RH patients ($P < 0.05$).

3.5. Analysis of the Predictive Value of Intestinal Microbiota-Related Indexes for MACCE. According to the ROC curve of intestinal microbiota-related indexes to predict MACCE, we found that the combined detection had the highest AUC (Figure 1 and Table 5).

4. Discussion

Diastolic blood pressure and/or systolic blood pressure still cannot be effectively controlled after RH patients sufficiently take more than 3 types of antihypertensive drugs including diuretics. It is difficult to control blood pressure in such patients, and the risk of MACCE increases accordingly [6]. Thus, it is necessary to investigate MACCE in RH patients. Intestinal flora is an important component of intestinal microecology, and it is in a dynamic and stable state under a physiological state, which is crucial for maintaining body health. The blood pressure of healthy germ-free mice was significantly increased after being treated with the stool of hypertensive mice [7]. However, the supplementation of Bifidobacterium breve could improve vascular endothelial function and prevent systolic blood pressure from rising [8]. Yan et al. [9] reported that the intestinal flora of healthy rats could significantly reduce the blood pressure of hypertensive rats and reshaped the composition, metabolism, and interrelationship of intestinal flora in hypertensive animal models induced by high salt and increased intestinal-derived corticosterone production, serum levels, and intestinal corticosterone levels, thereby promoting the increase of blood pressure. The above evidence suggested that the pathogenesis of high blood pressure involved the intestinal flora.

At the level of phylum classification, Bacteroidetes and phylum Firmicutes are the two most dominant phyla in the intestinal flora of healthy people and hypertensive people [10]. The present study found the similar phenomenon that the abundances of Bacteroidetes and phylum Firmicutes were the highest in the intestinal flora of RH patients regardless of whether they were complicated with MACCE. Moreover, the study showed that the abundances of Actinomycetes and Verrucomicrobia were higher in the MACCE group than in the no-MACCE group, while the abundance of unnamed virus had the opposite results, indicating that Actinomycetes, Verrucomicrobia, and unnamed virus were associated with MACCE in RH patients. As reported, in RH patients with MACCE, both Actinomycetes and Verrucomicrobia can regulate energy metabolism and further affect the occurrence of obesity, which is recognized as a MACCE-related risk factor [11], demonstrating that their upregulation may affect the occurrence of MACCE through the energy metabolism. Unnamed viruses can produce butyrate, maintain intestinal mucosal barrier function, and prevent harmful metabolites such as trimethylamine and lipopolysaccharide from entering the peripheral circulation through intestinal mucosa by upregulating the expression of intestinal epithelial tight junction protein [12]. Therefore, theoretically, reducing of abundances of Actinomycetes and Verrucomicrobia and increasing the abundance of unnamed viruses may help prevent damage to target organs such as the heart and brain in RH patients. However, how to regulate intestinal flora and whether it can bring substantial benefits to RH patients in the clinic remain to be further explored.

At the level of species classification, the number of Escherichia coli, Clostridium hathewayi, and Ruminococcus gnavus is higher in hypertensive patients than in healthy people [13]. Our data showed that the abundances of Eubacterium eligens, Akkermansia muciniphila, Prevotella stercorea, and Eubacterium rectale were significantly decreased in the MACCE group compared with the no-MACCE group, while the abundances of Escherichia coli, Clostridium hathewayi, and Ruminococcus gnavus were opposite. Among them, Escherichia coli parasitizes the human large intestine in the physiological state, harmless to the human body, but under certain conditions, it can produce coagulase, enterotoxin, and other harmful substances, causing inflammatory reaction, affecting the occurrence of MACCE through the brain-intestinal circulation pathway. A previous study explained that the increased abundance of Escherichia coli was a potential biomarker for predicting cardiovascular events after acute coronary syndrome [14], and our results were similar to the finding. According to the investigation of Li et al., the intestinal microflora Clostridium hathewayi increases in patients with diabetes, which is related to

Table 1: Comparison of general information between the two groups.

Data	MACCE group ($n = 169$)	No-MACCE group ($n = 186$)	t/χ^2	P
Age (year)	57.48 ± 9.64	55.87 ± 11.30	1.437	0.152
Gender			0.351	0.554
Female	88 (52.07)	91 (48.92)		
Male	81 (47.93)	95 (51.08)		
Body mass index (kg/m^2)	23.70 ± 0.59	23.58 ± 0.67	1.783	0.075
Diastolic blood pressure (mmHg)	114.58 ± 6.72	113.95 ± 5.24	0.990	0.323
Systolic blood pressure (mmHg)	153.84 ± 5.01	149.60 ± 5.31	7.718	0.001
Duration of disease (years)	7.92 ± 1.36	7.85 ± 1.42	0.473	0.636
Diabetes			0.679	0.410
No	146 (86.39)	166 (89.25)		
Yes	23 (13.61)	20 (10.75)		
Hyperlipidemia			0.733	0.392
No	110 (65.09)	129 (69.35)		
Yes	59 (34.91)	57 (30.65)		
Smoking			0.319	0.572
No	135 (79.88)	144 (77.42)		
Yes	34 (20.12)	42 (22.58)		
Drinking			0.307	0.580
No	141 (83.43)	151 (81.18)		
Yes	28 (16.57)	35 (18.82)		
Chronic renal insufficiency			1.387	0.239
No	158 (93.49)	179 (96.24)		
Yes	11 (6.51)	7 (3.76)		
Medication history				
Calcium antagonists	132 (78.11)	152 (81.72)	0.723	0.395
Diuretics	115 (68.05)	123 (66.13)	0.148	0.701
Beta-blockers	108 (63.91)	115 (61.83)	0.087	0.768
ACEI/ARB	161 (95.27)	180 (96.77)	0.532	0.466

Table 2: Comparison of abundance of intestinal flora at the phylum level between the two groups (±s).

Phylum	MACCE group ($n = 169$)	No-MACCE group ($n = 186$)	t	P
Actinomycetes	3.61 ± 1.02	0.34 ± 0.11	43.451	0.001
Chlamydiae	0.07 ± 0.02	0.07 ± 0.02	0.000	1.000
Unnamed virus	0.38 ± 0.12	0.75 ± 0.21	20.113	0.001
Bacteroidetes	25.42 ± 8.35	26.30 ± 9.48	0.924	0.356
Verrucomicrobia	12.72 ± 4.11	2.49 ± 0.82	33.231	0.001
Euryarchaeota	0.86 ± 0.23	0.83 ± 0.19	1.344	0.180
Phylum Firmicutes	51.35 ± 12.26	53.11 ± 14.73	1.217	0.225
Proteobacteria	12.22 ± 3.54	11.73 ± 3.25	1.360	0.175
Synergistetes	2.20 ± 0.70	2.09 ± 0.68	1.501	0.134
Fusobacteria	0.37 ± 0.11	0.39 ± 0.12	1.632	0.104

MACCE, which supports the role of Clostridium hathewayi in MACCE [15]. However, it is a pity that Clostridium hathewayi is rarely studied in the field of acute cardiovascular and cerebrovascular diseases, and the specific mechanism of Clostridium hathewayi in the occurrence of MACCE is still not clear. Ruminococcus gnavus is a member of the phylum Firmicutes and has a low abundance among the intestinal flora. Considerable evidence suggested that the increased

Table 3: Comparison for the abundance of intestinal flora at the species level between the two groups.

Species	MACCE group ($n = 169$)	No-MACCE group ($n = 186$)	t	P
Eubacterium eligens	1.34 ± 0.40	2.58 ± 0.83	17.647	0.001
Akkermansia muciniphila	0.09 ± 0.03	10.24 ± 3.11	42.420	0.001
Prevotella stercorea	0.04 ± 0.01	3.87 ± 1.29	35.591	0.001
Escherichia coli	6.25 ± 2.18	1.60 ± 0.55	28.126	0.001
Eubacterium rectale	0.79 ± 0.22	7.93 ± 2.34	39.503	0.001
Clostridium hathewayi	2.88 ± 0.94	0.09 ± 0.02	40.475	0.001
Ruminococcus gnavus	2.07 ± 0.60	0.66 ± 0.21	30.089	0.001

Table 4: Logistic regression equation analysis of RH complicated with MACCE.

Influence factors	β	SE	Wald x^2	OR	95% CI	P
Systolic pressure	2.458	0.659	13.907	11.676	1.835~74.293	0.001
Actinomycetes	1.847	0.512	13.009	6.339	1.148~35.002	0.001
Unnamed virus	-1.485	0.455	10.646	0.227	0.105~0.489	0.001
Verrucomicrobia	2.616	0.688	14.456	13.678	2.194~85.277	0.001
Eubacterium eligens	-0.846	0.236	12.845	0.429	0.258~0.714	0.001
Akkermansia muciniphila	-1.322	0.414	10.199	0.267	0.078~0.911	0.001
Prevotella stercorea	-0.680	0.203	11.206	0.507	0.394~0.652	0.001
Escherichia coli	2.579	0.732	12.409	13.178	4.662~37.251	0.001
Eubacterium rectale	-0.995	0.279	12.713	0.370	0.163~0.839	0.001
Clostridium Hathewayi	2.682	0.505	28.196	14.607	3.522~60.584	0.001
Ruminococcus gnavus	1.920	0.576	11.112	6.821	1.039~44.784	0.001

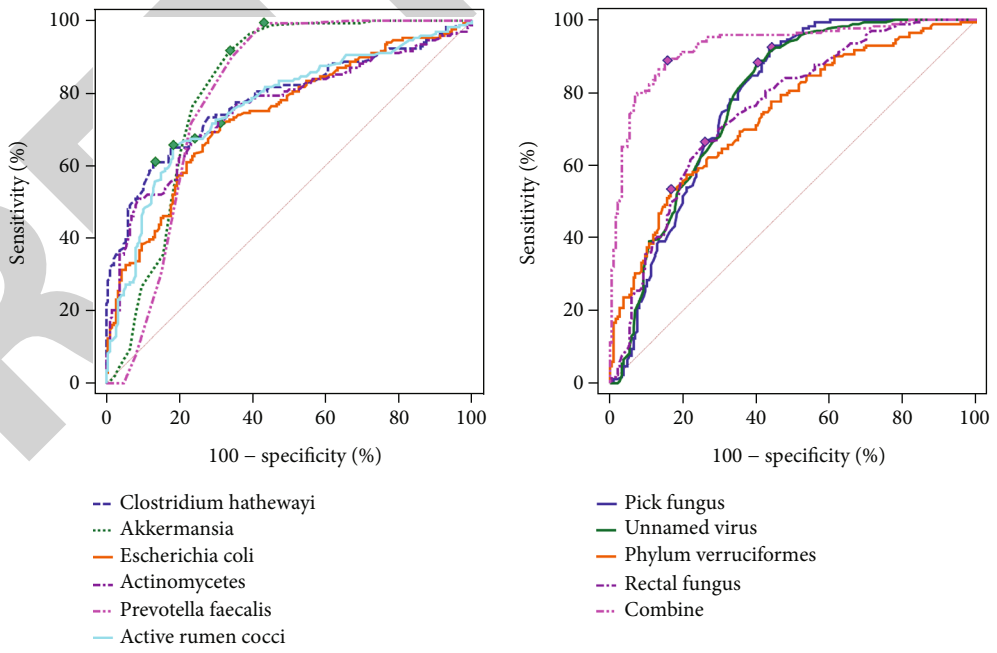

Figure 1: ROC curves of intestinal flora-related indexes to predict MACCE.

Table 5: Results of ROC analysis.

Index	AUC	95% CI	Cut-off value	Sensitivity (%)	Specificity (%)	*P*
Actinomycetes	0.757	0.708~0.800	3.36	67.46	75.81	0.001
Unnamed virus	0.783	0.736~0.824	0.50	88.17	59.68	0.001
Verrucomicrobia	0.739	0.690~0.784	12.08	53.25	83.33	0.001
Eubacterium eligens	0.780	0.733~0.822	1.89	92.31	55.91	0.001
Akkermansia muciniphila	0.815	0.770~0.854	0.13	91.72	66.13	0.001
Prevotella stercorea	0.797	0.751~0.838	0.06	99.41	56.99	0.001
Escherichia coli	0.739	0.690~0.783	5.21	71.60	68.82	0.001
Eubacterium rectale	0.754	0.706~0.798	0.85	66.27	74.19	0.001
Clostridium Hathewayi	0.781	0.734~0.832	2.61	60.95	86.56	0.001
Ruminococcus gnavus	0.764	0.717~0.808	1.92	65.68	81.72	0.001
Combination treatment	0.926	0.894~0.951		88.76	84.41	0.001

abundance of Ruminococcus gnavus could lead to oxidative stress and intestinal barrier damage [16]. Eubacterium eligens and Eubacterium rectale are symbiotic bacteria of the human intestinal flora that can produce butyric acid and reduce the risk of atherosclerosis [17]. Akkermansia muciniphila is a kind of probiotic that widely exists in animals and humans, and its decrease is associated with many metabolic diseases, such as diabetes, obesity and hypertension [18]. Prevotella stercorea is a kind of important symbiotic bacterium of human intestinal flora, which can protect the gastrointestinal mucosa, inhibit inflammation, and maintain the stability of the intestinal mucosa [19]. Thus, the decreased abundances of Eubacterium eligens, Akkermansia muciniphila, Prevotella stercorea, and Eubacterium rectale and the increased abundances of Escherichia coli, Clostridium hathewayi, and Ruminococcus gnavus were associated with MACCE in RH patients.

In the present study, according to the results of ROC analysis, we found that the AUC of each intestinal flora in predicting MACCE was >0.7, showing their predictive value in MACCE. In particular, the AUC of Akkermansia muciniphila was the highest compared with other intestinal flora, suggesting that Akkermansia muciniphila had the highest predictive value in MACCE among these intestinal florae. However, the AUC of combined detection of the intestinal flora was 0.926, which was significantly higher than that of other single intestinal flora, suggesting that the combined detection of the intestinal flora could improve the reliability of predicting MACCE. The reason may be that these intestinal florae are associated with the occurrence of MACCE, and the combined detection covers more mechanisms of MACCE occurrence. However, intestinal flora detection has certain requirements on hospital hardware and software configuration, which may limit its application in primary medical centers. Thus, further studies are needed to study more convenient intestinal flora detection methods.

Taken together, the increased number of Actinomycetes, Verrucomicrobia, Escherichia coli, Clostridium hathewayi, and Ruminococcus gnavus and the decreased number of unnamed virus, Eubacterium eligens, Akkermansia muciniphila, Prevotella stercorea, and Eubacterium rectale were associated with MACCE in RH patients. The combined detection can provide a method and idea for predicting and preventing MACCE.

Data Availability

The labeled dataset used to support the findings of this study is available from the corresponding author upon request.

Conflicts of Interest

The authors declare that there are no conflicts of interest.

References

[1] N. Sun, Y. Huo, and J. Wang, "Chinese expert consensus on diagnosis and treatment of refractory hypertension. Chinese," *Journal of Interventional Cardiology*, vol. 2, 2013.

[2] G. Lamirault, M. Artifoni, M. Daniel, N. Barber-Chamoux, and Nantes University Hospital Working Group on Hypertension, "Resistant hypertension: novel insights," *Current Hypertension Reviews*, vol. 16, no. 1, pp. 61–72, 2020.

[3] Q. Tang and L. Cao, "Intestinal flora and neurological disorders," *Sheng Wu Gong Cheng Xue Bao*, vol. 37, no. 11, pp. 3757–3780, 2021.

[4] R. R. Muralitharan and F. Z. Marques, "Diet-related gut microbial metabolites and sensing in hypertension," *Journal of Human Hypertension*, vol. 35, no. 2, pp. 162–169, 2021.

[5] N. G. Vallianou, E. Geladari, and D. Kounatidis, "Microbiome and hypertension," *Journal of Cardiovascular Medicine*, vol. 21, no. 2, pp. 83–88, 2020.

[6] S. Kim, J. J. Park, M. S. Shin et al., "Apparent treatment-resistant hypertension among ambulatory hypertensive patients: a cross-sectional study from 13 general hospitals," *The Korean Journal of Internal Medicine*, vol. 36, no. 4, pp. 888–897, 2021.

[7] P. Louca, C. Menni, and S. Padmanabhan, "Genomic determinants of hypertension with a focus on metabolomics and the gut microbiome," *American Journal of Hypertension*, vol. 33, no. 6, pp. 473–481, 2020.

Hindawi
Computational and Mathematical Methods in Medicine
Volume 2023, Article ID 9815867, 1 page
https://doi.org/10.1155/2023/9815867

Retraction

Retracted: Study on Strength and Quality Training of Youth Basketball Players

Computational and Mathematical Methods in Medicine

Received 26 September 2023; Accepted 26 September 2023; Published 27 September 2023

This article has been retracted by Hindawi following an investigation undertaken by the publisher [1]. This investigation has uncovered evidence of one or more of the following indicators of systematic manipulation of the publication process:

(1) Discrepancies in scope

(2) Discrepancies in the description of the research reported

(3) Discrepancies between the availability of data and the research described

(4) Inappropriate citations

(5) Incoherent, meaningless and/or irrelevant content included in the article

(6) Peer-review manipulation

The presence of these indicators undermines our confidence in the integrity of the article's content and we cannot, therefore, vouch for its reliability. Please note that this notice is intended solely to alert readers that the content of this article is unreliable. We have not investigated whether authors were aware of or involved in the systematic manipulation of the publication process.

In addition, our investigation has also shown that one or more of the following human-subject reporting requirements has not been met in this article: ethical approval by an Institutional Review Board (IRB) committee or equivalent, patient/participant consent to participate, and/or agreement to publish patient/participant details (where relevant).

Wiley and Hindawi regrets that the usual quality checks did not identify these issues before publication and have since put additional measures in place to safeguard research integrity.

We wish to credit our own Research Integrity and Research Publishing teams and anonymous and named external researchers and research integrity experts for contributing to this investigation.

The corresponding author, as the representative of all authors, has been given the opportunity to register their agreement or disagreement to this retraction. We have kept a record of any response received.

References

[1] Q. Meng, "Study on Strength and Quality Training of Youth Basketball Players," *Computational and Mathematical Methods in Medicine*, vol. 2022, Article ID 4676968, 11 pages, 2022.

Hindawi
Computational and Mathematical Methods in Medicine
Volume 2022, Article ID 4676968, 11 pages
https://doi.org/10.1155/2022/4676968

Research Article

Study on Strength and Quality Training of Youth Basketball Players

Qinghui Meng

Shanxi University, Taiyuan City, Shanxi Province 030006, China

Correspondence should be addressed to Qinghui Meng; 202023705033@email.sxu.edu.cn

Received 7 July 2022; Revised 22 July 2022; Accepted 28 July 2022; Published 18 August 2022

Academic Editor: Min Tang

In order to scientifically explore the effective path of strength quality training of basketball players and improve the effect of strength quality training of basketball players, this paper takes young basketball players as the research object and comprehensively observes the changes and improvement of strength quality by building a strength training monitoring system for basketball players. On this basis, it is proposed to integrate blood flow restriction and basketball players' special strength training. Through the comparison with the traditional resistance strength training method, it is found that after 8 weeks of experimental comparison, the athletes' strength quality test indicators show that the average 3RM of the experimental group 1 bench press is 65.2 kg, the experimental group 2 is 65.7 kg, and the experimental group 3 is 72.2 kg. The average performance of the traditional control group was 55.4 kg. Compared with the traditional group, the average performance of the three experimental groups in bench press was significantly improved, which also verified the feasibility of this method in strength quality training.

1. Introduction

Any sports event is completed by the muscle tissue as an active sports organ with different compliance intensity and contraction speed and then drives the movement of bones of specific sports organs to complete the action. If the strength brought by the contraction and relaxation of human muscles is improved in the process of sports, the effect of sports is bound to be affected. The running, jumping, and confrontation in the process of sports are inseparable from the strength quality of athletes, and a good strength quality will have a higher sports effect. Especially for basketball players, because basketball itself is a competitive sport, basketball players will face a lot of physical confrontation in the process of competition [1, 2]. Physical confrontation must rely on good strength quality as support, so special strength training of athletes is very important. This paper introduces a blood flow restriction training method and discusses the feasibility of special strength training by comparing with traditional resistance strength training.

2. Literature Review

Leng et al. analyzed the impact of core strength training on swimmers through empirical research. The results show that athletes can effectively improve their core strength through a period of core strength training. When athletes make various technical actions, they can greatly improve the coordination between the muscle groups involved, which is conducive to athletes' better control of the body's focus, so as to improve athletes' special technical ability and improve their sports performance [3]. Gómez-Carmona et al. conducted empirical research on the core strength training of fencing athletes. The research shows that fencing athletes can significantly improve their core strength, core endurance, core explosive power, and other abilities after a period of training by choosing their own core strength training methods [4]. Zou et al. conducted core stability training experiments on track and field athletes. The results of the experiments show that after receiving a period of core stability training, middle- and long-distance runners can greatly improve their running

efficiency and respiratory muscle ability and effectively reduce the probability of athletes' sports injury [5]. Li and Wang believe that because core strength training plays an important role in the performance of throwing athletes, athletes can significantly improve their body coordination and flexibility after a period of core strength training and maximize the strength of all parts of athletes [6]. Mwanzia et al. believe that in modern basketball, athletes need to have good core strength quality as support and guarantee when making basic technical actions such as moving, shooting, changing direction, passing, and breakthrough [7]. Only basketball players have strong core strength quality; they can ensure the stability of their bodies when making various technical movements. Especially in the process of physical confrontation, the importance of core strength training is self-evident, so that all links of the athlete's body can form a powerful whole, so as to ensure the coordination and flexibility between the upper and lower limbs, and improve the athlete's ability to use skills and tactics. Chao et al. believe that athletes need the participation of core areas in the process of making various difficult technical actions in training and competition. The core area plays an important role in the stability, coordination, and continuity of athletes in the process of completing various technical movements. They also proposed that the core strength area mainly refers to the lumbar and abdominal muscles, back muscles, hip muscles, and deeper muscle groups [8].

3. Athlete Training Monitoring System

3.1. Pneumatic Strength Training System. This paper studies a set of training equipment driven by air pressure as a load-bearing load [9]. This series of training equipment includes many horizontal equipment. Although each equipment has slightly different appearance and structure for different limb parts, the load source is all driven by air pressure, which is the same as training resistance. The training system studied in this topic includes two parts: the first level system is the service host for information storage and instruction distribution, and the second level system is the equipment directly involved in training, and its structure is shown in Figure 1.

As a service host, the primary system is carried on the PC side and is operated by the training center specialist to record and store data and issue training tasks. In terms of information exchange between the upper and lower systems, RFID wireless technology is integrated into each training mode with ID card as the medium, integrating the service system of the service host and the training needs of the training customers, so as to realize the real-time feedback analysis of training information.

3.2. Pneumatic Load Transfer Scheme. The scheme design of converting air pressure into load-bearing load mainly includes two aspects: on the one hand, the layout and structure of air pressure, on the other hand, the design logic of controlling air pressure, and at the same time, the mechanical structure of training equipment should be considered comprehensively in many aspects. As for the design of air circuit structure of air pressure perfusion, this research has high requirements for supplementing and unloading air pressure, which not only requires the control accuracy of proportional solenoid valve but also has corresponding requirements for the design structure of air circuit. After repeated tests, select the appropriate air pipe diameter and cylinder volume [10, 11]. The structure of pneumatic circuit is shown in Figure 2.

About the air pressure control, the embedded control system detects and adjusts the simulated load of the training equipment, that is, the air pressure value in the cylinder. During training, the sensor detects the air pressure value in the cylinder in real time and feeds it back to the master control to make corresponding adjustments. The design of pneumatic load feedback control of instruments and equipment is shown in Figure 3, forming a closed-loop control. The execution process of pneumatic load is as follows.

This research adopts the compound control of additional inverse model feedforward compensation and detecting current feedback PWM drive. In the PWM drive of proportional solenoid valve, in order to meet the control requirements at the same time, it is necessary to collect the current value on the coil at all times, and resistance is the simplest and most effective method, which is actually to adjust the deviation of the controlled quantity. It obtains the control deviation $e(t)$ according to the present value $r(t)$ and the test value $c(t)$:

$$e(t) = r(t) - c(t). \tag{1}$$

Then, taking $e(t)$ as the input, the arithmetic unit performs PI and PD control. The output is as follows:

$$u(t) = Kp\left[e(t) + \frac{1}{Ti}\int_0^t e(t)dt + \frac{T_d de(t)}{dt}\right] + u_0(1). \tag{2}$$

After conversion,

$$u(t) = Kpe(t) + K_i\int_0^t e(\tau)d\tau + K_d\frac{d}{dt}e(t) + u_0(1), \tag{3}$$

where at time t, $u(t)$ is the actual quantity, $e(t)$ is the deviation, and u_0 is the given value. Since STM32 is a digital component and belongs to discrete control, it should be discretized and converted into discrete state space expression:

$$u(KT) = K_p e(KT) + K_i\sum_{j=0}^{k} e(jT) + K_d[e(KT) - e(T(k-1))]. \tag{4}$$

In the above formula, KT is the number of time of the collected object, where $u(KT)$ is the output value of the time [12], K_i is the integral coefficient:

$$K_i = \frac{K_p T}{T_i}. \tag{5}$$

T_i is the integral time constant.

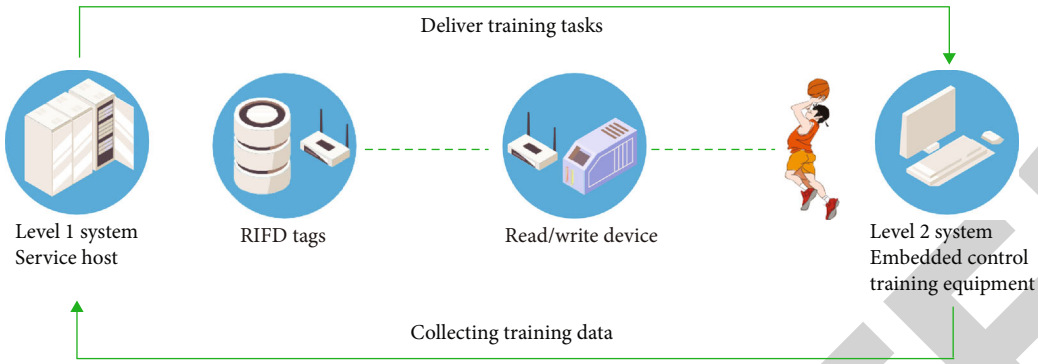

Figure 1: System operation structure.

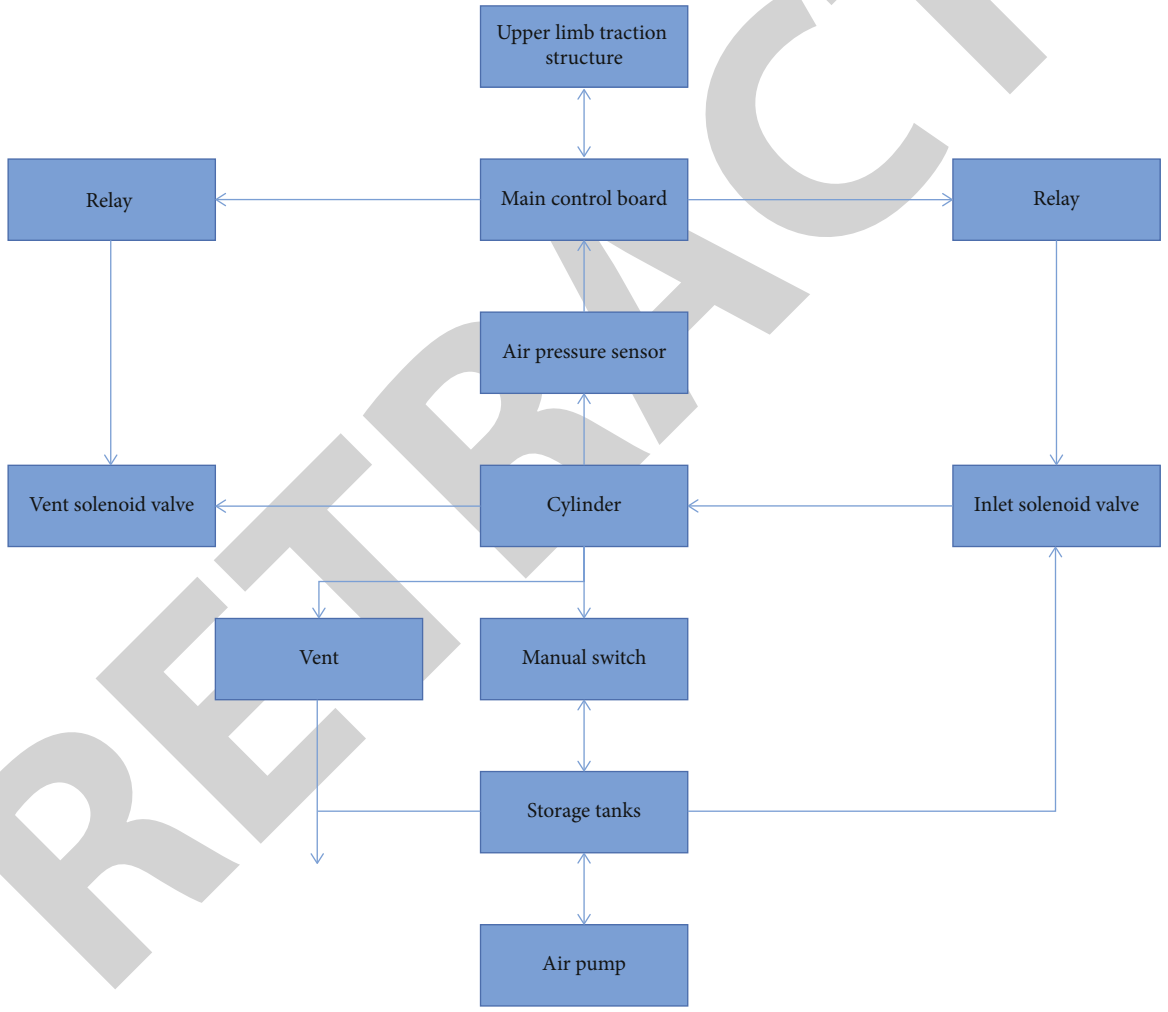

Figure 2: Pneumatic circuit structure.

K_d is the differential coefficient:

$$K_d = \frac{K_p T_d}{T}. \tag{6}$$

T_d is the differential time constant.

In this pneumatic control system, the sampling frequency is jointly determined according to the air path aperture and the response speed of the proportional valve, as well as the air pressure feedback value in the cylinder, and then according to the deviation generated in the upper limb training process, the control quantity is calculated by proportion, integration, and differentiation for control. As for parameter

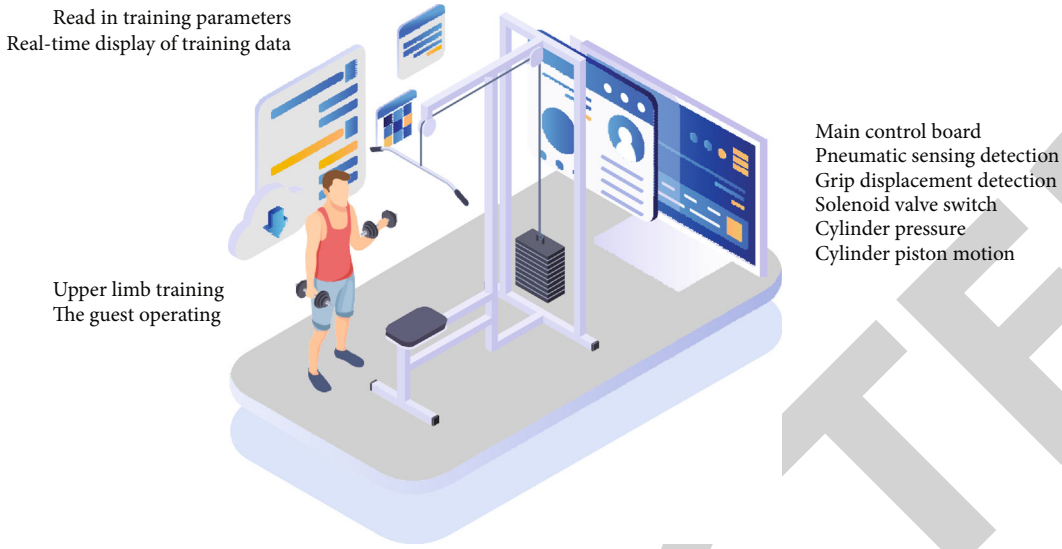

Figure 3: Pneumatic load control flow chart.

setting, the critical proportional method is better than the failure curve method according to the control demand. The air pressure control of the trainer is adjusted at any time according to the specific requirements of the training equipment in the use process. The general operation flow chart of the training equipment is shown in Figure 4, and the specific steps are as follows [13, 14].

The training system has two methods to increase or decrease the air pressure load of the equipment:

(a) There is a mechanical addition button on the equipment shell to increase or decrease the load manually, and the size of the increase or decrease load is determined by the individual's will

(b) There is a control system that automatically replenishes or releases the load according to the feedback of the trainers, or when the system self-checks the equipment, it replenishes the load to reach the initialization value

3.3. Pneumatic Load Calibration. Due to the difference in the manufacturing process of the sensor, the air pressure value may correspond to different voltage values, and the detection voltage value provided to the main control will also be different. In order to ensure that the measured air pressure value and the detected and collected voltage value correspond correctly, the air pressure transmitter should be calibrated before use to determine the compensation, which is the significance of calibrating the initial value of the air pressure sensor. First, set the starting point and any point to determine the corresponding relationship between voltage and pressure. We select the initial value and the intermediate value (roughly determined) as 0 MPa and 0.3 MPa as the calibration standards, and set 0 MPa as the free state, that is, the atmospheric pressure. The output voltage of the sensor at 0 MPa is a, and the output voltage of the sensor at 0.3 MPa is B [15, 16]. The linear relationship between the collected voltage value and the detected pressure is as follows:

$$\mathrm{Gas}P = \mathrm{Gas}V * \frac{0.3\ \mathrm{MPa}}{B - A}. \tag{7}$$

We set it as gross weight (w), which is the starting amount. According to physical mechanics, the load corresponding to air pressure is calculated as follows. P is the pressure in the cylinder, and S is the cross-section of the movable piston, where K is the weight proportion coefficient of the load. For this external instrument, that is, the ratio of the force on the cylinder piston to the force on the grip is pulled by the training customer. The purpose of adding the proportion coefficient is to eliminate the adverse effects such as friction. The weight of the load displayed on the LCD screen of the instrument is

$$W = P * S * K + w. \tag{8}$$

Since the pneumatic simulator is used to load the machine, the above calculated tension value is the theoretical tension value FS. Then, we actually test the tension value of the bracelet grip as F_C, and the relationship is shown in Figure 5 through actual repeated tests.

According to the experimental data, the measured arm tension F_C of the grip has the following relationship with the actual pressure Gas$P$ in the cylinder, where k is the linear coefficient:

$$F_C = \mathrm{Gas}P * k + 2.1. \tag{9}$$

In this paper, the diameters of the two proportional valves provided by KOFLOC3050 and KOFLOC3040 are selected, and the proportional solenoid valve is fitted and tested on the flow hysteresis curve according to the above fitting scheme. Two types of proportional valves were tested

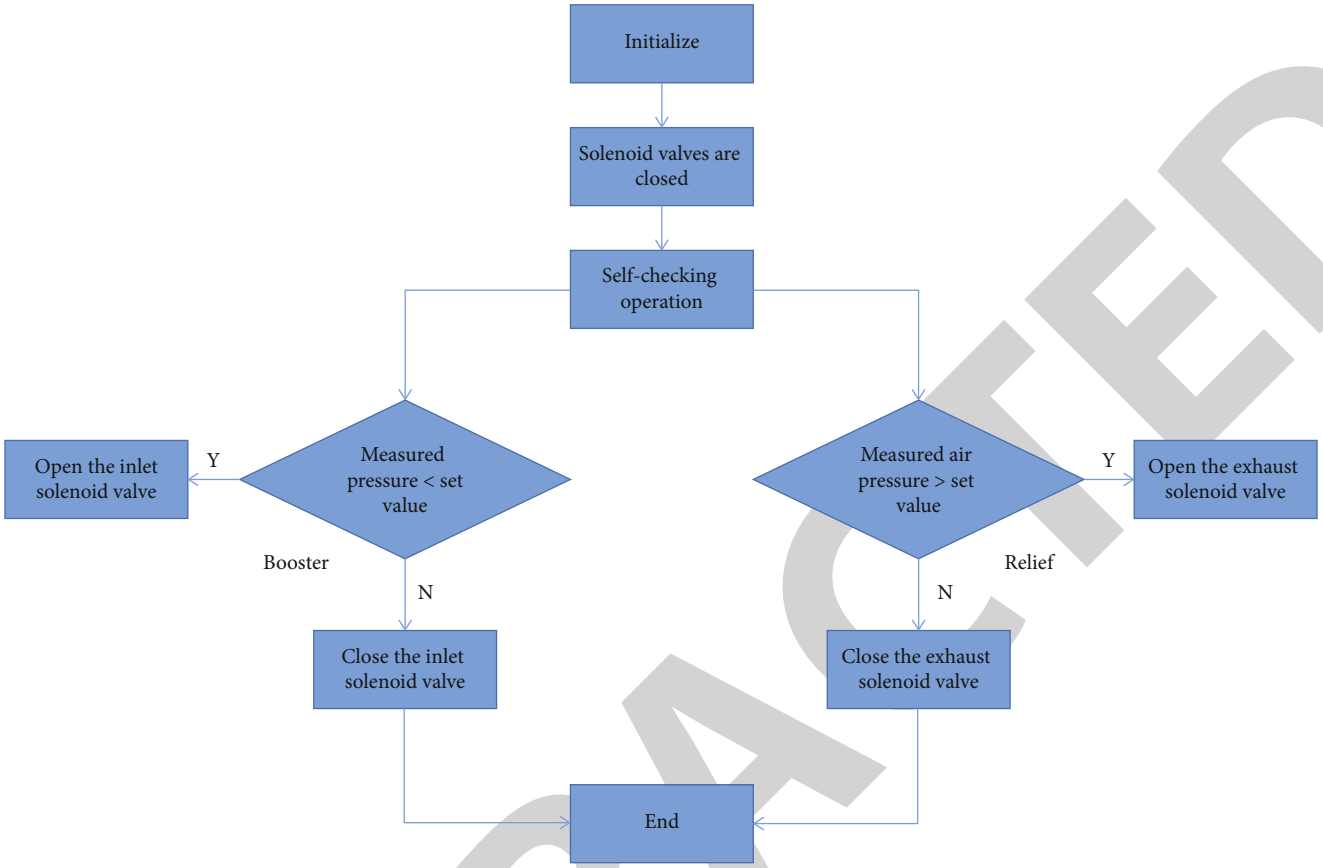

Figure 4: Operation process of solenoid valve.

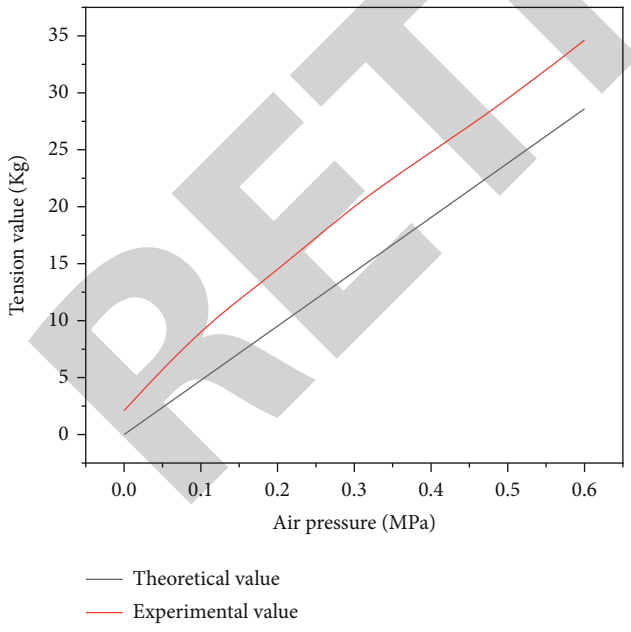

Figure 5: Comparison between theoretical tension and measured tension.

under 0.1 MPa air pressure. The air source was air, the input voltage was 24 V; the operation structure of the controller and the error parameters were obtained in the actual debugging [17]. Considering that this subject adopts incremental PID control, the calculation formula is

$$u(k) = u(k-1) + \Delta u(k), \tag{10}$$

$$\Delta u(k) = K_p[e(k) - e(k-1)] + K_I(e) + K_D[e(k) - 2e(k-1) + e(k-2)]. \tag{11}$$

The magnitude of K_p directly determines the amplitude oscillation, and the amplitude oscillation will increase with the increase of K_p amplitude, but the oscillation frequency is small, and the system needs more time to achieve stability; K_I determines the action response speed, and K_D is used to eliminate static errors. Variables in the formula are as follows:

$e(k)$: the error between the air flow through the flow valve and the theoretical value

$e(k-1)$: the error value of the previous time

$e(K-2)$: the error value of the previous sampling time

When $|e(k)|$ is higher than the amplitude of PWM wave, the error is too large. At this time, the control quantity is directly output at the maximum value to reduce the error to the allowable range as soon as possible, where

$$\Delta u(k) = \Delta u_{\max}, \tag{12}$$

$$\text{or } \Delta u(k) = -\Delta u_{\max}. \tag{13}$$

At this time, the system is equivalent to implementing open-loop control. When $e(k) \cdot \Delta e(k) \geq 0$, it means that it is a positive error at the moment, and the size of the error cannot be determined. The controller implements control, taking the absolute value of the reduced error as the control direction, and the controller output is as follows:

$$\Delta u(k) = K_I \left\{ \begin{array}{c} K_p[e(k) - e(k-1)] + K_I e(k) \\ +K_D[e(k) - 2e(k-1) + e(k-2)] \end{array} \right\} \quad K_I > 1. \tag{14}$$

If $|e(k)|$ is less than the set error limit, that is, the error is within the allowable range, there is no need for forced limit control, and general PID control can be implemented. When $e(k) \cdot \Delta e(k) < 0$ and $e(k) \cdot \Delta e(k-1) > 0$, the control reduces the error to the equilibrium state and keeps the control unchanged, and the output is $\Delta u(k) = 0$. When $|e(k)|$ is less than a minimal positive number, the error is very small at this time. The controller adds integral control to reduce the steady-state error. The operation formula is proportional plus integral control:

$$\Delta u(k) = K_p[e(k) - e(k-1)] + K_I e(k). \tag{15}$$

When $e(k) = 0$, it is proved that the system is basically error free at this moment and continues to maintain the current control relationship. After the fuzzy PID control processing of the variables by the master controller, the proportional valve drive circuit is driven by PWM wave, and the amplified PWM signal is supplied to the proportional valve to control the flow [18].

4. Comparative Study on Strength Quality Training of Juvenile Basketball Players

4.1. Research Design

4.1.1. Research Object. In this article, a total of 20 members of the basketball special class of basketball school are selected as the experimental objects of this study. All of them are male teenagers aged 14-16 and have a certain foundation of professional basketball training. The basic information of each research object is shown in Table 1, and the basic physical information is shown in Figure 6.

4.1.2. Experimental Method. The experiment period is from August 2020 to October 2020, and the training experiment lasts for 8 weeks. The duration of each experimental training should be controlled at about 35 minutes. In the training three times a week, the members of the experimental group wear pressure bandages for blood flow restriction training, while the members of the control group do not wear pressure bandages for traditional strength training (before the training officially begins, all experimental subjects need to carry out the pretest without blood flow restriction training device, and after all experiments, the posttest without blood flow restriction training device is required). Precautions and screening process before blood flow restriction training are shown in Figure 7.

Table 1: Basic information of experimental objects in basketball special class of basketball school.

Age	Height (cm)	Weight (kg)	BMI
16	180	75	23.1
16	190	85	23.5
14	179	70	21.8
16	179	72	22.4
15	182	65	19.6
16	174	71	20.9
14	180	76	23.4
14	177	70	22.3
16	176	72	23.2
16	180	68	20.9
16	178	72	22.7
14	186	70	20.2
16	183	77	22.9
16	174	81	23.9
16	185	74	21.6
16	186	83	23.9
16	195	86	22.6
15	182	71	21.4
16	192	82	22.2
14	187	73	20.8

Before the blood flow restriction training with a training load of 40% 1RM, the heart rate of the subjects was relatively flat, and there was no change in the heart rate after pressurization. After the blood flow restriction training for about 30 minutes, the immediate heart rate among the subjects did not fluctuate and deviate much, and the rate of heart rate recovery was basically the same as that of conventional resistance strength training [19].

4.2. Research Results and Analysis

4.2.1. Comparison and Analysis of the Test Results of the Special Strength Quality of the Subjects before the Experiment. Before the formal experiment, the original data of 20 people in the four experimental groups were statistically analyzed by using the four strength quality indicators in the youth basketball special strength quality for this experiment. The mathematical statistics method is used to carry out the t-test of independent samples, and the one-way variance homogeneity test and ANVOA difference analysis are carried out uniformly, so as to ensure the scientificity and rationality of the selection of experimental objects and help to ensure the official start of the experiment and the smooth progress of the whole experimental cycle.

Before the official start of this experiment, four groups of experimental objects were tested to obtain the results, and the original data were passed through the one-way variance homogeneity test in SPSS mathematical statistics and

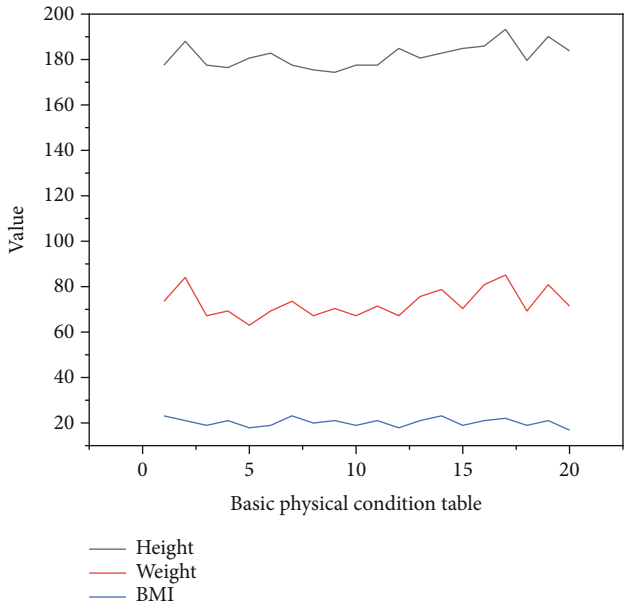

Figure 6: Basic physical conditions of objects in basketball special class of basketball school.

ANVOA variance analysis to draw the conclusion, as shown in Table 2. Before the experiment was officially started, there was no significant difference between the three experimental groups and the control group in the 3RM test item of free bench press ($f = 0.206$, $p = 0.891$, $p > 0.05$). In the barbell free squat 3RM project ($f = 0.118$, $p = 0.948$, $p > 0.05$), there is no significant difference. In the 3/4 sprint events ($f = 0.717$, $p = 0.556$, $p > 0.05$), there is no significant difference. In 17(m) × 15(m) endurance turnaround runs, $f = 0.088$, $p = 2.606$, $p > 0.05$. In the test item of one-step vertical take-off and height touch on both feet, $f = 1.821$, $p = 0.184$. Among the above five items related to basketball special strength quality, the p value is greater than 0.05. There is no significant difference in special strength quality between the three experimental groups and the control group, and everyone's level is relatively similar.

From the data in Table 3, it can be concluded that the T value of the first group and the second group in the bench press 3RM test project is 0.188, the p value is 0.855 ($p = 0.855$), and p is greater than 0.05. There was no significant difference in the strength quality of bench press between the first group and the second group. The value of the independent sample t-test of the subjects of the first and third groups in the bench press 3RM project is $t = -0.271$ and $p = 0.794$, where $p > 0.05$, indicating that there is no significant difference between the two groups. The comparative analysis between the experimental group 1 and the traditional control group ($t = 0.461$, $p = 0.657$, $p > 0.05$) shows that there is no significant difference between the two groups before the official start of the experiment. After comparing the experimental group 2 with the experimental group 3, the conclusion is drawn as follows: $t = -0.487$, $p = 0.639$, and $p > 0.05$. There is no significant difference in the test results between the two groups. The comparison between the experimental group 2 and the traditional control group can be drawn as follows: $t = 0.318$, $p = 0.759$, and $p > 0.05$; there is no significant difference between the experimental group 2 and the control group. Finally, the comparison between the experimental group 3 and the control group shows that $t = 0.318$, $p = 0.759$, and $p > 0.05$. To sum up, experimental group 1, experimental group 2, experimental group 3, and the traditional control group have independent sample t-test, and the p value is greater than 0.05, which has no significant difference. The three groups of the experiment cross compare with each other, and the p value is also greater than 0.05. It is proved that there is no significant difference among 20 subjects in total between all groups in the 3RM maximum strength test of bench press before the start of the experiment, which meets the starting requirements of this experiment.

From the data in Table 4, it can be concluded that the t value of experimental group 1 and experimental group 2 in the squat 3RM test project is 0.352, p value is 0.734 ($p = 0.734$), and p is greater than 0.05. There is no significant difference in the strength quality of bench press between experimental group 1 and experimental group 2, while the value of independent sample t-test between experimental group 1 and experimental group 3 in the squat 3RM project is $t = -0.04$ and $p = 0.969$, where $p > 0.05$. It shows that there is no significant difference between the two groups. The comparison and analysis between the experimental group and the traditional control group ($t = 0.436$, $p = 0.674$, $p > 0.05$) show that there is no significant difference between the two groups before the official start of the experiment. After comparing the experimental group 2 with the experimental group 3, it is concluded that $t = -0.399$, $p = 0.7$, and $p > 0.05$; there is no significant difference in the test results between the two groups. Comparing the experimental group 2 with the traditional control group, it can be concluded that $t = 0.67$, $p = 0.948$, and $p > 0.05$; there is no significant difference between the experimental group 2 and the control group. Finally, the experimental group 3 is compared with the control group, and it is concluded that $t = 0.488$, $p = 0.639$, and $p > 0.05$. To sum up, experimental group 1, experimental group 2, experimental group 3, and the traditional control group have independent sample t-test, and the p value is greater than 0.05, which has no significant difference. The three groups of the experiment cross compare with each other, and the p value is also greater than 0.05. It is proved that there is no significant difference among 20 subjects in total between all groups in the squat 3RM maximum strength test before the start of the experiment, which meets the starting requirements of this experiment [20].

After the 8-week training experiment, the paired sample t-test in the SPSS statistical software was used to calculate and compare the test results of the four test indicators selected from the basketball special strength quality of boys in the traditional control group before and after the experiment, so as to verify the changes and effects of traditional special resistance strength training compared with blood flow restriction training on the basketball special strength

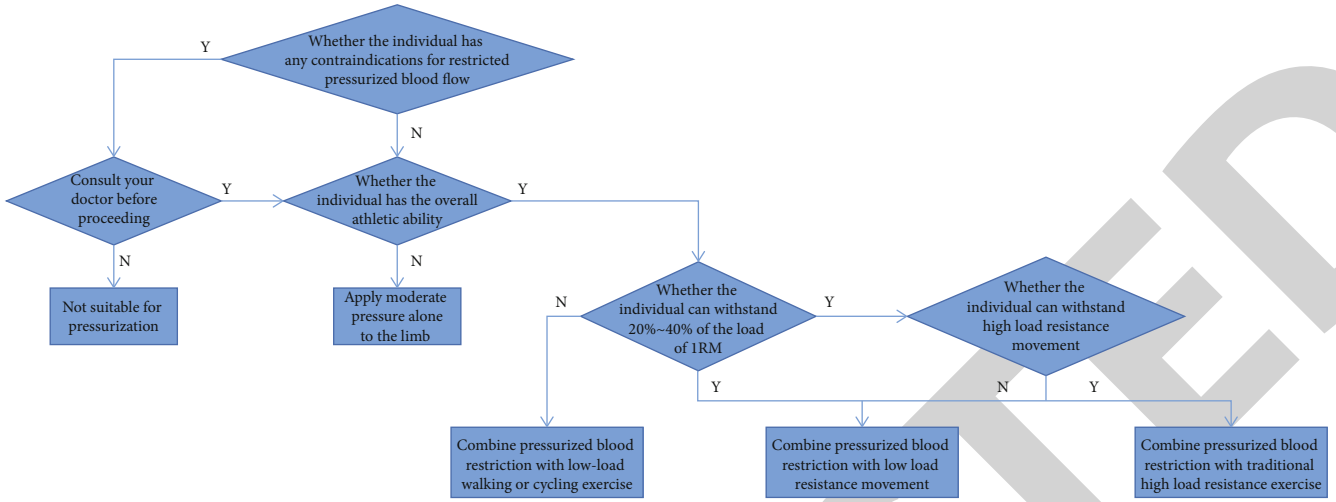

Figure 7: Flow chart of selecting pressure training strategy.

Table 2: One-way ANOVA of special strength indicators of subjects before the experiment.

$N = 5$	Bench press 3RM (kg)	Squat 3RM (kg)	3/4 full court run (s)	17×15 running (s)	Jump and touch high (cm)
Experiment group 1	53.2 ± 9.31	69.6 ± 8.26	4.08 ± 0.34	74.01 ± 4.89	315.60 ± 7.23
Experiment group 2	52.2 ± 7.36	67.6 ± 9.65	3.82 ± 0.48	66.89 ± 4.01	310.20 ± 7.46
Experimental group 3	54.8 ± 9.39	69.8 ± 7.66	3.91 ± 0.31	72.29 ± 4.91	309.00 ± 9.30
Control group	50.6 ± 8.50	67.2 ± 9.12	3.78 ± 0.26	70.71 ± 2.58	318.00 ± 2.91
p	0.891	0.948	0.556	2.606	1.821
f	0.206	0.118	0.717	0.088	0.184

Table 3: Multiple interactive comparative analysis of bench press items in the special strength of the subjects before the experiment.

Comparison group A	Comparison group B	Bench press 3RM mean ± standard deviation (kg)		t value	p value
Experiment group 1	Experiment group 2	53.2 ± 9.31	52.2 ± 7.36	0.188	0.855
Experiment group 1	Experimental group 3	53.2 ± 9.31	54.8 ± 9.39	-0.271	0.794
Experiment group 1	Control group	53.2 ± 9.31	50.6 ± 8.50	0.461	0.657
Experiment group 2	Experimental group 3	52.2 ± 7.36	54.8 ± 9.39	-0.487	0.639
Experiment group 2	Control group	52.2 ± 7.36	50.6 ± 8.50	0.318	0.759
Experimental group 3	Control group	54.8 ± 9.39	50.6 ± 8.50	0.741	0.480

Table 4: Multiple interactive comparative analysis of squat items in the special strength of the subjects before the experiment.

Comparison group A	Comparison group B	Squat 3RM mean ± standard deviation (kg)		t value	p value
Experiment group 1	Experiment group 2	69.6 ± 8.26	67.6 ± 9.65	0.352	0.734
Experiment group 1	Experimental group 3	69.6 ± 8.26	69.8 ± 7.66	-0.040	0.969
Experiment group 1	Control group	69.6 ± 8.26	67.2 ± 9.12	0.436	0.674
Experiment group 2	Experimental group 3	67.6 ± 9.65	69.8 ± 7.66	-0.399	0.700
Experiment group 2	Control group	67.6 ± 9.65	67.2 ± 9.12	0.670	0.948
Experimental group 3	Control group	69.8 ± 7.66	67.2 ± 9.12	0.488	0.639

Table 5: Comparative analysis of special strength indicators of traditional control group.

$N = 5$	Bench press 3RM (kg)	Squat 3RM (kg)	3/4 full court run (s)	17×15 run (s)	Vertical jump height (CM)
Before experiment	50.6 ± 8.50	69.6 ± 8.26	3.782 ± 0.257	70.71 ± 2.58	318.0 ± 2.91
Eight weeks of experiment	55.4 ± 7.34	74.7 ± 6.96	3.678 ± 0.256	69.35 ± 2.04	319.6 ± 2.30
p	0.082	0.058	0.007	0.630	0.016
f	-2.311	-2.627	5.039	2.561	-4.000

quality of young basketball players. The results are shown in Table 5.

Moreover, on the premise of not carrying out the training of wearing compression devices, the effect of the traditional control group has a large gap compared with the three experimental groups in terms of the pre- and postcomparison results of bench press and squat events. The degree of improvement of the control group before and after the training was about 4.8 kg, which was very balanced and regular. Perhaps because it did not carry out the same heavy and high-intensity load training as the traditional resistance strength training, it led to the improvement, but compared with the three experimental groups of blood flow restriction training, it did not have satisfactory effect.

4.2.2. Comparative Analysis of the Test Results of the Maximum Strength Quality in Basketball Special Strength Quality after the Experiment. After the experiment of blood flow restriction basketball special strength training three times a week for eight weeks, a postexperiment test was carried out for a total of 20 subjects in four groups in the experiment after the experiment was completed and the four test indicators of teenagers' basketball special strength in the postexperiment test. In order to further explore the relationship between these indicators among the four groups participating in this experimental training, the SPSS statistical software will be used to conduct one-way ANOVA and independent sample t-test on all the original data of the postexperimental test, analyze the relationship between the test data of different strength qualities in different groups, and analyze and discuss the reasons for the changes of these data. The specific results are shown in Table 6.

As shown in Table 7, after 8 weeks of blood flow restriction basketball special strength training, the average value of the bench press 3RM test of the experimental group 1 was 65.2 kg, that of the experimental group 2 was 65.7 kg, that of the experimental group 3 was 72.2 kg, and that of the traditional control group was 55.4 kg. Among them, experimental group 2 has an advantage of 0.5 kg compared with experimental group 1, experimental group 3 has an advantage of 7 kg compared with experimental group 1, and experimental group 2 has a disadvantage of 6.5 kg compared with experimental group 3, while the traditional control group has a disadvantage of 9.8 kg compared with experimental group 1, 10.3 kg compared with experimental group 2, and 16.8 kg compared with experimental group 3.

In the one-way variance test results of the 3RM item of bench press in the relevant special strength quality after the experiment is completed, $f = 6.403$. Next, we can see that the later p value is 0.005, $p < 0.01$, indicating that there is an extremely significant difference between the four groups of bench press after the experiment has trained eight groups. Next, it can be seen from Table 7 that the p value of the experimental group 1 and experimental group 2 is 0.855, and the mean difference is 0.5 kg, indicating that the training effect of bench press quality in low-intensity compression group and medium-intensity compression group is roughly the same after eight weeks of training, and there is no significant difference. The p value of the first group and the third group is 0.145, and the mean difference is 7 kg. The mean difference between the second group and the third group is 6.5 kg. Look back at the mean difference between the first group and the second group. The test results of the three groups are compared with each other, which shows that although the difference between the low-intensity pressure group and the high-intensity pressure group is still not significant, there is a relatively obvious gap compared with the medium pressure group. It also preliminarily shows that within the safe and reasonable range of values, with the continuous increase of the pressure load, the performance of the recumbent push of the athletes who carry out blood flow restriction basketball special strength training will also be improved more significantly.

By analyzing the bench press performance of the three experimental groups and the traditional control group, the average difference between the experimental group 1 and the traditional control group is 9.8 kg, the difference between the experimental group 2 and the traditional control group is 10.3 kg, and the difference between the experimental group 3 and the traditional control group has reached an amazing 16.8 kg. However, the p values obtained by the experimental group 2 and the experimental group 3 and the control group are all less than 0.05, and the p values obtained by the experimental group 3 have been less than 0.01, which is still significantly improved compared with the traditional control group, and the p values also decreased significantly compared with those before the experiment. This shows that under the same training load, the same interval time between groups and the same training plan, compared with the traditional resistance strength training, the blood flow restriction training has a very obvious improvement and progress in the strength quality of bench press 3RM of juvenile basketball players in basketball school. And under different pressure load conditions, the same training results will be different. The performance of bench press will increase with the increasing pressure value, and there is a positive correlation between the two.

Table 6: One-way ANOVA of the 3RM test results of bench press in basketball special strength quality after the experiment.

Control group ($N = 5$)	Mean ± standard deviation (kg)	Homogeneity test	f value	p value
Experiment group 1	65.2 ± 5.76			
Experiment group 2	65.7 ± 1.39	0.600	6.403	0.005
Experiment group 3	65.7 ± 1.39			
Traditional control group	55.4 ± 7.34			

Table 7: Independent sample t-test analysis table of 3RM test results of bench press in basketball special strength quality after the experiment.

Group A	Group B	Mean difference	t value	p value
Experiment group 1	Experiment group 2	-0.5	-0.189	0.855
Experiment group 1	Experimental group 3	-7.0	-1.614	0.145
Experiment group 1	Traditional control group	9.8	2.348	0.470
Experiment group 2	Experiment group 3	-6.5	-1.834	0.104
Experiment group 2	Traditional control group	10.3	3.081	0.015
Experiment group 3	Traditional control group	16.8	3.507	0.008

5. Conclusion

This paper combines the blood flow restriction training method with basketball special strength training, in order to explore the advantages of this training method for young basketball players' special strength quality, compared with the traditional resistance strength training, and the changes in body shape and function. This paper attempts to provide some references and suggestions for the training plan of the combination of the two and the optimization of the pressure value within the safe range of pressure application. Through the research, it is found that (1) blood flow restriction training can effectively improve the special strength quality of juvenile basketball players in basketball school, and it is the most significant to improve the maximum strength quality and strength endurance quality, which is significantly better than the control group. Although the speed strength and explosive force quality have been improved, the effect is not obvious, and the explosive force quality effect of the high pressure load group is less than that of the control group; (2) blood flow restriction training can effectively improve the cardiopulmonary function of juvenile basketball players. The heart rate decreased in quiet state, and the rate of heart rate returning to calm increased after exercise, indicating that blood flow restriction training enhanced the pumping function of the heart and indirectly improved the adaptability of muscles to high load intensity training; (3) through the test, it is found that the experimental group has a significant effect on the improvement of maximum strength no matter whether it compares itself before and after or with the control group. For strength endurance, explosive force, and speed force, the greater the pressure load, the better the effect. It shows that within the scientific and safe pressure range, the greater the pressure on the body, the better the training effect. Appropriate pressure value and interval time, as well as more targeted training programs, can achieve twice the result with half the effort compared with traditional resistance strength training.

Of course, it is necessary to make necessary preparations before trying blood flow restriction training. Before training, fully prepare for the preparatory activities and special warm-up exercises, and then carry out the adaptive activities of blood flow restriction training, and timely report to the coach whether the blood flow restriction training device is suitable and stable, as well as whether the physical condition of the experimental object is uncomfortable in the process of gradually increasing pressure. It is suggested that the team members who first try blood flow restriction training should be equipped with team doctors for real-time monitoring and risk and safety assessment, so as to ensure the health of the team members and prevent accidents. After blood flow restriction training, the pressure band must be removed as soon as possible with the guidance and help of the coach and team doctor. It is recommended to use various physical means to relax and stretch after strength training after the blood pressure and heart rate return to the normal range. To prevent excessive lactic acid accumulation and fascia adhesion, which will affect the training effect, it is suggested to carry out comparative training according to the flow chart of blood flow restriction training safety strategy, so as to ensure the scientific and safe training content.

Data Availability

The labeled data set used to support the findings of this study is available from the corresponding author upon request.

Conflicts of Interest

The author declares that there are no conflicts of interest.